Short course

Advanced Design for Ships and Offshore Floating Systems

September 1992

Sponsored by the European Commission's COMETT Programme

A five day course held at the Jury's Pond Hotel, Glasgow

Organised by:

MTD Ltd (through the UETP in Marine Science and Technology)

The University of Glasgow

ABOUT WEGEMT

WEGEMT is a European Association of 37 Universities in 17 countries. It was formed in 1978 with the aim of increasing the knowledge base and updating and extending the skills and competence of engineers and postgraduate students working at an advanced level in marine technology and related sciences.

WEGEMT achieves this aim by encouraging universities to be associated with it, to operate as a network and therefore actively collaborate in initiatives relevant to this aim.

WEGEMT considers collaborative research, education and training at an advanced level, and the exchange and dissemination of information, as activities which further the aim of the Association.

NB For marine technology and related sciences, WEGEMT includes all aspects of offshore oil and gas exploration and production, shipping and shipbuilding, underwater technologies and other interdisciplinary areas concerned with the oceans and seas.

ABOUT THE PUBLICATION

This publication represents a series of lecturers' notes which were presented at a short course and Workshop entitled *Advanced Design of Ships and Offshore Floating Systems* first presented at the Jury's Pond Hotel, Glasgow in September 1992. The course was coordinated by MTD, and hosted by the University of Glasgow. It was part funded by the EU COMETT Programme through the University Enterprise Training Partnership in Marine Science and Technology (MARTRAIN).

Published by WEGEMT
Originally published by The Marine Technology Directorate Limited

This volume has been made available so that it contains the original authors' typescripts and where possible, overheads used during the presentation. The method may from time to time display typographical limitations. It is hoped however, that they do not distract the attentions of the reader. Please note that the expressed views are those of the individual authors and the publishers cannot accept responsibility for any errors or omissions.

ADVANCED DESIGN FOR SHIPS AND OFFSHORE FLOATING SYSTEMS

GLASGOW - 21-25 SEPTEMBER 1992

COURSE PROGRAMME

Sunday, 20th September:

19.30 - 21.30	*Welcome Reception*

Monday, 21st September:

08.30 - 09.15	*Registration*
09.15 - 09.30	Welcome and Introduction by Professor D. Faulkner
09.30 - 10.30	Introduction to probability methods in design by Professor D. Faulkner
10.30 - 11.00	*Coffee*
11.00 - 12.00	Environmental design considerations by Dr. A. Incecik
12.00 - 13.00	Linear wave induced motions and loads on floating structures by Dr. A. Incecik
13.00 - 14.00	*Lunch*
14.00 - 15.00	Non-linear wave induced second-order motions of floating and compliant structures by Mr. G.E. Hearn
15.00 - 15.30	*Coffee*
15.30 - 16.30	Non-linear wave induced second-order motions of floating and compliant structures by Mr. G.E. Hearn
16.30 - 17.30	Introduction to advanced marine vehicles by Dr. A. Incecik

Tuesday, 22nd September:

08.30 - 10.30	Probability based offshore design for extreme lifetime loads and ultimate strength by Professor D. Faulkner
10.30 - 11.00	*Coffee*
11.00 - 12.00	Review of reasons for selecting a floating production system by Mr. N.S. Miller
12.00 - 13.00	Tanker based production and storage systems by Mr. N.S. Miller
13.00 - 14.00	*Lunch*
14.00 - 15.00	Buoy type production and storage systems by Mr. N.S. Miller
15.00 - 15.30	*Coffee*
15.30 - 17.30	Practical seakeeping design tools for monohulls by Mr. G.E. Hearn

Course Programme (Cont'd)

Wednesday, 23rd September:

08.30 - 10.30	Rule based and reliability based design for ship structures by Professor D. Faulkner
10.30 - 11.00	*Coffee*
11.00 - 12.00	Conceptual design of semi-submersible exploration platforms by Mr. H. Boonstra
12.00 - 13.00	Conceptual design of semi-submersible production platforms by Mr. H. Boonstra
13.00 - 14.00	*Lunch*
14.00 - 15.00	Practical seakeeping and structural design tools for advanced marine vehicles by Mr. N. Barltrop
15.00 - 15.30	*Coffee*
15.30 - 16.30	Practical seakeeping and structural design tools for advanced marine vehicles by Mr. N. Barltrop
16.30 - 17.30	Design to avoid material failure by Professor M.J. Cowling

Thursday, 24th September:

08.30 - 09.30	In-service assessment and maintenance by Mr. N. Barltrop
09.30 - 10.30	Life-cycle design of semi-submersible production platforms using probabilistic methods by Mr. H. Boonstra
10.30 - 11.00	*Coffee*
11.00 - 12.00	Life-cycle design of semi-submersible production platforms using probabilistic methods by Mr. H. Boonstra
12.00 - 13.00	Product prototyping at the design stage by Dr. R. Kattan
13.00 - 14.00	*Lunch*
14.00 - 15.00	Developments in design which support product proto-typing by Mr. W. Hills
15.00 - 15.30	*Coffee*
15.30 - 16.30	The use of a product modelling approach to create ship design and associated production information by Dr. B. Douglas
16.30 - 17.30	Design and dictates of production - small shipbuilding perspective by Mr. K. Fulford

19.30 - 22.00 *Course Dinner at University of Glasgow*

Course Programme (Cont'd)

Friday, 25th September:

08.30 - 09.30	Design and analysis of station keeping systems: D.P. systems by **Professor J.A. Pinkster**
09.30 - 10.30	Design and analysis of station keeping systems: Mooring Design by **Mr. N.S.Miller**
10.30 - 11.00	*Coffee*
11.00 - 12.00	Design and analysis of station keeping systems : Mooring Design by **by Mr. N.S.Miller**
12.00 - 13.00	Full scale testing and monitoring of the behaviour of ships and floating offshore structures by **Professor J.A. Pinkster**
13.00 - 14.00	*Lunch*
14.00 - 15.00	Model testing of ships and floating offshore structures by **Professor J.A. Pinkster**
15.00 - 15.30	*Coffee*
15.30 - 16.30	Model testing of ships and floating offshore structures by **Professor J.A.Pinkster**

ADVANCED DESIGN FOR SHIPS AND OFFSHORE FLOATING SYSTEMS

21-25 September 1992

Jury Pond Hotel, Glasgow

Delegates List

1. BLOEM, W., Marine Technology Engineer, Shell International Petroleum Mij, P.O. Box 162 - EPD/53, 2501 AN The Hague, The Netherlands.

2. CLELAND, Graham, Student, Univ. of Newcastle upon Tyne, Engineering Design Centre, Armstrong Building, Newcastle upon Tyne, NE1 7RU.

3. de VRIES, M.H., Royal Netherland Naval College, Her Nieuwe Diep 8, 1781 CA Den HelderR, The Netherlands

4. HUISMAN, J.M., Chief Naval Architect, Nedlloyd Lines, P.O. Box 240, 3000 DH Rotterdam, The Netherlands.

5. HULL, Alistair , Naval Architect, Aker Engineering plc.,10 North Silver Street, ABERDEEN, AB1 1RL

6. KARLINSKY, S.L., Leading Engineer, Central Design Bureau "Rubin", Marat Str. 90, 191126 ST. PETERSBURG, Russia.

7. KLINGE, P., Research Scientist, VTT Ship Laboratory, P.O. Box 114, SF-02151 Espoo, Finland.

8. LEWIS, T.C., Offshore Engineer, Global Maritime, 12 Craven Street, LONDON, WC2N 5PB

9. McCAIG, J., Director, G.L. Watson Naval Architects Limited, 6.13 Kelvin Campus, West of Scotland Science Park, GLASGOW, G 20 OSP (Part-time only)

10. STAUNTON-LAMBERT, Mark J., The Marine Technology Directorate Limited, 19 Buckingham Street, London, WC2N 6EF.

11. THORKILDSEN, Harald, Senior Engineer, Det norske Veritas Classification AS, P.O. Box 300, N-1322 Hovik, Norway

12. TOLIKAS, C., Research Student, University of Glasgow, Glasgow, G12 8QQ. (Part-time only)

13. UNO, Kiyotaka, Senior Researcher, NKK Corporation, 1 Kokan-Cho Kumozu, Tsu-City, MIE Pref., Japan

14. WOLFF, Ir. Ph. A., Senior Designer, Royal Netherlands Navy, Ministerie von Defensie, DMKM afd. Scleepsbouw, Van der Burghaus 31, Posthus 20702, 2200 ES Den Haag, The Netherlands.

INTRODUCTION TO PROBABILITY METHODS IN DESIGN

by

DOUGLAS FAULKNER

GLASGOW

CONTENTS

		Page No.
1.	INTRODUCTION	1
1.1	Structural Limit States	2
1.2	Analysis Levels	2
1.3	Transformation or First-Order Reliability Method	3
2.	UNCERTAINTY MODELLING	4
2.1	Physical Uncertainty	4
2.2	Knowledge Based Uncertainties	5
	Statistical Uncertainty	
	Modelling Uncertainty	
	Phenomenological Uncertainty	
2.3	Human Errors	9
2.4	Hidden Human Errors	13
2.5	Notional Reliability	13
2.6	Fuzzy Modelling	13
3.	USE OF RELIABILITY THEORY	14
3.1	Characteristic Values	15
3.2	Partial Safety Factors and Code Format	16
3.3	Economic Based Safety Decisions	19
	Economic Risk Evaluation	
	In-Service Assessments	
4.	RANDOM VARIABLE RELIABILITY THEORY	21
4.1	One Dimensional Random Variable	21
4.2	Basic Concepts	23
4.3	Reliability Analysis Steps	23
4.4	Single Failure Mode Structures	24
4.5	Special Case	27
	Reliability Index (β)	
	Importance of Low v_R	
4.6	Lognormal Distributions	29
4.7	General Case	30
4.8	Time Dependent Loads	31

Page No.

5. SECOND MOMENT TRANSFORMATION METHODS 34

5.1 Transformations 34
Rackwitz-Fiessler Transformation
R and Q Idealisation
Multi-dimensional Space
Solution
5.2 Hasofer-Lind Reliability Index 39
5.3 Derived Equations 41
Reliability Index
Partial Safety Factors
5.4 Summary 43

REFERENCES 44-46

FIGURES:

Fig. 1: Test Data and Modelling Uncertainties for Compressed Axially Stiffened Cylinders 8
Fig. 2: Factors which Influence Structural Reliability 12
Fig. 3: Reliability Index and Partial Safety Factors 17
Fig. 4: Design Points in Design Variable Space 17
Fig. 5: Economic Based Safety Decisions 20
Fig. 6: Time-Varying Load 22
Fig. 7: Out-crossing from a Safe Region 22
Fig. 8: Up-crossing of a Threshold Level 22
Fig. 9: Basic R-Q Representation 26
Fig. 10: Illustration of Reliability Index 26
Fig. 11: Region of Integration for Failure Probability 26
Fig. 12: Idealisation of Slow and Fast Random Variables 33
Fig. 13: Flow Chart for Structural Safety Evaluations 35
Fig. 14: Basic Variable Space and Transformed Variable Space 38

ANNEX - Glossary of Terms and Definitions

APPENDIX A Summary of Probability Theory

APPENDIX B Code Formats and Structural Reliability

APPENDIX C Standard Normal Distribution Table

ADVANCED DESIGN FOR SHIPS AND OFFSHORE FLOATING SYSTEMS
21-25 September 1992

INTRODUCTION TO PROBABILITY METHODS IN DESIGN

by

Douglas Faulkner

1. INTRODUCTION

This lecture is concerned with lifetime structural safety, how much is required and how this can best be achieved in design. As an introduction the lecture can make no claim to completeness, but merely introduce and hopefully illustrate some of the more important basic concepts in the context of safety of marine structures as designed.

Recently, probabilistic methods have been further developed to account for new information which becomes available after the design process. Such information can come from fabrication quality control or from in-service inspection and monitoring. If any proof testing were undertaken then a minimum strength is known. With this additional information some of the uncertainty present at the design stage is reduced or eliminated, and improved estimates of the reliability may be obtained. This 'updating' activity is particularly important in fatigue reliability, and is now well established in nuclear power, aerospace and offshore engineering. In this, the reliability of the inspection methods is itself important.

It is wise to recognise that structural reliability only has to do with failures of the structure resulting from excessive service loads and/or too low structural strength. It is therefore but one aspect of *Risk Analysis* which aims to account for all possible failure scenarios in the operation of the structure. This uses fault-trees to assess event failure rates, and aims to quantify the probability of occurrence of the top event. The risk is then assessed as a combined measure of the probability of occurrence of this *hazard* and its consequences and measures are taken to reduce both.

Two recommended texts are Thoft-Christensen & Baker (1982) and Melchers (1987). A glossary of terms and definitions is given in the Annex.

1.1. Structural Limit States

Typical limit states for marine structures are shown in Table 1:

Table 1: Limit States for Marine Structures

Limit state	Description	Examples
Ultimate	collapse of part (component) or all (system) of a structure	buckling of a brace, collapse of whole framework; buckling of ship deck; jackknife of cross-section; rupture leading to progressive collapse
Damage	fatigue cracking or permanent inelastic deformation	through-thickness cracking of tubular or plate; plastic bending of plates and stiffeners
Service-ability	disruption of normal use	excessive deflection, vibrations, accidental damage, etc.

Very few structures collapse or require major repairs, so violation of the ultimate strength or serious damage limit states rarely occur. When they do the consequences may be extreme, for example the spectacular collapse of the Tay Bridge, Ronan Point flats, Kielland drilling platform, and most probably the *MV DERBYSHIRE*.

Structural reliability is concerned with the calculation and *prediction* of the probability of limit state violation. In particular, the violation of the ultimate limit state is that which is first evaluated as a governing criterion which controls the major disposition of material, and hence cost. But, because of the alternating nature of wave induced loads, fatigue design assumes considerable importance for the more heavily loaded details, especially as the cost of in-situ repair is very high.

1.2 Analysis Levels

Reliability methods are usually classified in three levels of generally increasing complexity:

Level 1: code level methods in which reliability based partial safety factors (PSF) are applied to characteristic values of load components and resistance factors in the safety check equations used in design; this is a deterministic format most commonly advocated for limit state design codes at present

Level 2: second moment methods in which the random variables are defined only in terms of means and variances, (that is, they are assumed to be normally distributed) and the joint probabilistic behaviour is reflected in a covariance matrix; the measure of reliability is based on the reliability (or safety) index β. In *Advanced* or *Extended* Level 2 methods the design variables can have any type of probability distributions

Level 3: "exact methods" require the integration of the multi-dimensional joint probability distributions of the design variables extended over the failure domain; the measure of reliability is the calculated probability of failure p_f.

A fourth *Level 4* is sometimes referred to (Melchers, 1987 and Marley, 1991) as incorporating engineering economic analysis to give design for minimum total cost or maximum utility; but this is really a *decision* method not related to the complexity of the reliability method used.

It should also be noted that many design codes use PSFs which have not been properly derived using reliability methods. No less an authority than Melchers (1987) regards the Level 1 method in this way, but then it should not be included in the hierarchy of structural reliability measures! This confusion should be avoided, and these notes will show how PSFs are derived for any code format using reliability theory.

1.3 Transformation or First-Order Reliability Method

It is convenient if only the first two moments of each random variable are considered in the probability calculation. This can be achieved by using the Rosenblatt transformation (1952) in which non-normal distributions are transformed into equivalent normal distributions. The disadvantage is that the limit state functions become more complex and usually more non-linear.

In what follows, the transformations are best made about the checking or "design" points at which the variables combine to give the minimum reliability index β. As a further sufficiently accurate simplifying assumption for most purposes, all the limit state functions are piecewise linearised at their design points and the method is therefore referred to as a first-order reliability method (FORM). Historically, the transformation approach was developed as an extension of the first-order second moment method (FOSM), and it is still often referred to as the advanced (or extended) first-order second moment method (AFOSM). But it is sometimes felt to be less confusing to call the method FORM.

In passing, we can note that it is sometimes assumed that the failure surface is approximated by a quadratic surface at the design point. This approach is then referred to as a second-order reliability method (SORM). But, this refinement is not considered here and is seldom justified in any case because of the "notional" nature of the calculated reliability.

2. UNCERTAINTY MODELLING

Reliability is concerned with *uncertainties* related to randomness, bias errors, etc. The uncertainties we need to consider are those associated with the predicted still-water and environmentally-induced load effects on structural elements and with the predicted resistance of these elements to the various limit states. Broadly, formal uncertainties may be classified into two groups: aleatory (physical) or epestemic (knowledge). These latter may be reduced, at a cost, by collecting more information more carefully, or by adopting more realistic and/or sophisticated models. A third less formal group are human uncertainties - particularly important as we shall see.

2.1 Physical Uncertainty

This is also referred to as *inherent, intrinsic* or *fundamental* uncertainty, and is related to the natural randomness of a basic variable and cannot be reduced and are therefore also referred to as being *objective* uncertainties. Examples include variations of yield strength, wind loading, dead loads, etc. Variability in the physical dimensions of a structural component is also usually included, but in principle this can be reduced by improving the quality of construction. Typical values affecting strength and described in terms of coefficients of variation (v_i) and bias (ζ_i) are given in Table 2.

Table 2: Typical Random and Systematic Physical Uncertainties

Item	cov v_i%	Bias ζ_i%
Yield stress	6-9	10 to 15
Youngs modulus	1-3	-2 to 2
Plate thickness	1-4	-2 to 2
Cross-section of scantlings	2-4	-2 to 2
Welding stresses	10-15	
Plate distortions	30-50	
Stiffener distortions	10-15	

2.2 Knowledge Based Uncertainties

As stated above these uncertainties can in principle be reduced. Their estimation requires a considerable amount of judgement and they are therefore referred to as being *subjective* uncertainties.

Statistical Uncertainty: arising because of a limited number of observations. Statistical estimators, such as sample mean and higher moments, are derived from available data using standard procedures. These are then used to suggest an appropriate probability density function and associated parameters. But, generally, the observations of the variable do not perfectly represent it. In addition, different sample data sets will usually produce different statistical estimators and this causes statistical uncertainty.

Statistical uncertainty is seldom evaluated by engineers. But it can be incorporated in reliability analyses by letting the parameters which describe the probability distributions (such as the mean, variance, etc.) themselves be random variables. Bayesian analysis can provide the framework to incorporate this uncertainty in the analysis. But, in many cases, they are assessed on the basis of *expert opinion*. Typical covs would be 5-10%.

Modelling Uncertainty: is caused by the use of simplified relationships involving the basic variables to represent the real phenomenon or behaviour of interests. In its simplest form it concerns, for example, the uncertainty in modelling of the loads and structural response, such as limit state equations. Modelling uncertainty is usually incorporated into a reliability analysis by introducing the modelling parameter to represent the ratio:

$$X_m = \frac{\text{actual response}}{\text{predicted (modelled) response}}$$

It is usual to assume a normal distribution defined by $\overline{X}_m$ and v_{Xm}, derived where possible from measured or test data. Examples are given in Table 3 and Figure 1. At this stage three things are worth noting (Faulkner et al, 1987):

(i) modelling uncertainty is usually by far the largest uncertainty in both loading (actions) and strength (resistance) with v_{Xm} typically in the range 15% to 30% or more

(ii) v_{Xm} alone is often loosely referred to as the "modelling uncertainty", but the mean bias $\overline{X}_m$ can be equally important to assess - especially when using lower bound strength equations

(iii) the prediction model may be *analytical, numerical,* or based on *physical* tests, all aimed at representing real actions and resistances; in hydrodynamic tests flow regime related scaling errors can and frequently do occur which lead to uncertain bias in making predictions from model tests.

Statistical and *Engineering* criteria for establishing good analytical models have been developed by Faulkner (1988,1991) and applied by Faulkner et al (1992) to modelling the strength of stiffened cylinders under combined loads: $0.95 \leq \overline{X}_m \leq 1.05$, $v_{X_m} \leq 0.15$, etc.

Modelling uncertainty is usually implicit (and to an unknown degree) in permissible stress or *working stress design* philosophy, which is still used extensively. This is unfortunate as the maximum stress correlates poorly with "strength" in thin stiffened plate and shell structures made of ductile metals.

We should also note that the process of calculating the extreme design point load effect is usually based on linear analysis of stresses averaged over the element or component considered. This is then compared for reliability assessment with the modelled limit state resistance of the component based on inelastic non-linear ultimate collapse. This process itself introduces a lot of modelling uncertainty because of the implicit assumptions and the local degree of static indeterminacy of the structure. Again, this is seldom accounted for but can be overcome by incorporating the non-linear load effects and structural analysis more formally in the reliability analysis as a *system*.

Table 3: Typical Modelling Uncertainties

Item	cov v_{Xm}%	Bias ζ_{Xm}%
Factors affecting strength		
Flat panel collapse - best	10-15	-5 to 5
- typical codes	15-30	0 to 20
Unstiffened cylinder - codes	20-40	20 to 50(1)
Stiffened cylinders - best	12-18(2)	-20 to 40(1)
- typical codes	20-40(2)	0 to 30(1,3)
Submarine pressure hull		
- interframe collapse	5-10	-5 to 5
- general instability	15-20	0 to 20
Fatigue strength	30-70	50 to 150(4)
Factors affecting loads		
Dead loads	5-10	
Live loads	10-20	-10 to -30(5)
Ship extreme bending		
- initial distribution	5-10	-30(6) to 0
- extreme distribution	15-25	
Fixed offshore platforms	20-40	-10 to 10(7)
Compliant offshore platforms	15-30	-20 to 50(8)
Fatigue loads	10-20	-20 to 0

Notes:
(1) 'lower bound' curves are mainly used
(2) for all load combinations
(3) there are some much more extreme examples
(4) large scatter on life predictions - see more details elsewhere
(5) no reliable data available but 'growth factor' essential
(6) relates to overprediction of Linear Strip Theory
(7) based on Morison recipe
(8) based on ITTC and ISSC diffraction modelling studies

Assuming the objective physical uncertainties (Table 2) are independent from these subjective knowledge based uncertainties then the total random uncertainty (v_t) is given by:

$$v_t^2 = v_o^2 + v_s^2$$

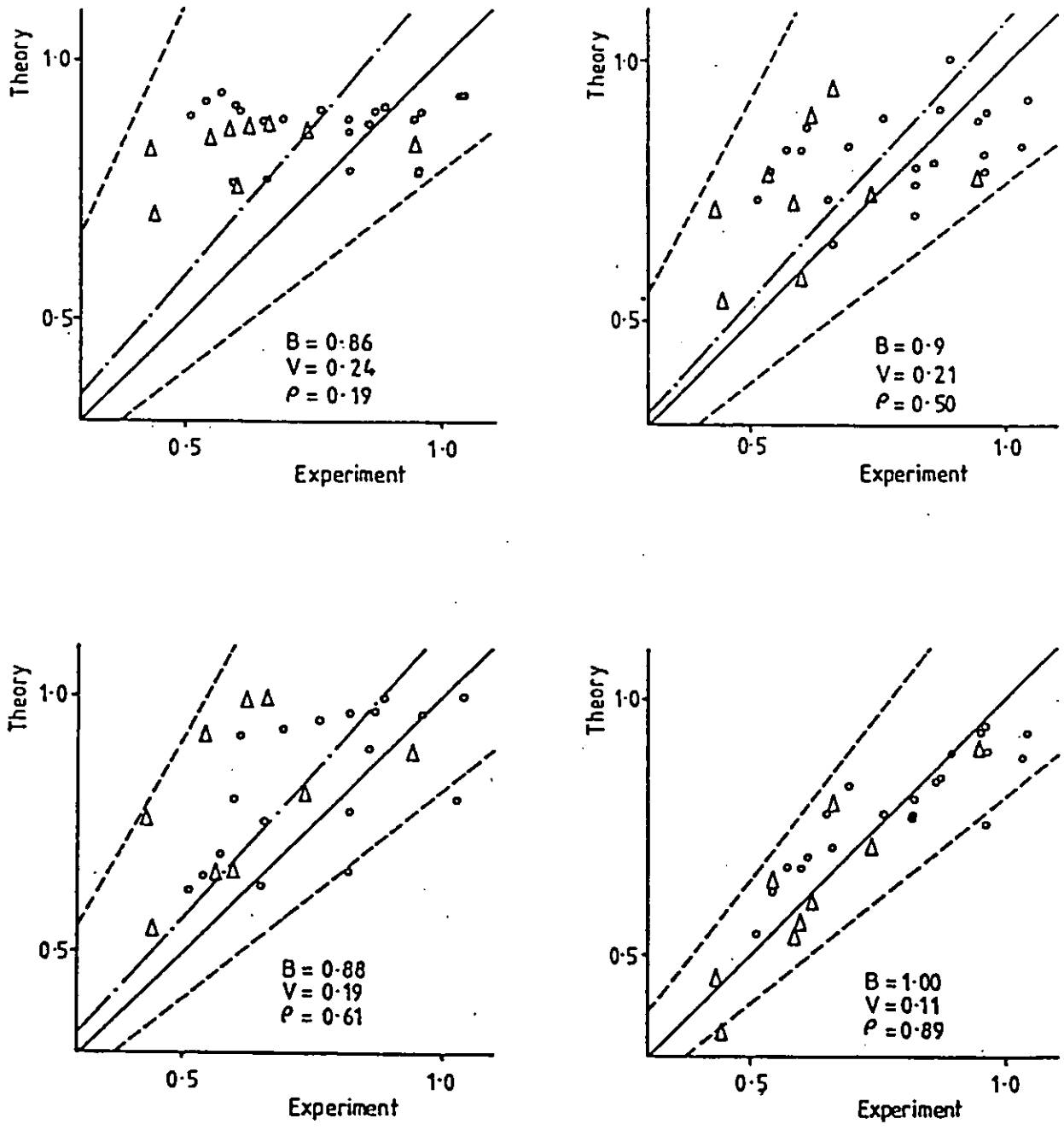

Δ Conoco – ABS data.
∘ U.K. test data.

Fig. 1: Test Data and Modelling Uncertainties for compressed axially stiffened cylinders

Phenomenological Uncertainty: arises because an apparently "unimaginable" phenomenon occurs to cause structural failure. The Tacoma Narrows suspension bridge collapse is one such case, where wind-induced aero-elastic resonant effects had not previously been considered. It was also a design which departed considerably from earlier designs.

This form of uncertainty may be considered to arise whenever the form of construction or the design technique generates any uncertainty about any aspect of the possible behaviour of the structure. It is therefore of particular importance for *novel* projects, or those which attempt to extend the "state of the art" (Pugsley, 1962). It is clear that only subjective estimates of the effect of this type of uncertainty can be given.

2.3 Human Errors*

It is generally accepted that the vast majority of recorded structural collapse or losses have very little to do with prescribed safety and are much more influenced by unpredicted human errors, sometimes involving a chain of events. Various estimates from 50% to 90% have been made for the frequency of such errors, and 85% has been quoted as a typical value for marine structures.

If reliability assessments are to relate to design human error must then be considered. But our understanding of it is limited and mainly qualitative. Following Matousek and Schneider (1976), Baker and Wyatt (1979) divided human errors into those due to:

- *Variability* in task performance but in which the structure nevertheless failed in a mode considered in design

- *Gross errors* which led to a mode of behaviour and failure against which the structure was <u>not</u> designed.

The latter are a direct result of ignorance or oversight of fundamental structural behaviour or service requirements, or "unimaginable" unknown situations.

* Sometimes referred to as *Blunders* and more commonly referred to as *Gross Errors*, but see distinction later.

Table 4: Prime Causes of Failure

Cause	%
- mistakes in drawings and calculation	7
- inadequate information in contract documents or instructions	4
- inadequate execution of erection procedures	13
- random variations in loading, structure, materials, workmanship, etc.	10
- Others	7
Performance variability errors	41
- contravention of requirements in contract documents or instructions	9
- unforeseeable misuse, abuse and/or sabotage, catastrophy, deterioration (partly "unimaginable")	7
- inadequate appreciation of loading or structural behaviour	43
Gross human errors	59

The relative importance of human errors can be gauged from Table 4 adapted from Walker (1981) who analysed 120 building failures. From this we see that about 40% fall into the variability category of low technical and professional standards, and about 60% are due to gross errors. The findings of Matousek and Schneider show a 36% to 64% ratio. Both suggest that unimaginable events constitute a rather low risk of about 5%. It is naturally much more difficult to provide similar data for marine structures, but as the human activities of design, construction and checking are similar we may expect a similar breakdown for human errors.

Safety factors can cater for some degree of human variability. However, it is unlikely that merely strengthening a structure against well understood hazards will obviate the effects of Gross human error. Some form of positive action is required. Melchers (1987) identifies seven strategies for *human intervention* to improve the situation. These are shown in Table 5.

Table 5: Human Intervention Strategies

Facilitative measures	Control measures
- Education	- self-checking
- Work environment	- external (independent) checking and inspection
- Reduce complexity	- sanctions (legal, others)
- Personnel selection	-

This formal and informal *human intervention* can also occur in operation. For example, controlling instruments are fitted to an increasing number of ships to show the Captain what level of bending load his ship is experiencing. He can then more easily avoid exceeding the maximum allowed still-water bending moments during loading and unloading, which otherwise could occur as a consequence of human errors. The other application is the voluntary manoeuvring of ships to minimise excessive rolling or avoid capsizing. But such manoeuvres may result in increased longitudinal bending moments, and the recorder enables the Captain to control extreme bending by changing course and/or speed. "Weather routeing" of ships to avoid extreme rough weather is also another example of human intervention, which reduces the probability of extreme loads. Guedes Soares (1984) has paid special regard to such measures and to loading uncertainties.

Pugsley (1973) pointed out that because errors are human they are very dependent on the working environment. He identified various factors which may affect "proneness to structural accidents":

- novelty that is new or unusual
  - types of structure
  - materials and /or construction
- experience and organisation of design and construction teams
- research and development background
- financial, industrial and political climate

The highest risks occur when several or all of these adverse features are present.

Pate-Cornell and Bea (1989) have more recently examined the influence on failure risks of the organisational weaknesses in firms concerned with design and construction. Their report is a useful complement to Pugsley's findings. Some idea of the complexity of all the factors which may influence structural reliability is shown in Fig. 2.

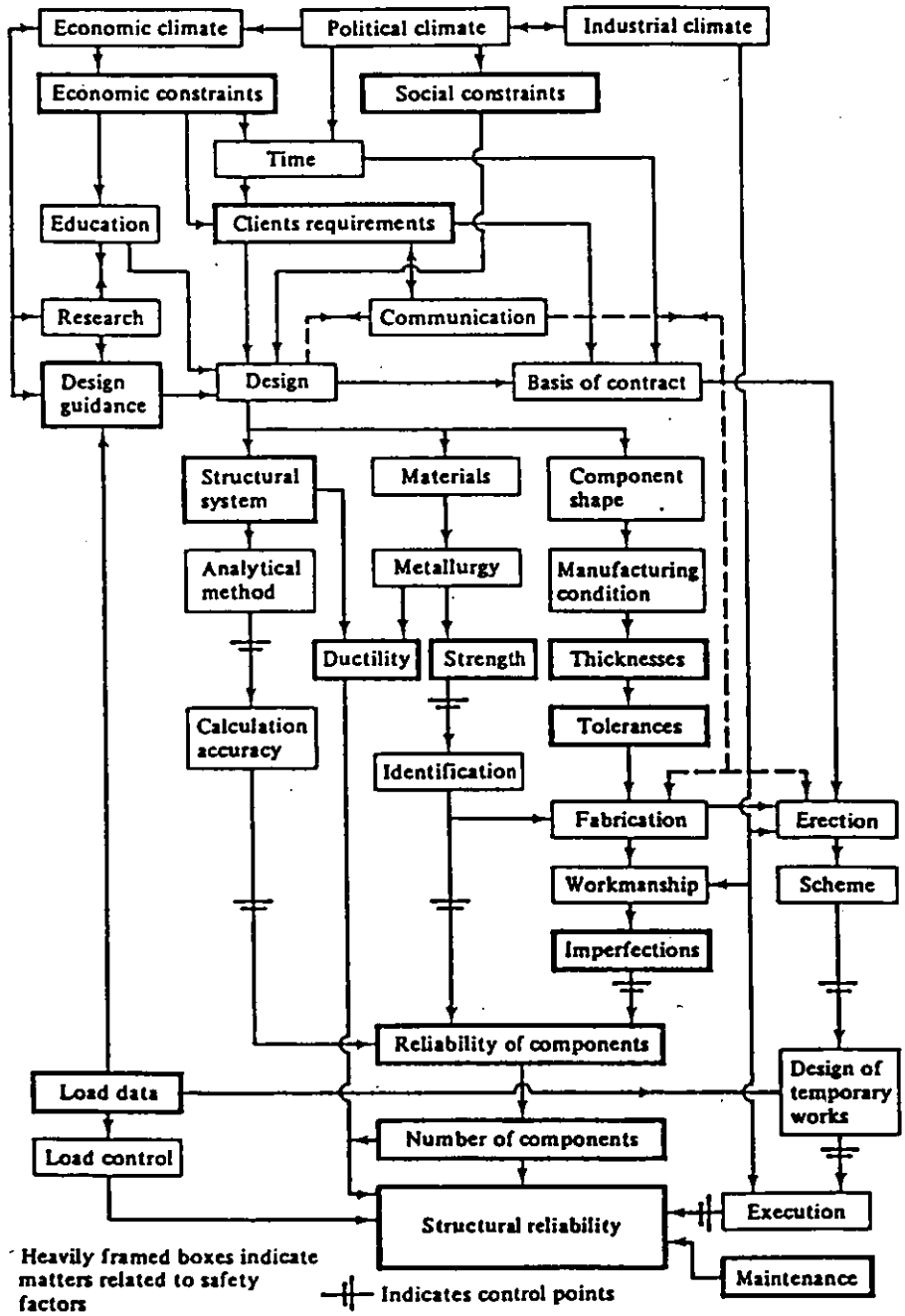

Fig. 2: Factors which influence Structural Reliability

2.4 Hidden Human Errors

Kendrick (1984) has outlined various unsafe features in pressure vessel design codes. This includes an example of an incorrect strength equation which could lead to designs 2:1 out on the unsafe side. Faulkner (1987, 1991) has quantified modelling uncertainties against structural tests and shown that in one popular offshore rules these uncertainties can vary by nearly 5:1. That is to say, within one code in particular, which has an extreme degree of skewness, it is possible to design a slender and a stocky component to resist the same load with the same supposed implicit safety level. But in truth the strengths of these two components would differ by 5:1. This leads to the distinct possibility that the least safe structure could be unacceptably unsafe, depending upon how badly the loading is modelled. But it would be attractive to the designer because of its light weight.

Both of these errors have been pointed out but the codes are still unchanged and in use. They are perhaps outside the scope of normal modelling or phenomenological uncertainties and are really examples of dangerous human errors arising in code draft modelling. They were caused by the carelessness and/or incompetence of the code drafters who have long since moved on to other things. These extreme errors will not be apparent to the average practising designer and must therefore be regarded as *hidden* human errors of the worst kind.

2.5 Notional Reliability

The difference between the *actuarial* or experienced real risk of structural failure or loss and the modelled or predicted p_f (which is lower) is sometimes referred to as the *adjunct* probability of failure. It is mainly attributed to human errors. But as indicated in sections 2.2 and 2.4 modelling errors can also be very large, and this must account for some of the difference.

So long as human errors and modelling uncertainties remain, there will always be a gap between predicted and experienced risks. At present this gap is typically 1 to 3 orders of magnitude. For these reasons any predicted reliability index or probability of failure is referred to as being *notional*.

2.6 Fuzzy Modelling

Blockey (1977) treated the adjunct probability of failure in the light of the concepts of Pugsley. He predicted the likelihood of structural accidents due to

human error and applied it to 23 major structural accidents. Brown (1979) on the other hand compared accident statistics with the theoretical probability of failure, and suggested one safety measure to represent both, that is, that could be associated with the total (real) probability of failure.

An interesting aspect of the work of Blockey and Brown is that they do not use a probabilistic framework that is common to structural safety studies, but they operate with the new concept of *fuzzy* sets. This theory has been developed to deal with vague or imprecise (fuzzy) concepts. This is fundamentally different from probability theory which deals with uncertain but precise concepts.

Guedes Soares (1984) argues that because they are based on different postulates it is difficult to relate the two concepts with each other. Although fuzzy sets may still be useful in relation to assessing the behaviour and safety of existing structures, it appears that in the near future it may be difficult to combine a gross error analysis based on fuzzy sets with the theoretical probability of failure, which is conditional on the avoidance of gross errors.

Error models based on a probabilistic approach have a better potential for estimating human errors. Mention is made of the work of Lind (1983) and Melchers (1987). Lind addressed also the question of the influence of gross errors in the total probability of failure. This is an important aspect that requires clarification as mentioned earlier.

3. USE OF RELIABILITY THEORY

Before embarking on the theory it is important to understand why we use reliability theory and what it can do for us. We really use it for two reasons:

- because it enables uncertainties to be handled in a rational and logical way in design and assessment; in particular it enables the sensitivity of the reliability to the various design variables and decision to be determined

- it follows that it also provides a more rational basis for decision making than is possible with purely deterministic analysis.

Decisions are seldom clear cut and will never be perfect, but it is preferable to take them using a probabilistic basis.

3.1 Characteristic Values

Traditionally, engineers concerned with safety have used 'lower bound' curves for fatigue, column strength, etc. and for 'nominal' or 'minimum' value for yield strength in metals. Likewise, 'upper bound' values for design loads are often used. These are nowadays increasingly called *characteristic values* defined as a fractile of the probability distribution of the variable. Many variables can reasonably be modelled by the normal (or Gaussian) distribution. For 'Resistive' variables the design or characteristic values are defined on the low side of the mean reistance:

$$R_k = \mu_R(1 - k_R v_R) \tag{3.1}$$

where R_k is the characteristic resistance (or other variable), μ_R its mean value* and v_R the coefficient of variation. k_R is a constant appropriate for the fractile chosen and is determined from the standardised normal distribution function - see the Tables in Appendix C. For example, if R_k is to be the value of resistance below which 5% of samples will fail then k_R is evaluated from:

$$0.05 = \Phi(-k_R)$$

hence $k_R = 1.645$ from Appendix C.

If the resistance has a cov = 10% say then from (3.1):

$$R_k = \mu_R(1 - 1.645 \times 0.1)$$

$$= 0.836\,\mu_R$$

For 'Loading' variables characteristic values are estimated on the high side of their mean. The characteristic or design load effect is:

$$Q_k = \mu_Q(1 + k_Q v_Q) \tag{3.2}$$

* Note: Other notations used for mean values are R_m and $\overline{R}$.

For convenience typical k values for percentage probabilities are:

%	15.9	5.0	2.32	1.0	0.1	0.01
k	1.0	1.645	2.0	1.28	3.09	3.72

Lower bound 5% values are often assumed for yield stress, and (incorrectly) for strength curves used in offshore design; 2 standard deviation values (2.32% probability) are generally used for fatigue strength design.

3.2 Partial Safety Factors and Code Format

Level 1 codes nowadays use partial safety factors (PSFs). If they have been calibrated to a specified safety level by using a higher level reliability method, they provide for the designer a deterministic design method which nevertheless is probability-based. A typical *code format* for safety checking might be, for example:

$$\gamma_c \gamma_f Q_k \leq \phi_m R_k \tag{3.3}$$

in which γ_c and γ_f are load effect PSFs > 1.0 and ϕ_m is a resistance PSF <1.0. They are illustrated diagrammatically in Fig. 3.

Appendix B gives the general principles for PSF code formats and compares some European and North American codes. The values of the PSFs will of course depend on the code format and are evaluated using level 2 reliability methods. Faulkner (1976) pointed out that with simple code formats like eq. (3.3) in common use, large unwanted random biases can occur with interactive load components and/or when using interaction equations for combined load strength limit states.

Also, with just 2 or 3 PSFs the resulting spread in reliability for a variety of structural components will be unnecessarily large and wasteful. This has been recognised in part and more recent safety checking equations tend to include up to five PSFs often spread within load combination equations. With PCs in general use this presents no real problem to the designer, and certainly achieves a more uniform reliability. Reliability can be an important tool in code drafting to aid code format decisions as well as for determining PSF values.

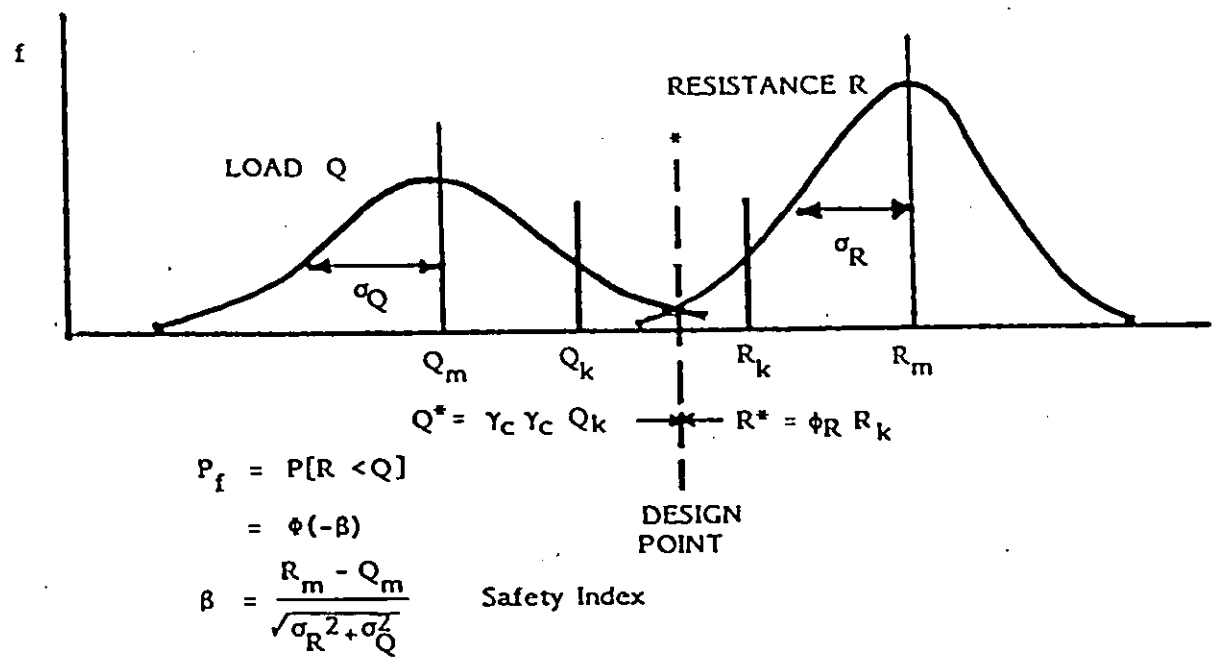

Fig. 3: Reliability Index and Partial Safety Factors

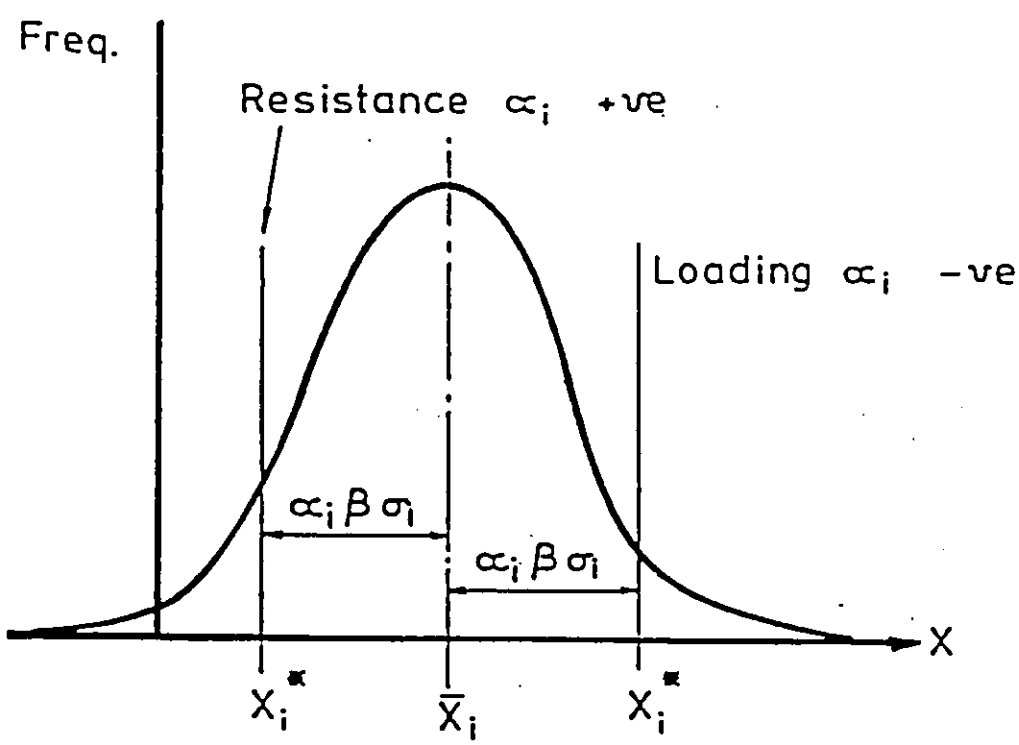

Fig. 4: Design Point in Design Variable Space

It follows that most code formats use PSFs which are *grouped*, for example, linked to 'static' or 'dynamic' loads, to material variability, etc. Recently 'modelling' PSFs have been included in advanced concepts, for example, for TLP structural and fatigue design (see Faulkner et al 1983 and and the derived ABS Model Code 1983 and Wirsching and Chan 1987).

In principle every design variable could have its own PSF, but this would be unnecessarily complex, moreover in general rather few variables are influential. Whatever the format the PSFs (γ_i, ϕ_i) are evaluated using level 2 reliability methods:

$$\gamma_i, \phi_i = \frac{x_i^*}{x_{ik}} = \frac{1-\beta_O \alpha_i v_i}{1 \pm k_i v_i} \tag{3.4}$$

where γ_i are loading PSFs usually ≥ 1.0 and for which the second denominator term is +ve, ϕ_i are resistance PSFs usually ≤ 1.0 and the second term in the denominator is −ve. For each variable x_i the *design point* value of greatest probability of failure (or minimum β) is x_i^*, and x_{ik} is the characteristic value, v_i are the coefficients of variation, β_O is the target reliability index for the code and α_i are the sensitivity factors for each variable and are −ve for loading variables. Figure 4 illustrates these design point relationships. Note that the PSFs can be 'mean value' PSFs in which case $x_{ik} = \mu_{xi}$ and $k_i = 0$.

The derivation of α_i is given later; it provides a useful parameter when judging the influence of each design variable. The sensitivity factor and derived PSFs are helpful in deciding which variables to include or to group in the code format. In submarine pressure hull design four different PSFs are effectively used in resistance terms, and each is linked to a different structural mode of failure because they vary widely - see Faulkner and Das (1990).

Finally, at this time of Eurocodes and internationalisation of design codes, one cannot overstate the importance of including modelling PSFs in the code format, and in particular to recognise the considerable weight and cost benefit to be gained by choosing only the code which has good analytical strength models as illustrated by Warwick and Faulkner (1989).

3.3 Economic Based Safety Decisions

As this subject is somewhat outside the scope of this course (which is aimed at design) just two items will be mentioned. However, the wider use of the reliability concept as an aid to more general decisions in relation to the safe design and operation of structures has been described by Baker (1985).

Economic Risk Evaluation: This approach, which is illustrated in Fig. 5, has been outlined by Marshall (1969) for establishing target reliability for use in design based on a minimisation of total lifetime cost including all the consequential costs arising from failure. These "deferred" costs when multiplied by p_f decrease as the reliability index β increases. In contrast the initial costs of design and acquisition increase with β. The total (sum) cost therefore has a saddle with a minimum cost and an associated optimum β_o. However, because of the notional nature of reliability such analyses have been used merely as a guide to such decisions in one or two companies. More recently the approach has been extended to enhanced life decisions as oil prices and other factors change.

In-Service Assessments: Although reliability theory is often thought of as being most important in design, many engineers first gain their experience of its use during in service reviews of their structures. Such reviews can be aimed at:

- Assessing the present state of structural safety in the light of 'updating' information from measurements, knowledge of storms survived, crack surveys, damage, etc.

- establishing an optimum inspection, maintenance and repair policy to minimise expenditure on this by deciding optimum repair periods based on reliability estimates of crack propagation, etc.

- making decisions related to extended use, for example of an offshore production platform to allow additional new satellite wells to be hooked up to it.

The scope for such decisions is wide, but many of these in-service assessments make use of probability based detection of cracks and predictions of crack propagation - refer, for example, to Madsen, Krenk and Lind (1986).

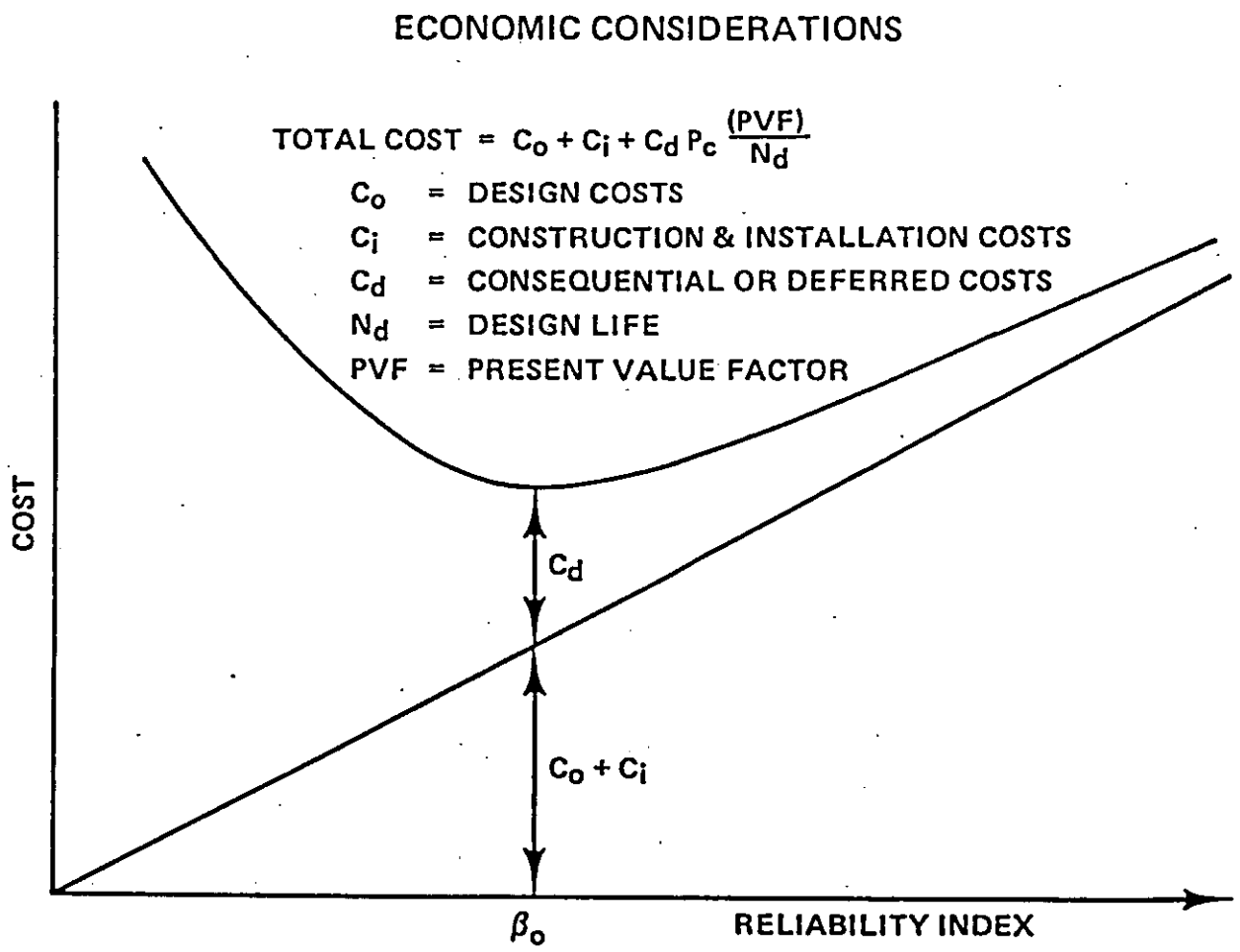

Fig. 5: Economic Based Safety Decisions

4. RANDOM VARIABLE RELIABILITY THEORY

In what follows only the case of *continuous* random variables is discussed. For *discrete* random variables (which take on only a finite countable number of discrete values) the results are analogous with integration being replaced by summation.

Appendix A provides a brief summary of the set theory mathematics of probability together with a description of the *probability* density functions (pdf) denoted by $f_X(x)$ and *cumulative* distribution functions (cdf) denoted by $F_X(x) = \int^x f_X(x)dx$ and their main parameters and moments. Appendix C provides standard normal table values for β values from 0 to 9.9 which are useful for evaluating p_f.

4.1 One-Dimensional Random Variables

Examples of a one-dimensional random variable are the normal shape imperfections in plates and cylinders and water surface variations above the mean level. Figure 6 shows a realisation of a one-dimensional stochastic process X(t) as a continuous time varying wave elevation, bending moment, or whatever.

There are two types of random variable model which can be used to represent the characteristics of the random process:

- random point-in-time distributions, and
- extreme value distributions.

The former is of relevance if the response of the structure is to be predicted at some random time t and is shown as f_X in Fig. 6. As the name suggests, it is the probability distributiuon of the variable X corresponding to sample values taken at random points in time. It is referred to as the *first-order* distribution or *initial* distribution and can be thought of as the 'parent' distribution from which extreme value distributions can be generated.

It is more likely, however, that the response of the structure is required under the maximum load that will occur *during* some time period T. For such an analysis, knowledge of the extreme value distribution f_Y corresponding to the period T is required. This is also shown in Fig. 6 and is the distribution we shall henceforth refer to as the lifetime extreme load effect Q or L.

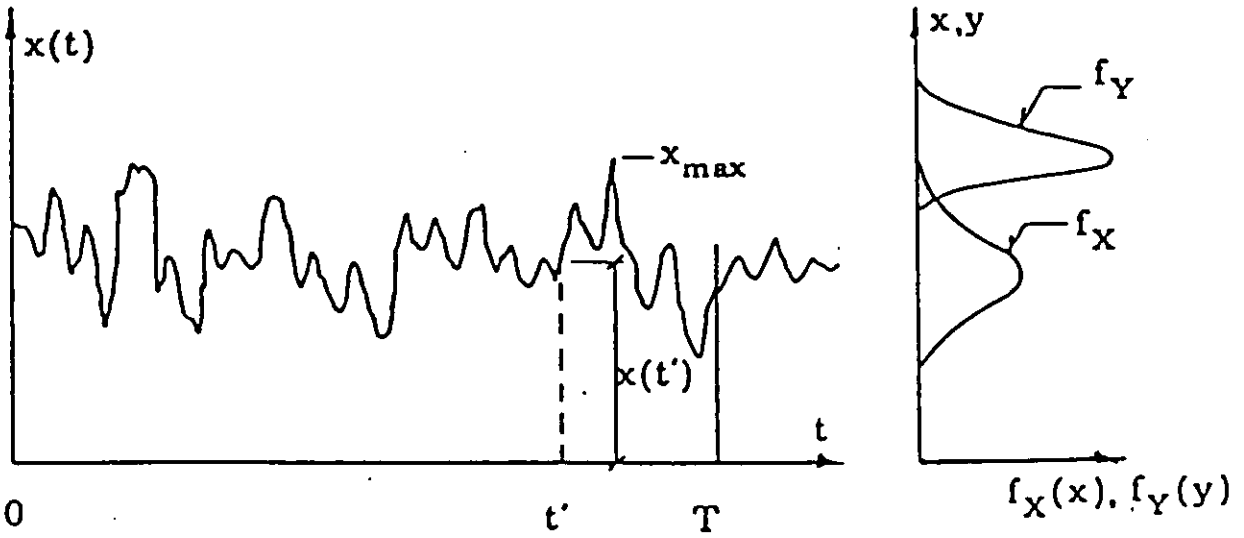

Fig. 6: Time-varying Load

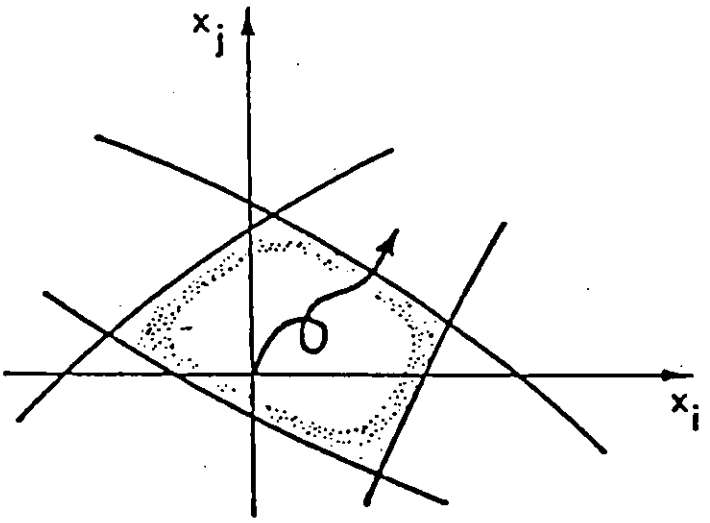

Fig. 7: Out-crossing from a Safe Region

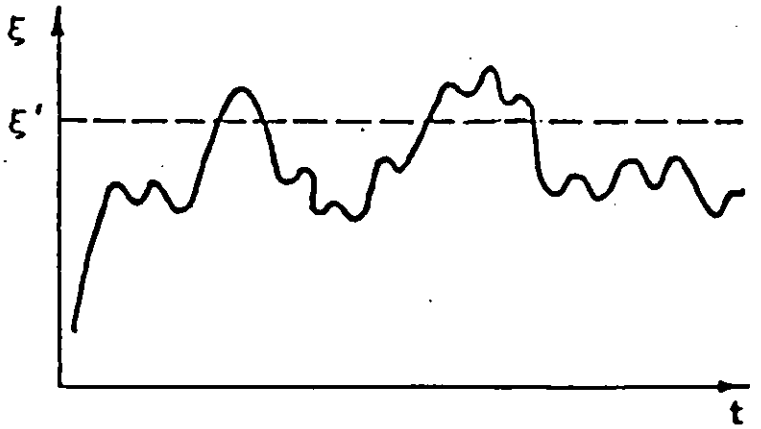

Fig. 8: Up-crossing of a Threshold Level

4.2 Basic Concepts

The reliability of a structure is its ability to fulfil its design purpose for some specified time. The design purpose may include several performance requirements to be satisfied through a specified reference or 'return' period. This may be chosen to be the same as the anticipated design life of the structure or some different period - usually longer. Performance requirements can be divided into:

(a) those associated with generally *irreversible* physical events, for example, the elasto-plastic collapse of all or part of the structure, and

(b) those associated with events which may occur with or without increments of permanent damage, several times during the life of the structure, for example, the gradual accumulation of fatigue damage locally.

For (a) one only needs to know the probability that the event will occur, the *first passage* probability, and is illustrated in Fig. 7 as the first *out-crossing* of any of the failure boundaries (failure modes) dividing the central safe region from the failure regions in multi-variable space. For (b) the proportion of time spent in the 'failure state' or the number of *up-crossings* of some *threshold* response level is of importance - as in fatigue crack propagation. This is illustrated in Fig. 8.

4.3 Reliability Analysis Steps

It is helpful to list more or less independent steps in the process (adapted from Baker):

1. Identify required performance for the structure, both at a member or *component* level and at a structural *system* level.

2. Select appropriate deterministic mathematical models which relate required performance to a set of engineering basic variables, for example, load and strength parameters.

3. Estimate the model uncertainties associated with the above models using data, judgement and appropriate statistical techniques.

4. Choose the basic physical variables, their probability distributions and parameters.

5. Use appropriate procedures to determine the reliability of critical parts of the structure for each performance requirement.

6. Use of the derived reliabilities as an input to some decision problem.

The last final step is essential, since the computed reliabilities have no absolute meaning. Such a final step might be evaluation of partial safety factors for use in a structural code of practice.

The model uncertainties in particular play a critical role in governing realistic standards of safety. The precise mathematical procedure used in step 5 is relatively unimportant provided it is sufficiently accurate. The more important part of the process is the basic modelling of the engineering problem.

4.4 Single Failure Mode Structures

In continuous plated structures the concept of a 'structural member' is in fact an idealisation generally corresponding to a discretisation of a structural continuum. However, it is a useful concept since structural codes tend to be organised in relation to the design (or assessment) of different types of member or component. Acting alone, or as part of a statically determinate structure, failure of the component corresponds to failure of the whole system. Its load-carrying capacity R can generally be expressed as a deterministic function of design variables x_i:

$$R = R(x_1, x_2 \ldots x_i \ldots x_m) \tag{4.1}$$

where x_i are quantities like dimensions, material properties and perhaps fabrication imperfections. If these design variables do not vary with time and Q is the maximum load applied to the component (including self weight) during the reference period T, then the reserve load-carrying capacity or 'safety margin' is given by:

$$M = R - Q \tag{4.2}$$

In general we have already seen that the design variables that make up R and Q are not known deterministically and are thus uncertain quantities. The safety margin M is then also an uncertain quantity and the reliability may be expressed as the probability that M is negative:

$$\left.\begin{aligned} p_f &= P(M \le 0) \\ &\quad P(R \le Q) \end{aligned}\right\} \tag{4.3}$$

In general, the safety margin may be expressed as:

$$M(t) = \min_t g(\underline{X}) \tag{4.4}$$

where the vector of random variables $\underline{X}$ includes all the quantities which act on and affect the structural behaviour. $g(X)$ is referred to as the *limit state function* and represents the *surface* between the safe set and failure set in the space of basic variables. The probability of failure is identical with the limit state violation.

This basic structural reliability idealisation of only one random load effect Q acting on one resistance whose strength R is uncertain is illustrated in Fig. 3. The two *probability* density functions are $f_Q(q)$ and $f_R(r)$ respectively. They are sometimes referred to as *marginal* density functions and must, of course, be expressed in the same units. *A structural component as built will, of course, have only one unique but unknown strength.* After design and construction the probability that the strength R of the component is ≤ some value x is given by the *cumulative* distribution $F_R(x)$. For the probability of failure (p_f) equation (4.3) is then replaced by:

$$\begin{aligned} p_f &= p(R - Q \le 0) \\ &= \int_{-\infty}^{\infty} F_R(x) f_Q(x)\,dx \end{aligned} \tag{4.5}$$

under the condition that R and Q are *statistically independent*. The integral is widely known as the *convolution integral* and is best understood by referring to Fig. 9 and by noting that the term $f_Q(x)$ represents the probability that the load effect Q acting on the member has a value between x and $x + dx$ in the limit as $dx \to 0$. By considering all possible values of x, that is, by taking the integral over all values of x in the loading and strength domains, the total probability of failure is obtained. Since in general it is not meaningful to have negative strengths, the lower limits of integration in eq. (4.5) may in practice be replaced by zero.

$$P_f = \int_0^\infty F_R(s)\, f_S(s)\, ds$$

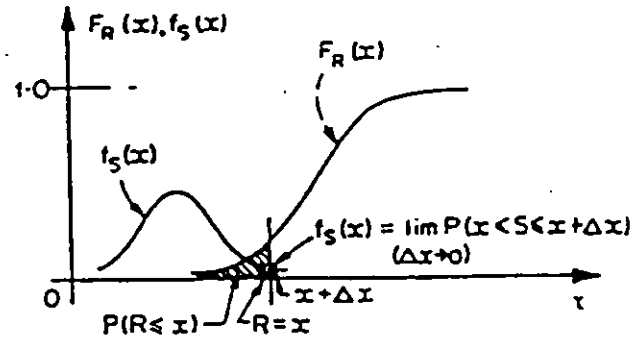

Fig. 9: Basic R-Q Representation

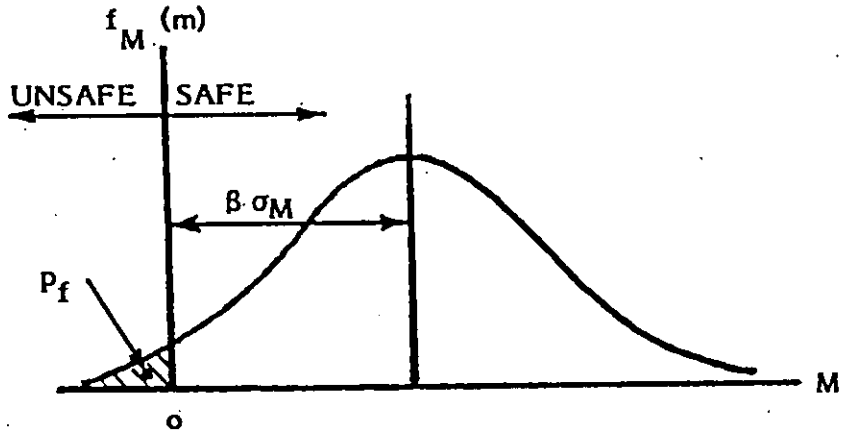

Fig. 10: Illustration of Reliability Index

$$P_f = \iint_D f_{RS}(r, s)\, dr\, ds$$

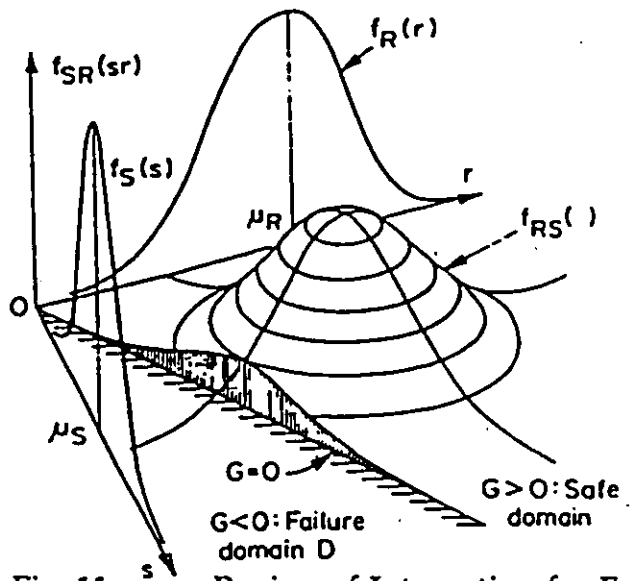

Fig. 11: Region of Integration for Failure Probability

4.5 Special Case

If R and Q are not only independent but are normally distributed variables then we can make use of the properties of the normal distribution function. Expressing p_f as in eq. (4.3) the safety margin is:

$$M = R - Q \tag{4.2}$$

$$\left.\begin{aligned} &\text{Thus} \quad \mu_M = E(M) = \mu_R - \mu_Q \\ &\text{and} \quad \sigma_M^2 = \text{var}(M) = \sigma_R^2 + \sigma_Q^2 \end{aligned}\right\} \tag{4.6}$$

Since R and Q are normal, M, a linear function of R and Q, is also normal and $(M - \mu_M)/\sigma_M$ is the unit standard normal. Referring to Fig. 10, and using the definition of the standard normal distribution function $\Phi(\ )$, the probability of failure is then:

$$p_f = \Phi\left\{\frac{0 - \mu_M}{\sigma_M}\right\} = \Phi\left\{-\frac{1}{v_M}\right\} \tag{4.7}$$

where $v_M = \sigma_M / \mu_M$ is the coefficient of variation of the safety margin M.

Reliability Index (β): the reliability index β is often referred to as the *safety index* and is defined as the ratio $\mu_M / \sigma_m = v_m^{-1}$ or the number of standard deviations by which μ_M exceeds zero, as illustrated in Fig. 10. Then, using eqs. (4.6) the reliability index is:

$$\beta = v_M^{-1} = \frac{\mu_R - \mu_Q}{\sqrt{\sigma_R^2 + \sigma_Q^2}} \tag{4.8}$$

$$\left.\begin{aligned} &\text{or} \quad \beta = \frac{\theta - 1}{\sqrt{v_R^2\theta^2 + v_Q^2}} \\ &\text{where} \quad \theta = \mu_R / \mu_Q \end{aligned}\right\} \tag{4.9}$$

$$\text{and} \quad p_f = \Phi(-\beta) \tag{4.10}$$

Note, θ is referred to as the *central safety factor.*

For the more general case where R and Q are jointly normally distributed with *correlation coefficient* $\rho_{R,Q}$ eqs. (4.9) and (4.10) still hold but σ_M is then given by:

$$\sigma_M = \left(\sigma_R^2 + \sigma_Q^2 + 2\rho_{R,Q}\sigma_R\sigma_Q\right)^{\frac{1}{2}} \tag{4.11}$$

Although this sub-section is headed "Special Case" there are many problems in practice where the reliability index approach using equations (4.8) to (4.11) is useful and sufficiently accurate. This follows in fact from the *central limit theorem* which states that the sum of a large number of random variables approaches the normal distribution, irrespective of the individual distributions of the random variables (Benjamin and Cornell, 1970). But there is a risk of 'lack of invariance problems', i.e. the results may vary with the dimensions chosen for M.

Equation (4.8) is also the simplest measure of safety which embodies the four most influential factors that affect safety, namely, the mean values of R and Q and their standard deviations.

Cornell (1969) is generally credited with introducing the safety index concept, and there is no doubt the analytical development of eq. (4.8), and the fact that the safety index is simply the inverse of the cov of the safety margin, is due to him But historically, such formats were introduced in Denmark in the 1940s; also, in 1955 there was a major debate in the Institution of Structural Engineers, London, where a Mr Thomas introduced eq. (4.8) as a measure of safety - see Pugsley et al (1955).

Importance of Low v_R: naval architects were traditionally taught that the main uncertainty in structural design arose from wave-induced loads. That this is not generally true can be seen by differentiating the safety index eq. (4.9) with respect to v_R and v_Q and equating for the variations in each to be of equal importance:

$$\frac{\partial\beta}{\partial v_Q} = \frac{\partial\beta}{\partial v_R}$$

$$\text{then} \quad v_Q = \theta^2 v_R$$

A typical ship central safety factor against jack-knifing would be $\theta = 2.5$ say. From Table 3 assume a modelling uncertainty for deck collapse of $v_{Xm} = 12.5\%$ and assume a physical uncertainty dominated by yield stress of 7.5% from Table 2, then:

$$v_R = \sqrt{0.125^2 + 0.075^2} = 0.146$$

Then, for v_Q to be as influential as v_R, it would need to be $v_Q = 2.5^2 \times 0.146 = 0.91$. But this is 3.6 times higher than the worst extreme load effect modelling uncertainty which is 25% from Table 3. It is clear that v_R has much greater influence on the safety index (which in this example is 3.4). This again highlights the crucial importance of reducing strength modelling uncertainties.

4.6 Lognormal Distributions

Lognormal distributions are frequently used, for example, to represent the pdf of material properties. They are also attractive in not admitting negative values, which is realistic for many physical variables, and this is also convenient for integration, etc. Moreover, because the natural logarithm of the random variables has a normal distribution (see Appendix A) then we can still use the results of the special case above. For example, if R and Q are both lognormally distributed, p_f may be expressed as:

$$p_f = P(M' \leq 1) \tag{4.12}$$

where $$M' = R/Q \tag{4.13}$$

Take natural logarithms (to base e) and putting $M = \ell n M'$ gives the margin:

$$\left.\begin{aligned} M &= \ell n R - \ell n Q \\ &= A - B \end{aligned}\right\} \tag{4.14}$$

where $A = \ell n R$ and $B = \ell n Q$. Failure occurs when $M' \leq 1$ or when $M \leq 0$. But, if R and S are lognormally distributed, A and B are normally distributed. It then follows that M is also normally distributed. Thus:

$$p_f = \Phi\left\{\frac{\mu_B - \mu_A}{\sqrt{\sigma_B^2 + \sigma_A^2}}\right\} \tag{4.15}$$

The properties of the lognormal distribution are such that if Y is lognormally distributed and $X = \ell n Y$, then:

$$\sigma_X^2 = \ell n\left(v_Y^2 + 1\right)$$

$$\tilde{m}_Y = \mu_Y e^{\left(-\sigma_x^2/2\right)} \text{ median value of Y.}$$

Substituting in eq. (4.15) and using the relations between A and R and B and Q leads to:

$$\beta = \frac{-\ell n\left\{\frac{\mu_Q}{\mu_R}\sqrt{\frac{v_R^2+1}{v_a^2+1}}\right\}}{\sqrt{\ell n\left(v_R^2+1\right)\left(v_Q^2+1\right)}} \tag{4.16}$$

and $p_f = \Phi(-\beta)$ as before.

Analytical expressions for β and p_f do exist for some other combinations of distributions of R and Q. However, they are not convenient, so in general the convolution integral eq. (4.5) needs to be evaluated in some other way.

4.7 General Case

Where the distributions of R and Q are non-normal, or are not known, or where R and Q are not statistically independent, then the simple case solution cannot be applied. Setting:

$$g(X_1, X_2 \ldots X_i \ldots X_n) = 0 \tag{4.17}$$

defines an $(n-1)$ dimensional *hyper-surface* in the n-dimensional basic variable space. This surface is the *failure surface* for the limit state being considered. It divides all possible combinations of the variables which cause failure from those combinations which do not. Note that this is an entirely deterministic concept. The probability of failure may then be expressed as:

$$p_f = P[g(X) \le 0] \tag{4.18}$$

$$= \iint \ldots \int_{g(X)\le 0} \prod_{i=1}^{n} f_{X_i}(x_i)\, dx_1\, dx_2 \ldots dx_n \tag{4.19}$$

where the integrand re presents the *joint* probability density functions for the n basic variables, and the integration is over the failure region. $f_{X_i}(x_i)$ is the marginal pdf for the ith basic variable X_i.

Except for some special cases, the integration over the failure domain $g(X) \leq 0$ cannot be performed analytically, and direct numerical integration is feasible only for problems of low dimension. Various approximate methods have been developed to evaluate eq. (4.19), and they are essentially of two types:

- *Transformation methods* in which the original problem is transformed into a probability space where the variables are mutually independent, standard normal variates (zero mean, unit variance). The integral is approximated by simplifying the boundary of the integration domain in the transformed space

- *Simulation methods* in which the integral is approximated by Monte Carlo (MC) simulation. For small p_f crude MC is efficient, however several variance reduction techniques are available, and importance sampling and directional simulation methods have been developed which greatly reduce computing time.

Only the first will be considered here as it forms the basis for the advanced first order second moment method referred to earlier. Melchers (1987) is a good reference for both methods.

4.8 Time Dependent Loads

Section 4.1 showed how a single time-varying load may be treated. The correct approach is to use the probability distribution for the load corresponding to the maximum intensity (extreme value) in the reference period T. Provided the correct distribution is used the time element may then be neglected in the reliability calculation.

When more than one time-varying load is present the problem is more complex. This is especiallly true when their frequencies are significantly different as, for example, with wind excited and wave excited forces, with first and second order wave forces, etc., with still-water and wave-induced forces, and so on. Then to find the maximum value of combined time dependent loads two models are recommended:

(a) the Ferry Borges-Castanheta model (1968)

(b) Turkstra's Rule (1980)

The first is very suitable for use with Level 2 methods and is greatly simplified to avoid the mathematical problems in estimating the sum of loading processes. For each load process X_i the reference period T (for example, one year) is divided into n_i equal elementary intervals or 'pulses' of time τ_i:

$$\tau_i = T / n_i \tag{4.20}$$

n_i is called the repetition number and is integer. It is further assumed that the load is constant in each elementary interval. For a load process having the marginal distribution $F_{X_i}(x_i)$ the extreme value distribution in the reference period T is taken as:

$$F_{\max X_i}(x_i) = \left[F_{X_i}(x_i)\right]^{n_i} \tag{4.21}$$

Therefore, for this rectangular pulse process it is a simple task to calculate the maximum value in the reference period T.

When combinations of load processes $X_1, X_2 \ldots X_k$ are considered it is assumed that the loads are stochastically independent with integer repetition numbers n_i where $n_i \leq n_2 \leq \ldots \leq n_i \leq \ldots \leq n_k$ and certain limits are placed on the repetition numbers for each process. Equation (4.21) is then generalised. Although this Ferry Borges-Castanheta model is a gross simplification, experience seems to verify that the model is capable of reflecting the most important characteristics of load combinations.

Turkstra's rule (1980) is an approximation to determine the largest maximum of the sum of load effects. By this rule the reliability is only checked when individual load processes reach their maximum value. Therefore the reliability will be over-estimated. However, it has been shown that this over-estimation is usually very small.

These studies confirm that adding the absolute values of the extremes of several environmental processes, or even assuming that these occur simultaneously, is conservative. For a fuller discussion with illustrations refer to Thoft-Christensen and Baker (1982) and Rackwitz and Fiessler (1978).

An idealisation for combining slow and fast random variables is provided by Prince-Wright (1992) in Fig. 12. The study has achieved major advances in joint

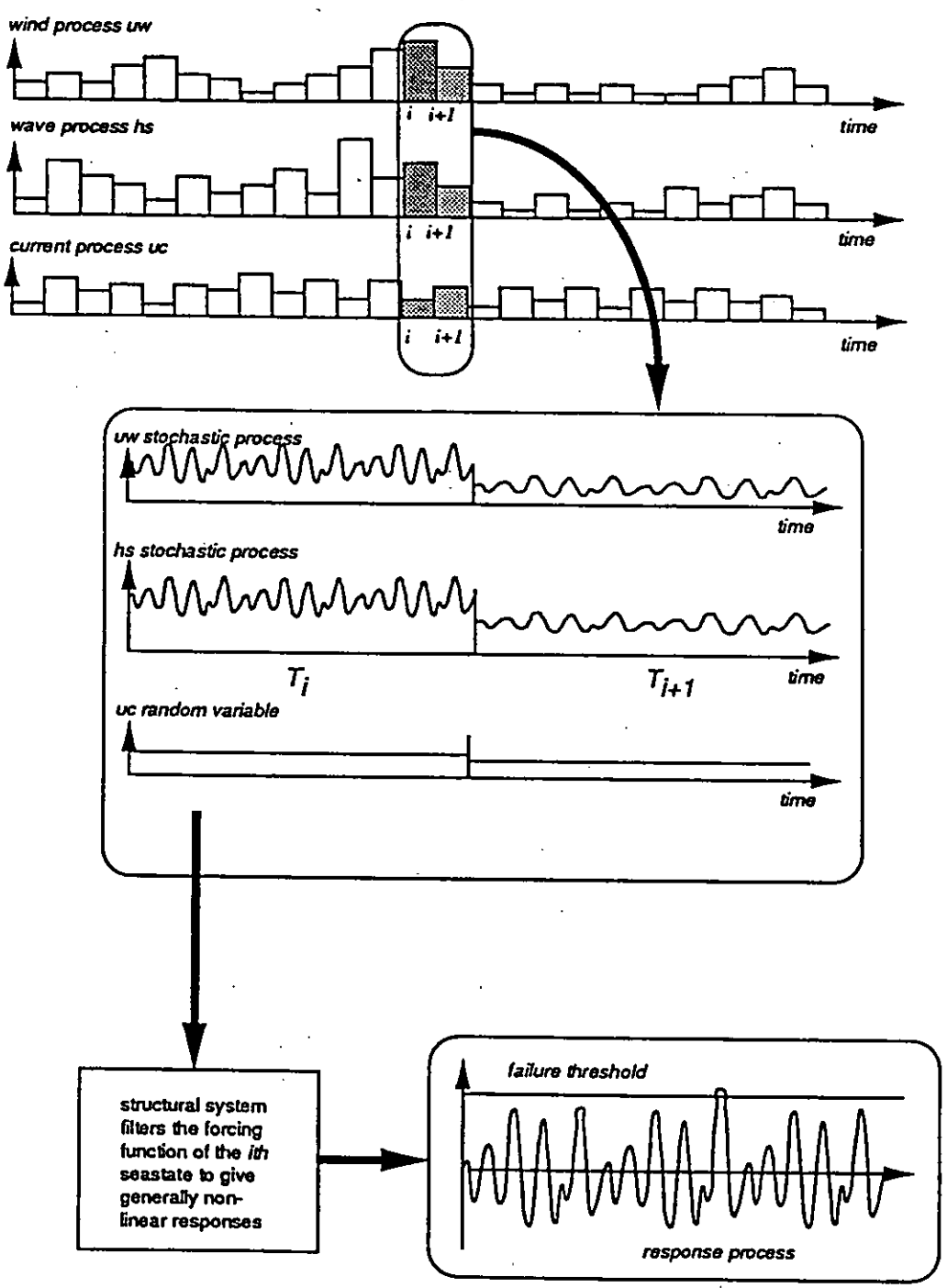

Fig. 12: Idealisation of Slow and Fast Random Variables

probability modelling, including also the effects of directionally spread seas. This will be important for future more realistic load effect modelling in offshore structures, and especially for compliant platform design. Figure 13 shows the flow chart used when developing the first Tension Leg Platform 'Model Code' for reliability based design (Faulkner et al, 1983).

5. SECOND MOMENT TRANSFORMATION METHODS

Rather than using approximate integration methods to evaluate eqs. (4.5) or (4.19), in transformation methods the probability density functions themselves are simplified. This was introduced in Section 1.3 where we saw that if the design variables are transformed to 'equivalent normal' distributions then they are completely defined by their first two moments, i.e. by their means and standard deviations. The transformation is to achieve the same behaviour in the tails.

Because of their inherent simplicity second-moment methods have become very popular, particularly in design code calibration work. Early ideas stem from Mayer in the 20s and Freudenthal, Rzhanitzyn and Basler in the 50s. Not until the late 1960s, however, was the time ripe for the ideas to gain a measure of acceptance (Cornell, 1969). Since then a number of extensions and refinements have flowed from Hasofer, Lind, Rackwitz, Ditlevsen, Fiessler and others who were advancing the ideas in the 70s and this continued into the 80s with Hohenbichler and Rackwitz, Moses, Madsen, Thoft-Christensen and Murotsu (1986), and others extending the reliability concept to *structural systems*.

5.1 Transformations

Given the joint distribution $F_X(x)$ for continuous random variables, there always exists a probability distribution transformation $\underline{U} = \underline{T}(\underline{X})$ where $\underline{U}$ is a vector of independent normal variables. If the basic variables X_i are mutually independent, a simple and generally effective transformation is:

$$\underline{T}: u_i = \Phi^{-1}\left[F_{X_i}(x_i)\right],\ i = 1,2...n \tag{5.1}$$

For dependent variables, the Rosenblatt (1962) transformation may be used:

$$\underline{T}: u_i = \Phi^{-1}\left[F_{X_i}\left(x_i | x_1, x_2 ... x_{i-1}\right)\right] \tag{5.2}$$

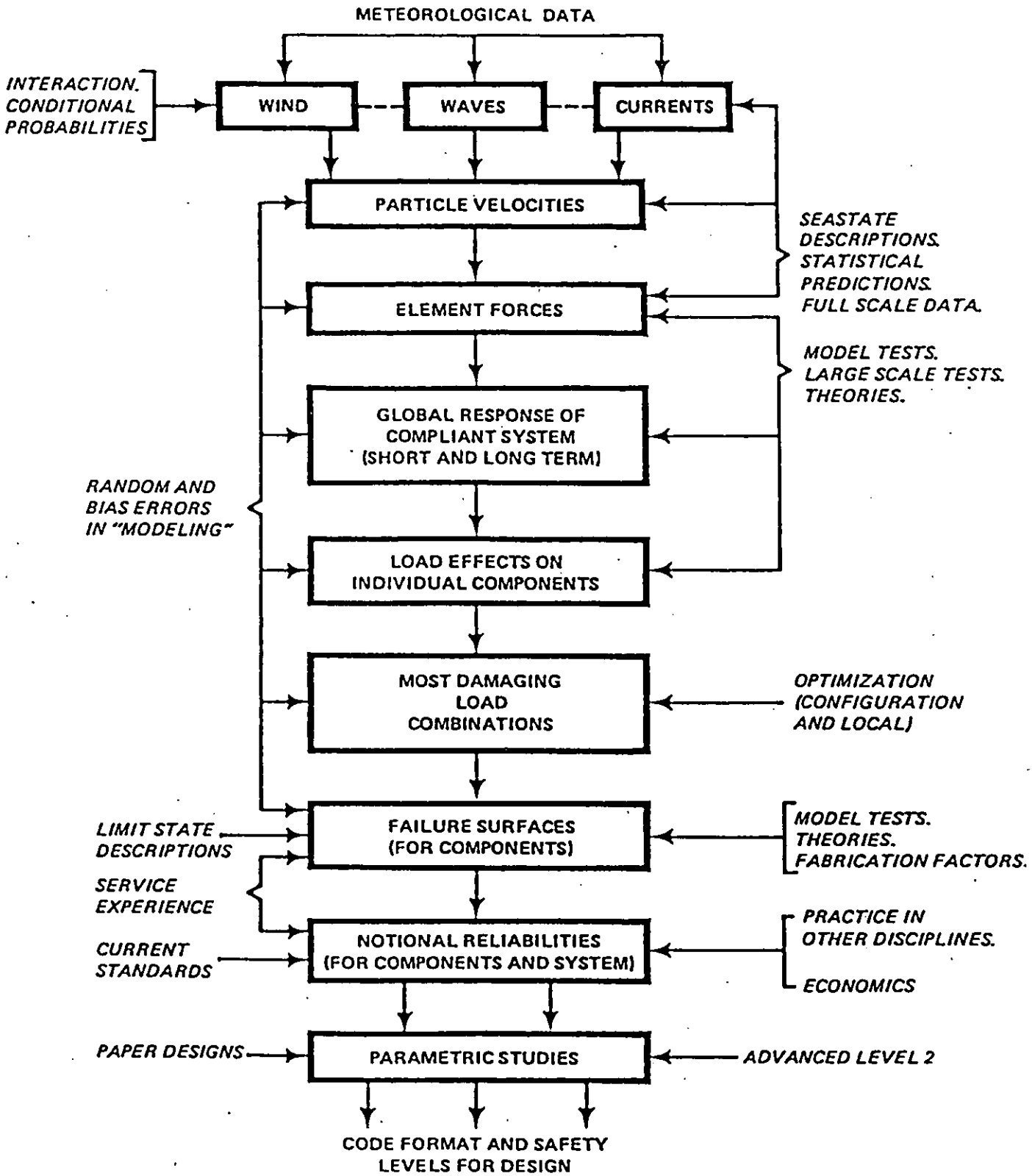

Fig. 13: Flow Chart for Structural Safety Evaluations

where $F_{X_i}(|)$ is the distribution function of X_i conditioned on $(X_1, X_2 \ldots X_{i-1})$. Equation (5.2) reduces to (5.1) in the case of independent variables. The transformation proceeds in a stepwise manner: first transforming the variables X_i into standardised normal variables having zero mean and unit variance:

$$U_i = \frac{X_i - \mu_{X_i}}{\sigma_{X_i}} \tag{5.3}$$

then the conditional variables $X_2|X_1$ etc. are transformed.

The inverse transfer is given by:

$$\underline{T}^{-1}: x_i = F_{X_i}^{-1}\left[\phi(u_i)|x_1, \ldots x_{n-1}\right] \tag{5.4}$$

The transformation to u-space is exact. In practice, however, the transformations $\underline{T}$ and $\underline{T}^{-1}$ must be performed numerically.

Rackwitz-Fiessler Transformation: This transformation is chosen in such a way that (a) the original density and (b) the distribution functions f_X and F_X for the random variable are equal to the corresponding values for the normally distributed variable at the design point. We need the mean value u_{Xt} and standard deviation σ_{Xt} where the subscript t refers to the new transformed variables. From condition (a):

$$\Phi\left[\frac{x_i^* - u_{Xt}}{\sigma_{Xt}}\right] = F_X(x^*)$$

$$\text{whence } u_{Xt} = x^* - \Phi^{-1}\left[F_X(x^*)\right]\sigma_{Xt} \tag{5.5}$$

Condition (b) gives:

$$\frac{1}{\sigma_{Xt}}\phi\left[\frac{x^* - u_{Xt}}{\sigma_{Xt}}\right] = f_X(x^*)$$

$$\text{whence } \sigma_{Xt} = \frac{\phi\left\{\Phi^{-1}F_X(x^*)\right\}}{f_X(x^*)} \tag{5.6}$$

The solution proceeds iteratively as part of the process in calculating β.

R and Q Idealisation: Section (4.2) introduced the resistance R and load effect Q, and in Section (4.5) the reliability index β was defined. The limit state functions can be represented by:

$$g(X) = R(X) - Q(X)$$

For this two-dimensional idealisation this is represented in the top part of Fig. 14 in which the joint density function contours of $f_X(x)$ are shown in basic space. The bottom part of Fig. 14 shows the transformed normal u-space in which the normal joint density contours are seen as circles.

Multi-dimensional space: the extension to multi-variable space is nicely described by expanding a sphere at the origin of the u-space until it first touches one of the limit state failure surfaces at some point called the *design point*. The distance to the origin is the reliability index β, and as this is the shortest distance to a failure surface the design point is also the point $\underline{u}^*$ of most likely failure.

The failure probability is then estimated using an important property of the multivariate standard normal, that is, the volume contained within this multi-dimensional hypersphere (or circle in two-dimensional space) is given very simply by $\Phi^{-1}(\beta)$, where Φ is the univariate standard normal (cumulative) distribution referred to earlier. Hence β is determined directly and eq. (4.10) gives the probability of failure:

$$p_f = \Phi(-\beta) \qquad (4.10)$$

Solution: Taking one transformed limit state surface at a time it is described by:

$$g(X) = g\left[\underline{T}^{-1}(\underline{u})\right] = g_u(\underline{u}) \tag{5.7}$$

The *design point* $\underline{u}^*$ is the solution to a minimisation procedure subject to the constraint:

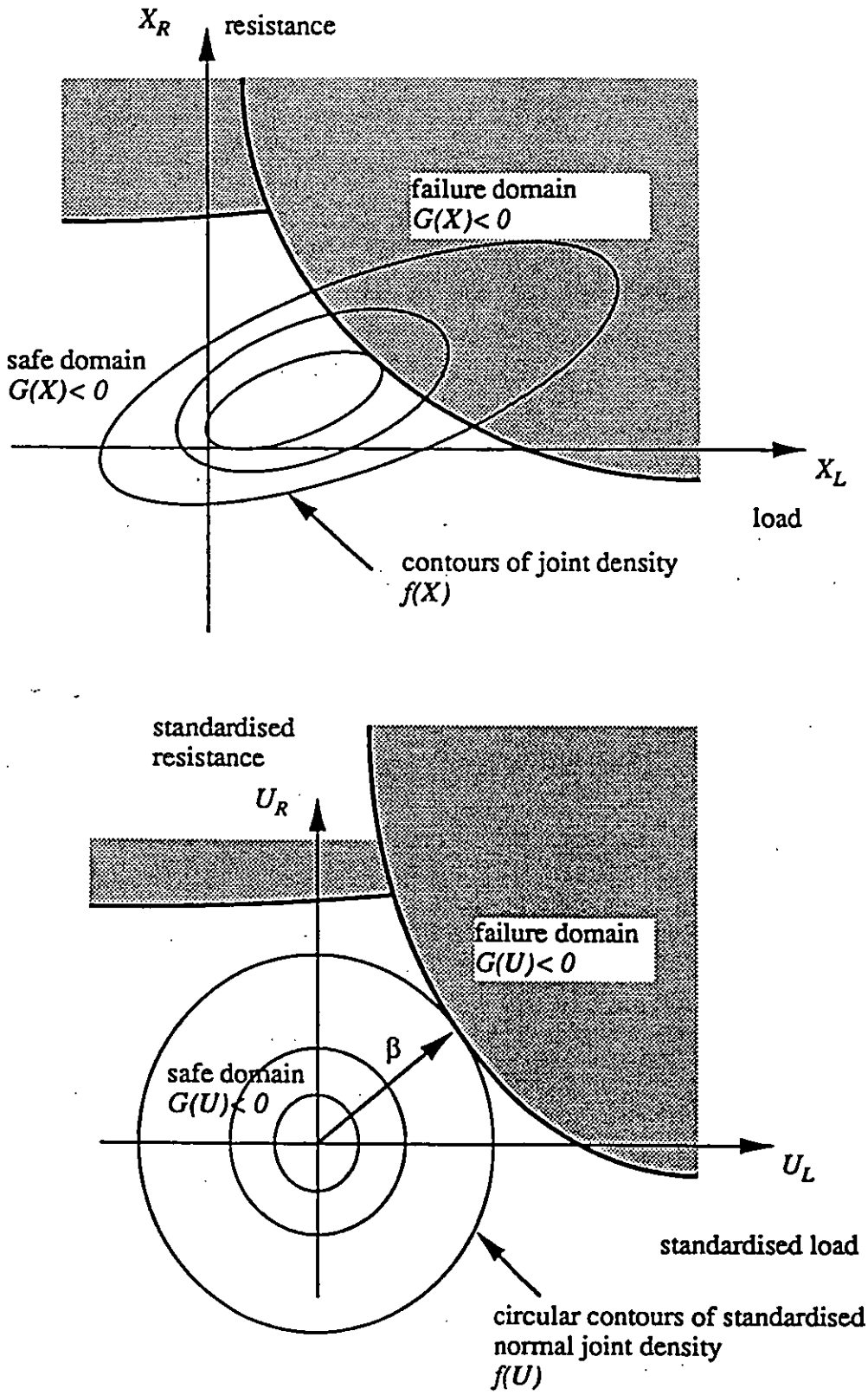

Fig. 14: Basic Variable Space and Transformed Variable Space

$$g_u(\underline{u}) = 0 \tag{5.8}$$

$\underline{u}^*$ is found by a suitable search algorithm (Rackwitz and Fiessler, 1978) in which checks are made to ensure all the gradients $\partial\beta / \partial u_i$ are zero and the matrix of second derivatives must be positive definite at $\underline{u}^*$. The second derivatives also give an indication of the tangent-hyperplane assumption which is implicit in the use of $\Phi(-\beta)$ as an approximation for p_f.

5.2 Hasofer-Lind Reliability Index

The Hasofer and Lind (1974) transformation provided a major advance in second-moment methods for two reasons. First, because they extended the method to include *correlated* basic variables, which can sometimes affect the value of β appreciably. Also, their reliability index is failure function invariant, that is, equivalent failure functions result in the same β.

As Appendix A does not address ***correlation*** then basic definitions may be helpful. Let X_1 and X_2 be two random variables with expected values $E[X_1] = u_{X_1}$ and $E[X_2] = u_{X_2}$. The *mixed central moment* defined by:

$$\left.\begin{aligned} \operatorname{cov}[X_1, X_2] &= E\left[\left(X_1 - u_{X_1}\right)\left(X_2 - u_{X_2}\right)\right] \\ &= E[X_1 X_2] E[X_1] E[X_2] \end{aligned}\right\}$$

is called the *covariance* of X_1 and X_2. The ratio

$$\rho_{X_1, X_2} = \frac{\operatorname{cov}[X_1, X_2]}{\sigma_{X_1} \sigma_{X_2}}$$

is called the *correlation coefficient*. It can be used as a measure of mutual linear dependence between a pair of random variables and lies between -1 and +1. If $\rho_{X_1, X_2} = 0$ the variables are *uncorrelated*. If the covariance is numerically large but negative, then the values of X_1 tend to be large when the values of X_2 are small, and vice versa. If both variables are simultaneously large and small then the correlation coefficient is positive and tends to 1.0 as the standard deviations decrease.

As before, the Hasofer and Lind's reliability index β is defined as the shortest distance from the origin to the failure surface in normalised u-space. This is the design point. By defining β where it is related to the non-dimensional failure surface and not to the failure function, a safety measure is obtained which is failure function invariant because all equivalent failure functions result in the same failure surface. The reliability index previously defined:

$$\beta = \frac{\mu_M}{\sigma_M} = v_M^{-1} \qquad (4.8)$$

will coincide with the β just defined when the failure surface is linear (a hyperplane). Therefore, in this case the important relation:

$$p_f = \Phi(-\beta) \qquad (4.10)$$

can also be used, provided the basic variables are normally distributed. The linearity requirement is achieved if the Taylor Series expansion of the terms in M is made about the design point. Then, Hasofer and Lind's safety index is formulated:

$$\beta = \min\left\{\sum_{i=1}^{n} u_1^2\right\}^{\frac{1}{2}} \qquad (5.9)$$

The calculation of β can be undertaken in a number of ways, and in the general case when the failure surface is non-linear an iterative method must be used. Many good programs exist for achieving this.

A very good approximation to β is obtained by first evaluating the direction cosines α_i^* at the design point using eqs. (5.6) and (5.7). The design point for any variable is then by definition:

$$X_i^* = u_{X_i} - \alpha_i^* \sigma_i \beta \qquad (5.10)$$

These are then substituted into the limit state equation g( ) and taking g = 0 leads to an equation involving β. This can then be solved for minimum β by any standard method. The procedure will be illustrated for simple limit states. Thoft-Christensen and Baker (1982) is an excellent text with examples.

5.3 Derived Equations

To recap, the first-order reliability index β is defined as the minimum distance in u-space from the origin to the failure surface; and the sign of β is determined as the sign of $g_u(0)$. The design point is expressed as a vector:

$$\underline{u}^* = \beta\underline{\alpha}^* \tag{5.11}$$

where $\underline{\alpha}^*$ is a unit normal vector to the failure surface at $\underline{u}^*$ and directed towards the failure set. It is given by a gradient vector of derivatives of the $g(\underline{u})$ limit state function and using (5.7) it can be shown that the individual basic variable components of $\underline{u}^*$ are:

$$\alpha_i^* = \frac{\partial\beta(\underline{u})}{\partial u_i} \tag{5.12}$$

$$\alpha_i^* = \frac{\left.\frac{\partial g_i}{\partial x_i}\right|_{x_i^*}\sigma_i}{\left\{\sum_1^n\left[\left.\frac{\partial g_i}{\partial x_i}\right|_{x_i^*}\sigma_i\right]^2\right\}^{\frac{1}{2}}} \tag{5.13}$$

where the *direction cosine* α_i is a measure of the sensitivity of β to changes in u_i. The quantity α_i^2 is commonly referred to as the *importance* or *sensitivity factor* for the variable, as discussed earlier. The value is an indication of the (first-order) uncertainty fraction that can be associated with any variable X_i. It follows from eq. (5.13) that:

$$\sum_1^n \alpha_i^2 = 1 \tag{5.14}$$

and this should be used as a check.

Reliability Index: the derivation of β from optimisation has already been described, and approved algorithms exist which determine β, α_i and other parameters. However, it is helpful to understand and useful for simple cases, to be able to derive an approximate solution for β directly. This can be done using linear error theory in which a first-order Taylor series expansion of the variables is about their design

points x_i^*. It can then be shown that the variance of the safety margin M is given by:

$$\sigma_M^2 \cong \sum_{i=1}^{n} \left(\frac{\partial G}{\partial X_i} \right)_{x_i^*}^2 \sigma_i^2 \tag{5.15}$$

where $G = g(X) = M$, the safety margin or limit state function. If any of the variables are correlated then additional terms need to be added to (5.15) for each correlated pair as follows:

$$\sum_i \sum_j \left(\frac{\partial G}{\partial X_i} \right)_{x_i^*} \left(\frac{\partial G}{\partial X_j} \right)_{x_j^*} \rho_{i,j} \sigma_i \sigma_j \tag{5.16}$$

Dividing eq. (5.15) by $\overline{M}^2$ the equation becomes:

$$v_M^2 \cong \sum_{i=1}^{n} \left\{ \frac{\partial G}{\partial X_i} \frac{X_i}{G} \right\}_{x_i^*}^2 v_i^2 \tag{5.17}$$

where v_i is the cov of the basic variables. In general these must include the modelling uncertainty v_{X_m}, but if these are judged separately then the total uncertainty v_t is given by:

$$v_t^2 = v_o^2 + v_{X_m}^2 \tag{5.18}$$

where v_o, for example, is given from eq. (5.17). Then $v_M = v_t$. Then from eq. (4.8) the safety index is:

$$\beta = v_M^{-1} \qquad (4.8)$$

Eq. (5.17) will be most accurate when the important variables are evaluated at their design points. These of course will not be known since from Section (3.2) we note:

$$x_i^* = \mu_{xi}(1 - \beta v_i \alpha_i) \tag{5.19}$$

However, one can either start the iteration process with $x_i = \mu_{xi}$ or with a judged value in the direction of the design point. The process is best illustrated with examples (Melchers, 1987).

Partial Safety Factors: in Section (3.2) eq. (3.4) for PSFs was given and can be calculated now that α_i and β are available. Examples will illustrate which variables are influential.

5.4 Summary

Whether first- or second-order, transformation methods nowadays are usually very fast and efficient. FORM directly provides sensitivity factors - not readily available from simulation methods. For many reliability calculations FORM is highly accurate, although the level of accuracy will be unknown. Also, the method requires differentiable failure functions, and no general, fail-safe and practical algorithm is available to be certain of identifying the most likely failure point(s). The method is only directly applicable to continuous random variables, and cannot deal with discrete variables or with random processes.

In contrast simulation is less efficient but may be applied to almost all problems. In principle it can achieve any desired level of accuracy, at the cost of extra computation. Often, a combination of the methods can be beneficial: use of FORM to locate the design point, thus identifying a good sampling density for importance sampling. Simulation can be used to provide accuracy checks on FORM and SORM results.

REFERENCES

Ang, A.H.S. and Tang, W.H. (1975): Probability Concepts in Engineering Planning and Design, vol. 1, Basic Principles, John Wiley.

Baker, M.J. and Wyatt, T. (1979): 'Methods of Reliability Analysis for Jacket Platforms', in Proc. 2nd Int. Conf. on Behaviour of Offshore Structures, London, BHRA, Cranfield, Berks., pp 499-520.

Baker, M.J. (1985): 'The Reliability Concept as an Aid to Decision Making in Offshore Engineering', in Proc. 4th Int. Conf. on Behaviour of Offshore Structures, Technical University Delft.

Benjamin, J.R. and Cornell, C.A., (1970): Probability, Statistics and Decisions for Civil Engineers, McGraw-Hill, New York.

Blockey, D.J., (1977): 'Analysis of Structural Failures', Proc. Instn Civ. Engrs, Part A, vol. 62, pp 51-74.

Brown, C.B., (1979): 'A Fuzzy Safety Measure', J. Engg, Mech. Div., ASCE, vol. 105, pp 855-872.

Cornell, C.A., (1969): 'A Probability Based Structural Code', J. of American Concrete Institute, vol. 66, no. 12.

Das, P.K., Faulkner, D. and Zimmer, R.A., (1992): 'Efficient Reliability Based Designs of Ring and Stringer Stiffened Cylinders under Combined Loads', in Proc. 6th Int. Conf. on Behaviour of Offshore Structures, London, vol. 1, BBP Technical Services Ltd., London, pp 180-193.

Faulkner, D., (1976): 'Safety Factors?', in Steel Plated Structures, ed by P.J. Dowling et al, Crosby Lockwood, pp 764-790.

Faulkner, D., Stiansen, S.G. and Birrell, N.D., (1983): 'Development of a Reliability Based Design Code for the Structure of Tension Leg Platforms', Paper OTC 4648, OTC Conf. Houston

Faulkner, D., Guedes Soares, C. and Warwick, D.M., (1988): 'Modelling Requirements for Structural Design and Assessment, in Integrity of Offshore Structures, ed by D. Faulkner et al, Elsevier Applied Science, pp 25-54.

Faulkner, D., (1991): 'What is wrong with Offshore Design Codes?', Trans. Institution of Engineers and Shipbuilders in Scotland, vol. 134, 1990-91, pp 35-48.

Ferry Borges, J. and Castanheta, M., (1968): Structural Safety, Laboratorio Nacional de Engenharia Civil, Lisboa, (2nd edition 1971).

Guedes Soares, C., (1984): 'Probabilistic Models for Load Effects in Ship Structures', Report No. UR-84-38, Division of Marine Structures, NTH, Trondheim.

Hasofer, A.M. and Lind, N.C., (1974): 'Exact and Invariant Second Moment Code Format', J. Engg Mech. Div., ASCE, vol. 100, EMI, pp 111-121.

Kendrick, S., (1984): 'How Safe are Design Codes?', in Marine and Offshore Safety, ed by P.A. Frieze et al, Elsevier, pp 363-379.

Lind, N.C., (1983): 'Models of Human Error in Structural Reliability', J. Structural Safety, vol. 1, pp 167-175.

Madsen, H.O., Krenk, S. and Lind, N.C., (1986): Methods of Structural Safety, Prentice-Hall Inc.

Marley, M.J., (1991): 'Time Variant Reliability under Fatigue Degradation', Doctor of Engineering Thesis, NTH, Trondheim (MTA rapport 1991:83)

Marshall, P.W., (1969): 'Risk Evaluation for Offshore Structures', J. Str. Div., ASCE, No. ST12, December 1969.

Matousek, M. and Schneider, J., (1976): 'Untersuchungen Struktur des Sicherheitsproblems bei Banwerken', Institut für Baustatik und Konstruktion, Eidgenössiche TH, Zurich.

Melchers, R.E., (1987): Structural Reliability Analysis and Prediction, Ellis Horwood, Chichester.

Pate-Cornell, E. and Bea, R., (1989): 'Organizational Aspects of Reliability Management: Design, Construction and Operation of Offshore Platforms', Research Report No. 89-1, Dept of Industrial Engineering and Engineering Management, Stanford University.

Prince-Wright, R., (1992): 'Structural Models of Environmental Data for Marine Structure Design', PhD Thesis, University of Glasgow.

Rackwitz, R. and Fiessler, B., (1978): 'Structural Reliability under Combined Random Load Sequences', J. Computers and Structures, vol. 9, pp 489-494.

Rand Corporation (1955): 'A Million Random Digits with 1,000,000 Normal Deviates', Free Press, New York.

Rosenblatt, M., (1952): 'Remarks on a Multivariate Transformation', Ann. Math. Stat., vol. 23, pp 470-472.

Pugsley, A.G. et al, (1955): 'Report on Structural Safety', Struct. Eng., vol 33, no. 5, pp 141-149.

Pugsley, A.G., (1962): Safety of Structures, Edward Arnold, London.

Pugsley, A.G., (1973): 'The Prediction of Proneness to Structural Accidents', Struct. Eng., vol 51, no. 6, pp 195-196.

Thoft-Christensen, P. and Baker, M.J., (1982): Structural Reliability Theory and its Applications, Springer-Verlag, Berlin.

Thoft-Christensen, P. and Murotsu Y., (1986): Application of Structural Systems Reliability, Springer-Verlag.

Turkstra, C.J. and Madsen, H.O., (1980): 'Load Combinations in Codified Structural Design', J. Struct. Div., ASCE, vol. 106, pp 2527-2543.

Walker, A.C., (1981): 'Study and Analysis of the First 120 Failure Cases', in Structural Failures in Buildings, Inst. Struct. Engrs, pp 15-39.

Warwick, D.M. and Faulkner, D., (1989): 'Economic Structures from Improved Design Code Modelling', 4th Int. Colloq. on Stability of Metal Structures', Proc. Code Differences Around the World, New York, SSRC.

Wirsching, P.H. and Chen, Y.N., (1987): 'Fatigue Design Criteria for TLP Tendons', J. Struct. Engr, vol. 113, no. 7.

Wirsching, P.H. and Chen, Y.N. (1988): 'Considerations of Probability-Based Fatigue Design for Marine Structures', J. Marine Structures, vol. 1, no. 1, pp 23-45.

ANNEX

GLOSSARY OF TERMS AND DEFINITIONS

Acknowledgements to

Det norske Veritas

1.3 Definitions

1.3.1 The following terms are important in the field of structural reliability:

Basic variables: A set of variables entering the limit-state equation including variables accounting for model uncertainties in the limit-state function itself.

Characteristic value: A nominal value to characterise the magnitude of a stochastic variable. The characteristic value is to be defined as a fractile of the probability distribution of the variable.

Confidence level: Probability, in percent, that a given observation is not the result of sampling error. A confidence level of 75 percent means that there is a probability of 25 percent that sampling error (chance fluctuations of sampling and testing) could have produced the result.

Design condition: Combination of design loads to be used in reliability checking. For the design of a marine units, two main groups of design conditions should be considered:

- Normal operation design conditions.
- Temporary design conditions.

Design life: The time period from commencement of construction until condemnation of a structure.

Design point: The most probable outcome of the basic variables when failure occurs, i.e. the point on the limit-state surface with the highest probability density.

Design value: Value to be used in the practical design, i.e., characteristic value modified by the material or load coefficient.

Failure: An event to a component or a system causing loss of component or system function, or deterioration of functional capability to such an extent that the reliability of the unit, personnel or environment is significantly reduced.

First-order reliability index: The approximation to the reliability index resulting from use of a first-order reliability method.

First-order reliability method: A reliability method in which the limit-state surface in the standardised normal space is approximated by a linear surface at the design point.

Limit-state: A state beyond which the structure no longer satisfies the requirements. For marine structures categories of limit-states are:

ULS - Ultimate limit-state.
FLS - Fatigue limit-state.
PLS - Progressive collapse limit-state.
SLS - Serviceability limit-state.

Limit-state function: Function of the basic variables which has negative values when the structure component fails, and which has positive values when the structure component is safe.

Limit-state surface: The surface separating the region of failure states from the region of safe states in the space spanned by the basic variables.

Load: Any action causing stress or strain in the structure. Load categories are:

P - Permanent loads.
L - Live loads, or variable functional loads.
D - Deformation loads.
E - Environmental loads.
A - Accidental loads.

Load coefficient: Partial safety coefficient by which the characteristic load effect is multiplied to obtain the design load effect.

Load effect: Effect of a single load or combination of loads on the structure, such as stress, deformation, displacement, motion, etc.

Material coefficient: Partial safety coefficient by which the characteristic strength is divided to obtain the design strength.

Model uncertainties: The inherent uncertainties of the calculation models (load model, strength model, function model for the structure, etc.)

Normal operation design conditions: Combinations of design loads in the period after the installation phase until condemnation or removal from location with the unit operation normally.

Omission sensitivity factor: A factor giving the change in the reliability index when a random variable is replaced by a fixed value.

Parametric sensitivity factor: A factor giving the change in the reliability index by a unit change in a distribution parameter or a fixed value.

Partial coefficient: Coefficient by which the characteristic value of a variable is modified to give the design value (i.e. a load or material coefficient.)

Probability of failure: Probability density of the limit-state variable integrated over the failure region of the space spanned by the basic variables.

Random (stochastic) process: A sequence of outcomes in which the values of variables are to some degree unpredictable.

Random (Stochastic) variable: A variable participating in a random (stochastic) process.

Redundancy: The ability of a component or system to maintain or restore its function when one failure has occurred. Redundancy can be achieved for instance by installation of more units or elements to restrain the loads, or by alternative means for performing a function.

Reliability: Ability of a component or a system to perform its required function without failure during a specified time interval. Failure probability density integrated over the region of safe states in the space spanned by the basic variables.

Reliability index: Fractile of the normalised normal probability function corresponding to the reliability.

Resistance: Capability of a structure or part of a structure to resist load effect.

Second-order reliability method: A reliability method in which the limit-state surface in the standardised normal space is approximated by a quadratic surface in the design point.

Serviceability: A condition in which a structure is considered to perform its design function satisfactorily.

Standardised normal space: A space of normally distributed random variables with zero mean values, unit standard deviations and zero correlation coefficients.

Temporary design conditions: Combinations of design loads occurring during temporary phases, such as: Construction, transportation, installation, retrieval, modification etc.

Uncertainty Importance factors: Factors giving the fraction of variance caused by variance in each basic variable.

1.3.2 The following terms are applied in connection with probability functions and related items:

Probability density function $f(x)$: The probability that a random variable x shall appear in the interval $[x, x+dx]$ is $f(x)dx$.

Cumulative probability function $F(x)$: $F(x) = \int_{-\infty}^{x} f(x)\,dx$

Exceedance probability function $Q(x)$: $Q(x) = 1 - F(x)$

Statistical moment of order k about zero, M_k: $M_k = M_k(x) = \int x^k f(x)dx$

Expectation value, $E(x)$: $E(x) = M_1 = M_1(x)$

Central moment of order n, m_n: $m_n = \int (x-E(x))^n f(x)dx \qquad m_1 = M_1$

Variance σ^2, Standard deviation σ: $\sigma^2 = m_2 \qquad \sigma = \sqrt{m_2}$

Coefficient of variation, COV: $COV = \dfrac{\sigma}{E(x)} = [\dfrac{M_2 - M_1^2}{M_1^2}]^{1/2} = \dfrac{\sqrt{m_2}}{m_1}$

Skewness coefficient, λ_3: $\lambda_3 = \dfrac{m_3}{\sigma^3} = \dfrac{M_3 - 3M_1M_2 + 2M_1^3}{[M_2 - M_1^2]^{3/2}}$

Coefficient of curtosis, λ_4: $\lambda_4 = \dfrac{m_4}{\sigma^4} = \dfrac{M_4 - 4M_1M_3 + 6M_1^2M_2 - 3M_1^4}{[M_2 - M_1^2]^2}$

Simultaneous (Joint) probability distribution, $f(\mathbf{x})$: The probability that any random variable x_i in a set shall appear within an interval $[x_i, x_i + dx_i]$ at the same time as any other variable x_j in the same set appears within an interval $[x_j, x_j + dx_j]$, is $f(\mathbf{x})d\mathbf{x}$.

Joint moment of order i,j, · · about zero, $M(\mathbf{x})_{i,j,\cdots}$:

$$M(\mathbf{x})_{i,j,\cdots} = \int\int x_1^i x_2^j \cdots f(\mathbf{x})d\mathbf{x}$$

Covariance between x and y, $R_{x,y}$: $R_{x,y} = M(x,y)_{1,1} - E(x)E(y)$

Correlation coefficient of x and y, $\rho_{x,y}$: $\rho_{x,y} = \dfrac{R_{x,y}}{\sigma_x \sigma_y}$

APPENDIX A

Appendix A: Summary of probability theory

A.1 PROBABILITY

Probability can be considered as a numerical measure of the likelihood that an event occurs relative to a set of alternative events that do not occur. The set of all possible events must be known.

The determination of the probability that an event occurs can be based on:

(1) *a priori* assumptions about the underlying mechanisms governing event(s);
(2) relative frequency of empirical observations in the past;
(3) intuitive or subjective assumptions.

The probability of an event E is denoted $P(E|X)$ where P is the probability operator, and $|X$ denotes the condition "subject to X", where X denotes whatever may be known or assumed in determining $P(E|X)$. Hence any probability depends on the state of knowledge (and ignorance) (or more generally "the state of nature") at the time that the probability is calculated. Seen in this way, all probabilities are conditional (as indicated by $|X$) [e.g. Tribus, 1969]. In many cases $P(E|X)$ will be denoted simply $P(E)$, the state of nature X being understood.

A.2 MATHEMATICS OF PROBABILITY

A.2.1 Axioms

(a) The probability $P(E)$ of an event E is a real non-negative number: $0 \leq P(E) \leq 1$.

(b) The probability of an inevitable event C is $P(C) = 1.0$. Hence the probability $P(0)$ of an impossible event equals 0.

(c) Addition rule. The probability that either or both of two events E_1 and E_2 occur is

$$P(E_1 \cup E_2) = P(E_1) + P(E_2) - P(E_1 \cap E_2) \tag{A.1}$$

Hence for two *mutually exclusive* events

$$P(E_1 \cup E_2) = P(E_1) + P(E_2) \tag{A.2}$$

A.2.2 Derived results

(d) Multiplication rule. The probability that both events E_1 and E_2 occur is

$$P(E_1 \cap E_2) = P(E_1|E_2)P(E_2) \tag{A.3}$$

If E_1 and E_2 are independent,

$$P(E_1|E_2) = P(E_1) \text{ and } P(E_1 \cap E_2) = P(E_1)\,P(E_2) \tag{A.4}$$

This provides the definition of *independent* events.

(e) If $\overline{E}$ is the event that E does not occur,

$$P(E \cup \overline{E}) = P(E) + P(\overline{E}) = P(C) = 1$$

Therefore

$$P(\overline{E}) = 1 - P(E) \tag{A.5}$$

(f) Conditional probability

$$P(E_1|E_2) = \frac{P(E_1 \cap E_2)}{P(E_2)} \tag{A.3a}$$

follows direction from (A.3).

(g) Total probability theorem. For events E_i, $i = 1, \ldots, n$, mutually exclusive and collectively exhaustive (i.e. covering all possiblities without overlap),

$$P(A) = P(A|E_1)P(E_1) + P(A|E_2)P(E_2) + \ldots + P(A|E_n)P(E_n) \tag{A.6}$$

by virtue of the multiplication rule.

(h) Bayes' theorem. From the multiplication theorem, for a particular event E_i and the event A,

$$P(A \cap E_i) = P(A|E_i)P(E_i) = P(E_i|A)P(A)$$

but $P(A)$ is given by the total probability theorem, so that

$$P(E_i|A) = \frac{P(A|E_i)P(E_i)}{\sum_{i=1}^{n} P(A|E_i)P(E_i)} = \frac{P(A|E_i)P(E_i)}{P(A)} \tag{A.7}$$

A.3 DESCRIPTION OF RANDOM VARIABLES

In what follows, only the case of continuous random variables will be noted; for discrete random variables the results are exactly analogous with integration being replaced by summation. The probability that the random variable X takes on a value less than or equal to x (a specific value) is given by:

$$P(X \leq x) \equiv F_X(x) = \int_{-\infty}^{x} f_X(x)\,dx \tag{A.8}$$

where $F_X(x)$ is the cumulative distribution function of X, and $f_X(x)$ is the probability density function. Obviously $f_X(x) = dF_X(x)/dx$; thus $f_X(x)$ is not a probability, but its local derivative. Specific cases of $f_X(x)$ and $F_X(x)$ are considered in section A.5. Any function satisfying $F_X(-\infty) = 0$, $F_X(+\infty) = 1.0$, $F_X(x) \geq 0$, $f_X(x) \geq 0$, and for which the derivative $dF_X/dx = f_X$ exists is a possible cumulative distribution function. However, in practice, attention is restricted to a restricted set

$$\begin{aligned} P(a < X \leq b) &= \int_{-\infty}^{b} f_X(x)\,dx - \int_{-\infty}^{a} f_X(x)\,dx \\ &= F_X(b) - F_X(a) \end{aligned} \tag{A.9}$$

A distribution may be described by a number of derived properties, commonly called "moments", without specific reference to either f_X or F_X. Also, for discrete functions, the probability density function is replaced by the probability mass function p_X.

A.4 MOMENTS OF RANDOM VARIABLES

A.4.1 Mean or expected value (first moment).

This is a "weighted average" of all the values that a random variable may take:

$$E(X) \equiv \mu_X = \sum_i x_i p_X(x_i) \overset{\text{or}}{=} \int_{-\infty}^{\infty} x f_X(x)\,\mathrm{d}x \tag{A.10}$$

It is called the "first moment" since it is the first moment of area of the probability density function. (The mean μ_X is analogous to the centroidal distance of a (beam) cross-section.)

Other central tendency measures are the *mode* which is most probable value, i.e. the value of x for which p_X or f_X is greatest and the *median* which is the value of x for which $F_X(x) = 0.5$, i.e. values above and below the median are equally likely.

A.4.2 Variance and standard deviation (second moment)

The variance of a random variable is a measure of the degree of randomness about the mean

$$\begin{aligned} E(X-\mu_X)^2 = \operatorname{var}(X) &= \sum_i (x_i-\mu_X)^2 p_X(x_i) = \\ &\overset{\text{or}}{=} \int_{-\infty}^{\infty} (x-\mu_X)^2 f_X(x)\,\mathrm{d}x \\ &= E(X^2) - (\mu_X)^2 \end{aligned} \tag{A.11}$$

which is a useful result. The standard deviation is

$$\sigma_X = [\operatorname{var}(X)]^{1/2} \tag{A.12}$$

The coefficient of variation is

$$V_X = \frac{\sigma_x}{\mu_X} \tag{A.13}$$

A.4.3 Bounds on deviations from the mean

For all discrete and continuous random variables there are bounds on the relationship between the standard deviation and the mean. The most well-known is due to Bienayme and Chebychev. For a random variable X, with mean μ_X and standard deviation σ_X,

$$P(|X-\mu_X| \geq k\sigma_X) \leq \frac{1}{k^2} \tag{A.14}$$

where $k > 0$ is a real number. This is a (weak) general bound on the amount of deviation $|X-\mu_X|$ from the mean relative to the standard deviation. If it is known that $f_X(x)$ has a single peak and has so-called "high order" contact with the x axis at $x = \pm\infty$, the right-hand side of expression (A.14) may be

replaced by $1/2.25k^2$. This is the "Camp–Meidall" inequality [Freeman, 1963, p. 30]

A.4.4 Skewness γ_1 (third moment)

A measure of skewness or lack of symmetry of a distribution is given by the third central moment about the mean:

$$E(X-\mu_X)^3 = \sum_i (x_i-\mu_X)^3 p_X(x_i) \overset{\text{or}}{=} \int_{-\infty}^{\infty} (x-\mu_X)^3 f_X(x)\,\mathrm{d}x \tag{A.15}$$

$E(X-\mu_X)^3$ will be positive if there is greater dispersion of values of $X \geqslant \mu_X$ than for values of $X < \mu_X$; the sign and magnitude of $E(X-\mu_X)^3$ governs the sign and degree of skewness

$$\gamma_1 = \frac{E(X-\mu_X)^3}{\sigma_X^3}$$

Positive skewness is indicated by the larger "tail" of the distribution in the positive direction.

A.4.5 Coefficient γ_2 of kurtosis (fourth moment)

The fourth central moment gives a measure of the "flatness" of the distribution. The greater the moment, the "flatter" (less peaked) is the distribution.

$$E(X-\mu_X)^4 = \sum_i (x_i-\mu_X)^4 p_X(x_i) \overset{\text{or}}{=} \int_{-\infty}^{\infty} (x-\mu_X)^4 f_X(x)\,\mathrm{d}x \tag{A.16}$$

For a standard normal distribution,

$$\gamma_2 = \frac{E(X-\mu_X)^4}{\sigma_X^4} = 3.0$$

The measure is used in statistics only for large samples.

A.4.6 Higher moments

Higher-order moments can be developed. A systematic way of developing moments indirectly employs the "moment-generating function" [e.g. Ang and Tang, 1975]. In general, the set of all moments of a probability density function describes the function exactly; any subset of moments represents an approximation to the probability density function. For some probability density functions, a limited set of moments is sufficient to describe the

function completely. Thus, the normal, or Gaussian distribution, is completely described by its first two moments.

A.5 COMMON UNIVARIATE PROBABILITY DISTRIBUTIONS

A.5.1 Binomial B(*n*, *p*)

It gives the probability of exactly x "successes" in n trials.

The probability mass function is

$$P(X=x) = p_X(x) = \binom{n}{x} p^x (1-p)^{n-x}, x = 1, 2, \ldots, n \quad (A.17)$$

The cumulative distribution function is

$$P(X \leq x) = F_X(x) = \sum_{\mu=0}^{x} \binom{n}{\mu} p^\mu (1-p)^{n-\mu}, x = 1, 2, \ldots, n \quad (A.18)$$

where

$$\binom{n}{x} = \frac{n!}{x!(n-x)!} \quad (A.19)$$

is the binomial coefficient.

The parameters are the number n of independent trials and the probability p of success per trial (= constant).

The moments are

$$E(X) = \mu_X = np \quad (A.20)$$

$$\mathrm{var}(X) = \sigma_x^2 = \mathrm{np}(1-\mathrm{p}) \quad (A.21)$$

It is applicable where there are only two discrete alternatives per independent trial, with probability p and $1-p$ respectively, with p = constant. The "multinomial" distribution applies where there are more than two discrete alternatives possible.

It has the useful property that

$$B(n_1, p) + B(n_2, p) = B(n_1 + n_2, p) \quad (A.22)$$

A.5.2 Geometric *G*(*p*)

It gives the probability that the nth trial is a success given that the first $n-1$ trials are failures.

The probability mass function is

$$P(N=n) = p_N(n) = (1-p)^{n-1} p \qquad n = 1, 2, 3, .. \quad (A.23)$$

The cumulative distribution function is

$$P(N \leq n) = F_N(n) = \sum_{i=1}^{n}(1-p)^{i-1}p = 1-(1-p)^n \qquad \text{(A.24)}$$

The parameters are the number n of independent trials and the probability p of success per trial (= constant).

The moments are

$$E(N) = \mu_N = \frac{1}{p} \qquad \text{(A.25)}$$

$$\text{var}(N) = \sigma_N^2 = \frac{1-p}{p^2} \qquad \text{(A.26)}$$

For applications, see those for the binomial distribution. It is assumed that the trials are independent. A case in which this is not so occurs in sampling without replacement. The corresponding distribution is the hypergeometric $HG(p)$ [Ang and Tang, 1975, p. 127; Freeman, 1963, p. 113].

A.5.3 Negative binomial $NB(k, p)$

It gives the probability that the kth occurrence of a success occurs at the tth trial.

The probability mass function is

$$P(T=t) = p_T(t) = \binom{t-1}{k-1}(1-p)^{t-k}p^k,\ t = k, k+1, \ldots \qquad \text{(A.27)}$$

The parameters are the number k of successes, the probability p of success per trial (= constant) and the number t of trials before k successes ($t \geq k$).

The moments are

$$E(T) = \mu_T = \frac{k}{p} \qquad \text{(A.28)}$$

$$\text{var}(T) = \sigma_T^2 = \frac{k(1-p)}{p^2} \qquad \text{(A.29)}$$

The number of trials can also be interpreted as the number of time units. It is also known as the Pascal distribution. Other forms also exist.

A.5.4 Poisson $PN(\upsilon t)$

It gives the probability of a number of occurrences of a random event in a given (time) interval given that the mean rate of occurrences is known.

The probability mass function is

$$P(X_t = x) = p_X(x) = \frac{(\upsilon t)^x}{x!} e^{-\upsilon t} \tag{A.30}$$

The cumulative distribution function is

$$P(X_t \leq x) = F_X(x) = \sum_{r=0}^{x} \frac{(\upsilon t)^r}{r!} e^{-\upsilon t} \tag{A.31}$$

The parameters are the mean occurrence rate (per unit time or space units) υ, the time or space interval t, the average number $\lambda (\equiv \upsilon t)$ of events in t and the number X_t of occurrences in t.

The moments are

$$E(X) = \mu_x = \upsilon t \tag{A.32}$$

$$\mathrm{var}(X) = \sigma_X^2 = \upsilon t \tag{A.33}$$

The Poisson distribution results from (approximates) the Binomial distribution $B(n, P)$ as $n \to \infty$ and p is small. The Poisson distribution replaces the time interval for the number of trials. The relationship is given by $np = \upsilon t$ in the limit as $n \to \infty$, $p \to 0$. In practice, this is satisfied if, say, $n = 50$ for $p < 0.10$, or $n = 100$ for $p < 0.05$. It has wide application in its own right and not merely as an approximation to the binomial distribution. When the Poisson distribution is used in terms of time or space units, with independence of events, a Poisson process results (see Chapter 6). Note that $(\upsilon t)^0/0! = 1$.

It has the useful property that

$$PN(\lambda_1) + PN(\lambda_2) = PN(\lambda_1 + \lambda_2) \tag{A.34}$$

A.5.5 Exponential $EX(\upsilon)$

It gives, for events occurring according to a Poisson process, the probability of the time to the first occurrence of an event.

The probability density function is

$$P(T = t) = f_T(t) = \upsilon e^{-\upsilon t}, \qquad t \geq 0 \tag{A.35}$$

The cumulative distribution function is

$$P(T \leq t) = F_T(t) = 1 - e^{-\upsilon t}, \qquad t \geq 0 \tag{A.36}$$

or

$$P(T \geqslant t) = e^{-\upsilon t}$$

The parameters are the mean occurrence rate υ and the time or space interval t.

The moments are

$$E(T) = \mu_T = \frac{1}{\upsilon} = \overline{\Delta t} \tag{A.37}$$

where $\overline{\Delta t}$ is the average time between arrivals or mean life

$$\text{var}(T) = \sigma_T^2 = \left(\frac{1}{\upsilon}\right)^2 = (\overline{\Delta t})^2 \tag{A.38}$$

The exponential distribution is the continuous analogue of the geometric distribution. Since a Poisson process is stationary by definition, any starting time can be used, and hence T can refer to "inter-arrival time", which is therefore exponentially distributed.

A.5.6 Gamma $GM(k, \upsilon)$ [Fig. A.1]

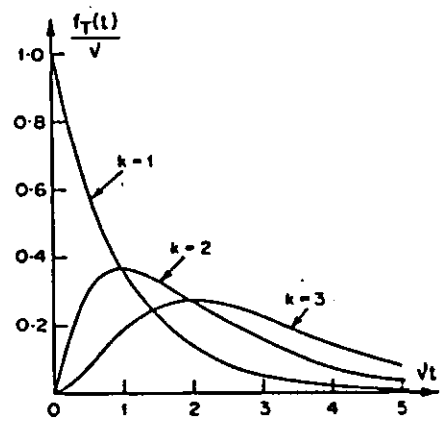

Fig. A.1 — Gamma probability density function.

It gives, for events occurring according to a Poisson process, the probability of the time T to the kth occurrence of an event. More generally, k need not be an integer.

The probability density function is

$$P(T=t) = f_T(t) = \frac{\upsilon(\upsilon t)^{k-1}}{\Gamma(k)}e^{-\upsilon t}, \qquad t \geqslant 0 \tag{A.39}$$

The cumulative distribution function is

$$P(T<t) = F_T(t) = 1-\sum_{x=0}^{k-1}\frac{(\upsilon t)^x}{x!}e^{-\upsilon t}, \; t \geqslant 0, \; k \text{ integer} \tag{A.40}$$

$$= \frac{\Gamma(k,\upsilon t)}{\Gamma(k)} \qquad t \geqslant 0, \text{ all } k$$

where

$$\Gamma(k) = \int_0^\infty e^{-u}u^{k-1}du = (k-1)! \qquad \text{for } k \text{ integer} \tag{A.41}$$

and

$$\Gamma(k,x) = \int_0^x e^{-u}u^{k-1}du \tag{A.42}$$

The parameters are the mean occurrence rate υ and the time or space interval t.

The moments are

$$E(T) = \mu_T = \frac{k}{\upsilon} \tag{A.43}$$

$$\text{var}(T) = \sigma_T^2 = \frac{k}{\upsilon^2} \tag{A.44}$$

$$E(T-\mu_T)^3 = 2k^{-1/2}\sigma_T^{-3} \text{ (skewness)} \tag{A.45}$$

The gamma function $\Gamma(k)$ is the generalization of the factorial for non-integer k. It is tabulated as the "incomplete gamma function" $\Gamma(k,\upsilon t)$ [Ang and Tang, 1975, p. 127; Benjamin and Cornell, 1970, p. 247].

For k integer, the distribution is also known as the "Erlang" distribution, and is the continuous analogue of the negative binomial distribution.

It has the useful property that, if X_i is $GM(k_i,\upsilon)$, then

$$\sum_i^m X_i = GM\left(\sum_i^m k_i, \upsilon\right) \tag{A.46}$$

A.5.7 Normal (Gaussian) $N(\mu,\sigma)$ (Fig. A.2)

It gives a distribution which arises frequently in practice as a limiting case of other probability distributions. It is also a reasonable description for many physical observations.

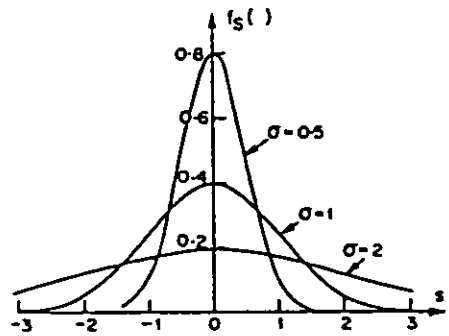

Fig. A.2 — Normal probability density function.

The probability density function is

$$f_X(x) = \frac{1}{(2\pi)^{1/2}\sigma_X}\exp\left[-\frac{1}{2}\left(\frac{x-\mu_X}{\sigma_X}\right)^2\right], \quad -\infty \leq x \leq \infty \quad \text{(A.47)}$$

The cumulative distribution function is

$$P(X \leq x) = F_X(x) =$$
$$= \frac{1}{(2\pi)^{1/2}}\int_{-\infty}^{s} e^{-\frac{1}{2}v^2}\,dv, \quad -\infty \leq x \leq \infty \quad \text{(A.48)}$$

where $s = (x-\mu_X)/\sigma_X$.

There is no simple expression for $F_X(x)$. However, there are many approximations (see below).

The parameters are the mean value μ_x and the standard deviation σ_x.

The moments are

$$E(X) = \mu_X \quad \text{(A.49)}$$

$$\text{var}(X) = \sigma_X^2 \quad \text{(A.50)}$$

$$E(X-\mu_X)^3 = 0 \text{ (no skewness)} \quad \text{(A.51)}$$

$$E(X-\mu_X)^4 = \frac{3}{\sigma_X^4} \quad \text{(A.52)}$$

The standard normal distribution $N(0,1)$ is usually tabulated for both $f_X(x)$ and $F_X(x)$ (see Appendix C). The variate is then $s = (x-\mu_X)/\sigma_X$ and $F_S(s)$ is commonly denoted $\Phi(s)$, while $f_S(s)$ is sometimes denoted $\phi(s)$. Note that, if X is $N(\mu_X, \sigma_X)$, then

$$f_X(x) = \frac{1}{\sigma_X}\phi\left(\frac{x-\mu_X}{\sigma_X}\right), \quad F_X(x) = \Phi\left(\frac{x-\mu_X}{\sigma_X}\right)$$

It has the useful properties that

$$\Phi(-s) = 1-\Phi(s) \tag{A.53}$$

$$s = \Phi^{-1}(p) = -\Phi^{-1}(1-p) \tag{A.54}$$

$$P(a<x\leq b) = \Phi\left(\frac{b-\mu_X}{\sigma_X}\right)-\Phi\left(\frac{a-\mu_X}{\sigma_X}\right) \tag{A.55}$$

If $Y = \sum_i X_i$ where X_i are independent $N(\mu_{Xi}, \sigma_{Xi})$,

$$\mu_Y = \sum_i \mu_{Xi} \tag{A.56}$$

$$\sigma_Y^2 = \sum_i \sigma_{Xi}^2 \text{ (cf. section A.11.1(a))} \tag{A.57}$$

Approximate expressions [Abramowitz and Stegun, 1966; Hastings, 1955] are as follows:

(i) $$\Phi(-\beta) \approx \frac{1}{\beta(2\pi)^{1/2}}e^{-\frac{1}{2}\beta^2} \tag{A.58}$$

(ii) $$\Phi(s) = P(s\leq s) = 1-\frac{1}{(2\pi)^{1/2}}e^{-\frac{1}{2}s^2}\left[\sum_{i=1}^{5} b_i t^i + \varepsilon(s)\right] \tag{A.59a}$$

where

$$t = (1+0.2316419s)^{-1}$$
$$|\varepsilon(s)| < 7.5\times 10^{-8}$$
$$b_1 = 0.319381530$$
$$b_2 = 0.356563782$$
$$b_3 = 1.781477937$$
$$b_4 = 1.821255978$$
$$b_5 = 1.330274429$$

(iii) $$\Phi(s) = P(S\leq s) = 1-0.5\left(1+\sum_{i=1}^{6} d_i x^i\right)^{-16} + \varepsilon(s) \tag{A.59b}$$

where

$$
\begin{aligned}
|\varepsilon(s)| &< 1.5 \times 10^{-7} \\
d_1 &= 0.0498673470 \\
d_2 &= 0.0211410061 \\
d_3 &= 0.0032776263 \\
d_4 &= 3.80036 \times 10^{-5} \\
d_5 &= 4.88906 \times 10^{-5} \\
d_6 &= 0.53830 \times 10^{-5}
\end{aligned}
$$

(iv) for $\beta \geq 1$ [Rosenblueth, 1985b],

$$\Phi(-\beta) \approx \left[\frac{\beta}{1+\beta^2} + \left(\sum_{i=0}^{5} a_i \beta^i\right)^{-1}\right]\phi(\beta) + \varepsilon(\beta) \qquad \text{(A.59c)}$$

where

$$
\begin{aligned}
|\varepsilon(\beta)| &< 5 \times 10^{-5} \\
a_0 &= \left(\frac{2}{\pi}\right)^{0.5} \\
a_1 &= 1.280 \\
a_2 &= 1.560 \\
a_3 &= 1.775 \\
a_4 &= 0.584 \\
a_5 &= 0.427
\end{aligned}
$$

A.5.8 Central limit theorem

This famous theorem states that the sum of a large number of random variables approaches the normal distribution, irrespective of the individual distributions of the random variables [Freeman, 1963, p. 181; Benjamin and Cornell, 1970, p. 251].

A.5.9 Lognormal $LN(\lambda, \xi)$ (Fig. A.3)

In this distribution, the natural logarithm of the random variable X, rather than X itself, has a normal distribution.

The probability density function is

$$f_X(x) = \frac{1}{(2\pi)^{1/2} x\varepsilon} \exp\left[-\frac{1}{2}\left(\frac{\ln x - \lambda}{\varepsilon}\right)^2\right], \quad 0 \leq x < \infty \qquad \text{(A.60)}$$

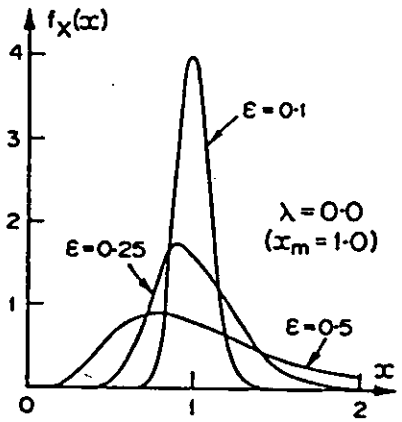

Fig. A.3 — Lognormal probability density functions.

The cumulative distribution function is

$$F_X(x) = \int_{-\infty}^{u} f_X(u)\,du = \Phi\left(\frac{\ln x - \lambda}{\varepsilon}\right) \quad \text{(no explicit form)} \qquad (A.61)$$

The parameters are

$$\lambda = E(\ln X) = \text{mean of } \ln(X) = \mu_{\ln X} \qquad (A.61a)$$

$$\xi^2 = \text{var}(\ln X) = \sigma^2_{\ln x} \qquad (A.61b)$$

The moments [e.g. Ang and Tang, 1975, p. 105] are

$$E(X) = \mu_X = \exp(\lambda + \tfrac{1}{2}\xi^2) \qquad (A.62)$$

$$\text{var}(X) = \sigma^2_X = \mu^2_X(e^{\xi^2} - 1) \qquad (A.63)$$

Because

$$P(a < x \leq b) = \Phi\left(\frac{\ln b - \lambda}{\xi}\right) - \Phi\left(\frac{\ln a - \lambda}{\xi}\right) \qquad (A.64)$$

this allows use of standard normal tables for evaluation of probabilities with X lognormal.

The lognormal distribution has the following useful properties.

(1) From equation (A.62),

$$\lambda = \mu_{\ln X} = \ln \mu_X - \tfrac{1}{2}\xi^2$$

or

$$\lambda = \ln x_m = \ln\left[\frac{\mu_X}{(1+V_X^2)^{1/2}}\right]$$

or

$$x_m = \mu_X e^{\frac{1}{2}\xi^2}$$

ϑηερε x_m is the median of x ($P(X \leq x_m) = 0.5$).

(2) From equation (A.63),

$$\xi^2 = \sigma_{\ln X}^2 = \ln\left(1+\frac{\sigma_X^2}{\mu_X^2}\right) = \ln(1+V_X^2) \approx V_X^2 \quad \text{for } V \leq 0.30$$

where V_X is the coefficient of variation.

(3) Also

$$x_m = \frac{\mu_X}{(1+V_X^2)^{1/2}}$$

so that $x_m \leq \mu_X$.

(4) *If* $Y = \prod_{i=1}^{n} X_i$ where X_i are lognormal, $LN(\lambda_i, \xi_i)$, then

$$\mu_{\ln Y} = \sum_{i=1}^{n} \mu_{\ln X_i} \quad \text{or} \quad y_m = \prod_{i=1}^{n} x_{m_i} \quad \text{and} \quad \sigma_{\ln Y}^2 = \sum_{i=1}^{n} \sigma_{\ln X_i}^2 \qquad \text{(A.65)}$$

A.5.9.1 Central limit theorem for lognormal

Because of the relationship between the normal and lognormal distributions, the central limit theorem extended to the lognormal distribution states that the *product* of a large number of random variables approaches the lognormal distribution, irrespective of the individual distributions of the random variables.

A.5.10 Beta *BT*(*a*, *b*, *q*, *r*) (Fig. A.4)

Although the beta distribution may arise from physical considerations, its chief advantage is its great flexibility in being able to be fitted to observed data. It is given in various, essentially equivalent forms.

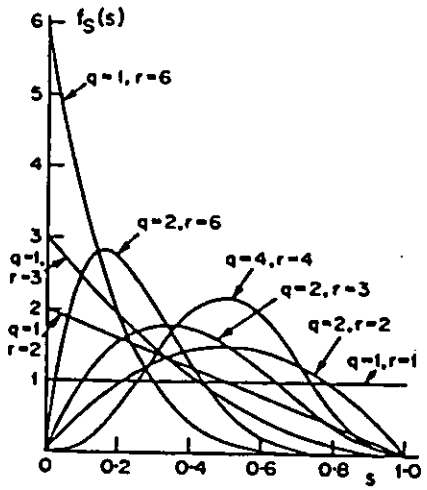

Fig. A.4 — Beta distribution probability density functions for different parameters.

The probability density function is

$$f_X(x) = \frac{1}{\beta(q,r)} \frac{(x-a)^{q-1}(b-x)^{r-1}}{(b-a)^{q+r-1}}, \qquad a \leq x \leq b \qquad \text{(A.66)}$$
$$= 0, \qquad \text{elsewhere}$$

where the Beta function $\beta(q,r)$ is given by

$$\beta(q,r) = \int_0^1 x^{q-1}(1-x)^{r-1}\,dx$$
$$= \frac{\Gamma(q)\Gamma(r)}{\Gamma(q+r)}$$
$$= \frac{(q-1)!(r-1)!}{(q+r-1)!} \qquad \text{for } q,r \text{ integer}$$

If $a=0$, $b=1$ (standard beta distribution),

$$f_S(s) = \frac{1}{\beta(q,r)} s^{q-1}(1-s)^{r-1}, \qquad 0 \leq s \leq 1 \qquad \text{(A.67)}$$
$$= 0, \qquad \text{elsewhere}$$

The cumulative distribution function

$$F_S(s) = \frac{\beta_s(q,r)}{\beta(q,r)}, \qquad 0 \leq s \leq 1 \qquad (A.68)$$

where the incomplete beta function $\beta_s(q,r)$ is given by

$$\beta_s(q,r) = \int_0^s y^{q-1}(1-y)^{r-1}\mathrm{d}y$$

The parameters a and b describe the intervals for the general beta distribution.

The moments are

$$E(x) = \mu_x = a + \frac{q(b-a)}{q+r} \qquad (A.69)$$

$$\mathrm{var}(X) = \sigma_x^2 = \frac{qr(b-a)^2}{(q+r)^2(q+r+1)} \qquad (A.70)$$

The coefficient of skewness is

$$\gamma_1 = \frac{2(r-q)}{(q+r)(q+r+2)\sigma_x} \qquad (A.71)$$

The *incomplete Beta function ratio* $\beta_s(q,r)/\beta(q,r)$ has been tabulated [Pearson and Johnson, 1968]. If q,r are both integral, $BT(0,1,q,r)$ *is* binomially distributed such that

$$f_S(s) = (q+r-1)p_X(x) \qquad (A.72)$$

where $p_X(x)$ is binomially distributed as $B(q+r-2,s)$ with $x = q-1$.

A special case of the general beta distribution is the *rectangular* or *uniform* distribution $BT(a,b,1,1) = R(a,b)$:

$$F_X(x) = \frac{1}{b-a} \qquad a<x<b \qquad (A.73)$$

$$= 0, \qquad \text{elsewhere}$$

$$F_X(x) = \frac{x-a}{b-a}, \qquad a<x<b \qquad (A.74)$$

$$= 0, \qquad x \leq a$$

$$= 1, \qquad x \geq b$$

with moments

$$\mu_X = \frac{(a+b)}{2}, \quad \sigma_X^2 = \frac{(b-a)}{12} \tag{A.75}$$

A.5.11 Extreme value distribution type I $EV\text{-}I(\mu, \alpha)$ (Fig. A.5)

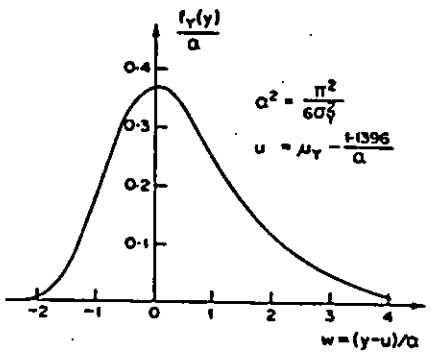

Fig. A.5 — Extreme value distribution type I (Gumbel).

The limiting (asymptotic) distribution of the largest (smallest) of n random variables X_i as $n \to \infty$. The distribution of the X_i must be of the form $F_X(x) = 1 - e^{-g(x)}$, $f_X(x) = e^{-g(x)}$, with $dg/dx > 0$. The normal, gamma and exponential distributions are of this type. The distribution Y, the *largest* of many independent X_i, is given asymptotically [Gumbel, 1958, pp. 159, 169], for the probability density function, by

$$f_Y(y) = \alpha \exp[-\alpha(y-u) - e^{-\alpha(y-u)}], \quad -\infty < y < \infty \tag{A.76}$$

and, for the cumulative distribution function, by

$$F_Y(y) = \exp[-e^{-\alpha(y-u)}], \quad -\infty < y < \infty \tag{A.77}$$

The parameters are the mode u of the distribution and α which is a measure of the dispersion of the distribution. α^{-1} is sometimes known as the "slope" of the distribution (obtained when plotting the distribution on so-called "Gumbel" paper).

Both u and α may be obtained, via the moments, from curve fitting to observed data.

The moments are

$$E(Y) = \mu_Y = u + \frac{\gamma}{\alpha} \tag{A.78}$$

where $\gamma = 0.577215\ \ 664\ \ 9\ldots$ is Euler's constant.

$$\mathrm{var}(Y) = \sigma_Y^2 = \frac{\pi^2}{6\alpha^2} \tag{A.79}$$

The skewness is

$$\gamma_1 = 1.1396 \tag{A.80}$$

(i.e. independent of u and α).

The following points should be noted in applications using this distribution.

(1) In practice, the X_i of the underlying population need not be completely independent nor completely identical [Gumbel, 1958, p. 166]. Also it may be difficult to determine the appropriate underlying distribution of the X_i, and convergence to the asymptotic distribution may be slow. Nevertheless extreme value distributions are useful for fitting to experimental data even where the underlying mechanisms are not fully understood.

(2) The distribution is tabulated by the National Bureau of Standards (NBS) (1953) in terms of a reduced variate $W = (Y - u)\alpha$ for which $u = 0$, $\alpha = 1$ and $F_W(w) = e^{-e^{-w}}$. The probability density function and cumulative distribution function in terms of Y are recovered from

$$f_Y(y) = \alpha f_W[(y - u)\alpha] \tag{A.81}$$

$$F_Y(y) = F_W[(y - u)\alpha] \tag{A.82}$$

(3) This distribution is also termed the "double exponential", "Gumbel" or "Fisher–Tippett Type I" distribution.

The complementary result is as follows. The distribution Y^S of the *smallest* of many independent X_i is given asymptotically by, for the probability density function,

$$f_{Y^S}(y^S) = \alpha \exp[\alpha(y^S - u) - e^{\alpha(y^S - u)}], \quad -\infty < y^S < \infty \tag{A.83}$$

and, for the cumulative distribution function,

$$F_{Y^S}(y^S) = 1 - \exp[-e^{\alpha(y^S - u)}], \quad -\infty < y^S < \infty \tag{A.84}$$

with

$$\mu_{Y^S} = u - \frac{\gamma}{\alpha} \tag{A.85}$$

$$\sigma^2_{Y^S} = \frac{\pi^2}{6\alpha^2} \tag{A.86}$$

$$\gamma_1 = -1.1396 \tag{A.87}$$

The distribution for Y^S is related to that for the reduced variable W above, by:

$$f_{Y^S}(y^S) = \alpha f_W[-(y^S - u)\alpha] \tag{A.88}$$

$$F_{Y^S}(y^S) = 1 - F_W[-(y^S - u)\alpha] \tag{A.89}$$

Hence, the tabulated results for the reduced variable W can be applied.

The extreme value distribution Y^S for the minimum has less practical application than that for Y; the Weibull distribution (type III) is more commonly used for smallest values.

A.5.12 Extreme value distribution type II $EV\text{-}II(u, k)$ (Fig. A.6)

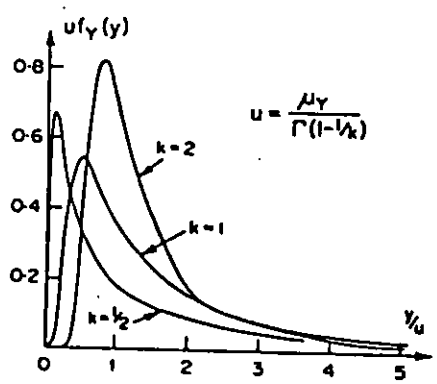

Fig. A.6 — Extreme value distribution type II (Frechet).

The limiting (asymptotic) distribution of the largest of n random variables X_i as $n \to \infty$. The distribution of the X_i must be of the form $F_X(x) = 1 - Ax^{-k}$, $x \geq 0$, A = constant [Gumbel, 1958, pp. 160, 255–272]. Typically of this form is the Pareto distribution, and the Cauchy distribution for $x \geq 0$.

The probability density function is

$$f_Y(y) = \frac{k}{y}\left(\frac{u}{y}\right)^k e^{-(u/y)^k}, \qquad y \geq 0 \qquad \text{(A.90)}$$

The cumulative distribution function is

$$F_Y(y) = e^{-(u/y)^k}, \qquad y \geq 0 \qquad \text{(A.91)}$$

The parameters are the characteristic value u of the distribution (median $> u >$ mode; median $\approx u \approx$ mode for $k > 4$) and k which is a dimensionless inverse measure of the dispersion of the distribution.

The moments are

$$E(Y) = \mu_Y = u\Gamma\left(1-\frac{1}{k}\right), \qquad k>1 \qquad \text{(A.92)}$$

$$\text{var}(Y) = \sigma_Y^2 = u^2\left[\Gamma\left(1-\frac{2}{k}\right) - \Gamma^2\left(1-\frac{1}{k}\right)\right], \qquad k>2 \qquad \text{(A.93)}$$

so that

$$V_Y^2 = \frac{\mu_Y^2}{\sigma_y^2} = \frac{\Gamma(1-2/k)}{\Gamma^2(1-1/k)} - 1 \qquad \text{(A.94)}$$

Moments of order $l \geq k$ do not exist; this complicates the estimation of parameters u and k.

The following points should be noted in applications using this distribution.

(1) If it is known that $k > 2$, equation (A.94) for V_Y^2 may be used to evaluate k, and u may be evaluated from equation (A.92) for μ_Y.
(2) The type II distribution for Y ($EV\text{-}II(u, k)$) may be transformed to the type I for Z ($EV\text{-}I(u, \alpha)$) by letting $Z = \ln Y$. Then

$$f_Y(y) = \frac{1}{y} f_Z(\ln y) \qquad \text{(A.95)}$$

$$F_Y(y) = F_Z(\ln y) \qquad \text{(A.96)}$$

$$\alpha = k \qquad \text{(A.97)}$$

Hence, in terms of the reduced variable W, which is tabulated (see section A.5.11),

$$f_F(y) = \frac{k}{y} f_W[(\ln y - \ln u)k] \qquad \text{(A.98)}$$

$$F_Y(y) = F_W[\ln y - \ln u)k] \tag{A.99}$$

(3) The above properties hold for $y \geqslant 0$. A more general result, for $y \gtrless \varepsilon$, $\varepsilon \gtrless 0$, can be obtained by linear transformation by writing $u - \varepsilon$ for u and $y - \varepsilon$ for y.
(4) This distribution is also termed the "Frechet" distribution.
(5) The distribution for the smallest extreme values is of no practical interest.

The distribution has a useful property in that the underlying distributions X_i for the type II distributions typically have longer tails ($x \geqslant 0$) than those for the type I distribution. This is also evident for the corresponding asymptotic distributions.

A.5.13 Extreme value distribution type III *EV-III*(ε,u,k) (Fig. A.7)

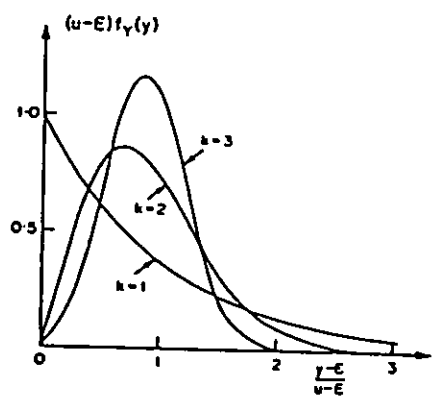

Fig. A.7 — Extreme value distribution type III (Weibull).

The limiting (asymptotic) distribution of the largest (smallest) of n random variables X_i as $n \to \infty$, with X_i limited *in the tail of interest* to some maximum (minimum) value w (or ε), and X_i having a distribution of general form

$$F_X(x) = 1 - A(w - x)^k, \qquad x \leqslant w,\ k > 0,\ A = \text{constant}$$

The rectangular ($k = 1$), triangular ($k = 2$) and the Gamma distribution ($\varepsilon = 0$) are of this form. The distribution Y^L *of the largest* of many independent X_i is given by [Gumbel, 1958, p. 275], for the probability density function,

$$f_{Y^L}(y^L) = \frac{k}{w-u}\left(\frac{w-y^L}{w-u}\right)^{k-1} F_{Y^L}(y^L), \qquad y \leq w \quad \text{(A.100)}$$

and, for the cumulative distribution function,

$$F_{Y^L}(y^L) = \exp\left[-\left(\frac{w-y^L}{w-u}\right)^k\right], \qquad y \leq w \quad \text{(A.101)}$$

More useful is the distribution Y of the *smallest* of many (independent) X_i [Gumbel, 1958, p. 277]; the probability density function is

$$F_Y(y) = P(Y \leq y) = 1 - P_Y(y). \qquad y \geq \varepsilon \quad \text{(A.102)}$$

where

$$P_Y(y) = \exp\left[-\left(\frac{y-\varepsilon}{u-\varepsilon}\right)^k\right], \qquad y \geq \varepsilon \quad \text{(A.103)}$$

which equals the probability of a value Y larger than y, i.e. $P(Y > y)$. Also,

$$f_Y(y) = \frac{\mathrm{d}F_Y(y)}{\mathrm{d}y} = \frac{k}{u-\varepsilon}\left(\frac{y-\varepsilon}{u-\varepsilon}\right)^{k-1} P_Y(y), \qquad y \geq \varepsilon \quad \text{(A.104)}$$

The parameters are the minimum value ε of X_i (and hence Y), the characteristic value u of the distribution (which converges to μ_Y as $k \to \infty$) and the "scale parameter" $1/k$ (usually $k > 1$).

The moments are

$$E(y) = \mu_Y = \varepsilon + (u-\varepsilon)\Gamma\left(1+\frac{1}{k}\right) \quad \text{(A.105)}$$

$$\mathrm{var}(y) = \sigma_Y^2 = (u-\varepsilon)^2\left[\Gamma\left(1+\frac{2}{k}\right) - \Gamma^2\left(1+\frac{1}{k}\right)\right] \quad \text{(A.106)}$$

The following point should be noted in applications using this distribution.

(1) Estimation of the parameters ε, u and k is not generally straightforward. If the underlying distribution in X_i is known, k is known, and ε and u can be estimated from the estimates for μ_Y and σ_Y^2. Otherwise, k may be estimated from sample skewness [Gumbel 1958, p. 289] or u may be estimated from order statistics [Gumbel 1958, p. 291]. If the lower limit ε

is known, or is zero, then u and k can be evaluated from equations (A.105) and (A.106) for μ_Y and σ_Y^2 by writing y for $y-\varepsilon$ and hence

$$\mu_Y = u\Gamma\left(1+\frac{1}{k}\right)$$

$$\sigma_Y^2 = u^2\left[\Gamma\left(1+\frac{2}{k}\right)-\Gamma^2\left(1+\frac{1}{k}\right)\right]$$

and

$$1+V_Y^2 = \frac{\Gamma(1+2/k)}{\Gamma^2(1+1/k)} \quad \text{or} \quad k \approx V_Y^{-1.09}$$

all of which can be estimated from sample data [Gumbel, 1958, p. 293]. However, the procedure is cumbersome [see also Mann *et al.*, 1974, p. 189].

(2) The distribution $F_Y(y)$ is pseudo-symmetric for $3.2<k<3.7$.

(3) *If* Y is *EV-III*(ε, u, k) for smallest values, then $Z=\ln(Y-\varepsilon)$ is *EV-I*$[\ln(u-\varepsilon), k]$ for smallest values. This enables the third extreme value distribution to be evaluated using the tables for *EV-I* (largest) in terms of the reduced variable W:

$$F_Y(y) = 1-F_W\{-k[\ln(y-\varepsilon)-\ln(u-\varepsilon)]\}, \qquad y \geqslant \varepsilon \qquad \text{(A.107)}$$

$$f_Y(y) = \frac{k}{y-\varepsilon}f_W\left[-k\ln\left(\frac{y-\varepsilon}{u-\varepsilon}\right)\right], \qquad y \geqslant \varepsilon \qquad \text{(A.108)}$$

(4) The distribution $P_Y(y)$ is also known as the Weibull distribution.

(5) If $\varepsilon = 0$, $k=2$, the distribution is also known as the Rayleigh distribution:

$$f_Y(y) = \frac{y}{\sigma_Y^2}\exp\left(-\frac{y^2}{2\sigma_Y^2}\right) \qquad \text{(A.102a)}$$

$$F_Y(y) = 1-\exp\left(-\frac{y^2}{2\sigma_Y^2}\right) \qquad \text{(A.103a)}$$

A.6 JOINTLY DISTRIBUTED RANDOM VARIABLES

A6.1 Joint probability distribution.

If an event is the result of two (or more) continuous random variables, X_1 and X_2 say, the probabilities that the event occurs for given values of x_1 and x_2 are described by the joint cumulative distribution function

APPENDIX B

Codes and structural reliability

9.1 INTRODUCTION

The design of structures using a structural design code, or an equivalent regulation, may be described as "structural proportioning by delegated professional authority" [Lind, 1969]. All designers required to use a particular design code are forced to follow one algorithm (usually) to achieve "their" design. Key steps in the structural proportioning process have been predetermined for the designer by code rules. Any structural design for which a particular code was used therefore reflects the "design" of the code itself. It follows that the formulation of a structural design code is the same as the bulk detail proportioning of all structures that will be designed using that code. The individual designer is left free to determine structural modelling, layout, main dimensions, connection types, support and loading conditions, etc., largely independent of the structural design code, but once such decisions have been made, the detail design is largely prescribed by code rules.

The objective of structural engineering design may be reasonably taken to be the maximization of the total expected utility of the structure, given a prescribed reference data set and availability of materials and labour. There are then two complementary aspects of the design task that must be considered:

(a) optimization of the total expected utility of the structure (by the designer);
(b) optimization of the structural design code (by code-writing committee).

The aim of this chapter will be to consider item (b), i.e. how a code should be formulated to be optimum for the range of structures for which it is likely to be used. In particular, attention will be confined to:

(1) safety-checking rules in code theory;
(2) the likely formats for so-called limit state design codes;
(3) the relationship of these codes to the theoretical reliability concepts introduced in the previous chapters.

Practical matters such as proper wording of requirements, interpretation, etc., will not be discussed. It will be assumed that physical models, such as those describing column strength, etc., are given and not subject to optimization, although that would clearly be a possibility. Fundamental aspects of code-writing philosophy have been discussed by Lind (1969, 1972), Legerer (1970), Veneziano (1976), Turkstra (1970) and others.

9.2 STRUCTURAL CODE OPTIMIZATION

A structural design code can be viewed as a predictive tool, in the sense that the designer, having followed the requirements of the code, would expect the resulting structure to be sufficiently safe and sufficiently serviceable during the period of its expected life. However, at the design stage, some matters are not known with any degree of certainty and can only be predicted (see Section 2.2). The way that a code is structured to allow for these uncertainties will affect the expected utility of any structure designed using it.

The degree of optimality of expected utility of a code will depend on the interests of those affected by it. The various requirements which a particular structure should satisfy will also depend on whose viewpoint is considered. Undoubtedly some of the requirements have the potential for conflict. Interested parties usually include the builder, the owner, the eventual user and various regulatory authorities.

Of these, regulatory authorities and structural engineers tend to rate structural safety as a very important requirement to be met. However, from the point of view of the other parties, safety might be seen as "necessary but not sufficient"; other matters such as serviceability and costs are also important. Mostly, in countries with well-established rules and traditions and a legacy of successful engineering, structural safety for other than major or unusual structures is largely a "non-issue" [Bosshard, 1979]. The functions of a structural design code tend, in these circumstances, to be seen more in economic and decision-making terms.

A further complication is that structural design codes must be applicable to whole families of structures each with details and with requirements which a code-writing committee can only guess at on the basis of previous experience. Again, prediction is involved. It is unlikely that in a single Code the differing requirements of the many structures and the many interested parties within its scope can be reconciled. As a result, it is very unlikely that optimization of a code *ab initio* will be successful.

An alternative approach is:

(1) to recognize that many structural design codes have been in existence for some considerable time;
(2) to assume that the codes represent the collective wisdom of the profession and reflect a degree of consensus arrived at over many years.

This process can be viewed as representing an alternative form of code optimization, now via refinement, or the gradual improvement of code provisions (if not necessarily their presentation and complexity) through accumulated experience and trade-offs.

Changes to a design code should be only gradually introduced since all the effects will not be known until the longer term. They should also be sufficiently small not to cause uncertainty and anxiety to code-writing committees, to code users and to other interested parties within its scope. Code revisions which result in safety level changes greater than about 10% are generally considered to alarm practitioners [Sexsmith and Lind, 1977].

Code changes which do not involve safety levels should also be treated carefully. Perceived code complexity increases dramatically with the introduction of changes of philosophy (e.g. from permissible stress to limit state design format), with the introduction of more comprehensive rules and with the change of measurement units (e.g. Imperial to SI units). All three changes were made at once in Britain's CP110 reinforced concrete code, with the result that "limit state design" was commonly held responsible for making design more complex.

The major inconsistency in traditional (non-limit state design) codes is in dealing with safety checking, and in particular the load combination rules for safety checking. It is typical for structural design codes each to deal with only one material or form of construction, such as steel, reinforced concrete, prestressed concrete and timber structures. By tradition, each of these codes has (had) a different set of load combination requirements. These are seldom consistent from one code to the next.

The main thrust of the introduction of limit state design code formats is to overcome the inconsistencies between various structural design codes and to employ reasonably rational rules for safety and serviceability checking. Such rules should require the designer to check all relevant limit states explicitly. A further, and important, aim is to make all code requirements "transparent" to the code user, so that it is clear which limit state is actually being checked.

9.3 IMPROVED SAFETY-CHECKING FORMATS

9.3.1 General

All the improved safety-checking formats are developments of existing deterministic formulations, rather than fully or partially probabilistic formulations. Hence they are all at Level 1 (see Table 2.10), involve no obvious probability calculations for the code user and will be largely similar in

appearance to traditional safety-checking formats (even though there are substantial conceptual differences). Thus, the partial factors system already widely used in concrete codes is likely be retained as a basis for development.

In principle, codes could employ level 2 procedures for safety checking, provided that codes also prescribed the basic variables for each design situation, the statistical parameters and the appropriate distributions, as well as notional acceptable p_f values. Each limit state would also need to be prescribed in an appropriate form. In view of the difficulty likely to be faced on reaching decisions about these matters, the gaps in the data required, the general unpreparedness of practitioners and the need to use computers even for simpler design problems involving reliability calculations, it is at present unlikely that safety-checking methods other than at level 1 will be used for day-to-day design application in the foreseeable future.

9.3.2 Unified rules of the Comité Européen du Béton and others

Common design rules to form the basis of all codes have been proposed by the Joint Committee on Structural Safety (JCSS) acting for Comité Européen du Béton (CEB) and five other European structural engineering groups. The rules are modifications of earlier code formats. The safety-checking analysis is formulated in the space of the load effects (stress resultants) and has the following general form [CEB, 1976]:

$$g_R\left(\frac{f_k}{\gamma_{m1}\gamma_{m2}\gamma_{m3}}\right) \geqslant g_S(\gamma_{f1}\gamma_{f2}\gamma_{f3}Q_k) \tag{9.1}$$

where g_R and g_S are resistance and load effect functions which convert the ( ) terms to resistance and load effects respectively, f_k and Q_k are characteristic material strengths and loads respectively (see section 1.4.4) and γ_{mi} and γ_{fi} are the respective partial factors.

The partial factors γ_{mi}, on material strength, take account of the following factors [CEB, 1976]:

(a) the possibility of unfavourable deviations of the strengths of materials or elements from the specified characteristic value;
(b) possible differences between the strength of the material or element in the structure from that derived from control test specimens;
(c) possible local weaknesses in the structural material or element arising principally from, or in, the construction process;
(d) the possible inaccurate assessment of the resistance of elements derived from the strength of the material including the variations of the dimensional accuracy achieved in construction as they affect the resistance.

The partial factors γ_{fi} on actions take account of the following factors:

γ_{f1} deviation of actions from their characteristic values;
γ_{f2} (load combination factor) allows for the reduced probability that all actions are at their characteristic value; it is given by three factors;

$$\psi_{pi} \leqslant 1 \qquad (i = 1, 2, 3) \ ;$$

γ_{f3} possible inaccurate assessment of the action effects, including dimensional inaccuracies.

In addition, either γ_m or γ_f may be modified to allow for low consequences of failure and/or the possibility of brittle failure.

A particular form of expression (9.1) adopted by CEB (1976)] is

$$g_R\left(\frac{f_{k1}}{\gamma_{m1}}, \frac{f_{k2}}{\gamma_{m2}}, \ldots\right) \geqslant$$

$$g_S\Big[\gamma_{f1_{max}}\gamma_{f3}\sum Q_{max} + \gamma_{f1_{min}}\gamma_{f3}\sum Q_{min} + \gamma_{f1_{mean}}\gamma_{f3}\sum Q_{mean}$$

$$+ \gamma_{f1}\gamma_{f3}\left(\psi_{p1}Q_{k1} + \sum_{i=2}^{n}\psi_{pi}Q_{ki}\right)\Big] \tag{9.2}$$

where $\psi_{pi} \leqslant 1$ are load combination factors with $\psi_{p1}Q_{k1}$ denoting the most unfavourable loading. The ψ_{pi} may be considered as the ratio of the arbitrary-point-in-time loading (see Chapter 7) to the characteristic value of that loading. Q_{max} and Q_{min} denote the dead load action (and other permanent actions) acting in the most unfavourable manner for the limit state being considered. Values for the parameters in expression (9.2) for various limit states are given in Tables 9.1 and 9.2. In this particular implementation, γ_{f3} has been incorporated into γ_{f1}.

Values for γ_{mi} would be fixed by code committees dealing with specific materials. For reinforced concrete, for example, typical values are $\gamma_m = 1.5$ for concrete and $\gamma_m = 1.15$ for steel reinforcement, given normal control, average inspection and "normal" consequences of failure.

The characteristic values of the loads and resistances are considered as their 95 or 5 percentile values as appropriate, or their currently accepted values in lieu.

9.3.3 National Building Code, Canada

A somewhat less complex safety-checking format [National Research Council of Canada (NRCC) (1977), Canadian Standards Association

Table 9.1 — Partial factors for CEB code format [CEB, 1976]

Partial factor	Limit states for the following combinations ultimate			serviceability	
	Fundamental loads	Accidental loads	Infrequent loads	Quasi-permanent loads	Frequent loads
$\gamma_{f1\,max}$	1.2	1.0	0	0	0
$\gamma_{f1\,min}$	0.9	1.0	0	0	0
$\gamma_{f1\,mean}$	0	0	1.0	1.0	1.0
γ_{f1}	1.4	1.0	1.0	1.0	1.0
ψ_{p1}	1.0	B	1.0	C	B
ψ_{pi}, $i \geq 2$	A	C	B	C	C

See Table 9.2 for A, B and C.

Table 9.2 — Load combination factors [CEB, 1976]

	Load combination factors ψ_p		
	A	B	C
Domestic buildings	0.5	0.7	0.4
Office buildings	0.5	0.8	0.4
Retail premises	0.5	0.9	0.4
Parking garages	0.6	0.7	0.6
Wind	0.55	0.2	0
Snow	0.55		
Wind and snow	0.55 and 0.4		

(CSA) (1974). [Allen (1975)] has been adopted for use in Canadian building codes. Typically it takes the form

$$\phi R \geq g_S[\gamma_D D_n + \psi(\gamma_L L_n + \gamma_W W_n + \gamma_T T_n + \ldots)] \tag{9.3}$$

The left hand-side represents factored resistance, composed of the resistance R, based on characteristic strengths and material properties, dimensions, etc., and a partial factor ϕ. The right-hand side represents factored load effects. The function $g_S[\ ]$ converts the loads to load effects.

The partial factors γ_D, γ_L, γ_W and γ_T apply to the nominal dead load D_n, live load L_n, wind load W_n, etc. The partial factors are related to an "important factor" γ_I which is a measure of the consequences of failure. For

most ordinary structures, $\gamma_I = 1.0$. For structures, such as hospitals, which must survive a disaster γ_I would be set at greater than unity. The partial factors are then related to γ_I, e.g. $\gamma_D = 1.25\gamma_I$ normally, and $0.85\gamma_I$ when D_n counteracts L_n, etc. For structures of lesser importance, or for structures subject mainly to deadload, $\gamma_I = 0.8$–1.0.

The load combination factor ψ accounts for the reduced probability that L_n, W_n and T_n reach their nominal values simultaneously. Typically it takes on values 1.0, 0.7 and 0.6 respectively for one, two or three loadings to which it applies acting concurrently.

The NBC safety-checking format is derived partly from the earlier (non-probabilistic) safety-checking format of the American Concrete Institute (ACI) [e.g. MacGregor, 1976]. It is similar to the CEB format for load combinations, although the numerical values are somewhat different. However, the major difference lies in the treatment of resistance calculations. Whereas the CEB format uses factored material strengths, factored dimensions, etc., in design to allow for the possibility that the material, dimensions, etc., may be less than anticipated, the NBC format (and the load and resistance factor design format of section 9.3.4) combines all the member understrength and geometrical error terms into the factor ϕ. This factor is intended to reflect the probability that the member as a whole is understrength.

The main disadvantage of the NBC safety-checking format is that it does not always allow adequately for the strength variance of members composed of different materials. If the axial load and moment are calculated for a given eccentrically loaded column using a Monte Carlo approach, a spread of results will be obtained [Grant *et al.*, 1978]. As can be seen from Fig. 8.5, the spread of results is much smaller for columns failing in tension. This could be predicted using the CEB safety-checking format, but not the NBC (or load and resistance factor design) format. Other examples, indicating that partial factors on material strengths are preferable to those on member strength, have been given by Allen (1981b). However, the major advantage of the NBC safety-checking format is that of simplicity, i.e. ϕ needs to be considered only once in calculations.

9.3.4 Load and Resistance Factor Design [LRFD]

The load and resistance factor design safety-checking format was proposed by Ravindra and Galambos (1978) for use in US codes. It has the following form:

$$\phi R_n \geqslant \sum_{k=1}^{i} \gamma_k S_{km} \tag{9.4}$$

where ϕ and R are the "resistance factor" and "nominal resistance" as used already in US practice in the (non-probabilistic) ACI safety-checking

format, the γ_k are the "load factors" or partial factors, and S_{km} the "mean load effects". Note that in this format the load effects rather than the loads themselves are combined. Where the relationship between loading and load effect is linear, such forms are, of course, equivalent.

Based on a series of calibration exercises involving only simple second-moment concepts (see also section 9.6) it was recommended that four specific versions of expression (9.4) would be sufficient for most design situations, i.e. only four load combinations need be examined [Ravindra and Galambos, 1978]. These are

$$\phi R_n \geq \gamma_D \overline{D} + \gamma_L \overline{L} \tag{9.5a}$$

$$\phi R_n \geq \gamma_D \overline{D} + \gamma_{apt} \overline{L}_{apt} + \gamma_W \overline{W} \tag{9.5b}$$

$$\phi R_n \geq \gamma_D \overline{D} + \gamma_{apt} \overline{L}_{apt} + \gamma_S \overline{S} \tag{9.5c}$$

$$\Phi R_n \geq \gamma_W \overline{W} - \gamma_D \overline{D} \tag{9.5d}$$

where $\overline{D}$ is the load effect due to the mean dead load, and $\overline{L}$, $\overline{W}$ and $\overline{S}$ are the means of the maximum lifetime live load, maximum lifetime wind load and maximum lifetime snow load respectively; γ_D, γ_L, γ_W and γ_S (each > 1.0) are the corresponding load factors and $(\ )_{apt}$ represents the arbitrary-point-in-time value (or "sustained" values; see Chapter 7). The load factor $\gamma_D < 1.0$ refers to the minimum dead load effect $\overline{D}$.

Expression (9.5b) is equivalent to the CEB format with $\gamma_{apt}\overline{L}_{apt}$ equivalent to $g_S(\gamma_{f1}\gamma_{f3}\Psi_{pi}Q_{ki})$ in expression (9.2) for the case of wind and live and dead load, except that Q_{ki} refers to the characteristic load (a "maximum") whereas $\overline{L}_{apt}$ is in the nature of a mean load. Similar comparisons can also be made for the other formulations [Ellingwood *et al.*, 1980]. Compared with the CEB format, the LRFD format has the advantage of being very similar to safety-checking formats at present in use in many countries, as well as having fewer load combinations which need to be considered. Thus, for a situation with dead, live, wind and snow loading, the CEB safety-checking format requires checking of 32 load combinations, the NBC format requires 14 and the LRFD format requires four (including in each case load reversal due to wind uplift).

9.3.5 Some observations

The safety-checking formats sketched above show different complexities; this implies that code-writers have considerable freedom in choosing a format. If too many partial factors are chosen, it will not generally be possible to derive consistent values for them all; the ideal number of partial factors is dependent on the number of degrees of freedom in the problem. Conversely, if for simplicity and practicality only a few partial factors are used, it must be expected that they will not strictly be constant over all design

situations, since the safety-checking format then has to apply to too great a range of possibilities. In effect, each partial factor has to allow for a number of sources of uncertainty or variability. The net effect of simplicity is that conservative values for partial factors must be used in order to cover all likely design situations. This obviously has a cost penalty.

Finally, it is often considered desirable to have the same safety-checking format for all codes, in particular in terms of load combinations. In principle these should be independent of the material used for the structure. Variation in material strength and behaviour would then be included in the ϕ or γ_{mi} factors only.

9.4 RELATIONSHIP BETWEEN LEVEL 1 AND LEVEL 2 SAFETY MEASURES

Safety factors were traditionally selected largely on the basis of intuition and experience [e.g. Pugsley *et al.*, 1955]. However, the availability of level 2 probability methods has made it possible to relate probabilistic safety measures such as p_{fN} or β to the partial factors of the level 1 safety-checking formats, provided that some simplifications and approximations are accepted. As will become evident later, the relationships which will be developed below are not strictly necessary for practical code calibration, but they are useful in illustrating that there is a reasonable link between level 1 and level 2 safety measures.

The discussion to follow will be in terms of the time-integrated approach of section 6.2. This means that specific reference to time-dependent behaviour of loads and resistances, etc., may be neglected provided that the appropriate (extreme value) probability distributions are used for the variables, and an appropriate load combination rule is employed.

Also, as noted earlier, reliability assessments for code work are made without detailed knowledge of the specific loads, materials and workmanship which will be involved in the actual project. Thus all such properties are predictions of some possible future implementation, and conservative parameters and probability density functions must be used. This means that the nominal failure probability and the corresponding safety index so calculated do not necessarily bear a close relationship to the nominal failure probability and safety index which would be obtained on the basis of data for the completed structure.

Largely in order to keep in mind that it is a predicted value on the basis of quite uncertain information, the nominal failure probability and the corresponding safety index used in this chapter for code calibration will be denoted p_{fC} and β_C respectively. The distinction between p_{fN} and p_{fC} (and β and β_C) is not normally made in the structural reliability literature; however, failure to have done so might appear to be a reason for the common lack of understanding of the meaning of the nominal failure probability as used in code work.

APPENDIX C

Appendix C: Complementary standard normal table

Table C.1 gives the $N(0,1)$ distribution; $\Phi(-\beta) = 1-\Phi(\beta)$ (see section A.5.7).

Table C.1

β	$\Phi(-\beta)$	β	$\Phi(-\beta)$	β	$\Phi(-\beta)$
0.00	0.5000	0.40	0.3446	0.80	0.2119
0.01	0.4960	0.41	0.3409	0.81	0.2090
0.02	0.4920	0.42	0.3372	0.82	0.2061
0.03	0.4880	0.43	0.3336	0.83	0.2033
0.04	0.4841	0.44	0.3300	0.84	0.2005
0.05	0.4801	0.45	0.3264	0.85	0.1977
0.06	0.4761	0.46	0.3228	0.86	0.1949
0.07	0.4721	0.47	0.3192	0.87	0.1922
0.08	0.4681	0.48	0.3156	0.88	0.1894
0.09	0.4642	0.49	0.3121	0.89	0.1867
0.10	0.4602	0.50	0.3085	0.90	0.1841
0.11	0.4562	0.51	0.3050	0.91	0.1814
0.12	0.4522	0.52	0.3015	0.92	0.1788
0.13	0.4483	0.53	0.2981	0.93	0.1762
0.14	0.4443	0.54	0.2946	0.94	0.1736
0.15	0.4404	0.55	0.2912	0.95	0.1711
0.16	0.4364	0.56	0.2877	0.96	0.1685
0.17	0.4325	0.57	0.2843	0.97	0.1660
0.18	0.4286	0.58	0.2810	0.98	0.1635
0.19	0.4247	0.59	0.2776	0.99	0.1611
0.20	0.4207	0.60	0.2743	1.00	0.1587
0.21	0.4168	0.61	0.2709	1.01	0.1563
0.22	0.4129	0.62	0.2676	1.02	0.1539
0.23	0.4091	0.63	0.2644	1.03	0.1515
0.24	0.4052	0.64	0.2611	1.04	0.1492
0.25	0.4013	0.65	0.2579	1.05	0.1469
0.26	0.3974	0.66	0.2546	1.06	0.1446
0.27	0.3936	0.67	0.2514	1.07	0.1423
0.28	0.3897	0.68	0.2483	1.08	0.1401
0.29	0.3859	0.69	0.2451	1.09	0.1379
0.30	0.3821	0.70	0.2420	1.10	0.1357
0.31	0.3783	0.71	0.2389	1.11	0.1335
0.32	0.3745	0.72	0.2358	1.12	0.1314
0.33	0.3707	0.73	0.2327	1.13	0.1292
0.34	0.3669	0.74	0.2297	1.14	0.1271
0.35	0.3632	0.75	0.2266	1.15	0.1251
0.36	0.3594	0.76	0.2236	1.16	0.1230
0.37	0.3557	0.77	0.2207	1.17	0.1210
0.38	0.3520	0.78	0.2177	1.18	0.1190
0.39	0.3483	0.79	0.2148	1.19	0.1170

β	Φ(−β)	β	Φ(−β)	β	Φ(−β)
1.20	0.1151	1.80	0.3593E-01	2.40	0.8198E-02
1.21	0.1131	1.81	0.3515E-01	2.41	0.7976E-02
1.22	0.1112	1.82	0.3438E-01	2.42	0.7760E-02
1.23	0.1094	1.83	0.3363E-01	2.43	0.7550E-02
1.24	0.1075	1.84	0.3289E-01	2.44	0.7344E-02
1.25	0.1057	1.85	0.3216E-01	2.45	0.7143E-02
1.26	0.1038	1.86	0.3144E-01	2.46	0.6947E-02
1.27	0.1020	1.87	0.3074E-01	2.47	0.6756E-02
1.28	0.1003	1.88	0.3005E-01	2.48	0.6569E-02
1.29	0.9853E-01	1.89	0.2938E-01	2.49	0.6387E-02
1.30	0.9680E-01	1.90	0.2872E-01	2.50	0.6210E-02
1.31	0.9510E-01	1.91	0.2807E-01	2.51	0.6037E-02
1.32	0.9342E-01	1.92	0.2743E-01	2.52	0.5868E-02
1.33	0.9176E-01	1.93	0.2680E-01	2.53	0.5703E-02
1.34	0.9013E-01	1.94	0.2619E-01	2.54	0.5543E-02
1.35	0.8851E-01	1.95	0.2559E-01	2.55	0.5386E-02
1.36	0.8692E-01	1.96	0.2500E-01	2.56	0.5234E-02
1.37	0.8535E-01	1.97	0.2442E-01	2.57	0.5085E-02
1.38	0.8380E-01	1.98	0.2385E-01	2.58	0.4940E-02
1.39	0.8227E-01	1.99	0.2330E-01	2.59	0.4799E-02
1.40	0.8076E-01	2.00	0.2275E-01	2.60	0.4661E-02
1.41	0.7927E-01	2.01	0.2222E-01	2.61	0.4527E-02
1.42	0.7781E-01	2.02	0.2169E-01	2.62	0.4397E-02
1.43	0.7636E-01	2.03	0.2118E-01	2.63	0.4269E-02
1.44	0.7494E-01	2.04	0.2068E-01	2.64	0.4145E-02
1.45	0.7353E-01	2.05	0.2018E-01	2.65	0.4025E-02
1.46	0.7215E-01	2.06	0.1970E-01	2.66	0.3907E-02
1.47	0.7078E-01	2.07	0.1923E-01	2.67	0.3793E-02
1.48	0.6944E-01	2.08	0.1876E-01	2.68	0.3681E-02
1.49	0.6811E-01	2.09	0.1831E-01	2.69	0.3573E-02
1.50	0.6681E-01	2.10	0.1786E-01	2.70	0.3467E-02
1.51	0.6552E-01	2.11	0.1743E-01	2.71	0.3364E-02
1.52	0.6426E-01	2.12	0.1700E-01	2.72	0.3264E-02
1.53	0.6301E-01	2.13	0.1659E-01	2.73	0.3167E-02
1.54	0.6178E-01	2.14	0.1618E-01	2.74	0.3072E-02
1.55	0.6057E-01	2.15	0.1578E-01	2.75	0.2980E-02
1.56	0.5938E-01	2.16	0.1539E-01	2.76	0.2890E-02
1.57	0.5821E-01	2.17	0.1500E-01	2.77	0.2803E-02
1.58	0.5706E-01	2.18	0.1463E-01	2.78	0.2718E-02
1.59	0.5592E-01	2.19	0.1426E-01	2.79	0.2635E-02
1.60	0.5480E-01	2.20	0.1390E-01	2.80	0.2555E-02
1.61	0.5370E-01	2.21	0.1355E-01	2.81	0.2477E-02
1.62	0.5262E-01	2.22	0.1321E-01	2.82	0.2401E-02
1.63	0.5156E-01	2.23	0.1287E-01	2.83	0.2327E-02
1.64	0.5050E-01	2.24	0.1255E-01	2.84	0.2256E-02
1.65	0.4947E-01	2.25	0.1222E-01	2.85	0.2186E-02
1.66	0.4846E-01	2.26	0.1191E-01	2.86	0.2118E-02
1.67	0.4746E-01	2.27	0.1160E-01	2.87	0.2052E-02
1.68	0.4648E-01	2.28	0.1130E-01	2.88	0.1988E-02
1.69	0.4552E-01	2.29	0.1101E-01	2.89	0.1926E-02
1.70	0.4457E-01	2.30	0.1072E-01	2.90	0.1866E-02
1.71	0.4363E-01	2.31	0.1044E-01	2.91	0.1807E-02
1.72	0.4272E-01	2.32	0.1017E-01	2.92	0.1750E-02
1.73	0.4182E-01	2.33	0.9903E-02	2.93	0.1695E-02
1.74	0.4093E-01	2.34	0.9642E-02	2.94	0.1641E-02
1.75	0.4006E-01	2.35	0.9387E-02	2.95	0.1589E-02
1.76	0.3921E-01	2.36	0.9138E-02	2.96	0.1538E-02
1.77	0.3836E-01	2.37	0.8894E-02	2.97	0.1489E-02
1.78	0.3754E-01	2.38	0.8657E-02	2.98	0.1441E-02
1.79	0.3673E-01	2.39	0.8424E-02	2.99	0.1395E-02

β	Φ(−β)	β	Φ(−β)	β	Φ(−β)
3.00	0.1350E-02	3.60	0.1591E-03	5.00	0.2859E-06
3.01	0.1306E-02	3.61	0.1531E-03	5.05	0.2203E-06
3.02	0.1264E-02	3.62	0.1473E-03	5.10	0.1694E-06
3.03	0.1223E-02	3.63	0.1417E-03	5.15	0.1299E-06
3.04	0.1183E-02	3.64	0.1363E-03	5.20	0.9935E-07
3.05	0.1144E-02	3.65	0.1311E-03	5.25	0.7582E-07
3.06	0.1107E-02	3.66	0.1261E-03	5.30	0.5772E-07
3.07	0.1070E-02	3.67	0.1212E-03	5.35	0.4384E-07
3.08	0.1035E-02	3.68	0.1166E-03	5.40	0.3321E-07
3.09	0.1001E-02	3.69	0.1121E-03	5.45	0.2510E-07
3.10	0.9676E-03	3.70	0.1077E-03	5.50	0.1892E-07
3.11	0.9354E-03	3.71	0.1036E-03	5.55	0.1423E-07
3.12	0.9042E-03	3.72	0.9956E-04	5.60	0.1067E-07
3.13	0.8740E-03	3.73	0.9569E-04	5.65	0.7985E-08
3.14	0.8447E-03	3.74	0.9196E-04	5.70	0.5959E-08
3.15	0.8163E-03	3.75	0.8837E-04	5.75	0.4436E-08
3.16	0.7888E-03	3.76	0.8491E-04	5.80	0.3293E-08
3.17	0.7622E-03	3.77	0.8157E-04	5.85	0.2438E-08
3.18	0.7363E-03	3.78	0.7836E-04	5.90	0.1800E-08
3.19	0.7113E-03	3.79	0.7527E-04	5.95	0.1325E-08
3.20	0.6871E-03	3.80	0.7230E-04	6.00	0.9716E-09
3.21	0.6636E-03	3.81	0.6943E-04	6.10	0.5220E-09
3.22	0.6409E-03	3.82	0.6667E-04	6.20	0.2778E-09
3.23	0.6189E-03	3.83	0.6402E-04	6.30	0.1463E-09
3.24	0.5976E-03	3.84	0.6147E-04	6.40	0.7636E-10
3.25	0.5770E-03	3.85	0.5901E-04	6.50	0.3945E-10
3.26	0.5570E-03	3.86	0.5664E-04	6.60	0.2018E-10
3.27	0.5377E-03	3.87	0.5437E-04	6.70	0.1023E-10
3.28	0.5190E-03	3.88	0.5218E-04	6.80	0.5130E-11
3.29	0.5009E-03	3.89	0.5007E-04	6.90	0.2549E-11
3.30	0.4834E-03	3.90	0.4804E-04	7.00	0.1254E-11
3.31	0.4664E-03	3.91	0.4610E-04	7.10	0.6107E-12
3.32	0.4500E-03	3.92	0.4422E-04	7.20	0.2946E-12
3.33	0.4342E-03	3.93	0.4242E-04	7.30	0.1407E-12
3.34	0.4189E-03	3.94	0.4069E-04	7.40	0.6654E-13
3.35	0.4040E-03	3.95	0.3902E-04	7.50	0.3116E-13
3.36	0.3897E-03	3.96	0.3742E-04	7.60	0.1445E-13
3.37	0.3758E-03	3.97	0.3588E-04	7.70	0.6636E-14
3.38	0.3624E-03	3.98	0.3441E-04	7.80	0.3017E-14
3.39	0.3494E-03	3.99	0.3298E-04	7.90	0.1359E-14
3.40	0.3369E-03	4.00	0.3162E-04	8.00	0.6056E-15
3.41	0.3248E-03	4.05	0.2557E-04	8.10	0.2673E-15
3.42	0.3131E-03	4.10	0.2062E-04	8.20	0.1169E-15
3.43	0.3017E-03	4.15	0.1659E-04	8.30	0.5058E-16
3.44	0.2908E-03	4.20	0.1332E-04	8.40	0.2167E-16
3.45	0.2802E-03	4.25	0.1067E-04	8.50	0.9197E-17
3.46	0.2700E-03	4.30	0.8524E-05	8.60	0.3864E-17
3.47	0.2602E-03	4.35	0.6794E-05	8.70	0.1608E-17
3.48	0.2507E-03	4.40	0.5402E-05	8.80	0.6623E-18
3.49	0.2415E-03	4.45	0.4285E-05	8.90	0.2701E-18
3.50	0.2326E-03	4.50	0.3391E-05	9.00	0.1091E-18
3.51	0.2240E-03	4.55	0.2677E-05	9.10	0.4363E-19
3.52	0.2157E-03	4.60	0.2108E-05	9.20	0.1728E-19
3.53	0.2077E-03	4.65	0.1656E-05	9.30	0.6773E-20
3.54	0.2000E-03	4.70	0.1298E-05	9.40	0.2629E-20
3.55	0.1926E-03	4.75	0.1015E-05	9.50	0.1011E-20
3.56	0.1854E-03	4.80	0.7914E-06	9.60	0.3847E-21
3.57	0.1784E-03	4.85	0.6158E-06	9.70	0.1450E-21
3.58	0.1717E-03	4.90	0.4780E-06	9.80	0.5408E-22
3.59	0.1653E-03	4.95	0.3701E-06	9.90	0.1998E-22

PROBABILITY BASED OFFSHORE DESIGN FOR EXTREME LIFETIME LOADS AND ULTIMATE STRENGTH

by

DOUGLAS FAULKNER

GLASGOW

Invited lecture presented at:

Fourth International Conference on Behaviour of Offshore Structures, Delft, July 1985.

THE RELIABILITY CONCEPT AS AN AID TO DECISION MAKING IN OFFSHORE ENGINEERING

M.J. BAKER

Department of Civil Engineering, Imperial College of Science and Technology, London, SW7 2BU, U.K.

SUMMARY

The paper describes some of the recent developments in structural reliability theory and discusses their application to offshore structures. Attention in focussed on the reliability analysis of structural systems and on the failure of structures by fatigue. Progress in applying these methods to real structures is discussed in the context of decision making. The areas requiring further research and development are highlighted.

1. INTRODUCTION

Not many years ago, papers on reliability assessment tended to attract only a specialist audience but recently there has been increasing interest in the subject. The main purpose of this paper is to address the wider audience concerned with the behaviour of offshore structures so that judgements can be made as to whether the tools of reliability analysis have been developed sufficiently far to be of significant value.

In many respects, the position of the reliability analyst is a difficult one, since the reliability of an offshore structure, or indeed any other complex system, depends on the behaviour of many components and subsystems: on such quantities as the peak magnitudes of the many loads and their occurrence in time, and on the skills of a wide range of people. For the assessment of this reliability, the analyst requires a sufficiently detailed knowledge of all the various related fields which in practice have some bearing on safety and reliability, but at the same time he should be sufficiently expert in his own field. However, it is only by using a reliability approach that questions of loading, materials specification, design, inspection and control can be treated in an integrated and rational way.

In this paper an attempt is made to review some of the key areas of structural reliability theory, to note some of the recent developments, to examine the use that has already been made of the reliability approach in offshore engineering, to assess the possibilities for future use and finally to discuss those areas where more development work is still needed.

In keeping with the theme of this conference, the paper focusses on the structural aspects of offshore systems and does not discuss the reliability of plant and process equipment, although the latter is clearly of importance from an overall viewpoint.

2. STRUCTURAL PERFORMANCE REQUIREMENTS

Most offshore structures are used for the extraction of oil and gas from below the sea bed and it is obvious that the prime requirement of the system is to allow this operation to continue uninterrupted until the reserves are exhausted or until further production becomes uneconomic. This implies continued structural integrity throughout the useful life of the field, together with the need to satisfy many specific operational requirements - for example, limitations on pitch and heave in a compliant structure. These operational requirements, which will generally be related to the safe operation of plant and equipment, may or may not be well-defined and will often be subject to change during the design phase. Realistic, as opposed to conservative, specification of these operational requirements is clearly of importance in governing the economy of the structural design.

Loss of structural integrity, and the resulting inability of the structure to support some or all the loads, can occur in a number of ways, such as by:

- foundation failure
- overall instability
- general plasticity
- fatigue
- fracture
- corrosion, etc.

or by a combination of these mechanisms. In general, each of these failure modes requires separate attention.

Loss of structural integrity may seem to be a more clearly defined condition than many of the above operational requirements, but in practice this is not the case. For example, although a designer does not want his structure to fail by fatigue, it is often by no means clear whether the 'failure event' against which to design is the through-thickness crack, the propagation of the crack around the perimeter of a structural member, the loss of a member, or the eventual loss of several members, followed by complete collapse.

Often in current practice, 'failure events' which in reality might not even affect the safe operation of the structure are selected for the purposes of design and analysis, because they are relatively easy to deal with computationally. Except for simple cases where plastic collapse analysis can be applied, failure criteria are often chosen in relation to structural member behaviour rather than the structural system as a whole. This conservative approach must lead to loss of economy in the usage of materials, but it will undoubtedly lead to savings in design time. In many cases, the ideal solution may lie far beyond our current capabilities. Nevertheless, it is clear that there are often overall cost benefits to be gained by adopting a systems approach to safety and reliability assessment, and to design itself.

Acceptable structural performance at the beginning and throughout the life of a structure is achieved in practice by a combination of techniques, including: data analysis, initial design, structural analysis, specification, quality control, inspection, defect assessment, repair, structural monitoring and maintenance. Some of these steps are carried out before the structure comes into service and some after.. Each is likely to influence the safety and reliability of a structure in a different way and in general will have a different degree of influence on each of the various failure modes.

For example, in a steel jacket structure, the risk of failure by fatigue is likely to be reduced by the detection and removal of weld defects, whereas the risk of failure of a tubular bracing member in axial compression is governed to a large extent by the correct estimation of the distribution of extreme wave heights and the choice of partial coefficients (partial safety factors) on loads and materials. The latter failure mode is largely uninfluenced by inspection procedures, except for the detection of gross errors, whereas, in the case of fatigue, inspection may be of critical importance.

3. STRUCTURAL RELIABILITY AND SAFETY

3.1 Basic Concepts

In a general sense, the reliability of a structure is its ability to fulfil its design purpose for some specified time. This implies first achieving and then maintaining the conditions under which the various structural performance requirements mentioned above will be satisfied. In a more specific sense, reliability can be interpreted as the probability that the structure will satisfy each performance requirement throughout a specified period of time - the reference period.

Performance requirements can be divided into those associated with generally irreversible physical events - e.g. the plastic collapse of all or part of a structure - where one only needs to know the probability that the event will occur (the first-passage probability), and those associated with events which may occur, with or without increments of permanent damage, several or more times during the life of the structure and where the proportion of time spent in the 'failure state' or the number of up-crossings of some threshold response level, is of importance - e.g. static deflections or vibration amplitudes greater than a given magnitude.

In the above, 'failure' is used in the general sense of 'failure to comply with a performance requirement' and does not necessarily mean structural collapse. These two types of performance requirement are illustrated in Figs. 1 and 2.

In Fig. 1, failure corresponds to the first out-crossing of any of the failure boundaries dividing the safe region from the failure regions, or, alternatively, the realisation at some point in time (e.g. when the structure is first loaded) of a combination of values of the design variables which will cause failure. Typically, the normal design variables can be divided into those that are time-varying (e.g. most loads or actions) and those that are not (e.g. most material prop-

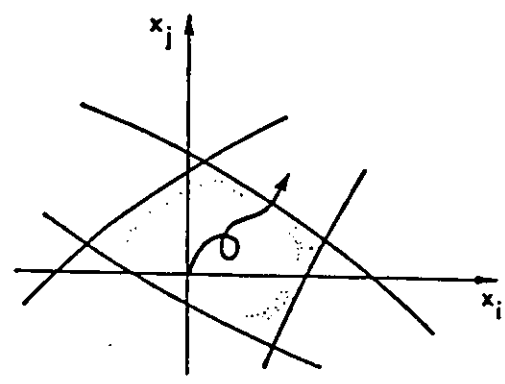

Figure 1: Out-crossing from safe region

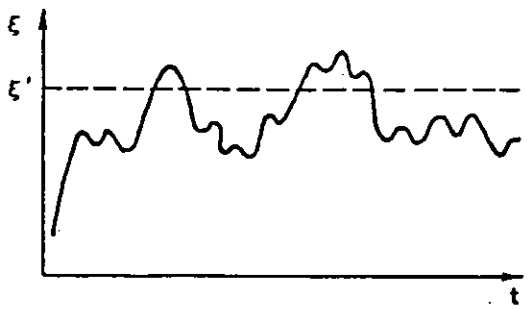

Figure 2: Up-crossing of threshold ξ'

erties and dimensions), but such a classification may need to be varied according to the performance requirement being considered. As discussed below, the various safe and failure regions are best represented in the n-dimensional space of the design variables, or sometimes more fundamental quantities, but, in Fig. 1, the problem is idealised for the purposes of representation as being two-dimensional.

For failure modes involving the total or partial collapse of the structure, the overall reliability is the probability that the structure will survive - i.e. remain in a 'safe state' for the duration of the reference period. This may be expressed as

$$P_s = P(S_1 \cap S_2 \cap \ldots \cap S_n) \qquad (1)$$

$$= 1 - P(E_1 \cup E_2 \cup \ldots \cup E_n)$$

where the event E_i is failure in mode i, S_i (not E_i) is the complement of E_i and P_s is the overall reliability or survival probability, and where the symbols $\cap$ and $\cup$ represent respectively the intersection (joint occurrence) and union (occurrence of at least one) of a number of events. The survival event corresponds to the shaded area in Fig. 1. The events $E_i \ldots E_k$ include the set of all possible plastic collapse mechanisms for the structure, together with other failure events.

Generally, it is convenient and realistic to consider the reliability of a structure with respect to each performance requirement separately and to analyse each set of failure modes independently. Nevertheless, the possibility of a sequence of events involving different failure mechanisms must not be overlooked. A possible scenario for a dynamically sensitive jacket-type structure might be:

- weak soil conditions, leading to
- increased dynamic response, leading to
- local fatigue failure, leading to
- overall failure by buckling and plastic collapse.

However, with the present state of knowledge, such a sequence of events is difficult to assess in a rigorous way, both deterministically and probabilistically.

Returning now to the second type of performance requirement illustrated in Fig. 2; in this case, non-compliance corresponds to a selected component of the structural response ξ_i being above some chosen threshold level ξ_i'. If the structure does not deteriorate with time, or with successive up-crossings of the threshold level or other higher levels, and provided that the loading can be idealised as a stationary process, the probability of 'failure' occurring at least once in an interval of time dt remains constant with time (provided the probability can be interpreted in a frequency sense).

3.2 Interpretation of Reliability Measures

For mass-produced, nominally identical, components subjected to nominally similar 'loading' for a specified period of time, reliability may be interpreted as the long-run survival frequency.

For unique, 'one-off', systems such as typical offshore structures, the relative frequency concept is not valid and the reliability or probability of survival must be interpreted in a subjective sense. This probability changes with time as more information becomes available - during the design, fabrication, float-out, installation and production phases - and should be used at each stage in the context of decision making.

For example, after the fabrication of a structure, some of the uncertainties in the material properties can be eliminated as a result of material testing, with a consequent reduction in the overall uncertainty in structural performance and a corresponding change (increase or decrease) in the computed reliability. The types of decisions that have to be made are:

- at the design stage - appropriate member sizes
- at the fabrication stage - appropriate geometric tolerances and defect sizes
- during use - suitable inspection and repair strategies

At each stage, the computed reliability may be used to optimise the decision to be taken, with a view to reducing costs.

4. ANALYSIS OF FIRST-PASSAGE FAILURES

4.1 Failure of single members

Single structural members are found in isolation as simple structures, and as components of statically determinate and statically indeterminate structures. The concept of 'structural member' is in fact an idealisation and tends to imply an element of

constant cross-sectional dimensions with uniform material properties along its length (e.g. simple beams, columns, cables, ties, hangers, etc.). In general, a single structural member will have a relatively small number of possible failure modes.

For a single structural member acting alone, or as part of a statically determinate structure, failure of the member corresponds to failure of the whole system. If the load-carrying capacity R of the member (expressed in units of load) is a deterministic function of m design variables $\bar{X} = \{X_1, X_2, \ldots, X_m\}$, R may be expressed as

$$R = R(X_1, X_2, \ldots, X_m) \qquad (2)$$

where X_i are quantities such as dimensions and material properties.

If $\bar{X}$ do not vary with time and Q is the maximum load applied to the member during the reference period t, then the reserve load-carrying capacity or 'safety margin' is given by

$$M = R - Q - f(W) \qquad (3)$$

where W is the self-weight of the member ($W = W(\bar{X})$), and where the function f allows for the different spatial distribution of W in relation to that of Q. Eq.(3) may also be re-written as an equation in load effects. M will then have units of say, kNm if the predominant response to load being considered is bending.

If $\bar{X}$ and Q are not known deterministically and are thus 'uncertain' quantities, either because they are physically variable or because their current values are not known, then the safety margin M also becomes an uncertain quantity and the reliability P_s may be expressed as

$$P_s = P(M > 0) = 1 - P(M \le 0) \qquad (4)$$

where P(.) stands for the probability of the event (.). See, for example, [1].

If M relates to the ultimate strength of the member, then $M \le 0$ corresponds to failure of the member and collapse of the whole structure, if the structure is statically determinate. For statically indeterminate structures, the failure of one member will generally not lead to failure of the whole structure, and the corresponding reliability evaluations become more difficult (see below).

In general, the safety margin may be expressed as

$$M(t) = \min_t g(X_1, X_2, \ldots, X_n)$$

$$= \min_t g(\bar{X}) \qquad (5)$$

where the vector of random variables $\bar{X}$ includes all the quantities which affect the failure of the structure, e.g. loads, material properties and dimensions, t is the specified reference period, and g(.) is the particular 'limit state function' or 'failure function'.

For the case of a single member acted upon by a single time-varying load, the probability $P(M \le 0)$ in Eq.(4) may then be expressed as

$$P_f(t) = P(g(\bar{X}) \le 0)$$

$$= \int_{g(\bar{X}) \le 0} f_{\bar{X}}(\bar{x})dx \qquad (6)$$

where X_n is the maximum load that will occur during the reference period t, and where $f_{\bar{X}}(\bar{x})$ is the multi-variate joint probability density function of the vector of random variables $\bar{X}$. The integral is taken over the region of the n-dimensional space in which $g(\bar{x}) \le 0$.

The apparent simplicity of Eqs.(5) and (6) should not mislead readers unfamiliar with this field. Although the mathematical form of the function $g(\bar{x})$ may be very simple for an isolated structural member (e.g. a single uniform beam in bending), this formulation is completely general and $g(\bar{x})$ could represent all the components of a dynamic and structural analysis of a complete structure together with the failure criterion for the member under consideration. See for example [2], [3]. Moreover, the form of Eq.(6) is such that analytical solutions or even solutions by direct numerical integration are rarely possible, except for a number of special cases. Other approaches, often referred to as Level 2 methods, are generally used in practice for the evaluation of P_f, as described below.

It should also be understood that the function $g(\bar{x})$ is entirely deterministic and simply distinguishes those combinations of design variables (when considered as deterministic quantities) which would cause 'failure' from those combinations that would not. In practice, however, the situation is not as simple as this since the methods of structural analysis and design methods which are used are generally not mathematically exact. They are often empirically based and are generally conservative - e.g. most rules for design against buckling. This gives rise to a further class of uncertainties, namely uncertainties in the accuracy and bias of the mathematical models represented by $g(\bar{x})$. This

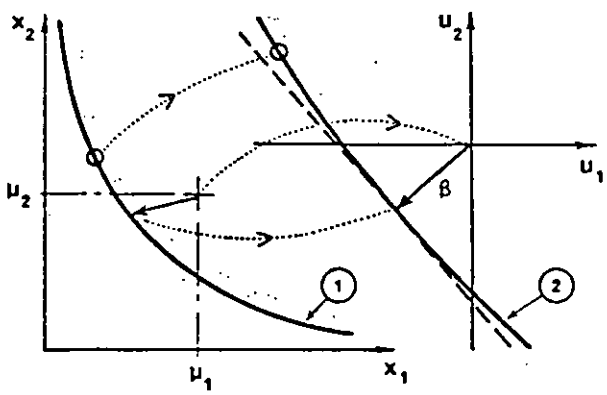

Figure 3: Failure surface transformation

is referred to as model uncertainty and will be discussed again later.

Setting $g(\bar{x}) = 0$ defines an (n-1) dimensional surface, known as the failure surface, in the n-dimensional space representing the n-dimensional vector of random variables $\bar{X}$. This is illustrated for the case n = 2 in Fig. 3, curve (1), (with both quantities being resisting as opposed to loading variables).

In general, some of the random variables X_i will be non-normal and often non-independent quantities. Since many probability calculations are more readily carried out in the space of independent standard normal variables $\bar{U}$ (u-space), it is convenient to map the failure surface $g(\bar{x}) = 0$ from the original x-space to u-space, where the failure surface is given by $g'(\bar{u}) = 0$. This is illustrated by curve (2) in Fig. 3. In u-space, the distance β from the origin to the closest point on the failure surface is referred to as the (Hasofer-Lind) reliability index, which is related to the reliability P_s by

$$P_s \simeq 1 - \Phi(-\beta) \qquad (7)$$

where Φ is the normal distribution function.

The closest point, $\bar{u}^*$, is generally referred to the design point and corresponds to the point on the failure surface where the joint probability density $f_{\bar{U}}(\bar{u})$ is a maximum. It gives the values of $\bar{u}$ at which failure is most likely to occur. If the point $\bar{u}^*$ is mapped back into the original x-space, $\bar{x}^*$ are the values of the design variables at which failure is most likely to occur (exactly in the case of normally distributed variables, or approximately in the case of non-normal quantities).

If $g'(\bar{u})$ is linear in $\bar{u}$, then Eq.(7) is exact, but this is rarely the case since even if $g(\bar{x})$ is linear, the mapping generally makes $g'(\bar{u})$ non-linear (unless $\bar{X}$ are jointly normal). However, if considered necessary, improvement in accuracy can be obtained by approximating the failure surface at the design point by a hyper-parabolic surface (see [6]), but not without a considerable amount of additional computational effort. Other possibilities also exist [7].

The ease with which the function $g'(\bar{u})$ can be derived from the function $g(\bar{x})$ depends on the inter-relationship between the random variables $\bar{X}$ (see [1]). If the variables are mutually independent then

$$u_i = \Phi^{-1}(F_{Xi}(x_i)) \qquad i = 1,n \qquad (8)$$

$$x_i = F_{Xi}^{-1}(\Phi(u_i)) \qquad i = 1,n \qquad (9)$$

and

$$g(\bar{x}) = g(F_{X1}^{-1}(\Phi(u_1)),\ldots,F_{Xn}^{-1}(\Phi(u_n)))$$

$$= g'(\bar{u}) \qquad (10)$$

where Φ^{-1} is the inverse standard normal distribution function and F_{Xi} is the probability distribution function of the random variable X_i.

If $\bar{X}$ is a jointly normal random vector with non-zero off-diagonal terms in the co-variance matrix $\bar{C}_{\bar{X}}$, a vector of uncorrelated variables $\bar{Y}$ can be found by an orthogonal transformation of $\bar{X}$. $g'(\bar{u})$ may then be found by the application of Eqs.(9) and (10).

If $\bar{X}$ are non-normal dependent variables, a possible but more complex approach is to use the so-called Rosenblatt transformation [8], as suggested by Hohenbichler and Rackwitz [9].

Having determined the transformed failure function $g'(\bar{u})$, the shortest distance from the origin to the failure surface may be found by a variety of algorithms [1], and hence an estimate of the member reliability from Eq.(7).

4.2 Failure of Structural Systems

4.2.1 General remarks. Most structures are complex systems which are generally thought of as being made up of members, elements or components connected together in a particular way. The sub-division of a structure into these parts is a necessary stage in the process of undertaking any stress analysis. It generally requires considerable simplification and idealisation of the structure. It is assumed here that this can be done without introducing any significant bias into the computed structural behaviour, but this requires considerable skill and is part of

the art, as opposed to science, of engineering. The detailed modelling of all parts of a large structural system is generally not feasible and the strengthening effects of nominally non-structural components are often neglected or considerably simplified.

In a normal deterministic analysis, it is common to make conservative assumptions with respect to the structural modelling, but in a reliability assessment the aim should be for a model which on average will be unbiased, with probabilistic allowances being made for possible positive or negative deviations.

In the following, it is assumed that a structure can be idealised in such a way that there is only a finite number of possible locations or nodes at which local failure can occur. For example, in a bracing member of a fixed jacket platform under the action of axial loads and bending moments, plasticity is likely to develop either at the ends or towards the centre, giving three possible failure locations. If the material properties and cross-sectional dimensions do not vary significantly along the length of the member, then the exact location at which the maximum load effects occur does not need to be known a priori.

4.2.2 Statically determinate systems. For statically determinate structures, the occurrence of failure at any node (i.e. the local load effect becoming equal to the structural resistance at the node) will cause failure of the structure. In practice, the form of failure will depend on the load-displacement characteristics of the component which fails (Fig.4) and whether the load or loads can be rapidly reduced. In general, the latter is not possible and complete collapse or very large deformations of the structure will occur.

If there are m possible nodes and the failure of node i is denoted E_i and occurs when $g_i(\bar{x}) \leq 0$, then the reliability, or probability of survival of the system is given by

$$P_s = 1 - P(\bigcup_{i=1}^{m} E_i) \quad (11)$$

$$= P(\bigcap_{i=1}^{m} S_i) \quad (12)$$

where S_i is the survival event.
The corresponding system failure probability is

$$P_f = 1 - P_s = P(\bigcup_{i=1}^{m} E_i) \quad (13)$$

This is illustrated in Fig. 5. The central shaded area (safe region) represents the event corresponding to the intersection of all the survival events S_i, and gives all the pairs of values (u_i, u_j) for which the structure remains safe. The failure region corresponds to the union of all the failure events E_i. Further, it should be noted that Fig. 5 shows only two dimensions in an n-dimensional space so the lengths of the vectors β, as shown, are not necessarily representative of their respective magnitudes.

Since the structure fails if failure occurs at any of the nodes, such a statically determinate structure is referred to as a 'series' system.

The probability P_f may be determined in a number of ways:

- by numerical integration of $f_{\bar{X}}(\bar{x})$ over the safe or failure regions
- by simulation
- by computing simple bounds on P_f
- by linearising the various failure boundaries at their design points and computing bounds on P_f
- by linearising the various failure boundaries at their design points and using the multi-variate normal distribution function
- various other approaches.

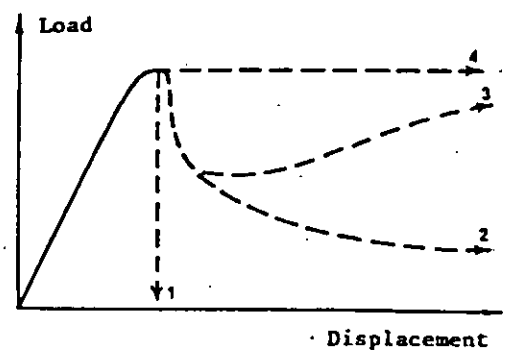

Figure 4: Typical load-displacement curves

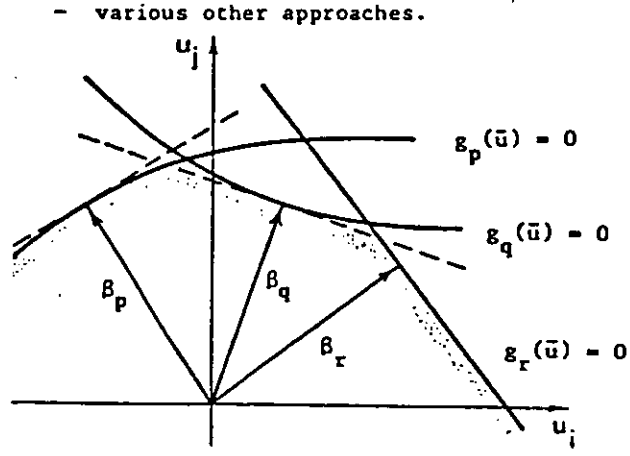

Figure 5: Multiple failure modes

The first two approaches tend to be impractical for small failure probabilities. Simple bounds on P_f have been known for a long time (see e.g.[10]) but are generally too wide to be of practical value, unless one failure mode dominates, i.e.

$$\max_k[P(E_i)] \le P(\bigcup_{i=1}^{m} E_i) \le \min[(\sum_{i=1}^{m} P(E_i),1] \quad (14)$$

The above are first-order bounds involving the probabilities of single events of a linear combination of these quantities. Better (second-order) bounds can be established by including the probabilities of the pairwise intersections $(E_p \quad E_q)$, as follows

$$P(E_1) + \sum_{i=2}^{m} \max[P(E_i) - \sum_{j=1}^{i-1} P(E_i \cap E_j),0]$$

$$\le P(\bigcup_{i=1}^{m} E_i) \le \quad (15)$$

$$\sum_{i=1}^{m} P(E_i) - \sum_{i=2}^{m} \max[P(E_i \cap E_j)]$$

In the area of structural engineering, these bounds are often referred to as Ditlevsen bounds [11]. Contributions to this field have also been made by others, as reviewed in [12]. The magnitude of the bounds given by (15) depend on the order in which the pairwise intersections are taken and how they are evaluated. Use may be made of the bi-variate normal distribution function:

$$P(E_p \cap E_q) = \Phi_2(-\beta_p,-\beta_q;\rho_{pq}) \quad (16)$$

This implies the linearisation of the failure functions at the design point, as shown in Fig. 5. The correlation coefficient ρ_{pq} can be shown to be the cosine of the angle between the normals to the linearised failure boundaries (i.e. the lines joining the design points to the origin).

The Ditlevsen bounds are a considerable improvement over the simple bounds (Eq.14), but tend to be rather wide for high positive correlations. More general bounds on the failure probability of series systems including higher order intersections are also available [13], but the computational requirements tend to increase dramatically.

An exception to this is the second-order non-linear lower bound on P_f developed by Ramachandran and reported in [14]. This is an approximation to the third-order linear bound and makes use of the following lower bound on the tri-variate normal integral

$$P(E_p \cap E_q \cap E_r) > \frac{P(E_p \cap E_q)\ P(E_p \cap E_r)}{P(E_p)} \quad (17)$$

for $\rho_{qr} > \rho_{pq}\rho_{pr}$ (18)

Finally, it should be noted that a good approximation to the m-dimensional normal distribution function $\Phi_m(\bar{\beta},\bar{\rho})$ has been developed by Hohenbichler [15] which allows the evaluation of P_s in Eq.(11) directly for the linearised failure functions, but not without considerable computational effort.

4.2.3 Statically indeterminate structures. Most structures are not statically determinate mainly for practical reasons and because redundancy provides some tolerance against accidental damage - e.g. minor ship collisions. In consequence, however, such structures are more difficult to analyse and in practice there may be a very large number of possible failure paths, i.e. node failure sequences.

In this section, some of the recent developments in systems reliability theory are reviewed, but the implications for offshore structures are not discussed until Section 5.

The probability of failure P_f for a statically determinate structure, defined in Eq.(13), is also the probability of an initial local failure occurring in a statically indeterminate structure, the bounds on which can be determined by any of the methods discussed above. P_f, as so defined, is therefore an upper bound on the overall system failure. Furthermore, any upper bound on P_f is also an upper bound to the system failure probability. [Whether computed lower bounds on P_f are also upper bounds on the system failure probability depends on particular circumstances]. However, as is well known, the economic benefits of a statically indeterminate structure derive from the fact that when considering the partial or overall collapse conditions, a significant degree of plasticity (i.e. local nodal 'failures') and load-effect re-distribution can be permitted. Thus, the use of P_f, as defined in Eq.(13), as an estimate of the overall system failure probability is likely to be uneconomic.

It is clear, therefore, that for the realistic assessment of a structure's system reliability it is necessary to perform either a non-linear structural analysis, or a sequence of step-wise linear analyses or a collapse load analysis.

Brittle behaviour. The most conservative assumption that can be made about a structural element's (node's) load-carrying capacity is that it behaves linearly up to some

maximum load and then ruptures. This idealised behaviour is a good approximation to curve 1 in Fig. 4 and is often referred to as 'brittle' behaviour. In practice, it is perhaps not as uncommon as might be expected; for example, as when two members are connected with a low strength weld. In this case, the weld metal may experience large strains and be acceptably ductile, but the connected structural member will show only a small elongation/rotation before sudden failure.

In the case of idealised elastic-brittle behaviour, the structure will behave elastically under increasing load until the first node fails, when a re-distribution of the member forces must take place. At this load, the structure may be in equilibrium or a further node or nodes may fail. If, at any value of imposed load, there remains a suitable load path to support the load, the structure can be defined as being safe at that load, irrespective of the number of node failures that have occurred.

In theory, the reliability of such a structure can be evaluated by determining all the possible sequences of node failures (link set sequences) which can take place while still leaving the structure in a state where it can carry the applied load or loads. The probability of survival of the structure is then the sum of the probabilities that each link set sequence will occur, since each link set sequence is a mutually exclusive event [16], [17]. For most structures, however, the number of link set sequences is immense and it is necessary to compute a lower bound on the system reliability (upper bound on the system failure probability) by considering only a reasonably small number of link set sequences. Some examples are given in [17]. This topic will not be considered further here.

Ductile behaviour. A very large percentage of routine deterministic structural designs and analyses are undertaken assuming either perfectly elastic or idealised elastic/pefectly-plastic material or member behaviour. The latter is a good approximation to curve 4 in Fig. 4, which is not infrequently seen in practice.

For structures whose elements or nodes can be assumed to follow perfectly-plastic behaviour, the system failure probability P_x can be written in the same form as Eq.(13) as

$$P_x = P(\bigcup_{i=1}^{m} E_i) \qquad (19)$$

where, in this case, the event E_i is the occurrence of ith plastic collapse mechanism, there being a total of m. As before, the event E_i can be expressed as $M_i = g_i(\bar{X}) \leq 0$, where $\bar{X}$ is a vector of basic variables such as material properties, dimensions and loads and with

$$P(E_i) = P(g_i(\bar{X}) \leq 0) \qquad (20)$$

Eq.(19) may be evaluated using the same techniques as described in Section 3.4.2. The individual plastic collapse mechanisms can be thought of as forming a series system, the occurrence of any one event E_i causing system failure. In practice, the various safety margins M_i are likely to be highly correlated, because not only are they each influenced by the uncertainties in the loads but also the various mechanisms may have one or more plastic hinges or yielded sections in common.

In the deterministic application of the theorems of plasticity, it is only necessary to search for the mechanism corresponding to the lowest value of the load factor, using trial and error, linear programming, the combination of elementary mechanisms or some other approach. However, when the loads and material properties are random variables, none of the feasible mechanisms can be excluded and each contributes to the overall system failure probability P_x.

If Eq.(19) is correctly evaluated by one of the methods described above, and none of the potential failure modes is neglected, then the value obtained for P_x is exact. If any of the mechanisms are excluded, the probability P_x' obtained from

$$P_x' = P(\bigcup_{i=1}^{k} E_i) \qquad k < m \qquad (21)$$

will clearly be a lower bound on P_x (upper bound on the system reliability P_s).

Since for most practical structures, including typical offshore structures, the number of potential plastic collapse mechanisms is very large, the practical problem to be solved is the identification of the most significant ones; i.e. to find k modes (k<<m) which when considered as a set contribute most to P_x. A number of solutions to this problem have been proposed.

Moses, Gorman and Rashedi [18-22] have developed an 'incremental load method' which uses a stepwise linear-elastic analysis of the structure under incremented loads and successive nodal failures, with the singularity of the stiffness matrix as the criterion for the development of a mechanism. This approach was originally proposed for use with the mean values of the structural properties [18], but a criterion involving the change in member 'utilisation ratios' (a deterministic measure) [21] provides a method for identifying at least some of the most important

mechanisms. This approach has also been used with 'brittle' and 'semi-ductile' members [22].

Murotsu et al. [23] and later Thoft-Christensen and Sorensen [24] have used the above incremental load approach but have used a probabilistic criterion for identifying the most likely failure mechanisms - namely, by identifying the node with the lowest reliability index at each stage of the incremental procedure. This has been termed the 'β-unzipping method'. A probabilistic criterion has also been proposed for truncating the search process.

More recently, Melchers and Tang [25] have developed the 'truncated enumeration method' for systematically identifying all the possible node failure sequences and then eliminating those that are unimportant.

All the above methods, however, are somewhat arbitrary in their approach to the problem and rely on the use of elastic analysis to derive the plastic collapse equations. Nevertheless, judged by their application to a number of example structures, they are all moderately successful. However, there is no easy way of telling how they would perform on reasonably realistic structures.

The most rigorous approach is undoubtedly that due to Ditlevsen and Bjerager [26,17], as described below.

Identification of significant collapse mechanisms. Ditlevsen and Bjerager's approach to identifying the most significant mechanisms can be summarised as follows for the case of a statically indeterminate frame loaded by ℓ point loads of random magnitude $\bar{Q}$ and in which bending effects are dominant.
If the frame is n degrees statically indeterminate and has m critical sections where plastic hinges could form, then by the lower bound (safe) theorem of plasticity [27], if the bending moments S_k at the m possible hinge positions can be chosen so that

$$|S_k| < R_k \qquad k = 1,2,\ldots,m \qquad (22)$$

and are such that the structure is in equilibrium with the applied loads, then plastic collapse will not occur. R_k is the random plastic moment capacity of the kth critical section, and is assumed here to have the same magnitude for both positive and negative rotations.

If n of the m unknown bending moments are selected as the indeterminacies and are assigned values $\bar{z} = \{z_1, z_2, \ldots, z_n\}$, then from considerations of equilibrium alone

$$S_k = z_k \qquad k = 1,2,\ldots,n \qquad (23)$$

and

$$S_{n+k} = \sum_{j=1}^{\ell} a_{k,j} Q_j + \sum_{i=1}^{n} b_{k,i} z_i \qquad (24)$$

$$k = 1,2,\ldots,m-n$$

where the influence coefficients $a_{k,j}$ and $b_{k,i}$ depend on the structural dimensions (assumed to be deterministic).

By considering all possible values for the values $\bar{z}$ $(\bar{z} \in R^n)$ satisfying Eq.(22), the system reliability may be expressed as

$$\begin{aligned} P_s &= 1 - P_x \\ &= P(\bigcup_{\bar{z} \in R^n} [((z_1<R_1)\cap(z_2<R_2)\cap\ldots\cap(z_n<R_n))\cap \\ &\quad ((\sum_{j=1}^{\ell} a_{n+1,j} Q_j + \sum_{i=1}^{n} b_{n+1,i} z_i) < R_{n+1})\cap \\ &\quad \ldots\ldots\cap \\ &\quad (\sum_{j=1}^{\ell} a_{m,j} Q_j + \sum_{i=1}^{n} b_{m,i} z_i) < R_m)]) \end{aligned} \qquad (25)$$

but, in general, this expression is very difficult to evaluate. If, however, only one set of values $\bar{z}$ is selected, as opposed to the infinite number of sets implied by Eq.(25), then it is clear that

$$\begin{aligned} P_s > P[&((z_1<R_1)\cap(z_2<R_2)\cap\ldots\cap(z_n<R_n))\cap \\ &((\sum_{j=1}^{\ell} a_{n+1,j} Q_j + \sum_{i=1}^{n} b_{n+1,i} z_i) < R_{n+1})\cap \\ &\ldots\ldots\cap \\ &(\sum_{j=1}^{\ell} a_{m,j} Q_j + \sum_{i=1}^{n} b_{m,i} z_i) < R_m)] \end{aligned} \qquad (26)$$

i.e. the right hand side of (26) is a lower bound on the system reliability P_s (upper bound on P_x).

If 'lower bound safety margins' M_k are now defined such that

$$M_k = R_k - z_k \qquad k = 1,2,\ldots,n \qquad (27)$$

and

$$M_k = R_k - \sum_{j=1}^{\ell} a_{k,j} Q_j + \sum_{i=1}^{n} b_{k,i} z_i$$

$$k = 1,2,\ldots,m-n \qquad (28)$$

inequality (26) becomes

$$P_s > P[(M_1>0)\cap\ldots\cap(M_m>0)] \qquad (29)$$

or, identically,

$$P_s > P[\min_{k=1}^{m} M_k > 0] \qquad (30)$$

The right hand side of inequality (27) can be seen to be the same as the right hand side of Eq.(12) and can be evaluated by any of the methods suggested for series systems. The best (highest) lower bound on the system reliability can now be found by selecting the arbitrary values of the n moments $\bar{z}$ so as to maximise the right hand side of (28). For normally distributed random varables and deterministic dimensions, this is a linear optimisation problem and can be solved by linear programming [17]. For more general conditions, non-linear programming is required.

The safety margin M_k for the critical section k which contributes most to the failure probability after optimisation of the $\bar{z}$ values has taken place is referred to as the dominant safety margin [17]. It should also be noted that different lower bounds to P_s will be found depending on which of the m critical sections are initially selected to have the n values $\bar{z}$ assigned to them.

The primary purpose of the present discussion, however, is not to examine ways for calculating a lower bound on P_s but rather an upper bound, as defined by Eq.(21).

From the theorem of virtual work

$$\sum_{j=1}^{\ell} Q_j\delta_j = \sum_{k=1}^{m} S_k\vartheta_k \qquad (31)$$

where $\delta_j=f(\vartheta)$, ϑ are a set of compatible displacements and hinge rotations, and Q_j, S_k are a set of forces and moments which are in equilibrium. [Note: Some of the values of ϑ_k in Eq.(31) may be zero, since the summation on the left hand side of Eq.(31) is taken over all m possible hinge positions]. From the upper bound theorem of plasticity, the collapse load for the structure will be less than or equal to $\bar{Q}$ when $S_k = R_k$, k = 1,m and where R_k is the plastic moment capacity of critical section k. Eq.(31) can then be re-written as an 'upper bound safety margin' as

$$M_u = \sum_{k=1}^{m} R_k\vartheta_k - \sum_{j=1}^{\ell} Q_j\delta_j \qquad (32)$$

and the probability of failure in this collapse mode is given by

$$P_f = P(M_u \le 0) \qquad (33)$$

Since the lower bound safety margins correspond to a set of forces and moments that are in equilibrium, the lower bound safety margins can be used to generate a set of upper bound safety margins by multiplying the terms in Eqs.(27 and 28) by a compatible set of rotations and displacements and forming a linear combination of these terms, i.e.

$$M_u = \sum_{k=1}^{m} \gamma_k M_k \qquad (34)$$

where γ_k are non-negative coefficients which are chosen so that M_u is independent of the arbitrary vector of indeterminate bending moments $\bar{z}$. The result is an upper bound safety margin corresponding to a particular plastic mechanism. As shown by Ditlevsen and Bjerager [26] a set of n dominant lower bound safety margins can be used to generate an upper bound safety margin. In general, there will q (> n+1) lower bound safety margins and a maximum of κ corresponding upper bound safety margins (where κ is the number of ways of selecting a subset of size n from a set of size q). These are then used to determine a close upper bound on the system reliability using Eq.(21). The closeness of this bound depends on how many upper safety margins are included and whether all the important ones are identified. However, because the upper bound safety margins are formed from a combination of dominant lower safety bound safety margins, it is reasonable to assume that this might be the case. Furthermore, it is clear that this approach is to be preferred to any of the incremental load procedures for determining collapse mechanisms, at least from a theoretical point of view.

The procedure may be modified to take into account axial stresses in place of bending stresses, or, with more computational effort, axial and bending effects together.

This seemingly complex procedure has been used on a number of example structures [17] and has been shown to provide a workable basis. The most complex resembles a simple offshore jacket and is shown in Fig. 6. 41 upper bound safety margins were identified with reliability indices ranging from 2.30 to 7.79, leading to a system reliability index of 1.91. In practice this reliability would be too small, but the example is of importance as it illustrates the range of applicability of these methods. However, the amount of computational effort may still be very considerable for large structures.

Intermediate behaviour. In practice, the moment-rotation or load-elongation characteristics of a structural member differ from the idealised brittle or ductile

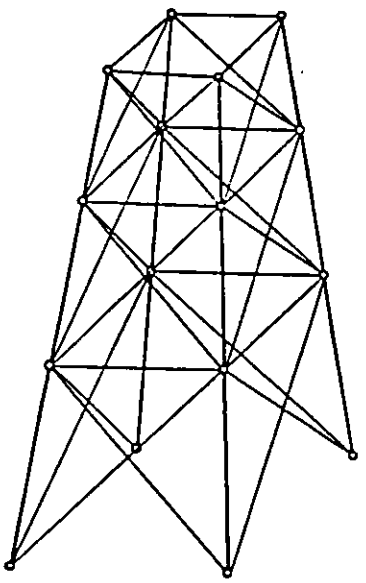

Figure 6: Simplified jacket structure (from [17])

behaviour analysed above. However, if the idealised behaviour is a reasonable good approximation to the true behaviour, no further action is required. On the other hand, if the members exhibit the characteristics shown by curves 2 or 3 in Fig. 4, some modified approach is required. To date, the problems of undertaking a reliability analysis of a structure exhibiting this type of member behaviour have not been thoroughly investigated, although some studies have been carried out, e.g. [22,25].
However, for structural members which exhibit sufficient ductility, it is clear that the reliability can be approximated either by assuming 'brittle' member behaviour with strengths corresponding to the first peaks of the load-deflection (or moment-rotation) curves or by assuming idealised plastic behaviour with plasticity occurring at some reduced load level.

5. APPLICATION TO OFFSHORE STRUCTURES

5.1 General remarks

Before discussing applications, it is necessary to review the assumptions that have been made in the preceding sections. The theory that has been outlined applies to structural systems in which the material properties, dimensions and loads can be modelled as random variables and in which the criteria governing first-passage failure can be written as a function of these quantities, the failure function. Furthermore, it is implicitly assumed that material properties are time-invariant, but with no restrictions on distribution type.

Most loads, however, vary with time, but no mention of this has been made in the above analysis. For the case of a single time-varying load acting together with any number of permanent loads (or other actions), the analysis can be undertaken by using the probability distribution of the maximum extreme load in the reference period t for which the reliability is being determined. See, for example [1].

For the case of more than one independent time-varying load, the problem is considerably more difficult. If the structure remains in a linear-elastic state, one solution is to derive an approximation to the probability distribution of the combined load-effect in the member of interest from the individual stochastic processes which characterise the separate loads. See, for example, [28]. However, if the probability of structural collapse is being determined, the assumption of linear elastic behaviour does not apply and this approach cannot be followed. In this case, the load combination rule developed by Bosshard [29] using the Borges-Castanheta load model can be used. However, this requires 2(r-1) different load combinations to be analysed, where r is the number of time-varying loads. Nevertheless, this approach can be integrated with the system reliability methods described above.

A further important consideration in connnection with deep water offshore structures is the contribution of the dynamic component of the response to the environmental loading (i.e. that component of the response due to inertia effects). For compliant structures and for dynamically sensitive fixed platforms, the dynamic behaviour of the structure is likely to have a profound influence on reliability in respect of both first-passage and damage-accumulation (e.g. fatigue) failure modes. The latter is discused separately in Section 6.

5.2 The present position

Offshore structures are complex structural systems which even under deterministic assumptions are costly to analyse. In view of this and the recent nature of many developments in structural reliability theory, particularly systems theory, it is not surprising that progress in the applications of these theories has been relatively modest. The applications that have been undertaken which relate to offshore structures fall into four broad categories:

- studies undertaken as part of the development of systems theory, e.g. [20,17].
- studies involving first member failure of dynamically sensitive systems, [30].

- studies of offshore components treated as isolated elements, e.g. [31].
- studies undertaken as part of code development work, e.g. [32].

As far as the author is aware, no comprehensive integrated analyses have yet been undertaken, but the time is approaching when this will certainly be attempted. Wide-ranging work was undertaken by the Conoco/ABS Rule Case Committee for the Design of Tension Leg Platforms [33], but this work did not extend to full system reliability studies.

Some further comments on two of the above items are appropriate. The work contained in [17] and [20] has already been discussed.

5.2.1 Reliability of dynamically sensitive systems. Many offshore structures fall into the category of being dynamically sensitive and there is generally no substitute for undertaking a full dynamic analysis either in the time-domain or in the frequency domain. However, either approach adds considerable complexity to the problem of undertaking a reliability assessment.

Working in the time-domain allows a step-by-step analysis of the structure to a simulated (or actual) wave force time-history to be conducted, using a realistic wave theory and damping. However, this tends to be very expensive in computer time and it is currently not feasible to contemplate Monte-Carlo trials involving a series of time-domain analyses. The basic problem with this approach within a reliability analysis for first-passage failure is the difficulty of choosing a suitable 'extreme' time-history. The Level 2 (reliability index) methods discussed in Section 3 are theoretically incompatible with the time-history approach, for the analysis of first-passage problems, since the extremes of the time-history are random. This is not true in the case of fatigue because the damage is cumulative and is closely related to the underlying parameters of the time-history, and not the extreme values.

Most reliability analyses of complex dynamically sensitive offshore structures have been conducted in the frequency domain [2,3,30]. The various models and calculation steps that are required in this process are shown in summary in Fig. 7. and have been discussed in some detail in [2]. Together they define the safety margin M given by Eq.(5). Using such an approach, it is possible to compute the reliability of each member of a jacket structure acting as part of a complex structural system subject to random wave and current excitation, in a completely rigorous way. In this approach, information also becomes available about the relative importance of the various design

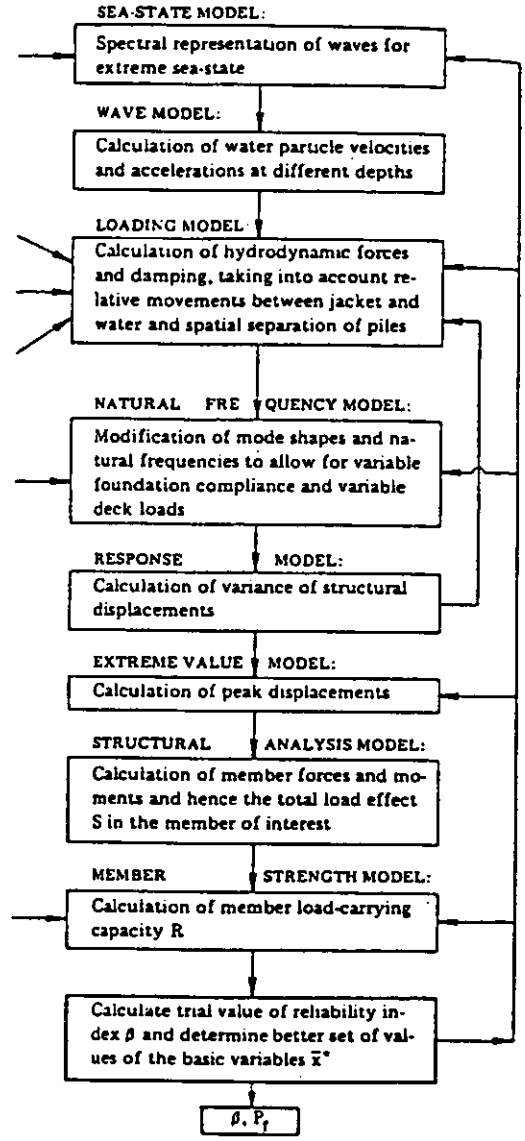

Figure 7: Models required for dynamic reliability analysis, from [1]

variables with respect to the probability of failure (i.e. the failure probability's sensitivity to uncertainty). This is illustrated in Fig. 8 for a six-leg jacket platform in 150m water depth. By including the failure criterion for the particular structural member and all aspects of the hydrodynamic loading and structural response within the reliability calculations, it is possible to see which source of uncertainty has the greatest effect on the failure probability. Frequently, the variability in extreme significant wave height or the associated wind speed, is found to be of greatest importance. In [30], it was shown that the fabrication tolerance for ring-stiffened cylindrical members could be reduced for certain forms of

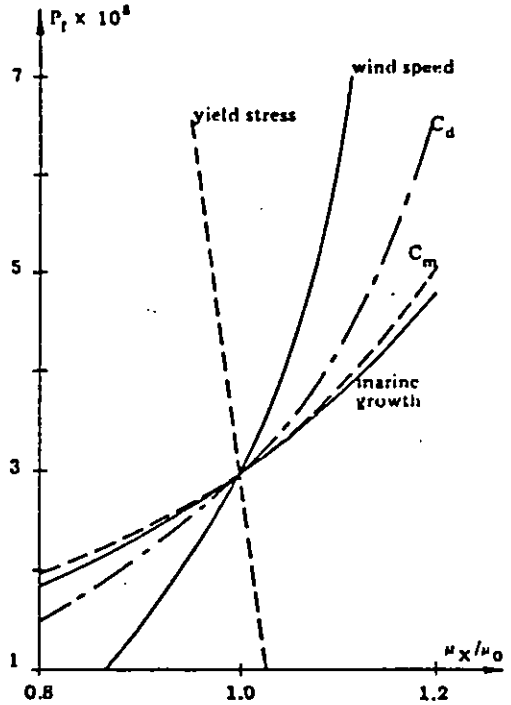

Figure 8: Sensitivity of failure probability to changes in mean values of parameters [1]

construction without having a significant effect on the reliability.

The probability that no member will fail during any reference period t (e.g. the design life) can be computed using the methods for series systems discussed in Section 4. However, as a single member failure does not generally cause system failure, this probability will in general be a conservative lower bound to the true system reliability.

To the author's knowledge, no work has yet been done, except in the area of earthquake engineering, to examine the reliability of dynamically sensitive structures to progressive collapse. This would require a classification of member failure modes into those that result in some permanent loss of system strength (e.g. buckling followed by low residual member strength) and those associated only with an increment of irreversible displacement (e.g. local yielding of a stocky member, or pile overload). The consequences of the peak dynamic response of a dynamically sensitive structure momentarily exceeding the response level which causes local 'failure' in one member are clearly very different in these two cases. In both cases the consequences are probably less severe than when the loads are applied statically and with long duration.

For dynamically sensitive structures with reasonably small degrees of statical indeterminacy, a 'brittle' buckling failure of one member during a particular extreme sea-state would generally lead to increased dynamic response with an increased risk of other local failures occurring. For highly redundant systems, or for systems with members or nodes behaving in a reasonably ductile manner, the initial 'failure' would not increase the probability of further failures. The latter would occur only at some higher value of peak structural response at a reduced level of probability.

5.2.2 Reliability of structual components.
A number of studies have been undertaken to examine the reliability of various structural components considered in isolation from the structure of which they are part. The main reason for this type of approach is that until recently the inclusion of the structural and response analysis of the complete system, as indicated by Fig. 7, within the failure function has often seemed too difficult. However, if the simpler approach is used, it is difficult to model the load effects acting on the component in a realistic way or to include the effect of combined loading from different sources. Nevertheless, such studies are of use as preliminary investigations to examine the significance of various design changes to the components concerned - for example, geometric tolerances.

This approach has also been used in the assessment of partial coefficients for use in design codes, but the results of such studies need to be used with care, as discussed later.

5.3 Buckling of stiffened cylinders

Stiffened and unstiffened cylindrical members are used extensively in all types of offshore steel structures and their behaviour has been widely researched over the last five years [34]. This has led to a set of semi-empirical deterministic design equations for different configurations. Although some of the design formulae for both ring- and stringer-stiffened cylinders have been improved as a result of the work of the Conoco/ABS Rule Case Committee, as reported by Faulkner [33], comparison of test data with the strength predictions of these mathematical models still shows considerable scatter (Fig. 9). Faulkner reports a coefficient of variation of 11.5% for the ratio of actual to predicted strength using the most recent design formulae for stringer-stiffened shells.

As mentioned in 4.1, the inability of strength formulae to predict the true load-carrying capacity of a structural component is referred to as strength model uncertainty. It can have a significant influence on reliability predictions. With coefficients of

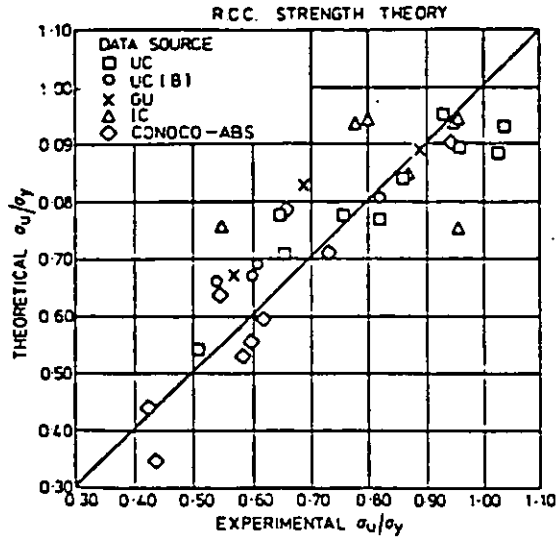

Figure 9: Predictions of compression strength for stringer-stiffened cylinders [33]

variation for the model uncertainty as large as 12%, or larger, this is likely to be the most important factor governing the predicted strength, since the coefficients of variation of basic material and geometric parameters are likely to be much less than this in practice (yield strength, typically 6-8%; dimensions, typically 1-2%).

The main reason for the large model uncertainties in structural components of this type is the fact that initial imperfections are not included explicitly in the strength formulae, an allowance being made only through an empirical 'knock-down' factor. Recent work [35] using non-linear finite element (FE) modelling of stringer-stiffened shells has shown that the peak load-carrying capacity of such components failing in a local buckling mode depends not only on the magnitude of the initial geometrical imperfections but also on the initial deformed shape, as is to be expected. Although residual stresses due to welding also have an influence, comparisons of FE results with those of laboratory model tests are typically very good and much better than the semi-empirical design formulae. This leads to the conclusion that, if possible, use should be made of finite element methods in shell reliability studies.

Even with modern computers, the direct use of non-linear finite element analysis within reliability programs is not currently feasible, so an indirect approach has to be used. Fig. 10 shows the results of using a mathematical model developed by multiple regression analysis from a extensive set of finite element calculations covering a wide range of shell geometries. This work is being carried out by Mr. M. Chryssanthopoulos at Imperial

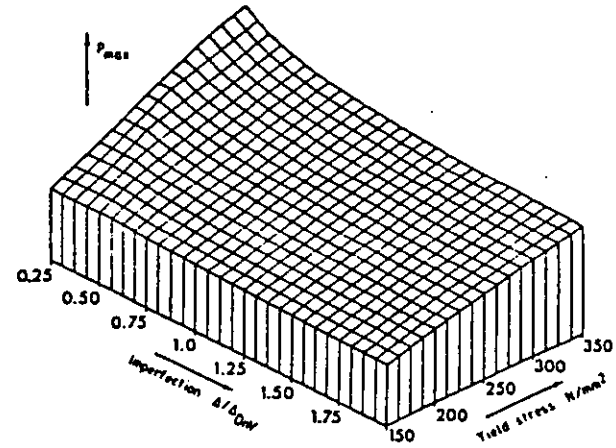

Figure 10: Response surface from regression analysis

College. The graph shows the response surface (in this case the axial load-carrying capacity of a cylindrical shell with 20 longitudinal stiffeners) for variations in material yield stress and magnitude of initial imperfection.

Once the regression model has been obtained, it may be used in place of the direct FE analysis within a structural reliability calculation. As might be expected, however, the use of a regression model based on data from a wide range parametric study may be rather inaccurate for some parameter combinations. In general, it will be necessary to supplement the general model with a few additional FE analyses in the region of interest. This is shown in Fig. 11. Although the resulting response surface becomes more irregular, it is well defined in the region of the 'design point'; i.e. with those combinations of parameters at which failure is most likely to occur. This work is continuing and will be reported at a later date.

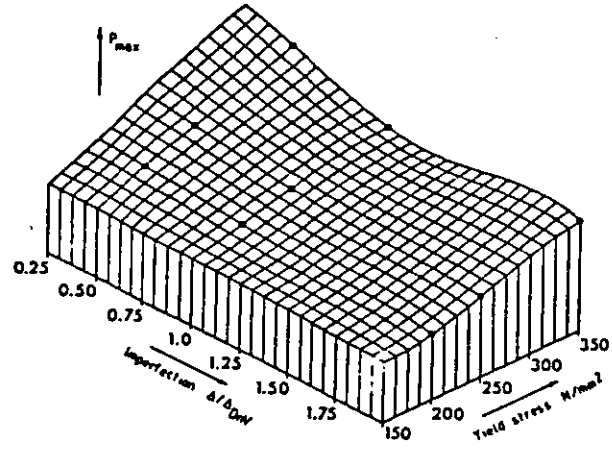

Figure 11: Modified response surface

6. FATIGUE RELIABILITY

6.1 General remarks

Fatigue is possibly the most frequently observed process leading to the failure of components of steel offshore structures. It is also one in which there is very large uncertainty in the number of cycles of load which will actually cause failure, and is therefore a natural candidate for the use of reliability methods.

During the last few years considerable developments have taken place in the understanding of fatigue crack growth, in quantifying the statistical scatter in fracture toughness and fatigue crack growth data, e.g. [36], in developing probabilistic models for fatigue damage, e.g. [37,38,39], and in developing methods suitable for the fatigue reliability assessment of offshore structures, e.g. [40]. Many of these techniques are now being applied but they have yet to be integrated with the systems reliability concepts discussed above. This is an important area for future research.

6.2 Fatigue models for reliability analysis

In the earlier sections of this paper it was seen that the usual deterministic models for assessing structural strength could be converted for use as failure functions for a probabilistic reliability assessment by transforming them into the form of Eq.(5), provided that appropriate account is taken of the inherent uncertainties in the model itself. The same technique can be applied to failure by fatigue, but the time dependent nature of the loading and the damage accumulation must be correctly taken into account.

6.2.1 The S-N approach. The most commonly used model for fatigue behaviour under constant amplitude loading is the linear logarithmic model

$$N_i S_i^m = K \tag{35}$$

where N_i is the number of cycles to failure, S_i is the range of applied stress and m and K are selected constants. Hence, failure can be assumed to occur when the number of cycles n is such that the damage D defined by

$$D = nS_i^m/K \tag{36}$$

exceeds unity. Furthermore, using Miner's rule it is also assumed that the damage D_1 due to one cycle of stress range S_i is given by

$$D_1 = S_i^m/K \tag{37}$$

and that the total damage is

$$D = (1/K) \sum_{i=1}^{N} S_i^m \tag{38}$$

For normal design purposes, m and K are chosen to give a curve which is a conservative lower bound on the relevant test data or a selected number of standard deviations below the mean curve.

However, for the purposes of reliability assessment, m and K need to be considered as random variables to allow for the large scatter in the number of cycles to failure experienced in practice; and a model uncertainty needs to be introduced into Eq.(38) to allow for the fact that the Miner's rule summation is subject to uncertainty.

The safety margin M, Eq.(37), may now be expressed as

$$M_1 = N - N_o \tag{39}$$

where N is the number of cycles of stress to cause failure and N_o is the required number to achieve a given design life, or as

$$M_2 = (\text{actual life}) - (\text{required life}) = L_a - L_r \tag{40}$$

The reliability P_s is thus

$$P_s = 1 - P(M_1 \le 0) = 1 - P(m_2 \le 0) \tag{41}$$

Provided M can be expressed in a suitable form, the techniques of Section 4.1 can be used to evaluate P_s.

For example, as shown by Wirsching [38], Manners [39] and others, for cases where the long-term distribution of wave height can be assumed to have a two-parameter Weibull distribution

$$F_H(h) = 1 - \exp(-(h/c)^\alpha) \tag{42}$$

and when the stress spectrum is narrow-banded and the structure is dynamically insensitive so that the stress range is closely related to wave height by

$$S = bH \tag{43}$$

where b is a constant, then from Eq.(37) the damage caused by one cycle of random wave height H is given by

$$D_1 = (bH)^m/K \tag{44}$$

and the expected damage per cycle is

$$E[D_1] = \int_0^\infty (bh)^m/K \; f_H(h)\, dh$$

$$= (bc)^m/K\ \Gamma(1+m/\alpha) \qquad (45)$$

where $\Gamma(.)$ is the gamma function.
If n is then the number of stress cycles per year and X_m is the model uncertainty in the operation of Miner's rule, the actual life will be

$$L_a = \frac{X_m K}{n(bc)^m \Gamma(1+m/\alpha)} \qquad (46)$$

and the safety margin is

$$M = \frac{X_m K}{n(bc)^m \Gamma(1+m/\alpha)} - L_r \qquad (47)$$

It should be noted that Eq.(45) gives the expected damage per cycle. However, because there are a large number of cycles per year, the scatter in the amount of damage from cycle to cycle does not affect the annual damage rate which can be obtained by multiplying the expected damage per cycle by the number of cycles per year. The uncertainty in the safety margin M results from uncertainties in the parameters X_m, K, and m. In other words, the expected damage per cycle given by Eq.(45) is a conditional expectation.

No restrictions are placed on the distributions of X_m, K and m above; but if it is assumed that they are lognormal, then a new safety margin M' may be defined as

$$M' = \frac{X_m K}{L_r n(bc)^m \Gamma(1+m/\alpha)} \qquad (48)$$

where M' is also a lognormal variable so that

$$P_s = 1 - P(M' \le 1) = 1 - P(\log M' \le 0) \qquad (49)$$

Analytical solutions can also be obtained for other long term distributions of wave height [39].

Spectral methods. In the case of dynamically sensitive offshore structures, some of the above assumptions do not apply and it is necessary to resort to spectral analysis of the structure's response to wave loading. The approach that can be followed is somewhat similar to that described in Fig. 7 for peak response analysis, but includes a fatigue failure criterion in place of an ultimate load failure criterion. It requires a number of simplifying assumptions, such as narrow band response. Such analyses have been carried out by Karadeniz et al. [41] and are still a fruitful area for further development.

6.2.2 The fracture mechanics approach.

Fatigue failure generally occurs as the result of a fatigue crack growing from some initial surface defect usually in a weld zone.

Assuming that the crack growth is governed by linear elastic fracture mechanics, Paris's law gives

$$\frac{da}{dN} = C(\Delta K)^m \qquad (50)$$

where $\frac{da}{dn}$ is the rate of crack growth

a is the current crack size,
ΔK is the range of stress intensity factor at the crack tip, and C and m are crack growth parameters.

In normal fracture mechanics calculations C and m are taken to be constants but in a reliability assessment they need to be treated as random variables, to account for the associated uncertainty. The range of stress intensity factor, ΔK, is related to the normalised stress intensity factor, Y, by

$$\Delta K = Y\Delta\sigma\sqrt{(\pi a)} \qquad (51)$$

where $\Delta\sigma$ is the range of applied stress, giving

$$\frac{da}{dn} = C(Y\Delta\sigma\sqrt{(\pi a)})^m \qquad (52)$$

Y depends on local geometry and the nature of the stress field. For the special conditions where both Y and the stress range $\Delta\sigma$ are independent of a, Eq.(52) gives

$$\int_{a_o}^{a_N} a^{-m/2} da = \int_o^N CY^m(\Delta\sigma)^m \pi^{m/2} dn \qquad (53)$$

which for $m \neq 2$ yields

$$a_N = W^{2/(2-m)} \qquad (54)$$

$$\text{where } W = a_o^{(2-m)/2} + \frac{2-m}{2} CY^m(\Delta\sigma)^m \pi^{m/2} N \qquad (55)$$

a_o is the initial defect size
and a_N is the crack size after N cycles of applied stress. Hence a_N may be expressed as

$$a_N = f(a_o, Y, C, m, \overline{\Delta\sigma}, \bar{N}) \qquad (56)$$

which is of the same form as Eq.(2). If the performance requirement is that the crack should not exceed a length a_f, the reliability, or the probability that this condition will hold true, for a period of exposure t is

$$P_s = P((a_f - a_N) > 0) \qquad (57)$$

This may be evaluated by the methods discussed in Section 4.1. Failure criteria other than the final crack size may also be considered by suitable modification of the governing equations; for example, the probability that, in any desired reference period, the component will not fail by unstable crack growth.

In practice, however, many of the conditions mentioned above do not hold true and Eq.(54) cannot be used. Instead, the crack growth must be determined from a cycle by cycle (or cycle block) application of the various stress ranges and this must be included within the reliability calculations. For example, components of offshore structures are subjected to a number of widely differing stress ranges, or more generally a stress spectrum; and the normalised stress intensity factor Y is not independent of crack size a but must be expressed as

$$Y = Y(a) \tag{58}$$

with the result that a_N cannot be expressed in closed form. A further constraint is that crack growth does not occur, and hence Eq.(52) does not apply, below a threshold value of ΔK, ΔK_{th}. The conditions which govern the magnitude of ΔK_{th} are not fully understood and the latter is therefore subject to considerable uncertainty. This gives rise to a more complex analysis procedure than indicated above.

When the location of the initial defect is known, the stress intensity factor Y(a) can be obtained by finite element modelling of the crack tip region and the relationship between Y and a obtained. In practice, this relationship should be considered to subject to model uncertainty, particularly when the exact location and orientation of any initial defect is not known, which is invariably the case.

For most offshore structures, the fatigue stress spectrum is likely to be associated with considerable uncertainty, mainly as a result of the uncertainties in the response of the structure to the fluid loading. Since the main contribution to the fatigue damage is from large numbers of medium waves and not from the less frequently occurring extreme waves, the prediction of the sea-state statistics is not the major source of uncertainty. The major source of uncertainty is in the transfer functions from sea-state to hydrodynamic forces, from hydrodynamic forces to dynamic response, from dynamic response to member force and from member force to stress intensity. The major uncertainties in loading can thus be expressed in terms of uncertainty in the magnitude of the various stress ranges rather than in terms of the numbers of cycles of loading.

If at a particular position in an offshore structure the numbers of cycles N_i of each of a complete set of discretised stress ranges $\Delta\sigma_i$ can be determined by analysing the dynamic response of the structure to the various sea states that will be experienced over the design life, the reliability of that particular component against fatigue failure may be determined. In general, it will be necessary to assume that the dynamic behaviour of the structure is not affected by the presence of the fatigue crack.

<u>Example: Fatigue growth leading to fracture.</u> If failure of the structural component is assumed to occur when the crack tip opening displacement (CTOD), δ, is greater than some critical material toughness, δ_{crit}, the safety margin is defined by

$$M = \delta_{crit} - \delta \tag{59}$$

where δ is given by [42] as

$$\delta = aY^2(a)\frac{2\pi\sigma_y}{E}\cdot\frac{\sigma_{pa} + \sigma_y}{\sigma_y} - 0.25 \tag{60}$$

and where a is the current crack size after fatigue growth
e_y is the yield stress of the material in which the crack tip is located
E is Young's modulus
e_{pa} is the peak applied stress

For a particular weld geometry and for given values of the fracture mechanics parameters C and m, the final crack size, a, can be taken as a deterministic function of the initial defect size, a_o, and the stress history. Hence, the safety margin M may be expressed as a deterministic function g(.) of eight parameters, the set of $\bar{N}$ stress ranges $\overline{\Delta\sigma}$ characterising the loading, and the model uncertainty affecting the magnitude of the computed stress range X_m, i.e.

$$M = g(\delta_{crit}, a_o, \Delta K_{th}, \sigma y, E, \sigma_{pa}, C, m, \bar{N}, \overline{\Delta\sigma}, X_m) \tag{61}$$

The probability $P(M \leq 0)$ can be obtained using the methods of Section 4.1, modelling the parameters in Eq.(61) as random variables as appropriate.

Some typical results shown in Fig. 12 illustrate how the probability of failure changes for different initial defect sizes. The probability depends on the parameters of the distributions of the various random variables in Eq.(61). Fig. 12 shows results for three different mean values of material toughness (e.g. corresponding to the crack tip being in the parent plate, the weld metal

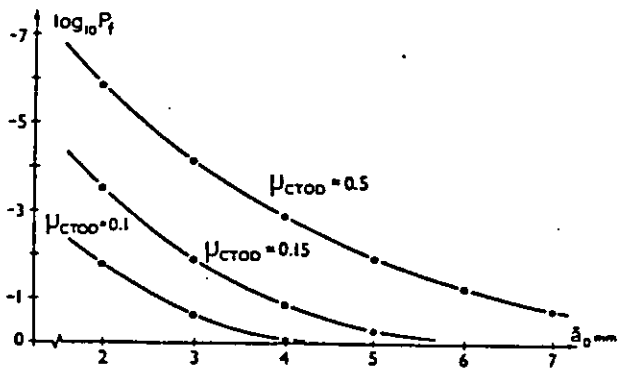

Figure 12: Effect of defect size on probability of fracture

and the heat affected zone).

It should be noted that the probability of failure depends on the peak stress σ_{pa}, which is generally not a constant. In this case, the overall probability of fracture has to be determined from a knowledge of the distribution of peak stress and the formulation of reliability problem is more complex than described above.

7. RELIABILITY AND DECISION

The value of a reliabilty assessment is that it enables uncertainties to be handled in a rational and organised way. In particular, reliability assessment enables the sensitivity of the reliability to the various design variables to be determined. Questions such as: are there sufficient data?, which components of the structure have the greatest influence on the safety of the structure?, etc., can then be answered, and appropriate practical measures taken.

It is sometimes stated that the application of reliability theory requires more data than are currently available. The aim of any reliability assessment, however, should be to improve decision making, and to make best use of both data and other information. This does not mean that the acquisition of more data is often not a desirable objective, but in this case it will be true irrespective of approach adopted. It is simply that probabilistic methods highlight those areas where data are lacking, whereas deterministic approaches effective ignore the problem.

Doubts are also sometines expressed about the validity of probabilistic reliability methods. In general, however, the competing deterministic design procedures are just a special case of more general probabilistic methods, and so this line of reasoning is invalid. This does not mean that the results of any reliability assessment should not be interpreted with caution, just as with any deterministic assessment. It is found not infrequently that the underlying engineering assumptions, whilst satisfactory for a conservative deterministic assessment of safety are inappropriate for an unbiased reliability assessment - for example, the neglect of the beneficial effects of membrane action on the collapse strength of restrained slabs.

In the opinion of the author, it is very important that the reliability analysis of a structure is not undertaken in an automated, mechanical fashion, but in an iterative way, incorporating the judgement of the various design specialists. Having undertaken a preliminary analysis, the question should be asked: Do these results, in terms of relative reliabilities, relative sensitivities, indicated courses of action, etc., correspond with the prior judgements of the associated specialists? And if not, why not? At this stage it may be necessary to revise some of the mathematical models of the structure and some of the probabilistic models of the design variables, or to get more data, and then to re-run the analyses. If the results are essentially the same, it may be necessary for some of the specialists to amend their judgements. This process should continue until all concerned with the project are satisfied that the best decision has been reached. The decision will never be 'perfect', since some information will always be missing, but will be the best that is possible at the time the decision has to be made, and within the time available.

The procedure that has been outlined above is a dynamic procedure involving all those involved in the structural design process. It differs from the more formalised statistical decision theory approach as described by Bea [43] which could be used as part of this approach. As mentioned at the beginning of this paper, the reliability of a structure may need to be determined at different stages in a structure's life and to answer essentially different decision questions.

Much effort has been put into the use of reliability methods for determining suitable partial factors for use in deterministic design procedures, e.g. [32]. This work will need to continue, as it is likely that deterministic procedures will remain common place for normal structures for the foreseeable future. However, for complex unique structures, particularly those with large failure consequences, the direct use of reliability analysis may be a practical alternative which will show economic benefits.

8. FUTURE RESEARCH

A number of topics requiring research have been mentioned above and a comprehensive list will not be given here. However, three subjects deserve special mention. First, the extension of methods of system reliability analysis to dynamically sensitive structures; second, the use of systems reliability methods in connection with failure by fatigue; and last, the development of methods for determining optimal strategies for defect assessment. Progress is needed in all these areas.

ACKNOWLEDGEMENTS

Many people have now contributed to the growing subject of structural reliability theory and it is not possible to mention all by name. The references given below comprise only a small fraction of the useful literature.

Thanks are due to Mr M Chryssanthopoulos for contributing Figures 10 and 11, and to the Marine Technology Directorate of the U.K. Science and Engineering Research Council (SERC) for financial support for some of the current and previous work referred to.

REFERENCES

[1] THOFT-CHRISTENSEN, P. and BAKER, M.J., Structural reliability theory and its applications. Springer-Verlag, 1982.

[2] BAKER, M.J., Reliability of offshore structures. NATO ASI on Reliability Theory and Application in Structural and Soil Mechanics, 1982. Martinus Nijhoff, 1983, 613-642.

[3] KARADENIZ, H., VAN MANEN, S. and VROUWENVELDER, A., Probabilistic reliability analysis for the fatigue limit state of gravity and jacket-type structures. 3rd BOSS Conference, Cambridge, Mass. USA, 1982.

[4] HASOFER, A.M. and LIND, N.C., Exact and invariant second-moment code format. J. Eng. Mech. Div., ASCE, Vol.100, No.EM1, Feb.1974.

[5] BAKER, M.J. and WYATT, T.A., Methods of reliability analysis for jacket platforms. 2nd BOSS Conference, London, 1979.

[6] TVEDT, L., Two second order approximations to the failure probability. Veritas Report RDIV/20-004-83.

[7] BREITUNG, K., Asymptotic approximations for multinormal integrals. J. Eng.Mech. Div.,ASCE, Vol 110, No.EM3, March 1984.

[8] ROSENBLATT, M., Remarks on a multivariate transformation. Annals of Mathematical Statistics, Vol. 23, 1952.

[9] HOHENBICHLER,M. and RACKWITZ, R., Nonnormal dependent vectors in structural safety. J. Eng. Mech. Div., ASCE, Vol. 107, No.EM6, Dec. 1981.

[10] CORNELL, C.A., Bounds on the reliability of structural systems. J. Str. Div., ASCE, Vol.93, NO.ST1, Feb. 1967.

[11] DITLEVSEN, O., Narrow reliability bounds for structural systems. J. Eng. Mech. Div., ASCE, Vol.', No.4, Dec. 1979.

[12] RAMACHANDRAN, K., System bounds - a critical study. Civil Engineering Systems, Vol.1, 1984.

[13] HOHENBICHLER, M. and RACKWITZ, R., First-order concepts in system reliability. Structural Safety, Vol. 1, No.3, 1983.

[14] RAMACHANDRAN, K. and BAKER, M.J., New reliability bounds for series systems. Proc. 4th International Conference on Structural Safety and Reliability, Kobe, 1985 (to be published).

[15] HOHENBICHLER, M., An approximation to the multi-variate normal distribution. Proc. EUROMECH 155 Reliability Theory of Structural Engineering Systems, DIALOG 6-82, Danish Engineering Acadamy, Lyngby, 1982.

[16] BARLOW, R.E. and PROSCHAN, F., Statistical theory of reliability and life testing. Holt, Rinehard and Winston, 1975.

[17] BJERAGER, P., Reliability analysis of structural systems. Report No.183, Department of Structural Engineering, Technical University of Denmark, 1984.

[18] MOSES, F., Structural system reliability and optimization. Computers and Structures, Vol.7, 1977.

[19] GORMAN, M.R., Reliability of structural systems. Report CE 79-2, Dept. Civil Eng., Case Western Reserve University, Cleveland, Ohio, 1979.

[20] MOSES, F. and STAHL, B., Reliability analysis format for offshore structures. Paper OTC 3046, Offshore Technology Conference, Houston, Texas, May 1978.

[21] MOSES, F., System reliability developments in structural engineering. Structural Safety, Vol.1, No.1, Sept 1982.

[22] RASHEDI, M.R. and MOSES, F., Studies on reliability of structural systems. Report No.R83-3, Dept. Civil Eng., Case Western Reserve Univ., Cleveland, Ohio, Dec. 1983.

[23] MUROTSU, Y., OKADA, H., NIWA, K. and MIWA, S., Reliability analysis of truss structures by using matrix method. J. Mech. Design, ASME, Vol. 102, No. 4, Oct. 1980.

[24] THOFT-CHRISTENSEN, P. and SORENSEN,J.D. Calculation of failure probabilities of ductile structures by the β-unzipping method. Report 8208, Instituttet for Bygningsteknik, Aalborg University Centre, Denmark, 1982.

[25] MELCHERS, R.E. and TANG, L.K., Dominant failure modes in stochastic structural systems. Structural Safety, Vol. 2, No. 2, Oct. 1984.

[26] DITLEVSEN, O. and BJERAGER, P., Reliability of highly redundant plastic structures, J. Eng. Mech Div., ASCE, Vol. 110, May 1984.

[27] NEAL, B.G., The plastic methods of structural analysis. Chapman Hall, 1956.

[28] MADSEN, H.O., Load models and load combinations. Thesis. Technical University of Denmark, Lyngby, Feb. 1979.

[29] BOSSHARD, W., Informal communication to the Joint Committee on Structural Safety, 1976.

[30] BAKER, M.J. and RAMACHANDRAN, K., Reliability analysis as a tool in the design of fixed offshore platforms. The Integrity of Offshore Structures, Proc. 2nd Int. Symp., Glasgow, 1981. Applied Science Publishers, 1981, 135-153.

[31] DAS, P.K., FRIEZE, P.A. and FAULKNER, D., Structural reliability modelling of stiffened components of floating structures. Structural Safety, Vol. 2, No. 1, May 1984.

[32] MOSES, F., Utilizing a reliability-based API RP2A Format. Final report, API PRAC Project 82-22, API, Nov. 1983.

[33] FAULKNER, D., Development of a code for the structural design of compliant deep water platforms. IESS/RINA Joint Meeting, Glasgow, Dec. 1984, Paper No.1461.

[34] KENNY, J.P. and PARTNERS, Buckling of Offshore Structures. Granada Publishing, 1984.

[35] AGELIDIS, N., Collapse of stringer-stiffened cylinders, PhD Thesis, Imperial College of Science and Technology, University of London, Sept. 1984.

[36] JOHNSTON, G. O., Statistical scatter in fracture toughness and fatigue crack growth data. Probabilistic Fracture Mechanics and Fatigue Methods. ASTM STP 798, 1983.

[37] MADSEN, H.O., Deterministic and probabilistic models for damage accumulation due to time-varying loading. DIALOG 5-82, Engineering Acadamy of Denmark, 1982.

[38] WIRSCHING, P.H., Fatigue damage assessment models for offshore structures. Earthquake Behavior and Safety of Oil and Gas Storage Facilities, PVP-Vol 77, ASME, 1983.

[39] MANNERS, W., Reliability analysis of the fatigue resistance of offshore structures. PhD Thesis. Imperial College of Science and Technology, University of London, Sept. 1983.

[40] WIRSCHING, P.H., Probability-based fatigue design criteria for offshore structures. API-PRAC Project No. 81-15, Final Report, Jan. 1983.

[41] KARADENIZ, H., VROUWENVELDER, A. and BOUMA, A.C., Stochastic fatigue analysis of jacket type offshore structures. NATO ASI on Reliability Theory and Application in Structural and Soil Mechanics, 1982. Martinus Nijhoff, 1983, 613-642.

[42] SMITH, I.J., PISARSKI, J.H. ELLIS, N. and PRESCOTT, N.J., A defect assessment method, using finite elements and the CTOD design curve, for use in the design of offshore welded structures. Paper 21, International Conference on Welded Structures, Welding Institute, London, Nov. 1982.

[43] BEA, R.G., HONG, S.T. and MITCHELL, J.S., Decision analysis approach to offshore platform design. Jounal of Structural Engineering, Vol. 110, No.1, ASCE, Jan. 1984

RULE BASED AND RELIABILITY BASED DESIGN FOR SHIP STRUCTURES

By

DOUGLAS FAULKNER

© 1978 The Royal Institution of Naval Architects

Toward a Unified Approach to Ship Structural Safety

by D. Faulkner* (Fellow) and J. A. Sadden** (Member)

Read in London at a meeting of the Royal Institution of Naval Architects on April 12, 1978. Professor J. B. Caldwell, B. Eng., Ph.D. (Vice-President) in the Chair.

SUMMARY: A completely rational approach to primary safety is not possible at present. But two closely linked semi-probabilistic or second-moment methods which take some account of the statistical nature of the loading and collapse (or limit state) strengths may now commend themselves to designers, owners, and certifying authorities. These are the partial safety factor approach (closest to the conventional safety factor) and the safety index. The paper outlines them both but concentrates on the second concept which is applied to five naval designs varying in length from 91-154 m and for which measured strain records exist. The safety indices are compared with those for pseudo-merchant ships designed by rule and having the same lengths, and then with those for larger merchant ships having a length range 158-328 m.

If one accepts the traditional design approach, in which comparisons are made with the best 'successful' past designs, then the heterogeneous nature of the results suggests two closely linked findings. First, that there are some obvious shortcomings in the conventional use of the safety factor. Secondly, notwithstanding the possible fatigue implications, it does seem that there is appreciable scope for better weight and cost compromises in both naval and merchant designs, and especially for the larger merchant ships.

It would, perhaps, be premature to accept by itself either of these hybrid approaches to design until further statistical data are available. Nevertheless, the authors advocate a design policy which adopts one or both of these approaches in parallel with current methods. This would assist in building up a data bank of relevant information for future use. But even more important, it could provide a stimulus to rational design thinking and to the necessary further research.

NOTATION

B, D	beam, depth
C_b, C_w	block, waterplane coefficient
$\{C\}$	capability (strength) matrix
$\{D\}$	demand (load) matrix
$\bar{C}_u$	mean capability
C_k, D_k	characteristic capability, demand
$D_e \bar{D}_e$	modal, mean values of extreme total demand
$f(x), F(x)$	probability density, distribution function
F	scalar safety factor
H_e	effective wave height
L_w, L	length on waterline, BP
M	C − D margin
M_w, M_s	wave, still water moment
p_f, p_o	probability of failure, lower bound
s, S	plastic shape factor, standard deviation
Z, Z_e	elastic, effective section modulus
v_c, v_d, v_m	c.o.v. capability, demand, margin
α	$1 + \zeta$, correction parameters for mean values
β_f	safety index
$\gamma_c \cdot \gamma_d \cdot \gamma_s$	partial safety factor components
γ_o	$\gamma_c \gamma_d \gamma_s$ overall partial safety factor
$\sigma_y, \bar{\sigma}_y$	nominal, mean yield strength
σ_s, σ_w	still water, wave bending stress
$\sigma_{te}, \bar{D}_e$	$\sigma_{we} + \sigma_s$ mean total extreme bending stress
σ_u, σ_{eu}	average, effective ultimate compression strength of critical gross-panel
θ	$\bar{C}_u/\bar{D}_e$ central safety factor
$\zeta_c, \zeta_s, \zeta_y$	systematic errors in compression strength, section effects, yield strength
$\rho_{c,d}$	correlation coefficient between C and D
ϕ	σ_u/σ_y compression strength parameter

* Professor of Naval Architecture and Ocean Engineering, The University of Glasgow.

** Constructor, Ship Department, MOD(PE), Bath.

1. SAFETY CONCEPTS

1.1 Classification and Recent History

It is convenient to classify safety concepts according to their degree of sophistication.

1.1.1 Level-1 or first moment methods:

Essentially the 'safety factor' approach in which a single valued worst 'demand' design or working load D_d is related to similarly dimensioned failure or limit 'capability' (resistance or strength) of the structure C_u by a scalar quantity F

$$C_u \geq F\, D_d \qquad (1)$$

The strengths C_u can in principle allow for interactive failure modes, but the concept of a single unique scalar safety factor F is then illusory[1]. It should also be noted that it is usual for nominal or minimum specified material and section properties to be used. Perhaps the most common example is the allowable stress basis for design where a limiting strength is assumed when the stress reaches the yield stress, but this approach has been criticised recently[1,2] as it has in the past[3].

1.1.2 Level-2 or second moment methods:

These assume that the load and strengths are independent random variables which can be represented by two distribution curves as shown in Fig. 1, and that it is possible to

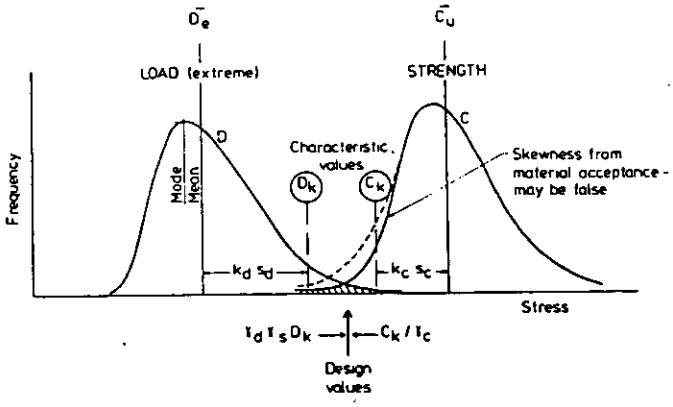

Fig. 1 Second moment characteristics of ships load and strength frequencies

estimate their second moment statistical properties of the means and standard deviations; they are therefore sometimes referred to as first-order probabilistic methods. These methods are hybrid in the sense that they combine conventional determinism with statistics. The best known is the partial safety factor concept which is now in use in Civil Engineering [4,5], in concrete codes [6,7] and for masonry, timber and in certain offshore codes. But historically it was preceded in discussion at least by the safety index concept [8,9] which has recently been applied to ships [10]. Both these semi-probabilistic methods will be described more fully later.

1.1.3 Level-3 fully statistical approach:

Probabilities of failure are assessed and 'added' using purely statistical data and methods—indeed it is the only method which can rigorously combine all loads and modes of failure. Symbolically from Fig. 1

$$p_f = p\{C < D\} \tag{2}$$

Or, if f(x) are the probability density or frequency distributions and F(x) the distribution functions of two uncorrelated random strength and load variables C and D, and both are time invariant, it follows [9] that

$$\left.\begin{aligned} p_f &= \int_0^\infty \{F_C(x)\}\, f_D(x)\, dx, \text{ or} \\ &= 1 - \int_0^\infty \{F_D(x)\}\, f_C(x)\, dx \end{aligned}\right\} \tag{3}$$

Pugsley [11] and Freudenthal [12] were the pioneers for aircraft and civil structures more than three decades go.

In truth the expression for p_f as required to be applied to ships to solve the lifetime extreme value problem is somewhat more complicated than above and order statistics are required. Moreover, the transfer functions to convert wave excitation into loads and then into load-effect vectors are much more complex than land-based structures or even aircraft. Thus it took nearly two decades from the first major breakthrough [13], and much encouragement [14,15] and intermediate research [16,17,18], before any attempt was made to apply the theory to ships on a life-time basis [19,20].

It is interesting that the chronological sequence in these three approaches is levels-1, 3 and 2. The current interest in second-moment methods reflects the formidable difficulties in the most rational level-3 approach (see Ref. 20 and discussion) which, when coupled with the insufficiency of data, has compelled designers and code-drafters to adopt a less sophisticated level [21]. Whether this proves only to be an intermediate stage remains to be seen as most structures fail by 'blunders' [20,22]. Moreover it is vital for design procedures to be as simple as possible as well as being soundly based. They must also be in a format which is easily modified as our knowledge improves.

Meanwhile, research continues on level-3 approaches [23,24] which seems to confirm earlier findings [10,25,26] that large ships in particular are several orders safer than smaller ships and seem to offer plenty of scope for weight and cost saving. This research has also included a statistical dynamics approach after Bolotin [27] which claims [28] to take account of quality of production and time dependent effects such as deterioration in strength due to corrosion or cracking.

1.2 Limit State Conditions

This paper is concerned with primary hull girder strength in the traditional vertical bending mode [29,30] which most directly affects structural weight and ship safety. The limit state considered is based on upper deck compression strength in the sagging condition because

(a) decks are usually considerably lighter than bottom structures and hence are more susceptible to buckling failure

(b) distance to the neutral axis is greatest

(c) sagging wave-induced bending moments are likely to be higher than hogging values [31] and this is amply supported by measurements at sea [32], by static balance calculations [33] and by model tests [34].

These conclusions point clearly to failure in a sagging condition as the most likely mode of hull-girder collapse [35,36].

Fatigue is not considered in the paper, partly for reasons of space, but also because fatigue failures are most unlikely to be catastrophic. Also, it has been argued [1,35] that, allowing steel weight to be determined by fatigue considerations, for example by placing limits on nominal hull bending stresses as is done at present, will not usually lead to the most efficient designs. That is, designs which are adequately safe but costing least.

This may seem to challenge the recent very elegant defence of the classification society approach [37], and there is no denying that as section modulus requirements slowly reduce then fatigue design per se requires closer attention. Also good structural details and quality control, to avoid or minimise fatigue damage, are themselves costly. But recent experience in box-girder bridges, and indeed in ships [38,39], confirms that the same attention to the detailed design of joints is also required and justified to enable the structure to achieve its required inelastic buckling strength. Naval experience is relevant. In spite of generally appreciably higher stress levels and lower structural weight than in merchant ships, naval designs are relatively fatigue free, which justifies the emphasis on inelastic buckling collapse in design.

2. CONVENTIONAL APPROACHES

The effective wave concept and the statutory rule section modulus approach are linked in the sense that they are explicitly and implicitly based on the static wave balance principle coupled with still water loads. Neither approach makes any allowance for different mission profiles or ship motion effects (excepting Ref. 26 which presents a simplified statistical analysis with a generalised wave load and some allowance for dynamic flexibility). Nominal scantlings and material properties are used throughout, and it is usually assumed that instability failure must be designed out of existence (irrespective of the structural loading index) by placing restrictions on cross section slendernesses.

2.1 Effective Wave Height

This can be defined as the height of a trochoidal wave of ship length which by a conventional static balance calculation (Smith effect excluded) gives the same wave bending moment as the maximum that a ship would experience during her lifetime. To this of course is added the worst still water loads.

Chapter 6 of Ref. 40 provides a very good historical review of the traditional static wave balance and the various approximations for wave and still water moments, etc. The White-Biles[41] $H_e = L_w/20$, used initially (1893) by the RN, was universally adopted for well over half a century as a basis for comparing primary structures from ship to ship. Nevertheless, as early as 1910 wave measurements[42] suggested the $L_w/20$ wave would over-estimate wave bending for long ships as compared with short ones. Cornish's data in fact suggested a design wave height to give a more uniform probability which was proportional to $\sqrt{L_w}$. But, instead of responding rationally to this more up to date data naval architects, with their customary mystique, compensated for the inadequacies of the $L_w/20$ wave by using it with Tobin's 'allowable stress' $\sqrt[3]{L_w}$ (ton/in², ft).

About the time of World War II the US Navy finally adopted the $1{\cdot}1\sqrt{L_w}$ wave, and classification societies eventually followed suit in the 1960s. However, the US Navy soon moved on to the rather more severe wave[43]:

$$\left.\begin{aligned} H_e &= 34 \sin(\pi L_w/1100) \text{ ft} \\ &= 34 \text{ ft for } L_w > 550 \text{ ft} \end{aligned}\right\} \quad (4)$$

A similar extreme design wave based on North Atlantic weather ship data was advocated by the senior author for RN frigate designs in the middle 1960s as an extreme lifetime wave:

$$\left.\begin{aligned} H_e &= 5\, L^{0{\cdot}3} \text{ ft} \\ &= 2{\cdot}2\, L^{0{\cdot}3} \text{ m} \end{aligned}\right\} \quad (5)$$

and maximum strains measured so far at sea[32] seem to agree reasonably well with static stresses derived from Eq (5), as indicated for five frigate and destroyer designs in Tables I and II. For shorter naval designs an L/9 wave has been used[44] which is close to the L/7 theoretical stability limit. See also Fig. 2.

TABLE I: Particulars of certain naval frigates and destroyers designed in the 1950s and 60s

Design	L m	B m	C_b	Z deck m³
A	91·4	10·1	0·48	0·52
B	109·7	12·5	0·47	1·05
C	106·7	12·9	0·51	1·30
D(i)	109·7	12·5	0·50	1·96(ii)
E	153·9	16·5	0·49	3·74(iii)

Notes

(i) somewhat idealised in Ref. 20

(ii) assumes superstructure partially effective[45]; 1·12 m³ ignoring superstructure[20]

(iii) 01 deck—all other values are for 1 deck.

In advocating maximum effective wave heights Eqs (4) and (5) it was recognised that appreciably higher waves have been recorded by various authorities, including the Admiralty Ship Welding Committee[46] and Getz[47] who advocated a 15 m wave. Nevertheless, it was argued that for frigates and destroyers (and indeed for other low freeboard ships) increased wave heights do not necessarily produce larger bending moments[40].

By dimensional analysis it can be shown that excluding the Smith effect wave bending moments are given by

$$M_w = k\rho g B L^2 H_e\, f(C_w) \quad (6)$$

The $1{\cdot}1\sqrt{L}$ effective wave is very close to that derived from Eq (8) of Ref. 17 (same as Eq (6) above but with $f(C_w)$ simply equal to C_w) and lies above all the merchant ship results[49]

TABLE II: Naval Designs: theoretical and measured wave-induced and still water sagging stresses in the upper deck (N/mm²)

Designs	A	B	C	D	E
L/20	125	117	91	65(i)	114
$2{\cdot}2\, L^{0{\cdot}3}$	232	192	152	107(i)	148
maximum measured(ii)	184	137	110	66	147
extrapolation for 3000 days return period(iii)	219	170	128	81	167
σ_{we} = most probable extreme for 3×10^7 cycles(iii)	253	211	159	116(i)	155
σ_s = still water	−28	−33	−29	−11(i)	−11

Notes

(i) theoretical stresses assume superstructure partially effective[45]

(ii) measured up to 1969

(iii) corresponds to about 25 years life—see Section 3. 3. 1.

except for the two ships around 240 m length. See Fig. 2 which compares certain effective wave heights with those derived from SSC and RN maximum strain measurements extrapolated for total ship life.

Murray in 1955[48] was the first to advance a wave height which would be nearly tangential to L/20 for small ships but which would eventually diminish for long ships:

$$H_e = 80\, L e^{-L/900} (C_b + 0{\cdot}3)\, 10^{-3} \text{ feet} \quad (7)$$

The inclusion of C_b is curious and permeates rule requirements to this day. Assuming C_b increases linearly with length and has values 0·5 when L = 100 m and 0·8 when L = 310 m the lower curve in Fig. 2 is obtained from Eq (7). It would diminish for L greater than about 400 m.

It is interesting that the merchant ship strain measurements show that as ship length increases beyond 300 m, H_e appears to decrease. This has been observed elsewhere[10,26] and is now reflected in recent classification society section modulus rules[50] where the coefficient increases up to 300 m lengths

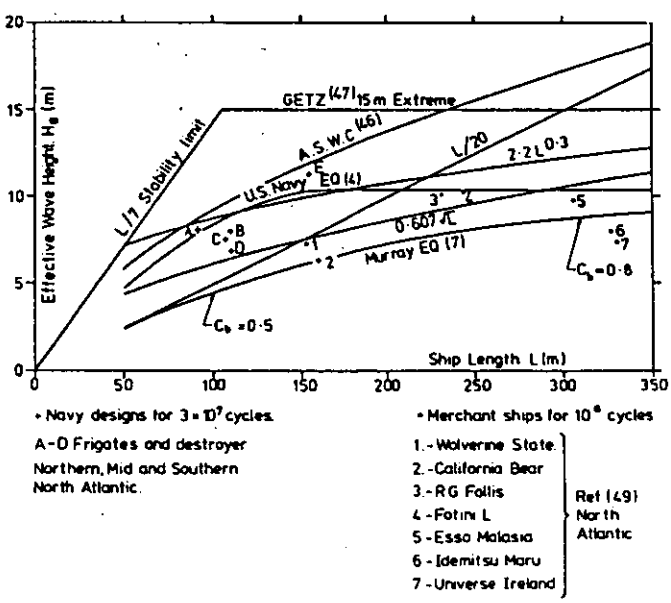

Fig. 2 Effective wave heights compared with derivations from measured strains

and decreases beyond 350 m. For intermediate ship lengths of 90-250 m or so an analysis of these rules using Eq (6) suggests that H_e is proportional to L^n where n varies from 0·25 to 0·3, which is similar in form to Eq (5).

2.2 Section Modulus Requirements

The major classification societies presently have an almost unified requirement that the hull midship section modulus should not be less than the greater of[50]:

$$\text{(a)} \quad Z = C_1 L^2 B(C_b + 0{\cdot}7)\ \text{cm}^3 \tag{8}$$

where C_1 is tabulated as a fraction of L which increases approximately as $L^{0{\cdot}25}$ till 300 m and decrease beyond 350 m

$$\text{or (b)} \quad Z = (M_w + M_s)/\sigma_c \tag{9}$$

where σ_c is the rule combined stress ($\sigma_w + \sigma_s$) which is either 161 N/mm² or 178 N/mm² depending on the ship type; and certain limits are placed on σ_w and σ_s for differing operating conditions and for sea service are σ_w = 98 N/mm² irrespective of ship type and σ_s = 63 and 80 N/mm².

Where higher tensile steel is used extensively in the main hull structure, Z as determined above, is to be multiplied by whichever is the greater factor of $245/\sigma_y$ (N/mm²) or 0·059 (L/D).

Formula (a) is clearly easier to evaluate than (b) and in general represents a greater value than (b) which will only be greater in a few extreme cases. Even the still water loading may be altered to leave (a) as the limiting case. The bracket term in (a) is purely empirical,* as is the L/D restriction on the use of higher strength steels.

Ship types have an influence on the application of these formulae generally as follows:

- Tankers—both deck and bottom usually at or close to lower limit
- Bulk Carriers—deck close to lower limit but bottom not so as presence of inner bottom prevents it
- General Carriers with two or more decks—possibly both deck and bottom close to lower limit
- Ro-Ro Ships—local strength requirements for wheel loads etc. mean that Z values for both deck and bottom may be up to 60% above minimum values
- Smaller and Special Craft—again local strength considerations will generally ensure Z is above the minimum (this may also apply to warships).

It should be noted that corrosion control may have an important influence on the actual Z values. Also, acceptance of service restrictions and hence lower values of M_w can be important for smaller vessels.

Naval ships do not of course have to comply with Classification Society rules. It is nevertheless interesting to compare Eq(8) with the section moduli for the five naval designs A-E previously considered as follows: 0·783, 1·440, 1·448, 1·482 and 4·151 m³ respectively. These are 11-50% greater than the actual values in Table I. Although correcting for yield stress would narrow this gap, buckling considerations would increase it even more, as we shall see later. Moreover, these naval ships are 15 to 25 years old (and are being compared with 1976 merchant ship rules), and only one class has experienced fatigue problems of any significance.

3. SECOND MOMENT METHODS

3.1 General Remarks

The merit of these methods is that they reply on four parameters only, the mean values and variances of load and strength.

These can be measured or assessed objectively, and adjusted for subjective uncertainties. No knowledge is required about the nature of the distributions in the tails, or even of truncation of one or both distributions (though this latter fact where known may be used when selecting safety parameters). All random uncertainties are treated uniformly, through the simplest measure—the coefficient of variation. Systematic errors affect the mean values.

With wave loading one may use either the mean value and variance

A of the 'long-term' probability distribution, that is, the probability of exceeding a certain load in any wave cycle selected at random from the total cycles expected to be experienced in the ship's life (see the approximate straight line distribution of Fig. 3), or

B of the probability distribution of the highest bending moment ever likely to be experienced in the ship's expected life (see Gaussian type distribution in Fig. 3).

Of course, two different sets of safety measures will result, the latter yielding appreciably smaller margins. For comparisons with other ships one has to be consistent in the choice, and in keeping with the statistical analyses in Refs. 10, 19 and 20 the latter approach B is adopted. This will give a more normal extreme load distribution with a relatively high mean value. Normal distributions are particularly convenient. They are completely defined by first- and second-order moments, and in particular random *errors* in measurements and assessments are often regarded as normally distributed sums of many elementary errors. The use of a normal distribution is also frequently justified by the central limit theorem.

We should also remind ourselves that semi-statistical methods cannot combine the risks of failure for independent modes of failure, or even provide a rigorous procedure for proportioning a structure against different load combinations and multi-modal failures. Consequently three main stages have to be distinguished:

(a) the definition of critical loads and load factors

(b) the transformation of load into load-effects, and the definition of load-effect factors

(c) the definition of critical resistances.

These three aspects are closely related. Decisions concerning one affect the others. The density of the load-effect vector[1] $\{Q\}$ will be general be given by a multi variate distribution

$$\{\vec{Q}\} = \{A\}\ \{\vec{D_i}\}$$

where $\{A\}$ is the transformation matrix and the loads $D_i = D_1, D_2, \ldots D_N$ are usually assumed to be normally distributed. This and other simplifying assumptions have been developed in a comprehensive engineering approach to structural safety by Ferry Borges[51].

Also, for a given structure there exist some stochastic dependencies (random but ordered) between external forces, internal forces, strength characteristics, failure mechanisms, etc., that generally diminish the expected frequency of failure[52]. Ang overcomes some of these difficulties with his extended reliability concept[53] which admits of some degree of ignorance through the introduction of a subjective deterministic judgment factor ν such that

$$p\ \{C < \nu D\} = p_0$$

where p_0 is a lower bound objective probability of failure. He later defined the judgment factor in probability terms[54], and the reader is referred to recent developments in North America[55,56] which have led to new codes[57,58].

Meanwhile, two rather simpler concepts will be outlined and

* C_w would be a more relevant parameter than C_b, but in either case the relation would be highly non-linear. Naval architects have a passion for linearising, but in this case it obscures the truth quite severely.

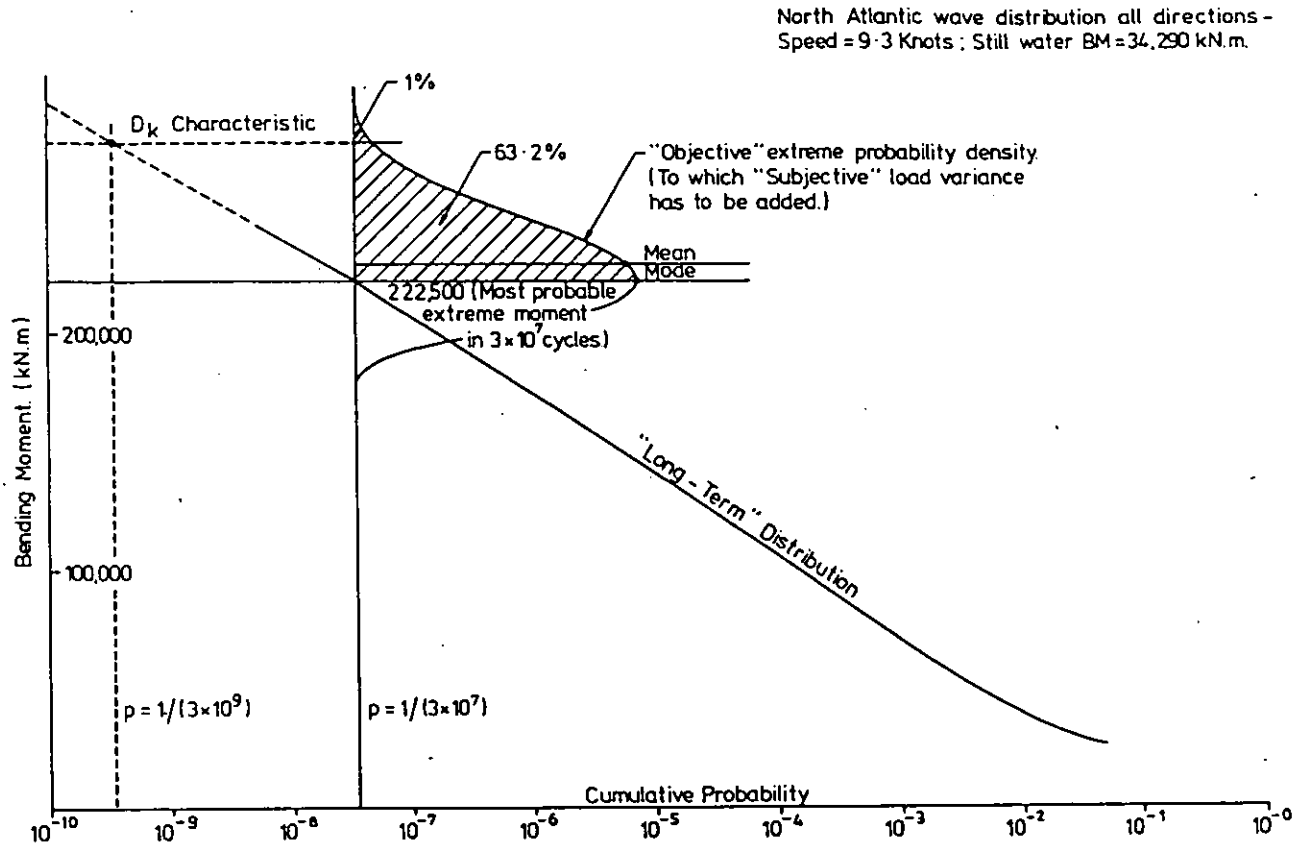

Fig. 3 Theoretical wave bending moment probabilities for naval design B

applied here. Greater emphasis will be placed on the Safety Index, although many may favour the Partial Safety Factor approach as being closer to the conventional safety or load factor. The statistical aspects of strength are considered in Section 3.2, whilst those for loading are considered in Section 3.3.

3.2 Partial Safety Factors

The relationship between the characteristic loads $\{D_k\}$ and strengths $\{C_k\}$ will generally be of the form

$$\{\vec{C}_{kj}\} \geq \gamma_c \gamma_s \left[\sum_{i=1}^{N} \gamma_{di} \{A\} \{\vec{D}_{ki}\} \right]_j \qquad (10)$$

where the subscripts i refer to the different loads factored by the correct transformation matrix to give the load-effect for load combination j in the n-dimensional space. The transforms of co-ordinates will be tensors if they are linear or homogeneous, although the approach to the failure surface may very often be anything but linear in ships[1]. Also, the stochastic nature of each load will be different and in some cases correlated, in others not.

However, even with mixed tensors of higher rank than two (rank one is a vector, rank zero is a scalar, and Kronecker's delta is an important high rank mixed tensor) it can be shown that the process of summation over the repeated index contracts the mixed tensor on transformation so that its rank is reduced by two. The outcome would appear to justify at most a simple vectorial approach to safety[1] if we restrict ourselves to a tri-variate failure surface approached linearly. Any varying directionality of the load strength vectors, for example due to loss of structural stiffness which causes load redistributions particularly at higher loads, can be allowed for by computer based incremental methods in which the transformation matrices are instantaneously assessed.

A formula of the type of Eq(10) should be written for each limit state and for each load combination applicable for the structure whose safety is being assessed. However, if we ignore interactive effects between different failure modes and adopt a weakest-link model for ultimate collapse of the ship's hull[20,30], and make use of the fact that p_f is dominated more by variability in load than in strength, no serious errors should arise. (This would not of course be the case with fracture modes of failure).

For illustration, therefore, we shall consider only one limit state (upper deck inelastic interframe buckling which is the most likely mode) and we shall approximate by assuming a linear relation between load and stress. We shall take stress to be a measure of all values of C and D. Then all transformations are tensors of zero rank (scalars) and Eq(10) reduces to

$$C_k/D_k = \gamma_c \gamma_d \gamma_s (C_d/D_d) \qquad (11)$$

where C_d and D_d are design values for strength and load, and are usually assumed to be equal when applying the partial safety factor concept. Then

$$C_k = \gamma_o D_k \qquad (12)$$

where $\gamma_o = \gamma_c \gamma_d \gamma_s$ is an overall partial safety factor*, and we recognise at once the similarity to the traditional safety factor F of Eq(1).

The subjective (requiring judgment) partial safety factors by which the objectively derived characteristic loads are multiplied to obtain the design loads are

* We should note that although the inequality in Eq (10) suggests that $\gamma_o \geq 1$, this will depend upon the choice of k_d and k_e for the characteristic loads and strengths, see Fig. 1. Refs. 20 and 25 showed that for 'successful' naval frigates γ_o could be less than unity, and we shall return to this point later.

γ_d which takes account of the variability of the applied loading and also the variation of behaviour from the idealised assumptions in design (both should be assessed separately)

γ_s which takes account of the nature of the structure (fail-safe, etc.) and the seriousness of failure in economic and loss of life terms.

The partial safety factor by which the characteristic strengths are divided to obtain the design strength is

γ_c which takes account of the differences between the strength of the material as determined by tests and the effect of possible local defects on full-scale strength.

The draft BS 449 for steel seems to be advocating 0·95 and 0·05 percentiles (k = 1·645 for normal distributions), and suggested values are in the range γ_d = 1·2 to 1·6, γ_c 1·1 or slightly less. British codes have not yet accepted γ_s but values in the range 1·0 to 1·2 might be expected. Thus γ_o values in the range 1·2 to 2·1 appear to be implied in the draft BS 449. It does not follow that similar values would be advisable in ships.

3.2.1 Ships strength model

The ISSC[4] in 1970 supported the use of the simple model related to the average compression strength σ_u in a critical gross-panel in the midship section

$$M_u = Z\,\sigma_u \tag{13}$$

Some of the shortcomings of this were discussed five years ago[20]. It would be inappropriate to review all these, but the following sections highlight some of the more important recent findings regarding the systematic and random errors in Eq (13), and offer alternative advice. We should note, however, that the simple linear relation (13) which relates failure stress to failure moment is a good example of an incorrect load-effect transformation mentioned in Section 3.1. It is only justified for convenience to avoid iteration and to enable direct use to be made of σ_u from compression tests or theory. We must therefore acknowledge and take some account of the approximation. A better 'effective width' type approximation might be

$$M_u = Z_e\,\sigma_{eu} \tag{14}$$

which certainly leads to a better estimate of edge stresses and strains at failure but although it can allow for some stress redistribution in the cross section (see for example Eq(14) Ref. 20) it does not allow for residuary strength after gross-panel failure[30,36,59]. It is non-linear, since both Z_e and σ_e vary with load, and it requires a complex iterative solution which is not justified by the fact that it is still approximate. Even more approximate but often used[10,40] is

$$M_u = Z\,\sigma_y \tag{15}$$

An upper limit may be provided by

$$M_p = Z\,\sigma_y s \tag{16}$$

where s is the fully plastic shape factor which for certain naval studies[61] was 1·28 and 1·48 (the latter would not be typical). The shakedown limit[62] has been proposed but challenged[63].

3.2.1.1 Systematic errors

The model chosen for the mean ultimate moment is

$$\overline{M}_u = \sigma_y Z\,\{(1 - \alpha_y + \alpha_y\alpha_c\phi)\,\alpha_y\}\,\alpha_s \tag{17}$$

where $\alpha = 1 + \zeta = 1 +$ systematic errors and $1 \geq \phi \geq \alpha_y/(1 + \alpha_y)$.

The term in curly brackets is the modification to the nominal average compression failure stress σ_u in a critical upper deck gross-panel[35,40] brought about by the systematic errors. For example, yield strength has three main systematic errors:

(a) acceptance tests based on a nominal or 'minimum' specified yield strength—often used in design as σ_y; permission to retest also raises the mean of the accepted test data

(b) variations in testing technique[9,21] such as size of specimen, alignment of the testing machine, strain rate, which in mill testing will often be high enough to provide the unstable upper yield which is against the customer's interest

(c) compression yield is often somewhat higher than tensile yield, but this also usually affects test results on which ϕ is based.

A figure of ζ_y = 0·10 (which may be optimistic for high strain rate testing) has been assumed throughout, and is reasonably consistent with the data used for the frigate and tanker designs which will be used as comparisons[20]. Lehigh tests[56] suggest ζ_y = 0·05. Values greater than 0·20 are appropriate for certain mild steels as supplied to shipyards.

ζ_c is the systematic error which may arise in using idealised design codes to evaluate σ_u. For example, the extensive design data[35] from tests of single bays of longitudinally stiffened panels[64] when compared with larger scale multi-bay tests[65] do seem to be somewhat pessimistic, perhaps due to the stabilising influence of adjoining longitudinals, etc. Moreover, in practical structures other contraints may be provided by secondary structure ignored in the idealisation. Also, conservative assumptions are made in design, and in some cases lower bound curves are used. Each of these represent a systematic error which may be judged subjectively. For the present calculations a value ζ_{co} = 0·15 has been assumed for very slender cross-sections when $\phi \simeq$ 0·5. This may seem somewhat arbitrary but it is evident that ζ_c must diminish as ϕ approaches unity otherwise σ_u would exceed σ_y. A relation of the form

$$\zeta_c = (1 - \phi)\,(2 + \zeta_y)\,\zeta_{co} \tag{18}$$

would seem sensible and has been assumed—to be published[70].

Lastly, ζ_s represents the margin between the moment at which compression collapse occurs in the weakest portion of the hull and the ultimate bending moment. It arises from redistribution of compression load as the structure deforms laterally and buckles, and from residuary strength after local compression failure. This has been studied using an incremental inelastic finite element approach[36]. It seems that ignoring the post-buckling reduction in load[30] can be exceedingly optimistic especially for slender geometries. Overestimates in M_u may vary from 15 to 50%, the former value being for a stocky cross-section. The 'hard corners' in the cross-section also affect strength appreciably. A previous approximation[20] ignoring residuary strength can be shown to yield

$$M_u/M_p = \phi\,(1 + k\nu)/s \tag{19}$$

where $k\nu$ is a function of web/deck area etc.

Taking the bracket term as 1·1, ϕ = 0·6 and s = 1·25 for a frigate cross-section, gives M_u/M_p = 0·53. This is only slightly lower than the results for a slender cross-section derived more rigorously[36]. It may therefore still serve as a useful design approximation, especially if used in conjunction with the slightly optimistic interframe ϕ data presented at the time the debate started[59].

These more rigorous calculations[36] for naval hulls indicate ζ_s was never less than 0·13 and in some special cases it was much more. A value of ζ_s = 0·15 has been assumed throughout.

3.2.1.2 Random errors

This has been discussed rather fully using linear error theory although little general agreement has been reached on realistic values. In ships the total random uncertainties for compression strength vary from $v_c = 9{\cdot}2$ to $11{\cdot}3\%$ in Ref. 20 to a global figure of 13% in Ref. 10. It should strictly bear some relation to the cross-section dimensions since plate widths do not vary greatly. For example, a critical gross panel has rather arbitrarily been defined as 20% of the beam[20]. On this basis the component of v_c which represents the objective uncertainty in yield strength could on statistical grounds be taken as being inversely proportional to $\sqrt{B}$. This would indicate higher values for the naval frigates and destroyers than for the larger merchant ships with which they will later be compared.

Against this the relatively light and slender cross-sections of the naval ships indicate a greater sensitivity to fabrication imperfections. Uncertainties in column strengths range from 5 to 14·3% at Lehigh[66,55] to 2 to 11% at Imperial College[67]. Plate tests in the stocky and intermediate ranges[68] show a subjective c.o.v. of about 5%. Strut panel tests on identical Tee stiffened ship panels in the critical yield elastic buckling range[64] gave a total c.o.v. = 10·9% from which the subjective uncertainty is perhaps 9-10%. 'Adding' in the independent objective uncertainties, especially in yield stress (of say 8 to 10% at the stocky end of the range) supports an overall choice of $v_c = 0{\cdot}13$ as used in Ref. 10.

3.2.2 Application to existing naval designs

In evaluating γ_o from Eq (12) the 5 percentile characteristic strength was chosen so

$$C_k = \bar{C}_u\,(1 - 1{\cdot}645\,v_c)$$
$$= 0{\cdot}786\,\bar{C}_u \text{ when } v_c = 0{\cdot}13$$
$$\bar{C}_u = \bar{M}_u/Z \text{ from Eq (17, 18).}$$

The nominal interframe compression strength factors ϕ were derived from current design data[69] and all required parameters are given in Table III. Two theoretical characteristic loads were taken from Table II, along with one extrapolated from strain measurements.

It will be seen that the $2{\cdot}2\,L^{0{\cdot}3}$ effective wave provides overall partial safety factors between 1·1 and 1·9, while extrapolated lifetime values from strain measurements lie between 1·2 and 2·5. If the superstructure had not been fitted in design D (the original design condition) the upper end of each of the ranges would have been reduced to 1·6 and 1·7 respectively.

3.2.3 Application to 'rule' design warships

Taking the rule section modulus for the 5 naval designs (Section 2.2) and assuming $\sigma_y = 245$ N/mm² and $\phi = 0{\cdot}9$ but otherwise the same values as in the previous section, Table IV presents results similar to those in Table III, but with the effective wave $0{\cdot}607\sqrt{L}$ m ($1{\cdot}1\sqrt{L}$ feet) included for comparison. It follows that for all the designs from Eq (17, 18) $\bar{C}_u$ is constant and = 286 N/mm². Hence the 0·5% C_k = 225 N/mm².

The results not surprisingly indicate somewhat greater consistency and appreciably greater strength than for the actual naval designs. Using the $2{\cdot}2\,L^{0{\cdot}3}$ total wave results, for example, comparisons of 'rule' and actual designs are given in Table V.

Ignoring the superstructure for design D does provide a valid comparison because this was an original design requirement (no doubt because deckhouse superstructures are not always permanent structures throughout the ship's life). Its importance is apparent as noted in Ref. 20.

The increased strength of the rule designed ships is due mainly to the increased section modulus, but is also affected by the appreciably higher compression strength $\phi = 0{\cdot}9$ which corresponds to reasonably stocky stiffeners and

TABLE III. Characteristic strength and total load parameters and partial safety factors γ_o for naval designs (stress N/mm²)

Design	A	B	C	D	E
Strength parameters:					
σ_y nominal	286	286	232	309	309
σ_u nominal	212	179	161	165[i]	208[iii]
ϕ nominal	0·74	0·63	0·69	0·54	0·68
$\bar{C}_u = M_u/Z$	282	244	215	227	283
$C_k = 5\%$	222	201	169	178	222
Theoretical total loads[iv]:					
$D_k = 2{\cdot}2\,L^{0{\cdot}3}$	204	159	123	96[ii]	137
$\gamma_o = C_k/D_k$	1·1	1·3	1·4	1·9	1·6
$D_k = \sigma_{te}$ for 3×10^7 cycles[v]	225	178	130	105[ii]	144
γ_o	1·0	1·1	1·3	1·7	1·5
Extrapolated from strain measurements[iv,v]:					
D_k	191	137	99	70	156
γ_o	1·2	1·5	1·7	2·5	1·4

Notes

(i) upper deck strut-panel[20]

(ii) assuming superstructure partially effective—neglecting it would give $\gamma_o \simeq 0{\cdot}57$ those above

(iii) 01 deck

(iv) from Table II

(v) 25 year life

TABLE IV: 'Rule' design warships: Partial safety factors γ_o, and section modulus comparisons

Design	A	B	C	D	E
Theoretical total loads:					
$D_k = 2{\cdot}2\,L^{0{\cdot}3}$	136	116	110	127	123
γ_o	1·7	1·9	2·0	1·8	1·8
$D_k = 0{\cdot}607\sqrt{L}$	86	75	70	86	91
γ_o	2·6	3·0	3·2	2·6	2·5
Extrapolated from strain measurements: [ii]					
D_k	127	100	89	93	141
γ_o	1·8	2·2	2·5	2·4	1·6
Actual Z m³	0·520	1·054	1·299	1·962[iii]	3·739
Rule Z m³	0·783	1·440	1·448	1·482	4·151

Notes

(i) $C_k = 225$ N/mm², and all load stress values corrected for rule Z

(ii) 25 year life

(iii) 1·121 m³ if superstructure is ignored.

$b/t \simeq 44$. Naval cross-sections are slender, presumably in an attempt to save structural costs. No reduction was made to the rule section modulus for the somewhat higher strength steels used by the navy because it would not have affected the rule strength.

3.3 Safety Index

The margin $M = C - D$ (which at this stage we will consider as scalar quantities) is a measure of the safety (or structural performance), whether it be inadequate $M < 0$, or overdesigned M large. Even if the joint distribution of C and D is unknown their first and second moments are sufficient to find the mean and variance of M by making use of the linearity property of expectation. They also provide a lower bound to reliability, the probability that C exceeds D[52]. The probability of failure has an upper bound given by the, admittedly coarse, Tchebycheff inequality as

$$p_f = p\{M < 0\} \leq v_m^2 \tag{20}$$

where v_m is the coefficient of variation of M

$$v_m = \frac{\sqrt{\theta^2 v_c^2 + v_d^2 - 2\rho_{c,d}\,\theta v_c v_d}}{\theta - 1} \tag{21}$$

If C and D are independent random variables then the correlation coefficient is zero and we can define a safety index $\beta_f = v_m^{-1}$

$$\beta_f = \frac{\theta - 1}{\sqrt{\theta^2 v_c^2 + v_d^2}} = \frac{\bar{C}_u - \bar{D}_e}{\sqrt{S_c^2 + S_d^2}} \tag{22}$$

where from Eq (20) we see that

$$\beta_f \leq \frac{1}{\sqrt{p_f}} \tag{23}$$

TABLE V. Partial safety factor comparisons

Design	$\bar{\gamma}_o$	cov γ_o
Rule designs	1·85	8%
Actual designs	1·46	21%
Actual designs ignoring superstructure for D ($D_k = 176, \gamma_o = 1·0$)	1·28	19%

that is, high probabilities of failure will be associated with low safety indices. If the distributions of C and D are known

$$p_f = \Phi\beta_f \tag{24}$$

where Φ is available in graphs and tables in many sources from Freudenthal[9] to the most recent comprehensive survey[51]. These show variations of p_f with θ; v_c and v_d for a wide range of frequency distributions of C and D. Ferry Borges[51] also includes data on the obvious link with partial safety factors using 0·05 and 0·005 fractiles. Similar data have been provided recently for ship designers[14,10]. As far as the authors are aware the first reference to the safety index was 22 years ago by Thomas—p 308 of Ref. 8. Alternative similar safety indices have been advanced, including the rather popular use[71] of $\ln\theta$ in the numerator of Eq (22). Most of these arise either from certain assumptions about the distributions or attempts to overcome distribution sensitivity problems and the stochastic nature of the subjective uncertainties concerning the distributions. The serious reader should consult Ang and recent surveys[55,56].

Meanwhile, the authors favour the simplicity and intuitive appeal of β_f as defined by Eq (22). No knowledge is required about the probability densities of C and D other than some consistent assessment of their mean values and c.o.vs. Even the act of defining these is a sound discipline which should bring home to the serious designer some of the uncertainties facing him. The other attraction of β_f is that as v_c and v_d tend to zero β_f tends to infinity, which of course from Eq (23) means there is no risk of failure. Although this is not practical in man made structures, it is conceptually more attractive than, for example, γ_o tending to θ, a finite safety factor. This implies, incorrectly, that even in such an extreme case there is some upper limit on safety.

3.3.1 Ship loading theory

Since still water loads vary little and are relatively small in most naval designs, a static balance in the deep condition was made to evaluate σ_s. In all five designs this gave a hogging moment, which improves safety.

To this was added the mean value of the extreme wave bending stress extrapolated over the assumed 25 year ship life. The analysis followed the by now familiar three broad stages:

(a) evaluate the bending response to regular waves

(b) use short-term statistics to calculate response variance for a given speed, heading and weather conditions

(c) summation of probabilities over all anticipated speeds, headings and weather conditions to evaluate long term statistics.

These will now be described in a little more detail.

The linear strip theory analysis was based on the SCORES program[72] which calculates the vertical mean square wave-induced bending moments amidships at a number of headings and speeds in a variety of seas of unit wave height. The ISSC (1967) two-parameter spectrum was used and short-crested seas assumed. The following conditions were assumed:

(1) mean periods of 2·5, 4·5, 6·5, 8·5, 10·5, 12·5, 14·5, 16·5 18·5 and 20·5 seconds in conjunction with unit significant wave heights;

(2) relative headings of 0°, 30°, 60°, 90°, 120°, 150° and 180°;

(3) a speed of about 10 knots (this is usually sufficient because bending moments are not very sensitive to speed and 10 knots is a reasonable maximum to expect in very severe weather).

Sufficient accuracy was achieved for ships longer than 60 m if component wave frequencies of 0·1, 0·2, 0·3..... 1·7, 1·8 rads/sec were specified. To avoid anomalies associated with very low frequencies of encounter wave frequencies were chosen in conjunction with ship speed to ensure that $|\omega_e| \geq 0·05$ rads/sec.

The results of these strip theory calculations were then used to estimate the long-term probabilities of exceeding given bending moments using a statistical program. To do this it was necessary to assess the probability of meeting each combination of wave height and mean period and the amount of time that ships spend at different speeds and headings with respect to the predominant wave direction. This was done as follows:

(i) The probabilities of meeting particular combinations of wave height and period depend on the areas in which the ship will operate. However, sufficiently detailed forecasts are seldom available and a standard operating pattern must be assumed. In such circumstances the probabilities set out in Table III, Chapter 9 of Ref. 60 were used.

(ii) Head seas usually cause the highest vertical bending moments and the probability of Commanding Officers changing course to meet seas head on increases with increasing wave height. Therefore the probabilities of encountering waves of various heights from different sectors were based on the analysis of bridge logs of frigates and destroyers.

(iii) The sea areas in which the ships were assumed to operate were taken from Ref. 73 and are:

Zones 1-2, northern N. Atlantic
Zones 6-11, mid N. Atlantic
Zones 16-18, southern N. Atlantic.

A 25 year life of 33% time spent at sea with a mean wave encounter period of about 8·5 seconds gives 3×10^7 total wave cycles.

It can be shown that the probability of the peak wave bending moment b^+ in any one cycle (crest-to-crest), which might occur in any one of a whole range of conditions, equalling or exceeding a given value B_w is

$$Q = P\{b^+ \geq B_w\}$$
$$= \iiiint p\{V/H, \alpha/H\}\, p\{H,T\} e^{-B_w^2/2m_{OH}}\, d\alpha dV dT dH \tag{25}$$

where $m_{OH} = m_{OH}(V, \alpha, H, T)$ is the mean square response at ship speed in seas of wave height H, mean period T with predominant direction α. That is, we do not even need to assume linearity of response with wave height if we have, for example, enough data from model tests. However, we do not in general have such data, and in practice Eq (25) can only be evaluated arithmetically taking discrete values of H, T, α and V. We therefore made use of the usual linearity of response assumption which leads to the far more tractable

$$Q = \sum p\{V/H, \alpha/H\}\, p\{H,T\} e^{-B_w^2/2H^2 m_o} \tag{26}$$

where $m_o = m_o(V, \alpha, 1, T)$ the more usual mean square response in seas of unit wave height. A typical wave bending moment derived in this way is given for naval design B in Fig. 3. Superimposed at a probability level $P = (3 \times 10^7)^{-1}$ is a random uncertainty which will be discussed below and in Section 3.3.1.2.

3.3.1.1. Extreme value statistics

Curves such as Fig. 3 are often referred to as long term probability curves. But as Karst has pointed out (Appendix A of Ref. 16) this is a misnomer. Such curves show, in effect, the probabilities of exceeding specified wave bending moments during any one cycle at *any* time in a ship's life.

However, it is usually more important to determine the probabilities of specified bending moments being exceeded at least once during the life of a ship in which n waves are met. Karst showed this probability is given by the Binomial distribution

$$p(x) = \binom{n}{x} Q^x (1-Q)^{n-x} \tag{27}$$

where p(x) is the probability of exceeding the bending moment, B_w, x times in n independent cycles. In fact one cycle is not statistically independent of the few hundred cycles immediately preceding or following it. Nevertheless, the Binomial distribution is still valid if one is considering the whole of a ship's life.

If n is very large and Q is very small so that the expected or average number of exceedences m(= nQ) remains finite it has been shown that the Binomial frequency function is approximated by the one parameter (m) discrete Poisson distribution

$$p\{x\} = m^x e^{-m}/x! \tag{28}$$

where m is both the population mean and the population variance. Thus the probability that the given wave bending moment B_w is not exceeded in n wave cycles is found by putting x = 0 and is

$$p\{0\} = e^{-nQ} \tag{29}$$

The cumulative probability of the moment being exceeded at least once in n cycles is

$$P\{0\} = 1 - p\{0\} = 1 - e^{-nQ} \tag{30}$$

and we may note that for the special case where the wave bending moment is chosen such that Q = 1/n (which leads to the most probable extreme moment) the probability of exceedence is $1 - e^{-1} = 0{\cdot}632$ as discussed elsewhere[20,74].

Using this approach Fig. 4 shows the theoretical probability of the highest moment experienced by naval design B in a 25 year life of 3×10^7 cycles exceeding certain values. The figure also includes a histogram showing the distribution of the highest wave bending moment that would ever be experienced in the ship's life, as predicted by theory. This corresponds to the Poisson distribution superimposed on the cumulative probability of Fig. 3. By taking first and second moments of this histogram, and by adding a $(\Delta M_w)^2/12$ variance correction for the interval width, the mean values and standard deviations are obtained. For naval design B they are

$$\overline{M}_{we} = 222{\cdot}9 \text{ MNm}$$
$$S_{ow} = 16{\cdot}6 \text{ MNm}$$

and the mean value is only 3·3% greater than the mode $M_{we} = 222{\cdot}5$ MNm. This fact was used to simplify the calculations of the mean total extreme demand (load) for all the designs by assuming

$$\overline{D}_e \simeq 1{\cdot}033\, \sigma_{we} + \sigma_s \tag{31}$$

where $\sigma_{we} = M_{we}/Z$ the modal wave bending stress for 3×10^7 cycles evaluated directly from figures such as Fig. 3. The objective random uncertainty for the total wave bending moment (see next section) is then

$$v_{ow} = S_{ow}/Z\overline{D}_e \tag{32}$$

Since we were talking earlier about characteristic loads we can make use of Eq(29) to find the wave-induced moment which, for example, has only a 1% chance of being exceeded. It is necessary to find Q such that

$$e^{-nQ} = 0{\cdot}99$$
$$\text{i.e. } Q = 0{\cdot}0101/n \simeq n^{-1}/_{100}$$

that is, we simply move two orders of probability to the left (lower values) of n^{-1} in Fig. 3 and read off the appropriate moment. This provides a more conservative *design extreme value*, which is also the most probable extreme value in 100 n wave encounters. Had we chosen this for the characteristic load of naval design B in Table III we would find $D_k = 268 - 33 = 235$ N/mm² which is 96% of the expected mean strength and gives an overall partial safety factor on a 5% strength basis of $\gamma_o = 0{\cdot}9$, less than unity.

Alternatively, if there were 100 design B sister ships operating with the same mission profile, the same statistical arguments[16] lead to the conclusion that one of these ships would be expected (with 0·632 probability) to exceed this stress = 235 N/mm² in its lifetime.

We should note that the above method for predicting the lifetime extreme moment has made no use of order statistics[18,74] which recognise that wave (or stress) records

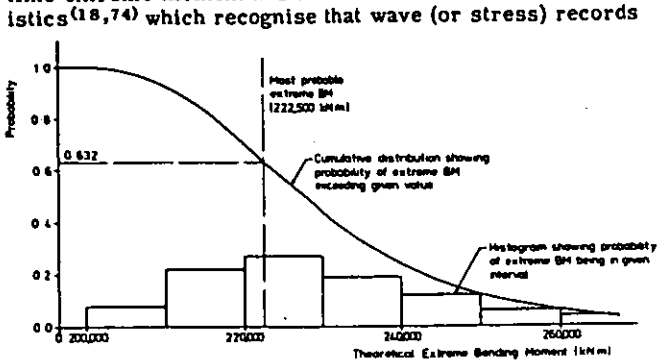

Fig. 4 Theoretical extreme bending moment probabilities for naval design B during 3×10^7 cycles

are not of sufficient duration to accurately reflect all of the possible extreme stresses in a ship's lifetime. However, if a *design extreme value* is used with a sufficiently small probability of exceedence (0·01 was used above) it follows from analyses similar to those presented by Ochi[74] that the statistical approximations implicit in the present method would agree reasonably with the more exact solution derived by applying order statistics.

3.3.1.2 Random errors

Equation (32) in the last section for the five naval designs considered here gives v_{ow} 8·6, 8·5, 9·5, 8·0 and 7·7% respectively with an average value of 8·5%. The subscripts indicate that this represents the objective uncertainty in the wave induced total bending moment—'objective' in the sense that S_{ow} is calculable from the Poisson distribution. For naval designs S_{os} due to still water variations is ignored, as is correlation between still water and wave induced moments (only minor effects detected in experiments). In general the still water variance would have to be added to S_{ow}^2 to give a total variance. To this we have to add the 'subjective' components of load variance to obtain S_d for use in Eq(22). This requires considerable judgment.

Subjective errors in calculating wave-induced distributions can arise from many sources. Perhaps the main sources include uncertainties in

(a) accuracy of wave height and period statistics

(b) variation in spectral shape and in particular the adequacy of two-parameter spectra

(c) accuracy of assumed course and speed and their variations with wave height

(d) actual time and zones of service operation differing from assumed mission profile

(e) accuracy of linear strip-theory.

Working backwards we may expect (e) to cause mainly systematic errors (discussed in the next section) and little can be said at present about (c) and (d). Some Captains alter heading and speed to avoid the worst seas, and a study of operating service profiles like those being recorded in naval ships logs could ultimately prove very useful.

Much has been written about (b) but at present there is little hope of improvement on a world wide basis, even though the sensitivity of response to the selection of wave parameters has recently been demonstrated[75].

In the introduction of their tome[73] Hogben and Lumb include some comparisons between visual estimates and measurements of waves. It was found possible to derive a linear fit between the measured significant height H_m and the visually estimated H_v (generally lower) as follows

$$\left.\begin{aligned} H_m &= 1{\cdot}23 + 0{\cdot}88\, H_v \text{ m} \\ \text{RMS deviation} &= 1{\cdot}27 \text{ m} \end{aligned}\right\} \qquad (33)$$

Wave period estimates were even less reliable.

For sea-states 6, 7 and 8 this corresponds to random subjective uncertainties from source (a) of $v_{sw} \simeq 25\%$, 14% and 9% respectively. As was shown by SSC research[16,17] for cargo ships operating in the North Atlantic the highest expected bending moment is more likely to be caused by the moderate to severe storms than by the much rarer and elusive 'worst possible storm'—which many Captains would probably avoid anyway nowadays with more attention paid to weather routing. Lewis[17] also refers to other relationships[76,77] and appears to have adopted an uncertainty in extreme prediction due to weather—waveheight uncertainty of 14·9%. Fig. 5 of Ref. 14 also provides wave height data by various observers from which it can be deduced that for ships around 110 m long (as for most of the presented naval designs herein) $v_{sw} \simeq 15\%$.

Recent observed strains in naval ships suggest an overall random uncertainty in measured data as compared with linear strip theory (LST) predictions of greater than 20%. If we 'subtract' $v_{ow} \simeq 8{\cdot}5\%$ and assume statistical independence this suggests subjective uncertainties from all causes of *at least* $v_s = 18\%$. The biggest contribution is likely to be from sources (a) and (b) and this result is approximately in accord with the derivations of the previous paragraph.

Thus, the total uncertainty in ship loading $v_d = S_d/\bar{D}_e$, where $S_d \simeq (S_o^2 + S_s^2)^{1/2}$, is likely to exceed 20%, perhaps appreciably. For many fixed offshore structures it has recently been argued that for extreme loads v_d is likely to exceed 30%[78].

3.3.1.3 Systematic errors

It is well known that linear strip theory approaches generally overestimate extreme bending predictions. Indeed it is claimed[79] that theoretical methods of predicting wave-induced bending stresses in warships (as in this paper) give values which are higher than measured stresses by up to 60%. There seems to be no consistent pattern to this overestimate. The values in Table III show the ratios of theory to measurement for total lifetime loads vary from 0·92 to 1·50, with a mean of 1·24 and c.o.v. of 0·17 (somewhat smaller than the 20% mentioned earlier no doubt due to the smaller sample size).

The sources of error which may arise from the use of linear strip theory (LST) *per se* are[80]

(a) neglect of non-linear buoyancy effects because extreme wave profiles seldom intersect the hull where it is entirely vertical

(b) in addition to linear force terms additional higher order terms in heave and pitch will exist; it is well known that in a moderate sea the exciting waves are non-linear, and the hydrodynamic forces are not linear either and decay exponentially with depth.

To these must be added systematic errors arising from sources (a) to (d) in Section 3.3.1.2 which are to do with uncertainties in sea wave statistics and operating conditions. See also the last paragraph of Section 3.3.1.1 concerning the relatively short duration of recorded data.

The non-linear buoyancy effects were mentioned earlier. Static considerations show that the ratio of sagging to hogging bending moments increases rather more than proportionately with wave height[31,33] and this has been confirmed by strain measurements in warships[32], in containerships[81] and in models[34]. Moreover, this and other non-linear force effects have been examined together and shown recently[80] to increase theoretical predictions of the probabilities of failure for a frigate[20], cargo ship[19] and large tanker[20]. So error sources (a) and (b) above appear only to increase the discrepancy. Results from wave tests on a model destroyer offer some support for this because measured response amplitude operators are slightly higher than the theoretcial LST values, although this is not generally true.

It also seems[75] that errors in spectral distribution will have some effect on the mean and variance of the short-term analysis. We must therefore conclude that whilst the discrepancy cannot yet be explained the major source of error (apart from storm avoidance actions) is likely to be in defining extreme sea conditions for the long-term statistics. The results are very sensitive to significant wave height and mean wave period assumptions for extreme waves, particularly for ships of frigate size[79]. The shortage of wave energy data for large waves (H_s above 8 m) is a matter for concern.

Nevertheless, the use of the theory described above for predicting the extreme wave-induced bending moment is advocated for naval designs with corrections (a) for nonlinear buoyancy determined from static balance calculations. The procedure is justified on the basis that the implicit pessimism means that instead of there being a 63% chance of exceeding the theoretical modal value of the extreme the actual probability based on measured strains is only about 2%.

3.3.2 Application to existing naval designs

The theory has been applied to the five designs described earlier. The four parameters required for safety index β_f are means of load and strength ($\overline{D}_e$ and $\overline{C}_u$), and their variances (S_d^2 and S_c^2). $\overline{C}_u = M_u/Z$ was derived in Section 3.2.2 using Eq(17, 18) and $\overline{D}_e$ is given by Eq(31) in Section 3.3.1. v_c was chosen as 0·13 (see Section 3.2.2.2) which is thought to be reasonably realistic. However, a v_d of 0·16 was selected which is almost certainly an underestimate (see Section 3.3.1.2) but does enable comparisons to be made with other data in which similar assumptions are implicit[10,19,20]. The effect of variation in v_c and v_d, and in other variables is examined parametrically later.

On these bases β_f was calculated using Eq(22), and the results which include central safety factor θ are given in Table VI. Values based on lifetime extrapolations from measured strain data are also presented in Table VI. Fig. 5 is a plot of β_f against ship length.

Theoretical values for β_f range from 0·9 to 3·4 with an average value of $\bar{\beta}_f = 2·2$ and c.o.v. = 0·48 (or 1·7 and 0·56 respectively if the superstructure is ignored in design D). Equivalent lifetime measured extrapolations are $\bar{\beta}_f = 3·2$ and c.o.v. = 0·36 (or 2·8 and 0·21 ignoring superstructure in D). Clearly, the effect of the superstructure is dramatic for design D. It corresponds to a Caldwell efficiency[45] of about 0·85, which is somewhat greater than was assumed in Ref. 20.

TABLE VI: Naval Designs: Theoretical and measured estimates of safety indices and central safety factors

Design	A	B	C	D	E
$\overline{C}_u$ Table III	282	244	215	227	283
Theory(ii):					
$\overline{D}_e \simeq 1·033\ \sigma_{we} + \bar{\sigma}_s$ Eq(31)	233	185	135	109(ii)	149
$\theta = \overline{C}_u/\overline{D}_e$	1·2	1·3	1·6	2·1	1·9
β_f Eq(22)	0·9	1·4	2·3	3·4	3·1
Measured Extrapolations(iii):					
$\overline{D}_e$	191	137	99	70	156
θ	1·5	1·8	2·2	3·2	1·8
β_f	1·9	2·8	3·6	5·0	2·9

Notes:

(i) $v_c = 0·13$, $v_d = 0·16$ throughout

(ii) assuming superstructure partially effective—neglecting it would give $\overline{D}_e = 190$ N/mm², $\theta = 1·2$ and $\beta_f = 0·9$

(iii) total stress for 25 year life, see Table II.

3.3.3 Application to merchant ships

3.3.3.1 'Rule' naval designs

As in Section 3.2.3 the same approach has been applied to the five naval designs using rule requirements for section modulus and $\phi = 0·9$ appropriate for stocky sections. The theoretical results in Table VII and Fig. 5 indicate a range of β_f from 2·9 to 3·9 with $\bar{\beta}_f = 3·4$ and c.o.v. = 0·11. Thus the results are on average appreciably safer and much more consistent than for the actual naval designs.

Actual merchant ships of the same size would have a worldwide mission profile, which is about 1 order of magnitude less severe in terms of p_f than for the North Atlantic bias for naval ships. Against this they would probably spend more than twice as many days at sea, and so the β_f values probably apply equally to such vessels.

3.3.3.2 Larger merchant ships

Eighteen existing merchant ships have been analysed in a comparable way previously[10] and the results presented for comparison in Fig. 5. They range in deadweights from 26,500 to 190,000 tonnes and in length from 160 m to 330 m. Sixteen of the ships have an Indian Ocean, South and North Atlantic mission profile in zones[73] 1, 7, 11, 18, 20, 23, 28, 29, 34, 41, 42 and 45. The remaining two ships were the MARINER[19] (ship 16) operating in the North Atlantic and which has been the subject of much SSC research, and a large tanker[20] (ship 12) operating worldwide. The analyses differed from that in this paper in several respects, notably

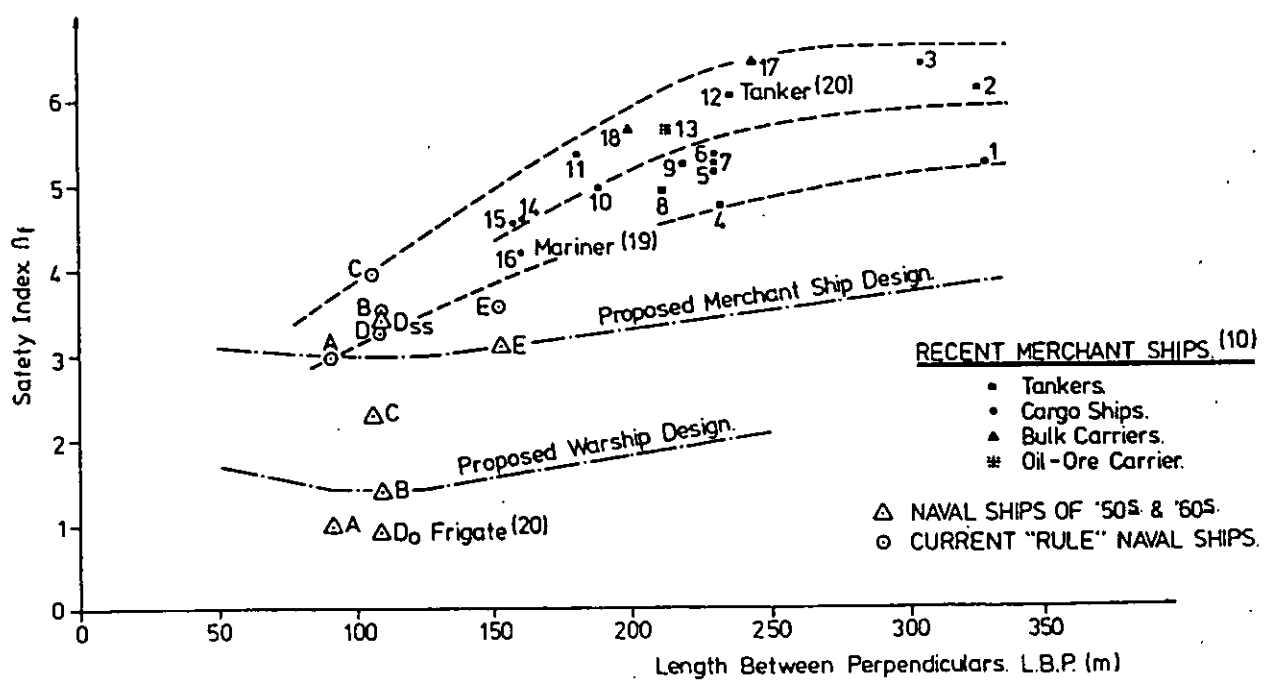

Fig. 5 Safety indices for naval and merchant ships

TABLE VII: 'Rule' design warships: safety indices and central safety factors based on theory

Design	A	B	C	D	E
$\bar{D}_e$ (iii)	155	135	121	144	134
$\theta = \bar{C}_u/\bar{D}_e$	1·9	2·1	2·4	2·0	2·1
β_f Eq(22)	2·9	3·5	3·9	3·3	3·5

Notes:

(i) $v_c = 0{\cdot}13, v_d = 0{\cdot}16$ throughout

(ii) $\bar{C}_u = 286$ N/mm² throughout

(iii) $\bar{D}_e$ stresses for Table VI corrected for rule Z (Table IV)

(a) longer time at sea ≃ 10^8 cycles

(b) long-crested head seas assumed

(c) less severe operational zones

(d) $M_u = \sigma_y Z$, that is, stronger generally

and no account was taken of variation of ship speed with wave height—a minor effect. Overall, it is thought the pessimism of (a) and (b) nearly but not quite compensates for the optimism of (c) and (d). But we should remember the optimism implicit in the low choice of v_d.

The justification for the former statement is twofold. Firstly the band of large merchant ship results in Fig. 5 broadly extends slightly downwards to cover the five 'rule' design naval ships, especially bearing in mind the 10% reduction in rule section modulus over the three years from 1973-76. Secondly, Ref. 20 analysed the present naval frigate D and tanker (ship 12) of Ref. 10. Their respective probabilities of failure were about 10^{-5} (with superstructure effective) and 10^{-8} respectively. Over the range of β_f considered this would correspond to a difference of about 1·5 compared with actual values

frigate D $\beta_f = 3{\cdot}4$

tanker[10] $\beta_f = 6{\cdot}0$.

We may reasonably conclude that the present analysis is slightly more pessimistic than that of Ref. 10. This may be one or two orders of probability difference, which is hardly of any consequence for most merchant ships[23]. Any method adopted will in any case have to be used comparatively for the present.

3.3.4 Parametric studies

We have seen there are still many uncertainties in strength and loading of a random and systematic kind. The effect of some of these on safety has been examined in Tables VIII, IX and X for naval design B. Her basic 'as designed' characteristics are

strength $\phi = 0{\cdot}63$

safety $\theta = 1{\cdot}3, \beta_f = 1{\cdot}5$

random $v_c = 0{\cdot}13, v_d = 0{\cdot}16$

systematic $\alpha_y = 1{\cdot}1, \alpha_{co} = \alpha_s = 1{\cdot}5$.

3.3.4.1 Change in compression strength

Table VIII shows that in naval designs reduction in ϕ reduces safety drastically. Clearly, compromising with structural cost (which is probably illusory anyway) must not be carried too far.

3.3.4.2 Change in load and strength variability

In view of the probable optimism in the selection of $v_d = 0{\cdot}16$ Table IX should be of interest. For values of strength variability $v_c \geq 0{\cdot}10$ and values of load variability $v_d \geq 0{\cdot}20$ the safety index is nowhere greater than 1·3 and is sometimes less than unity in the naval designs. Rule design ships are appreciably safer and more resilient to these changes.

TABLE VIII: Change in $\bar{C}_u$, θ and β_f for change in compression strength ϕ for naval and rule designs 'B'

ϕ	0·52 (i)	0·6	0·7	0·8	0·9 (ii)
Naval designs:					
$\bar{C}_u$	204	233	269	302	333
θ	1·1	1·3	1·5	1·6	1·8
β_f	0·5	1·1	1·8	2·4	2·8
'Rule' design warships:					
$\bar{C}_u$	174	199	230	259	286
θ	1·3	1·5	1·7	1·9	2·1
β_f	1·3	1·9	2·6	3·1	3·5

Notes:

(i) Lower limit at which Eq(17) applies $= \alpha_y/(1 + \alpha_y)$

(ii) Upper limit may approach 1·0 but seldom does in practical structures

(iii) All other parameters as previously

3.3.4.3 Change in strength systematic errors

The strength model chosen for this study is unusual in form, and includes the systematic strengthening factors ζ (Section 3.2.1). Many will regard it as optimistic although the authors regard it as more realistic than most. Any optimism it has may in any case be justified if it is to be used in conjunction with the implicit pessimism of lifetime predictions of extreme load using present extreme wave data (see the end of Section 3.3.1.3).

Table X shows the effect of changes in the systematic factors. In particular Case (A) shows that reduction in the compression strength and section effect uncertainties leads quickly to drastic reductions in safety. Yet these factors are ignored in most designs (that is, $\alpha_{co} = \alpha_s = 1$) in which case design B would have a theoretical safety index of zero.

4. DISCUSSION

Although some conclusions may be drawn, the authors prefer to avoid the word since second moment methods are at a very formative stage. These closing remarks will be philosophical in the hope that the ensuing discussion will add considerably to any merit the paper may have.

4.1 General Remarks

The above procedure for wave load predictions owes much in a statistical sense to Lewis and his very talented associates in the 60s[16,17]. Perhaps the three most important changes in the intervening years have been

(a) defining the sea state by wave height and period statistics[73]

(b) inclusion of short crested analysis

(c) inclusion of probability distributions for ship heading and speed, based on an analysis of bridge logs.

It seems, however, that only a few combinations of speed, heading and sea conditions make a significant contribution to the probability of exceedence, which may simplify future calculations. Nevertheless, much remains to be done, to improve the definition of extreme wave data in particular.

The strength model is novel and may appear too sophisticated. It is justified because evidently some naval designs have quite low safety levels compared with most merchant ships. And so some knowledge of the reserve of strength beyond local failure is clearly desirable. In this respect much more needs to be known about the capability of man-made imperfect structures.

TABLE IX: Change in β_f for varying values of v_d and v_c for warship design B—all other parameters remaining unchanged

v_c \ v_d	0·05	0·10	0·15	0·20	0·25	0·30
Navy:						
0·05	3·9	2·7	2·0	1·5	1·2	1·0
0·10	2·3	1·9	1·6	1·3	1·1	1·0
0·15	1·6	1·4	1·3	1·1	1·0	0·9
0·20	1·2	1·1	1·1	1·0	0·9	0·8
0·25	1·0	0·9	0·9	0·8	0·8	0·7
Rule:						
0·05	9·6	7·7	6·1	4·9	4·1	3·5
0·10	5·1	4·8	4·3	3·8	3·4	3·0
0·15	3·5	3·4	3·2	3·0	2·8	2·6
0·20	2·6	2·6	2·5	2·4	2·3	2·2
0·25	2·1	2·1	2·0	2·0	1·9	1·8

TABLE X: Change in $\overline{C}_u$, θ and β_f for changes in systematic errors—naval design B

Case (A) $\Delta\alpha = \alpha_{co} = \alpha_s, \alpha_y = 1{\cdot}1$ throughout

Case (B) $\Delta\alpha = \alpha_y, \alpha_{co} = \alpha_s = 1{\cdot}15$ throughout

$\Delta\alpha$	1·00	1·05	1·10	1·15	1·20	1·25
Case (A):						
$\overline{C}_u$	187	205	224	244	265	286
θ	1·0	1·1	1·2	1·3	1·4	1·6
β_f	0·0	0·5	0·9	1·4	1·8	2·1
Case (B):						
$\overline{C}_u$	230	237	244	250	256	261
θ	1·2	1·3	1·3	1·4	1·4	1·4
β_f	1·1	1·2	1·4	1·5	1·6	1·7

The so-called 'successful' ship approach, beloved by naval architects, is a useful concept for most hydrodynamic and stability features of design. But it is quite incomplete as a concept for good structural design. Success is not just the avoidance of failure, but also providing the owner with the least total cost at an adequate but not excessive level of safety. This, we believe, is not being achieved in merchant ships or consistently in naval ships. Nor will it be generally achieved until we step forward to take advantage of decades of research and really learn from our so-called successful ships.

If we do this then we must look at Fig. 5 and ask ourselves such questions as

(a) why are the safety levels of ships so widely spread when modern methods are applied?

(b) why are merchant ships generally several orders safer than naval ones?

(c) should we not be designing to the lowest demonstrably 'successful' safety standards, and thereby certainly save weight and presumably in many cases cost also?

The answers seem reasonably clear, but are seldom acted on. Nor are our ship owners always sufficiently well informed, perhaps.

Taking only question (b) there seem to be three plausible answers from merchant ship designers:

(i) still water loads vary considerably and can lead to adverse loading

(ii) structural details are poorer than in warships and so fatigue can be, or become, a problem

(iii) the capital investment is greater?

None of these seem very inhibiting when compared with naval experience, but we welcome enlightenment. Perhaps the idea of a benefit for good structural details should be re-examined?

The biggest shortcoming of the method presented (apart from the concentration only on the lowest mode of failure) is the absence of any treatment of slamming. This, we believe, is the biggest unknown now in ship primary loading-especially so for limber warships and certain merchant ships which might well attract slam-induced vibratory response on top of wave-encounter bending. It is to be hoped that recent work at University College London, will help establish answers to this problem[82] in conjunction with high frequency strain records from sea.

4.2 Use in Design

The Royal Navy has taken a major step forward in proposing to adopt as part of its structural loading assessments a reasonable, if arguable, semi-statistical method. The present paper perhaps opens the door to marrying it to a semi-statistical approach to 'jack-knifing' strength predictions, using second moment methods.

The senior author has previously advocated[1] a Partial Safety Factor approach, simply to start the ball rolling and because it is now being used in civil engineering. It might also commend itself to many designers as being closer to the conventional safety factor approach. It seems even that a well chosen effective wave, which agrees best with strain derived data (Fig. 2), could be used on an extended static balance basis[33] to provide characteristic primary loads.

However, the four-parameter Safety Index approach also has much to commend it, and can be equally easily used in a design context[10]. Much will be learned, and useful comparisons made, if both of these second moment methods can be introduced into ship design alongside more conventional methods. The safety levels ultimately adopted must emerge from this process.

In this respect proposed design curves, inserted only for discussion, appear in Fig. 5. There seems no good reason why ships should not have a reasonably uniform safety index. Some may argue that small naval ships with thin plating which is reduced quickly by corrosion, should have a higher β_f than larger ships. Against this larger ships represent a greater capital investment, and perhaps should have higher safety standards.

Any method adopted must at present be used comparatively. Comparing small and large ships is legitimate, providing we argue as above. Comparing acceptable safety indices for ships with ones similarly defined for aeroplanes or civil engineering structures is less legitimate. Their loading, even when stochastic, will be sufficiently different to provide different results. Also, as pointed out in Section 3.1, different interpretations may be placed on the 'mean load'. Even offshore structures may expect somewhat different acceptable values of the safety index because of drag and depth-penetration effects. There is little doubt that offshore structures are designed closer to the bone than are merchant ships[78].

Finally, there is no in service measure (other than the low incidence of fatigue cracks, which is only partially relevant) of a good structural design. This is one reason why, for example, the safety levels in naval designs vary so much. Perhaps greater unity can now be achieved, and economies can safely be made in many merchant ships.

ACKNOWLEDGMENTS

We are indebted to the Ship Department, MOD(PE) Bath, for much of the data in the paper. We also gratefully acknowledge the permission of the Society of Naval Architects and Marine Engineers to reproduce data for Figs. 2 and 5 from Refs. 49 and 10. This has enabled us to compare naval and merchant ships, we hope for the benefit of both. Any views expressed are those of the authors and do not necessarily reflect those of the Ship Department.

REFERENCES

1. Faulkner, D.: 'Safety Factors ?', Steel Plated Structures, Crosby Lockwood Staples, 1977, p 764-790.
2. Kendrick, S.: Chapter 9, The Stress Analysis of Pressure Vessel and Pressure Vessel Components, ed. by S. S. Gill, Pergamon Press, 1970.
3. Weck, R.: 'A Rational Approach to Standards for Welded Construction', Br. Welding Jnl., Nov. 1966, p 658-668.
4. Bate, S. C. C.: 'Partial Safety Factors in Structural Engineering Codes of Practice', The Structural Engineer, Vol. 53, no. 8, Aug. 1975, p 333-334.
5. Comité Européen du Béton, Fédération Internationale de la Précontrainte—Recommendation Internationales pour le calcul et l'éxécution des ouvrages en béton, Seconde Edition, Juin 1970.
6. Building Code Requirements for Reinforced Concrete, Proposed Revision of ACI 318-63, American Concrete Institute Jnl., Feb. 1970. (See also Ref. 57).
7. The Structural Code for Concrete, CP 110: 1972.
8. 'Report on Structural Safety', with Discussion, The Structural Engineer, Vol. 33, no. 5, May 1955, and Vol. 34, no. 9, Sept. 1956.
9. Freudenthal, A. M.: 'Safety and Probability of Structural Failure', Trans. ASCE, Vol. 121, 1956.
10. Mansour, A. E.: 'Approximate Probabilistic Method of Calculating Ship Longitudinal Strength', Jnl. Ship Res. Vol. 18, no. 3, Sept. 1974, p 203-213.
11. Pugsley, A. G.: 'A Philosophy of Aeroplane Strength Factors', Report and Memo no. 1906, British Aeronautical Research Committee, 1942.
12. Freudenthal, A. M.: 'The Safety of Structures', Trans ASCE, Vol. 102, 1947.
13. St. Denis, M. and Pierson, W.: 'On the Motions of Ships in Confused Seas', Trans SNAME, Vol. 61, 1953, p 280.
14. Caldwell, J. B.: Report of Committee 10 on 'Design Philosophy and Procedure', Proc. 3rd ISSC, Oslo, 1967.
15. Proc. 4th ISSC, Tokyo, 1970.
16. Hoffman, D. and Lewis, E. V.: 'Analysis and Interpretation of Full-scale Data on Midship Bending Stresses of Dry Cargo Ships', Ship Structures Committee, Report SSC-196, June 1969.
17. Lewis, E. V.: 'Predicting Long-term Distributions of Wave-induced Bending Moment on Ship Hulls', Paper No. 6, SNAME, Spring Meeting, 1967, p 1-18.
18. Mansour, Alaa: 'Methods of Computing the Probability of Failure under Extreme Values of Bending Moment', Jnl Ship Res., Vol., 16, no. 2, June 1972, p 113-123.
19. Mansour, A. E.: 'Probabilistic Design Concepts in Ship Structural Safety and Reliability', Trans SNAME, Vol. 80, 1972, p 64-97.
20. Mansour, A. E. and Faulkner, D.: 'On Applying the Statistical Approach to Extreme Sea Loads and Ship Hull Strength', Trans RINA, Vol. 115, 1973, p 277-314.
21. Flint, A. R. and Baker, M. J.: 'Rationalisation of Safety and Serviceability Factors in Structural Codes', CIRIA Report 63, Oct. 1976.
22. Pugsley, Sir Alfred: 'The Prediction of Proneness to Structural Accidents', The Structural Engineer, Vol. 51, no. 6, June 1973, p 195-196.
23. Goodman, R. A. and Mowatt, G. A.: 'Application of Strength Research to Ship Design', Steel Plated Structures, Crosby Lockwood Staples, 1977, p 676-712.
24. Lewis, Edward V.: 'Ship Structural Design for Extreme Loads', Paper prepared for special issue of Schiffstechnik in honour of the birthday of Professor O. Grim, 7 Sept. 1976.
25. Faulkner, D.: Discussion of the Report of Committee 10 on Design Procedure, Proceedings 5th ISSC, Hamburg, 1973, p 6-11.
26. Planeix, J. M., Huther, M. and Latché, M: 'Dynamic and Stochastic Aspects in the Structural Analysis of VLCCs and ULCCs', Trans NECIES, Vol. 90, 1974, p 133-150.
27. Bolotin, V. V.: Statistical methods in Structural Mechanics, Holden-Day Inc., 1969.
28. Ivanov, L. D. and Caldwell, J. B.: 'The use of Statistical Dynamics in the Calculation of the Reliability of Ship Structures', International Shipbuilding Progress, Vol. 23, no. 259, March 1976, p 55-62.
29. Yuille, I. M.: 'Longitudinal Strength of Ships', Trans RINA, Vol. 105, 1963, p 1-33.
30. Caldwell, J. B.: 'Ultimate Longitudinal Strength', Trans RINA, Vol. 107, 1965, p 411-430.
31. Conn, J. F. and Miller, N. S.: 'The Effect of Various Factors on Wave Bending Moments', Trans NECIES, 1960-61, p 107.
32. Smith, C. S.: 'Measurement of Service Stresses in Warships', Conf. Stresses in Service, ICE, March 1966.
33. Thomas, Geoffrey O.: 'An Extended Static Balance Approach to Longitudinal Strength', Trans SNAME, Vol. 6, 1968, p 238.
34. Dalzell, J. F.: 'An Investigation of Midship Bending Moments Experienced in Extreme Regular Waves by Models of a Tanker and Destroyer', Ship Structures Committee Report, SSC-156, Feb. 1964.
35. Faulkner, D.: Compression Strength and Change, MIT thesis, 1972 (see also chapters 21 and 22 of Ref. 40).
36. Smith, C. S.: 'Influence of Local Compressive Failure on Ultimate Longitudinal Strength of a Ship's Hull', PRADS—Int. Conf. on Practical Design in Shipbuilding, Tokyo, Oct. 1977, p 73-79.
37. Planeix, J. M., Raynard, J. and Huther, M.: 'New Outlooks for Guardians of Safety: Explicit versus Implicit Risk Analysis in Classification/Certification', Second WEMT Conference, Safety at Sea, RINA, 1977.
38. Faulkner, D.: 'Welded Connections used in Warship Structures', Trans RINA, 1964, p 39-70.
39. Caldwell, J. B. and Woodhead, R. G.: 'Ship Structures: Some possibilities for Improvement', Trans NECIES, 1972-73.
40. Evans, J. H., ed.: Ship Structural Design Concepts, Cornell Maritime Press, 1975.
41. Biles, J. H.: 'The Strength of Large Ships', Trans IESS, 1893-94, p 39.
42. Cornish, V.: Waves at Sea, T. F. Unwin, London, 1910.
43. St. Denis, M.: 'On the Structural Design of the Midship Section', DTMB Report C-555, Oct 1954.
44. Dixon, R. H., Ramsay, B. W. and Usher, P. J.: 'Design and Build of the GRP hull of HMS WILTON', Symp. on GRP Ship Construction, RINA, 1972.

45. Caldwell, J. B.: 'The Effect of Superstructures on the Longitudinal Strength of Ships', Trans RINA, Vol. 99, 1957, p 664-689.

46. 'Structural Trials on S.S. OCEAN VULCAN and S.S. CLAN ALPINE—Discussion of Results', The Admiralty Ship Welding Committee Report no. R12, 1954. (See also Turnbull, J.: 'Longitudinal Strength', Trans RINA, 1953, p 103).

47. Getz, J. R.: 'Longitudinal Strength and Minimum Weight', Scandinavian Ship Technical Conference, Oslo, Oct. 1960.

48. Murray, J. M.: 'Development of Basis of Longitudinal Strength Standards for Merchant Ships', Trans RINA, Vol. 97, 1955, p 217-244.

49. Little, Robert S., Lewis, Edward V. and Bailey, Fred C.: 'A Statistical Study of Wave-induced Bending Moments on Large Ocean-going Tankers and Bulk Carriers', Trans SNAME, Vol. 79, 1971, p 117-168.

50. Lloyd's Register of Shipping, Rules and Regulations for the Construction and Classification of Steel Ships, 1976.

51. Ferry Borges, J. and Castanheta, M.: Structural Safety, Advanced Course 101, Laboratorio Nacional de Engenharia Civil, 2nd ed, Lisbon, March 1971.

52. Cornell, C. A.: 'Bounds on the Reliability of Structural Systems', Proc. ASCE, vol. 93, no. ST1, Feb. 1967 (see also vol. 95, no. ST8, 1969).

53. Ang, A. H-S.: 'Extended Reliability Basis of Structural Design Under Uncertainties', Annals of Reliability and Maintainability, Vol. 9, 1970, p 642-649.

54. Ang, A. H-S. and Amin, M.: 'Safety Factors and Probability in Structural Design', Proc. ASCE, Jnl Str. Div., Vol. 95, no. ST7, 1969, p 1389-1405.

55. Modern Concepts of Structural Safety and Design, ASCE National Structural Engineering Meeting, April 1973.

56. Canadian Structural Engineering Conference, Montreal, 1976.

57. American Concrete Institute Code, 1976.

58. Canadian Limit States Design Specification, 1976.

59. Faulkner, D.: Discussion of Ref. 30.

60. Price, W. G. and Bishop, R. E. D.: Probabilistic Theory of Ship Dynamics, Chapman and Hall, London, 1974.

61. Betts, C. V. and Attwell, D. M.: 'The Ultimate Longitudinal Strength of Ships', Shipbuilding and Shipping Record, Dec. 30, 1965, p 889-890.

62. Jones, Norman: 'On the Shakedown Limit of a Ship's Hull Girder', Jnl Ship Res., Vol. 19, no. 2, June 1975, p 118-121.

63. Faulkner, D. and Betts, C. V.: Discussion of Ref. 20, Jnl Ship Res. Vol. 20, no. 1, March 1976, p 61.

64. Faulkner, D.: 'Compression Tests on Welded Eccentrically Stiffened Plate Panels', Steel Plated Structures, Crosby Lockwood Staples, 1977, p 581-617.

65. Smith, C. S.: 'Compressive Strength of Welded Steel Ship Grillages', Trans RINA, Vol. 117, 1975, p 325-359.

66. Bjorhoude, R.: Deterministic and Probabilistic Approaches to the Strength of Steel Columns, Doctoral Dissertation, Lehigh University, 1972.

67. Perry, S. H. and Chilver, A. H.: 'The Statistical Variation of the Buckling Strengths of Columns', Proc. ICE, Vol. 61, part 2, March 1976, p 109-125.

68. Faulkner, D.: 'A Review of Effective Plating for use in the Analysis of Stiffened Plating in Bending and Compression', Jnl Ship Res., Vol. 19, no. 1, March 1975, p 1-17.

69. Sadden, J. A.: 'Primary Strength Design for Destroyers and Frigates', Steel Plated Structures, Crosby Lockwood Staples, 1977, p 658-675.

70. Faulkner, D.: 'On the Systematic and Random Uncertainties Associated with the Prediction of Ultimate Strength of Ships' (to be published).

71. Røren, E. M. Q. and Furnes, O.: 'Behaviour of Offshore Structures and Structural Design—State of the Art', BOSS '76 Conf. Trondheim, Aug. 1976.

72. Kaplan, P.: 'Development of Mathematical Models for Describing Ship Structural Response in Waves', Ship Structure Committee Report SSC-193, Jan. 1969.

73. Hogben, N. and Lumb, F. E.: Ocean Wave Statistics, HMSO, 1967.

74. Ochi, M.: 'On Prediction of Extreme Values', Jnl Ship Res., Vol. 17, no. 1, March 1973, p 29-37.

75. Hoffman, D.: 'Analysis of Measured and Calculated Spectra', UCL Conf. The Dynamics of Marine Vehicles and Structures in Waves, I. Mech. E, 1-5 April 1974, p 45-50.

76. Roll, H. U.: 'Height, Length and Steepness of Waves in the North Atlantic and Dimensions of Sea waves as Functions of Wind Force', SNAME T & R Bulletin no. 1-19 (translation from German), 1958.

77. Moskowitz, L., Pierson, W. J. and Mehr, E.: 'Wave Spectra Estimated from Wave Records obtained by the OWS Weather Explorer', New York University Research Division Report, Parts I, II and III, Nov. 62, March 63 and June 1965.

78. Faulkner, D.: 'Some Thoughts on the Nature of Hazards affecting Structures in Deeper Water', Jnl. Soc. for Underwater Technology, Vol. 3, no. 1, April 1977, p 16-21.

79. Clarke, J. D.: 'Factors Affecting the Long Term Statistics of Wave Loading', unpublished MOD(PE) Report, 1977.

80. Jensen, J. Juncher and Pedersen, P. Tendrup: 'The Effect of Non-linearities on the Probability of Failure of Ship Structures', The Technical University of Denmark, DCAMM Report No. 122, Aug. 1977.

81. Meek, M., Adams, R., Chapman, J. C. and Wieske, P.: 'The Structural Design of The O.C.L. Container Ships', Trans RINA, Vol. 114, no. 2, 1972, p 241-292.

82. Bishop, R. E. D., Price, W. G. and Tam, P. K. Y.: 'A Unified Dynamic Analysis of Ship Response to Waves', Trans RINA, Vol. 119, no. 6, 1975, p 363-390.

DISCUSSION

Mr J. F. Coates M.A., R.C.N.C. (Fellow): This is a valuable paper in that it addresses itself to a fundamental question of naval architecture and indeed of many other fields in engineering. I would like to underline one of the authors' conclusions in making one general point.

The identities of the naval designs taken as examples are obscure, and possibily deliberately so, but it is not surprising to me that they do not consistently follow any strength and loading criterion, logical or otherwise. This is simply because in practice there are, as I am sure every warship designer knows, many factors which cause a warship designer to depart from purely structural criteria in designing structures. For instance, a design of a ship may be volume-determined and there may be good reasons for maintaining a minimum thickness of plating greater than that called for by criteria for overall bending such as those considered so ably in this paper.

Such departures in practical design in no way diminish the importance, however, of striving for the soundest possible design criteria. Indeed, I believe that, paradoxically, if one

may say so, the very need to depart from them makes it more important that what has to be departed from has the greatest possible physical significance, so that the risk or penalty which is involved in the actual design decision may be properly appreciated.

We have adopted the approach which has been put to us this morning in the Ministry of Defence for warship design, but, following what I have just said, I expect that we shall continue to depart from it in practice! That will be not only for those reasons but also because, like most design concerns with responsibility spread over many years, we are very cautious, and I believe quite properly cautious, about changing from one design criterion to another. We shall certainly think twice about accepting a design which would be acceptable by the new criteria but which is a long way from meeting any old ones, illogical though those may be.

The authors are therefore absolutely correct in saying that any method adopted must at present be used comparatively, and in doing just that we are moving responsibly towards a more logically based design for structural safety.

Mr B.N. Baxter, M.Sc., Ph.D. (Fellow): The authors postulate two new approaches to ship structural strength and whilst there are weaknesses in the present traditional design procedures, there are too many unresolved questions in the present paper to allow me to accept either of the alternatives other than as a basis for discussion.

When considering the design of a ship, be it warship or merchant ship, one of the fundamental design requirements is the determination of a maximum stress level which is satisfactory to the designer and based on accepted calculations and experience.

In statical strength experiments carried out on warships, the final stresses at collapse for the USS PRESTON, USS BRUCE and HMS ALBUERA were 13·7 tons/in^2, 12·1 tons/in^2 and 17·08 tons/in^2 respectively. For the last ship, the ratio of stress at failure to design stress was 3·23. Similar experiments have not been carried out on merchant ships and, therefore, comparable values are not known.

However, calculated maximum design stresses for merchant ships would be of the same order and, even for larger ships, would probably not exceed 10 tons/in^2, particularly after reductions for the Smith correction. In addition, stresses recorded at sea indicate that values of more than 8 tons/in^2 are rare, even in bad weather.

In Section 4.1, the authors state that merchant ships are several orders safer than naval ships. The basis for this is quoted as:

(i) Still water bending moments for merchant ships vary considerably compared with those for naval ships.

This is true, but the total stress is composed of still water and wave bending stresses, the latter varying considerably with waves and weather, and there is no reason to believe that warships at sea are not stressed as highly as merchant ships.

(ii) Structural details are poorer in merchant ships than in warships and, therefore, structural fatigue can become a problem.

This is also true although Lloyd's Register of Shipping published in 1967 a guide to assist shipyard drawing offices, entitled 'Detailed Design in Ships'.

In addition, quality control in warship construction and greater attention to structural design detail result in a more efficient use of material. Nevertheless, the basic hull material is now similar for both types of ship.

Although naval ships have much thinner plating than merchant ships, the maintenance of modern naval ships is such that hull corrosion is almost non-existent. A corrosion allowance is included in the determination of the thickness of merchant ship plating and some decrease in thickness is permitted with age.

However, competition among the leading Classification Societies is intense and no Society willingly includes unnecessary material.

(iii) The capital investment is greater.

It is difficult to see the validity of this since a modern warship about 130 metres in length and 4,000 tonnes displacement now costs about £60M to build and equip and has a through life cost over 37 years of probably £300M. A 140,000 dwt bulk carrier costing about £30M to build will have a life cost over 20 years of about £100M.

Another reason why it is difficult to believe that merchant ships are generally several orders safer than naval ones is because of world shipping losses. The average tonnage lost annually for ships of 500 gross tons and above for the period 1972 to 1976 was 0·36% of the total world tonnage, i.e. more than 1 million tons.

Of 2,102 ships lost between 1969 and 1975, 7% were lost because of structural failure[83].

In 1977, of the 203 ships lost, 37 were lost because of weather, 25 because of founderings and abandonments, 41 because of strandings, 18 because of collisions and 65 because of fires and explosions. All of these were merchant ships, some new, and whilst fires, strandings and collisions can occur to both merchant ships and warships, it could be argued that had the merchant ships been stronger, the number under this heading would have been smaller.

If serious casualities, i.e. those causing pollution, are added, then for tankers of about 10,000 dwt and above, the average annual loss for the years 1968 to 1976 is 2·2% of the tonnage at risk, i.e. 4·84 million tons.

More information required to strengthen the arguments used in the paper should include:

(a) The measurement of waves and accompanying stresses in ships under severe weather conditions.

(b) An analysis of the recent stresses in warships in service using data between 1966 and 1978.

(c) The assumed factor of safety between design stress and stress at failure.

(d) The effect on the safety of structures of variances in the quality control procedures.

(e) The inclusion of dynamic effects among waves, including slamming.

One historical point may be of interest. The authors state that the Royal Navy first used the L/20 wave in 1893. In a paper[84] published in 1888, Bergstrom refers to ships 290 ft long and gives details of longitudinal strength calculations performed by Bureau Veritas for longer ships. The ships were assumed to rest on trochoidal waves with a length equal to the length of the ship and a height equal to L/20.

I agree in principle with the validity of a statistical approach to the determination of maximum bending moments and stresses but any long term values obtained by extrapolation must fit existing engineering standards.

Despite what might appear to be strictures in my comments, I enjoyed this useful paper and look forward very much to the next advance proposed by the authors.

REFERENCES

83. Hansen, H.R.: 'Structural Design—Safety and Reliability Considerations behind the Classification Society Requirements'. Proc. Second West European Conference on Marine Technology (WEMT 77) published by RINA.

84. Bergstrom, G.: 'The Structural Strength of Cargo Steamers'. Trans. NECIES, Vol. 5, 1888/9.

Mr R.A. Goodman, B.Sc., Ph.D. (Member): This is a very stimulating paper and it raises many questions which are of great interest to me.

I am in full agreement with the use of the general safety concepts which the authors have summarised, and, as the authors are aware, we in Lloyd's Register have been exploring such methods more or less continuously since about 1965. Murray's 1966 RINA paper[48], and several others published around that time, contained a great deal of the early work. In recent years, Lloyd's Register has moved a long way towards what the authors call 'second moment methods' and the 'fully statistical approach'[23,85]. The strength concepts outlined by the authors are certainly not novel as far as Lloyd's Register and several other Classification Societies are concerned.

In my opinion, there are two aspects which are causing great difficulty in practical application at the present time. First, there is no general agreement about how the various parts which make up the safety concept should be put together to form an application methodology which gives practical, stable and consistent results. The concept requires the use of, among other things, strip theory, a wave energy spectrum formulation to represent individual sea states, long-term sea state information, allowance for wave energy spread, ship speed, ship heading, etc. Nearly every worker in the field has his own ideas about each of these items, and the way in which they should be put together to produce a safety concept, and the results produced by each worker using apparently similar input rarely agree; all have good and reasonable reasons as to why their answers are the correct ones. The second aspect which is causing difficulty is the fact that, given any particular application methodology, small changes to certain input items will result in big changes in results. For example, many applications are strongly dependent on the most extreme sea conditions for some sea routes or sea areas. Estimation of extreme conditions is very difficult and, as the authors point out, is an item requiring particular attention. If we are to make significant progress towards practical day-to-day application, these two difficulties must be resolved.

With regard to the comparison presented in the paper of safety levels in naval and merchant ships, Dr Baxter has already covered far more ably than I can the arguments there. I would also suggest that the differences follow mainly because of the simplified and restricted strength model. When irksome practical difficulties such as corrosion rates, material quality variability and slamming effects are allowed for, as they should be, then the picture may not be so clear. There does not seem to be any good reason why similar ship types should not have a reasonably uniform safety index, but it is not clear to me why naval ships should have the same index as merchant ships, which is what the authors seem to be suggesting. In any event, I would wish to proceed on the basis of a more complete strength model than the one outlined.

It would seem to me that the main justification at this time for developing the type of strength models outlined is that they can embrace most aspects of strength in a comprehensive and logical way, and the practical means to make the concepts work are available. In my opinion, one of the main uses of the concepts at the present time is to employ them to gain an understanding of what aspects of ship structural design are important[23]. For example, the methods have been used recently in Lloyd's Register to investigate the effect on structural safety of ship construction tolerances[85].

REFERENCE

85. Goodman, R. A., and Mowatt, G. A.: 'Assessment of Imperfections in Ship Structural Design', Conference on the Influence of Residual Stresses and Distortions on the Performance of Steel Structures, Institution of Mechanical Engineers, London, October, 1976.

Mr D. W. Chalmers, R.C.N.C. (Member): I congratulate the authors on a very valuable summary of the position on design margins, and I agree very strongly with the need to rationalise margins—they are certainly not very rational at the moment, as is implied by the paper—and particularly the need for a simple design method that a designer can use.

The complete statistical method, even if we had enough data to make it usable at present, would be difficult to apply, because I do not believe anybody would ever agree on an acceptable probability of failure, particularly when human life is involved.

One of my tasks is teaching structural design to students at University College London, and in the lecture which we have on design margins both the methods touched on in this paper are discussed. The partial safety factor method always produces some amusement, because the assigning of values to the partial factors is as essentially subjective as assigning a value to the good old single safety factor. The other, and more important method I believe, the safety index method, goes down very well. It makes sense. The students all like it. One gets to the end and then has to let them down because there are very little data on which to base the coefficient of variation, especially the one on material strength. I make a plea then for more published data on material strength, in particular of made-up deck grillages.

I would, however, take issue with the authors on two points. First, in Fig. 5 they propose that a warship should have a lower safety index than a merchant ship. I cannot see that. As one of the purposes of a warship is to fight, strictly speaking it should have a higher safety index because in fighting it will lose some material, or is likely to do so; it carries around an enormous amount of very valuable equipment and it is desirable to get that equipment back to harbour again.

The second point, which is perhaps rather more contentious, is that I do not believe that we should be designing to the lowest acceptable margins to save weight and cost, which is what is suggested. In most warships and in many merchant ships the proportion of structural weight and cost to the whole is relatively small, so the savings in reducing margins are essentially in material. These will be small and, what is more, will tend to lead to a more complex structure. This structure is likely to be difficult to build and maintain. We should not be trying to aim to build ships like aircraft, with their attendant costs. I think that in the future we should be aiming towards simplification of the structure, to reduce labour costs, which are very high, and to allow for more use of automation. In this the margins may be higher, which will allow more room for error, there will be likely to be fewer modes of failure, and more chance of finding them. The cost of the extra material is very likely to be offset by labour savings through the life of the ship. For such a design the simplified safety index method which is proposed would be ideal; the balance of simplicity and complexity would fit well.

I think this argument also answers, or partly answers, another of the authors' questions on why merchant ships are safer than naval ones—that the market forces and perhaps to a lesser extent the Classification Society rules tend towards a simpler, stronger structure.

Professor G. Aertssen (Fellow): I see in Section 1.2 the following statement: 'The limit state considered is based on upper deck compression strength in the sagging condition'. I think that is right for many types of ships, but I have a feeling that it is not right for container ships.

If we calculate the longitudinal stress amidships on the main deck, we have to take account, first, of the stress due to waves and, second, of the still water stress. Now on the DART EUROPE[86] stress records were taken in extreme sea-states. I referred to the condition of that ship in a sea-state of 15 m significant wave height. The figure of 15 m is also the figure given in the Getz formula in Fig. 2 (effective wave heights). The worst record was published in a paper to the North East Coast Institution[87]. We transformed the stresses to the inertia modulus of the ship, so translating the stresses into longitudinal bending moments. We cali-

brated the ship, transferring ballast from forward to aft. After that, correcting the stress by means of the calibration results, the worst stress we obtained was 10 kg/mm². In this wave stress are included low frequency and high frequency effects. Adding to it 10 kg/mm² for the hogging stress due to still water conditions, we came to 20 kg/mm². At the time we thought that we should add 50% for the stress concentration effect, so we came to 30, and 30 is below the yield point of 36 so that we felt we were on the safe side.

This means that the worst state for a container ship is the hogging condition and not the sagging condition. On the other hand, it is true that damage may be caused by deck compression, and here I think about flare slamming. Indeed, flare slamming is bad. I agree on that. But the captain does not react to it. The captain does not, I think, bother about it. His speed is reduced in bad weather. He reduces speed when he feels concern for the longitudinal strength, so he reacts to the classic slamming of Ochi, and nothing else. Some naval architects feel that the captain should react also to flare slamming and they advise putting sensors on the fore deck, but I do not think that this is satisfactory. At any rate, the ship has to proceed in bad weather, and even buckling of the fore deck, in the absence of fracture, is not catastrophical.

REFERENCES

86. Ferdinande, V., De Lembre, R. and Aertssen, G.: Spectres de vagues de l'Atlantique Nord'. ATMA Bulletin, 1975.
87. Aertssen, G.: 'Reduced Draught at Sea: Its Problems'. Trans. NECIES, Vol. 93, 1976/77.

The Chairman, Professor J. B. Caldwell, B.Eng, Ph.D. (Fellow): I think it was Dr Goodman who expressed the view that there was almost too much in this paper, and certainly it is full of material for discussion, dealing as it does with the very essence of structural design and the philosophy which will underpin our design methods in the future. So I hope that those who have not had an opportunity to contribute verbally this morning will send their contributions in writing so that we can give this paper the thorough discussion which it deserves.

The authors have given us a very comprehensive presentation of what is still a relatively new philosophy of structural design. It is arguable—and this has been hinted in some of the comments made in discussion—that we might appear to be moving too quickly towards new and much more complex methods of structural design. It could be said, with justification, that the gap between people in the forefront of structural development and the users, particularly in the shipyards, appears to be widening. This may create problems for the future, and it certainly lends strength to the plea which Mr Chalmers has made for some effort to be made to distil from this paper some practical methods which designers can appreciate and readily apply. A first reading of the paper may well convey the impression that the probabilistic approach to ship structural safety is all too complicated; whereas I believe, as the authors do, that in principle it can offer a more logical and more consistent method for the design and assessment of marine structures. That the methods are still difficult to put into practice is a consequence of lack of statistical data rather than of inadequacy of the basic methodology.

It was very nice to hear Professor Faulkner in his presentation recall our association as colleagues some fifteen years ago at the Royal Naval College at Greenwich when we had many discussions about the then state of the art of structural design. It is a pleasure to see the work of our two authors now brought to such good fruition in this paper. I have no doubt that many of us will make much use of this paper in future, because it is a mine of information on the present position and philosophy in regard to reliability analysis of ship structures. It will, therefore be an extremely valuable contribution to have in our Transactions for which I express our grateful thanks to the authors.

The vote of thanks proposed by the Chairman was carried with acclamation.

WRITTEN DISCUSSION

Mr C. S. Smith, B.Sc., Ph.D. (Fellow): The authors have provided a useful description of the semi-probabilistic 'Level-2' methods of structural design and their application to ships. The comparative results shown in Fig. 5 and Tables II to X add most interestingly to those of Ref. 20, indicating a startling difference in safety levels between naval and merchant ships. Presumably Mr Sadden, as a naval designer, would stand by the adequacy of safety standards in existing RN frigates and destroyers; it would be interesting to hear the views of those responsible for merchant ship design practice (Classification Societies?) on the apparent conservatism of their position.

The writer is glad to see that the authors advocate a cautious approach to introduction of statistics into ship design (properly emphasised by their use of the words 'toward' and 'approach' in the paper's title) and agrees that a sensible approach is introduction of safety index and partial safety factor methods alongside traditional design procedures in the expectation that the former will evolve and in due course take over from the latter. This process will probably take many years. In the meantime it is desirable that design authorities should establish a formal framework of alternative Level-2 and Level-3 statistical design procedures, duly programmed for computers but with appropriate flexibility to allow updating, covering various forms of structural and non-structural failure in addition to the primary hull-girder bending failure mode discussed by the authors. (It will presumably be necessary to consider non-structural or semi-structural failure modes such as collision, fire, explosion and grounding together with structural modes in order to satisfy any requirement for net probability of non-occurrence of ship loss).

There is of course a danger, as statistical design methods become more familiar and readily applied, of their indiscriminate use on a 'black-box' basis leading to unsound design decisions. This seems clearly to have happened in the case of linear strip theory/linear superposition analysis as embodied in computer programs such as SCORES where, as the authors are no doubt well aware, quite undue credence has sometimes been given to long-term statistical estimates of extreme wave-induced loads without recognition of uncertainties regarding statistics of extreme wave conditions, non-linearity of ship response and slamming effects. The development of statistical design methods should perhaps be associated with a licensing procedure which confines their application in design to a limited number of qualified operators, all other prospective users (including of course the present writer) being confined to comparative studies and obliged to wear conspicuous L-plates.

Professor E. V. Lewis, M.S. (Fellow): This paper clarifies a number of areas in the field of ship structural safety, as well as making several new contributions. The favourable comments (Section 4) on work at Webb Institute[16,17,24] are greatly appreciated. Furthermore, we are gratified to find such a complete demonstration (Section 3.3.1.1) of the thesis that order statistics are not *necessarily* required to obtain a 'design extreme value'. (This actually contradicts the statement in Section 1.13 that 'to solve the lifetime extreme value problem ..... order statistics are required'. We have long maintained that the load or stress expected to be exceeded once in the lifetime of 100 ships (lifetime probability of 0·01) obtained from a cumulative distribution should be very nearly the same as the expected highest value in 100 ship lifetimes obtained by order statistics. In other words, the 'extreme probability density' distribution in Fig. 3 could be replaced

by the lifetime probability of exceedance. For in a given statistical population the highest value is the highest value no matter how one selects it. Hence, the suggestion at the end of Section 3.3.1.1 that applying order statistics leads to 'a more exact solution' is questioned.

This writer feels that, although we may not yet be ready to implement the 'Level-3' fully statistical approach, we should continue to press our efforts towards this goal. Referring to Fig. 1, the paper stresses that load and strength (or demand and capability) must be expressed in consistent formats, i.e., either probability per cycle of loading or per lifetime. The strength depends on factors involving the materials in the ship, the way it was built, etc., and hence varies from ship to ship but not with time for one particular ship (if one neglects corrosion and fatigue). Hence, the strength curve in Fig. 1 represents what may be called lifetime probability. Our statistical load data, on the other hand, are usually expressed as probability per cycle of wave bending. To convert the corresponding distribution function to lifetime probability one can proceed in the manner discussed in the preceding paragraph (equation (30) and Fig. 4).

If we attempt to follow the Level-3 approach (Fig. 1 and equation (3)) it is undesirable to simplify the loading information by utilising only a mean and c.o.v. (equation (32)). Furthermore, many of the random and systematic errors discussed in Sections 3.3.1.2 and 3.3.1.3 should already be accounted for in curve D of Fig. 1. Perhaps more rapid progress can be made by proceeding as suggested in Fig. 3—start with the 'objective' extreme probability density function (or lifetime cumulative probability) and then add the relatively small 'subjective' load variance to it.

At present it seems to be the strength probabilities rather than loads that are insufficiently well known to permit the immediate adoption of the Level-3 approach. However, this paper has advanced knowledge considerably—in particular by introducing the factor ζ_s which 'represents the margin between the moment at which compression collapse occurs in the weakest portion of the hull and the ultimate bending moment'. This is a significant factor and hence it seems to be rather unsatisfactory to assume a single value of 0·15 in all cases when studies show that 'in some special cases it was much more'. Furthermore, it is suspected that the coefficient of variation (Section 3.2.1.2) is actually significantly less for merchant ships than assumed in previous work[10,20] because of heavy plating and the difference between local bending and total collapse. It is hoped that work will continue in this area, differentiating among different types of ships and structural configurations.

A few comparatively minor comments follow:

Conventional approach (Section 2)

The concept of 'effective wave height' is not limited to the *maximum* bending moment in a ship's lifetime (see, for example, the scale in Fig. 2).

The American Bureau of Shipping has adopted a curve of effective wave height to be used in association with an essentially constant allowable stress (some variation occurs as a result of corrosion allowance effects). This trend is roughly comparable to the $0{\cdot}607\sqrt{L}$ curve in Fig. 2 but levels off above L = 225 m and is constant at 8·15 m above L = 305 m.

Random errors in load (Section 3.3.1.2)

Variation in spectral shape (item b) can be taken into account by using 'families' of measured spectra, not idealised 'two-parameter' formulations[17].

Furthermore, the difference between observed and significant wave height is not a direct source of error, and was not considered so in my earlier work[17]. One introduces a correction factor that is applied overall, and any variation in this factor is automatically taken care of by the wide range of wave heights included in a long-term calculation.

Systematic errors (Section 3.3.1.3)

There is some doubt that they are as large as suggested in the paper. They are all subject to accurate assessment by model tests, and therefore it should not be necessary to accept arbitrary values of c.o.v. as high as 0·17 to 0·20.

General remarks (Section 4.1)

Regarding changes from our earlier work[16,17], we have always made use of short-crested seas (item 6) in our research at Webb Institute.

In conclusion, it seems to me that the authors have made a great contribution to the structural safety problem by pointing out explicitly the many sources of doubt and uncertainty. Perhaps the greatest progress can now be attained by concentrating on obtaining realistic values for all these variations, taking into account differences in ship types and services.

Mr A. E. Mansour, Ph.D.: I would like to congratulate Professor Faulkner and Mr Sadden for this fine and interesting paper. I introduced the semi probabilistic safety analysis into ship design in 1974 by a paper published in the Journal of Ship Research (see Ref. 10) with application to 18 commercial vessels. The work was sponsored by the American Bureau of Shipping. I am glad to see now that, in the present paper, this approach is extended and further applied to five naval designs.

I do agree with Professor Faulkner and Mr Sadden that the time is right for the application and use of semiprobabilistic methods in ship design. On the one hand, when compared with the deterministic factor of safety used currently in design, the semi probabilistic methods offer the advantage of modelling explicitly the uncertainties associated with the design variables through coefficients of variation of the bending moment and hull strength. On the other hand, when compared with the fully probabilistic approach (Refs. 18, 19, 20) the semi probabilistic methods have the virtue of simplicity, and more importantly, do not depend on information that is not available at the present time. Specifically, information regarding the form of the long term distributions of the bending moment and the hull strength is not necessary. Such distributions seem to be controversial at the present time and may require years of data collection and analysis before their exact forms are known, particularly at the 'tails'.

In Fig. 5, the authors compare the safety indices of the 18 commercial vessels given in Ref. 10 with those of the five naval designs computed in their paper. I have noticed that the method of computing the required design parameters used in the semi probabilistic analysis and in equation (22) is slightly different from the one I used for the 18 vessels[10]. My concern is now, are we comparing these vessels on an equal basis? If the 'yard stick' is not exactly the same, this may explain, or have something to do with, the lower values of the safety indices computed for the naval vessels.

In my opinion, one of the most important considerations lacking in the current semi probabilistic methods is that there are no means available for combining the different modes of failure; something which can be done in the fully probabilistic methods. Combining such modes of failure and developing a safety index which reflects them can be a challenging task, but indeed deserves our attention and future effort.

Once again I congratulate the authors for an excellent paper which brings us one step closer to a unified approach to ship safety.

Professor Sir Alfred Pugsley, Kt, OBE, DSc, FRS: This paper makes proposals for another step forward in the 'tailoring' of the strength of a ship to meet its duties economically, and does so in a statistical form related to methods now coming into use in other branches of engineering. I hope with the authors that their proposals will commend themselves to ship designers for use, at the present stage, 'in parallel with current methods'.

I would, however, draw attention to a lesson of history in the matter of close tailoring of strengths to duties. Early aeroplanes were designed for strength to withstand particular manoeuvres, including acrobatic ones. It was only when large passenger aircraft came into being and were not, of course, required to be strong enough for such extreme manoeuvres, that it was realised that gust loads, previously 'covered' by manoeuvre loads, must be studied. In the same way, suspension bridges in the early decades of this century were progressively tailored to meet realistic traffic loads, and thus consequentially failed to provide the torsional stiffness to prevent flutter, which designers had either not thought of or had deemed impossible with such large and heavy structures.

I wonder if the authors would agree that ship designers should now look again at loading conditions *other than those linked directly with a ship's operational duties*. Recent tanker accidents make a layman, for instance, wonder if such long ships should have more bending strength to resist breaking under tidal and wave actions when caught at the bow upon beach or rock. And whether warships should have more reserve strength to complement their reserve buoyancy when holed; to minimise the chance, for example, of breaking in two when damaged as well as of sinking? Ship designers will think of better questions of this sort.

Mr J. C. Adamchak: In their closing remarks the authors indicate their feeling that the absence of any treatment of slamming represents the biggest shortcoming of the method presented. In this regard I think the authors should be particularly interested in some research in this area which has been carried out for several years and is currently continuing in the Structures Department of the David W. Taylor Naval Ship R&D Center. This research is directed towards the development of procedures and techniques for providing basic load information which includes the effects of both vertical and lateral low-frequency wave induced bending moments and vertical and lateral dynamic bending moments (whipping moments) due to slamming. This information is required for performing a variety of naval research and design tasks, such as (i) the determination of ship loading spectra for conducting fatigue crack growth and cumulative damage studies and model tests, and (ii) the prediction of maximum lifetime loads for use in the design of ship longitudinal strength members. The procedures developed to date were first applied to the determination of a lifetime load spectrum for a 90 ft Aluminium Ship Evaluation Model (ASEM) of a conceptual 300 ft aluminium naval vessel. The development of the load spectrum for this model is described in Ref. 88. At present, work is continuing in this area to generalise these procedures for application to naval ships in the 300 to 1000 ft length range. It is anticipated that a report on this subject will be available in the near future.

REFERENCE

88. Birmingham, J. T., Marchica, N. V. and Borriello, F. F.: 'Development of a Fatigue Lifetime-Load Spectrum for a Large Scale Aluminum Ship Model'. Paper presented at the ASTM Symposium on Service Fatigue Loads, Monitoring, Simulation and Analysis, Atlanta, Georgia, Nov. 14-15, 1977.

Dr Y. Akita: I would like to congratulate Professor Faulkner and Mr Sadden on their presentation of a quite interesting and suggestive paper on the recent design philosophy of ships. As a fellow researcher into the rational design of ship structures. I would like to ask just one question on this instructive paper.

The authors indicate the usefulness of the second moment method and introduce the concept of the partial safety factors which are considered to be easily adopted in practical design in shipyards.

I suppose, however, a method of obtaining directly the probability of failure by equation (3), in the fully statistical method as stated by the authors in Section 1.1.3 assuming the approximate probability distribution curves (one of them is a Gaussian) for the load as well as the strength is easy and useful in practical usage, since the value of the probability of failure seems to have clearer physical meaning than the partial safety factors.

I would like to hear the authors' opinion on such an approach.

Mr T. J. Cook, R.C.N.C. (Member): As pointed out in the paper it is important that design procedures are simple as well as soundly based. One reason for the move away from effective wave height calculations, which are simple to undertake, is the lack of theoretical support for the method. However alternative methods are often more time consuming in application. This explains the current interest in the Level-2 methods which represent a compromise between a simple and a theoretically justified solution. Looking ahead there would appear to be three alternatives for the designer:

(a) undertake strength calculations using Level-2 methods,
(b) progress to a Level-3 method which would seem to offer some theoretical gain at the expense of simplicity,
(c) return to a carefully selected effective wave height which would give strains that agreed closely with values measured on ships at sea.

From the designers viewpoint, alternative (c), which is simple to use and has a practical basis, would be an attractive solution.

The application of the Level-2 method seems to depend on the assumption that the distributions of strength and loading are the same in all structures. Is the strength distribution likely to be the same in warships (where, for example, torsional bending is not a problem, long stalk tees are used, etc) and merchant ships (where torsional bending is often a problem, long stalk tees are not used, etc)?

As explained in the paper, one of the weaknesses of the methods described is the absence of a treatment of slamming. It is hoped that the results of the present studies at University College London on the prediction of slamming bending moments will produce methods which can readily be combinded with the methods for predicting wave bending moments.

Mr C. V. Betts, M.A., M.Phil., R.C.N.C. (Member): The authors' case for an interim second-moment approach to an eventual fully rational structural design process is well argued. While some doubts remain for this contributor, the illustrative value and insight afforded by the proposed use of partial safety factors or safety indices are considerable, particularly when coupled with sensitivity analyses such as those shown in Section 3.3.4 and Tables VIII-X.

My reservations concern (i) the continuing large discrepancy in apparent safety of merchant ships and warships and (ii) the great dependence of the results of second moment methods on the design assumptions made.

(i) Relative safety of merchant and warships: the problems arising from the fact that the major differences between estimated probabilities of failure for merchant ships and warships do not seem to accord with experience were well covered in the discussion to Ref. 20. However, the credibility problem remains and I begin to wonder whether the 'safety gap' is due not only to the items discussed in Section 4.1 but also, in part, to the deliberate concentration on primary longitudinal strength. Perhaps the interaction between primary and secondary strength is significant in this context. Tankers have certainly suffered transverse strength problems in the recent past, so possibly the *combined* probability of longitudinal and transverse failure of tankers is closer to that of warships. This, if true, would further complicate the already difficult task of introducing probabilistic methods into structural design. I would welcome the authors' views, as I suspect this problem remains a significant obstacle to general acceptance of their proposals.

(ii) Second moment methods: the authors are undoubtedly right to try to find an interim design method for current use

that can be used to gather data for the next step towards a fully rational design process. Unfortunately, whether one uses partial safety factors or safety indices the resulting safety measure is highly dependent on the assumptions (in demand, capability *and* statistical theory) made in its derivation. Thus, as the authors recognise in Section 3.3.3.2, comparisons between different designs are meaningful only when accompanied by a list of the implied assumptions (this is true of present methods also, of course, but then the assumptions are more generally understood and accepted). One consequence of this is that proposed design curves such as the authors offer in Fig. 5 should surely be replaced by design 'bands', of considerable width! Indeed, despite the simplicity and greater 'purity' of the safety index, I think I incline marginally to the partial safety factor concept at this stage of development as having more intuitive 'meaning'.

Finally, if designers are to invest in the future and contribute to the next stage of progress some common pooling of data is presumably required. If the authors agree with this, perhaps they would suggest how it might best be done.

Mr J. Wolfram, B.Sc. (Member): I found this paper very interesting. The approach to safety suggested is a logical step forward which makes good use of the recent research contained in the extensive list of references.

In the final section the authors ask the question 'Why are merchant ships generally several orders safer than naval ones?' I would like to suggest three reasons why merchant ships should have a higher safety index, as calculated by the authors; and I would invite the authors' comments on these.

The first relates to the estimation of the coefficient of variation of the strength. The accuracy of the estimate depends on the amount of data available. So the greater the number of representative experiments performed, the greater the confidence in the estimate. This can be represented explicitly by 'confidence intervals'. If the data are, or are assumed to be, normally distributed, then a chi-squared test may be employed. Alternatively, if the distribution is only assumed to be finite then the 'jack knife' technique developed by Tukey (Ref. 89) may be used to give approximate confidence intervals. Applying these methods to the data given by Professor Faulkner[64] on the compressive strength of 13 nominally identical stiffened panels, for which the c.o.v. is 10·9%, the confidence intervals given in Table XI are obtained:

TABLE XI

	95% Confidence Intervals	
	Two-sided Limits	One-sided Limit
Chi-squared	7·8% < c.o.v. < 18·0%	c.o.v. < 16·5%
'Jack knife'	6·2% < c.o.v. < 16·2%	c.o.v. < 15·3%

These figures give a measure of the uncertainty of the c.o.v. of strength when using the amounts of data currently available. With more data the uncertainty is reduced, although after a while the law of diminishing returns sets in. On the other hand with very few items of data the uncertainty increases dramatically. The paper states the subjective c.o.v. is about 9-10%. Now as the objective parts of the c.o.v. are derived from relatively larger samples most of the uncertainty in the estimated c.o.v. is concerned with the subjective element.

The compression tests just referred to and the majority of other similar work have employed panels with symmetrical stiffeners of slenderness ratios representative of naval ship construction. In merchant ship construction unsymmetrical sections for deck longitudinals are very common and classification society rules make no explicit distinction between the two types. The buckling of the unsymmetrical section is a somewhat different problem from that of the symmetrical section (Refs. 40 and 90). Distortions during construction may also be different. Seah (Ref. 91) has collected data on the variation in 'uprightness' of unsymmetrical stiffeners as welded to plates. These show bias in one direction which may influence tripping. Hence the uncertainty concerning the subjective elements of c.o.v. of strength is greater for merchant vessels than naval ones. This uncertainty could be reflected in the greater safety index for merchant vessels.

Such a view ties in with the ISSC Design Procedure Committee's view that there should be some reward for increased knowledge and understanding of structural response[15].

The second reason for a higher safety index concerns the different loading pattern on the two types of vessels. Consider a partially laden cargo vessel in extreme seas. Here not only is the primary loading a maximum but so are most of the other design loads, particularly if the cargo comes adrift and is thrown around the holds. In such circumstances damage to transverse structure is likely. Now the longitudinal compressive strength depends very much on the support provided by the transverse structure[40,65]. Damage to transverse structure may reduce such support, increasing the effective length for buckling, and hence reducing the strength.

A naval ship designed 15 to 25 years ago would be designed to carry transverse loads from gun recoil and other loads imposed whilst in action. I doubt very much that naval vessels engage one another in extreme seas when they are in danger of breaking up. Hence the naval vessel is unlikely to be subjected to maximum loading from all sources in the same short time interval and damage to transverse structure when maximum primary strength is required is less likely. A larger safety index for merchant ships could reflect this difference in loading patterns. The factor of safety for the transverse structure could also reflect the role of contributing indirectly to primary strength.

The third reason for a higher safety index is concerned with the variation of strength of vessels in service. Classification society rules apply to a variety of ship types and sizes constructed using a variety of different methods and equipment all over the world. British naval vessels are designed on a 'one off' basis and are constructed in four or five British yards using similar techniques and equipment. Consequently, variation in strength about the designed level will be greater for merchant ships initially. In addition, maintenance and repair work for naval vessels is carried out at a few dockyards on a regular basis. Notwithstanding the classification societies' periodic surveys, maintenance of merchant ships depends very much on the shipowners' standards which are varied and the standards of the repair facilities employed which are also varied. Hence the variation in strength of merchant vessels towards the end of their lives is likely to be greater than for naval vessels. A higher safety index for Rule designed vessels would therefore seem logical.

REFERENCES

89. Mosteller and Tukey: 'Data Analysis and Regression'. Addison-Wesley 1977.

90. Bleich, F.: 'Buckling Strength of Metal Structures'. McGraw-Hill 1952.

91. Seah, A.K.: 'Ideal and Real Ship Structures'. M.Sc. Thesis, University of Newcastle, 1971.

Professor T. Moan: The authors are to be commended for taking up the important topic of rationalisation of the structural design of ships by introducing probabilistic formats. My remarks refer both to the probabilistic analysis for design and the more philosophical question of establishing the target safety level with reference to merchant ships.

Regarding the probabilistic formulation, its chief merit is that it allows all uncertainties/variabilities to be consistently taken into account. Paradoxically enough, one of the major difficulties with the approach is to identify and, in particular, quantify inherent, model and statistical uncertainties[92].

In connection with Section 3.2.1, I would like to know to what extent the authors think that fracture may occur before the longitudinal 'post-buckling' strength of real ships can be developed by redistribution of forces. In addition to the uncertainties mentioned in Section 3.3.1 associated with the ship loading process, the departure of the sea elevation process from the Gaussian character should be recognised[93]. This effect becomes great for seas of great intensity. The question whether there is an upper bound to the wave height and, hence, load effects then naturally arises. Also, the statistical uncertainty, due to limited data samples, e.g. for the short-term spectral and the long-term wave description has often been treated unfairly.

In the wave load effect analysis the necessity of considering the flexural behaviour of the ship in some cases must be noted. The load transfer model of slender ships should account for springing behaviour[94]. But, above all, the effect of ship handling on the response is emphasised. The effect of combining a system for hull surveillance and ship handling procedures is noted[95].

It would be interesting to know what advantages the authors see in deriving extreme load effects in the way they have in Section 3.3.1 compared to using order statistics.

The knowledge of uncertainties is often such that subjective (degree of belief) probabilities in a Bayesian framework must be applied. For instance, the captain's attitude towards avoiding heavy weather could be formalised in such a framework.

Following the arguments described in Section 1.2 the authors limit their discussion to the sagging 'jack-knifing' mode of failure. I feel that others may be important. If, for instance, designers simply design the ship deck and bottom for approximately equal safety, equal weight should be placed on the corresponding failure modes in the reliability analysis of the system. Furthermore, local failures, e.g. of hatch covers, cargo tank arrangements of LNG ships, etc. have proved to be, or may be, catastrophic and should be considered.

Let me start my comments on probabilistic design formats with some remarks on terminology. I do not agree that the Level 1 format, based on characteristic load effects and strengths is a first moment method (Section 1.1.1), when the special case of central safety factor concept is excluded. The partial safety factor method should be termed (semi-probabilistic) Level 1 method rather than a second moment method (Sections 1.1.2 and 3)[96].

As to the introduction of new design formats in codes I feel that the present lack of data, and the complexity of analysis in a consistent application of e.g. the Level 2 methods as compared to Level 1 methods for all modes of failure on all hierarchical levels of a ship structure suggest that the partial safety factor concept be applied in codes. However, the partial coefficients ought to be rationally derived so as to comply in a certain best way with a given safety level over a class of structures[97]. It is noted that the Danish code[98] allows an optional use of a Level 2 method.

The authors touch on the question of establishing the target safety level in Section 4. In the following I would like to comment on this interesting and complex problem.

The target safety level should, in general, be set on the basis of the objectives to codes, related to social, economic, legal, insurance and statutory criteria. The principal objective is to prevent fatal accidents. Considering that consequence of structural failure only, the target level, p, of the probability of failure could be set on an accident rate basis for workers in various, related industrial environments[99]. (The more general problem of finding the acceptable safety level in man's technical apparatus, of course, is beyond the jurisdiction of engineering). Now, by using approximate relations between p and the safety index, β, the target safety index can be obtained. This social criterion suggests that a uniform safety level is optimal. One commonly experiences, however, a risk aversion of the general public in the sense that the death of 10 people (or spillage of 10,000 tons of oil) in one accident in one year is worse than many incidents resulting in the same total consequences in the same period of time. This implies that the acceptable failure probability should be lower for vessels with the larger crew (holds). If the crew (amount of cargo which may cause pollution) increases with the size of the vessel (for a given type of ship), the target safety level should follow the trend of the 'notional' safety level in Fig. 3. (Obviously, the argument presupposes that risk is 'rational', and, hence is to be accounted for). The target safety level should also depend on the actual relation between structural failure and the consequences of the actual failure, as implied, for instance, by the type and number of compartments into which the ship is subdivided, the efficiency of the life-saving equipment etc. On the other hand, I feel that the target safety level should not depend upon the effect of corrosion (mentioned in Section 4.2) which ideally should be reflected in the probabilistic design by accounting for its variability.

Alternatively, an economic code objective based on a minimisation of total costs comprising initial costs, capitalised expected maintenance and direct and indirect failure costs, may be introduced. In this context it becomes important to include the whole spectrum of local and global failures and unserviceability modes such as those caused by fatigue. The occurrence of small cracks, which are seldom catastrophic, may have a considerable influence on maintenance costs[100]. Clearly, the rationalisation effort will be very complex in this case.

Consider the simple case where the initial cost, C_I, varies linearly with the logarithm of the probability of failure, ln p_f, associated with a single failure mode. The optimal (target) p_f — level is then equal to the slope of the C_I — ln p_f curve divided by the capitalised failure cost, C_F. The absolute level of initial investment itself does not enter the criterion.

Applying the economic principle to the component design of a system results in the intuitively reasonable conclusion that the probability of failure should be smallest for components which have a significant effect on the system safety but involve relatively small initial costs. Of course, the allowable safety level should also, in principle, depend on the degree of system redundancy in cases where the code design check is carried out for individual components.

The cost-benefit characteristic of e.g. a hull surveillance system may be investigated in the socio-economic optimisation framework. The system is advantageous if the cost of equipment and its operation is less than the expected saving of maintenance and failure costs of the ship.

Because the loss of reputation of the parties involved is greater when the failure is due to material or fabrication defects than extreme loads, it has been proposed[101] to let the target safety level increase with the dead/live load ratio. For ships the required safety level, therefore, should increase with the still-water/wave load ratio.

There are a number of difficulties with the application of the economic optimisation approach. One is the assessment of intangibles such as the loss of life and loss of reputation, confidence, etc. The principal consideration of loss of life, however, should be reflected in a constraint on the risk level according to the social criterion mentioned above. The value of life, as given by insurance, courtroom compensation findings etc. could be included in a socio-economic optimisation. Another difficulty with the rationalisation of safety is gross errors associated with human decisions in design construction and operation. They cause the majority, say 90% or more, of the accidents[102]. Flint[99] suggested that the 'true' probability of failure be obtained by multiplying the 'notional' probability of failure (as calculated on the basis of identifiable uncertainties) by a constant, say, of 10 or greater. This is, however, only a partial solution. If the 'true' probabilities are not estimated in some acceptable manner, the optimisation cannot be other than a suboptimisation. Therefore, an important area for study should be 'human reliability' and its dependence upon organisational and administrative procedures etc.

Clearly, the deficiencies of current reliability methods and data indicate that they should not be followed blindly.

The methodology is just another tool to translate the physical environment into a designers 'feel' for the problem and improve his engineering judgement to rationally control the risk problem. An additional benefit is a clearer insight into the relative effect of uncertainties and variabilities of load effects and strength, control and inspection procedures etc. This information can, among other things, be used to direct research to maximise the improvement in predicting structural performance.

REFERENCES

92. Benjamin, J. and Cornell, C. A.: 'Probability, Statistics and Decision for Civil Engineers'. McGraw-Hill, 1970.

93. Moan, T.: 'Structural Aspects of Floating and Fixed Offshore Structures'. Proc. Int. Seminar on Safety of Structures under Dynamic Loading, TAPIR, Trondheim, 1978.

94. Skjørdal, S. O.: 'A Rational Strip Theory Approach for the Evaluation of Springing'. Division of Marine Hydrodynamics, The Norwegian Institute of Technology, 1978.

95. Lindeman, K. and Nordenstrøm, N.: 'A System for Ship Handling in Rough Weather'. Proc. Fourth Ship Control System Symposium, Royal Netherlands Naval College, Vol. 7, 1975, 45-68.

96. Proc. Second Conference on Structural Safety and Reliability, Technical University of Munich, 1977, published by Werner-Verlag, Düsseldorf, 1977.

97. Lind, N. C.: 'Reliability-based Structural Codes Optimisation Theory and Practical Calibration'. Proc. Int. Seminar on Safety of Structures under Dynamic Loading. TAPIR, Trondheim, 1978.

98. Nordic Committee on Building Regulations. Proposals for safety codes for load-carrying structures. NKB Draft 74-10-04, October 1974.

99. Flint, A. R.: 'Design Objectives for Offshore Structures in Relation to Social Criteria'. Proc. Conference on the Behaviour of Offshore Structures. The Norwegian Institute of Technology, Trondheim, 1976, 574-578.

100. Lewis, E. V. et al.: 'Load Criteria for Ship Structural Design'. Ship Structure Committee Report, SSC-240, US Coast Guard Headquarters, Washington D.C., 1973.

101. Sexsmith, R. G. and Lind, N. C.: 'Policies for Selection of Target Safety Levels'. Proc. Second Conference on Structural Safety and Reliability, Technical University of Munich, 1977. Published by Werner-Verlag, Düsseldorf, 1977.

102. Cashman, J. P.: 'Analysis of World Merchant Ship Losses 1967-75'. Proc. Second West European Conference on Marine Technology, Safety at Sea, May 1977, London. Published by RINA.

Mr J. Odland: This is a very interesting paper giving a systematic presentation of different safety concepts. When it comes to application, however, the lack of relevant data is always an obstacle for reliable conclusions.

The general strength model which is defined by equation (17) is very interesting, but it should have been supported by a more detailed discussion and argumentation. Whether it is optimistic or not depends on the choice of numerical values for the coefficients. As used in the paper they seem to be chosen rather arbitrarily. This is of course due to lack of available data, but the parametric study (Table X) demonstrates very clearly that the theoretical safety index is very sensitive to this choice. The systematic error due to use of idealised design codes has been given a value which is quite significant because as it stated, practical structures will generally be stiffened by secondary structure. Although this is correct in many cases, it should also be kept in mind that the many irregularities and details in actual ships may initiate yielding or cracking due to insufficient local deformation capacity, which has the opposite effect.

These arguments are also relevant to the safety margin which arises from redistribution of stresses after initial buckling. It does not seem quite reasonable to justify the use of unconservative coefficient by taking into account any possible conservatism in the load representation (Section 3.3.4.3).

Interframe buckling of deck only has been considered. This is often the most interesting mode of failure and it is probably also most convenient for analysis.

However, many ships, including warships (Section 3.3.1) may be designed with still water hogging moments even in the loaded condition. This fact tends to increase the probability of the additional and more complicated modes of failure:

(a) tensile failure modes in the deck,

(b) compressive failure modes in the bottom structure.

When this has been mentioned, it is even more interesting that the five warships with their low safety margins have been operated successfully. According to this paper, merchant ships are designed with considerably larger safety margins. Some possible reasons for this have already been suggested by the authors. It should also be mentioned that the experience with wave-load predictions for extremely large ships is limited, and that the wave-loads also depend on the operation of the ships (contrary to the situation for fixed offshore structures).

Ships designed according to rules are assumed to be given an 'ordinary seamanlike' treatment. By various manoeuvres it is possible for the navigator to reduce ship motions and thereby possibly also the stresses.

This is much more difficult with large ships where the contact between ship and navigator has deteriorated. The consequences of cargo outflow from damaged oil tankers or LNG carriers may also be so serious that an increased safety margin should be required.

Considering the partial safety factor approach, the coefficient γ_S could be used for differentation here.

Uncertainties associated with dynamic loads are generally larger than uncertainties associated with capability. Most of the shortcomings of existing methods for wave load predictions have been well described by the authors. The longitudinal stresses may also be affected considerably by hull openings, superstructures, action of horizontal bending moment and wave-induced hull vibrations. It is quite obvious that a hull surveillance system with instrumentation for direct measurement of stresses would represent a large step in the direction of the elimination of such uncertainties.

Such a system can also help to re-establish the contact between navigator and ship. In principle, all uncertainties regarding the theoretical response analysis could be eliminated, and only questions regarding stress measurement devices and extrapolation of measured stresses would remain. The possibilities of such a system have been discussed in Ref. 103.

A significant reduction of the safety margins of merchant ships as indicated in the paper, Fig. 5, can hardly be recommended without the use of such systems which not only give warnings during operation, but also increase the information about sea loads.

REFERENCE

103. Lindemann, K., Odland, J. and Strengehagen, J.: 'On the Application of Hull Surveillance Systems for Increased Safety and Improved Structural Utilization in Rough Weather'. Annual Meeting, SNAME, New York 1977.

Mr E. P. Wierzchowski, Dr Techn.Sc.: It is my pleasure to comment on this valuable paper, which really is a step ahead in the practical application of semi-probabilistic methods to the safety assessment of ships.

I share the authors' opinion that the so-called second moment methods, which were advocated by ISCC more than ten years ago, are the most promising and tractable for the practical design of ship structures. These deterministic formats for the probabilistic design of structures have recently acquired a more axiomatic background—an outline of theory of structural design codes—due to the works of Lind, Cornell, and Murzewski et al[104].

As far as the comparison between safety levels for naval and merchant ships is concerned, as given in Fig. 5, I would hesitate to draw any firm and general conclusion as to excessive levels of safety for merchant ships. First of all because it is not true that the upper deck inelastic buckling is the lowest, or the most likely, mode of failure for merchant ships. It may be, at the most, true when failure modes which do not involve fracture only are considered, but not for all possible modes, which should be taken into account.

In fact, in all the 40 merchant ships that have broken in two parts in the last three decades, failures had started in the tension flange of the hull girder and were caused by brittle fractures triggered by structural discontinuities or by fatigue cracks.

On the other hand all reported buckling damage in modern large merchant ships was of the local type in webs of deep frames, frame corners, bulkhead plating etc. Moreover, even fast cargo ships in the length range L = 140 – 160 m, which did suffer buckling damage in the deck and side structure[105] and which more nearly resemble the naval ships analysed in the paper, would presumably show a sufficient level of safety within the presumptions adopted by the authors, i.e., taking into account the low frequency wave load and the midship hull structure only. The real type of failure for these ships is mainly governed by the bow impact and slamming loads and the distribution of 'capability' and 'demand' along the ship hull, i.e., by factors not included in authors' analysis.

In fact, one should not worry about the compressive strength of the hulls of other current merchant ships, even for poorly designed structure; other modes of failure like brittle fracture or combined fatigue and brittle fracture constitute a more real danger[106]. Therefore the nominal stress level is to be limited because of the possible occurrence of cracks. How to implement the above philosophy in the rules of a classification society with the use of modern analytical tools has been clearly demonstrated elsewhere[107].

For the naval ships considered, the 'gap' between the fracture involving modes of failure and the buckling modes may be far smaller due to higher standards of strength and of notch toughness of the materials used, better workmanship and more careful design of structural details, which allow higher nominal stress levels and in turn result in smaller structural scantlings and relatively lower buckling properties.

In conclusion the structural safety of modern ships is such a complex matter involving, apart from quantifiable factors, so many important but as yet unquantifiable ones (based mainly on the feed-back of information from service), that any practical method of assessment of ship structural safety should reflect all this complexity and previous experience. In this context the authors' proposals regarding the minimum acceptable values of safety indices, as shown in Fig. 5, seem to be premature—at least for merchant ships. They are too incompletely evaluated and too arbitrarily outlined to be accepted as a sound basis for the assessment of the longitudinal strength of the hull girder.

Nevertheless I would like to congratulate the authors on their very interesting study of the application of modern methods to ship structural design and their courage in presenting such a discussion-provoking paper, which is indispensable for any progress.

REFERENCES

104. 'Stochastic Structural Mechanics'. Lectures given on Conf. on Stochastical Methods in Structural Mech., Jablonna, June 1972, Edited by J. Murzewski, Polish Academy of Sciences, Ossolineum, 1973.

105. McCallum, J.: 'The Strength of Fast Cargo Ships'. Trans. RINA, Vol. 117, 1975.

106. Nibbering, J. J.: 'Permissible Stresses and their Limitations'. Ship Structure Committee Report SSC-206, 1970.

107. Spinelli, L.: 'A Few Notes on RINa Rules 1971 considered in the Light of the Present Knowledge on Ship Structural Design'. Technical Bull. of RINa No. 46, July 1971.

AUTHORS' REPLY

Looking back at the discussion six years ago of Ref. 20 (Mansour and Faulkner) to which this paper may be considered a sequel, we are struck by several facts. Both papers attracted a wide ranging discussion (18 contributions in each case) of generally high quality which appreciably enhanced the paper's value. For this we are grateful and encouraged. Neither paper was intended or claimed to be comprehensive, merely illustrative. Similar calculations, for example, must be done for each one of the other significant failure mode and load combinations in each of the critical regions of the primary structure. Both papers mentioned the importance of other factors, such as fracture, costs, etc., which could not be considered because of the need for reasonable brevity. Some of the former omissions we shall cover in reply; elsewhere, where we make no comment, it may be assumed we generally agree with contributors' remarks. In this respect we are particularly grateful to Mr Coates for his words of wisdom.

The authors are encouraged by the general belief, by all except one contributor, that some form of reliability method is now desirable in ship structural design. However, to take up a point mentioned by the Chairman, Professor Caldwell, we would be discouraged if the gift of gradualism, which is so frequently paraded as the naval architect's sheet anchor, impedes progress under the respectable guise of 'caution'. It seems to us that caution should be exercised in two ways:

(a) in the methods one uses, and

(b) with the final check on scantlings to see if they make engineering sense.

We believe that excessive caution in (a) can be bad if it impedes progress, as it frequently does, whereas caution is often insufficiently exercised in (b).

It is highly desirable that design methods and codes match our improved knowledge, otherwise we will not achieve a better blend of adequate and reasonably uniform safety with best economy which should be the fruit of our labours. Reliability indices defined by use of second moment information have been used for the last decade within safety code committee work in other fields. So let us advance with these improved methods used alongside the old, and in the process equip ourselves with better understanding and data with which to tackle new problems for which there may be no past comparisons.

Revised and additional naval data

At the time the paper was prepared the extrapolations from measured statistical strain gauge records made by the senior author were from readily available reports. For a variety of reasons NCRE subsequently re-appraised these records and discarded much of their earlier data as being of limited validity, for one reason or another. Since Dr Baxter has raised the question of measured bending stresses, we present this revised data and 5% characteristic partial safety factors

TABLE XII: Naval Designs: revised stress (N/mm²), effective wave height (m) and partial safety factor data based on a re-appraisal of measured strain data; theoretical partial safety factors for 5% characteristic values

Designs	A	B	C	D	E
Measured wave induced stress extrapolated to a return period of 3000 days (to be compared with Table II line 4)	211	148	95	82	123
Corresponding effective wave height (to be compared with Fig. 2)	7·7	6·9	5·6	6·9	8·3
Theoretical 5% characteristic strength (N/mm²) (Table III line 5)	222	201	169	178	222
5% characteristic total bending stress extrapolated from statistical strain data	244	159	96	97	151
Partial safety factor γ_0 based on statistical strain data	0·91	1·26	1·76	1·84	1·47
Theoretical 5% characteristic total bending stress $p = 1/20 \times 3 \times 10^7$	273	215	158	126	168
Partial safety factor γ_0 based on strip theory predictions	0·81	0·94	1·07	1·41	1·32

in the top part of Table XII. The bottom part of the table gives theoretical psf values for comparison. It will be seen that psf's based on measurements range from 0·9 to 1·5, whereas theoretical values range from 0·8 to 1·4. The agreement of these ranges would seem to be encouraging but may be fortuitous in view of the relatively poor agreement for individual designs. In both ranges values less than unity exist in supposedly successful ships.

The data based on revised measured strains go a long way towards explaining the apparent discrepancy for Design E between the high theoretical safety index ($\beta_f = 3{\cdot}1$) and the very severe effective wave heights (11·3 m) shown in Fig. 2—the revised value of the latter is 8·3 m. If Fig. 2 were adjusted in accordance with the revised strain gauge data ship A would then stand out as an unusually high equivalent wave height for its length. This, however, can be explained by referring to the particularly stormy waters in which this class of frigates were operating during the period when strain gauges were fitted.

This illustrates the, perhaps obvious but sometimes overlooked, sensitivity of extreme wave loads and hence of actual safety levels to the zones of ship operation. For this purpose a simple effective wave height is inadequate. Thus for critical designs reasonably realistic mission profiles are important. In this respect most of the naval designs were originally conceived for a less arduous world wide mission profile than that in which they now find themselves. Naval ships used to operate for extended periods east of Suez, whereas nowadays, operating more as a NATO force, they experience a greater content of North Atlantic and North Sea conditions. However, this is not a contributory reason for their lower safety against upper deck failure, as demonstrated in this paper, since comparisons with merchant ships have been made for similar mission profiles.

The Strength Model

We are pleased to provide Mr Odland with a fuller justification for equation (17). This strength model is a very minor extension only to the popular equation (13) in that it is based on the expression

$$M_u = Z\,\sigma_u\,(1 + \zeta_s) \tag{34}$$

ζ_s is the cross-section systematic error which we believe is explained fully enough in the paper. We agree its choice is arbitrary without further research work, but it seems important for designers to appreciate that it can be a significant factor. The curly bracket term in equation (17) is $\bar{\sigma}_u/\sigma_y$ and endeavours to allow for the effects on $\bar{\sigma}_u$ of the systematic errors in yield strength (σ_y) and compression strength (ϕ) over a range of relevant slenderness parameters likely to be used in practical designs. We assume that the systematic errors in scantlings are negligible and that σ_y and ϕ have corrections for systematic errors defined by mean as-built values

$$\left.\begin{aligned}\bar{\sigma}_y &= \alpha_y\sigma_y\\ \bar{\phi} &= \alpha_c\phi\end{aligned}\right\} \tag{35}$$

where σ_y and ϕ are nominal values used in design. We have previously[39] defined compression strength as

$$\sigma_u = \phi\sigma_y \tag{36}$$

Let λ be a general slenderness parameter for compression strength and assume it is a function of scantling slenderness and proportional to $\sqrt{\sigma_y/E}$. Test data for most compression modes of failure suggest that a reasonable approximation to elasto-plastic collapse is given in the design range by

$$\phi = 1 - k\lambda^2 \tag{37}$$

A typical example is $k = 0{\cdot}25$ for the Johnson parabola defining column collapse in the range $1 \geq \phi \geq 0{\cdot}5$. A similar expression could be used, slightly conservatively, for other modes of failure. If we consider first the effect of the systematic error in yield strength this will alter the slenderness parameter to a truer mean value $\bar{\lambda} = \lambda\sqrt{\alpha_y}$. These two changes will in turn alter the mean compression strength. From equations (36) and (37)

$$\bar{\sigma}_u = (1 - k\bar{\lambda}^2)\,\bar{\sigma}_y = (1 - k\bar{\lambda}^2\alpha_y)\alpha_y\sigma_y$$

To eliminate $k\lambda^2$ use equation (37) again to give

$$\bar{\sigma}_u/\sigma_y = \{1 - (1 - \bar{\phi})\alpha_y\}\alpha_y \tag{38}$$

Now consider the effect of the systematic error in compression strength by substituting $\bar{\phi}$ from equation (35) to give

$$\bar{\sigma}_u/\sigma_y = (1 - \alpha_y + \alpha_y\alpha_c\phi)\alpha_y \tag{39}$$

which is the curly bracket term in equation (17). Two of its virtues are that it requires no knowledge of cross section slenderness parameters and it does compel the designer to think seriously about ϕ.

The Loading Model

There were few comments on the load prediction method used. This is probably a reflection of the fact that the techniques used are now common place, even if they are seldom applied as a matter of routine.

Dr Goodman pointed out the difficulties inherent in applying techniques which require the selection of appropriate wave statistics, energy spectra, and course and speed statistics, when apparently small changes in certain inputs result in much larger changes in final predictions. Whilst these are real problems (they could easily account for subjective uncertainties in loading of greater than the 18% referred to in Section 3.3.1.2) the authors do not believe that we can afford to wait until every worker in the field is agreed. For many years to come it will still be necessary to make more or less arbitrary selections, relying on comparison with successful past practice and assessments of the degree of uncertainty in each set of data to ensure safety. It is appreciated that this is probably easier for a centralised organisation like the Ministry of Defence than for classification societies that have to operate worldwide.

Professor Aertssen takes us to task on our bald statement that the most likely mode of collapse is in the sagging condition. The statement is certainly true for the warships studied and is true for most of the merchant ships studied earlier. However, it is acknowledged that hogging still water bending moments in many merchant ships are enough to swamp the effect of sagging wave-induced bending moments being higher than hogging wave-induced moments. Even so it is arguable that in a rational design code the strength of the lower flange of the hull girder should always be significantly higher than that of the upper flange: after all there are no stability penalties associated with strengthening the bottom and it has to withstand much higher transverse loads, more severe corrosion, and grounding damage. We will return to this topic later in the discussion.

Professor Aertssen also refers to slamming and distinguishes between the response of masters to slamming of the keel or the flare of the bow. His remarks emphasise how important it is that any rational design procedure includes the effect of slamming *and the response of ships' officers to that slamming*. The authors, therefore, look forward to the day when the work of Birmingham et al[88], so helpfully mentioned by Dr Adamchak, and of Bishop et al[108] can be matched by a better understanding of human reactions.

Dr Smith points out the dangers of indiscriminate use of linear strip theory and wave statistics without regard for the limitations of the theory used or the uncertainties associated with the statistics of extreme waves. This is a danger associated with any change of technique. (As Mr Betts points out, more traditional methods are equally dependent on only partially justifiable assumptions but at least traditional assumptions are usually well understood). The authors believe the potential dangers can be overcome if, as Dr Smith suggests, new methods are introduced alongside old ones. In the final analysis, however, everything depends on the integrity and competence of the designer, and it is hoped that this paper has helped by describing the limitations and quantifying the uncertainties associated with the methods used by the authors.

Professor Lewis raises the question of the need for order statistics in extreme bending moment analysis. He is right in believing they are not needed, and we apologise for the confusion caused. In Section 1.1.3 we should have said 'order statistics *may* be used'. Insofar as no one has yet demonstrated that the use of order statistics is more exact than that used in the paper we would agree that our last sentence in Section 3.3.1.1 may be incorrect. However, if high probabilities of exceedence were used, for example, 0·1 or more, then we believe the use of order statistics *may* be more accurate. But in essence, and for all practical purposes, we agree with Professor Lewis.

Professor Lewis suggests that the subjective variances in loading are small. The authors cannot agree—subjective load variances, however assessed, are at least as great as objective variances, and are probably much greater. Although the use of families of spectra[75] rather than idealised formulations can reduce the degree of pessimism (the systematic error) that is built into the method used by the authors (see Table VI) such changes cannot reduce the subjective uncertainty of 17-20% which is mainly a result of the paucity of data on extreme wave heights, wave spectra in extreme conditions, and the statistics of ship handling. Nor can this uncertainty be reduced by model testing since it is almost entirely due to environmental factors.

Mr Cook wonders whether the complexity of statistical methods is worthwhile, especially in respect of bending moment predictions, and suggests the use of a modernised equivalent static wave for design purposes. This would certainly eliminate the problems of the choice of statistical data referred to by Dr Goodman, but it is not favoured by either of the authors. It is inconceivable that future developments in load prediction will be based on anything but some form of spectral analysis and all rigorous analyses must recognise the random nature of environmental forces. Whilst an equivalent static wave can be devised to give moments which correspond to those derived by strip theory and wave statistics, it would be incapable of further development: thus it is the opinion of the authors that now is the time to become familiar with the more comprehensive methods which, hopefully, can be gradually modified as our understanding of the nature of wave-induced loads advances.

Mr Odland mentions the importance of seamanship in reducing wave loads on ships and draws attention to the dangers in very large ships where, perhaps, loads are larger than the motions of the ship would suggest. (These dangers could be even more pressing in vessels with the bridge well aft). The authors believe that a significant proportion of the subjective uncertainties associated with loading are caused by the different responses of different mariners and thus Mr Odland's interesting suggestion of a stress-monitoring system might well reduce the c.o.v. of the demand. However, the complication may not be worthwhile: for Frigate B *if* subjective uncertainties could be halved by such a surveillance system v_d could be reduced to 0·11 and thus β_f increased from 1·4 to about 1·5; for the equivalent 'Rule' design frigate the changes would be from 3·5 to about 3·9.

Comparison of Merchant Ships and Naval Vessels

Dr Baxter was the first of many contributors to question the truth of the finding that there are far greater reserves of strength against upper deck compressive collapse in merchant ships than in warships, quoting casualty statistics in support of his arguments. Unfortunately these statistics do not distinguish between different modes of failure and therefore cannot be used to test the validity of the paper. It must be re-emphasised that the paper related to the rather specialised topic of upper deck compressive collapse at amidships only and it is certainly not the authors' contention that merchant ships are much stronger than warships in every respect. Indeed it now appears that safety indices for the outer bottom structures of merchant ships could be as low as those for the upper decks of frigates.

Dr Baxter seems to be in agreement with the authors' views that differences in still water loads, structural details, and capital investment do not justify the large differences in strength discovered. It is, however, worth qualifying his comments on capital cost by pointing out that his comparison does not include the value of the cargo, nor does it allow for the far greater numbers of merchant ships built—these factors must be taken into account when investments at risk are compared.

Dr Goodman questioned why warships and merchant ships should have the same safety index, even if a more comprehensive analysis were used. We were not, in fact, suggesting that the two types should share a common safety index: apart from different standards of construction and maintenance, the size of the world merchant fleet would indicate the need for a somewhat greater level of safety, and this is reflected in the proposals on Fig. 5. No, the aims of the paper were to demonstrate the need to take the various uncertainties that confront the naval architect into account when specifying strength requirements, to suggest how this might be done, and

to question the justification for such very wide differences between the criteria being applied to the upper deck strength of merchant ships and warships.

Mr Chalmers suggests that the safety indices for warships should be higher than those for merchant ships to take account of the possibility of action damage. However, the authors consider that if one were to do that one would be designing against the simultaneous occurrence of two very, very rare events—a point made in a slightly different context by Mr Wolfram. If it were wished to make special provision for action damage, the authors would suggest a procedure along the lines of that devised for assessing the adequacy of the stability of warships[109]: that is to say, the strength of the hull after damage would be compared, not with the most probable extreme bending moment likely to be experienced in 20-30 years, but with the most probable extreme bending moment likely to be experienced in the few weeks it might take to return to harbour.

Mr Chalmers also suggests that we should be proposing higher safety indices in order to encourage the design of simpler and cheaper structure. In fact, the reverse would be the case. With a safety index of 1 to 2 one has the choice between lightweight but complex structure or moderately heavy but simple structure: with a safety index of, say, 3 to 4 the choice would be between complex and moderately heavy structure or simple and very heavy structure. Only in those ships where weight was of no significance at all would it be possible to afford simple structure.

Dr Mansour rightly points out that there are differences between his 1974 analysis[10] and the analysis used in the present paper. Whilst the yardsticks are not exactly the same, the differences are not great enough to invalidate our findings. This is discussed fully in Section 3.3.3.2.

Mr Betts suggests that the differences between the safety indices of merchant ships and warships result from our concentration on longitudinal strength. He goes on to suggest that if transverse loadings were taken into account calculated probabilities of failure of the two types might be much closer, thus correspnding better with actual loss rates. The authors agree that this could well be the case. However, except in way of the double bottom, this may not prove to be an undue complication: the interaction between transverse loads and longitudinal strength has been found to be slight in single-skin warships[69] and it is believed that the same is true for merchant ships—certainly classification society rules *appear* to treat the two loadings separately. There then remains the problem mentioned by Dr Mansour of the choice of safety indices to guarantee acceptable combined probabilities of failure, but this is, in principle, no more difficult than choosing two independent safety factors—one for longitudinal strength and one for transverse—as is done at present. Further remarks on the extension of the philosophies described to other load cases are included later in the reply.

Mr Wolfram's remarks on confidence limits for strength are noted and agreed. He lists three reasons why merchant ships should have higher safety indices than warships

- because of the use of unsymmetrical sections
- because the possibility of damage to transverse structure by cargo in heavy seas may reduce longitudinal strengths
- because of the supposedly reduced degree of control during design, construction and service.

With regard to the first of these points, it is true that the strength model did not take into account torsion buckling. On the other hand, the authors do not believe its inclusion would significantly affect their findings since a structure fabricated of Tee-bars will, in most circumstances, be no less likely to suffer a torsional form of collapse than a structure fabricated of bulb-flats. In other words, the bulb-flat is no more inefficient in torsion than it is inefficient in flexure.

The authors would certainly agree with Mr Wolfram's second point that the transverse structure of ships is crucial in the maintenance of longitudinal strength. However, they would suggest that this problem ought to be tackled directly by appropriately high safety indices for the transverse structure rather than by increasing longitudinal strength to a degree that is bound to be somewhat arbitrary. Admittedly superficial and limited studies by the authors suggest that the safety indices for the transverse strength of merchant ships and warships are more comparable than the corresponding indices for the longitudinal strength of the upper deck.

The authors are not in a position to refute Mr Wolfram's third point (although the classification societies may not entirely agree with his sentiments) nor do they propose exactly the same safety index for naval vessels and merchant ships (see Fig. 5).

Dr Wierzchowski rightly points out that much more work needs to be done before our proposals could be implemented, drawing particular attention to the failures of merchant ships due to brittle fracture or compressive collapse in the forebody.

Taking the latter of these two observations first, Fig. 12 of Ref. 105 certainly indicates that in a typical vessel which suffered damage the safety index must have been very much lower in the forebody than at amidships. However, it must be noted that this was as much due to decreased compressive strength forward as to increased stresses. Thus low stress levels (to prevent fatigue) are not necessarily linked with high margins against compressive buckling. This point can also be inferred from Tables IV, VI and VII. For Frigate B the rule section modulus is 37% more than the built section and this would imply a safety index of 2·8 if the compressive strength of the Rule-designed vessel were the same as the frigate: in fact the safety index is greater than this at 3·5.

Nevertheless, the authors accept Dr Wierzchowski's main contention that the work has to be extended to cover a number of other important considerations such as hogging moments, slam-induced whipping, shear (not mentioned by any contributors), transverse loadings in all forms, and, in the largest ships, wave-induced vibration.

Choice of Safety Measure and Values for Designs

Dr Mansour is correct in pointing out that semi probabilistic methods (such as level-2) are unable at present to combine all modes of failure, and we agree that this challenging development deserves future attention. This is certainly a shortcoming of level-2 methods (and more so for conventional level-1 methods) and further work would be required to establish how important this is.

Dr Akita expressed a preference for level-3 methods. However, he did not suggest how acceptable probabilities of failure should be chosen. Professor Moan fills this gap by describing how probabilities of failure might be chosen with reference to social, economic and other factors. In contrast Mr Chalmers foresees great difficulty in ever applying the level-3 approach because it brings us face to face with accepting a small but finite probability of failure and therefore risk of loss of life. Thus he prefers level-2 methods and particularly the use of the safety index.

As indicated in the paper, the authors favour level-2 methods at the present time, though not for the same reasons as Mr Chalmers. They do not see insurmountable difficulties in choosing or agreeing acceptable probabilities of failure in the manner described by Professor Moan. After all we weigh risks against benefits, albeit subconsciously, every time we choose between different modes of transport for a journey. Furthermore, the selection of target safety levels which are related to risks of failure and its consequences is now routine in other branches of engineering. The greater difficulty would appear to be the exact definition of the tails of the load and strength distributions when there are so little full-scale data available. Thus the authors prefer, for the time being, a method which does not depend on assumptions

about the shape of the strength and load distributions, relying instead on the less tenuous assumption that the distributions are similar from one ship to another and can be characterised by their means and variances. It also avoids the problems of truncation.

Accordingly the authors strongly believe in selecting design safety levels by judicious comparison with past practice *over as wide a field as can reasonably be considered*. This was the basis upon which Fig. 5 was drawn and the proposed design curves chosen. The authors stand by their contention that merchant ships can be compared directly with warships with regard to the longitudinal strength of the upper deck (and for many other aspects) although they accept that the comparison needs greater refinement than space or time permitted when the paper was written. Nevertheless, they remain convinced that greater sophistication would not change the nature of Fig. 5 although it might reduce the apparent differences between merchant ships and warships slightly.

To return to the problem of the safety index for bottom structure we have studied the strength of the outer bottom of the WOLVERINE STATE as far as available data permits[110,100]. With transverse framing compression collapse of the outer bottom ignoring the effect of pressure is likely to occur at 127 N/mm^2 according to Ref. 111 or 171 N/mm^2 according to the more recent Ref. 35. Taking $\zeta_s = 0{\cdot}15$ as in the paper the ultimate stresses are 146 and 196 N/mm^2 respectively. The mean extreme compression stress in the outer bottom is estimated to be about 133 N/mm^2. The corresponding safety indices for the two strength data used are $\beta_f = 0{\cdot}5$ and $1{\cdot}2$ respectively. These are lower than for the upper deck of most of the naval designs. The same procedure for upper deck collapse gives safety indices of 3·2 and 4·5 respectively. The latter figure is close to the value of 4·2 for design 16 (MARINER) Fig. 5, which is encouraging. In these calculations, a value of $v_c = 0{\cdot}13$ and $v_d = 0{\cdot}16$ was assumed as in the paper. These figures appear reasonable when compared with test data[111] and the variability of the still water moment in the light condition[100].

Thus the bottom structure in these designs is much more critical than the upper deck, which seems quite irrational. It will also be noticed that the safety index is in this case very sensitive to the particular compression strength design data chosen which implies a large subjective systematic uncertainty. In view of the low safety indices this is rather unsatisfactory. Similar studies for 'Rule' design naval vessels less than 120 m long (all except design E) show that their bottom structure may be transversely framed according to current classification society rules. If this were done their safety indices would be extremely low and in some cases negative. Indeed the inner bottom of a particular ship designed in accordance with published rules would have been in a state of collapse before leaving harbour! It would of course be prevented from doing so by the intact outer bottom but we suggest this is far from satisfactory.

Thus, we must conclude that safety indices can vary very appreciably in critical structure in any given design, as well as between one design and another. This is irrational and supports many of our earlier contentions about the desirability of moving toward a more unified approach. It is not possible at present to state what levels of β_f or γ_0 to use in design. These must emerge from the adoption of second moment methods alongside more conventional approaches as described earlier. Moreover, it is important, of course, to compare safety indices based on similar density functions[112].

Since there has been much discussion of the importance of fatigue, and opinions obviously still differ, this matter *must* also be resolved if we are to make progress. The most recent Russian work[113] supports our view that it should not be a governing factor in distributing primary steel weight (and cost) and hence in deciding safety levels.

Finally, this leads to the question of semantics raised by Professor Moan. We would not wish to take issue with him since first-order reliability analyses are equivalent to second moment probabilistic methods. His discussion is excellent.

Closure

Professor Sir Alfred Pugsley draws attention to lessons of history and other relevant matters which call for no special answer. But we are particularly privileged to have his contribution because he has been the pioneer of much of the basic thinking in safety for aircraft and civil structures.

As a final general remark, much has been said in discussion about the comparisons of naval and merchant ships. As we have illustrated, just as large inconsistencies exist between high safety indices in the upper decks of certain merchant ships and low safety indices in their bottom structure. This is quite irrational and wasteful in structural cost and can only lead to the disturbing conclusions that many shipowners and designers have very little idea about structural safety and present classification rules still offer considerable scope for improvement.

The authors are very grateful to the contributors. We never realised that by answering some of their remarks we have exposed further important conclusions which support our general plea to make progress with modern knowledge.

REFERENCES

108. Bishop, R. E. D., Price, W. G. and Tam, P. K. Y.: 'On the Dynamics of Slamming'. Trans. RINA, Vol. 120, 1978, p 259.

109. Sarchin, T. H., and Goldberg, L. L.: 'Stability and Buoyancy Criteria for US Naval Surface Ships'. Trans. SNAME, 1962.

110. St. Denis, Manley: 'A Guide for the Synthesis of Ship Structures, Part One. The Midship Hold of a Transversely-Framed Dry Cargo Ship!. Ship Structures Committee Report SSC-215, 1970.

111. Evans, J. H.: 'Strength of Wide Plate under Uniform Compression'. Trans SNAME, Vol. 68, 1960, p 585.

112. Ditlevsen, Ove: 'Generalised Second Moment Reliability Index'. Danish Centre for Applied Mathematics & Mechanics, Report no. 144, Oct. 1978.

113. Korotkin, Ya. I.: 'Principles and Criteria for Assessing the Overall Strength of Ship's Hulls' (in Russian). Sudostroenie, No. 8, 1977, p. 3.

ENVIRONMENTAL DESIGN CONSIDERATIONS

by

ATILLA INCECIK

GLASGOW

ENVIRONMENTAL DESIGN CONSIDERATIONS

by

ATILLA INCECIK

GLASGOW

ENVIRONMENTAL DESIGN CONSIDERATIONS

INTRODUCTION

An accurate knowledge of the environmental parameters is fundamental to the sound design of marine structures. In order to calculate the loads likely to be imposed by the natural phenomena and to predict the resulting motion and structural response characteristics under normal and extreme conditions various meteorological and oceanographical parameters (metocean parameters) have to be established. Metocean parameters important for the design analysis of marine structures are:

Wind:	Mean Wind Speed Mean Wind Direction Wind Power Spectral Density Function Variation of Wind Speed above the Sea Level
Wave:	Significant Wave Height Mean Wave Period Wave Amplitude Spectral Density Function Mean Wave Direction Wave Directional Spreading Function Identification of effect of currents, seabed topography and other factors likely to modify the above parameters
Current:	Surface Current Speed Surface Current Direction Current Profile (speed and direction) Tidal Current Speed and Direction Identification of low frequency components in current velocities
Tide:	Astronomical Tide Storm Surge
<u>Air and Sea Temperatures</u>	
Ice	The extent of snow and ice accumulation
Marine Growth:	The extent to which marine growth may form on the submerged sections of the marine vessels

The number of parameters involved cause the primary shortcoming of a deterministic design analysis. While a rigid offshore structure is typically dominated by wave forces, response characteristics of a compliant structure are also strongly affected by wind, tide and storm surge, low frequency wave drift forces, currents and wind dynamics (see Fig.1). Simultaneous occurrence of independent extremes for each of the above metocean parameters produces results which range from overly conservative for some responses to non-conservative for others. In order to produce a cost effective and safe structure the designer must evaluate and specify the design event or condition for each response.

Most metocean parameters vary with time in a random manner, and extreme values to be used in design can only be selected on a probabilistic basis. The probability that a metocean parameter will exceed a given value leads to the concept of a 'return period'. The definition of return period given in the U.K. DEn Guidance Notes is:

> *The return period of a stated value of a metocean variable is the average period of time between exceedance of that value.*

In practice, offshore structures are designed against extreme metocean parameters using 50 or 100 year conditions, and for most practical engineering purposes these numbers provide a convenient and well-proven standard for design. During normal operational conditions design calculations are usually carried out using environmental parameters which are not less then those likely to be exceeded, on average, once a month.

If an offshore structure has a design life of 30 years, the probability that it will experience at least one event with a return period of 50 years during its life, is about 0.45. If the event has a return period of 100 years, the probability reduces to 0.26.

The above probability values can be found from the following equation:

$$P = 1 - p^n \qquad (1)$$

where p = annual probability that the event will not occur
n = platform life in years.

A return period of 50 years means an annual probability of occurrence of 1/50 = 0.02, or a probability of non-occurrence of 1- 1/50 = 0.98. In the above example:

$$P = 1 - (0.98)^{30} = 0.45$$

If the structure was designed so that exceedance of the load imposed during this event was to cause catastrophic failure, then both the 50 year and the 100 year return periods would not be acceptable as design criteria. To reduce the probability of experiencing such an event to, say, 1% during a 30 year life, the event should have a return period of about 3500 years.

This simple example demonstrates the need for a probabilistic approach to design involving the establishment of risk-based design criteria based on reliability and uncertainty analyses.

WIND

Wind is an important parameter in predicting the steady wind forces on marine structures. In addition, fluctuating wind forces (dynamic wind effects) due to wind gust may also be important in the design of moored and compliant structures.

Time average wind speeds over prescribed time periods are used in calculating the steady wind forces on N marine structures. During wind load and response calculations estimates of wind speeds with N year period are required with averaging times from 3 seconds (i.e. an extreme gust value) to 24 hours. The estimated wind speeds are referenced to a standard height of 10 m above still water level. The estimates of wind speeds at different heights are also required for design calculations.

Estimates of 50 year return omni-directional hourly-mean wind speeds at 10 m above still water level around the British Isles are shown in Fig.2. (From Ref.1).

The wind speed values for the N year return period wind speed, V_N, may be estimated from the following equation (see also Ref.1):

$$V_N = 0.71(1+0.106 \ln N)\, V_{50} \qquad (2)$$

Relationship between the 50 year return hourly wind speeds of Fig. 2 and 50 year return wind speeds with shorter averaging times and at greater heights above sea levels is extracted from Ref. 1 and given in Table 1.

Reference 2 gives the following equation to define the wind speed at any arbitrary height from the sea level in terms of hourly wind speed at 10 m above the sea level:

$$V_{t,z} = \alpha\, V_{1hr,\,10}\, (z/10)\, \beta \qquad (3)$$

where: $V_{t,z}$ = the wind speed averaged over a time interval t as defined by α and β, z meters above the mean water level

$V_{1hr,10}$ = the wind speed averaged over one hour, 10 m above the mean water level.

α = gust factor

β = height exponent

α and β for different averaging time intervals are given in the following Table:

FACTOR	AVERAGING TIME INTERVAL					
	1 hr.	10 min.	1 min.	15 sec.	5 sec.	3 sec.
α	1	1.06	1.18	1.26	1.31	1.33
β	0.15	0.13	0.133	0.106	0.102	0.1

To represent the gustiness of the wind field, the power spectral density of the wind must be specified. The following spectral definitions derived from land based wind data may be adapted for offshore use with care:

Harris wind spectrum: (Ref. 3)

$$Sw(f) = \frac{4\kappa\bar{f}\,V_{10}^2}{f(2+\bar{f}^2)^{5/6}} \tag{4}$$

where $\bar{f} = \frac{Lf}{\overline{V}_{10}}$; f is frequency (Hz.); L, length scale(= 1200 m); $\overline{V}_{10}$, wind speed at height of 10 m (m/sec) and κ, drag coefficient which may be calculated as function of the wind speed as:

$$\kappa = 0.0008 + 0.000064\,\overline{V}_{10} \tag{5}$$

The Davenport spectrum: (Ref.4)

$$S_w(f) = \frac{4\kappa\bar{f}^2\overline{V}_{10}^2}{f(1+\bar{f}^2)^{4/3}} \tag{6}$$

Kaimal Spectrum: (Ref. 5)

$$S_w(f) = \frac{200\kappa \tilde{f}^2 \overline{V}_{10}^2}{f(1+50\tilde{f})^{5/3}} \tag{7}$$

where $\tilde{f} = \frac{fz}{\overline{V}(z)}$

Ochi proposed the following formulation for the average wind spectra obtained from measured data over a seaway (Ref.6):

$$S_w(f) = 583\, z\, \kappa\, \overline{V}_{10} \quad \text{for } 0 < f_* < 0.003$$

$$S_w(f) = \frac{420\, f_*^{0.7}}{f(1+f^{0.35})^{11.5}} \kappa V_{10}^2 \quad \text{for } 0.003 < f_* < 0.1$$

$$S_w(f) = \frac{838\, f_*}{f(1+f^{0.35})^{11.5}} \kappa V_{10}^2 \quad \text{for } f_* > 0.1 \tag{8}$$

where $f_* = f z / \overline{V}_{10}$

WAVES

The forces due to surface waves contribute significantly to the first and second order dynamic response of, and structural loading on, marine systems. The information relating to waves used in design should include heights, periods and directions. There are two basic approaches used in selecting the design wave conditions. One approach is based on a *single design wave* method in which the design wave is represented by a wave height, period and direction. One of the reasons for using this approach is the simplicity in determining the maximum wave loading and resulting response of marine structures. In this approach usually the extreme amplitude design wave, which has either 50 or 100 year return period, and its associated period are used to determine the maximum response on a marine structure. However, it should be borne in mind that the waves inducing maximum response in the structure as a whole may be different from those having the most severe effect on structural elements and the maximum dynamic motion response of a structure will be due to waves other than the extreme amplitude design waves. It should also be noted that the fatigue life will be governed by frequently occurring low amplitude waves. The second approach is based on the use of *wave energy spectra.* In this method a suitable wave

spectrum model is chosen representing the proper energy density distribution of the sea waves at site or travel routes under consideration. In design, wave spectra are used:

a) to predict the relative importance of waves of different frequencies in exciting the dynamic and structural response of floating or compliant systems

b) to determine the force spectrum in fatigue calculations.

Single Design Wave Approach: The wave parameters used in design should ideally be based on a series of site specific wave measurements. A programme of site specific measurements yields values of significant wave height, H_s, and associated zero-up-crossing period T_z. These parameters are typically measured at 3 hourly intervals over a sampling period of at least 1000 seconds. If sufficient years of data is available an asymptotic extreme value analyses should be used to obtain an estimate of the significant wave height having a 50 or 100 year return period (H_{s50} or H_{s100}). Otherwise, individual values of H_s from the data set should be fitted to a recognised probability distribution and this should be used to obtain an estimate of the 50- or 100-year value. The choice between the different distributions (e.g. Fisher-Tippett, Weibull, etc.) should be made on the basis of goodness of fit. Figure 3 which is extracted from Ref.1 shows the estimates of 50-year return significant wave heights H_{s50} around the British Isles. The Fisher-Tippet I distribution was used to estimate the significant wave height values given in Fig.3. From the Fisher-Tippet I distribution one can determine a wave height that will not be exceeded with a given level of probability as:

$$h = A + B\,[-\ln(-\ln P)] \qquad (9)$$

where A and B are the location and scale parameters of the distribution

P = Prob (Hs < h) or

P = 1-(expected number of exceedances/total number of values)

or P(H<h) = 1- (1/Nn)

For example, for three hourly values of H_s, the 50-year return value can be estimated as, $P(H_{s50} < h) = 1 - (1/\,50 \times 365.25 \times 8\,) = 0.999993$.

Typical values of A and B, as obtained from various locations around the British Isles, are given as follows (Ref.7):

1.	Seven Stones Light Vessel Data (1962-1982)	A = 1.78, B = 1.09
2.	Dowsing Light Vessel Data (1970-1980)	A = 0.94, B = 0.65
3.	Seven Stones Data	A = 1.83, B =1.12

Assuming that waves in a three (or six) hourly record follow a Rayleigh distribution, the following relationship between the significant wave height H_S and h may be written:

$$h / H_S = (0.5 \ln(N / n))^{1/2} \tag{10}$$

The maximum wave height for a sequence of N waves with known H_S can be expressed as:

$$H_{max} = H_S (0.5 \ln N)^{1/2} \tag{11}$$

Assuming that there are 1000 waves in a three hourly record H_{max} can be calculated in terms of H_S as:

$$H_{max} = H_S (0.5 \ln (1000))^{1/2} = 1.86 H_S$$

In deep water (when the ratio between wave length and water depth is greater than about 0.25) the wave elevation above still water may be estimated as:

$$a_{crest} = 1.03 H \tag{12}$$

Reference 1 gives the following relationships to estimate the crest elevation and maximum height of individual waves with a given return periods:

$$a_{crest,N} = 0.74 (1 + 0.1 \ln N) H_{s50} \tag{13}$$

$$H_{max,N} = 1.34 (1 + 0.1 \ln N) H_{s50} \tag{14}$$

An estimate of the zero-downcrossing or upcrossing wave period T_Z at the time when the significant wave height has an extreme value, such as H_{s50}, is obtained by assuming a specific value for wave steepness. Often a value of 1/18 is used so T_z is obtained from:

$$\frac{2 \pi H_{s50}}{g T_z^2} = \frac{1}{18} \tag{15}$$

or

$$T_z = 3.4 (H_{s50})^{1/2}$$

Measurements indicate that 1/18 is appropriate for open ocean sites, but larger values of about 1/14 apply at sites where waves are fetch limited. In practice, a value is often obtained by a visual inspection and extrapolation of the H_S - T_Z scatter plot. These

rather crude estimates of T_Z are often sufficient, but if the exact value of T_Z is important, for example, if a structure being designed is sensitive to small changes in T_Z then a range of values should be specified. Reference 8 recommends a range from approximately 2.6 $H_S^{0.5}$ to 3.9 $H_S^{0.5}$.

Wave Energy Spectra Approach: A non-directional wave frequency spectrum represents the distribution with frequency of the sea surface variance in a given sea state. The sea surface variance is itself proportional to wave energy. Apart from severe storms, the wave spectrum in the open ocean is generally a complicated mixture of swell from distant storms, 'old wind sea' from recent nearby winds, and a sea generated by present local wind. Site-specific data should ideally be used to establish these spectra. In the absence of such data mathematical models are used to define wave energy distributions. The general form of a wave spectrum may be written as:

$$S(\omega) = A\,\omega^{-N} \exp(-B\omega)^{-M} \tag{16}$$

where A and B are usually functions of wind speed and fetch. The values of the exponents N and M were obtained by various researchers by fitting eq. 1 to the energy spectral form of field data and they have been found to be widely different ($3 < N < 7$, $1 < M < 4$). The most common two forms of spectra models are given in the following.

Pierson-Moskowitz Spectrum: This spectrum model describes a fully-developed sea determined by the wind speed assuming that the fetch and duration are infinite. For the applicability of this model the wind has to blow over a large area at a nearly constant speed for many hours prior to the time when the wave record is obtained and the wind should not change its direction more than a certain specified small amount. The PM spectrum can be expressed as:

$$S(\omega) = \alpha\, g^2\, \omega^{-5} \exp\left[-\beta\, (g / \overline{V}_{19.5}\, \omega)^4\right] \tag{17}$$

where:

$$\alpha = 0.0081$$
$$\beta = 0.74$$

However, for predicting responses of marine structures for design consideration, the Pierson-Moskowitz spectrum may be expressed in terms of the significant wave height, H_S, instead of the wind speed $\overline{V}_{19.5}$. For this it is assumed that waves are representative of a Gaussian random process and that the spectrum is narrow banded. Then the area under the spectrum is equal to $(H_S/4)^2$, and the Pierson-Moskowitz spectrum can be expressed in the following form:

$$S(\omega) = \alpha\, g^2\, \omega^{-5} \exp\left[-0.032\, (g / H_S\, \omega^2)^2\right] \tag{18}$$

JONSWAP Spectrum: The JONSWAP spectrum has been derived from measurements made in the North Sea off Denmark (Ref.9). It describes fetch-limited growing seas in the absence of swell and is given by:

$$S(\omega) = \alpha \frac{g^2}{\omega^5} e^{-1.25\left(\frac{\omega_m}{\omega}\right)^4} \gamma^{e^{-\frac{(\omega-\omega_m)}{2\sigma^2\omega_m^2}}} \tag{19}$$

where:

$$\gamma = 3.3$$

$$\sigma = \begin{matrix} 0.07 \\ 0.09 \end{matrix} \text{ for } \begin{matrix} \omega \le \omega_m \\ \omega \ge \omega_m \end{matrix}$$

$$\alpha = 0.076(\overline{X})^{-0.22}$$

$$\omega_m = 7\pi\left(\frac{g}{U}\right)(\overline{X})^{-0.33}$$

$$\overline{X} = \frac{gX}{U^2}$$

X = fetch in nautical miles
U = wind speed in knots

Response Spectrum: If the response characteristics of a marine vehicle are a linear function of the wave amplitude, the response spectra can be obtained as the product of the wave spectrum and the response amplitude operators. Various statistical descriptions of the responses, such as average value, significant value, extreme value, etc. can be obtained from the response spectra.

Short Term Statistics: If the wave height values are assumed to be Rayleigh distributed, so are the response values. The probability density function of a response amplitude value R_o can be written as:

$$p(R_o) = \frac{R_o}{\sigma_R^2} e^{\left(-\frac{R_o^2}{2\sigma_R^2}\right)} \tag{20}$$

The probability of exceeding the value of R_o is

$$Q(R>R_o) = e^{\left(-\frac{R_o^2}{2\sigma_R^2}\right)} \tag{21}$$

where:

$$\sigma_R^2 = \int_0^\infty S(\omega) RAO^2(\omega)$$

RAO = Response Amplitude/Wave Amplitude.

The most probable extreme response amplitude value in N waves may be written as:

$$R = (2\sigma_R \ln(N))^{1/2} \tag{22}$$

The probability of exceeding the response value given in eq. (20) for large N values is 0.632 (Ref.10). The design extreme response amplitude value that will not be exceeded in N encounters with a probability of 0.99 is given by:

$$R = (2\sigma_R \ln(N/0.01))^{1/2} \tag{23}$$

Long Term Statistics: If the short term calculations summarised above are carried out for different sea states which may be represented by significant wave height H_s and the associated average period T_z the long term statistics of the response values can be calculated as follows:

The probability of exceeding the value of R_o is:

$$Q(R>R_o) = \sum_{i=1}^{N}\sum_{j=1}^{N} e^{\left(-\frac{R_o^2}{2\sigma_{R,i,j}^2}\right)} P_{i,j} \tag{24}$$

where $P_{i,j}$ is the probability of occurrence of a sea state described by H_s and T_z. Probability of occurrence of a given set of H_s and T_z can be obtained from scatter diagrams (see for example Ref. 11). To calculate the long term probabilities of response values using the scatter diagrams, the Pierson-Moskowitz spectrum may be redefined in terms of H_s and T_z as follows:

$$S(\omega) = k\omega^{-5} e^{\left[-1.25\left(\frac{\omega_{max}}{\omega}\right)^4\right]} \tag{25}$$

where:

$$k = 173H_s^2 / T_z^4 \quad \text{and} \quad \omega_{max}^4 = 553 / T_z^4$$

Similarly, in order to utilise the JONSWAP spectrum using the scatter diagrams for long term predictions, H_s and T_z values are expressed in terms of γ and $T_M = 2\pi/\omega_M$ by Chakrabarti in Ref. 12 as follows:

$$H_s = (0.1161 + 0.01581\gamma - 0.00065\gamma^2)\, T_0^2 \tag{26}$$

$$T_0 = (1.49 - 0.102\gamma + 0.0142\gamma^2 - 0.00079\gamma^3) T_z \tag{27}$$

For given H_S and T_Z which are to represent a particular sea state by the JONSWAP spectrum, then eqs 26 and 27 may be solved for T_0 and γ by a simple iterative technique.

Reference 1 gives an alternative definition of the JONSWAP spectrum as a function of H_S and T_Z as follows:

$$S(\omega) = 116.73 H_S T_Z (T_Z \omega)^{-5} 3.3^q e^{-711.78(T_Z\omega)^{-4}} \tag{28}$$

where: $q = e - \frac{(0.2046 T_z \omega - 1)^2}{2\sigma^2}$

Directional Spectra: The directional wave spectrum, $S(\omega,\theta)$, describes the distribution of surface variance with frequency, ω, and direction θ, where θ is the direction from which the wave component is travelling. The directional wave spectrum is generally represented by the following equation:

$$S(\omega,\theta) = S(\omega)\, G(\omega;\theta) \tag{29}$$

where: $G(\omega;\theta)$ is the directional spreading function which represents the directional distribution of the total sea energy.

Our knowledge of the directional distribution of sea energy is very limited due to lack of field measurements. However, there are a number of proposed equations which can be utilised to model short crested waves (see Ref. 13).

The first proposed form of directional spreading is a cosine-squared distribution in the range of $\pm\frac{\pi}{2}$ (Ref.14):

$$G(\theta) = \begin{cases} \frac{2}{\pi}\cos^2\theta & |\theta| \le \frac{\pi}{2} \\ 0 & |\theta| > \frac{\pi}{2} \end{cases} \tag{30}$$

Ref.1 gives the following expression for $G(\omega;\theta)$:

$$G(\omega;\theta) = N \operatorname{Cos}^{2s}[(\theta-\theta_m)/2] \tag{31}$$

where θ_m, the dominant direction, and s, a spreading factor, are both functions of ω. N is a normalising constant which ensures $G(\omega;\theta)$ integrates to 1, and is given by:

$$N=\frac{\Gamma(s+1)}{2\sqrt{\pi}\ \Gamma(s+0.5)} \tag{32}$$

where Γ is the Gamma function.

Mitsuyasu et al in Ref. 15 propose the following equations for the calculation of s values:

$$s=\begin{cases} s_{max}(\frac{\omega}{\omega_p})^5 & \text{when } \omega \le \omega_p \\ s_{max}(\frac{\omega}{\omega_p})^{-2.5} & \text{when } \omega > \omega_p \end{cases}$$

where ω_p is peak frequency. The recommendations based on the measured data for s_{max} are given as follows:

- wind waves, $s_{max} = 10$
- swell with short decay distance, $s_{max} = 25$
- swell with long decay distance, $s_{max} = 75$

The directional response spectrum may be formulated by combining the directional wave spectrum with the directional transfer functions as follows:

$$RS(\omega,\theta_m) = S(\omega)\int_{\theta_{min}}^{\theta_{max}} G_0 Cos^{2s}(\frac{\theta-\theta_m}{2})[RAO(\omega,\theta)]^2 d\theta \tag{33}$$

Various statistical descriptions of the responses, such as average value, significant value, extreme value, etc. for each dominant wave direction can be obtained from the response spectra defined in eq.33 utilising the statistical equations given in the previous sections.

For grater accuracy it is often recognised that the effect of wave directionality should now be considered when predicting the motion and structural behaviour of offshore platforms. Uni-directional wave approach is assumed to yield more conservative design values. While this assumption can be shown to be true in the case of

extreme motion and structural response of certain types and configurations of offshore platforms, one has to question the application of this assumption to directionally sensitive structures and fatigue load calculations. Refs. 16, 17 and 18 describe the effect of wave directionality on loads and responses of various offshore platforms.

CURRENTS

The current at any position is the vector sum of tidal and storm surge and other components. Tidal currents are regular and predictable and the maximum tidal current is associated with the highest or lowest astronomical tide. Table 2 extracted from Ref.1 gives a general indication of the range of current speeds which can be expected in the continental shelf seas around the U.K. Theoretically, the number of variables involved and, in particular, the different levels of turbulence have limited the development methods for predicting the current profiles. The collection of suitable field data is very difficult and expensive. As a consequence, if any measurements are available through the water column for the site concerned these are generally used to define the shape of the current profile. Otherwise, some combination of power law or logarithmic law variation near the seabed and sea surface are used as a starting point for the development of a plausible profile associated with the specified depth-averaged current magnitude.

Reference 1 gives the following power law formulae for tidal current profiles:

$$u_{t(s)} = \left(\frac{s}{0.32h}\right)^{1/7} \bar{u}_t \quad \text{for } 0 \le s \le 0.5h$$

$$u_{t(s)} = 1.07\bar{u}_t \qquad \text{for } 0.5h \le s \le h \tag{34}$$

where:

$u_{t(s)}$	=	speed of the tidal current at a height s above the seabed
$\bar{u}_t$	=	depth-averaged speed of the tidal current
h	=	total water depth

Estimates of maximum depth-averaged current speed and direction are given in Figs. 4 and 5 respectively (Ref.1).

Storm surge current profile is defined with the following equation in Ref.1:

$$u_{s(s)} = \left(\frac{s-h'}{10}\right) u_w + \bar{u}_s \quad \text{for } h' \le s \le h$$

$$u_{s(s)} = \bar{u}_s \qquad \text{for } 0 \le s \le h' \tag{35}$$

where:

$u_{s(s)}$ = speed of storm surge current plus wind drift at a height 's' above the seabed

$\bar{u}_s$ = depth-averaged storm surge current

s = height above the seabed (in m)

h = total height between the seabed and still water level (in m)

h' = height above the seabed at which the current profile changes slope (in m)

h' = $h - 10(u_w - \bar{u}_s)$

u_w = 0,03 x wind speed (hourly-mean speed given in Fig. 2)

If $u_s > u_w$ $\quad u_{s(s)} = \bar{u}_s \quad$ for $0 \le s \le h$

$\bar{u}_s$ values can be obtained from Fig. 6 (Ref. 1).

It is necessary to introduce a multiplying factor throughout the bi-linear profile to ensure that the average current obtained by integrating the profile from the sea surface to the seabed is equal to the depth-averaged storm surge current. The factor is given in Ref.1 as:

$$\left[\frac{5(u_w - \bar{u}_s)^2}{h\bar{u}_s} + 1\right]^{-1}$$

COMBINATION OF EXTREME WIND, WAVE AND CURRENT PARAMETERS

There are three possible ways of combining extreme metocean parameters in determining the extreme design loads and responses. (See also Ref. 19).

(a) 50 (or 100) year wave height is combined with the 50 (or 100) year return period wind speed and the 50 (or 100) year return period current speed. If these events are uncorrelated this method will yield the most conservative extreme design load and response with return period of 50^3 (or 100^3). If they are totally correlated this method will yield design load and response values with return period of 50 (or 100) year.

(b) Any "reasonable" combination of wind speed, wave height, and current speed that results in the 50 (or 100) year return period combined motion and structural response. This method requires the use of joint statistics of the metocean parameters to arrive at the combination yielding 50 (or 100) year return period load or response. (See Ref. 20 for the estimation of joint probability of

metocean parameters). Having obtained metocean combinations with required return period, in order to estimate the combined extreme load and response values one has to simulate various combinations of wave, wind, and current parameters as their directions vary. References 21 and 22 give results to illustrate the effect of various load combinations and directionality on motion and structural response of compliant offshore platforms.

(c) 50 (or 100) year return period wave height with "associated" wind and "associated" current for structures dominated by wave loads; 50 (or 100) year return period wind with "associated" wave and "associated" current for structures dominated by wind loads and 50 (or 100) year return period current with "associated" wave and "associated" wind for structures dominated by current loads (see Fig.1). "Associated" may be interpreted as the statistically expected value of metocean parameters co-existing with the parameter which has return period of 50 (or 100) year. For structures, where more then one one environmental parameter is important, the first or second methods should be used.

REFERENCES

1. Offshore Installations: *Guidance on Design, Construction and Certification*, Department of Energy, Fourth Edition, 1990, London.

2. *Det norske Veritas Rules for the Design, Construction and Inspection of Offshore Structures*, Appendix A: Environmental Conditions, 1979, Hovik.

3. Harris, R.I., *The Nature of the Wind, Proc. of the Seminar on the Modern Design of Wind Sensitive Structures*, The Inst.of Civil Engineers, 1970, London

4. Davenport, A.G. *Gust Loading Factors*, Jnl of the Structural Division, ASCE, vol.93, no.ST3, 1967.

5. Kaimal, J. C. et al *Spectral Characteristics of Surface Layer Turbulence*, Jnl of Royal Meteorological Society, vol. 98, 1972.

6. Ochi, M.K. and Shin, Y.S., W*ind Turbulent Spectra for Design Consideration of Offshore Structures*, Proc. of Offshore Technology Conference,1988, Houston.

7. Carter, D.J.T., *A Simple Model for Estimating Return Value of Wave Height*, Proc. of Intl Conference on Modelling the Offshore Environment, SUT, 1987, London.

8. *ISSC Report of Committee I.1 (Environmental Conditions)*, 7th Intl Ship Structures Congress, 1979, Paris.

9. Hasselman, K. et al, *Measurements of Wind-Wave Growth and Swell Decay During JONSWAP*, Dt. Hydrography. Reihe A (8), NR. 12, 1973.

10. Ochi. M.K., *On the Prediction of Extreme Values*, Jnl of Ship Research, 1973.

11. *Global Wave Statistics*, Compiled and Edited by the British Maritime Technology Ltd. and Published by Unwin Brothers Ltd., 1985.

12. Chakrabarti, S.K., *Technical Note: On the Formulation of JONSWAP Spectrum*, Applied Ocean Research,vol.6, no.3, 1984.

13. Goda, Y., *Random Seas and Design of Maritime Structures*, University of Tokyo Press, 1985.

14. Arthur, R.S, *Variability in Direction of Wave Travel in Ocean Surface Waves*, Ann. New York Academy of Science, vol. 51, no.3,1949.

15. Mitsuyasu et al, *Observation of the Directional Spectrum of Ocean Waves Using a Coverleaf Buoy*, Jnl of Physical Oceanography, vol. 5, no.4, 1975.

16. Standing, R.G., Rowe, S.J. and Brendling, W.J., *Jacket Transportation Analysis in Multidirectional Waves*, Proc. of the 18th Annual Offshore Technology Conference, Paper No. OTC 5283, Houston, 1986.

17. Steele, K.,Tvestad,T. and Remseth,S., *Compliant Tower Response Prediction Procedures*, Proc. of the Offshore Technology Conference, Paper No. OTC 5783, Houston, 1988.

18. Helvacioglu, I.H. and Incecik, A., *Second-Order and Short-Crested Wave Effects in Predicting the Behaviour of a Compliant Structure*, Proc. of the Offshore Mechanics and Arctic Engineering Conference, The Hague, 1989.

19. *Draft Recommended Practice for Planning, Designing and Constructing Fixed Offshore Platforms- Load and Resistance Factor Design*, API Recommended Practice 2A-LRFD (RP 2A-LRFD) First Edition, 1989.

20. Prior-Jones, R.L., Beiboer, F.L., *The Use of Joint Probability*, Proc. of the Intl Conference on Environmental Forces on Offshore Structures and their Prediction, Society of Underwater Technology, London, 1990.

21. Incecik, A., Helvacioglu, I.H. and Prince-Wright, R., *Effects of Joint Probability and Short Crestedness in Designing a Compliant Structure*, Proc. of the Intl Conference on Environmental Forces on Offshore Structures and Their Prediction, Society of Underwater Technology, London, 1990.

22. Yilmaz, O. and Incecik, A., *Identification of Non-Linear Effects in Predicting the Motion Response of a 'CALM' System*, Proc. of the Offshore Mechanics and Arctic Engineering Conference, Calgary, 1992.

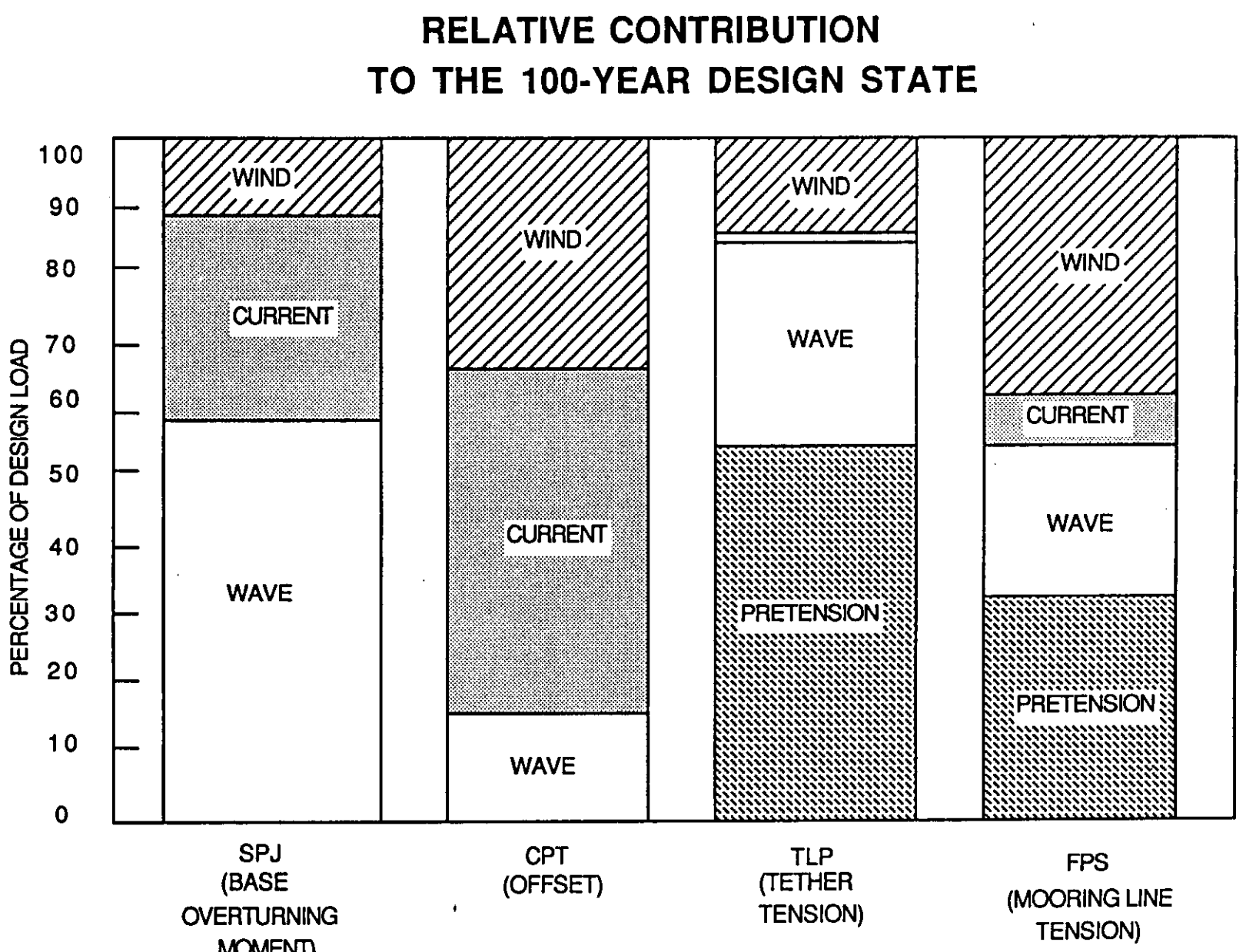
RELATIVE CONTRIBUTION
TO THE 100-YEAR DESIGN STATE
PERCENTAGE OF DESIGN LOAD
100
90
80
70
60
50
40
30
20
10
0
WIND
CURRENT
WAVE
WIND
CURRENT
WAVE
WIND
WAVE
PRETENSION
WIND
CURRENT
WAVE
PRETENSION
SPJ
(BASE
OVERTURNING
MOMENT)
CPT
(OFFSET)
TLP
(TETHER
TENSION)
FPS
(MOORING LINE
TENSION)

FIG. 1

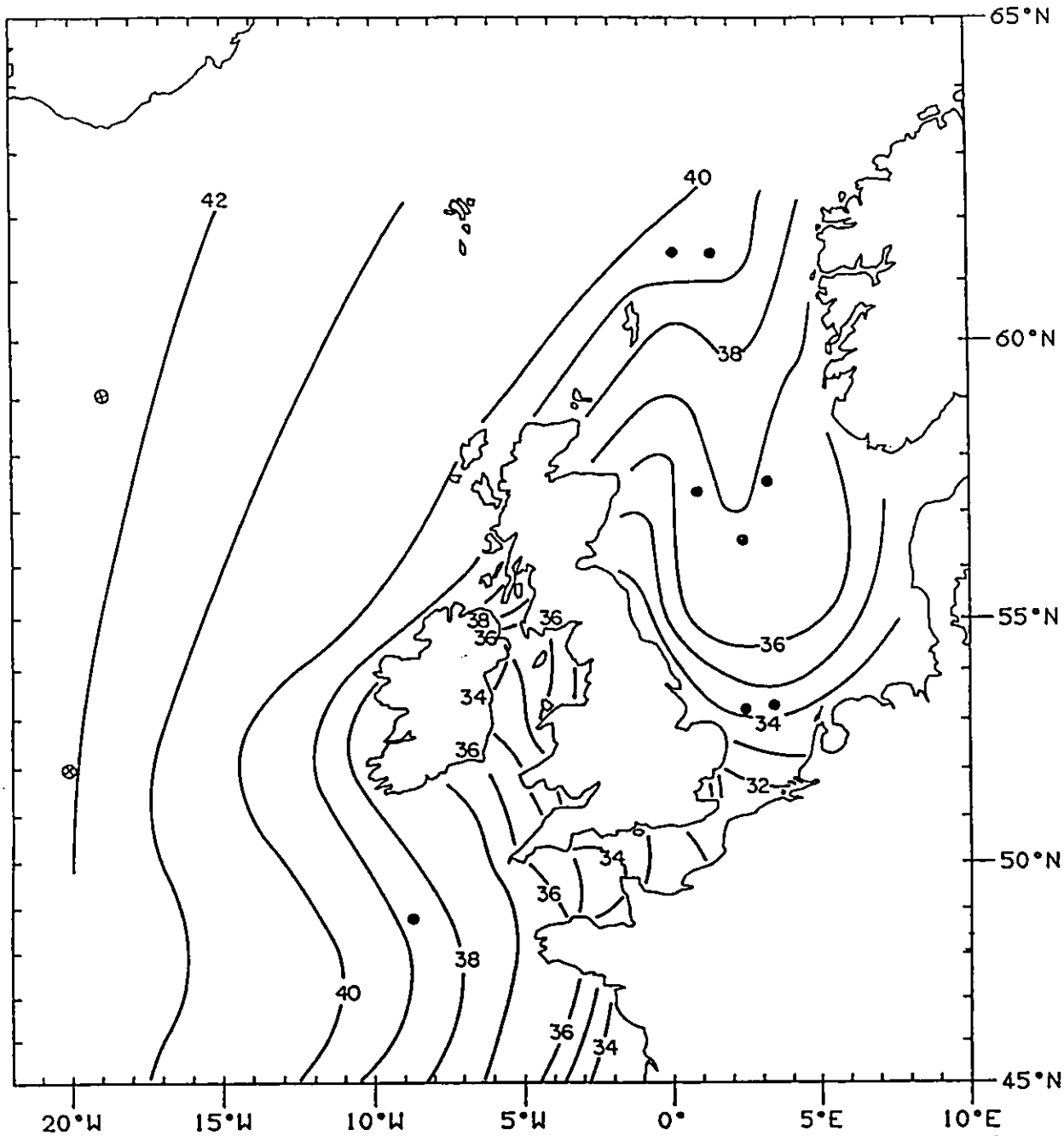

FIG. 2 **: Estimates of 50-year return omnidirectional hourly-mean wind speeds at 10 m above still water level**

Contours are in m/s. Estimated maximum error is ± 2 m/s.

Ocean Weather Stations, where wind speeds have been measured for many years at fixed locations, are shown ⊕.
Sites used for verification purposes are shown • (see OTH 89 299).

Source: Analysis of VOF and instrumental data (OTH 89 299). Details of the analysis method used are to be found in this reference.

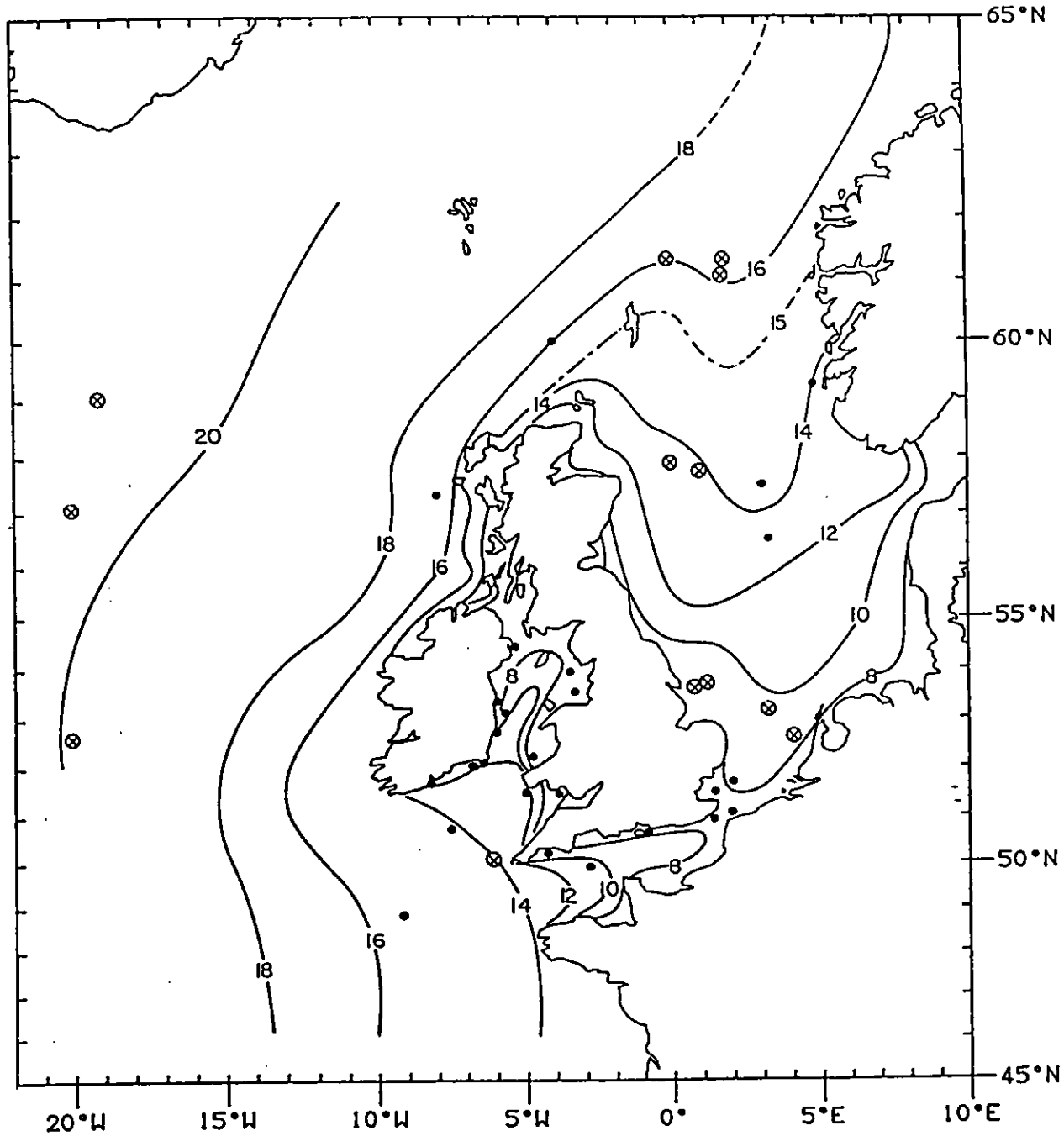

FIG. 3 : Estimates of 50-year return significant wave heights, H_{s50}

Contours are in metres.

Wave measurement sites are marked •. Measurement sites where accuracy of estimates is likely to be relatively high are marked ⊗.

Shallow water effects should be taken into account where applicable

Source: Analysis of measured wave data and wind data (OTH 89 300).

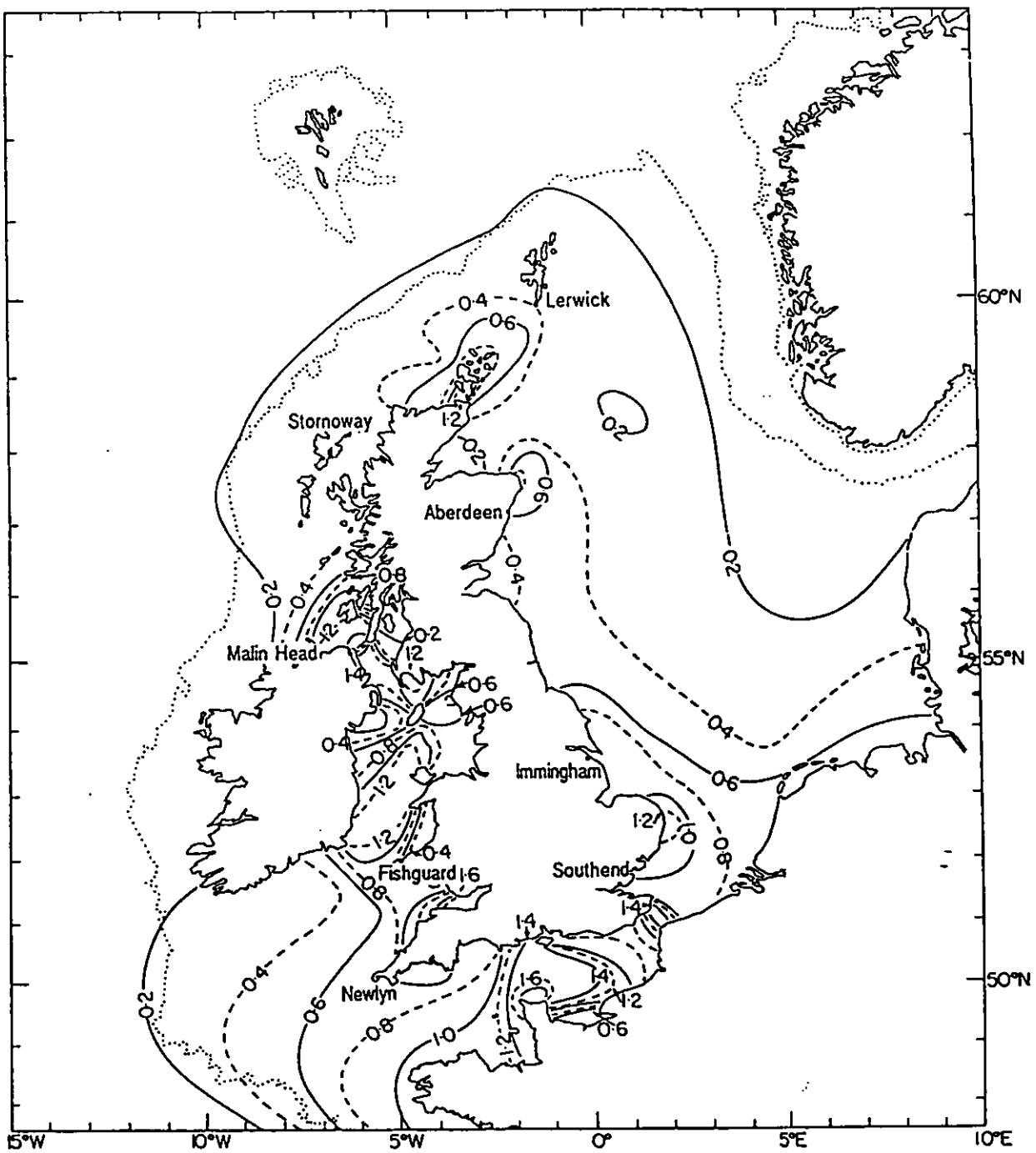

FIG. 4 : **Estimates of maximum depth-averaged flow of an average spring tidal current**

Contours are in m/s

See Section 6 for definition of spring tidal current

Dotted line is the 100 fathom (183 m) depth contour

Source: Observations (OTH 89 299)

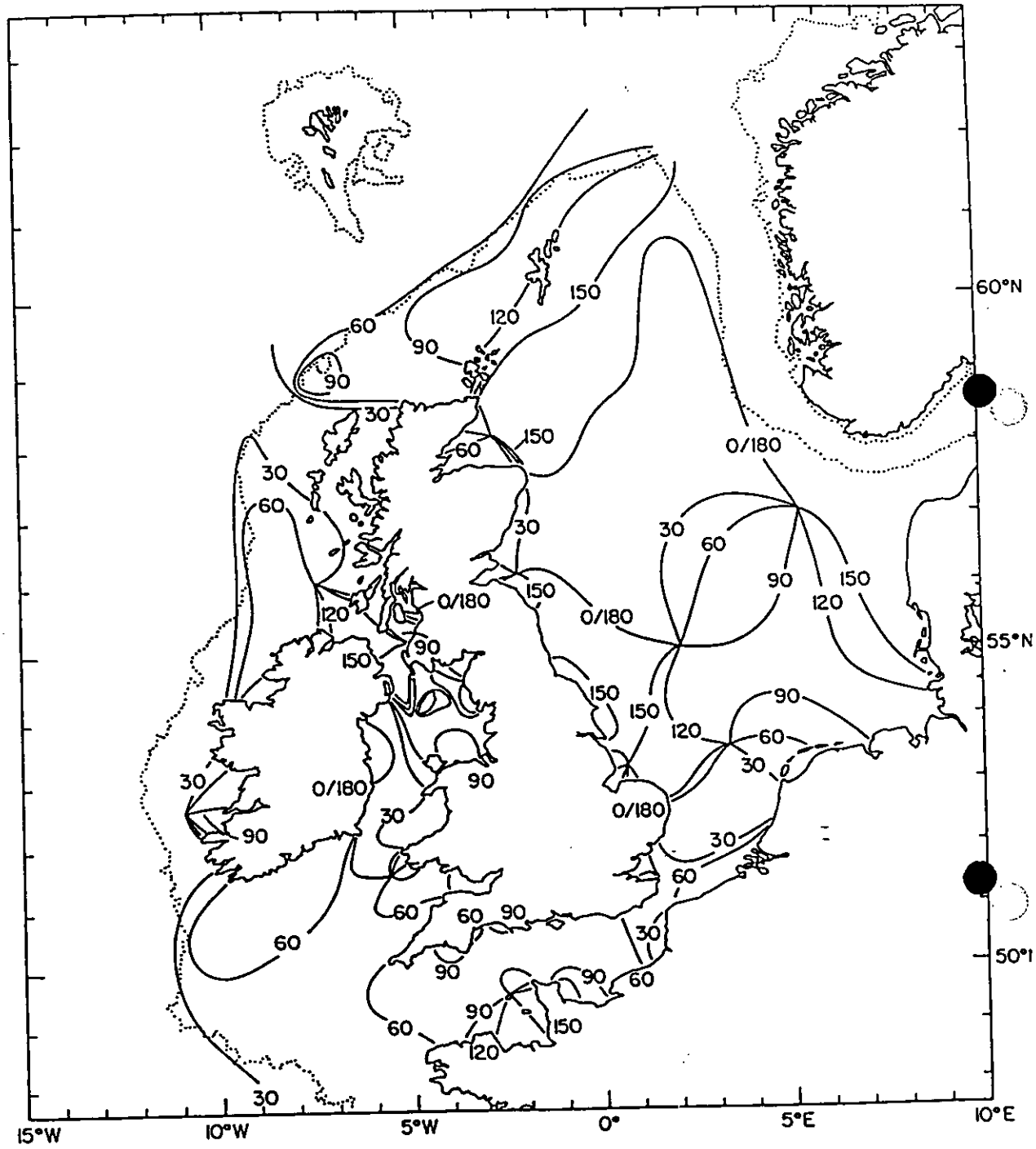

FIG. 5 : **Direction of the maximum flow of the average spring tidal current**

Contours are in degrees clockwise relative to north or south

0° and 180° are the same direction

Dotted line is the 100 fathom (183 m) depth contour

Source: Observations (OTH 89 299)

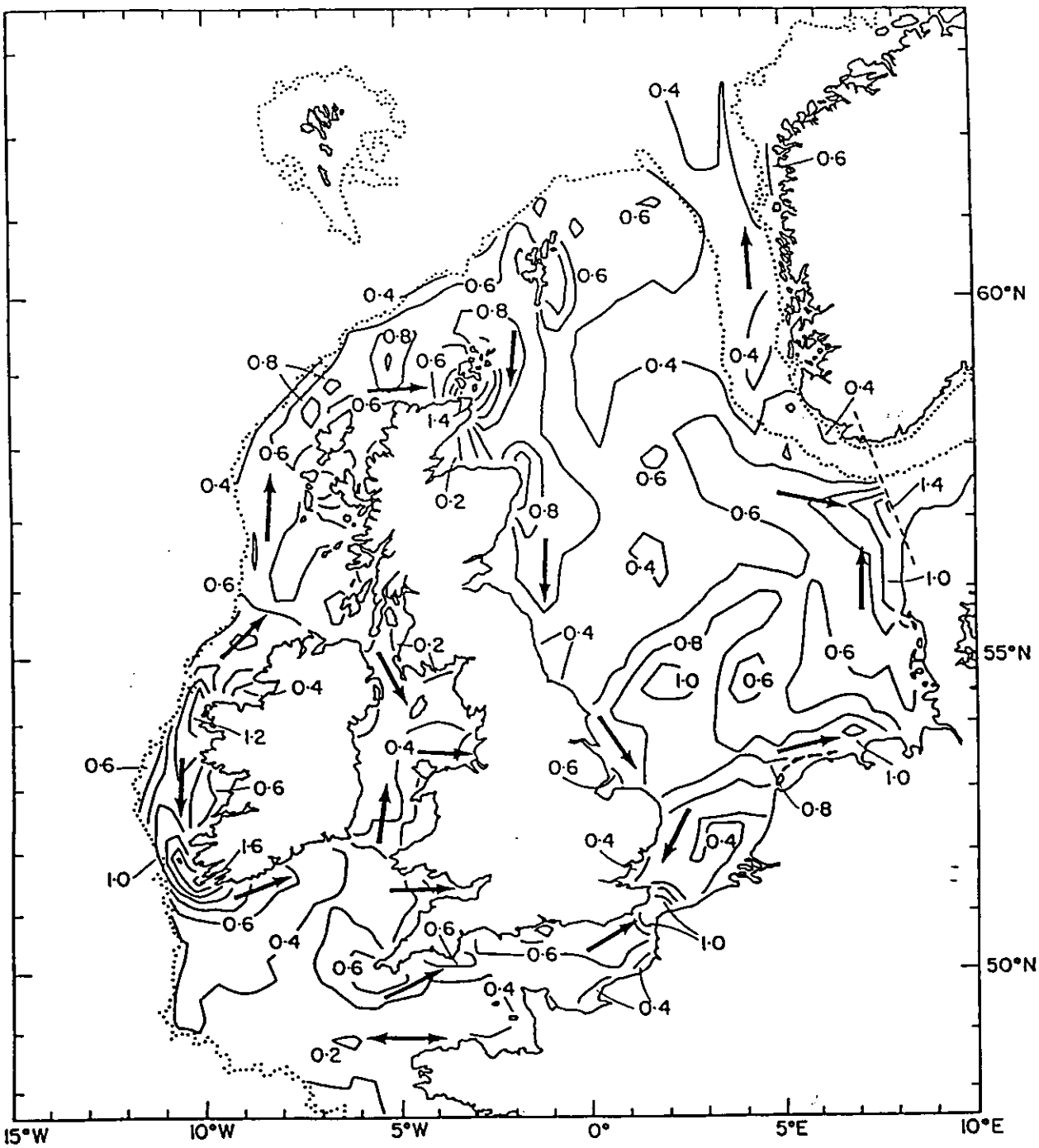

FIG. 6 : Estimates of 50-year return depth-averaged hourly-mean storm surge currents

Bold arrows indicate the direction of the maximum current in regions where the computed surge currents have preferred directions

Contours are in m/s

Dashed line is the 100 fathom (183 m) depth contour

Source: Numerical model simulations (OTH 89 299)

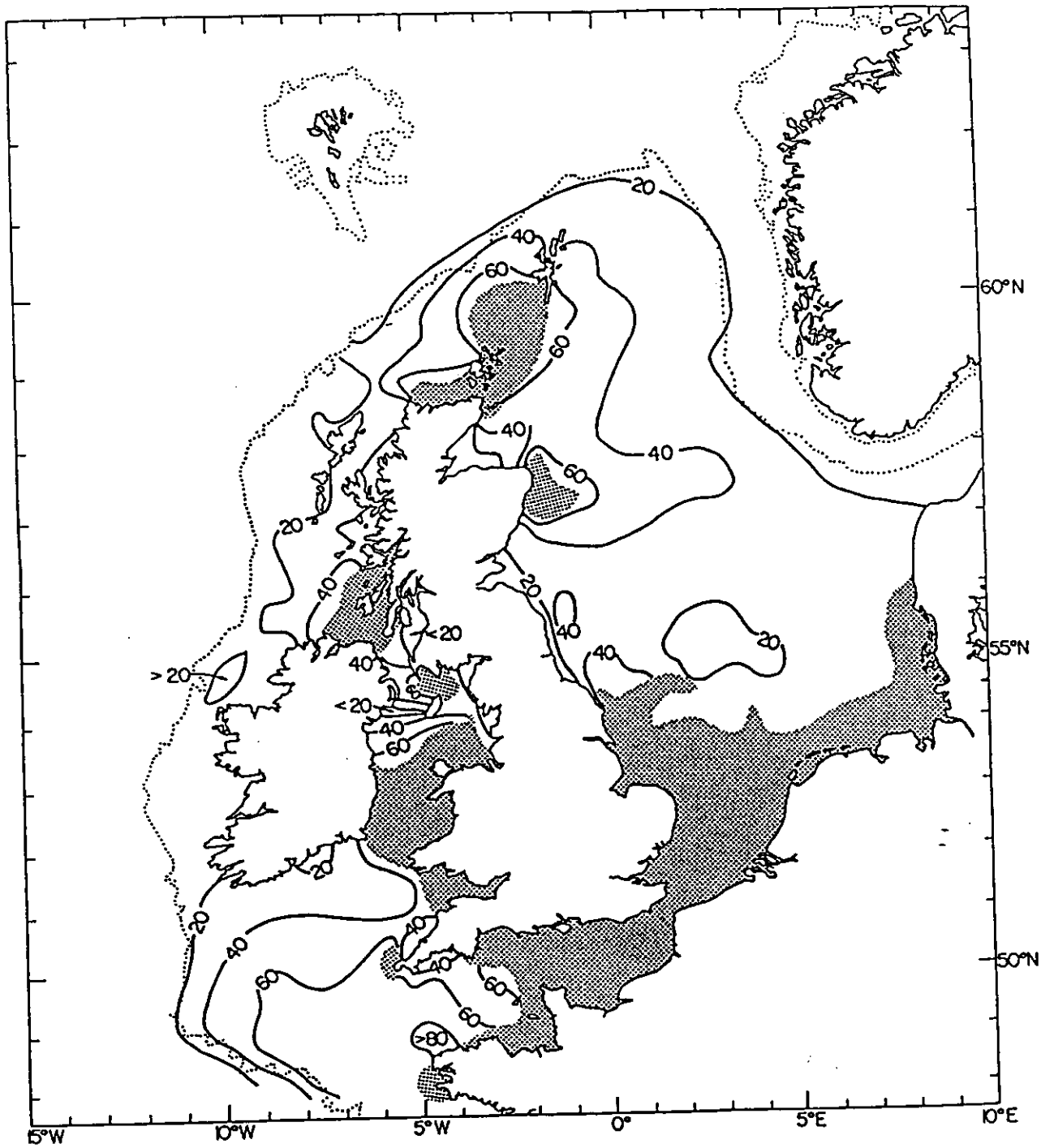

FIG. 7 : **Boundary-layer thickness, δ**

Contours are in metres

In the shaded regions, and in coastal reginns shallower than 20 m, δ should be assumed to be equal to the water depth

Source: OTH 89 299

TABLE 1

Relationships between the 50-year return hourly wind speeds of Figure 2 and 50-year return wind speeds with shorter averaging times

Extreme wind speed (m/s) with an averaging time of: (hour)	(mins)					(secs)				
1	15	10	5	2	1	30	15	10	5	3
30	31	31	32	34	35	37	38	39	40	41
31	32	32	33	35	36	38	40	41	42	43
32	33	33	34	36	37	39	41	42	43	44
33	34	34	35	37	39	41	43	43	45	46
34	35	35	36	38	40	42	44	45	46	47
35	36	36	38	40	41	43	45	46	48	49
36	37	38	39	41	42	45	47	48	49	50
37	38	39	40	42	44	46	48	49	51	52
38	39	40	41	43	45	47	50	51	52	53
39	40	41	42	44	46	49	51	52	54	55
40	41	42	43	45	47	50	53	54	55	56
41	42	43	44	47	49	52	54	55	57	58
42	43	44	45	48	50	53	55	57	58	60

Source: Mathematical modelling (OTH 89 299)

TABLE 2

Range of maximum current speeds in the continental shelf seas around the UK

Current	Range of maximum speed (m/s)	Period	Relevant Section	Location
Tidal depth-averaged	0.3-2.5	12.4 hours	11.6.3 a)	For spatial variation see Figure 4.
Storm surge depth-averaged	0.2-1.4 (1)	2-10 days	11.6.3 c)	For spatial variation see Figure 6. More extreme in winter
Surface wind drift	0.9-1.2 (1)	1-2 days	11.6.3 d)	For spatial variation see Figure 11.1, Section 11.3. More extreme in winter
Internal waves	<0.4 (2)	30 minutes	11.6.3 g)	In the unshaded areas of Figure 11.8, particularly near the shelf edge. May-October
Inertial currents	<0.2 (2)	14-16 hours	11.6.3 g)	In the unshaded areas of Figure 11.8. May-October
Currents along fronts	<0.3 (2)	Long period	11.6.3 g)	At the boundaries of the shaded areas in Figure 11.8. May-October
Circulation	<0.15 (2)	Longer than 10 days	11.6.3 g)	

(1) 50-year return value

(2) Maximum observed, but higher speeds may be possible

LINEAR WAVE INDUCED MOTIONS AND LOADS ON FLOATING STRUCTURES

by

ATILLA INCECIK

GLASGOW

LINEAR WAVE INDUCED MOTIONS AND LOADS ON FLOATING STRUCTURES

INTRODUCTION

In this lecture three different approaches used to predict the linear wave forces and resulting motion responses and loads on floating offshore platforms will be discussed. The results of various international co-operative studies to investigate the correlation between the different methods will be summarised. Finally, the recent advances in various techniques will be highlighted.

MOTION RESPONSE PREDICTIONS USING THE MORISON APPROACH

Since the early 1970s various investigators have adopted the Morison approach to predict wave exciting forces and the resulting responses and loads on various types of floating and compliant offshore platforms. The features common in the linear analysis tools developed and described in Refs 1, 2 and 3 can be summarised as follows:

(a) Airy wave theory is adopted. Amplitudes of wave and platform motions are assumed to be small. This assumption permits the linear superposition of the wave forces acting on the restrained structure due to the wave particle motions and hydrodynamic forces acting on the structure due to rigid-body oscillations of the platform in calm water.

(b) The platform can be divided into several volume elements. If the sectional dimensions of these elements are less then about 1/5th of the wave length, the wave and motion induced forces can be assumed to be concentrated in the centre of these volume elements. If one of the dimensions of these volume elements is large compared to the wave length, the two or three dimensional source distribution methods which are discussed in the next sections should be adopted.

(c) The wave and motion induced forces are calculated on each volume element, assuming that the rest of the structure is not present. In other words, the interference between the elements of the structure is not taken into account. The total force acting on the structure is obtained by summing the forces on each volume element.

(d) Hydrodynamic forces due to rigid body velocity are linearised and the wave forces due to wave particle velocities are neglected.

In the following, a brief summary of the Morison approach and the application of this method to predict wave wave exciting forces and response will be discussed.

Wave Induced Forces:

The wave induced force on each member of an offshore structure is assumed to consist of the following force components:

(a) Dynamic Pressure Force: This force is due to the hydrodynamic pressure change below the surface of a wave train while the wave is proceeding. It is assumed that the presence of the member does not interfere with the flow field. The pressure forces can be calculated in the following form :

$$\vec{F} = p\vec{n}ds = \iint_S 0.5H_w \rho e^{ky} \cos(kx - \omega t)\vec{n}ds \qquad (1)$$

where:

$\vec{n}$: Unit normal vector

ds : Area element of surface S

When the sectional dimensions of the volume element (say, height H, and beam B) in the wave field are small compared to the wave length, i.e. $H/\lambda \ll 1$ and $B \ll 1$, it can be shown that the pressure force vector given with the above surface integral equation can be calculated as:

$$F_{Px} = \rho\, a_x\, A_s \quad \text{[Force/unit length]} \qquad (2)$$

$$F_{Py} = \rho\, a_y\, A_s \quad \text{[Force/unit length]} \qquad (3)$$

where:

A_s : Cross-sectional area

a_x : Horizontal wave particle acceleration at the centre of A_s

a_y : Vertical wave particle acceleration at the centre of A_s

(b) Acceleration Force: The presence of the volume element in the wave field causes disturbance of the pressure field and this results in the acceleration forces on it. These forces can be calculated as follows:

$$F_{Ax} = K_{Mx}\, \rho\, a_x\, A_s \quad \text{[Force/unit length]} \tag{4}$$

$$F_{Ay} = K_{My}\, \rho\, a_y\, A_s \quad \text{[Force/unit length]} \tag{5}$$

where: K_{Mx} = Added-mass coefficient in horizontal mode of oscillation
K_{My} = Added-mass coefficient in vertical mode of oscillation

When the pressure and acceleration forces are summed the following form of total wave inertia force equation is obtained:

$$F_{Ix} = F_{Px} + F_{Ax} = \rho\, a_x\, A_s\, (1+K_{Mx}) \tag{6}$$

$$F_{Iy} = F_{Py} + F_{Ay} = \rho\, a_y\, A_s\, (1+K_{My}) \tag{7}$$

$(1+K_{Mx})$ and $(1+K_{My})$ can be replaced with the horizontal inertia coefficient $C_{M,x}$ and the vertical inertia coefficient $C_{M,y}$ respectively.

(c) Drag Force: Viscous effects existing in the real flow domain give rise to drag forces. Drag forces mainly result from turbulent flow of body downstream. These forces can be calculated as follows:

$$F_{Dx} = 1/2\, \rho\, C_{Dx}\, B\, U_x\, |U_x| \quad \text{[Force/unit length]} \tag{8}$$

$$F_{Dy} = 1/2\, \rho\, C_{Dy}\, H\, U_x\, |U_x| \quad \text{[Force/unit length]} \tag{9}$$

where:

C_{Dx} : Drag coefficient in X direction
C_{Dy} : Drag coefficient in Y direction
U_x : Horizontal wave particle velocity at the centre of A_s
U_y : Vertical wave particle velocity at the centre of A_s

The wave particle kinematics for deep water and added mass and damping coefficients for various geometrical shapes are given in Tables 1 and 2 respectively.

Motion Induced Forces:

(a) Acceleration Force: When the volume element is subjected to sinusoidal acceleration in calm water, the forces on it induced by fluid can be calculated as follows:

$$F_{HA_x} = -K_{Mx}\, \rho\, \ddot{X}\, A_s \quad \text{[Force/unit length]} \tag{10}$$

$$F_{HA_y} = -K_{My}\, \rho\, Y\, A_S \quad \text{[Force/unit length]} \tag{11}$$

(b) Drag Force: When the volume element is subjected to sinusoidal velocity in calm water, the forces acting on it can be written as follows:

$$F_{HD_x} = -1/2\, \rho\, C_{Dx}\, B\, \dot{X}\, |\dot{X}| \quad \text{[Force/unit length]} \tag{12}$$

$$F_{HD_y} = -1/2\, \rho\, C_{Dy}\, H\, \dot{Y}\, |\dot{Y}| \quad \text{[Force/unit length]} \tag{13}$$

In order to linearise the drag force equations, $C_{Dx}\, \dot{X}\, |\dot{X}|$ and $C_{Dy}\, \dot{Y}\, |\dot{Y}|$ can be replaced by $C_{DL,x}\, X$ and $C_{DL,y}\, Y$ respectively. The linearised drag coefficients can be given as:

$$C_{DL} = C_D\, (8\omega/3\pi)\, \dot{X} \tag{14}$$

As is seen from eq. (14) C_{DL} is dependent on motion amplitudes. The solution must therefore involve an iteration procedure in which a value of resultant velocity is assumed and C_{DL} is computed as the motion equation is solved. A new value of the rigid body velocity is calculated using the first computed C_{DL} and compared with the measured velocity. Iteration is continued until the last two velocity values are close to each other within an acceptable limit.

(c) Restoring Force: Restoring forces occur when the platform is displaced from its equilibrium position in calm water. The restoring forces can arise due to change in the underwater geometry of the platform and/or system which connects the platform to earth. The restoring force vector can be expressed as:

$$F_R = -[K]\, \{X\} \tag{15}$$

Motion Response Equation:

When the offshore platform is considered as an oscillating rigid-body having six degrees of freedom, the motion equation of the platform can be derived from Newton's second law as follows:

$$F_T = [I]\, \{\ddot{X}\} \tag{16}$$

where F_T is the total force/moment vector, [I] mass matrix, and $\{X\}$ acceleration vector of the platform. In this equation the total force vector, F_T can be replaced by the sum of the force and moment components which has been derived in the preceding sections.

$$F_I + F_D + F_{HA} + F_{HD} + F_R = [I]\, \{\ddot{X}\} \tag{17}$$

When the force/moment components are rearranged as motion dependent terms on the left hand side and time dependent forcing terms on the right hand side, the following form of six linear, second-order differential equations can be obtained:

$$[M]\{\ddot{X}\} + [C]\{\dot{X}\} + [K]\{X\} = \{F_W\} \tag{18}$$

where :

$[M]=I+\sum_i K_M V_i$	Mass + added mass matric
$[C]=\sum_i C_{DL,i}$	Hydrodynamic damping matrix
$[K]$	Restoring coefficient matrix
$\{F_W\}$	Wave force/moment vecotr
$\{\ddot{X}\},\{\dot{X}\},\{X\}$	Acceleration velocity and displacement vectors

It is assumed that there is no coupling between the different modes of motion. Equation (18) reduces to six uncoupled linear second-order differential equations, for which the standard solution can be written as:

$$X_{j,o} = F_{j,o}/\ ((K_j - M_j\omega^2))^2 + C_j^2\omega^2)^{0.5} \tag{19}$$

where $X_{j,o}$ and $F_{j,o}$ are motion and force/moment amplitudes respectively

Equation (19) can also be written in terms of frequency ratio, r_i, and damping ratio, d_i, as :

$$X_{j,o} = F_{j,o}/\ (K_j\ ((1- r_j^2))^2 + (2r_jd_j)^2)^{0.5} \tag{20}$$

where :

r_j = $\omega/\omega_{n,j}$ = (Forcing Frequency)/(Natural Frequency) in (j) mode of oscillation

$\omega_{n,j}$ = $(K_j / M_j)^{0.5}$

d_j = $C_j/(2(M_jK_j)^{0.5})$ = (Damping/Critical damping)

EXAMPLES

1. Determine the total wave exciting forces on the structure shown in the following Figure; what should be the ratio between column separation B and the wave length λ so that there will be no wave force acting on the structure? Calculate the surge response.

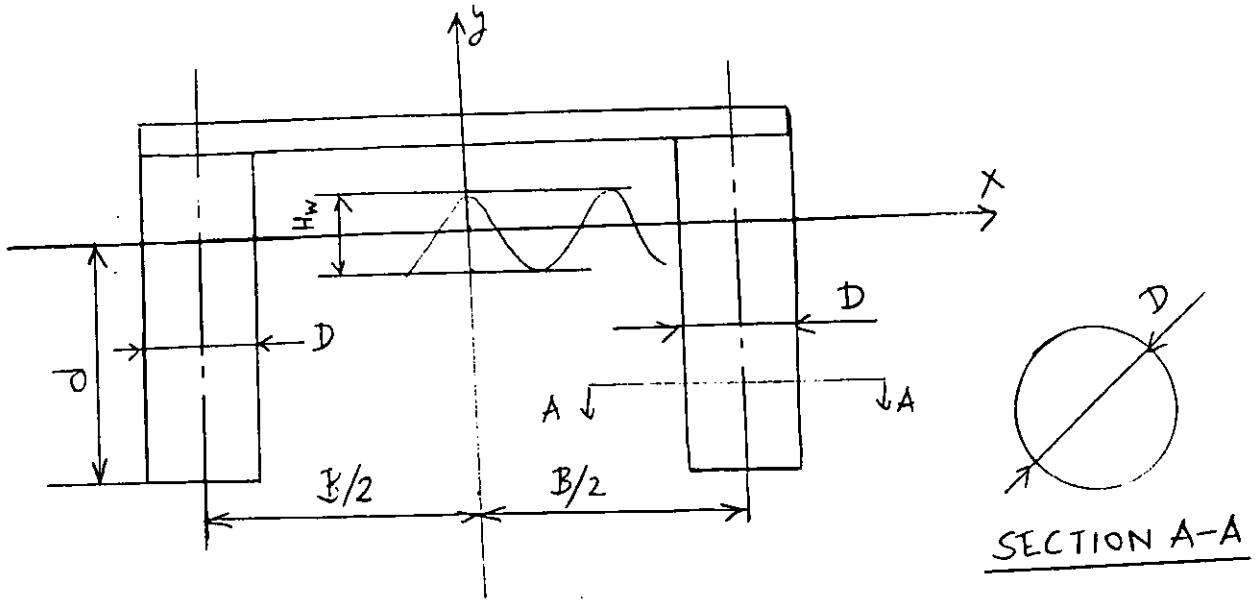

Horizontal wave forces on column (1):

$$F_{T,1} = F_{Px} + F_{Ax} + F_{Dx}$$

$$F_{T,1} = \rho\, C_M \int_{-d}^{0} a_{x,1} A_s\, dy + 1/2\, \rho\, C_D\, U_{x,1} |U_{x,1}| \int_{-d}^{0} D\, dy$$

where:

$$C_m = 2,\ \rho = 1.025,\ C_D = 0.6,\ A_s = \pi D^2/4$$

$$a_{x,1} = 0.5\, H_w\, \omega^2 e^{ky} \operatorname{Sin}(kB/2 - \omega t)$$

$$U_{x,1} \quad 0.5\, H_w\, \omega\, e^{ky} \operatorname{Cos}(kB/2 - \omega t)$$

$$F_{T,1} = \rho\, C_M\, \pi D^2/4\; 0.5\, H_w\, \omega^2 \operatorname{Sin}(kB/2 - \omega t) \int_{-d}^{0} e^{ky}\, dy$$

$$+1/2\, \rho\, C_D\, D\, (0.5\, H_w\, \omega)^2 \operatorname{Cos}(kB/2 - \omega t)\, |\operatorname{Cos}(kB/2 - \omega t)| \int_{-d}^{0} e^{2ky} dy$$

or

$$F_{T,1} = \rho\, C_M\, \pi D^2/4\; 0.5\, H_w\, \omega^2 (1/k)(1 - e^{-kd}) \operatorname{Sin}(kB/2 - \omega t)$$
$$+1/2\, \rho\, C_D\, D\, (0.5\, H_w\, \omega)^2 \operatorname{Cos}(kB/2 - \omega t)\, |\operatorname{Cos}(kB/2 - \omega t)|\, (1/2k)(1 - e^{2ky})$$

Similarly, horizontal wave exciting forces on column (2) can be written as:

$$F_{T,2} = \rho C_M \pi D^2/4\ 0.5 H_w \omega^2 (1/k)(1-e^{-kd}) \mathrm{Sin}(-kB/2 - \omega t)$$
$$+1/2\ \rho C_D D (0.5 H_w \omega)^2 \mathrm{Cos}(-kB/2 - \omega t) |\mathrm{Cos}(-kB/2 - \omega t)| (1/2k)(1- e^{2ky})$$

and the total horizontal wave force on the structure becomes:

$$F_T = F_{T,1} + F_{T,2}$$

or

$$F_T = \rho C_M \pi D^2/4\ 0.5 H_w \omega^2 (1/k)(1-e^{-kd}) [\mathrm{Sin}(kB/2-\omega t) - \mathrm{Sin}(kB/2 + \omega t)]$$
$$+1/2\ \rho C_D D (0.5 H_w \omega)^2 (1/2k)(1- e^{2ky})\{\mathrm{Cos}(kB/2 - \omega t) |\mathrm{Cos}(kB/2-\omega t)|$$
$$\mathrm{Cos}(kB/2 +\omega t) |\mathrm{Cos}(kB/2+\omega t)| \}$$

The following trigonometric relationships can be used to simplify the total wave force equation given above:

$$\mathrm{Sin}(kb/2 - \omega t) = \mathrm{Sin}(kb/2)\mathrm{Cos}(\omega t) - \mathrm{Sin}(\omega t)\mathrm{Cos}(kb/2)$$
$$\mathrm{Sin}(kb/2 + \omega t) = \mathrm{Sin}(kb/2)\mathrm{Cos}(\omega t) + \mathrm{Sin}(\omega t)\mathrm{Cos}(kb/2)$$
$$\mathrm{Cos}(kb/2 - \omega t) = 8/(3\pi)\ \mathrm{Cos}(kb/2 - \omega t)$$
$$\mathrm{Cos}(kb/2 + \omega t) = \mathrm{Cos}(kb/2)\mathrm{Cos}(\omega t) - \mathrm{Sin}(\omega t)\mathrm{Sin}(kb/2)$$
$$\mathrm{Cos}(kb/2 - \omega t) = \mathrm{Cos}(kb/2)\mathrm{Cos}(\omega t) + \mathrm{Sin}(\omega t)\mathrm{Sin}(kb/2)$$

Total wave force expression becomes:

$$F_T = \rho C_M \pi D^2/4\ 0.5 H_w \omega^2 (1/k)(1-e^{-kd})(-2\ \mathrm{Cos}(kB/2))\mathrm{Sin}(\omega t)$$
$$+1/2\ \rho C_D D (0.5 H_w \omega)^2 (1/2k)(1- e^{-2kd})(64/9\pi^2)(2\mathrm{Cos}(kB/2))\mathrm{Cos}(\omega t)$$

Before we calculate B/λ for zero horizontal surge force, let us determine the relative importance of drag and inertia forces by calculating the ratio of drag to inertia forces:

$$\alpha = \frac{\text{Inertia Force}}{\text{Drag Force}} = \frac{\rho C_M 0.5 H_w \omega^2 e^{ky} \pi D^2/4}{1/2 \rho C_D (o.5 H_w \omega)^2 e^{2ky} D}$$

$$\alpha = \frac{C_M \pi D}{C_D H_w e^{ky}}$$

Assuming, $C_M = 2$ $C_D = 0.2$, $H_w = 10$ m, $y = 0$ and $D = 10$ m

$$\alpha = (2\ \pi\ 10)/(0.6 \times 10 \times 1) = 10$$

and taking $y = -10$ m and $\omega = 0.6$ rad/sec

$$\alpha = (2\pi 10) / (0.6 \times 10 \times e^{-k10}) = 15$$

where: $k = \omega^2 / g = (0.6)^2 / 9.81 = 0.03669$

If we neglect the drag forces on this structure, the total horizontal wave force expression becomes:

$$F_T = -C_M \rho\, 2\pi D^2/4\, d\, 0.5\, H_w\, \omega^2 (1/kd)(1-e^{-kd}) \mathrm{Cos}(kB/2)\mathrm{Sin}(\omega t)$$

The physical meaning of each term in the above equation can be explained as follows:

$2\pi D^2/4\, d$	=	Volume of the structure
$\rho\, 2\pi D^2/4\, d$	=	Mass of the structure
$\mathrm{Cos}(kB/2)$	=	Spacing dependent term

$-C_M \rho\, 2\pi D^2/4\, d\, 0.5\, H_w\, \omega^2 (1/kd)(1-e^{-kd}) \mathrm{Cos}(kB/2)$ = Wave ext. force amplitude

In order to arrive at zero horizontal wave force on the structure, the spacing dependent term should be set to zero. Thus:

$$\mathrm{Cos}(kB/2) = 0$$
$$kB/2 = \pi/2(2n+1)\ ,\quad n=0,1,2,3,$$

since $k = 2\pi/\lambda$ and $B/\lambda = (2n+1)/2$

Surge Motion Equation:

$$(M + M_{AVM})\ddot{X} + C\dot{X} + k_s X = F_0 \mathrm{Sin}(\omega t)$$

where:

$$M + M_{AVM} = 2\rho(\pi D^2/4)d + 2\rho K_M(\pi D^2/4)d = 2(1 + K_M)\rho(\pi D^2/4)d$$
$$= 2C_M\rho(\pi D^2/4)d$$

and, assuming that:

$$C = 0$$
$$X = X_0 \mathrm{Sin}(\omega t)$$
$$X = X_0\, \omega\, \mathrm{Cos}(\omega t)$$
$$X = -X_0\, \omega^2 \mathrm{Sin}(\omega t)$$

The surge motion equation becomes:

$$-(M + M_{AVM})\, X_0\, \omega^2 \operatorname{Sin}(\omega t) + k_s X_0 \operatorname{Sin}(\omega t) = F_0 \operatorname{Sin}(\omega t)$$

or

$$X_0(k_s - \omega^2(M + M_{AVM})) = F_0$$

and X_0 from the above equation can be calculated as

$$X_0 = F_0 / (k_s - \omega^2(M + M_{AVM})) = (F_0 / k_s) / (1 - (\omega/\omega_n)^2)$$

where:

$$\omega_n = \sqrt{\frac{k_s}{M + M_{AVM}}}$$

2. Determine the heave response of the simplified structure shown in the following Figure:

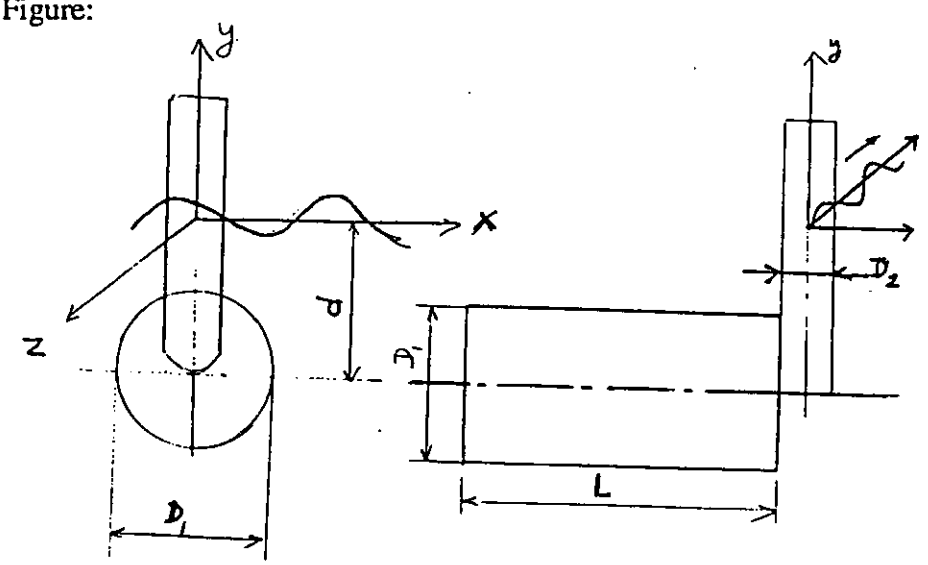

Vertical Forces on the horizontal cylinder:

$$F_{VH} = -C_M\, \rho\, (\pi D_1^2/4)\, L\, 0.5\, H_w\, \omega^2\, e^{-kd} \operatorname{Cos}(\omega t)$$

Vertical forces on the vertical cylinder:

$$F_{VV} = \rho\, g\; 0.5\, H_w\; e^{-kd}\; (\pi D_2^2/4) \operatorname{Cos}(\omega t) - (4/3)\rho\, (D^2/2)^3\, 0.5\, H_w\, \omega^2\, e^{-kd} \operatorname{Cos}(\omega t)$$

Total force on the structure:

$$F_{TV} = F_{VH} + F_{VV}$$

or

$$F_{TV} = \rho\; 0.5\, H_w\; e^{-kd}\, [-C_M\, (\pi D_1^2/4)\, L\, \omega^2 + g(\pi D_2^2/4) - (D^2/2)^3 \omega^2] \operatorname{Cos}(\omega t)$$

Assuming that:

$$D_1 = 10 \text{ m}, D_2 = 5 \text{ m}, L = 50 \text{ m}, \omega = 0.5 \text{ rad./sec.}, C_M = 2, g = 9.81$$

Hull pressure + acceleration dependent term = $2 \times (\pi \times 10^2/4)\,(0.5)^2\,50 = 1963.5$ kN
Vertical column pressure dependent term = $9.81 \times \pi \times 25 / 4 = 192.6$ kN
Vertical column acceleration dependent term = $125 \times (0.5)^2 / 6 = 5.20$ kN

The above calculations show that the acceleration forces on the vertical column can be neglected and the total heave force on the structure can rewritten as:

$$F_{TV} = \rho\, 0.5\, H_w\, \pi\, e^{-kd}\, g(D_2^2/4)[1 - C_M\,(\omega^2 D_1^2 L / D_2^2 g)]\, \mathrm{Cos}(\omega t)$$

In order to have zero heave force on the structure, the term in the bracket should be set to zero:

$$1 - \frac{C_M\, \omega^2\, D_1^2\, L}{D_2^2\, g} = 0$$

or

$$\omega = \frac{D_2^2\, g}{C_M\, D_1^2\, L} = \frac{D_2^2\, g \frac{\pi}{4}}{C_M\, D_1^2\, L \frac{\pi}{4}}$$

or

$$\omega = \sqrt{\frac{g\, A_w}{C_M\, V_H}}$$

A_w : Water plane area of the vertical cylinder = $(\pi D_2^2 / 4)$
V_H : Volume of the horizontal cylinder = $(\pi D_2^2 L / 4)$

Heave response equation:

$$(M + M_{AVM})\,\ddot{Y} + C\,\dot{Y} + k_s Y = F_{TV}$$

where:

$M = (\pi D_1^2 L / 4 + \pi D_1^2 d / 4)\,\rho = \rho\,(V_H + A_w)$

$M_{AVM} = \rho\, K_M\, V_H + 4/3\, \rho\, D_2^3 / 8$ where $K_M = 1$ for circular cylinders

$C = 0$

$k_s = \rho\, g\, A_w$

and the solution of heave response equation may be written as:

$$Y = (F_{TV} / k_s) / (1 - (\omega/\omega_N)^2)$$

where:

$$\omega_N = \sqrt{\frac{k_s}{M + M_{AVM}}}$$

$$Y = \frac{0.5\, H_w\, \rho\, e^{-kd} A_w\, g\, [1 - C_M \frac{\omega^2 V_H}{A_H g}]\, \mathrm{Cos}(\omega t)}{\rho\, g\, A_w\, (1 - \omega^2 g\, [\, (2\, V_H + A_w\, d) + \frac{D_2^3}{6}\,]\,)}$$

and the R.A.O. for the heave motions can be determined as:

$$\mathrm{R.A.O.} = \frac{y}{0.5\, H_w} = \frac{e^{-kd}[1 - C_M \frac{\omega^2 V_H}{A_H g}]}{1 - \omega^2 g\, [\, (2\, V_H + A_w\, d) + \frac{D_2^3}{6}\,]}$$

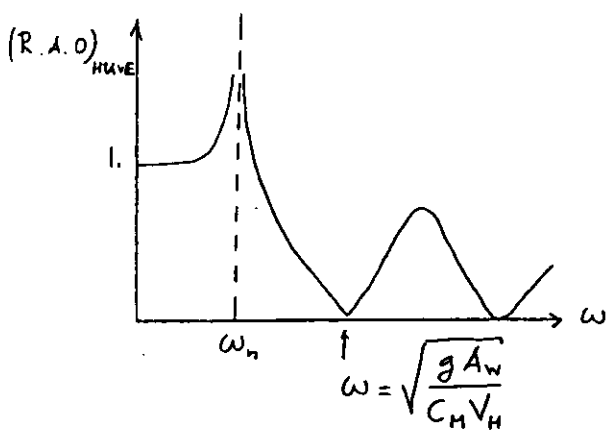

3. *Simplified Heave Response Predictions for Design Optimisation of Semi-Submersibles*

In the following simplified design, equations for predicting the heave response of a semi-submersible comprising twin hulls with multi columns are given (see also the following Figure). The course participants are recommended to derive these equations following the Morison approach described in this section and the calculation procedures illustrated in the above examples.

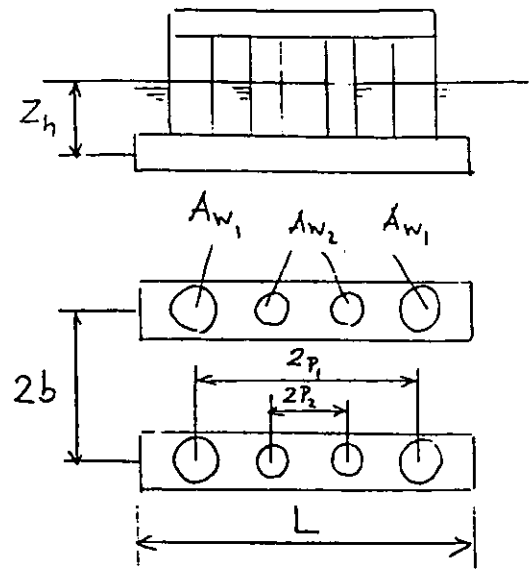

The heave forces in head seas for a semi-submersible with 4 columns per hull:

$$F_{TV} = \rho\, g\, 0.5\, H_w\, e^{-kz_h} \{k\, V(\alpha+K_M) - 4(1+k\, z_h)\,(Aw_1 \cos(kp_1) + Aw_2 \cos(kp_2)\}$$

where: $\alpha = \mathrm{Sin}(kL/2)/(kL/2)$
V = Total Volume

The heave response in head seas:

$$\text{R.A.O.} = e^{-kz_h}\{(1+k\, z_h)(C_1 \mathrm{Cos}(kp_1) + C_2 \mathrm{Cos}(kp_2) - k/k_H + (k\, V/Aw)(1-\alpha)\}/(1-k/k_H)$$

where:

$$k_H = \omega_n^2/g = \rho\, Aw/(M + M_{AVM})$$
$$C_1 = 4\, Aw_1/Aw$$
$$C_2 = 4\, Aw_2/Aw$$

The heave response amplitude operator given above may be modified for 3 and 2 column per hull semi-submersible configurations by modifying C_1 and C_2 as follows:

For 2 columns $C_1 = 1$, $C_2 = 0.0$

For 3 columns $C_1 = 4\, Aw_1/Aw$, $C_2 = 2\, Aw_2/Aw$, $p_2 = 0$

The heave forces in beam seas for a semisubmersible with N columns per hull

$$F_{TV} = \rho\, g\, 0.5\, H_w\, e^{-kz_h} \{k\, V(1+K_M) - 4(1+k\, z_h)\, Aw \cos(kp)\}$$

The heave response in beam seas:

$$\text{R.A.O.} = e^{-kz_h}\{1 + (k\, z_h)/(1-k/k_H)\}\cos(kp)$$

MOTION RESPONSE PREDICTIONS USING THE SOURCE DISTRIBUTION METHODS

In the source distribution methods the wave acceleration and rigid-body motion induced forces are calculated from the solutions of scattering and radiation potentials respectively. In two or three dimensional source distribution methods the unknown potentials of scattering and radiation are represented in terms of the Green's function. The solutions of these potentials can be obtained from the kinematic boundary conditions. The Green's function integral equation can be solved by dividing the three dimensional underwater geometry into N panels and assuming that source strengths remain constant over each panel (3-D Source Distribution Method). Alternatively, the underwater geometry is first divided into M number of two dimensional strips and each strip is subdivided into L segments on which source strengths are assumed to be constant. It is also assumed that there is no interaction between the strips (2-D source distribution Method). Once the potential functions are determined the pressure due to wave scattering or rigid-body motions can be calculated from Bernoulli's equation. The forces and moments can be obtained from the surface integrals, as in eq. (1)

The derivation and solution of motion response equations in source distribution methods are identical to those given in the Morison approach.

The two dimensional source distribution method to calculate wave and motion induced forces on floating structures has been described in detail in Refs. 4, 5 and 6. The three dimensional source distribution procedures for hydrodynamic load and response calculations have been detailed in Refs. 7, 8 and 9

COMPARATIVE STUDIES ON MOTION RESPONSE PREDICTIONS

The 17th ITTC Ocean Engineering Committee carried out an extensive study to compare the different methods used in predicting the motion response of a semi-submersible. The study was performed using 34 programs from 28 different organisations, and a summary of the committee's work has been published in Ref. 10. The methods implemented in the computer programs included the Morison approach, as well as two or three dimensional source distribution techniques. This study concluded that motion response predictions from most of the programs correlate well for surge and sway motions and they are also in good agreement with the experimental measurements. However, heave, roll, pitch and yaw response predictions show large scatter. The study also concluded that the three dimensional source distribution technique does not yield better predictions than the Morison approach.

The 9th ISSC initiated a case study to compare different diffraction/radiation analysis methods of predicting wave and motion induced forces acting on a tension leg platform. The resulting first-order motion and mean drift forces were compared. Seventeen organisations took part in the study and most of the organisations employed the three dimensional source distribution or boundary element methods to perform the task. The results of this study have been published in Ref.11. The results revealed that there is a good correlation in the prediction of surge, sway and yaw motions. However, the other modes of motion, as well as wave and motion induced forces, show large scatter.

A recent comparative study of computer programs for floating systems was sponsored by the Royal Norwegian Council for Scientific and Industrial Research as part of a larger study on floating production systems for oil and gas - FPS 2000 (Ref.12). Twentythree Institutions worldwide took part in the study and predicted first and second-order forces and resulting motions of a ship and a deeep draught floater (semi-submersible).

While first-order force and motion predictions carried out for the ship geometry by different institutions correlated well with each other, there were significant differences between the predictions carried out for the semi-submersible and for the second order force and motions of the ship. The typical variations in results are summarised in the following table:

Table: Standard Deviation in Per Cent of the Mean Values

Quantity	*Ship*	*Semi-submersible*
First-order Forces	3	15
Added-Mass	3	15
Damping	30	25
Steady Surge and Sway Force	40	50
Steady Heave Force	>50	>50
Steady Roll, Pitch and andYaw Moments	>50	>50
Slowly varying second-order forces	>50	>50

Currently the 20th ITTC Conference Ocean Engineering Committee is undertaking another comparative study by correlating the first-order wave exciting force and resulting response values as well as wave drift force and moment coefficients predicted for a semi-submersible by about twenty different organisations using their computer programs. The predictions will also be correlated with the measurements.

Although the comparative studies undertaken to date show generally poor correlations when the results are closely examined, one may say that the spread in results from different computer programs based on identical hydrodynamic theory was just about as large as that from programs based on different theories. This may lead us to conclude that the problem of disagreement in the first-order motion response predictions reduces to a problem of validation of computer software and accurate modelling rather than inaccuracy of the underlying hydrodynamic theory.

ADVANCES IN FIRST ORDER WAVE FORCE AND RESPONSE CALCULATIONS

Zero Speed Unsteady Flow Problem:

This problem has almost reached the most advanced state in its reduction to a computationally efficient and reliable form. It is therefore of interest for direct application to vessels without forward speed, but also as a model to provide guidance for the more difficult cases involving steady and unsteady forward motion.

A substantial number of computer programs has been developed to solve this problem for arbitrary three dimensional floating or submerged bodies in water which is infinitely deep or of constant depth. These programs were widely used in the design of offshore platforms. However, as discussed in the previous section, the limitations of the 'first generation' programs were apparent when various comparative studies were carried out (Refs. 10,11).

In order to improve this unsatisfactory situation the 'second - generation' panel programs have been developed with various numerical refinements. These include fast algorithms for evaluating the free surface Green function with controlled accuracy, and the use of an iterative solver for the linear system of algebraic equations leading to the value of the unknown potential on each panel. The use of these programs has made it possible to increase the maximum number of panels from a few hundred to several thousand, and to establish convergence of the solution as this number is increased. Comparisons of the first-order wave and rigid-body induced forces and motion responses obtained for a deep water floater and a ship using the 'second - generation' panel programs show significant improvements, as illustrated in the previous section. Full details of the comparative study are given in Ref. 12.

The Forward - Speed Steady Problem:

One of the most difficult problems in ship hydrodynamics involves steady or unsteady motion with forward speed. The difficulties are associated with the analytical

formulation and the numerical problems in developing solutions. The uncertainties regarding the analytical formulation are associated with the issue of linerisation of the free-surface. Well known integral expressions exist for the steady free-surface Green function, with forward velocity included. However, these functions, and presumably also the exact solution of the linearised problem, contain subtle and very complicated mathematical singularities.

An approximate linearisation of the free-surface condition, without restricting the geometry or Froude Number, is known as the Kelvin-Neumann approach in wave resistance theory. Several computer programs have been written utilising the Kelvin-Neumann approach and excluding the short-wave component of the spectrum in evaluating the Green function. However, due to numerical convergence problems the routine use of these programs is not as yet practicable. Of course this situation could change if fast algorithms are used for the Green function, and if effective numerical filtering of the short-wave length singularity can be implemented in a rational manner.

The Forward - Speed Unsteady Problem:

The same techniques used for the steady problem can be extended to unsteady ship motions in waves. Having developed and validated computer programs based on 3-D source distribution technique for zero forward speed, Chan (Ref. 9) extended the formulation of Green's function to determine the wave loading on a marine vessel travelling with a forward speed in deep and shallow water. The Green function formulation developed by Chan represents a translating and oscillating source in infinite and finite water depths. Newman (Refs. 13, 14) and Telste and Noblesse (Ref. 15) have developed algorithms for the computation of a Green function representing an oscillating source or translating source for infinite water depth. However, the oscillating source potential, or translating source potential, cannot satisfy the undisturbed free surface condition for the unsteady forward motion problem. Inglis and Price (Ref. 16) and Wu and Eatock Taylor (Ref. 17) have independently modified the expression for Green's function representing a translating and pulsating source which satisfies the undisturbed free-surface condition for the unsteady forward motion problem. However, these modified expressions of the Green function are only applicable to deep water. The formulations derived in Ref. 9 are also applicable to finite and infinite water depths and allow for the interaction between steady waves (Kelvin Waves) and the unsteady waves (Radiation Waves) and satisfy the undisturbed free surface conditions.

REFERENCES/

REFERENCES

1. HOOFT, J.P.: 'A Mathematical Model of Determining Hydrodynamically Induced Forces on a Semisubmersible', Trans. of SNAME, Vol. 79, 1971.

2. PAULLING, J.R.: 'Elastic Response of Stable Platform Structures to Wave Loading', Proc. of the Intl. Symposium on the Dynamics of Marine Vehicles and Structures, London, 1974.

3. OO, K.M. and MILLER, N.S.: 'Semi-submersible Design: The Effect of Different Geometries on Heaving Response and Stability', Trans. R.I.NA., 1977.

4. FRANK, W.: 'Oscillation of Cylinders in or below the Free Surface of Deep Fluids', NSRDC Report 2375, 1967.

5. SALVESEN, T., TUCK, E.O and FALTINSEN, O.: 'Ship Motions and Sea Loads', Trans. SNAME, Vol. 78, 1970.

6. KIM,C.H., CHOU, F-S and TIEN. D.: 'Motions and Hydrodynamic Loads of a Ship Advancing in Oblique Waves', Trans. SNAME, Vol.88, 1980.

7. GARRISON, C.J.: 'Hydrodynamic Loading of Large Offshore Structures: Three-Dimensional Source Distribution Methods', in Numerical Methods in Offshore Engineering, Ed. Zienkiewicz, Lewis, and Stagg, Wiley Series in Numerical Methods in Engineering, 1978.

8. HOGBEN, N and STANDING, R.G.: 'Wave Loads on Large Bodies', Proc. of Intl. Symposium on Dynamics of Marine Vehicles and Structures in Waves, London, 1974.

9. CHAN, H.S.: 'A Three Dimensional Technique for Predicting First and Second Order Hydrodynamic Forces on a Marine Vehicle Advancing in Waves', PhD Thesis, University of Glasgow, 1990.

10. TAKAGI, M., ARAI, S.I., TAKEZAWA, S., TANAKA. K. and TAKARADA, N.: 'A Comparison of Methods for Calculating the Motion of a Semi-Submersible', Ocean Engineering, Vol. 12, No. 1, 1985.

11. EATOCK TAYLOR, R. and JEFFERYS, E.R.: 'Variability of Hydrodynamic Load Predictions for a Tension Leg Platform', Ocean Engineering, Vol. 13, No. 5, 1986.

12. NIELSEN, I.G., HERFJORD, K. and LOKEN, A.: 'Floating Production Systems in Waves: Results from a Comparative Study on Hydrodynamic Coefficients, Wave Forces and Motion Responses', Report of the Workshop on FPS200, Bergen, Norway, 1989.

13. NEWMAN, J.N.: 'Evaluation of the Wave Resistance Green Function: Part 1 - The Double Integral', Journal of Ship Research, Vol. 13, No.2 , 1987a.

14. NEWMAN, J. N.: 'Evaluation of the Wave Resistance Green Function: Part 2 - The Single Integral on the Centreplane', Journal of Ship Research, Vol. 13, No. 3, 1987b.

15. TELSTE, J.G. and NOBLESSE, F.: 'Numerical Evaluation of the Green Function of Water-Wave Radiation and Diffraction', Journal of Ship Research, Vol. 30, No. 2, 1986.

16. INGLIS, R.B. and PRICE, W.G.: ' Calculation of the Velocity Potential of a Translating, Pulsating Source ', Trans. RINA, Vol. 123, pp 163-175, 1981.

17. WU, E.X. and EATOCK TAYLOR R.: 'A Green's Function Form for Ship Motions at Forward Speed', International Shipbuilding Progress, Vol. 34, 1987.

18. SARPKAYA, T. and ISAACSON, M.: 'Mechanics of Wave Forces on Offshore Structures', Van Nostran Reinhold Company, New York, 1981.

19. HALLAM, M.G., HEAF, N.J. and WOOTTON, L.R.: 'Dynamics of Marine Structures: Methods of Calculating the Dynamic Response of Fixed Structures Subject to Wave and Current Action', CIRIA Underwater Engineering Group, London, 1978.

TABLE 1: (From Ref. 18)

Deep water approximation to linear wave theory (Sarpkaya and Isaacson (1982))

Range of validity	$kd > \pi$ or $\frac{d}{\lambda} > \frac{1}{2}$
Velocity potential	$\phi = \frac{g}{\omega}\zeta_a e^{ky} \sin(kx - \omega t)$
Dispersion relation	$c^2 = \frac{\omega^2}{k^2} = \frac{g}{k}$
Wave length	$\lambda = \frac{gT^2}{2\pi}$
Surface elevation	$\zeta = \zeta_a \cos(kx - \omega t)$
Pressure	$p = \rho g \zeta_a e^{ky} \cos(kx - \omega t)$
Horizontal particle displacement	$\xi = -\zeta_a e^{ky} \sin(kx - \omega t)$
Vertical particle displacement	$\eta = \zeta_a e^{ky} \cos(kx - \omega t)$
Horizontal particle velocity	$U_x = \zeta_a \omega e^{ky} \cos(kx - \omega t)$
Vertical particle velocity	$U_y = \zeta_a \omega e^{ky} \sin(kx - \omega t)$
Horizontal particle acceleration	$\dot{U}_x = \zeta_a \omega^2 e^{ky} \sin(kx - \omega t)$
Vertical particle acceleration	$\dot{U}_y = -\zeta_a \omega^2 e^{ky} \cos(kx - \omega t)$

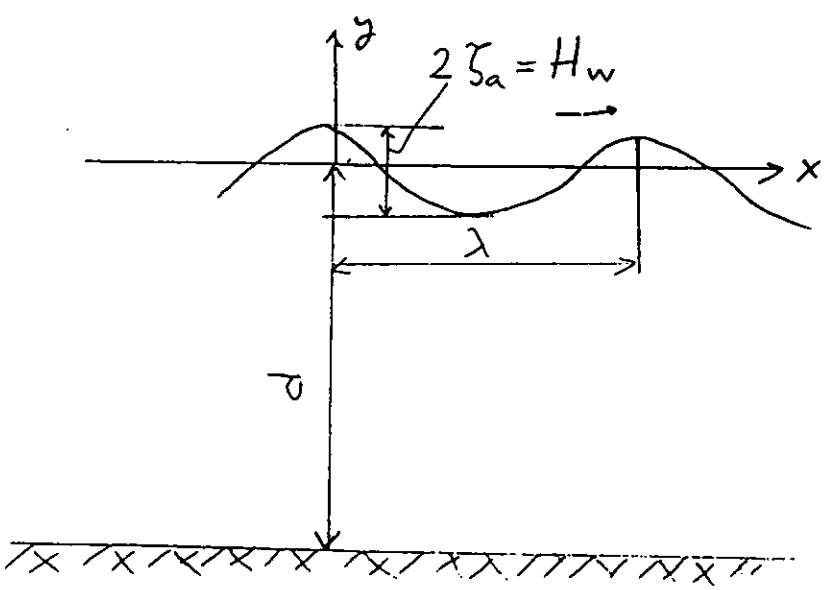

Table 2 Added Masses of Various Bodies (From Ref. 18)

SHAPE	ADDED MASS PER UNIT LENGTH ← MOTION					
CIRCLE	$\rho\pi c^2$					
ELLIPSE	$\rho\pi b^2$					
ELLIPSE	$\rho\pi a^2$					
PLATE	$\rho\pi w^2$					
RECTANGLE	a/b			a/b		
	—	1.00	$\rho\pi a^2$	1	1.51	$\rho\pi a^2$
	10	1.14	"	0.5	1.70	"
	5	1.21	"	0.2	1.98	"
	2	1.36	"	0.1	2.23	" (Wendel 1950)
DIAMOND	2	0.85	"			
	1	0.76	"			
	0.5	0.67	"			
	0.2	0.61	"	(Wendel 1950)		
I-BEAM						
a/c = 2.6, b/c = 3.6		2.11	$\rho\pi a^2$	(Patton 1965)		
REGULAR POLYGON	n = 3	0.654	$\rho\pi a^2$			
	4	0.787	"			
	5	0.823	"			
	6	0.867	"			
OR	—	1.000	"	(Wendel 1950)		

n SIDED

Table 2 (Continued)

SPHERE $\frac{2}{3}\rho\pi R^3$

ELLIPSOID OF REVOLUTION $k\,\frac{4}{3}\rho\pi b^3$

a/b	k
0.01	0.6348
0.10	0.6148
0.20	0.6016
0.40	0.5712
0.60	0.5447
0.80	0.5211
1.00	0.5000
2.00	0.4200
3.00	0.3660
5.00	0.2956
7.00	0.2511
10.00	0.2071

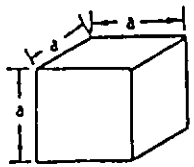

CUBE $0.7\rho a^3$

(Sarpkaya 1960, Yu 1945)

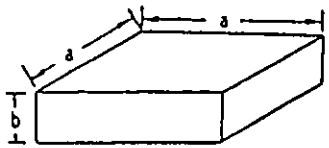

RECTANGULAR BLOCK $k\,\rho a^2 b$

b/a	k
0.5	1.32
0.6	1.15
0.8	0.86
1.0	0.70
1.2	0.57
1.6	0.45
2.0	0.35
2.4	0.30
2.8	0.26
3.6	0.22

(Sarpkaya 1960)

Table 2 (Continued)

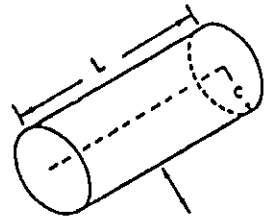

L/(2c)	
1.2	0.62 $\pi\rho c^2 L$
2.5	0.78 "
5.0	0.90 "
9.0	0.96 "
∞	1.00 "

(Wendel 1950)

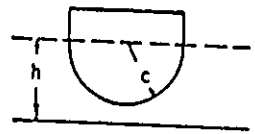

FLOATING CYLINDER $k\,\frac{\pi}{2}c^2$

h/c	k
1.2	1.83
1.5	1.45
2.0	1.22
3.0	1.09
5.0	1.03
∞	1.00

(Bai 1977)

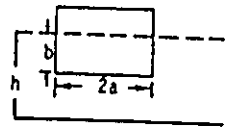

FLOATING RECTANGLE

$2k_1\rho ab$

b/h	k_1 a/b = 0.2	0.5	1.0	2.0
0.0	4.75	2.14	1.18	0.67
0.2	4.92	2.25	1.29	0.78
0.4	5.43	2.63	1.66	1.16
0.6	6.63	3.56	2.53	2.02
0.8	10.15	6.46	5.23	4.62

$2k_2\rho ab$

h/b	k_2
1.1	5.52
1.2	3.49
1.5	2.11
3.0	1.35
8.0	1.21
∞	1.19

(Bai 1977, Flagg and Newman 1971)

Table 2 (Cont'd)

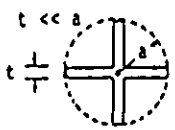

EQUALLY SPACED MULTIPLE FINS $2\rho\pi a^2/2^{4/n}$ for $n \geq 3$ (Bryson 1954)

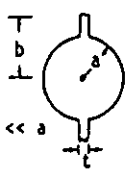

CIRCLE WITH TWO SYMMETRIC FINS

$\rho\pi a^2$

$\rho\pi b^2\left(1 - \frac{a^2}{b^2} + \frac{a^4}{b^4}\right)$

(Newman 1977)

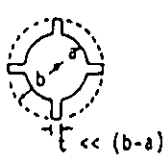

CIRCLE WITH EQUALLY SPACED MULTIPLE FINS

$$2\rho\pi b^2\left\{\left[\frac{1 + (a/b)^n}{2}\right]^{4/n} - \frac{1}{2}\left(\frac{a}{b}\right)^2\right\}$$

for $n \geq 3$

n = number of fins (Bryson 1954)

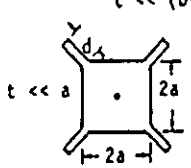

FINNED SQUARE

d/a	
0.05	1.61 $\rho\pi a^2$
0.10	1.72 "
0.25	2.19 "

(Wendel 1950)

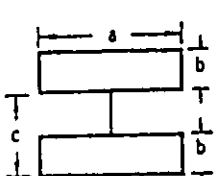

TANDEM RECTANGLES

$2\Lambda ab$

	Λ			
	b/a			
c/a	0.1	0.2	0.4	1.0
0.5	3.2	1.6	0.75	---
1.0	3.8	2.0	1.1	0.35
1.5	4.4	2.3	1.3	0.45
2.0	4.9	2.7	1.5	0.55
3.0	5.4	2.9	1.6	0.60
4.0	5.6	3.0	1.6	0.70

(Sarpkaya 1960)

CIRCULAR DISK* $\frac{8}{3}\rho c^3$

ELLIPTICAL DISK

b/a		
∞	1.000	$(\pi/6)\rho ba^2$
3	0.900	"
2	0.826	"
1.5	0.758	"
1.0	0.637	"

(Munk 1934)

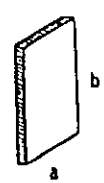

RECTANGULAR PLATE

b/a		
1.0	0.579	$(\rho/4)\pi a^2 b$
1.25	0.642	"
1.59	0.704	"
2.0	0.757	"
2.5	0.801	"
4.0	0.872	"
5.0	0.897	"
8.0	0.934	"
10.0	0.947	"
∞	1.000	"

(Meyerhoff 1970)

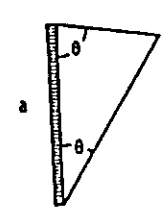

TRIANGULAR PLATE

$$\frac{\rho a^3(\tan\theta)^{3/2}}{3\pi}$$

(Nielsen 1960)

* All bodies shown above are assumed to be very thin.

Table 2 (Cont'd) (From Ref. 19)

Drag coefficients for common structural forms

Section shape	C_D
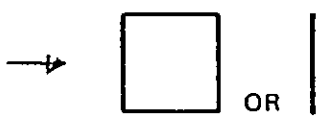	2.0
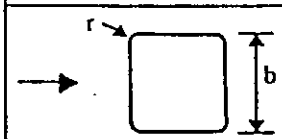	0.6
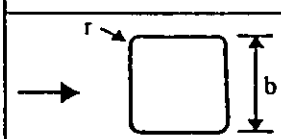	0.5
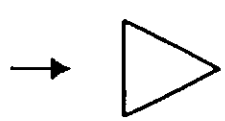	2.0
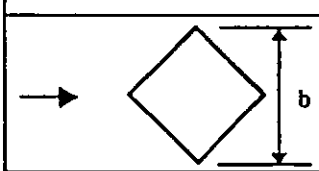	1.5

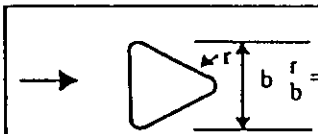	1.9
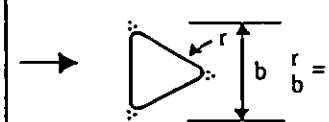	1.3
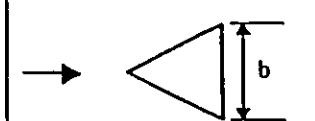	1.3
	1.3
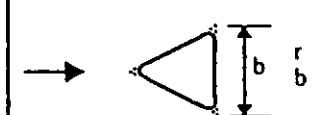	0.5

Delany and Sorensen, 1953

Table 2 (Cont'd) (From Ref. 19)

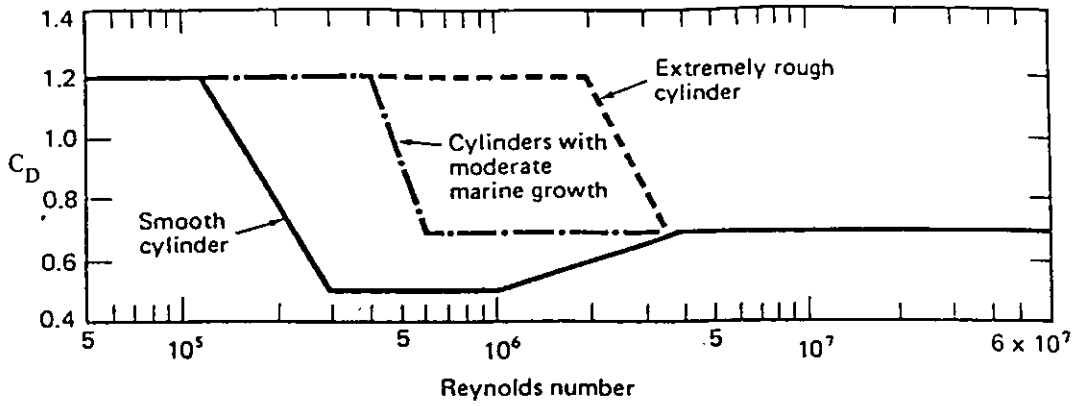

Drag coefficient values recommended by Olsen, 1974 (see also Miller, 1976 and BSRA, 1975)

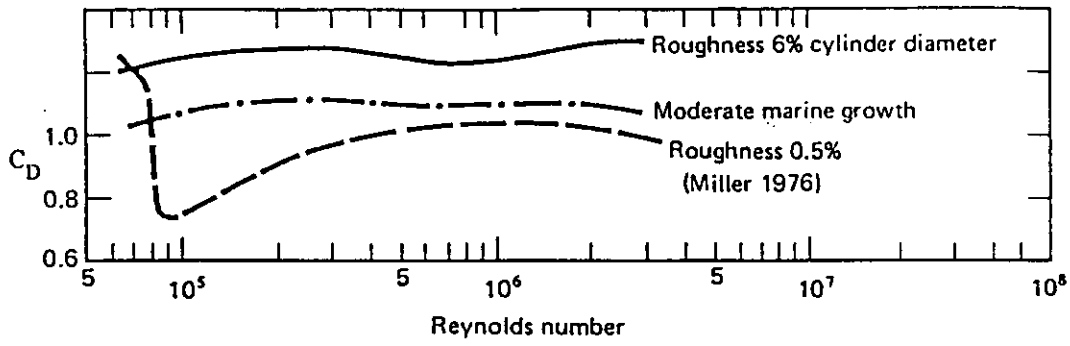

Some factors that affect the values of C_D in Morison's Equation

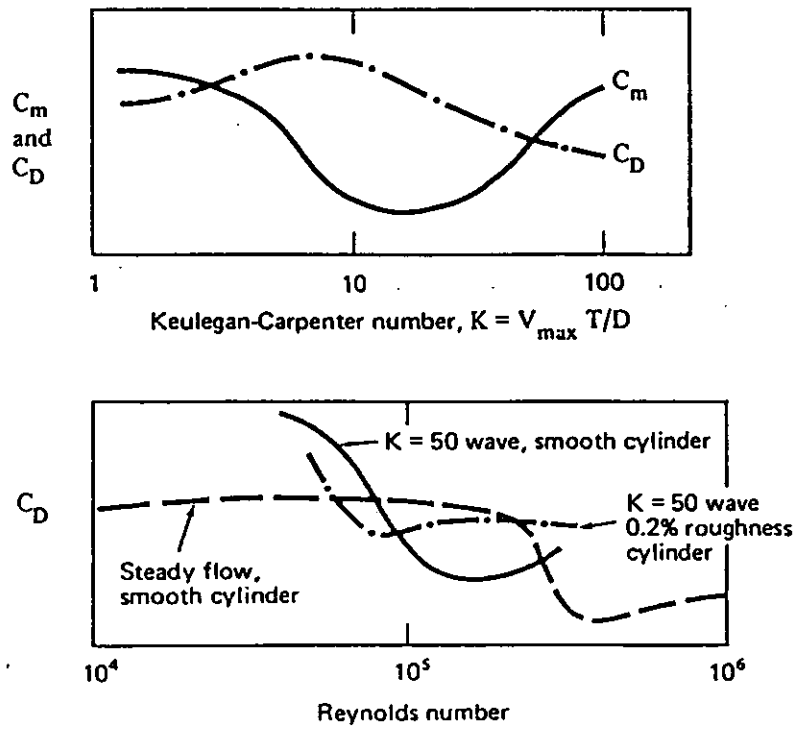

Schematic representation of effect of wave flow on values of C_D and C_m (Sarpkaya, 1976)

INTRODUCTION TO ADVANCED MARINE VEHICLES

by

ATILLA INCEICK

GLASGOW

INTRODUCTION TO ADVANCED MARINE VEHICLES

INTRODUCTION

Advanced marine vehicles which are exemplified by the hydrofoil, air cushion vehicle, surface effect ship, small water plane area twin hull ship (SWATH) and of various hybrid form concepts are of increasing importance in both passenger and cargo transportation and military missions. Extensive research and development programmes are being carried out in Norway and Japan to design and construct optimum vessel forms for fast cargo and passenger transportation. This lecture will start by introducing the investigations of Hybrid Surface Ship forms carried out at the David Taylor Research Centre in the 1970s and will detail the research and development programmes on AVM forms being carried out in Japan and Norway.

U.S. NAVY HYBRID SHIP CONCEPTS

The U.S. Navy Hybrid Ship Concept programme considered three types of lift for surface ships and generated various hybrid forms, as summarised in the following. Figure1 and Table 1 extracted from Ref. 1 show the U.S. Navy Hybrid Ship form concepts.

1. *Small Water Plane Area Single Hull (SWASH) Ship*: In this concept, the single submerged hull and centreline surface piercing strut provide about 85% of the total lift force. At zero speed the remaining buoyancy is obtained from side hulls with sufficient waterplane area to provide transverse as well as longitudinal stability. The side hulls are integral parts of the above water platform. At operating speeds sufficient lift is generated by the surface piercing hydrofoils to lift the side hulls clear of the water. The seakeeping and calm water resistance performance of this concept are detailed in Ref. 2

2. *Hydrofoil Small Waterplane-Area Ship (HYSWAS)*: This form consists of a single submerged hull with a fully submerged foil system and an upper hull structure supported above the water surface by a single, slender, longitudinal strut. At low speed the buoyancy is provided by the submerged hull, the strut and a small segment of the upper hull. As speed increases the lower hull and submerged strut provide 70% of the total lift, with the foil system providing 30%. A main foil is located just forward of mid-ship position and carries about 75% of the dynamic lift. A secondary aft foil carries 25% of the dynamic lift and maintains appropriate trim and pitch stability.

3. *Large Hydrofoil Hybrid Ship (LAHHS):* This concept consists of a slender submerged hull and foil system connected to the upper hull by three struts. The underwater hull provides 50 to 70% of the total lift through buoyancy and has a circular cross-section, a length-to-diameter ratio of about 20, and a prismatic coefficient of 0.8. The hydrofoils proposed for this concept have span-to-beam ratios that vary from about 1.0 to 1.7 and provide forward and aft dynamic force distributions of 30% and 70% respectively.

4. *Hydrofoil Air Cushion Ship (HYACS):* This concept consists of an air cushion surrounded by a rigid side hull extending downward from each side of the upper hull, with flexible seals fore and aft, a fully submerged aft foil connected to the side hull by struts, and a forward foil supported by a strut on the centreline of the upper hull. The air cushion provides 70% of the buoyancy and the remaining 30% is provided by the submerged foil system.

5. *Small Waterplane Area Air Cushion Ships (SWAACS):* This concept consists of an air cushion surrounded by a rigid side hull with flexible seals fore and aft and a single, slender, longitudinal strut. The air cushion provides 70% of the buoyancy and the remaining 30% is provided by the submerged foil system.

The performance characteristics, speed and operational range of the above concepts are detailed in Ref. 3. Reference1 gives the following conclusions with regard to operational characteristics of the Hybrid Surface Ship Forms summarised above:

1. If a vessel is to be operated at speeds of less than 30 knots and in high sea states on a year round basis, the HYSWAS and, to a lesser extent, LAHHS configurations have superior performance over the other hybrid ship concepts.

2. If a vessel is to be operated at a speed range of 18 to 40 knots in high sea states, the HYSWAS and LAHHS concepts have relatively better speed and range performance.

3. If a vessel is to be operated at a speed range of about 30-50 knots in high sea states, the LAHHS configuration appears to be superior.

4. Although the cushionborne hybrids described above have a higher speed capability in calm water, the effect of rough water tends to negate this advantage and speed drops rather rapidly under such adverse conditions.

JAPANESE TECHNO-SUPERLINER PROGRAMME

The research and development programme started in 1989 in Japan aims at designing and building a super high speed cargo transportation vessel which will satisfy the following design requirements:

a. Cargo carrying capacity = 1,000 Tonnes
b. Service range = 500 Nautical miles
c. Service speed = 50 Knot
d. Regular service at Sea State 6

This five year R&D programme is being funded by the Japanese Ministry of Transport and seven major shipbuilding companies (Ref.4). The project has a total budget of about 10 billion Yen. (£50M). Currently two basic concepts are being investigated through an extensive multi-disciplinary programme which includes studies on overall design, hydrodynamic hull performance; structural aspects and new materials; propulsion and motion control systems. This programme has kept the R&D activities in Shipbuilding in Japan alive during a brief downturn in the Shipbuilding Industry. The two basic concepts being studied are a hydrofoil hybrid ship: TSL-F and an air cushion-borne ship: TSL-A.:

1. *Hydrofoil Hybrid Ship Concept (TSL-F):* The configuration selected for the development of this hydrofoil hybrid ship concept consists of:

   a. A main Hull
   b. A fully submerged lower hull
   c. Fully submerged foils
   d. Struts

   Figure 2 (extracted from Ref. 5) illustrates the TSL-F concept. In the initial design the submerged foil dimensions were selected so that they could provide about 20% of the buoyancy at the service speed. However, earlier experiments gave much less lift than required due to complex hull-strut and foil interaction phenomena. The foils submerged 6.8 m below the surface were being optimised for the required lift forces. The prototype tests carried out with a 1/20 scale model proved very satisfactory seakeeping, manoeuvring and course keeping characteristics of the design. Waterjet propulsors driven by gas turbines have been selected for the vessel.

2. *Air Cushion-borne Ship Concept (TSL-A):* This vessel concept consists of two slender catamaran hulls enclosed by bow and aft seals which are made of flexible membrane and underwater fins for motion control - see Fig. 3 (extracted from Ref. 6). The air cushion provides about 70% of the buoyancy. The other design features in this concept are as follows:

(a) In order to reduce the weight corrosion resistant aluminium alloy will be used to construct the hulls and the superstructure

(b) Jet propulsors driven by gas turbines will be employed

(c) The vessel will be equipped with a ride control system which controls the cushion pressure to reduce vertical motions, and small waterplane fins to reduce pitch and roll motions of the vessel in high seas states

(d) The freight capacity will be equivalent of 150 ordinary 20 feet containers and all will be loaded on the upper deck. The proposed vessel dimensions allow the ship to use existing harbour facilities.

NORWEGIAN ACTIVITIES ON HYBRID SHIPS

There are three Norwegian companies which are actively working on the hybrid foil-borne and air cushion-borne catamarans:

The Westamarin Foilcat 2900 Project: Westamarin have recently completed the main technical trials with the 29 metre Foil-borne catamaran. The vessel is designed for a service speed of 50 knots for passenger transportation. This vessel is equipped with diesel engines which derive CP propellers (see Fig. 4 and Ref. 8). At low speeds the vessel is fully hull-borne, above 12 knots some lift is available, increasing with speed until 28 knots the vessel can be fully foil-borne. The under keel clearance is determined by the Master according to the weather conditions. The material used in constructing the structure is aluminium.

The Kvaerner Fjellstrand Foilcat: This is a 40 metre foil-borne craft to be operated at 50 knots with water jet propulsors driven by gas turbines. The designers of this vessel predicted that motions of this foil-borne catamaran are reduced by about 60 to 70% compared to a traditional catamaran. The design is described as a low-flying catamaran supported by foils, combining dynamic lift and displacement (Ref.9).

The CIRRUS Aircushion Catamarans : The company has been building air cushion-borne catamarans since 1984. The air cushion-borne catamarans built by Cirrus comprises vessels from 18 m to 60 m with maximum speeds in excess of 50 knots. All the vessels are in FRP/sandwich materials and payload capability varies from 7 tonnes to 150 tonnes. The Cirrus series of catamarans are equipped with jet propulsion driven by diesel engines (Ref.10).

TECHNO-ECONOMICAL ASPECTS

In order to complete the introduction to AVMs described in this lecture, a summary of their techno-economical characteristics are given as follows:

Since most of the new hybrid ship concepts utilise water jets for propulsion, in Fig. 5 propulsive efficiency for different propulsors is given (Ref.11).

The advantages of the water propulsion system are:

1. Low draft
2. High power
3. High speed
4. Elimination of external underwater appendages
5. Free choice of location of the propulsive machinery
6. Elimination of complex transmission machinery
7. No underwater radiated propeller cavitation noise
8. Direct control of steering and manoeuvring (no rudder)
9. Less propeller vibration
10. Better manoeuvring qualities.

The disadvantages of the water jet propulsion system are:

1. More expensive
2. Less efficient
3. Heavier
4. More complicated
5. Cavitation in the inlet system
6. Poor impeller access
7. Pump cavitation

Table 2, obtained from Ref.12, shows the operational limits for AVMs.
Figure 6 shows the accelerations versus frequencies for different levels of sea sickness and fatigue.
Figure 7 indicates the drag component breakdown for air cushion drag/weight ratio for different Froude Numbers (Ref.13).
Reference 14 describes structural design aspects of AMVs and discusses the requirements for research and development to establish new design codes for AVMs.
In Fig. 8 (obtained from Ref. 15) the transport efficiency of various marine vehicles for different speeds are compared. The transport efficiency is defined as Installed Power/(All-up-weight x Speed). The transport efficiency of hybrid marine vehicles is compared in Fig.9.

REFERENCES

1. MEYER, J.R.: 'Hybrid Hydrofoil Technology - An Overview', Proc. of the First International Conference on Fast Sea Transportation, Norway, 1991.

2. GERSTEN, A.: 'A Small Waterplane Area Single Hull with Stabilising Hydrofoil (SWASH); Seakeeping Characteristics and Calm Water Performance', NSRDC SPD-599-01, November, 1974.

3. MEYER, J.R.: 'A Comparison of Several Hybrid Surface Ship Concepts', Naval Engineers Journal, 1977.

4. SUGAI, K. and YAMAGUCHI, M.: ' Research and Development Programme of Tecno-Superliner', Proc. of the First International Conference on Fast Sea Transportation, Norway, 1991.

5. YAMANAKA, N. et al: 'A Submerged Hull and Foil Hybrid Super-High Speed Liner', Proc. of the First International Conference on Fast Sea Transportation, Norway, 1991.

6. OZAWA, H. et al: 'A Concept Design Study of "Techno-Superliner"', Proc. of the First Intl Conference on Fast Sea Transportation, Norway, 1991.

7. HIRANO, M. et al: 'Research on Hydrodynamic Aspects of "Techno-Superliner-A"', Proc. of the First Intl Conference on Fast Sea Transportation, Norway, 1991.

8. 'FOILCAT READY FOR SERVICE', Ship and Boat International, July ,1992.

9. 'Dyanamic Support - Where Next?', Ship and Boat international, July/August, 1989.

10. 'Jane's High Speed Marine Craft and Air Cushion Vehicles', Edited by Robert L. Trillo, 1989.

11. ARCANT, L.: 'Waterjet Propulsion for High- Speed', Proc. of the AIAA/ SNAME Advanced Marine Vehicles Conference, Norfolk, Virginia, 1967.

12. FALTINSEN,O.: 'High Speed Marine Vehicle Lecture Notes', Norwegian Institute of Technology, 1991.

13. WILSON, R.A.: 'Powering Prediction for Surface Effect Ships Based on Model Results', Proc. of the AIAA/SNAME Advanced Marine Vehicles Conf., California, 1978.

14. FAULKNER, D.: 'Classification Societies - Are they up-to -date?', Proc. of the Conference on High Speed Marine Craft, Norwegian Society of Chartered Engineers, Kristiansand, 1992.

15. AKAGI, S.: 'Synthetic Aspects of Transport Economy and Transport Vehicle Performance with Reference to High Speed Marine Vehicles', Proc. of the First Intl Conference on Fast Sea Transportation, Norway, 1991.

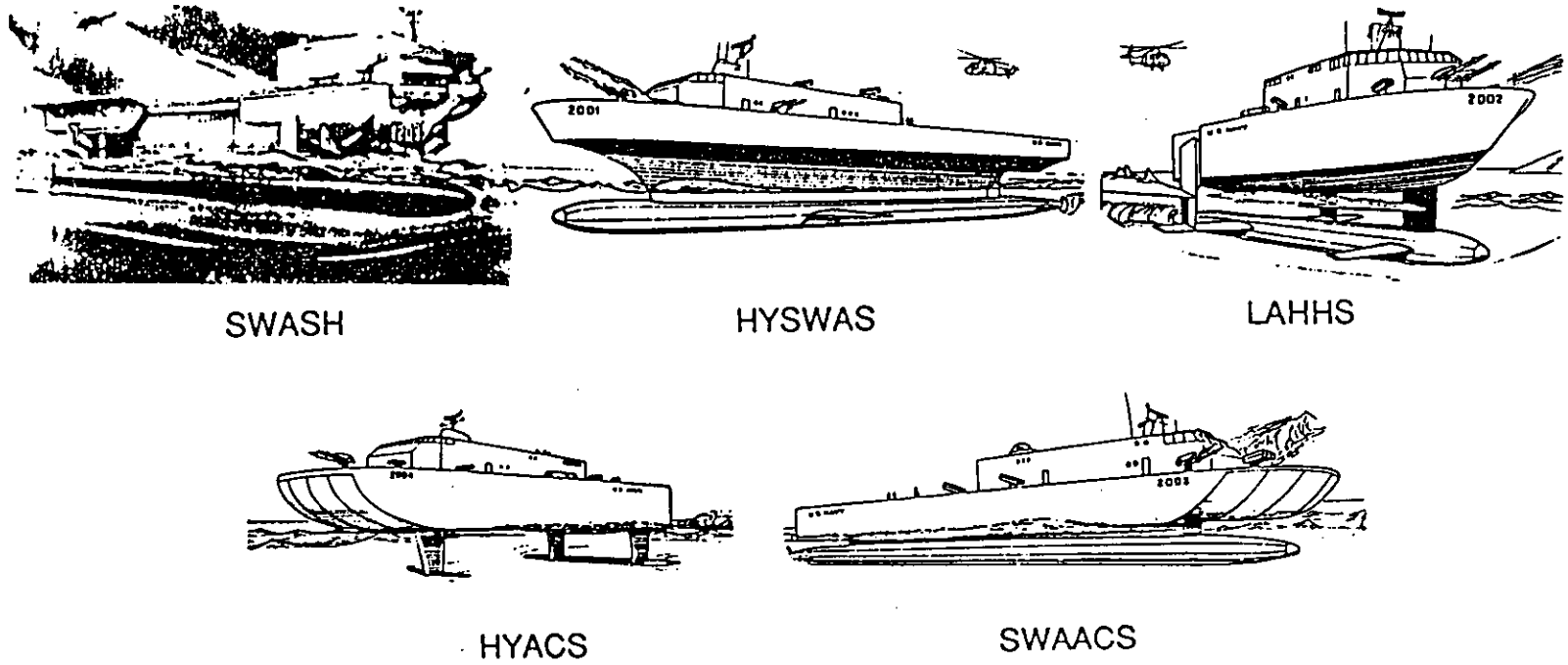

Figure 1 - Sketches of Early Hybrid Marine Interface Vehicle Concepts

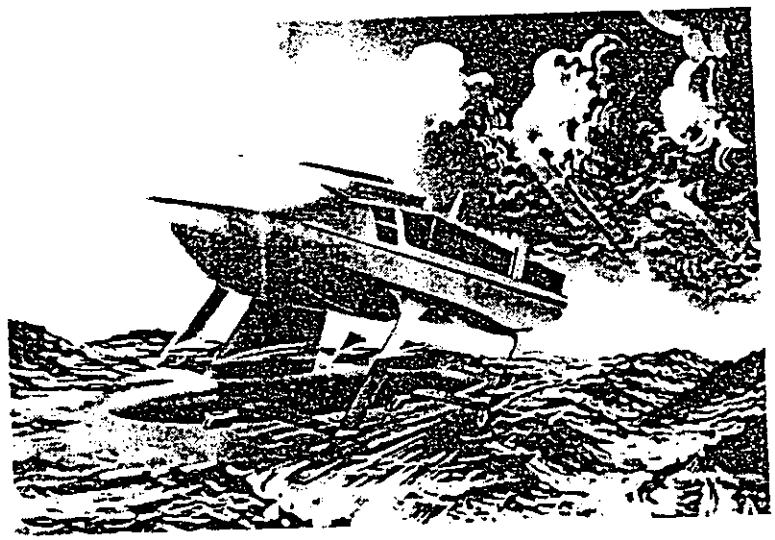

Figure 2 Artist impression of TSL-F

Principal dimensions of model ship

Length of upper hull	... ...	3.721 m
Length of lower hull	... ...	3.953 m
Breadth of upper hull	... ...	1.395 m
Diameter of lower hull	... ...	0.26 m
Depth	... ...	0.865 m
Draft in hullborne	... ...	0.693 m
Draft in foilborne	... ...	0.447 m

V = 50 Kn
PL = 1000 Tonnes
Scale = 1/21.5

R = 500 Nautical Miles
R&D Cost = £50 M

Principal particulars of the TSL-A

Length(OA)	abt.127.0m	Cargo Payload(max)	abt.1000t
Breadth(mld)	27.2m	Hull Material	Aluminum Alloy
Depth(mld)	11.0m	Machinery	
Draft off cushion	abt. 5.0m	Main Engine(GT)	25,000PS*4
on cushion	abt. 1.4m	Lift Engine(GT)	4,300PS*4
Speed(max)	abt. 50kt	Propulsor	Waterjet Pump*4
Cruising Range	abt. 500nm	Lift Fan	Centrifugal Fan*4

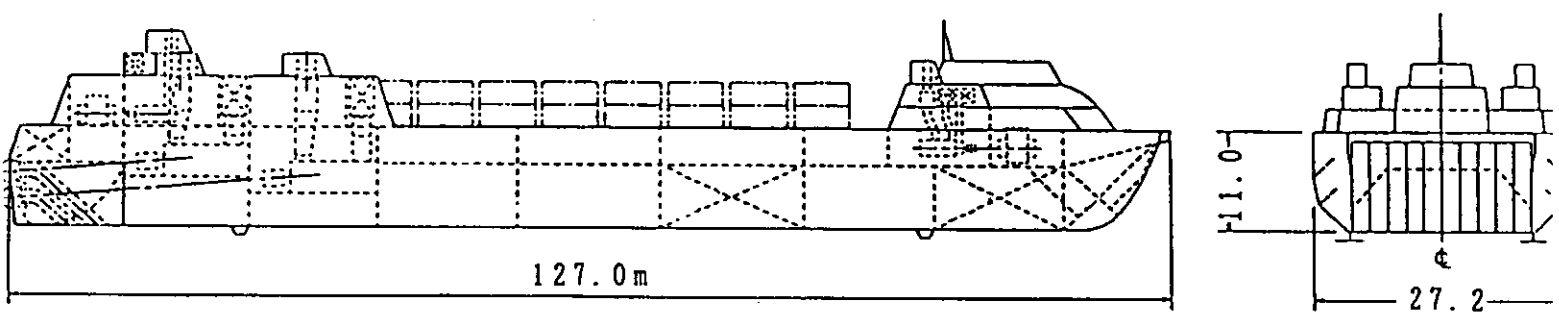

Fig.3 Outline of the TSL-A

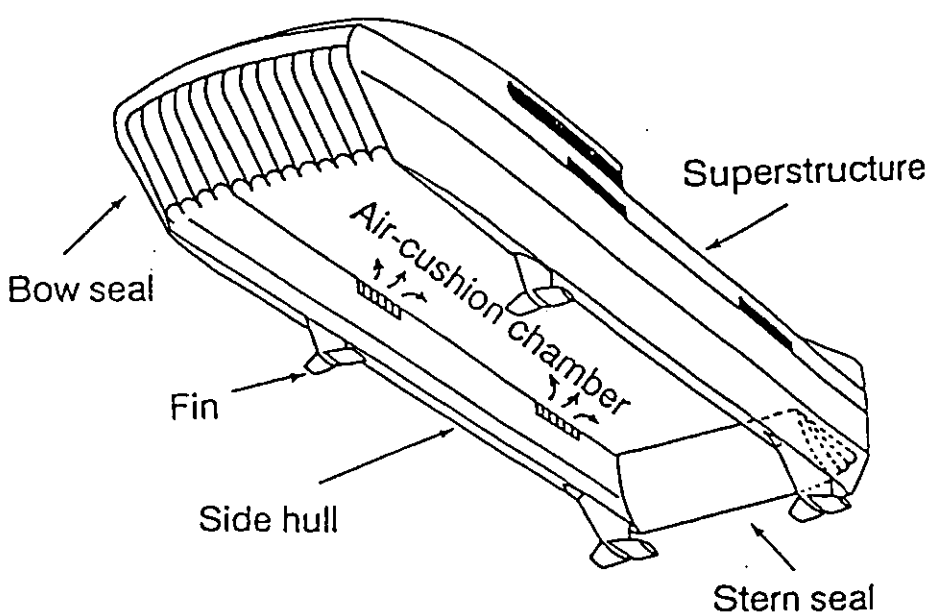

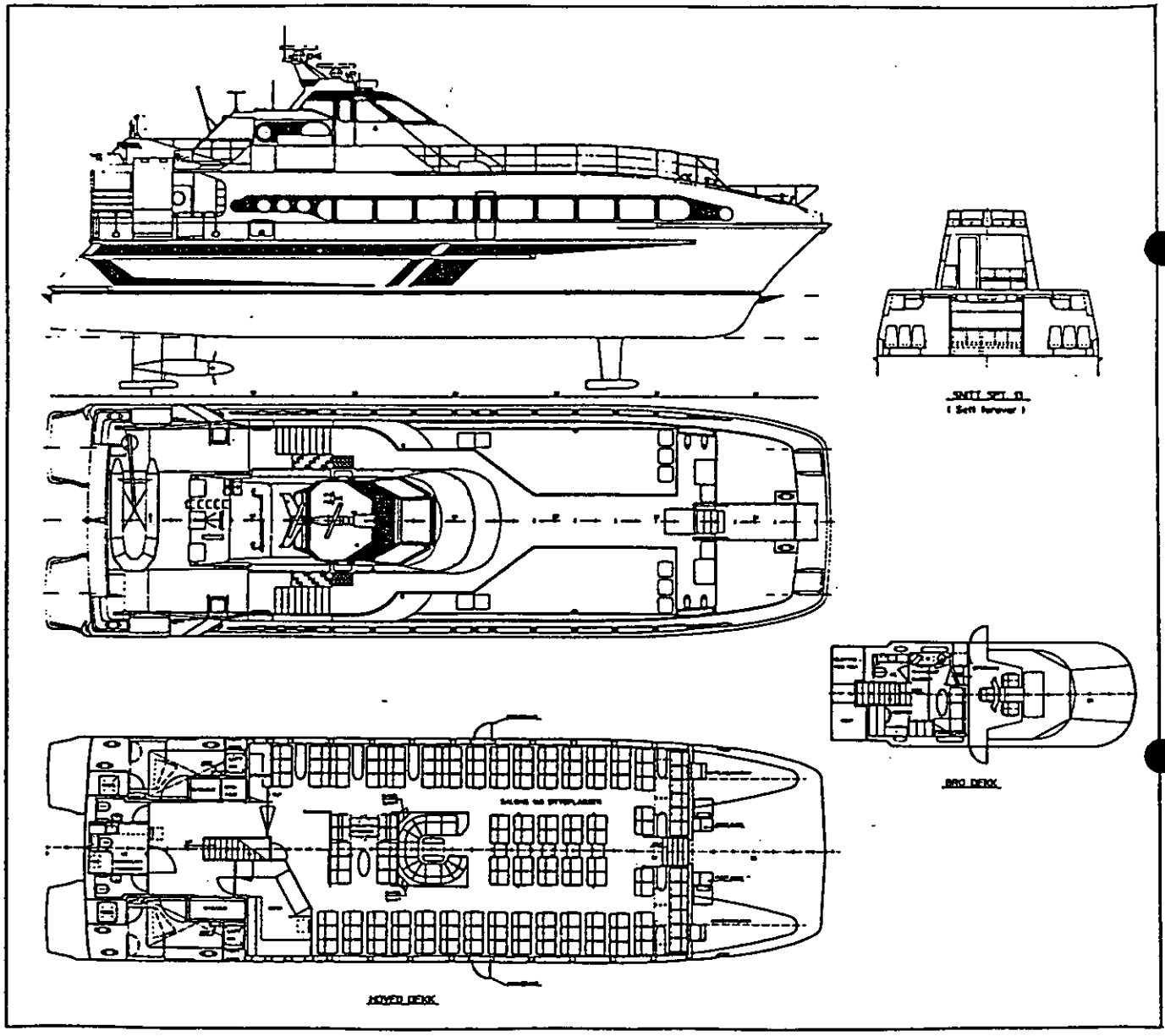

Fig. 4: Westamarin Foilcat 2900

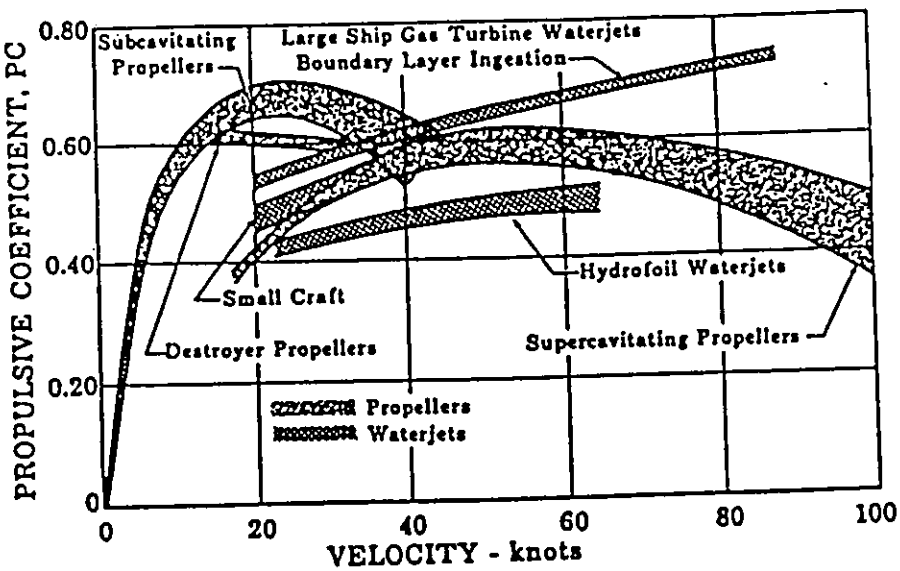

Fig. 5: DESIGN PROPULSOR COMPARISONS

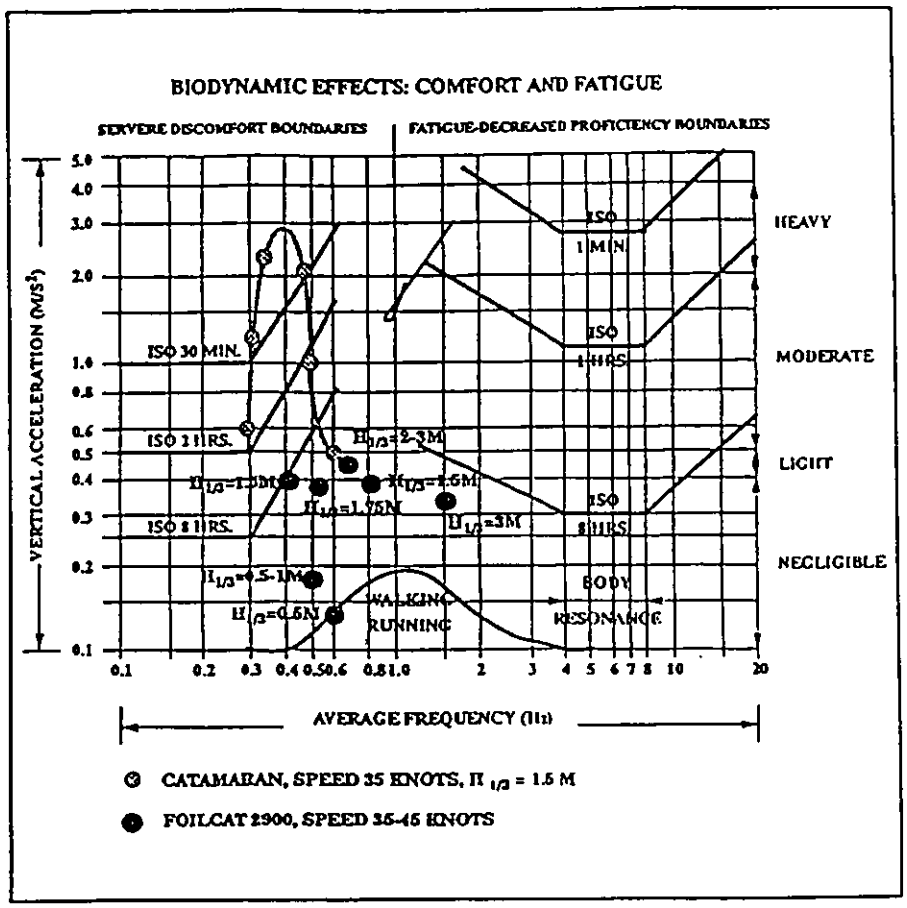

Fig. 6

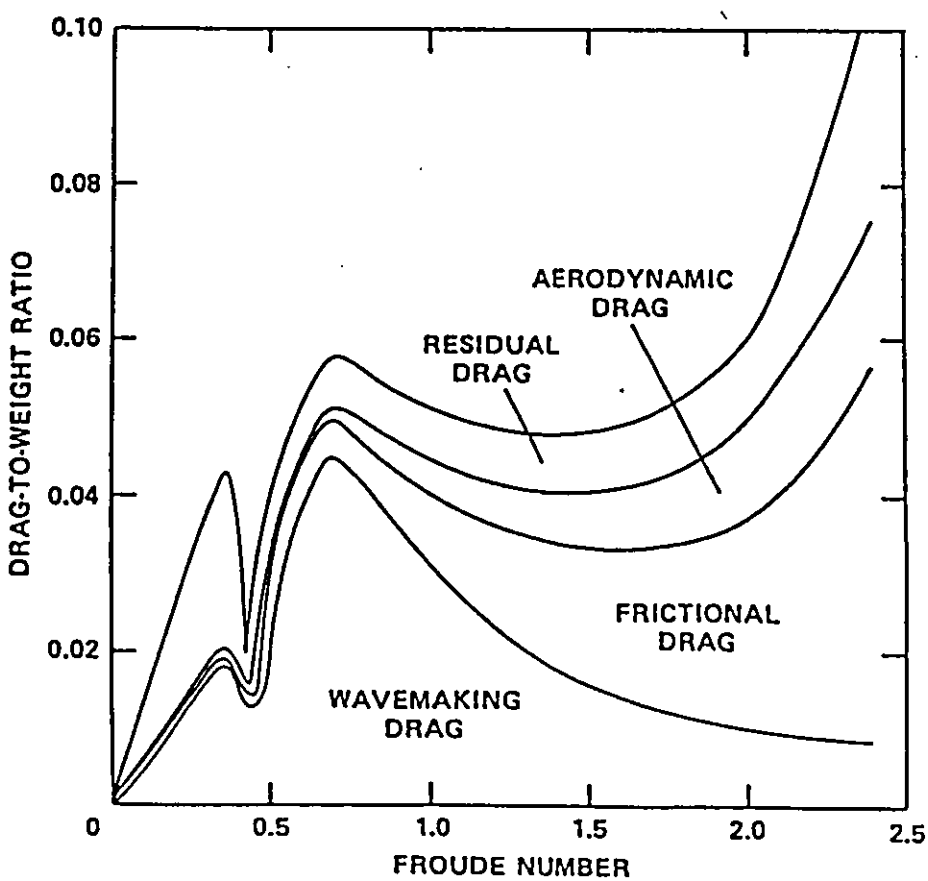

Fig. 7: – Drag Component Breakdown for the SES-100B in State 1 Sea

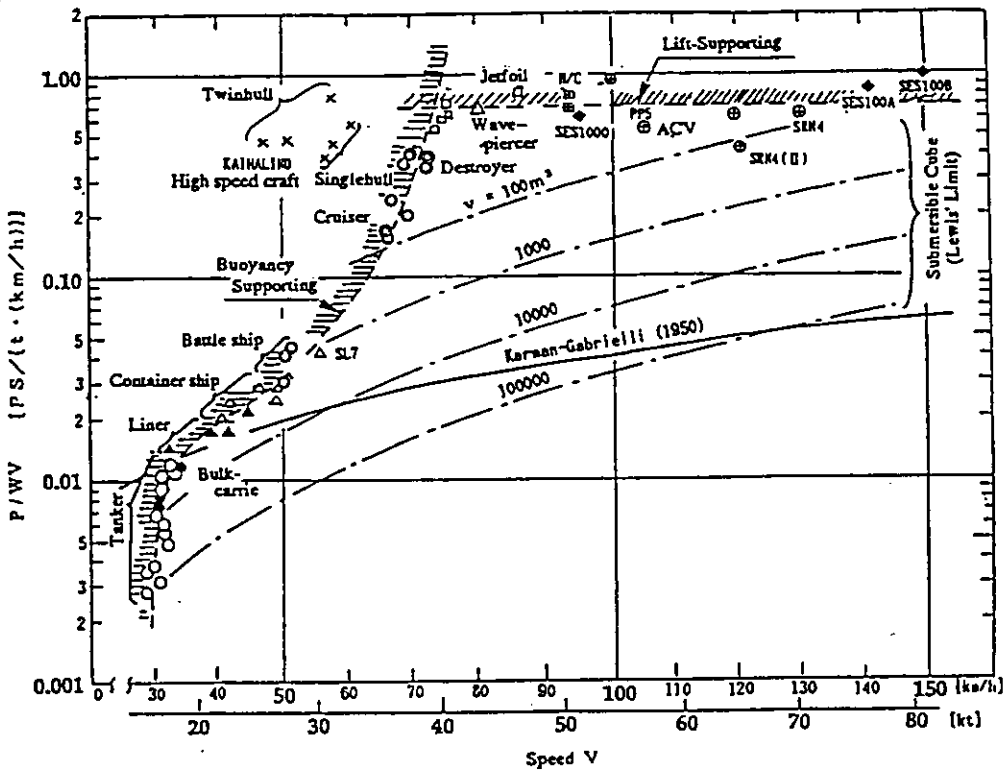

Fig. 8: Transport efficiency of various marine vehicles

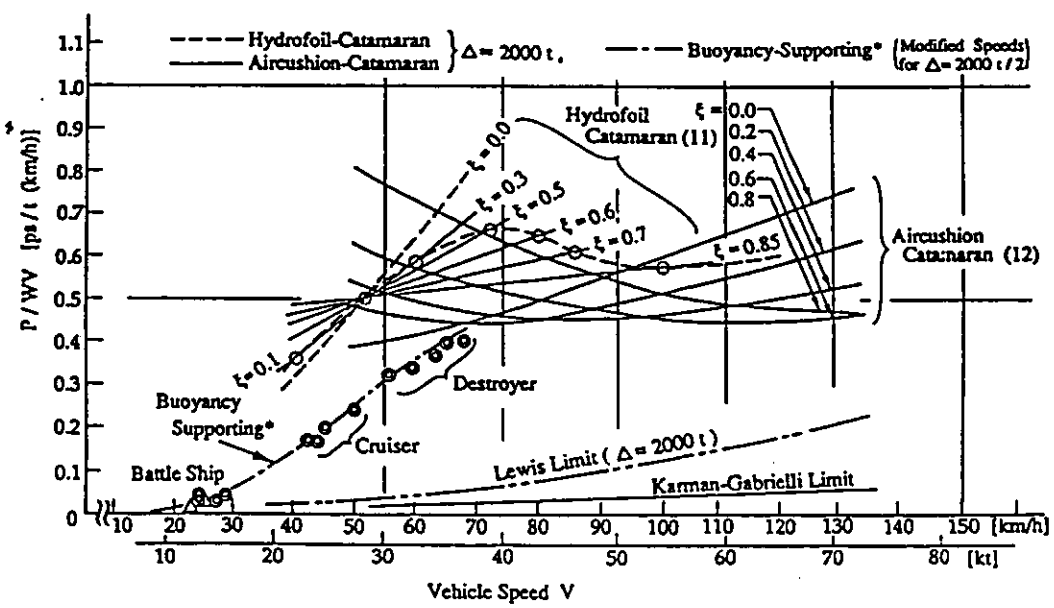

Fig. 9: Transport efficiency of hybrid marine vehicles (K-G diagram)

Table 1 - Hybrid Surface Ship Forms

HYBRID TYPE	SOURCES OF SUSTENTION	
SMALL WATERPLANE AREA SINGLE HULL (SWASH) SHIP	BUOYANCY (85%) FROM SINGLE SUBMERGED SLENDER HULL AND STRUT AND DYNAMIC LIFT (15%) FROM SURFACE-PIERCING FOIL SYSTEM.	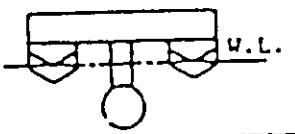
HYDROFOIL SMALL WATERPLANE AREA SHIP (HYSWAS)	BUOYANCY (70%) FROM SINGLE SUBMERGED HULL AND SINGLE STRUT AND DYNAMIC LIFT (30%) FROM FULLY-SUBMERGED FOILS.	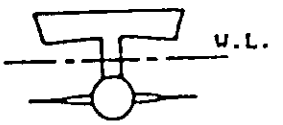
LARGE HYDROFOIL HYBRID SHIP (LAHHS)	BUOYANCY (70%) FROM SINGLE SUBMERGED HULL AND DYNAMIC LIFT (30%) FROM FULLY-SUBMERGED FOILS (MULTIPLE STRUTS ARE EMPLOYED TO JOIN UPPER AND LOWER HULLS).	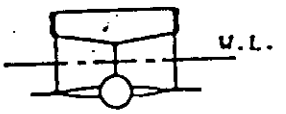
HYDROFOIL AIR CUSHION SHIP (HYACS)	POWERED STATIC LIFT (70%) FROM HIGH LENGTH-TO-BEAM AIR CUSHION/RIGID SIDEHULL SYSTEM AND DYNAMIC LIFT (30%) FROM A FULLY SUBMERGED FOIL SYSTEM.	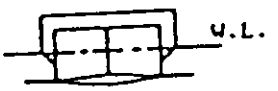
SMALL WATERPLANE AREA AIR CUSHION SHIP (SWAACS)	POWERED STATIC LIFT (70%) FROM HIGH LENGTH-TO-BEAM AIR CUSHION/RIGID SIDEHULL SYSTEM AND BUOYANT LIFT (30%) FROM A SINGLE SUBMERGED SLENDER HULL AND SINGLE STRUT	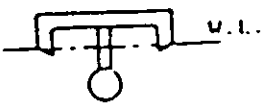

TABLE 2: OPERATIONAL LIMITS

	MERCH. VESSEL	NAVAL VESSEL	HIGH SPEED SHIP
VERTICAL ACC. (RMS), FP	LENGTH DEPEND.	0.275 g	0.65 g
VERTICAL ACC. (RMS) BRIDGE	0.15 g	0.2 g	0.275 g
LATERAL ACC. (RMS) BRIDGE	0.12 g	0.2 g	0.275 g
ROLLING (RMS)	6°	4°	4°
SLAMMING PROBABILITY	LENGTH DEPEND.	0.03	0.03
WATER ON DECK PROBABILITY	0.05	0.05	0.05

NON-LINEAR WAVE INDUCED SECOND-ORDER MOTIONS OF FLOATING AND COMPLIANT STRUCTURES

by

GRANT E. HEARN

NEWCASTLE UPON TYNE

Advanced Design for Ships & Offshore Floating Structures

Nonlinear Wave Induced Second-Order Motions of Floating and Compliant Structures

Grant E. Hearn

University of Newcastle Upon Tyne

Introduction.

The fluid-structure interaction analysis of a floating or compliant structure can be viewed with different levels of complexity. The first task is to decide upon the level of complexity to be associated with the modelling of the wave system responsible for the fluid-structure interaction. This so called 'incident' wave is generally considered to be regular (in terms of its geometric form) and harmonic in time. The waves are also usually described as 'progressing', as they travel from their region of generation to other parts of the seaway. Description of the fluid flow resulting from the wave motion will be linear or non-linear depending upon the wave slope, and hence the amplitude of the fluid velocities induced by the progressing regular harmonic wave upon the water particles. Irrespective of the nature of the associated induced fluid velocities the waves will ultimately interact with some structure. The structure may be an advancing ship, a fixed jacket structure, a compliant structure or a floating offshore structure. In this case our attention is drawn to the scale of the structure and how this might affect the wave structure interaction.

For slender structures or structures made up of slender members, the viscous nature of the associated fluid flow can be considered more important that the pressure loading resulting from the contact made by the incident wave system. In fact from an 'inviscid' viewpoint the structure or structural members are often considered to be transparent to the wave system. In this case the potential wave loading is known as Froude-Krylov loading and the nonlinear aspects of the loading are attributed to viscous drag through the Morison formula.

For the larger displacement structures the concept of transparency is inappropriate and so it is necessary to recognise the development of a scattered wave field due to the incident wave structure interaction. The phenomenon of wave scattering is clearly to be associated with the transfer of momentum from the fluid to the

structure. If the structure is floating the loading due to the reversal of momentum will lead to the structure moving. For each degree of freedom of motion additional so called 'radiation' wave systems will be set up as a consequence of the water now being excited by the motions of the structure. Thus the structure will experience fluid loading as a result of the incident wave system and its own motions.

Irrespective of whether the floating structure is steadily advancing or moored the impact of forward speed effects upon the modelling of the fluid structure interactions and hence the fluid loading and motions is very critical, and a number of choices have to made regarding the sophistication of the analysis to be undertaken. In the following sections we shall therefore consider:

- formulation of the zero speed and forward speed fluid structure interaction problems,
- alternative solutions of the first order problem,
- calculation of mean second order forces,
- the impact of first order models upon second order force predictions,
- the prediction of low frequency damping and its impact upon the calculation of low frequency motions of moored structures.

2. Modelling Fluid-Structure Interactions.

In this section we remind ourselves of the basic fluid equations and then generate a general fluid structure interaction analysis model with forward speed dependence. Thereafter different levels of simplification are discussed with respect to different situations of interest.

2.1 *Some Basic Fluid Equations.*

The fluid is assumed to be inviscid and incompressible and subject to irrotational flow. The condition of incompressibility reduces the continuity equation

$$\frac{\partial \rho}{\partial t} + \nabla \cdot (\rho \vec{V}) = 0 \tag{1a}$$

to

$$\nabla \cdot \vec{V} = 0. \tag{1b}$$

Since irrotational flow means there is no circulation then

$$\nabla \wedge \vec{V} = 0, \tag{2}$$

and so Equation (2) and the vector operator identity

$$\nabla \wedge (\nabla \Phi) \equiv 0, \tag{3}$$

applicable to any scalar function Φ which is sufficiently continuously differentiable, suggests that the fluid velocity vector $\vec{V}$ may be treated as

$$\vec{V} = \nabla \Phi. \tag{4}$$

In this case we refer to Φ as a velocity potential.

The Cartesian rectangular reference system Oxyz is assumed to advance with steady speed U, with x positive forward, z positive upwards, and the origin O located in the undisturbed free surface. Assuming (u, v, w) denote the fluid velocity components, the scalar form of Equation (1a) is

$$\frac{\partial u}{\partial x} + \frac{\partial v}{\partial y} + \frac{\partial w}{\partial z} = 0. \tag{5}$$

Also, noting that Equation (4) means that the velocity potential function $\Phi(x, y, z, t)$ and the fluid velocity components (u, v, w) satisfy the basic relationships

$$u = \frac{\partial \Phi}{\partial x}, \; v = \frac{\partial \Phi}{\partial y} \text{ and } w = \frac{\partial \Phi}{\partial z}, \tag{6}$$

we may combine Equations (1b) and (4) to produce the well known Laplace equation

$$\nabla \cdot (\nabla \Phi) \equiv \nabla^2 \Phi = 0. \tag{7a}$$

The Laplace equation may also be expressed in the form

$$\nabla^2 \Phi = \frac{\partial^2 \Phi}{\partial x^2} + \frac{\partial^2 \Phi}{\partial y^2} + \frac{\partial^2 \Phi}{\partial z^2} = 0. \tag{7b}$$

upon combining Equations (5) and (6). This equation clearly applies everywhere in the fluid since it encompasses the conditions of incompressibilty and irrotational flow.

2.2 *Formulation of General Interaction Problem.*

If the fluid is considered to be bounded by the surface S, then in the context of general offshore related fluid structure interaction analysis S may be considered to comprise of the wetted surface of the structure, S_w, the free surface, S_f, and

the seabed, S_b. For reasons which will become clear a little later in the notes we also introduce a closed vertical arbitrarily shaped cylindrical surface, S_r, which terminates at its intersections with S_f and S_b. In the theoretical studies of models operating in a tank, S_b will become the tank floor and S_r will be partitioned into tank walls and appropriate control surfaces. Both the surfaces S_w and S_b are to be considered impermeable. The impermeability of the seabed, or the tank floor, and the assumption that the fluid is inviscid, means that

$$\frac{\partial \Phi}{\partial z} = 0 \text{ on } z = -d, \tag{9}$$

where d is the depth of the water.

Since the location of the free-surface is not known a 'priori we shall assume that it is described by an equation of the form

$$S_f(x, y, z, t) = 0. \tag{10}$$

Since fluid particles on the surface are not allowed to leave the surface their velocity relative to the free surface is zero. Equivalently, using the substantial or material derivative, to follow the particle on the surface this condition may be expressed as

$$\frac{DS_f}{Dt} = 0. \tag{11}$$

The operator $\frac{D}{Dt}$ takes into account the local changes due to the passage of time and the changes brought about by changes in spatial location. If the structure advances with speed U in the positive x direction, then $\frac{D}{Dt}$ relative to the steady advancing reference system Ox, y, z can be expressed as

$$\frac{D}{Dt} \equiv \frac{\partial}{\partial t} - U\frac{\partial}{\partial x}. \tag{12}$$

On the free-surface continuity of atmospheric pressure and fluid pressure is to be assumed. Since pressure gradient rather than absolute pressure is responsible for fluid flow, the atmospheric pressure can be taken as zero without any loss of generality. Also the Eulerian equations of motion of the fluid, with respect to the steady translating reference system, can be reduced to the composite pressure equation of Bernoulli, namely

$$p = -\rho\left[\left(\frac{\partial}{\partial t} - U\frac{\partial}{\partial x}\right)\Phi + \frac{1}{2}(\nabla\Phi)^2 + gz\right]. \tag{13}$$

Here p is the hydrodynamic pressure.

Expressing the free-surface $S_f(x,y,z,t) = 0$ in the form

$$S_f(x,y,z,t) = z - \varsigma(x,y,t) \tag{14}$$

a composite free-surface condition, applicable on the instantaneous position of the free-surface, is expressible in the form

$$\frac{\partial^2\Phi}{\partial t^2} + U^2\frac{\partial^2\Phi}{\partial x^2} - 2U\frac{\partial^2\Phi}{\partial x\partial t} + 2\nabla\Phi\cdot\nabla\left[\frac{\partial\Phi}{\partial t} - U\frac{\partial\Phi}{\partial x}\right]$$
$$+\frac{1}{2}\nabla\Phi\cdot\nabla(\nabla\Phi)^2 + g\frac{\partial\Phi}{\partial z} = 0 \text{ on } z = \varsigma. \tag{15}$$

This equation is determined from the condition $\frac{Dp}{Dt} = 0$, and Equations (11) and (13), and some manipulation!

On the instantenous position of the wetted surface of the vessel, continuty of the structural and fluid normal velocity components leads to the kinematic boundary condition

$$\begin{aligned} V_n &\equiv \bar{n}\cdot(\nabla\Phi - U\hat{\underline{i}}) \\ &\bar{n}\cdot(\underline{v}_o + \underline{\Omega}\wedge\underline{r}), \end{aligned} \tag{16}$$

where $\underline{r}$ is the position vector of a wetted surface point with respect to the body fixed frame, Ox', y', z', $\underline{v}_o$ is the velocity of the origin O′ of the body fixed reference system relative to the steadily advancing reference system Ox, y, z and Ω is the angular velocity of the body fixed reference system, and hence of the vessel.

Since Equation (7) is to be satified at every point in the fluid, this equation may be considered the governing partial differential equation. Since the form of the equation is elliptic, in terms of the classification of partial differential equations, its solution demands specification of boundary conditions for Φ on all subsurfaces of a closed bounding surface S. On the control surface S_r this can be quite difficult. For the moment it is sufficient to note that an appropriate boundary condition must be applied on S_r.

At present both the rigid body motion and the fluid structure interaction problems must be solved simultaneously in the time domain, because of the dependence on the instantaneous positions of the free surface and the wetted surface of the vessel. It is also necessary to note that the total velocity potential Φ in the case of the forward speed problem will consist of the exact solution to the steady forward

speed problem, Φ_s, and the unsteady problem potential Φ_u associated with the interactions of the vessel and the incident wave system. That is, Φ_u represents a perturbation of the steady wavemaking problem. Hence we must consider the two different free surface elevations ς_s, associated with the vessel steadily advancing in otherwise calm water, and the final profile ς resulting from the perturbation of ς_s as a result of introducing the incident wave system and hence the additional fluid structure interaction.

It is the implied, but as yet unquantified, interactions of the normally two distinct hydrodynamic problems of wavemaking and wave scattering, the obvious nonlinearities of Equation (15) and the hidden complexities of the wetted surface boundary condition of Equation (16) that make the forward speed dependent interaction analysis complex. Likewise it is not possible at this stage to be precise about what we intend to mean by nonlinear, or even second order, forces.

Clearly, some simplifications are required to make the mathematical problem tractable.

2.3 *Linearisation of General Interaction Problem.*

A formal approach to identifying the simplifications is perturbation analysis. Thus both Φ and ς are to be expanded as series of the form

$$\Phi(x,y,z,t) = \Phi_s(x,y) + \epsilon\Phi_1\,(x,y,z,t) + \epsilon^2\Phi_2(x,y,z,t) + \ldots \tag{17}$$

and

$$\varsigma(x,y,t) = \varsigma_s(x,y) + \epsilon\varsigma_1(x,y,t) + \epsilon^2\varsigma_2(x,y,t) + \ldots \tag{18}$$

That is, different order governing equation pairs $[\varsigma_n(x,y,t), \Phi_n(x,y,z,t)]$ may be obtained for the unsteady potential Φ_u given (ς_s, Φ_s) are known.

The value of Φ on the instantaneous free surface in terms of its value on $z = \varsigma_s$ is given by

$$\Phi(x,y,\varsigma;t) = \Phi_s(x,y,\varsigma_s) + \epsilon\left[\Phi_1(x,y,\varsigma_s;t) + \varsigma_1\frac{\partial\Phi_s}{\partial z}\right] + O(\epsilon^2)\,, \tag{19}$$

and upon substitution into the composite free surface condition of Equation (15)

this leads to the linearised (first order) unsteady potential Φ_1 satisfying [1]

$$\begin{aligned}
&\varsigma_1\left[g\frac{\partial^2\Phi_s}{\partial z^2}+U^2\frac{\partial^3\Phi_s}{\partial z\partial x^2}-2U\left(\nabla\Phi_s\cdot\nabla\frac{\partial^2\Phi_s}{\partial z\partial x}+\nabla\frac{\partial\Phi_s}{\partial z}\cdot\nabla\frac{\partial\Phi_s}{\partial x}\right)\right.\\
&\left.+\frac{1}{2}\frac{\partial}{\partial z}(\nabla\Phi_s\cdot\nabla(\nabla\Phi_s)^2)\right]+\left[\frac{\partial^2\Phi_1}{\partial t^2}+g\frac{\partial\Phi_1}{\partial z}+U^2\frac{\partial^2\Phi_1}{\partial x^2}-2U\frac{\partial^2\Phi_1}{\partial x\partial t}\right]\\
&+2\left[\nabla\Phi_s\cdot\nabla\frac{\partial\Phi_1}{\partial t}-U\nabla\Phi_s\cdot\nabla\frac{\partial\Phi_1}{\partial x}-U\nabla\Phi_1\cdot\nabla\frac{\partial\Phi_s}{\partial x}\right]\\
&+\frac{1}{2}\nabla\Phi_1\cdot\nabla(\nabla\Phi_s\cdot\nabla\Phi_s)+\nabla\Phi_s\cdot\nabla(\nabla\Phi_s\cdot\nabla\Phi_1)=0\ \text{ on } z=\varsigma_s(x,y),
\end{aligned}\tag{20a}$$

with ς_1 the first order correction of the free surface satisfying

$$\varsigma_1=-\frac{\frac{\partial\Phi_1}{\partial t}+\nabla\Phi_s\cdot\nabla\Phi_1-U\frac{\partial\Phi_1}{\partial x}}{g+\nabla\Phi_s\cdot\nabla\frac{\partial\Phi_s}{\partial z}-U\frac{\partial^2\Phi_s}{\partial z\partial x}}\,. \tag{20b}$$

Similarly, to satisfy the wetted surface continuity condition the outward normal on the instantaneous location of S_w is required and since this is not possible a' priori the outward normal vector $\bar{n}$, the origin velocity $\bar{v}_0$ and the angular velocity Ω are also expressed as series of the form

$$\bar{n}=\bar{n}_s+\epsilon\bar{n}_1+\epsilon^2\bar{n}_2+O(\epsilon^3)\ ,$$

$$\bar{v}_o=\epsilon\bar{v}_{01}+\epsilon^2\bar{v}_{02}+O(\epsilon^3)\ ,$$

and

$$\Omega=\epsilon\Omega_1+\epsilon^2\Omega_2+O(\epsilon^3). \tag{21}$$

Hence, it follows that Equation (16) may be expressed in the form

$$\bar{n}_s\cdot\bar{V}_s+\epsilon[\bar{n}_s\cdot\nabla\Phi_1+\bar{n}_1\cdot\bar{V}_s]=\epsilon\bar{n}_s\cdot[\bar{v}_{01}+\Omega_1\wedge\bar{r}]+O(\epsilon^2) \tag{22}$$

where $\bar{V}_s=\nabla\phi_s-U\hat{i}$ is the fluid velocity caused entirely by the steady forward motion relative to the translating reference system. Next using Taylor series expansions of $\bar{V}_s$ and Φ_1 on the instantaneous surface, in terms of their values on the steady forward speed surface, ς_s, leads to

$$\bar{n}_s\cdot\bar{V}_s+\epsilon\bar{n}_s\cdot(\bar{\delta}_1\cdot\nabla)\bar{V}_s+\epsilon[\bar{n}_s\cdot\nabla\phi_1+\bar{n}_1\cdot\bar{V}_s]=\epsilon\bar{n}_s\cdot[\bar{v}_{01}+\Omega\wedge\bar{r}]. \tag{23}$$

This equation is correct to first order. Since the zero-order term vanishes identically and the first-order outward normal component $\bar{n}_1$ can be expressed in terms of $\bar{n}_s$, further vector identity manipulation leads to

$$\frac{\partial\Phi_1}{\partial n}=\bar{n}_s\cdot\dot{\bar{\delta}}+\bar{n}_s\cdot[(\bar{V}_s\cdot\nabla)\bar{\delta}_1-(\bar{\delta}_1\cdot\nabla)\bar{V}_s] \tag{24}$$

where $\bar{\delta}_1$ is the first-order displacement

$$\bar{\delta}_1 = \bar{\xi}_1 + \bar{\theta} \wedge \bar{r} \ , \tag{25a}$$

and the corresponding first order velocity is given by

$$\dot{\bar{\delta}}_1 = \bar{v}_{01} + \Omega_1 \wedge \bar{r}. \tag{25b}$$

So far, the time dependence of the rigid floating or compliant structure, and the fluid motions resulting from the 'unsteady' motions have not been specified. From this point on the incident waves and hence the responses to their excitation will be considered harmonic, and so, typically, the first-order translations and angular velocities will be expressed as

$$\xi_1 = (\eta_1, \eta_2, \eta_3) \exp(-i\omega_e t) \equiv (\tilde{\eta}_1, \tilde{\eta}_2, \tilde{\eta}_3) \tag{26a}$$

and

$$\Omega_1 = -i\omega_e(\eta_4, \eta_5, \eta_6) \exp(-i\omega_e t) \equiv -i\omega_e(\tilde{\eta}_4, \tilde{\eta}_5, \tilde{\eta}_6) \ , \tag{26b}$$

where ω_e, the encounter frequency, satisfies

$$\omega_e = \omega_0 - \frac{2\pi}{\lambda} U \cos\beta. \tag{27}$$

Here ω_0 denotes the incident wave fequency and β defines the wave heading of the incident wave relative to the negative x axis. Hence a wave heading of 180 degrees corresponds to a head sea. If the first-order unsteady potential is now partitioned as

$$\Phi_1(x, y, z; t) = \Phi^I(x, y, z; t) + \Phi^D(x, y, z; t) + \sum_{k=1}^{6} \eta_k \Phi^k(x, y, z; t) \tag{28}$$

then Equation (24) reduces to

$$\begin{aligned} \frac{\partial \Phi_1}{\partial n} =& \left[\frac{\partial \phi^I}{\partial n} + \frac{\partial \phi^D}{\partial n} + \sum_{k=1}^{6} \eta_k \frac{\partial \phi^k}{\partial n} \right] \exp(-i\omega_e t) \\ =& \bar{n}_s \cdot \dot{\bar{\delta}}_1 + \bar{n}_s \cdot [(\bar{V}_s \cdot \nabla)\bar{\delta}_1 - (\bar{\delta}_1 \cdot \nabla)\bar{V}_s] \text{ on } S_w. \end{aligned} \tag{29}$$

Alternatively, expressing the right-hand side of the wetted surface boundary condition as

$$\sum_{k=1}^{6} (-i\omega_e n_k)\eta_k + U \sum_{k=1}^{6} m_k \eta_k \tag{30}$$

it can be shown, after some manipulation, that

$$\begin{aligned}\sum_{k=1}^{3} m_k\eta_k &= -\,\bar{\xi}_1\cdot[(\bar{n}_s\cdot\nabla)\bar{v}_s]\ \text{, and}\\ \sum_{k=4}^{6} m_k\eta_k &= -\,\bar{\theta}_1\cdot[(\bar{n}_s\cdot\nabla)(\bar{r}\wedge\bar{v}_s)]\ ,\end{aligned} \tag{31}$$

where $\bar{v}_s = \bar{V}_s/U$ corresponds to the unit forward speed case. Hence, on the mean wetted surface S_w, we have

$$\frac{\partial\phi_k}{\partial n} = -i\omega_e n_k + Um_k \ :\ k = 1,2,...,6$$

and

$$\frac{\partial\phi^D}{\partial n} = -\frac{\partial\phi^I}{\partial n}. \tag{32}$$

However, we must note that after all this manipulation to simplify the problem by replacing calculations on unknown surfaces to calculations on assumed known surfaces, and the linearisation of the unsteady problem, now assumed to be harmonic, the oscillatory and steady forward speed potentials interact in a nonlinear manner! In fact only if we neglect the steady potential Φ_s and its associated free surface ς_s, will the free surface and wetted surface boundary conditions simplify any further.

Therefore neglecting the effect of Φ_s the free surface condition, Equation (15), reduces to the more commonly quoted form of the forward speed free surface, namely

$$\frac{\partial^2\Phi_1}{\partial t^2} + g\frac{\partial\Phi_1}{\partial z} + U^2\frac{\partial^2\Phi_1}{\partial x^2} - 2U\frac{\partial^2\Phi_1}{\partial x\partial t} = 0 \ \text{ on } \ z = 0\,, \tag{33}$$

whereas in the corresponding wetted surface boundary condition the forward speed related m_k terms may be simplified to

$$\begin{aligned} m_k &= 0 \ :\ k = 1,2,3,4,\\ m_5 &= n_3\,,\\ m_6 &= -\,n_2\,.\end{aligned} \tag{34}$$

The terms (n_1, n_2, n_3) are the direction cosines associated with the first order definitions of the outward normal $\bar{n}_1$.

The free surface condition expressed in Equation (33) can in some instances still be considered too complex for the situation being analysed. In the case of moored

structures the large amplitude low frequency excursions of the structure can be viewed as a low variable forward speed. On the otherhand for ships the orders of the magnitude of the wave s associated with the forward speed and the oscillatory interactions may be considered comparable. Therefore further enhancement of the free surface condition can provide a compromise between the intractable form of Equation (20a) and the much simplified form of Equation (33).

2.4 *Different Forward Speed Formulations.*

The first three formulations will presented assume no interaction between Φ_u and and Φ_s. The fourth formulation will assume a 'weakened' interaction between the steady and unsteady potentials on the basis of low forward speeds. In each case linearisation will have been performed. The results are simply quoted as they can be deduced from earlier sections of the notes.

Formulation A

The simplest approach to treating low forward speed is to assume it enters the calculations through the encounter frequency only at the basic interaction analysis. In this case we have

$$\begin{aligned} \nabla^2\Phi_u &= 0 \\ \left[g\frac{\partial}{\partial z} + \frac{\partial^2}{\partial t^2}\right]\Phi_u &= 0 \text{ on } S_f, \\ \frac{\partial}{\partial n}\left[\phi^I + \phi^S\right] &= 0 \text{ on } S_w \\ \frac{\partial}{\partial n}\phi^k &= -i\omega_e n_k + U m_k \text{ on } S_w. \end{aligned} \qquad (A)$$

Setting $U = 0$ obviously provides the corresponding zero speed formulation.

Formulation B

In this formulation the explicit dependence of the composite free-surface boundary condition upon U is recognized to the extent that Equation (33) is applied. That is,

$$\left[g\frac{\partial}{\partial z} + \left(\frac{\partial}{\partial t} - U\frac{\partial}{\partial x}\right)^2\right]\Phi_u = 0 \text{ on } S_f, \qquad (B)$$

with the remaining equations unchanged.

Formulation C

In this formulation the Green function associated with Formulation A is either expanded to remove the U^2 dependence[2-3] or the U^2 dependence is removed from the composite free-surface condition on the basis of low forward speed[4]. In either case the free-surface boundary condition is effectively reduced to

$$\left[g\frac{\partial}{\partial z} + \frac{\partial^2}{\partial t^2} - 2U\frac{\partial^2}{\partial x \partial t}\right]\Phi_u = 0 \text{ on } S_f. \tag{C}$$

As before the remaining equations of the formulation are as above for Formulation (A).

Formulation D

When including the steady and unsteady wave interaction the dynamic free-surface condition derived by applying Bernoulli's equation leads to

$$\eta = -\frac{1}{g}\left[\frac{D}{Dt}\Phi + \frac{1}{2}|\nabla\Phi|^2\right], \tag{35}$$

as the Lorentz transform implies that $\frac{\partial}{\partial t}$ be replaced by

$$\frac{D}{Dt} = \frac{\partial}{\partial t} + \nabla\Phi_s \cdot \nabla. \tag{36}$$

Using these equations and neglecting higher order terms of $\nabla\Phi_s$ the new proposed free-surface boundary condition may be written[5] as

$$\left[g\frac{\partial}{\partial z} + \left(\frac{\partial}{\partial t} - U\frac{\partial}{\partial x}\right)^2\right]\Phi_u + 2\left(\frac{\partial}{\partial t} - U\frac{\partial}{\partial x}\right)(\nabla\Phi_s \cdot \nabla\Phi_u) = 0 \text{ on } S_f. \tag{D}$$

2.5 *The General Zero Speed Problem*

Having considered the forward speed problem in general terms the simpler zero speed problem is now examined so that one can appreciate how the higher order representations of the incident wave are derived. This is of relevance when determining the nonlinear forces modelled by the Morison formula used to estimate the fluid loading on the slender structural members of offshore jackets and platforms.

Introducing, for convenience, the shorthand notation

$$\frac{\partial\Phi}{\partial t} = \Phi_t, \quad \frac{\partial\Phi}{\partial x} = \Phi_x, \quad \frac{\partial\Phi}{\partial y} = \Phi_y \text{ and } \frac{\partial\Phi}{\partial z} = \Phi_z, \tag{37}$$

with the normal derivative denoted by Φ_n, the nonlinearised set of governing equations are:

$$\begin{aligned} \nabla^2\Phi &= 0 \text{ everywhere in the fluid,} \\ \Phi_n &= 0 \text{ on } z = -d, \\ \Phi_t + \frac{1}{2}\left(\Phi_x^2 + \Phi_y^2 + \Phi_z^2\right) + g\varsigma &= 0 \text{ on } z = \varsigma, \text{ and} \\ \Phi_x\varsigma_x + \Phi_y\varsigma_y + \Phi_z\varsigma_z + \varsigma_t &= 0 \text{ on } z = \varsigma. \end{aligned} \tag{38}$$

In this case we may use the Taylor's series

$$\Phi(x,y,\varsigma,t) = \Phi(x,y,0,t) + \varsigma\left(\frac{\partial\Phi}{\partial z}\right)_{z=0} + \varsigma^2\left(\frac{\partial^2\Phi}{\partial z^2}\right)_{z=0} + \ldots. \tag{39}$$

to reduce the 'exact' kinematic and dynamic free-surface conditions of Equations (11) and (13) to provide the linear equation pair

$$\begin{aligned} g\varsigma_1 + \Phi_{1t} &= 0 \\ \varsigma_{1t} - \Phi_{1z} &= 0, \end{aligned} \tag{40}$$

and the second-order equations pair

$$\begin{aligned} g\varsigma_2 + \Phi_{2t} &= -\varsigma_1\Phi_{1tz} - \frac{1}{2}\left[\Phi_{1x}^2 + \Phi_{1y}^2 + \Phi_{1z}^2\right] \\ \varsigma_{2t} - \Phi_{2z} &= +\varsigma_1\Phi_{1zz} - \eta_{1x}\Phi_{1x} - \varsigma_{1y}\Phi_{1y}. \end{aligned} \tag{41}$$

Both sets of equations now apply on the undisturbed free surface $z = 0$. In fact, in general one can generate the nth order equations pair with the general form[6]

$$\begin{aligned} g\varsigma_n + \Phi_{nt} &= F_{n-1} \\ \varsigma_{nt} - \Phi_{nz} &= G_{n-1}. \end{aligned} \tag{42}$$

The expressions denoted by F_{n-1} and G_{n-1} refer to combinations of ς_k and Φ^k with $k \leq n-1$. As n increases so the complexity of the equations increases quite significantly.

2.6 *Specifying the Incident Wave Velocity Potential*

Solution of Laplace's equation, Equation (7), using the boundary conditions expressed in Equations (9) and (40) for the first order problem, and subject to Equations (9) and (41) for the second order problem, leads to

$$\epsilon\phi_1^I = \frac{\alpha g a}{\omega}\frac{\cosh k(z+d)}{\cosh(kd)} exp(ikx) \tag{43}$$

and

$$\epsilon^2\phi_2^I = \frac{\alpha 3a^2}{8}\frac{\cosh 2k(z+d)}{\sinh^4(kd)}exp(i2kx) \tag{44}$$

the first and second-order incident wave potentials. The first order waveis assumed to have an amplitude 'a'. Hence for k the wave number $\epsilon = ka$ corresponds to the wave slope, which is assumed small. The coefficient α simply determines the actual wave form characteristic at the origin at time zero. Strictly speaking the pressure equation, Equation (13), is only unique, regarding the pressure p to within an additive constant. So recognising the constant is different for each different order of solution it is possible to show that

$$\epsilon^n\Phi_n^I = \epsilon^n R_e[\phi_n^I exp(-in\omega t) + C_n(t)], \tag{45}$$

with R_e denoting the real part of the quantity in parenthesis. The $C_n(t)$ term is there to eliminate the Bernoulli equation constant. In particular

$$C_1(t) = 0 \text{ and } \mathrm{C_2(t) = g\bar{\varsigma}_2 t} \tag{46}$$

where

$$\bar{\varsigma}_2 = \frac{ka^2}{2sinh(2kd)} \tag{47}$$

is the wave set-down[7], so called because it represents the time average of the second-order elevation, and this corresponds to a negative offset from the undisturbed free-surface. Other higher order contributions are available[8-9].

2.7 *The General Diffraction Problem.*

Having seen how the complexity of the incident wave models may be generalised the next natural step is to introduce the presence of a structure of sufficient displacement to ensure wave scattering takes place. The structure is assumed to be fixed whether it is a gravity type offshore structure or some general floating structure. As already noted earlier the introduction of the structure necessitates two additional boundary conditions. The first represents continuity of the normal velocity across the wetted-surface of the structure (assumed impermeable). The second condition must be imposed to ensure uniqueness of Φ^D and to control the far-field nature of the solution.

This second condition is imposed because of the elliptic nature of the governing equation expressed in Laplace's equation. Since in these notes steady-state boundary value problem formulations are to be favoured in preference to an initial value

problem approach, we have two choices regarding the determination of the boundary condition on S_r. We may either introduce a real or fictitious damping term or use physical insight. When introducing additional damping it is normal to require the harmonic solution satisfying the other boundary conditions to vanish at infinity. When the additional artificial damping is allowed to tend to zero the final result will satisfy the appropriate radiation condition. The boundary S_r is often referred to as the radiation surface, and hence the condition satisfied by the fluid flow on this surface is designated the radiation condition. The artificial damping approach was suggested by Rayleigh. Sometimes the physical situation suggests the form of the radiation condition, but this intuitive approach may also lead to incorrect formulations.

The radiation condition is a condition imposed on the scattering potential Φ^D not Φ^I. This scattering potential exists to model the interaction of the incident waves with the structure. Treating Φ as the sum of the potentials Φ^I and Φ^D the perturbation analysis leads to the following first order and second order diffraction analyses. In particular the time independent potential ϕ_1^D must satisfy

$$\begin{aligned} \nabla^2\phi_1^S &= 0 \text{ everywhere in the fluid,} \\ \phi_{1n}^S &= 0 \text{ on } z = -d, \\ \phi_{1z}^S - m_0\phi_1^S &= 0 \text{ on } z = 0, \\ \phi_{1n}^S + \phi_{1n}^I &= 0 \text{ on the wetted surface of the structure,} \end{aligned} \tag{48}$$

whereas ϕ_2^D must satify

$$\begin{aligned} \nabla^2\phi_2^S &= 0 \text{ everywhere in the fluid,} \\ \phi_{2n}^S &= 0 \text{ on } z = -d, \\ \phi_{2z}^S - 4\nu\phi_2^S &= \alpha_2^S \text{ on } z = 0, \text{ and} \\ \phi_{2n}^S + \phi_{2n}^I &= 0 \text{ on wetted surface of structure.} \end{aligned} \tag{49}$$

Here m_0 is the wavenumber defined by $m_0 = \omega^2/g$.

The free-surface forcing function α_2^S may be expressed as

$$\alpha_2^{SI} = \alpha_2^{SI} + \alpha_2^{SS} \tag{50}$$

with

$$\alpha_2^{SI} = -\frac{iw}{2g}\phi_1^S\left(\phi_{1zz}^I - \nu\phi_{1z}^I\right)$$
$$-\frac{iw}{2g}\phi_1^I\left(\phi_{1zz}^S - \nu\phi_{1z}^S\right) \tag{51}$$
$$+\frac{2iw}{g}\left(\phi_{1x}^I\phi_{1x}^S + \phi_{1y}^I\phi_{1y}^S + \phi_{1z}^I\phi_{1z}^S\right)$$

and

$$\alpha_2^{SS} = -\frac{iw}{2g}\phi_1^S\left(\phi_{1zz}^S - \nu\phi_{1z}^S\right)$$
$$+\frac{iw}{g}\left[\left(\phi_{1x}^S\right)^2 + \left(\phi_{1y}^S\right)^2 + \left(\phi_{1z}^S\right)^2\right]. \tag{52}$$

For the first-order diffraction problem intuition suggests that the character of the disturbance at some distance from the source of the disturbance, the structure, should correspond to a progressing wave moving away from the structure. Certainly, there is no obvious reason for the scattered waves to travel out to 'infinity' and then suddenly start travelling back towards the structure. Mathematically this can be expressed as

$$lim_{r\to\infty}[\phi_{1r}^S - i\nu\phi_1^S] = 0 \text{ in the far} - \text{field.} \tag{53}$$

The subscript r denoting differenting radially in the horizontal plane. The second-order diffraction problem is less straight forward. Ogilvie and Tuck[10] discussed the difficulties of providing higher-order solutions in the context of strip-theory some twenty years ago. The three-dimensional problem has only relatively recently been dealt with satisfactorily[11]. Here the formulation used by Clark et al [12–13] has been presented.

To define the radiation condition at second-order the general forcing function

$$\alpha_2 = \alpha_2^S + \alpha_2^{II} \tag{54}$$

and and its far-field behaviour must be considered carefully. The incident wave forcing term α_2^{II} is similar to α_2^{SS} with Φ_1^I components replacing those of Φ_1^S. The disturbances due to α_2^S have been designated 'locked waves' by Molin, whereas the third disturbance associated with α_2 is called a free-wave. Whereas the free-wave part of the disturbance does satisfy a Sommerfeld radiation condition and a double frequency dispersion equation the asymptotic behaviour of the locked waves is the key to identifying the full radiation condition. The associated analysis is

not reported here for reasons of space and complexity, but the interested reader should consult cited references[7,10–14] for further details and other appropriate bibliographic details.

2.9 *Summarising the Results.*

Analysis consists of choices. With each choice there is a different level of computational effort and a different degree of 'correctness' regarding the modelling of the selected fluid structure interactions of interest. In practical offshore engineering the trick is to try to minimise the computational effort, whilst maintaining a level of modelling appropriate to the situation being analysed. Having looked at the choices of modelling the interactions, we now consider the selection of different solution techniques.

In the literature many papers on finite element, boundary element and hydrid methods of solution are to be found. In this discourse only the different boundary element technique based procedures will be considered and applied in later sections.

3. Solution of Linearized Formulations.

Since Φ is harmonic the fluid flow may be described using either the time independent velocity potential ϕ or a corresponding distribution of source strengths σ . The solution domain in either case depends upon whether the selected Green function automatically satisfies the free-surface condition, the sea-bed condition and an appropriate radiation condition or some subset of these boundary conditions. Since the formulations now presented are primarily for deep water, the impermeability condition and the behaviour of the Green function G will usually remove S_b from the integral equation formulations generated from Green's second identity[1]. The only exception considered here is in the eigenfunction matching technique described.

3.1 *Low Order Boundary Element (LOBE) Formulations.*

By LOBE we mean the elements used to discretise the surfaces are plane and the variation of the unknown velocity or source strength is assumed invariant over each element.

3.1.1 *Zero Speed Open Water Formulation*

Assuming the velocity potential is to be solved directly the choice of second kind

Fredholm integral equations are[15]

$$-\alpha\phi + \int_{S_w} \phi \frac{\partial G}{\partial n} ds = \int_{S_w} G\, v_n ds, \tag{55}$$

for a pulsating source Green function satisfying all the required boundary conditions except the wetted-surface boundary condition, whereas

$$\begin{aligned} -\alpha\phi + \int_{S_w} \phi \frac{\partial G}{\partial n} ds + \int_{S_r} \Big[\phi \frac{\partial G}{\partial n} - G \frac{\partial \phi}{\partial n}\Big] ds \\ + \int_{S_f} \Big[\phi \frac{\partial G}{\partial n} - \frac{\omega^2}{g} \phi G\Big] ds = \int_{S_w} G\, v_n ds\ , \end{aligned} \tag{56}$$

if G corresponds to the simpler Rankine source defined by $G = \frac{1}{r}$ where r is the distance between the fluid singularity point and some generic point in the fluid. The term $\frac{\partial \phi}{\partial n}$ on S_r is now replaced using either the Sommerfeld radiation condition expressed in the form

$$\frac{\partial \phi}{\partial r} = \Big[i m_0 - \frac{1}{2r}\Big]\phi, \tag{57}$$

where r indicates a radial derivative on some conveniently selected cylindirical radiation boundary. Alternatively if we know the far-field behaviour of the velocity potential then matching of the inner and the outer solutions can be undertaken to satisfy[16–17]

$$\phi_{\Omega^I} = \phi_{\Omega^O} \text{ and } \Big(\frac{\partial \phi}{\partial n}\Big)_{\Omega^I} = \Big(\frac{\partial \phi}{\partial n}\Big)_{\Omega^O}, \tag{58}$$

with Ω^I and Ω^O indicating inner and outer solutions. Using the full pulsating source Green function the corresponding integral equation for the unknown source strength is

$$-\alpha\sigma = \int_{S_w} \sigma \frac{\partial G}{\partial n} ds - v_n\ , \tag{59}$$

3.1.2 *Forward Speed Open Water Formulation*

The corresponding translating-pulsating source Green function based integral equations are

$$\begin{aligned} -\alpha\phi + \int_{S_w} \phi \frac{\partial G}{\partial n} ds - 2i \frac{U\omega_e}{g} \oint_{L_0} G\phi dy \\ + \frac{U^2}{g} \oint_{L_0} [\phi \frac{\partial G}{\partial x} - G \frac{\partial \phi}{\partial x}]\, dy = \int_{S_w} G\, v_n ds, \end{aligned} \tag{60}$$

for determining the velocity potential directly and

$$-\alpha\sigma = \int_{S_w} \sigma \frac{\partial G}{\partial n} ds + \frac{U^2}{g} \oint_{L_0} n_1 \sigma \frac{\partial G}{\partial n} dy - v_n\ , \tag{61}$$

for determining the unknown source strength, with ϕ recoverable from

$$\phi = \int_{S_w} \sigma G ds \ ,$$

The contour L_0 is the undisturbed free-surface waterline[15].

3.1.3 *Slow Forward Speed Open Water Formulation*

If the pulsating-translating source Green function is expanded in terms of the parameter $\tau = U\omega_e/g$, and terms involving τ^2 and higher orders are considered negligible because of the low forward speed, then we may assume that $G = G_0 + \tau G_1$ and similarly $\sigma = \sigma_0 + \tau\sigma_1$. Consequently the single second-kind Fredholm integral equation (61) may be reduced to the coupled second-kind Fredholm equations[31-32]

$$-\alpha\sigma_0 = \int_{S_w} \sigma_0 \frac{\partial G_0}{\partial n} ds - v_{n_0}$$

and

$$-\alpha\sigma_1 = \int_{S_w} \sigma_1 \frac{\partial G_0}{\partial n} ds - \int_{S_w} \sigma_0 \frac{\partial G_1}{\partial n} ds - v_{n_1} \ , \tag{62}$$

with ϕ recoverable from $\phi_0 = \int_{S_w} \sigma_0 G_0 ds$ and

$$\phi_1 = \int_{S_w} \sigma_1 G_0 ds + \int_{S_w} \sigma_0 G_1 ds \ . \tag{63}$$

G_0 is in fact the zero speed Green function and G_1 is a forward speed correction[3] which is also expressible in terms of G_0. Any computer code capable of solving the zero speed problem can be immediately used to solve this forward speed problem. This is readily justified upon observing that the first integral equation has exactly the same form as the zero speed integral equation, and once G_0 is known, the second integral equation also reduces to a zero speed form with G_0 replaced by G_1.

3.1.4 *Eigenfunction Matching Technique for Zero or Low Forward Speeds*

In this case the inner problem is formulated by applying Green's second identity. The resulting integral equation is

$$\begin{aligned} \alpha\phi + \int_{S_w} \phi \frac{\partial G}{\partial n} ds + \int_{S_f} \Big[\phi \frac{\partial G}{\partial n} - \frac{\omega_e^2}{g} \phi G\Big] ds \\ + \int_{S_{b,c}} \phi \frac{\partial G}{\partial n} ds + \int_{S_r} \Big[\phi \frac{\partial G}{\partial n} - G \frac{\partial \phi}{\partial n}\Big] ds = \int_{S_w} v_n G ds \end{aligned} \tag{64}$$

where G is the steady velocity potential associated with the Rankine source. Implicit in this formulation is the assumption that U is sufficiently small that it does

not occur explicitly in the free-surface condition. When U is zero this integral equation corresponds to the finite depth form of Equation (56).

Here the surfaces $S_{b,c}$ represent the tank bottom and the tank walls and S_b is the seabed or tank bottom in water of depth d. The linearised free-surface conditions, the sea-bed or tank bottom conditions and the tank wall conditions are implicitly satisfied by the above formulation. The usual wetted-surface diffraction and radiation boundary conditions are embedded in v_n. On the radiation surface, S_r, continuity of velocity potential and normal velocity are facilitated through the eigenfunction expansions in the sense of Equation (58).

For the *open water case* the polar form of the eigenfunction[16–17] may be expressed as

$$\phi(r,\theta,z) = \sum_{l=-L}^{L} \Big\{ A_{l0} \frac{H_l(m_0 r)}{H_l(m_0 R)} \cosh m_0(z+d) + \sum_{j=1}^{J} A_{lj} \frac{K_l(m_j r)}{K_l(m_j R)} \cos m_j(z+d) \Big\} exp(il\theta) \tag{65}$$

whereas in the *in-tank* problem[94–95] we use

$$\begin{aligned}\phi(x,y,z) = &\sum_{l=0}^{L_c} A_{l0} exp\mp(iD_{l0}x) \cosh m_0(z+d) \cos[(\frac{l\pi}{W})y'] \\ &+ \sum_{l=L_c+1}^{L} A_{l0} exp\pm(D_{l0}x) \cosh m_0(z+d) \cos[(\frac{l\pi}{W})y'] \\ &+ \sum_{l=0}^{L}\sum_{j=1}^{J} A_{lj} exp\pm(D_{lj}x) \cos m_j(z+d) \cos[(\frac{l\pi}{W})y']\end{aligned} \tag{66}$$

with W the tank width and

$$y' = (y - \frac{W}{2}). \tag{67}$$

The A_{lj} eigenfunction coefficients are determined with the unknown potentials on the surfaces S_w, S_f and $S_{b,c}$ or S_b. The functions denoted by H_l and K_l are the Hankel function of the first kind and the modified Bessel function of the second kind respectively with:

$$m_0 \tanh(m_0 d) = \frac{\omega_e^2}{g}, \qquad m_j \tan(m_j d) = \frac{-\omega_e^2}{g}, \tag{68}$$

$$D_{l0} = \Big[m_0^2 - (\frac{l\pi}{W})^2\Big]^{\frac{1}{2}} \quad \text{and} \quad D_{lj} = \Big[m_j^2 + (\frac{l\pi}{W})^2\Big]^{\frac{1}{2}}. \tag{69}$$

The in-tank eigenfunction expansion can have imaginary values of D_{l0} when m_0 is less than $\frac{l\pi}{W}$. Hence L_c denotes the highest values of l for which D_{l0} is real. The

wave numbers corresponding to $m_0 W = l\pi$ are the resonant modes of the tank. For $l > L_c$ the exponential terms associated with the imaginary values of D_{l0} are modified to correspond to decaying contributions as x becomes very large in either direction. The double summation, involving the coefficients D_{lj}, represents the evanescent modes. The upper limits L and J indicate that a finite number of terms are used in the applications.

3.1.5 *Green Function Matching Technique*

Zero Speed Problem

Here the inner problem is exactly the same as for the zero speed open water formulation i.e.

$$\begin{aligned} -\alpha\phi + \int_{S_w} \phi \frac{\partial G}{\partial n} ds + \int_{S_r} \Big[\phi \frac{\partial G}{\partial n} - G \frac{\partial \phi}{\partial n}\Big] ds \\ + \int_{S_f} \Big[\phi \frac{\partial G}{\partial n} - \frac{\omega^2}{g} \phi G\Big] ds = \int_{S_w} G\, v_n ds \end{aligned} , \tag{70}$$

but now rather than specify $\frac{\partial \phi}{\partial n}$ on S_r using a Sommerfeld radiation condition, or some other matching condition, the required radiation boundary derivative is determined using the first-kind Fredholm integral equation[18–19]

$$-\alpha\phi' + \int_{S_r} \phi' \frac{\partial G}{\partial n} ds = \int_{S_r} G \frac{\partial \phi'}{\partial n} ds. \tag{71}$$

The negative sign correctly takes into account the difference in the sign of the outward normal on S_r for the inner and outer problems and ϕ' is the other solution.

Forward Speed Problem

The inner Rankine source based formulation is now given by

$$\begin{aligned} -\alpha\phi + \int_{S_w} \phi \frac{\partial G}{\partial n} ds + \int_{S_r} \Big[\phi \frac{\partial G}{\partial n} - G \frac{\partial \phi}{\partial n}\Big] ds \\ + \int_{S_f} \Big[\phi \frac{\partial G}{\partial n} - \frac{1}{g}\Big[\omega_e + iU \frac{\partial}{\partial x}\Big]^2 \phi G\Big] ds = \int_{S_w} G\, v_n ds \end{aligned} , \tag{72}$$

whereas the outer integral equation is[18–19]

$$\begin{aligned} -\alpha\phi' + \int_{S_r} \phi' \frac{\partial G}{\partial n} ds - 2i \frac{U\omega_e}{g} \oint_{L_r} G\phi' dy \\ + \frac{U^2}{g} \oint_{L_r} [\phi' \frac{\partial G}{\partial x} - G \frac{\partial \phi'}{\partial x}]\, dy = \int_{S_r} G\, \frac{\partial \phi'}{\partial n} ds. \end{aligned} \tag{73}$$

Again the latter equation is treated as a first-kind integral equation in terms of the normal derivative of the velocity potential on the radiation boundary.

3.2 *The Higher Order Boundary Element (HOBE) Formulation*

In the formulations presented the solutions are usually generated using flat panels and the assumption that the sought unknown function (velocity potential or source strength) is invariant over the individual panels. In the higher-order boundary element method[20–21] curved panels and higher order functional representations of the unknown velocity potential, or source strength, are used. We therefore require appropriate interpolation functions within each element. Serendipity elements, in the terminology of finite elements have been used at Newcastle University. In particular both quadratic and cubic representations of the unknown function over quadrilateral and triangular elements have been considered. The number of nodes per element are therefore 8 and 6, and 12 and 10 for the quadratic and cubic representations respectively. For plane boundary elements it is normal to have one node only at the element centroid.

If $\underline{r}\ (\xi, \eta, \varsigma)$ denotes the position vector of a generic point of an element then

$$\underline{r}(\xi, \eta, \varsigma) = \sum_{k=1}^{n} \underline{r}(\xi_k, \eta_k, \varsigma_k) N_k(u, v)$$

and (74)

$$\phi(\xi, \eta, \varsigma) = \sum_{k=1}^{m} \phi(\xi_k, \eta_k, \varsigma_k) M_k(u, v),$$

where n and m indicate the degree of the representation of the element geometry and velocity potential respectively for the selected element geometry, and N_k and M_k are the shape functions evaluated at the kth node of the element located at $(\xi_k, \eta_k, \varsigma_k)$. Thus (ξ, η, ς) represents the coordinates of a generic point on an element and $(\xi_k, \eta_k, \varsigma_k)$ denotes the specific points used to define the element representation.. In terms of the local element coordinate system (u, v) the elemental area ds will satisfy

$$ds = J(u, v) du\ dv, \tag{75}$$

where $J(u, v)$ is the Jacobian. It may be shown[19] that the discretised form of the zero speed Green function formulation of Equation (1) may be expressed in

the higher-order boundary element form

$$-\alpha\phi + \sum_{j=1}^{N}\sum_{k=1}^{m}\phi(q_k^j)\int_{S_j}\int M_k(u,v)\Big(n_\xi\frac{\partial G}{\partial\xi} + n_\varsigma\frac{\partial G}{\partial\varsigma} + n_\eta\frac{\partial G}{\partial\eta}\Big)J(u,v)du\,dv = \sum_{j=1}^{N}\int_{S_j}\int Gv_nJ(u,v)du\,dv\,, \tag{76}$$

where N is the total number of elements used to model the wetted-surface boundary S_w. We may also approximate normal derivatives of the velocity potential to the same degree m, thus

$$\frac{\partial\phi'}{\partial n} = \sum_{k=1}^{m} M_k(u,v)\frac{\partial\phi'(\xi_k,\eta_k,\varsigma_k)}{\partial n} \tag{77}$$

may be used in the zero speed Green Function Matching formulation of Equation (16). Other HOBE formulations for zero and forward speed have been implemented and tested[18].

3.3 *Some General Comments.*

In Section 2 the parameter α was used to control the profile of the incident wave, and for this purpose may assume the value ± 1 or $\pm i$.

In all of the integral equation formulations the parameter α is the solid angle subtended at the node where the integral equation is applied. The consequence of using the incorrect solid angle at the free-surface has been demonstrated for the 2D HOBE method [21]. For the 3D HOBE approach ita assignment is even more critical and care in its evaluation is very important. For example, for the corner point of a rectangular box form of S_r the solid angle is $\pi/2$ for the inner problem formulation and $7\pi/2$ for the outer problem formulation!

Since α is the angle subtended at a point by a surface S then it only has the value 2π , in 3D formulations, when S is smooth at the point of interest. Otherwise a scheme investigated by Hearn and Donati [20] is used. For nodal points on the intersection of the wetted-surface, S_w, and the free surface, S_f, the solid angle definition must also take into account the contribution from the image part of the Green function. For more details of the HOBE method see Hearn [18–19].

Completeness of the formulations requires explicit definitions of the zero speed and forward speed Green functions. These may be found in reference(1) for both finite and infinite water depths for both 2D and 3D formulations. In Section 4 they

will be simply quoted without derivation since the calculation of nonlinear forces is critically dependent upon the ability of the software to robustly determine the value of second derivatives of the Green functions.

In strip-theory the wetted-surface of the vessel S_w is simply replaced by the sectional contours C_w, with a corresponding reduction in the dimensionality of the associated integrals and a different value for the solid angle α.

4. Evaluation of First and Second Order Forces

In this section the differences between evaluation of first and second order forces is considered. In general the first order forces are derived from application of the linearized form of Bernoulli equation given in Equation (13). The first order forces are generally classified as active and reactive. The active or wave excitation forces are determined from knowledge of the incident potential Φ_1^I and the scattering potential Φ_1^D. The reactive forces are determined from the radiation potentials Φ_1^k and these forces are usually partitioned into components in phase with the acceleration and velocity associated with a particular mode.

Second order forces can be seen as being generated from the linearized Bernoulli equation using a second order incident and diffraction potential, or, they may be determined from application of the full nonlinear Bernoulli equation, using all the available first order potentials. Here we shall only consider the latter case since the former case is still in a state of development and most applications relate to regular simple bottom standing geometric forms for water of finite depth. In fact if the second order diffraction potential is not required explicitly the second order wave excitation forces can be found using Green's second identity to provide a eqiuvalent second order force Haskind relationship[22].

The two particular methods of evaluating second order forces discussed here are generally known as the near-field and far-field approaches. Having described each procedure an outline and provided some indication of the associated difficulties of calculation we shall discuss the impact of the calculation of first order quantities upon the calculation of second order forces,

The fluid force and moments acting upon the structure are obtained through integration of the resolved pressure over the wetted surface using the relationships

$$\vec{F} = -\int_{S_w} p\vec{n}ds \tag{78}$$

and

$$\vec{M} = -\int_{S_w} p\vec{n} \wedge \vec{r} ds, \tag{79}$$

where $\vec{n}$ is the unit outward normal.

4.1 *The Near-Field Approach.*

The unsteady pressure and force are assumed to be expressible in the form

$$p = \sum_{i=0}^{N} \epsilon^i p^{(i)} + O(\epsilon^{N+1}), \tag{80}$$

and

$$\vec{F} = \sum_{i=0}^{N} \epsilon^i \vec{F}^{(i)} + O(\epsilon^{N+1}). \tag{81}$$

The bracketed superscript on p and F denote the 'order' of the term. Substitution of these perturbation expansions into Equations (78) and (79), and the collection of all terms of like order leads to the following expressions for the zeroth, first and second-order forces:

$$\vec{F}^{(0)} = -\int_{S_w^{(0)}} p^{(0)} \vec{n}^{(0)} \, ds, \tag{82}$$

$$\vec{F}^{(1)} = -\int_{S_w^{(0)}} p^{(1)} \vec{n}^{(0)} \, ds - \int_{S_w^{(0)}} p^{(0)} \vec{n}^{(1)} \, ds - \int_{S_w^{(1)}} p^{(0)} \vec{n}^{(0)} \, ds, \tag{83}$$

$$\begin{aligned} \vec{F}^{(2)} = & \int_{S_w^{(0)}} p^{(0)} \vec{n}^{(2)} \, ds - \int_{S_w^{(1)}} p^{(1)} \vec{n}^{(1)} \, ds - \int_{S_w^{(0)}} p^{(2)} \vec{n}^{(0)} \, ds \\ & - \int_{S_w^{(1)}} p^{(0)} \vec{n}^{(1)} \, ds - \int_{S_w^{(0)}} p^{(1)} \vec{n}^{(0)} \, ds - \int_{S_w^{(2)}} p^{(0)} \vec{n}^{(0)} \, ds. \end{aligned} \tag{84}$$

The Bernoulli fluid pressure equation, Equation (13), coupled with the perturbation expansion for p in Equation (80) upon rearrangement leads to

$$p^{(0)} = -\rho g z, \tag{85}$$

$$p^{(1)} = -\rho \left(\frac{\partial}{\partial t} - U \frac{\partial}{\partial x} \right) \Phi_u^1, \tag{86}$$

and

$$p^{(2)} = -\rho \left[\frac{1}{2} (\nabla \Phi_u^1)^2 + \left(\frac{\partial}{\partial t} - U \frac{\partial}{\partial x} \right) \Phi_u^2 \right]. \tag{87}$$

The zeroth order forces are the hydrostatic buoyancy forces

$$\vec{F}^{(0)} = \rho g \int_{S_w^{(0)}} z \vec{n}^{(0)} \, ds. \tag{88}$$

The first order force consists of the reactive and wave excitation forces, together with hydrostatic restoration forces, that is

$$\vec{F}^{(1)} = \rho \int_{S_w^{(0)}} \left(\frac{\partial}{\partial t} - U \frac{\partial}{\partial x} \right) \Phi_u^1 \vec{n}^{(0)} \, ds + \rho g (0, 0, \tilde{\eta}_3 A_w - \tilde{\eta}_5 A_w x_{cf}). \tag{89}$$

Here A_w and x_{cf} are the waterplane area and the longitudinal coordinate of the centre of flotation respectively.

The corresponding second order force is extremely complex and provides steady and slowly varying force components. Considering the average value of the second order force over a wave period it may be shown that

$$\begin{aligned} \overline{F}_m^{(2)} = & -\frac{1}{4}\rho g \int_{Lw} |\zeta_a|^2 \overline{N} dl + \frac{1}{4}\rho \int_{Sw} |\nabla \phi|^2 \overline{n} ds \\ & - \frac{1}{2} Re[\theta_{1a}^* \cdot F_a^{(1)}] + \frac{1}{2}\rho \omega_e \int_{Sw} Im[\delta_{1a}^* \cdot \nabla \phi] \overline{n} ds \\ & - \frac{1}{2}\rho U \int_{Sw} Re[\delta_{1a}^* \cdot \nabla \phi_x] \overline{n} ds \\ & - \frac{1}{2}\rho g A_w x_{cf} Re[\eta_4^* \, \eta_6] \hat{k} \end{aligned} \tag{90}$$

with

$$\begin{aligned} \overline{F}^{(1)} = & \rho \int_{Sw} (\frac{\partial}{\partial t} - U \frac{\partial}{\partial x}) \phi \overline{n} ds \\ & + \rho g (0, 0, \tilde{\eta}_3 A_w - \tilde{\eta}_5 A_w x_{cf}) \end{aligned} \tag{91}$$

and

$$\overline{N} = (n_1, n_2, n_3)/(n_1^2 + n_2^2)^{\frac{1}{2}}. \tag{92}$$

Here, $\overline{N}$, has been introduced to account for the slope of the wetted-surface. That is, wall sidedness is not assumed. The above expressions and notation are consistent with Hearn and Tong [1], but differ slightly to the zero forward speed expressions presented by Standing et al [23] and Pinkster[24].

The components of Equation (90) are readily interpreted.

- component I represents the contribution from the changing wetted-surface area due to the relative free surface elevation,
- component II gives the velocity squared effect of Bernoulli's equation,
- component III accounts for the effect of the first order fluid force due to rotation of the body axis,

- component IV represents the change of the pressure field on the wetted-surface due to the body displacement,
- component V corrects for the convective effect of the pressure field variation due to the steady forward speed and
- component VI accounts for the second order effect in rotation of the axis on the vertical force and is zero for pure head sea incidence.

Evaluation of Equation (90) is critically dependent on the solution of the first order potentials and the motion responses, in particular the diffraction potential is required explicitly.

The evaluation of higher order derivatives is important in both the evaluation of the second-order forces[16,17,25] and in the HOBE fluid-structure interaction formulations[18]. In particular in the HOBE formulation the speed associated term $U\nabla\phi_x$ has required the development of special transformations to allow evaluation of Equation (78). These transformations have been derived [18–19] and implemented.

It is clear that evaluation of the second order wave loads can only occur after the first order interaction analysis for regular harmonic waves and the corresponding motion analysis has been undertaken in the frequency domain.

In more general terms Standing et al [23] noted that wave drift forces have a mean and low-frequency component, which are the combined result of the second-order pressures and interactions associated with first-order wave field, and the pressures in the second-order wave (e.g. 'set-down').

Salvesen [26] demonstrated that the second-order wave gives rise to low-frequency forces, but not to mean drift force components. The 'set-down' wave is one particular effect of non-linear interactions within a wave field, whereby the water surface is depressed beneath the wave group surface but elevated between such groups. This is due to the orbital velocity of the fluid particles being larger within wave groups of large waves than those occurring due to the interaction between such groups. It is the variation in pressure between these two regions which cause this effect.

4.2 *The Far-Field Approach.*

Rather than integrate directly the pressure over the wetted surface of structure we may appeal to the conservation of momentum or energy. That is, we assume V

is the volume of fluid bounded by the surface S and the total momentum, $\vec{M}_{tum}$ is given by

$$\vec{M}_{tum} = \rho \int_V \vec{q} dV \tag{93}$$

where q is the velocity of any point in the fluid. The rate of linear momentum is determined from

$$\begin{aligned} \frac{D\vec{M}_{tum}}{Dt} =& \rho \frac{D}{Dt} \int_V \vec{g} dV \\ =& \rho \int_V \frac{\partial \vec{q}}{\partial t} dV + \rho \int_S \vec{q} V_n dS \end{aligned} \tag{94}$$

where V_n is defined in Equation (16). After considerable manipulation it may be shown that the longitudinal component of the second order force in the negative x-direction, the added resistance, is expressible in the form

$$R_W = R_{IB} + R_{BB} \tag{95}$$

with

$$R_{IB} = 2\pi\rho\varsigma_A w_o cos\beta Re[H(\beta, m_o)] \tag{96}$$

and

$$\begin{aligned} R_{BB} = 2\pi\rho \left[\int_{-\pi/2}^{-\alpha_o} + \int_{-\alpha_o}^{\pi/2} - \int_{\pi/2}^{3\pi/2} \right] \left[|H(\theta, K_2)|^2 \frac{K_2^2 cos\theta}{\sqrt{1 - 4\tau cos\theta}} d\theta \right] \\ + 2\pi\rho \int_{\alpha_o}^{2\pi - \alpha_o} |H(\theta, K_1)|^2 \frac{K_1^2 cos\theta}{\sqrt{1 - 4\tau cos\theta}} d\theta. \end{aligned} \tag{97}$$

The other parameters are :

$$\begin{aligned} \alpha_o &= cos^{-1}(1/4\tau) \ : \ \tau = Uw_e/g > 1/4, \text{ and is zero otherwise ,} \\ \begin{matrix} K_2 \\ K_1 \end{matrix} &= \frac{m_o\left(1 - 2\tau cos\theta \pm \sqrt{1 - 4\tau cos\theta}\right)}{2cos^2\theta}, \\ H &= \sum_{j=1}^{6} \eta_j H_j + H_7 \quad \text{and} \\ H_j(\theta, K) &= \int_{S_w} \sigma_j exp[Kz_o - iK(x_o cos\theta + y_o sin\theta)] ds \ . \end{aligned} \tag{98}$$

Here σ_j is the source strength associated with the six radiation problems ($j = 1, 2, ..., 6$) and the diffraction problem ($j = 7$). m_o is the zero-speed wave number,

whereas K_1 and K_2 correspond to poles of the free-surface contribution of the translating-pulsating Green function[27]. The derivation of the final expressions is dependent upon Newman's asymptotic limits for the radiation and scattering potentials expressed in terms of the Kochin functions[28] H_j. The body-body interaction term, R_{BB}, is much more complicated and generally smaller than the wave-body term, R_{IB}. The R_{IB} term can be partitioned into four distinct components $R_{IB_i} : i = 1,2,3,4$. The calculations undertaken are based upon direct evaluation of the following expressions:

$$\begin{aligned}
R_{IB_1} &= \frac{i}{2}\rho m_o cos\beta \sum_{j=1}^{6} \eta_j \int_{S_w} \phi_j \frac{\partial \phi_I^*}{\partial n} ds, \\
R_{IB_2} &= \frac{i}{2} m_o cos\beta \sum_{j=1}^{6} \eta_j F_{Kj}^*, \\
R_{IB_3} &= \frac{i}{2}\rho m_o cos\beta \int_{S_w} \phi_7 \frac{\partial \phi_I^*}{\partial n} ds, \quad \text{and} \\
R_{IB_4} &= -\frac{i}{2}\rho m_o cos\beta \int \phi_I^* \frac{\partial \phi_7}{\partial n} ds.
\end{aligned} \tag{99}$$

A superscript $*$ indicates the complex conjugate of a quantity, ϕ_I is the incident wave velocity potential, and the Froude-Krylov force, in the jth direction, is defined by

$$F_{Kj} = \rho \int_{S_w} \frac{\partial \Phi_I}{\partial t} n_j ds. \tag{100}$$

It is to be understood that only real parts of the expressions for the R_{IB_i} components are to be evaluated.

5.0 First Order Models and Second Order Forces.

The second order forces are not trivial calculations and the predictions generated through computer software are greatly affected by differences in implementation. Assuming Formulations A and B of Section 3 are to be used with the near-field and far-field second order force predictors, the four methods may be designated 1A, 1B, 2A and 2B where the designators 1 and 2 identify the near-field and far-field predictors.

Typically differences in software can occur with regard to:

- the discretisation process and the geometric handling
- evaluation of the Rankine source $\frac{1}{r}$ - each Green function has the form $G = \frac{1}{r} + I_{fs}$ where I_{fs} denotes free surface influence.

- evaluation of the hydrostatic restoration terms in the sense of standard waterplane calculators versus wetted surface integrals.
- determination of the active and reactive forces.

Each is now considered in terms of different techniques actually implemented at Newcastle.

5.1 *Boundary element generation.*

The discretisation process can be described as a simple partitioning of S_w and any other subsurface of S into a number of plane surface elements. From an applications viewpoint this means selecting co-ordinates on the actual surface and indicating how the points are to be used to make up individual triangular, quadrilateral and polygonal boundary elements. To indicate how differences in implementation evolve the associated details for a quadrilateral element (facet) are presented. In this part of the notes $\underline{r}_i$ is defined as the position vector of the ith node of a facet, assuming clockwise numbering of nodes. Since Geometric Method 1 includes all the steps of Geometric Method 2 their details are presented in reverse order.

5.1.1 *Geometric Method 2*

Defining vectors $\underline{t}_1$ and $\underline{t}_2$ as $\underline{t}_1 = \underline{r}_1 - \underline{r}_3$ and $\underline{t}_2 = \underline{r}_4 - \underline{r}_2$, the wetted-surface outward normal, $\underline{n}$, and the area of the quadrilateral element are given respectively by

$$\underline{n} = (n_x, n_y, n_z) = \frac{\underline{t}_1 \wedge \underline{t}_2}{|\underline{t}_1 \wedge \underline{t}_2|} \quad \text{and} \quad A = \frac{1}{2}\ |\underline{t}_1 \wedge \underline{t}_2|. \tag{101}$$

Clearly $\underline{t}_1$ and $\underline{t}_2$ are the diagonals of the quadrilateral element. Treating the 'mean point' of the associated nodes as the 'centroid', $\underline{r}_c$, of the element it follows that

$$\underline{r}_c = \frac{1}{4} \sum_{i=1}^{4} \underline{r}_i \,. \tag{102}$$

5.1.2 *Geometric Method 1*

This method includes all the previous steps of Method 2. However, the definition of the element centroid is refined. The logic behind the modification is that specifying four points in space does not necessarily mean they all lay on a flat plane. In the steps now indicated an 'equivalent' mean plane is generated. The modified nodes, $\underline{r}_i^m$, are defined by

$$\underline{r}_i^m = \underline{r}_i + c_i \underline{n} \quad \text{where} \quad c_i = (\underline{r}_c - \underline{r}_i)\cdot\underline{n} \ : \ i = 1,2,3,4. \tag{103}$$

Defining the additional vectors

$$\underline{t}_i' = \underline{r}_{i+1}^m - \underline{r}_1^m \ : \ i = 1,2,3, \quad \text{and the areas} \quad A_i = \frac{1}{2} \ |\underline{t}_i' \wedge \underline{t}_{i+1}'| : i = 1,2, \quad (104)$$

the centroid of the equivalent plane element can be shown to be given by

$$\underline{r}_c' = \frac{1}{3} \left\{ \underline{r}_1^m + \underline{r}_3^m + \frac{A_1 \underline{r}_4^m + A_2 \underline{r}_2^m}{A_1 + A_2} \right\}. \quad (105)$$

5.2 *Rankine source evaluation*

The Rankine source, its associated image singularity, and their derivatives, can be treated separately because they are not frequency dependent. Initially very simple strategies were developed for evaluating these quantities. However, realising that predictions could be affected by the strategy used, more refinements were developed[29]. To present the different strategies adopted $\triangle S_i$ and $\triangle S_j$ are defined as the areas of the 'influenced' and 'influencing' facets respectively. The following terms are then introduced to indicate different procedures for evaluating terms of the form $\int \frac{1}{r} ds$ and their associated derivatives:

'Simple pole' implies evaluation of the integrand at the centroid of the 'influenced' facet, and weighting this value by the facet area.

'Numerical' integration implies product Gaussian quadrature using 1 to 64 points, depending upon the ratio $\frac{1}{r} \ (\triangle S_i \ \triangle S_j)^{\frac{1}{4}}$.

'Analytic' integration means direct application of the Hess and Smith[30] equivalent line integration procedures.

'Extended Analytic' integration treats the special case of '$r = 0$' using extensions of Hogben & Standing[31] analogous to those of Hess and Smith.

5.2.1 Integration Strategy 1

This strategy was used in Method 1 of Reference [1]. Defining a distance scale, $r_s = (\triangle S_i \ \triangle S_j)^{\frac{1}{4}}$ the integrands of the fundamental source, the image source and their derivatives are evaluated as follows:

- Simple pole method when $r \geq 3r_s$.
- Numerical integration when $2r_s < r < 3r_s$.
- Analytic integration when $r \leq 2r_s$ and $r \neq 0$.
- Extended analytic integration when $r = 0$.

5.2.2 Integration Strategy 2

The second simpler strategy was used with Method 2 of Reference [1]. In this case the integration of the Rankine source and its derivatives are evaluated according to:

- Simple pole method when $r > \sqrt{\Delta S_i}$.
- Analytic integration when $r \leq \sqrt{\Delta S_i}$.
- Extended analytic integration when $r = 0$.

The image source and its derivatives are evaluated only for non-self-induced cases using the simple pole method.

5.3 *Hydrostatic restoration terms*

The fact that the wetted surface of the structure is defined explicitly means that the hydrostatic terms may be evaluated by direct application of Archimedes principle, that is, direct integration of the hydrostatic pressure, or, mathematically equivalent, from a knowledge of the waterplane area, and the appropriate first or second moments of the waterplane area The hydrostatic force and moment components are derivable from

$$\underline{F}_H = -\rho g \int_{S_w} \underline{n} ds, \quad \text{and} \quad M_H = -\rho g \int_{S_w} [(\underline{r} - \underline{r}_{cr}) \wedge n] ds, \tag{106}$$

where $\underline{r}_{cr}$ is the location of the assumed centre of rotation. Existence of port-starboard symetry will remove the need to calculate some of the forces and movements. Numerically the evaluations can be carried out using either of the following procedures.

5.3.1 Hydrostatic Method 1

In Method 1 of Reference [1] knowledge of the surface area and the normal direction to the individual facets was used. Thus, given the N facet discretisation of S_w , say, the implied necessary integrals were evaluated using

$$c_{33} = -\rho g \sum_{i=1}^{N} n_{z_i} \triangle S_i \quad c_{35} = c_{53} = \rho g \sum_{i=1}^{N} (x_{c_i} - x_{cr}) n_{z_i} \triangle S_i$$

$$c_{44} = -\rho g \sum_{i=1}^{N} (y_{c_i} - y_{cr})^2 n_{z_i} \triangle S_i + \rho g \sum_{i=1}^{N} (y_{c_i} - y_{cr})(z_{c_i} - z_{cr}) n_{y_i} \triangle S_i \tag{107}$$

$$c_{55} = -\rho g \sum_{i=1}^{N} (x_{c_i} - x_{cr})^2 n_{z_i} \triangle S_i + \rho g \sum_{i=1}^{N} (x_{c_i} - x_{cr})(z_{c_i} - z_{cr}) n_{x_i} \triangle S_i$$

where the ith boundary element centroid is $(x_{c_i},\ y_{c_i},\ z_{c_i})$, and $(n_{x_i},\ n_{y_i},\ n_{z_i})$ denotes the outward normal. Effectively all integration is carried out using the mid-point value based argument of the 'simple pole' procedure of Section 5.2.

5.3.2 Hydrostatics Method 2

Knowledge of the indicated mathematical equivalences for the case of $\mathbf{r}_{cr} = \mathbf{r}_g$, also allows evaluation of the hydrostatic restoration coefficients using

$$c_{33} = \rho g A_{wp} \quad c_{35} = c_{53} = -\rho g A_{wp}^{1L}$$

$$c_{44} = \rho g[(z_b - z_g)V + A_{wp}^{2T}] \quad c_{55} = \rho g[(z_b - z_g)V + A_{wp}^{2L}], \tag{108}$$

where A_{wp} denotes waterplane area, and A_{wp}^{iL} and A_{wp}^{iT} denotes i^{th} longitudinal and transverse moment of the waterplane area respectively. Evaluation of these terms, in Method 2 of Reference [1], was undertaken using analytic integrations of the Lagrangian polynomials fitted to the waterline. Here z_b, z_g and V denote location of vertical centre of buoyancy, vertical centre of gravity and the displaced volume of the vessel.

5.4 *Rationalisation of Prediction Methods.*

In these notes, and other recent publications[27,36,37], rationalisation of the implementations means selecting Geometric Method 1, with Integration Strategy 1 and Hydrostatic Method 2. This is to remove subject differences of computer coding and ensure differences are only due to differences in model or second order force predictor.

5.5 *Differences in first-order hydrodynamic quantities.*

Considering the motion analysis as a first step in the second-order force calculation process, any noted differences in the motion response procedure can be identified in terms of the procedure designations 1A through 2B. The differences in processing the first-order hydrodynamic quantities will arise from the availability of derivatives of G and the forward-speed corrections applied.

Availability of $\partial\phi^j/\partial x$ $(: j = 1, 2, ..., 7)$, in Method 1A, means direct calculation of terms of the form $Un_k\partial\phi^j/\partial x$, whereas in the other methods an equivalent operator $Um_k\phi^j$ is used in the integration associated with the reactive and wave excitation force components[26].

In Methods 1A and 2A, treating ϕ_A^j as the directly calculated ϕ from Formulation A, the equivalent forward-speed velocity potentials are determined using the corrections

$$\phi^j = \phi_A^j : j = 1,2,3,4 \quad \text{and} \quad \phi^j = \phi_A^j \pm \frac{U}{i\omega_e}\phi_A^k \ : j = \begin{matrix}5\\6\end{matrix} \quad \text{with} \quad k = \begin{matrix}3\\2\end{matrix}. \tag{109}$$

5.6 *Second-order force evaluations.*

The differences introduced in the post processing of the fluid-structure interaction analysis to match a particular second-order force calculation procedure are concerned with the evaluation of $\nabla\phi_x$ in the near-field procedure, and the evaluation of the Kochin functions in the far-field method.

The need to calculate $\nabla\phi_x$ arises for two reasons. The first is associated with determination of the free-surface elevation. Since σ, rather than ϕ, is determined in both Formulations A and B, application of the kinematic free-surface boundary condition to determine ς_{fs}, the wave elevation at the free-surface, from Φ at the facet centroids, requires a first-order Taylor series correction, that is

$$\varsigma_{fs} = \varsigma_A - \frac{1}{g}\left(\frac{\partial\Phi}{\partial t} - U\frac{\partial\Phi}{\partial x}\right) - \frac{\delta \underline{r}_{fs}}{g}\cdot\nabla\left(\frac{\partial\Phi}{\partial t} - U\frac{\partial\Phi}{\partial x}\right), \tag{110}$$

where Φ is the time dependent total velocity potential including both radiation and diffraction influences. The second reason is the need for direct evaluation of $\nabla\phi_x$ in component V of Equation (90).

σ_j determined from Formulation A cannot be corrected directly for forward-speed and so in Method 2A σ_j should be replaced by the 'equivalent' term $\partial\phi^j/\partial n - \phi^j\partial/\partial n$ in the Kochin function, where $\partial\phi^j/\partial n$ and ϕ_j forward-speed corrected, as discussed above. That is the boundary condition, as well as the velocity potential, is forward-speed corrected in the Kochin function evaluations.

5.7 *Evaluation of harmonic parts of Green's function.*

For the pulsating source Green's function of Formulation A the harmonic part is also evaluated using the same 'numerical integration' procedure described in the discussion of the Rankine singularity. However, the finite integral representation of Hearn for G and its first derivatives[32] have been extended to include evaluation of the required second derivatives[29].

For the translating-pulsating source Green function the derivatives were not evaluated originally in Formulation B[1]. Hence to implement the Method 1B they

had to be derived analytically and then determined numerically. Consistent with the free-surface integral of the Green function, the derivatives are expressed as one-fold integrals of the standard complex Exponential Integral. The latter function is evaluated using a series approximation for small arguments and a rational function approximation[30] for the larger arguments.The one-fold cylindrical coordinate based integral representation of G is found to be computationally less demanding than the corresponding Cartesian two-fold integral form and is undertaken using procedures based on Patterson's method[33] .

5.8 *Green's function derivative evaluation.*

The purely pulsating source Green's function is numerically stable in terms of function and first and second derivative evaluation. In contrast the translating-pulsating source is singular for both the subcritical ($\tau < 1/4$) and supercritical ($\tau > 1/4$) flow regimes. Whereas the singular nature is not always clearly evident in evaulations of G the instabilities are very much in evident in the derivatives

$$\frac{\partial^2 G}{\partial x \partial z} \quad \text{and} \quad \frac{\partial^2 G}{\partial x \partial y}.$$

The singular nature is dependent upon the type of cubature procedures used and the particular combinations of field and source points, which are a function of the discretisation process. In the subcritical regime the $\omega = \pi/2$ value causes K_2 to become singular. For supercritical conditions both endpoint singularities and a singular K_2 cause numerical problems. Hence we introduce Method 1A$'$ as Method 1A with all second derivative contributions included. A robust Method 1B$'$ has yet to be implemented, but the nature of the associated numerical problems are gradually being understood.

To give some appreciation of the complexity of the evaluating the derivatives consider two alternative mathematically equivalent descriptions of the Green function for the simpler pulsating source case. The Green function may be written as

$$G(p,q) = \frac{1}{r} + \frac{1}{r'} + 2m_o \mathrm{PV} \int_o^\infty \frac{J_o(KR)}{K - m_o} e^{K(z+z_o)}\, dK + i2\pi m_o e^{m_o(z+z_o)} J_0(m_o R), \tag{111}$$

or

$$\begin{aligned} G(p,q) = \frac{1}{r} + \frac{1}{r'} - \pi m_o [H_0(m_o R) + Y_0(m_o R) - i2J_0(m_o R)] e^{m_o(z+z_o)} \\ - 2m_o e^{m_o(z+z_o)} \int_{z+z_o}^0 \frac{e^{-m_o t}\, dt}{\sqrt{R^2 + t^2}}, \end{aligned} \tag{112}$$

Equivalently we may write

$$G(p,q) = \frac{1}{r} + \frac{1}{r'} + 2m_o I_1 + iIm_1, \tag{113}$$

where

$$I_1 = \mathrm{PV}\int_0^\infty \frac{e^{K(z+z_o)} J_0(KR)\, dk}{K - m_o}, \tag{114}$$

and

$$Im_1 = 2\pi m_o e^{m_o(z+z_o)} J_0(m_o R). \tag{115}$$

Derivatives with respect to x and y will lead to differentiation of J_o and hence the derivatives (first and second) can be expressed in terms of I_1, Im_1, and the additional functions

$$I_2 = \mathrm{PV}\int_0^\infty \frac{e^{K(z+z_o)} J_1(KR)\, dk}{K - m_o}, \tag{116}$$

$$Im_2 = 2\pi m_o^2 e^{m_o(z+z_o)} \frac{J_1(m_o R)}{R}. \tag{117}$$

The alternative Green function representation has the form

$$G(p,q) = \frac{1}{r} + \frac{1}{r'} - m_o e^{m_o(z+z_o)}(\pi HY_o(m_o R) + 2IF_1) + Im_1, \tag{118}$$

where

$$IF_1 = \int_{z+z_o}^0 \frac{e^{-m_o t}\, dt}{\sqrt{R^2 + t^2}}, \tag{119}$$

$$HY_n(X) = H_n(X) + Y_n(X), \tag{120}$$

and the additional auixilary function

$$IF_2 = \int_{z+z_o}^0 e^{-m_o t}\sqrt{R^2 + t^2}\, dt, \tag{121}$$

The principal value (P.V.) of the derivatives of the pulsating (zero-speed) Green function necessary for the near-field added resistance computation can be written as follows[29]:

$$\frac{\partial G(p,q)}{\partial x} = -(x - x_o)\left[\frac{1}{r^3} + \frac{1}{(r')^3} + \frac{2m_o}{R^2}\left(1 + \frac{(z+z_o)}{r'}\right) + \frac{2m_o^2}{R} I_2 + iIm_2\right], \tag{122}$$

$$\frac{\partial G(p,q)}{\partial y} = -(y - y_o)\left[\frac{1}{r^3} + \frac{1}{(r')^3} + \frac{2m_o}{R^2}\left(1 + \frac{(z+z_o)}{r'}\right) + \frac{2m_o^2}{R} I_2 + iIm_2\right], \tag{123}$$

$$\frac{\partial G(p,q)}{\partial z} = -\frac{(z - z_o)}{r^3} - \frac{(z + z_o)}{(r')^3} + \frac{2m_o}{r'} + 2m_o^2 I_1 + im_o Im_1, \tag{124}$$

$$\frac{\partial^2 G(p,q)}{\partial x^2} = -\frac{1}{r^3}\Big[1-\frac{3(x-x_o)^2}{r^2}\Big] - \frac{1}{(r')^3}\Big[1-\frac{3(x-x_o)^2}{(r')^2}\Big]$$
$$-2m_o\frac{(y-y_o)^2}{R^3}\Big[m_oI_2+\frac{1}{R}\Big(1+\frac{(z+z_o)}{r'}\Big)\Big]$$
$$+2m_o\frac{(x-x_o)^2}{R^2}\Big[m_o\Big(\frac{I_2}{R}-m_oI_1\Big)+\frac{1}{R^2}\Big(1+\frac{(z+z_o)}{r'}\Big) \tag{125}$$
$$+\frac{1}{(r')^2}\Big(\frac{(z+z_o)}{r'}-m_or'\Big)\Big]$$
$$-\frac{i}{R^2}\Big[(x-x_o)^2(m_o^2Im_1-Im_2)+(y-y_o)^2Im_2\Big],$$

$$\frac{\partial^2 G(p,q)}{\partial x\partial y} = (x-x_o)(y-y_o)\Big[3\Big(\frac{1}{r^5}+\frac{1}{(r')^5}\Big)-\frac{2m_o^2}{R^2}(m_oI_1-\frac{2I_2}{R})$$
$$+\frac{2m_o}{R^2}\Big[\frac{1}{(r')^2}\Big(\frac{z+z_o}{r'}-m_or'\Big)+\frac{2}{R^2}\Big(1+\frac{(z+z_o)}{r'}\Big)\Big] \tag{126}$$
$$-\frac{i}{R^2}(m_o^2Im_1-2Im_2)\Big],$$

$$\frac{\partial^2 G(p,q)}{\partial x\partial z} =(x-x_o)\Big[3\frac{(z-z_o)}{r^5}+3\frac{(z+z_o)}{(r')^5}-\frac{2m_o}{(r')^3}-\frac{2m_o^2}{R^2}\Big(1+\frac{(z+z_o)}{r'}\Big)$$
$$-2\frac{m_o^3I^2}{R}-im_oIm_2\Big]. \tag{127}$$

In a similar manner introduction of auxiliary functions for the alternative form Green function lead to the equations[29]

$$\frac{\partial G(p,q)}{\partial x} = -(x-x_o)\Big[\frac{1}{r^3}+\frac{1}{(r')^3}+\frac{2m_o}{R^2}\Big(m_or'+\frac{(z+z_o)}{r'}\Big)$$
$$-\frac{m_o^2}{R}e^{m_o(z+z_o)}\Big(\pi HY_1(m_oR)+\frac{2m_o}{R}IF_2\Big)+iIm_2\Big], \tag{128}$$

$$\frac{\partial G(p,q)}{\partial y} = -(y-y_o)\Big[\frac{1}{r^3}+\frac{1}{(r')^3}+\frac{2m_o}{R^2}\Big(m_or'+\frac{(z+z_o)}{r'}\Big)$$
$$-\frac{m_o^2}{R}e^{m_o(z+z_o)}\Big(\pi HY_1(m_oR)+\frac{2m_o}{R}IF_2\Big)+iIm_2\Big], \tag{129}$$

$$\frac{\partial G(p,q)}{\partial z} = -\frac{(z-z_o)}{r^3}-\frac{(z+z_o)}{(r')^3}+\frac{2m_o}{r'}-m_o^2e^{m_o(z+z_o)}\Big[\pi HY_0(m_oR)+2IF_1\Big]$$
$$+im_oIm_1, \tag{130}$$

$$
\begin{aligned}
\frac{\partial^2 G(p,q)}{\partial x^2} = & -\frac{1}{r^3}\left[1-3\frac{(x-x_o)^2}{r^2}\right]-\frac{1}{(r')^3}\left[1-3\frac{(x-x_o)^2}{(r')^2}\right] \\
& + \frac{m_o^2}{R}e^{m_o(z+z_o)}\Big[m_o(x-x_o)^2\left(\pi HY_0(m_oR)+2IF_1\right) \\
& + \frac{(y-y_o)^2-(x-x_o)^2}{R}\left(\pi HY_1(m_oR)+\frac{2m_o}{R}IF_2\right)\Big] \\
& - 2\frac{m_o(y-y_o)^2}{R^4}\left[\frac{(z+z_o)}{r'}+m_or'\right] \\
& + 2\frac{m_o(x-x_o)^2}{R^2}\left[\frac{1}{(r')^2}\left(\frac{(z+z_o)}{r'}-m_or'\right)+\frac{1}{R^2}\left(\frac{(z+z_o)}{r'}+m_or'\right)\right] \\
& - \frac{i}{R^2}\left[(x-x_o)^2(m_oIm_1-Im_2)+(y-y_o)^2Im_2\right],
\end{aligned}
\tag{131}
$$

$$
\begin{aligned}
\frac{\partial^2 G(p,q)}{\partial x\partial y} = & (x-x_o)(y-y_o)\Big[3\left(\frac{1}{r^5}+\frac{1}{(r')^5}\right) \\
& + \frac{m_o^2}{R^2}e^{m_o(z+z_o)}\Big[\pi\left(m_oHY_0(m_oR)-\frac{2}{R}HY_1(m_oR)\right) \\
& + 2m_o\left(IF_1-\frac{2}{R^2}IF_2\right)\Big]+\frac{2m_o}{R^2(r')^2}\left[\frac{(z+z_o)}{r'}-m_or'\right] \\
& + \frac{4m_o}{R^4}\left[\frac{(z+z_o)}{(r')}+m_or'\right]-\frac{i}{R^2}\left(m_o^2Im_1-2Im_2\right)\Big],
\end{aligned}
\tag{132}
$$

$$
\begin{aligned}
\frac{\partial^2 G(p,q)}{\partial x\partial z} = & (x-x_o)\Big[3\frac{(z-z_o)}{r^5}+3\frac{(z+z_o)}{(r')^5}-\frac{2m_o}{(r')^3}-\frac{2m_o^2}{R^2}\left(\frac{(z+z_o)}{r'}+m_or'\right) \\
& + \frac{m_o^3}{R}e^{m_o(z+z_o)}\left(\pi HY_1(m_oR)+\frac{2m_o}{R}IF_2\right)-im_oIm_2\Big].
\end{aligned}
\tag{133}
$$

6. Analysis of the Wichers' Tanker

Having been given some insight regarding the complexity of the calculations and the choices regarding the implementation we will now look at the application of some of the different analyses to a moored 200,000 dwt tanker. This example is selected because of the large amount of theoretical data and experimental measurements available. All of which are public domain.

Exploiting geometric symmetry the Wichers' tanker specified in Table 1 is analysed using a 268 facet discretisation of Figure 1.

The equations of motion used were formulated with respect to the centre of rotation and LCG is assumed amidships. Using post processed solutions for the source strength, σ, the added resistance, R_W, is calculated for a variety of forward

Table 1. Principal particulars Wichers' 200k dwt tanker.

L_{pp}	B	T	V	D	KG	k_{yy}	C_b
310.0m	47.20m	18.90m	234994m^3	20.70m	13.32m	77.47m	0.85

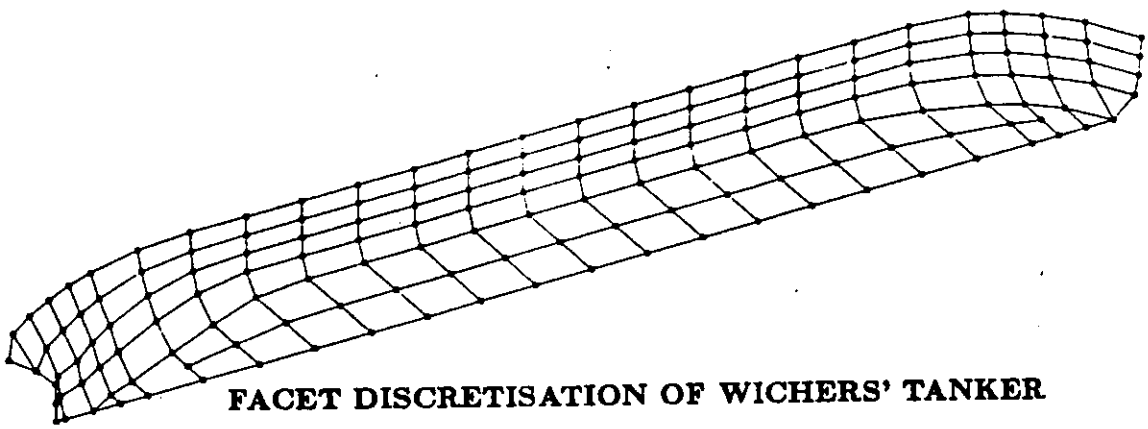

Figure 1. Boundary Element Discretisation of Wichers' Tanker.

and reverse speeds for a range of incident wave frequencies. Thereafter the added resistance is treated as a function of ship speed, and the low-frequency damping is evaluated, for each method, for each wave-frequency from

$$b_w = \frac{1}{\varsigma_A^2}\left(\frac{\partial R_W}{\partial U}\right) \mid_{U=0}. \tag{134}$$

The non-dimensionalised incident wave-frequency, added resistance and low-frequency damping are defined by

$$f_o = \omega_o\sqrt{(L_{pp}/g)}, \quad R'_W = R_W/[\rho g \varsigma_A^2 B^2/L_{pp}] \quad \text{and} \quad b'_w = b_w B^2/[\rho V\sqrt{(g/L)}], \tag{135}$$

where B is beam and L is the length of the structure.

The low frequency damping is of importance in designing mooring system. In some cases the low frequency damping is so important that if time domain analyses are run without inclusion of its effect the difference between predicted excursions and measured excursions is 100 % in error due to over prediction. Using such information in a design scenario could be an expensive error. In this section we consider

the impact of coupling different first order solvers with the two second order force predictore. It is also worth noting that since the low-frequency damping requires evaluation of the velocity derivative of R_W its prediction[27] is dependent upon the particular speed combinations selected. In the application now reported the speed-combinations and analysis combinations, defined in Tables 2 and 3, are considered. Speed combination 9 of Table 2 corresponds to the selected forward-speeds of Wichers' study[34], whereas speed combination 1 corresponds to that used in the earlier Newcastle studies [1,35,36,29]. In developing prediction Methods 1A', 1A, 1B, 2A and 2B the default combination of analyses adopted is combination 1 of Table 2, both here and in References [37,38].

Table 2.
Definitions of Speed Combinations.

Speed Comb.	Froude Numbers $(U/\sqrt{gL})$				
1	- 0.02	- 0.01	0.001	0.01	0.02
2	- 0.02	- 0.01	0.001	0.01	0.04
3	- 0.02	- 0.01	0.001	0.02	0.04
4	- 0.04	- 0.01	0.001	0.01	0.02
5	- 0.04	- 0.01	0.001	0.01	0.04
6	- 0.04	- 0.01	0.001	0.02	0.04
7	- 0.04	- 0.02	0.001	0.01	0.02
8	- 0.04	- 0.02	0.001	0.01	0.04
9	- 0.04	- 0.02	0.001	0.02	0.04

Table 3.
Definition of Analysis Combinations

Analysis Comb.	1	2	3	4	5	6	7	8
Geometry Method	1	1	2	1	2	1	2	2
Integration Strategy	1	1	1	2	2	2	1	2
Hydrostatic Method	2	1	2	2	2	1	1	1

In Figures 2 & 3 the Method 1A' and 1A added resistance predictions, together with the experimental measurements[34], for the Wichers' tanker are presented as a function of non-dimensional incident wave-frequency f_o. The predicted added resistances are almost identical. Comparing Figures 3 & 4 the Method 1A and 1B predictions also show very similar trends, although there is a 7% variation in the highest peak and a 10% variation in the group of lower peak values of R'_W. The generally small differences between Methods 1A & 1B suggest that the radiation and diffraction potential contributions to $\nabla\phi_z$ of Equation (90) are neglegible in

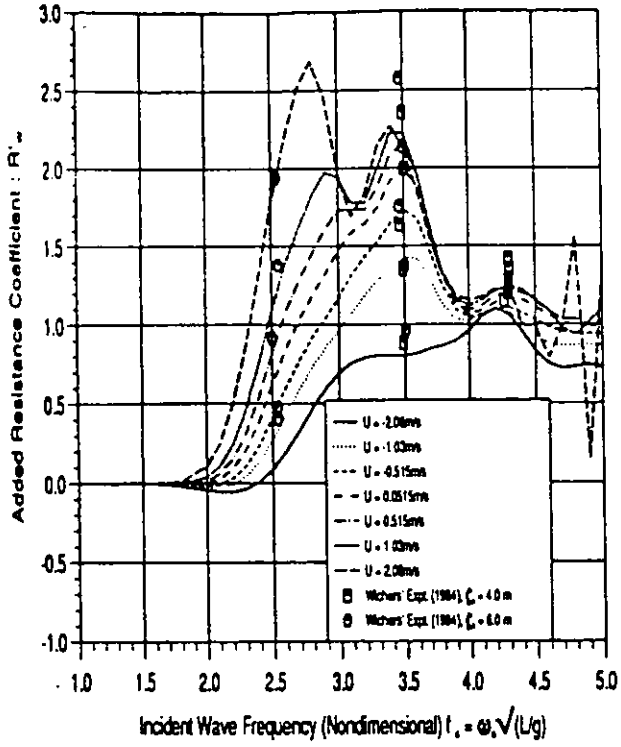

Figure 2. Non-dimensionalised added resistance using Method 1A′ i.e. second derivatives of G included.

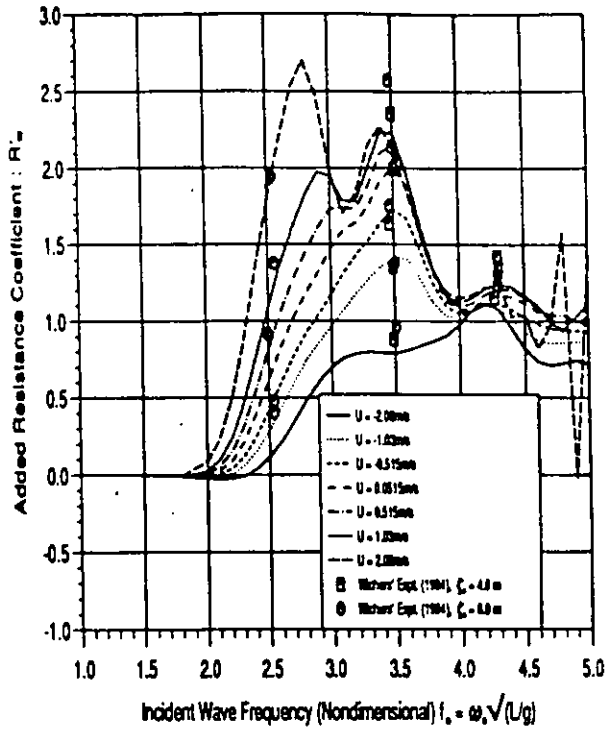

Figure 3. Non-dimensionalised added resistance using Method 1A i.e. second derivatives of G excluded.

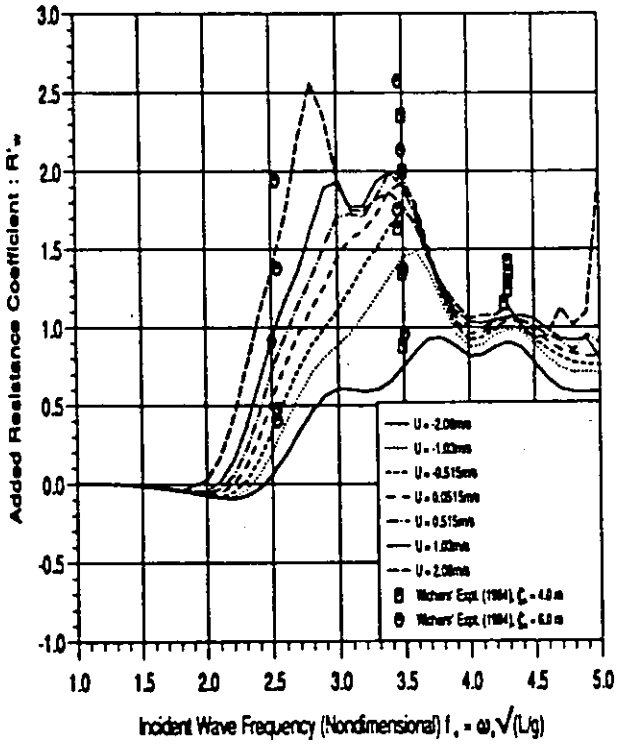

Figure 4. Non-dimensionalised added resistance using Method 1B i.e. second derivatives of G excluded.

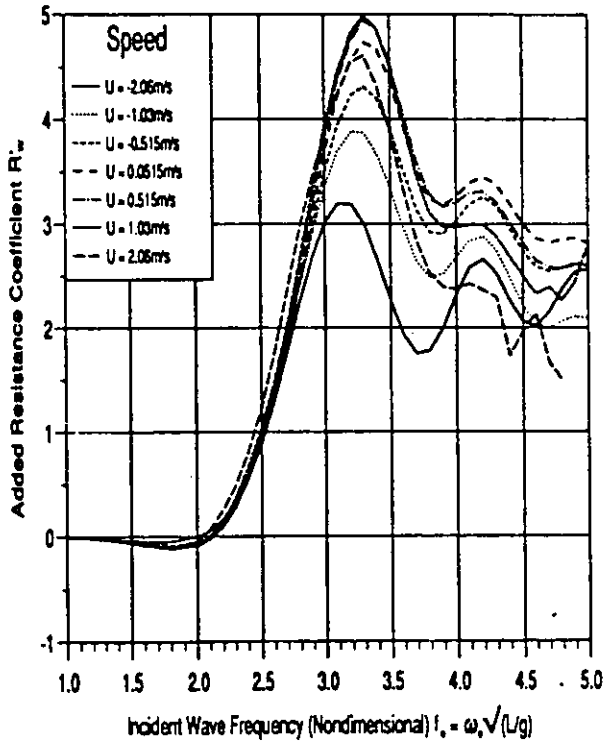

Figure 5. Non-dimensionalised added resistance using Method 2A.

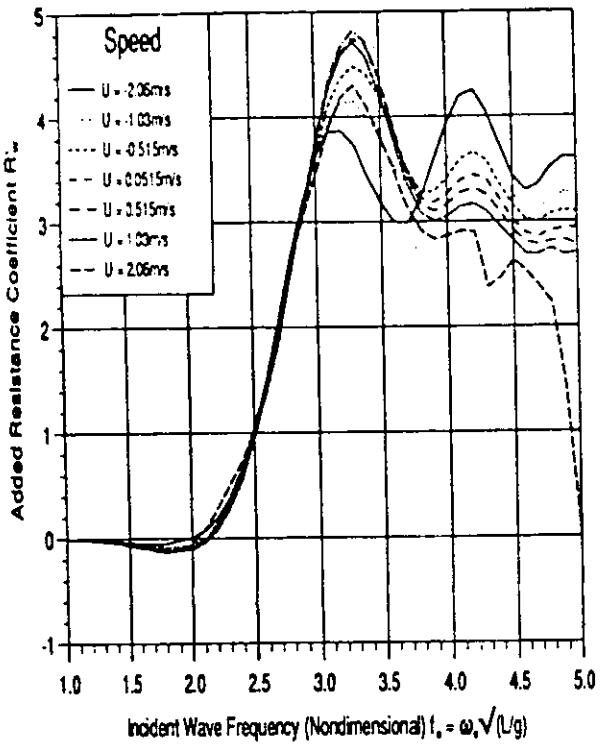

Figure 6. Non-dimensionalised added resistance using Method 2B.

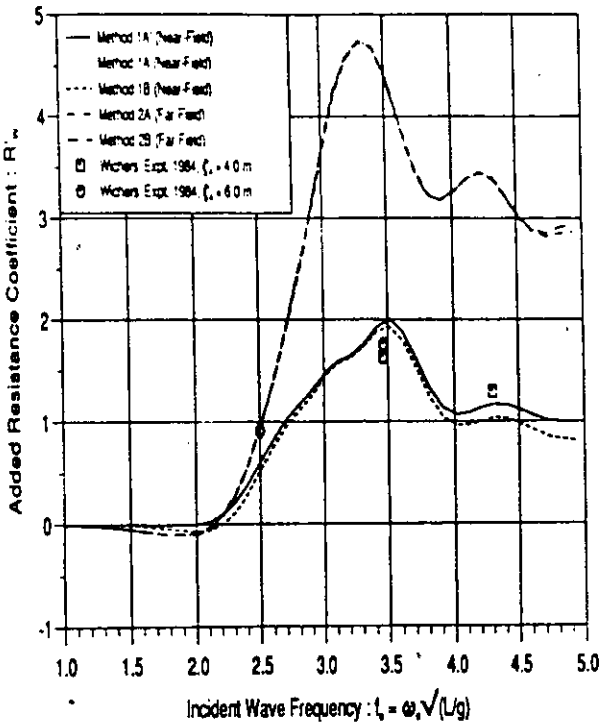

Figure 7. Non-dimensionalised added resistance comparing all five methods and experimental results [1].

comparison to the incident wave contribution.

It should be noted that whereas the spatial correction of the $\partial\Phi/\partial t$ term of Equation (110) was included in the Method 1B calculations, because it only included first-order derivatives of G, it is not possible to conclude that boundary element centroidal evaluations of free-surface elevation are sufficient. In general Method IB seems to produce smaller mean second-order forces in the low forward and reverse-speed regimes. The near-field added resistance also reflects a sensitivity to the fluid-structure interaction formulation used. To complete the study the numerical instabilities identified will require special quadrature techniques, capable of handling the cited numerical problems, to be establish absolutely the conclusions drawn.

Comparing Methods 2A & 2B, Figures 5 & 6, the band of oscillation at the higher frequencies is significantly lower when applying Method 2B. Plots of R'_{IB} demonstrate[37] that the wave-body interaction term accounts for 80% of the mean second-order forces. The body-body interaction term R'_{BB} of Method 2B also displays a radically different frequency dependence than the Method 2A, having larger peaks and a narrower oscillation band at the higher wave frequencies[37]. In both

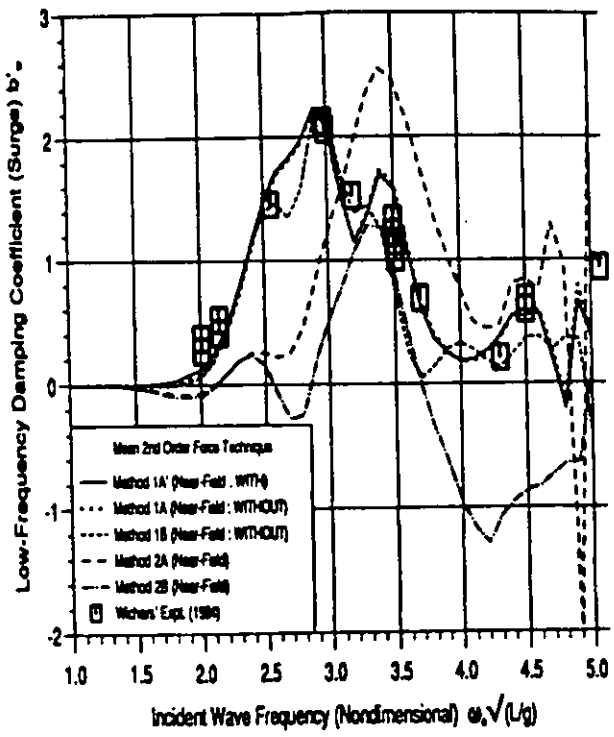

Figure 8. Non-dimensionalised low-frequency damping comparing all five methods and experimental results [1].

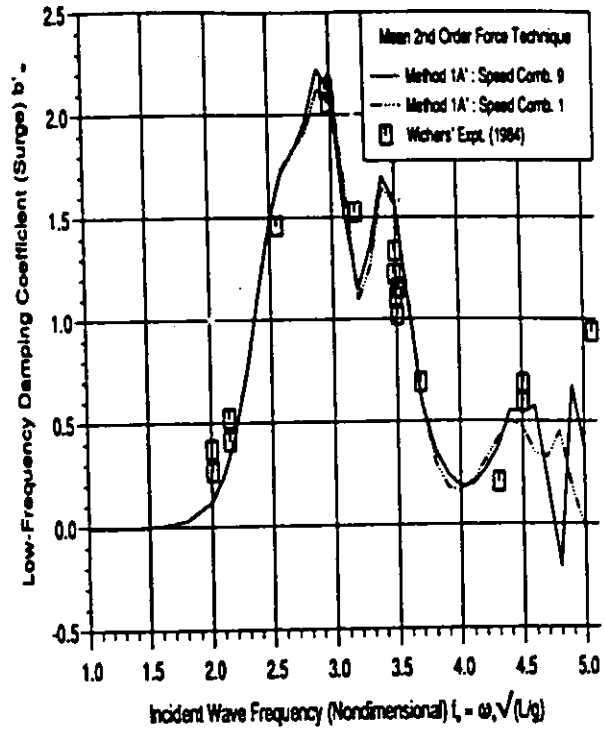

Figure 9. Non-dimensionalised low-frequency damping using Method 1A′ with Speed Combinations 1 and 9, and experimental results [1].

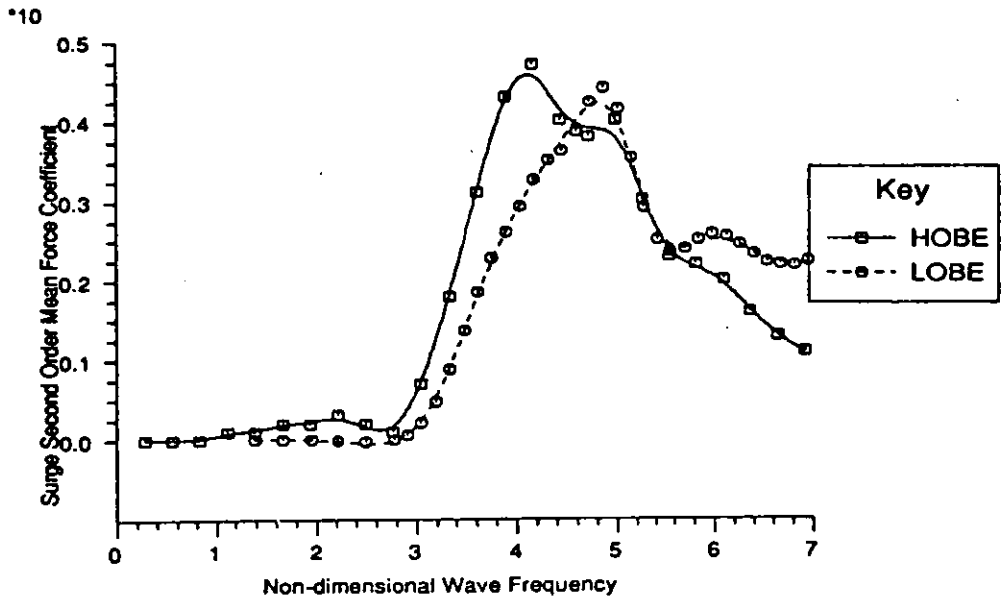

Figure 10. Comparison of HOBE and LOBE Analyses of Tanker.

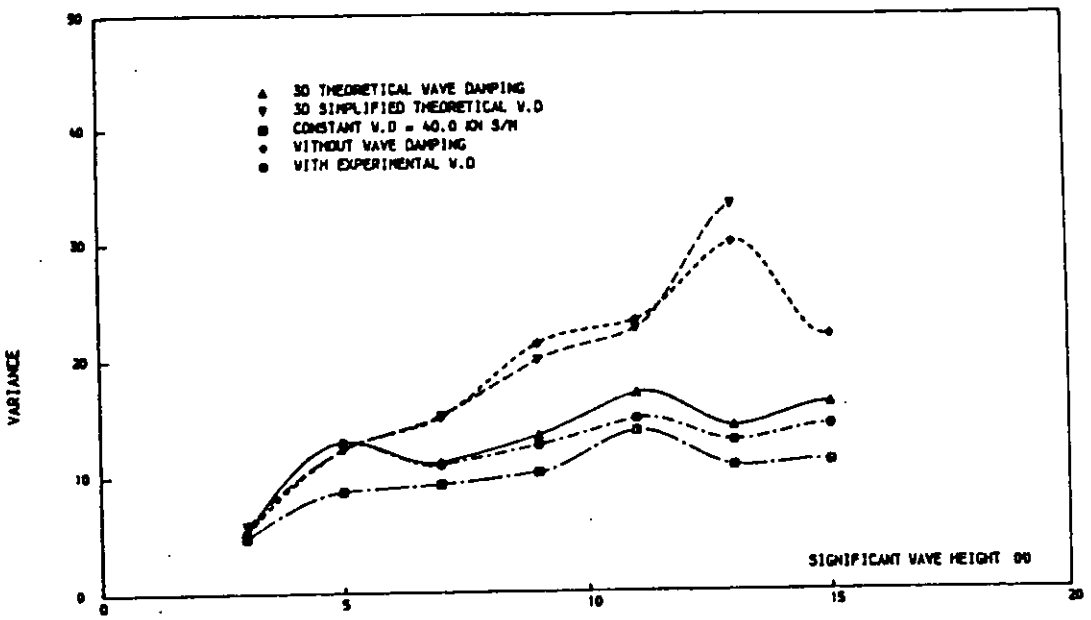

Figure 11. Surge Variance versus Significant Wave Height.

methods the heave and diffraction Kochin functions dominate the low f_o region of R'_{BB} and the pitch Kochin function contributes more significantly in the central f_o range.

Comparing all five sets of predictions we note that:

- The peak far-field prediction is twice the peak near-field added resistance prediction, see Figure 7.
- The far-field added resistance does not increase in a straight forward manner with increases in forward-speed, as does the near-field approach.
- For the low forward-speeds considered, use of Formulation B, rather than A, generally reduces the predicted added resistance.
- The position of the peaks and observed differences in their location is due more to the differences in the second-order force calculation analyses than the interaction formulations employed.
- The near-field procedure remains the preferred approach to calculate the added resistance.

In contrast the far-field low-frequency predictions are quite insensitive to speed combination selected for $f_o < 4.0$. However, the peak values of Method 2A are higher and occur at a higher incident wave-frequency. The character of Method 2B is closer to that of Method2A than Method 1B, but is greatly reduced[37]. The wide spread of predictions is perhaps more readily appreciated upon studying Figure 13. This compares all five sets of predictions, for speed combination 9, with the experimental measurements based on this same speed combination. In Figure 14 the Wichers' experimental data is compared with Method 1A′ predictions for speed combinations 1 and 9. The superiority of the near-field approach whether using Formulation A or B for the hydrodynamic data does clearly appear to be established if the results of this note and those of references [1,34,39] are combined.

The exclusion of second order derivatives in component V of the near-field procedure makes this term independent of radiation and diffraction effects, whereas the influence upon component I is not too significant at the low speeds examined. In future research, steps to overcome numerical instabilities associated with higher order derivatives of G in Formulation B could lead to an even more reliable and robust prediction procedure.

The predictions of low-frequency damping for each of the five methods, as a function of speed-combination and incident wave-frequency, indicate that the difference between the Method 1A′ and Method 1A predictions are negligible. For frequencies below $f_o = 2.5$ the trends and magnitude of Method 1A & 1B predictions are remarkably similar. Likewise, beyond $f_o = 3.5$ the low-frequency predictions are similar in character, if not equal in levels. The real differences are in the central region $2.5 < f_o < 3.5$, particularly in terms of the shape character of the low-frequency transfer function. The peak low-frequency damping value (around $f_o = 3.0$) is extremely sensitive to the selected speed combination, with a 25% spread in value upon comparison with the lowest predicted peak value.

For the same vessel Figure 10 shows a recent comparison[40] between the LOBE based Method 1A and an equivalent HOBE based implementation of the same approach. At this point it is difficult to say that the differences are purely due to the differences in LOBE and HOBE formulations. Some researchers have suggested using a very simplistic method of deducing low frequency damping. Some years ago I named it the drift force gradient (DFG) to distinguish it from the added resistance gradient based definition of Equation (134). The impact of using these predictions of low frequency damping in a time domain solution was to predict

rms excursions larger than if no damping had been included. Figure 11 represents a plot of surge variance as a function of significant wave height. The analysis producing the poor values of damping was less costly to execute, but is that a justifiable reason for selecting a poor procedure?

7. Some Final Comments.

In general the near-field methods 1A/, 1A and 1B have proven to be the most robust approach so far, whether comparing added resistance of ships, barges or semi-submersibles. The low frequency damping is an important parameter for the analysis of moored structures. It too is best predicted using the near-field methods implemented. Another advantage of the near-field approach is that the dominance of the added resistance by component I for ships, and component II for offshore barges, agrees with a common sense appreciation of the contributions of these components.

Understanding analysis from a mathematical point of view can be involved and difficult. Trying to reason out why analysis produces the results it does when the calculation procedures are long and involved can prove to be even more difficult. Endeavouring to rationalize why different theories lead to predictions with sometimes very narrow, and sometimes widely varying bands of inequality, for apparently minor changes of problem specification, probably defies understanding or reasoning.

References

1. Hearn, G.E., Tong, K-C. & Lau, S-M., "Sensitivity of Wave Drift Damping Coefficients to the Hydrodynamic Analysis Models used in the Added Resistance Gradient Method", J. Offshore Mechanics and Arctic Engineering, Vol. 110, No. 6, pp. 337-348, Nov. 1988.

2. Huijsmans, R.H.M & Hermans, A.J., "A Fast Algorithm for Computation of 3D Ship Motions at Moderate Forward Speed", Proc. 4th Int. Conf. on Numerical Ship Hydrodynamics; Sept. 1985; Washington, USA.

3. Lau, S-M. & Hearn, G.E., "Simplified Low Forward Speed Green Function", SERC MTD, Floating Production Systems Managed Programme, Interim Progress Report form Project A1, Low Frequency Damping Predictions and Behaviour of Marine Structures in a Seaway, 22p., April 1988.

4. Grue, J. & Palm, E., "Currents and Wave Forces on Ships and Marine Structures", IUTAM Memorial Symposium to Professor R.E.D. Bishop on the Dynamics of Marine Vehicles and Structures in Waves; June 1990, Brunel Univ., Proc. in press.

5. Hearn, G.E. & Kwok, T., "Formulating the 3D Low Forward Speed Problem to Include Steady-Unsteady Interactions", Newcastle University, SERC MTD/MoD Interim Progress Report, Dec. 1990.

6. Stoker, J.J., "Water Waves: The Mathematical Theory with Applications", Interscience, Section 1.2, Helmholtz's theorem, pp. 7-9, Section 1.3, Potential flow and Bernoulli's law, pp. 9-10, Section 2.1, Theory of waves of small amplitude, pp. 19-22, 1957.

7. Mei, C.C., "The Applied Dynamics of Ocean Surface Waves", John Wiley & Sons, Section 4.1.3, Further Remarks on the Radiation Condition, p. 13; Section 12.9, Second-Order Wave Forces on a Fixed Body, pp. 657-665 & p. 472, 1983.

8. Fenton, J.D., "A Fifth-Order Stokes Theory for Steady Waves", ASCE, J. Waterway, Port, Coastal & Ocean Engineering, Vol. 111, No. 2, pp. 216-234, March 1985.

9. Marshall, A.L., "On Implementing Fifth-Order Gravity Wave Theory", Underwater Technology, Vol. 13, No. 1, pp. 2-4, Spring 1987.

10. Ogilvie, T.F. & Tuck, E.O., "A Rational Strip-Theory of Ship Motion: Part I", University of Michigan, Dept. of Naval Architecture & Marine Engineering, Report No. 013, 1969.

11. Molin, B., "Second-Order Diffraction Loads upon Three-Dimensional Bodies", Applied Ocean Research, Vol. 1, No. 4, pp. 197-202, Oct. 1979.

12. Clark, P.J., Bettess, P., Hearn, G.E. & Downie, M.J., "Second-Order Wave Diffraction by the Finite Element Method", Newcastle University, Department of Marine Technology, Report, 1990.

13. Clark, P.J., Bettess, P., Hearn, G.E. & Downie, M.J., "The Application of Finite Element Analysis to the Solution of Stokes Wave Diffraction Problems", In press: Int. J. Num. Methods in Fluids.

14. Wehausen, J.V. & Laitone, E.V., "Surface Waves", Handbuck der Physik,

Vol. IX, Sect. 12, Other Boundary Conditions, pp. 471-472, 1960.

15. Hearn, G.E., "Using Mathematics to Simplify Free Surface-Interaction Analysis", Int. Conference on Computational Methods in Flow Analysis; 5-8 Sept. 1988; Okayama, Japan. 35p.

16. Hearn, G.E. & Liou, S-Y., "Finite Depth and Tank Wall Effects Upon First and Second Order Forces", Proc. 9th Int. Conf. Offshore Mechanics and Arctic Engineering Conference; 18-23 Feb. 1990; Houston, TX, USA, Vol. I, Part A, pp. 171-180, Feb. 1990.

17. Liou, S-Y., "Hybrid Boundary Integral Equation Method for the Hydrodynamic Analysis of Marine Structures in Open and Confined Water", Newcastle University, Dept. Marine Technology, Ph.D. Thesis, 1990.

18. Hearn, G.E. & Lau, S-M., "Low Frequency Damping Predictions and Behaviour of Marine Structures in a Seaway: Final Report", SERC MTD, Floating Production Systems Managed Programme of Research, 1987-89, Final Reports, Vol. 1, Project A1, ca. 150p, 13 Dec. 1989.

19. Hearn, G.E., "Higher Order Boundary Elements: An Applicable Concept for Hydrodynamic Analysis", Advanced Experimental Techniques and CAE Methods in Ship Hydro- and Aerodyanmics; SMSSH '90; 19th Scientific and Methodological Seminar on Ship Hydrodynamics, Oct. 1990. Varna. Proc. BSHC, Vol. 2, Ppr No. 60, pp (60-1)-(60-8), 1990

20. Donati, E, & Hearn, G.E. "Higher Order Boundary Elements for Free-Surface Structure Interaction Analysis: Final Report", John Brown Offshore Ltd., SERC MTD Dynanmics of Compliant Structures Cohesive Programme 1983-85, Final Report, Vol. 1, Vessel Loads and Response 'A', pp. 1-161, Nov. 1985.

21. Hearn, G.E. & Donati, E., "A New Fluid-Structure Interaction Analysis Based on Higher-Order Boundary Elements", Int. J. Num. Methods in Fluids, Vol. 8, No. 2, pp. 199-225, Feb. 1988.

22. Lighthill, M.J., "Waves and Hydrodynamic Loading", BOSS '79, Proc. 2nd. Int. Conf. on the Behaviour of Offshore Structures: Aug. 1979; London, UK. Vol. 1, Ppr No. 1, pp. 1-40, 1979.

23. Standing, R.G., Dacunha, N.M.C. & Matten, R.B., "Mean Wave Drift Forces: Theory and Experiment", National Maritime Institute, Report R124,

1981.

24. Pinkster, J.A., "Low Frequency Second Order Wave Exciting Forces on Floating Structures", Netherlands Ship Model Basin, Report 650, 1980.

25. Tong, K-C., "Second-Order Wave Excitation and Damping Forces on Floating Bodies", Newcastle University, Dept. Marine Technology, Ph.D. Thesis, 1988.

26. Salvesen, N., "Second-order Steady-State Forces and Moments on Surface Ships in Oblique Regular Waves", Proceedings of the Dynamics of Marine Vehicles and Structures in Waves , University College London, April 1974, pp. 225-239.

27. Hearn, G.E. and Goodwin, P., "Low-Frequency Damping Predictions: Assessing the Choices", Proceedings of Offshore Mechanics and Artic Engineering (OMAE) , June 1992.

28. Newman, J.N., "Marine Hydrodynamics", MIT Press, Section 6.4, Nonlinear Effects, pp. 247-251, 1977.

29. Hearn, G.E. and Tong, K-C., "Second-Order Fluid Damping", Final Progress Report for 1985-87 SERC MTD Dynamics of Compliant Structures Managed Programme , Vol. II, December 1987, pp. 250.

30. Hess, J.L. and Smith, A.M.O., "Calculation of Potential Flow About Arbitrary Bodies", Progress in Aeronautical Sciences , Vol. 8, Pergamon Press, 1967, pp. 1 - 138 (See Section 4.4 in particular).

31. Hogben, N. and Standing, R., "Wave Loads on Large Bodies", Proceedings International Symposium on Dynamics of Marine Vehicles and Structures , University College London, April 1974, pp. 273 - 292.

32. Hearn, G.E., "Alternative Methods of Evaluating Green's function in 3D Ship - Wave Problems", Journal of Ship Research , Vol. 21, No. 2, June 1977, pp. 89 - 93.

33. Patterson, T.N.L., "The Optimum Addition of Points to Quadrature Formulae", Mathematics of Computation , Vol. 22, 1968, pp. 847 - 856.

34. Wichers, J.E.W. and Huijsmans, R.M.H., "On the Low-Frequency Hydrodynamic Damping Forces Acting on Offshore Moored Vessels", Proceedings of Offshore Technology Conference , Paper 4813, May 1984, Vol. 3, pp.

315-324.

35. Hearn, G.E. and Tong, K-C., "Evaluation of Low-Frequency Damping", Proceedings of Offshore Technology Conference , Paper 5176, May 1986, Vol. I, pp. 229-241.

36. Hearn, G.E. and Lau, S-M., "Low-Frequency Damping Predictions and Behaviour of Marine Structures in a Seaway", 1987-89 SERC MTD Floating Production Systems Managed Programme , Vol. I, January 1990, pp. 160.

37. Hearn, G.E. and Goodwin, P., "Low-Frequency Damping Predictions: The Identification of a Reliable and Robust Method", Proceedings of Conference on Behaviour of Offshore Structures, Imperial College London, July 1992.

38. Hearn, G.E. and Goodwin, P., "Far-Field and Near-Field Investigations of Second-Order Force Prediction", Proceedings of Practical Design of Ships and Mobile Units (PRADS) , May 1992.

39. Hearn, G.E., "Low-Frequency Damping: The Development of its Theoretical Prediction", Proceedings of an International Union of Theoretical and Applied Mechanics Memorial Symposium on the Dynamics of Marine Vehicles and Structures in Waves , Edited by Price, W.G., Temarel, P. and Keane, A.J., Developments in Marine Technology, Vol. 7, Elsevier, 1991, pp. 237-252.

40. Hearn, G.E. and Kwok, T., "Steady-Unsteady Fluid-Structure Interaction Influences on the Behaviour of Moored Structures", Final Contract report, SERC/MOD, August 1992.

PRACTICAL SEAKEEPING DESIGN TOOLS FOR MONOHULLS

by

GRANT E. HEARN

NEWCASTLE UPON TYNE

Advanced Design for Ships & Offshore Floating Structures

Practical Seakeeping Design Tools for Monohulls

Grant E. Hearn

University of Newcastle Upon Tyne

Introduction.

In the past there has been a tendency to use seakeeping software as an analysis tool rather than a design tool. Certainly the development of the 'workstation', by the computer industry, has facilitated the application of such analyses at the conceptual design stage. However, desktop computing power and blind application of seakeeping analysis does not, in itself, constitute a practical design tool. Similarly ad hoc variations of an initial design with a multiplicity of applications of the seakeeping analysis will certainly not provide a hydrodynamically optimal design. Practical seakeeping design tools must not only undertake any required standard seakeeping analysis, but also assist the designer with the generation of 'sensible' alternative designs. 'Sensible' is a difficult concept to define objectively, but should certainly imply that other related hydrodynamic and hydrostatic properties should not be adversely affected by any attempts to improve seakeeping. In some cases it will be used synonymously with the term 'practical' when discussing the lines of the alternative generated designs.

Coupled with the application of analysis goes that other important, but quite undefinable, quantity called 'experience'. For would be young designers 'experience' can be a hard commodity to acquire, especially in a modern world in which one-off innovative designs are to be generated and tendered for without risk, either financial or technical. To assist such designers, new procedures must and are being sought which permit a rational investigation of a design and, if necessary, facilitate provision of 'experience' generating activities specific to the design under consideration. Rather than simply present those procedures in isolation we will first address the following points:

- What does the available wealth of knowledge, buried in the open literature, tell us regarding the sensitivities (perceived or actual) of seakeeping characteristics and geometric variation?

- How is seakeeping capability to be assessed and quantified?
- How are the methods of assessment to be used to design a better ship?

Having discussed these points in turn we shall then consider two alternative approaches to using seakeeping analysis in the design context. The first approach is based upon 'design charts' and the second process is most readily described as an 'inverse analysis' based design procedure.

2. Seakeeping Design Parameters.

Although forward speed is an important parameter in the context of voluntary and involuntary speed reductions, in the following discussions we limit our attention to the influence of geometric changes upon the behaviour of a ship in a seaway. The parameters to be addressed can be grouped as follows:

- displacement (∇), main dimensions (L, B, T), and block coefficient (C_B)
- coefficients which define the details of the hull form, e.g. C_{WP}, LCB and LCF.

These parameters are primarily concerned with the specification of the underwater characteristics of the vessel. They are the principal parameters responsible for the motion of the ship. For deck wetness and water impact forces the above water form characteristics, such as freeboard and flare are important. However these will not be considered here, since in the context of theoretical analyses most of the available software cannot account for their influence.

It is known from hydrodynamics that the inertia forces consisting of the structural mass and the hydrodynamic mass (the added mass) are directly related to the total displaced volume, as well as the longitudinal distribution of both the cross sectional area and the sectional beam-draught ratio. On the otherhand the fluid damping forces are related to the longitudinal distribution of the sectional area and beam, and the hydrostatic or restoring forces are governed by the total waterplane area and the longitudinal distribution of beam. Therefore, it should be clear that the motions of a ship in a seaway are governed by the form of its waterplane area and the distribution of sectional area and draught, in addition to its main dimensions, speed, and heading.

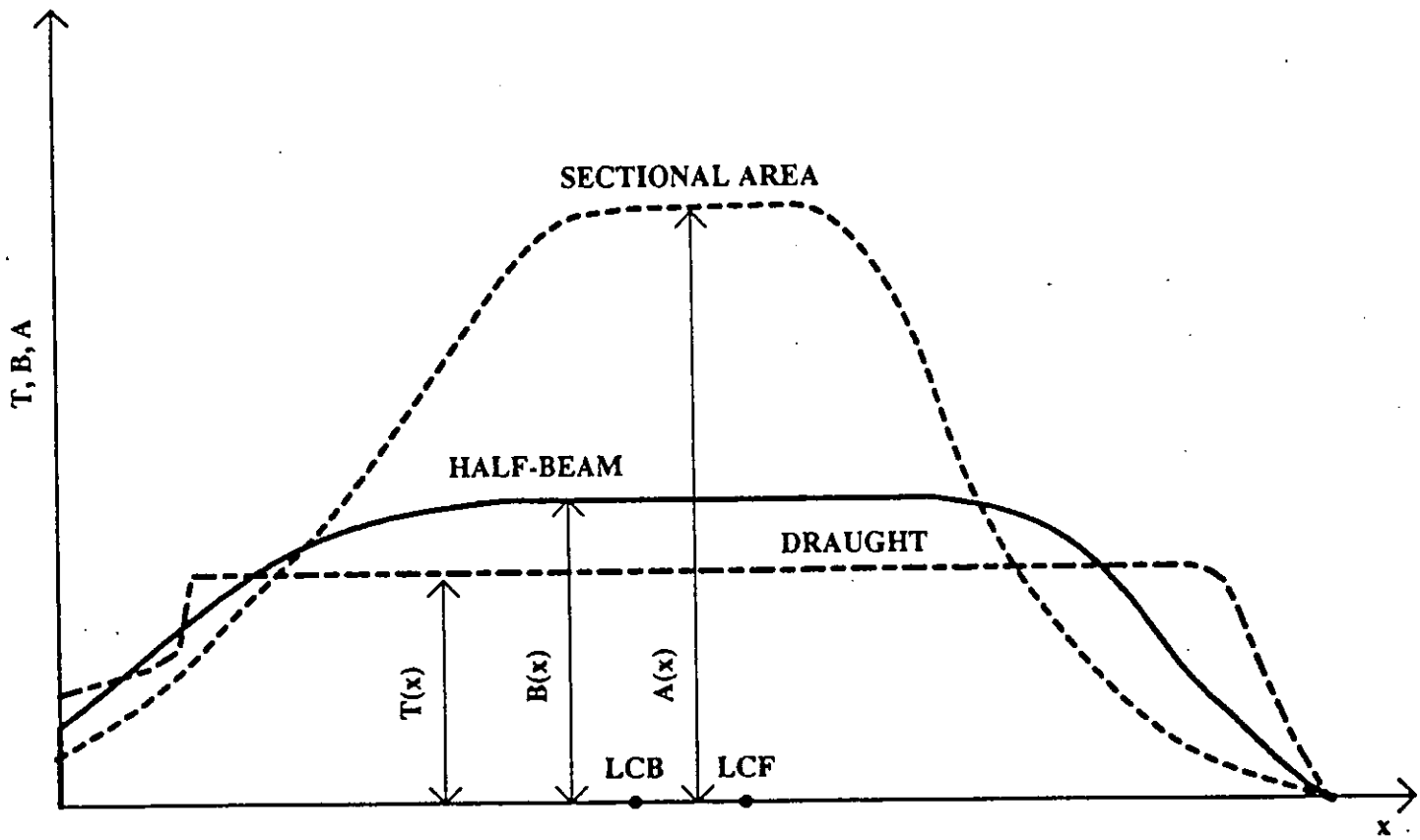

Figure 1. Definition of Hull Form Parameters.

In Figure 1 schematic curves of longitudinal distribution of the sectional area and beam at the loaded waterline are shown. In view of the earlier comments this simple figure can be considered as containing useful information concerning both the hydrodynamic characteristics and the naval architectural hull form parameters. Clearly, the area under the sectional area curve provides the displaced volume and the longitudinal centre of buoyancy, LCB, whereas the area under the beam curve provides the waterplane area and the longitudinal centre of flotation, LCF.

These parameters are sufficient to provide a complete description of the hull form in the case of fixed block coefficient and main dimensions, provided we assume the transverse sections can be generated using either Lewis sections or other conformal mapping techniques. The parameters LCB and LCF also receive considerable attention in the literature regarding the seakeeping behaviour of different ships.

Once the size and the underwater hull form of the ship have been selected the motion characteristics of the vessel in a seaway has largely been predetermined. Whereas the above water form of the vessel does not significantly influence the motion of the ship, it strongly affects its spray and deck wetness characteristics. The freeboard near the bow, particularly at the forward perpendicular, is the most important aspect of the above water form of the ship with respect to taking water over the bow. Other features of the above water shape, which primarily affect its spray characteristics, are the flare of the bow, the use of knuckle or spray rails in the bow, and the roundness of the bow at the stem. It is summary statements such as those just expressed that we sometimes express as 'experience' and therefore use in our decision making. Additional experience is gained by studying the results of other researchers. Space does not permit a full review of each of the many available published papers and reports. However, from reading a limited number of different sources it is possible to distil the following qualitative measures of seakeeping behaviour regarding the influence of:

- displacement
- ship length
- ship beam
- ship draught

and their related ratios as expressed in terms of

- L/B
- L/T
- B/T
- C_B.

The information will be presented in tabular form, and will indicate the influence of the selected geometric parameter upon the heave, pitch and relative bow motion (RBM) responses, together with vertical acceleration, slamming frequency, deck wetness frequency and the added resistance. In the tables + and − are used to indicate beneficial and detrimental effects respectively, while 0 indicates that a change in the selected parameter does not cause any beneficial or detrimental effect. The effects of parameter changes noted in each case assume an increase in the selected geometric parameter.

2.1 Influence of displacement and main dimensions.

Each of the listed parameters will now be considered in turn. The presentation might seem a little artificial as it appears that each parameter has been studied in isolation. In reality all the quoted references, and others, have to be considered in some detail to generate the conclusions presented.

2.1.1 *Influence of displacement on seakeeping characteristics.*

The influence of displacement is presented in Table 1.

Table 1. Influence of Displacement on Seakeeping Characteristics

Source	Heave	Pitch	RBM	Acc.	Slam.	Wet.	Add.Res.
Lewis (1955)		+					
Beukelman&Huijser (1977)	+	+	+	+			+
Lloyd (1988)				+	+	+	

The specific ship types considered and the approach adopted in the associated references are as follows:

Lewis (1955) investigated the influence of ship size on seakeeping by expanding the predicted pitch response spectra based on measured RAOs, for a Series 60 model, to shorter and longer ship length values.

Beukelman and Huijser (1977) investigated the effects of displacement and forebody variations upon the seakeeping qualities of Series 60 ship forms using strip theory.

Lloyd (1988) investigated the effects of the hull form on seakeeping characteristics using a simple mathematical frigate hull form.

2.1.2 *Influence of length on seakeeping characteristics.*

The results of our observations are found in Table 2.

The additional sources of information required in this case can be summarised as:

Lewis (1960) reports the results of a comparative testing of two cargo ship models to investigate the influence of length on ship motions.

Table 2. Influence of Length on Seakeeping Characteristics

Source	Heave	Pitch	RBM	Acc.	Slam.	Wet.	Add.Res.
Lewis (1960)		+		+		+	
Muntjewerf (1963)	+	+					+
Schmitke&Murdey (1980)	+	+	0	+			
Lloyd (1988)				+	−	−	

Muntjewerf (1963) investigated the effect of hull form and length on destroyers using a series of five destroyer models.

Schmitke and Murdey (1980) carried out a methodical series of model tests on frigate type hull forms and presented results showing the effect of hull form parameters on calm water resistance and seakeeping characteristics.

2.1.3 *Influence of beam on seakeeping characteristics.*

The results of our observations are found in Table 3.

Table 3. Influence of Beam on Seakeeping Characteristics

Source	Heave	Pitch	RBM	Acc.	Slam.	Wet.	Add.Res.
Lewis (1960)		+					
Muntjewerf (1963)	+	+					−
Abkowitz et al.(1966)	0	0	0	0			
Schmitke&Murdey (1980)	−	−	−	−			

The additional information required in this case is:

Abkowitz et al.(1966) studied the effects on motions of variations in length, beam, draught, prismatic coefficient, and midship coefficient of a Series 60 form.

2.1.4 *Influence of draught on seakeeping characteristics.*

The results of our observations are found in Table 4.

2.1.5 *Influence of L/B on seakeeping characteristics.*

Our observations are presented in Table 5.

Table 4. Influence of Draught on Seakeeping Characteristics

Source	Heave	Pitch	RBM	Acc.	Slam.	Wet.	Add.Res.
Lewis (1960)		−			+		
Abkowitz et al.(1966)	−	−	−	−			
Schmitke&Murdey (1980)	−	−	−	−			

Table 5. Influence of Length/Beam on Seakeeping Characteristics

Source	Heave	Pitch	RBM	Acc.	Slam.	Wet.	Add.Res.
Vossers et al.(1961)	0	0	0				
Swaan (1961)	0	0					
Wijngaarden (1984)	−	−	−	−			
Robson (1987)	+	+	+	+			
Lloyd (1988)				−	+	0	

The additional sources of information required in this case are as follows:

Vossers et al.(1961) carried out systematical experiments on the series 60 models to investigate the influence of main dimensions and displacement on seakeeping characteristics.

Swaan (1961) published model test results on the heaving and pitching and on the added resistance in waves of a Series 60 form.

Wijngaarden (1984) developed a seakeeping ranking technique for research vessels of differing dimensions and hull form parameters.

Robson (1987) experimentally investigated the influence on seakeeping of variations in L/B, B/T and C_B for a high speed displacement form.

2.1.6 *Influence of L/T on seakeeping characteristics.*

The conclusions drawn are given in Table 6.

Additional information in this case can be gained from:

Bales (1980) developed an analytical model relating ship underwater geometry and ship responses to an index of seakeeping merit using 20 destroyer forms.

Table 6. Influence of Length/Draught on Seakeeping Characteristics

Source	Heave	Pitch	RBM	Acc.	Slam.	Wet.	Add.Res.
Vossers et al.(1961)	+	+	+				+
Swaan (1961)	+	+					−
Abkowitz et al.(1966)	+	+	+	+			
Bales (1980)	+	+	+	+			
St.Denis (1983)	+	+					
Wijngaarden (1984)	+	+	+	+			
Lloyd (1988)				+	−	+	

St. Denis (1983) untook a review of the available literature with the purpose of identifying and highlighting any inconsistent conclusions which could be drawn from the results of published research.

2.1.7 *Influence of B/T on seakeeping characteristics.*

The results of our observations are found in Table 7.

Table 7. Influence of Beam/Draught on Seakeeping Characteristics

Source	Heave	Pitch	RBM	Acc.	Slam.	Wet.	Add.Res.
Schmitke&Murdey (1980)	+	+	+	+	−		
Robson (1987)	+	+	+	+			

2.1.8 *Influence of C_B on seakeeping characteristics.*

The results of our observations are found in Table 8.

2.2 Influence of forebody shape on seakeeping characteristics.

The influence of forebody is presented in Table 9.

In the table a U or a V has been used to indicate a preference for a more U-shaped or a more V-shaped forebody. Some of the sources cited in Table 9 were referenced in earlier tables. Here, we summarise again, in some cases, their contribution in the context of Table 9.

Table 8. Influence of Block Coefficient Seakeeping Characteristics

Source	Heave	Pitch	RBM	Acc.	Slam.	Wet.	Add.Res.
Vossers et al.(1961)	0	0	0				
Swaan (1961)	–	0					
Beukelman&Huijser (1977)	+	+	+	+	+	+	+
Schmitke&Murdey (1980)	–	–	–	–	–		
Robson (1987)	0	0	0	0			
Lloyd (1988)				0	–	–	

Table 9. Influence of forebody form on motions

Source	Heave	Pitch	RBM	Acc.	Add. Res.
Lewis (1955)	V	V	V	V	
Swaan & Vossers (1961)	V	V	U	V	U
Abkowitz et al.(1966)	V	V	V	V	
Ewing (1967)	V	0	V	V	
Moor (1970)	V	U	U	U	
Yourkov (1973)	V	V			
Beukelman & Huijser (1977)	V	0	V	V	0
St. Denis (1983)	V	V			
Athanassoulis&Loukakis (1985)	U	U	U	U	U

Lewis (1955) investigated the effect of forebody form on speed loss in regular and irregular head seas.

Swaan and Vosser (1961) tested six Series 60 models with same principal dimensions and displacement, but with different section form in the forebody and in prismatic coefficient.

Ewing (1967) made computations for four Series 60, 0.70 block coefficient form with different form of forebody which were similar but not identical to those experimentally investigated by Swaan and Vosser.

Moor (1970) tested a series of sixteen models derived from the form of a large twin screw ship with block coefficient 0.573, to investigate the influence of secondary hull form parameters (LCB, LCF, CWP and C_B) on motion and propulsive characteristics in waves.

Yourkov (1973) investigated the influence of forebody form on seakeeping characteristics of a cargo ship using a strip theory based computer program.

Athanassoulis and Loukakis (1985) investigated seakeeping characteristics of a destroyer hull form. Section forms of the parent hull and its four variants were represented with three parameter extended Lewis descriptions. The vertical centre of bouyancy of each hull form was varied independent from other parameters.

2.3 Influence of secondary form parameters.

In addition to LCB, C_{WP} and LCF we shall also consider the forward and aft water plane area coefficients C_{WPF} and C_{WPA}.

2.3.1 *Influence of LCB on seakeeping characteristics.*

Our observations are presented in Table 10.

Table 10. Influence of LCB on Seakeeping Characteristics

Source	Heave	Pitch	RBM	Acc.	Slam.	Wet.	Add.Res.
Ewing (1967)	aft	fwd	0	0			
Moor (1970)	aft	fwd	fwd	fwd			
Beukelman&Huijser (1977)	aft	aft	aft	aft	aft		
Bales (1980)	aft	aft	aft	aft			
St. Denis (1983)	fwd	fwd					
Wijngaarden (1984)	fwd	fwd	fwd	fwd			

In Table 10 'aft' and 'fwd' indicate a preference for moving the LCB as far aft or as far foreward as possible.

2.3.2 *Influence of LCF on seakeeping characteristics.*

Our observations are summarised in Table 11.

Table 11. Influence of LCF on Seakeeping Characteristics

Source	Heave	Pitch	RBM	Acc.	Slam.	Wet.	Add.Res.
Bales (1980)	fwd	fwd	fwd	fwd			
St. Denis (1983)	aft	aft					
Blok&Beukelman (1984)	fwd	fwd	fwd	fwd			fwd
Wijngaarden (1984)	aft	aft	aft	aft			

Here we need only note that:

Blok and Beukelman (1984) reported the results of a systematic subseries of high speed displacement ship models, with Robson (1987) carrying out the major investigation.

2.3.3 *Influence of C_{WP} on seakeeping characteristics.*

The influence of C_{WP} and the related C_{WPF} and C_{WPA} coefficients are summarised in Tables 12, 13 and 14 respectively.

Table 12. Influence of C_{WP} on Seakeeping Characteristics

Source	Heave	Pitch	RBM	Acc.	Slam.	Wet.	Add.Res.
Moor (1970)	+	0	0	0			
Schmitke&Murdey (1980)	+	+	+	+	+		
Blok&Beukelman (1984)	+	+	+	+			+
Wijngaarden (1984)	−	−	−	−			

Table 13. Influence of C_{WPF} on Seakeeping Characteristics

Source	Heave	Pitch	RBM	Acc.	Slam.	Wet.	Add.Res.
Schmitke&Murdey (1980)	+	+	+	+	+		
Bales (1980)	+	+	+	+			
Lloyd (1988)				+	+	+	

Table 14. Influence of C_{WPA} on Seakeeping Characteristics

Source	Heave	Pitch	RBM	Acc.	Slam.	Wet.	Add.Res.
Schmitke&Murdey (1980)	0	0	0	0	0		
Bales (1980)	+	+	+	+			

2.3.4 *Influence of C_M on seakeeping characteristics.*

This parameter has received very little attention, as shown in Table 15, as it is generally regarded as an unimportant parameter.

Table 15. Influence of C_M on Seakeeping Characteristics

Source	Heave	Pitch	RBM	Acc.	Slam.	Wet.	Add.Res.
Abkowitz et al.(1966)	0	0	0	0			
Lloyd (1988)				0	+	+	

2.3.5 *Influence of Inertia on seakeeping characteristics.*

The influence of mass distribution, as measured through the radius of gyration, on the seakeeping characteristices is summarized in Table 16.

Table 16. Influence of Radius of Gyration on Seakeeping Characteristics

Source	Heave	Pitch	RBM	Acc.	Slam.	Wet.	Add.Res.
Kent (1922)		–					
Lewis (1955)	0	–		–	–	–	
Newton (1960)						0	
Vossers&Swaan (1960)	–	–					–
Swaan&Rijken (1964)			–	+		–	–
Ewing (1967)	–	–	–	–			
Beukelman&Huijser (1977)	–	0	–	0	–	0	–

Additional information required can be summarised as:

Kent (1922) conducted experiments with three models at three different ballast conditions to provide low, medium and high radii of gyration.

Newton (1960) simply suggested that radius of gyration would not affect wetness characteristics to any extent.

2.4 Influence of above water form.

An important criterion of seakeeping performance is the probability of bow submergence and hence of shipping water on deck, particularly in head seas, since this greatly affects attainable speed and operational performance of the ship. Predicting the shipping of water involves the comparison of the relative bow motion with the available bow freeboard. Therefore, shipping water depends not only on the relative bow motion but on the above water form and section shapes. The designer must make every effort to ensure that the freeboard selected is adequate and bow section shapes are suitable. However, since the theoretical analyses available do not take into account the above water form this subject will not be discussed in any great detail. However we can reproduce a summary of the influence of different above water form characteristics on deck wetness, due to Lloyd et al (1986), see Table 17.

2.5 Summarising the data.

The information presented is very qualitative and whilst it appears to provide an appreciation of the sensitivities of seakeeping to ship size, dimensions and form it is not necessarily helpful in an actual design situation when quantitive data must be generated and assessed. In particular the designer requires to know which particular parameter changes are the most effective to remove a particular detrimental seakeeping characteristic. Also conflicts of requirement exist within the tables provided.

3. Assessment of Seakeeping Capability.

The seakeeping performance of a ship in a seaway is of major importance with regard to its overall operational effectiveness. The ability of a ship to accomplish its mission objectives successfully is determined by the complex interactions between the various ship subsystems and the ocean environment. In general terms, the fulfillment of mission objectives requires the efficient operation of all ship subsystems. However poor at-sea performance can prevent or degrade the effectiveness of the design when operations are undertaken in increasingly severe seas. Therefore, a comprehensive seakeeping performance assessment methodology must account for and properly weigh, and model these interactions.

Table 17. Literature survey on effects of above water form on deck wetness [based on Lloyd et al.(1986)]

SOURCE	Freeboard	Flare	Rake	Knuckle
Hovgaard(1889)			+	
Kent(1950)		+	+	
MacDonald and Telfer(1938)		+		
Edward and Todd(1939)	+	+		
Allan(1951)		+		
Saunders(1957)	+	−	−	
Abkowitz(1957)		+		
Newton(1960)	+	+		+
Tasaki(1960)		−		
Swaan and Vossers(1961)		+		
Van Sluijs and Gie(1972)		+		+
Lloyd(1983)	+	−	+	
Lloyd et al.1986)	+	0	+	0
O'Dea and Walden(1985)		+	+	0

In order to evaluate the seakeeping performance of a ship in an ocean environment, it is necessary to represent the environment in a meaningful way, to predict the responses of the ship to the seaway, and to quantify those variables which would affect the performance of potential missions of the ship. Here Figure 2 provides an overview of the various elements of seakeeping performance analysis.

3.1 Seakeeping criteria.

Knowledge of the sea environment and ship response alone is not sufficient to determine the mission success or the survivability of the ship. It is necessary to determine what magnitude of response will cause degradation of performance, or in the extreme, loss of the ship. The result of this evaluation is the determination of limiting response criteria which are mission dependent. The availability of clear statements on limiting response criteria for different ship type and missions is, unfortunately, very limited. Traditionally, such data has been acquired by ship

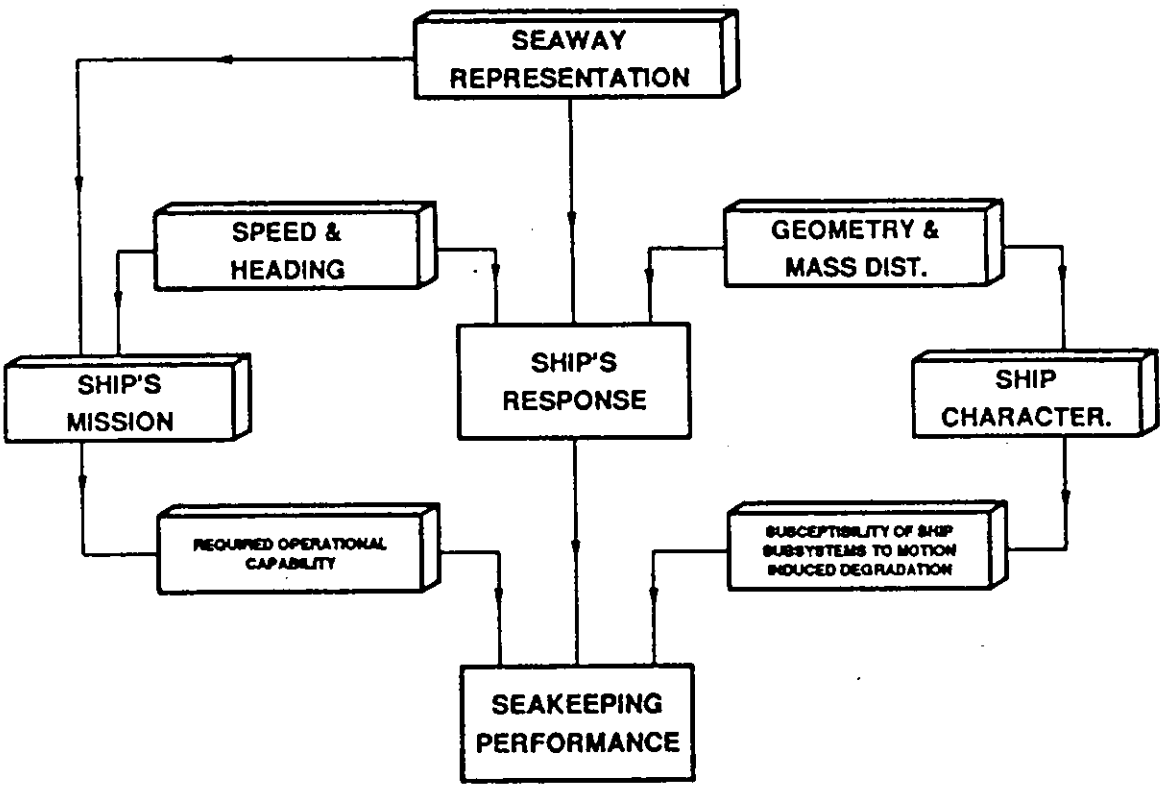

Figure 2. Overview of Seakeeping Performance Assessment.

operators through years of experience. This experience base is essential to the safe and successful operation of a particular ship. Ideally we would like to assess the ability of the ship to operate in different sea states, within the design process.

The selection of size, principal dimensions and ship form in the preliminary design stage will determine the ability of the vessel to operate in heavy weather. Thus a knowledge of the limiting factors and acceptable ways of identifying them in practice is required in the early stages of design to produce a seakindly vessel. The previous section identified some of the important ship hull form parameters and their influence upon seakeeping. Here we seek to identify possible seakeeping criteria for use in design.

Seakeeping criteria are essentially objective expressions of 'subjective' or perceived performance indicators which may be used to specify the preferred limits to be imposed on the responses of a vessel in heavy weather. Thus they should express the practical limits to be placed upon the vessel with respect to: structural response, motion magnitudes, crew and passenger comfort and cargo integrity. In short they are required to reflect the limitations imposed on the vessel by circumstances and the operators. Ideally, operators would like to accomplish their missions at the highest practical speeds possible in all weather conditions. Since this is not always possible, in practice, the criteria will have to reflect the mission of the ship and be ship type dependent. For example, a cargo liner's mission is to transport cargo between designated ports on a regular schedule, and good seakeeping performance is measured by on-time arrival even in stormy, winter weather. On the other hand, the mission of an aircraft carrier is to be able to station itself anywhere in the oceans of the world and launch and receive aircraft whenever required to do so. Hence, good seakeeping performance or operability can be judged by the ability of the ship to handle its aircraft in a specified sea condition. These examples show that different ships require different sets of criteria depending on their missions. This situation makes it far from easy to develop mathematical methods, that would provide a systematic basis for evaluation of the seakeeping performance of all types of ships in relation to their environment.

The methods which have been used to determine seakeeping criteria, for use in evaluating the seakeeping performance of a ship near the limits of its operability, are:

- Special seakeeping trials in which ships are driven as fast as their captain dares in rough seas, and the performance characteristics at the point the captain decides to reduce speed are taken to be critical responses.
- Prolonged seakeeping monitoring in which the maximum responses over a long period, including typical rough weather conditions, are taken to be the critical values, assuming that the captain will operate near the limits on occasions, but will never exceed them. This approach is suitable to merchant ships which cannot be spared for special trials, but it neglects the probability that special circumstances or severe weather may force the ship to exceed the normal limits of the captain.

- Questionnaires of ship operators, asking for the conditions which cause them to reduce speed or change heading, and taking a statistical average of their answers.

In an analogous fashion to the tabular presentation of Section 2 we now present different criteria distilled from the literature for different characteristics of ship behaviour.

3.1.1 *Slamming criteria.*

Slamming is the phenomenon that occurs when the bow of a ship emerges from the water and reenters with considerable impact, frequently causing a shudder throughout the ship. Kehoe(1973) defined a slam as occuring when the forefoot and the first 15 per cent of the keel aft of the bow emerges from the water and then re-enters with a vertical velocity relative to the water surface greater than a certain threshold value. This definition follows the work of Ochi (1964) who defined the critical re-entry velocity as $0.093(g/L)^{\frac{1}{2}}$, where L is the ship length. Another version of critical velocity, which takes into account the underwater hull shape was given by Conolly (1974) and may be expressed in the form

$$V_{cr} = 4.56\sqrt{\frac{gD}{k}}, \tag{1}$$

where $k = \pi^2(\cot\beta)^2/4$, D is draught and β is the deadrise angle of an equivalent wedge at the section $0.2L$ abaft of FP.

The information pertinent to slamming and available in the open literature is summarised in Table 18.

3.1.2 *Deck wetness.*

Deck wetness criteria can be expressed in terms of the number of times green seas break over the bow per hundred oscillations. Such definitions are attractive to the analyst because they can be calculated theoretically and hence used to assess the satisfaction of design requirements. The definition is not so clear in practice as water from one wetting may not have cleared before the next occurrence.

The different suggested upper bands for deck wetness are displayed in Table 19.

3.1.3 *Accelerations.*

Vertical and lateral accelerations are of major importance for ship habitability because of their strong association with the incidence of seasickness. Limits which have been proposed by various authors are summarized in Table 20.

Table 18 Limit criteria for slamming frequency

SHIP TYPE	Slamming Freq.	Location	Source
Cargo liner	6 per 100 pitches	bow	Aertssen(1968)
Cross-channel	5 per 100 pitches	bow	Aertssen(1968)
Large tanker	3 per 100 pitches	bow	Aertssen(1968)
Bulk carrier	3 per 100 pitches	bow	Aertssen(1968)
Trawler	6 per 100 pitches	bow	Aertssen(1968)
Merchant (M)	1 per 100 pitches	0.15L aft FP	Chrysosstimidis(1972)
Destroyer	60 per hour	0.15L aft FP	Kehoe(1973)
Merchant	3 per 100 pitches	0.15L aft FP	Ochi&Motter(1974)
Merchant	8 per 100 pitches	bow	Hoffmann(1976)
Merchant	4 per hour	bow	Hoffman(1976)
Naval (N)	3 per hour	bow	Olson (1978)
M & N	3 per 100 pitches	0.15L aft FP	Chilo&Sartori(1979)
Naval	20 per hour	0.15L aft FP	Bales&Cieslowski(1981)
Trawler	20 per hour	0.15L aft FP	Spouge(1985)

For mortals, such as myself, acceleration is all too readily appreciated through our state of health in rough seas. However, in order to provide a better seakeeping criteria for vertical and lateral accelerations, several estimators have been developed. Thus the concept of Motion Sickness Indicator(MSI) was developed in a study sponsored by the U.S. Navy in 1976 to investigate the effect on humans of motions in an 'at-sea' environment. The work attempted to quantify the incidence of actual vomiting (emesis) of individuals subjected to vertical sinusoidal motion. The MSI value indicates the percent of subjects that experienced emesis in a two-hour test period.

The original concept of subjective motion magnitude, SMM, was proposed by **Schoenberger (1975)** who subjected a number of USAF pilots to vertical sinusoidal motions at a given reference frequency (1.0 Hz) and amplitude (± 0.46g). This particular motion was assigned an SMM value of 10.0. The pilots were then

Table 19 Deck Wetness Frequency Criteria

SHIP TYPE	Deck Wetness Frequency	Source
Merchant	10 per hour	Lewis(1967)
Cargo liner	5 per 100 pitches	Aertssen(1968)
Ore carrier	5 per 100 pitches	Aertssen(1968)
Cargo ship	5-7 per 100 pitches	Ferdinande(1969)
Naval	60 per hour	Kehoe(1973)
Naval	1 every 110 sec.	Conolly(1974)
Merchant	5 per 100 pitches	Landsburg et al(1976)
Naval	30 per hour	Olson(1978)
Merchant&Naval	7 per 100 pitches	Chilo&Sartori(1979)
Naval	30 per hour	Bales&Cieslowski(1981)
Naval	30 per hour	Andrew &Lloyd(1981)
Trawler	36 per hour	Spouge(1985)

subjected to motions at other frequencies and amplitudes and asked to quantify their severity relative to the reference motion. Thus, for example, if a particular motion seemed twice as uncomfortable as the reference motion it was to be assigned an SMM value of 20.0.

The empirical relationship

$$\mathrm{SMM} = A\left[\frac{\bar{s}}{g}\right]^{1.43} \tag{2}$$

was derived from Schoenberger's results, where $A = 30 + 13.53(\ln f)^2$, $\bar{s}$ is the amplitude of vertical acceleration in m/sec^2, g is the acceleration due to gravity ($9.81 m/sec^2$), and f is the frequency in Hz.

These results apply only to sinusoidal motions and in order to apply them to the random motions occuring on the ship it would be necessary to assume, say, that

$$\bar{s} = 2\sqrt{m_4} \tag{3}$$

Table 20 Vertical Acceleration Criteria

SHIP TYPE	Limit Vertical Acc.	Location	Source
Merchant	$\Pr\{amp. > 0.4g\} < 0.04$	Working areas	Lewis(1955)
Cargo liner	0.45g sig. amp.	Bow	Aertssen(1968)
Cross-Channel	0.5g sig. amp.	Bow	Aertssen(1968)
Merchant(125m)	0.55g sig. amp.	Bow	Aertssen(1968)
Merchant(190m)	0.35g sig. amp.	Bow	Aertssen(1968)
Merchant(260m)	0.25g sig. amp.	Bow	Aertssen(1968)
Large Tanker	0.25g sig. amp.	Bow	Aertssen(1968)
Ore Carrier	0.25g sig. amp.	Bow	Aertssen(1968)
Trawler	0.7g sig. amp.	Bow	Aertssen(1968)
Merchant	average $1/10 < 1.0$	Cargo spaces	Chryssostomidis(1972)
Merchant-full load	$\Pr\{amp. > 0.4g\} < 0.07$	Bow	Ochi&Motter(1974)
Merchant-ballast	$\Pr\{amp. > 0.4g\} < 0.03$	Bow	Ochi&Motter(1974)
Merchant	0.5g max.	Bow	Landsburg et al(1976)
Merchant	0.5g max.	Bow	Hoffman(1976)
Merchant	0.4g sig. amp.	Bow	Ferdinande(1978)
Merchant&Naval	0.4g sig. amp.	FP	Chilo&Sartori(1979)
Naval	0.2g rms amp.	Bridge	Comstock et al(1980)
Naval	0.2g rms amp.	Bridge	Andrews&Lloyd(1980)
Naval	0.4g sig. amp.	Bridge	Bales&Cieslowski(1981)

and

$$f = \frac{1}{2\pi}\sqrt{\frac{m_6}{m_4}}, \tag{4}$$

where m_4 and m_6 are the variances of the vertical acceleration and rate of change of vertical acceleration respectively. Thus $\bar{s}$ is equated to the significant vertical acceleration and f to the average zero crossing frequency of the acceleration.

3.2 Summarising the data.

The foregoing sections indicate a number of different facts. The seakeeping criteria for a given mission, if they exist, will certainly impose limits on the design. However criteria in themselves do not assist the designer to provide a hull form which meets its mission requirements. At best they indicate constraints to keep the behaviour of the vessel within preferred bands of operability for a wide range of sea states. Quantifying human responses to vessel response is not trivial, especially if it is to be used as a design constraint. We next turn our attention to seakeeping for design methodologies in which our appreciation of seakeeping parameter dependence will be used, with or without criteria, to provide better alternative designs.

4. Seakeeping For Design Methodologies.

In this section three distinct approaches are considered. A fourth and obvious approach is the development of regression equations from model test results. This only remains a practical tool if the data base is continuously updated and the regression analyses reworked to reflect dependencies on all parameters considered important at the time of use. An early example of this approach is provided by Moor and Murdey (1968).

In particular, they presented the results of experiments in waves of 34 models of practical ship designs in the form of regression equations of significant pitch and heave and mean power increase in irregular head waves as a function of different hull form parameters and speed. The models covered a wide range of single screw ocean going cargo liners and tankers with block coefficients 0.55 to 0.88.

4.1 Seakeeping tables.

A different approach in seakeeping for design is to make use of extensive systematic computer calculations of the responses of the hull forms for a particular ship type for a wide range of characteristics. Bales and Cummins (1970) claimed to have developed a computational design tool to predict the trends in seakeeping variables with changes in hull geometry. The methodology discussed in the paper was said to consist of a hull form generator, a mathematical model to calculate ship motions in a specified sea environment, and a response surface representation of the trends in hull form geometry. In the case of cargo ship they assumed a simplified hull form series could be specified using seven defining hull form parameters, including length, beam, draught, waterplane area coefficient, and nominal values of sectional

area coefficient at the forward and aft perpendiculars. The profile was assumed to be rectangular. The waterlines consist of a parallel midship segment, together with fourth degree polynomial descriptions of the fore and aft bodies. Actual section forms were replaced by 'Lewis' forms having the same breadth, draught and sectional area. All calculations were carried out for head seas with a constant radius of gyration for all forms. In order to compare the seakeeping performance of different hull forms a seakeeping efficiency criterion was used. This took into account heave, pitch, relative motion and absolute acceleration. The latter two responses were considered at a location ten percent of ship length abaft the forward perpendicular.

Loukakis and Chryssostomidis (1975) calculated ship responses for a set of Series 60 hull forms and presented the results in the form of seakeeping tables as a function of the ship speed, geometry and sea state. Selected ship responses include: heave and pitch motions, relative motion, velocity and accelerations at selected locations along the ship length, bending moment amidships, and added resistance in waves. In addition, slamming, deck wetness, keel emergence and propeller racing information were included in tables. The tables presented are for seventy two hull forms based on eight values of block coefficient. The responses for long crested head seas were calculated using a strip theory based computer program. Lewis form representation of the ship sections was used for the calculation of added mass and damping forces. The results obtained through interpolation of seakeeping tables were compared with theoretical predictions and experimental measurements and generally a good agreement was obtained.

Comparisons are presented by Loukakis and Chryssostomidis (1975) of responses obtained by interpolation from their tables and results for the six specific hulls given by Bales and Cummins (1970). Agreement is excellent for heave, pitch, and accelerations. Relative motion is slightly overpredicted in high seas in some cases, but differences are within acceptable limits.

Chryssostomidis (1972) proposed a design procedure whereby any number of alternative designs can be explored and their seakeeping performances evaluated. It involves the following steps for each design:

- determine power requirements in different sea states as a function of speed,

- estimate attainable speed in different sea states, considering effects of motions on vertical accelerations, shipping water and slamming, with certain specified acceptable limits,
- determine average speed for the distribution of sea states expected in service, considering both the above power and motion limits on speed,
- calculate voyage fuel consumption from the above powers and speeds,
- estimate costs and hence probability of the alternative designs.

In the first two steps the seakeeping tables of Loukakis and Chryssostomidis (1975) are intended to be used with a one-parameter spectrum. No examples of application in a design context are given. St.Denis' discussion makes interesting reading.

Hearn et al (1990 & 1991b) suggested the use of design charts (rather than tables) to indicate the sensitivity of an initial design to systematic changes in hull form parameters. Initially (1990) only secondary hull form parameters were considered. Then both principal ship dimensions and secondary parameters were investigated (1991). This is discussed in Section 5.

4.2 Ranking of seakeeping.

Bales (1980) developed an analytical model relating ship underwater hull geometry to an index of seakeeping merit and quantified it using 20 existing destroyer-type hull forms scaled to 4300 metric ton displacement. Eight seakeeping responses were selected to represent the most essential measures of seakeeping performance. These responses were: heave, pitch, ship-to-wave relative motions at stations 0 and 20, slamming at station 3, absolute vertical acceleration at station 0, heave acceleration and absolute vertical motion at station 20. To establish a comparative measure of seakeeping performance in head waves, a seakeeping rank, R, was defined as the unweighted summation of selected responses averaged over five modal wave periods per significant wave height and five Froude numbers. To facilitate comparison, numerical values of the seakeeping rank, R, were normalized within the database population. According to this normalized scale, the R values ranged from 1 to 10, representing the worst and the best performing hulls, respectively.

To develop an early stage design tool, Bales further postulated that the R value of a given hull design may be closely approximated by an equation of six hull form parameters that are readily available in the early stages of design development.

These six parameters were chosen on the basis of insight gained from an earlier analytical investigation of the seakeeping systematic series of Bales and Cummins (1970). These parameters, as a group, provided three basic set of descriptors for the waterplane, the profile, and the sectional fullness of the fore and aft bodies. Such an approximated value of R was defined by $\hat{R}$. Selected hull form parameters are listed, in order of their impact on $\hat{R}$, as follows:

- Waterplane coefficient forward of amidships, C_{WPF}
- Draught-to-length ratio, T/L
- Vertical prismatic coefficient forward of amidships, C_{VPF}
- Vertical prismatic coefficient aft of amidships, C_{VPA}
- Waterplane coefficient aft of amidships, C_{WPA}
- Cut-up ratio, c/L, where c is the distance from the forward perpendicular to the cut-up point.

By applying a linear regression analysis to the six hull form parameters and to the R value of each hull in the database, an equation for $\hat{R}$ was derived in the form

$$\begin{aligned} R =& 8.422 + 45.104C_{WPF} + 10.078C_{WPA} - 378.465(T/L) \\ &+1.273(c/L) - 23.501C_{VPF} - 15.875C_{VPA}. \end{aligned} \tag{5}$$

This equation could indeed very closely reproduce values of the seakeeping rank, R, for all ships in the database. However, its validity is subject to certain limitations, such as type of hull and range of hull form parameters of the database. Furthermore, the ranking is based on ship responses in head seas only. Nevertheless, within these limitations the equation may be exploited to find a seakeeping optimised hull form. Bales produced such a hull form by adopting appropriate form parameters to maximize the $\hat{R}$ value within the bounds of the database. This hull form was designated Hull 21 and extensive theoretical calculations and experimental analyses were performed to predict its seakeeping performance. The results indicated that Hull 21 had superior seakeeping performance characteristics compared with similar ships of 'ordinary' design. The results of resistance experiments also indicated that Hull 21 had a considerably higher level of resistance in the higher speed range compared with similar 'ordinary' designs.

Later Walden (1983), using a similar methodology, added a term to the seakeeping rank equation expressing the effect of displacement. That is, the term $a_7(\Delta - 4300)/4300$ was to be added to Equation (5). However, a_7 was not specified.

From the numerical values for the coefficients of the seakeeping rank given by Bales and the applicable range of permissible values for the hull form parameters, it can be concluded from Equation (5) that superior seakeeping performance requires C_{WPF} and C_{WPA} to be as large as possible, whereas the parameters $T/L, C_{VPF}$ and C_{VPA} are to be as small as possible within the permissible ranges of values. The effect of c/L was found to be minor.

On the basis of Walden's extension it can be concluded that doubling the displacement results in approximately doubling the value of R.

Wijngaarden (1984), using a procedure similar to Bales', developed a regression equation to predict the seakeeping performance of a systematic series of 17 small ship forms derived from a research vessel form. The alternative forms were generated through variation of the main dimensions, prismatic coefficient, and longitudinal position of the centre of bouyancy while the displacement was kept fixed. Heave, pitch, absolute vertical acceleration, and relative bow motion were calculated using a ITTC fetch limited spectrum for 6 mean wave periods and one significant wave height (of 1.9 m.) in head seas for a speed value corresponding to F_n=0.30. These responses were weighted with the probabilities of occurrence of the wave periods. A seakeeping index, R_n, for each hull was obtained. By applying a regression analysis to the seakeeping indices, a seakeeping rank in terms of six hull form parameteres was obtained as follows:

$$\begin{aligned} R_n = & -11.624 + 111.409C_p^4 + 5.042LCB - 20.064C_{WP} - 3.236(L/B) \\ & + 1.743(L/T) - 5.663LCF. \end{aligned} \tag{6}$$

Thus Wijngaarden uses quite different parameters to Bales with a nonlinear dependence of R_n on C_p. He concludes that, for constant displacement, ship seakeeping responses are mainly influenced by C_p and LCB.

McCreight (1983) extended the original Bales data base to include 45 different hull forms with displacements of 4300, 5800, 7300 and 8800 t. In addition to considering several alternative definitions of R, he carried out a stepwise regression analysis on the resulting 180 hull form data base using 73 hull form parameters

and combination of parameters. From this he determined that the significant parameters for seakeeping performance are expressed in the ranking equation

$$\begin{aligned} R =& a_0 + a_1 BM_L \Delta + a_2 C_{VPF} + a_3 C_{VPA} + a_4 BM_L/(BL^3) + a_5 L + a_6 T/B \\ &+ a_7 A_{WA}/\Delta^{2/3} + a_8 (LCF - LCB)\Delta + a_9 LCB/\Delta^{1/3} + a_{10} L^2/(BT). \end{aligned} \tag{7}$$

It is clear from the above summary of different ranking approaches that different researchers have proposed different form parameters as the principal independent variables affecting seakeeping performance. For instance McCreight's seakeeping rank includes 10 form parameters only two of which are the same as Bales' rank. Similarly, Wijngaarden's rank has 6 parameters, only one of which is the same as Bales' rank and none belongs to the McCreight rank.

4.3 Optimization of hull forms for seakeeping.

The first attempt at developing a seakeeping optimisation method is due to Bales (1980). Bales used motion data for 20 existing destroyer type hull forms, and linear regression analysis techniques to correlate averaged seakeeping performance (in head seas at various speeds) to certain selected hull form parameters. He then used the resulting optimum combination of these parameters and conventional lines drawing methods to design an 'optimum' seakeeping hull form.

Grigoropoulos and Loukakis (1988) developed a computer based methodology for developing hull forms with optimised seakeeping performance. To investigate the validity of the methodology, the hull form of a reefer vessel was selected and defined by a family of four curves, namely, the sectional area curve, the waterplane curves, the longitudinal profile curve, and the longitudinal distribution curve of the centroids of ship sections. Since the methodology was developed to be used in the preliminary design stage, main dimensions and displacement were kept constant and section forms were obtained using a three parameter 'extended Lewis' form representation. To obtain variant hull forms from the parent hull, the linear transformation method of Lackenby (1950) was used. To reduce the required computer time, only the peak values of the response curves were compared.

In their optimization problem the objective function was really a ranking function, insofar as they used a weighted sum of the peak values of a prescribed set of ship responses in regular waves. This problem was solved using a Hooke and Jeeves' algorithm. To verify the results, models of the parent and the optimum hull were built and tested in regular waves. Theoretical and experimental results were compared and it was concluded that, although both hulls have similar resistance characteristics, the optimum hull had a significantly improved seakeeping performance.

Hearn et al (1991a & 1992) have developed a radically different optimisation procedure based upon addressing particular responses. They do not use either the ranking concept or a criteria based approach. This is discussed in greater detail in Sections 5.5 to 5.8.

Lloyd (1991) developed a computer aided design tool which automatically creates a destroyer type hull form to achieve a specified seakeeping performance. To avoid 'over-optimisation', the objective function of the optimisation process is defined that a hull form which has the closest match between the given probabilistic criteria and their corresponding target values. The optimal values of the specified hull form parameters are obtained by searching a database consisting of regression equations for each response in terms of the selected form parameters. Having determined the optimal form parameters, the optimal lines plan is obtained by using polynomial representation. In reality it is analogous to a ranking based optimisation approach.

4.4 Summarising the results.

Personally, I do not find ranking techniques very attractive since the single index summarises a great deal of information. Radically different hulls could produce the same ranking. It is also not clear how exactly differences of ranking are to be interpreted in a quantitative sense. Having looked at the underlying philosophy of other researchers' design methodologies we now look at two alternative procedures developed at Newcastle University.

5. Two Particular Practical Seakeeping Design Tools.

The tools to be described have evolved as a result of step by step investigation of the choices regarding:

- facilitating seakeeping analysis in the design office
- systematic hull form generation

- alternative methods of executing seakeeping analysis
- development of design charts
- development of 'inverse analysis' based optimisation techniques.

In this section the development will be outlined and examples of application provided.

5.1. Seakeeping analysis for design office use.

To appreciate the sensitivity of a particular design to hull form changes requires the use of appropriate software or a lot of tank time. Taking the former option, we usually have to get involved in the formulation and solution of appropriate Fredholm integral equations and the associated process of discretisation which involves the detailed specification and processing of appropriate waterline and offset data.

Hearn et al (1988) presented a fully automated seakeeping analysis which untook all the data processing necessary to invoke the hidden mathematical analysis, whilst allowing the designer to specify the data where it was most convenient for him/her. The software matched the 'design office' reference system to the mathematical reference system by generating spline based representations of the hull form defined. This software provided the designer with the ability to very rapidly assess the effects of design changes on motion responses without having to be reasonable expert at the associated hydrodynamics and marine dynamics. However such designer friendly software simply leads to 'black box' use of the analysis, with no guidance on the generation of alternative hull forms capable of exhibiting better seakeeping characteristics. That is, the enhanced software simply transformed the problem of 'how to undertake seakeeping analysis' into one 'of knowing how best to use the analysis'. Something radically different was required.

5.2. Systematic hull form generation.

To provide a hull form which meets the specified requirements the designer should, ideally, investigate the sensitivity of his initial design or basis ship to changes in some of the parameters identified in Section 2. To appreciate 'cause' and 'effect' regarding changes in the parameters, one requires the generation of a systematic series of hull forms in which the differences between alternative hulls are generated on the basis of controlled changes of one parameter, subject to all others remaining invariant. Also to ensure that the predicted trends in performance with hull form

parameters are representative, the variations in the selected parameters must be as large as possible while keeping within practical limits.

Once a series of alternative hull forms has been generated the software of Hearn et al. (1988) based on the earlier work of Salvesen et al (1970) and Hearn and Donati (1981) can be used in the manner indicated in Figure 3.

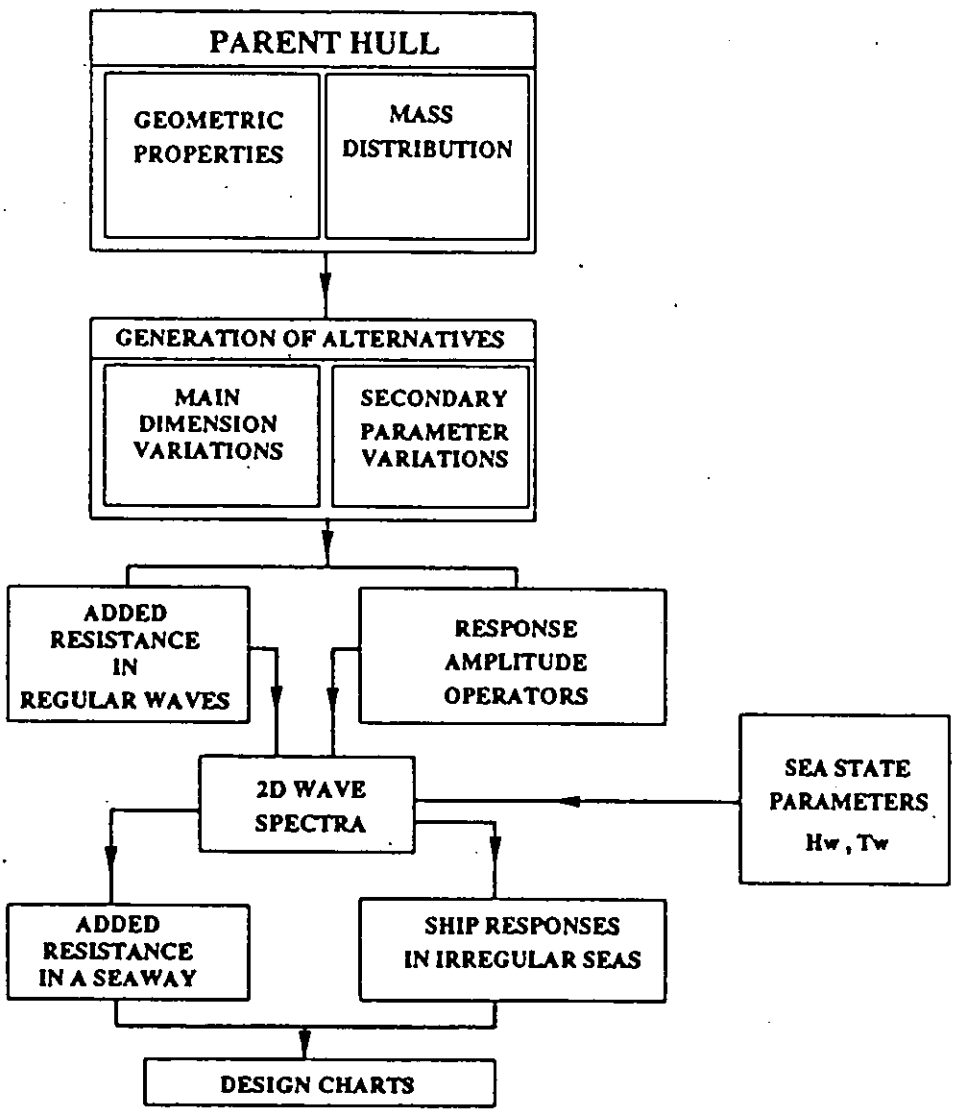

Figure 3. Forward Analysis Approach in Design for Seakeeping.

To modify the principal parameters of length, beam, or draught, the hull offsets may simply be multiplied by corresponding constant expansion or contraction factors. This does not affect the secondary parameters, i.e. C_B,C_M,C_P,C_{WP},LCB,

and LCF. However, this variation will alter the displacement. In order to change length, for fixed B/T and displacement, the midship section area is altered in an inverse ratio to the length. The block coefficient and all secondary form parameters will then remain unchanged. The new main dimensions for a change of L are:

$$L' = (1 + \delta L)L, \quad B' = \frac{B}{\sqrt{1 + \delta L}}, \quad \text{and} \quad T' = \frac{T}{\sqrt{1 + \delta L}}. \tag{8}$$

Since B'/B and T'/T are equal and L'/L is designer specified, the waterlines and offsets of corresponding stations can be found using standard naval architectural procedures.

With L fixed and B/T changing by a factor of $1 + \delta x$, say, the changes in B and T now correspond to

$$B' = B\sqrt{1 + \delta x} \quad \text{and} \quad T'\frac{T}{\sqrt{1 + \delta x}}. \tag{9}$$

The corresponding changes in offsets and waterlines are undertaken in the usual manner.

The details related to generation of the hull form for secondary parameter variation can be based upon

- linear distortion of sectional area and beam curves combined with conformal mapping techniques.
- linear distortion of sectional area and beam curves combined with linear distortion of waterlines.
- Moor's (1970) linear distortion method.

In the first two procedures the linear distortion could be undertaken using the well known 'one-minus prismatic' method. However there are two major disadvantages with such an approach

- for a given change in fullness the longitudinal distribution of the displacement added (or removed) cannot be controlled, and
- there is no control over the extent of the parallel middle body in the derived forms.

To overcome such disadvantages the Lackenby (1950) method can be employed so that

- C_{WP} can be varied subject to LCB and LCF remaining unchanged
- LCB may be changed subject to other two parameters remaining unchanged
- LCF may be changed subject to other two parameters remaining unchanged

given displacement (and hence C_B) are to remain invariant in general. Details of the transformation techniques implemented, courtesy of Kadir Sarıöz, are provided in Appendix A.

The conformal mapping can be undertaken using either Lewis section definitions or the Landweber-Macagno approach. Related details of conformal mapping transformation techniques are provided in Appendix B.

Moor indicated how new sections can be generated from a given parent form using a section shape factor corresponding the ratio of sectional area and half beam.

With details of the different transformation procedures adopted outlined we now consider in greater detail the generation of the alternative hull forms and hence their use. The distinct steps are now identified.

- Define initial design or basis ship using either offset data or simple sets of design curves based on sectional area curve, design waterline curve and profile. In latter case transverse sections are automatically generated using well known two or three parameter conformal mapping transformations (see Appendix B).
- Next choose parameters to be modified and the limits of their modification.
- Generate alternative forms automatically, together with the geometric data files if direct standard 'forward' use of the seakeeping analysis is to be undertaken.

In Figure 4 the standard 24 alternative hull forms for variation in L and B/T are presented for a trawler. Each alternative hull is generated from the parent hull located in the centre of the figure. Thus the bottom left corner corsponds to a 'short - fat' ship and the bottom right corner corresponds to a 'long - thin' ship relative to the parent hull.

In Figure 5 similar alternative hull forms are developed for changes in LCF and

LCB in the vertical and horizontal directions respectively, with the C_{WP} corresponding to that for the parent hull. For each increase or decrease in C_{WP} a corresponding set of 25 ship sections is generated.

For the specific transverse sections presented in Figure 5 a Lewis transformation was used in their generation. In this particular example a range of LCF and LCB variations of $\pm 2\%$ relative to the parent hull is possible without infringement of the mathematical transformation limitations.

In Figure 6 the corresponding sections generated using Moor's method are presented. In this case variations are limited to $\pm 1\%$ before the procedure breaks down. Whilst the Moor transformation produces more ship like forms, compared with the Lewis transformation, it limits the scope of the parametric studies.

Here moving LCF forward and LCB abaft leads to fine V - shaped forebody sections (see lower right corner of Figures 5 & 6). Shifting LCB forward and LCF abaft leads to fuller U - shaped forebody sections (see upper left corner of figures).

5.3 Alternative methods of executing seakeeping analysis.

With the original and alternative ship form sections defined, appropriate hydrodynamic analyses may be undertaken explicitly or implicitly. By explicit we mean the Lewis transformation is used to reassign the solutions of corresponding problems for a circular cylinder, based on Ursell (1949) multipole analyses, to each actual section. The obvious explicit method is use of numerical solvers based on the Frank (1967) Close - fit approach. Given many of the sections will be analysed time and time again the hydrodynamic coefficients (pure and coupled) might be calculated once and stored. That is, a large number of possible ship transverse sections, assumed to be described by their Lewis tranformation parameters (see Table 21) are generated, and each is then analysed explicitly using the Frank Close-fit approach. At Newcastle cubic spline surfaces have been fitted so that for any section generated subsequently the hydrodynamic coefficients (pure and cross coupling) can be determined through interpolation of the appropriate spline surface. In earlier publications we have described the stored information as Grim diagrams, as he suggested a corresponding graphical approach for pure heave coefficients in the early 1950s, see Grim (1953). A presentation of typical Grim diagrams used to define a spline surface is illustrated in Figure 7. The availability of the Grim surfaces means that hydrodynamic - motion analysis task

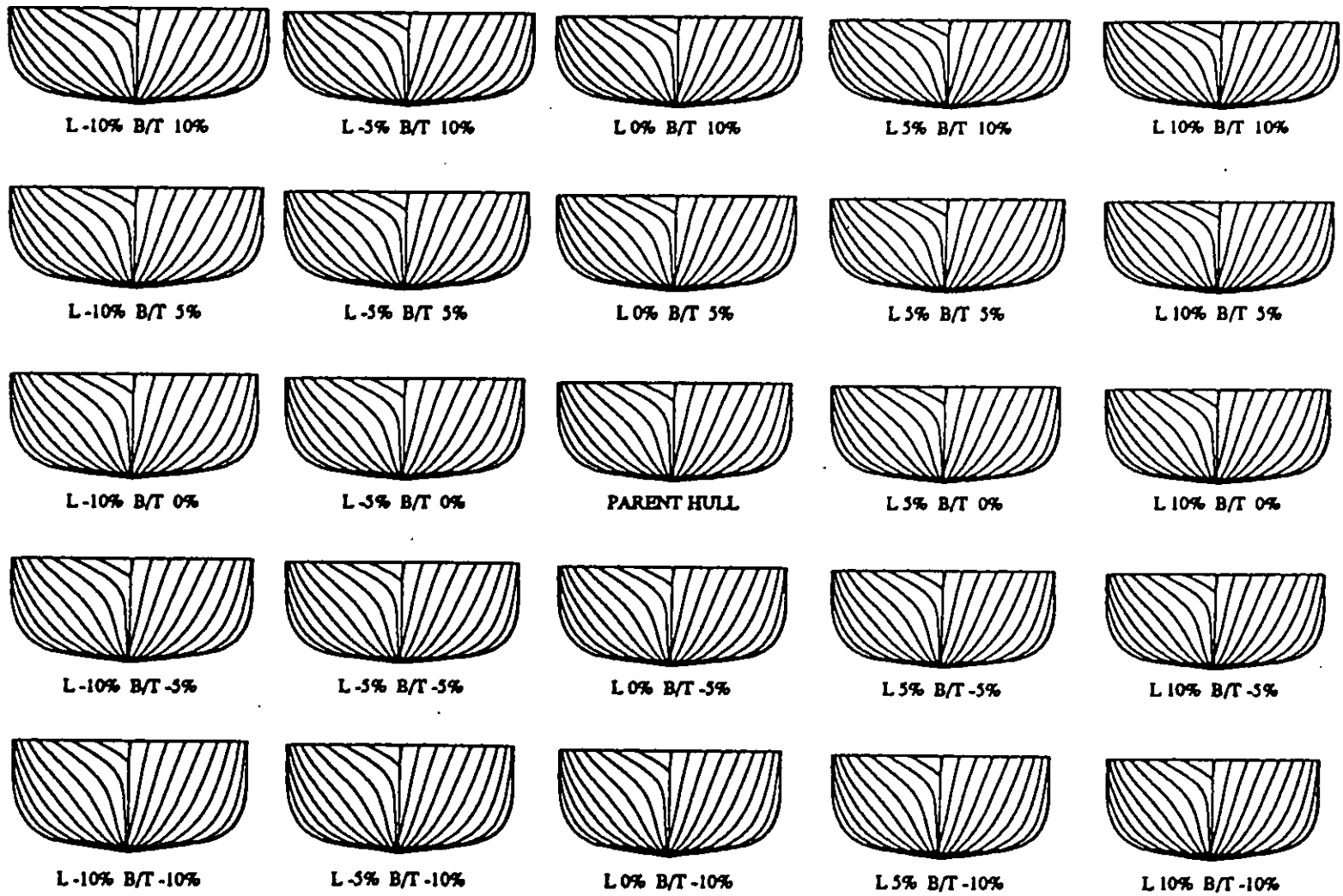

Figure 4. Main Dimension Variations for Trawler.

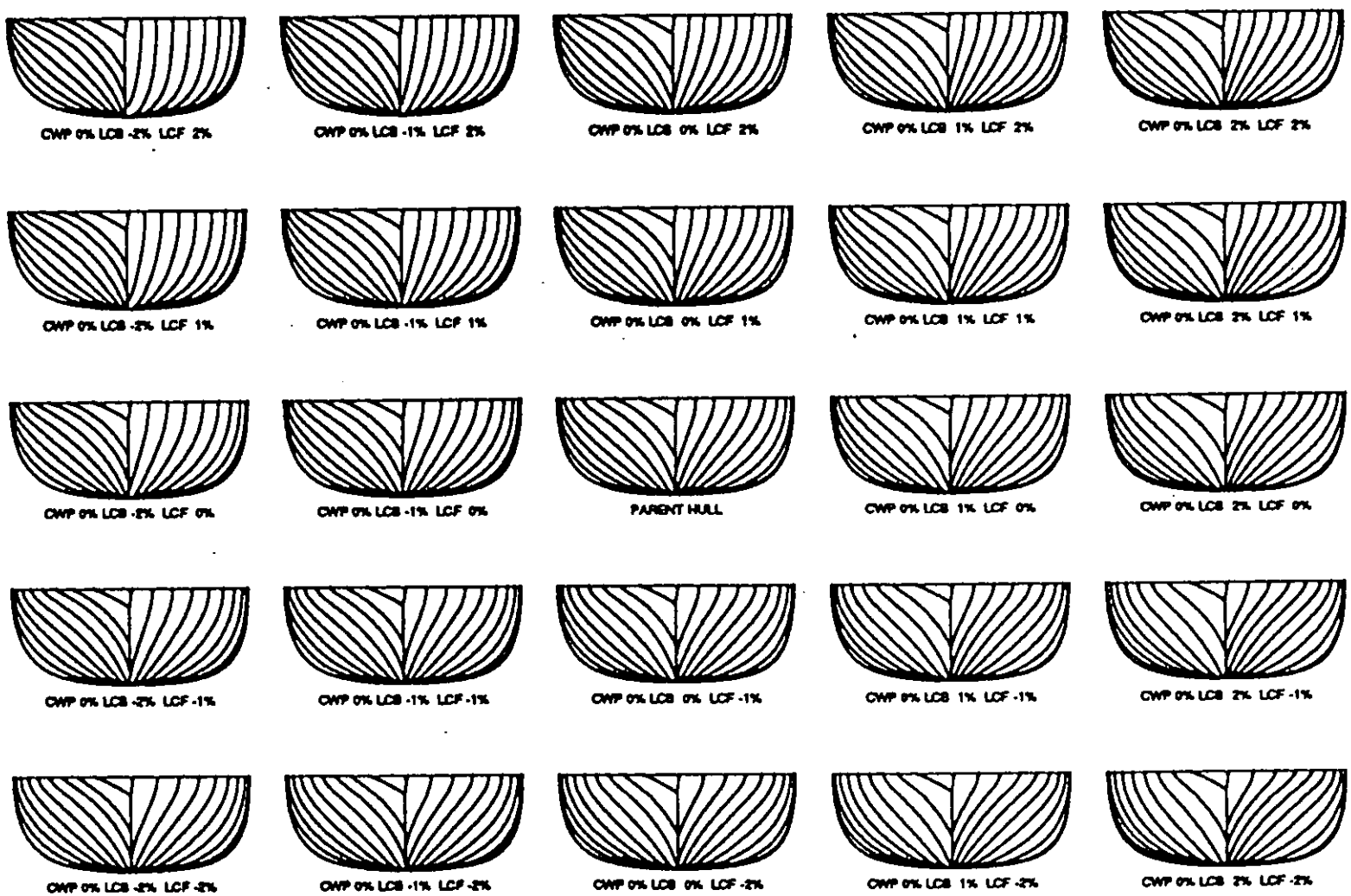

Figure 5. Secondary Parameter Variations for Trawler.

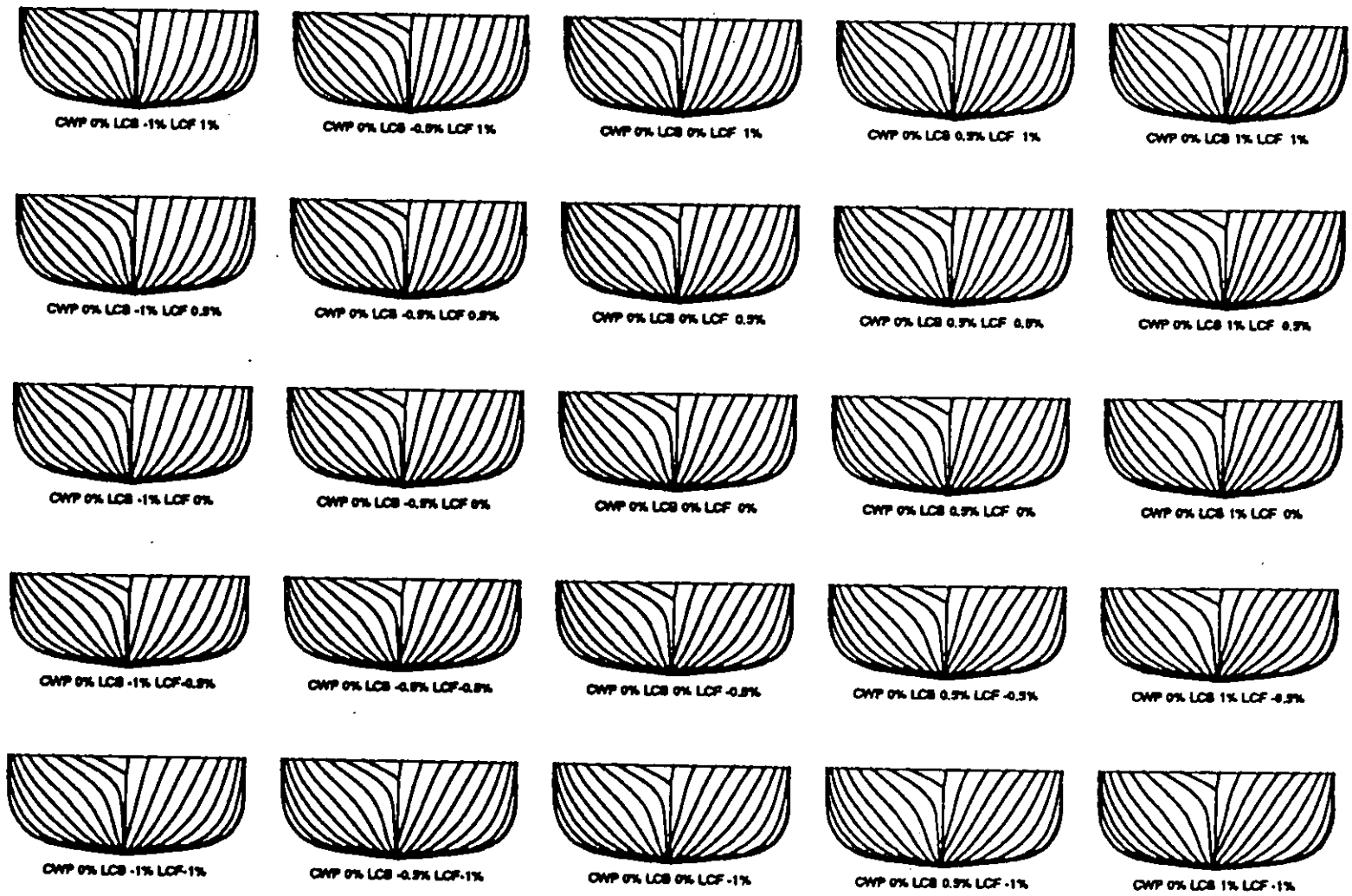

Figure 6. Secondary Parameter Variations for Trawler by Moor's Method.

is reduced to interpolation of hydrodynamic data and direct motion response calculations. This facilitates very rapid analysis of the many alternative ship forms to be considered in a design study. Typically, allowing for primary and secondary parameter variations a minimum of a 100 alternatives will be analysed.

Table 21. Range of Parameters for Lewis Sections.

Parameter	Lower Limit	Upper Limit
Area Coefficient ($S/2BT$)	0.5	1.0
Beam/Draught (B/T)	0.4	4.4
Nondimensional frequency ($\frac{\omega^2 B}{2g}$)	0.0	1.6

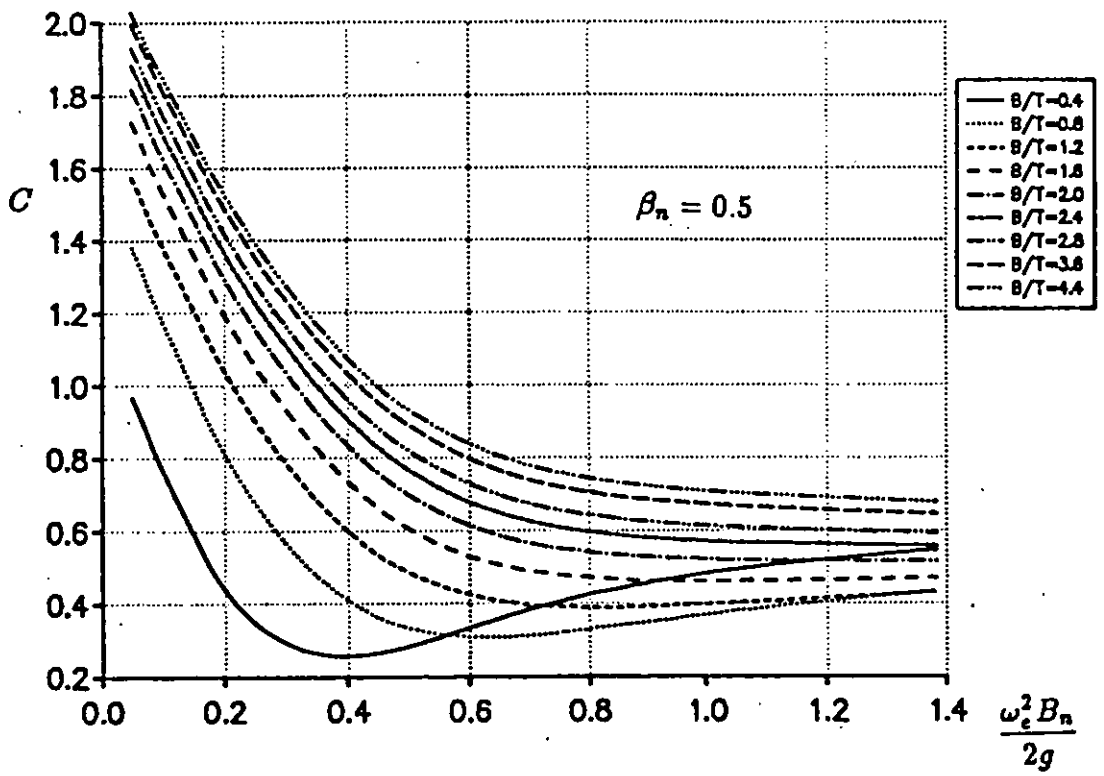

Figure 7. Typical Grim Diagram for Heave Added Mass.

5.4 Development of design charts.

Through direct analysis of the series of alternative hulls generated and selection of appropriate sea spectra the root mean square, rms, values of different responses or response related quantities can be determined. Thereafter the changes in the

rms levels, relative to rms levels of the parent hull, can be plotted in a three dimensional parameter space to provide indicators of which changes in hull form parameters or dimensions leads to detrimental and beneficial effects. For the trawler of Section 5.3, variations of heave rms for sea-state 6 (H_s equal to 5.0m and T_m of 12.4s.) are shown in Figure 8 for primary parameter changes. Figure 9 provides the corresponding secondary parameter design chart for trawler heave.

This sort of presentation provides information similar to the general observations presented in the tables of Section 2 for different geometric variations. But in this case the information is both qualitative and quantitative and is specific to the vessel under consideration in the design process for specific sea-states. The process is readily applied to any other vessel type, see Hearn et al (1990 & 1991b) for sensitivity studies undertaken for trawlers, destroyers and cargo ships.

Rather than consider a fixed number of discrete changes in the various geometric parameters continous variations could be imposed and the consequences investigated. However, the volume of output (graphical and otherwise) would be overwhelming. On the other hand if all the results were available within the computer, searches for an optimal form might be considered. This naturally leads to the idea of formulating an optimisation approach.

5.5. Formulation of the Optimisation Procedure.

Under the assumption that motion responses are linear, or at least can be linearized, and are harmonic the equations of motion for the advancing ship in regular waves may be written in the general form

$$L_{kj}(H,\omega,V)\eta_j = F_k \; ; \quad k = 1,2,...,6. \tag{10}$$

The operator L_{kj} is of the form

$$L_{kj} = -(M_{kj} + A_{kj})\omega^2 + iB_{kj}\omega + C_{kj}, \tag{11}$$

where M is the generalised structural mass matrix, A and B represent the added mass and fluid damping matrices associated with the forces induced in the kth mode, as a consequence of motion in the jth mode, and C is the hydrostatic restoring force matrix. In Equation (10) H represents the hull geometry and the degrees of freedom, k, corresponds to surge, sway, heave, roll, pitch, and yaw as k assumes the value 1 to 6 respectively. The above formulation is general, but for conceptual design strip-theory rather than full 3D analysis will be employed.

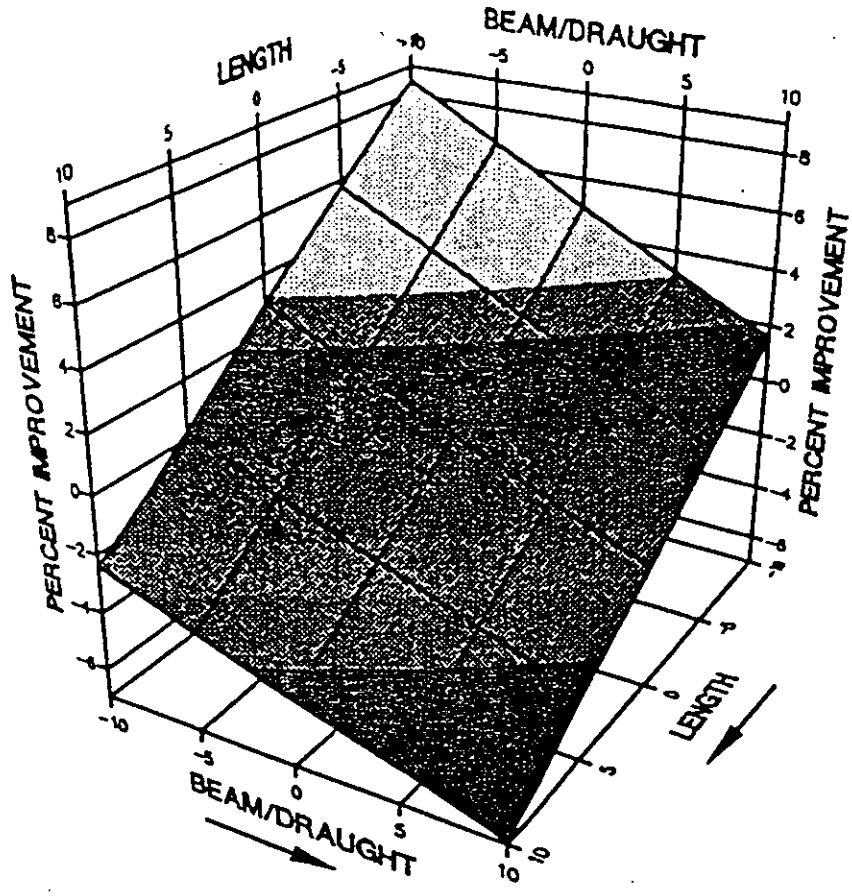

Figure 8. Typical Main Dimension Design Chart for Heave.

In this case the effects of forward speed are present only in the cross-coupling coefficients and we may write

$$\begin{aligned} A_{kj} &= A^0_{kj} + A^V_{kj} \\ B_{kj} &= B^0_{kj} + B^V_{kj}, \end{aligned} \tag{12}$$

where the superscript V indicates a forward speed correction. The strip theory approach enables us to evaluate the speed independent part of total added mass and damping coefficients in terms of the zero speed sectional hydrodynamic coefficients, thus for example

$$A^0_{35} = \int_L a_{33} x dx \tag{13}$$

and

$$A^V_{35} = -\frac{V}{\omega_e^2} B^0_{33}.$$

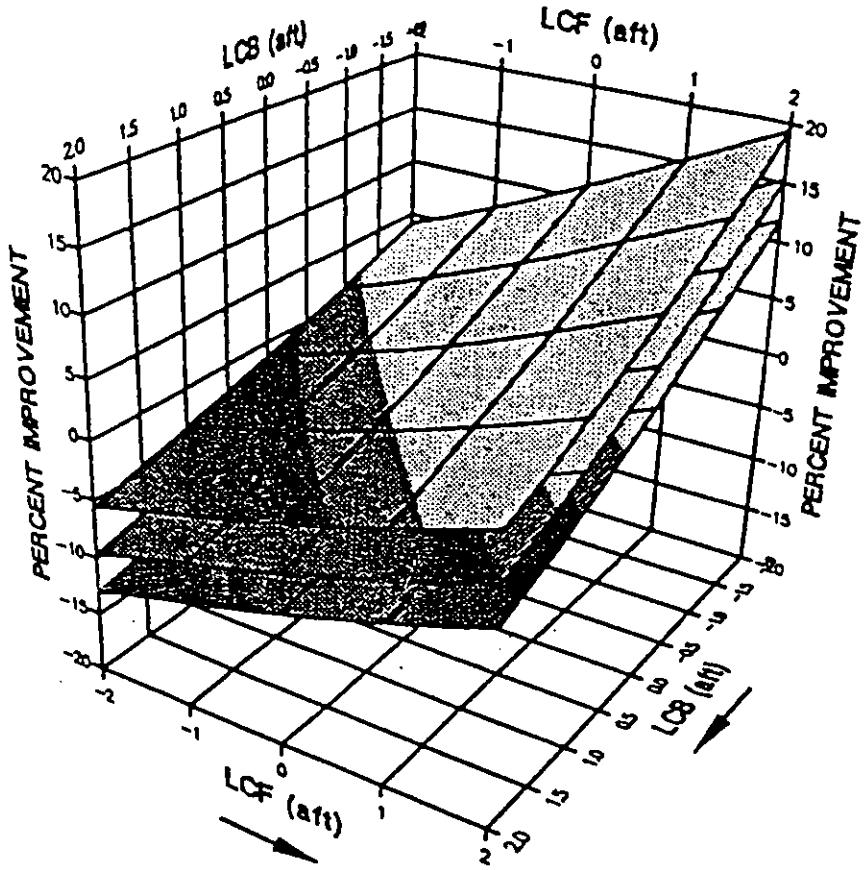

Figure 9. Typical Secondary Parameter Design Chart for Heave.

Therefore the problem can be reduced to the calculation of two dimensional hydrodynamic coefficients for a limited number of transverse sections. If the hull surface is assumed to be represented by $y = f(x, z)$, for the Frank Close-Fit approach we may consider

$$\begin{aligned} A_{kj} &= A^0_{kj}\{f(x,z),\omega\} + A^V_{kj}\{\omega, V\} \\ B_{kj} &= B^0_{kj}\{f(x,z),\omega\} + B^V_{kj}\{\omega, V\}, \end{aligned} \tag{14}$$

where ω is the wave frequency and V is the forward speed. The hydrostatic restoring force coefficients, which are independent of wave frequency and forward speed are then viewed as

$$C_{kj} = C_{kj}\{f(x,z)\}. \tag{15}$$

The exciting force and moments can be expressed in terms of hull surface coordinates, wave frequency, speed and heading and so

$$F_k = F_k\{f(x,z), \omega, V, \beta\}. \tag{16}$$

Therefore, the linearized matrix for equations of motion become

$$\{-\omega^2(M + A_{kj}) + C_{kj} + i\omega B_{kj}\}\eta_j = F_k \tag{17}$$

or,

$$\{M_{kj} + iN_{kj}\}\eta_j = F_k. \tag{18}$$

If D represents the determinant of the complex matrix M, N and D_{kj} represent the kj^{th} minor of D, then the complex displacement η_k is given by

$$\begin{aligned} \eta_j &= \frac{1}{D}\sum_{k=1}^{6} D_{kj} \cdot F_k \\ &= \{T_k + iU_k\} \cdot F_k, \text{ say.} \end{aligned} \tag{19}$$

Hence the amplitude of the motion is

$$\eta_j = \{T_j^2 + U_j^2\}^{1/2} \tag{20}$$

and the phase lag is

$$\epsilon_j = \arctan(\frac{U_j}{T_j}). \tag{21}$$

The resulting motions, η_j, are thus a function of hull form, the forward speed, and the wave properties ω and β, that is

$$\eta_j = \eta_j\{f(x,z), \omega, V, \beta\}. \tag{22}$$

The corresponding response spectrum is given by

$$\begin{aligned} &S_{\eta_j}\{f(x,z), \omega, V, \beta \mid H_s, T_m\} = \\ &S_w\{\omega \mid H_s, T_m\} \cdot \mid \eta_j\{f(x,z), \omega, V, \beta\} \mid^2 . \end{aligned} \tag{23}$$

and the variance, or rms value of the jth response is thus

$$rms_j = \sqrt{\int_0^\infty S_{\eta_j} d\omega}. \tag{24}$$

The seakeeping responses of a vessel can be viewed as a function of the hull surface coordinates. Hence, potentially, each point on the hull surface is a design variable to be varied during an optimisation procedure to obtain an optimised hull surface equation.

As ship motions do not appear to be sensitive to very localised sectional details of hull shape, the actual section shape through the 'Lewis section' concept can be seen as a function of beam, draught, and area. Thus, the total added mass and damping forces can be viewed as

$$\begin{aligned} A_{kj} &= A^0_{kj}\{b(x), T(x), S(x)\} + A^V_{kj}\{\omega, V\} \\ B_{kj} &= B^0_{kj}\{b(x), T(x), S(x)\} + B^V_{kj}\{\omega, V\}. \end{aligned} \tag{25}$$

The hydrostatic restoring force coefficients can be viewed as

$$C_{kj} = C_{kj}\{b(x), T(x), S(x)\}, \tag{26}$$

where $b(x), T(x)$, and $S(x)$ are the beam, draught, and cross-sectional area respectively at the station located at x. In strip theory the exciting forces and moments can be expressed in terms of sectional added mass and damping coefficients and so

$$F_k = F_k\{b(x), T(x), S(x), \omega, V, \beta\}. \tag{27}$$

Therefore, the linearized equations of motion can be viewed as

$$\eta_j = \eta_j\{b(x), T(x), S(x), \omega, V, \beta\}, \tag{28}$$

and in this case the response spectrum functional dependencies are expressed as

$$\begin{aligned} &S_{\eta_j}\{b(x), T(x), S(x), \omega, V, \beta \mid H_s, T_m\} = \\ &S_w\{\omega \mid H_s, T_m\} \cdot \mid \eta_j\{b(x), T(x), S(x), \omega, V, \beta\} \mid^2 . \end{aligned} \tag{29}$$

Rather than treat sectional beam, $b(x)$, sectional draught, $T(x)$, and sectional area, $S(x)$, as the fundamental independent variables we can use the hull form generation procedures of Section 5.4 to develop complete alternative hulls, and then search for those changes in $L, B/T, LCF, LCB$ and C_{WP} , say, that will lead to an optimal hull form. In this case rather than restrain parameter variations to the discrete increments of the design chart approach, we may now search continously the designer specified parameter space to seek out the optimal form.

5.6 Solution of Optimisation Problem.

Having derived an analytical form of the response of a ship to an irregular seaway as a function of its underwater form, the formal formulation and solution of the

optimization problem can now be considered. The problem can be formalised as requiring to 'Minimization of the objective function $f(x)$, subject to constraints expressed by inequalities $g_i(x) > 0, \ : i = 1, 2, ..., N$.'

In practice an equality constraint, such as $A \cdot x = B$, can be converted into the two inequality constraints $A \cdot x > B$ and $A \cdot x < B$.

In our problem, $f(x)$ is the user selected seakeeping related response quantity such as the maxima of a selected RAO or a complex seakeeping operability index, and x is the vector representation of the design variables defining the hull surface or hull form characteristics. Both geometrical constraints and practical design constraints about the hull form are included in $g_i(x)$. For the purpose of the numerical treatment of these constraints, one can apply an internal penalty function technique, which transforms the problem into a unconstrained optimization problem in which the objective function is expressed in the form

$$F(x, r_k) = f(x) + r_k \sum_{i=1}^{N} \{\frac{1}{g_i(x)}\} \quad : \quad r_k > 0. \tag{30}$$

The optimisation problem outlined is amenable to solution by nonlinear programming techniques and the Hooke and Jeeves' (1961) direct search method has been found to work well for the problem under discussion.

The structure of an optimisation problem consists of the following system descriptors, namely the

- Optimisation (design) variables
- Geometric and functional constraints, and the
- Object function

Various choices of optimisation (design) variables and the problems of the different approaches have been discussed by Hearn et al. (1991a).

In our now standard formulation linear distortion of the sectional area curve can be achieved by maintaining constant displacement and block coefficient without extra geometric constraints. Therefore 10 geometric bounds on the design variables are sufficient to restrict the procedure.

The specific constraints used in the Newcastle software are:

$$L_{min} \leq L \leq L_{max} \tag{31}$$

$$(B/T)_{min} \leq B/T \leq (B/T)_{max} \tag{32}$$

$$LCB_{min} \leq LCB = \frac{\int_0^L S(x)xdx}{\int_0^L S(x)dx} \leq LCB_{max} \tag{33}$$

$$C_{WP_{min}} \leq C_{WP} = \frac{1}{LB}\int_0^L b(x)dx \leq C_{WPmax} \tag{34}$$

$$LCF_{min} \leq LCF = \frac{\int_0^L b(x)xdx}{\int_0^L b(x)dx} \leq LCF_{max} \tag{35}$$

An optimal solution can be found if a measure of merit function is defined. Such a function is called an object function.

Provided the designer wishes to minimise a specific seakeeping response, an obvious choice for the object function is the mean variance of the response for a selected spectrum and associated characterisation. To reduce computational effort the peak value, rather than the mean rms value of the RAO of the selected response may be used as the object function. It is assumed that an alternate design with a reduced peak RAO will also have a reduced rms value. This assumption has been shown to be valid for most practical situations. This selection will significantly reduce computational effort since calculation of the rms value for each variant may require the calculation to be repeated for up to, say 20, wave frequency values.

A different object function for minimisation is the Bales (1980) seakeeping rank expressed as

$$R = \sum_{i=1}^{n} \omega_i R_i. \tag{36}$$

Here the designer supplies a set of response weights, ω_i, $i = 1$ to n, for each of the n responses included in the object function. The assignment of weights is a value of judgement, which the designer must make on the basis of the mission requirements which he is attempting to satisfy.

Since the sea conditions prevailing at any instant of time in the future cannot be predicted exactly, they have to be approximated using probabilistic methods. Similarly, the response of the ship will be probabilistic in nature. This suggests use of the joint probability of different seakeeping events as a multi-objective function in the search for an optimal hull form. Such an objective function may be written as

$$\Pr\{R_1 > c_1 \cup R_2 > c_2 \cup ...R_n > c_n\}, \tag{37}$$

where R_i is the ith seakeeping response and c_i is the corresponding criterion limit or specified limit for this response. This procedure requires knowledge of an applicable set of seakeeping criteria.

Yet another alternative object function is the Lloyd's (1991) criteria-based seakeeping multi-objective function in which the objective of the search process is to minimize the sum of the squares expressed as

$$\epsilon = \sum_{i=1}^{n} \Big(\Pr\{R_i - c_i\} \Big)^2. \tag{38}$$

The application of all three forms of object function were considered by Sarıöz et al. (1992) in the optimisation analysis of a container ship.

5.7 The Newcastle Implemented Optimisation Procedure.

The structure of the inverse analysis procedure is illustrated in Figure 10. The procedure consists of a data unit, a hull form generator, an optimizer, a seakeeping theory module, and a data base for added-mass and fluid-damping coefficients. A number of prerequisites, all of which can easily be obtained in the early stages of design, have to be prepared in advance. The most important is the information related to the geometry of parent hull. For hydrodynamic applications, only the portion of the hull from the design waterline on down is required. Given only a waterline curve, the keel line, and a sectional area curve as initial input, a unique Lewis form hull can easily be generated using the technique described earlier. The Lewis forms generally provide fairly good first approximations to the ship sections. An exception occurs for those ships with very large bulbs.

During the optimisation process a large number of variant forms which are geometrically derived from a parent hull are generated. Since the mass distribution is not one of the optimisation variables, these alternative 'ships' are assumed to

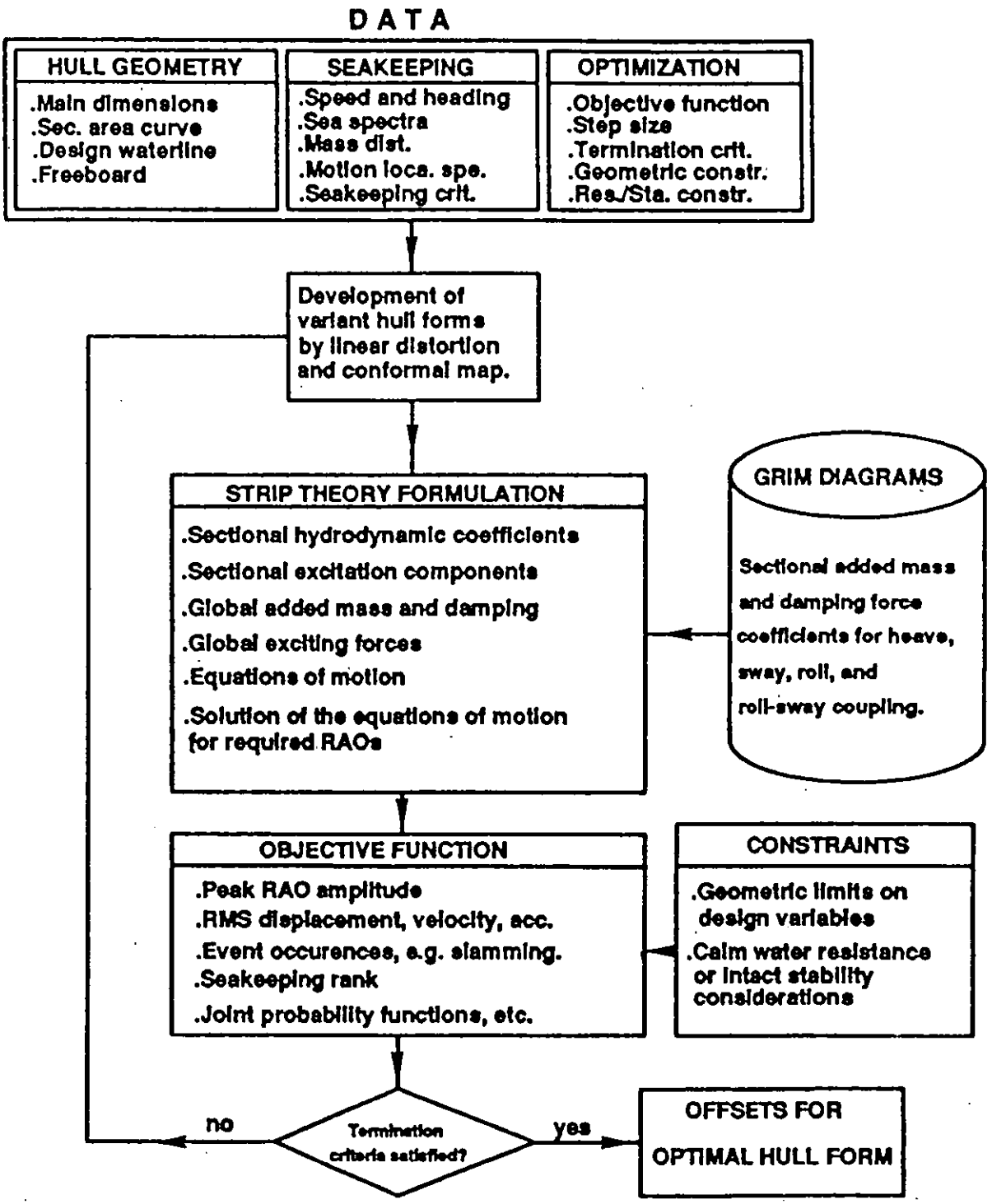

Figure 10. Structure of Inverse Analysis Procedure.

have similar mass distribution characteristics which can be represented by the coordinates of the centre of gravity and the radii of gyration.

The second group data includes selection of an appropriate spectral formulation, with required significant wave height and modal period values to represent a given sea-state, and an objective function. A variety of options exist regarding the objective function to be optimized and these are provided in a menu, as shown in Figure 11. The choices range from peak heave RAO to complex multi-objective formulations.

In the search for an optimal combination of the specified hull form parameters an important activity is to be able to generate alternative forms to the parent hull which vary in one parameter only. Thereafter, the optimizer provided has an inbuilt ability to judge the relative positive/negative influence of each parameter using any one of the different hull generation procedures described.

5.8 Some Typical Applications.

The optimisation procedure described in the previous sections have been applied to a wide range of ship types including: trawlers, cargo vessels, destroyers, and small patrol vessels. To illustrate the process the trawler form, used with the forward analysis procedure of Section 5.4, is reinvestigated. The most intriguing question to be explored is whether or not the optimisation methodology just outlined can lead to appreciable seakeeping improvements in a heavily constrained case.

Example 1

For the initial example, we will consider a redesign of the parent trawler form to produce a minimal peak heave RAO. The main dimensions and form parameters of this form are given in Table 22. In the redesign the dimensions and displacement of the parent hull are assumed to be fixed. Its form parameters will be allowed to vary over limited ranges, encompassing their original values, as follows:

$$\begin{aligned} 0.730 &< C_{WP} < 0.776 \\ 0.466 &< LCB < 0.506 \\ 0.439 &< LCF < 0.479. \end{aligned} \tag{39}$$

These limits correspond to ±2% for LCB and LCF, and ±3% for C_{WP} which are the geometric limits commented upon earlier.

```
****************************************
****************************************
***                                  ***
***     O B J E C T I V E            ***
***                                  ***
****************************************
****************************************

  1. PEAK AMPLITUDE OF HEAVE RAO
  2. PEAK AMPLITUDE OF PITCH RAO
  3. PEAK AMPLITUDE OF VERTICAL ACCELERATION RAO
  4. PEAK AMPLITUDE OF RELATIVE MOTION RAO
  5. RMS HEAVE
  6. RMS PITCH
  7. RMS VERTICAL ACCELERATION
  8. RMS RELATIVE MOTION
  9. PROBABILITY OF SLAMMING
 10. PROBABILITY OF DECK WETNESS
 11. PEAK AMPLITUDE OF ADDED WAVE RES. RAO
 12. USER SPECIFIED WEIGHTED SUMMATION
 13. JOINT PROBABILITY FUNCTION
 14. ERROR SUM

****************************************
****************************************
***                                  ***
***     C O N S T R A I N T S        ***
***                                  ***
****************************************
****************************************

 0. NO CONSTRAINTS OTHER THAN IMO
    STABILITY REQUIREMENTS
 1. INTACT STABILITY - AREA UNDER GZ
    CURVE NOT LESS THAN THE PARENT
 2. SMOOTH WATER RESISTANCE
    LESS OR EQUAL TO PARENT
 3. (1) AND (2) BOTH APPLIED
```

Figure 11. A Typical Menu for Selecting Object Function and Constraints.

The redesigned version of the trawler, designated OPT1, has a more V shaped forebody as shown in Figure 12. It is seen from Table 22 that OPT1 has the same main dimensions as the parent hull, however the *LCB* and *LCF* have the aftmost and foremost positions allowed within the limits specified. Similarly the waterplane area coefficient has increased by 3% to assume the upper limit specified.

Example 2

In this case only the main dimensions are allowed to vary. Thus the displacement and the secondary form parameters are kept constant. In this case L and B/T are to be constrained according to

$$54.864 < L < 67.056$$

$$2.183 < B/T < 2.668. \tag{40}$$

The final optimal form, designated OPT2, has similar section shapes and the same breadth as the parent hull, but the length and draught have the maximum and minimum values allowed within the respective specified limits. This form is shown in Figure 13 and the main dimensions and form parameters are given in Table 22.

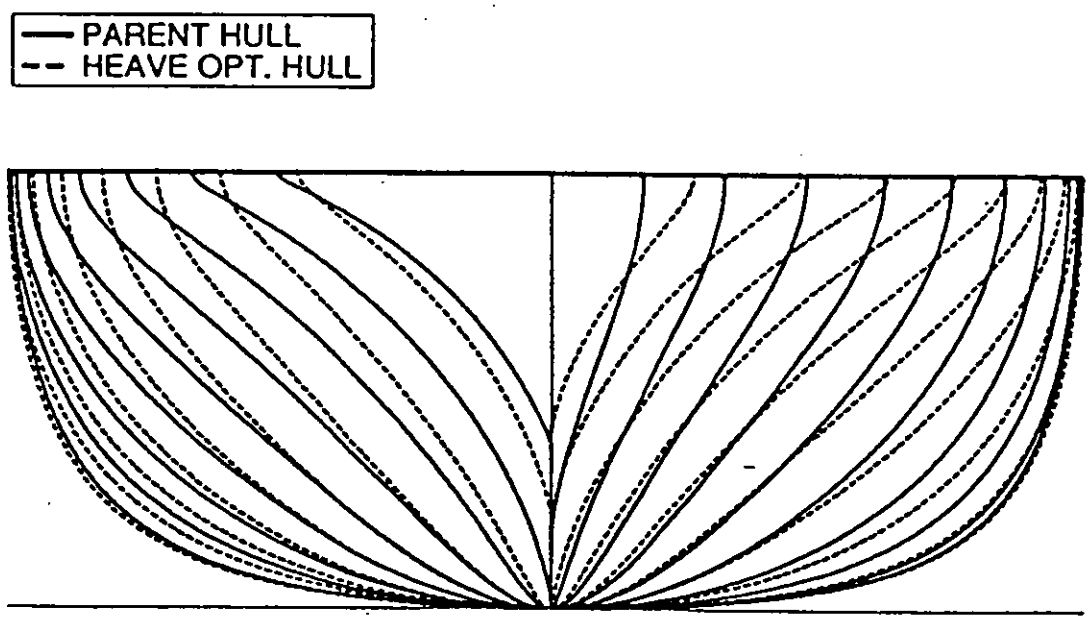

Figure 12. Comparison of Parent Trawler and Secondary Parameter Optimised Hull Forms.

Example 3

Finally both the main dimensions and the secondary form parameters are allowed to vary subject to C_B and displacement being kept constant. The optimal form, OPT3, as shown in Figure 14 combines the best features of OPT1 and OPT2. Table 22 presents the details of the example. Inspection of this table indicates that best values are attained for all parameters.

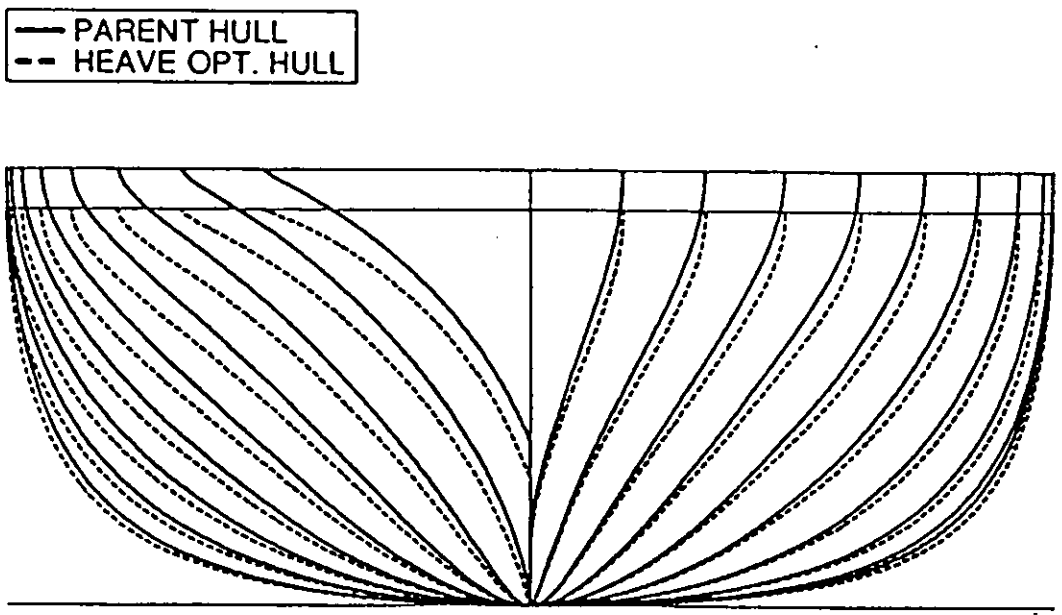

Figure 13. Comparison of Parent Trawler and Primary Parameter Optimised Hull Forms.

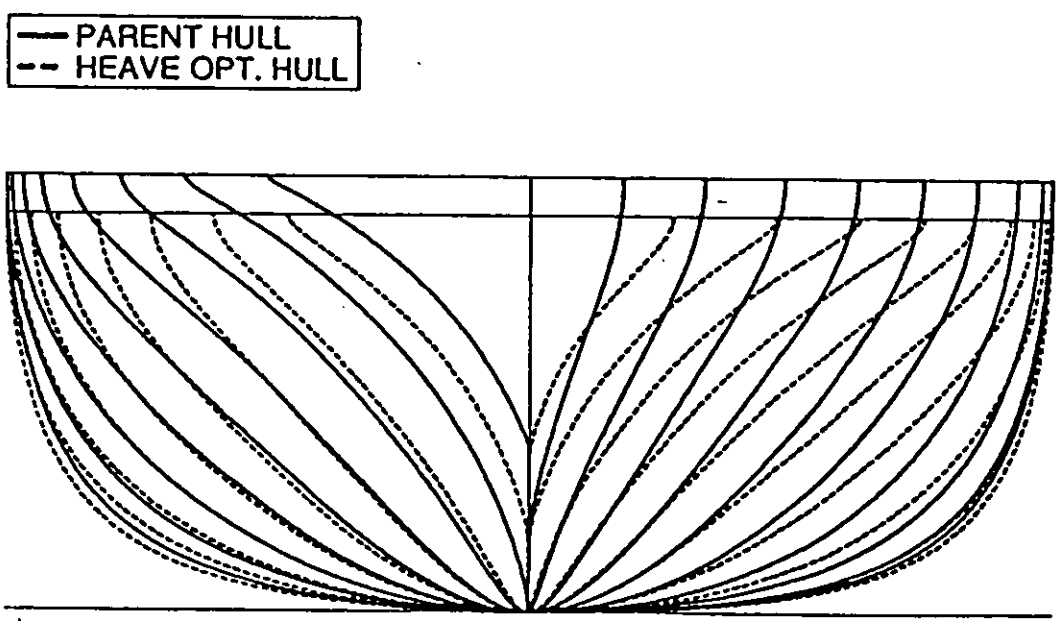

Figure 14. Comparison of Parent Trawler and Global Optimised Hull Form.

Table 22. Form Characteristics of Parent and Optimal Trawler Forms

PARAMETER	PARENT HULL	OPT1	OPT2	OPT3
$L[m]$	60.960	60.960	67.056	67.056
$B[m]$	12.200	12.200	12.200	12.200
$T[m]$	5.030	5.030	4.574	4.574
$LCB\%L$	0.486	0.466	0.486	0.466
$LCF\%L$	0.459	0.479	0.459	0.479
C_{WP}	0.753	0.776	0.753	0.776

Further examination of the optimised hull forms

To check the validity of the foregoing optimization results, seakeeping responses of the optimal forms are compared with those predicted for the parent hull. In Figures 15 to 26 comparisons of heave, pitch, vertical acceleration, relative motion, added resistance, deck wetness probability and slamming probability are presented. Excepting minor differences at the small wave lengths, each of the OPT1, OPT2 and OPT3 hull forms provide heave responses which are superior to those of the parent trawler form, see Figure 15. Furthermore, it is seen that secondary parameter optimization provides improvements equally significant to the primary parameter optimization. The corresponding pitch RAOs (for the heave optimized forms) shown in Figure 16 indicate that whereas the main dimension and global optimized forms have better pitch behaviour than the parent hull, the secondary parameter optimization are worse for this response. The vertical acceleration, relative motion, and added resistance RAOs presented in Figures 17, 18 and 19 show similar trends. That is the secondary parameter optimization consistently and significantly reduces the peak response amplitude while the main dimension based optimization shifts the frequency of resonance at the peak RAO value.

In order to provide more realistic comparisons, the different RAOs are combined with a standard ITTC spectrum to obtain statistical seakeeping response characteristics in an irregular seaway. These comparisons appear in Figures 20 to 26.

The rms pitch, acceleration, relative motion and added resistance responses presented in Figures 21 to 24 confirm the trends indicated by the RAO comparisons of Figures 16 to 19. Apart from the pitch response, the improvements obtained

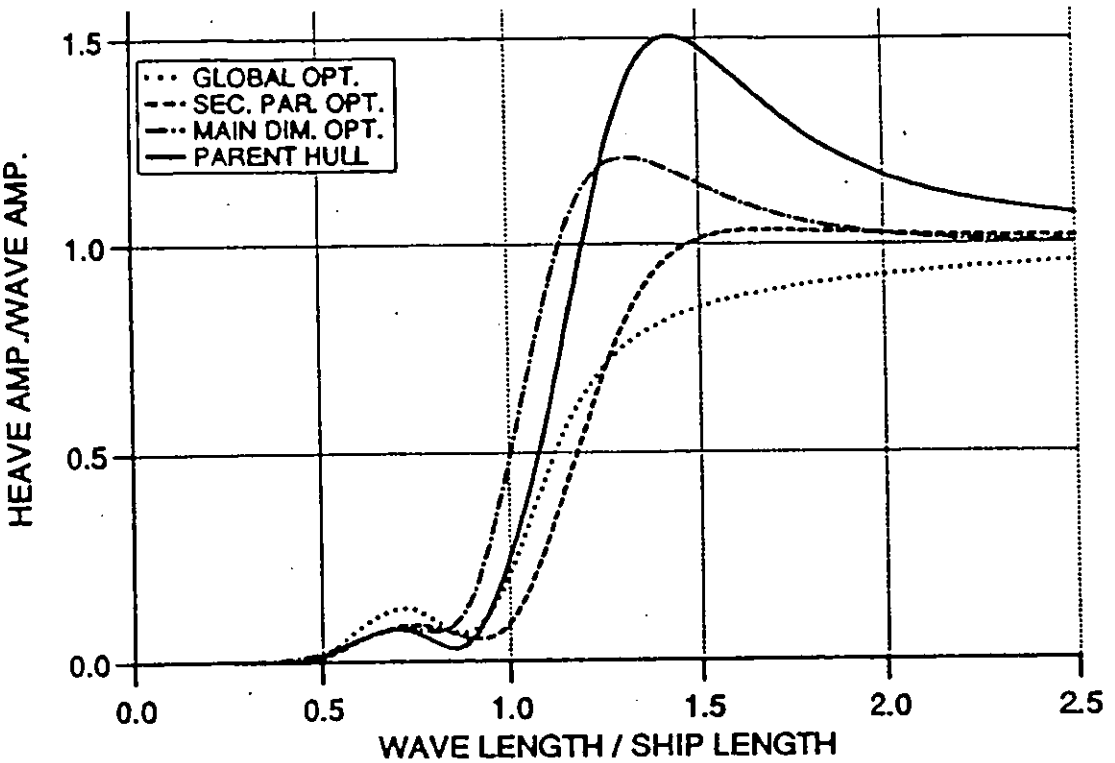

Figure 15. Heave Comparison of Parent Trawler and Heave Optimised Alternatives.

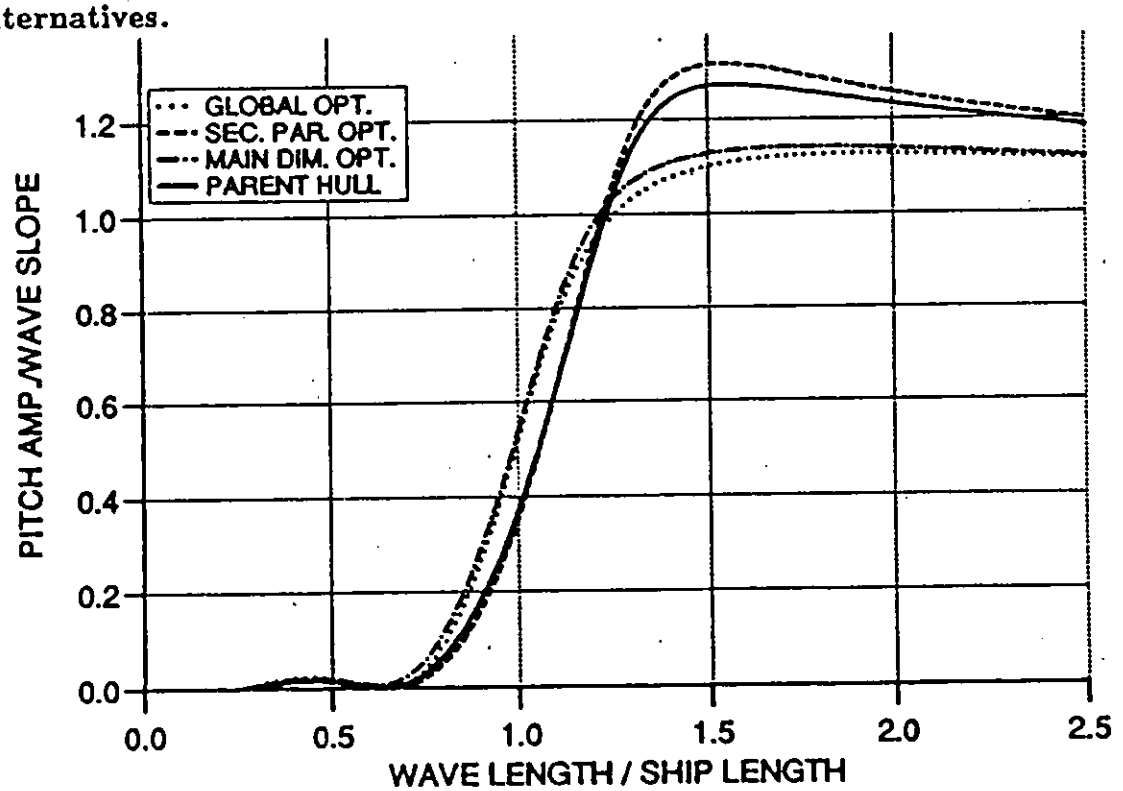

Figure 16. Pitch Comparison of Parent Trawler and Heave Optimised Alternatives.

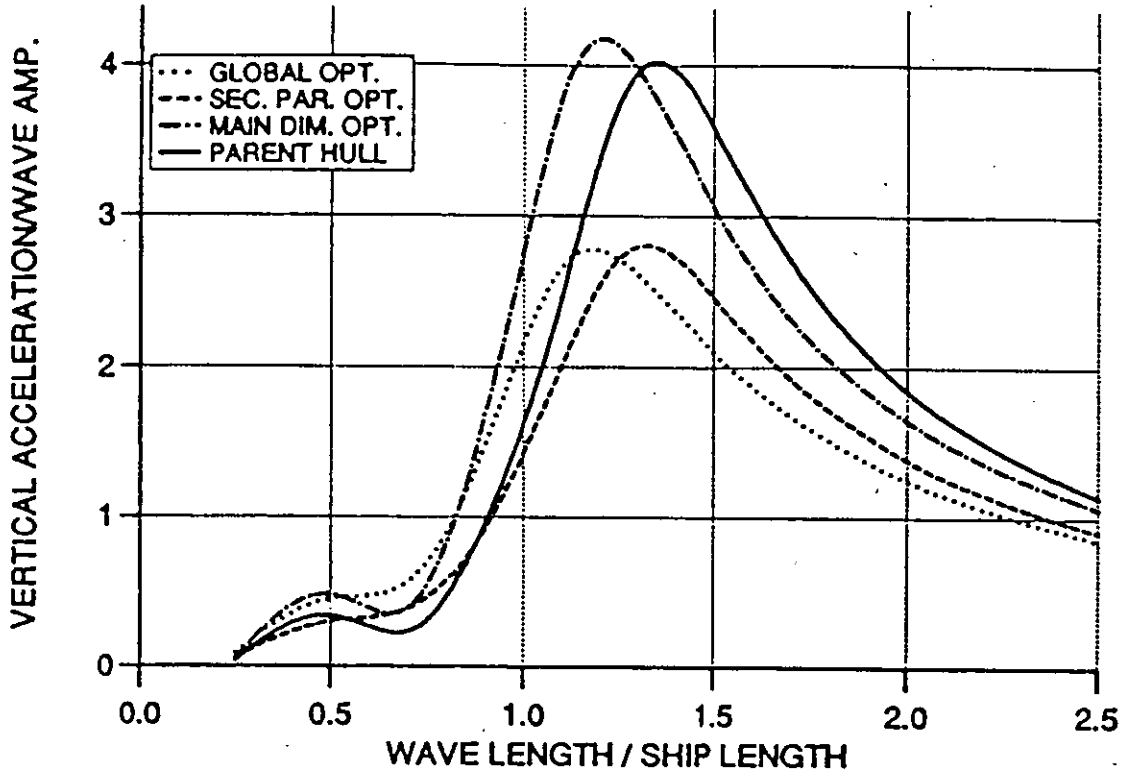

Figure 17. Acceleration Comparison of Parent Trawler and Heave Optimised Alternatives.

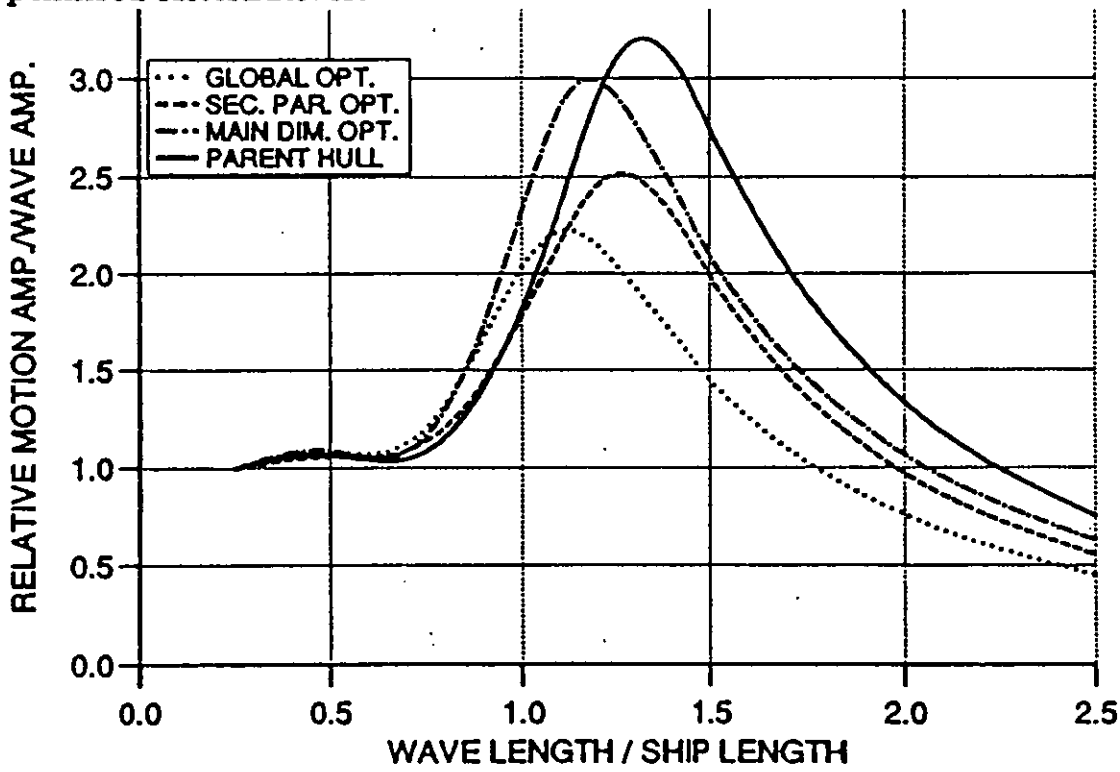

Figure 18. Relative Motion Comparison of Parent Trawler and Heave Optimised Alternatives.

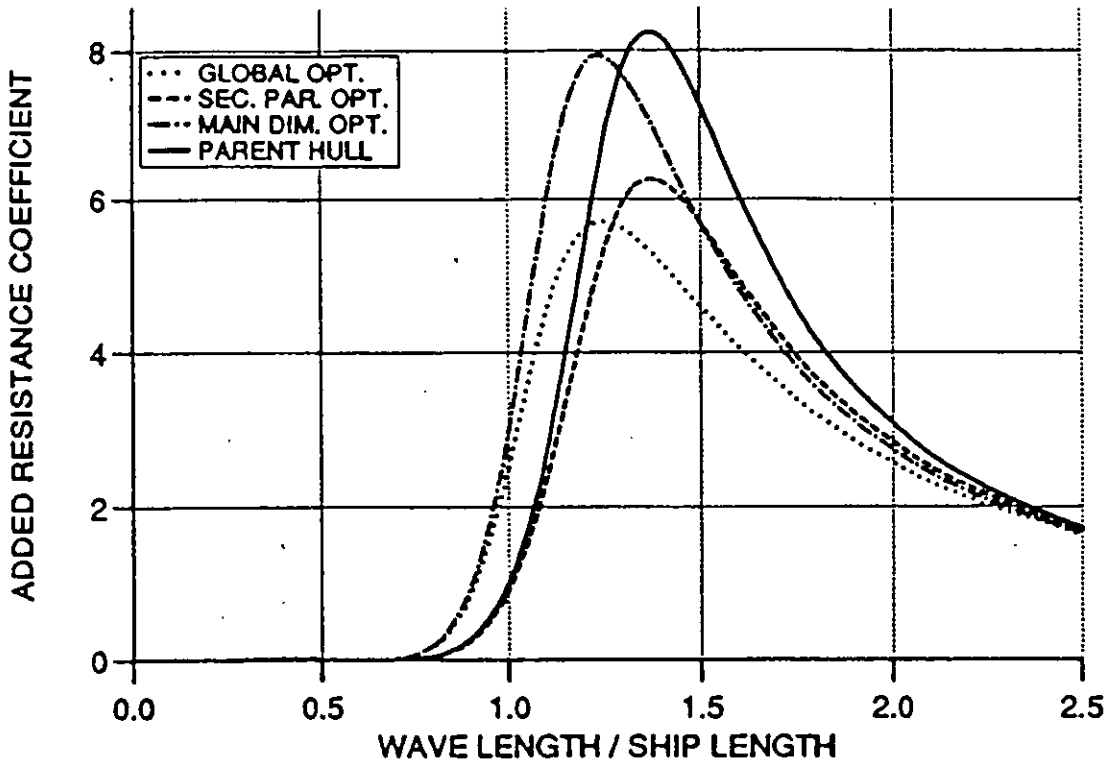

Figure 19. Added Resistance Comparison of Parent Trawler and Heave Optimised Alternatives.

by secondary parameter optimisations are greater than those obtained by primary parameter optimisations. However, consistent with the pitch RAO of Figure 16, the secondary parameter optimisation for heave related pitch rms response is worse for all sea states. The rms heave comparisons of Figure 20 indicate an unusual trend with the increasing sea state, in that the secondary parameter heave optimisation consistently provides improvements for the range of sea states, whereas the global heave optimisation actually increases the rms heave response at the higher sea states.

Slamming and deck wetness probabilities shown in Figures 25 and 26 are significantly improved by secondary parameter heave optimisation. However global heave optimisation provides small improvements in deck wetness probability, whereas the slamming probability worsens for this case.

Similar optimisation procedures have been carried for the cases where the objective function used has been one of the following:

- rms pitch,
- rms vertical acceleration at 0.25 L aft of FP,

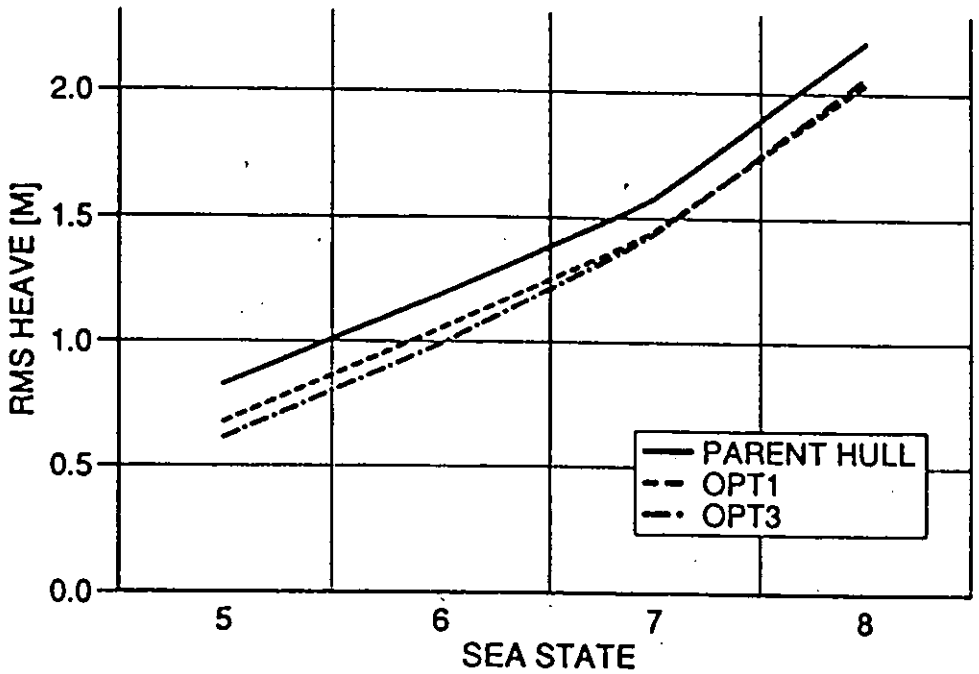

Figure 20. Comparison of rms Heave for Parent Trawler and Heave Optimised Alternatives.

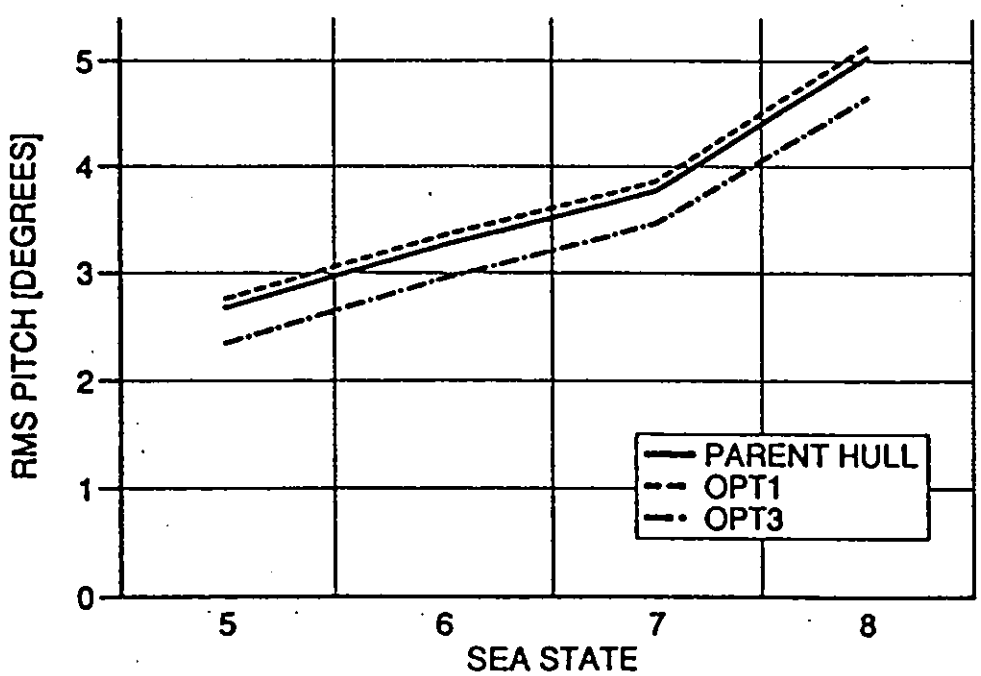

Figure 21. Comparison of rms Pitch for Parent Trawler and Heave Optimised Alternatives.

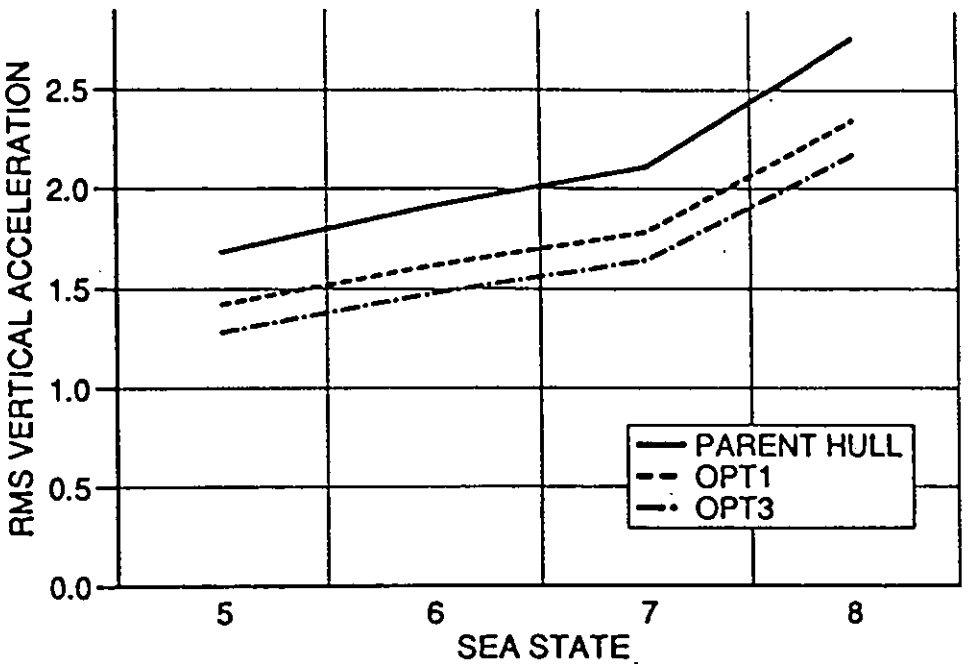

Figure 22. Comparison of rms Acceleration for Parent Trawler and Heave Optimised Alternatives.

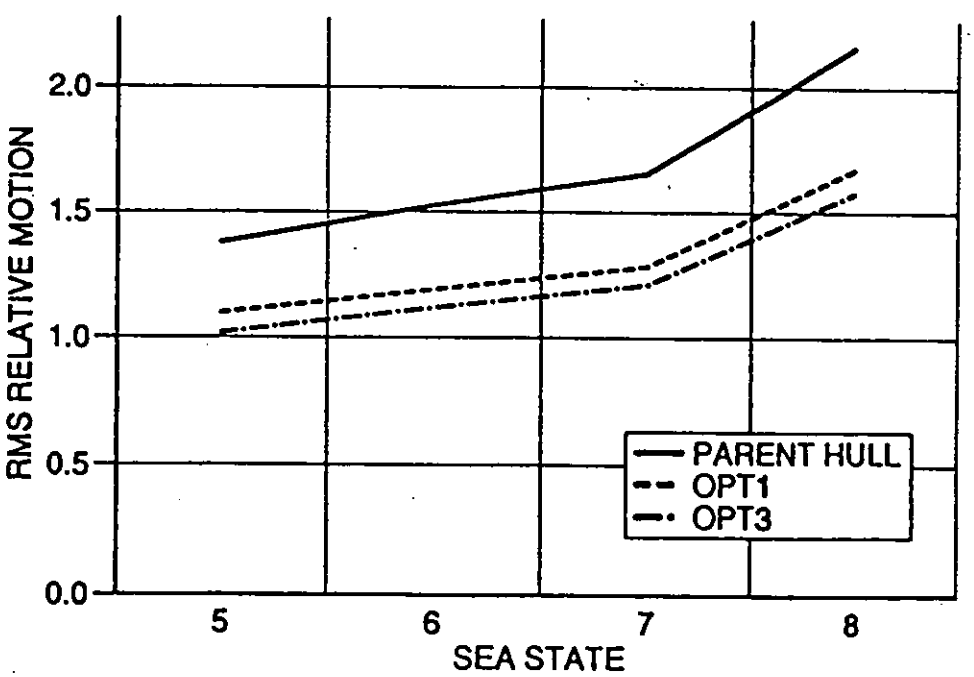

Figure 23. Comparison of rms Relative Motion for Parent Trawler and Heave Optimised Alternatives.

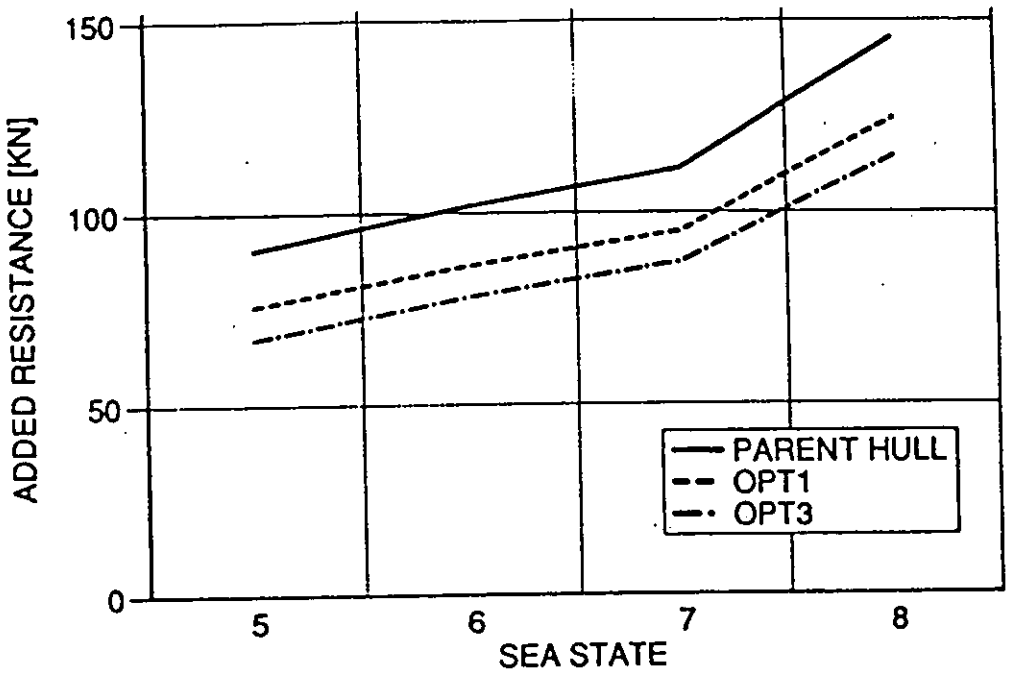

Figure 24. Comparison of Mean Added Resistance for Parent Trawler and Heave Optimised Alternatives.

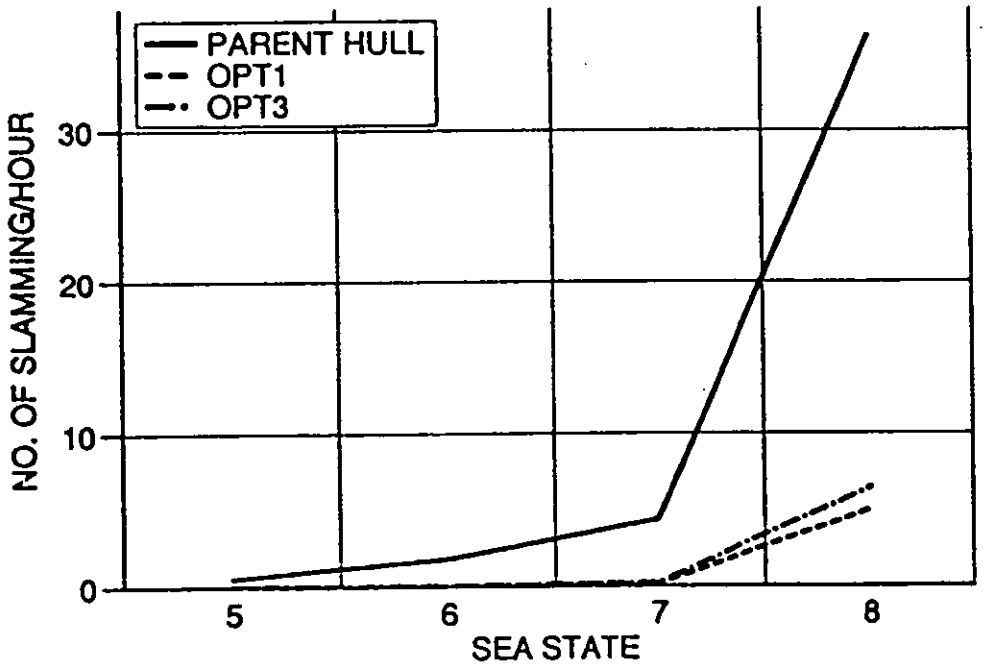

Figure 25. Comparison of Slamming Probability for Parent Trawler and Heave Optimised Alternatives.

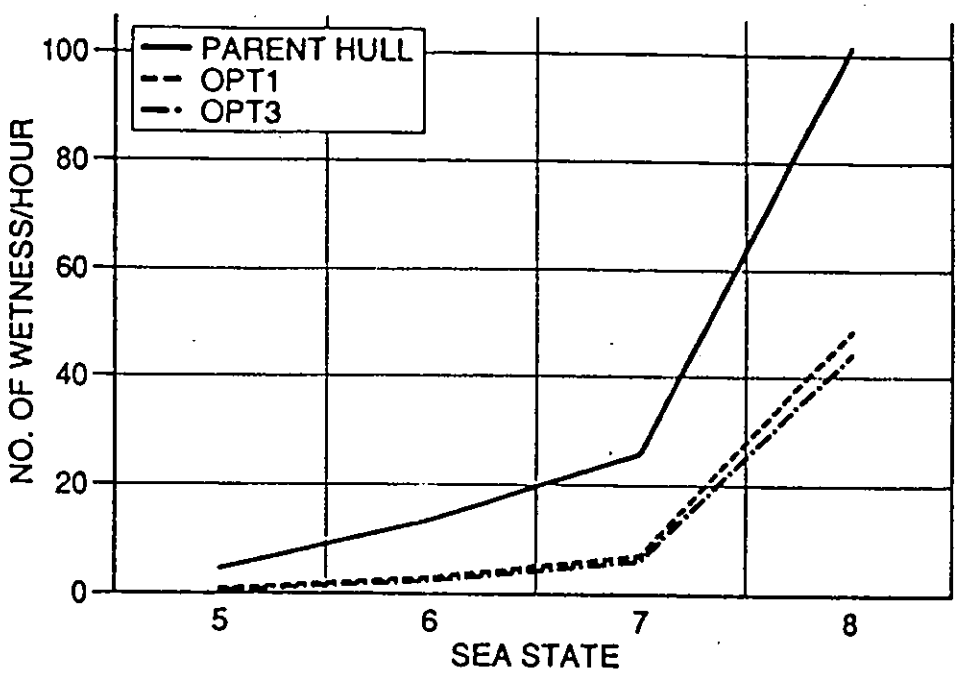

Figure 26. Comparison of Deck Wetness Probability for Parent Trawler and Heave Optimised Alternatives.

- rms relative motion at 0.15L aft of FP,
- Probability of slamming,
- Probability of deck wetness, or
- Mean added resistance.

Many more results for the trawler and other vessels exist. Space does not allow presentation here.

6. Some Closing Remarks.

The application of very sophisticated 3D analyses has not been considered as they do not represent practical tools for normal conceptual design. Once a potentially workable design has been recognised then such tools come into their own at the detailed stages of design. In the foregoing text relatively simple analyses have been considered as there is a need at the conceptual design stage to consider as many options as possible quickly.

In comparing the seakeeping analysis of Section 5.2 and the previous Section 5.8 the underlying reasons for introducing the term 'forward' and 'inverse' analysis becomes relatively clear. 'Forward' analysis simply relates to determining the seakeeping characteristics of a given specified hull form or some systematically generated variation of the parent hull. 'Inverse' analysis implies determination of the changes in the parameters of the initially selected parent hull form to provide a vessel with improved seakeeping responses. That is, we start with a definition of a hull form and then identify a better hull form.

In the course of traditional design any seakeeping analysis undertaken would generally be performed upon a hull form with satisfactory stability and 'R & P' characteristics. In the case of moving to an inverse analysis approach the output optimised hull form may not satisfy the stability conditions and its resistance could be much worse. Such a situation occurred in one of the ranking analyses cited. Hence the constraints associated with the inverse procedure should include the more obvious design constraints of stability and resistance requirements.

The stability calculations are relatively straightforward and so satisfaction of appropriate IMO stability requirements can be readily imposed upon the optimised hull form produced. In fact as seakeeping responses are improved so the alternative hull stability improves, and so in practice imposing such a constraint makes no impact upon the form of the identified optimised hull form. With or without the constraint the generated hull is the same. Resistance is quite a different issue.

For global parameter changes regression based resistance predictors can be used. However most published regression formulae are not dependent upon the majority of the secondary parameters recognised as having impact upon the seakeeping characteristics. Therefore if the size, principal dimensions and block coefficient are unchanged the resistance predictions will remain unchanged for all alternative hull forms. This is not very satisfactory.

For secondary parameter changes either thin ship theory must be used or some other procedure devised. For long slender ships the thin ship theory is adequate and the basis of the analysis is consistent with the assumptions bound up with the strip theory methods used to solve the fluid structure interaction problems associated with seakeeping. For other fuller ships either full 3D methods must be considered or other ad hoc methods devised to reflect dependencies upon all the parameters affecting resistance and seakeeping. A tall order.

Similarly the parameters included in 'form factor' formulae used in the calculation of the viscous resistance do not include the secondary seakeeping parameters identified in the foregoing text. Thus a clear challenge exists to develop alternative resistance predictor methods if stability, seakeeping and resistance are to be sensibly assessed in parallel. Only then we will have identified a practical design tool capable of providing optimal hydrodynamic hull forms.

References.

Abkowitz, M. A. (1957), "Seakeeping Considerations in Design and Research", *SNAME*, New England Section.

Abkowitz, M. A., Vassilopoulos, L. A. and Sellars, F. H. (1966), "Recent developments in Seakeeping Research and Its Application to Design", *Trans. SNAME*, Vol. 74.

Aertssen, G. (1968), "Labouring of Ships in Rough Seas with Special Emphasis on the Fast Ship", *SNAME Diamond Jubilee International Meeting.*

Allan, J. F. (1951), "Research on Design of Drifters", *Trans. INA*, Vol. 93.

Andrew, R. N. and Lloyd, A. R. J. M. (1981), "Full Scale Comparative Measurements on the Behaviour of Two Frigates in Severe Head Seas", *Trans. RINA*, Vol. 123.

Athanassoulis, G. E. and Loukakis, T. E. (1985), "An Extended Lewis Form Family of Ship Sections and Its Application to Seakeeping Calculations", *International Shipbuilding Progress*, Vol. 32, No. 366.

Bales, N. K. and Cummins, W. E. (1970), "The Influence of Hull Form on Seakeeping", *Trans. SNAME*, Vol. 78.

Bales, N. K. (1980), "Optimizing the Seakeeping Performance of Destroyer Type Hulls", *13th Symposium in Naval Hydrodynamics*, Tokyo.

Bales, N. K. and Cieslowski, D. S. (1981), "A Guide to Generic Seakeeping Performance Assessment", *Naval Engineers Journal*, Vol. 94, April.

Beukelman, W. and Huijser, A. (1977), "Variation of Parameters Determining Seakeeping", *International Shipbuilding Progress*, Vol. 24, No. 275.

Blok, J. J. and Beukelman, W. (1984), "The High Speed Displacement Ship Systematic Series of Hull Forms", *Trans. SNAME*, Vol. 92.

Chilo, B. and Sartori, G. (1979), "Seakeeping Merit Rating Criteria Applied to Ship Design", *International Shipbuilding Progress*, Vol. 26, No. 304.

Chryssostomidis, C. (1972), "Seakeeping Considerations in a Total Ship Design Methodology", *9th Symposium in Naval Hydrodynamics*, Paris.

Comstock, E. N. and Keane, R. G. (1980), "Seakeeping by Design", *Naval Engineers Journal*, Vol. 92, No. 2, April.

Conolly, J. E. (1974), "Standards of Good Seakeeping for Destroyers and Frigates in Head Seas", *Int. Symp. on the Dynamics of Marine Vehicles and Structures in Waves*, University College, London.

Edward, J. and Todd, F. H. (1939), "Steam Drifters: Tank and Sea Tests" *Transactions of Institute of Engineers and Shipbuilders in Scotland*, Vol. 82.

Ewing, J. A. (1967), "The Effect of Speed, Forebody Shape and Weight Distribution on Ship Motions", *Trans. RINA*, Vol. 109.

Ferdinande, V. (1969), "Some Notes on the Shipping of Water on a Model of a Cargo Ship in Irregular Waves", *International Shipbuilding Progress*, Vol. 16, February.

Frank, W. (1967), "Oscillation of Cylinders in or Below the Free Surface of Deep Fluids", *DTNSRDC* , Report No. 2375.

Grigoropoulos, G. J. and Loukakis, T. A. (1988), "A New Method for Developing Hull Forms with Superior Seakeeping Qualities", *Proceedings of CADMO 88*, Southampton.

Grim, O. (1953), "Berechnung der durch Schwingungen eines Schiffskorper Erzeugten Hydrodynamischen Krafte", *Jahrbuch der Schiffbautechnischen Gesselschaft*, Vol. 47.

Hearn, G. E. and Donati, E. (1981), "Seakeeping Theories: Applying Some Choice", *Trans. NECIES*, Vol. 97.

Hearn, G. E., Hills, W., and Colton, P. (1988), "Incorporating a Seakeeping Capability in a Computer Aided Preliminary Design System", *SNAME STAR Symposium*, June.

Hearn, G. E., Hills, W., and Sarıöz, K. (1990), "Making Seakeeping Analysis Work for the Designer - A New Practical Approach", *19th Scientific and Methodological Seminar on Ship Hydrodynamics*, Varna, October.

Hearn, G. E., Hills, W., and Sarıöz, K. (1991a), "Practical Seakeeping for Design: A Ship Shape Approach", *RINA Spring Meetings*, April.

Hearn, G. E., Hills, W., and Sarıöz, K. (1991b), "A Hydrodynamic De-

sign Methodology for Conceptual Ship Design", *Proceedings of ICCAS 91*, Brazil, September.

Hoffman, D. (1976), "The Impact of Seakeeping on Ship Operations", *Marine Technology*, Vol. 13, No. 3.

Hooke, R. and Jeeves, T.A. (1961), "Direct Search Solution of Numerical and Statistical Problems", *Journal of the Association for Computing Machinery*, Vol. 8, No. 4.

Hovgaard, W. (1889), "Trials on Three Danish Torpedo Boats", *Engineering*, Vol. 26.

Kehoe, J. W. (1973), "Destroyer Seakeeping: Ours and Theirs", *Proceedings of the U.S. Naval Institute*, Vol. 99, No. 11.

Kent, J. L. (1922), "Experiments on Mercantile Ship Models in Waves", *Trans. INA*, Vol. 62.

Kent, J. L. (1950), "The Design of Seakindly Ships", *Trans. NECIES*, Vol. 66.

Lackenby, H. (1950), "On the Systematic Geometrical Variation of Ship Forms", *Trans. INA*, Vol. 92.

Landsburg, A.C. and Cruikshank, J.M. (1976), "Tanker Ballasting: How Light Can You Go?", *Trans. SNAME*, Vol. 83.

Landweber, L. and Macagno, M. (1959), "Added Mass of a Three-Parameter family of Two-Dimensional Forms Oscillating in a Free-Surface", *Journal of Ship Research*, Vol. 2, No. 4, March.

Lewis, F. M. (1929), "The Inertia of the Water Surrounding a Vibrating Ship", *Trans. SNAME*, Vol. 37.

Lewis, E. V. (1955), "Ship Speeds in Irregular Seas", *Trans. SNAME*, Vol. 63.

Lewis, E. V. (1960), "Increasing the Sea Speed of Merchant Ships", *Trans. SNAME*, Vol. 67.

Lloyd, A. R. J. M. (1983), "Deck Wetness Experiments", *20th ATTC*, Hoboken.

Lloyd, A. R. J. M., Salsich, J. O. and Zseleczky, J. J. (1986), "The Effect of Bow Shape on Deck Wetness in Head Seas ", *Trans. RINA*, Vol. 128.

Lloyd, A. R. J. M. (1988), "The Effect of Hull Form and Size on Seakeeping", *Proceedings of CADMO 88*, Southampton.

Lloyd, A. R. J. M. (1991), "The Seakeeping Design package (SDP)", *RINA Spring Meetings*, London, April.

Loukakis, T. A. and Chryssostromidis, C. (1975), "Seakeeping Standard Series for Cruiser-Stern Ships", *Trans. SNAME*, Vol. 83.

Macdonald, K. E. and Telfer, E. V. (1938), "Seakindliness and Ship Design", *Trans. NECIES*, Vol. 54.

McCreight, K. K. (1983), "Estimating the Seakeeping Qualities of Destroyer Type Hulls", *DTNSRDC Report*, SPD-1074-01, January.

Moor, D. I. and Murdey, D. C. (1968), "Motions and Propulsion of Single screw Models in head Seas (Part 1)", *Trans. RINA*, Vol. 110.

Moor, D. I. (1970), "Effects on Performance in Still Water and Waves of Some Geometric Changes to the Form of a Large Twin-Screw Ship", *Trans. SNAME*, Vol. 78.

Muntjewerf, J. J. (1963), "The Influence of Shipform and Length on the behaviour of Destroyer Type Ships in head and Bow Seas", *International Shipbuilding Progress*, Vol. 10, No. 102.

Newton, R. N. (1960), "Wetness Related to Freeboard and Flare", *Trans. RINA*, Vol. 102.

Ochi, M. K. (1964), "Extreme Behaviour of a Ship in Rough Seas- Slamming and Shipping of Green Water", *Trans. SNAME*, Vol. 72.

Ochi, M. K. and Motter, L. E. (1973), "Prediction of Slamming Characteristics and Hull Responses for Ship Design", *Trans. SNAME*, Vol. 81.

O'Dea, J.F. and Walden, D.A. (1985), "Effect of Bow Shape and Nonlinearities on the prediction of Large Amplitude Motions and Deck Wetness", *15th ONR Symposium on Naval Hydrodynamics*, Hamburg.

Olson, R.S. (1978), "An Evaluation of the Seakeeping Qualities of Naval Combatants", *Naval Engineers Journal*, Vol. 90, February.

Robson, B. L. (1987), "Systematic Series of High Speed Displacement Hull Forms for Naval Combatants", *Trans. RINA*, Vol. 130.

Salvesen, N., Tuck, E. O. and Faltinsen, O. (1970), "Ship Motions and Sea Loads", *Trans. SNAME*, Vol. 78.

Sarıöz, K., Hearn, G. E., and Hills, W. (1992), "Practical Seakeeping for Design: An Optimised Approach", *Proceedings of PRADS 92*, Newcastle Upon Tyne, May.

Saunders, H. E. (1957), "The Influence and Behaviour of the Above Water Form", *Hydrodynamics in Ship Design*, Chapter 26, Vol. I, SNAME.

Schmitke, R. T. and Murdey, D. C. (1980), "Seakeeping and Resistance Trade-offs in Frigate Hull Form Design", *13th Symposium on Naval Hydrodynamics*, Tokyo.

Schoenberger, R. W. (1975), "Subjective Response to Very Low Frequency Vibration", *Aviation, Space and Environmental Medicine*, June.

Spouge, J. R. (1985), "The Prediction of Realistic Long-term Ship Seakeeping Performance", *Trans. NECIES*, Vol. 101.

St. Denis, M. (1983), "On the Empiric Design of Seakindly Ships", *Proceedings of PRADS 83*, Tokyo.

Swaan, W. A. (1961), "The Influence of the Principle Dimensions on Ship Behaviour in Irregular Waves", *International Shipbuilding Progress*, Vol. 8, No. 82.

Swaan, W. A. and Vossers, G. (1961), "The Effect of Forebody Section Shape on Ship Behaviour in Waves", *International Shipbuilding Progress*, Vol. 8, No. 83.

Swaan, W. A. and Rijken, H. (1964), "Speed Loss at Sea as a Function of Longitudinal Weight Distribution", *International Shipbuilding Progress*, Vol. 11, No. 15.

Ursell, F. (1949), "On the Heaving Motions of a Circular Cylinder on the Surface of a Fluid", *Quarterly Journal of Mechanics and Applied Mathematics*, Vol. 2.

Van Sluijs, M. F. and Gie, T. S. (1972), "Behaviour and Performance of Compact Frigates in Head Seas", *International Shipbuilding Progress*, Vol. 19, No. 210.

Von Kerzcek, C. and Tuck, E. O. (1969), "The Representation of Ship Hulls by Conformal Mapping Functions", *Journal of Ship Research*, Vol. 13, No. 4.

Vossers, G. and Swaan, W.A. (1960), "Some Seakeeping Tests with a Victory Model", *International Shipbuilding Progress*, Vol. 7, No. 69.

Vossers, G., Swaan, W.A. and Rijken, H. (1960), "Experiments with Series 60 Models in Waves", *Trans. SNAME*, Vol. 68.

Walden, D. A. (1983), "Extension of the Bales Seakeeping Rank Factor Concept", *20th ATTC*, Hoboken.

Wijngaarden, A. M. (1984), "The Optimum Form of a Small Hull for the North Sea", *International Shipbuilding Progress*, Vol. 31, No. 359, July.

Yourkov, N. (1973), "Vertical motions of Ships with Different Forms of Forebody", *International Shipbuilding Progress*, Vol. 20, No. 223.

APPENDIX A.
Linear Distortion Methods.

A common technique used to derive an alternative design with the same main dimensions, but different prismatic coefficient or LCB, is to change the location of stations whilst preserving the offsets defining each station. That is, the shape of the sections remain the same as in the parent hull, but they are moved forward or aft to bring about a desired change in the sectional area curve.

Let us consider Figure A.1 . Here $F(x)$ represents the dimensionless sectional area curve of one half-body of the ship. The curve $F(x)$ need not be given in mathematical form; it is assumed to be an empirical design curve. It is convenient to consider the half-body to be of unit length with the maximum ordinate of the sectional area curve also equalling unity. All horizontal dimensions are therefore fractions of the half length, and the area under the curve $F(x)$ is numerically equal to the prismatic coefficient of the half-body.

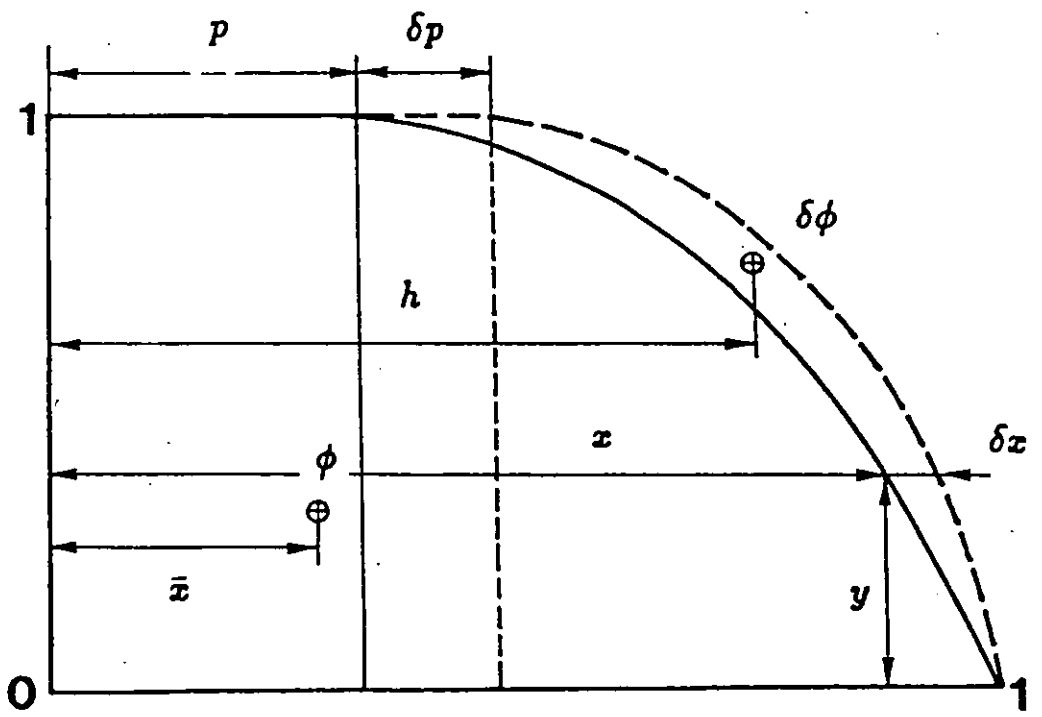

Figure A.1. Dimensionless Half Body Sectional Area Curve.

In accordance with the "one-minus prismatic" method, the new spacing of the sections from the end of the body is made proportional to the difference between

the respective prismatics and unity, that is

$$\delta x = \frac{\delta\phi}{1-\phi}(1-x) \tag{A.1}$$

where ϕ is the prismatic coefficient of the half body, $\delta\phi$ is the required change in the prismatic coefficient of the half-body, x is the fractional distance of any transverse section from midships, and δx is the necessary longitudinal shift of the section at x to produce the required change in prismatic coefficient. The change in the parallel middle body δp will equal δx at $x = p$, therefore

$$\delta p = \frac{\delta\phi}{1-\phi}(1-p). \tag{A.2}$$

Although, the 'one-minus prismatic' method is useful and simple to apply, it has two major disadvantages:

- for a given change in fullness the longitudinal distribution of the displacement added (or removed) cannot be controlled, and
- there is no control over the extent of the parallel middle body in the derived forms.

Lackenby (1950) describes a simple method for deriving the amount by which each offset station should be moved to generate given changes in the following parameters:

- total prismatic coefficient,
- forward and aft prismatic coefficients,
- longitudinal centre of bouyancy, and
- length and location of parallel middle body.

In this method the ship is partitioned into two halves, the forebody and the afterbody. To transform the parent form to a desired ship form with different C_P and / or LCB position the two halves of the parent hull are transformed separately. Thus the calculated changes in the prismatic coefficient of both the afterbody and the forebody are required. This approach can be used in the distortion of the sectional area curve to change fullness as expressed by C_P, or location of centroid, as measured by LCB. Alternatively the design waterline curve can be distorted to change C_{WP} or LCF.

Lackenby assumed an expression for δx of the form,

$$\delta x = c(1-x)(x+d), \tag{A.3}$$

where c and d are constants in a given case. The end conditions are

$$\begin{aligned} \delta x &= 0 \quad \text{at} \quad x = 1 \text{ , and} \\ \delta x &= \delta p \quad \text{at} \quad x = p. \end{aligned} \tag{A.4}$$

These conditions and the observation that the additional area $\delta\phi = \int_0^1 \delta x dy$ yields

$$c = \frac{\delta\phi - \delta p \frac{1-\phi}{1-p}}{\phi(1-2\bar{x}) - p(1-\phi)} \tag{A.5}$$

and

$$d = \frac{\delta p}{c(1-p)} - p. \tag{A.6}$$

Hence

$$\delta x = (1-x)\left\{\left[\delta\phi - \delta p \frac{1-\phi}{1-p}\right]\frac{x-p}{A} + \frac{\delta p}{1-p}\right\} \tag{A.7}$$

where

$$A = \phi(1-2\bar{x}) - p(1-\phi). \tag{A.8}$$

So far only the individual half-bodies have been dealt with. Now they will be considered together, in order to determine the effect of the variations in LCB and C_P in the separate half bodies upon the total prismatic coefficient and the position of the LCB of the vessel. Consider Figure A.2. Each half-body is of unit length with a maximum ordinate of unity. It is desired to change total prismatic coefficient by $\delta\phi_t$ and change the position of the centroid by $\delta\bar{z}$. The amount of changes in prismatic coefficients of fore and after bodies can be calculated using the simple relationships

$$\delta\phi_f + \delta\phi_a = \delta\phi_t$$

$$\delta\phi_f(h_f - \bar{z}) + (\phi_t + \delta\phi_t)\delta\bar{z} = \delta\phi_a(h_a + \bar{z}).$$

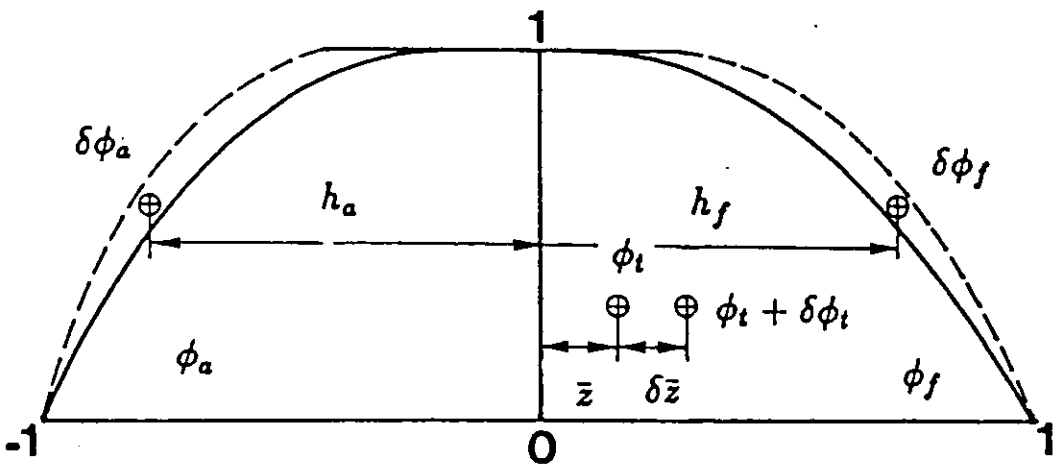

Figure A.2. Variation of Sectional Area Curve

Hence

$$\begin{aligned} \delta\phi_f &= \frac{2[\delta\phi_t(h_a - \bar{z}) - \delta\bar{z}(\phi_t + \delta\phi_t)]}{h_f + h_a} \\ \delta\phi_a &= \frac{2[\delta\phi_t(h_f + \bar{z}) + \delta\bar{z}(\phi_t + \delta\phi_t)]}{h_f + h_a}, \end{aligned} \tag{A.9}$$

where $\bar{z}$ is the distance of the LCB in the basis ship from midships expressed as a fraction of the half length.

The moment of the added "sliver" of area about midships is given by:

$$\delta\phi \cdot h = \int_0^1 \delta x \cdot x \cdot dy.$$

Using Equations (A.3) and (A.6)

$$\begin{aligned} \delta\phi \cdot h =& c\int_0^1 (x^2 - x^3 - px + px^2)dy + \frac{\delta p}{1-p}\int_0^1 (x - x^2)dy \\ =& c(2\phi\bar{x} - 3\phi k^2 - p\phi + 2p\phi\bar{x}) + \frac{\delta p}{1-p}(\phi - 2\phi\bar{x}) \\ =& c\phi[2\bar{x} - 3k^2 - p(1 - 2\bar{x})] + \frac{\delta p\phi}{1-p}(1 - 2\bar{x}). \end{aligned}$$

Substituting for c from Equation (A.5) and dividing by $\delta\phi$ we have the lever

$$h = \phi\left\{\frac{\left[1 - \frac{\delta p(1-\phi)}{\delta\phi(1-p)}\right]}{\phi(1-2\bar{x}) - p(1-\phi)}[2\bar{x} - 3k^2 - p(1-2\bar{x})] + \frac{\delta p}{\delta\phi}\frac{1-2\bar{x}}{1-p}\right\}$$

or,

$$h = \phi\left\{\frac{B}{\phi}\left[1 - \frac{\delta p}{\delta\phi}\frac{1-\phi}{1-p}\right] + \frac{\delta p}{\delta\phi}\frac{1-2\bar{x}}{1-p}\right\}. \tag{A.10}$$

Hence B is a constant depending only on the geometrical properties of the basis form, that is

$$B = \frac{\phi[2\bar{x} - 3k^2 - p(1-2\bar{x})]}{A} \tag{A.11}$$

where k is the radius of gyration (or lever of the second moment) of the original curve about midships. Therefore the levers h_f and h_a can be written as follows:

$$h_f = \phi_f\left\{\frac{B_f}{\phi_f}\left[1 - \frac{\delta p_f}{\delta\phi_f}\frac{1-\phi_f}{1-p_f}\right] + \frac{\delta p_f}{\delta\phi_f}\frac{1-2\bar{x}_f}{1-p_f}\right\} \tag{A.12}$$

$$h_a = \phi_a\left\{\frac{B_a}{\phi_a}\left[1 - \frac{\delta p_a}{\delta\phi_a}\frac{1-\phi_a}{1-p_a}\right] + \frac{\delta p_a}{\delta\phi_a}\frac{1-2\bar{x}_a}{1-p_a}\right\} \tag{A.13}$$

Having calculated h_f and h_a for the fore and aft bodies the required adjustments to the fore and after body prismatics to give any desired change in LCB position and total prismatic coefficient can be determined from Equations (A.9). From these the revised spacing of the transverse sections can be calculated using the appropriate expressions for δx, as given in Equation (A.7).

In this study it is assumed that the alternative hull forms have the same parallel middle body length as the parent hull, i.e. $\delta p = 0$. Therefore, h_f and h_a do not involve $\delta\phi_f$ or $\delta\phi_a$. However, in the general case where $\delta p \neq 0$, the relations for h_f and h_a themselves involve the required changes in fineness $\delta\phi_a$ and $\delta\phi_a$. This difficulty can be overcome by substituting the expressions for h_f and h_a in the Equations (A.9) and solving for $\delta\phi_f$ and $\delta\phi_a$. The resulting general expressions are:

$$\delta\phi_f = \frac{2\left[\delta\phi_t(B_a + \bar{z}) + \delta\bar{z}(\phi_t + \delta\phi_t)\right] + C_f\delta p_f - Ca\delta p_a}{B_f + B_a} \tag{A.14}$$

$$\delta\phi_a = \frac{2\Big[\delta\phi_t(B_f - \bar{z}) + \delta\bar{z}(\phi_t + \delta\phi_t)\Big] - C_f\delta p_f + Ca\delta p_a}{B_f + B_a} \tag{A.15}$$

where C is a constant for the parent form given by

$$C = \frac{B(1-\phi) - \phi(1-2\bar{x})}{1-p}. \tag{A.16}$$

There are definite limits to which the fullness of a given form can be varied for this method. In this connection it can be shown that the absolute limit of the fullness is

$$\delta\phi = \frac{\delta p(1-\phi) \pm A(1 - \frac{\delta p}{1-p})}{1-p}. \tag{A.17}$$

This result is derived in detail by Lackenby (1950) in Appendix II of his paper.

APPENDIX B

Conformal Mapping Transformation Techniques

The suitability of conformal mapping techniques for the approximate representation of underwater sections of ships is well known, especially since Lewis (1929) adopted this approach to calculate the added mass of ships. Lewis used a three termed mapping function. Therefore it is necessary to specify three parameters such as beam, draught and sectional area to determine the coefficients of the mapping function so as to produce a specific section form. Evidently, by including more terms and free coefficients in the mapping transformation it is possible to control more features of section shape. Von Kerzcek and Tuck (1969) demonstrated that it takes relatively few terms of the mapping function to obtain very close approximations to a broad range of realistic ship section shapes.

A principal advantage of conformal mapping is that the sections generated are represented by a single set of mathematical equations and this greatly simplifies certain hydrostatic and hydrodynamic calculations. Moreover, the section shapes generated by conformal mapping tend to be automatically fair in the manner of streamline shapes and do not exhibit rapid oscillations.

However, in the context of design the designer may want to control the section character in the direction of more U-shaped or V-shaped sections, keeping the other section parameters the same. This is feasible, within the scope of the conformal mapping method, provided extra parameters are introduced. One particular drawback of section shapes derived by mapping on to a circle is that the tangent to the section at the waterline is vertical, making it difficult to represent sections with flare. This can be avoided by using polynomials for the above water form and matching the underwater form at a point slightly below the waterline.

The fundamental problem to be solved in applying the conformal mapping technique is the determination of the mapping function corresponding to a given sectional curve. Unfortunately, this problem cannot be solved in closed form, except in some simple special cases. In general, approximate methods and numerical techniques should be used. A successful choice of the mapping technique is primarily dependent upon the desired accuracy and the kind of data used in defining the sectional curve. Such data can be classified into three categories:

- a set of points on the curve,
- a number of local properties of the curve, such as the slope of the curve

or the curvature at given points, and

- a number of global properties of the curve, such as the area, breadth, draught, or various moments with respect to specified axes.

When the problem is to accurately represent an actual section shape, the first two categories of data are used. However, in the systematic hull form variation problem it is necessary to be able to create a section shape using a small number of parameters. For this purpose several families of conformal mapping functions have been developed. The most convenient ones being the two-parameter family introduced by Lewis (1929) and the three-parameter family of Landweber and Macagno (1959).

Limiting the problem to conventional port starboard symmetric ship sections and assuming a mirror image in the undisturbed free surface the mapping function can be reduced to

$$z = a_0\varsigma + \sum_{n=1}^{N} a_{2n-1}\varsigma^{1-2n} \tag{B.1}$$

where z and ς are the complex variables

$$z = x + iy \quad \text{and} \quad \varsigma = \xi + i\eta = re^{i\theta} \tag{B.2}$$

and the coefficients a_n are real due to the symmetry about both the x and y axes. In practice the two planes of symmetry mean that only a single quadrant need be considered, as illustrated in Figure B.1

In the ς-plane a unit radius circle is described by

$$\varsigma = e^{i\theta} = \cos\theta + i\sin\theta. \tag{B.3}$$

Substituting B.3 into B.1 and separating real and imaginary terms leads to

$$\begin{aligned} x(\theta) =& a_0\cos\theta + a_1\cos\theta + a_3\cos 3\theta + \ldots + a_{2N-1}\cos(2N-1)\theta \\ y(\theta) =& a_0\sin\theta - a_1\sin\theta - a_3\sin 3\theta - \ldots - a_{2N-1}\sin(2N-1)\theta. \end{aligned} \tag{B.4}$$

The coefficients a_i are called mapping coefficients and as θ varies from 0 to $\pi/2$ so the section contour is described.

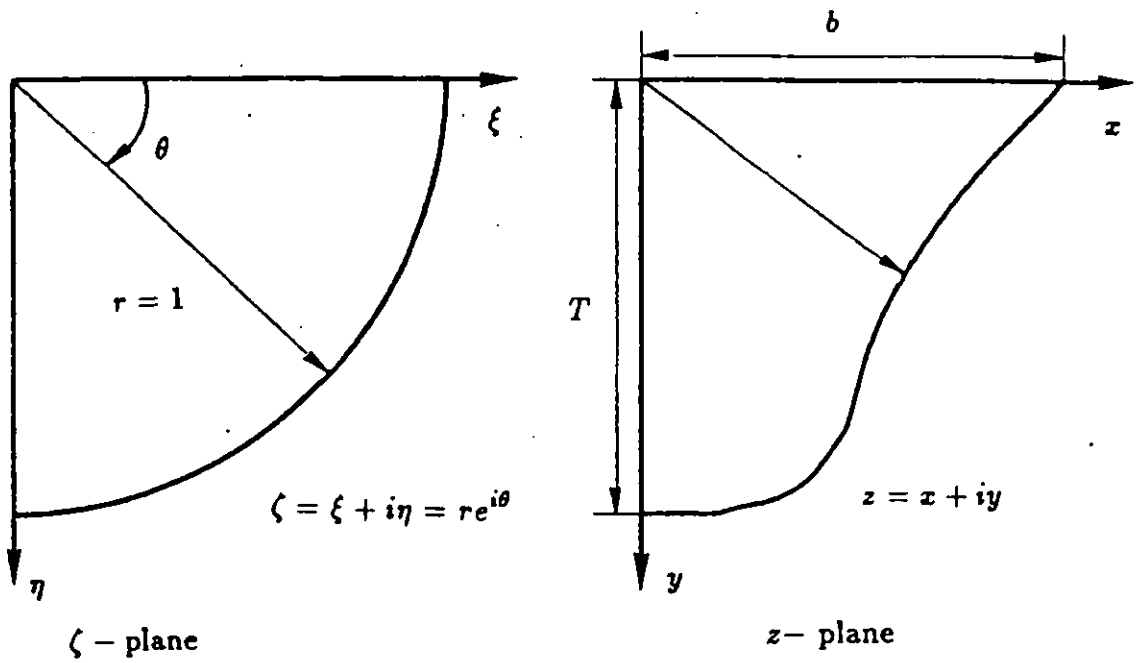

Figure B.1. Mapping a Ship Section to a Circle

The two parameter mapping introduced by Lewis (1929) utilizes the first three terms of the Equations (B.4), that is

$$\begin{aligned} x(\theta) &= a_0 \cos\theta + a_1 \cos\theta + a_3 \cos 3\theta \\ y(\theta) &= a_0 \sin\theta - a_1 \sin\theta - a_3 \sin 3\theta. \end{aligned} \tag{B.5}$$

Next let b denote the half-beam of the section at the waterline, and T the draught. Since $x = b$ when $\theta = 0$, and $y = T$ when $\theta = \pi/2$, then Equation (B.5) reveals the relationships

$$\begin{aligned} b &= a_0 + a_1 + a_3 \\ T &= a_0 - a_1 + a_3. \end{aligned} \tag{B.6}$$

The sectional area of the half section at the selected station is given by

$$S = \int_C x dy = \int_0^{\pi/2} x(\theta) \frac{dy(\theta)}{d\theta} d\theta \tag{B.7}$$

and this reduces to

$$S = \frac{\pi}{2}(a_0^2 - a_1^2 - 3a_3^2). \tag{B.8}$$

Given the sectional half-beam, b, the draught, T, and the area, S, the corresponding mapping coefficients satisfy

$$\begin{aligned} a_0 &= \frac{1}{2}(b+T) - a_3 \\ a_1 &= \frac{1}{2}(b-T) \\ a_3 &= -\frac{1}{4}(b+T) + \frac{1}{4}\left[(b+T)^2 + 8(bT - \frac{2}{\pi}S)\right]^{\frac{1}{2}}. \end{aligned} \tag{B.9}$$

Dividing these coefficients by the draught yields the new coefficients

$$a_0' = \frac{a_0}{T}, \quad a_1' = \frac{a_1}{T}, \quad \text{and} \quad a_3' = \frac{a_3}{T}. \tag{B.10}$$

Defining the half-beam/draught ratio, $\lambda = b/T$, and the sectional area coefficient as $\sigma = S/2bT$, and then dropping the primes, gives

$$\begin{aligned} a_0 &= \frac{1}{2}(\lambda+1) - a_3 \\ a_1 &= \frac{1}{2}(\lambda-1) \\ a_3 &= -\frac{1}{4}(\lambda+1) + \frac{1}{4}\left[(\lambda+1)^2 + 8\lambda(1 - \frac{4}{\pi}\sigma)\right]^{\frac{1}{2}}. \end{aligned} \tag{B.11}$$

Landweber and Macagno (1959) introduced the third parameter and defined a family of forms given as follows

$$\begin{aligned} x &= (1+a_1)\cos\theta + a_3\cos 3\theta + a_5\cos 5\theta \\ y &= (1-a_1)\sin\theta - a_3\sin 3\theta - a_5\sin 5\theta. \end{aligned} \tag{B.12}$$

Since $x = b$ when $\theta = 0$, and $y = T$ when $\theta = \pi/2$, then Equation (B.12) implies that

$$\begin{aligned} b &= 1 + a_1 + a_3 + a_5 \\ T &= 1 - a_1 + a_3 - a_5. \end{aligned} \tag{B.13}$$

The sectional area can be expressed as

$$S = \frac{\pi}{2}(1 - a_1^2 - 3a_3^2 - 5a_5^2). \tag{B.14}$$

Introducing the nondimensional parameters

$$\alpha = \frac{2}{b}, \quad \lambda = \frac{T}{b} \text{ and } \quad \sigma = \frac{S}{2bT}$$

Equations (B.13) can be solved for a_1 and a_3, that is

$$\begin{aligned} a_1 &= \frac{1-\lambda}{\alpha} - a_5 \\ a_3 &= \frac{1+\lambda}{\alpha} - 1. \end{aligned} \tag{B.15}$$

Substituting these relationships into Equation (B.14) gives

$$S = \frac{\pi}{2}\Big\{-2 - 6a_5^2 + b[3(1+\lambda) + a_5(1-\lambda)] - b^2(1+\lambda+\lambda^2)\Big\}. \tag{B.16}$$

The sectional area coefficient σ is then given by

$$\sigma = \frac{\pi}{8\lambda}\Big\{-\alpha^2(1+3a_5^2) + \alpha[3(1+\lambda) + a_5(1-\lambda)] - 2(1+\lambda+\lambda^2)\Big\}. \tag{B.17}$$

Now the sectional area coefficient σ and λ are known, while a_5 and α are unknown. However assuming a value for a_5, and solving the above quadratic equation in α yields

$$\alpha = \frac{B \pm \sqrt{B^2 - 4AC}}{2A} \tag{B.18}$$

where

$$A = 1 + 3a_5^2$$

$$B = 3(1 + \lambda) + a_5(1 - \lambda)$$

$$C = 2(1 + \lambda + \lambda^2) + \frac{8\lambda\sigma}{\pi}$$

When the shape characteristics b, T, and S are given, the corresponding values of λ, σ, a_1 and a_3 can be readily obtained from Equations (B.13), (B.14), and (B.15).

Next we consider the practical application of the given theory. Initially we may assume that a_5 is known and has a value of 0.0, say. Then one can calculate α using Equation (B.18) and so determine a_1 and a_3 using Equation (B.15). Having determined the mapping coefficients, the offsets of the section can be calculated using the three-parameter form of mapping function. These calculated offsets can then be used to calculate the vertical distance of the centroid of the section from the keel. If the calculated centroid compares favourably with the actual KB value of the original section the coefficients may be used, otherwise the process continues until the assumed value of a_5 gives a KB value which is very close to the actual centroid position.

The vertical position of the centroid may be considered as a measure of the U-ness or V-ness of the section. The lower values corresponding to V-shaped sections. It therefore follows that by changing the vertical position of the centroid, one may transform an U-shaped section into a V-shaped one, and vice versa whilst keeping constant the values of breadth, draught and sectional area. In theory this device can be used to generate alternative transverse sections.

REASONS FOR SELECTING A FLOATING PRODUCTION SYSTEM

by

NEIL S. MILLER

GLASGOW

REASONS FOR SELECTING A FLOATING PRODUCTION SYSTEM

INTRODUCTION

The technology associated with oil and gas production is under continuous research and development. Advances such as the introduction of horizontal drilling and multi-phase pumping open up fresh possibilities for developing new fields. In a well developed oil province like the North Sea where there is already a considerable infrastructure in the form of existing pipelines and platforms development engineers are bound to look first at avoiding the construction of any form of platform and to use a subsea completion to some adjacent existing facility.

If this is not possible for technical or economic reasons - it is frequently very difficult to come to a satisfactory agreement to use some other companies facilities - consideration must be given to the construction of either a fixed or floating platform. The analysis must include the export arrangements. If it is an oil field a good deal will depend on the amount of gas present and any restrictions on how it may be disposed.

If it is a small amount and of the order of the requirements for power generation there is little problem but if it is sufficiently large that the regulatory authorities insist on it being either marketed or re-injected it can affect the selection of platform type.

If an oil or gas line passes close by it may be possible to connect into it and reduce the export problem. However, if the complete platform and export facilities must be created this will greatly increase the capital expenditure. It is then necessary to decide whether the field reserves and possibly the reserves of other fields in the neighbourhood justifies the construction of fixed facilities, both platform and pipeline, or whether part of the infrastructure must come from floating units.

A pipeline can only be justified if there are large reserves which will give a long field life and the route to a suitable terminal is comparatively short in water depths of less than 250 m. The most suitable terminal is a company owned refinery but if the oil must be stored ashore and then reshipped to its eventual market the cost of these operations must be taken into account.

If these conditions are not met a floating export system may meet the economic restraints. In a mild sea area this can consist of a CALM buoy some form of articulated column with the shuttle tanker moored directly to it and the only

downtime will be due to the time required for shuttle tanker change over the occasional storm which may be too severe for the tanker to remain connected. Such conditions are rare and more often it will be necessary to have some limited storage in the system to cover for bad weather and change over times.

This storage may either be obtained on the platform itself or at the loading unit but will inevitably add to capital costs. At the unit the storage may either be a large buoy e.g. the Shell SPAR buoy, or by a tanker. Such tankers can have a variety of moorings from simple CALM buoys in mild conditions to articulated columns (FULMAR unit) and turret moorings (the ALBA storage unit) in severe weather conditions.

If it is necessary to use such a unit the question arises as to whether it can also carry the production equipment and eliminate the platform.

DRILLING CONSIDERATIONS

For many fields it is highly desirable to have a drilling rig continuously employed in development drilling and carrying out workover operations. An example is fields where large amounts of sand and sediments are expected in the flow stream. Most drilling engineers would prefer a fixed platform to eliminate the problems associated with floating drilling. Drilling is only possible from multi-point moored floating structures e.g. semi-submersibles, buoys, unless the drilling rig is installed above the turret in a turret moored tanker unit e.g. PETROJARL. This requires a very large turret which is mechanically and structurally difficult.

On the other hand there are several platforms in the North Sea where large drilling installations have been little used after development drilling was completed and much closer attention is now being paid to the long term requirements for a drilling spread on a fixed platform. Other means of well servicing are being actively sought. The techniques of sub-sea completions have greatly improved and so it is possible to have all the wells in the immediate area under a platform pre-drilled before the platform is brought over them. This makes possible the use of floating production vessels with little or no well servicing facilities.

WEIGHT OF PRODUCTION EQUIPMENT

As we shall see semi-submersibles and buoys are limited in their capability for carrying heavy equipment on decks where atmospheric ventilation is possible and where the effects of wave action are minimised. Thus the weight of production equipment is of crucial importance in considering the use of floating facilities. This will be particularly true where it is necessary to carry out water and gas injection as the treatment and power requirements drive up the necessary weight of equipment.

Tanker type vessels have few weight restrictions but the necessity to have a single point mooring with the oil and gas flows going through some form of swivel restricts the volume of output (and input) which can be handled. Recent developments in swivel design are claimed to have overcome this but the industry still lacks confidence in multi-path high pressure swivels or the mechanical equivalents. In deep water it may be possible to avoid swivels by allowing the risers to twist up to 720°.

As a result floating production systems have been limited to production rates of less than 100,000 barrels per day (bbls/d) although the larger semi-submersibles and tanker type vessels can probably cope with twice this rate.

AVAILABILITY OF VESSELS SUITABLE FOR CONVERSION

In the early 80's, following a slump in oil consumption after price rises, there was a surplus of large oil tankers which could be obtained relatively cheaply for conversion to a floating production and storage unit (FPSO) or merely a storage unit. Due to a combination of scrapping due to age and an increase in the demand for tankers (See Figs. 1 and 2 from Ref.1) this surplus has largely disappeared and more and more of these units are being specially constructed but at much greater costs than the surplus ships of the 80's. There are considerable gains in having a new vessel instead of a conversion in terms of expected life, geometry and layout and overall safety and risk of pollution. The increased attention to some form of double skin arrangement to lessen the risk of a serious oil spillage following a collision has meant that many old designs of tanker are no longer acceptable to the authorities for conversion to FPSO's.

The demand for semi-submersibles tends to follow the oil price with fluctuations in day rates from 10,000$ per day in 'bad' times to 50,000$ per day in 'good' times. These rates apply to the older type of vessels which have been found suitable for conversion to production vessels. Their deck load capacity is rarely greater than 4000 tonnes and often much smaller so that the weight of production equipment they can carry is limited. Deck space is also fairly critical bearing in mind that it is not possible to go upwards without raising the centre of gravity and increasing the wind loading, both of which adversely affect the vessels stability.

It is possible that some of the large semi-submersibles which have been built as crane barges will become surplus to requirements because of the continual improvements in lifting capacity achieved in recent years. Such vessels may make satisfactory production units for large fields, especially in areas where the environment is not very severe. One large semi-submersible, which has been specially designed as a production and limited storage unit, is being completed in

Italy but it remains to be seen if this will set a new trend. A large concrete semi-submersible with storage is planned for the West Troll field.

TECHNICAL CONSIDERATIONS

The above discussion has concerned general field development considerations with, apart from the deck weight problem, little discussion of the technical problems associated with floating systems.

The field environment in terms of the wind, wave and current conditions will determine the size of the vessel necessary to avoid unacceptable downtime due to vessel motions or an inability to connect with a mooring or having connected to stay connected. Generally wave conditions are the most important with their period characteristics having the greatest influence but in some areas of the world wind and current can be the decisive factors.

The larger the vessel the longer will be the natural periods of its heave, pitch and roll motions and the less its susceptibility to wave induced motions. Unfortunately increased size also implies increased capital costs.

A second drawback to increased size is the greater mooring loads involved with additional costs implications. Mooring costs are very dependant on water depth with mooring being difficult in either shallow water (less than 100 m) or very deep water (greater than 1500 m) and most convenient in depths of 150 to 300 m. When using converted vessels it is important to balance the gains in motion characteristics which may be obtained by a large size against the increased mooring loads and associated mooring costs.

In very deep water serious consideration is being given to the continuous use of dynamic positioning to avoid mooring. The power required tends to rise rapidly in severe sea states and to obtain the necessary degree of reliability means much duplication of equipment with a high capital cost. Nevertheless in calmer sea areas where gas is available to provide cheap power this may prove to be the cheapest option. Such a vessel will need to be designed to have a low resistance in waves in order to limit it's power consumption. There appears to be limited scope for the BP 'SWOPS' approach where the vessel only connects with the wells in sea conditions below some fixed limit.

Many existing floating systems have been conversions from other roles. In such cases it is vital that an accurate assessment be made of the current condition of the vessels structural condition and state of all its power generation and other services to see how far they comply with current offshore regulations and what will be required to bring them up to the required standard. There have been many examples of conversions costing far more than was originally budgeted for.

It is particularly important to carry out a detailed fatigue analysis to make sure the structure is capable of carrying the loads it will suffer during the anticipated field life. In certain sea areas these can be much higher than would be anticipated during the normal life of for example a tanker or a bulk carrier.

Safety considerations must always be borne in mind, particularly the layout of the accommodation block in relation to the production equipment and other potential hazards such as the swivel in a turret moored vessel. Many existing floating production systems have weaknesses in this respect and it should not be assumed that the same layout and standards of equipment is acceptable in current practice. A safety assessment should be carried out at all stages of the design but particularly in deciding on the initial layout and operating procedure. For single point moored systems this may require the fitting of azimuthing thrusters at the stern so that the vessel can be turned beam on to the wind in the event of fire or a gas leak.

PURELY GAS FIELDS

The above discussion relates to oil fields with some gas present. There are known to be a large number of gas fields offshore with considerable reserves but in locations remote from any sizable market. Various alternatives have been considered for developing these by production systems such as floating LNG plants and methanol plants. So far the economics has proved unacceptable although it is probable that current technology is adequate. In the Europe/Asia area the availability of vast reserves of gas on land makes the likelihood of such developments remote but in the Gulf of Iran and in the Australia/Indonesia region markets may exist in Japan and Korea where there is already extensive investment in LNG facilities and possibly in the USA.

There is enormous scope for developing cheaper systems to get both petroleum gases and natural gas (methane) from remote offshore locations to the consumer markets.

SUMMARY

It will be clear from the above discussion that there is no defined set of circumstances which dictates that a floating production will be preferable to a fixed platform or some combination of sub-sea completion to existing facilities. With the continual improvement in technology associated with all types of production systems each new field must be analysed to determine the most economic system for its development at that time.

The most likely scenario for floating systems is an oil field with a low gas/oil ratio remote from existing platforms and pipelines and from local markets in water deeper than 200m. This would appear to exclude much of the North Sea but floating systems, using conversions of existing vessels, have been preferred in a number of cases in recent years confirming that their economics can be decisive in special circumstances.

GENERAL TECHNICAL CONSIDERATIONS

One of the prime concerns of all oil engineers is that the production vessel's motions should be as low as possible and that any downtime due to motions should be less than 2% per year. In the early days of semi-submersible floating production systems in the North Sea much higher downtimes were experienced mainly due to weaknesses in the export system which involved tankers tying up to CALM buoys. Downtimes could average nearly 20% per year but be much higher in the winter months. Improvements in heave compensation equipment, in the design of the internals of separators and other pieces of equipment and in the vessel designs has reduced the downtime on the production side to around 2% maximum.

Conventional separators have been designed to cope with the following levels of motion:

Angular motions	0 to 7.5°
Linear motions	0 to 0.25g
Period	3 to 15 secs.

New designs (see Ocean Industry p.51, June 1992 and p.25 Dec. 1991/Jan. 1992) are claimed to still further reduce the sensitivity to motions. The introduction of hydrocyclones has made oil/water separation much easier and more efficient.

Some of these improvements have been achieved by simply increasing the size of the production unit which should always lead to a reduction in motions since its natural periods will be longer. Since increased size generally means increased capital costs it is necessary to consider carefully whether this size is really necessary in the weather conditions in the field.

It is important to consult the reservoir engineers to find out how they expect the wells to behave if they are shut in for a day or more. If this is likely to lead to a build up of pressure so that when operations are restarted the product flow is increased there may be little or no loss of revenue in the short or long term and downtime may be acceptable if it involves less capital cost. There will be other cases where the well characteristics will dictate that the flow must be kept as steady as possible and it is very important to select the best type and size of vessel for the environmental conditions.

ENVIRONMENTAL CONDITIONS

In the early stages of design it will be important to obtain wave scatter diagrams, wind rose data (velocity and direction) and current data (again velocity and direction). Ideally these should be obtained by instrumented measurements over several years but in a new development area this will rarely be possible.

In such a case it is necessary to use one of the large sets of predicted wave conditions such as Global Wave Statistics prepared by Dr Hogben and his colleagues at British Maritime Technology and published by Unwins - (see Fig.3 for the worldwide coverage and Fig. 4 for a typical diagram). For each sea area the amount of data available to make the predictions is quoted above the Tables and allows one to judge the confidence which can be placed in it, e.g. for the North Atlantic a very large amount of data was available from weather ships, coastal stations and merchant ships reporting daily. It will be noted that the data is also given by direction and by season throughout the year.

From the motion point of view the most important data is the wave period content and particularly long period waves as this will dictate the vessel size to a large extent. Wave scatter diagrams usually quote the zero crossing period of the waves as determined from the wave spectrum. Of more importance to motion considerations is the spectrum peak period. Unfortunately it's relationship to the zero crossing period depends on the type of spectra, the theoretical ones in common use being the JONSWAP and the Pierson-Moskowitz. The ratio of peak period to zero crossing is approximately 1.29 and 1.41 for the respective cases. In continental shelf areas it is probably preferable to use the JONSWAP formula while in open sea areas such as off the West coasts of the U.K. the Pierson-Moskowitz would be preferable. Measured data on site can give the best indication of which approximation to use.

Table 1.1 gives period and wave length data for four sea areas to illustrate the problems involved:

Central North Sea
Northern North Sea - East of Shetland
West of Shetland
Brazil.

The zero crossing periods which are exceeded for less than 2% of the time vary from 8.7 secs in the Central North Sea to 11.3 secs West of Shetland. The corresponding variation in peak period is from 11.2 to 14.6 secs for a JONSWAP spectrum and 12.3 to 15.9 secs for the Pierson-Moskowitz formula. The range of wave lengths covered by these figures is from 196m to 395m i.e. a factor of nearly 2. For a new sea area, it will be wise to use the Pierson-Moskowitz figures when deciding on the desirable natural period for a vessel.

NATURAL MOTION PERIODS

The periods of greatest concern from the motion point of view are those of heave, pitch and roll. The surge, sway periods are important for mooring design and will be discussed at greater length in that section.

The formulae governing the heave and pitch/roll natural periods of motion are:

Heave $Th = 2\pi\left[(M + M_{AVM} / \rho g A_w)\right]^{1/2}$; Pitch/Roll $Tp/Tr = 2\pi\left[(I + I_{AVM}) / \rho g \nabla GM\right]^{1/2}$

where	M	=	displacement mass of vessel (tonnes)
	M_{avm}	=	added virtual mass in heave (tonnes)
	ρ	=	mass density of sea water (1.025 tonnes/m^3)
	g	=	acceleration of gravity (m/sec^2)
	Aw	=	waterplane area of vessel (m^2)
	Ip or Ir	=	mass inertia of vessel about a transverse/ longitudinal axis through the CG. (tonnes m^2)
	Iavmp/r	=	inertia of added virtual mass in pitch/roll about the CG (tonnes m^2)
	GM_L or GM_T	=	height of longitudinal/transverse metacentre above the the CG (m)

The metacentric height GM is determined from the formula:

	GM	=	KB + BM - KG
where	KB	=	height of centre of buoyancy above the keel or lowest point on vessel (m)
	BM	=	Ial or Iat/∇ (m)
	Ial or Iat	=	2nd moment of water plane area about a transverse/ longitudinal axis throughout the centroid of the water-plane. (m^4)
	∇	=	volume of displacement (m).
	KG	=	height of the CG above the keel.(m)

If these formula are examined it will be seen that in all cases, as the vessel size increases, the numerator will increase at a faster rate than the denominator and so the period or BM value will increase. In heave the increase will be as the square root of the increase in dimensions for a geometrically similar body but the pitch/roll periods depend on the height of the CG which is governed by the mass distribution and is restricted by stability considerations. Although it may appear possible to have very long pitch/roll periods by having low values of GM_L or GM_T this would lead to high static angles of trim/list under wind forces and non-symmetric loads and so there are regulations governing the minimum values which can be used. Thus the designer must strike a happy medium between statical stability and motion considerations.

The detailed application of these formula to the three general types of vessel which may be considered for a floating production system:

Semi-submersible
Ship/barge shaped vessel
Buoy

are considered in the lectures dealing with these particular designs.

Tension leg platforms (TLP) are not being treated although they represent an important variation on a floating vessel where the heave motion is restricted by the tension in the tethers. Although many of its design problems are similar to those of semi-submersibles the compliant nature of the moorings introduces many new aspects which have been treated extensively in papers to the Offshore Technology Conferences (OTC), the Offshore and Arctic Engineering (OMAE) symposia and the meetings of the International Society of Offshore and Polar Engineers (ISOPE).

In all cases the general objective is to design the vessel so that its natural periods of motion lie as far away from the predominant wave periods as possible.

In the range of wave periods it is important to keep the motion exciting forces and moments low and it will be shown how this is achieved by careful selection of the dimensions and mass distribution in each case.

REFERENCE

1. The Tanker Industry in the 1990s - Shell Briefing Service, no. 5, 1991.

TABLE 1.1: Period and Wave Length Data for a Number of Sea Areas

	PERIOD AND WAVE LENGTHS EXCEEDED 2% OF TIME				
		PIERSON MOSKOWITZ		JONSWAP	
AREA	T_Z secs	T_p	(m)	T_p Secs	(m)
CENTRAL NORTH SEA	8.7	12.3	236	11.2	196
NORTHERN NORTH SEA	10.9	15.4	370	14.1	310
WEST OF SHETLAND	11.3	15.9	395	14.6	333
BRAZIL	10.0	14.1	324	12.9	260

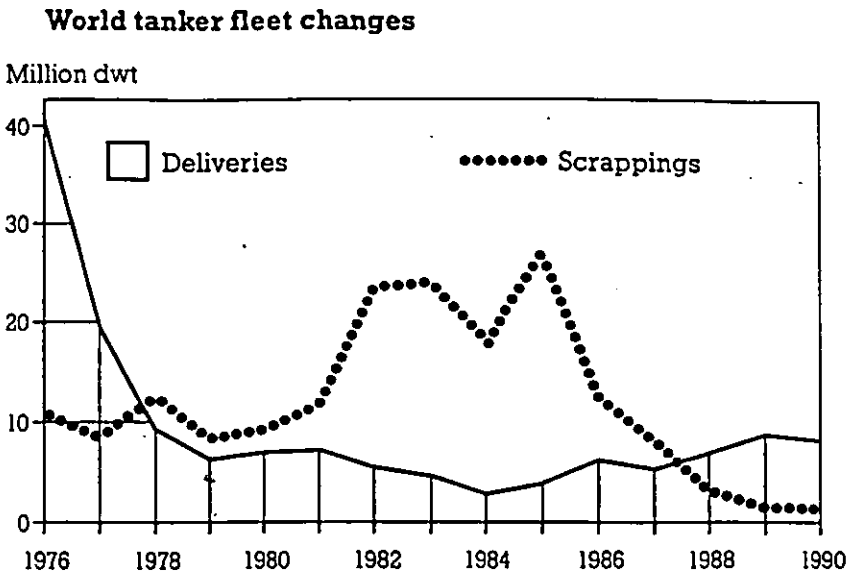

Fig. 1 World Tanker Fleet Changes.

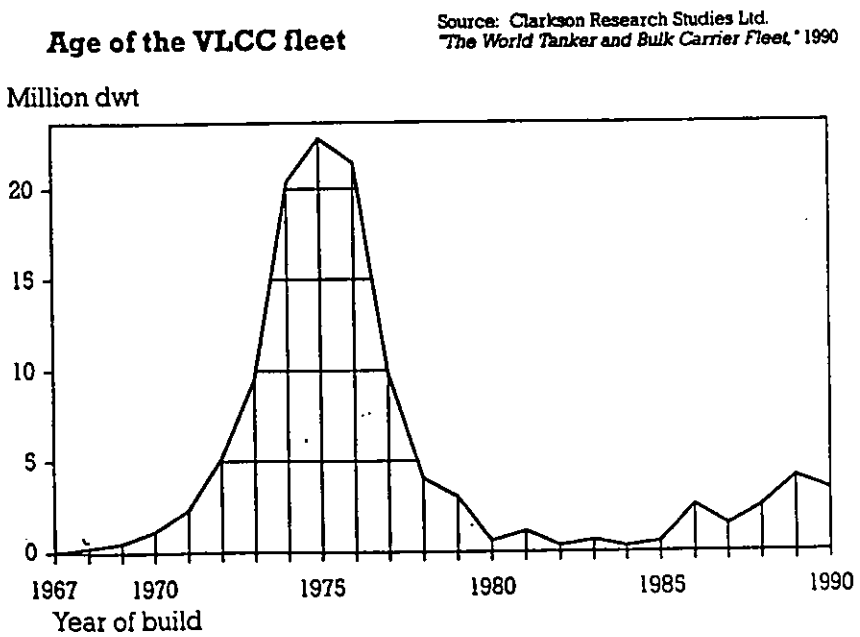

Fig. 2 Age of the VLCC Fleet.

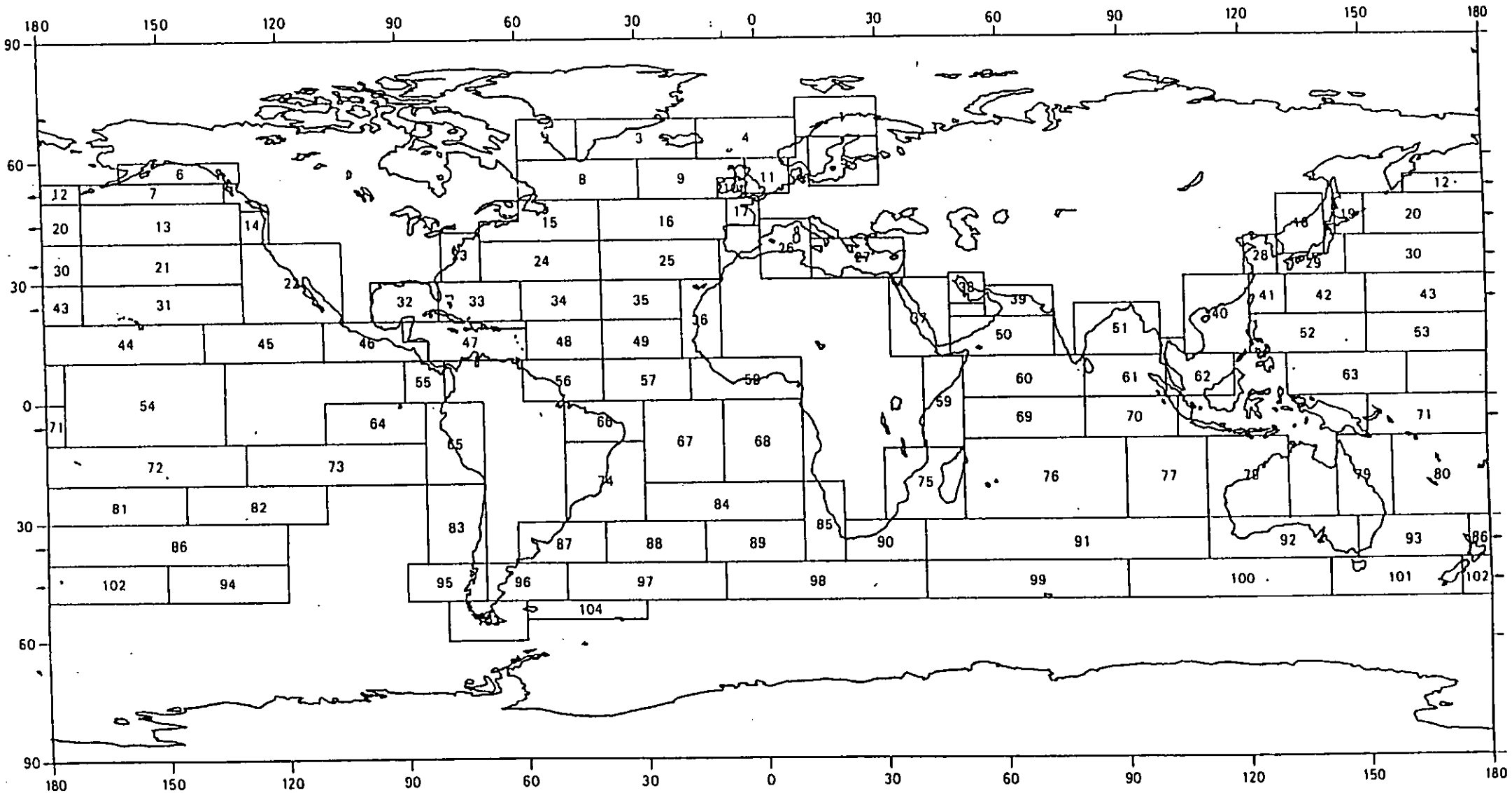

Fig. 3 Sea Areas covered by Global Wave Statistics

TOT. NO. OF OBS. WIND/WAVE = 68729
ALL WIND = 913426

ANNUAL

AREA 11

NORTH WEST

PERCENTAGE OF OBS = 12.80%

SIGNIFICANT WAVE HEIGHT (m)	<4	4-5	5-6	6-7	7-8	8-9	9-10	10-11	11-12	12-13	>13	TOTAL
TOTAL	35	206	348	262	114	34	8	2	-	-	-	1000
>14	-	-	-	-	-	-	-	-	-	-	-	1
13-14	-	-	-	-	-	-	-	-	-	-	-	1
12-13	-	-	-	-	-	-	-	-	-	-	-	1
11-12	-	-	-	-	-	-	-	-	-	-	-	1
10-11	-	-	-	1	1	-	-	-	-	-	-	2
9-10	-	-	1	1	1	1	-	-	-	-	-	3
8-9	-	-	1	2	2	1	-	-	-	-	-	5
7-8	-	-	2	3	3	1	-	-	-	-	-	9
6-7	-	1	3	6	4	2	1	-	-	-	-	17
5-6	-	1	7	10	7	3	1	-	-	-	-	30
4-5	-	3	15	20	12	5	1	-	-	-	-	56
3-4	-	8	32	37	20	6	2	-	-	-	-	105
2-3	1	22	66	62	28	8	2	-	-	-	-	189
1-2	5	58	119	82	28	6	1	-	-	-	-	298
0-1	29	112	103	39	8	1	-	-	-	-	-	291
TOTAL												

ZERO CROSSING PERIOD (s)

NORTH

PERCENTAGE OF OBS = 11.34%

SIGNIFICANT WAVE HEIGHT (m)	<4	4-5	5-6	6-7	7-8	8-9	9-10	10-11	11-12	12-13	>13	TOTAL
TOTAL	28	173	328	278	135	45	11	2	1	-	-	1000
>14	-	-	-	-	-	-	-	-	-	-	-	-
13-14	-	-	-	-	-	-	-	-	-	-	-	-
12-13	-	-	-	-	-	-	-	-	-	-	-	-
11-12	-	-	-	-	-	-	-	-	-	-	-	-
10-11	-	-	-	-	-	-	-	-	-	-	-	-
9-10	-	-	-	1	1	-	-	-	-	-	-	2
8-9	-	-	1	1	1	1	-	-	-	-	-	4
7-8	-	-	1	2	2	1	-	-	-	-	-	7
6-7	-	-	2	4	4	2	1	-	-	-	-	13
5-6	-	1	5	9	7	3	1	-	-	-	-	26
4-5	-	2	11	18	13	6	2	-	-	-	-	52
3-4	-	6	26	36	23	9	2	1	-	-	-	103
2-3	1	18	60	66	35	11	3	1	-	-	-	192
1-2	4	50	117	94	37	9	2	-	-	-	-	313
0-1	23	96	106	48	12	2	-	-	-	-	-	288
TOTAL												

ZERO CROSSING PERIOD (s)

NORTH EAST

PERCENTAGE OF OBS = 8.47%

SIGNIFICANT WAVE HEIGHT (m)	<4	4-5	5-6	6-7	7-8	8-9	9-10	10-11	11-12	12-13	>13	TOTAL
TOTAL	154	358	308	135	39	8	2	-	-	-	-	1000
>14	-	-	-	-	-	-	-	-	-	-	-	-
13-14	-	-	-	-	-	-	-	-	-	-	-	-
12-13	-	-	-	-	-	-	-	-	-	-	-	-
11-12	-	-	-	-	-	-	-	-	-	-	-	-
10-11	-	-	-	-	-	-	-	-	-	-	-	-
9-10	-	-	-	-	-	-	-	-	-	-	-	1
8-9	-	-	-	-	-	-	-	-	-	-	-	1
7-8	-	-	1	1	-	-	-	-	-	-	-	2
6-7	-	1	2	2	1	-	-	-	-	-	-	5
5-6	-	2	4	3	1	-	-	-	-	-	-	10
4-5	1	5	9	7	3	1	-	-	-	-	-	24
3-4	2	13	22	15	6	1	-	-	-	-	-	60
2-3	7	40	56	31	10	2	-	-	-	-	-	148
1-2	29	114	115	49	13	2	-	-	-	-	-	323
0-1	116	183	100	27	5	1	-	-	-	-	-	431
TOTAL												

ZERO CROSSING PERIOD (s)

WEST

PERCENTAGE OF OBS = 15.85%

SIGNIFICANT WAVE HEIGHT (m)	<4	4-5	5-6	6-7	7-8	8-9	9-10	10-11	11-12	12-13	>13	TOTAL
TOTAL	69	273	353	209	74	19	4	1	-	-	-	1000
>14	-	-	-	-	-	-	-	-	-	-	-	-
13-14	-	-	-	-	-	-	-	-	-	-	-	-
12-13	-	-	-	-	-	-	-	-	-	-	-	-
11-12	-	-	-	-	-	-	-	-	-	-	-	-
10-11	-	-	-	-	-	-	-	-	-	-	-	-
9-10	-	-	-	1	1	-	-	-	-	-	-	2
8-9	-	-	1	1	1	-	-	-	-	-	-	3
7-8	-	-	2	2	1	1	-	-	-	-	-	6
6-7	-	1	3	4	3	1	-	-	-	-	-	12
5-6	-	2	7	8	4	2	-	-	-	-	-	23
4-5	-	5	15	15	8	2	1	-	-	-	-	47
3-4	1	13	34	30	13	4	1	-	-	-	-	95
2-3	3	35	71	51	19	5	1	-	-	-	-	184
1-2	12	85	124	66	19	4	1	-	-	-	-	310
0-1	53	132	96	30	6	1	-	-	-	-	-	317
TOTAL												

ZERO CROSSING PERIOD (s)

ALL DIRECTIONS

PERCENTAGE OF OBS = 100.00%
(INCLUDING 2.40% DIRECTION UNKNOWN)

SIGNIFICANT WAVE HEIGHT (m)	<4	4-5	5-6	6-7	7-8	8-9	9-10	10-11	11-12	12-13	>13	TOTAL
TOTAL	23	160	324	288	145	50	13	3	1	-	-	1000
>14	-	-	-	-	-	-	-	-	-	-	-	-
13-14	-	-	-	-	-	-	-	-	-	-	-	-
12-13	-	-	-	-	-	-	-	-	-	-	-	-
11-12	-	-	-	-	-	-	-	-	-	-	-	1
10-11	-	-	-	-	-	-	-	-	-	-	-	1
9-10	-	-	-	1	1	-	-	-	-	-	-	2
8-9	-	-	-	1	1	1	-	-	-	-	-	4
7-8	-	-	1	2	2	1	1	-	-	-	-	7
6-7	-	-	2	4	4	2	1	-	-	-	-	13
5-6	-	1	4	9	7	4	1	-	-	-	-	26
4-5	-	2	11	19	14	6	2	1	-	-	-	55
3-4	-	6	27	39	26	10	3	1	-	-	-	112
2-3	1	17	63	73	40	13	3	1	-	-	-	210
1-2	3	49	121	99	40	10	2	-	-	-	-	323
0-1	19	86	94	41	10	2	-	-	-	-	-	253
TOTAL												

ZERO CROSSING PERIOD (s)

EAST

PERCENTAGE OF OBS = 9.15%

SIGNIFICANT WAVE HEIGHT (m)	<4	4-5	5-6	6-7	7-8	8-9	9-10	10-11	11-12	12-13	>13	TOTAL
TOTAL	121	340	329	153	44	9	2	-	-	-	-	1000
>14	-	-	-	-	-	-	-	-	-	-	-	-
13-14	-	-	-	-	-	-	-	-	-	-	-	-
12-13	-	-	-	-	-	-	-	-	-	-	-	-
11-12	-	-	-	-	-	-	-	-	-	-	-	-
10-11	-	-	-	-	-	-	-	-	-	-	-	-
9-10	-	-	1	1	-	-	-	-	-	-	-	2
8-9	-	-	1	1	1	-	-	-	-	-	-	3
7-8	-	1	2	2	1	-	-	-	-	-	-	6
6-7	-	2	4	4	2	1	-	-	-	-	-	11
5-6	-	3	8	6	3	1	-	-	-	-	-	22
4-5	1	8	16	12	5	1	-	-	-	-	-	42
3-4	2	19	33	22	8	2	-	-	-	-	-	86
2-3	6	44	65	36	11	2	-	-	-	-	-	164
1-2	20	99	107	46	11	2	-	-	-	-	-	285
0-1	91	164	92	24	4	1	-	-	-	-	-	375
TOTAL												

ZERO CROSSING PERIOD (s)

SOUTH WEST

PERCENTAGE OF OBS = 15.79%

SIGNIFICANT WAVE HEIGHT (m)	<4	4-5	5-6	6-7	7-8	8-9	9-10	10-11	11-12	12-13	>13	TOTAL
TOTAL	122	341	330	154	45	10	2	-	-	-	-	1000
>14	-	-	-	-	-	-	-	-	-	-	-	-
13-14	-	-	-	-	-	-	-	-	-	-	-	-
12-13	-	-	-	-	-	-	-	-	-	-	-	-
11-12	-	-	-	-	-	-	-	-	-	-	-	-
10-11	-	-	-	-	-	-	-	-	-	-	-	-
9-10	-	-	-	-	-	-	-	-	-	-	-	1
8-9	-	-	1	1	-	-	-	-	-	-	-	2
7-8	-	-	1	1	1	-	-	-	-	-	-	4
6-7	-	1	3	3	1	-	-	-	-	-	-	8
5-6	-	2	6	5	2	1	-	-	-	-	-	17
4-5	1	7	14	11	5	1	-	-	-	-	-	38
3-4	2	18	33	22	8	2	-	-	-	-	-	85
2-3	7	48	70	39	12	2	-	-	-	-	-	179
1-2	25	115	121	50	12	2	-	-	-	-	-	324
0-1	87	150	82	21	3	-	-	-	-	-	-	344
TOTAL												

ZERO CROSSING PERIOD (s)

SOUTH

PERCENTAGE OF OBS = 14.12%

SIGNIFICANT WAVE HEIGHT (m)	<4	4-5	5-6	6-7	7-8	8-9	9-10	10-11	11-12	12-13	>13	TOTAL
TOTAL	111	327	335	164	49	11	2	-	-	-	-	1000
>14	-	-	-	-	-	-	-	-	-	-	-	-
13-14	-	-	-	-	-	-	-	-	-	-	-	-
12-13	-	-	-	-	-	-	-	-	-	-	-	-
11-12	-	-	-	-	-	-	-	-	-	-	-	-
10-11	-	-	-	-	-	-	-	-	-	-	-	-
9-10	-	-	-	-	-	-	-	-	-	-	-	1
8-9	-	-	-	1	-	-	-	-	-	-	-	2
7-8	-	-	1	1	1	-	-	-	-	-	-	3
6-7	-	1	2	2	1	-	-	-	-	-	-	7
5-6	-	2	5	5	2	1	-	-	-	-	-	15
4-5	1	6	13	11	5	1	-	-	-	-	-	38
3-4	2	17	33	24	9	2	-	-	-	-	-	88
2-3	6	47	74	44	14	3	1	-	-	-	-	188
1-2	22	110	124	55	14	2	-	-	-	-	-	326
0-1	81	144	82	22	4	-	-	-	-	-	-	333
TOTAL												

ZERO CROSSING PERIOD (s)

SOUTH EAST

PERCENTAGE OF OBS = 10.08%

SIGNIFICANT WAVE HEIGHT (m)	<4	4-5	5-6	6-7	7-8	8-9	9-10	10-11	11-12	12-13	>13	TOTAL
TOTAL	185	386	290	110	27	5	1	-	-	-	-	1000
>14	-	-	-	-	-	-	-	-	-	-	-	-
13-14	-	-	-	-	-	-	-	-	-	-	-	-
12-13	-	-	-	-	-	-	-	-	-	-	-	-
11-12	-	-	-	-	-	-	-	-	-	-	-	-
10-11	-	-	-	-	-	-	-	-	-	-	-	-
9-10	-	-	1	1	-	-	-	-	-	-	-	2
8-9	-	1	1	1	-	-	-	-	-	-	-	4
7-8	-	1	2	2	1	-	-	-	-	-	-	6
6-7	-	2	4	3	1	-	-	-	-	-	-	11
5-6	1	5	8	5	2	-	-	-	-	-	-	21
4-5	1	10	15	9	3	1	-	-	-	-	-	39
3-4	4	22	29	15	4	1	-	-	-	-	-	75
2-3	10	49	55	24	6	1	-	-	-	-	-	146
1-2	33	112	92	32	6	1	-	-	-	-	-	276
0-1	137	184	82	17	2	-	-	-	-	-	-	422
TOTAL												

ZERO CROSSING PERIOD (s)

TABULATED PROBABILITIES ARE IN PARTS PER THOUSAND OF THE POPULATION IN EACH TABLE

Fig. 4 Typical Page of Data from Global Wave Statistics.

TANKER BASED PRODUCTION AND STORAGE SYSTEMS

by

NEIL S. MILLER

GLASGOW

TANKER BASED PRODUCTION AND STORAGE SYSTEMS

INTRODUCTION

The factors which govern the size of floating production and storage units have been briefly discussed in the introductory lecture. The following material assumes that a new purpose built vessel is to be used. Some of the ideas are applicable to the analysis of existing tankers if it is proposed to look for a conversion. However in such a case it is probably more important to look closely at the present condition of the ship's structure and equipment rather than its motion behaviour.

Recent changes in IMO regulations regarding the need for a double skin approach to reduce the possibility of an oil outflow following a collision or a grounding may well become mandatory for floating production vessels and can affect the use of existing tankers. Although tankers may have to have double bottoms there appears to be little advantages in having a double bottom in an FPSO since it is never likely to ground while loading with oil. Double bottom tanks involve a poorer use of the steel than if it is concentrated in the outer shell and adds considerably to inspection and repair difficulties. For these reasons they should be avoided.

The wing ballast tanks must have sufficient capacity to give the vessel a draft which will ensure it is unlikely to have a 'bow out' condition and slamming at its light operating draft. It is also undesirable to have any large change in draft between the light and loaded condition because of the effect of such changes on the mooring stiffness and response.

Thus it will be usual to retain the ballast water in the wing tanks while the normal export cargo is being loaded and only pump it out when bad weather leads to a delay in the shuttle tanker connecting and extra days output must be stored. In this way there will be little change in draft during the export downtime period. During the majority of the time the ballast tanks will be full and corrosion inhibiting measures can be at their most effective.

The above considerations govern the required volumes for both ballast and oil storage.

Although a number of different single point mooring systems have been used in the past modern design practice is increasingly towards some form of turret mooring. In sea areas with very stormy conditions either the turret is installed within the forward 25% of the length in order to reduce the combined effects of

pitch and heave on the risers or some form of disconnectable turret is used and a disconnection made when motion levels exceed some preset value.

The mechanical design of the turret and its integration into the main structure of the vessel is best carried out by a specialist contractor and is not considered here. Some companies have designed large turrets which incorporate either drilling or work-over facilities, e.g. the PETROJARL, but this leads to a large weight increase with more complex bearing arrangements.

Since the turret must incorporate some form of swivel plus other piping connections it represents one of the potential risk areas in the design. For this reason ideally the accommodation should be at the forward end with the turret and all production and storage facilities aft of it so that it will always weathervane to be up wind of any fire or gas leakage.

Additionally two azimuthing thrusters should be fitted aft so that in the event of a fire the vessel can be turned to a heading which will send the flames over the side. These thrusters, which need not have high power since they have a large leverage to the turret, can also be very beneficial in reducing mooring loads due to slow drift forces. This will be discussed further in the lectures on mooring.

They are also of benefit during the export operations as they can steady the heading of the FPSO and make it easier for the shuttle tanker to follow it's motion. Finally they can provide steerage way on the FPSO in the event of a catastrophic failure of the moorings.

Such an event is unlikely with a multi-line catenary system where the breaking of any single line will be noted and some remedial action taken. Mooring systems which rely on a single mechanical joint have a poor history of reliability and it is important that thrusters be available on such units.

Thus a typical purpose built vessel might look as shown in Fig. 1. but many variations are possible.

THE EFFECT OF PRINCIPAL DIMENSIONS ON THE MOTION CHARACTERISTICS OF A RECTANGULAR BARGE.

The following analysis applies strictly to a rectangular barge. In practice it is desirable to apply some rounding at the bow and stern in order to reduce current and wind loading but a purpose built vessel will have a block coefficient between 0.90 and 0.92 compared to tankers with coefficients in the range of 0.80 and 0.85. It is normal to apply some rounding at the bilge for constructional reasons but a bilge

keel must then be fitted to reduce rolling and this would be avoided by a rectangular bilge. These changes from the purely rectangular vessel have little effect on the motion characteristics and the following theory has been found applicable to the initial design of tankers and bulk carriers.

The most important factors determining the motion behaviour are:

1. the natural periods of motion
2. the shape of the heave force and pitch moment curves.

These depend primarily on the choice of principal dimensions although the mass distribution with the vessel has an influence on the pitch behaviour. However to main low still water shear forces and bending moments the internal mass must be nearly equal to the external water pressure so that the mass distribution is also largely fixed by the geometry.

There is little interaction between pitch and heave and both may be treated as linear single degree of freedom systems. The objectives of a good design are to get the natural motion periods longer than the peak period of the spectra which is exceeded for less than 2% of the time and to get low heave forces and pitch moments at all shorter periods.

As indicated earlier the heave natural period:

$$T_H = 2\pi\left[\frac{M + M_{AVM}}{\rho g A_W}\right]^{1/2} \qquad (1)$$

For a rectangular vessel this becomes:

$$T_H = 2\pi\left[\frac{\rho LBT + \frac{\pi}{2}\rho\left(\frac{B}{2}\right)^2 C_V L}{\rho g LB}\right]^{1/2}$$

$$= \frac{2\pi}{g^{1/2}}\left[T + \frac{\pi}{8}BC_V\right]^{1/2} \qquad (2)$$

where L,B and T are the length, breadth and draft of the barge respectively and Cv is the added virtual mass coefficient. It depends on the ratio of B/2T in the following manner:

B/2T	0.1	0.2	0.5	1	2	5	10
C_V	2.23	1.98	1.70	1.51	1.38	1.21	1.14

These values apply to an infinite frequency and strictly they are frequency dependent, but since the added mass affects both mass and exciting force/moment terms in the equations of motion the neglect of this effect has a small influence on the motions.

The pitch natural period:

$$T_p = 2\pi\left[\frac{I_L + I_{AVM_L}}{\rho g \nabla GM_L}\right]^{1/2} \tag{3}$$

If the mass is assumed to be evenly distributed:

$$I_L = \frac{1}{12}(\rho LBT)L^2 \tag{4}$$

$$I_{AVM_L} = \frac{1}{12}\left(\rho\frac{\pi}{2}\left(\frac{B}{2}\right)^2 C_V L\right)L^2 \tag{5}$$

$$\nabla = LBT \tag{6}$$

For a barge of the type being considered GM_L is approximately equal to BM_L i.e. the height of the longitudinal metacentre above the centre of buoyancy.

$$\text{Thus } GM_L = BM_L = \frac{\frac{1}{12}BL^3}{LBT} = L^2/12T \tag{7}$$

$$\text{and} \qquad T_p = 2\pi\left[\frac{\frac{1}{12}\rho\left(L^3BT + \frac{\pi}{\theta}B^2L^3C_V\right)}{\rho gLBT.\frac{L^2}{12T}}\right]^{1/2}$$

$$= \frac{2\pi}{g^{1/2}}\left[T + \frac{\pi BC_V}{8}\right]^{1/2} \tag{8}$$

Generally the centre of gravity will be above the centre of buoyancy so that equation (8) will slightly underestimate the pitch period.

It is important to note that the expressions for the two periods are identical and depend purely on the breadth and draft i.e. they are not affected by the length.

The formula can be written in the form:

$$T_H, T_P = \frac{2\pi T^{1/2}}{g^{1/2}}\left[1+\frac{\pi}{8}\frac{B}{T}C_V\right]^{1/2} \qquad (9)$$

Table 1 gives typical values of these variables. From this Table it can be seen that to get long periods one must have a deep draft but even then it is difficult to get a natural period greater than the spectral peak period which is only exceeded for 2% of the time. If a period greater than 12 secs is to be achieved the breadth must be greater than 40 m. The minimum length/breadth ratio will be close to 5 so this infers a length of 200 m which will give a storage capacity around 50,000 tonnes and confirms that this is about the minimum size for the North Sea. To achieve a 14 sec period requires a beam greater than 60 m and a draft greater than 16m which infers a length around 300 m and a displacement greater than 260,000 tonnes. It has to be a large field to justify such capital expenditure.

EXCITING FORCES AND MOMENTS AND DYNAMIC RESPONSE

The principal forces affecting the dynamic behaviour are those due to pressure and inertia effects. Velocity forces are low compared to these and can be ignored except in rolling where viscous effects contribute greatly to the damping. The equations for the exciting forces and moments and the heave and pitch dynamic response are given in Appendix 1.

The pressure and inertia inertia forces will generally act in opposite directions as shown in Fig 2. Under a wave crest there will be an upward pressure force on the bottom of the hull but the inertia forces act in the downward direction because of the direction of the wave particle acceleration. The reverse is true in a wave trough.

The heave exciting force due to pressure plus inertia effects is:

$$F_H = \rho g a_o e^{-kT} B\left[\frac{\lambda}{\pi}-\frac{\pi B C_V}{4}\right]\sin\frac{\pi L}{\lambda}\cos kct \qquad (10)$$

where a_0 = wave amplitude

λ = wave length

k = $2\pi/\lambda$ = wave number

c = wave velocity = $\left(g/k\right)^{1/2}$

t = time

TABLE 1: Values of Heave/Pitch Natural Periods for Various B/2T Ratios and Drafts

B/2T	C_v	$\left[1+\frac{\pi B C_v}{8T}\right]^{1/2}$	T = 12 m		T = 13 m		T = 14 m		T = 15 m		T = 16 m	
			T_H, T_p(Secs)	B (m)	T_H, T_p(Secs)	B (m)	T_H, T_p(Secs)	B (m)	T_H, T_p(Secs)	B (m)	T_H, T_p(Secs)	B (m)
1.4	1.43	1.60	11.1	33.6	11.6	36.4	12.0	39.2	12.4	42.0	12.8	44.8
1.6	1.40	1.66	11.5	38.4	12.0	41.6	12.5	44.8	12.9	48.0	13.3	51.2
1.8	1.38	1.72	12.0	43.2	12.4	46.8	12.9	50.4	13.4	54.0	13.8	57.6
2.0	1.36	1.77	12.3	48.0	12.8	52.0	13.3	56.0	13.8	60.0	14.2	64.0

The pitch exciting moment is:

$$M_P = \rho g a_o B e^{-kT} \frac{L}{2}\left[\frac{\lambda}{\pi} - \frac{\pi B C_v}{4}\right]\left[\cos\frac{\pi L}{\lambda} + \frac{\lambda}{\pi L}\sin\frac{\pi L}{\lambda}\right]\sin kct \qquad (11)$$

From equations (10) and (11) the following points may be noted:

(1) Both the heave force and the pitch moment are zero when:

$$\lambda = \frac{\pi^2 B C_v}{4} \qquad (12)$$

At this wave length the pressure and inertia forces cancel one another. This length does not depend on the ship length but on the breadth and draft as indicated by Table 2.

Table 2: Variation of λ/B ratio to give Zero Heave Force and Pitch Moment for various B/2T Ratios

$B/2T$	C_v	λ/B
0.5	1.70	4.19
1.0	1.51	3.72
2.0	1.36	3.36
3.0	1.29	3.18

(2) The heave force is zero when $L/\lambda = 1,2$ and 3 ($\sin(\pi L/\lambda = O)$ and there are one, two, or three wave lengths in the vessel length.

(3) The pitch moment is zero when $\tan\pi L/\lambda = \pi L/\lambda$ which is approximately true when $L/\lambda = 1.43, 2.46, 3.47$.

(4) Both the heave and pitch expressions have the term e^{kT} which indicates that the forces and moments will be reduced by an increased draft.

Thus the designer has four wave lengths for both heave and pitch where the force or moment will be zero. One of these wave lengths is the same for both motions. It is important to select a combination of dimensions which gives the best spread of these zeros along the frequency axis for the particular sea area. Dimensions which makes the zero due to pressure/inertia cancellation coincide

with one of the other zeros due to balance of the forces in the trough and crest represents a poor design.

It is shown in textbooks on vibration that the response of a single degree of freedom system to a harmonic exciting force FCoswt is given by the equation (see Fig. 3)

$$x = \frac{\frac{F}{k}\cos(\omega t - \phi)}{\left[\left(1-\left(\frac{\omega}{\omega_n}\right)^2\right)^2 + \left(2\gamma\frac{\omega}{\omega_n}\right)^2\right]^{1/2}} \tag{13}$$

where
- x = displacement from the at rest position
- F = exciting force(moment)
- K = spring stiffness of the system
- ω_n = the natural frequency of the system
- γ = is the ratio of the damping of the system to its critical damping $2m\omega_n$ where m is the complete mass of the system

ϕ is the phase angle and is given by the expression:

$$\phi = \mathrm{Tan}^{-1}\left[\frac{2\gamma\frac{\omega}{\omega_n}}{1-\left(\frac{\omega}{\omega_n}\right)^2}\right] \tag{14}$$

If the values for the exciting heave force and pitch moment, the natural frequencies in heave and pitch and the relationship between wave frequency and wave length are inserted in equations 13 and 14, the following formulae result:

$$\text{Heave response} = \frac{\frac{\lambda}{L}a_o e^{-kT}\left(\frac{\lambda}{\pi} - \frac{\pi BC_v}{4}\right)\sin\frac{\pi L}{\lambda}\cos(\omega t - \phi)}{\left[\left(\lambda - 2\pi\left(T + \frac{\pi BC_v}{8}\right)\right)^2 + 8\gamma^2\lambda\pi\left(T + \frac{\pi BC_v}{8}\right)\right]^{1/2}} \tag{15}$$

$$\text{Pitch response} = \frac{6\frac{\lambda}{L}\frac{a_o}{L}e^{-kT}\left(\frac{\lambda}{\pi} - \frac{\pi BC_v}{4}\right)\left(-\cos\frac{\pi L}{\lambda} + \frac{\lambda}{\pi L}\sin\frac{\pi L}{\lambda}\right)\sin(\omega t - \phi)}{\left[\left(\lambda - 2\pi\left(T + \frac{\pi BC_v}{8}\right)\right)^2 + 8\gamma^2\lambda\pi\left(T + \frac{\pi BC_v}{8}\right)\right]^{1/2}} \tag{16}$$

$$\text{Heave Phase Angle} \quad \phi_4 = \text{Tan}^{-1} \frac{2\gamma\left[2\pi\lambda\left(T + \frac{\pi}{8}BC_v\right)\right]^{1/2}}{\left[\lambda - 2\pi\left(T + \frac{\pi BC_v}{8}\right)\right]} \tag{17}$$

The expression for the phase angle for pitch is the same as for heave, but since the pitch is 90° out of phase to the heave (equations 15,16) the phase angles to the wave crest are also always 90° different (pitch lagging heave by 90°)

The first term in this denominator gives an expression for the wave length corresponding to the natural frequency and could be deduced from equation (2):

$$\lambda = 2\pi\left(T + \frac{\pi BC_v}{8}\right)$$

$$\text{or } \lambda = 2\pi T\left(1 + \frac{\pi B}{T}\frac{C_v}{8}\right) \tag{18}$$

Equations (15) to (17) can form the basis of a program to determine the heave/pitch characteristics of any rectangular barge.

Equations (15) to (17) can be rewritten in a form which non-dimensionalises the expressions within brackets:-

$$\text{Heave Response} = \frac{\frac{\lambda}{\pi L}e^{-\kappa T}\left(1 - \frac{\pi^2 BC_v}{4\lambda}\right)\sin\frac{\pi L}{\lambda}\cos(\omega t - \phi)}{\left[\left(1 - 2\pi\left(\frac{T}{\lambda} + \frac{\pi BC_v}{8\lambda}\right)\right)^2 + 8\gamma^2\pi\left[\frac{T}{\lambda} + \frac{\pi BC_v}{8\lambda}\right]\right]^{1/2}} \tag{19}$$

$$\text{Pitch Response} = \frac{\frac{6}{\pi}\frac{\lambda}{L^2}e^{-\kappa T}\left(1 - \frac{\pi^2 BC_v}{4\lambda}\right)\left(-\cos\frac{\pi L}{\lambda} + \frac{\lambda}{\pi L}\sin\frac{\pi L}{\lambda}\right)\sin(\omega t - \phi)}{\left[\left(1 - 2\pi\left(\frac{T}{\lambda} + \frac{\pi BC_v}{8\lambda}\right)\right)^2 + 8\gamma^2\pi\left[\frac{T}{\lambda} + \frac{\pi BC_v}{8\lambda}\right]\right]^{1/2}} \tag{20}$$

$$\text{Heave Phase Angle} = \text{Tan}^{-1} \frac{2\gamma\left[2\pi\left(\frac{T}{\lambda} + \frac{\pi}{8}\frac{BC_v}{\lambda}\right)\right]}{\left[1 - 2\pi\left(\frac{T}{\lambda} + \frac{\pi}{8}\frac{BC_v}{\lambda}\right)\right]} \tag{21}$$

From these equations it is possible to see that if λ is very large the denominator

tends to 1 in all cases and for heave the numerator tends to 1 also while for pitch it tends to zero (due to trignometric term). The phase angle ϕ tends to 0° i.e. the barge is following the waves up-hill and down-dale with no motion relative to the wave surface.

At the natural frequency, the first term in the denominator becomes zero and the second becomes 2γ. The expression for λ which gives the natural frequency (equation 18) is not compatible with the value of λ which makes the heave force or pitch moment zero (equation 12). The two equations can only be satisfied at zero draft. It is thus impossible to make the exciting forces and moments zero at the natural frequency.

Considering equation (15a), the non-dimensional heave response is going to be reduced by having as large a value of L as possible since none of the other terms, apart from the first contain L. This is even more true for the pitch response per metre wave height since the factor L^2 appears in the denominator. Thus although the natural periods and zero force/moment period are independent of the length, the dynamic response, particularly in pitch, is very dependent on the choice of length in relation to the wave lengths in the area of operation.

DAMPING

The value of γ is obviously very important in determining the level of response at the natural frequency, although as indicated above if L is large, a low response will be obtained. A rectangular box with sharp corners will have very high resistance to heaving and pitching motions. Ideally it would be desirable to avoid round bilges but if these are fitted they should have large bilge keels over the maximum length in order to provide a high degree of roll damping as well as heave/pitch damping.

Since damping is largely due to viscous effects i.e. is a function of the square of the heaving/pitching velocity, it is strictly non-linear and linearisation has to be applied to use equations (15) to (17). From model experiments the damping factor γ is found to vary between 0.06 and 0.09 and for design it would be advisable to use the lower value although this may over-predict the motions.

STATICAL STABILITY AND NATURAL ROLLING PERIOD

The second major factor governing the principal dimensions is the need to ensure an adequate reserve of statical stability while at the same time keeping the rolling period as high as possible. Since the vessel will weathervane about its single point mooring it should normally experience few seas coming from the beam-on

direction but in swell conditions this is a possibility. Such conditions may be much more common off the Australian coast and in the Timor Sea. Swell waves may be generated by storms thousands of miles away and travel in a direction at right angles to the locally prevailing wind and sea conditions. Such a situation can be difficult to handle even if thrusters are available as it is necessary to strike the best balance between mooring loads and motion response.

It is thought that the natural rolling period should be greater than the peak period which is exceeded for 2% of the time. It is possible to get a long rolling period by having a low GM_T but this is undesirable as experience shows that in most oil fields there is a desire to increase the weight of production equipment throughout the field life. Further a purpose built FPSO must be expected to have a life of at least 25 years and perhaps be used on a number of fields which may call for different types and weights of production equipment.

Therefore a new design should have a GM_T in the region of 2 to 3m in both its loaded and ballast conditions.

The production modules will normally be sited on a deck 3m above the main deck for safety reasons. An alternative is to fit an upper double skin ballast tank which is kept permanently filled with water and to have the production units mounted on the main deck.

The natural rolling period is more difficult to estimate than the pitching period due to possible errors in estimating the values of GM_T and the mass inertia. Figure 4 illustrated the changes in mass distribution between the ballast and loaded conditions. The addition of the process equipment above the main deck will increase the mass inertia as will items such as flare stacks, cranes etc.

For a preliminary estimate for the loaded condition it is suggested that the mass be treated as if it is evenly spread over the cross section. Although the oil will be confined to the centre tanks the inertia associated with the process modules and accommodation will have the effect of giving a near even mass distribution.

Assuming that the mass ρBT per section is uniformly spread over a cross section of breadth B and depth D, the mass inertia:

$$I_R = \frac{\rho BT}{12}\left(B^2 + D^2\right) \qquad (22)$$

The added virtual mass inertia of a rectangular section in rolling can be expressed in the form:

$$\frac{1}{2}\rho\pi C_{VR}\left(\frac{B}{2}\right)^4 \qquad \text{per unit length} \qquad (23)$$

where C_{VR} is the added mass coefficient in roll. Over the practical range of B/2T values it is approximately 0.15 so that:

$$I_{AVMR} = \frac{\rho B^4}{67.9} \qquad \text{per unit length} \qquad (24)$$

The centre of gravity of the hull structure is normally below the half-depth due to the heavier plating in the bottom and the effect of heating coils, pumps etc. The effect of the process plant will be to raise this centre but it is not very sensitive to the weight and height as the following example will show.

Suppose 10,000 tonnes of equipment is added 4.5m above the deck of a ship of 85,000 tonnes displacement whose CG is 11m above the keel. If the depth of the ship is 22m the new CG is:

$$\frac{10{,}000 \times 26.5 + 85{,}000 \times 11}{95{,}000} = 12.63\text{m above keel}$$

i.e. the CG has been raised by 1.63m. This figures indicates why a fairly high initial GM_T has been suggested to allow for changes in process equipment in later life.

For preliminary design it is suggested that the CG be assumed 1m above the half-depth. Since the value of BM for a rectangular barge is $B^2/12T$ this gives the following formula for GM:

$$GM_T = \left[\frac{B^2}{12T} + \frac{T}{2} - \left(\frac{D}{2} + 1\right)\right] \qquad (25)$$

This figure will need to be rigorously checked early in the design but it will give an adequate indication of dimensions which are unsuitable either because of too low or too large a value of GM>

Substituting these various values into the general formula for the natural rolling period:

$$T_R = 2\pi\left[\frac{\rho\frac{BTL}{12}\left(B^2 + D^2\right) + \frac{\rho B^4 L}{67.9}}{\rho BTLg\left(\frac{B^2}{12T} + \frac{T}{2} - \left(\frac{D}{2} + 1\right)\right)}\right]^{1/2}$$

or $$T_R = 2\pi\left[\frac{\frac{(B^2+D^2)}{12}+\frac{B^3}{67.9T}}{g\left(\frac{B^2}{12T}+\frac{T}{2}-\left(\frac{D}{2}+1\right)\right)}\right]^{1/2} \qquad (26)$$

e.g. if B = 35m, D = 20m and T = 10m; T_R = 13.8 secs.

As for the other natural periods, the length of the vessel does not enter the formula.

MORE GENERAL DESIGN CONSIDERATIONS

In sea areas where high waves may be expected it is necessary to provide a high freeboard to reduce the possibility of water on deck and poor conditions for staff operating the process plant. A figure of 10m in the loaded condition is typical of North Sea practice but it could be lower in other parts of the world with calmer seas. The resulting high depth tends to give rather more internal volume than is required for the cargo and ballast and this aspect has to be watched.

The question of minimum size has been discussed earlier and in North Sea conditions is about 50,000 tonnes storage (370,000 bbls at 0.85 spec.grav.). This will give a vessel about 200m in length which is the minimum necessary to give reasonable pitch motions and an export downtime of no more than 4 days in severe weather. Such an FPSO can cope with an output up to 60,000 bbls/day with 3 to 4 days excess storage provided the shuttle tankers (two) round trips vary from 3 to 7 days which is typical of North Sea conditions. This implies that for fields with lower outputs the vessel size is dictated by motion criteria and that it will have excess capacity for the field output with shuttle tankers calling as required.

The high freeboard requirement indicates a relatively deep vessel compared to equivalent capacity tankers. Its length is likely to be less due to the high internal volume and high block coefficient. Structurally this is very beneficial as the wave bending moments (BM) is a function of $BL^{2.3}$ to $BL^{2.5}$ and thus increases rapidly with length. As a result of all these factors high tensile strength steels with consequential worries about corrosion margins can be avoided in the deck and bottom plating. High quality steels must be used, i.e. no grade A mild steels, in order to achieve the necessary fatigue life. Great attention must be paid to corrosion prevention measures and provision made for easy inspection (and if necessary repair) of the internal structure.

A higher degree of subdivision than is normal in tankers may be required in order to achieve low levels of still water bending moments during the loading and,

if necessary, deballasting process. The sequences for these operations must be worked out very carefully beforehand and incorporated in the control system so that it is impossible to cause an accidental overload of the hull girder. Provision must be made for inspection and maintenance of all tanks including a system of isolation valves which will ensure that no oil can enter the tank concerned during these operations.

The natural periods of the oil in the storage tanks must be checked for both pitching and rolling motion at a number of levels to ensure that the chosen length and breadth of each tank does not produce undesirable synchronism with the vessel periods. All bulkheads must be designed against fluid impact forces.

SUMMARY OF PRELIMINARY DESIGN OBJECTIVES

Before going on to consider a design example it is worth while summarising some of the design objectives in this complex problem:

(1) The storage volume must be capable of taking the output during the average interval between shuttle tanker calls plus 3.5 days.

(2) The value of GM must be around 3m in the loaded condition with the process plant and all associated equipment on board.

(3) The natural rolling period must be greater than 12 secs.

(4) The natural pitching and heaving periods must be as long as possible.

(5) The zero force frequencies for heave and pitch must be spread out as much as possible to give a good motion response.

(6) From structural considerations L/D must be less than 13.

(7) The underdeck volume should be no greater than 1.8 times the displacement in order to accommodate the segregated ballast and produced water storage capacity.

(8) The external surface area should be as small as possible consistent with the above requirements. This implies low values of L/B and L/D.

Design Example

The example chosen is that of an FPSO having a storage capacity of 500,000

bbls with specific gravity of 0.87 i.e. a deadweight of approximately 70,000 tonnes. This corresponds to 11 days output at 45,000 bbls per day and use of a single shuttle tanker.

The mass of process plant is estimated at 15,000 tonnes and the vessel lightweight (structure, accommodation, basic power plant, pumps, metering) at 25,000 tonnes giving a loaded displacement of 110,000 tonnes.

Table 3 gives the results of an analysis of a range of dimensions to produce the above displacement.

It begins with three choices of draught 11, 13 and 15 m which have been supplemented at a later stage by a set at 14 m. For each draft a series of lengths have been chosen with the lowest length in each case being 200 m corresponding to a wave period of 11.3 secs. The values of the breadth B were calculated to give the correct displacement assuming a block coefficient of 0.90. The depth D was based on a freeboard of 10 m in all cases.

From these figures and using the assumptions outlined above the values of KM_T, and T_R, the rolling period were calculated. For the 11 m draught the values of GM_T are very high leading to low values of T_R and the first two designs have been rejected for too low periods. For the 15 m design the values of GM_T are low and the last two designs in this group have been eliminated for this reason.

The next two columns gives the ratio of B/2T and the corresponding value of C_V determined from the curve in Fig. 5. This enables the wave length $[\pi^2 BC_V / 4]$ where the pressure and inertia forces will cancel giving zero heave force and pitch moment to be determined. The next three columns give the values of the wave lengths where the heave forces are zero due to balance of the forces in the crest and trough. Examining these figures it can be seen that for the remaining design at 11m draught two of the zeros (145.5 m and 125 m) are close together compared to the first case at 13 m draught (156.2 and 100 m). For longer vessel lengths the separation decreases.

The following two columns give the additional zeros in the pitch moment. The separation of the zeros is much smaller than for heave and it will be noted that the order in which they occur changes as the length increases. The best separation is achieved at the longest length for each draught. For the 15 m draught there is a very poor separation for the only design left in this section and it should be dismissed at this stage.

The next two columns give the heave and pitch natural periods in seconds

and expressed as the corresponding wave length. There is a very small range of values with the shorter vessels always giving the longest period. However, since the pitch stiffness is a function of the length this may not produce the best response.

The remaining columns all give measures of the economic efficiency of the design since low values of L/B, L/D, hull volume and hull area all indicate low capital costs. The indications are that a deep draught short vessel will be the most economic, as one might expect, since it gets nearest to the sphere which might be the ultimate on this consideration alone.

Overall it is clear that in this case the 13 m draught provides the best design balance with the suggestion that some increase in this draft could be beneficial. For this reason the set of results at 14 m draught were added. This produces only one viable design. The best combination will be with a draught somewhere between 13 and 14 m and a length near to 200 m although this may give a poor pitch response and it may need to be lengthened for this reason.

The motion performance of the three 13 m draught designs is shown in Figs. 6 and 7. Figure 6 showing the heave response indicates the very good behaviour which can be obtained for wave lengths shorter than the natural heaving period and that at longer wave lengths the R.A.O. is always below 1 m/m.

The pitch response curves (Fig. 7) show the improvements which are obtained by increasing length but if the natural period is low enough very good response characteristics can be obtained.

APPLICATION OF THEORY TO PRACTICAL FORMS

In practice it is necessary to apply some rounding at the bows to reduce wind, current and wave drift loads. At the stern a cut up must be fitted in order to accommodate the azimuthing thrusters. A circular bow tends to produce undesirable hydrodynamic instabilities so it is suggested that a parabolic ending be applied which extends 0.18B forward of the rectangular block form and extends 0.36B aft of this point. A similar extension (0.18B) is suggested at the aft end to accommodate the cut-up so that the total length is now:

$$= L + 0.36B$$

where L is the length of the best rectangular block design.

This extension of the length will improve the pitch performance over that of the rectangular block.

SUMMARY

A series of formulae have been produced which enables an initial set of dimensions to be chosen for an FPSO to meet specific field output and environmental conditions. It is emphasised that for fields with large outputs (60,000 bbls/day) a very careful analysis must be made of the shuttle tanker sizes, numbers and schedules in order to arrive at the necessary size of storage unit. This should be as small as possible so long as it has a storage capacity greater than 50,000 tonnes plus 3.5 days output. These figures which are governed by motion considerations apply to North Sea conditions and smaller vessels may be acceptable in calmer areas of the world.

TABLE 3: Analysis of Different Rectangular Block Designs for a Displacement of 110,000 Tonnes

T m	L m	B m	D m	KM m	GM_T m	T_R Secs	B/2T	C_V	HEAVE ZERO $\frac{\pi^2 BC_v}{4}$ m	HEAVE ZERO L m	HEAVE ZERO L/2 m	HEAVE ZERO L/3	PITCH ZERO $\frac{L}{1.43}$	PITCH ZERO $\frac{L}{2.46}$	T_H, T_P Secs	$T_H T_P$ m	L/B	L/D
11	210	51.62	21	25.69	14.19	11.20	-	-										
11	230	47.13	21	22.45	10.95	11.53	-	-										
11	250	43.36	21	19.74	8.24	12.16	1.97	1.36	145.5	250	125	83.3	174.8	101.6	11.72	214.4	5.76	11.90
13	200	45.86	23	19.98	7.48	13.30	1.76	1.38	156.2	200	100	66.7	139.9	81.3	12.34	237.7	4.36	8.70
13	220	41.69	23	17.64	5.14	14.57	1.60	1.40	144.0	220	110	73.3	153.8	89.4	12.02	225.6	5.28	9.56
13	240	38.22	23	15.86	3.36	16.56	1.47	1.42	133.9	240	120	80.0	167.8	97.6	11.75	215.6	6.28	10.43
15	200	39.75	25	16.28	2.78	18.84	1.325	1.44	141.2	200	100	66.7	139.9	81.3	12.28	235.4	5.03	8.00
15	220	36.13	25	14.75	1.25	-	-											
15	240	33.12	25	13.59	0.09	-	-											
14	210	40.55	24	16.78	3.78	16.48	1.45	1.42	142.1	210	105	70.0	146.8	85.4	12.13	229.7	5.17	8.75
14	220	38.71	24	15.92	2.92	17.95	1.38	1.43	136.6	220	110	73.3	153.8	89.4	11.99	224.4	5.68	9.17
14	230	37.03	24	15.16	2.16	-												
14	240	35.49	24	14.50	1.50	-												

TABLE 3 (Cont'd)

	Hull Volume $\times 10^{-3}$ m^3	Hull Area $\times 10^{-3}$ m^3	Comment on Design
11	-	-	T_R too low, GM_T too high
11	-	-	" " " "
11	205	32.18	L/D , L/B too high
13	190	27.54	Good separation of zero
13	190	28.46	
13	190	29.38	
15	179	25.90	GM_T too low, poor separation of pitch zero
15	-	-	
15	-	-	
14	184	27.11	
14	184	27.59	GM_T too low, poor zero separation
14	-	-	
14	-	-	

OUTLINE ARRANGEMENT OF 120,000 DWT FPSU

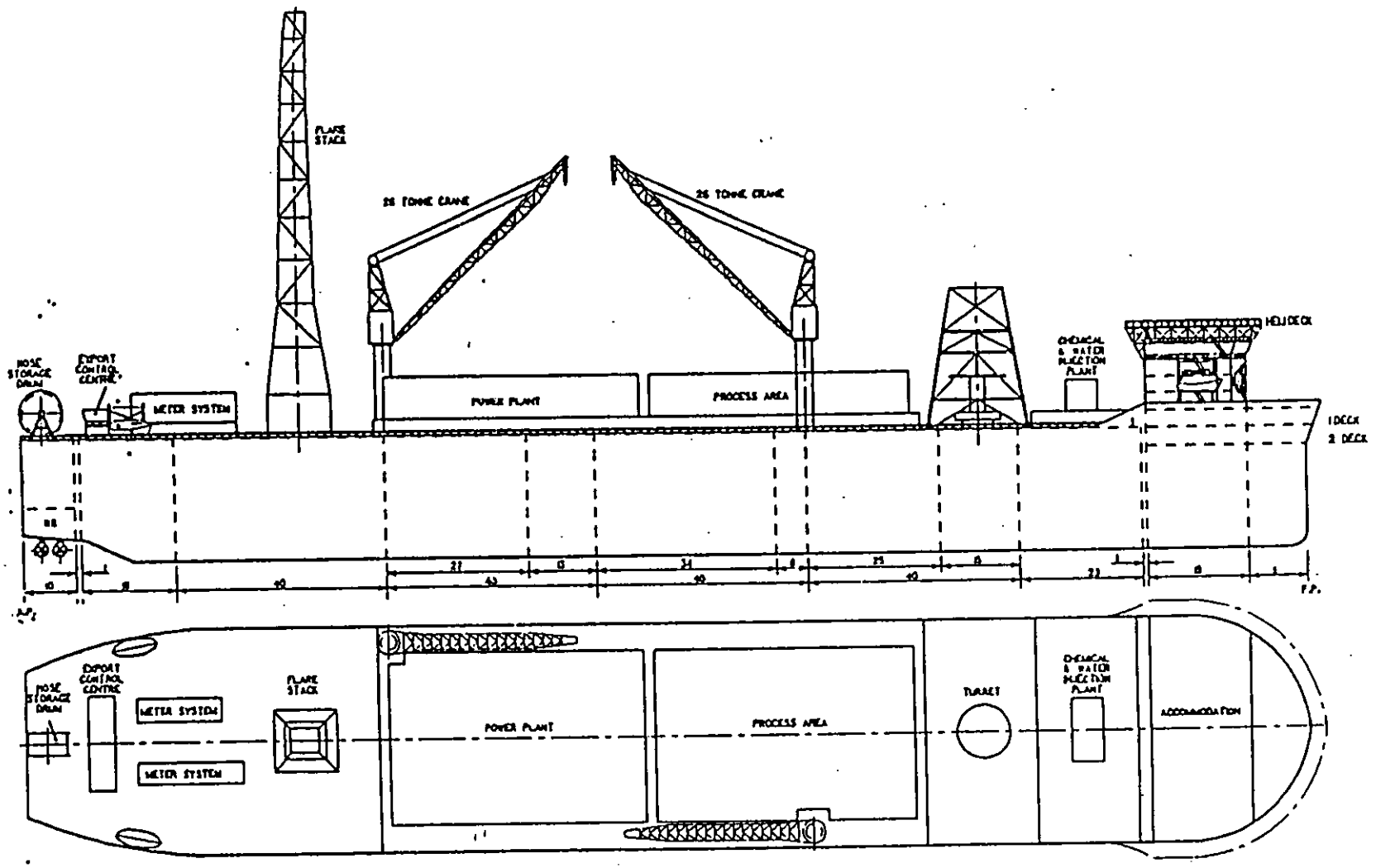

FIG. 1.

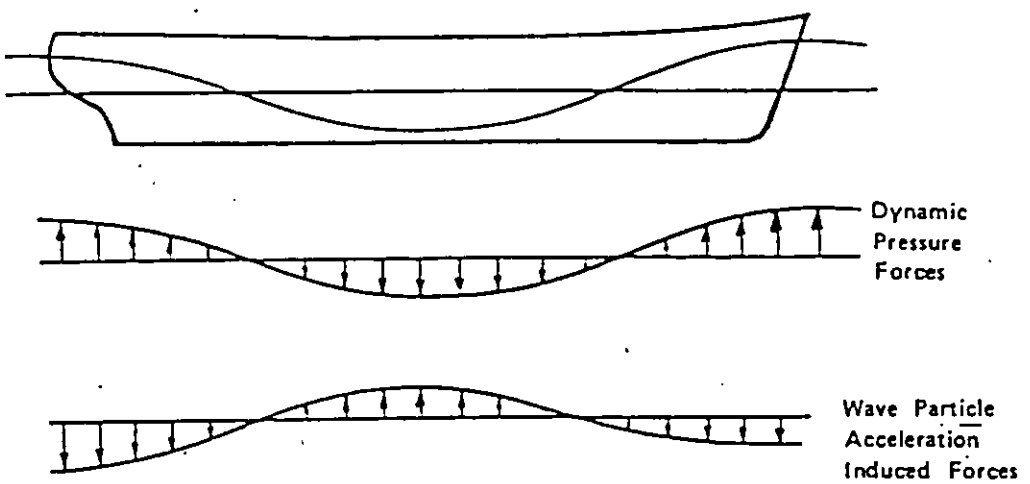

FIG 2 *Wave Force Components on Surface Vessel*

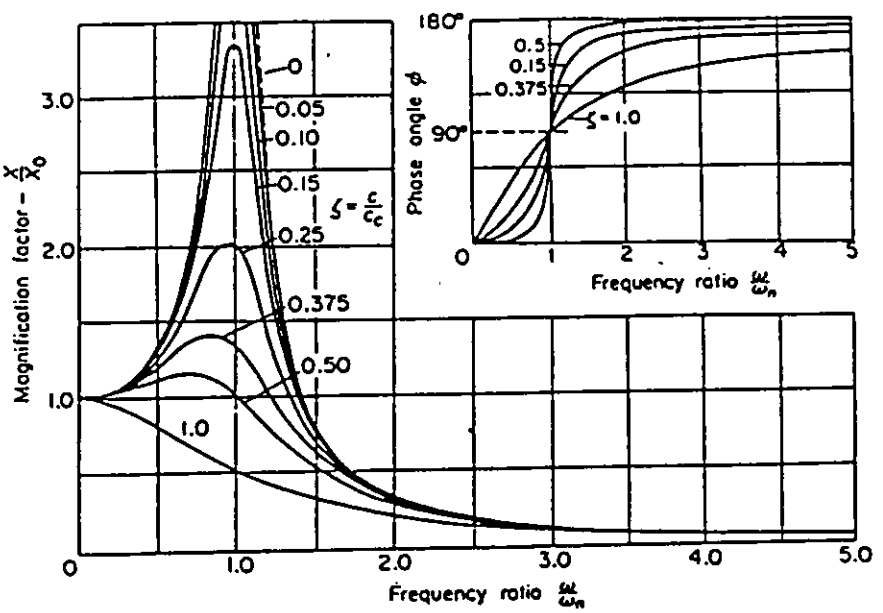

FIG MOTION RESPONSE OF A LINEAR SINGLE DEGREE OF FREEDOM SYSTEM

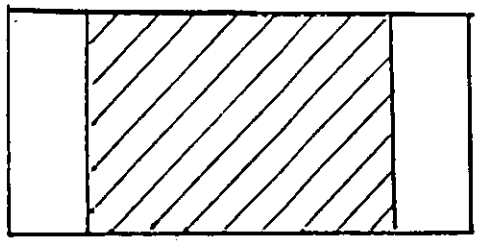

Fig. 4 Change in Cross Section Loading from Ballast to Loaded Condition.

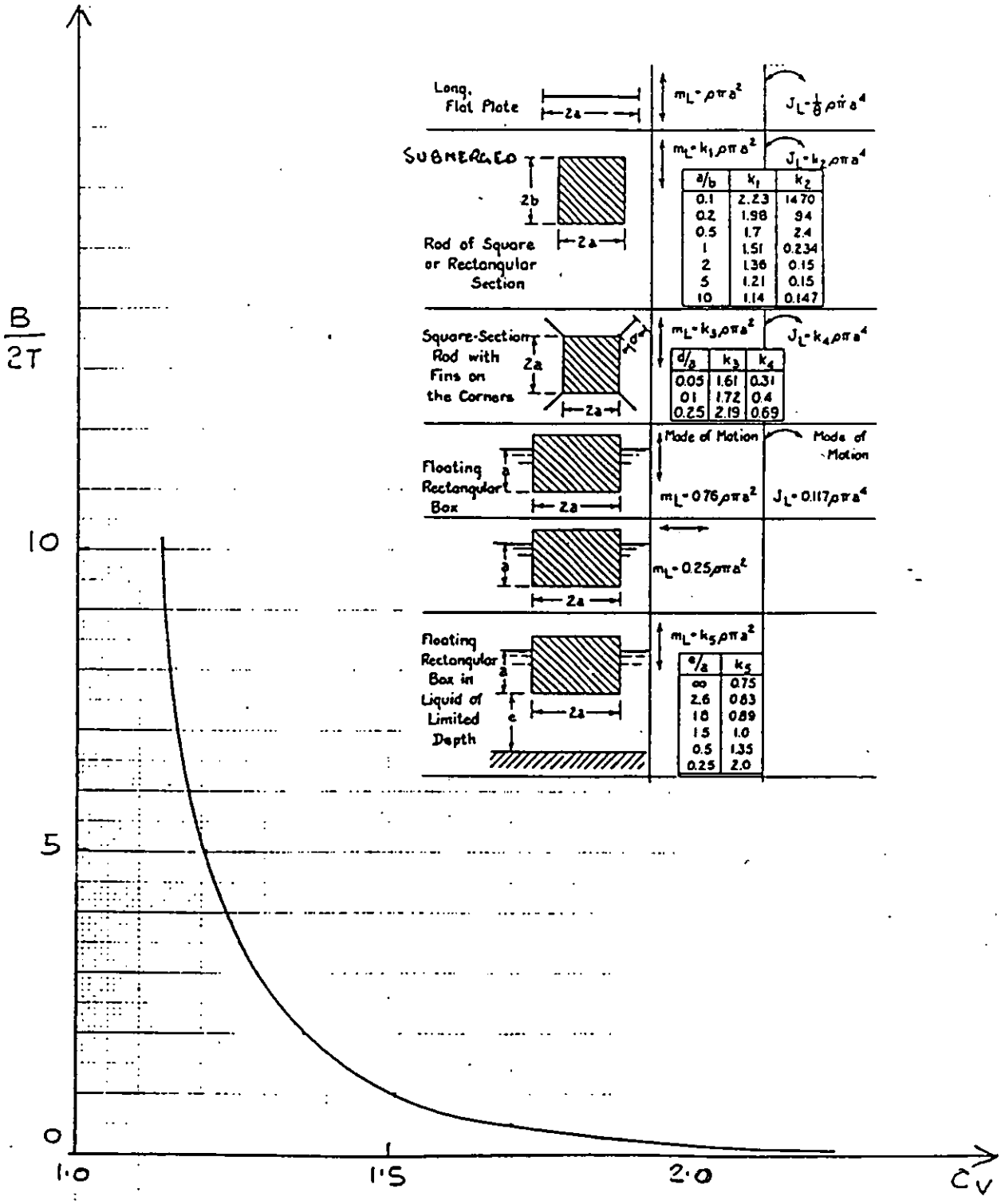

Fig 5. CURVE OF ADDED VIRTUAL MASS COEFF

Figure 6. Heave response for three designs with draft of 13m

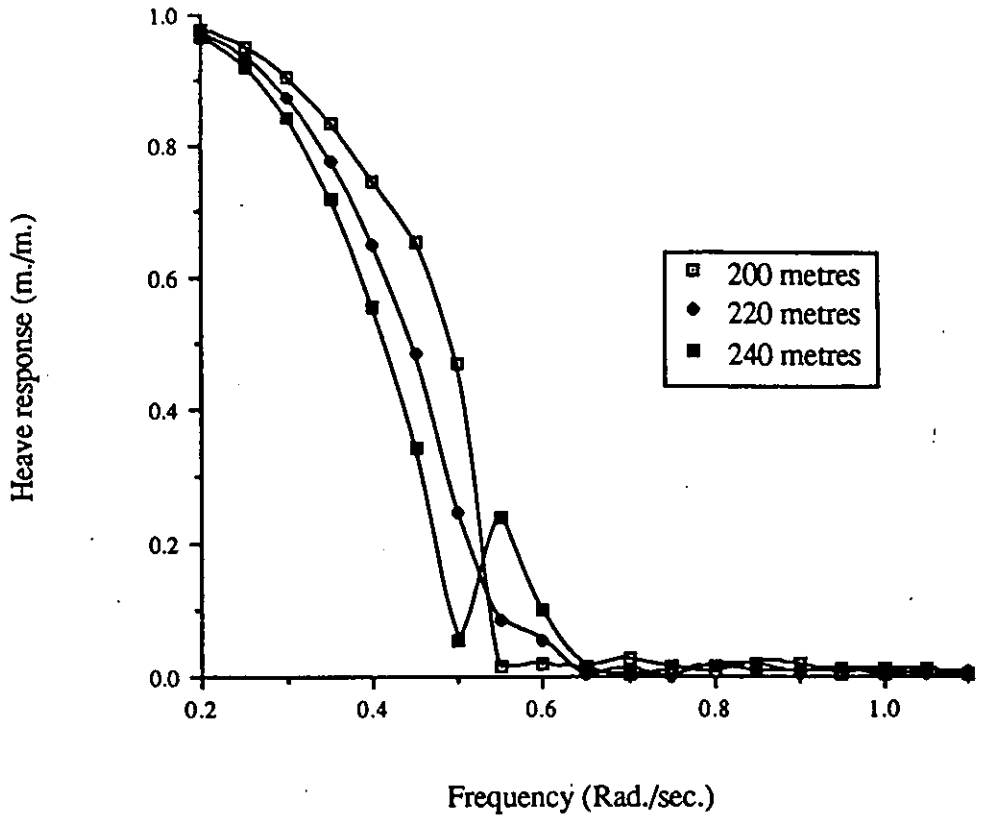

Figure 7. Pitch response for three designs with draft of 13m

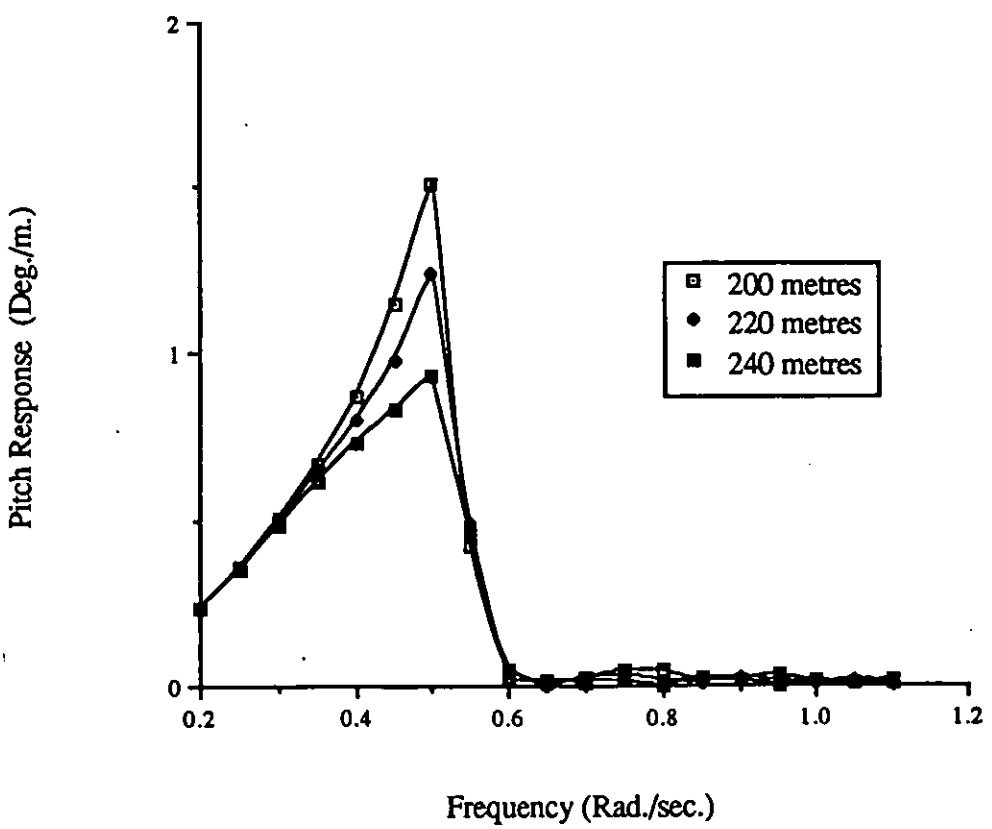

FORCES AND MOMENTS DUE TO WAVES

Waves in Longitudinal Direction - Heaving Forces

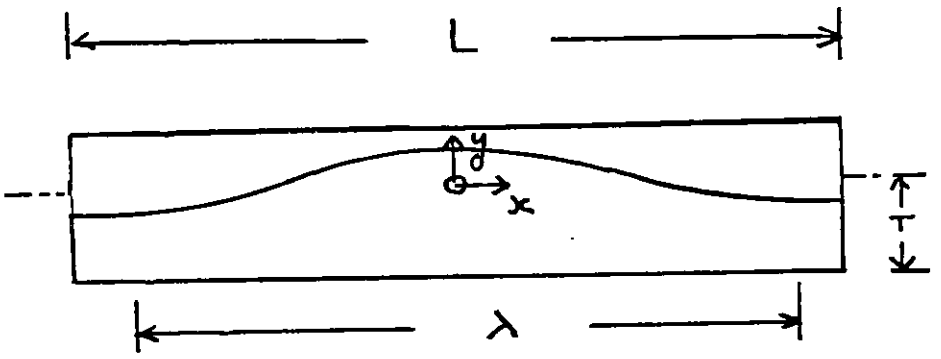

1. To develop the equations it is assumed that the origin of the wave is at the centre of the length and at the still water level. The equation to the wave will be:

$$y = a_o \mathrm{Cos}k(x - ct)$$

where a_o is the wave amplitude

k = $2\pi / \lambda$ where λ is the wave length

c = wave velocity = $[g\lambda / 2\pi]^{1/2}$ (neglecting shallow water effects on the wave)

2. The wave will cause three sets of forces on the hulls:

(a) pressure forces due to change in pressure on the bottom

(b) inertia forces due to the particle accelerations in the wave acting on the added virtual mass

(c) viscous forces due to the particle velocities in the wave acting on the transverse projected area normal to the particle velocity.

The latter are small compared to those due to (a) and (b) and may be neglected in the early design stage.

The dynamic pressure at a depth T below the surface:

$$= \rho g a_o e^{-kt} \mathrm{Cos}k(x-ct)$$

Therefore the heaving force on an element of length dx:

$$= \rho g a_o e^{-kt} \mathrm{Cos}k(x-ct)(Bdx)$$

and the total force $= \rho g a_o B e^{-kT} \mathrm{Cos}k(x-ct)dx$

$$= \rho g a_o B e^{-kT} \left[\int_{-L2}^{+L2} (\mathrm{Cos}kx\mathrm{Cos}kct + \mathrm{Sin}kx\mathrm{Sin}kct) \right] dx$$

$$= 2\rho g a_o \frac{Be^{-kT}}{k} \mathrm{Sin}\frac{kL}{2} \mathrm{Cos}kct \qquad \text{A1}$$

since the Coskx term disappears on the application of the limits.

(d) the vertical component of particle acceleration is:

$$- kga_o e^{-kT} \mathrm{Cos}k(x-ct)$$

the added virtual mass in: $\rho \frac{\pi}{2} \left(\frac{B}{2} \right)^2 C_V dx.$

the vertical inertia force $= -\rho g \frac{\pi}{8} B^2 k a_o C_V e^{-kT} \int_{-L2}^{+L2} \mathrm{Cos}k(x-ct)dx$

$$= -\rho g \frac{\pi}{4} B^2 a_o C_V e^{-kT} \mathrm{Sin}\frac{KL}{2} \mathrm{Cos}kct \qquad \text{A2}$$

Adding the pressure and inertia terms, the heave force:

$$= \rho g a_o B e^{-kT} \left[\frac{2}{k} - \frac{\pi B C_v}{4} \right] \qquad \text{A3}$$

3. The most interesting term is the term in brackets:

$$\left(\frac{2}{K}-\frac{\pi BC_v}{4}\right)$$

4. This term suggests that for any rectangular pontoon it is possible to choose a breadth such that the pressure and inertia heave forces will cancel at a particular wave length.

Pitching Moments

5. The pitching moment due to the pressure forces is given by:

$$\rho g a_o B e^{-kT}\int_{-\frac{1}{2}L}^{+\frac{1}{2}L} x\,\mathrm{Cos}k(x-ct)\,dx$$

where the integral becomes:

$$\int_{-\frac{L}{2}}^{+\frac{L}{2}}(x\mathrm{Cos}kx\mathrm{Cos}kct+x\mathrm{Sin}kx\mathrm{Sin}kct)dx$$

which becomes on integration:

$$\left[\left(x\frac{\mathrm{Sin}kx}{k}+\frac{\mathrm{Cos}kx}{k^2}\right)\mathrm{Cos}kct+\left(-x\frac{\mathrm{Cos}kx}{k}+\frac{\mathrm{Sin}kx}{k^2}\right)\mathrm{Sin}kct\right]_{-\frac{L}{2}}^{+\frac{L}{2}}$$

$$=\frac{1}{k}\left[\left\{-\frac{L}{2}\mathrm{Cos}\frac{kL}{2}-\left(-\frac{L}{2}\right)\mathrm{Cos}\frac{kL}{2}+\frac{1}{K}\left(\mathrm{Sin}\frac{kL}{2}-\mathrm{Sin}\left(\frac{-kL}{2}\right)\right)\right\}\mathrm{Sin}kct\right]$$

and the complete expression becomes:

$$\rho g a_o\frac{Be^{-kT}}{k}\left[-L\mathrm{Cos}\frac{kL}{2}+\frac{2}{k}\mathrm{Sin}\frac{kL}{2}\right]\mathrm{Sin}kct \qquad \text{A5}$$

Similarly the pitching moment due to inertia forces becomes

$$-\rho g a_o\frac{\pi}{8}B^2C_v e^{-kT}\left[-L\mathrm{Cos}\frac{kL}{2}+\frac{2}{k}\mathrm{Sin}\frac{kL}{2}\right]\mathrm{Sin}kct \qquad \text{A6}$$

The complete expression for the pitching moment becomes:

$$\rho g a_o B_e^{-kT}L\left[\left(\frac{1}{K}-\frac{\pi BC_v}{8}\right)\left(-\mathrm{Cos}\frac{kL}{2}+\frac{2}{kL}\mathrm{Sin}\frac{kL}{2}\right)\right]\mathrm{Sin}kct \qquad \text{A7}$$

$$\text{The heave response} = \frac{\text{Heave Force / Heave Stiffness x Cos}(kct+\phi)}{\left[\left(1-\left(\frac{\omega}{\omega_n}\right)^2\right)^2+\left(2\gamma\frac{\omega}{\omega_n}\right)^2\right]^{\frac{1}{2}}}$$

$$\text{The numerator} = \frac{\rho g a_o B e^{-kT}}{\rho g L B}\left[\frac{2}{K}-\frac{\pi B C_V}{4}\right]\text{Sin}\frac{kL}{2}\text{Cos}(kct+\phi)$$

which, on substituting $k = \frac{2\pi}{\lambda}$:

$$= \frac{a_o e^{-kT}}{L}\left[\frac{\lambda}{\pi}-\frac{\pi B C_V}{4}\right]\text{Sin}\frac{\pi L}{\lambda}\text{Cos}(kct+\phi)$$

$$\text{The denominator} = \left[\left(1-\frac{2\pi g/\lambda}{T+\frac{\pi}{8}BC_v}\right)^2+\frac{4\gamma^2\cdot\frac{2\pi g}{\lambda}}{T+\frac{\pi BC_v}{8}}\right]^{\frac{1}{2}}$$

$$= \frac{1}{\lambda}\left[\left(\lambda-2\pi\left(T+\frac{\pi}{8}BC_V\right)\right)^2+8\gamma^2\pi\lambda\left(T+\frac{\pi BC_V}{8}\right)\right]^{\frac{1}{2}}$$

$$\text{Heave Response} = \frac{\frac{\lambda}{L}a_o e^{-kT}\left[\frac{\lambda}{\pi}-\frac{\pi BC_V}{4}\right]\text{Sin}\frac{\pi L}{\lambda}\text{Cos}(kct+\phi)}{\left[\left(\lambda-2\pi\left(T+\frac{\pi BC_V}{8}\right)\right)^2+8\gamma^2\pi\lambda\left(T+\frac{\pi BC_V}{8}\right)\right]^{\frac{1}{2}}} \qquad \text{A8}$$

$$\text{Pitch response} = \left(\frac{\text{Pitch Moment / Pitch Stiffness Sin}(kct+\phi_2}{\text{Same Denominator as for Heave since}}\right.$$

$$(\omega_n)_p = (\omega_n)_H$$

$$\text{Numerator} = \frac{\rho g a_o B e^{-kT} L}{\rho g L B T\frac{L^2}{12T}}\left[\frac{\lambda}{2\pi}-\frac{\pi BC_v}{8}\right]\left[-\text{Cos}\frac{\pi L}{\lambda}+\frac{\lambda}{\pi L}\text{Sin}\frac{\pi L}{\lambda}\right]\text{Sin}kct$$

$$= \frac{6a_o}{L^2}\left[\frac{\lambda}{\pi}-\frac{\pi BC_v}{4}\right]\left[-\text{Cos}\frac{\pi L}{\lambda}+\frac{\lambda}{\pi L}\text{Sin}\frac{\pi L}{\lambda}\right]\text{Sin}kct$$

$$\text{Pitch response} = \frac{\frac{6a_o}{L}\cdot\frac{\lambda}{L}\left[\frac{\lambda}{\pi}-\frac{\pi BC_v}{4}\right]\left[-\mathrm{Cos}\frac{\pi L}{\lambda}+\frac{\lambda}{\pi L}\mathrm{Sin}\frac{\pi L}{\lambda}\right]\mathrm{Sin}kct+\phi}{\left[\left(\lambda-2\pi(T+\frac{\pi BC_v}{8})\right)^2+8\gamma^2\pi\lambda(T+\frac{\pi BC_v}{8})\right]^{1/2}} \qquad \text{A9}$$

$$\text{The phase angle } \phi = \mathrm{Tan}^{-1}\frac{\left[2\gamma\left(\frac{2\pi g}{\lambda}\left(\frac{T+\frac{\pi}{8}BC_v}{g}\right)\right)^{1/2}\right]}{\frac{1}{\lambda}\left[\lambda-2\pi(T+\frac{\pi}{8}BC_v\right]}$$

$$= \mathrm{Tan}^{-1}\frac{2\gamma\left[2\pi\lambda\left(T+\frac{\pi}{8}BC_v\right)\right]^{1/2}}{\left[\lambda-2\pi\left(T+\frac{\pi}{8}BC_v\right)\right]}$$

6. The phase angles for pitch and heave are equal, but since the equation for heave (A8) is a function of Coskct, whereas the equation for pitch (A9) is a function of Sinkct, heave and pitch are always 90° out of phase with the pitch lagging the heave.

THE DESIGN OF BUOY BASED SYSTEMS

by

NEIL S. MILLER

GLASGOW

THE DESIGN OF BUOY BASED SYSTEMS

INTRODUCTION

By far the widest use of buoys has been for carrying the equipment necessary for mooring a storage or export tanker and the associated riser, swivel and hoses. These are generally known as Catenary Anchor Leg Moorings (CALMS). There are a very large number of such installations throughout the world and they have given good service. A number of different designs are in use ranging from simple cylindrical structures, with perhaps a small horizontal bilge keel, to large buoys such as the ELSBM designed for the AUK field which was originally fitted with a sophisticated turntable for the oil loading facilities and with a heli-pad (see Figs 1 and 2)

Due to their relatively small size such buoys will have low natural periods in heave, pitch and roll - somewhere between 6 and 8 secs. for heave - and thus in North Sea conditions will experience severe motions for over 30% of the time in winter months. This caused the abandonment of most of the CALM based offshore loading systems in the 1980's.

The only large buoy installation was the Shell SPAR buoy installed in the Brent field in 1976 to provide a storage and offloading facility. It is still in use although its present storage capacity is below the originally designed 300,000bbls. due to an accidental overload of one of its storage cells.

At the time of the SPAR installation there was considerable interest in large buoy design particularly concrete structures and there are a number of papers describing such ideas from that period.

Recently there has been renewed interest amongst oil companies, consultants and construction firms, in designing buoys which can carry limited amounts of production equipment (see Refs (1) to (3). They are intended for fields with small reserves where production is only expected to last a few years and the production facility can then be moved on to another similar situation.

In other cases larger buoys are being considered with sufficient storage capacity to cover for bad weather delays in export. Because of their increased size such buoys are capable of carrying a greater mass of production equipment. It is also desirable that they provide direct offloading without intermediate facilities.

Thus the advantages which it is hoped to achieve with such designs are:

(1) Low capital cost compared to other vessels to perform the same tasks. The structure may be of steel or concrete.

(2) A multi-point moored system with low mooring forces capable of carrying a number of risers, umbilicals etc. and sufficient deck weight capacity for the necessary production equipment.

(3) An ability to move from field to field as their reserves become exhausted.

(4) Direct offloading without intermediate sub-sea piping plus loading facility.

NATURAL PERIOD, MOTION, STABILITY AND GEOMETRY CONSIDERATIONS.

The simplest form of buoy is to use a circular cylinder. It is instructive to consider some of the basic equations for such a design in order that the changes necessary to create a vessel capable of carrying out the desired tasks can be determined.

Referring to Fig. 3 which shows a circular cylinder of radius R floating at a draught T.

The displaced volume $= \pi R^2 T$ (M^3) (1)

The waterplane area $= \pi R^2$ (M^2) (2)

KB $= \frac{T}{2}$ (M) (3)

BM $= \frac{\left(\frac{\pi R^4}{4}\right)}{\pi R^2 T} = \frac{R^2}{4T}$ (M) (4)

KM $= \frac{T}{2} + \frac{R^2}{4T}$ (M) (5)

The added mass in heave $= \frac{4\rho R^3}{3}$ (Tonnes) (6)

Natural heave period $= 2\pi\sqrt{\frac{\rho\pi R^2 T + \frac{4\rho R^3}{3}}{\rho g \pi R^2}}$

$= 2\pi\sqrt{\frac{T + \frac{4R}{3\pi}}{g}}$ (secs.) (7)

In the above equations the formula for added virtual mass is approximate in that it has been assumed equal to half that of a fully immersed disc of radius R. A slightly more accurate method of taking account of the buoy dimensions is shown in Appendix 2 and will be used in subsequent design equations. It must be realised that this quantity is strictly frequency dependant and more accurate values can only be obtained by three dimensional diffraction programs. These are too elaborate and costly to use at the early design stage. Appendix 1 shows that in the equations of motion the added mass term appears on both sides of the equation and thus small errors do not greatly affect the computed motions.

The Table of environmental data given in the introductory lecture showed that the buoy natural heave period had to be greater than 12.3 secs. in the Central North Sea and greater than 14.6 secs. West of Shetland if its downtime was to have any prospect of being around 2%.

From equation 7 this means that the term:

$$\sqrt{\frac{T + \frac{4R}{3\pi}}{g}}$$

must be greater than 2, inferring either a deep draught or a large radius or some combination of these two possiblities. These conditions clash with the requirements for stability inferred from equation (5) in that it will be impossible to carry much deck load at a height which will keep it clear of wave action if the value of KG must be less than KM. The $\frac{R^2}{4T}$ term in KM will be small and this is tantamount to saying that for stabililty the CG must be below half the draught. In practice this can only be achieved by using a high density ballast in the bottom to partially offset the deck weight which will be at least 17 to 20 above the sea surface.

It is therefore necessary to look at geometry changes which will improve the natural periods and also allow ballast weights to be low down.

The most obvious way of increasing the natural have period is to increase the added mass since it must be remembered that the mass must be kept low for economy. If a horizontal bilge keel is added it will behave like a submerged disc and the added mass will be of the form:

$$8\rho\left[R2^3 - R1^3\right]$$

where R1, R2 are the radii of the buoy and the disc respectively. This suggests that if R2 is made large, the necessary increase in period will be achieved. Since the horizontal added mass of a cylinder is $\rho\pi R^2$ tonnes/m this will also increase the added inertia in pitch/roll.

If the disc is given some depth it will be capable of carrying some of the required ballast. On the other hand an increase in volume near the base lowers the centre of buoyancy and the metacentric height and thus the centre of gravity so that it is clear some compromise must be sought.

There are other reasons connected with the exciting forces in pitch/roll why the radius and depth of the disc must be restricted. This can be seen from Fig. 4.

The horizontal wave forces are chiefly inertia dominated and depend on the square of the radius so that a deep, high radius disc will cause large horizontal forces low down and will lead to high pitch/roll moments. Their magnitude depends on the height of the CG and will be less for a low CG but this infers more ballast and less pay load and so some more happy medium must be found.

Note that the depth from the waterline to the top of the lower caisson must be made larger than the trough depth of the largest wave which may be encountered i.e. the wave must not drop below the top of the lower caisson or rapid changes in waterplane area will occur with unpleasant motions. This greatly restricts the geometry for small buoys.

STRUCTURAL LAYOUT

The structural/sub-division layout must conform with the regulations laid down by the statutory authorities and the classification societies for floating production systems. The most important for this type of buoy are the stability regulations (section 31 of Offshore Installations: Guidance on Design, Construction and Certification - 4th Edition : Department of Energy).

The minimum value of GM for a surface floating unit is 0.3m, but the wind loading on a production buoy will be comparatively high and to limit static angles of heel it is thought that the GM will need to be nearer to 1.5m in a non-storage buoy. In a storage buoy it can be much closer to the minimum because the much greater displacement means that it is less sensitive to heeling caused by environmental loads.

The unit must be able to withstand the flooding of any one watertight compartment. The extent of damage must be assumed to be from 5 m above to 3 m below the waterline under consideration and to a depth of 1.5 m in a horizontal direction normal to the outside shell with a lateral or circumferential extent of 3m and a vertical extent of 3 m. Due to its low waterplane area it must be expected that in operational conditions the buoy draft will vary over ± 1 m due to changing consumables on board.

The damage requirements infers that there must be an inner cylinder with a clearance to the outer shell greater than 1.5m and with horizontal and vertical

bulkheads positioned so as to meet both the extent of damage regulation and the one compartment sub-division. All these bulkheads must be able to withstand the full pressure to which they may be subjected. This should be assumed as the maximum still water head plus the maximum wave elevation above this level including run-up on the outer surface of the buoy.

It should be noted that this double skin arrangement provides an extremely stiff structure since the outer and inner shells form the flanges of a series of circular web frames which are over 1.5m deep. If the stiffening arrangements are such as to reduce shear lag effects much of the plating will be effective in reducing bending.

Construction of these buoys is simplified since the hull radius is generally large enough for the hull plating to take the required contour of the web frames under its own self weight, without costly plate bending operations.

DECK DESIGN

Circular decks are in general wasteful of space since so many pieces of equipment are rectangular in shape. There is therefore a strong incentive to go from the circular buoy main body to a square shaped deck which will overhang the buoy sides. Because deck area is so important the buoy may well be increased in diameter to conical form at this section below the junction with the deck. This conical portion may start a few metres above the waterline and extend to the highest level the waves are expected to reach, including any run-up. The conical shape will reduce run-up, will deflect spray outwards, and will provide greater waterplane area which is advantageous from the damaged stability and motion viewpoints. However, the advantages must be balanced against the fact that it leads to more steel weight high up.

RISER ARRANGEMENTS

There exists a number of possibilities for running risers up to the operating deck level. A central moonpool can be created for this purpose, but this makes the deck arrangements more difficult and it will be necessary to construct a cofferdam around the moonpool in case its sides are accidentally holed and the buoy flooded. This need only be of 1 m width but, since its plating must also be able to withstand the external pressures, it adds considerable structural weight.

Since the decks will overhang the main buoy structure, rigid risers may be brought up externally and attached to the buoy structure up to deck level. This has advantages because any gas leaks are fully vented, but from the base upwards there is an increased risk of damage which will need to be designed against. It should be impossible to have supply ship or export tanker impact due to the deck overhang, but floating objects can have high impact velocities in steep waves.

A third alternative is to use the cofferdam space between the inner and outer hulls to create one or more moon pools, but the effects on sub-division requirements must be borne in mind.

Oil companies will have their own views on which of these alternatives offers the greatest safety and utility for their operations.

STORAGE BUOY DESIGNS.

The above discussion applies to minimum size buoys for production in small fields.

If it is necessary to incorporate storage in the unit, the design restrictions are somewhat less onerous. If the field is in fairly benign waters where offloading can take place during the majority of the time, all that may be required is two or three days storage for the duration of a storm.

In North Sea conditions continuous loading is only possible in the summer months and even then there will be several periods of storm conditions when the shuttle tanker will not be able to stay connected. For a small field it is likely that only one shuttle tanker will be necessary, and even it may not be fully employed. Under such circumstances it will be better to share the export facilities of some other field with offshore loading.

The smallest shuttle tankers in regular use are of 50,000 tonnes dwt. This is about the smallest size which can give reasonable offloading downtime in winter weather. Reasonable in this context is a maximum of 4 days delay in connecting due to the environmental conditions. Thus the buoy storage capacity should be around 50,000 tonnes (about 370,000 bbls. of oil at 0.85 specific gravity) plus four days output.

It must be emphasised that offloading downtime depends on the size of the shuttle tanker, being less for large vessels, and on the degree of sophistication of its positioning system, but vessels less than 50,000tonnes dwt are likely to have natural motion periods in the range of commonly occurring wave periods and will thus more frequently encounter problems in staying connected to a buoy

One important difference from tanker storage vessels is that the oil must be stored by the load on top method, i.e. there is always a mixture of oil and water in the tanks with oil on top due to its lower specific gravity. This is necessary to avoid the high external pressures which would occur if the deep tanks were emptied while separate ballast tanks were filled, as in a tanker. It does require that oil be always sucked from the top of the tank and pumping must stop when the oil/water interface approaches the suction. The depth of this interface will depend on the oil characteristics. If the oil requires heating for pumping concrete buoys storage are more efficient.

The subdivision of the storage compartments must be carefully thought out from the point of view of restricting possible leakage if a tank is accidentally damaged. Care must be given to the cathodic protection and other special measures which may be called for because of the oil's chemical characteristics. A double bottom will be required to take the permanent ballast which is likely to be needed for stability reasons and a double skin tank top to give protection from dropped weights, etc.

MOTION AND STABILITY OPTIMISATION

The foregoing discussion indicates that it is necessary to develop the hydrostatic and motion equations for buoys with the general shape and nomenclature shown in Fig. 5. A moonpool has been inserted although this may not be incorporated in practice if other arrangements are made for the risers. For a given displacement it has a beneficial effect on stability but leads to higher motion exciting forces and higher mooring loads. In a storage buoy the depth of the lower caisson, H2, will be greatly increased to provide the storage volume and the horizontal bilge plate may be omitted since the mass plus added mass are sufficiently large to give long natural periods. The hydrostatic and natural period equations for this geometry are given in Appendix 3. At this stage it is assumed that a GM of 1.5 m can be obtained, which dictates the position of the centre of gravity

HEAVE EXCITING FORCES

Figure 6 shows a wave crest at the buoy centreline with an origin in the stillwater surface. The equations in Appendix 3 apply when the wave length is greater than five times the buoy diameter, and for shorter wave lengths small corrections should be applied to take account of diffraction effects. The designer is generally not interested in accurate results at these wave lengths in the design stage and is primarily concerned with the performance in wave with periods greater than 8 secs. (100m. wave length).

In the crest there will be upward forces on all the lower surfaces due to the increase in pressure experienced on the bottom of the buoy. However, on top of the lower caisson, the force will be downward and due to the exponential fall off in pressure change below the surface the dynamic pressure on the top of the caisson will be greater than on the bottom - see Fig. 6a.

On the other hand, since the wave particle acceleration is downwards in the crest the inertia forces will act downwards on all parts of the buoy - see Fig. 6b.

There will always exist a wave length where these two sets of forces will balance one another and the designer should ensure that this zero force point lies in a useful part of the wave frequency range, i.e. generally near the most severe wave periods likely to be encountered. It can be shown theoretically that the zero force

point cannot be made to coincide with the natural heave period, but it should lie at a shorter period but close to the natural period in order to get most benefit. Later we shall see that this is important for the phase relationship between the waves and the heave response.

The upward pressure force will predominate for periods longer than that at which the balance occurs, while at shorter periods inertia forces will be largest.

Since the horizontal bilge keel has very little depth the difference in pressure on its upper and lower face may be ignored, but it will contribute considerable inertia forces.

Although not negligible, velocity forces are small relative to the pressure and inertia forces and may be neglected in the early stages of design

The equations governing these forces are developed in Appendix 3.

SURGE FORCES AND PITCH/ROLL MOMENTS

The horizontal forces which govern the pitch/roll behaviour are also mainly due to pressure plus inertia effects and velocity forces are neglected in the equations that follow. The moorings will provide a restraint and the fairleads should be sited close to the centroid of the horizontal forces at the wave period which is likely to cause the largest surge.

The pitch/roll moment depends greatly on the position of the centre of gravity which will be variable as deck load changes so that the effect on different levels of GM must be investigated in the design stage. The moment is also very dependent on the depth and radius of the lower caisson since the forces are proportional to the square of the radius. Practical access problems for ballast stowage will dictate the minimum depth which is unlikely to be less than 1.5 m.

Relevant horizontal force and moment equations are given in Appendix 3.

DESIGN EXAMPLE

In order to demonstrate the usefulness of the above simplistic approach to the problem of selecting a geometry which will meet a given set of requirements, consider the case of designing a buoy to carry a payload of 1200 tonnes at a local centre of gravity (cg) of 16 m above the waterline. This represents the mass of production, power generation equipment and utilities, but excludes the mass of the crew quarters, helideck and safety related structures such as blast walls, etc. In order to achieve a reduction in capital costs compared to a semi-submersible it is aimed to design a buoy with a displacement no greater than 9000 tonnes.

If the total deck weight excluding the structure is estimated at 1600 tonnes, i.e. crew quarters, helideck, etc. is estimated at 400 tonnes with a cg. of 1.5 m higher than that of the production equipment, this leaves 7400 tonnes for the steel weight, consumable fluids plus the permanent ballast. The steel weight will depend on the riser arrangements as a moonpool and its attendant cofferdam will add to the steel weight compared to a design with external risers.

As a starting point for the design, the dimensions shown in Fig. 7, and in the tabulated details below it, will be used to perform the motion calculations and to see the direction in which changes may be made to improve the performance.

The displacement is just over 9000 tonnes and includes an allowance of 25 tonnes for the buoyancy of the horizontal bilge keel and its structural stiffening. The value of KB is 7.6 m and the BM is 2.55 m, giving a KM value of 10.15 m. If the GM is to be around 1.5 m the KG must be 8.65 m. The small diameter moonpool has little effect on the displacement or on the second moment of area of the water-plane and this diameter could be increased without having a large effect on the external dimensions. Such an increase would produce a higher value of KM and allow a higher KG.

The depth of the main body of the buoy, 14.4 m, has been chosen to try to eliminate the possibility of the wave trough dropping below the top of the lower caisson.

To obtain the heave natural period it is necessary to determine the added mass factors appropriate to each portion of cylinder. The values of the mean aspect ratio are as follows:

Main body of buoy	$\frac{\pi R1}{2(H1+H2)}$	= 0.196,	CvR1	= 2.0
	$\frac{\pi R3}{2(H1+H2)}$	= 1.276	CvR3	= 1.45
Lower caisson	$\frac{\pi R3}{2H2}$	= 12.01	CvR34	= 1.1
	$\frac{\pi R4}{2H2}$	= 14.78	CvR4	= 1.0

Those for the lower caisson are tending to 1.0 - the value for a disc.

The heave added mass is equation 9 of Appendix 3:

$$M_{AVM} = 1.33\,\rho\left(C_{VR3}R_3^3 - C_{VR1}R_1^3\right) + 2.66\rho\left(C_{VR4}R_4^3 - C_{VR34}R_3^3\right) + {}^{8}/_{3}\,\rho\left(R_5^3 - R_4^3\right) \text{ Tonnes} \qquad (9)$$

$$= 4321+5524+3445 \text{ Tonnes}$$

$$= 13290 \text{ Tonnes}$$

The bilge keel makes a significant contribution. The heave natural period is:

$$T_h = 2\pi\sqrt{\left[\frac{9000+13290}{\pi\rho g(13^2-2^2)}\right]}$$

$$= 2\pi\sqrt{\left[\frac{22290}{5212.3}\right]}$$

$$= 12.99 \text{ sec.}$$

and $\omega_h = 0.483$ rads/sec.

If the bilge keel were omitted the period would be reduced to 11.9 secs.

The added inertia in pitch/roll comes mostly from the effects of the added mass in surge/sway and the contribution from the bottom of the buoy and the lower caisson's upper and lower surfaces can be ignored initially as this produces a conservative pitch natural period. The various terms in the added mass inertia are:

Main body of buoy:

$$= \rho\left[\frac{\pi\times 13^2\times 14.3^3}{12} + \pi x 13^2 x 14(1.7+7.15-8.65)^2\right]$$

$$= \rho[129379 + 304]$$

Lower caisson:

$$= \rho\left[\frac{\pi\times 16^2\times 1.7^3}{12} + \pi\times 16^2\times 1.7(8.65-1.7/2)^2\right]$$

$$= \rho[19+83182]$$

Total inertia:

$$= 218{,}206 \text{ tonnes m}^2$$

The mass inertia of the buoy can only properly be determined once the full structural design and layout has been completed. An approximation must be made in the early design stages. Initially the mass of steel will be taken as 2000 tonnes with a cg at 10.7 m above the baseline. Thus the preliminary figures for the mass distribution are as follows:

PRELIMINARY ESTIMATE OF MASS DISTRIBUTION:

Item	Mass Tonnes	vcg above base m	moment about base Tonnes m.	Inertia about CG Tonnes m^2	Inertia about local cg. Tonnes m^2
Payload	1200	32.0	38,400	654,827	
Accom. etc	400	33.5	13,400	247,207	
Steel wt.	2000	10.7	21,400	8,487	192,666
Ballast	5400	0.85	4,590	327,694	
TOTAL:	9000		77,790	1,238,215	192,666

The vertical CG above base = $KG = \frac{77,900}{9000} = 8.64m$

The total mass inertia is greater than 1,430,880 Tonnes m^2 since the mass inertia about their own cg has been neglected for all items other than the steel weight.

Using the above data the natural pitch/roll period is:

$$Tp/r = 2\pi\sqrt{\left[\frac{1,430,880 + 218,233}{9.81 \times 9000 \times 1.5}\right]}$$

$$= 22.17 \text{ secs. and}$$

$$\omega p/r = 0.283 \text{ rads/sec.}$$

This is a very satisfactory period and is longer than many semi-submersibles, but the natural heave period is lower than desirable. Little can be done to improve it without increasing the displacement since to reduce the waterplane area also reduces the value of KM and is likely to reduce the payload. Some improvement may be achieved by increasing the size of the moonpool, but this will add to the steelweight and needs to be approached cautiously as the surge forces and pitch/roll moments will also increase.

MOTION CALCULATIONS

Heave

The motion calculations for this design are given in some detail in Tables (1) to (3). This has been done so that the contribution of each term to the forces or moments may be seen and the effect of changes in their dimensions gauged.

Table (1) deals with the heave response. Columns (1) to (4) give the particulars of the wave conditions investigated. The wave periods range from 5.2 to 25.1 secs. The exponential fall off in the wave disturbance at the top and bottom of the lower caisson is given in columns (5) and (6). In the long waves there is very little attenuation, but it is very large in the short waves, even for this comparatively shallow draught.

The upward pressure force (divided by ρga) on the bottom of the caisson is given in column (7), while the downward force on top of the caisson is in column (8). The algebraic addition of these two is in (9), showing a net upward force which declines at the shorter periods due to the exponential effect. Columns (10) to (12) contain the inertia forces (divided by ρga) on the base of the main body (radius R3), on the lower caisson and on the horizontal bilge keel respectively. They all act downwards in the crest and are of the same order with the lower caisson providing the highest forces.

The addition of these forces to the pressure forces is given in column (13). The net heave force is upward in all waves beyond approximately 10 secs period indicating that pressure effects dominate, but for shorter periods the acceleration forces are largest and the net force is downwards.

Columns (14) and (15) give the heave response and the phase angle to the wave crest respectively. A damping ratio of 0.06 has been assumed from experimental data, but the use of a large bilge keel may increase this. The response follows that of the familiar single degree of freedom system with a peak at the natural frequency. At wave periods longer than this the phase angle is less than 90° and the buoy tries to follow the wave contour - up hill and down dale. For periods just shorter than the natural period the exciting force is still upward, but the phase angle has changed to near 180°, so that the response becomes out of phase with the waves and can lead to large relative motions with water on deck.

A more serious problem can occur in the wave trough. The buoy will be moving upwards and the waterline can drop towards the top of the lower caisson. The value of KB + BM may drop below KG and the buoy become unstable with violent and erratic motions. To overcome this it may be necessary to use a conical shape instead of a cylinder for the lower part of the main body. The conical shape should be designed so that KB + BM is always greater than KG for any possible waterline. Unfortunately the conical shape leads to a lower KB. One method of partially compensating for this is to have an annular space underneath the buoy within the inner shell (radius R2) so as to raise the KB. It is necessary to ensure that there is sufficient bottom area to carry the ballast with the desired cg.

At wave periods below 10 secs the exciting force becomes downward in the wave crest, but since the response is 180 out of phase the buoy is moving in phase with the waves and the relative motion is low. The only problem region is

between the natural period and the period where the force changes from upwards to downwards in the wave crest.

SURGE/SWAY

These calculations are given in Table (2) using some of the data in Table (1).

Columns (2) and (3) give the contributions to the surge force from the main body and the lower caisson respectively. The latter is quite small for this design. The surge force per unit wave implitude is given in column (5), the force increasing steadily throughout the range of frequencies. However, the surge response is greatest at the low frequencies because the force has to be divided by the square of the frequency.

PITCH/ROLL RESPONSE

The relevant calculations are given in Table 3. Columns (2) to (4) contain the terms which are multiplied by R_3^2. It is worth noting that it is the difference between columns (2) and (4) which is being multiplied and this is a very small figure in comparison to the individual values in columns (2) or (4). A small change in the value of y_g, the distance of the CG below the waterline, could change the sign of this difference and this explains why the pitch response is so sensitive to the precise CG position. The operating staff need to be aware of this with clear guidance on the best position.

The same feature occurs in the terms which are multiplied by R_4^2 - columns (2), (6) and (7). The algebraic sum of these columns leads to a small number which could change sign if y_g was altered.

The sign of the moments due to the main body of the buoy and the lower caisson are different since one set of forces acts above the CG and the others below. In long waves the forces on the lower caisson dominate, but as the waves get shorter and the exponential term becomes more significant the forces on the body become the largest.

Columns (9) and (10) give the summation of the forces and the multiplication by the appropriate external factor. The pitch/roll response is given in column (11). It is quite large near the natural period but for the practical range of waves in the North Sea, i.e. shorter than 18 secs period, the response characteristics are good.

It is emphasised that no attempt has been made to optimise the position of the CG and the first thing to examine is whether any value of the metacentric height between 1.5 m and 0.5 m gives a better performance. Higher values would require such a low centre of gravity that they would severely limit the payload and are therefore not practical options. The second variable to examine is the depth and

radius of the lower caisson since it controls the size of the pitch moment in long waves.

GENERAL COMMENTS ON THE DESIGN

This type of design produces a buoy with a huge internal volume (over 11,000 m^3) between the top of the lower caisson and the 30 m level This is the level above which decks can be open to the environment since it is clear of wave action. These decks allow natural ventilation and will therefore be the optimum location for the utilities and process equipment because of this reduced risk of explosion.

Certain equipment, such as the water injection plant including its compressors, the fire-fighting pumps and domestic water supply, can easily be contained within this body of the buoy, but normal oil company practice dictates that any items of plant where there is any gas hazard must have natural ventilation and thus has to be on open decks above the effects of wave action. There is a preference for gas turbines for power generation and for them to be sited on open decks.

However, there is a history of marine practice, especially on liquefied gas carriers, of successful operation of dual fuel power generators in engine rooms below decks. It is felt that much greater use can be made of the internal volume to increase the payload without any sacrifice in safety if marine practice is followed. Only equipment and services involving the possibility of high pressure gases need to be on open decks.

The above design has assumed steel as the material, but if concrete were to be used for the main body with steel upper decks the buoy mass would be greater giving improved motions. Concrete construction is well established for this type of structure and economies may be possible in build cost and in through life costs due to reduced maintenance.

STORAGE DESIGNS

These cannot be produced by some geometric variation of a successful small buoy design. The lower caisson will now form the main body of the buoy and the upper portion only provides the support for the deck structures. The depth of the upper caisson can remain substantially the same, but the difference between the diameters at the two portions of the buoy will need to be changed since the bottom of the buoy will now be far below the surface and due to the exponential fall off the pressure changes and inertia forces on the bottom will be much lower. As a result, the area on the upper side of the lower caisson which experiences downward forces in a wave crest must be reduced if the balance between upward and downward forces is to be achieved within the practical range of wave periods, preferably at a long period.

Since the majority of the surge forces come from the upper part of the buoy, it is important to keep the diameter of the upper section as small as is practical from the point of view of the necessary deck areas. However, a storage buoy may be expected to carry a much higher mass of production equipment and will require more deck area.

It has been suggested earlier that the minimum size of a storage buoy for an open sea situation is 50,000 tonnes storage plus 4 days output. If an output of 30,000 bbls/d is assumed, this infers for an oil with specific gravity of 0.85, a total capacity around 500,000 bbls or 67,600 tonnes oil storage. Since the oil is being stored on top of water, an allowance must be made for the interface thickness which cannot be pumped. Thus the tanks must have a total capacity near to 70,000 tonnes.

Figure 7 gives an outline sketch and approximate dimensions for a buoy with the following tentative weight distribution

Table: TENTATIVE WEIGHT DISTRIBUTION FOR A 70,000 TONNES STORAGE BUOY.

Item	Mass Tonnes	cg above base (m)	Moment about base (tonnes m.)
Oil storage plus water	70,000	27.25	1,907,500
Ballast(solid)plus water	11,000	1.00	11,00 0
Production Equipment	10,000	88.00	880,000
Steel wt. plus outfit	25,000	40.00	1,000,000
Totals:	116,000		3,798,500

CG above base = 32.74m.

The hydrostatic particulars are:

Displacement mass = 117,128 tonnes
KB = 33.27 m
BM = 1.10 m
KM = 34.37 m
∴ GM = 1.63 m

Thus this geometry of buoy has excess capacity in both displacement and GM which can be used to increase the payload of production equipment or its height above the baseline.

A moonpool has not been inserted since it would need to be of a very large diameter if the risers are not to touch its sides during surging on the moorings or

alternatively the riser connections within the moonpool would be so low down as to cause difficulty in making connections.

The natural heave period of this buoy is in the region of 22 secs mainly due to the increased displacement compared to the small buoy. This will be adequate for most sea areas.

Part of the heave response is calculation given in Table 4. It shows that as before the upward pressure forces dominate in long waves, but the balance between upward and downward forces occurs around 17 second period which will be good in severe sea states when the peak frequency is in this region. This point can be tuned by adjustment of the ratio of the two diameters. The heave stiffness in this case is 12,636 kN/m so that the static response is always less than 0.5 and the dynamic response will be very good. This will also be the case for pitching/rolling due to the long natural period that will result from the high mass and added mass inertia. Thus the motion characteristics of this unit will be much better than a ship/barge shaped unit of the same capacity.

The final dimensions of such a unit may need to take into account the constructional and initial installation problems. As for the production buoy, concrete may offer some advantages as a material, but because of the much higher masses involved the resulting improvement in motion characteristics will be much smaller.

REFERENCES

1. Design of Mono-column Type FPSO - M.Miyagawa and Y. Isozaki - Soc. of Pet. Engrs. 22985 SPE Asia-Pacific Conf. 1991.

2. Minifloater - A deepwater production alternative. W.P.J.M. Kerchoff and G.L. Pijfers Ocean Ind., September 1990 p147.

3 Unmanned satellite FPS targets marginal fields - Article in Ocean Ind., April/ May 1992 p126.

Table 1 - 9000 Tonne Buoy Heave Response

(1)	(2)	(3)	(4)	(5)	(6)	(7)	(8)	(9)	(10)	(11)	(12)	(13)	(14)
ω Rad./Sec.	λ Wave (m)	T Wave (Sec.)	$k=\frac{2\pi}{\lambda}$ $(m)^{-1}$	e^{-kH_1} $H_1=14.3$ (m)	$e^{-k(H_1+H_2)}$ $H_1+H_2=16$	* See below	*	Net Press. Force / ρga	*	*	*	Net heave Force / ρga	Heave Response (m./m.)
0.250	985.9	25.1	0.0064	0.9125	0.9027	715	-249	446	-24	-31	-19	392	1.03
0.300	684.7	20.9	0.0092	0.8767	0.9631	683	-240	443	-33	-43	-27	340	1.07
0.350	503.0	18.0	0.0125	0.8363	0.8187	648	-228	420	-43	-56	-34	287	1.16
0.400	385.1	15.7	0.0163	0.7921	0.7704	610	-216	394	-53	-69	-42	230	1.35
0.450	304.3	14.0	0.0206	0.7448	0.7192	569	-204	365	-62	-81	-50	172	1.92
0.475	273.2	13.2	0.0230	0.7197	0.6921	548	-197	351	-67	-87	-54	143	2.25
0.500	246.5	12.6	0.0255	0.6944	0.6650	526	-190	336	-71	-93	-57	115	1.55
0.550	203.7	11.4	0.0308	0.6437	0.6109	484	-176	308	-79	-104	-63	62	0.37
0.600	171.2	10.5	0.0367	0.5916	0.5559	440	-162	278	-86	-113	-69	10	0.03
0.700	125.8	9.0	0.0499	0.4989	0.4500	356	-134	222	-95	-126	-76	-75	0.13
0.800	96.3	7.9	0.0652	0.3936	0.3523	279	-108	171	-97	-131	-77	-134	0.15
0.900	76.1	7.0	0.0826	0.3069	0.2667	211	-84	127	-93	-128	-74	-168	0.13
1.000	61.6	6.3	0.1020	0.2326	0.1955	155	-64	91	-84	-118	-67	-178	0.10
1.200	42.8	5.2	0.1468	0.1225	0.0955	76	-33	43	-59	-87	-47	-150	0.06

* (7) $\pi\left(R_4^2-R_1^2\right)e^{-k(H_1+H_2)}$

(8) $-\pi\left(R_4^2-R_3^2\right)e^{-kH_1}$

(10) $1.33k\left[C_{VR3}R_3^3-C_{VR1}R_1^3\right]e^{-k(H_1+H_2)}$

$C_{VR3}=1.45 \quad C_{VR1}=2.0$

(11) $1.33k\left[C_{VR4}R_4^3-C_{VR34}R_3^3\right]\left[e^{-kH_1}+e^{-k(H_1+H_2)}\right]$

$C_{VR4}=1.09 \quad C_{VR34}=1.11$

(12) $\frac{8}{3}k\left(R_5^3-R_4^3\right)e^{-k(H_1+H_2)}$

(14) $$\frac{1.025x9.81x(\text{Col.13})}{1.025x9.81x\pi x\left(13^2-2^2\right)}\frac{1}{\sqrt{\left(1-\left(\frac{\omega}{\omega_n}\right)^2\right)^2+\left(2\gamma\frac{\omega}{\omega_n}\right)^2}}$$

$\gamma=0.06 \qquad \omega_n=0.483\text{rad./sec.}$

Table 2 - 9000 Tonne Buoy Surge Forces

(1)	(2)	(3)	(4)	(5)	(6)
ω Rad./Sec.	* See Below	*	Net Force / $2\rho g a \pi$	Surge Force (kN/a.)	Surge Ampl. (m./m.)
0.250	15	2	17	1074	0.95
0.300	21	4	25	1579	0.97
0.350	28	4	32	2022	0.91
0.400	35	6	41	2590	0.89
0.450	43	7	50	3159	0.86
0.475	47	7	54	3412	0.84
0.500	52	7	59	3728	0.82
0.550	60	8	68	4296	0.78
0.600	69	9	78	4928	0.76
0.700	86	10	96	6065	0.68
0.800	102	11	113	7139	0.62
0.900	117	10	127	8024	0.55
1.000	130	9	139	8782	0.48
1.200	148	7	155	9793	0.38

(2) $R_3^2\left(1-e^{-kH_1}\right)$

(3) $R_4^2\left(e^{-kH_1}-e^{-k(H_1+H_2)}\right)$

$$\text{Added Mass In Surge} = \rho\pi R_3^2 \times H_1 + \rho\pi R_4^2 \times H_2$$
$$= 7687+1401$$
$$= 9088 \text{ Tonnes}$$
$$\therefore \left(M + M_{AVM}\right)_{Surge} = 18088 \text{ Tonnes}$$

Table 3 - 9000 Tonne Buoy Pitch/Roll Response

(1)	(2)	(3)	(4)	(5)	(6)	(7)	(8)	(9)	(10)	(11)
ω Rad./Sec.	$H_1 e^{-kH_1}$ $H_1 = 14.3$ (m)	$\frac{1}{k} + y_G$ $y_G = -7.35$m	* See Below	*	*	*	*	Net Mom. / $2\rho g a \pi$ (5) + (8)	Moment a KNm/m.	Response Deg./m
0.250	13.05	148.90	13.03	3.38	14.44	1.46	-17.92	-14.54	918.6	1.66
0.300	12.54	101.30	12.49	8.45	13.81	1.38	-28.16	-19.71	1245.0	3.04
0.350	11.96	72.65	11.89	11.83	13.10	1.28	-35.84	-23.97	1497.0	1.18
0.400	11.32	54.00	11.23	15.21	12.33	1.17	-40.96	-25.75	1627.0	0.69
0.450	10.65	41.19	10.51	23.66	11.51	1.05	-48.64	-24.89	1578.0	0.44
0.475	10.29	36.13	10.13	27.04	11.07	1.00	-56.32	-29.28	1850.0	0.44
0.500	9.93	31.86	9.74	32.11	10.64	0.94	-58.88	-26.77	1691.0	0.34
0.550	9.20	25.12	8.95	42.25	9.77	0.82	-64.00	-21.75	1374.0	0.21
0.600	8.46	19.90	8.13	55.77	8.89	0.71	-71.68	-15.91	1005.0	0.12
0.700	7.00	12.69	6.47	89.57	7.20	0.51	-79.36	10.21	-645.0	-0.05
0.800	5.63	7.99	4.84	133.51	5.64	0.33	-81.92	51.59	-3259.0	-0.20
0.900	4.39	4.76	3.30	184.21	4.27	0.14	-66.56	117.65	-7433.0	-0.35
1.000	3.33	2.45	1.88	245.05	3.13	0.04	-74.24	170.81	-10792.0	-0.41
1.200	1.75	-0.54	-0.47	375.18	1.53	-0.01	-58.88	316.30	-19984.0	-0.50

* (4) $\left(1 - e^{-kH_1}\right)\left(\frac{1}{k} + y_G\right)$ (7) $\left(e^{-kH_1} - e^{-k(H_1+H_2)}\right)\left(\frac{1}{k} + y_G\right)$

(5) $R_3^2[(2) - (4)]$ (8) $R_4^2\left[-H_1 e^{-kH_1} + (H_1 + H_2)e^{-k(H_1+H_2)} - \left(e^{-kH_1} - e^{-k(H_1+H_2)}\right)\left(\frac{1}{k} + y_G\right)\right]$

(6) $(H_1 + H_2)e^{-k(H_1+H_2)}$

$$\text{Pitch Response} = \frac{\text{P.moment}}{\rho g \nabla GM} \frac{\text{SIN}(\omega T + \vartheta)}{\sqrt{\left(1 - \left(\frac{\omega}{\omega_n}\right)^2\right)^2 + \left(2\gamma \frac{\omega}{\omega_n}\right)^2}}$$

$\omega_n = 0.283$ Rad./sec.

$\rho g \nabla GM = 9.81 \times 9000 \times 1.5 = 132435$ KNm

Table 4 - Storage Buoy Heave Response

(1)	(2)	(3)	(4)	(5)	(6)	(7)	(8)	(9)	(10)	(11)
w Rad./Sec.	l Wave (m)	T Wave (Sec.)	$k = \frac{2\pi}{\lambda}$ $(m)^{-1}$	e^{-kH_1} $H_1 = 15m$	$e^{-k(H_1+H_2)}$ $H_1 + H_2$ =70m	* See below	*	*	*	Net Heave Force / ρga
0.250	985.9	25.1	0.0064	0.9085	0.6389	1108	-434	-44	-100	530
0.300	684.7	20.9	0.0092	0.8711	0.5252	911	-417	-51	-130	313
0.350	503.0	18.0	0.0125	0.8290	0.4169	723	-396	-55	-158	114
0.400	385.1	15.7	0.0163	0.7831	0.3195	554	-374	-55	-182	-57
0.450	304.3	14.0	0.0206	0.7342	0.2364	410	-351	-52	-203	-196
0.500	246.5	12.6	0.0255	0.6822	0.1678	291	-326	-46	-220	-301
0.550	203.7	11.4	0.0308	0.6300	0.1158	201	-301	-38	-233	-371
0.600	171.2	10.5	0.0367	0.5767	0.0766	133	-276	-30	-243	-416
0.700	125.8	9.0	0.0499	0.4731	0.0304	53	-226	-16	-255	-444
0.8	96.3	7.9	0.0652	0.3761	0.1014	10	-180	-7	-256	-425

* (7) $\pi R_4^2 e^{-k(H_1+H_2)}$

(8) $-\pi\left(R_4^2 - R_3^2\right)e^{-kH_1}$

(9) $1.33k.C_{VR3}.R_3^3.e^{-k(H_1+H_2)}$

$C_{vVR3} = 1.74$

(10) $1.33k\left[C_{VR4}R_4^3 - C_{VR34}R_3^3\right]\left[e^{-kH_1} + e^{-k(H_1+H_2)}\right]$

$C_{VR4} = 1.63$ $C_{VR34} = 1.69$

Heave Stiffness = 1.025 x 9.81 x π 20^2 = 12635.8 KN/m

M = 117128 Tonnes

A_{VM} = 1.33 x 1.74 x 20^3 = 18514 Tonnes

+ 2.66 x 23.5^3 = 20306 Tonnes

Total = 38820 Tonnes

$$T_H = 2\pi\sqrt{\frac{117128 + 38820}{12635.8}} = 22.1 \text{ Secs}$$

ω_h = 0.284 Rad./Sec.

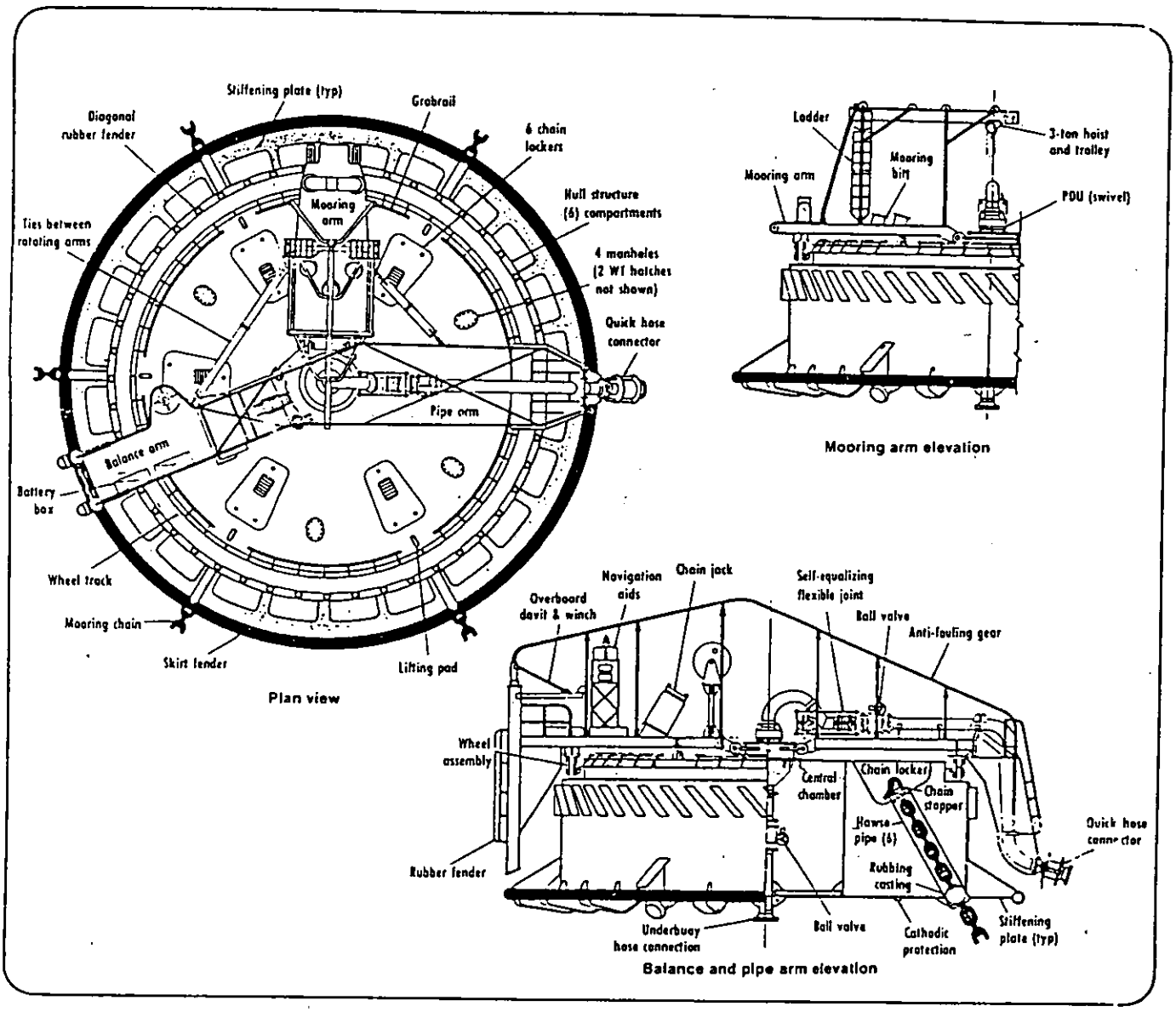

Figure 1 Typical CALM (Catenary Anchor Leg Mooring) Buoy.

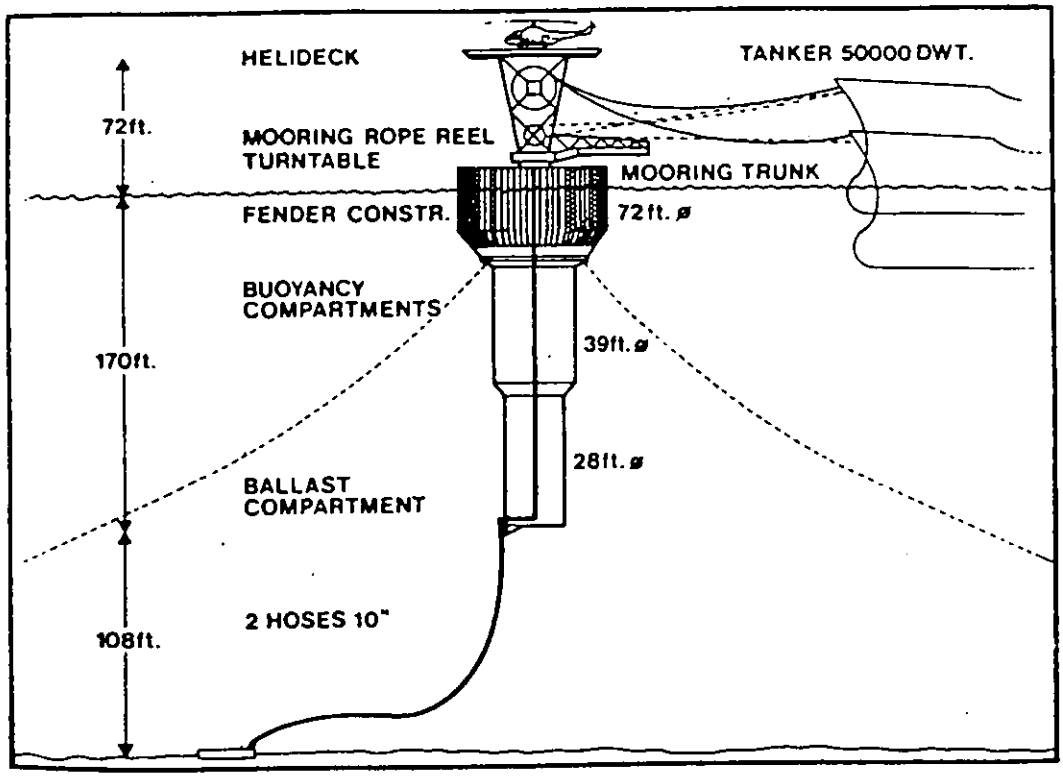

Figure 2 Loading Buoy at AUK Field

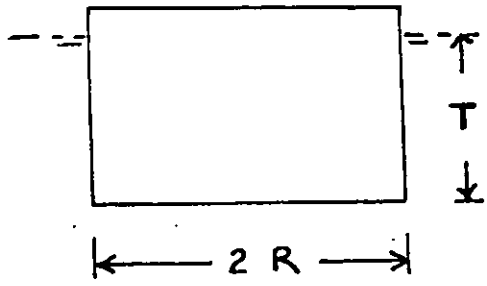

Figure 3 Simple Cylindrical Buoy.

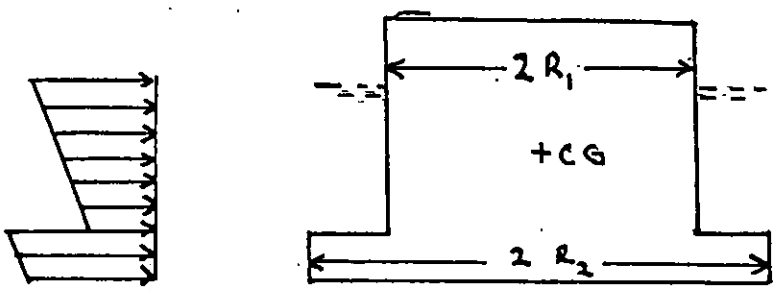

Figure 4 Cylindrical Buoy with Lower Caisson.

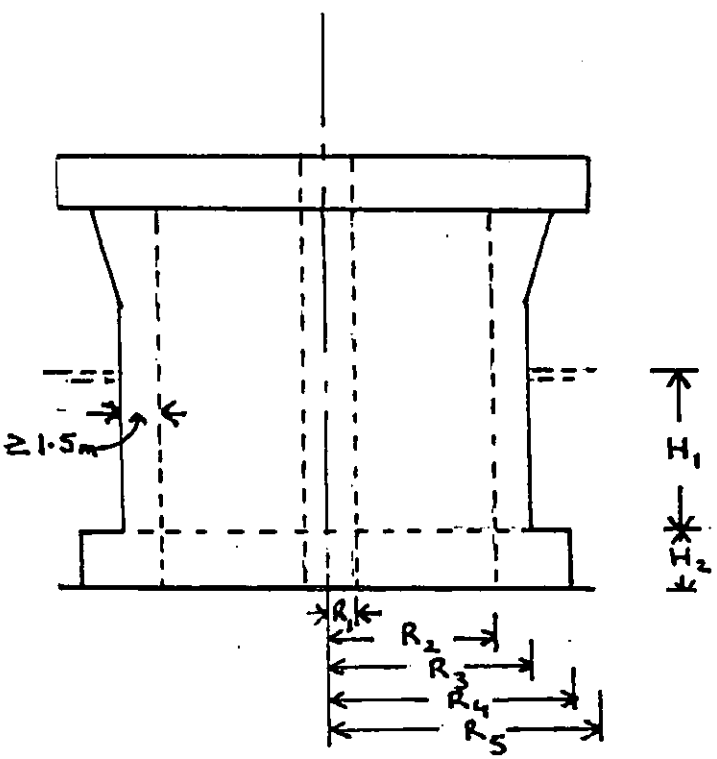

Figure 5 Diagram Showing Nomenclature Used in Developing Formulae in Appendix 3.

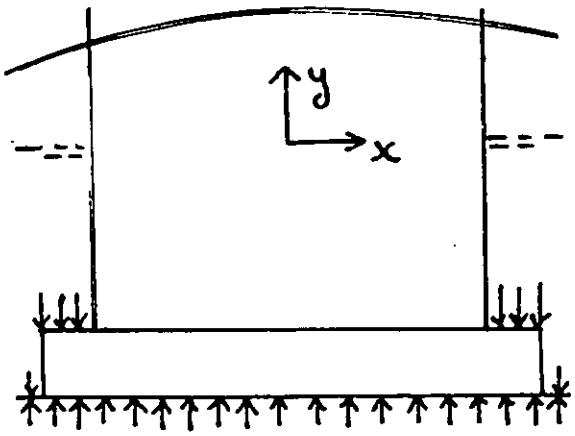

Figure 6a Pressure Forces.

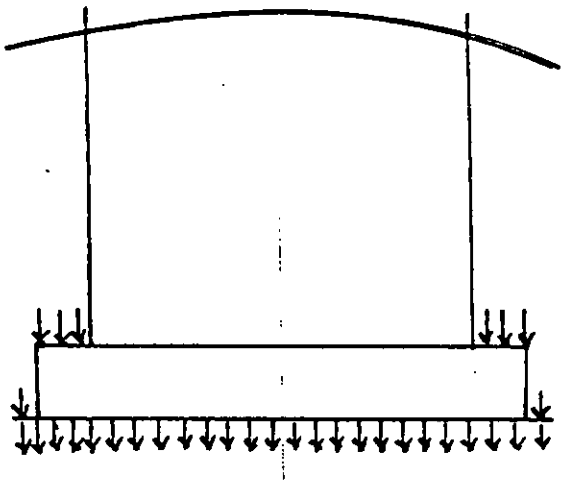

Figure 6b Inertia Forces.

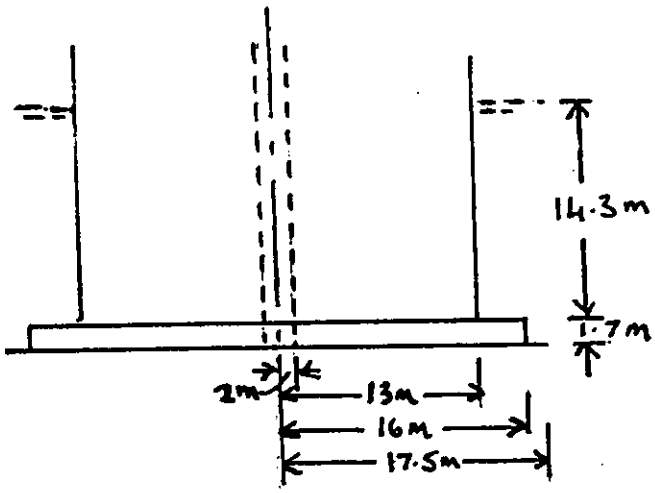

Figure 7 Leading Particulars of Underwater Portion of Small Production Buoy.

Immersed volume	= 8782 m
Displacement mass	= 9002 tonnes
KB	= 7.6m
BM	= 2.55m
KM	=10.15m
KG	= 8.65m

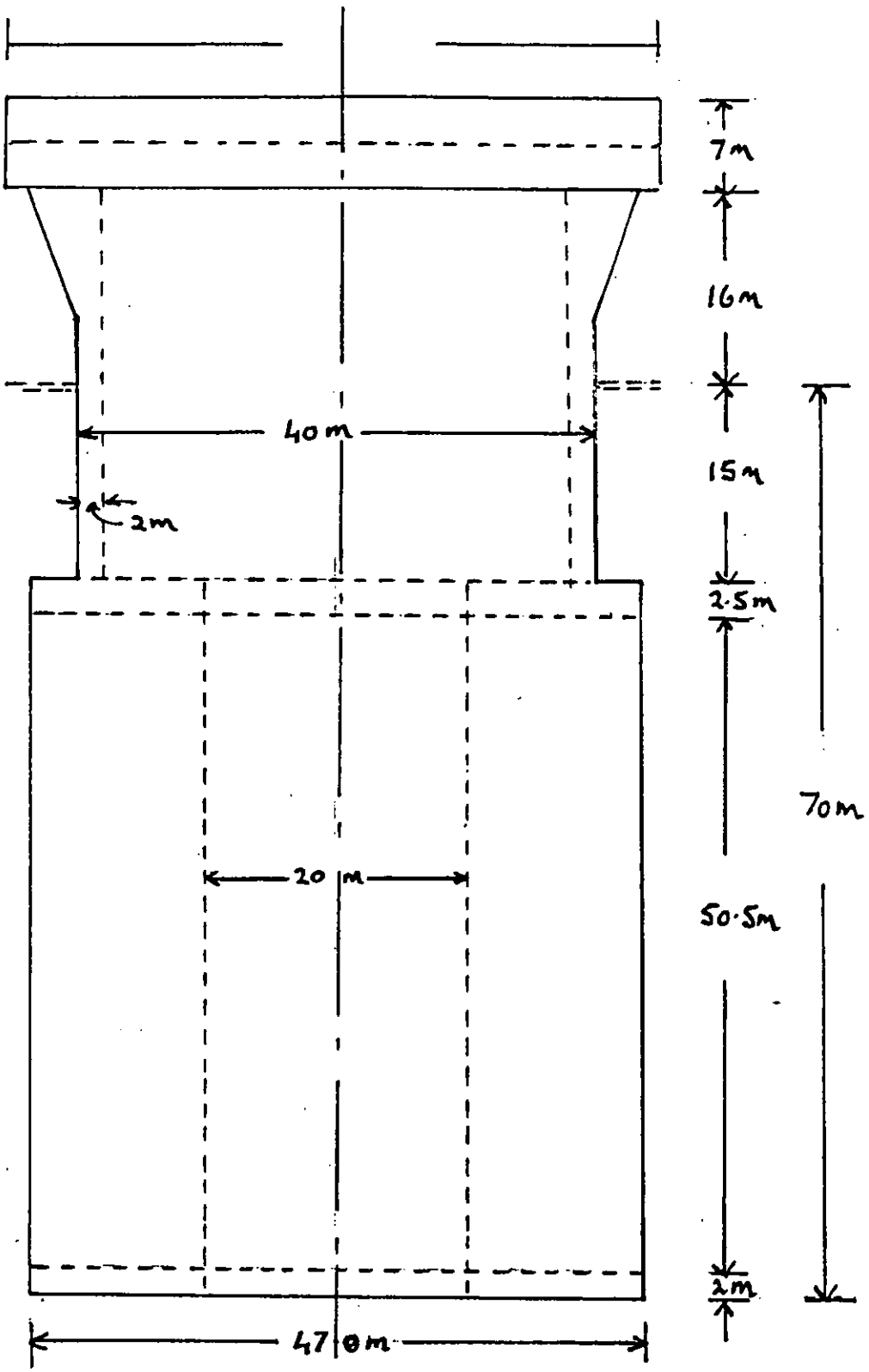

Figure 8 Initial Attempt at Storage Buoy Dimensions.

DYNAMIC RESPONSE TO WAVE EXCITING FORCES

Introduction

The dynamic response of a floating body to wave exciting forces is basically modelled on the forced single degree of freedom system which has an equation of motion:

$$M\ddot{x} + C\dot{x} + Kx = F\,\mathrm{Cos}\omega t \qquad 1.1$$

where F is the harmonic exciting force with a frequency ω.

The solution to the above equation consists of a transient part and a steady state part as follows:

$$x = x_1 e^{-\zeta\omega_n t}\mathrm{Sin}(\sqrt{1-\zeta^2}\,\omega_n t + \phi_1) + \frac{F\mathrm{Cos}(\omega t - \phi)}{\left[(K - m\omega^2)^2 + (c\omega)^2\right]^{1/2}} \qquad 1.2$$

where $\zeta = \dfrac{C}{c_c}$

and C_c(critical damping) $= 2m\omega_n$ 1.3

The first term normally quickly dies away due to the exponential term, but it may be of importance in certain cases of offshore structures, e.g. a Tension Leg Platform being struck by a single large wave may have a transient response which, when combined with the response to succeeding smaller waves, may still produce large motions and stresses.

The second term may be rewritten by dividing the numerator and denominator by K to give:

$$x = \frac{\frac{F}{K}\mathrm{Cos}(\omega t - \phi)}{\left[(1 - (\frac{\omega}{\omega_n})^2)^2 + (2\xi\frac{\omega}{\omega_n})^2\right]^{1/2}} \qquad 1.4$$

F/K is the static deflection under the applied force and so 1.4 may be written as :

$$\frac{x}{x_{STATIC}} = \frac{\mathrm{Cos}(\omega t - \phi)}{\left[(1-(\frac{\varpi}{\omega_n})^2)^2 + (2\xi\frac{\omega}{\omega_n})^2\right]^{1/2}} \qquad 1.4a$$

ϕ has the value:

$$\mathrm{Tan}^{-1}\frac{2\xi(\frac{\omega}{\omega_n})}{1-\frac{\omega}{\omega_n})^2} \qquad 1.5$$

Figures 1.1, 1.2 and 1.3 show the response curves for displacement x, velocity ωx, and acceleration $\omega^2 x$ for a range of values of ξ, the damping coefficient, while Fig. 1.4 shows the phase angle ϕ. The base of all the figures is the ratio of ω/ω_n and it will be seen that at $\omega / \omega_n = 1$ a very large response will occur if the damping is low since the response is then:

$$\frac{x}{x_{STATIC}} = \frac{1}{2\xi}\cos(\omega t - \phi) \qquad 1.6$$

For body motions ξ will be in the range of 0.05 to 0.12, but for elastic vibration of the structure it will be much lower, of the order of 0.001 to 0.005. Note that if ω/ω_n is much greater than 1.0, damping has little effect on the motions and so in semi-submersibles and some compliant structures which have natural frequencies much lower than the frequencies at which the wave energy occurs, increased damping is of little assistance in improving the motion. However, when such vehicles are moored the natural frequencies of the moorings may be very low indeed (periods around 60-200 secs) and it is important to have as much damping as possible at these frquencies.

The phase angle ϕ is close to zero for low frequencies, passes through 90° when $\omega/\omega_n = 1$ and for large values of ω/ω_n approaches 180° (see Fig. 4). It is very important to remember phasing when considering the relative motion of two vehicles such as a shuttle tanker moored to a storage buoy as it is probable that their natural frequencies will be considerably different and thus their motions may be out of phase with consequent high loadings on any attachments between the two vehicles.

Derivation of the Equations of Motion

In order to demonstrate the principles of calculating the motion of a floating body we will consider the motion of a circular cylinder floating vertically in waves when it is assumed that the dimensions of the cylinder are small, relative to the waves. Since we are dealing with a completely symmetrical body, when the

cylinder is pushed downwards in the water only an upward restoring force occurs, but most practical bodies are not symmetrical about all planes. Thus, for a ship a vertical displacement will set up both vertical (heave) forces and pitch moments due to the lack of symmetry of the waterplane fore and aft of the centre of water plane area. In such a case the equations of motion must be set up to include all these interactions and we get a set of six simultaneous equations in the six degrees of freedom. Fortunately many offshore structures show a fairly high degree of symmetry and wall-sidedness so that it is possible to create many of the motions independently of the others.

Consider a cylinder floating freely in a train of regular sinusoidal waves:

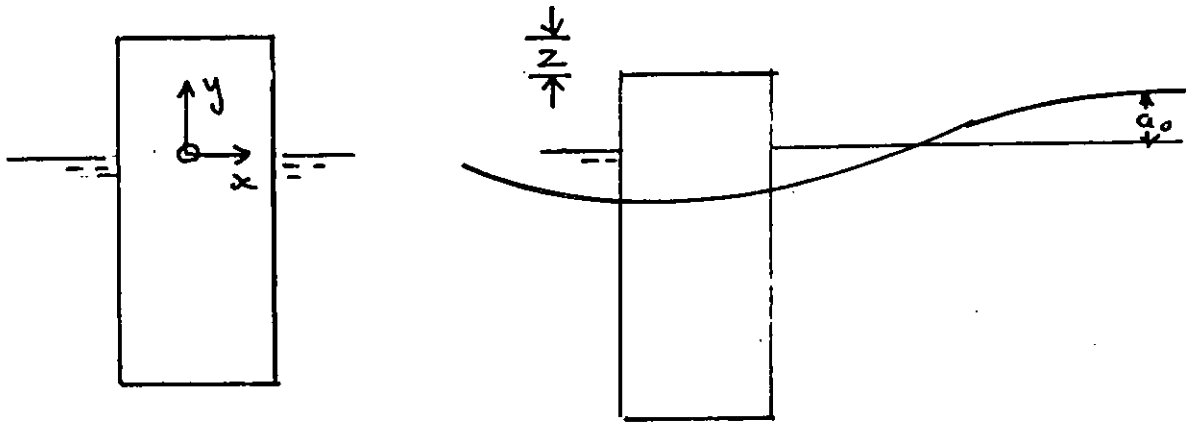

Fig. 1

The fundamental equation governing the behaviour of the cylinder is:

$$F = m\ddot{z} \qquad 1.7$$

where F is the summation of all forces acting on the cylinder
m is its mass
and $\ddot{z}$ is the vertical acceleration.

The force F is made up of hydrostatic and hydrodynamic forces as follows:

Hydrodynamic Hydrostatic

$$F = A(\ddot{y} - \ddot{z}) + C(\dot{y} - \dot{z}) + K(y - Z) \qquad 1.8$$

where the coefficients A, C and K are the forces per unit relative acceleration, relative velocity and relative vertical displacement from the still water position, $\ddot{y}, \dot{y}$ and y give the acceleration, velocity and displacement of the water level due to the wave, while $\ddot{z}, \dot{z}$ and z refer to the body's displacement from its still water position. A is the added virtual mass, while C must be regarded as an equivalent damping force coefficient since the actual force due to velocity is proportional to the square of the velocity.

If the wave and motion are both simple harmonic then the terms $(\ddot{y}-\ddot{z})$, $(\dot{y}-\dot{z})$, $(y-z)$ will be simple harmonic, although not necessarily in phase.

Rewriting (1) and (2) we have:

$$(m + A)\ddot{z} + c\dot{z} + kz = A\ddot{y} + C\dot{y} + Ky \qquad 1.9$$

The right hand side represents the exciting forces due to the wave acting on the body in its still water position, while the left hand side gives the reaction forces.

All the terms on the right hand side can be related to the wave profile $y = a_o e^{ky} \mathrm{Cos}k(x - ct)$ so that:

$$\begin{aligned} Ay + Cy + Ky &= -A\omega^2 a_o e^{ky} \mathrm{Cos}k(x - ct) - C\omega a_o e^{ky} \mathrm{Sin}k(x - ct) \\ &\quad + Ka_o e^{ky} \mathrm{Cos}k(x - ct) \\ &= a_o e^{ky} (K - A\omega^2) \mathrm{Cos}k(x - ct) - C\omega \mathrm{Sin}k(x - ct) \qquad 1.10 \\ &= F_1 \mathrm{Cos}k(x - ct) - F_2 \mathrm{Sin}k(x - ct) \\ &= F_0 \mathrm{Cos}k(x - ct + \phi) \end{aligned}$$

where $k = \dfrac{2\pi}{\lambda}$

λ = wave length

c = wave velocity

$$F_o = \left[F_1^2 + F_2^2\right]^{1/2} = a_o e^{ky}\left[(K - A\omega^{2)^2}\right]^{1/2} \qquad 1.11$$

$$\phi = \mathrm{Tan}^{-1}\left(+\frac{F_2}{F_1}\right) = \mathrm{Tan}^{-1}\frac{C\omega}{K - A\omega^2}$$

Note that if the value F_o is regarded as constant for each frequency we have the equation of motion in the standard form for a linear single degree of freedom system subject to a harmonic exciting force:

$$(m + A)\ddot{Z} + C\dot{Z} + KZ = F_o \mathrm{Cos}k(x - ct + \varphi)$$

with the solution:

$$\frac{F_o \cos k(x - ct - \phi)}{\left[(K - (m + A)\omega^2)^2 + (C\omega)^2\right]^{1/2}} \text{ where } \phi = \mathrm{Tan}^{-1}\frac{C\omega}{K - (m + A)\omega^2} \qquad 1.12$$

This can be rewritten by dividing numerator and denominator by K:

$$Z = \frac{F_o / K}{\left[(1-(\frac{\omega}{\omega_n})^2)^2 + (2\zeta\frac{\omega}{\omega_n})^2\right]^{1/2}} \qquad 1.13$$

where $\zeta = \frac{c}{c_c} = \frac{c}{2[K(m+A)]^{1/2}}$ 1.14

and $\omega_n = \left[\frac{K}{m+A}\right]^{1/2}$ 1.15

APPROXIMATE TREATMENT OF HEAVE ADDED VIRTUAL MASS OF VERTICAL CYLINDERS

When calculating the acceleration forces on vertical cylinders their dimensions may be large compared to the waves (e.g. a storage buoy). In such cases it is necessary to express the added virtual mass in terms of a length δx along the direction of travel of the wave. This in effect means treating the cylinder as a series of strips of width $2R\sin\theta/H$.

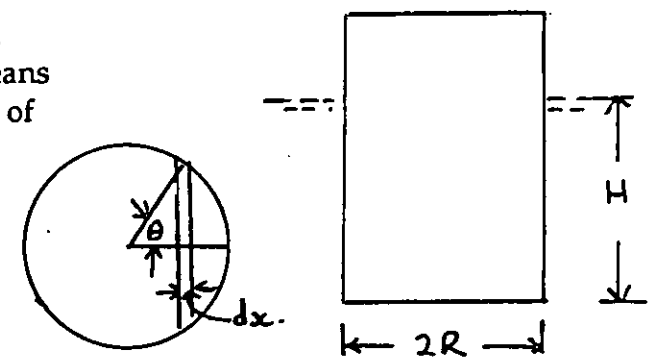

By integration of these values across the diameter an expression for the total virtual mass can be obtained. Since an analytic expression for C_V in terms of aspect ratio is relatively complicated, it is proposed to use a mean aspect ratio of $\pi R/2H$ and add a correction factor J to take account of the three dimensional effect. The value of J will be found from the limiting case of a disc.

Added virtual mass of strip of width $2R\sin\theta$ (for one face only)

$$= \frac{\pi}{2}\rho\,(R\,\mathrm{Sin}\,\theta)^2 JC_v \times R\,\mathrm{Sin}\,\theta\,d\theta \text{ since } \delta x = (R\delta\theta)\,\mathrm{Sin}\theta.$$

For a circular disc the total added mass (both faces)

$$= 2 \times \frac{\pi}{2}\rho R^3 c_v J \times 2\int_0^{\pi/2} \mathrm{Sin}^3\theta d\theta.$$

$$= 2\pi\rho R^3 JC_v\left[\frac{\mathrm{Cos}^3\theta}{3} - \mathrm{Cos}\theta\right]^{\pi/2}$$

$$= 2\pi\rho R^3 JC_v\left[-\frac{1}{3}+1\right] = \frac{4}{3}\pi\rho R^2 JC_v$$

For a thin disc, i.e. $H \to o$, C_v will tend to 1.0.

$$\therefore \quad \frac{4}{3}\pi\rho R^3 = \frac{1}{3}\rho R^3 \text{ (exact value for a disc)}$$

or $J = 0.635$.

Therefore an approximate value of the added mass for one face = $\frac{2\pi}{3}\rho R^3 J C_v$ = $1.33\ \rho R^3 C_v$ and for top and bottom faces = $2.66\ \rho R^3 C_v$ where C_v is for the mean aspect ratio.

FORMULAE FOR HYDROSTATIC, STABILITY AND MOTION QUANTITIES FOR BUOY - Fig. 5

Immersed volume:

$$\nabla = \pi(R_3^2 - R_1^2)H_1 + \pi H_2(R_4^2 - R_1^2) + \pi t_b(R_5^2 - R_1^2)(m^3) \quad (1)$$

$$\text{Displaced Mass } M = \rho\nabla \text{ Tonnes} \quad (2)$$

$$\text{2nd moment of waterplane area } I_A = \frac{\pi}{4}\left(R_3^4 - R_1^4\right) \quad (3)$$

$$BM = \frac{I_A}{\nabla} \quad (4)$$

$$KB = \left[\pi H_2\left(R_4^2 - R_1^2\right)\frac{H_2}{2} + \pi\left(R_3^2 - R_1^2\right)\left(H_2 + \frac{1}{2}H_1\right)\right] \div \nabla \quad (5)$$

$$KM = KB + BM \quad (6)$$

$$GM = 1.5 \quad (7)$$

$$KG = KM - 1.5m \quad (8)$$

Added mass in heave:

$$M_{AVM} = 1.33\,\rho\left(C_{VR3}R_3^3 - C_{VR1}R_1^3\right)$$

$$+ 2.66\rho\left(C_{VR4}R_4^3 - C_{VR34}R_3^3\right)$$

$$^8/_3\,\rho\left(R_5^3 - R_4^3\right) \text{ Tonnes} \quad (9)$$

where C_{VR3}, C_{VR1} are for aspect ratios $\frac{\pi R_3}{2(H_1 + H_2)}, \frac{\pi R_1}{2(H_1 + H_2)}$

C_{VR4}, C_{VR34}, are for aspect ratios $\frac{\pi R_4}{2H_2}, \frac{\pi R_3}{2H_2}$

Natural heave period:

$$T_H = 2\pi\left[\frac{M + M_{AVM}}{\rho g\pi\left(R_3^2 - R_1^2\right)}\right]^{1/2} \quad (10)$$

Mass inertia about CG = I_B

Added mass inertia of body in pitch I_{AVM}

$$= \pi R_3^2 \frac{H_1^3}{12} + \pi R_3^2 H_1 \left(\frac{H_1}{2} + H_2 - KG \right)^2 + \pi R_4^2 \frac{H_2^3}{12} + \pi R_4^2 H_2 \left(KG - \frac{H_2}{2} \right)^2 \qquad (11)$$

Natural pitch/roll period $T_{P/R} = 2\pi \left[\frac{I_B + I_{AVM}}{\rho g \nabla GM} \right]^{1/2}$ (12)

EXCITING FORCES IN HEAVE.

Dynamic presssure force on bottom of buoy = $\rho g a \pi \left(R_4^2 - R_1^2 \right) e^{-k_1(H_1+H_2)} \mathrm{Cos}k(x\text{-}ct)$

Pressure force on top of lower caission: $\rho g a \pi \left(R_4^2 - R_3^2 \right) e^{-k_1(H_1+H_2)} \mathrm{Cos}k(x - ct)$

where a = wave amplitude.

k = $2\pi/\lambda$ and λ = wave length.

c = wave phase velocity = $\left[g\lambda/2\pi \right]^{1/2}$

kc = ω = wave frequency.

The difference of the pressure forces on top and below the horizontal bilge keel is negligible.

The net pressure force = $\rho g a \pi \left[\left(R_4^2 - R_1^2 \right) e^{-k(H_1+H_2)} - \left(R_4^2 - R_3^2 \right) e^{kH_1} \right] x \mathrm{Cos}k(x\text{-}ct)$

The vertical inertia forces (13)

$$= \rho \omega^2 a \left[1.33 \left(C_{VR3} R_3^3 - C_{VR1} R_1^3 \right) e^{-k(H_1+H_2)} \right]$$

$$+ \left(C_{VR4} R_4^3 - C_{VR34} R_3^3 \right) \left(e^{-kH_1} + e^{-k(H_1+H_2)} \right)$$

$$+ \left[8/3 \left(R_5^3 - R_4^3 \right)_e^{-k(H_1+H_2)} \right] \mathrm{Cos}k(x - ct) \qquad (14)$$

Also $\omega^2 = gk$ (15)

SURGE FORCES

Dynamic pressure + inertia on upper cylinder:

$$= -(1+C_M)\rho\omega^2 a \int_{y=-H_1}^{y=o} \pi R_3^2 e^{ky} dy \, \mathrm{Sin}k(x-ct)$$

where $C_m =$ added virtual mass coefficient = 1.0

$$= 2\rho kga\pi R_3^2 \left[\frac{1}{K}\right](1-e^{-kH_1})\mathrm{Sin}k(x-ct)$$

Similarly on lower caisson:

$$\text{Surge Force} = 2\rho ga\pi R_4^4\left[e^{-KH_1} - e^{-k(H_1+H_2)}\right]\mathrm{Sin}k(x-ct)$$

$$\text{Total Force} = -2\rho a\pi\left[R^2\left(1-e^{-kH_1}\right) + R_4^2\left(e^{-kH_1} - e^{-k(H_1+H_2)}\right)\right]\mathrm{Sin}k(x-ct) \qquad (16)$$

PITCH/ROLL MOMENT DUE TO HORIZONTAL FORCES

Vertical forces neglected but they will affect the pitch in short waves.

Pitch moment =

$$-2\rho kga\pi\left[\int_{y=-H_1}^{y=0} R_3^2(y-y_G)e^{ky}dy + \int_{y==-(H_1+H_2)}^{y=-H_1} R_4^2(y-y_G)e^{ky}dy\right]\mathrm{Sin}k(x-ct)$$

$$-2\rho ga\pi\int R_3^2\left[H_1e^{-kH_1} - \left(1-e^{-kH_1}\right)\left(\frac{1}{k}+y_G\right)\right]$$

$$+R_4^2\left[-H_1e^{-kH_1} + (H_1+H_2)e^{-k(H_1+H_2)} - \left(e^{-kH_1} - e^{-k(H_1+H_2)}\right)\left(\frac{1}{k}+y_G\right)\right]\mathrm{Sin}k(x-ct)$$

where y_G is the distance of the CG below the waterline (17)

MOORING DESIGN

NEIL S. MILLER

GLASGOW.

MOORING DESIGN

INTRODUCTION

Although there is a considerable literature on mooring design it still rests on a considerable amount of empiricism mainly due to the lack of the environmental data which would allow greater precision in achieving specific objectives.

The following material relates to the design of catenary moorings for floating production vessels where the mooring may be expected to remain in use for periods of up to 25 years. In recent years various combinations of catenary mooring and a buoyant column have been designed and there are a few installations of this type but such hybrid systems are not considered in detail.

Articulated columns are not considered as although they were popular in the late 70's and early 80's they are now considered to be an expensive form of mooring which has a poor record in reliability. Much of the early design faults have been eliminated but currently the costs of such columns are too high to be competitive.

The design and installation of moorings is normally carried out by firms specialising in this work but frequently other engineers have to specify the environmental conditions which the design must withstand, the model tests and test conditions which must be used and the design criteria in respect of loads and materials. It will be shown that there is considerable differences between different design codes and that it is necessary for the oil company to satisfy itself that the design conditions and criteria are in line with its intentions for the unit concerned. The lectures will attempt to cover these aspects of the mooring problem.

A considerable amount of time will be devoted to consideration of all the factors affecting the loading on the moorings but since part of the loading is dynamic in nature and depends on the stiffness and damping behaviour it brings in the mooring line characteristics. Thus it is not easy to separate the loading on the system and its ability to resist these demands as one would wish to do to use a reliability approach in design. However, if mooring design is to be put on a more sound basis this is the direction in which the industry must move.

The determination of the design loading is common to all mooring problems so that some aspects of mooring drilling semi-submersibles and other service vessels will be covered. However, due to their need to be able to moor in a wide variety of water depths and environmental conditions special considerations go into the selection of the mooring equipment for such vessels.

It is now common to use some thruster assistance to reduce the excursions on the moorings and thus their loading but the design of such systems will not be dealt with. A key aspect in deciding to use such assistance are the costs associated with the degree of redundancy necessary to ensure that the thrusters will be operational when the need to use them arises.

This redundancy must cover all aspects of power generation, control systems and the thruster units themselves. Many companies have a philosophy of only using these units under the most severe or emergency conditions, but there is a danger that long periods of inactivity may reduce their reliability and they should certainly be tested at regular intervals.

MOORING LOADS

The mooring loads arise from various effects of the waves, wind and current and may be defined by the equation:

$$M = L_{WS} + L_{WD} + L_{CT} + L_{CW} + L_{DW} + L_{SD} + L_S + L_{LD}$$

L_{WS} = the steady wind load

L_{WD} = the wind gust induced loading

L_{CT} = the load due to tidal, storm surge and any ocean circulation current flows

L_{CW} = the load induced by wind driven current

L_{DW} = the steady drift force due to waves

L_{SD} = the slow drift dynamic force

L_S = the net force induced by the first order motions (mainly surge/sway but with contributions from heave, pitch and roll for single point moored vessels and additionally yaw in the semi-submersible and buoy cases)

L_{LD} = the tension force induced by the dynamic line behaviour

Such an equation applies at only one draft and one depth of water since changes in these variables will affect the mooring stiffness and its response to the dynamic forces.

Nearly all design codes specify that the wind, wave and current forces shall act co-linearly on the assumption that this provides a degree of conservatism when considering loads with a return period of 1 in 50 or 100 years. This is discussed in some detail in Ref. 1 which is primarily concerned with the joint probability of current and waves.

Such an assumption provides the highest load if the mooring is designed by what has come to be known as the quasi-static procedure where all steady loads are applied to the mooring and its offset determined and the excursion due to surge/

sway is then applied to give the total quasi-static excursion and with appropriate safety factors the design can be assessed. Surge/sway is always greatest in long waves and therefore the 1 in 50/100 year condition is appropriate.

However, it will be shown that the wave drift is unlikely to be at its highest value in the 1 in 50 year wave conditions and will be greater in much shorter period waves which have a higher probability of occurrence. Depending on the mooring stiffness and damping characteristics, the dynamic excursion due to wave drift forces may be much higher than that found in the quasi-static solution even although the surge/sway contribution will be much less. Under these wave conditions there is a good possibility that the wind, waves and current will not be in line with one another and it is necessary to consider the worst combination of directions. This may produce higher design loads in many cases and especially in deeper water.

Unfortunately our knowledge of many of the quantities involved such as damping, drift force coefficients and the effect of current on these quantities is still open to considerable errors in a particular case and the best design loads will be obtained by careful model tests in a facility which is able to accurately reproduce the environmental conditions - including depth of water and mooring line spread. There are very few such facilities and it may be necessary to resort to tests of parts of the system in different facilities and to combine the results theoretically.

Additionally, statistical data on the frequency of conditions when there are severe wave conditions (of the order of 1 year return period) with high winds at a different heading to the waves are rare. This must be a possibility as a low pressure area, which causes the wind and waves, moves across the ocean and can be seen in some published records from the Ekofisk field (see Fig. 1 from Ref. 2). Each time the wave conditions get above a significant height of 6 m. the wind direction changed within the next few hours by as much as 180°. Since it is impossible for the wave direction to change in such a time due to the inertia involved, the wind must have had varying angles to the waves.

Further it is possible for the wind to increase to a high velocity within a short time which will have little effect on the prevailing wave conditions. A case has been recorded (Ref. 3) of wind speed increasing from 16 to 60 knots in 20 minutes. It is therefore thought that it is possible for the 50 year return period wind to exist with 1 year wave conditions and that such a combination can provide a higher loading than the 50 year return, all co-linear, assumption.

The above discussion relates to the long term mooring of production or storage units and lesser criteria are applicable to drilling units where they have the possibility to disconnect their risers in very severe storm conditions and take other measures to reduce the loads on the most heavily loaded lines.

The API (Ref. 4) code recommends a level of wind,wave and current conditions which will be exceeded for 0.1% of the time at the site but to assume these are co-linear. The arguments given above apply to the wave drift forces and response for semi-submersibles, but they provide a much smaller proportion of the

loading and the mooring loads may not be much higher if the wind and waves are not in line.

WIND LOADING

The wind loading is calculated from the basic formulae:

$$L_{WS} = \tfrac{1}{2}\rho C_D A U^2 \qquad (1)$$

where:

ρ = air density which is commonly taken as 0.00123 tonnes/m^3 but which can range from 0.00134 at -6°C to 0.00118 at +25°C.

C_D = drag coefficient determined ideally from a wind tunnel test of the complete structure but may be taken for each component of the structure and the results added to give a total drag. The latter procedure always produces a less accurate result due to our inability to take account of interference effects.

A = transverse projected area normal to the wind direction. In cases where there are axes of symmetry the area is taken normal and parallel to these axes and the C_D values are derived from the forces and moments normal and parallel to the axes for all wind heading angles (m^2)

U = wind velocity (m/secs) at a reference height of 10 m above the sea surface.

The wind velocity provides the largest source of uncertainty in this formula. The classification societies and other regulatory bodies specify differing time averages to be used in determining U ranging from a 1 minute average to a 1 hour average with a growing tendency to specify a 10 minute average.

Since the natural period of the vessel on its moorings will be around 1 to 3 minutes or greater, a 1 minute average speed implies that gusts of shorter duration will have little effect on the mooring loads and may be neglected. If a 10 minute average is used gust effects should be taken into account.

There is no general agreement between the various authorities on the relationship between the 1 hour, 10 minute and 1 minute average speeds. Figure 2 gives the latest figures for the 1 hour average values prepared for the former Department of Energy and published in their Guidance Notes (Ref. 5). In the same publication, they give the relationship between the 1 hour average and various other averaging periods indicating figures of approximately 1.04 and 1.17 between the 1 hour and the 10 minute and 1 minute averages respectively. Much higher differences are given by other authorities such as Bureau Veritas.

The wind profile above the sea depends on the averaging period chosen. Reference 5 indicates that this is a complex relationship which cannot be represented by the commonly used relation

$$U_Z = U_{10}\left(z/10\right)^{1/n} \qquad (2)$$

where:
- z = height above the surface (m)
- U_{10} = reference velocity 10m above the surface
- n = an index which varies from around 7 for a 1 hour average to 11 for a 1 minute average. Lloyd's Rules use 8 and Det norske Veritas 11.1

A relationship which gives approximately the Guidance Rules values is:

$$U_{z,T} = V_{10,1HR}(1.49 + 0.125 \ln Z - 0.21 \ln t + 0.0144 (\ln t)^2) \qquad (3)$$

$U_{z,T}$ = velocity(m/sec) at a height z (m) and time average t (secs)

$U_{10,1HR}$ = 1 hour average velocity at 10m. above the sea surface.

The formula is applicable in the range of time averages from 1 hour to 1 minute and from sea level to 100 m above the surface with an accuracy of the order of + 2%. The tables of values in the Guidance Rules (p. 11.13 and 11.14) only quote values in integer form and this makes curve fitting difficult.

One weakness of equation (3) is that it indicates a velocity at the sea surface where theoretically it should be zero but since there will nearly always be waves present the boundary condition is poorly defined.

A comparison of the 1 hour, 10 minute and 1 minute average speeds with height is given in Table 1 along with the profiles for indices of 1/8 and 1/11 and for a 1 hour average speed of 38 m/sec at 10m above the sea. The corresponding 1 minute average is given(Ref. 5) as 45 m/sec and this has been applied to determining the profile for the 1/11 index.

From Table 1 it can be seen that, for this 1 hour average speed, equation (3) predicts a higher speed for the 1 hour average speed and lower values for the 1 minute average compared to the data in the Guidance Rules. The 1/8 index gives a close approximation to the 1 hour average profile while the 1/11 index is a very good approximation to that of the 1 minute average. At heights below 10m, which gives rise to the majority of the lateral wind forces on tankers there is no great difference between the equation (3) values and the index profile for the 1 hour average but significant differences for the 1 minute case.

Table 1:/

Table 1: **Comparison of 1 hour and 1 minute average speeds with profiles based on 1/8 and 1/11**

Height above sea(m)	Eqn (3) t=3600s m/sec	Table 11.5 Ref. 5 m/sec	Eqn (3) t=60secs m/sec	Table 11.5 Ref. 5 m/sec	$38(z/10)^{1/8}$ m/sec	$45(z/10)^{1/11}$ m/sec
0.0	28.0		33.1		0.0	0.0
1.0	28.0		33.1		28.4	36.5
2.5	32.3		37.5		32.0	39.7
5.0	35.6		40.8		34.8	42.2
10.0	38.9	38.0	44.1	45.0	38.0	45.0
20.0	42.2	42.0	47.3	48.0	41.4	47.9
30.0	44.1		49.3		43.6	49.7
40.0	45.5	45.0	50.6	51.0	45.2	51.0
50.0	46.5		51.7		46.5	52.1
60.0	47.4	47.0	52.6	53.0	47.5	53.0
80.0	48.8	49.0	53.9	54.0	49.3	54.4
100.0	49.9	50.0	55.0	55.0	50.7	55.5

At the 10 m level the 1 minute average speed is 18% higher than the 1 hour average, but at the 100 m level this difference has decreased to 10%. This indicates that the centre of action of the wind force will be at different heights for the two cases, especially bearing in mind that the force depends on the square of the wind speed.

One inconsistency in the Guidance Rules is that, in section 31 on stability, they give a recommended procedure for calculating the wind force which is based on practice in the American Bureau of Shipping and Lloyd's Register. The force is expressed by the formula:

$$F = \tfrac{1}{2}\rho A C_S C_H U^2 \qquad (4)$$

where:

C_S = shape coefficient depending on the shape of the structural member to the wind (see Table 2).

C_H = the height coefficient depending on the height above the sea of the structural member exposed to the wind (see Table 3).

Table 2/

Table 2: Values of the shape coefficient C_S

Shape	C_S
Spherical	0.4
Cylindrical	0.5
Large flat surface (hull deckhouse, smooth under deck areas)	1.0
Drilling derrick	1.25
Wires	1.2
Exposed beams and girders under deck	1.3
Small parts	1.4
Isolated shapes (crane, beam, etc.)	1.5
Clustered deck houses or similar structures	1.1

Table 3: Values of the height coefficient C_H

Height above sea level(m)			C_H
0.	-	15.3	1.0
15.3	-	30.5	1.10
30.5	-	46.0	1.20
46.0	-	61.0	1.30
61.0	-	76.0	1.37
76.0	-	91.5	1.43
91.5	-	106.5	1.48

Since the force depends on the square of the velocity the value of C_H is equivalent to the square of the non-dimensional profile. It is shown as 1.0 up to 15.3 m. above the surface and as 1.1 for the next 15.2 m. The American Bureau asks for a 1 minute average speed at 10m above the surface to be used with this profile. If the figures in Table 1 are examined, it will be seen that to use the $U_{10,1M}$ will lead to a considerable overestimate of the wind load on a tanker hull where in the beam on condition the majority of the area is below 10 m. The errors will be proportionately less for semi-submersibles since only the columns are exposed over this range but will be significant. This method also produces the wrong centre of wind pressure which is important to stability calculations. It is suggested that it is better to use the Guidance Rules Section 11 profiles if eq. (4) is used.

WIND TUNNEL RESULTS

If a C_D value is to be used for the complete unit (FPSO, semi-submersible, buoy), it must have been determined for the same wind profile as the mooring force calculation requires. This is the major difficulty for tanker type vessels as much of the data available have been determined for a 1 hour average profile and in many cases the profile used was not recorded.

It is common to use the OCIMF values (Ref. 6) but these were determined for a wind profile with a nominal index of 1/7 (Ref. 7) The measured profile differed from the 1/7 by as much as 5% although fortunately the differences were all in the direction of a higher value of the index i.e. a shorter averaging period. Ref. 6 does not state the height of the reference velocity used in determining the drag coefficients and whether this was a measured velocity or the theoretical 1/7 index value.

The models used were at small scales (1/300 to 1/340) and thus the model Reynolds Number were orders of magnitude less than the full scale and the results for the near circular bow cases must be somewhat suspect. No mention is made of turbulence stimulation devices. These points are mentioned since they should be covered in the specification for any future tests.

Gould (Ref. 8) has shown that accurate results can be obtained by testing the model in a uniform flow over its full depth to obtain the drag coefficient, but modifying the area at each height by the square of the non-dimensional profile to take account of the desired wind profile. Thus the vessel is split into a convenient number of horizontal layers and $\sum A\alpha^2$ is calculated for each layer where A is the area and α is the wind gradient profile factor. An example of such a calculation for a tanker is shown in Table 4 where large vertical intervals have been taken to reduce the size of the Table. It would be normal to use 1 m vertical intervals in a computer program. The wind profile in this case is a 1 hour average of 38 m/sec at 10m above the surface which using equation (3) gives a 10 minute average speed of 38.87 m/sec.

TABLE 4: Example of Longitudinal Wind Force Calculation for a Tanker 240 m long by 44.2 m beam. Using a 10 Minute Average Wind Gradient - $V_{10,1HOUR}$ = 38 m/sec

Height Above Sea Surface (m)	Description	Dimensions B x D (m)	Area AT (m^2) 0.125lnZ	$V_{x,t=a}$ / $V_{10,10m}$	Corrected Area(m^2) = $A_T\alpha^2$
0-5	Main Hull	44.2 x 5	221	0.850	159.7
5-10	Main Hull + Superstructure	44.2 x 5	221	0.987	215.3
10-15	Superstructure	32 x 5	160	1.051	176.7
15-20	Superstructure	29.0 x 5	145	1.093	173.2
20-25	Superstructure	32.0 x 1			
	Bridge	12.0 x 1.5			
	Funnel	3.5 x 2.5 Total = 59		1.124	74.5
25-30	Funnel	3.0 x 5	15	1.149	19.8
30-35	Funnel	3 x 1			
	Bridge Mast	6 x 1.5 Total = 12		1.170	16.4
	TOTAL		833.0		835.6

Longitudinal Wind Force (OCIMF) = $1/2 \times 0.00123 \times 0.955 \times 83.3 \times 38.87^2$
= 739KN

Longitudinal Wind Force (GOULD) = $1/2 \times 0.00123 \times 1.178 \times 835.6 \times 38^2$
= 874KN

In the example given in Table 4, there is very little difference between the corrected and uncorrected areas, but the distribution of the areas over the depth is very different e.g. for the first 5m above the sea the corrected area is 159.7 m against the actual area of 221 m and so the force distribution with depth is very different. In a beam on wind situation the majority of the area is below the 10 m level and thus the corrected area will be less than the true area due to the gradient effect

To sum up, for wind tunnel test to provide accurate mooring loads:

(a) the wind profile in the tunnel must be for the correct averaging profile - either a 10 minute average or a 1 minute average. Alternatively a uniform profile may be used but the layers of area on the full scale must be corrected for the wind profile when using the C_D from such a test.

(b) the drag (and lift) coefficients must be determined using the velocity at 10m above the sea surface.

(c) the model scales must be large enough to minimise scale effects (they cannot be eliminated) and where appropriate turbulence stimulation devices should be used.

DRAG COEFFICIENTS

As far as can be determined there are no published wind tunnel tests on an FPSO vessel with all the process units, cranes and export booms etc. on board. Many companies appear to have been content to use the OCIMF values since in the head on condition the transverse projected area is very similar to that of a tanker. If as will be suggested, it becomes necessary to consider wind loading at a heading to the waves for mooring design, it will become important to get accurate drag and moment coefficients which will properly reflect the above water structural layout.

The coefficients in common use i.e. the OCIMF and Gould values are summarised in Table 5, but it must be remembered that they are not directly comparable since the latter are for a uniform profile and are to be used with a corrected area. Allowing for this difference it will be seen that there are differences in the shape and magnitudes between the two sets of results. The example given in Table 4 shows an 18% difference in wind force.

The OCIMF values show large differences between a rounded and a conventional bow in the ballast condition, while Gould does not show this for a visually very similar bow. The result is that the longitudinal wind force calculated for an angle of 60° off the bow will be in opposite directions according to the two sets of results. This emphasises the need for well conducted wind tunnel tests on any tanker type FPSO.

The same arguments apply to semi-submersibles and buoys as the methods proposed for calculating the wind loads as illustrated by equation (4) and Tables (2) and (3) above are very crude and open to error. In the semi-submersible case the

presence of decks supported on columns gives rise to large lift effects especially after the vessel has developed an angle of inclination to the wind. This is the chief reason why there is poor agreement between wind tunnel tests and calculated loads and moments but scale effects are also serious.

An example is the use in many of the design codes of a drag coefficient of 0.5 for circular cylinders. The Reynolds Number (Rn) for a 10m diameter column in a 38m/sec wind is over 10^7 and the drag coefficient on the column will be of the order of 0.65 to 0.7 (see Figs 3, 4). The use of 0.5 is only justified since no interference effects are taken into account and these will reduce the drag on columns which are partially shielded by a column or columns in front of them. However, such a procedure does not distinguish between an Aker H3 design with 8 columns and considerable bracing and a GVA 4000 design with 4 columns and little bracing.,

The DNV rules are more detailed than those of Lloyds and the American Bureau in that they attempt to take account of interference effects, extent of rounding of corners etc. However, a number of papers (Ref.s 9 to 27) compare wind tunnel results with forces and moments calculated according to the various codes and the general conclusion is that the codes overestimate the forces and moments by between 10 to 40% with DnV giving the poorest agreement.

This is by no means conclusive as the wind tunnel tests have used different wind profiles and in some cases very dubious methods of compensating for the Rn problem on the columns have been applied. The full scale measurements made of mooring loads in one case (Ref. 21), indicated these to be 30% lower than the wind tunnel results. Part of this difference could be explained by differences in the wind profile and by scale effects, but a substantial amount remained unexplained.

Since wind loading will form the largest part of the mooring load on most semi-submersibles, it is important to carry out wind tunnel tests and make every effort to obtain the correct wind profile in the tunnel and to use a scale sufficiently large to offer the prospect of reducing Rn effects by turbulence stimulation. In the Norwegian sector such tests are mandatory from stability considerations, but they are also necessary to get more precise mooring loads. Design calculations using any of the code methods are likely to overestimate the mooring load and should be checked against the few wind tunnel tests available (with due note of the profile used).

For buoy design a drag coefficient of 0.7 should be used for the circular caisson, but the upper deck loadings will have to be estimated using existing codes.

WIND GUST EFFECTS

It has been suggested earlier that wind gust effects should be taken into account if a 10 minute average wind speed was used. Although a 1 minute average speed will be approximately 13% higher than a 10 minute average and thus the corresponding wind force 26% higher, it may be that a 10 minute average plus gust effects will produce a higher loading on the mooring. The response to the gust

effects depends on the mooring stiffness and most importantly on the damping. If this is low the dynamic excursion due to gusts may exceed the static excursion due to the higher average wind speed.

Little of no data exists on the degree of correlation which may exist between the wave drift dynamic response and the wind gust response. At the low natural periods of the moorings it appears likely that they will from time to time coincide in their actions and it may not involve much conservatism to assume that their effects are additive.

For a single point moorings, the action of wind gusts is probably more important when the wind and waves are not in line since they then induce yawing which may drive up the wave drift loads and the overall load on the moorings.

There are a number of different formulae in use for the wind gust spectrum. These were reviewed by Ochi and Shin (Ref. 28) who proposed a new formula to take better account of the low frequency measurements which were available - see Figs. 5 and 6 from Ref. 28.

Following the Ochi/Shin notation the spectra formulae are expressed as follows:

Dimensionless frequency:

$$f_* = \frac{fz}{\overline{U}_z} \tag{5}$$

Dimensionless spectral density:

$$S(f_*) = \frac{f\,S(f)}{u_*^2} \tag{6}$$

where:

f	=	frequency in cycles per second
z	=	height above sea level in metres
$\overline{U}_Z$	=	mean wind speed at height z in m/sec
$S(f)$	=	spectral density function in m^2/sec
u_*	=	shear velocity in m/sec

The values of $\overline{U}_Z$ and u_* used in deriving the spectral formulae were:

$$\overline{U}_Z = \overline{U}_{10} + 2.5u_* \ln\left(\frac{z}{10}\right) \tag{7}$$

$$u_* = \sqrt{C_{10}}\,\overline{U}_{10} \tag{8}$$

where:

$\overline{U}_{10}$ = 1 hour mean wind speed at 10m height in m/sec

C_{10} = surface drag coefficient evaluated from wind measurements at 10m height. It is given approximately by the formula

$$C_{10} = \left(0.75 + 0.067\,\overline{U}_{10}\right) \times 10^{-3}$$

Using the above notation the most commonly used wind gust spectral formulae are:

Davenport:

$$S(f_*) = \frac{4x^2}{\left(1+x^2\right)^{4/3}} \tag{9}$$

where:

$$x = 1{,}200\frac{f}{\overline{U}_{10}}$$

Harris:

$$S(f_x) = \frac{21.97x}{\left(1+6\pi^2x^2\right)^{5/6}} \tag{10}$$

where:

$$x = \frac{((1.09)(180)}{\overline{U}_Z}$$

Ochi/Shin:

$$S(f_*) = \begin{cases} 583\,f_* & \text{for } 0 \le f_* \le 0.003 \\ \dfrac{420 f_*^{0.70}}{\left(1+f_*^{0.35}\right)^{11.5}} & \text{for } 0.003 \le f_* \le 0.1 \\ \dfrac{838 f_*}{\left(1+f_*^{0.35}\right)^{11.5}} & \text{for } f_* > 0.1 \end{cases} \tag{11}$$

There are several variations on the Davenport and Harris formulae in use in oil companies - in particular the characteristic length is changed from 1200 to 1800 in the Davenport case. There is a scarcity of data measured above the sea to verify these formulae and so an allowance of ± 10% should be allowed on the $S(f_*)$ values.

Standing et al in Ref. (25) found that a modified form of the Kaimal spectrum gave the best fit to the wind data recorded at the West Sole platform. It has the form:

$$fS(f)/u^2 = \frac{0.66x}{\left(x^{0.15} + 9/8x\right)^{5/3}} \tag{12}$$

where: $x = 1667f/U$, U is the mean velocity at the height considered, u is the variance of the fluctuating velocity (i.e. the square of the turbulence level).

Gust Loading:

The fluctuating wind drag on a structure:

$$F(t) = \tfrac{1}{2}\rho_A C_D A_T U(t)^2 \tag{13}$$

where:

$U(t)$ = U+u and u is the fluctuation in the wind speed about the mean U.

Rewriting (12):

$$\begin{aligned} F(t) &= \tfrac{1}{2}\rho_A C_D A_T\left[U^2 + 2Uu + u^2\right] \\ &= \tfrac{1}{2}\rho_A C_D A_T U^2\left[1 + 2u/U + u^2/U^2\right] \end{aligned} \tag{13a}$$

The first term in (13a) is the steady wind drag determined in the normal manner. The second term $\rho_A C_D A_T Uu$ provides a fluctuating drag while the third term provides second order effects which are normally neglected but which may be important if the level of atmospheric turbulence is high. In open sea conditions this is unlikely to be the case except in tropical storm conditions.

The power spectrum of the fluctuating drag is:

$$S_D(f) = \left(\rho_A C_D A_T U\right)^2 S_u(f) \tag{14}$$

i.e. it is a constant times $S_u(f)$ where the constant depends on C_D and A_T. The units of the force spectrum will be $(kN)^2$ per unit of frequency i.e. $(kN)^2$ sec.

DYNAMIC RESPONSE TO WIND GUSTS

Once the steady loads due to wind, current and wave drift forces have been determined, it is possible to find the excursion corresponding to these loads. Normally the load excursion curve will be a curved line getting gradually steeper as the excursion increases. In the following it is assumed that the curved line can be replaced by a straight line over the region covered by the dynamic excursion i.e. that the system has a linear response. Once the dynamic excursion has been obtained the validity of the assumption over the range should be examined and if necessary the calculations repeated with a new value of the stiffness.

The natural frequency of the mooring in this state can be found from:

$$f_n = \frac{1}{2\pi}\left[\frac{K_s}{M + M_{AVM}}\right]^{1/2} \text{cycles / sec} \tag{15}$$

K_s = mean mooring stiffness over expected excursion range

where: M is the displacement mass of the vessel (tonnes)
and M_{AVM} is its added mass in the direction of motion

If the vessel on its moorings is now treated as a linear single degree of freedom system, its dynamic response spectrum is:

$$S_x(f) = \frac{1}{K_S^2}|H_f|^2 S_D(f) \tag{16}$$

where:

$|H_f|$ is the mechanical admittance or magnification factor and equals:

$$\frac{1}{\left[\left(1-\left(f/f_n\right)^2\right)^2+\left(2\gamma f/f_n\right)^2\right]^{1/2}}$$

where: γ is the ratio of the damping to critical damping for the mooring system. This is difficult to determine with any precision, being partly due to the motion of the mooring lines which in turn depends on the dynamics excursion.

If no better data is available it is suggested that a value $\gamma = 0.06$ be used in order to get a first estimate of the excursion and this may then be refined by subsequent calculations on the mooring line behaviour.

Since K_S is a constant equations (13) and (15) may be combined to give:

$$S_x(f) = \left(\frac{\rho_A C_D A_T U}{K_S}\right)^2 |H_f|^2 S_u(f) \tag{17}$$

Computationally what is required is to determine $S_u(f)$ and $|H_f|^2$ for a series of values of f, multiply them together and treat the quantity in brackets as a constant which can be introduced at the end of the calculation. The units of $S_x(f)$ are m^2 sec.

The effect of the low value of the damping is to give a very narrow peaked response spectrum so that it is common to apply a Rayleigh probability distribution to estimate the response

The mean square value of the response is:

$$E_X = \int_{\mu}^{\infty} S_x(f)df \tag{18}$$

This integral must be determined accurately so that the spectral values must be calculated at very closely spaced intervals near the natural frequency with wider spacings further away.

The Rayleigh distribution has the general form:

$$p(x) = \frac{2x}{E_x} e^{-x^2/E_x} \tag{19}$$

and its cumulative distribution is:

$$P(x)_{x > x_1} = e^{-x_1^2/E_x} \tag{20a}$$

$$P(x)_{0 < x < x_1} = 1 - e^{-x_1^2/E_x} \tag{20b}$$

The significant excursion (mean of the one third highest excursions - crest to trough values) $X_{1/3} = 2 \times \text{RMS value} = 2[E_x]^{1/2}$. The highest excursion will depend on the length of time the storm blows but an appropriate estimate for the early design stage is:

$$X_{MAX} = 0.95 X_{1/3} \tag{21}$$

This is the excursion beyond that due to the steady forces and it will be important to see how well the assumed value of stiffness represents the mooring behaviour at this point and if necessary repeat the calculation with a modified value.

CURRENT LOADING

It is common practice to add the 50 year return value of the tidal and ocean circulation/storm surge current to that generated by the wind and treat them as co-linear with the wind and the waves.

Since the tidal current has a definite time cycle with regard to both speed and direction apart from its monthly and di-urnal variations this assumption is very conservative. In the North Sea the tidal, storm surge and the wind driven elements of velocity with 50 year return period have values less than 1 m/sec so that when they are squared to get the current force the individual values are quite low. When the velocities are added, however, the value is greater than 1.0 and this produces a significant force. In certain areas it may be possible to determine the directions of the maximum tidal effects and only perform the addition for these particular directions.

Section 11.6 of the Guidance Notes provides data on the 50 year return period values of the currents in the U.K. and Norwegian waters. Figs (7) to (9) reproduce the average tidal velocity, tidal direction and storm surge velocity diagrams from the Guidance Notes. Table 11.13 of the notes gives factors to estimate the maximum tidal current from the average value. They are approximately 1.5 in the oil/gas producing areas of the North Sea. The 50 year values of the surface wind drift U_w is quoted as varying from 0.9 to 1.2 m/sec, which corresponds to 3% of the 50 year hourly wind speed.

Despite a considerable research effort there is still considerable doubt about the depth profile to use with the current. The Guidance Notes give considerable detail while stressing the lack of good long term data to confirm the figures.

For the tidal profile it suggests:

$$U_{t(z)} = (z / 0.32h)^{1/7}\,\bar{u}_t \qquad \text{for } 0 \le z \le 0.5h$$

$$U_{t(z)} = 1.07\,\bar{u}_t \qquad \text{for } 0.5h \le z \le h \tag{22}$$

where:

$U_{t(z)}$ = tidal velocity at a height z above the sea bed

$\bar{u}_t$ = depth-averaged tidal velocity

z = height above the sea bed

h = total water depth.

A detailed method of developing an overall vertical structure of the current is given in Ref (29) which provides the theoretical and experimental background to the Guidance Rules sections on wind and currents. A simplified approach to the storm surge plus wind driven current is suggested in the Guidance Rules as follows:

$$U_{S(z)} = \bar{U}_S + \frac{(z - h^1)}{10} U_W \qquad \text{for } h^1 \langle z \langle h$$

$$U_{S(z)} = \bar{U}_S \qquad \text{for } 0 \langle z \langle h \tag{23}$$

where:

$U_{S(z)}$ = speed of storm surge current plus wind drift at a height z above the sea bed (m/sec)

$\bar{U}_S$ = depth averaged storm surge current from Fig.

z = height above the sea bed in metres

h = total height between the sea bed and still water level (in m.)

h^1 = height above the sea bed at which the current profile changes slope = $h - 10(U_W - \bar{U}_S)$

If $U_S \ge U_W$, the profile is $U_{S(z)} = \bar{U}_S$

This profile has to be multiplied by a factor:

$$\left[1+\frac{S\left(U_w-\overline{U}_s\right)^2}{h\overline{U}_s}\right]^{-1}$$

to ensure that the average current obtained by integrating the profile from the sea bed to the surface is equal to the depth averaged storm surge current.

The classification societies tend to recommend that the wind driven current at the surface is 1.7% of the 50 year, 1 minute average at 10m above the sea wind speed and that it declines to zero at a depth of 50 m below the surface i.e.:

$$U_z = U_t + 0.017U_w[50-Z]/50 \tag{24}$$

Below 50 m the tidal plus surge current is assumed uniform to the bottom.

An alternative profile used by some of the companies engaged in the recording and analysis of environmental data is based on the following assumptions:

(a) The local wind induced current speed at the surface is 3% of the extreme 12 hour mean wind speed at 10m above sea level.

(b) The current profile due to local wind follows a logarithmic relationship where:

$$U_Z = U_0 - \left[\left(\frac{U^*}{K}\right)\ln\frac{z}{Z_0}\right] \; ; \; U_z > 0.0 \tag{25}$$

U_Z = wind drift current at depth z

U_0 = wind drift current at the surface (3% of the 12 hour average wind speed, 10 m above sea level)

U^* = friction velocity (0.12% of the wind speed at 10m above the surface)

K = von Karman's constant (0.4)

z = depth below surface

Z_0 = surface roughness length (0.0015 m)

(c) The profile above the sea bed can be approximated by a power law of the form:

$$\frac{U_h}{U_{h1}} = \left(\frac{h}{h_1}\right)^{0.1} \tag{26}$$

where:

U_h is the current speed at reference height h above the sea bed.
U_{h1} is the current speed at reference height h_1 above the sea bed.

sometimes scaling factors are added to get agreement with measured profiles.

Using the wind data in Ref. 5 a 1 min. average speed of 45 m/sec corresponds to a 1 hour average of 38 m/sec and a 12 hour average speed of 33 m/sec. Using these values Table 6 has been calculated to show the differences in these three profiles at a point in the North Sea where the tidal velocity is 0.3 m/sec and the storm surge velocity is 0.6 m/sec. The differences are greatest near the surface and could produce a 300% difference in current force. These differences are very important for ship type structures.

DRAG COEFFICIENTS

The classification societies and the Guidance Notes suggest the same drag coefficients for the underwater portions of semi-submersibles as used for the wind calculations. These have been discussed earlier and most of the comments are applicable in the underwater case.

There are a number of tank test results for the drag of ship type hulls in currents. Ref. (30) to (38) plus some of earlier reference on wind tunnel testing. They show a large scatter as will be seen from figures (10) to (12) which give the coefficients for ahead, lateral and moment coefficients against heading angle. As for the wind tunnel tests it was found that rounded bows produced suction forces which gave forces in the ahead direction when the current was at angles as low as 30° off the bow (see the OCIMF curve).

To make matters worse, Palo (Refs 34 to 36)) carried out full scale measurements on a tanker and a destroyer in an estuary and found that the drag coefficient was very dependent on the local current profile over the draft of the ships. The tanker was badly fouled and there must be some doubts about the absolute values of the drag coefficients measured but there is a clear indication that tank tests in a uniform flow may not be representative of the conditions surrounding a moored ship in a high wind where there will be a high shear in the surface water layers.

It is therefore with some diffidence that the following formulae for the current drag on full form vessels are put forward

$$C_{XC} = 0.40 + 0.002511\theta - 1.157 \times 10^{-4}\theta^2 + 4.285 \times 10^{-7}\theta^3$$

$$C_{YC} = 0.016133\theta - 9.10 \times 10^{-5}\theta^{-2}$$

$$C_{XYC} = -4.418 \times 10^{-3}\theta + 6.9098 \times 10^{-5}\theta^{-2} - 2.4897 \times 10^{-7}\theta^3$$

where: $0° < \theta < 180°$

$0°$ applies to current from astern

$180°$ applies to current from bows

$$C_{XC} = F_{CL} \Big/ \frac{1}{2}\rho A_T U^2$$

$$C_{YC} = F_{CT} \Big/ \frac{1}{2}\rho A_L U^2$$

$$C_{XYC} = M_C \Big/ \frac{1}{2}\rho A_L L U^2$$

F_{CL} = Longitudinal Current Force
F_{CT} = Transverse Current Force
M_C = Moment due to Current
V = Current Velocity
ρ = Water Density (1.025 Tonnes/m^3)
A_T = Transverse Projected Area = BT
A_L = Longitudinal Projected Area = LT
L = Length (m)
B = Beam (m)
T = Mean Draft (Mid Ships) (m)

WAVE DRIFT FORCES

Wave drift forces arise from second order effects in waves and are functions of the square of the wave height. As for first order forces they are made up of a combination of potential and viscous effects. In ships shaped bodies potential effects tend to dominate while in semi-submersibles viscous effects are of a similar order.

In recent years there has been very considerable advances in computational methods of calculating drift and the associated damping forces on arbitrarily shaped bodies and these are discussed elsewhere in this course. They all involve splitting the body shape up into a large number of elements in order to achieve adequate accuracy especially at the higher frequencies (shorter waves) and considerable computer time even on modern high speed computers

Recently there has been an extensive international collaborative program (Refs 39, 40) to verify the various computer programs in use and to try to establish the minimum number of elements to get accuracy for both the first and second

order forces and responses. This research has shown that there existed a large scatter between programs, some of which was due to poor modelling and efforts are being made to establish some quality assurance methods whereby the designer can have confidence in the results. These generally involve checking that the results converge as a higher number of elements are taken. There still remain questions regarding the agreement between computed forces and those measured in model tests. The latter are difficult to carry out accurately since the manner of mounting the model and generating the waves can influence its behaviour.

In the early stages of a design, the designer cannot afford the time and effort involved in such calculations or model tests and has to resort to empirical data from previous results to estimate the forces.

The drift forces on semi-submersibles are very dependent on the number and arrangement of the columns and to get a reliable estimate one must have computed or measured data from a semi-submersible with substantially the same geometry. Reference (41) to (58) give a list of papers providing such data. One of the difficulties in using this data is that different authors use different factors to non-dimensionsalise the coefficients and care must be taken in converting to a particular set of design dimensions.

The same problem exists for ship shaped forms where some authors non-dimensionalise the forces by dividing by $\frac{1}{2}\rho g a^2 L$and some by $\frac{1}{2}\rho g a^2 \nabla^{1/3}$. Neither of these factors reflect the shape of the body i.e. two ships can have the same volume of displacement but very different length to breadth ratios and the two methods of presentation would produce different forces. Additionally the data is frequently presented in different ways e.g. against heading angle for a constant frequency or against frequency for a constant heading. The latter is preferable as the former can easily miss some of the peaks which occur.

To try to present the available data (Refs 59-91) plus some unpublished results) in a more useable form, an analysis was made of different non-dimensionalising factors to try to reflect the vessel geometry more accurately. The best solution so far has been as follows:

$$\text{Force coefficients } C_x, C_y = \frac{F_{Dx}, F_{Dy}}{\frac{1}{2}\rho g a^2\left[\left(BT\cos^2\theta\right)^{1/4} + \left(LT\sin^2\theta\right)^{1/4}\right]\left(LC_B\right)^{1/2}}$$

where:

F_{DX}, F_{DY} are the drift forces in the longitudinal and lateral or transverse direction,

B = vessel breadth (m)

T = vessel draft (m)

L = vessel length between perpendiculars(m)

C_B = vessel block coefficient

a = wave amplitude (m)

The terms in the square brackets in the denominator reflect the submerged cross sectional area in the longitudinal and transverse directions when θ is 0° or 180° and 90° respectively. Using the above factors the available theoretical and experimental data were plotted and gave reasonable curves for the C_x and C_y coefficients, see Figs. (13) to (14) for typical examples. These curves include data for both loaded and ballast conditions indicating that the above factor appears to take reasonable account of such changes.

The frequency has been non-dimensionalised by multiplying by $\left[\nabla^{1/3}/g\right]^{1/2}$.

In the case of C_Y curve fitting is made difficult by nearly all the theoretical results showing peaks near the natural roll and heave frequencies while these are not reflected by the experimental results. In many cases the experiments were not carried out at the precise frequency concerned and may have missed the peak but it is thought that the explanation lies in viscous effects increasing the damping in roll well above the theoretical potential damping.

As a result the C_Y data has been curve fitted in two stages:

(a) A fifth order polynomial against frequency and a cubic polynomial against heading angle.

(b) A trigonometric expression which attempts to express the peaks.

Since the peaks are dependent on the natural rolling and heaving frequencies and the former changes with the radius of gyration there can be a considerable error in applying the comparatively few results available to a particular design. For this reason the forces from the general trend and from the peaks should be calculated separately and the results only combined if the natural period of the prototype is in the same frequency range as indicated by the formula.

The C_x coeffficients have been fitted by a 5 x 3 polynomial as for the C_y. Curves showing their variation with heading angle are shown in Figs (15) and (16).

It will be found that the frequency range covered is satisfactory for most FPSO type vessels, but it should be noted that as the heading angle approaches 90 the value of C_y becomes large at the higher frequencies and there may be an underestimation of the drift forces for the high frequency end of the wave spectrum. At the low frequency end the curve fit tends to produce negative values which agree with some sets of calculations but many of the experimental data show slightly positive values. This could lead to some underestimation in the 50 year return period spectrum where the peak will be close to these frequencies.

There is also a tendency of all the curves to have too low a slope in the region of a non dimensional value of 0.25 which could lead to an underestimate if the spectral peak is in this region. Because of the least squares nature of the curve fit these areas of under-estimate are balanced by areas of over-estimate but these are likely to be away from the peak of the spectra.

Despite these weaknesses it is felt that designers will benefit from these data as it gives a ready method of assessing the change in drift forces with heading angle. Although the longitudinal drift coefficient C appears to be nearly constant once the heading reaches 160 it must be remembered that the method of non-dimensionalising leads to a larger multiplying factor with decreasing angle and therefore higher forces. The C_y value increase rapidly as the heading angle approaches 90 and as the factor is also increasing the drift forces become very large. The drift force coefficients in the surge and sway directions for full form vessels $(0.8 < C_B < 0.92)$ were found to be approximately represented by the formulae in Appendix 1.

The moment coefficients showed no clear trend and varied from positive to negative signs for ships with the same leading particulars. The values of the moments were quite low in relation to the moments generated by the sway forces acting about the mooring point and thus their omission creates no large error for single point moored ships.

The above data applies to a ship in still water and the presence of a current will modify the values. Such current effects can be included in the drift force coefficient calculations but as seen earlier the precise current distribution over the depth of the wave disturbance is somewhat uncertain. No computations appear to have been made with something approaching a wind driven current profile. The available results indicate an increase in C_x coefficients of the order of 25% for a 2m/sec current which is high for North Sea conditions.

STEADY WAVE DRIFT FORCE

The theory of wave drift forces see Ref. 88), shows that the second order wave spectrum is made of three separate contributions:

(a) A steady force resulting from the sum of the forces due to each individual wave height making up the spectrum.

(b) A spectrum of forces at a frequency equal to twice the frequency of the first order spectrum.

(c) A spectrum of forces at the differences between the values of the first order spectrum frequencies.

Spectrum (b) is usually ignored as the frequencies are too high to have any effect on mooring but it is not certain that it is negligible for other types of behaviour of offshore structures.

Since the wave spectrum gives the values of: $\frac{1}{2}a^2$/unit of frequency (m^2 sec) the steady drift force can be obtained by multiplying each spectral ordinate by the drift force coefficient appropriate to that frequency, integrating over the practical range of frequencies and multiplying by the appropriate non-dimensionalising

factor and a factor 2 to eliminate the ½ associated with the spectrum. The frequency intervals must be small to ensure accurate integration especially in cases where the peak of the drift force curve coincides with the spectral peak.

Pinkster Ref. (88) shows that the spectrum of low frequency drift forces can be derived from the equation:

$$S_F(\mu) = 2\rho^2 g^2 \int_0^\infty S_\xi(w) S_\xi(w+\mu) R^4(w+\mu/2) dw$$

where $S_F(\mu)$ is the force spectrum, $S_\xi(w), S_\xi(w+\mu)$ are two values of the wave spectrum and $R(\omega+\mu/2)$ is the wave drift force at the mean of the two frequencies.

The dynamic surge can be estimated using the method outlined for wind gust with the spectrum of wave drift forces replacing the wind spectrum. This must be regarded as a first estimate of the dynamic excursion due to the assumptions of linearity in the mooring and a Rayleigh distribution but will be sufficient to determine if the selected mooring configuration is to satisfy the loading conditions.

1ST ORDER MOORING LOADS

These are mainly due to the horizontal movements of the vessel (surge/sway/yaw), but heave, pitch and roll all make contributions when the motions are severe. All these motions tend to be near their maxima in long period waves, i.e. the 50 year return period conditions, see Figs. (17, 18) for typical surge RAO curves for a ship and a semi-submersible. The inertia of the vessel is usually so great that the moorings do very little to restrain these motions and this in part explains the concentration in the design codes on 50 year return period conditions.

DESIGN LOAD CONDITIONS

One point which is not obvious in the foregoing is that the peaks of the wave drift force curves do not occur in the 50 year wave conditions - indeed they are near zero or negative at the peak of JONSWAP spectra for the 50 year return period. Figures (19, 20) taken from Ref. 92 show typical drift force curves for a ship and a semi-submersible together with the 50 year return period spectrum for a Central North Sea Field.

The highest steady and dynamic drift forces will be obtained by spectral peak periods much shorter than the 50 year period.

Tables (7-9) show the steady wave drift forces for a 120,000 tonne dwt tanker and a semi-submersible in part of a wave scatter diagram. The figure in the top right hand corner of each Table gives the 50 year return period steady drift force. Over large areas of these scatter diagrams the steady drift forces are much larger than the 50 year return value. Since at each zero crossing period they are highest at the highest significant height the key question is "What is the 50 year return period value of this height?". It will be limited by wave breaking but there is no agreed figure for the maximum steepness in wave spectra. The tables show a wave slope of

1/20 which is near the theoretical maximum for a JONSWAP spectrum but, as the Tables indicate, there have been many recorded spectra with a greater steepness in the Forties Field. Thus, vessels in this area will experience drift forces much higher than the 50 year return period value several times per year. The increases are not so great for the semi-submersibles but involve a 100% increase at the steepest waves.

In the wave conditions where the drift forces are high it would be unwise to assume that the wind and waves will be co-linear but it is possible for a 50 year return period wind to occur since most of the available data suggests that very high wind speeds only occur for short periods - of the order of less than 3 hours.

If the wind and waves are not in line single point moored vessel will take up some mean heading to the waves and yaw about this point under the varying forces of wind, waves and current. Table (10) shows how the wave drift force increases with heading angle. Again the forces in the 6 to 9 second zero crossing period range are larger than the 50 year return period value but they are significantly higher than the head on values. This is not conclusive proof of higher mooring forces as to have the heading to the waves there must exist wind and current forces which balance the wave lateral forces and moments about the mooring point. It is the head on component of all these forces which is important.

However, from observation of model tests conducted in such conditions, it appeared that the highest mooring forces occurred when the vessel had yawed to quite a large angle under the action of wind and in a quiet period in the wave spectrum but was at the extreme value of the slow drift motion and was then struck by a series of high waves in this position. It is not possible to estimate such behaviour in the frequency domain and use must be made of model tests or a mathematical simulation of the problem.

DYNAMIC DRIFT FORCES

Figure (21) shows the results of dynamic response calculations for the 120,000 tonne dwt tanker in the 50 year and a 1 year storm wave conditions. Note the different scales on the diagrams. Again the dynamic response in the 1 year conditions is much higher and is likely to be so over a considerable range of significant heights and zero crossing periods.

The estimated dynamic excursion resulting from these two cases was as follows:

Hs (m)	13.5	12.5
T_Z (secs)	12.5	8.5
Maximum excursion (m)	6.0	7.8
Force (kN)	2550	3287

i.e. a 28% increase in mooring force.

CHOICE OF WAVE SPECTRUM

The above calculations were done with the ITTC version of the JONSWAP spectrum but other versions of the spectrum where the enhancement factors are varied with the significant height and period show a larger increase in the dynamic response at the 8.5 second period.

It has been noticed that the Pierson-Moskowitz spectrum will generally give a higher mooring force in the 50 year conditions and in most other combinations of Hs, Tz values, except when the peak in JONSWAP spectrum coincides with a peak in the drift force coefficient curve.

In North Sea conditions the JONSWAP spectrum is usually accepted as being closer to actual conditions, but these differences must be borne in mind in the assessment of mooring loads.

CONDITIONS FOR HIGHEST MOORING LOAD

It is not possible to say with certainty that the mooring loads will be higher in a 1 year return period wave condition combined with the 50 year wind and current, since the forces in the mooring depend to a certain extent on the dynamic characteristics of that mooring. There is no doubt that conditions of high significant wave heights with zero crossing periods in the range of 6 to 10 secs combined with 50 year winds and currents from the worst heading to the waves should be investigated for all multi-point moored systems.

At present it is impossible to give guidance on the worst angle between wind and waves for single point moored vessels as so much depends on the relative magnitude of the wind and wave forces. This can only be resolved by extensive simulation calculations but, to be realistic, these must involve energy spreading in both the waves and the wind. Unfortunately there is little agreement on the best mathematical formulations for energy spreading (see Refs. 85, 93 to 96), and only further research will produce reliable guidance.

SUMMARY OF PROBLEMS IN DETERMINING MOORING LOAD

The foregoing has shown that at present many of the data necessary for the estimation of mooring loads are poorly defined and require further research. Despite what has been said above about the value of model tests, to the best of the author's knowledge there is no testing tank which can reproduce at model scale all the features of the full scale environment.

In particular, it is very difficult to produce the highly sheared current within the first few metres below the surface which is typical of the wind driven current. The wind loading must be produced either by fans blowing on the model and having their speed adjusted to give the correct order of force as determined from

wind tunnel tests or by fans sited on the model and again having their speed adjusted to give the correct order of force and moment. In either method the speeds may be varied to simulate gust effects. Due to the different velocity profiles between model and full scale it is generally impossible to satisfy both the force moment conditions, and any relationship between wind gusts and the wave conditions which may exist on the full scale will not be reproduced.

To get good results:

(1) a wind tunnel test must have been carried out on a model which is around 1/100 scale or larger with the correct wind profile for the method to be used in designing the moorings - either 10 min. average or 1 min. average or a uniform profile. If the latter, the results must be corrected for the design wind profile. The level of turbulence in the wind tunnel should attempt to reproduce the full scale. Where rounded surfaces are involved, the Rn during the tests should be greater than 10^5 and turbulence stimulation devices fitted. The drag and lift coefficients should be determined using the reference velocity at 10 m above the surface.

(2) a wind tunnel test should be carried out on the underwater structure in a highly sheared wind flow to simulate the profile of the tidal plus storm surge and wind driven currents. The remarks about scale effects in (1) above apply.

(3) using the results of(1) and (2) the wind and current forces to be applied to a hydrodynamic model to represent the model scale must be evaluated. On such a model it will be normal to generate a current which represents the tidal plus surge elements so that only the additional force due to the wind driven current needs to be added to the wind forces and moments.

(4) tests on the hydrodynamic model must be carried out in a tank which is sufficiently large to permit a model at 1/75 scale or larger with full reproduction of the designed mooring spread and depth of water. It is not acceptable to replace part of the scaled moorings by a spring system of equivalent stiffness as much of the damping comes from the moorings especially in deep water. `Unfortunately there is likely to be a considerable scale effect on this damping due to Rn effects and differences in the dynamic characteristics of individual lines between model and full scale. Any flexible riser system should be reproduced to physical scale but it is generally impossible to reproduce dynamic characteristics.

The wave makers must be capable of producing multi directional seas with specified energy spreading and the method of producing the spectrum must be free of any bias towards particular frequencies. It must also avoid any repetition in a time scale representing up to 10 hours on the full scale. The beaches must be capable of absorbing the waves so that the wave system near the model is stationary. Sufficient wave height probes must be deployed around the model to ensure that these conditions are being obtained. Wave probes too close to the model are likely to be affected by reflected waves and to give a false measurement of the input conditions.

Where current is being generated, its profile with depth and width of the tank and degree of turbulence must be measured.

The statical stability particulars (GM_T and GM_L) must be carefully checked. The corresponding radii of gyration, which should have been derived from an analysis of the range of full scale conditions to be encountered, must be accurately reproduced. Tests must be carried out with the steepest waves possible in the period range 6 to 10 secs (zero crossing period) and with the 50 year wind at several angles to the waves.

The analysis techniques to be used to forecast 50 year return period values from the measured data must be agreed beforehand and the methods of spectral analysis planned to provide the correct form of data.

RELIABILITY ASPECTS OF MOORING

The foregoing discussions indicates that the mooring load is a function of the significant wave height and zero crossing period, the energy spreading within the waves, the wind speed and direction relative to the wave direction and the speed and direction of the various elements of current. Strictly speaking it is necessary to know the joint probability functions of all these variables in order to determine the loading probability.

Although such data may be available from some well instrumented sites very little analysed data exists to built up the necessary statistics. The immediate priority is to get data on the probability distribution of wind speed and direction relative to the wave direction once the significant wave height exceeds 5m at any zero crossing period. Current loading is of lesser importance even with the all co-linear assumption and if each element of current were to be treated separately with their differing directions, it is likely the proportion of mooring load due to current would fall. However for single point moored vessels the current may be important in determining the heading angle and thus have a large impact on the total load.

Some efforts have been made to develop a reliability approach based on the all co-linear approach but this appears to be so unrealistic as not to be worth while pursuing.

LAYOUT OF MOORING

Environmental Considerations

The severity of the environmental loading will vary with direction. In the North Sea both the wind and waves are much less severe from the North Easterly direction and generally the worst wave conditions come from between West and North. The Guidance Notes give some indication of this in Table 11.6 which applies only to wind conditions. This indicates that in the Northern North Sea the maximum winds from the North East and East are 87% and 85% respectively of the maximum winds from the South East, South and North West. Thus the wind

loading from the East is about 30% lower and the wave loading is correspondingly reduced due to reduced fetches as well as reduced speed.

For a multi point moored vessel such as a semi-submersible where there may be a difference in the magnitude of the drift and wind forces between the head-on the beam-on conditions the vessel should be orientated so that the aspect producing the highest wind load is facing North East and South West. It may also be desirable to vary the angles between the mooring lines to reflect the directions of greatest load. Note however that although the 50 year return period wave conditions are most severe from the North West to North the 1 year return period conditions which produce high drift forces may be generated from other directions since they are probably due to high winds of short duration blowing over limited fetches.

In other parts of the world, e.g. Brazil and Indonesia, the wind and current directions remain sensibly constant for half the year and then reverse on to a diametrically opposed bearing. In such circumstances it is worth considering multi-point mooring tankers with their longitudinal axis along the predominant wind/current/wave direction.

PIPELINE RISER CONSIDERATIONS

If a pipeline, manifold and flexible riser system has to be accommodated through and within the mooring spread use may be made of the lower mooring loads from certain directions to open the spacing between the mooring lines so as to give a bigger clearance for the pipeline. No anchor should be within 300m of the pipeline. The siting of the riser manifold should take into account the possibility of a break in any of the mooring lines and the subsequent movement of the vessel and its lines.

PRESENCE OF OTHER SURFACE FACILITIES

If there are any other fixed platforms or oilfield facilities within a short distance of the proposed mooring site consideration must be given to the possibility of a catastrophic failing of the mooring leaving the vessel free floating and perhaps with little power available. There must be a warning system to alert the crew that this has occurred.

Under high wind conditions FPSO's can drift at the rate of approximately 1km. every 20 minutes and its heading to the wind direction can be somewhat unpredictable. If thrusters are available then the heading can be controlled and some element of steering achieved, but the control system must ensure that power generation is maintained even if it involves a switch from gas to diesel fuel. The navigational display system must be adequate to allow the executive officers to come to quick decisions on the best course of action to avoid a collision with another installation.

The mooring designer should site the vessel so that under the most probable direction of failure the vessel will tend to drift clear of any other installations in the vicinity.

VARIABLE STIFFNESS WITH DIRECTION

One method of dealing with varying directional environmental loading has been indicated above. An alternative in the case of FPSOs is to maintain equal heading angles and a symmetrical mooring layout, but to vary the properties and configuration of individual lines in order to provide an equal margin of safety in all directions. This is generally not an option in semi-submersibles unless a special mooring is fitted for a particular operation.

Thus there are a number of analyses to be carried out after the loading data has been determined before the designer can get down to the detailed design of the mooring lines.

DESIGN OF MOORING LINES

In depths of water from 100 to 300m it is probable that some combination of chain and wire rope will provide a satisfactory mooring system. Generally chain will be used for the section on the sea bed due to its better wear properties than wire rope. Wire rope is likely to be used for the suspended length under the initial tension with possibly chain being used on the connection point to the vessel, again because of its better resistance to wear in fairleads and stoppers. The latter decision depends on the method of tensioning and line adjustment to be adopted. On semi-submersibles winches or windlasses may be available but on an FPSO system which is to be semi-permanently moored it is normal to omit such equipment and use linear jacks or gripper systems with no great length of mooring line material on board.

For a floating production system in European waters it is unlikely that the mooring can be achieved with less than 8 lines. Increasing the number of lines will reduce the scantlings of individual lines which may lead to cheaper costs per line but the added costs of anchors, installation, inspection and renewal may offset such initial savings. It is therefore necessary to do detailed calculations to find which combination gives the lowest overall cost. Although in some cases initial capital cost may be a dominating factor it is important to examine through-life costs

These decisions may be influenced by the sea bed conditions and for an FPSO mooring a detailed survey should be available with soil samples over a depth of 30 m at a number of points in the possible mooring area. This may help to decide whether to use a piled anchor or a conventional anchor. Again a cost analysis may be the deciding factor but this may be influenced by the state of the offshore construction industry at the time as day rates can fluctuate greatly from one year to the next.

Apart from cost the objective in selecting the mooring line material configuration is to arrive at a satisfactory stiffness so, that the level of excursion is within the limits set by the riser system with the requisite factors of safety in the most heavily loaded line(s). To perform such calculations it is necessary to have a computer program for the solution of the catenary equations for the individual lines and to develop the stiffness characteristics for the complete mooring system.

There are a great many variables in this problem as will have become obvious from the earlier discussion on the general mooring lay-out, the options regarding number of lines, levels of pre-tension and the possible material combinations within one line. This may include the use of clump weights or buoys i.e. point loads with perhaps complex hydrodynamic properties. It is therefore uneconomic to develop a computer program which caters for all combinations and use should be made of one of the several highly developed programs on commercial offer. Some of these programs now include a treatment of the mooring line dynamics in the fluid flow and this is desirable as it can provide an estimate of the damping likely to arise from the mooring lines as well as giving an important part of the loading on the system. The treatment of the behaviour of the portion of the line on the sea bed when the excursion of the vessel produces a component of load transverse to its axis needs to be checked to ensure that the movement of the line on the sea bed is being taken into account.

All programs will give a treatment of the one line broken situation but one should check that this is not based on the assumption of an initially symmetrical system and allows for a varying angular stiffness, however that may be achieved. The movement of the lines on the sea bed then become significant and the importance of having some measured soil properties.

Some programs offer time domain solutions but although these may be necessary if model tests are not carried out they are not suitable for the initial design stages where many different variables have to be investigated in order to arrive in the regions where a final solution is likely to be found.

The Classification Society procedures and safety factors for mooring design are adequately described in their rules and will not be detailed here. They are still largely based on the quasi-static approach but as noted earlier there are significant differences in the definitions of the environment and the methods of calculating the environmental loads. There are slight differences in the safety factors employed but these are much smaller than the differences in load which would be obtained. In all cases they state that if dynamic calculations are carried out the safety factors will be specially considered so that there is scope for applying the latest technical knowledge.

Kwan Ref. (97) describes the thinking behind the latest API draft guidance on the mooring of floating production systems and another paper in the same publication Ref. (98) discusses the application to a particular design. The loading ideas are still largely based on the co-linear action of wind, wave and current and a 100 year return period for FPSO's which are to remain on station for many years.

It recommends a dynamic analysis be carried out although the quasi-static approach may be used for initial design. The comparative design calculations carried out using the two approaches indicated that the dynamic calculations always gave the highest loads and that the differences increased with increasing depth of water. At 1000 m. water depth the differences were 700%. The wave periods for the two sea states examined are not given, but it is unlikely they lay in the range where the wave drift response would be highest.

CALCULATION OF MAXIMUM OFFSET

Two methods are recommended, a combined spectrum method and a simple rule.

The combined spectrum method rests on the following assumptions:

(a) wave frequency and low frequency responses are statistically independent and can be lumped into a single combined spectrum.

(b) the combined process can be assumed Gaussian and the assumption of a Rayleigh peak distribution is sufficiently accurate to compute all statistical parameters.

The statistical value is obtained from the equation:

$$x = m_o x \sqrt{2\ell n(T / E_n T_z)}$$

where:

x	=	expected maximum of the combined effect
m	=	zero moment of the combined low and wave frequency response spectrum
T	=	storm duration
T_Z	=	zero crossing period of the combined spectrum = $2\pi[m_o / m_2]$
E_n	=	number of exceedances during time T and is normally set to 1.0 (maximum exceeded once in a duration of 3 to 6 hours)

The simple rules are as follows:

If $S_{\ell f\,max} > S_{wf\,max}$ then $S_{max} = S_{mean} + S_{\ell f\,max} + S_{wfsig}$

and if $S_{wf\,max} > S_{\ell f\,max}$ then $S_{max} = S_{mean} + S_{wf\,max} + S_{\ell fsig}$

where:

S_{mean}	=	mean vessel offset
S_{max}	=	maximum vessel offset
$S_{wf\,max}$	=	maximum wave frequency motion
S_{wfsig}	=	significant wave frequency motion
$S_{\ell f\,max}$	=	maximum low frequency motion
$S_{\ell fsig}$	=	significant low frequency motion

This makes the application of a frequency domain initial analysis fairly simple. Kwan gives results which indicate that the above rule gives results in the range of 0.94 to 1.16 times the values obtained by the combined spectrum method.

MOORING LINE TENSION - MAXIMUM TENSION

A similar rule is used to determine the maximum line tension:

If $T_{\ell f max} > T_{wf max}$ then $T_{max} = T_{mean} + T_{\ell f max} + T_{wf sig}$

If $T_{wf max} > T_{\ell f max}$ then $T_{max} = T_{mean} + T_{wf max} + T_{\ell f sig}$

Following a limited reliability analysis the maximum allowable line tensions are increased compared to those permitted with a quasi-static analysis as indicated by the following Table.

Method of Analysis	Tension Criteria (% of B.S.)	
	Intact	One line Broken
Quasi-static	50	71
Dynamic	60	75

The subject of the correct method of combining the wave frequency and low frequency effects due to wind and waves has been the subject of several papers (see Refs. 72,80,90-108). There is no general agreement since they frequently start from different aspects of the problem. However, a number of authors have shown that the drift forces are non-Gaussian and therefore the combined spectrum method is somewhat suspect.

Possibly the most detailed work has been carried out in Norway under the FPS 2000 research programme. Stansberg (Ref. 99) states that the Rayleigh assumption underestimates the largest maxima and that an exponential distribution gives better agreement with measured results. This is particularly true in cases where the damping is high when the extreme amplitudes may be 50 to 100% higher than those predicted using the Rayleigh assumption. He develops a theory to provide a method of estimating the response, but it depends on a good knowledge of the damping, which is one of the most poorly defined quantities.

The damping is made up of a combination of potential and viscous effects on the vessel plus largely viscous effects on the mooring lines. The size of the latter contribution depends on the vertical amplitudes of the mooring line as the vessel surges/sways backwards and forwards. Huse Ref. (109-111) has put forward a method of calculating this damping contribution which must be added to the other effects. It is a fairly simple matter to add this calculation to a mooring design program but requires an iterative approach to arrive at the correct order of value. There could be scale effects on the drag coefficients determined by Huse from his experiments.

Thus, although there is a reasonable theoretical understanding of all the elements which go to make up the loads and response characteristics of the moorings, there is a lack of accurate experimental data to validate the theories and give confidence that the environment is being adequately modelled.

SECONDARY EFFECTS ON MOORING LOADS

In considering the accuracy of mooring calculations it is important to bear in mind and if necessary evaluate the effect of certain changes in the basic variables due to the method of mooring installation or operation of the vessel.

Amongst these are:

(1) Water depth changes due to changing draft on the vessel, tidal and storm surge effects. This is clearly much more important in shallow water [< 100m] than in deep water where the percentage change in depth will be much less. Calculations for a 120,000 tonne dwt FPSO in 136 m depth of water showed that there could be a variation of ±5.5 m about the mean between the deep draft at the lowest water level and the ballast draft at the highest water level. This caused a ±15% change in line tension and a similar change in mooring stiffness. Such changes will be cyclical in nature due to the loading pattern and tidal effects and would need to be accounted for in any reliability analysis.

(2) Effective weight of line per unit length. Since the manufacture has to guarantee the breaking load, it is likely that there will be an initial bias towards a greater weight than the nominal. Ref. (112) suggests that this may be as high as 10%.

(3) Effective Youngs Modulus (E). This is determined from tests for both chain and wire rope with the latter showing the greatest variation since it is closely related to the method of manufacture, the previous history of handling, and the load history. The extension of the chain or wire rope under load leads to a change in the weight per metre which has to be taken into account in the catenary calculations so that an error in E has two effects. For chain, the E values will be within ±2%, but for wire rope this may increase to ±9%.

(4) Line length and orientation. The most likely source of error lies in the positioning of the anchor. With piled anchors it is probable that it will be within a radius of 10 m of the design point, but for conventional anchors the error may be larger since it has to be pulled into its final position and, depending on the soil characteristics, this may involve greater movement than desired. Both the line length and its orientation may be affected and in shallow water such an error can be significant. In the case of piled anchors the chain at the point of attachment may be some distance below the sea floor and the effective anchoring point closer to the vessel than intended.

(5) Accuracy of pre-tension. If a large number of lines have to be pre-tensioned by a jacking system a considerable time will be involved during which there will be changes in tidal level so that it is likely that there will be some differences in the tension achieved. The tension is commonly measured by the angle the line makes with the vertical. A change of 1 degree usually requires a change of tension of the order of 5% in the working range of pre-tensions.

LINE BREAKING STRENGTH

Designs are usually based on the catalogue breaking strength of the material. Test data which would allow a mean and standard deviation to be established have been scarce, but there are now a number of programmes to remedy this weakness - see Refs (113,114) for wire rope and (115,116) for chain. Within a short time it should be possible to produce probability distributions for these quantities.

FATIGUE

Since FPSOs are likely to be moored in the same position for many years it is necessary to consider the fatigue life, especially in view of the level of drift force which can be experienced at low wave periods which have a high frequency of occurrence.

The difficulty of such calculations is the lack of joint probability data for wave height and zero crossing period, wind speed and direction and current speed and direction. Strictly, this data must be available from each compass point, especially if the mooring is not symmetrical. In the absence of such data a wind speed appropriate to the sea state may be assumed to act co-linearly with the waves, but this is a very artificial condition as, for example, in North Sea conditions the wind rose rarely has the same characteristics as the wave height rose due to varying fetch conditions with direction. Also co-linearity may not produce the highest loading.

Accepting these qualifications on the initial data the calculations should be carried out for representative pairs of H_S, T_Z values from the wave scatter diagrams for each direction being considered. Due to the number of calculations required it is only practical to consider a frequency response method with its limitations.

For these calculations the stiffness of the mooring should be determined at a point equal to the mean wind, current and wave drift loading plus the significant wave frequency excursion. This stiffness should be used in the estimation of the low frequency excursion and loading. If model tests are available for a limited number of the conditions they can be used to scale the calculations. For an unsymmetrical mooring it would be extremely difficult and expensive to carry out model tests from each direction.

The API draft code provides T-N curves for chain, wire rope and connecting links in the form:

$$NR^M = K$$

where:

N	=	number of cycles to failure
R	=	ratio of tension range to a reference breaking strength
M	=	slope of the T-N curve
K	=	intercept of the T-N curve

Better guidance on the fatigue characteristics of both chain and wire rope may be expected from various ongoing research programmes Ref. (113 to 116).

Various approaches to calculating the annual fatigue damage are suggested in the API recommendations but the most practical appears to be a simple summation. In this approach low frequency and wave frequency fatigue damage are calculated separately. The total damage is assumed to be the sum of the two according to the following equation which is based on a Rayleigh distribution assumption:

where:

D	=	annual fatigue damage from wave and low frequency effects
N	=	number of wave frequency tension cycles per year calculated from: $N = (3.15576 \times 10^7 \times P)/T_Z$
P	=	the total probability of occurrence of the environmental condition, computed as Ps (probability of the environmental occurrence given the direction) times Pd (probability of directional occurrence)
T_Z	=	zero crossing period

R	=	ratio of rms wave frequency range to a reference breaking strength. The range should be taken as twice the rms tension.
Γ	=	Gamma function
N	=	number of low frequency tension cycles per year $= P \times 3.15576 \times 10^7/Tn$
TL	=	natural period of the vessel at the appropriate mean position
R	=	ratio of rms low frequency tension range to a reference breaking strength.

The total fatigue damage is obtained by summing the damage over all directions and wave periods, i.e.

$$D_t = \sum_{DIR} \sum_{SEAS} D$$

The fatigue life of the mooring is $L = 1/D_t$ (years).

The service life of the mooring should be less than the fatigue life divided by a factor of safety. In the API this is given as 3 but other authorities may call for higher values. It is reasonable to call for a higher standard than is required for a fixed platform due to the greater influence of wind loading and resulting uncertainty in total load.

The above fatigue calculation assumes that anti-corrosion and, where necessary (wire ropes), anti-wear measures are taken and regular inspections carried out to ensure they are effective.

CONCLUDING REMARKS

The foregoing notes will have indicated that there are still many areas of uncertainty in the design of moorings for vessels which have to remain on station for many years and some of these apply to short term moorings also. Some of these uncertainties can be removed by well planned model tests of the vessel, but many lie in the lack of joint probability data for wind, waves, and current, including their relative directions. Such data has been recorded for a number of stations and should be re-analysed to provide the statistics appropriate to mooring.

There are significant differences between the recommendations or requirements of classification and regulatory/advisory bodies which means that designers often have to exercise judgement of the best course to adopt in a particular case. This is an unsatisfactory position and the industry must try to reach a more widely accepted code of practice.

POLYNOMIAL FORMULAE FOR THE SURGE AND SWAY DRIFT COEFFICIENTS

The wave drift forces for tanker type vessels have been non-dimensionalised in the following manner:

$$C_x, C_y = \frac{F_x, F_y}{\tfrac{1}{2}\rho g a^2\left[\left(BT\cos^2\theta\right)^{1/4} + \left(LT\sin^2\theta\right)^{1/4}\right]\left[LC_B\right]^{1/2}} \qquad (1)$$

where: Fx, Fy are the surge/sway forces in kN

L	=	BP length (m)
B	=	beam (m)
T	=	draft (m)
C	=	block coefficient where $0.78 < c_b < 0.92$
θ	=	heading angle and must lie between 90° and 180° with 180° being head seas
ρ	=	water density (1.025 tonnes/m^3)
g	=	acceleration due to gravity = 9.81 m/sec^2
a	=	wave amplitude (m)

The frequency has been non-dimensionalised by the factor $\omega\sqrt{\nabla^{1/3}/g}$

where: ω = wave frequency (rad/sec)

∇ = volume of displacement (m^3)

The data were normalised to lie between ±1 so that in the following formulae:

$$X = \sqrt{\frac{\nabla^{1/3}}{g}} - 1.6 \text{ and } -0.8 \le x \le 1.0$$

and $$Y = (180^\circ - \theta)/45^\circ \text{ where } -1.0 < Y < 1.0$$

$C_x =$

$+0.16414$	$+0.06760X$	$-0.29955X^2$	$+0.14080X^3$	$+0.20735X^4$	$-0.14903X^5$
$-0.07575Y$	$-0.03621XY$	$+0.15680X^2$	$+0.17259X^3Y$	$-0.05413X^4Y$	$-0.11189X^5Y$
$-0.00897Y^2$	$-0.05398XY^2$	$+0.04909X^2Y^2$	$+0.15769X^3Y^2$	$-0.04629X^4Y^2$	$-0.10423X^5Y^2$
$+0.22539Y^3$	$+0.05663XY^3$	$-0.41185X^2Y^3$	$+0.10950X^3Y^3$	$+0.22517X^4Y^3$	$-0.13329X^5Y^3$

$$C_x = 0 \text{ at } 90^\circ$$

$C_y =$

$+0.74745$	$+1.07205X$	$-0.82060X^2$	$-0.74810X^3$	$+0.73479X^4$	$+0.26513X^5$
$-0.67876Y$	$-1.03204XY$	$+1.25461X^2Y$	$+1.67777X^3Y$	$-0.87388X^4Y$	$-0.89642X^5Y$
$+0.20708Y^2$	$-0.07963XY^2$	$-0.86990X^2Y^2$	$+0.15872X^3Y^2$	$+0.59370X^4Y^2$	$-0.19019X^5Y^2$
$-0.35820Y^3$	$-0.04581XY^3$	$+0.54697X^2Y^3$	$-1.07383X^3Y^3$	$-0.50596X^4Y^3$	$+0.87992X^3Y^3$

$$C_y = 0 \text{ at } 180^\circ$$

To cope with peaks in the C_y curves, the following terms may be added to C_y (see Text).

$$C_{ya} = 4\mathrm{Cos}^2 2\pi(x-0.1)e^{-5x} \cdot e^{5(90-\theta)/150}$$

where:

$$x = \left(\omega\sqrt{\frac{\nabla^{1/3}}{g}} - 1\right) \text{ and must lie within the range } 0 \le x \le 1.0$$

while θ lies in the range $90^\circ \le \theta \le 180^\circ$

REFERENCES

1. R.L. Prior-Jones and F.L. Beiboer: 'Use of Joint Probability in Deriving Environmental Design Criteria', Advances in Underwater Technology, Ocean Science and Offshore Engineering, vol. 26, Environmental Forces on Offshore Structures and their Prediction, Kluwer Academic Publishers.

2. EKOFISK Environmental Data, Loginfo Ltd., 1985.

3. J. Harding and A.A. Binding: 'The Specification of Wind and Pressure Fields on the North Sea and some Areas of the North Atlantic during 42 Gales for Period 1966-76, IOS Report No. 55.

4. Analysis of Spread Mooring Systems for Floating Drilling Units, API Recommended Practice 2P(RP2P), May 1987. Also recent Draft Code on Recommended Practice for Design, Analysis and Maintenance of Mooring Floating Production Systems.

5. Offshore Installations - Guidance on Design, Construction and Certification, Dept. of Energy, Fourth Edition 1990, HMSO.

6. Prediction of Wind and Current Loads on VLCCs, Oil Companies International Marine Forum, OCIMF, Wetherby and Co., 1978.

7. F.A. Benham, S.S. Fang and G.H. Fetters: 'Wind and Current Shape Coefficients for Very Large Crude Carriers', OTC 2739, 1977.

8. R.W.F. Gould: 'The Estimation of Wind Loads on Ship Superstructures', Marine Technology Monograph No. 8, Royal Institution of Naval Architects.

9: J.M. Macha and D.F. Reid: 'Semi-Submersible Wind Loads and Wind Effects', SNAME, vol. 92, pp 85-124, 1984.

10. K. Yoshida, N. Oka and T. Arima: 'Some Considerations of the Wind Load Evaluation and the Response Production of Tension Leg Platforms', OMAE, 1986.

11. P.E. Freathy and S. Taggart: 'Wind Loads on Floating Offshore Structures'. OMAE, 1986.

12. P.J. Ponsford: 'Wind Tunnel Measurements of Aerodynamic Forces and Moments on a Model of a Semi-Submersible Offshore Drilling Rig', National Maritime Institute, Technical Report R.34, 1982.

13. P.J. Ponsford: 'Wind Tunnel Measurements of Lift, Drag and Overturning Moment on a Semi-Submersible Offshore Drilling Rig', National Maritime Institute, Technical Report R.152, 1976.

14. K. Nishimoto, H. Maeda and S.E. Guchi: 'A Study of Components of Wind and Current Loads on Semi-Submersibles'.

15. G. Buresti, G. Lombari, et al: 'Wind Tunnel Tests on a Tension Leg Platform Model', OMAE.

16. P.E. Freathy and B.J. Vickery: 'Wind Loads on Semi-Submersible Offshore Platforms', OTC 5174, 1986.

17. A. Kareem, P.C. Lu et al: 'A Wind Tunnel Investigation of Aerodynamic Loads on a Typical Tension Leg Platform', OTC 5173, 1986.

18. P.H. Laurich: 'A Wind Simulation System for the *Ocean Ranger* Hydrodynamic Model Study', OTC 5361, 1987.

19. E. Willemsen and C. Leynse: 'Analysis of High Reynolds Number Wind Tunnel Tests on the Semi-Spar', OTC 4956, 1985.

20. H. Rolfsman and E.T.D. Bjerregaard: 'Wind Forces on a Semi-Submersible Equipped with Alternative Drilling Derricks', OTC 4531, 1983.

21. H. Boonstra and C. Leynse: 'Wind Tunnel Tests on a Model of a Semi-Submersible Platform and Comparison of the Results with Full Scale Data', OTC 4245, 1982.

22. A. Kareem and C. Dalton: 'Dynamic Effects of Wind on Tension Leg Platforms', OTC 4229, 1982.

23 E.T.D. Bjerregaard and E.G. Sorensen: 'Wind Overturning Effects Obtained from Wind Tunnel Tests with Various Semi-Submersibles', OTC 4124, 1981.

24. E.T.D. Bjerregaard et al: 'Wind Overturning Effects on a Semi-Submersible', OTC 3063, 1978.

25. R.G. Standing, J.A.B. Wills et al: 'Wind Loading and Dynamic Response of a Floating Production Platform in Waves', Advances in Underwater Technology, Ocean Science and Offshore Engineering, vol. 26, Environmental Forces on Offshore Structures and Their Prediction.

26. G. Grekoussis and N.S. Miller: 'The Resistance of Semi-Submersibles', Trans Inst. of Engineers and Shipbuilders in Scotland, 1978.

27. S. Singh: 'Uncertainties in the Estimations of Fluid Loading on Offshore Structures with Special Emphasis on Wind Forces', I.MarE, 1989.

28. M.K. Ochi and Y.S. Shin: 'Wind Turbulent Spectra for Design Consideration of Offshore Structures', OTC 5736, 1988.

29. Metocean Parameters (parameters other than waves), OTH 89, 299, Dept. of Energy, HMSO.

30. S.L.S. Fang: 'Field Measurement of VLCC Mooring Loads', OTC 3383.

31. E.T.D. Bjerregaard and E.G. Sorensen: 'Forces and Moments on Underwater Bodies, Obtained from Wind Tunnel Tests', OTC 4438.

32. R.Y. Edwards: 'Hydrodynamic Forces on Vessels Stationed in a Current', OTC 5032, 1985.

33. V. Jacobsen and D.B. Jones: 'Current Loads on Ships Moored in Shallow Water', OTC 5581, 1987.

34. P.A. Palo: 'Current Induced Vessel Forces and Yaw Moments from Full Scale Measurements', Ocean Science and Engineering, vol. 11 (1 and 2), pp 1-69, 1986.

35. P.A. Palo: 'Steady Wind and Current Induced Loads on Moored Vessels', OTC 4530, 1983.

36. P.A. Palo: 'Full Scale Vessel Current Loads and the Impact of Design Methodologies and Similitudes', OTC 5205, 1986.

37. O.M. Faltinsen et al: 'Hydrodynamic Analysis of Tankers at Single-Point Mooring Systems', BOSS 79.

38. J.E. Wichers: 'Progress in Computer Simulations of SPM Moored Vessels', OTC 5175, 1986.

39. C.T. Stansberg et al: 'Problems of Mooring and Positioning of Floating Production Systems', 6th Intl Conf. on Floating Production Systems, 1990.

40. K. Herfjord and F.G. Nielsen: 'A Comparative Study on Computed Motion Response for Floating Production Platforms', BOSS 92, p 19.

41. R. Eatock Taylor and P. Sincock: 'Wave Drift Enhancement Effects for Moored Systems in Random Waves', 6th OMAE Conf., 1986.

42. Y.S. Hong: 'Computation of Wave Drift Forces Acting on Semi-Submersible Platform', 6th OMAE Conf., 1986.

43. J.Z. Cao, Y.G. Fu and Y. Feng: 'The Low Frequency Hydrodynamic Coefficients in Surge for a Semi-Submersible', 6th OMAE Conf., 1986.

44. C. Aage, H. Lundgren et al: 'Scale Effects in Model Testing of Floating Offshore Structures, 6th OMAE Conf., 1986.

45. L.J. Wevers and R.W. Bos: 'Measurements of Wave Induced and Drift Induced Line Forces and Motions of Semi-Submersible DB100', OTC 4439, 1982.

46. J.A. Pinkster: 'Mean and Low Frequency Forces on Semi-Submersibles', OTC 3951, 1981.

47. H. Rye, S. Rynning and J. Moshagen: 'Calculated Draft Forces on Two Semi-Submersible Platform Types in Regular and Irregular Waves', OTC 2366, 1975.

48. S, Kato, S. Ando and T. Kinoshita: 'On the Statistical Theory of Total Second-Order Responses of Moored Floating Structures', OTC 5579, 1987.

49. G.E. Hearn and K.C. Tong: 'Wave Drift Damping Coefficient Predictions and Their Influence on the Motions of Moored Semi-Submersibles', OTC 5455, 1987.

50. M. Kobayashi, K. Shimada and T. Fujihira: 'Steady and Dynamic Responses of a TLP in Waves', OMAE 1985.

51. G.H. Kim and W. Bao: 'A Strip Method for Lateral Drift Force of a Semi-Submersible', Jnl of Energy Resources, vol. 107, September 1985.

52. S. Spangenberg and B.K. Jacobsen: 'The Effect of Wave Grouping on Slow Drift Oscillations of an Offshore Structure', Intl Symp. on Ocean Engineering and Ship Handling, Gothenburg, 1980.

53. R.H.M. Huijsmans and J.N. Dekker: 'Combined Effect of Waves and Current on the Motion Behaviour and Tether Forces of a deep Water Tension Leg Platform', OTC 6180, 1989.

54. S. Takase and S. Kato: 'Statistical Properties of Slow Drift Motion of a Vessel Moored in Random Seas' - Dynamics of Marine Vehicles and Structures in Waves, W.G. Price et al (editors, Elsevier Science Publishers, 1991.

55. Q. Tao et al: 'Negative Low Frequency Wave Drift Damping of TLP, ISOPE, 1991.

56. R.G. Standing, et al: 'Full-Scale Measured and Predicted Low Frequency Motions of the Semi-Submersible Support Vessel "*Uncle John*", ISOPE, 1991.

57. T. Matsui: 'Computation of Slowly Varying Second-Order Hydrodynamic Forces on Floating Structures in Irregular Waves', Jnl of Offshore Mechanics and Arctic Engg, vol. 111, p 223, 1989.

58. J. Angwin: 'Results of a Joint Semi-Submersible/Submersible Wave Drift Force Project', TNO Report.

59. G.R.G. Lewison: 'Experimental Determination of Wind, Wave and Drift Forces on large Tankers', Symposium on the Behaviour of Disabled Large Tankers, RINA, London, 1981.

60. I.D. Dand: 'Model Studies of Freely Drifting and Towed Disabled Tankers', Symposium on the Behaviour of Disabled Large Tankers, RINA, London, 1981.

61. S.K. Chakrabarti: 'Experiments on Wave Drift Force on Moored Floating Vessel', OTC 4436, 1982.

62. O.A. Olsen et al: 'Slow and High Frequency Motions and Loads of Articulated Single Point Mooring Systems for Large Tankers', Norwegian Maritime Research.

63. J.A. Pinkster and J.E.W. Wichers: 'The Statistical Properties of Low Frequency Motions of Non-Linearly Moored Tankers', OTC 5457, 1987.

64 R.G. Standing et al: 'Recent Developments in the Analysis of Wave Drift Forces, Low Frequency Damping and Response', OTC 5456, 1987.

65. J.E. McDowall and B.L. Thompson: 'Analysis of the Slowly Varying Motions of a Floating Production System', OTC 5206, 1986.

66. G.E. Hearn and K.C. Tong: 'Evaluation of Low Frequency Wave Damping', OTC 5176, 1986.

67. J.E.W. Wichers: 'Progress in Computer Simulations of SPM Moored Vessels', OTC 5175, 1986.

68. J.E.W. Wichers and R.M.W. Huijsmann: 'On the Low Frequency Hydrodynamic Damping Forces Acting on Offshore Moored Vessels', OTC 4813, 1984.

69. B. Molin: 'Three-Year Experience in the Numerical Prediction of the Slow-Drift Motion of Moored Tankers', OTC 4533, 1983.

70. J.E.W. Wichers: 'On the Low-Frequency Surge Motions of Vessels Moored in High Seas', OTC 4437, 1982.

71. G.E. Hearn, K.C. Tong and S.M. Lau: 'Sensitivity of Wave Drift Damping Coefficient Predictions to the Hydrodynamic Analysis Models Used in the Added Resistance Gradient Method', Jnl of Offshore Mechanics and Arctic Engineering, vol. 110, p 337, November 1988.

72. C.T. Stansberg et al: 'Model Tests on Non-Linear Slow Drift Oscillations Compared to Numerical and Analytical Data', BOSS 1988.

73. R.M.W. Huijsmann: 'Wave Drift Forces in Current', OMAE ????

74. J.A. Pinkster: 'Dynamic Positioning of Vessels at Sea', Intl Symposium on Ocean Engineering, Ship Handling, Gothenburg, 1980.

75. J.A. Pinkster: 'Low Frequency Second Order Wave Forces on Vessels Moored at Sea', 11th Symposium on Naval Hydrodynamics.

76. O.M. Faltinsen and A.E. Loken: 'Slow Drift Oscillations of a Ship in Irregular Waves', Modelling, Identification and Control, vol. 1, no. 4, pp 195-213, 1980.

77. S. Nakamura, K. Saito and M. Takagi: 'On the Increased Damping of a Moored Body During Low Frequency Motions in Waves', OMAE 1986.

78. O.M. Faltinsen, L.A. Oahle and B. Sortland: 'Slow Drift Damping and Response of a Moored Ship in Irregular Waves', OMAE, 1986.

79. I.K. Boroday and A.A. Roussetsky: 'Evaluation of Characteristics of Hydrodynamic Forces Causing Ship Drift in Irregular Seas', OMAE, 1986.

80. J.A. Pinkster: 'Statistics of High and Low Frequency Motions of a Moored Tanker', OTC 6178, 1989.

81. D.C. Cotter and S.K. Chakrabarti: 'Effect of Current and Waves on the Damping Coefficient of a Moored Tanker', OTC 6138, 1989.

82. G.E. Hearn and K.C. Tong: 'A Comparative Study of Experimentally Measured and Theoretically Predicted Wave Drifting Coefficients', OTC 6136, 1989.

83. G.E. Hearn, S.M. Lau and K.C. Tong: 'Wave Drift Damping Influences upon the Time Domain Simulations of Moored Structures', OTC 5632, 1988.

84. J.E. Wichers: 'Wave Current Interaction Effects on Moored Tankers in High Seas, OTC 5631, 1988.

85. J.A. Pinkster: 'The Influence of Directional Spreading of Waves on Mooring Forces', OTC 5629, 1988.

86. G.E. Hearn: 'Low Frequency Damping - The Development of its Theoretical Prediction', Dynamics of Marine Vehicles and Structures in Waves, W.G. Price et al as Editors.

87. R.G. Standing: 'The Verification and Validation of Numerical Models, with Examples Taken from Wave Diffraction Theory, Wave Loading and Response', Dynamics of Marine Vehicles and Structures in Waves, Elsevier Science Publishers, 1991.

88. J.A. Pinkster: 'Low Frequency Phenomenon Associated with Vessels Moored at Sea', Soc. of Pet. Engrs, Paper SPE 4837, 1974.

89. V. Aanesland et al: 'Wave Drift Damping of a Turret Moored Ship', Boss 92.

90. G.E. Hearn, P. Goodwin: 'Low Frequency Damping Prediction - The Identification of a Reliable and Robust Method', BOSS 92.

91. M.J. Krafft and C.H. Kim: 'Surge Drift Motion of a Moored Vessel in Random Waves', ISOPE 1991 (Vol. III).

92. N.S. Miller and P.M. Wilson: 'The Design Wave Conditions for Determining Wave Drift Forces on Moored Ships and Semi-Submersibles', BOSS 92.

93. T. Vinje: 'On the Effect of Short Crestedness on the Statistical Distribution of Slowly Varying, Second Order Forces', Applied Ocean Resarch, 1988, vol. 10, no. 3, p 155.

94. N.H. Kim and D.K.P. Yue: 'Slowly-Varying Wave Drift Forces in Short-Crested Irregular Seas', , Applied Ocean Resarch, 1989, vol. II, no. 1.

96. Y. Inoue and W.Y. Xue: 'Slowly Varying Drift Forces in Directional Waves', BOSSS 92.

97. C.T. Kwan: 'Design Practice for Mooring of Floating Production Systems', 1st Offshore Station Keeping Symposium, SNAME, Texas Section, 1990.

98. J.B. Usland: 'Aspects of Mooring System Design for Floating Production Units', 1st Offshore Station Keeping Symposium, SNAME, Texas Section, 1990.

99. C.T. Stansberg: 'A Simple Method for Estimation of Extreme Values of Non-Gaussian Slow-Drift Responses', ISOPE, 1991 (Vol. III).

100. A. Naess: 'Prediction of Extremes of Combined First-Order and Slow-Drift Motions of Offshore Structures', Applied Ocean Research, 1989, vol. II, no. 2.

101. A. Naess: 'The Statistical Distribution of 2nd Order Slowly Varying Forces and Moments', Applied Ocean Research, vol. 8, no. 2, 1986.

102. A. Naess: 'On the Statistical Analysis of Slow Drift Forces and Motions of Floating Offshore Structures', 6th OMAE Conference.

103. J.M. Johnson and A. Naess: 'Time Variant Wave Drift Damping and its Effect on the Response Statistics of Moored Offshore Structures', ISOPE 1991.

104. C.T. Stansberg: 'Model Scale Experiments on the Extreme Slow Drift Motions in Irregular Waves', BOSS 92.

105. T. Kinoshita, S. Takase and S. Kato: 'Statistical Properties of Slow Drift Motion of a Vessel Moored in Random Seas', Dynamics of Marine Vehicles and Structures in Waves, Elsevier Science Publishers, 1991.

106. S. Kato, T. Kinoshita and S. Takase: 'Statistical Theory of Total Second Order Responses of Moored Vessels in Random Seas', Applied Ocean Research, 1989, vol. 12, no. 2.

107. S. Kato and S. Ando: 'On the Statistical Theory of Total Second Order Responses of Moored Floating Structures, OTC 5579, 1987.

108. P.K. Shaw: 'Statistics of Mooring Line Tension in Random Waves', OTC 6035, 1989.

109. E. Huse: 'Influence of Mooring Line Damping Upon Rig Motions', OTC 5204, 1986.

110. E. Huse and K. Matsumoto: 'Practical Estimation of Mooring Line Damping', OTC 5676, 1988.

111. E. Huse and K. Matsumoto: 'Mooring Line Damping Due to First and Second Order Vessel Motion', OTC 6137, 1989.

112. R.C. Macdonald: 'Positional Mooring Offshore', Lloyd"s Register Staff Association Paper No. 4, 1984-85.

113. R.C. Chaplin: 'Mooring Ropes - The Prediction of Fatigue Endurance', Conf. on The Way Forward for Floating Production Systems, IBC Technical Services, 1987.

114. A.E. Potts, R.C. Chaplin and N.R.H. Tantrum: 'Factors Influencing the Endurance of Steel Wire Rope for Mooring Offshore Structures', OTC 5718, 1988.

115. J. Lereim: 'Summary of the 4 Year Project - Anchor Chain Cables Offshore', OTC 5060, 1985.

116. M. Lalani: 'Developments in Fatigue Design Guidelines for Anchor Chains as Mooring Lines', OTC 6452, 1990.

TABLE 5: Comparison of Wind Drag Coefficients for Large Tankers According to OCIMF and GOULD

$$C_x = \frac{F_x}{\frac{1}{2}\rho A_r U_w}$$

$$C_y = \frac{F_y}{\frac{1}{2}\rho A_L U_w}$$

where:

F_x, F_y	=	longitudinal, lateral wind force
ρ	=	density of air
A_T, A_L	=	actual transverse lateral projected area for OCIMF
	=	transverse lateral projected area corrected for the wind gradient in Gould
U_W	=	wind velocity at 10 m above sea surface

Heading Angle	LOADED				BALLAST				
	OCIMF		GOULD		OCIMF			GOULD	
	C_x	C_y	C_x	C_y	C^*_{x1}	C^*_{x2}	C_y	C_x	C_y
180°(Head on)	-0.95	0.00	-1.18	0.00	-0.88	-0.88	0.00	-0.90	0.00
170	-0.90	0.09	-0.99	0.10	-0.75	-0.75	0.12	-0.69	0.12
160	-0.82	0.19	-0.95	0.20	-0.60	-0.60	0.31	-0.60	0.25
150	-0.72	0.30	-0.83	0.36	-0.49	-0.49	0.51	-0.45	0.42
140	-0.61	0.43	-0.69	0.53	-0.33	-0.27	0.66	-0.36	0.58
130	-0.48	0.55	-0.52	0.66	-0.22	0.00	0.79	-0.22	0.75
120	-0.34	0.63	-0.36	0.80	-0.13	0.30	0.89	-0.16	0.84
110	-0.20	0.68	-0.15	0.91	-0.08	0.46	0.95	-0.14	0.90
100	-0.07	0.70	-0.04	0.96	-0.05	0.48	0.98	-0.07	0.96
90	0.02	0.72	0.08	0.95	0.00	0.30	0.98	-0.01	0.97
80	0.09	0.72	0.20	0.95	0.07	0.21	0.96	0.07	0.96
70	0.18	0.71	0.29	0.90	0.17	0.17	0.89	0.14	0.90
60	0.26	0.68	0.41	0.81	0.27	0.27	0.79	0.23	0.80
50	0.33	0.63	0.43	0.74	0.36	0.36	0.69	0.35	0.68
40	0.39	0.54	0.48	0.66	0.46	0.46	0.57	0.37	0.56
30	0.48	0.42	0.61	0.53	0.54	0.54	0.45	0.43	0.42
20	0.55	0.38	0.72	0.38	0.61	0.61	0.30	0.50	0.26
10	0.65	0.15	0.79	0.20	0.63	0.63	0.17	0.54	0.16
0 (Stem on)	0.60	0.00	0.79	0.00	0.61	+0.61	0.00	+0.56	0.00

$^*C_{x1}$ = conventional bow

$^*C_{x2}$ = Rounded bow

TABLE 6: Comparison of Current Profile According to Various Guides in Depth of Water 100 m

Depth below Surface (m)	Ref. (5) m/sec	Classification Society m/sec	MAREX
0	1.54	1.66	1.89
-5	0.96	1.59	0.97
-10	0.92	1.51	0.90
-15	0.92	1.44	0.89
-20	0.92	1.36	0.88
-50	0.92	0.90	0.83
-75	0.91	0.90	0.75
-99	0.78	0.90	0.57

ZERO CROSSING PERIOD, Tz (secs)

SIGNIFICANT WAVE HEIGHT, Hs (m)

	3.5	4.5	5.5	6.5	7.5	8.5	9.5	10.5	11.5	12.5
13.5										213
							1/10			1/50
12.25					1786	1479	892	497	293	175
11.75					1643	1360	820	456	270	161
11.25					1506	1247	752	420	247	148
10.75					1376	1139	687	383	226	135
10.25					1251	1035	624	348	205	123
9.75				1072	1132	937	565	315	186	111
9.25				965	1018	843	508	284	167	100
8.75				863	911	754	455	254	150	89
8.25				768	810	671	404	226	133	79
7.75				677	715	592	357	199	117	70
7.25				593	626	518	312	174	103	61
6.75			465	518	542	449	271	151	89	53
6.25			399	440	465	385	232	129	76	46
5.75			337	373	394	326	196	110	65	39
5.25			287	311	328	272	164	91	54	32
4.75		193	230	254	269	222	134	75	44	26
4.25		155	184	204	215	178	107	60	35	21
3.75		120	143	159	167	139	84	47	27	16
3.25		90	108	119	126	104	63	35	21	12
2.75	7	65	77	85	90	75	45	25	15	9
2.25	5	43	52	57	60	50	30	17	10	6

ABOVE AND TO THE LEFT OF THIS LINE THE 50 YEAR VALUES ARE EXCEEDED

+ WAVES OBSERVED ON WAVE SCATTER DIAGRAM

Table 7 Steady Wave Drift Force (kN). Ship (Head-On), Jonswap Spectra.

ZERO CROSSING PERIOD, Tz (secs)

SIGNIFICANT WAVE HEIGHT, Hs (m)

	3.5	4.5	5.5	6.5	7.5	8.5	9.5	10.5	11.5	12.5
13.5										415
							1/10			1/50
12.25					1059	758	557	435	368	342
11.75					975	697	513	400	338	315
11.25					893	639	470	367	310	288
10.75					816	584	429	335	283	263
10.25					742	531	390	304	257	239
9.75				975	671	480	353	275	233	217
9.25				878	604	432	318	248	210	195
8.75				785	540	387	284	222	188	175
8.25				698	480	344	253	197	167	155
7.75				616	424	303	223	174	147	137
7.25				539	371	266	195	152	129	120
6.75			792	467	322	230	169	132	112	104
6.25			679	401	276	197	145	113	96	89
5.75			574	339	233	166	123	96	81	75
5.25			479	283	195	139	102	80	68	63
4.75		474	392	231	159	114	84	65	55	51
4.25		379	314	185	128	91	67	52	44	41
3.75		295	244	144	99	71	52	41	34	32
3.25	145	222	184	108	75	53	39	31	26	24
2.75	104	159	131	78	53	38	28	22	19	17
2.25	70	106	88	52	36	26	19	15	12	12

ABOVE AND TO THE LEFT OF THIS LINE THE 50 YEAR VALUES ARE EXCEEDED

+ WAVES OBSERVED ON WAVE SCATTER DIAGRAM

Table 8 Steady Wave Drift Force (kN), Semi-Sub (Head-On), Jonswap Spectra.

ZERO CROSSING PERIOD, Tz (secs)

SIGNIFICANT WAVE HEIGHT, Hs (m)

	3.5	4.5	5.5	6.5	7.5	8.5	9.5	10.5	11.5	12.5
13.5										272
							1/10			1/50
12.25					1031	754	550	399	296	224
11.75					949	693	506	367	272	206
11.25					870	636	464	336	249	189
10.75					794	580	424	307	228	173
10.25					722	528	385	279	207	157
9.75				880	653	477	348	252	187	142
9.25				792	588	430	314	227	169	128
8.75				709	526	384	281	203	151	114
8.25				630	468	342	249	181	134	102
7.75				556	413	302	220	160	118	90
7.25				487	361	264	192	140	104	79
6.75			404	422	313	229	167	121	90	68
6.25			347	362	268	196	143	104	77	58
5.75			293	306	227	166	121	88	65	49
5.25			245	255	189	138	101	73	54	41
4.75		196	200	209	153	113	83	60	44	34
4.25		157	160	167	124	91	66	48	36	27
3.75		122	125	130	97	71	52	37	28	21
3.25	150	92	94	98	73	53	39	28	21	16
2.75	108	66	67	70	52	38	28	20	15	11
2.25	72	44	45	47	35	25	19	13	10	8

ABOVE AND TO THE LEFT OF THIS LINE THE 50 YEAR VALUES ARE EXCEEDED

+ WAVES OBSERVED ON WAVE SCATTER DIAGRAM

Table 9 Steady Wave Drift Force (kN), Semi-Sub (Beam-On), Jonswap Spectra.

STEADY DRIFT FORCES AT A PERCENTAGE OF 50 YEAR RETURN PERIOD FORCE (JONSWAP SPECTRA) IN HEAD-ON CONDITIONS. 120,000 TONNE dwt FSU - LOAD DRAFT

HEADING 180°

Hs(m)	Zero Crossing Period (secs) 5.5	6.5	7.5	8.5	9.5	12.5
4.25	86	96	101	84	50	
5.25		146	154	128		
6.25			218	181		
7.25				243		
7.75				278	168	
8.25					190	
10.5		584	616	510	308	
13.5						100

HEADING 160°

Hs(m)	Zero Crossing Period (secs) 5.5	6.5	7.5	8.5	9.5	12.5
4.25	212	215	198	149	100	
5.25		329	302	228		
6.25			428	323		
7.25				434		
7.75				498	334	
8.25					378	
10.5		1310	1207	912	614	
13.5						361

HEADING 140°

Hs(m)	Zero Crossing Period (secs) 5.5	6.5	7.5	8.5	9.5	12.5
4.25	477	495	416	291	204	
5.25		756	635	443		
6.25			900	628		
7.25				846		
7.75				966	679	
8.25					770	
10.5		3021	2542	1773	1247	
13.5						795

Table 10 Increase in drift force with heading angle.

Fig. 1

PLATFORM PROCESSED DATA JANUARY 1984

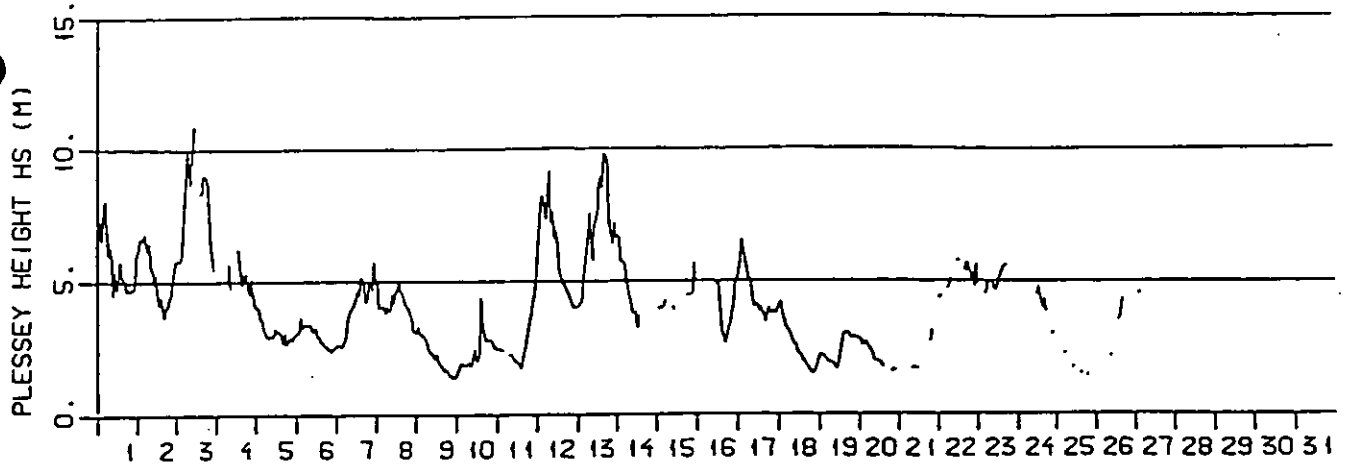

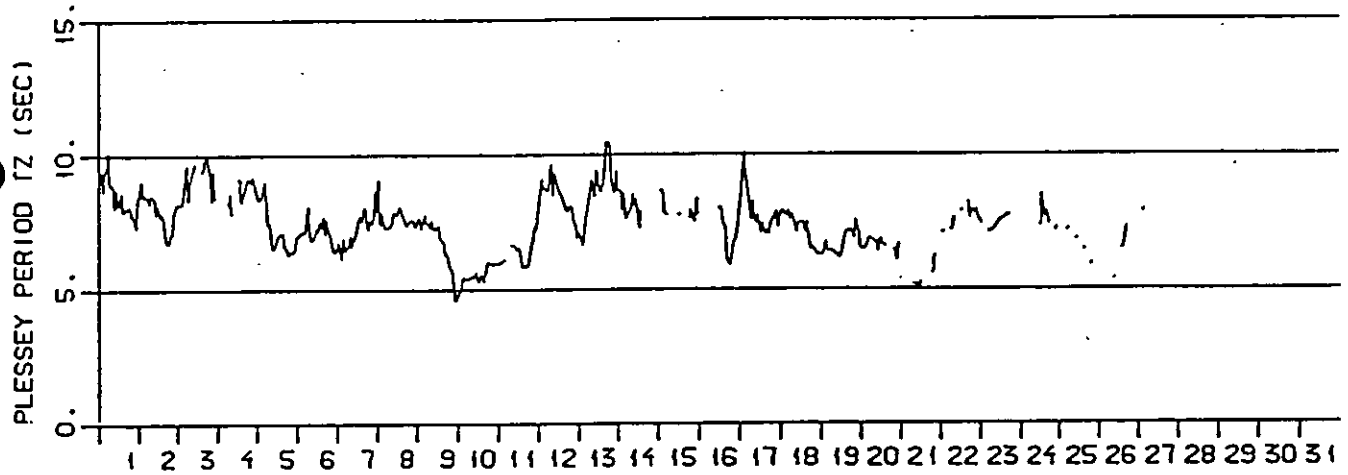

PLATFORM PROCESSED DATA JANUARY 1984

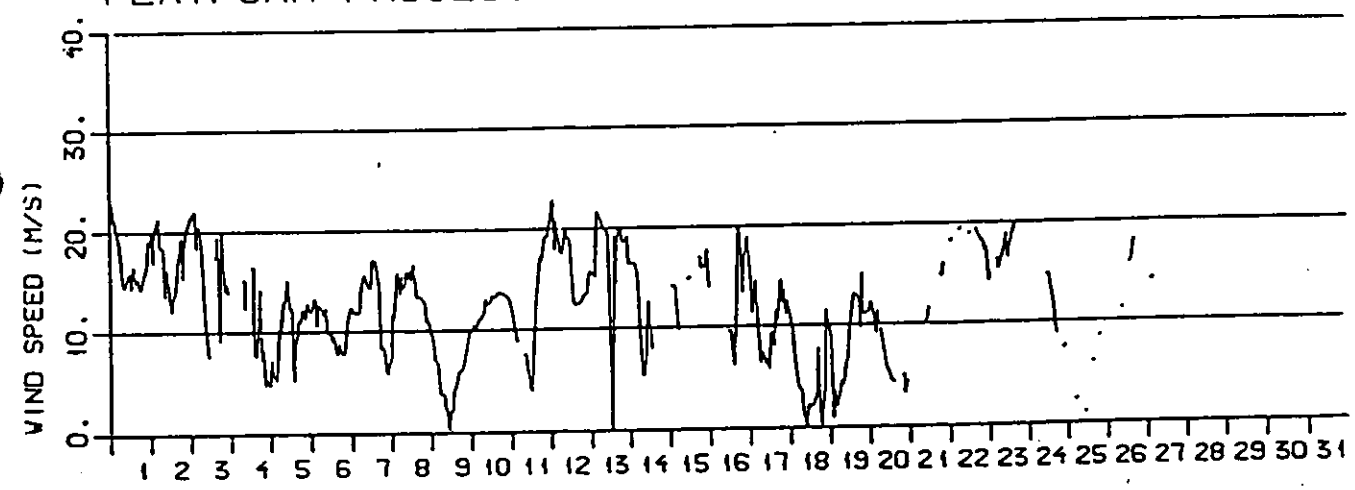

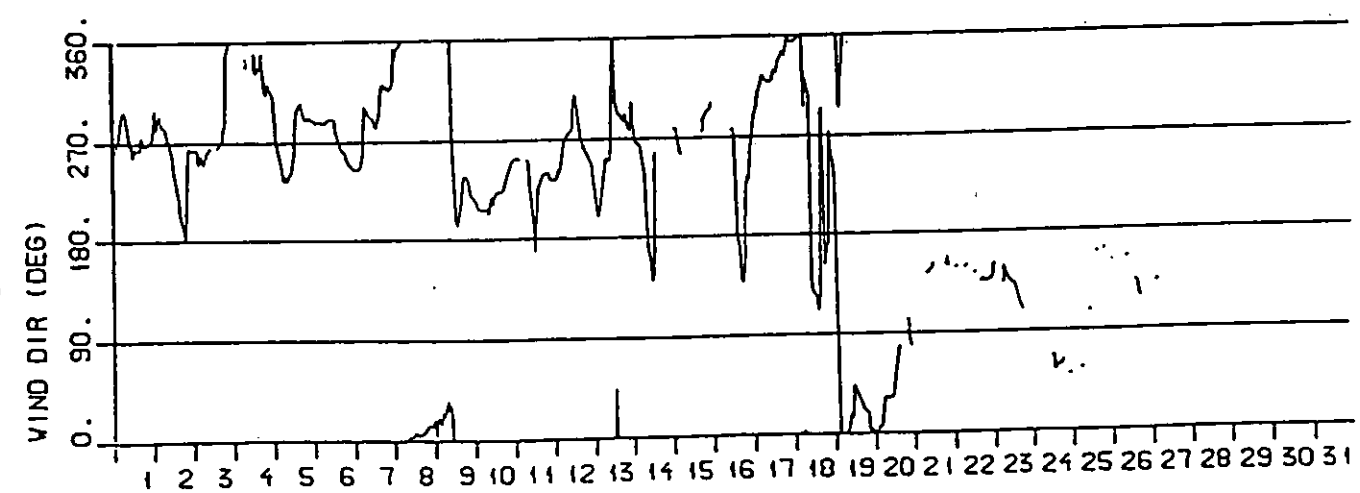

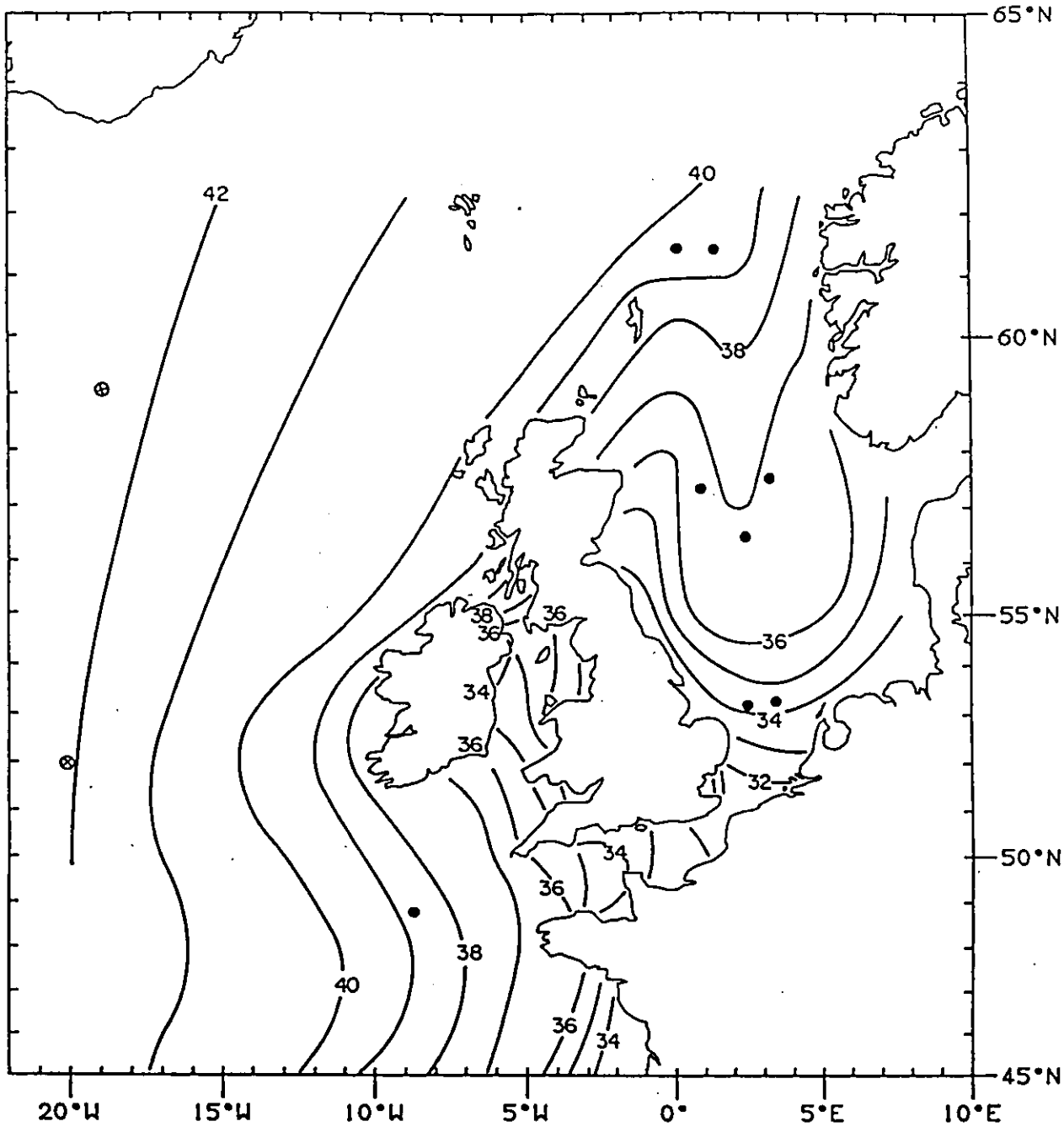

Estimates of 50-year return omnidirectional hourly-mean wind speeds at 10 m above still water level

Contours are in m/s. Estimated maximum error is ± 2 m/s.

Ocean Weather Stations, where wind speeds have been measured for many years at fixed locations, are shown ⊕.
Sites used for verification purposes are shown • (see OTH 89 299).

Source: Analysis of VOF and instrumental data (OTH 89 299). Details of the analysis method used are to be found in this reference.

Fig. 3

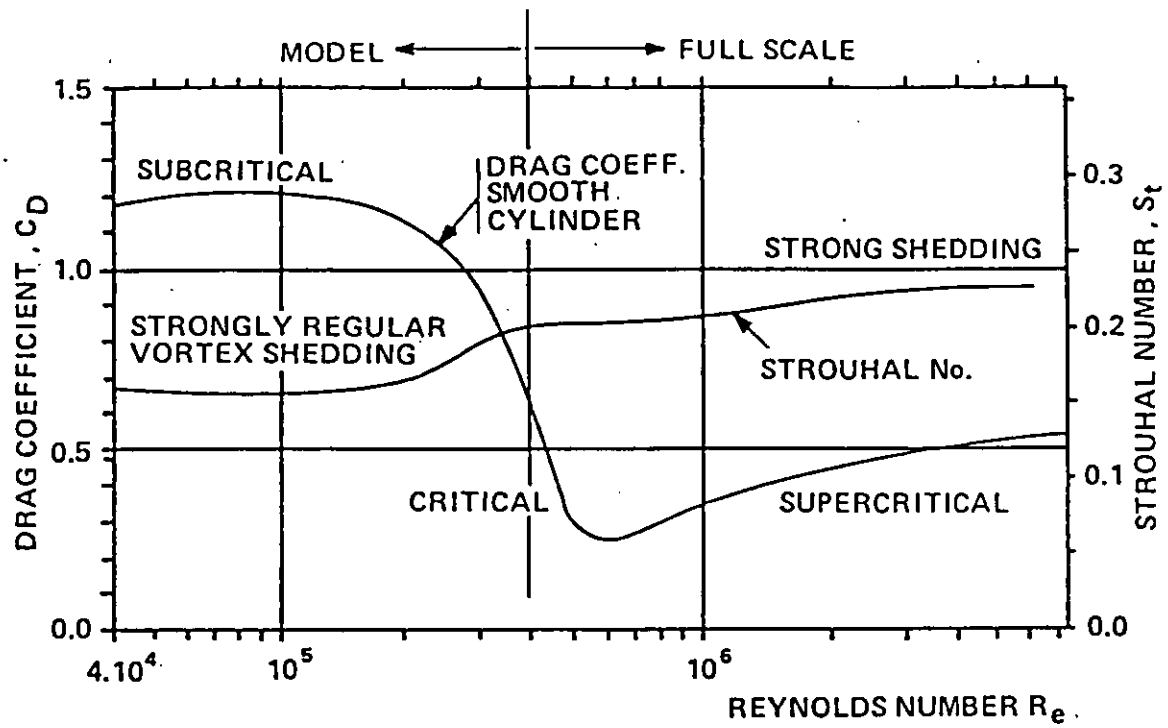
MODEL
FULL SCALE
SUBCRITICAL
DRAG COEFF. SMOOTH CYLINDER
STRONG SHEDDING
STRONGLY REGULAR VORTEX SHEDDING
STROUHAL No.
CRITICAL
SUPERCRITICAL
DRAG COEFFICIENT, C_D
STROUHAL NUMBER, S_t
REYNOLDS NUMBER R_e
1.5
1.0
0.5
0.0
0.3
0.2
0.1
0.0
4.10^4
10^5
10^6

Fig. 4

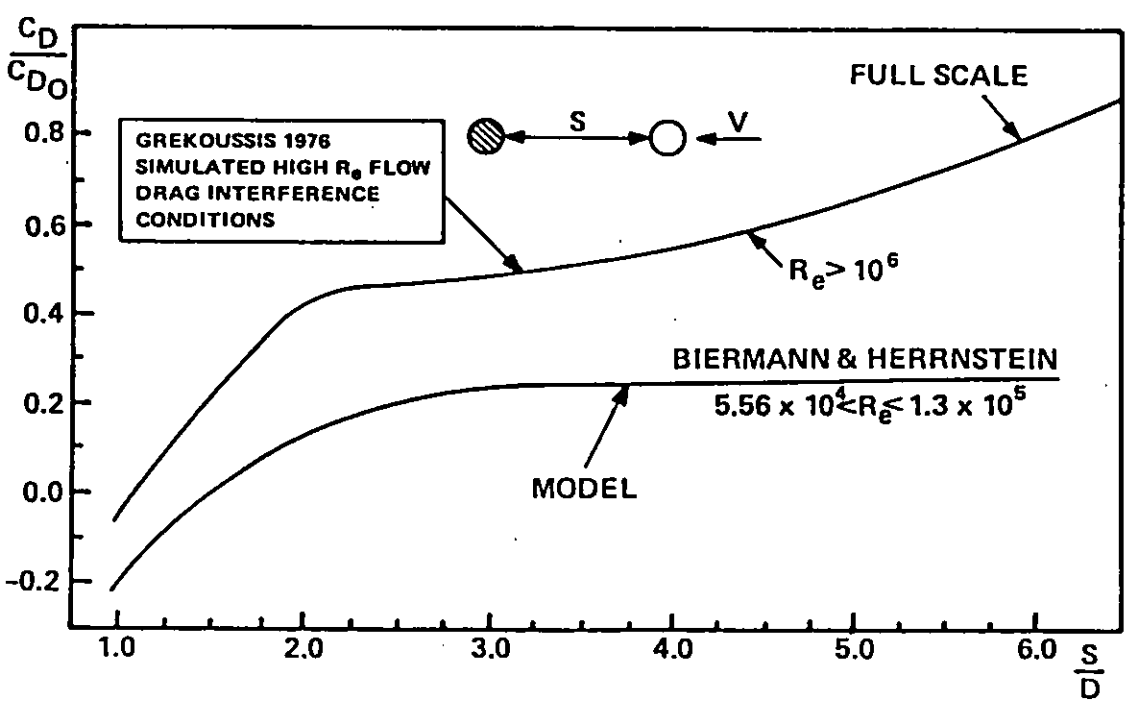
$\frac{C_D}{C_{D_O}}$
GREKOUSSIS 1976
SIMULATED HIGH R_e FLOW
DRAG INTERFERENCE
CONDITIONS
S
V
FULL SCALE
$R_e > 10^6$
BIERMANN & HERRNSTEIN
$5.56 \times 10^4 < R_e < 1.3 \times 10^5$
MODEL
0.8
0.6
0.4
0.2
0.0
-0.2
1.0
2.0
3.0
4.0
5.0
6.0
$\frac{S}{D}$

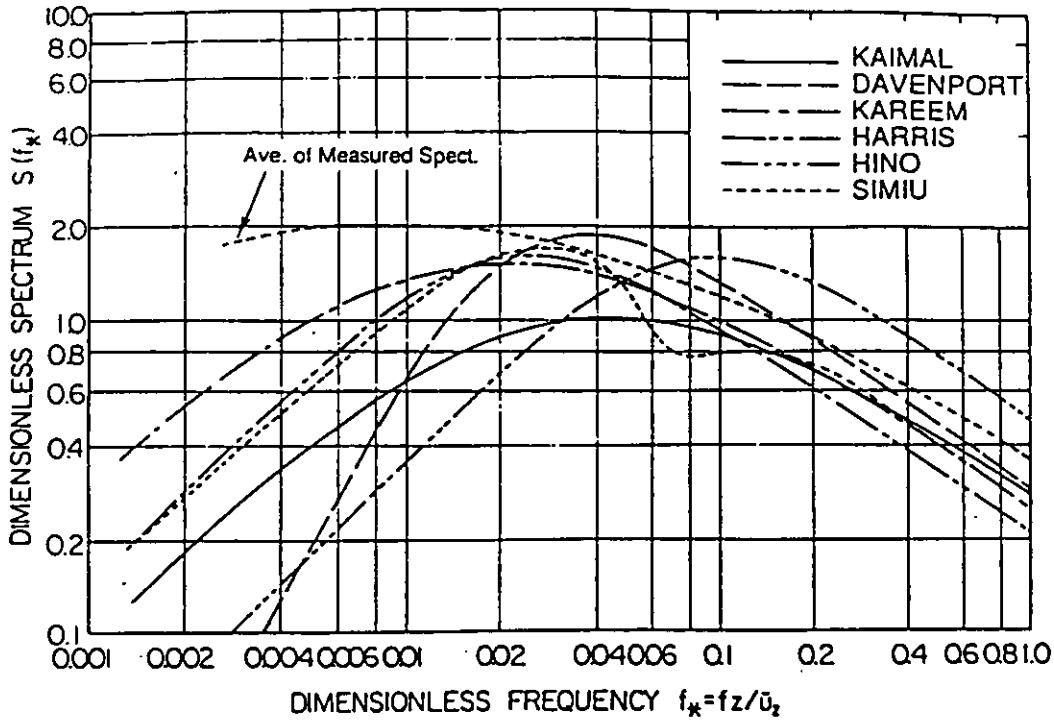

Figure 5 Comparison of various wind spectral formulations

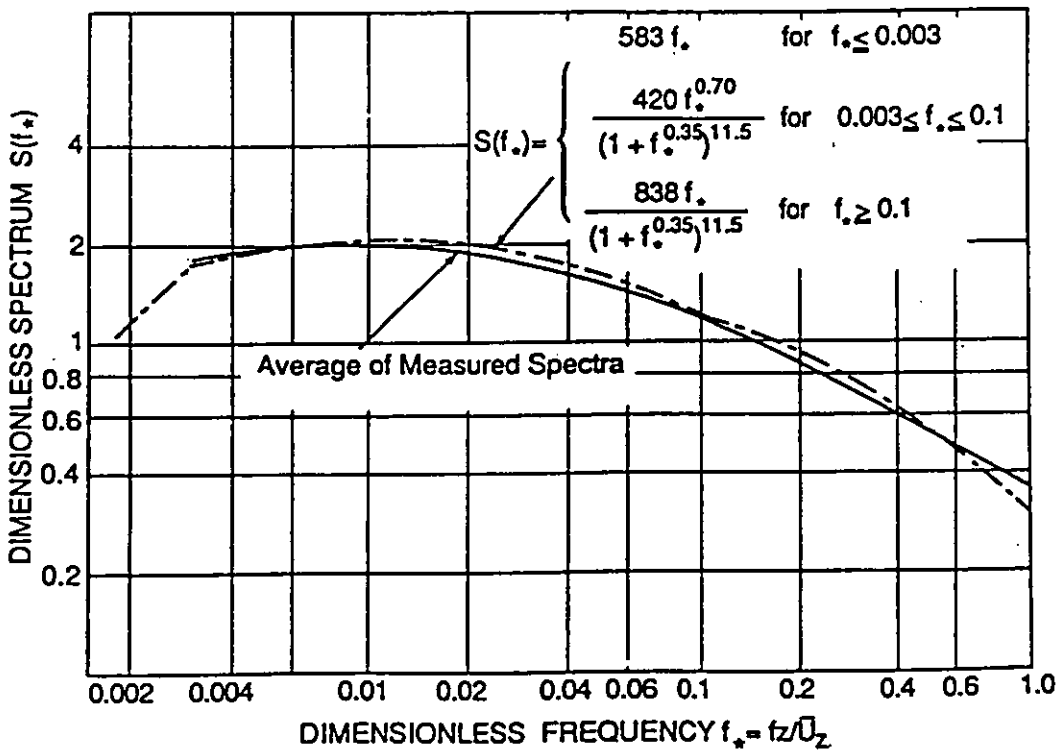

Figure 6 Mathematical presentation of average of measured wind spectra over a seaway

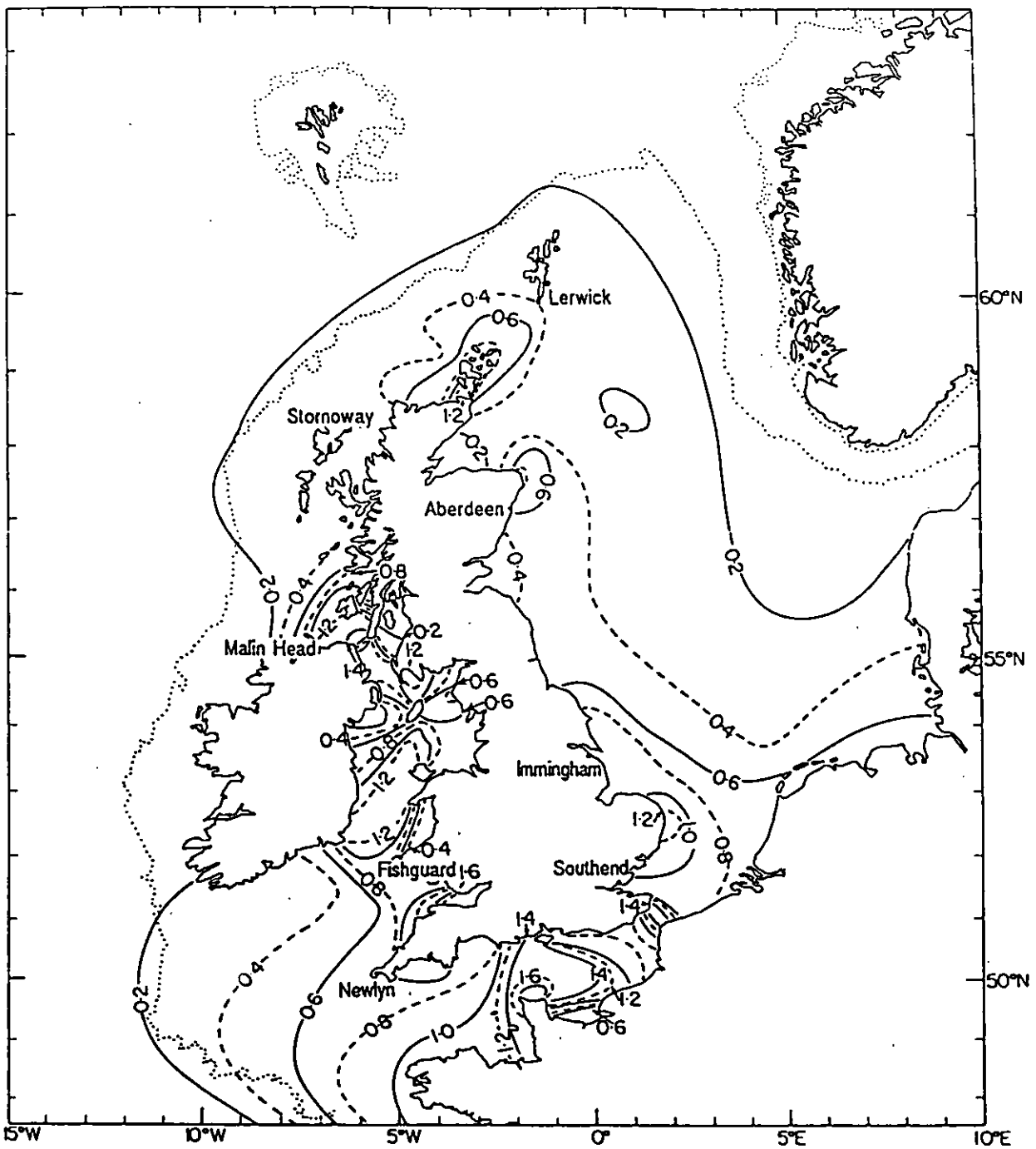

Estimates of maximum depth-averaged flow of an average spring tidal current

Contours are in m/s

See Section 6 for definition of spring tidal current

Dotted line is the 100 fathom (183 m) depth contour

Source: Observations (OTH 89 299)

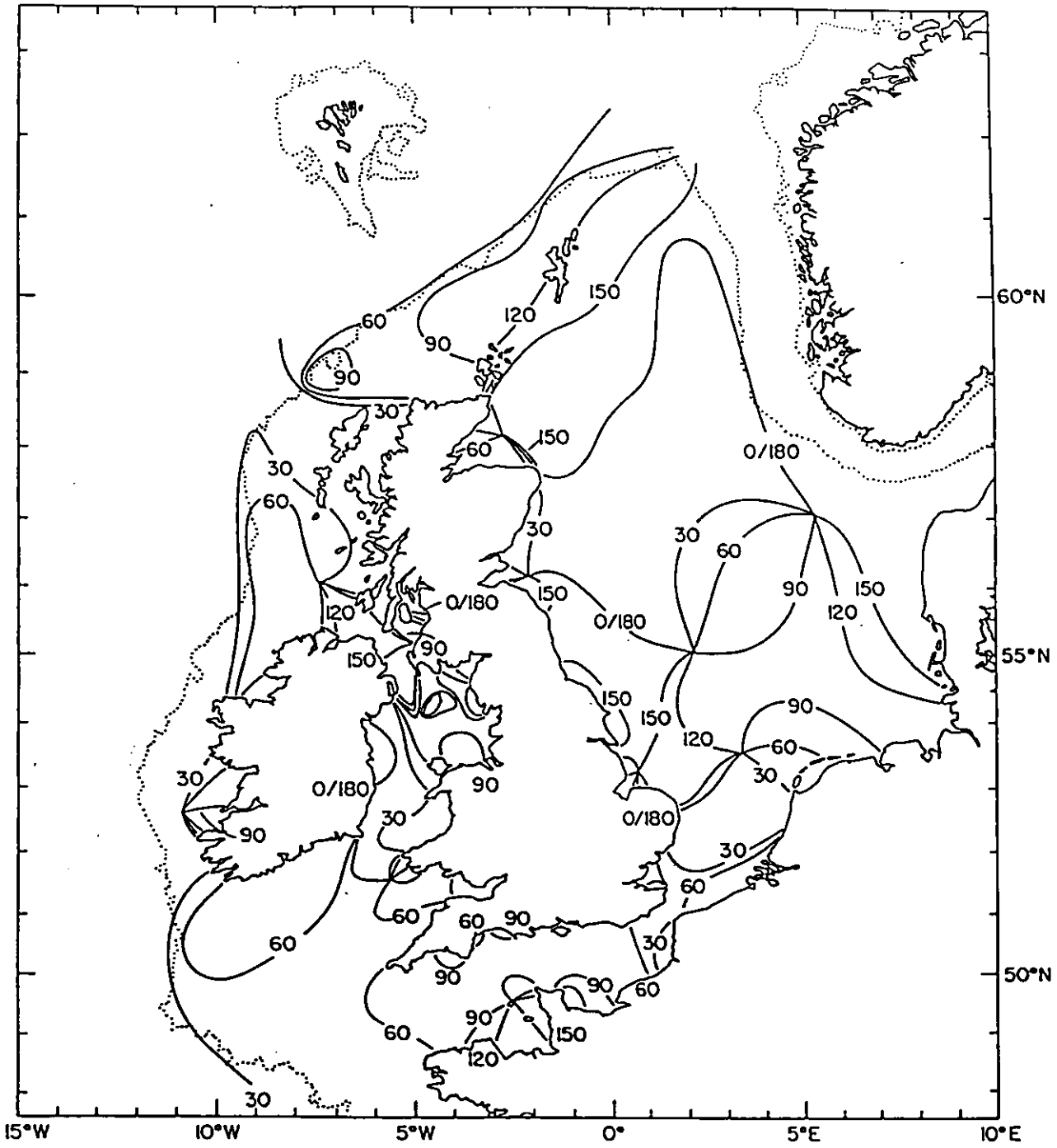

Direction of the maximum flow of the average spring tidal current

Contours are in degrees clockwise relative to north or south

0° and 180° are the same direction

Dotted line is the 100 fathom (183 m) depth contour

Source: Observations (OTH 89 299)

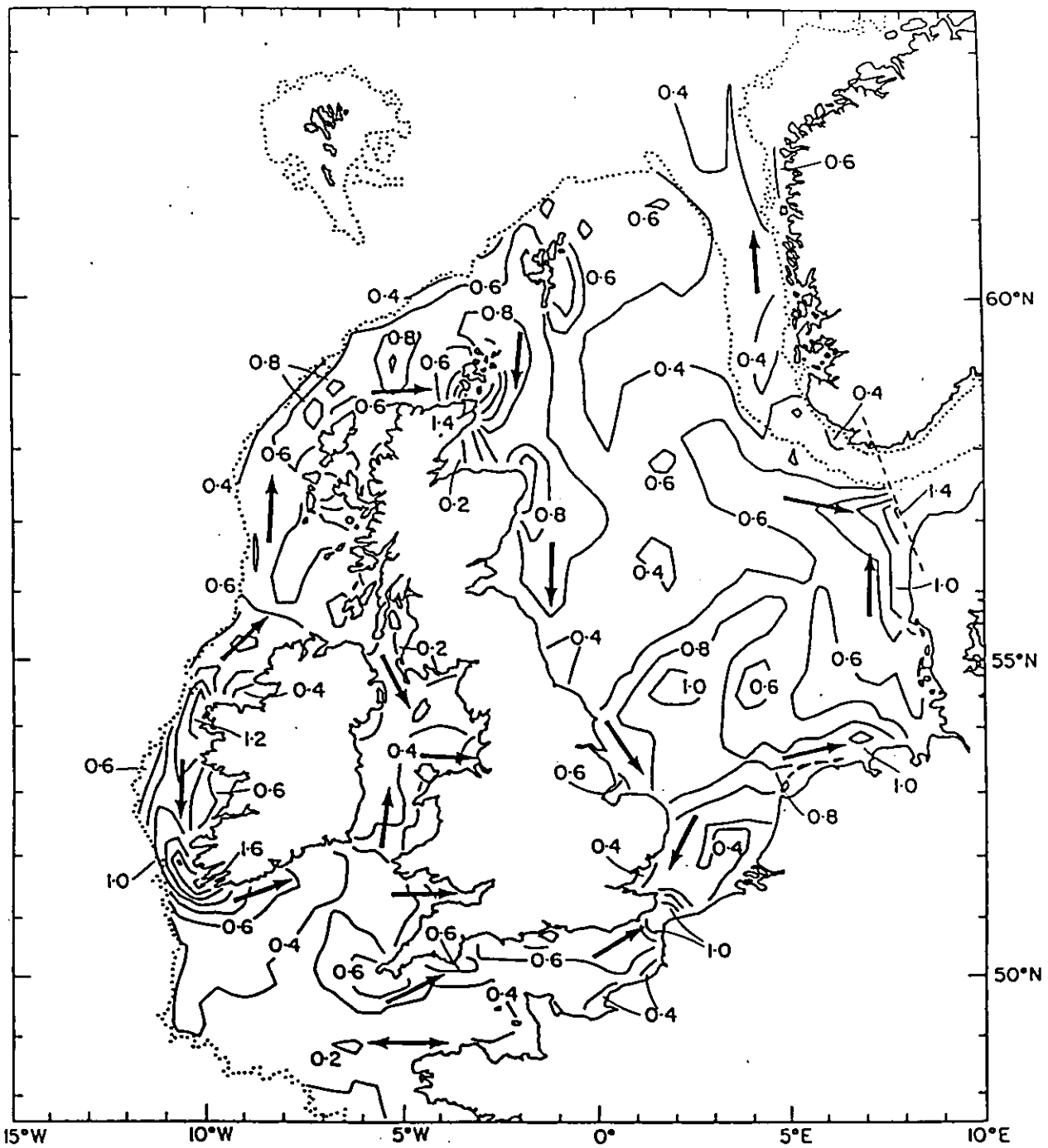

Estimates of 50-year return depth-averaged hourly-mean storm surge currents

Bold arrows indicate the direction of the maximum current in regions where the computed surge currents have preferred directions

Contours are in m/s

Dashed line is the 100 fathom (183 m) depth contour

Source: Numerical model simulations (OTH 89 299)

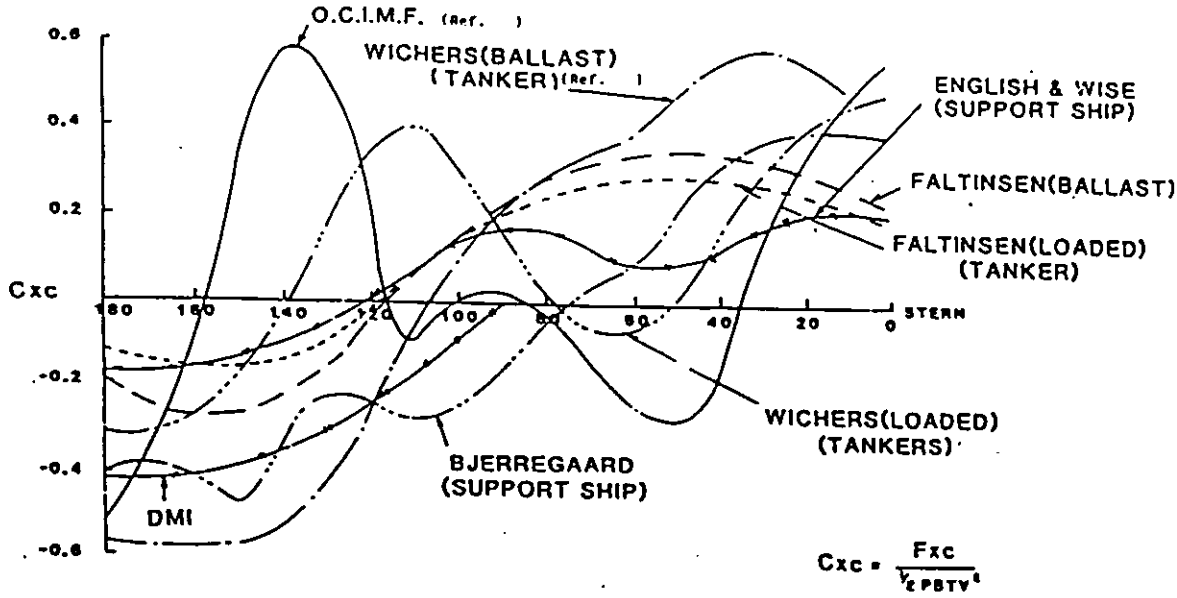

Fig. 10

LONGITUDINAL FORCE COEFFIENT VERSUS HEADING ANGLE

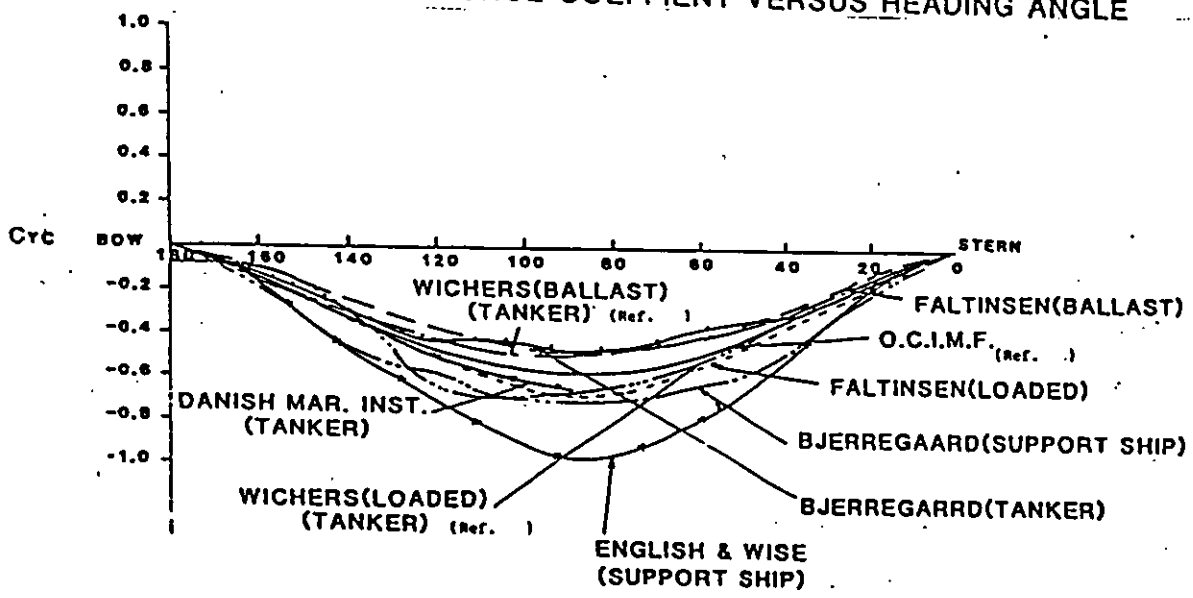

Fig. 11

LATERAL CURRENT FORCE COEFFICIENT

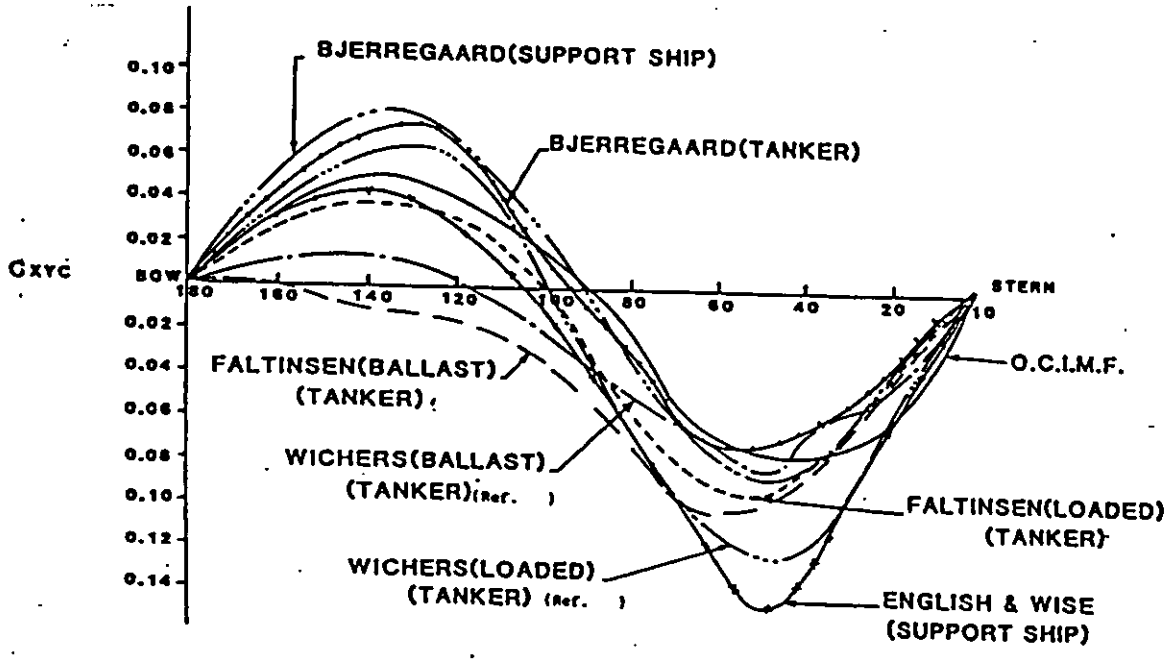

Fig. 12

CURRENT MOMENT COEFFICIENTS

135° HEADING

Fig. 13

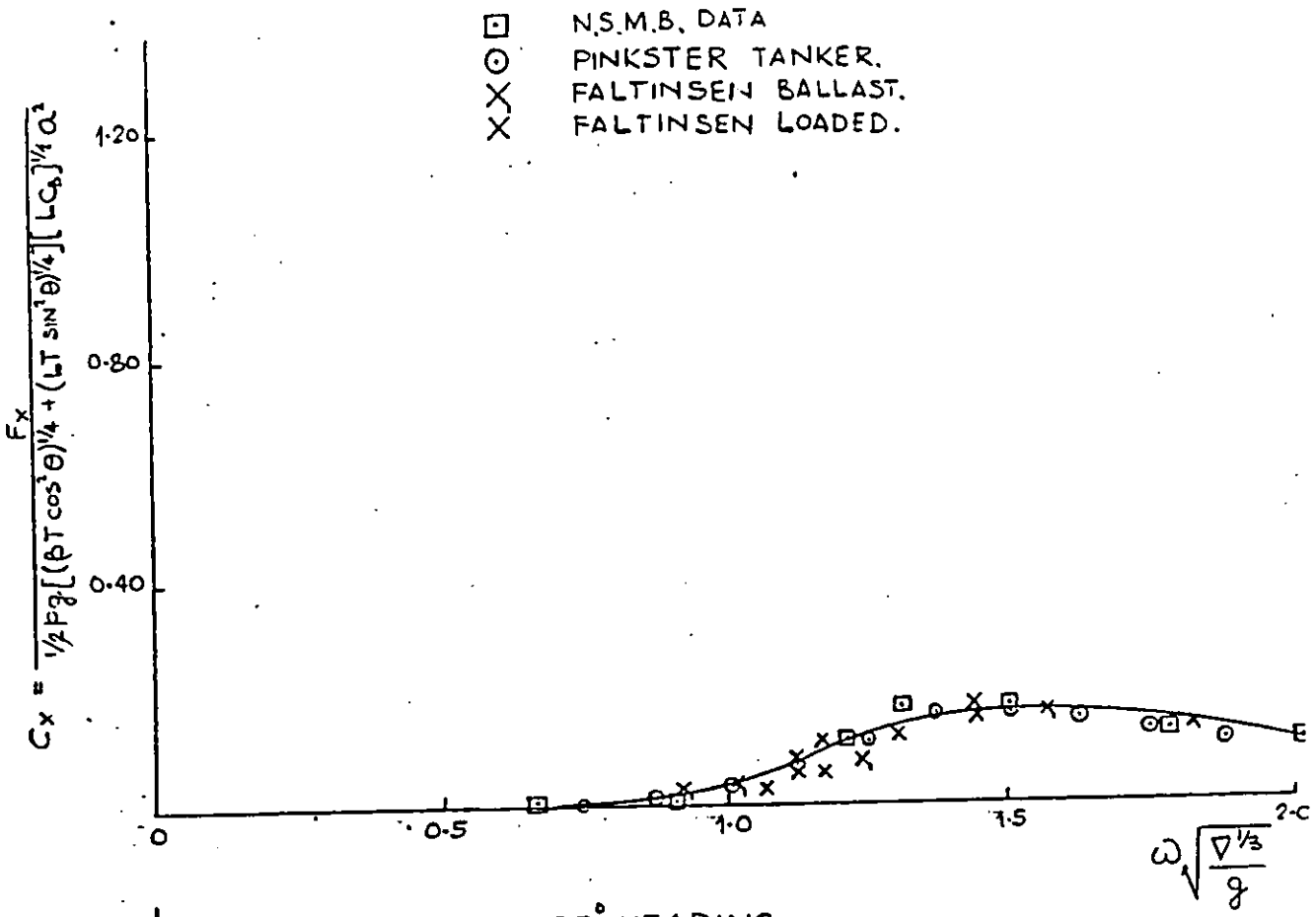

135° HEADING

Fig. 14

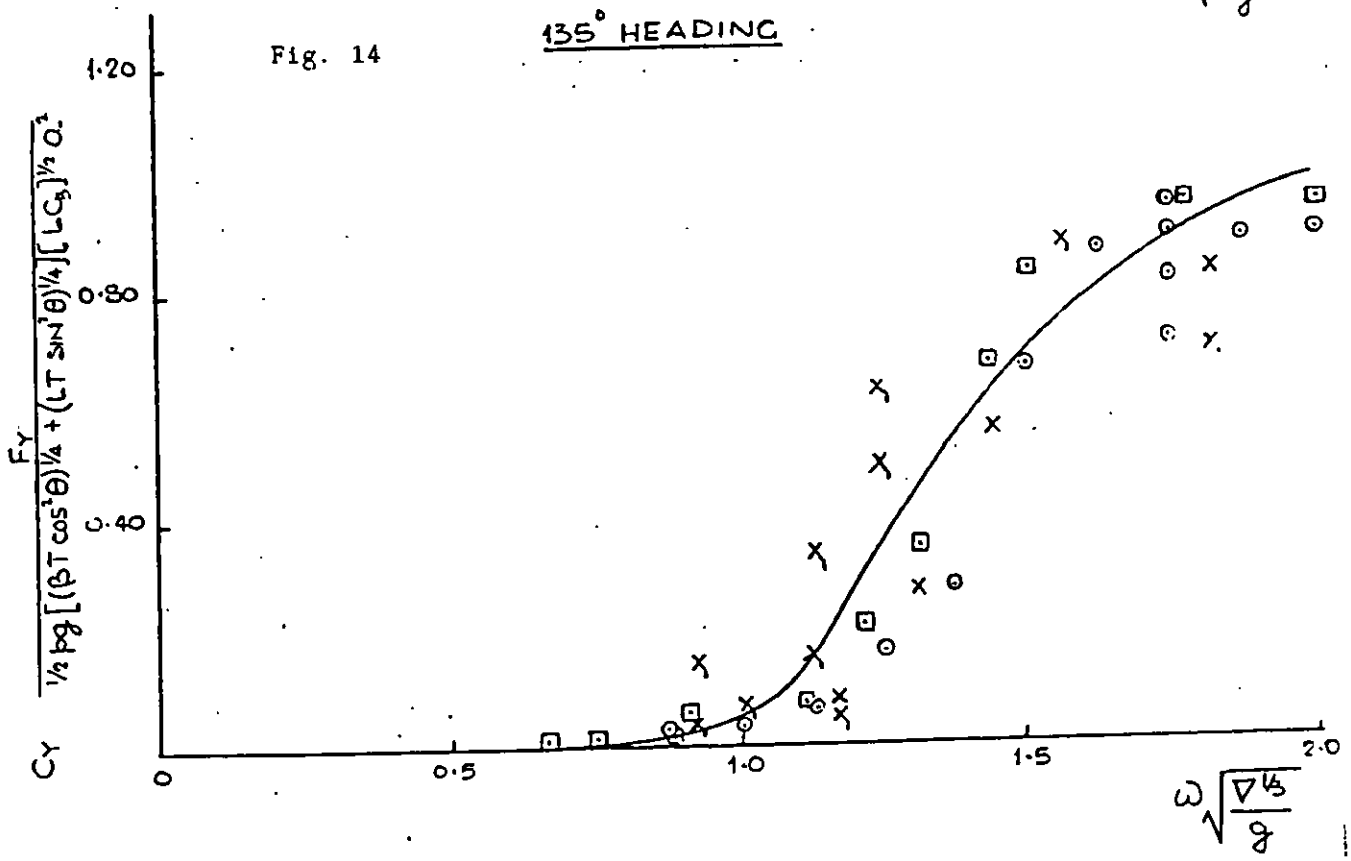

Fig. 15

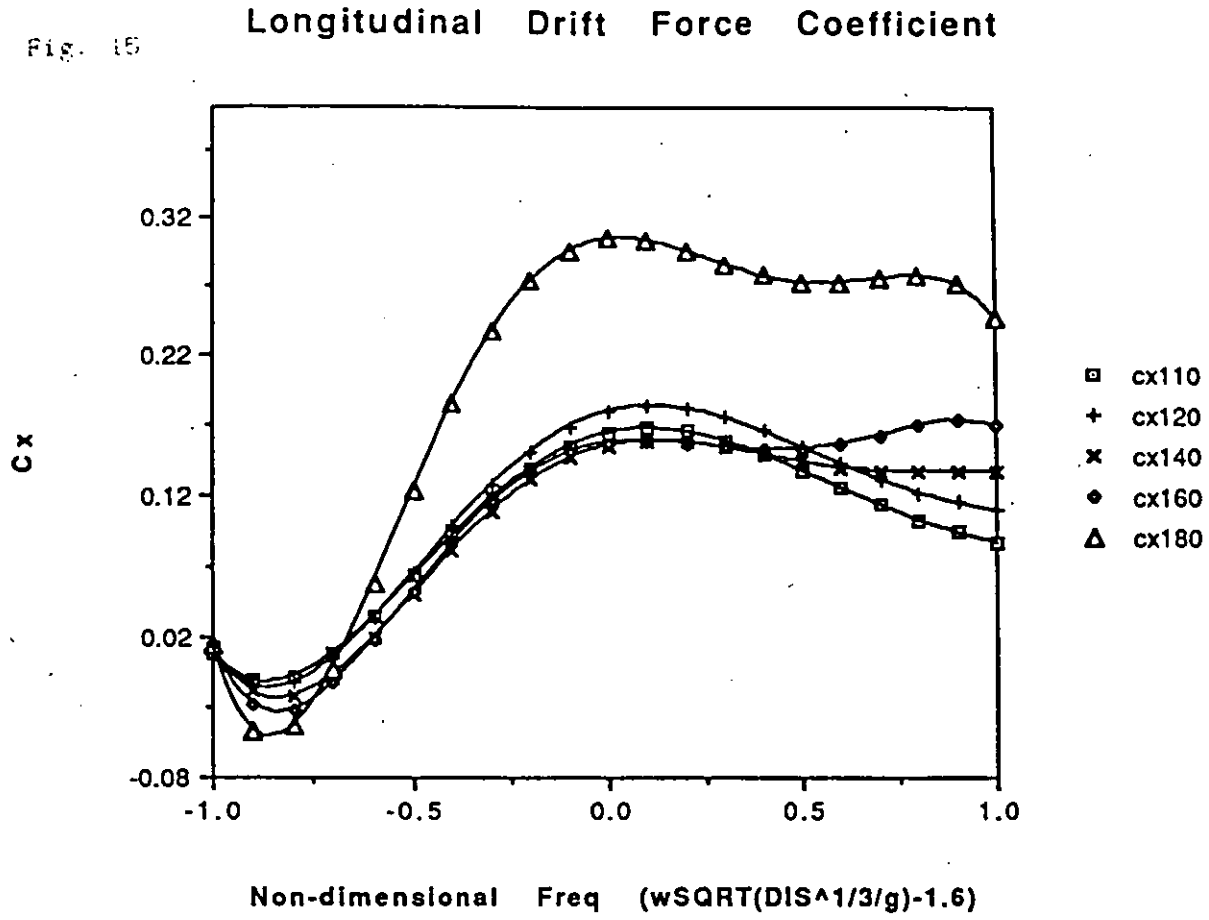
Longitudinal Drift Force Coefficient
0.32
0.22
0.12
0.02
-0.08
Cx
-1.0
-0.5
0.0
0.5
1.0
Non-dimensional Freq (wSQRT(DIS^1/3/g)-1.6)
cx110
cx120
cx140
cx160
cx180

Fig. 16.

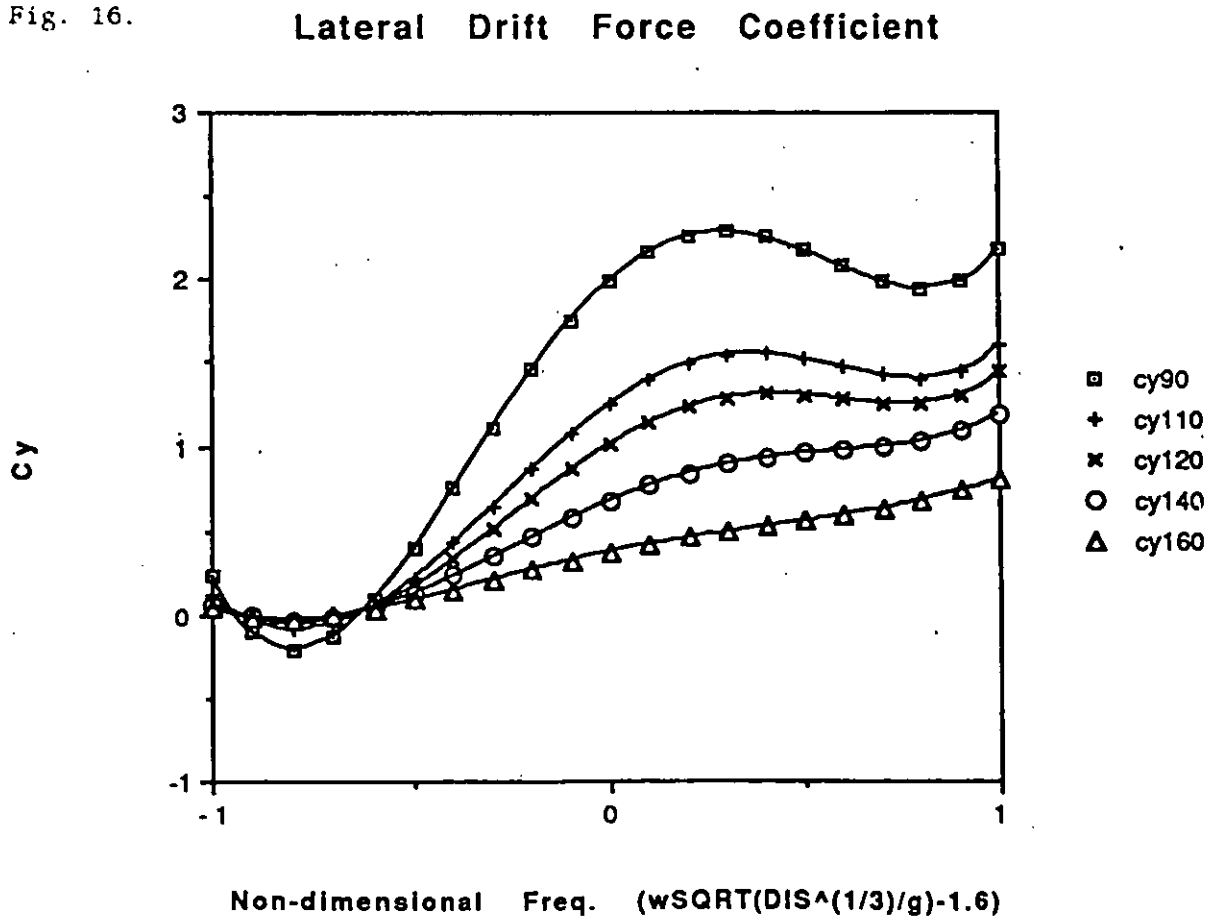
Lateral Drift Force Coefficient
3
2
1
0
-1
Cy
-1
0
1
Non-dimensional Freq. (wSQRT(DIS^(1/3)/g)-1.6)
cy90
cy110
cy120
cy140
cy160

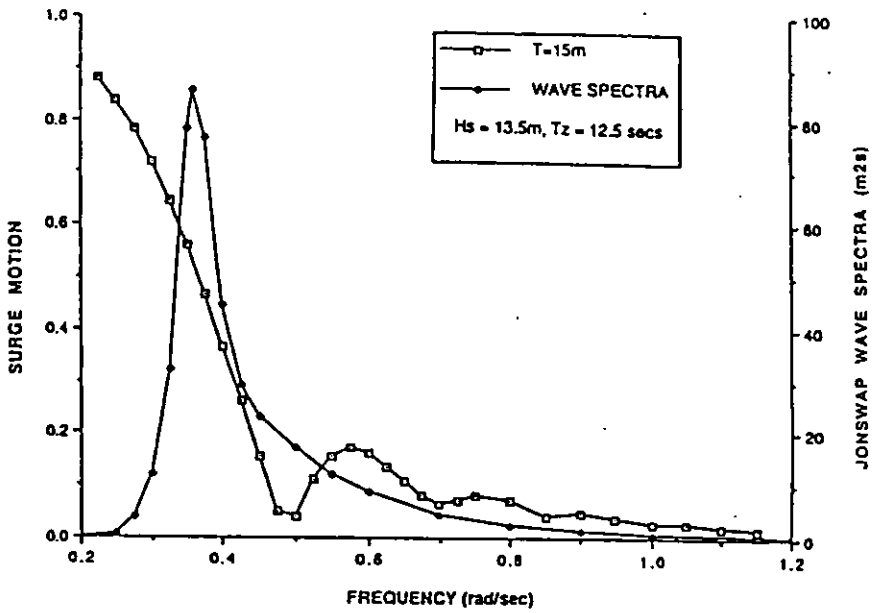

Fig. 17 Surge RAO (ship) and 50 year spectra.

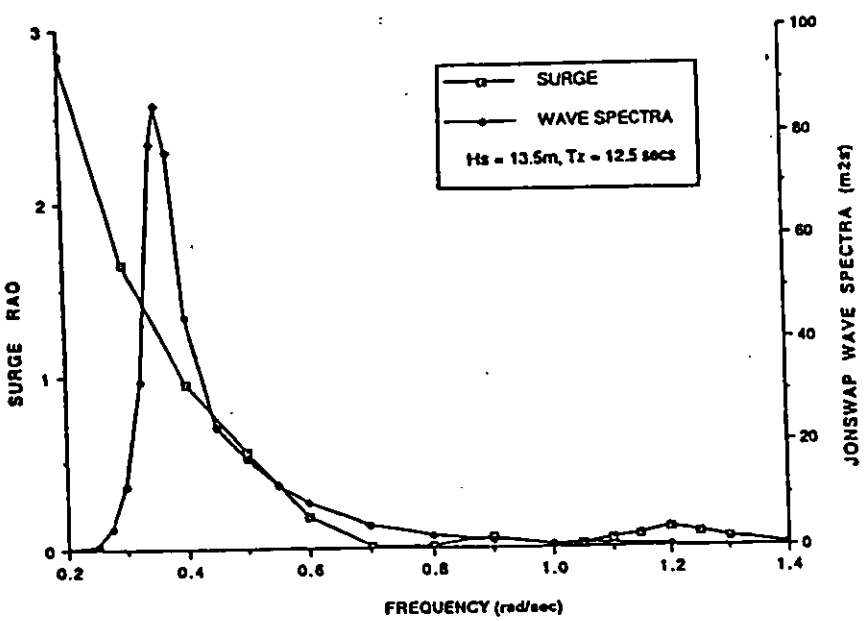

Fig. 18 Surge RAO (semi-submersible) and 50 year spectra.

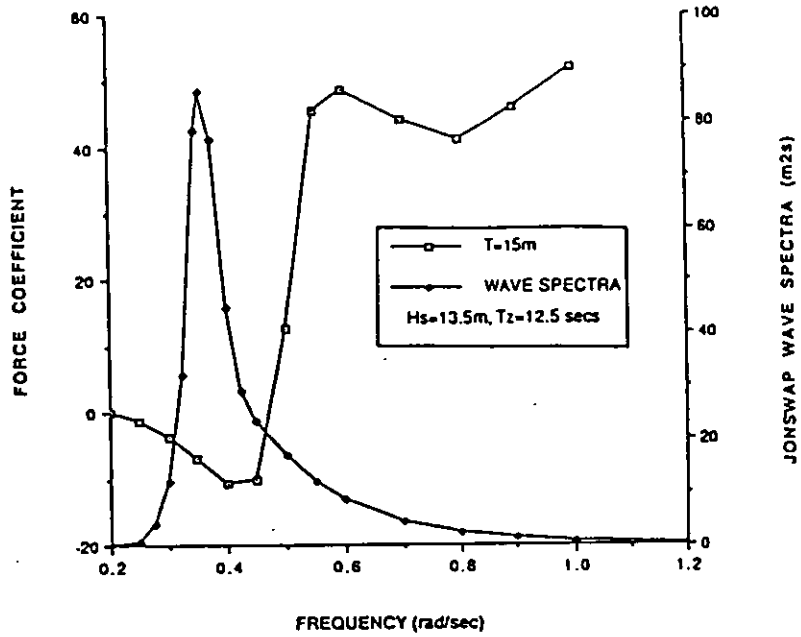

Fig. 19 Drift force curve (ship) and 50 year spectra.

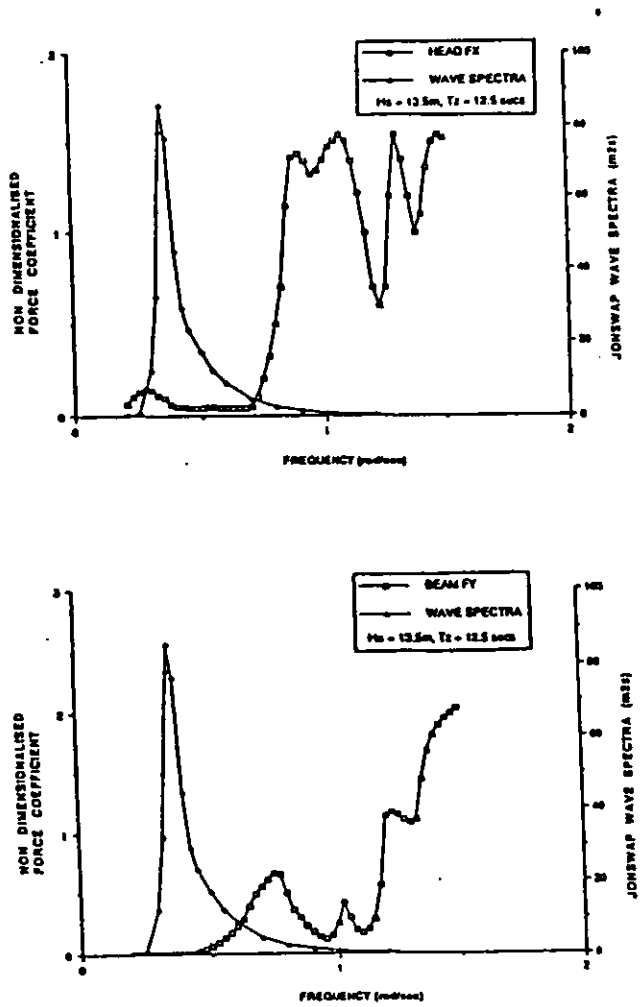

Fig. 20 Drift force curves (semi-submersible) and 50 year spectra.

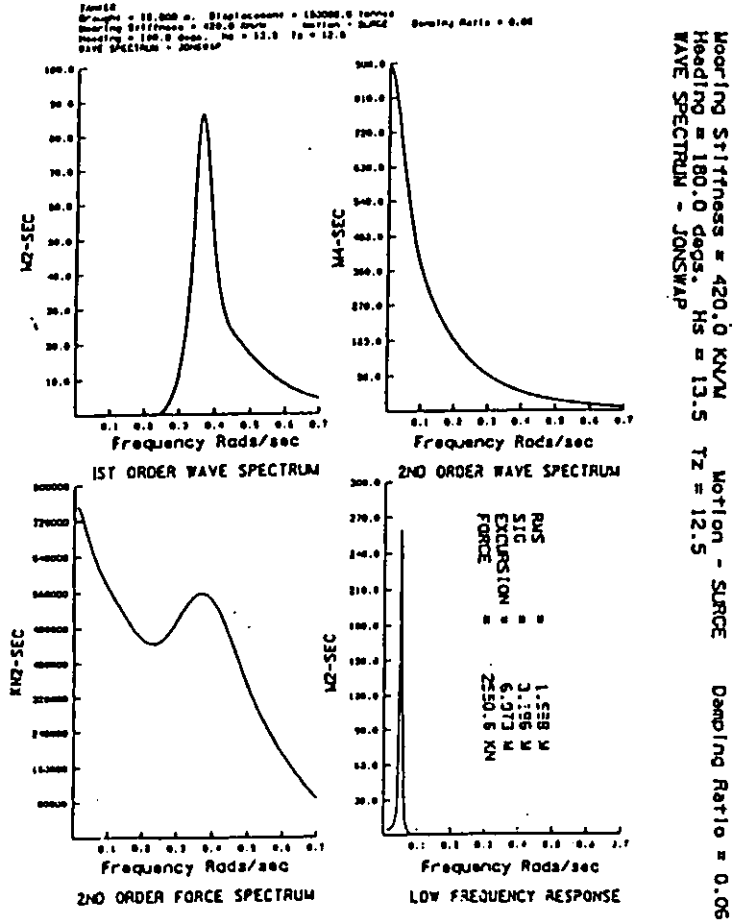

Low Frequency Response, 50 Year Condition (Ship)

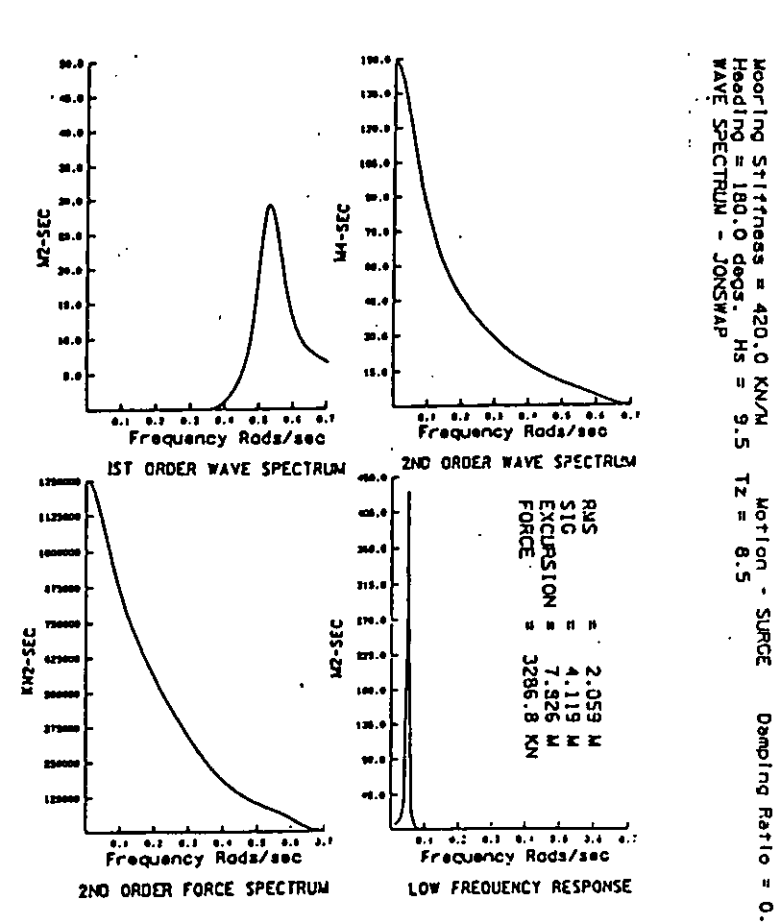

Low Frequency Response, 1 Year Condition (Ship)

Fig. 21 Low frequency drift calculation for a 120,000 tonne dwt tanker in two wave spectra.

CONCEPTUAL DESIGN OF SEMI-SUBMERSIBLE PRODUCTION PLATFORMS

by

HOTZE BOONSTRA

DELFT

CONCEPTUAL DESIGN OF SEMI-SUBMERSIBLE PLATFORMS FOR EXPLORATION AND PRODUCTION.

H. Boonstra
Delft University of Technology
The Netherlands

1. Introduction.

The design process of semi-submersible platforms is basically similar to the design of 'normal' ships. In both cases the designer (or the design-team) has to conceive an "optimal" structure, which complies with the generally limited number of design requirements, extensive rules and regulations from classification societies, safety requirements posed by governmental bodies, etc. There are however in practice a number of differences between semi-subs and conventional ships, which effects the design process considerably. The most notable of these differences are:

- The total number of existing semi-subs is very small compared to conventional merchant ships, (less than 250 units world-wide), whereas there is a great variety in configuration. This means that mostly the designer cannot make use of (statistical) data built up in the past, but has to use "first-principles" instead.
- A semi-sub requires a lot more analysis during the first stages of the design than a conventional ship: a preliminary design is not ready before aspects such as motions in seaway, overall strength, station keeping and (damage) stability are investigated.
- In contrast to most ship types there is a great variety in configuration and lay-out of semi-submersible platforms.
- Whereas the ship designer will try to keep the main dimensions of the design as small as possible, given the required deadweight and cargo volume, the designer of a semi-submersible has to search for an optimum balance between overall dimensions, seakeeping characteristics, draught, and stability.

The consequence of the differences above is that the approach of a preliminary design of a semi-submersible platform differs considerably from the way in which a conventional ship is designed.

In the first part of these notes mobile semi-submersible platforms (used for exploration) are discussed, in section 7 special aspects of stationary semi-submersible platforms (used for production of hydrocarbons) are treated.

2. Short history of semi-submersible platforms.

Semi-submersible drilling platforms have evolved from so-called "submersibles", a type of platform used extensively for exploration drilling in the Gulf of Mexico in the 50's and early 60's, consisting of pontoons and vertical columns, on which a deck was placed. In transit condition the structure was floating on its pontoons, when drilling the pontoons rested on the sea bed. The maximum allowable water depth was thus limited by the height of the columns. It was noticed that when operating the submersible in floating mode, with the pontoons submerged below the water line, a stable platform was created which did not respond very much to the waves. By adding mooring equipment and some other conversions to an existing submersible (Blue Water Rig no. 1, 1961) the semi-submersible was born (see e.g. Howe [1]).

In the following decade, 1965 to 1975, a great variety of semi-submersible platform configurations was designed and constructed. The number of columns could vary from three (the famous Sedco 135 type) to twenty or more, the lower hull consisted either of two or more parallel floaters or individual footings under each column. Structural integrity was generally provided by means of numerous horizontal, inclined and vertical braces.

A number of typical platform configurations are shown in Fig.1 (from ref.[6]). The early

structures were built up from individual columns and footings, kept together by means of a complex configuration of bracings and deck beams. The motion behaviour of these platforms is excellent, often better than that of two floater type platforms with a larger displacement. A disadvantage of these designs however is the poor towing characteristics: even with powerful tugs the speed is limited to a few knots. Another drawback is the difficulty in achieving a fully redundant structure, a requirement of most Classification Societies after the capsizing of the 'Alexander Kielland' in 1980 due to failure, initiated by a fatigue crack in a butt weld, of one of the bracings.

In later years, from about 1980 to present times, the design of exploration semi-submersibles conversed to more or less one type: two parallel floaters, a small number of columns (four or six) and as less braces as possible. The deck of modern designs almost invariably is built up from stiffened plate panels instead of box girders on which separate deck houses are supported. It is noteworthy that already in 1965 a modern looking type of semi-sub was designed (but unfortunately never built) for the Mohole drilling project, a research effort to investigate the layers of the crust of the earth underneath the ocean, and not intended to search for hydrocarbons (see McClure, [2]).

At present there are about 250 semi-submersible platforms in operation worldwide, of which some 180 are used as exploration drilling rigs, the remainder is deployed for production, installation, pipelaying, accomodation, general services and diving.

3. Basic data and environmental conditions.

The basic requirements needed to start the design of an exploration semi-submersible is relatively small and consists of:

Payload capability.

The payload includes all variable loads the platform carries on deck, in the columns and in the lower hulls. Also vertical components of mooring line forces, riser tension, guideline tension and drill string forces are included within this payload. Because loads at deck level decrease the stability of the platform, it is recommended that the payload be accommodated as much as possible in the lower hulls or in the columns.

Variable deck load.

The variable deck load is the payload at deck level. The variable deck load is an important item in the contract between the owner and the building yard (similar to the deadweight for a conventional ship).

Deck carrying capability.

The deck carrying capability can be defined as the amount of fixed equipment at deck level plus the variable deck load It should not be confused with the variable deck load or the payload capability as defined above. For a given platform the deck carrying capability is limited by the minimum required hydrostatic stability. The deck carrying capability is of utmost importance to the designer, because it determines to a great extent the size of the platform. Whereas the variable deck load is generally fixed during the whole design stage, the weight of fixed equipment is often not known in the early stages of the design because the amount of equipment, machinery and its make is not fixed yet. In most cases the designer has to make estimates for this part of the deck carrying capability, based on previous experience, brochures etc.

Number of crew.

The number of crew determines size and weight of the accommodation and safety equipment.

Heave response.

In most cases the minimum natural period for heave is specified, as well as the significant heave amplitude in maximum operational conditions. Heave requirements strongly effect the overall dimensions and operational draught of the design.

Mobility.

The mobility is generally specified as the sailing speed which can be obtained under own power during tow with a given bollard pull capacity of tugs. It influences the shape of the pontoons.

Operational water depth.

The maximum operational water depth determines to a great extent the type (chain, wire rope, combination of both, number of lines) and size (length of line, diameter) of the mooring equipment.

Environmental conditions.

Environmental conditions include wind velocity, wave height and period, current, maximum and minimum temperature. The wind, wave and current are often specified both for maximum operational conditions and for survival condition. The wind velocity is meaningful only when the averaging period is given (e.g. 3 seconds (for gust), 10 minutes or one hour). The wave condition can either be specified as a wave spectrum, with significant height and mean period (sometimes even the spectral shape is given), or as a maximum height and associated period. In most cases an exploration platform will be designed to operate worldwide, which means that the conditions prevailing in the most severe area of the world are governing.

The above items can be considered as minimum 'owners requirements', but of course other constraints, requirements or conditions can be posed, these may include for instance:

- Maximum overall dimensions and/or maximum draught.
- The configuration of the structure and lay out of the deck equipment.
- Type of mooring system.
- Make of equipment.

It may seem like a paradox, but generally the task of the designer becomes easier when the number of requirements and constraints are increased.

4. Design objectives and main design parameters.

In this section the design objectives, their interactions and design parameters involved are discussed.

Motions in seaway.

When compared to ships, semi-submersibles have a very poor payload capability in relation to the displacement. The sole reason for the existence of semi-subs is their excellent behaviour in waves. Therefore the most important objective for the designer is to establish a good dynamic behaviour in waves, in particular the heave motion. It appears that heave is also the motion component easiest to influence by variation of platform parameters. The most important parameters in this respect are:

- Area of water plane in relation to displacement: effects the natural heave period and the cancellation point.
- Shape of the lower hulls (width/height ratio, distribution of volume along the length of the lower hull): effects both natural heave period and wave excitation.
- draught of the platform: very effective in diminishing wave excitation.
- spacing of stabilizing columns (or overall dimensions): large overall dimensions diminish wave excitation, especially in moderate sea states.

Often a high natural period for heave is sought by designers, because it is presumed that this is synonymous with optimal heave characteristics. Motion analysis learns that this is not per definition the case, in a good design the natural period is chosen close to the cancellation point.

It is obvious that the parameters effecting the motion characteristics also are strongly linked with deck carrying capacity, stability and steel weight, therefore a good balance has to be sought between the various objectives. A computer program in which dimensions and other parameters

can be changed easily and systematically and in which motion characteristics, stability, steel weight, etc, are calculated is of great use to the designer. An example of heave Response Amplitude Operators (RAO's) for different semi sub designs is shown in Fig.2 (from ref. [6]).

Because it is difficult to compare and judge the heave characteristcs directly from the RAO, the significant heave motion is calculated in a given sea state (operational, or survival, or both) and in some cases a long term distribution is determined when a wave scatter diagram of the location under consideration is available. See Fig.3 for the schematic representation of these calculations.

Airgap.

As the stability, or in other words the maximum deck carrying capacity, of a semi-submersible strongly depends on the vertical position of the deck and its equipment, it is of utmost importance to keep the airgap as low as possible. Therefore the minimum required airgap should be established in an early stage of the design, taking into account the maximum immersion of the edges of the platform in waves (note that the maximum immersion depends on the motions and does not necessarily occur at maximum wave conditions). Also static heel due to wind and trochoïdal shape of waves has to be included in the calculation.

In many cases semi-submersible platforms have been designed to float in survival condition at a smaller draught than in operational condition. For most drilling platforms the effective gain in operational deck carrying capacity is relatively small and it is questionable if the additional risks involved like de-ballasting in severe weather are worthwhile.

Variable deck load.

The variable deck load is a major part of the deck carrying capacity as discussed above. Even more important, it is generally one of the main items in the building contract, comparable to the deadweight capacity of a ship. Therefore during the design stages the variable deck load must be monitored constantly. Each additional ton of steel weight at deck level or fixed equipment at deck level will decrease the variable deck load with the same amount. The variable deck load capacity is directly linked with stability requirements as, at a certain draught of the platform ballast water in the pontoons can be replaced by variable deck load, thus increasing the centre of gravity, until the stability just meets the requirements. Because the variable deck load is only about 10 percent of the displacement of the platform it is obvious that semi-submersibles are very weight-sensitive.

Steel weight.

A designer will generally try to keep the steel weight as low as possible. For the platform as a whole the main incentive is to minimize initial costs, for the upper part of the platform also stability and variable deck load capability play an important role. Efforts in weight saving should therefore be concentrated in particular on the deck structure.

Major parameters related to steel weight are:

- Draught: a small draught allows for smaller plate thickness, lighter stiffening of the lower hulls and a decreased height of column. The adverse effect on motion characteristics should be kept in mind.
- Frame spacing: a small frame spacing allows for smaller plate thickness and thus reduces steel weight. Construction costs will not decrease proportionally however, due to increase in welding length.
- Support of the deck by means of a great number of braces will decrease the structural weight of the deck. Bracing connections however are fatigue-prone construction details and should be avoided as much as possible. In most modern semi-submersible designs bracings supporting the deck are avoided and the penalty for additional steel weight is accepted.
- Vertical (instead of horizontal) stiffening of columns reduces plate thickness of the columns because the main loading of the columns is in vertical direction. For the same reason stiffening of pontoons should be in longitudinal direction.

Redundancy.

After the tragic accident with the Alexander Kielland in 1980, where a simple fatigue crack in one bracing caused the break away of a complete column which was followed by the capsizing of the platform, causing the death of 123 persons, the attention of designers and structural engineers was focussed very much on structural redundancy in offshore platforms. In fact Classification Societies require it is shown that the structure can withstand the fracture of a bracing or a bracing connection. In the past the redundancy was often achieved by redistribution of the loads over the remaining bracing system. In most modern designs the number of bracings is limited to a minimum and redundancy is found in the stiffened plate structure of columns and deck. Although the strength analysis of the damaged structure is generally not carried out in the preliminary design stage, the lay-out of the structure must be such that redundancy is catered for.

Mooring.

Station keeping of semi-submersible platforms is normally achieved by a spread mooring system. Sometimes the mooring system is assisted by thrusters which are primarily installed for field moves under own power. Installation of a full DP system is in principle possible and has been installed on one or two platforms, but will require an enormous power due to the heading insensibility for environmental loads, in contrast to ship shaped structures. In most cases chain is preferred for the anchor legs over steel wire rope because of ease of handling, lesser sensitivity for wear and tear and better mooring characteristics in smaller water depths. For deep water, say 300 m and more, a steel wire rope mooring system or a combination of chain and wire could be considered. In the latter case complex and expensive winches have to be installed. The number of anchor legs shall be in all cases at least 8 or 10 in order to achieve sufficient redundancy in the system. For a proper mooring analysis the environmental forces on the platform due to wind, current and wave drift have to be known as well as the (surge/sway) motion of the platform. Due to these environmental forces and due to the vertical component exerted by the mooring system on the platform there is an interaction between the platform dimensions, size and stability on one hand and the mooring system on the other hand. The interaction is relatively weak and generally disregarded in the conceptual design phase.

In these lecture notes no attention will be paid to the anchor point itself, relevant information can be found in e.g. Puech, ref. [3].

5. Platform configuration.

Although in the past an enormous variety of configurations has been developed and constructed, at present all designs of semi-submersibles for exploration are based on the two-floater type. However within this type a number of variations is possible as discussed below:

- The number of columns can be 4 or 6. The 4 column case will result in a square deck, with 6 columns the deck will have a rectangular shape. From lay-out point of view a rectangular deck is preferred. Also the unsupported length of the main deck girders is smaller in the latter case, which results in a smaller weight of the deck structure.
- The bracing configuration can vary from very simple (two horizontal bracings to absorb the split force between the pontoons) to a very complicated configuration of transverse and diagonal members which transfer all global loads on the platform. The first case results in a heavy deck structure but has the advantage that the lay-out of the deck is flexible. Another advantage is that fatigue sensitive bracing connections are avoided as much as possible.
- Pontoons may be tapered towards the ends (to improve sailing characteristics) or may be kept completely flat. The cross section of the pontoons (height to width ratio) influences the heave characteristics. Heave motions can also be affected by giving the pontoons a so called 'dogbone' shape (see the sketch of the platform "Trendsetter" in Fig.1).
- The deck structure can be built up from stiffened plates, from truss elements or a combination of these two.

6. Preliminary design calculations.

The environment to which a structure in the ocean is subjected to, is of a stochastic nature, and so are some aspects and processes in the construction, operation, maintenance and repair as well. These stochastic aspects therefore should ideally be reflected in the design of a platform from the early stage on. However this is often not possible: one important reason in this respect is that, in order to investigate probabilistic effects, a lot has to be known already about the structure and its behaviour. This means that in one way or another the designer has to come up with a fairly detailed preliminary design before expensive and time consuming analyses can be performed. It goes without saying that this preliminary design should preferably be good enough to pass the more detailed examinations instead of having to be adapted on essential points. Therefore reliable and up to date software should be available to the designer in the conceptual phase. In the last two decades abundant literature has been published on hydromechanical and structural analysis of floating offshore structures, often in the form of papers presented at conferences and symposia. In recent years the underlying theories have been compiled in a number of books, see for example Morgan [4], Patel [5] and Claus [6].
The most important design calculations to be used in the conceptual stage are reviewed below.

Motions in waves.

Hooft [7] has developed a method for the hydromechanical analysis of transparent floating structures built up from slender elements. The structure is modelled by means of simple geometrical bodies, representing columns, floaters, bracings etc. to which coefficients for added mass and (linearized) damping are attributed. It is assumed that individual elements do not influence each other, which makes it possible to calculate first order motions in waves and also to analyze overall loads in the structure. The advantage of this method, as compared to diffraction calculations, is that the modeling is simple and requires not much time, so parameter variations can be performed very fast. Oo and Miller [8] have analyzed and compared in a similar way the motion behaviour of various configurations and geometries. Van Santen (in [9]) has shown that for relatively transparent structures like most drilling semi-subs are, this method gives reliable results. For more solid structures the interaction cannot be neglected and a diffraction calculation is required. In contradiction to the case of moored tankers, slowly varying drift forces do not play an important role in the mooring analysis of semi-submersible platforms. Therefore, in the conceptual design stage slowly varying drift forces are generally not taken into account.

Wind and current loads.

Forces due to wind and current are required for the analysis of the mooring system and for the stability calculations. The way in which the loads are to be calculated can be found in the Rules and Regulations of Classification Societies (see eg. [10]). For these calculations the platform is split up into a number of elements (columns, deck houses, derrick, crane boom, ...) to which a drag coefficient C_D is attributed. With known area of the element, velocity and density of air (or water in the case of current) the force on the element can be calculated. The total load is then found by summation of the loads calculated on the individual elements, if necessary taking into account shielding effects. However in the conceptual design stage the lay-out of the platform, in particular at deck level is not very well detailed and is described only in a parametric way. Consequently it should be kept in mind that the forces and overturning moments calculated are not very accurate. Because the mooring system is not very strongly related to other design aspects and because an experienced designer can estimate the stability characteristics fairly well based on the initial metacentric height only, the calculation of wind and current loads is often omitted in the conceptual design. Although this may be acceptable from practical point of view, it is not very satisfactory.

Structural strength.

The loads on the primary structure of a semi-submersible can be split up in local loads (e.g.due to water pressure) and overall loads (see e.g. DnV [10]). Because the overall loads can only be determined when the structure is known, the first estimate of primary scantlings is based on

local loads only, in which case the permissible stress is kept low in order to allow additional stresses due to overall loading. In DnV regulations, ref.[10], guidance is given on the calculation of plate thickness and sectional modulus of stiffeners and girders. Main parameters are the local pressure, yield point, permissible stress in relation to yield, stiffener spacing, girder span and spacing. With a small database containing stiffener properties and dimensions of web plate and flange of girders a first estimate of the scantlings of pontoons and columns can be generated. In a similar way the global structure of the deck can be generated, although here the loads are less well defined as the lay-out of the deck is not yet known.

Steel weight.

From the first estimate of scantling as explained above the steel weight of the primary structure can be deducted by summation of all elements of pontoons, columns and deck. For a realistic steel weight of the complete structure an allowance, based on statistics and/or experience of the user of the programme has to be added.

Hydrodynamic stability.

The intact and damage stability has to comply with requirements of one of the classification societies and one or more national authorities. An almost complete overview (based on 1985 regulations) of these requirements is given in Kuo [12]. Factors playing a major role in the stability calculations are the wind overturning moment (for the intact case) and size of compartments in pontoons and columns (for the damaged case). Because both factors are not accurately known in the conceptual stage of the design, often the stability is judged based on the initial metacentric height only.

Mooring analysis.

The analysis of the mooring system of a semi-submersible exploration platform is normally done in a quasi-static way. The method is described amongst others in API [13] and DnV [10] Forces from wind, current and mean wave drift are considered as static loads which result in a static displacement of the platform in the horizontal plane. The first order surge (or sway) motion is treated as an excursion around the new equilibrium. Mooring line forces are calculated as if the mooring line is at each moment of time in equilibrium. As the mooring system does not interact strongly with other design parameters, the full mooring calculation is often reduced in the conceptual design to an estimate of the vertical component of the lines (used in the weight and stability analysis) and a linearized mooring stiffness in the horizontal plane (used in the motion analysis).

7. Aspects of semi-submersible platforms for production.

In the previous section design aspects of mobile semi-submersible platforms are discussed. These platforms are relocated every few months or so, often within a limited geographical area (e.g. the British sector of the North Sea), but sometimes they have to cross oceans. This mobility of course affects the design of the platform. In the present section we will discuss the consequences for the design of a platform intended to stay on one location for several years or even its total lifetime.

Basic data.

Whereas the variable deck load is a major part of the deck carrying capacity of a drilling platform, the variable load of a production platform is very small. As a consequence the difference between operational and survival loading condition does not exist. On the other hand, the required deck carrying capacity depends strongly on the amount and type of equipment to be installed and therefore production platforms show a much larger variation in size than drilling platforms do.

As a production platform has to operate in site-specific environmental conditions, the design of the main dimensions and the mooring system can be tuned to these conditions only.

Because mobility plays a minor role for production platforms, the ground for selection of

two parallel pontoons does not exist. Often a configuration based on a square ring pontoon (with four columns) or a rectangular pontoon (with six columns) is selected instead.

Design objectives.

Instead of ensuring a required variable deck load as in case of a drilling platform, the total deck carrying capacity is one of the major items the designer has to keep track of during the design process.

The mooring system for a production platform is even more critical than for a drilling platform. In the latter case the riser will generally be disconnected in survival condition and a large offset can be tolerated.

A production platform has to stay in contact with the sub-sea wellheads under all circumstances and too large an offset can be disastrous. As a consequence it is recommended to perform a dynamic mooring calculation instead of a quasi-static one (see API [14]) and to use piled anchor point instead of retrievable (ship-type) anchors.

The configuration of modern semi-submersible production platform designs differs considerably from mobile units, and is in almost all cases based on a pontoon consisting of a square (or rectangular) closed ring (see Fig.4). The cross sectional shape of pontoons an columns can vary from circular to square. The choice mainly depends on consideration related to production as from hydrodynamic point of view differences are relatively small (although when drag forces play an important role, for instance in case of high current velocity the consequences for the mooring system should be taken into account.

8. Systematic investigation into effects of parameter variations.

Until recently most engineering companies involved in the design and analysis of semi-submersible platforms used separate programmes for the various design calculations mentioned in the previous section, each with their own input. As a consequence a systematic variation of one or more parameters in the design required a lot of time when one wanted to keep track of all relevant aspects. By building a shell around the various application programmes which provides the required input for each programme from one data set, which can easily be varied systematically,it becomes possible to generate in a short period of time a great number of alternative designs. In this way a 'design space' can be generated and by introducing boundaries to the results of the calculations and rejection of designs which do not comply with the boundaries a number of 'acceptable' designs is left over. From these designs a good starting point for a detailed design can be derived, either by looking for an 'optimum' (for instance minimum steel weight) or by introduction of a merit function in which more than one variable is included. This procedure has been used successfully in the conceptual design of various types of ships and is generally known as Concept Exploration Model (CEM). At the Delft University of Technology a CEM for semi-submersible platforms is being developed in two graduation projects.

9. References.

[1] R.J. Howe: "Offshore Mobile Drilling Units", Ocean Industry, July 1968.

[2] A.C. McClure: "Development of the Project Mohole Drilling Platform", SNAME 1965.

[3] A. Puech: "The Use of Anchors in Offshore Petroleum Operations", Gulf Publishing Company, Houston, 1984.

[4] Nina Morgan (ed.): "Marine Technology Reference Book", Butterworth & Co. Ltd., London, 1990.

[5] M.H. Patel, J.A. Witz: "Compliant Offshore Structures", Butterworth-Heinemann Ltd., Oxford, 1991.

[6] G. Claus et.al.: "Offshore Structures, Vol. 1 - Conceptual Design and Hydromechanics",

Springer Verlag, Berlin, 1992.
[7] J.P. Hooft: "Hydrodynamic Aspects of Semi-submersible Platforms", PhD Thesis, Delft University of Technology, 1972.
[8] K.M. Oo, N.S. Miller: "Semi-submersible Design - The Effect of Differing Geometries on Heaving Response and Stability", London, Transactions RINA 1976.
[9] G. van Oortmerssen (ed.): "Floating Structures and Offshore Operations", Elsevier, Amsterdam, 1987.
[10] DnV: "Rules for the Construction and Classification of Mobile Offshore Units", Hovik, Oslo, Norway 1991.
[11] DnV: "Classification Note 31.4 - Column Stabilized Units (Semi-Submersible Platforms), Hovik, Norway, 1985.
[12] C. Kuo (ed.): "Stationing and Stability of Semi-Submersibles", Graham & Trotman Ltd., London, 1986.
[13] API RP 2P: "Recommended Practice for the Analysis of Spread Mooring Systems for Floating Drilling Units", 1984
[14] API RP 2FP1: "Draft Recommended Practice for Design, Analysis, and Maintenance of Mooring for Floating Production Systems", 1991.

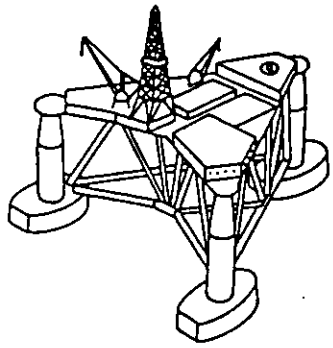

SEDCO 135 (1965)

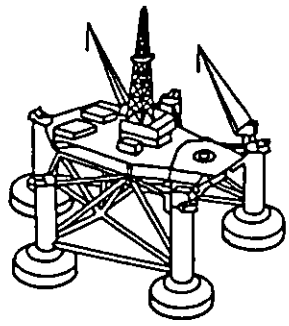

PENTAGONE (1969)

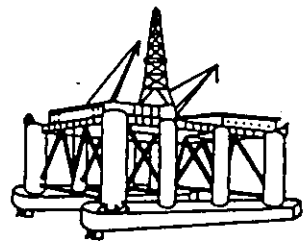

SEDCO 700 (1973)

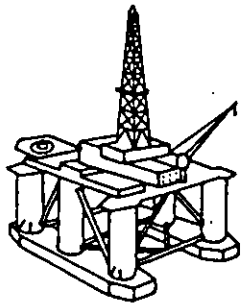

PACESETTER (1973)

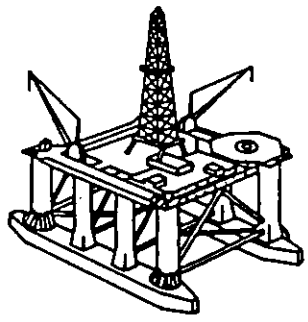

AKER H-3 (1974)

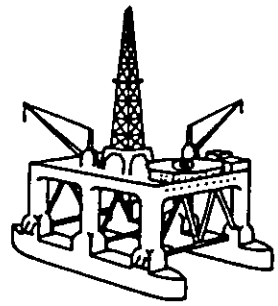

BINGO 3000 (1982)

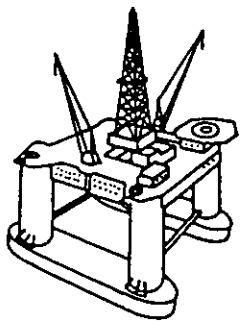

GVA 4000 (1983)

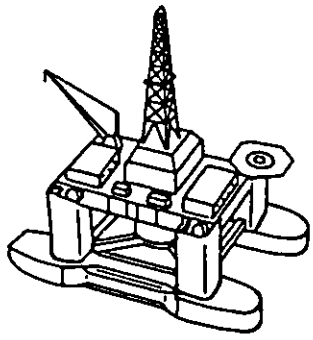

TRENDSETTER (1987)

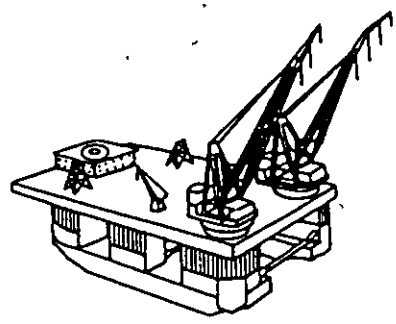

BALDER (1978)

Fig. 1 Example Semi-submersibles (From [6])

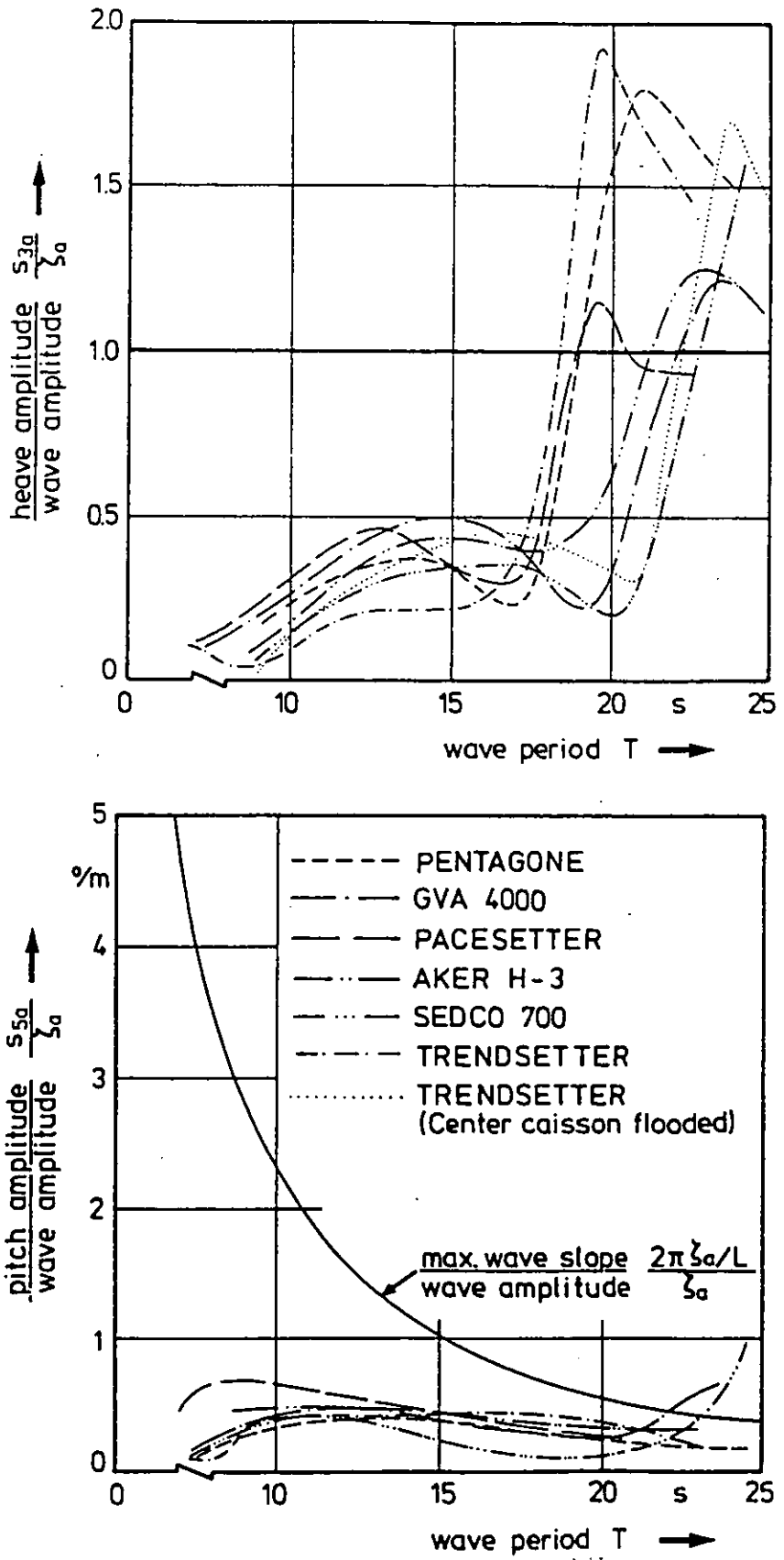

Fig.2 Heave and Pitch RAO for Semi-submersibles in Head Seas (From [6])

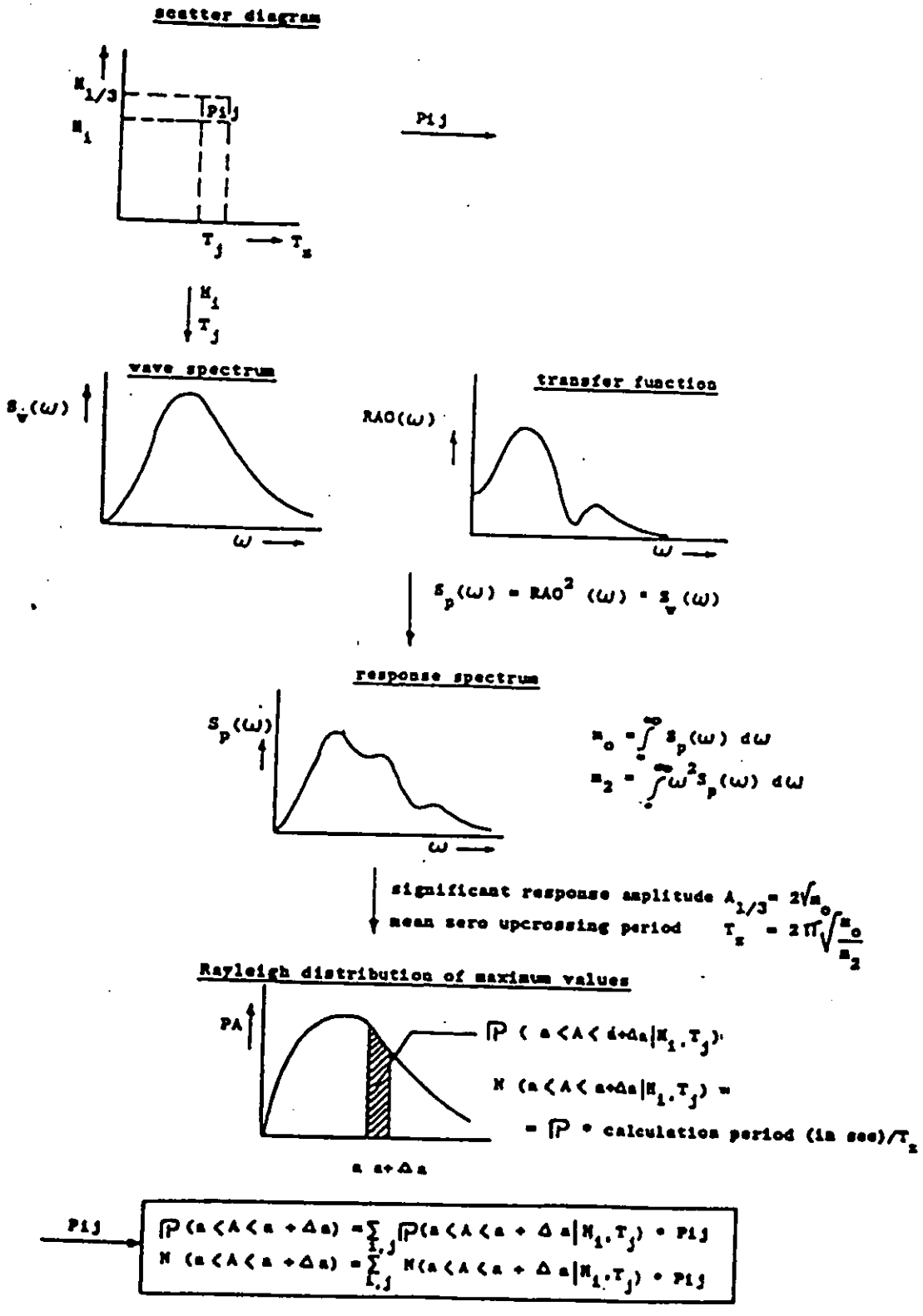

Fig.3 Short-Term and Long-Term Distribution of Wave Induced Effects

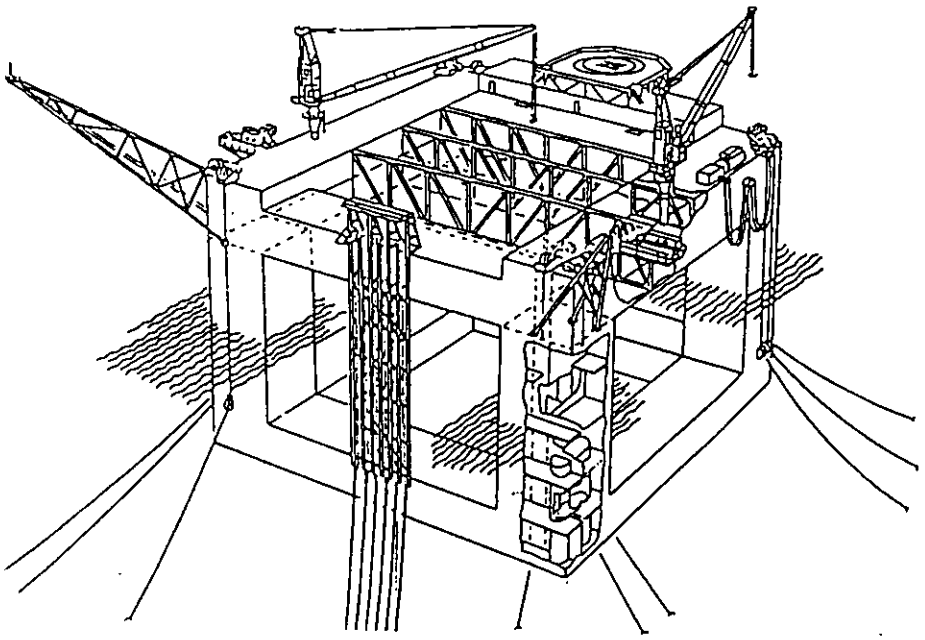

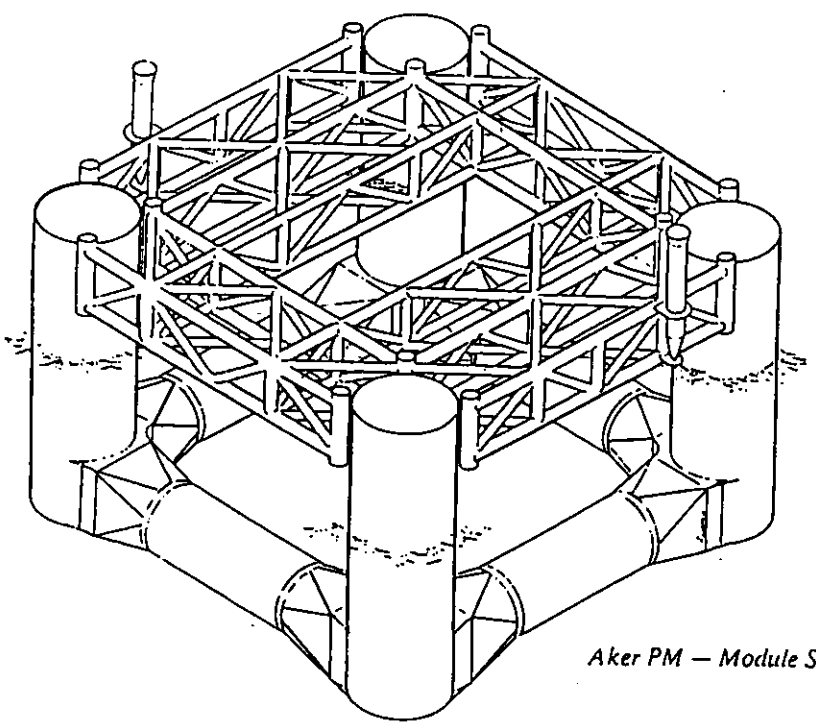

Aker PM — Module Support Deck.

Fig.4 Example Semi-submersible Platforms for Production of Hydrocarbons

LIFE-CYCLE DESIGN OF SEMI-SUBMERSIBLE PRODUCTION PLATFORMS USING PROBABILISTIC METHODS

by

HOTZE BOONSTRA

DELFT

LIFE-CYCLE DESIGN OF SEMI-SUBMERSIBLE PRODUCTION PLATFORMS USING PROBABILISTIC METHODS

H. Boonstra
Delft University of Technology
The Netherlands

Summary
This lecture is mainly based on activities and first results of the EC sponsored project "Cost Effective Life-Cycle Design of Robust Floating Structures".

This project was focused on floating structures which form the basis for production facilities for exploitation of sub-sea hydrocarbon reserves. Production systems, in contrast to exploration platforms, must remain on station for 15 to 25 years. Drydocking in this period would mean an expensive disruption of production. A high standard of reliability is thus required of floaters.

The project aims to optimize the life-cycle cost of a floater from initial design to scrapping. To this end, methods and procedures have been compiled and developed to quantify structural reliability and costs over the life-cycle.
Life-cycle cost calculations include initial cost as well as in-service costs, which are based on the estimated probability of repair.

Conventional means of assuring structural reliability are based on the use of safety margins on maximum design stresses. With the recognition of fatigue as a limiting design state, the fatigue life based on the Palmgren-Miner approach has been used in the past. This approach, however, does not allow for quantification of the risk of failure.

Reliability analysis, as developed in the project, includes determination of: internal forces and moments in response to relevant sea states; the influence matrix to convert forces and moments to stresses; long-term stress range distribution; crack growth calculation based on Paris' equation; reliability, taking into consideration inspection, repair and maintenance strategies.

The project is innovative in the sense that existing procedures are integrated into a coherent method for cost effective life-cycle design. Key procedures in the method developed have been consolidated in a prototype computer program to assist design activities.

The method developed can be applied to the design of alternative structural concepts which may be compared with designs based on conventional techniques. The ultimate objective is to be able to draw more general conclusions with regard to life-cycle design from this comparison.

1. INTRODUCTION

In the present lecture a description is given of a prototype system for the structural design of floating structures of the semi-submersible type based on satisfying not only initial design requirements but also those associated with the fabrication, installation and operational phases of the life-cycle of the structure. The system should allow for optimization of the cost of the structure over its life-cycle. For relevant literature reference is made to Chang [1], Madsen [2],[3] and Schall [4].

Because the loading on the structure due to the environment (in particular the loading due to waves) is of a stochastic nature, a realistic investigation of the results of that loading should also be based on a stochastic approach. But wave loading is not the only stochastic parameter, also aspects such as standard of fabrication, the detection of cracks during an inspection and the subsequent repair can be considered as stochastic variables.

An important aspect of the project is to use the system developed to investigate a robust but cost effective alternative design for comparison with a conventionally designed

equivalent. The method used integrates recent developments related to assessing the performance of structures during their lifetime into the design process.

The project was focused on the structural design of floaters for production of hydrocarbons, but the method could, with some modifications, be used for other types of complex structures as well.

2. FLOATERS FOR OIL AND GAS PRODUCTION

In the early days of offshore oil and gas production the interest was focused on locating and developing large fields which were easily accessible and exploitable. Today, however, new fields are often small and may be located in more remote or deeper waters. Development of new fields today requires advanced technology to overcome the difficulties of working in deep water and flexible production facilities which can be deployed elsewhere when fields are depleted. Furthermore, cost effective means of exploitation are needed for operations to be profitable at all. This requirement leads to a demand for low initial cost and high reliability to limit in-service cost. A further requirement is flexibility to accommodate different types of production equipment and ease of conversion.

In short, apart from specific technical requirements, today's situation calls for a life-cycle cost effective solution. Semi-submersible based floating production units could be such a solution as they can be moved with relative ease and costs do not rise extremely with increased water depth. Floater based production units enable motion sensitive processes to be continued in all kinds of weather.

The Marcon designed Norring 4 (Figure 1) is a good example of a floater based production platform and has served as the benchmark design for this project.

In contrast to floater based drilling rigs which are drydocked regulary, production floaters should preferably remain on station for 15 to 25 years. Removal for preventive maintenance or repair is out of the question for a production floater. Inspection, maintenance and repair (IRM) must be minimized and execution at sea should be possible. This requires a robust structure and the high cost of offshore maintenance activities should be taken into consideration in the design process.

3. COST EFFECTIVE LIFE-CYCLE DESIGN OF SEMI-SUBMERSIBLE PLATFORMS

Definition

The designing of a floater comprises the preparation of a design and the compilation of sufficient evidence that the design is the best solution to meet the operator's requirements. Which design is best depends on the relative importance attached by the operator to: cost, safety, etc.

Requirements

The requirement for life-cycle cost effectiveness is generally implicit in specific requirements. Classification Rules, for example, contain numerous provisions to ensure that a unit remains in operation for a reasonable period.

Operators pay attention to areas such as, e.g., corrosion protection and quality control during construction. Such matters are stressed, at a cost, during newbuilding because operators believe this pays off. In other words, life-cycle costs are believed to be lower!

The above demonstrates the interest of operators in reducing life-cycle cost and also their solution, i.e. requiring measures which are deemed beneficial. This, however, leaves the designer with little choice but to comply with such a requirement rather than stimulating him to provide alternative solutions leading to a life-cycle cost effective design.

The Design Process

A design cannot be logically deduced from the requirements. Therefore, a basic design cycle, covering the design as a whole, is completed in each succeeding phase of the design process. The following subdivision in phases is generally used:

0. problem formulation,
1. concept design,

2. preliminary design,
3. final design,
4. design detailing.

Concept Design

In the concept design phase, the general configuration of the design is chosen. Rough main dimensions and general arrangement layout are also determined here. Main parameters for initial dimensioning of floaters are the following requirements:

- deck carrying capacity,
- necessary deck area,
- air-gap,
- intact metacentric height,
- natural heave period.

In this phase, specific constraints such as restricted dock width, are also taken into account.

Preliminary Design

Preliminary design is the major synthesizing phase in the design process. The design is developed and analyzed to the stage where the designer is confident that requirements can be met and risks are identified and considered acceptable. Based on the results of the previous phases, the main dimensions and other general parameters are fixed. Preliminary design precedes more detailed evaluation of motions, forces and moments and reliability.

In this phase, main dimensions and layout are refined to meet specific client wishes, to accommodate practical considerations and cater for improved characteristics such as:

- overall strength,
- motions,
- providing whole numbers of frame spaces in the width of columns and pontoons,
- spacing of bulkheads to coincide with frame or girder positions,
- rounding off of overall dimensions,
- etc.

Subdivision of columns and pontoons deserves special consideration to allow for damage stability requirements. Suitable positioning of bulkheads and decks in the columns can reduce the extent of flooding as a result of damage. In the pontoons, the maximum size of compartments is limited by damage stability considerations.

Construction details, such as spacing of frames and girders, have a distinct influence on main dimensions. This influence is related to design aspects such as structural weight and initial costs. This influence must be evaluated and final values chosen before proceeding to the detailed design. By implication, determination of local scantlings, weight and cost estimates are part of the preliminary design stage.

Main dimensions and structural configuration also influence the presence and significance of local stress concentrations in the construction. A principle solution must be defined to accommodate the effects of such local stress concentration.

Final Design and Design Detailing

These phases are concerned with more thorough validation of the general design as well as design of components of the structure. This project does not cover these phases.

Cost Effective Life-Cycle Design

In the course of the project it was established that initial life-cycle cost considerations should be addressed in the preliminary design phase of the design process. In this phase, configurations are fixed which influence future as well as initial costs of the floater. It must be admitted, however, that attention to fatigue friendly design aspects at a lower level of detail can have a profound effect on in-service costs. The same applies to the quality of the fabrication work.

Evidence

Designers today cannot easily demonstrate life-cycle cost effectiveness on the drawing board. This hampers evaluation of concept solutions as a major step in the design process.

There are numerous guidelines on how to design a robust construction, the assumption being that robust is life-cycle cost effective. Examples of such guidelines are: the reduction of overall stress levels, the use of the minimum number of elements in the construction (what is not there cannot go wrong), the reduction of the outside surface area (less corrosion), the avoidance of stress concentrations, etc.

Although useful in the execution of the design work such guidelines have the disadvantage of not being quantifiable. The designer cannot make a trade-off between design solutions with different features.

Design Tools

From the above it was concluded that optimization of a design for life-cycle cost effectiveness is not possible without suitable tools for quantitative evaluation of alternative design solutions. Today's methods however, do allow for qualitative assessment of design aspects influencing life-cycle cost. In this project a system has been developed to integrate life-cycle reliability of structural components with high local stress concentrations in the design process.

4. LIFE-CYCLE COST

The following general formulation of life-cycle costs is used in the project:

$$C_{life-cycle} = C_{init} + \Sigma C_{is} + C_{dem} \tag{1}$$

The various cost items are defined as follows:

$C_{life-cycle}$ life-cycle costs.

C_{init} initial costs, all costs of design, engineering, fabrication, installation, certification, etc., prior to the start of operations.

Cis in-service costs, which are all costs incurred in maintaining the floater structure in an operational condition; the nett present value of these costs is used.

C_{dem} demobilization costs, the costs associated with shut-down of production and disposal of the floater to the satisfaction of relevant authorities.

In this project, life-cycle cost effective design is only concerned with C_{init} and C_{is}. It is assumed that demobilization cost is offset by the scrap value of the floater and C_{dem} may thus be disregarded.

C_{init} is determined primarily by the general size and overall design. Provisions for improved initial reliability and reduced reliability degradation in service are assumed to have only a minor influence on overall initial cost.

Within the project C_{is} includes only structural in-service costs such as inspection for cracks and their repair. It is acknowledged that, in practice, in-service costs, even if just related to the floater and not to the production facilities, include much more than just crack detection and repair. The cost associated with, e.g., corrosion protection or maintenance of mooring integrity may well exceed the cost of structural maintenance. Structural maintenance has been chosen as the focus of the project as there is a more direct relation to the initial design. The probability of detection of cracks and the necessity to repair them are determined by the inspection policy and the reliability of the platform. This reliability is characterized by an initial level, degradation in service, and upgrading by in-service inspection and repair.

The basic formula used for in-service costs is as follows:

$$C_u = \sum [Ci(1 - Pf_i) + Cr_i * Pr_i] + Cf * \int Pf dt \quad (2)$$

Where:
Ci = cost of inspection.
Cf = cost of failure.
Cr = cost of repair.
Pf = the probability of occurrence of failure.
Pr = the probability of necessity of repair.
t = time.
The rate of interest has been taken into account in the integration of in-service costs over the lifetime of the structure. The effect is not very large when future expenditures are small as the real rate of interest, actual bank interest minus the rate of inflation, amounts to only 2% or 3%.

5. STRUCTURAL DESIGN AND RELIABILITY

In the project, as already mentioned earlier, in-service cost is related to structural maintenance only. Thus, maintenance and associated cost is assumed to be primarily influenced by the structural reliability of the floater.

Initial Structural Design

In general, the construction of a floater is sized on the basis of extreme static limit states which are assumed to be the most severe combinations of environmental conditions and unfavourable operational load distribution. The underlying assumption is that such a combination would be extremely unlikely (100 year wave), and that, if the construction could withstand that, then it would be safe in all conditions. To account for inaccuracies in calculation procedures and to allow an extra margin against failure, safety margins are applied to allowable stresses.

A similar safety margin procedure is also applied to the fatigue strength of the construction. Cumulative fatigue damage over the design lifetime of the construction is evaluated on the basis of the Palmgren-Miner approach and compared with appropriate S-N curves. Normally, the cumulative damage is not allowed to exceed 50% of the fatigue strength. The basic philosophy is to avoid fatigue damage during the in-service life of the floater.

The use of the reliability based approach for structural design is a recent development. In this approach, global structural reliability is the consequence of the response to limit states and the probability of these limit states occurrence. The load carrying capacity (strength) has a probability distribution. This distribution is the result of inaccuracies in design calculations as well as fabrication errors and statistically distributed properties of the materials used. The load is variable and can be represented by a probability density distribution. The reliability of a floater is determined by combining the probabilistic characterization of load and strength to determine the probability of failure, as discussed by Faulkner [5].

$$PF = \int F_d(x) F_c(x) dx \quad (3)$$

with:
F_d = probability density distribution of loading (or demand).
F_c = probability density distribution of strength (or capacity).
PF = probability of failure.
The probability of failure equals the probability of strength being less than the extreme load and is shown as the shaded area in Figure 2b.

In practice, scantlings of floaters are determined on the assumption of perfect prediction of both load and strength (Figure 2d). A safety margin is generally applied to

allow for inaccuracies in the predicted values. The use of this approach is incorporated in most Classification Societies' Rules.

In-Service Reliability

The reliability approach as outlined in the previous paragraph only allows determination of in-service costs due to structural failure. Even here, one would have to account for the effect that aging would have on the probability distribution of strength.

The most important phenomenon affecting in-service reliability is fatigue crack growth. This crack growth may be modelled using the Paris-Erdogan equation.

$$\frac{da}{dn}=C(\Delta K)^m \tag{4}$$

C and m are material constants. ΔK is the stress intensity factor range (K_{max}-K_{min}) at the crack tip. ΔK is influenced by the overall geometry of the joint (Y(a)) and the far field reference stress (S).

$$\Delta K=SY(a)\sqrt{\pi a} \tag{5}$$

ΔK should always be positive but a threshold value can also be applied.

$$\Delta K>\Delta K_{threshold}\geq 0 \tag{6}$$

Substitution of equation 5 into equation 4 and separating the variables leads to:

$$\frac{da}{Y(a)\sqrt{\pi a}}=C(S^m)dn \tag{7}$$

The left hand side of equation 7 forms the basis for the evaluation of the limit damage (R) by integration from initial (a_0) to critical crack size (a_c) (equation 8).

$$R=\int_{a_0}^{a_c}\frac{da}{Y(a)\sqrt{\pi a}} \tag{8}$$

The right hand side of equation 7 is integrated from the initial number of cycles (N_0) to the number of cycles at time t (N_t) for evaluation of the long-term damaging effect (L, equation 9).

$$L=\int_{N_0}^{N_t}C(S^m)dn \tag{9}$$

In the project the damaging effect is determined by two different methods. In one approach, the expectation of S^m is determined directly on the basis of higher order moments of the long-term stress range distribution. In the other approach, a Weibull fit of this distribution is used as the basis for determination of S^m.

Failure is defined as the situation where L exceeds R. If the safety margin (M) is defined as the positive difference between R and L, the probability of failure follows from equation 10. An approximate solution for P_f is determined using SYSREL software which forms part of the STRUREL software package [6].

$$Pf=Prob[R-L\leq 0]=Prob[M\leq 0] \tag{10}$$

The probability of cracks being present, being found upon inspection and the necessity to

repair them are evaluated on the basis of an event tree describing the problem.
The probability of repair and the associated cost in the case of multiple subsequent inspections is again evaluated with SYSREL software. SYSREL is basically intended for the evaluation of structural system reliability. By modelling events as system components, combined probabilities can be established. Figure 3 shows the situation for two inspections.

6. HFES SYSTEM DESCRIPTION

As part of the project, a Computer Aided Design system was developed in which life-cycle cost and reliability calculations are integrated in the design process. The system is called the "Heavy Floater Expert System" (HFES).

The HFES can be used as a design system for concept and basic design of floaters. Detailed structural design is only covered where needed for reliability assessment of fatigue sensitive joints.

In the scope of the project the application domain of the design system has been limited to one floater concept only. The modular design of the HFES, however, is suitable for extension of the application domain to other floater concepts.

HFES System Architecture

The design system is set up as a complex conglomerate of miscellaneous programs or modules, different in nature and in use. Figure 4 shows the system architecture with the integration of the various modules. All functions of the system can be accessed through the graphic user-interface.

In order to be able to incorporate designers expertise into the design system in a more structured and coherent way it was decided to use expert system technology. The object-oriented features provide powerful means for the definition and the calculation of structural design in combination with integrated algorithms for evaluation of weight and hydrostatics.

The system runs on IBM-PC compatible computers using MS-WINDOWS. Most of the geometry definition and constructional layout, as well as a number of conventional naval architectural calculations, have been implemented using the Nexpert Object expert system shell. Calculations have further been implemented in C and FORTRAN programming languages. The design information is stored both in the Nexpert Knowledge Base and in the design database. Reliability and IRM calculations have been implemented using STRUREL software developed by the University of Berlin (ref. [6]).

HFES Program Flow

The general program flow is shown in Figure 5. The following five major groups may be discerned:

1. FPS, First Pass Sizing.
2. CPD, Conventional Preliminary Design, definition of the geometry, determination of scantlings, conventional design calculations.
3. LTSRD, determination of the long-term stress range distribution in the fatigue-sensitive locations.
4. R&IRM, determination of the reliability of the structure at local stress concentrations and the optimization of the IRM strategy and associated cost.
5. COST, determination of initial and life-cycle cost.

In FPS, the initial sizing of the floater is performed. Basically, main dimensions are determined on the basis of required deck load capacity, air gap, minimum heave period and stability.

In CPD, main dimensions are manually revised to cater for practical considerations such as ease of fabrication. On the basis of these revised main dimensions, local scantlings and naval architectural performance parameters are determined.

In LTSRD, the long-term stress range distribution at local stress concentrations is determined. It is assumed that the most critical locations, with regard to fatigue-sensitivity, occur in the column to pontoon connection. The following procedure is used (see Figure 6):

- wave loads are determined in the MOTSTRAN module,

- transformation to internal forces and moments using a simple beam model of the global structure,
- internal forces and moments are then applied to a FE model of the column to pontoon connection to determine local stresses.

This procedure is executed for waves of various frequencies and unit amplitude from three directions. In this way the stress Response Amplitude Operator (RAO) of the structure to these waves is determined.

In the subsequent module the RAO is combined with a scatter diagram and a wave spectrum to determine the long-term stress range distribution for the local stress concentrations under consideration.

In R&IRM the reliability of the construction is determined by integration of the Paris-Erdogan equation to determine the loading of the structure at a given time. This leads to a probability of occurrence of cracks of a certain size. The inspection and repair strategy is optimized with regard to cost, on the basis of the cost of inspection, and probability and cost of repair as well as of failure. The procedure has been worked out for upto three inspections over the lifetime of the structure.

In COST, initial and life-cycle cost are determined. Initial cost follows equation 2, presented earlier. Fabrication manhours are determined in a separate fabrication module in which welding and assembly hours are determined on the basis of the construction layout. In-service costs follow from R&IRM.

To date, the final evaluation of the cost effectiveness is still performed manually. The reliability calculation only applies to the column to pontoon connection. While important for structural integrity of the floater as a whole, the floater design cannot be said to be optimized if only the design of this part is covered.

7. FURTHER USE OF THE PROGRAMME

An integrated prototype computer aided design system has been developed for cost effective life-cycle design of floating structures. Structural reliability calculations and determination of associated IRM cost are presently confined to the column to pontoon connection.

Possible options which might be investigated to test their life-cycle effectiveness are the following:

1. Material Quality.
   Use of material with higher yield strength will decrease the steel weight of the platform, but because the fatigue properties of welded steel do not improve when material of a higher yield strength is used, costs of inspection and repair may well be increased. It is proposed to test the effectiveness of high tensile steel, yield strength 360 N/mm², against the original Norring 4 material choice, yield strength 270 N/mm².
2. Frame Spacing.
   The choice of frame spacing influences structural weight and fabrication cost as well as fatigue reliability. The life-cycle cost consequences of frame spacings ±150 mm as compared to the Norring 4 frame spacing of 750 mm may be investigated.
3. Alternative concepts for the column to pontoon connection may also be investigated. Some alternative concepts [7] are shown in Figure 7.
4. Optimization of the inspection schedule during the life time of a structure and selection of the most appropriate methods of inspection.

8. ACKNOWLEDGEMENT

This lecture is based on the first results of the project "Cost Effective Life-Cycle Design of Robust Floating Structures". The project was supported by a development credit from the European Community (EC), under project number TH-88-3284. The project started in September 1990 and was completed in August 1992.

The project was carried out as a joint venture by Marcon Engineering B.V., Leiden, The Netherlands; Nederlandse Verenigde Scheepsbouw Bureaus B.V., The Hague, The

Netherlands; Registro Italiano Navale, Genoa, Italy; Germanischer Lloyd, Hamburg, Germany; and the Delft University of Technology, Delft, The Netherlands.

References:

1. Chang, Pin Yu: "A State-of-the-Art Review of the Reliability Approach and Methodology for the Design of Aerospace and Ocean Systems", Marine Technology, September 1990.
2. Madsen, H.O. et. al.: "Methods of Structural Safety", Prentice-Hall Inc., Englwood Cliffs, New Jersey, 1986.
3. Madsen H.O. et. al.: "Optimal Inspection Planning for Fatigue Damage of Offshore Structures", ICOSSAR89, San Fransisco, 1989.
4. Schall G. et. al.:"Fatigue Reliability Investigation for Marine Structures Using a Response Surface Method", OMAE-91-1266
5. Faulkner D.: "Semi-Probabilistic Approach to the Design of Marine Structures", Extreme Loads Response Symposium, 1981.
6. Comrel-ti, Componental Reliability Analysis: Time Invariant Case, User Manual. RCP Gmbh, Munchen, Germany.
7. Structural Design of the Column to Pontoon and the Column to Deck Connection of a Semi-Submersible Production Platform, 2nd. interim report of graduation thesis project (in Dutch), I.D. Aryawan, 27 April 1992.

Symbols Used:

a	Crack size.
a_o	Initial crack size.
a_c	Critical crack size.
C	Material constant in the Paris equation.
C_{dem}	Demobilization cost.
Cf	Cost of failure.
Ci	Cost of inspection.
C_{init}	Initial cost.
C_{is}	In-service cost.
$C_{life\text{-}cycle}$	Life-cycle cost.
Cr	Cost of repair.
ΔK	Stress intensity factor range (K_{max}-K_{min}) at the crack tip.
L	Long-term damaging effect.
m	Material constant in the Paris equation.
M	Safety margin (R-L).
N	Total number of inspections during the lifetime.
n	The inspection number, i.e. the 1st, 2nd, 3rd, etc.
Pf	The probability of occurrence of failure.
Pr	The probability of necessity of repair.
R	Limit damage.
S	Far field reference stress.
t	Time.
$Y(a)$	Joint geometry function.

List of Abbreviations:

CEC	Commission of the European Communities.
COMREL	Component Reliability, commercial reliability software.
COST	Module for determination of initial and life-cycle cost.
CPD	Conventional Preliminary Design program module.
DUT	Delft University of Technology.
FLOATER	A semi-submersible type floating structure generally used as a basis for oil and gas operations.
FPS	First Pass Sizing, concept design module of the HFES.
GL	Germanischer Lloyd.
HFES	Heavy Floater Expert System.
HFP	Heavy Floater Project, internal title for the CEC project "Cost Effective Life-Cycle Design of Robust Floating Structures".
IRM	Inspection, Repair, Maintenance.
LOGOS	Automation subsidiary of Nevesbu.
LTSRD	Module for determination of the long-term stress range distribution at local stress concentrations.
MARCON	Marcon Engineering B.V.
MOTSTRAN	Marcon in-house program for determination of motion response in waves and associated forces on the structure.
NEVESBU	Nederlandse Verenigde Scheepsbouw Bureaus (Netherlands United Shipbuilding Bureaus).
NEXPERT OBJECT	Commercial expert system development software.
R&IRM	Module for determination of the reliability of the structure in the hot spots and the optimization of the IRM strategy and associated cost.
RAO	Response Amplitude Operator, response of the structure to waves of unit amplitude.
RESDIS	Marcon in-house program for determination of the long-term stress range distribution on the basis of wave scatter diagrams and RAO.
RINA	Registro Italiano Navale.
STRUREL	Structural Reliability, commercial reliability software package.
SYSREL	System Reliability, commercial reliability software, part of STRUREL package.

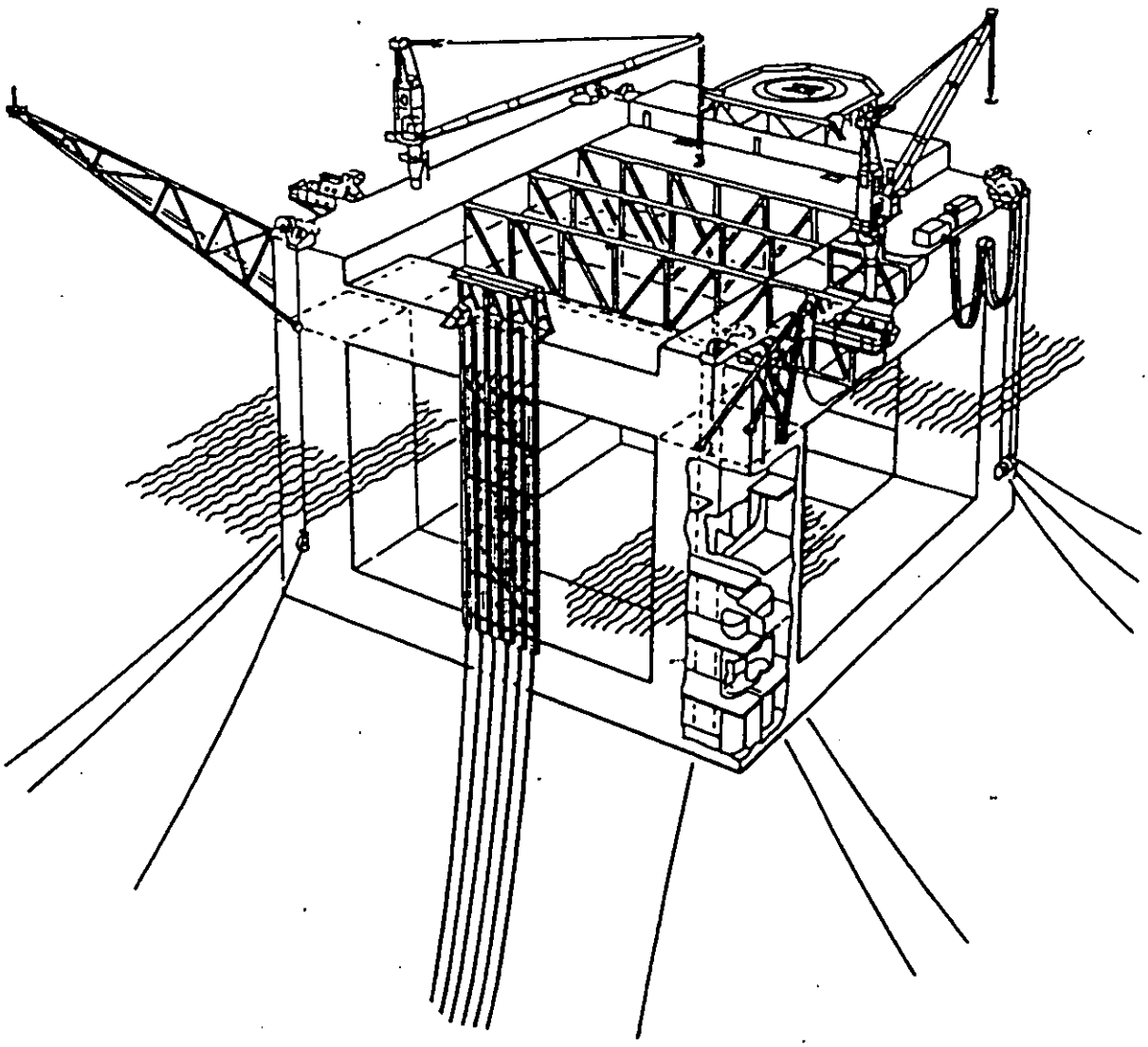

Fig. 1 Example Floating Production Platform.

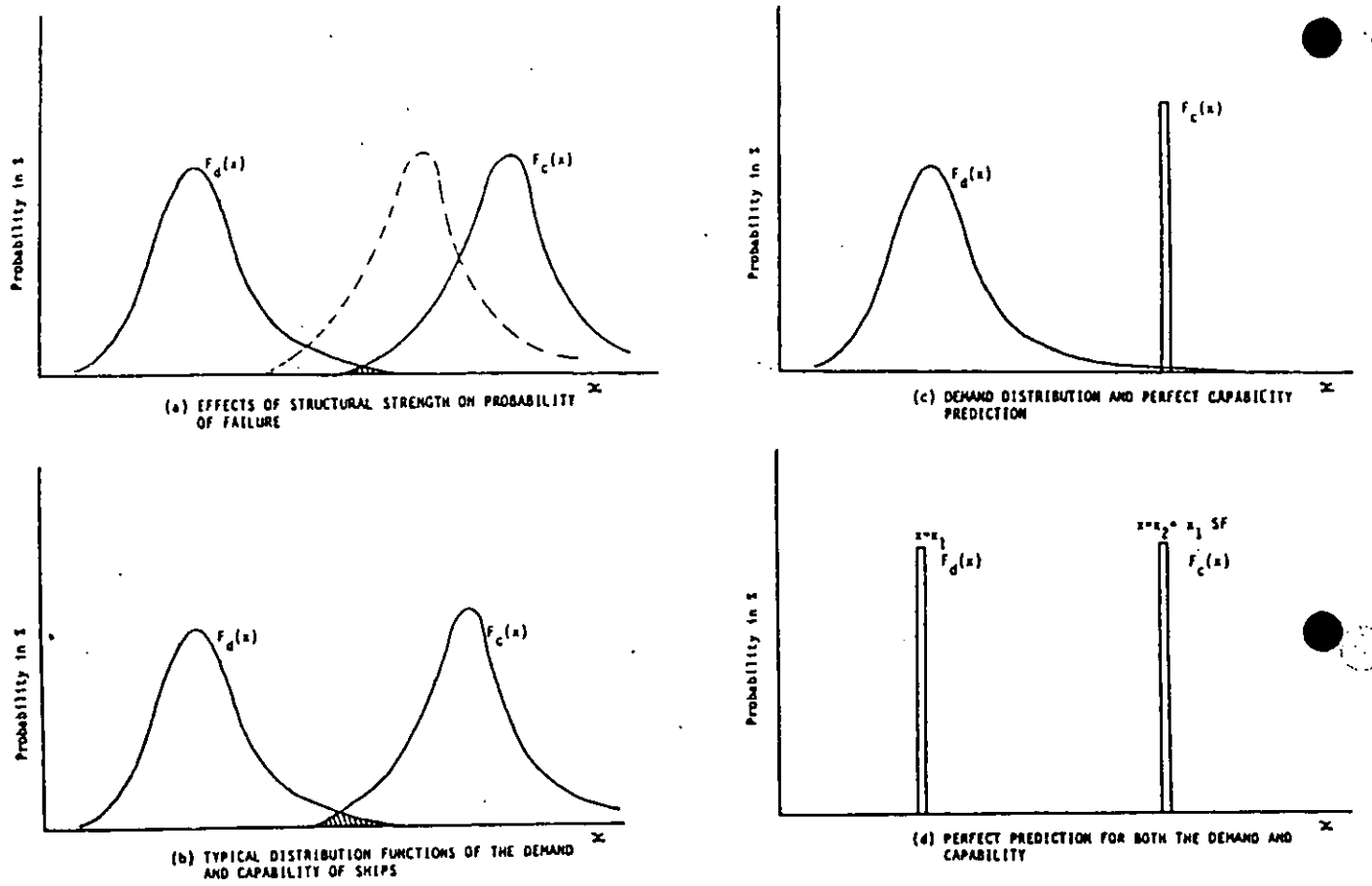

Fig. 2 Probability density function of loading and strength (from 5).

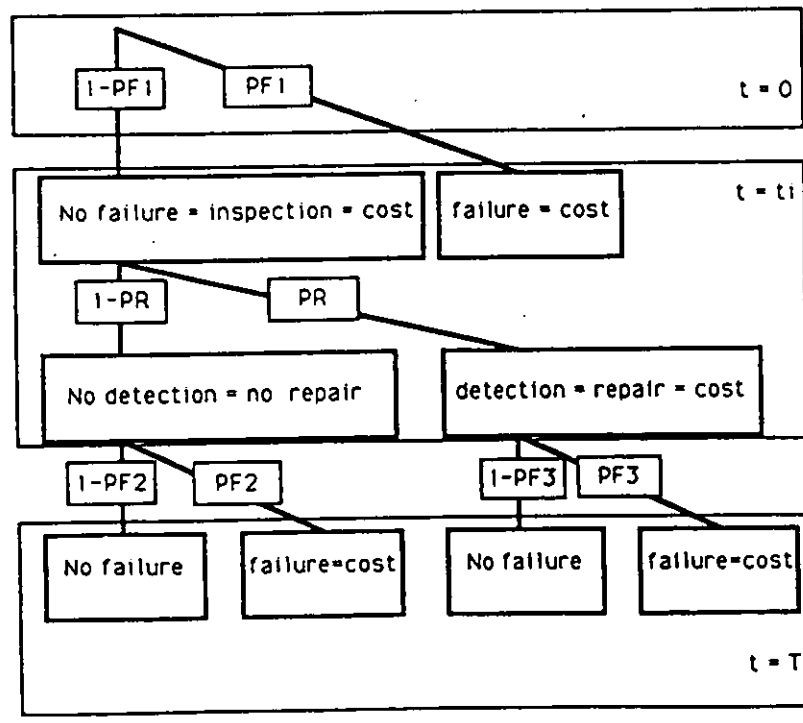

Fig. 3 Event tree for inspection and repair.

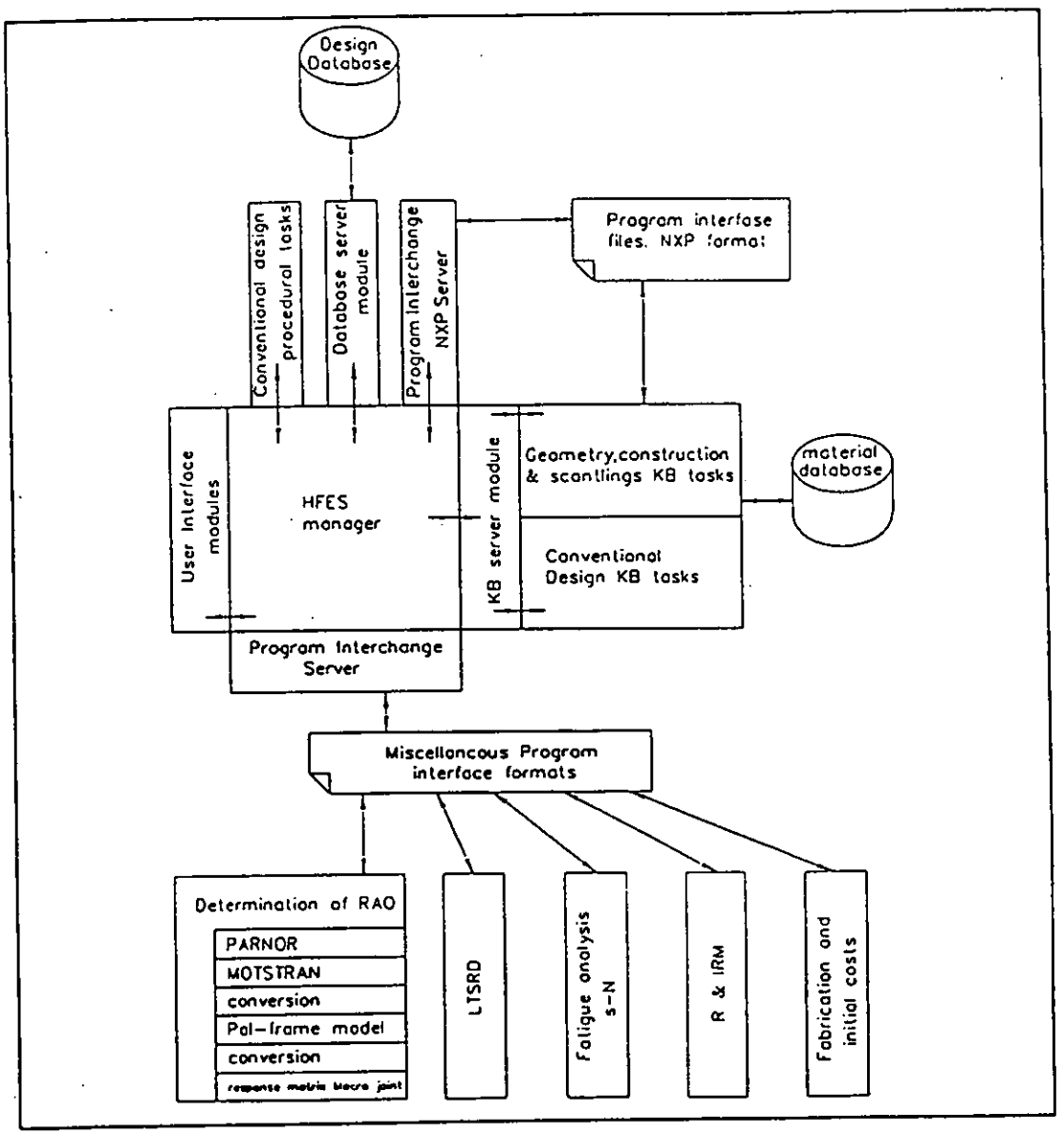

Fig. 4 System Architecture.

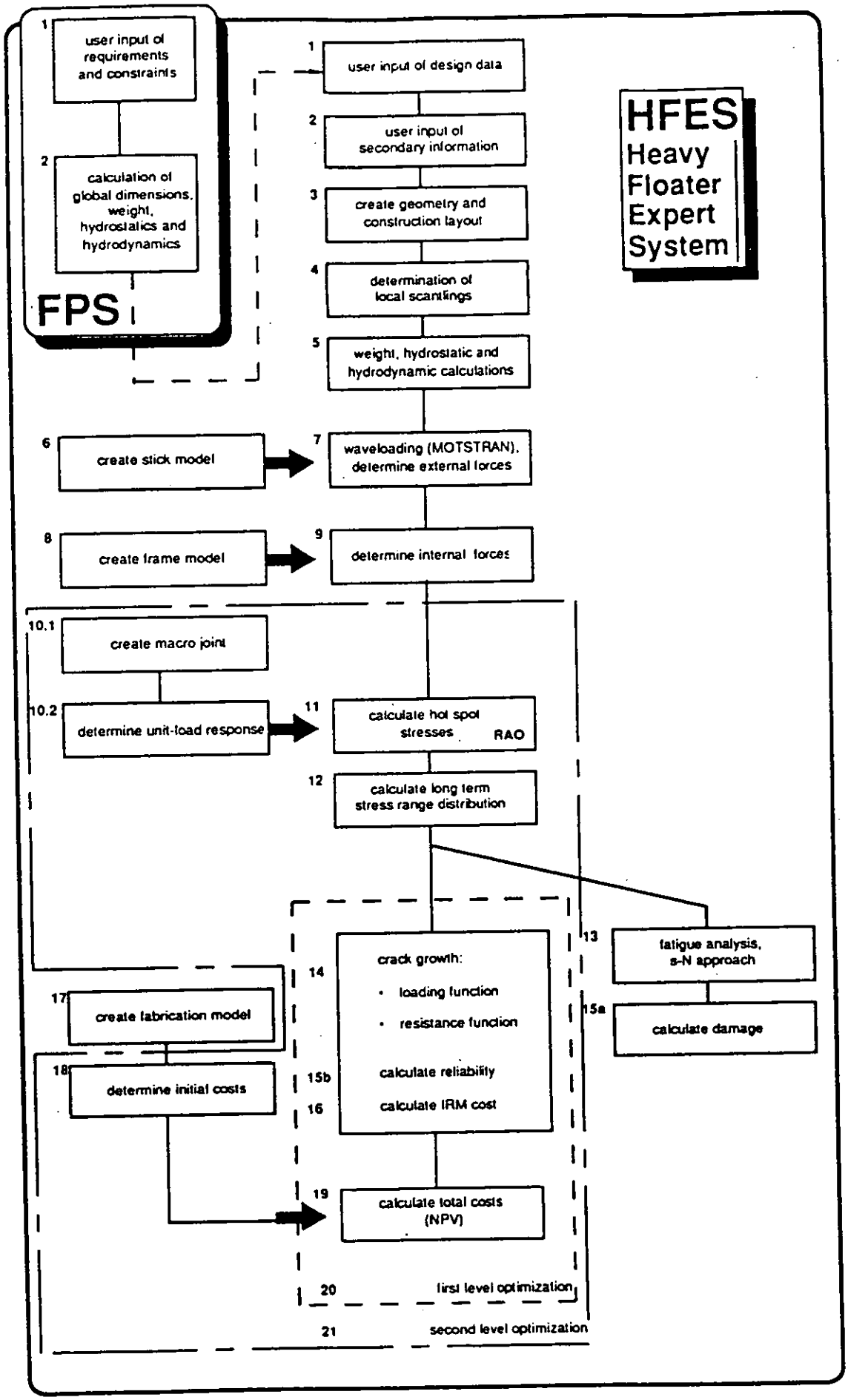

Fig. 5 Flow chart of the calculations.

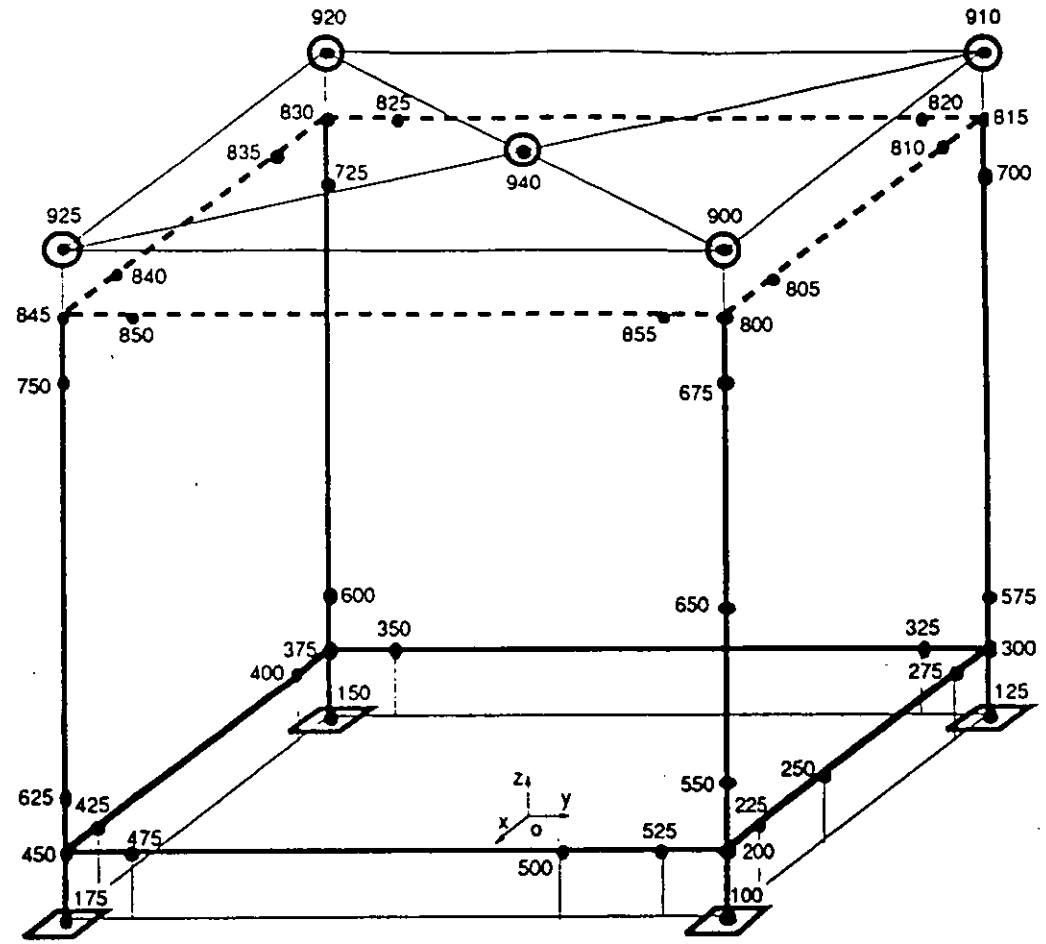

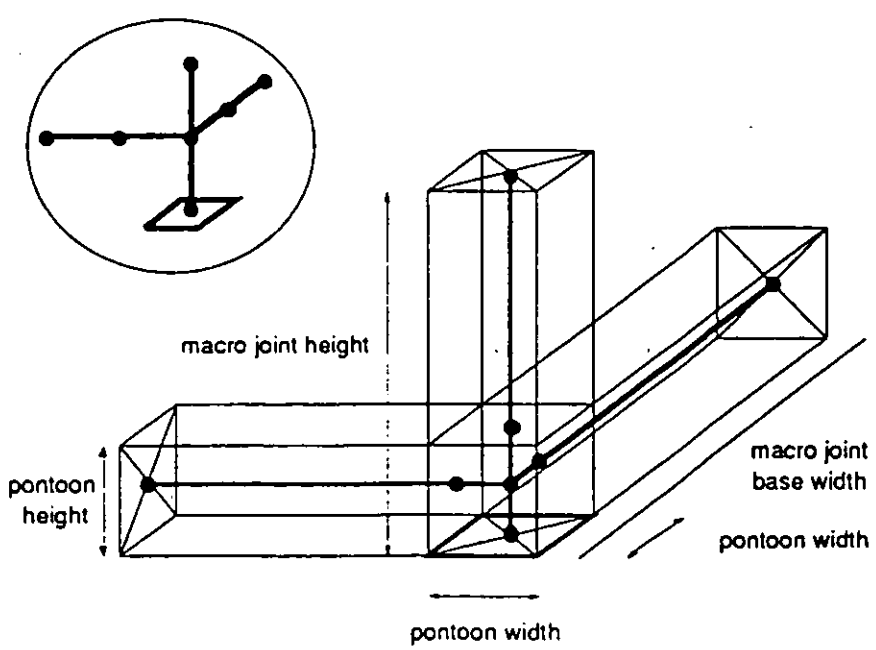

Fig. 6[a] Model for waveloading and overall structural analysis.

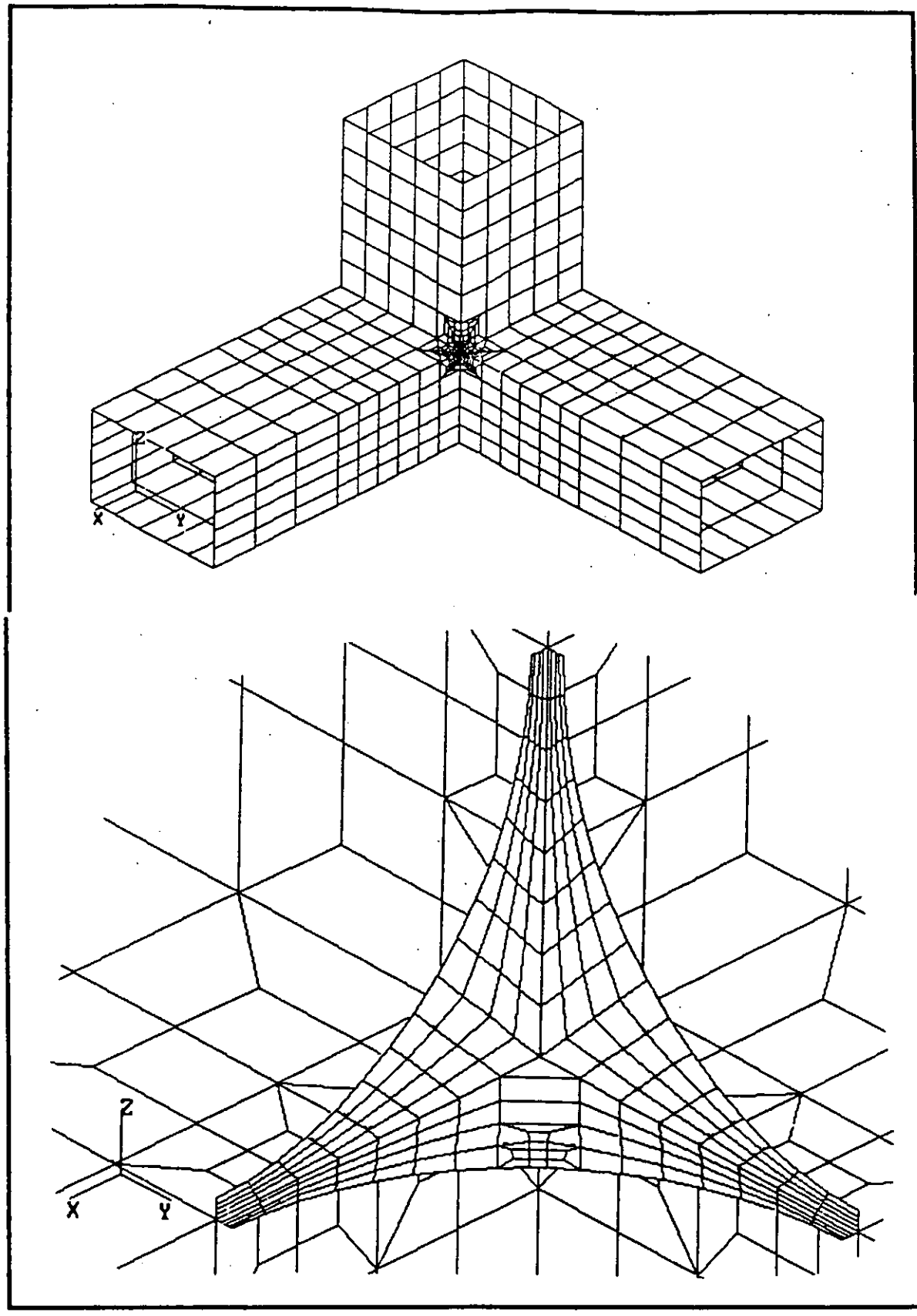

Fig. 6[b] Example of Macro-element and details.

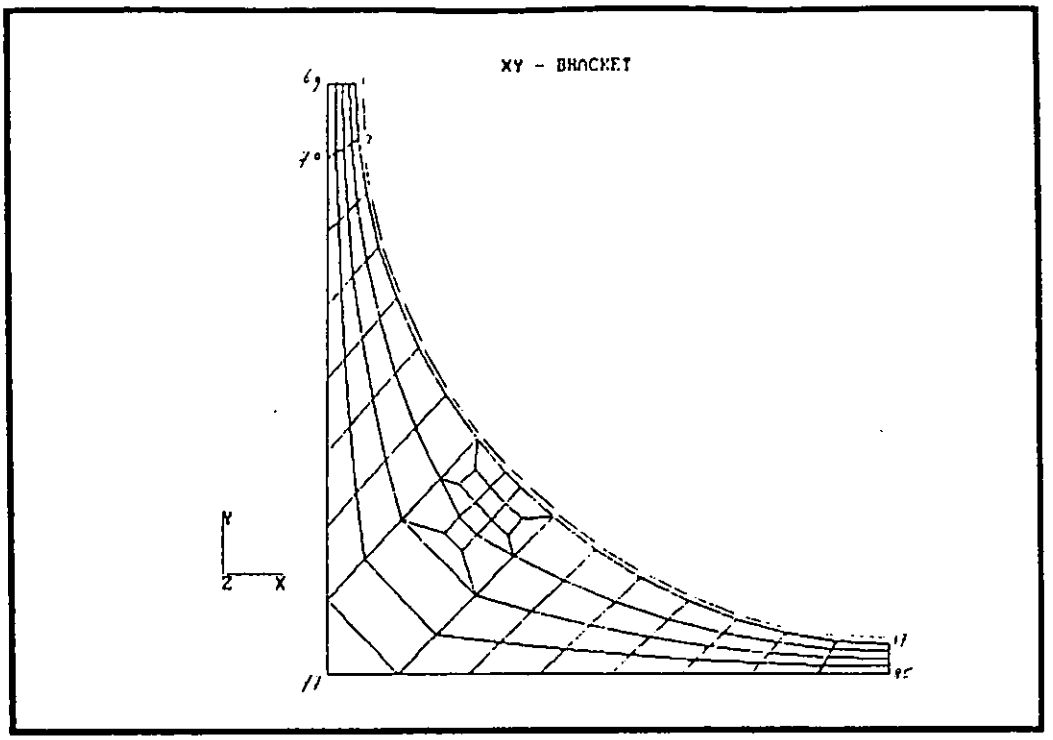

XY-bracket node 1301 – 1399

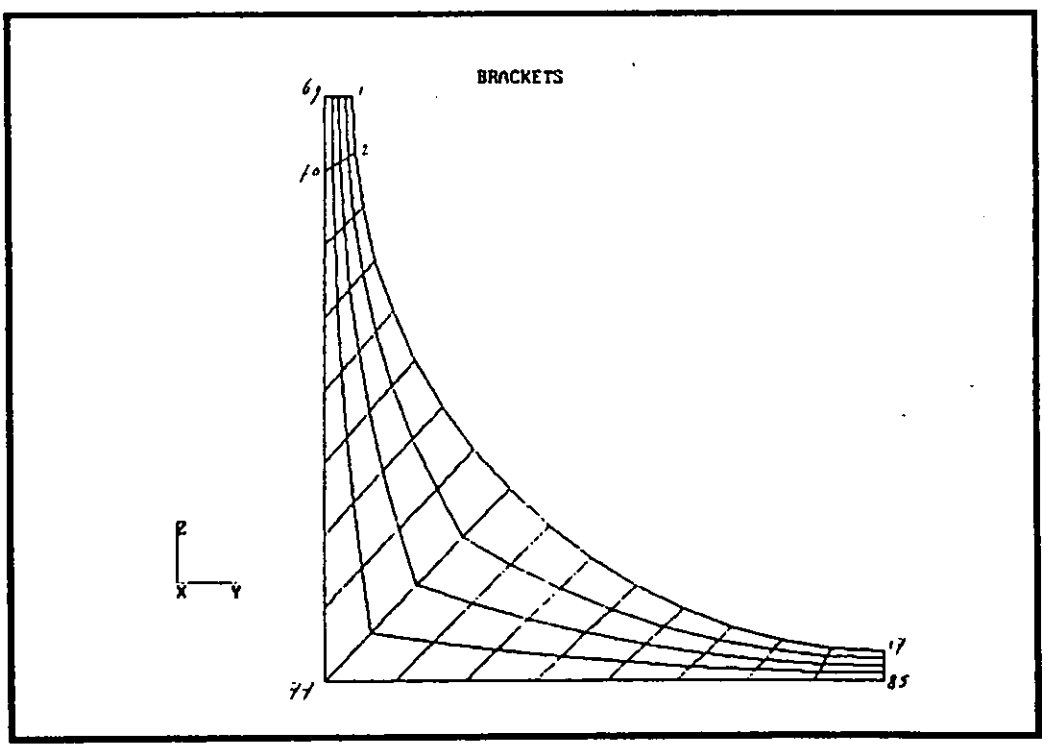

XZ-bracket node 1401 – 1485

YZ-bracket node 1501 – 1585

Fig. 6c Finite element modelling of brackets.

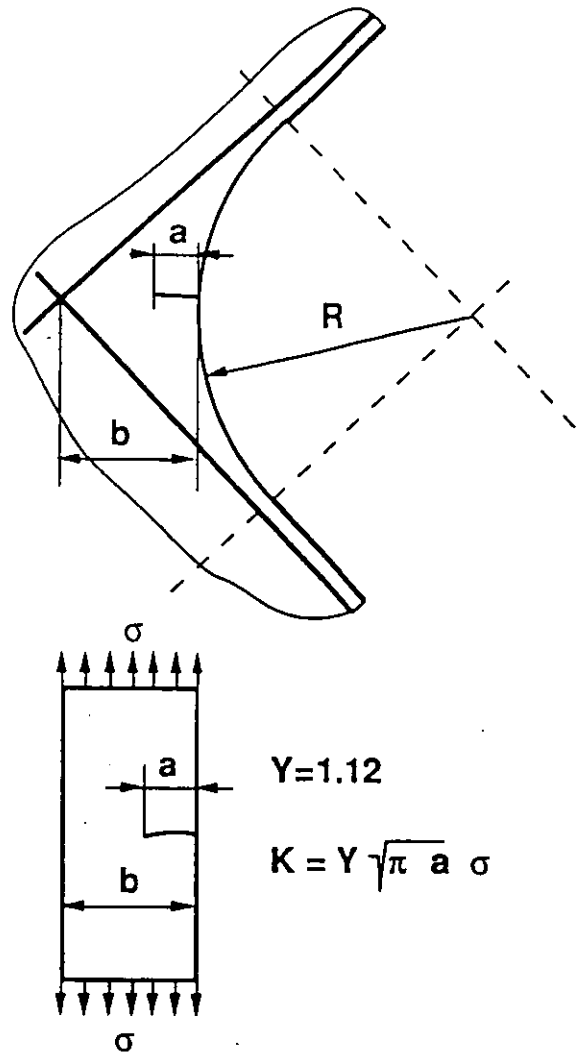

Fig. 6[d] Model for crack growth analysis.

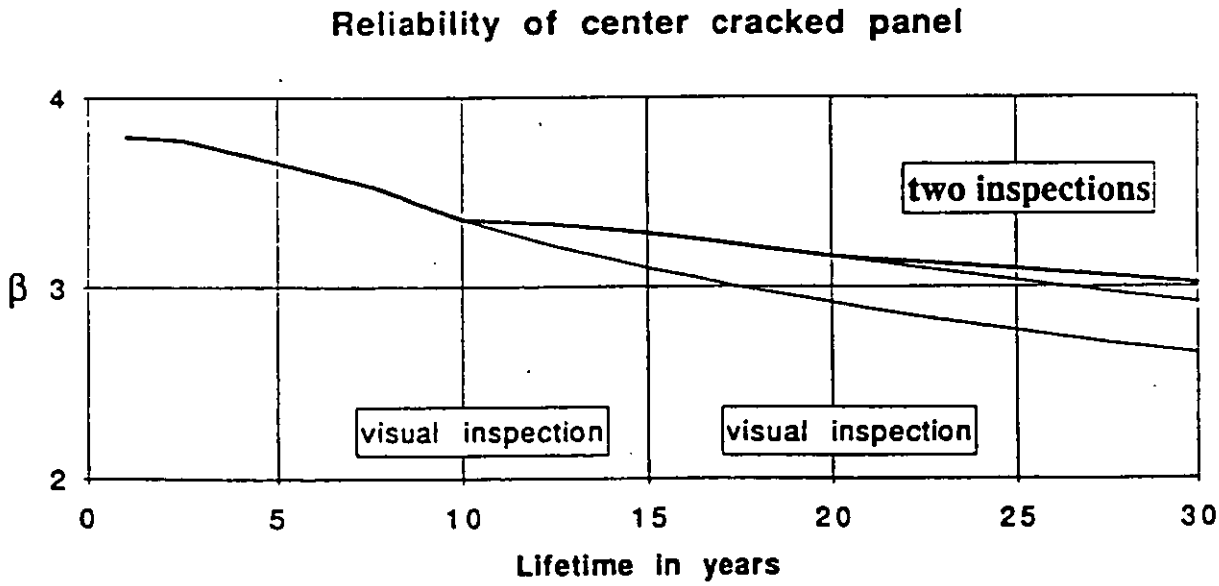

Fig. 6[e] Result of reliability analysis.

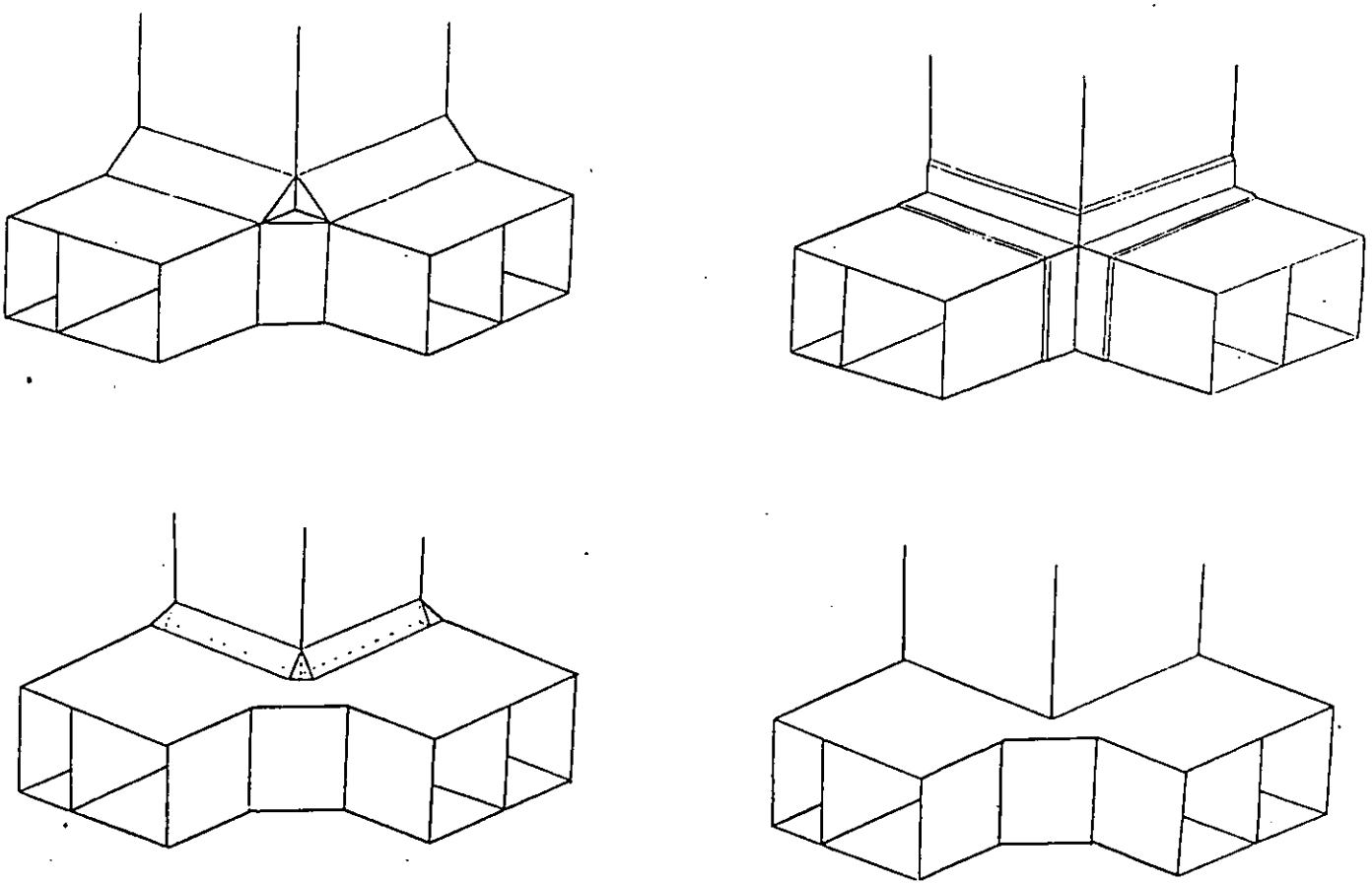

Fig. 7 Alternative concepts for connection between column and pontoon.

PRACTICAL SEAKEEPING AND STRUCTURAL DESIGN TOOLS FOR ADVANCED MARINE VEHICLES

(1) SEAKEEPING

by

NIGEL S. BARLTROP

EPSOM

Practical seakeeping and structural design tools for advanced marine vehicles: 1) Seakeeping

Purpose

Seekeeping calculations are performed:

- To check passenger comfort;
- For input to structural calculations, for which:
  - Structural acceleration loading and
  - Pressure loading are required.

The vehicle types for which this presentation is relevant are:

Displacement	Planing	Monohull
Multi-hull	SWATH	Hydrofoil

Hovercraft and Surface Effect Ships are outside the scope of this presentation.

Full problem to be solved

The equation of motion for the hull is 6 simultaneous differential equations :

$$M\ddot{x} + C\dot{x} + Kx = f(t)$$

These are in principle coupled with the Navier Stokes equation for the water:

$$\frac{Du}{Dt} = \frac{\partial u}{\partial t} + u\frac{\partial u}{\partial x} + v\frac{\partial u}{\partial y} + w\frac{\partial u}{\partial z} = -\frac{1}{\rho}\frac{\partial p}{\partial x} + \nu\left(\frac{\partial^2 u}{\partial x^2} + \frac{\partial^2 u}{\partial y^2} + \frac{\partial^2 u}{\partial z^2}\right)$$

$$\frac{Dv}{Dt} = \frac{\partial v}{\partial t} + u\frac{\partial v}{\partial x} + v\frac{\partial v}{\partial y} + w\frac{\partial v}{\partial z} = -\frac{1}{\rho}\frac{\partial p}{\partial y} + \nu\left(\frac{\partial^2 v}{\partial x^2} + \frac{\partial^2 v}{\partial y^2} + \frac{\partial^2 v}{\partial z^2}\right)$$

$$\frac{Dw}{Dt} = \frac{\partial w}{\partial t} + u\frac{\partial w}{\partial x} + v\frac{\partial w}{\partial y} + w\frac{\partial w}{\partial z} = -g - \frac{1}{\rho}\frac{\partial p}{\partial z} + \nu\left(\frac{\partial^2 w}{\partial x^2} + \frac{\partial^2 w}{\partial y^2} + \frac{\partial^2 w}{\partial z^2}\right)$$

Various boundary conditions have to be satisfied at the sea surface, hull surface and seabed.

It is unfortunately impractical to solve this full set of equations with the level of detail needed to model the small scale of the turbulence associated with the viscocity of the fluid.

In principle it is possible to make simplifying assumptions about the nature of the turbulence and to obtain solutions using a coarse finite element mesh to solve the, now approximate, Navier Stokes equation. Pressure integration over the moving hull and fin/foil surfaces couples in the rigid body hull dynamics. However the amount of numerical calculation is still inpractically large for complex 3-d problems. We therefore simplify the problem even further and simply add together various effects that in reality interact in complex non-linear ways.

Linear diffraction theory

This method is very good for large relatively slow ships. It also provides a useful insight and start for analysing fast craft operating essentially in a displacement mode.

Assume:

Small waves: *therefore almost flat water surface, small water particle velocities and no intermittent wetting of the hull surface.*
Viscocity unimportant: *therefore no drag forces*
Irrotational flow: *therefore no lift forces*
Small forward speed: *in conjunction with the small wave assumption this results in the* $0.5\rho v^2$ *pressure in Bernoulli's equation being small. This in turn results in slam and planing pressure effects being negligible.*

With the above assumptions the Navier Stokes equations given above can be simplified to Laplace's equation and the hull-water, water surface and seabed boundary conditions allow a relatively simple solution procedure of:

Laplace's equation for the water;
in conjunction with:
The rigid body hull dynamics equation.

This method is known as linear diffraction theory. For general hull shapes this is solved either using finite element or source sink methods.

Large wave calculations

As the wave heights get larger the straightforward linear diffraction theory method becomes a useful guide to the behaviour but the extra effects, described above, must be included and the shortcomings of the linear diffraction results must be taken into account.

The intermediate results of the linear diffraction analysis, particularly added mass and wave radiation damping are useful indicators of what may be expected in the non-linear behaviour. However slow speed linear diffraction results are not necessarily satisfactory in the large wave/high speed calculation.

Consider, for instance the wave pattern produced by each hull of a catamaran. At low speed the waves generated by one hull will cross to the adjacent hull and interfere with the primary wave loading effects. In contrast at high speed the wave pattern from each hull may be leaft behind and so there will be less hydrodynamic interaction between the two hulls.

Care also has to be taken when solving the six differential equations for the motion of the hull. Most conveniently the axis system for these calculations may be fixed relative to the hull. As the size of the response increases so the accelerations of the axis system become important and apparent forces such as centripetal forces become significant and must be taken into account.

With all these effects considered, and with careful use, software based on these principles can model extreme behaviour of fast craft. The technique has a broad applicability and has, for instance, also been used to track fishing boat broaching and capsize behaviour in following seas. It must however be used by experienced hydrodynamicists since great care is required in the modelling if good results are to be obtained.

Tank tests / mathematical modelling

Tank tests and model tests provide a useful means of obtaining an independent cross check for a particular analysis and also for software validation. In general it is beneficial to perform both types of modelling.

Mathematical modelling is able to provide much more detailed information than tank tests. The following examples demonstrate cases where mathematical modelling is particularly useful:

* When the response of high speed vehicles to quartering or beam seas is required. This is because the shape and size of conventional tanks means that it is not possible to determine the response to waves coming from other than the head or stern.

* Mathematical modelling is especially useful for catamaran and SWATHs when structural pressure loading is required for structural analysis purposes.

* Mathematical modelling can also provide an understanding of complicated responses that may be seen in tank tests but only speculatively explained from tank tests alone.

Case study

A linear diffraction and a large wave catamaran model will be described.

PRACTICAL SEAKEEPING AND STRUCTURAL DESIGN TOOLS FOR ADVANCED MARINE VEHICLES

(2) STRUCTURAL ANALYSIS

by

NIGEL S. BARLTROP

EPSOM

Practical seakeeping and structural design tools for advanced marine vehicles: 2) Structural Analysis

Selection of appropriate analysis method

We can select either:

a) One big Finite Element analysis or
b) Simple global analysis + local analyses

a) has the advantage of avoiding linking problems between the different levels of analysis.
b) has the advantages that:

At early stages of the design the detail is not usually settled. sing method (b) the detailed analyses can therefore easily follow on as the detail develops;

Each analysis is simpler, easier to undertake and much less dependent on the other analyses;

It is difficult in practice to refine a mesh which is suitable for a complete vessel of say 80m length down to element sizes of a few mm which may be required near complex intersection;

Repetition of details means that similar details will occur in many places. In principle substructure methods could be used to take advantage of this situation but the difficulty described in the above paragraph makes this difficult in practice;

It leads to the engineer being more aware of the structural behaviour and leads to a better understanding of the problem.

b) is therefore often a much more practical and economic route to follow. It requires more engineering judgment but also leads to the greater development of engineering judgment. However as time goes on and computers and software become more powerful the balance is constantly changing in favour of more complex global analyses.

Basic assumptions

1) Rigid/flexible body interaction with the hydrodynamic loading

For the hydrodynamic analysis the vessel can nearly always be considered as rigid body free to move in 6 degrees of freedom. This will usually also be the case for small fast craft. However if the encounter period of the waves becomes equal to a natural period of the hull structure then large springing oscillations can occur. We are not aware of any response of this sort with small high speed craft but they are important, especially for fatigue, on large, ocean going, trading vessels (bulk carriers and tankers).

2) Quasi-static structural analysis

If no structural natural periods are likely to be excited then quasi-static structural analysis is appropriate. The basic idea is that the full equation:

$$M\ddot{x} + C\dot{x} + Kx = f(t)$$

(which represents a set of N simultaneous equations, where N is the number of

degrees of freedom in the structural analysis model), does not need to be solved because the $M\ddot{x}$ forces are essentially those associated with the rigid body dynamics. Therefore instead of solving for $\ddot{x}$, it is known with sufficient accuracy at the beginning of the analyses as the global acceleration vector: $\ddot{x}_g$.

The $C\dot{x}$ forces are unimportant because the structure is not operating near a structural resonance.

It is therefore possible to replace the full equation with the quasi-static equivalent:

$$Kx = f(t) - M\ddot{x}_g$$

K is the structural stiffness matrix plus the hydrostatic stiffness matrix and sufficient additional supports to prevent rigid body motions of the hull.
M is the mass (excluding external hydrodynamic added mass)
f(t) is a loading vector including all hydrodynamic and hydrostatic pressure calculated for the undeformed hull.
$\ddot{x}_g$ is a vector of accelerations for each structural degree of freedom. It most conveniently also includes the gravity acceleration.

This equation can be solved using an ordinary static FE package.

3) Dynamic structural analysis for springing

If springing is to be taken into account, then a structural dynamic analysis is required. However the dynamics of the hull are affected by its immersion in the water. In particular:

The water resists vibratory acceleration of the hull, which can be regarded as an added mass effect (note however that care must be taken not to double count the added mass affecting the primary rigid body dynamics);

The vibrating hull generates waves which result in added damping;

The hydrostatic stiffness of the water contributes (usually only very slightly) to the overall hull girder stiffness, however this is already taken into account in the quasi-static method;

Local analysis

The details used in ship structures are commonly repeated thousands of times in any ship. Their cost therefore has a significant effect on the overall cost of the ship. However the simplest details to build tend to contain sharp right-angled corners.

These have very large stress concentrations which are difficult to calculate and to interpret. They are difficult to calculate because a finite element solution will usually give higher and higher stresses as the mesh is made smaller. This is because the stress may theoretically be infinite and the finite element solution is tending to infinity as the mesh is refined.

The significance of these high stresses varies according to the failure mode:

Fatigue

The difficulty of interpretation the high stresses is because the stress concentration is localised. When a fatigue crack is small it is completely

within the stress concentration and so will be totally affected by the SCF. As the crack grows the effect of the SCF becomes smaller. This is difficult to take into account using S-N curves but can be taken into account using fracture mechanics methods.

Cracks propagate by fatigue essentially when the local stress at the crack tip is cycling in tension. Conventionally in welded construction the assumption is made that welding residual tensile stresses will result in high mean tensions so that all stress fluctuations will propagate the cracks. Owing to the high stress concentration applied loads can shake out the residual stresses and this can sometimes be a beneficial effect.

The significance of fatigue for a design is dependent on many factors but greater care is required when dealing with high strength steels and aluminum than when working with mild steel. This is due to the ratio of yield stress to fatigue strength of the different materials.

Strength

Strength assessment is usually based on codes of practice used in conjunction with the computer predicted applied loads. Checks are required for yield and buckling. Suitable codes include DNV rules , BS5400 part 3 and API rules. Detailed stress analysis will usually predict localised high stresses which would not be found by simpler by hand calculation methods. These areas of high stress are not usually significant for strength checks and so can usually be ignored. Residual welding stresses and initial flatness imperfections need to be taken into account. These are usually taken into account by the code of practice. Self equilibriating stresses from differential temperature effects may usually be ignored.

Fracture

Fracture will be discussed in following lecture. The stresses to be taken into account are generally the same as those required for strength checks however the local high stresses, tensile welding residual stresses and other self equilibriating stresses may be important for fracture.

Case study

Some global and local analyses on ship structures will be presented and discussed.

IN SERVICE ASSESSMENT AND MAINTENANCE

by

NIGEL S. BARLTROP

EPSOM

In service assessment and maintenance

Introduction

The purpose of in service assessment and maintenance analysis is to assist with efficiently finding and repairing damage that may be detrimental to the safety or serviceability of the structure. For fixed offshore structures this involves planning the timing of the inspection of different parts of the structure. For ships this involves checking the inspection intervals required by the classification society and where necessary performing additional inspection.

The damage is likely to be caused by:

Fatigue
Corrosion } Decay with age;

Collision or other impact damage;
or:
Design deficiencies leading for example to local buckling.

Structural management

To properly plan inspections and act on the results some form of structural management system is required. The process should start at the design stage and continue through the life of the structure. Important decisions which may seem of limited importance at the design stage, eg the selection of steel toughness grade, the number of alternative load paths in a framed structure or the ease of access for inspection, can have a large effect on the amount of inspection needed to keep the structure safe during it's life. It is therefore sensible to consider inspection at the design stage.

During the life of the structure the actual defects found are a guide to the accuracy of the inspection and the actual behaviour of the structure. It is useful to interpret this information statistically in order to improve the guidance for future inspections. Stress monitoring can also be used to improve the inspection plans. When there is some control over static or dynamic stresses, as there is in a trading ship, then information from the inspections can be used to put additional limits on still water or wave bending moments. Other monitoring systems such as strain gauges and accelerometers can also be used to provide operational guidance aimed at avoiding fracture.

Damage assessment methods

Damage assessment involves analysis that can sometimes be similar to that performed at the design stage. The assessment of the effects of corrosion damage is an example. For fatigue cracks the analysis usually involves the assessment of the critical defect size for brittle fracture and the reason for the crack: Was it caused by a large initial defect or are the cyclic stresses too great? The decision can then be taken on:

* the urgency of the repair;
* whether a revised detail is desirable;
* whether more extensive examination of similar details is required;
* what the inspection plan should be for the joint in the future.

Differences between different structural types

It is worth noting that there are significant differences between different types of structure:

Offshore platforms

Redundant -

Localises fractures
Critical areas to some extent identifiable
Can use leak detection methods
Ideally requires system reliability models

Semis

Variable redundancy

Interaction with stability is important

Bulk carriers

Non-redundant

Many potentially critical areas
Corrosion and fatigue are important
Low toughness steels are used in many areas
Severe loading patterns
Inspection of side shell and deck head is difficult

Tankers

Non-redundant

Many potentially critical areas
Corrosion and fatigue are important
Low toughness steels used in some areas
Pollution is of considerable concern
Inspection of side shell is difficult

Fast ships

Light construction important
Aluminum: strong as mild steel but 1/3 fatigue strength
High toughness a useful benefit

Case studies

Some typical calculations for inspection planning of an offshore jacket structure and a tanker will be discussed.

Design to Avoid Material Failure

Prof. M.J. Cowling, Glasgow Marine Technology Centre,
Glasgow University, Glasgow, G12 8QQ

1.0 INTRODUCTION

The purpose of this lecture in an 'advanced' design course for offshore floating systems and ships is to focus attention on topics which take assessment beyond normal design codes. The reasons for doing this are to provide the tools for assessment for unusual design loads, unusual service history, economic benefits in terms of original fabrication cost or in-service inspection costs, or 'tuning' of the design to give a pre-determined level of structural integrity.

Given the time available this lecture can only deal with a limited number of topics. These are:

(i) Fatigue endurance based design.
(ii) Fracture mechanics based fatigue assessments.
(iii) Assessment for fracture.
(iv) A strategy for assessing new technology.

2.0 FATIGUE ENDURANCE BASED DESIGN

2.1 Background

With an increasing need for cost effective operation of offshore structures it is vital that inspection and maintenance planning is carried out on a rational basis with quantified benefits. Reliability analysis provides the capability to achieve such planning since it is possible to relate the failure of individual structural components to the failure of the overall structure. Maintenance planning may then be based on the target reliability required which relates to the consequences of failure. Considerable interest has been aroused in recent years into the quantifications of the effects of redundancy in offshore structures. Clearly, although adding redundant members creates additional cost at the time or original construction, the ability of the structure to tolerate damage to some individual members in service without loss of the complete structure may be a substantial benefit.

Most fatigue problems occur at connections. Hence initial fatigue design of joints in offshore structures should be carried out in accordance with the current version of the design code or certifying authority rules adopted for the specific case. When this initial assessment is complete more information may be added including:

(i) the actual failure probability
(ii) the sensitivity of the predicted life to the size of uncertainties in the input data
(iii) partial safety factors to be applied to deterministic design to achieve a target reliability
(iv) influence of redundancy
(v) system reliability
(vi) the ratios of fatigue design life to required service life

Fatigue life prediction is a particularly suitable candidate for reliability analysis since it is associated with many diverse uncertainties. These are primarily material variability and modelling uncertainty in damage summation but in fatigue analysis of offshore structures considerable uncertainty in stress range prediction can be added to this list. This arises from the compound effects of uncertainties in the magnitude of wave loading, combined with uncertainties in global stresses resulting from the real structural response and uncertainties in local stress concentrations and variations in local weld geometry. In estimating fatigue reliability the aim is to provide a tool, which will enable the user to arrange potential fatigue failure sites in order of increasing reliability and thereby provide a programme for inspection and repair.

2.2 Advanced Level II Method of Reliability Analysis

Reliability can be calculated by the advanced Level II method of analysis. The accuracy of this method has been proved[1] to be adequate for most purposes and reference[2] describes it in detail.

The outcome of the analysis is the solution for the safety index β and the probability of failure may then be obtained from

$$Pf = \Phi(-\beta)$$

where Φ represents the normal distribution function.

The Level II reliability evaluation procedure is readily carried out with significant computational facilities. However a hand calculation method is appropriate for quick calculations. Considering only one regime the failure function can be derived from Miner's sum and the S-N curve as

$$Z = 1 - \frac{NS^3}{AD} \tag{1}$$

Clearly failure will happen when the last part in Eq.(1) is greater than unity, i.e.,

$$L = \frac{NS^3}{AD} > 1 \tag{2}$$

Since distributions of fatigue capacity A, Miner's sum D and stress range S are often found to be lognormal, the distribution of variable L is also lognormal. This probability can be obtained by[3]

$$Pf\,(L > 1) = \Phi\,(\ln(1/m_L) / \sigma_{\ln L}) \tag{3}$$

where Φ is the widely tabulated Normal distribution function, m_L is median of random variable L and $\sigma_{\ln L}$ is the standard deviation of the lognormal distribution of L. Meanwhile for the Normal distribution the failure probability can also be expressed as

$$1 - Pf = \Phi(\beta)$$

where β is the safety index. Thus

$$Pf = 1 - \Phi(\beta) = \Phi(-\beta) \tag{4}$$

Comparing Eq.(3) with Eq.(4), we have

$$\beta = \ln(m_L) / \sigma_{\ln L} \tag{5}$$

where

$$m_L = (m_A\, m_D) / (N\, m_{S^3}) \tag{6}$$

and

$$\sigma_{\ln L}^2 = \ln (V_L^2 - 1) \qquad (7)$$

$$V_L^2 = (V_A^2 + 1)(V_D^2 + 1)(V_S^2 + 1)^9 - 1$$

in which V_A, V_D and V_S are coefficients of variation of the lognormal distribution of fatigue capacity A, Miner's sum D and stress range S, respectively.

Since design stress ranges often fall into the regime of m = 5, the influence of this regime should be included. In this case variable L in Eq.(2) can expressed as

$$L = \frac{1}{L_1 + L_2} = \frac{1}{\dfrac{N_1 S_1^3}{A_1 D} + \dfrac{N_2 S_2^5}{A_2 D}} \qquad (8)$$

where subscripts correspond to different regimes. The distribution of variable L here is no longer lognormal although L_1 and L_2 are still lognormal. The probability that variable L is less than unity cannot be simply given by Eq.(3) in principle. As an approximate estimate Eq.(3) is used here but the median of variable L is substituted by

$$m_L = \frac{1}{\dfrac{N_1 m_{S_1}^3}{m_{A_1} m_D} + \dfrac{N_2 m_{S_2}^5}{m_{A_2} m_D}} \qquad (9)$$

and the standard deviation is taken as

$$\sigma_{\ln L}^2 = (\sigma_{\ln L_1}^2 + \sigma_{\ln L_2}^2) / 2.4 \qquad (10)$$

where $\sigma_{\ln L_1}$ and $\sigma_{\ln L_2}$ are derived as in Eq.(7).

2.3 Uncertainties and Sensitivities

In examining the effects of changes in input parameters it is important to distinguish between (i) changes in mean values of input data, often used to examine deterministic sensitivity of calculated values to the input data, and (ii) changes in the degree of uncertainty associated with input variables which affect the reliability of a calculated value (i.e. design life).

Given the wide range of factors which combine to give the nominal stress at a point in an offshore structure, and the sensitivity to both mean value of stress and the sensitivity to the uncertainty in stress it is preferable to examine these sensitivities on a typical structure. This forms the basis of the results presented here which are given to draw the attention of fatigue designers to typical and relevant aspects of the design calculations.

2.3.1 Sensitivity to Changes in Mean Values

For a typical offshore structure the sensitivity, in terms of changes to calculated stress levels, as a result of changes in assumed wave height, SCF, thickness of marine fouling, current velocity, C_D and C_M are shown in Figure 1. Table 1 gives a summary of these relative results and compares them with another study using a different structural configuration.

2.3.2 Sensitivity to Changes in Uncertainties

In examining the effects of changes in uncertainties it is important to appreciate the extent of uncertainties associated with particular variables. Table 2 provides a summary of values from the literature and used in the background studies to this document. Figure 2 shows the overall relative sensitivities for splash zone and subsea portions of a typical structure.

2.4 Target Reliability

2.4.1 Philosophy

In probabilistic design the engineer should be able to show that a joint meets some specified minimum target reliability. The target safety index, β_T related to reliability $\mathbf{R}$ by $\beta_T = \Phi^{-1}(\mathbf{R})$ is considered in this section.

Factors which should influence the choice of target reliability are:

1. human, environmental and economic consequences of failure
2. warning time of impending collapse
3. accessibility of joint for purposes of inspection and repair
4. redundancy
5. limits of probabilistic model

The last item is important because it brings attention to the fact that it is of little value to recommend actuarial values of failure probabilities i.e. values that might compare with experienced failure frequencies. For such a value to be of use the model predicting failure probabilities would need to incorporate the way in which load shedding interacts with fatigue failure of a joint and the mechanisms of progressive collapse. For present purposes the probability of some lesser event, e.g. through thickness cracking of a single joint, is used as a means of parametising the failure event. Clearly prescription of design values of reliability, or β_T must be tailored to the capabilities of the probabilistic model.

2.4.2 Redundancy

A redundant structure in the civil engineering sense means one whose member forces cannot be determined by resolving in three dimensions and taking moments. Another commonly understood concept of redundancy is that a member is redundant if its removal will not lead to progressive collapse under the design loads. Neither of these definitions is adequate in the context of fatigue. The reason being that neither make reference to the notion, crucial to the concept of fatigue, of time; time to failure or life of the structure.

Clearly what is needed before any meaningful discussion is a definition of 'redundancy in fatigue' which takes into account the lifetime of the structure. To this end let redundancy in fatigue be defined such that a member is redundant in fatigue if its failure by fatigue would not initiate subsequent fatigue failures such that the structure would become disabled within its planned lifetime. By 'disabled' what is meant is an inability to support the design loads. With this definition the structure does not need to have collapsed before the planned life has expired for a member to be called non-redundant. Rather, a member should be called non-redundant if its failure causes, by load shedding, enough other fatigue failures for it to be sufficiently weakened that the design loads could no longer be supported.

2.4.3 Other Factors

The factors of human consequences of failure and joint accessibility for inspection and for repair can be adequately dealt with by creating four distinct categories and their associated target reliabilities $\mathbf{R}_1$ to $\mathbf{R}_4$ as follows:

	non-redundant	redundant (collapse)
inaccessible	R_1	R_2
accessible	R_3	R_4

Analysis described in reference 4 produced recommendations for appropriate target reliability indices, β_T. Hence the procedure is to determine which category describes the joint in question and select the appropriate β_T from the table:

	non-redundant	redundant
inaccessible	3.4	3.1
accessible	2.7	2.0

2.4.4 Design Curves

Section 2.2 presented a simple way of calculating fatigue reliability given the median number of lifetimes $\check{m}_L$ and the distribution moments V_B, V_A and V_D of the fatigue variables B, A and D. Once a value of V_L (Equation 4) has been established β can be plotted in terms of life for a particular structural detail.

Figure 3 is such a design curve i.e. given a target β the curve can be used to determine the required normal life. Figure 4 shows the effects of permitting a degree of redundancy in terms of improving the system reliability from that of the individual detail.

3.0 FRACTURE MECHANICS BASED FATIGUE ASSESSMENTS

3.1 Background

In the fatigue life assessment of offshore structures, the classic S-N curve approach which relates the stress range at a point under consideration to the number of cycles to failure is traditionally used. In order to assess the fatigue life of a cracked structure it is necessary to consider the depth of the fatigue crack. Here a modified S-N curve is introduced to predict the fatigue life which includes the contribution of crack size. This model establishes the relation between S-N curve approach and fracture mechanics method. The relations between time, initial

crack size and thickness of material are established to overcome the weakness of the classic S-N curve approach.

3.2 Linear Elastic Fracture Mechanics

In linear elastic fracture mechanics, the behaviour of a crack is characterized by the stress intensity factor, K. From a knowledge of the range of K occurring at the crack tip an estimate of the growth can be made.

The stress intensity factor can be expressed as

$$K = Y\sigma\sqrt{(\pi a)} \tag{11}$$

where Y is a correction factor and is a function of the crack length and dimensions of structural and crack geometries; σ is the nominal stress at the crack site; a is the crack depth.

It is usual to assume that the growth of a crack is according to the Paris law[5]

$$\frac{da}{dN} = C\,\Delta K^m \tag{12}$$

where C and m are empirically determined; da/dN is the crack growth rate per cycle; and ΔK is the range of stress intensity factor occurring at the crack tip.

Substitution of Eq.(11) into Eq.(12) leads to

$$\frac{da}{dN} = C\,(Y\,\pi^{1/2}a^{1/2}\Delta\sigma)^m \tag{13}$$

Prediction of total number of cycles required to grow the crack from an initial length of a_i to the final length of a_f under the constant amplitude loading can be obtained by directly integrating Eq.(13). If an individual stress range is $\Delta\sigma_i$, the allowable number of cycles is given by

$$N_i = \frac{1}{C\,\Delta\sigma_i^m\,\pi^{m/2}} \int_{a_i}^{a_f} \frac{da}{Y^m\,a^{m/2}} \tag{14}$$

The effect of random variations of stress range of the fatigue can be accounted for by substituting $\Delta\sigma_i$ with weighted average stress range

$$S = (\Sigma n_i \Delta\sigma_i^m / \Sigma n_i)^{1/m} \tag{15}$$

into Eq.(14), which gives

$$N = \frac{1}{C S^m \pi^{m/2}} \int_{a_i}^{a_f} \frac{da}{Y^m a^{m/2}} \tag{16}$$

where n_i is the number of cycles corresponding to the stress range $\Delta\sigma_i$.

3.3 The Modified S-N Curve Approach

In the classic S-N curve approach, the number of cycles that a structural component is subjected to in fatigue loading is represented by the following equation:

$$NS^m = A \tag{17}$$

where m and A are empirical constants, representing the slope and the intercept of the S-N curve in a log-log plot; and A represents the fatigue resistance. The stress range is as given in Eq.(15).

The crack size, a, does not appear in this formula. Comparing Eq.(16) and (17), it can be seen that the fatigue resistance, A, should actually be a function involving the failure mechanism of the structure under consideration and not a constant, i.e. the S-N curve should have the form

$$NS^m = A(a) \tag{18}$$

where A(a) can be expressed as

$$A(a) = \frac{1}{C \pi^{m/2}} \int_{a_i}^{a_f} \frac{da}{Y^m a^{m/2}} \tag{19}$$

It is clear that the fatigue resistance A is a function of structural and crack geometries, the type of loading and material property. For a structural component under a given type of loading the fatigue resistance can be calculated by integration of Eq.(19) for the different initial crack sizes a_i. Once the fatigue resistance A is determined, the remaining fatigue life can be easily predicted by using the same procedure of the classic S-N curve approach.

3.4 An Example

A structural detail is subjected to a series of nominal stress ranges $\Delta\sigma_i$, which are listed in Table 3.4 with the corresponding number of cycles n_i. The stress concentration factor applied to the nominal stress range is relatively low at 1.46. The weighted average stress range for the required 30 years of service life is calculated according to Eq.(15), which is

$$S = 6.17 \text{ N/mm}^2$$

The upper bound Paris law constant C is assumed to be 3.0E-13 and m is taken as 3. It is assumed that the structure will fail when the crack reaches the far surface therefore the final crack size a_f is taken as the thickness of the component. The fatigue resistance A can now be calculated by using Eq.(18), with three different formulae of the correction factor Y given in References 6, 7 and 8. The results are plotted against initial crack depth a_i/T in Figure 5. It is noted that the three formulae are the same when crack depth is small and the change of the fatigue resistance when the initial normalized crack size is less than about 10^{-5} is negligible, but it decreases rapidly when the initial crack size increases after it reaches the fractional depth of 10^{-5}.

For the given stress range S, the total fatigue lives can be evaluated by Eq.(18) for different initial crack sizes. Figure 6 shows that the relationship between fatigue life and initial crack size is similar to that between fatigue resistance and initial crack size. That is the remaining fatigue life will not change significantly if the normalised crack size is less than 10^{-5}. However fatigue life decreases rapidly when the initial normalised crack size is bigger than 10^{-5}.

Figure 7 shows several modified S-N curve for the corresponding initial crack sizes. Other examples may be used to show the influence of material, thickness and type of loading on fatigue resistance.

Table 3.4

Nominal Stress Range $\Delta\sigma_i$ (N/mm²)	No. of Cycles in 50 Years n_i
49.6	7.200E2
38.3	9.801E3
27.2	1.334E5
16.9	1.814E6
8.2	2.468E7
1.7	3.358E8

3.5 Life Estimates Incorporating Reliability

If the material failure is defined as when final crack size a_f is equal to the specimen thickness t, the failure function may be written as

$$z = t - a_f \tag{20}$$

where a_f is a function of Paris law constant and stress range. Assuming the distributions of all variables are lognormal, the probabilities of failure with time may be calculated by the Level II method. Results are shown in Figure 8 for four problems.

For these four problems the nominal stress range $\Delta\sigma_i$ and corresponding number of cycles n_i are listed in Table 3.5. The SCF applied to the nominal stress range is 1.46. The mean value of the Paris law constant C is taken as 9.5945E-14 (C = 3.0E-13 when calculating lower bound life). The initial crack size a_i, bias on stress range B_S and standard deviations for Paris law constant and stress range for the different problems are listed in Table 3.6.

Table 3.5

Nominal Stress Range $\Delta\sigma_i$ (N/mm²)	No. of Cyclesin 50 Years n_i
49.6	7.200E2
38.3	9.801E3
27.2	1.334E5
16.9	1.814E6
8.2	2.468E7
1.7	3.358E8

Table 3.6

	a_i(mm)	SD_C	SD_S	B_S	life(years)
Prob.1	0.9	0.57	0.396	1.	256
Prob.2	0.9	0.57	0.396	0.5284	1800
Prob.3	0.9	0.57	0.117	0.5284	1800
Prob.4	3.0	0.57	0.117	0.3171	1800

4.0 DETAILED FRACTURE MECHANICS ASSESSMENT FOR FRACTURE

4.1 Introduction

The procedure should be based on assessment of a postulated flaw, using the basic procedures of PD6493:1991[10] Level 2 with the additional specialist procedures relevant to the application[11]. The procedure can be adapted to determine acceptable flaw sizes, or used with other assessment methods if appropriate data are available.

It is necessary to decide the loading and minimum temperature for which the assessment is required. The loading effects should be determined in the first instance for best estimates of maximum loading, without any load factors prescribed by any limit state design codes. Where a probabilistic assessment is required estimates of the variability and distributions of the loading and all other input parameters are necessary.

Since a Two Criteria fracture assessment method, based around the Level 2 Failure Assessment Diagram (FAD)[10], has been adopted then fracture assessment involves calculating two failure parameters: The fracture driving force parameter (K_r or $\sqrt{\delta_r}$) and the plastic collapse parameter, S_r. These two parameters are plotted on the FAD, and if the coordinates fall outside the locus of the FAD the crack is unacceptable. To achieve the assessment the following calculation steps should be followed:

4.2 Data Required

4.2.1 Type and Geometry of Joints

4.2.1.1 The type of joint in which the flaw to be assessed lies must be specified from the following typical alternatives:

(a) Circumferential butt weld between lengths of tube.
(b) Longitudinal butt weld in tubular members.
(c) Flat plate butt weld.
(d) Type of tubular nodal joint, e.g. T, K, T-K, Y, with T-butt welds.
(e) T-butt or fillet welded attachment.

4.2.1.2 The relevant geometric parameters in the region of the flaw must be specified.

4.2.1.3 The extent and type of any deviations from intended geometry must be specified, e.g. misalignment in butt welds.

4.2.1.4 The weld toe profile and geometry must be specified, e.g. weld surface attachment length to thickness ratio L/T, weld toe angle θ, and weld toe radius-to-thickness ratio R/T.

4.2.2 Forces and Moments in Members

Results of structural analysis of the overall frame under the chosen critical loading conditions must be available to give the forces and moments in the members in the region being assessed. These should be provided as axial forces, in-plane and out-of-plane bending moments, and shear forces in two perpendicular directions. Both maximum load and fatigue load ranges are required.

4.2.3 Material Properties

4.2.3.1 Tensile

Information on the type of steel, welding consumables, weld procedures and post weld heat treatment is required. Where possible, data on the actual tensile strengths (yield and ultimate strengths) for the material in which the flaw lies should be provided. Both weld metal and parent metal strengths are required. Where specified data are not available, minimum specified values should be assumed.

4.2.3.2 Fracture Toughness

Fracture toughness data for material typical of the region in which the flaw lies are required. Where possible this should be obtained from procedure tests using the actual welding consumables and procedures as used in construction.

The data may be provided in either K_{mat} or δ_{mat} form depending on test methods used. The minimum value of at least 3 tests at the minimum temperature should be used. CTOD tests should be on the full thickness of concern wherever possible, and it is then permissible to use δ_c, δ_u, or δ_m values as occur in the tests.

If data are used from small scale tests, or converted from Charpy or other tests, the basis of the derivation of K_{mat} or δ_{mat} values must be stated and justified.

4.2.4 Flaw Dimensions and Location

The flaw should be categorised, as in PD6493:1991, as one of the following:

(a) surface breaking,
(b) embedded,
(c) through thickness.

The length, height, depth from the surface (if relevant), and orientation of the flaw must be stated as best estimates including the method by which these were determined and any likely uncertainties/ errors. The position and orientation relative to both welds and direction of stressing must be stated. This must include position relative to different bending moment axes.

4.3 Fracture Assessment Principles

A detailed statement of the methodology for fracture assessment is given in Reference[11]. The basic principles are for the use of the PD6493:1991 Level 2 Assessment Diagram, with the crack driving force parameters K_r or $\sqrt{\delta_r}$ and S_r calculated from the data of Section 4.2. Thus separate calculation of fracture and plastic collapse failure conditions is required, with interaction and plasticity effects covered by the shape of the assessment diagram.

In general the parameter S_r may be calculated either on the basis of local collapse or on the basis of global collapse. The local collapse approach will usually be very conservative and a check should be made first to see whether a defect is acceptable on this basis. If the defect is unacceptable on the local basis it should be checked again using the global collapse basis. It is most important that a lower bound solution is used with the global collapse approach.

4.4 Crack Assessment

4.4.1 As an initial assessment plot the coordinates of the point (K_r, S_r) or ($\sqrt{\delta_r}$, S_r) for the deepest point and surface point positions on the Level 2 FAD. If the points lie within the locus the crack may be acceptable, if any of the points lie on or outside the locus the crack is unacceptable.

4.4.2 If all points lie within the Failure Assessment Diagram re-evaluate the coordinates using the partial safety factors appropriate to the required level of reliability as described in 4.5. If all the reassessed points lie within the locus the crack is acceptable for the level of the reliability selected. If any of the points lie on or outside the locus the crack is unacceptable for the level of reliability selected.

4.5 Safety Factors

The safety factors to be applied in assessments depend on the acceptable or target probability of failure and on the uncertainties in the input data. In particular the uncertainties associated with stress, defect size and material toughness have a significant influence. Partial safety factors should be selected, as appropriate, from the table below and should be applied, in the case of defect size and stress, to mean values. For the material toughness the partial safety factor should be used to reduce the characteristic value (lowest of 3 results or equivalent).

Partial safety factors for case	Target probability of failure 2.3×10^{-1}	10^{-3}	10^{-5}
Stress measured (COV5%)	1.1	1.4	2.0
Stress estimated (COV30%)	1.2	1.6	2.4
Flaw size SD (2-5mm)	1.0	1.2	1.7
Flaw size SD (10mm)	1.1	1.4	1.8
Toughness (K_{1C})	1.0	1.2	1.3
Minimum of 3 toughness (CTOD)	1.0	1.4	2.6

The target partial reliability should be chosen from independent assessment, or from the table below, for the appropriate failure consequences and degree of redundancy.

Failure Consequences	Redundant Component	Non-redundant Component
Moderate	2.3×10^{-1}	10^{-3}
Severe	10^{-3}	10^{-5}

5.0 A STRATEGY FOR ASSESSING NEW TECHNOLOGY

5.1 Background

The major driving force of reducing cost of both original fabrication and whole life costs provides a fertile environment for technological change. The increasing impetus for change is visible in the rapid increase in use of polymer composite materials offshore for fire and blast protection applications. On the structural side there are a number of competing technologies. These include the use of higher strength steels (significant welding problems), the use of structural aluminium (often incorrectly viewed as expensive), the use of structural composites (established credibility in small ships) and adhesive bonding of steel and/or polymer composites (lacking in public credibility).

This section examines the case of adhesive bonding of steel structures as an illustration of the barriers to be overcome in progressing such technology. A similar scenario applies to each of the areas of new technology listed above.

5.2 Potential

This section addresses the problems of implementing adhesive bonding into the design and fabrication of steel structures traditionally joined by a fusion fillet welding process. These structures typically consist of flat or curved plate of 3-10mm thick to which stiffeners are bonded. The possible applications for such technology include large structures for the marine and offshore industries. The requirements for adhesives in such joint configurations are part of a methodology which must incorporate the original design requirements and the demands of through life performance. The fillet joints in such stiffened plate structures usually carry low to moderate forces mainly in shear and compression but may have to provide a substantial ultimate load carrying capacity as well as resistance to fatigue loading in service.

When considering substitution of adhesive bonding in traditional welded structures the driving forces for change include the avoidance of residual stresses. In relatively thick section structures residual stresses can dominate the fatigue life of the structure[12] even when the service loading is compressive. In thinner section structures, for example, ships, the consequence of residual stresses from welding is often extensive and costly distortion.

When considering the adoption of bonding the fundamental properties of adhesives have to be appreciated. The most important being the general characteristics of low strength, low modulus and, by structural steel standards, very

low toughness levels. These factors are coupled with great sensitivity of mechanical properties to temperature, a limited maximum service temperature and currently weak inspection capability for such joints.

Despite this apparently poor starting point the potential for adhesive bonding as a substitute for welding in large steel structures is immense and will improve as the understanding of the behaviour of such joints and the acceptance of the necessary design and assessment requirements increases. Overall the increasing use of adhesive bonding has to be accompanied with increasing technical confidence. This requires a rational design and assessment framework with the inevitable limitations well understood rather than being absorbed in ill defined safety factors. In this context the widely quoted and crudely applied safety factor of 10[13], applied to static stress levels at ambient temperatures, does little to enhance confidence in adhesive bonding among potential users.

5.3 Methodology Objectives

In modern design and assessment methodologies relating to welded steel structures (see sections 2, 3 and 4) there are free flowing strategies for assessing the demands on structures from the loading and the resistance available to combat these demands. Such strategies include the concepts of structures continuing to operate through the whole of life with a considerable population of defects but also include inspection and repair capabilities and the consequences of failure. In addition, the uncertainties associated with each stage of such assessments may now be included to provide a reliability based assessment[2]. None of these strategies is complete or perfect but in recent years considerable strides have been made in improving their technical content and defining areas of lack of knowledge.

Parallel developments are needed for adhesively bonded structures if this joining technology is to be employed in applications where full scale type testing is not available as a tool for design auditing. Currently there are large gaps in knowledge relating to both the detailed stress distributions arising from the loading on adhesive joints and material performance in terms of behaviour under simple and complex conditions of stress, rate of loading, temperature, long term environmental resistance and tolerance to imperfections (defects). A further factor is the relative difficulty of assessing the quality of fabricated joints and the criticality of defects. The filling of these gaps and the consolidation of data and assessment procedures into a credible and coherent methodology is a worthwhile but long term objective. The benefit should be design procedures incorporating adequate levels of safety consistent with the application and the consequence of failure.

5.4 Unknowns and Uncertainties

In attempting a complete structural integrity assessment of bonded structural connections when used as a substitute for welding several areas of inadequate knowledge are apparent. Principally these are the capability and performance of inspection processes and the behaviour of the various types of defects occurring in bonded joints. limited fracture mechanics studies of bonded butt joints with very stiff adherends and the adhesive joint subjected to tensile stresses have been undertaken but it is not clear that direct technology transfer from welded connections is appropriate[14]. However in fabricating structures it is necessary to set quality levels for inspection prior to service. These threshold acceptance levels for various types of defect ought to be part of the integrity assessment process and should take account of the capability of the inspection processes and the consequences for the structure resulting from the defects. With incomplete understanding of the failure process applicable to adhesive joints it is difficult to quantify the effects of the various types of defects which occur[15]. In addition the performance of the available inspection processes is very limited. Practical inspection capability is seen to be in need of improvement but the target inspection performance should be determined as a result of integrity assessment requirements. Identical arguments regarding the criticality of defects and inspection performance apply to in-service inspection and subsequent repair decisions.

As databases of results for mechanical properties expand then the uncertainties associated with adhesive performance can begin to be quantified. These together with the uncertainties in loading and quality of connection may then be assembled in a reliability format to provide guidance on safety factors for specific reliability levels.

5.5 Feasibility

To date the feasibility of bonding stiffeners to plating has been demonstrated[16]. The mechanical performance both under static loading and fatigue conditions[14] is adequate and in some cases superior to the welded case. Long term durability does not appear to be a significant problem[17] but a total strategy[18] incorporating design fabrication, inspection and assessment, from which structural integrity might be assured, is yet to be developed.

6.0 REFERENCES

1. Plane, C.A., Cowling, M.J., Nwegbu, V.K. and Burdekin, F.M., 'The role of redundancy in reliability based fatigue life assessments in offshore structures', Ch. 26 in 'Integrity of Offshore Structures - 4', ed. by D. Faulkner, M.J. Cowling and A. Incecik, Elsevier Applied Science, London, 1990.

2. Plane, C.A., Cowling, M.J., Nwegbu, V.K. and Burdekin, F.M., 'The determination of safety factors for defect assessment using reliability analysis methods', Ch. 19 in 'Integrity of Offshore Structures - 3', ed. by D. Faulkner, M.J. Cowling and A. Incecik, Elsevier Applied Science, London, 1988.

3. Plane, C.A. and Cowling, M.J., 'Reliability based defect assessment methodology', Defect Assessment in Offshore Structures Managed Programme, Phase 2 Progress Report, January 1989, Glasgow Marine Technology Centre.

4. Plane, C.A. and Cowling, M.J., 'A comprehensive method for the treatment of uncertainties in fatigue design based on Miner's sum', Defect Assessment in Offshore Structures Managed Programme, Phase 2 Progress Report, January 1989, Glasgow Marine Technology Centre.

5. Paris, P.C., The Growth of Fatigue Cracks due to Variations in Load, Ph.D. Thesis, Lehigh University, Bethlehem, Pa., 1962.

6. Isida, M., Nogudi, H. and Yoshida, T., International Journal of Fracture, 26 (1984) 157-188.

7. Raju, I.S. and Newman, J.C., Engineering Fracture Mechanics 11 (1979) 817-829.

8. Gross, B. and Srawley, J.E., National Aeronautics and Space Administration, NASA Report TND - 2603 (1965)

9. D.En./Lloyd's Register of Shipping, 'Sensitivity of fixed offshore platforms to uncertainties in design'. Offshore Technology Report OTH88/254, HMSO.

10. British Standards Published Document PD6493:1991, 'Guidance of methods for assessing the acceptability of flaws in fusion welded strucutres'.

11. Cowling, M.J. and Burdekin, F.M., 'A new Procedure for assessing defects in offshore structures'. To be published.

12. Hugill, P.N., Sumpter, J.D.G. and Nicholson, R.W., Integrity of Offshore Structures - 3 , Elsevier Applied Science, 1988, pp345-360.

13. Adams, R.D., Structural Adhesives in Engineering, I.Mech.E., London, 1986, pp17-24.

14. Cowling, M.J., Smith, E., Hashim, S.A. and Winkle, I.E., 'Performance of adhesively bonded steel connections for marine structures', Proc. EVALMAT 89, Kobe, Japan, November 1989.

15. Cawley, P. and Adams, R.D., Mater. Sci. and Technol. 5, 1989, pp413-425.

16. Winkle, I.E., Cowling, M.J., Hashim, S.A. and Smith, E.M., 'What Can Adhesives Offer to Shipbuilding?', Journal of Ship Production, Vol. 7, No. 3, pp137-152, August 1991.

17. Cowling, M.J., Hashim, S.A., Smith, E.M. and Winkle, I.E., 'Adhesive Bonding for Marine Structural Applications', Proc. 3rd Int. Conf. on Polymers in a Marine Environment, London, I.Mar.E., October 1991.

18. Hashim, S.A., Cowling, M.J. and Winkle, I.E., 'Design and Assessment Methodologies for Adhesively Bonded Structural Connections', Int. J. Adhesives and Adhesion, Vol. 10 No. 3, pp139-145, July 1990.

Parameter			Lloyd's	Present
Hydrodynamic coefficients	Cd = 0.6	+20%	u	u
	Cd = 0.7	+100%	R	R
	Cd = 1.2		R	R
	Cd = 1.2, Cm = 1.3		M	u(1.27)
	Cm	-25%	M	M
Wave	Period +2 sec		R	
	Period -2 sec		u	
	Period +10%			u(1/1.16)
	Period -10%			u(1.06)
Current	Zero current		u	u
Marine Growth	x 2		R	R
Directionality	Proportional occurrences		u	
Water depth	Min		u	u
Wave Exceedance	H_{max}	+10%	R	u(1/1.36)
	H_{max}	-10%	M	u(1.4)

R/M Reduction/Multiplication of fatigue life by a factor > 1.5

(1.27) Factor in current study when < 1.5

u Parameter not sensitive i.e. factor < 1.5
Blank indicates study not done.

Table 1 Comparison with Lloyds'[9] deterministic study

		List 1 COV	List 2 COV	List 3 COV	List 4 COV	List 4 Bias
1	H	30	16[2]	20	13[3,4]	1.05[4]
2	SCF	20	20	20	20	-
3	C_d	25	10[1]	10	40[3]	1.7
4	C_d	25	10[1]	10	40[3]	1.7
5	C_m	25	10[1]	10	28[3]	1.4
6	C_m	25	10[1]	10	28[3]	1.4
7	ρ_w	5	5	5	5	-
8	$MFOUL_{top}$	30	45[1]	30	30	-
9	$MFOUL_{bottom}$	30	45[1]	30	30	-
10	U_c	10	35[1]	20	-	-
11	SWH	5	5	5	5	-
12	S-N	38.6	38.6	38.6	38.6	-
13	MINRSUM	30	30	30	30	-

1. After Soares
2. 25 for wave kinematics used by Soares
3. After Fjeld
4. Includes current

Table 2 Uncertainties in variables

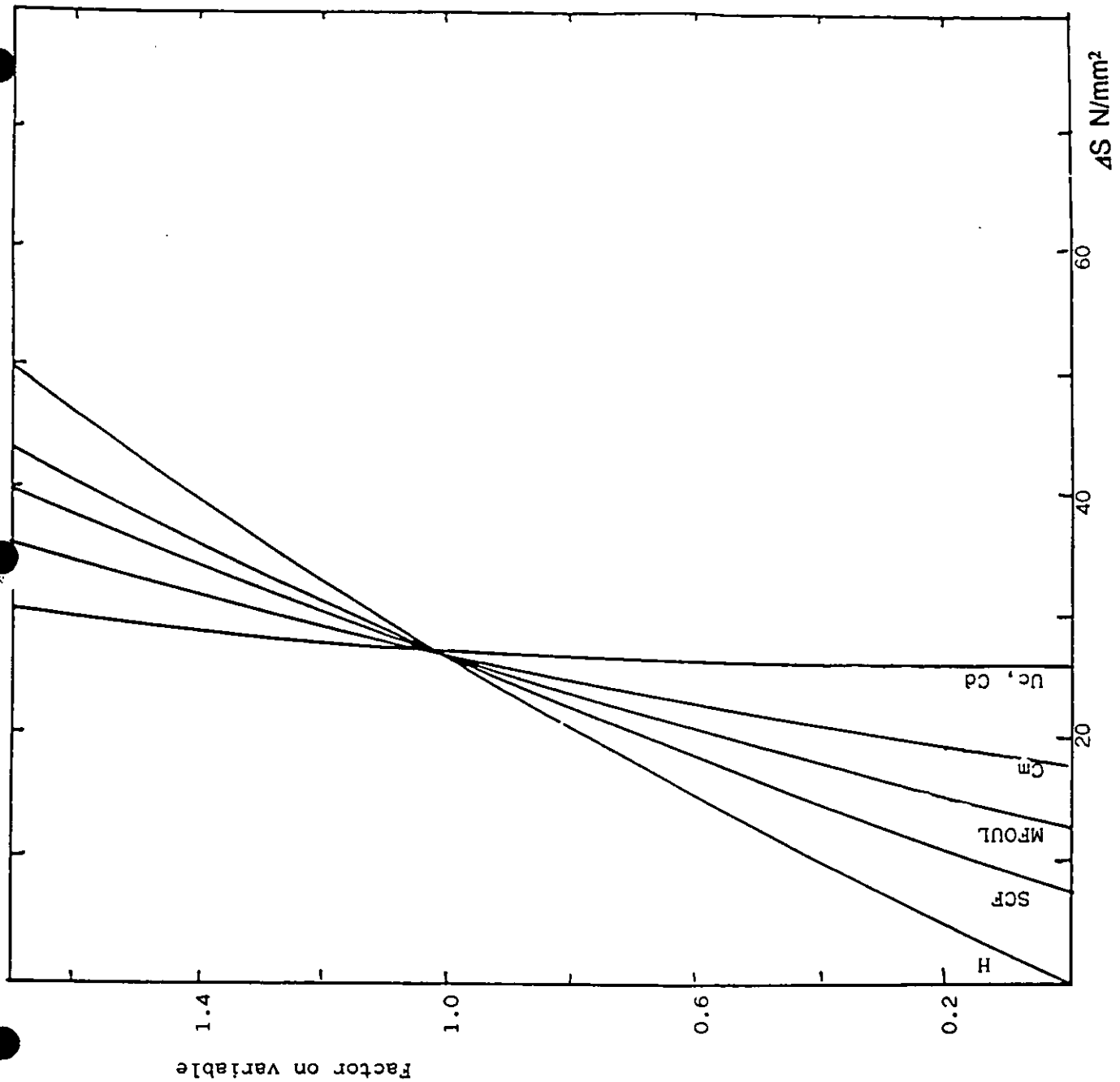

Figure 1 Deterministic Sensitivities

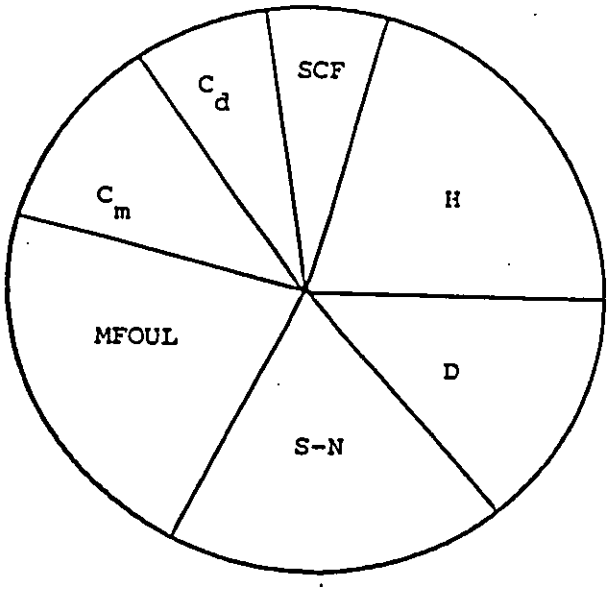

Splash Zone

COV(H) = 15%

C_d = 0.7

COV(SCF) = 20%

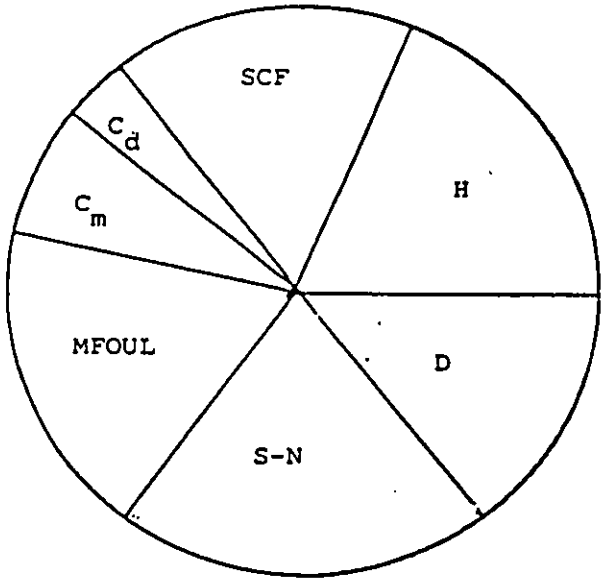

Subsea

COV(H) = 15%

C_d = 0.7

COV(SCF) = 20%

Figure 2 Relative sensitivities to uncertainties

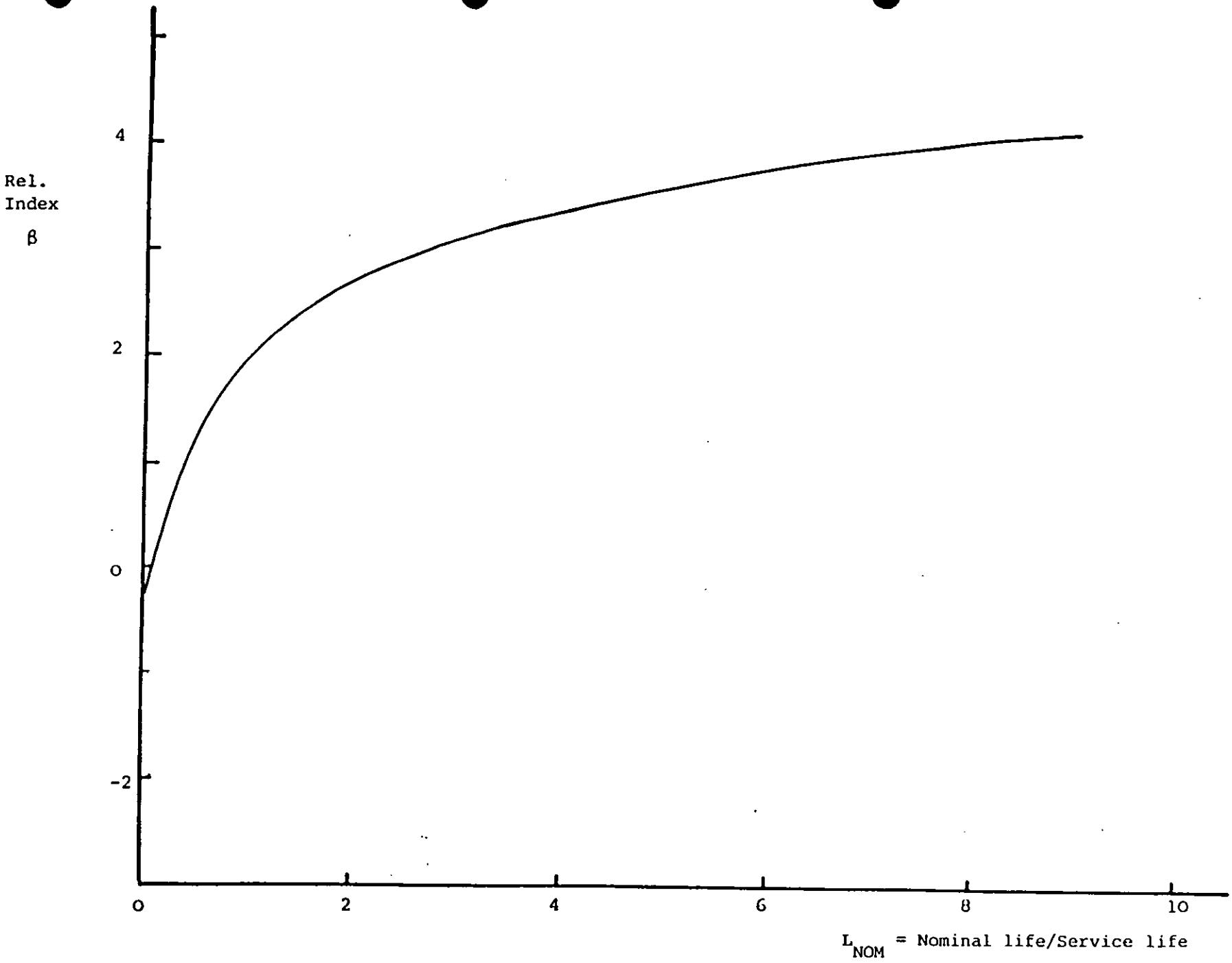

Figure 3 Design curves for nominal life

Figure 4 System Probability of Failure for Full Structure

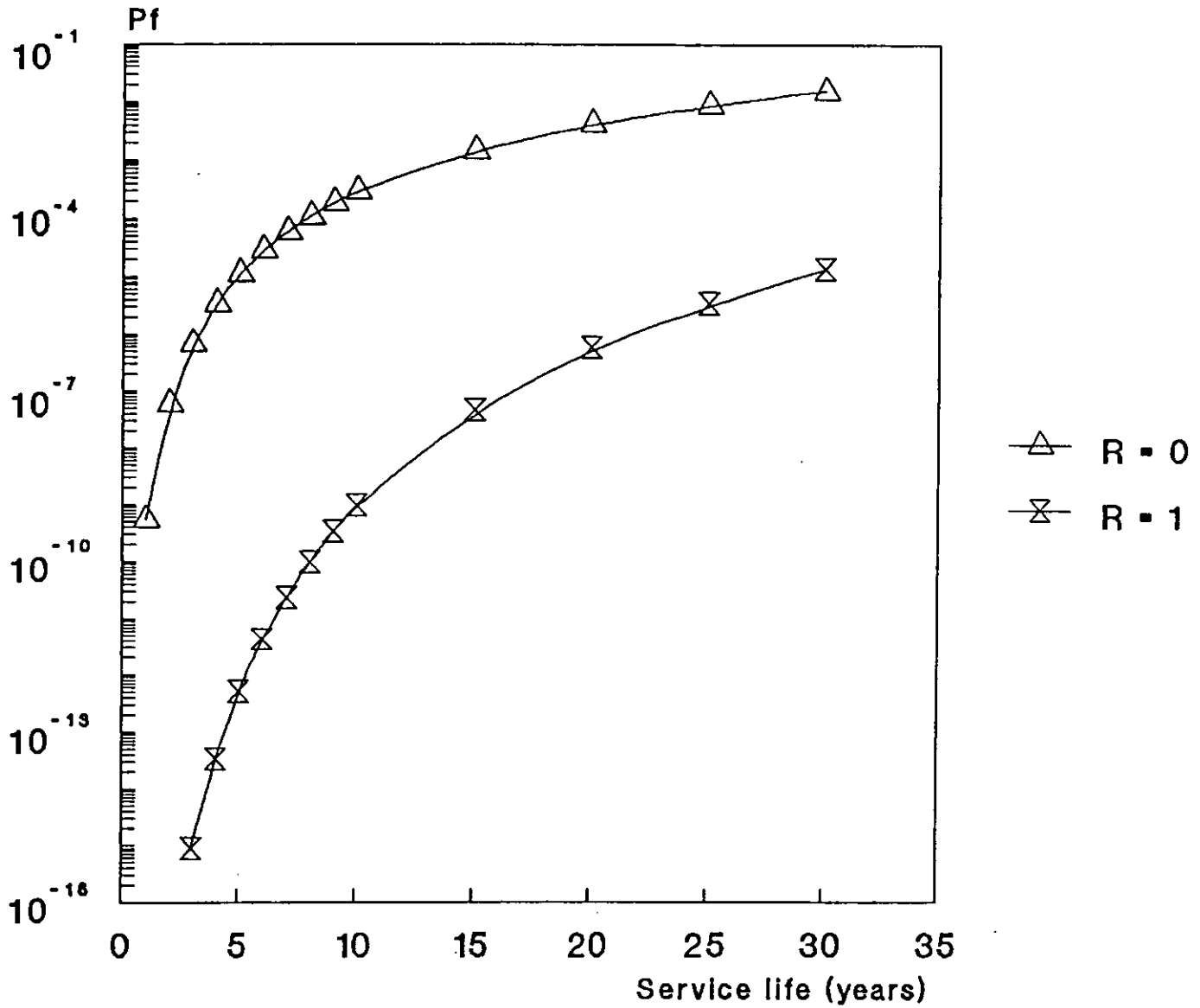

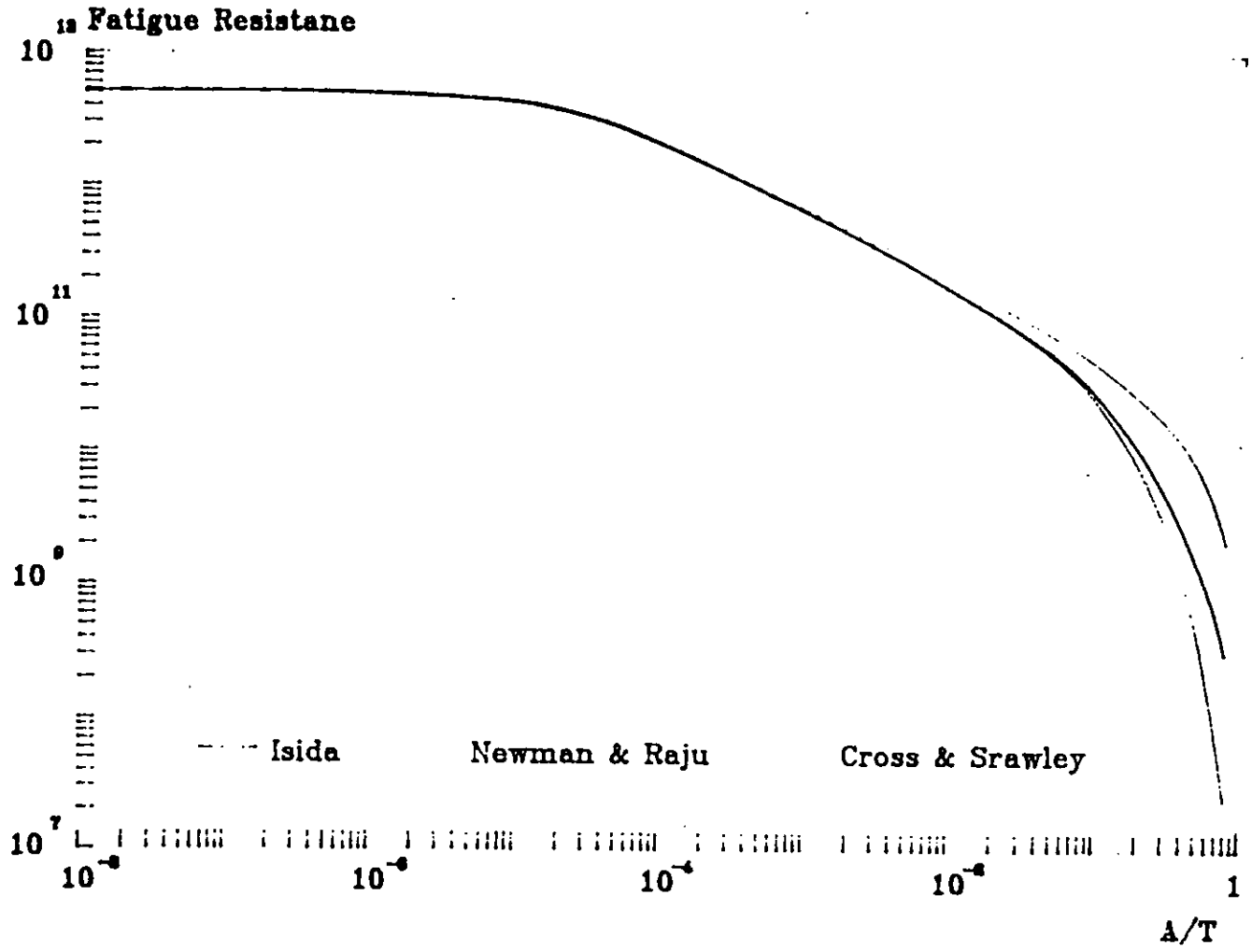

Figure 5 Fatigue Resistance as a Function of Different Value of Crack Depth

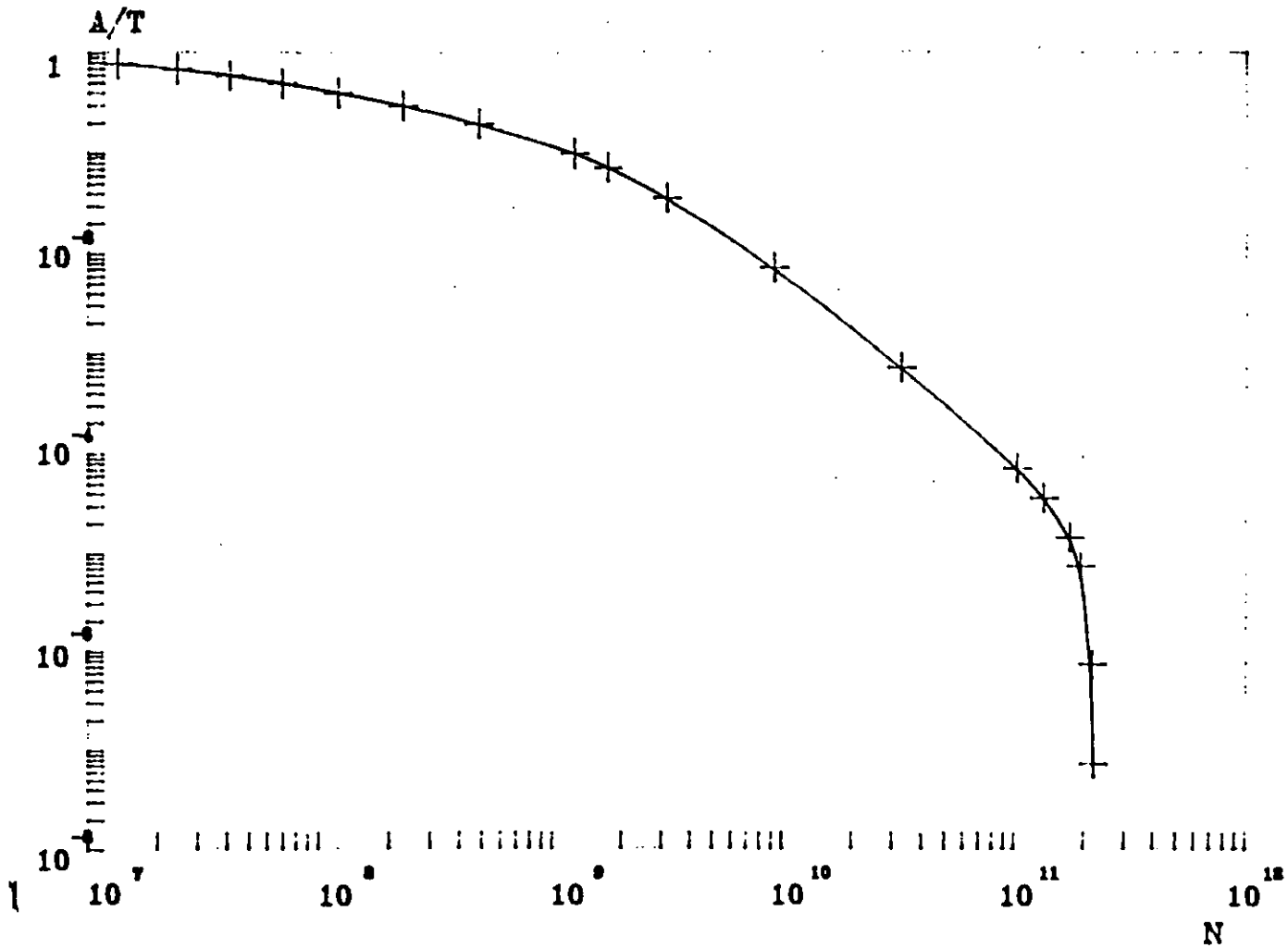

Figure 6 Initial Crack Size versus Fatigue Life (Cycles)

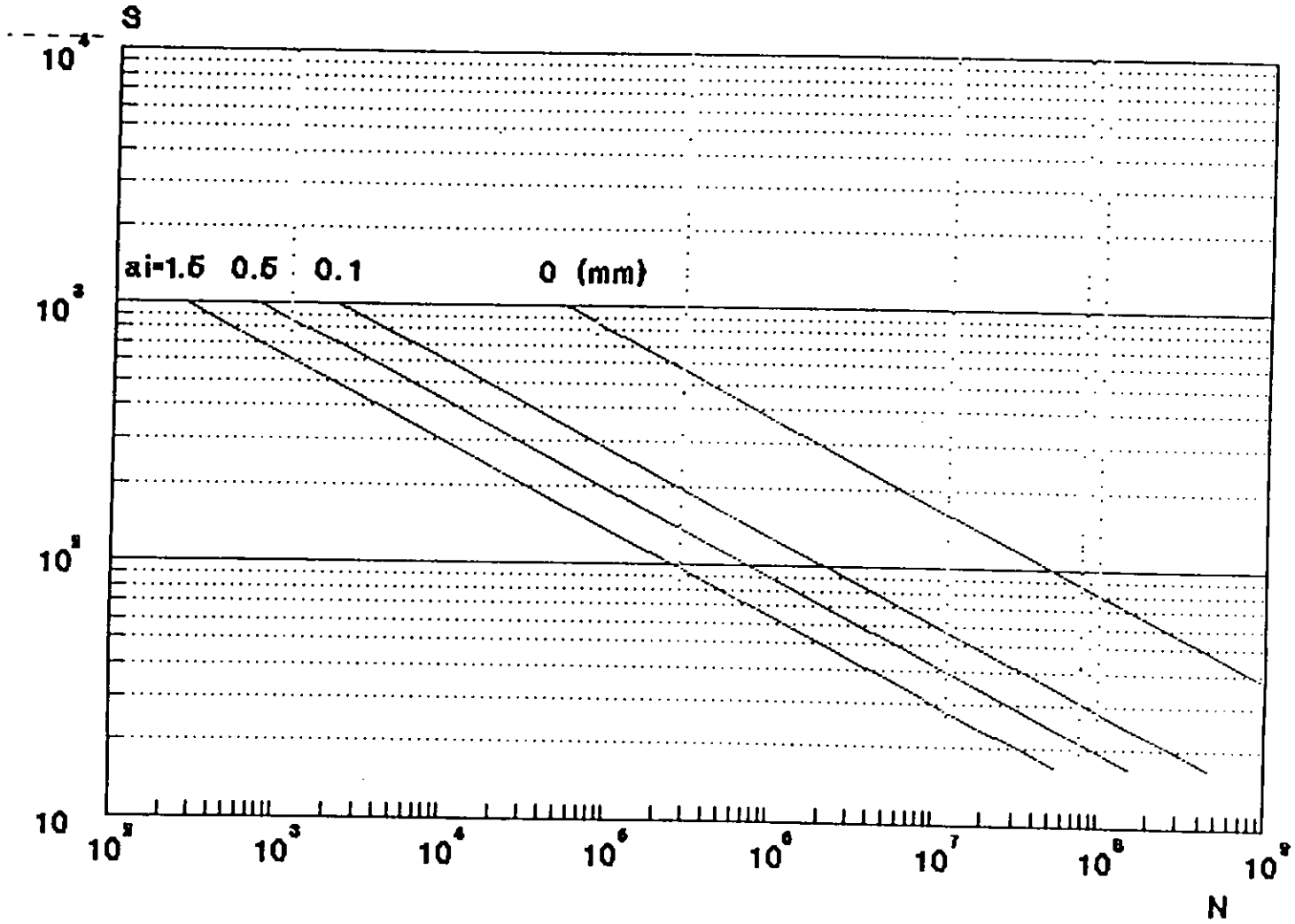

Figure 7 Modified S-N Curve of Different Initial Crack Depth for Light's Prob.

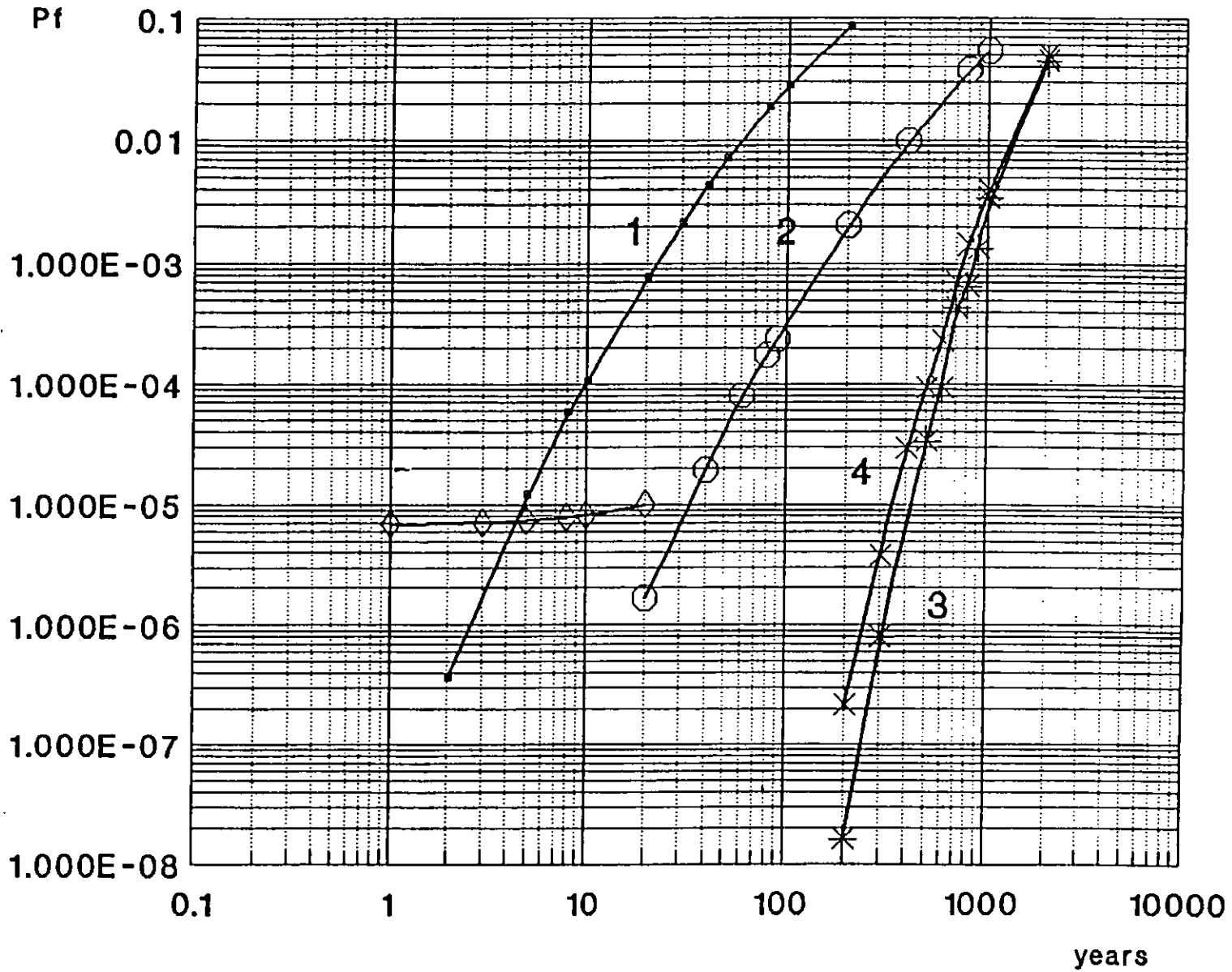
Pf
0.1
0.01
1.000E-03
1.000E-04
1.000E-05
1.000E-06
1.000E-07
1.000E-08
0.1
1
10
100
1000
10000
years
1
2
3
4

Figure 8

Advanced Design for Ships
and Offshore Floating Systems.

Glasgow 21-25 September 1992

Product Prototyping at the Design Stage.

DR. M.R. KATTAN
Newcastle University
August 1992.

1. INTRODUCTION.

The intense development activities for the construction of a large variety of unconventional marine structures, pose considerable problems not only for designers but also for constructors.

The increasing variety of structures reduces opportunities for standardisation which offer the constructor benefits more efficient and cost effective production, thus driving up construction costs as, invariably there is a design/construction mismatch. Or simply, the constructor experiences increased difficulty in building new structures.

The purpose of this paper is to investigate a possible method for helping both designers and constructors to work together to provide more production friendly designs.

The paper firstly discusses the progress of production technology in the marine construction field and indicates paths towards future development. It then considers the need for prototyping and offers a technique that will alleviate some of the design and construction problems.

2. THE DEVELOPMENT OF PRODUCTION TECHNOLOGY.

The development of Production technology and its relation to design can be traced through the production spectrum[1] this in turn, provides useful indications as to where production technology may lead us.

Marine manufacturing facilities at present span the complete range of the production spectrum. At the extreme many organisations are still employing fixed position methods of manufacture, whilst, at the other extreme, others are developeing fifth generation marine factories.

The production spectrum in figure 2.1 broadly outlines the development of marine manufacturing facilities up to the seventh generation.

Figure 2.1. Production Spectrum

PRODUCTION TYPE

JOB SHOP	BATCH	GROUP	FLOW

PRODUCTION LAYOUT

Fixed Position	Process	Group	Product

PRODUCTION PRE-INVESTMENT

Low → Relative → High

PRE-INVESTMENT THINKING

Low → Relative → High

POST-INVESTMENT THINKING

High → Relative → Low

PRODUCTIVITY

Low → High

FLEXIBILITY

Low → High

VARIETY

High → Low

1st Generation (site)	2nd Generation (shipyard)	4th Generation (vessel factory)	3rd Generatio (ship factory)
			5th Generatio (marine factor
			6th Generatio (process)
			7th Generatio (structu

Facilities that produce a high variety of products tend to be Job Shop in nature with minimum investment. Typical of these facilities were the offshore yards when they were first established they were no more than sites.

The second generation saw an increase in investment in equipment and facilities for treatment and preparation activities. Increased mechanisation early on in the production process, leaving the erection process as in the first generation. This is typical of many european offshore facilities at present. Making the erection stage the bottleneck.

The third generation facilities identified the benefits of mass production and identified specific products e.g.: jackets for offshore, tankers in shipbuilding. These could offer a repetitive standard product to enable high levels of efficiency to be attained.

These facilities found that they could not survive by being dependent on one product, so the natural development was to produce a limited variety of products, which by careful design could incorporate similar components. US offshore fabricators probably lead in this and Japanese shipyards also did well from this in the early 80's.

However, the increase in variety reduced efficiency. Thus a drive was made to continue to produce a limited variety of end products but by careful design, to make them from identical or very similar interim products. This enabled production efficiency to be increased. This in turn gave birth to the Marine factory. Capable of building any marine vehicle at high levels of efficiency. (The fifth generation).

This brings us up to date with the current level of Production technology with a number of marine factories now capable building structures and ships with equal ease and efficiency. However, to predict design and production needs, we must understand what will happen in the future to production technology.

The 6th Generation will see facilities investigate new processes for manufacture. There is already evidence of this in new cutting and joining processes, with prehaps Lasers and Adhesives hitting the headlines most often.

The 7th Generation facilities will, in turn, take advantage of the capabilities of these new processes, to develop new structural interim products from steel and

other materials that would be standard and useable for all marine vehicles. We will see the demise of the siffened plate panel in favour of sandwich structures in both steel and composites.

As these developments take place in production, there will be an increased onus placed on designers to understand what can and can't be done, so that they can maximise the production technology available in designing new products.

This must lead to a more integrated approach to computer aided design and production.

3. THE ROLE OF THE PROTOTYPE.

The concept of arithmetic of errors[2], identifies the fact that, as a mathamctical computation becomes more complex, rounding or computational erros, although individually small, can accumulate to create errors so large, that they can have a significant bearing on the final results of a calculation. This is exactly the same process that occurs in assembly industries.

The individual process errors, although small, can accumulate to make an assembly extremely difficult to manufacture to tolerance without extensive fairing or rework.

The ideal solution for any new design, would be the production and testing of a prototype before issue of the final drawings. Equally it is desirable to test the proposed production technology by having a test run or producing an "O" series.

The purpose of a prototype is to provide feedback to designers about problems presented by the new design that the production process cannot accommodate. This would either lead to extensive rework or in the extreme cases, a product that cannot be produced.

A Prototype then provides a feedback loop between production and design early on before full production starts (see figure 3.1).

In large or heavy manufacturing industries, most products are one off so called "made to order" products. The high capital cost and low numbers, provide little opportunity or economic justification, to fully investigate the integration of both design and production, before manufacture actually starts.

Consequently, although a physical prototype is not a viable option an alternative approach is a realistic possibility.

The use of merging equations as identified by the Japanese in 1967 (3), clearly indicated that the potential for the development of a theoretical prototype on paper could be achieved. This would enable a design of a large assembly to be evaluated for production before being committed to manufacture.

This is an important possibility because the ability for production to influence the build time and cost of manufacture diminishes with time (figure 3.2a). In addition, the number of design changes increase over the initial project life and then tail off towards the end of the project life (figure 3.2b).

Consequently, it is important for production to influence design but to do so based on quantative data rather qualatative opinions.

Through the use of techniques such as merging equation and the application of statistical process control, it is possible to predict the probable outcome of a series of processes that produce interim and final products.

The following sections describe how these techniques can be used but first it is necessary to dispel a number of common misconceptions.

Figure 3.1. The Coordination of Design and Production.

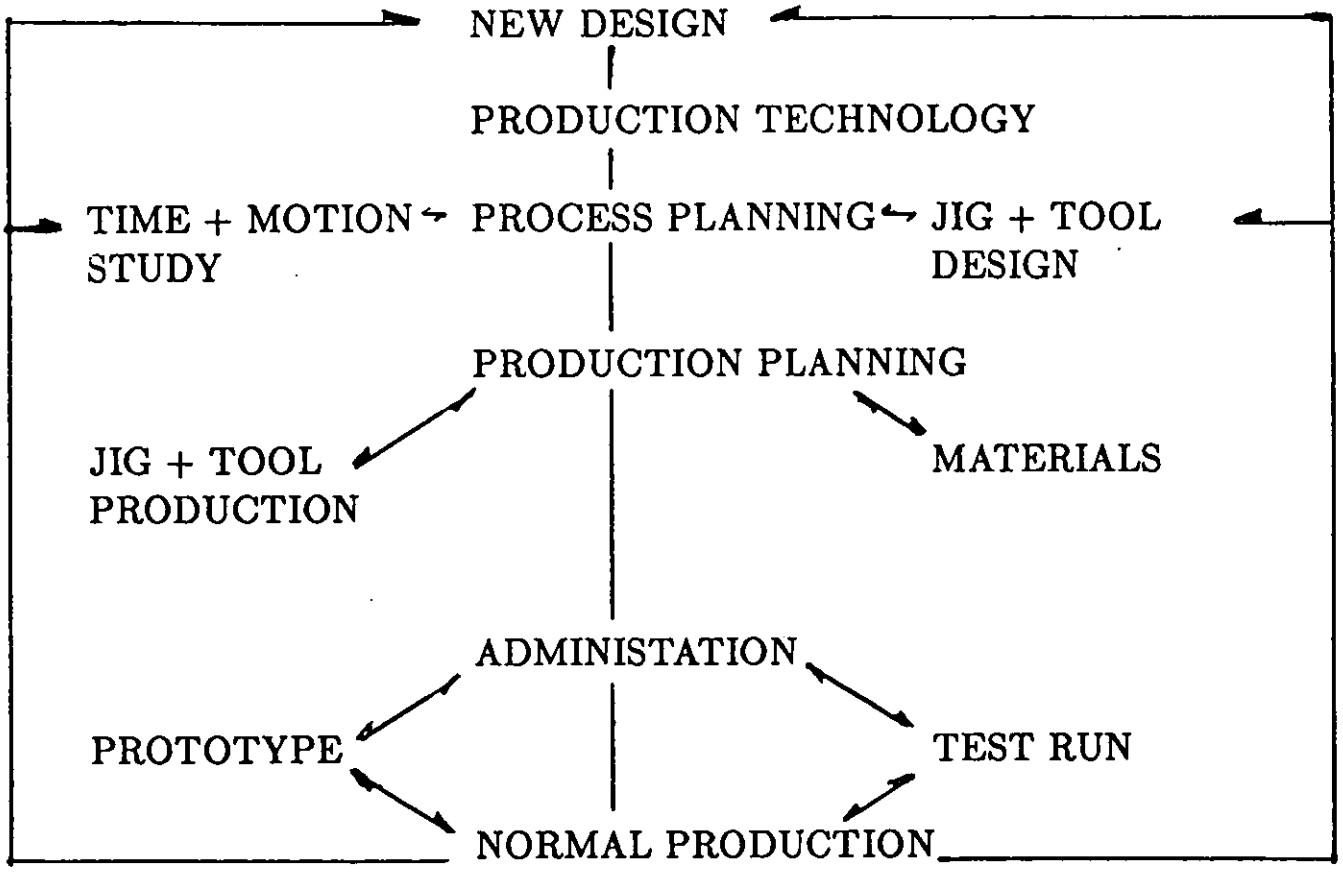

FIGURE 3.2

A) CONTROL OF COSTS OVER PROJECT LIFE

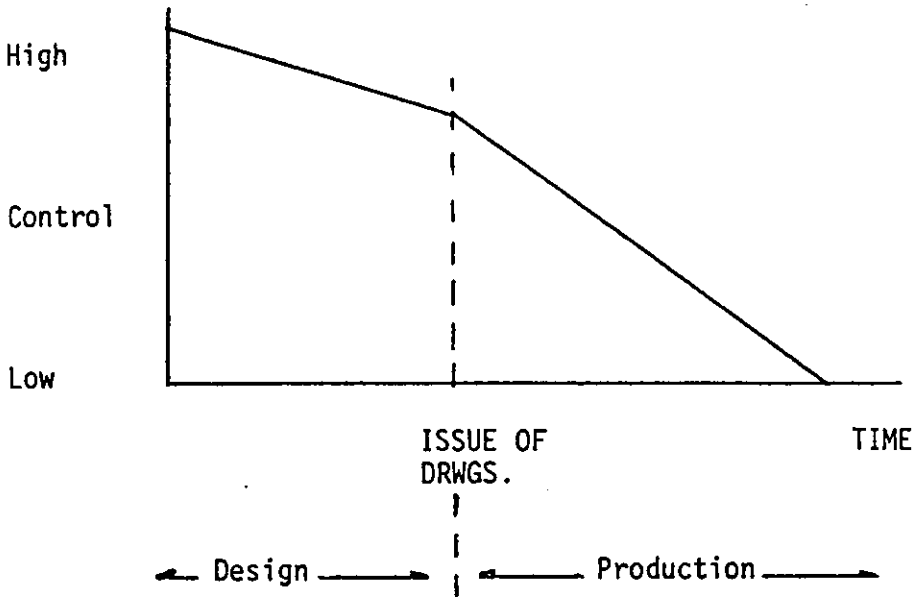

B) DESIGN CHANGES OVER LIFE OF PROJECT

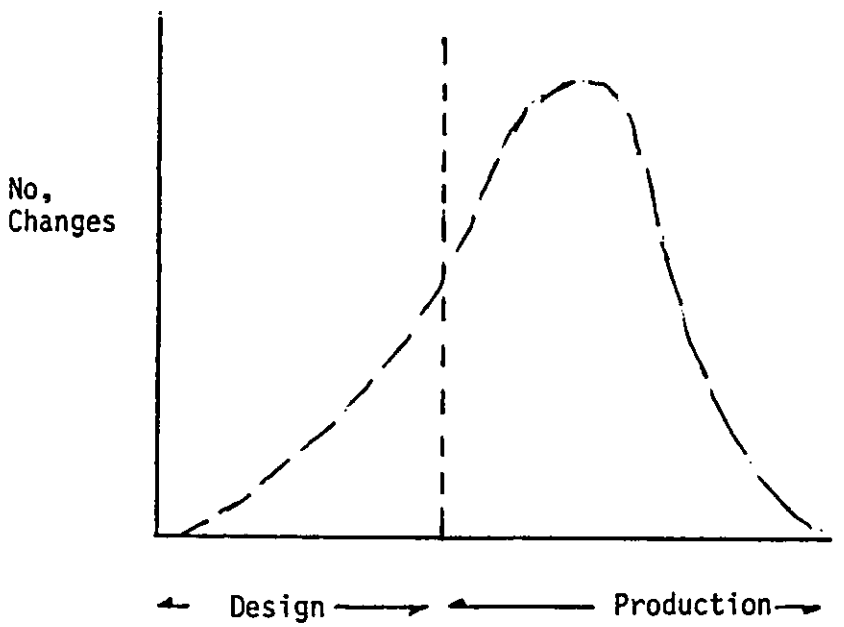

4. DESIGN AND PRODUCTION.

In the building of any particular marine structure, one of the more common arguments for lack of control of production systems is that the new product is unique and therefore no historic data can readily be used to predict the likely outcome of production.

Yet the structure is built in the same facility, by the same workers, using the same equipment. Therefore, the conclusion that can be drawn is; the products must be inherently similar but that those similarities are not maximised during the design phase.

So designs should maximise the similarity between products. Standardisation of interim products is possible. The Americans have demonstrated this in the offshore world and the Japanese and Germans have demonstrated this in ship production.

Advances in Computer Aided Design[4] have enabled designers to produce more sophisticated designs with less and less effort. However, these systems carry little or no production information so they have not encourage designers to improve the producibility element of the design.

From the manufacturers point if view, the pressure of competition means that they must often tender for contracts, not fully understanding the production problems a design presents. Hence they juggle with manhour budgets to try and accommodate considerable rework activities to overcome these problems. This rework is often carried out under the worst possible conditions and adding consdierable cost to the project thus compounding the problem.

A methodology that could be used in conjunction with a Computer Aided Design facility but providing data on producibility of the structure designed, would provide considerable benefits to designers and manufacturers. This would encourage the use of similar interim products and standardise manufacturing methods.

5. PRODUCT PROTOTYPING METHODOLOGY.

The technique for Product prototyping is essential, given the direction of development that is foreseen in production technology and the developments in computer aided design.

This section will review the technology required, and outline a methodology for prototype modelling. It will then illustrate the application to an appropriate structure, a built up stiffened panel.

5.1. Tolerances.

The first stage in developing a product prototype model is to clearly define tolerances. There are two types of tolerances. Global tolerances, that relate to overall dimensions of the final product on completion. Local tolerances, that relate to small assemblies or interim structures. These local tolerances may or may not contribute to the Global tolerance requirements but are identified because they are critical. An example of a Global tolerance may be on the length and breadth dimensions of a panel. A local tolerance would be on the stiffener spacing for slot fit up.

Given the final tolerance of a product individual process tolerances can be defined using a tolerance chain analysis as represented by equation 1[5]. This states that the final tolerance squared is equal to the sum of inidvidual process tolerances squared.

$$T^2_{\text{Final}} = t_1^2 + t_2^2 + t_1^2 \ldots\ldots + t_1^2 \tag{1}$$

Thus, from the tolerances on the final product tolerances for various assemblies could be established. Achieving the tolerances leads to a low probability of rework in the interim and final structure.

5.2 Process Capability.

Having identified the required tolerances the capability of a production process to meet the tolerance set must be established. The capability of a process is usually defined as:

$$\bar{X} \pm 3\sigma \ldots\ldots \tag{2}$$

where:
$\bar{X}$ = mean process performance.
σ = the standard deviation of the process.

The capability of the process can be evaluated using a process capability chart[6]. This can then be compared directly against the tolerance requirements (see figure 5.1).

The example in figure 5.1, shows a process that is capable of meeting the tolerance limits set. Clearly, data must be collected about the process and as a rule of thumb, about 30 samples of data are required to construct a capability chart.

If the process is not capable of meeting the tolerance requirements, then either, the process performance must be improved or, the design changed to alleviate the problem. If neither of these options is taken then production problems will result in rework. So design for production should ensure that designs are capable of being produced.

5.3. Statistical Process Control (SPC).

Data from capability studies can be further utilized on an ongoing basis for the development of X-bar and R-charts for each process. These provide ongoing information as to how a particular production process is performing over time and allows the adoption of SPC and problem solving techniques to improve performance. Thus, the responsibility of production is to continuously improve process capability (figure 5.2).

The result of using these charts is that the performance of each process is controlled and monitored. Each process can then be defined by a mean performance and a variance that reflects the range of possible performance. For example a cutting machine could have a mean performance of -1mm (that is it has a tendancy to cut 1mm short of the required length) with a variance of $2mm^2$ [7].

The value of the mean and variance define the performance distribution of the process. This enables the structure being produced to be evaluated against requirements.

This data could, in turn, be stored into a database linked to a CAD system. This would enable a designer to anlyse the capability of production to produce components to tolerance at a given work station.

FIGURE 5.I CAPABILITY CHART

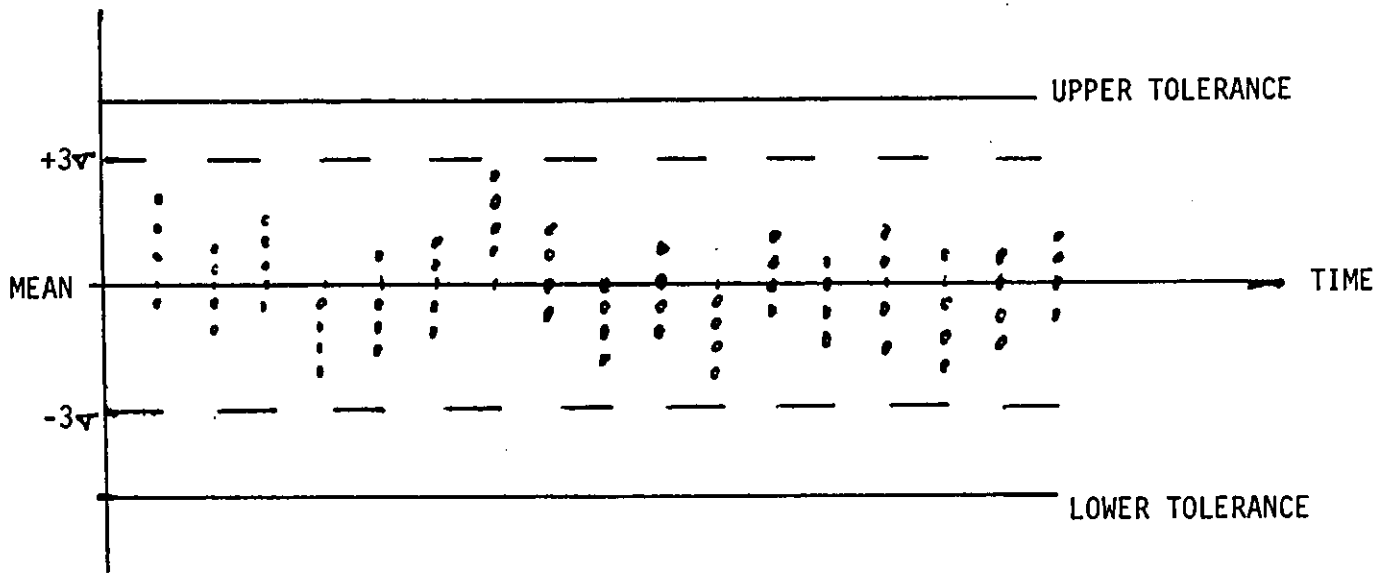

5.4. Merging Equations.

Having identified a methodology for predicting the performance of individual processes and therefore, the capability of producing components to tolerance. The next stage is to predict what would happen once these components are put together to create an interim or finished product.

To do this analysis, use is made of two basic statistical theories. The theory of summation of Means and the theory of summation of variance[8].

The concept of merging equations is used to predict the accumulation of error at various stages of manufacture. The total error for any manufacturing process is given by[9]:-

$$Z = \Sigma P_i + \Sigma S_i + \Sigma A_i + \Sigma E_i$$

where:
Z = total error
P = sum of errors in the process
S = sum of errors in subassembly
A = sum of errors in assembly
E = sum of errors in erection.

This enables us to generate two different but related equations.

i) Variation merging equation.

This equation sums the mean variation of processes using the theory of summation of means.

ii) Variance merging equation.

This equation sums the variance of processes using the theory of summation of variance.

The result for a structure, are two equations with a term by term correlation.

An example for a 2 plate panel is shown in figure 5.2.

Figure 5.2. Derivation of Merging equations for a two plate panel.

W = width overall

S = shrinkage

G = alignment gap

A = width plate 1

B = width plate 2

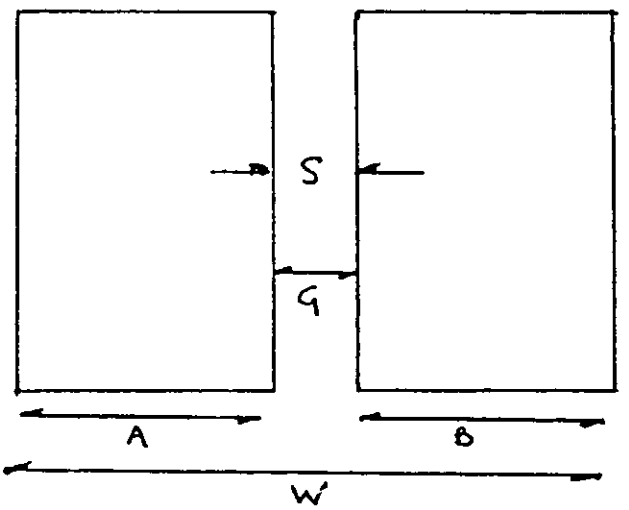

Sequence

Activity	Mean (mm)	Variance (mm^2)
cut plate 1	+1	2
cut plate 2	+2	1
Aign	-1	2
weld (shrinkage)	-3	3
	+1	8

current capability = -7.4mm to 9.4mm
on a tolerance of $\pm$3mm
percentage in tolerance = 68%

These simple techniques could be used, through a CAD system, to confirm the capability of production to produce a particular product. This would provide the designer with feedback on how the design may best be modified to enable the required structure to be produced first time. Applicability of the prototype method can be demonstrated by the example presented in the following section.

6. EXAMPLE OF THE PROTOTYPING MODEL.

Consider the built up stiffened deck plate panel shown in figure 6.1 which has been designed for manufacture at a facility.

The panel is required to be within a tolerance of -6mm to +2mm for the overall width. The designer having generated the design, now needs to confirm whether or not it is feasible to manufacture it and if not, how much rework is likely to be involved.

The following process data and information is available:

The panel is made of plates that are 6m x 1.5m

Process data (for axis O X)

	$\bar{X}$ (mm)	V (mm^2)
Plate cutting	+0.5	0.9
Plate alignment	+1	0.6
single sided welding shrinkage	-4	1.2
shrinkage per stiffener	-1	1.0
shrinkage per web	-1.5	1.3

a) Initial analysis.

The initial analysis gives the following results:

Variation merging equation.

$$\bar{X} = (5x0.5) + (4x1) + (4x - 4) + (8x - 1) + (3x - 1.5)$$

$$= -22mm$$

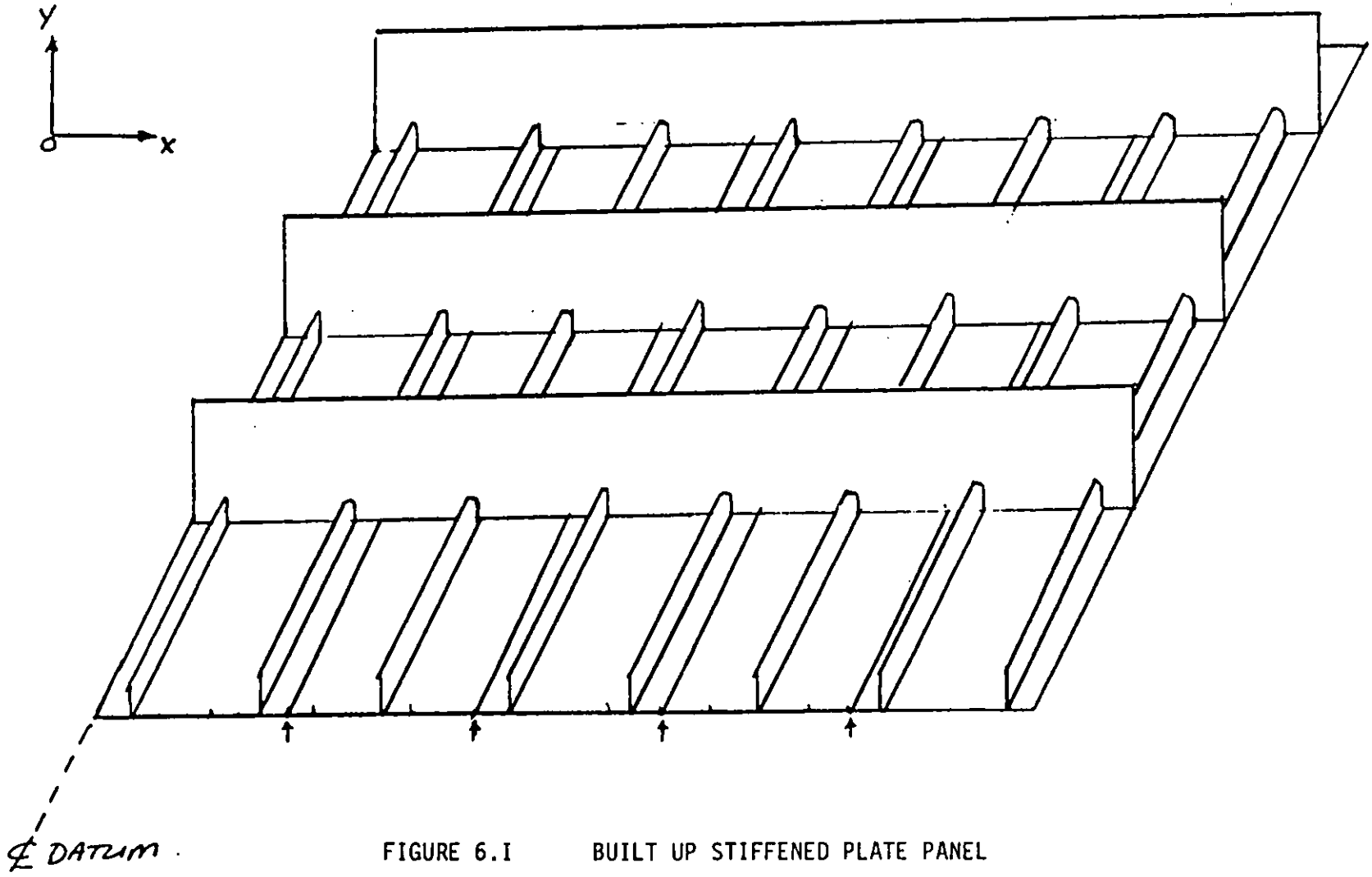

FIGURE 6.I BUILT UP STIFFENED PLATE PANEL

Variance merging equation.

$$V = (5x0.9) + (4x0.6) + (4x1.2) + (8x1) + (3x1.3)$$
$$= 23.6mm^2$$

The first thing the designer can note, is that the combined effect of shrinkage and cutting processes leaves the structure 22mm too narrow on average. Thus an allocation of +20mm would be required to bring the structure to -2mm (the middle of the tolerance band range).

The capability of the process is

$$\pm 3\sigma = \pm 3 \times \sqrt{23.6}$$
$$= \pm 14.57mm$$

This gives a probability of rework of 41.8% obtained from:

$$Z_1 = \frac{x - \bar{x}}{\sigma} = \frac{-6 - (-2)}{4.857} = \frac{-4}{4.857} = 20.9\%$$

$$Z_2 = \frac{x - \bar{x}}{\sigma} = \frac{2 - (-2)}{4.857} = \frac{4}{4.857} = 79.1\%$$

Rework = ((100 - 79.1) + 20.9) = 41.8% on a tolerance of -6mm to +2mm.

b) First modification.

Consider now what would happen if the designer changes plate size to 6 x 3m.

Variation merging equation.

$$\bar{X} = (3x0.5) + (2x1) + (2x - 4) + (8x - 1) + (3x - 1.5)$$
$$= -17mm$$

Variance merging equation.

$$V = (3x0.9) + (2x0.6) + (2x1.2) + (8x1) + (3x1.3)$$

$$= 18.2mm^2$$

Allocation = 15mm
Process capability = $\pm$ 13.0mm
Probability of rework = 35%

c) Second modification.

Reducation in number of stiffeners to 6 by increasing scantlings and improved cutting machine performance from production.

New process values.

	$\bar{X}$ (mm)	V (mm^2)
shrinkage per stiffener	-1.2	1.0
cutting machine performance	0.5	0.6

Then,

$$\bar{X} = (3x0.5) + (2x1) + (2x - 4) + (6x - 1.2) + (3x - 1.5)$$

$$= -16.2mm$$

$$V = (3x0.6) + (2x0.6) + (2x1.2) + (6x1) + (3x1.3)$$

$$= 15.3mm^2$$

Allocation = 14.2mm
Capability = $\pm$ 11.73mm
Percentage rework = 31%

Thus, it can be seen, that product prototyping can encourage a designer to use larger standard components and minimise the number of processes, to reduce the probability of rework and improve design for production. This is done by control of variation.

In addition, the prototype modelling process, can encourage designers to discuss problems with production to see what improvements to particular manufacturing processes can be made, again with a view to minimising rework.

Although the example shown is quite straightforward, it does clearly illustrate the benefits of prototype modelling. Thw whole process is relatively easy to computerise but needs to be accessed by the designer.

The example does clearly show the benefits that could be gained from prototype modelling however one important aspect must be demonstrated.

d) Third modification.

If the original structure is taken then an allocation of 20mm was required and process capability was $\pm$ 14.57mm.

If the tolerances could be relaxed to -7mm to +3mm then the probability of rework recalculated, a rework probability of 31% would be obtained.

This reinforces the need for clear and accurate definition of tolerances and for designs to take into account the nature of tolerance build up. Poor allocation of tolerances will lead directly to increased rework levels.

7. CONCLUSIONS.

Product Prototyping at the design stage offers consdierable benefits in improving the producibility of designed structures. It provides a mechanism by which the designer can appreciate and quantify production problems, that may arise as a result of design decisions.

Through the use of CAD, the designer can be provided with a powerful tool for rapidly changing designs and producing alternative configurations in response to operational criteria. The development of product prototyping would enable the designer to rapidly and simply optimistic the design for both operation and production. The process has been computerised as a stand alone system but in the short term, its integration into a CAD system would be essential for its broader application.

REFERENCES.

1. The Strategic Development of Ship Production Technology.
M.R. Hargroves, J.A. Teasdale and R. Vaughan. Trans. NECIES, APRIL 1975.

2. Engineering Mathematics.
Bajpai, Mustoe and Walker, Wiley, 1984.

3. A Study of Accuracy Control in Hull Construction Work.
Yokata, Minamizaki, Hori. J. Soc. Nav. Arch., Japan, 114 (1963) p. 242 (Dec.).

4. A Conceptual Ship Design System Incorporating Expert Knowledge.
M. Welsh, PhD Thesis 1990, Newcastle University.

5. Quality Planning and Analysis.
J. Juran, Gryna, McGraw Hill 1988.

6. Statistical Quality Control.
Grant and Leavenworth, McGraw Hill 1980.

7. Application of Statistical Process Control Techniques to Shipbuilding.
M.R. Kattan, Trans. NECIES, Vol. 105, No. 4, Sept. 1989.

8. Introduction to Statistics.
Walpole, Collier Macmillan 1974.

9. see reference 3.

ADVANCED SHIP AND OFFSHORE DESIGN TECHNIQUES

DEVELOPMENTS IN DESIGN WHICH SUPPORT PRODUCT PROTOTYPING

W. Hills
Director, Engineering Design Centre
University of Newcastle upon Tyne
Newcastle upon Tyne, NE1 7RU

1. INTRODUCTION

The characteristics of made-to-order products usually mean that prototypes cannot be produced. Effective prototype modelling of the design and manufacturing processes is crucial to the success of the design process. The decision making process in design takes place in an uncertain environment, management intervention will be necessary. It is inevitable that changes will be made during the design process. The guidance offered to those involved in design and the associated processes when making such decisions must be made in a way which does not impede the effectiveness of the design process. It is important that we develop our systems in this context. This lecture is intended to provide an overview of current research aimed at developing methods which support the process of prototype modelling.

The importance of effective databases in design cannot be over-emphasised and the concept of Object Oriented Data Base Management Systems (OODBMS) is introduced. The application of an OODBMS is described in detail via an example relating to cost estimating.

2. PRODUCT CHARACTERISTICS AND THEIR INFLUENCE ON THE DESIGN PROCESS

Marine vehicles, offshore production plant and made-to-order products can be characterised by; their complexity, they are made-to-order and often to an individual customer's specification. They are high value (often hundreds of millions of pounds) with many components and many sub-assemblies and often tens of thousands of different parts, they sell on functionality in which life cycle costs may be more important than first cost. There will be many technologies incorporated into the product. They are knowledge intensive and advances in technology have an immediate impact, the introduction of a new technology cannot be deferred. The design process can last several months and the production process several years. The advance has to be incorporated into the design process as it occurs and in some cases this means modifying the product during the manufacturing process. The products will

often have to operate in hostile environments and process hazardous materials in conditions where size and space requirements have to be minimised and safety is paramount.. Clearly the implications of the foregoing are far-reaching for both the designer and the systems he needs to support his activities. The product characteristics and the influence of manufacturing and operations imply a necessity for a wide range of design tools, which while being applicable to specific domains, also have features which are generic and support the design and associated decision making process across a range of product types.

3. RESEARCH ISSUES

The design of MTO products takes place in an environment in which there is a need to provide an interface with manufacturing. Each product may be unique, a major difficulty is the identification and development of generic methodologies and processes.

There are large amounts of data and there is a need to exchange this efficiently and in standard form, often between companies several thousands of miles apart. The need to represent design models in a manner which reflects the way in which they will eventually be produced suggests an object oriented approach. These issues support the more focussed activity of providing support for the decision making process.

Decisions relating to the design and product development of MTO products are taken in situations in which there is a high level of uncertainty, a complex cost structure, a requirement to minimise risk and optimise the usage of space. The problems have multiple criteria which may conflict and designers will have differing perceptions of the relative importance of their criteria. The requirement to provide flexible systems based upon generic principles which can be adopted in domain specific issues suggests that knowledge based systems could be used to advantage

These issues form part of the core of the research programme at the Engineering Design Centre at Newcastle University. The projects most closely related to the decision making process are:

1) Multiple Criteria Decision Making
2) Expert Systems in Spatial Layout Design
3) Cost Estimating
4) Design for Safety

It would be unrealistic to develop design tools and methods in isolation. The design decision process requires interaction between each of the models. This implies a level of integration, where the use of product information models facilitates such a process. This is utilized in a process of integration which is the topic of a major project:

5) Project Integration Methodologies

Summaries of these five projects follow:

3.1 Multiple Criteria Decision Making

Design takes place in a complex, multi-criteria environment and the principal aim of this project is to produce an engineering decision support environment based on multiple criteria decision making methods, and to demonstrate the use of the environment using two examples from different domains in engineering design. The first version of this environment is now ready. This incorporates eight distinct methods: four each for design selection and for design synthesis. A semi-submersible design model and several selection problems have been successfully solved using the environment. Several other problems are currently being dealt with in discussion with industrial partners like NEI Parsons (Optimal design of turbo-generators) and Swan Hunters (Engine selection) and the MOD (multi-role naval vessels). Supporting work has been done on: (i) Mathematical treatment of subjective attributes. (ii) Interactive analytical methods for estimating weighting factors representing the preference ordering of designers using minimum preference information. Initial effort has been concentrated on producing a working environment.

3.2 Expert Systems

Spatial engineering is often a crucial activity in the design of marine vehicles and offshore plant. The primary aim of this project is to apply knowledge-based and emergent-order programming techniques to conceptual layout problems in the field of large MTO products in order to develop a prototype for CAD tools which manipulate and analyse a product's topology, rather than its precise geometry. Numerous contacts with industry have been established, leading to identification of the key components necessary in a spatial information model for large MTO products, and insights into current practice which will be valuable for formulating a specification for an automated spatial design environment. The project now has demonstrable, working first-cut prototypes of a generic layout-oriented product model database schema, a layout annealing system and a means for converting attributes extracted from the former into associativity data to drive the latter. Whilst both still rely to a degree on manual coding to function as intended they are in active use, yielding rules and techniques which will be of use at later stages of the project. Current work proceeds on two fronts. The first is directed towards mechanising the generation of those parts of the overall product model database relevant to layout by adding detail to a template schema which, it is hoped, will prove generic across all the product domains concerned. On the second, the experience gained using the first-cut prototype layout annealing program is being applied to the specification of a second system which will allow ordinary users to perform similar layout generation experiments, adding their own rules to those supplied, and viewing and editing the resultant product topology. These methods are being applied to determine the layout of the topsides of an offshore production platform.

3.3 Cost Estimating

The thrust of the cost estimating project is to establish the extent to which it is possible to develop a generic estimating framework for complex made-to-order products. By linking cost estimating more closely with concept design, then improved designs can be developed and evaluated. In the short time the project has been running, industrial links have been built up, which show great support for improved cost estimating methods using new object oriented database technology. The means of creating generic classes of objects is currently being explored in the context of major components such as pumps and heat exchangers. The

methodology distinguishes between design and performance driven costs and manufacturing efficiency driven costs. These principles are being applied to the cost estimating process for naval vessels and further detail is given in section 6.

3.4 Design for Safety

The work consists of two parts: (i) Those created by problems of architecture and arrangement (e.g. structure subdivision). (ii) Those created by problems associated with engineering systems (e.g. electrical, mechanical, hydraulic etc). The progress to date included the mapping of the principal safety analysis methodologies onto the design plane to identify the inter-relationahips and data flows. This map is forming the basis of a range of analytical developments. These include (i) the Boolean representation of systems consisting of components with multiple potential states to obtain critical transition tables representing all failure paths. (ii) Generalised limit state analysis with elements of parameter control and (iii) Simulation models for examination of the statistical behaviour of critical paths and failure states. Some initial work has also been done on quantitative simulation. The current phase of work is concentrating on application of the developed safety framework with a view to enriching the methodology.

3.5 Project Integration Methodologies

In addition to individual projects a major initiative is being carried out to investigate the mechanisms and procedures necessary to facilitate their integration. The project integration was initially identified as the activity which would bring together the results of the individual projects. Early work in this regard took the approach based on developing a common product data model which would be used to demonstrate the exchange of product information between the projects. This was followed by a study of the functional and data requirements of the projects together with an overview of current approaches to integration. A new strategy was produced for project/design integration as driven by the requirements of the various projects. A layered architecture has been adopted which sees the objectives of integration in terms of a design information repository, design tools, project functionality, design process management and the communication between distributed design agents. These are organised in a distributed and open environment. An object-oriented approach has been adopted to deal with the design classes and the methods to effect design actions in them. A user interface is being prototyped which shows the breadth of the proposed integrated environment through the range of projects and design tools. The depth of the integration process is illustrated by the definition and control of the design process and the level of definition included in the product model as the design proceeds. The process of integration provides a further opportunity to continue the process of identifying and developing the generic features inherent in the individual projects.

4. ENGINEERING DATABASE REQUIREMENTS IN SHIPBUILDING AND OFFSHORE ENGINEERING

Database requirements and specifications for design vary according to the application and required functionality. However in terms of engineering system and component design our experiences are reflected in a project concerned with electrical systems cost estimation. The most recent work on the electrical cost estimation project has focused attention on detailing the information requirements of the electrical estimator/designer at the concept stage design.

What has transpired from the preliminary research is the diverse nature of information required by the estimator to complete an apparent simple task. For example, selecting the lighting requirements for accommodation area includes the correlation of information from:

- Accommodation layout
- Compartment type
- Owners specification
- BSI ISO, DTI, MOD, IEEE etc Standards
- Company Standards
- Range of possible vendors
- Geometry
- Characteristics of electrical systems
- Environmental factors governing lighting conditions
- Vessel type (eg commercial, MOD)

The derived engineering database will comprise of many different systems, such as the lighting system, which will vary in complexity. It is important to note that the engineering database will not treat data as discrete packets of information. It will take a wider view by associating other systems which will be necessary to complete the information model. Taking the lighting system again, the model would be incomplete without the cabling system, which requires distribution and section boxes etc. The sum of the lighting load will form part of the calculation to determine the generator capacity required to supply the total electrical system.

It is important within this environment to bind the physical data with the methods which will interpret the data. This will give the estimator/designer a flexible way of assembling information to form a unique solution to the design problem. The user is also freed from the task of having to determine what method to apply in a certain calculation as this is bonded with the input and output data. The job of the estimator/designer will be to use his/her experience in selecting the best option available.

The engineering database is not a standalone system. It should be a functional and important part of the whole CAD environment and support effective engineering data management. This environment should provide the estimator/designer with a consistent user interface from which the design can evolve using the engineering database. The CAD environment should, for example, meet or satisfy the following criteria:

- Use a third party database on which all the design information can be both stored and retrieved.
- The ability to enforce the use of standard building blocks such as cabin arrangements, having associative design information such as reflective indices, ie elements of the product model.
- allow access to information which is not native to the system.
- support and provide access to routines which are external to the CAD system, but which may affect directly the work of the user, eg finite element methods.
- Provide methods to customise functionality which best suits the needs of the user, eg menu structure and items available are specific to the user.
- Facilitate the storage of geometrical data in compliance with standards such as ISO STEP. (Standard for the Exchange of Product Model Data).

The time available to develop and test the implementation of the engineering database is usually short considering the complexities that have to be overcome to make it successful in operation. It is, therefore, imperative that the database and development language should be tightly integrated to reduce development time. The ISO STEP model should be easily developable on the database, making the engineering database CALS level 2 and 3 compliant (this is how data is represented in a database and communicated electronically). The use of STEP should ensure the adapability of the database to incorporate, for example, production information at the concept design stage. However, the ability to communicate technical and design information with other systems will be the real strength of the STEP model.

5. OBJECT-ORIENTED DATABASE MANAGEMENT SYSTEMS (OODBMS)

OODBMS represent the latest software technology in database management systems, which views the data, not as a series of discrete numbers, but as all the elements or attributes inherent in an "object" - dimensions, performance, inter-relationships etc. They incorporate all of the features found in Relational Data Base Management Systems (RDBMS), but also extend capability including the features found in object-oriented languages such as C++ and Smalltalk. Also included are notions of object identity, encapsulation, classes and inheritance (see Section 6). The appeal of OODBMS is derived from two salient factors:

a. The data model more precisely matches real world entities (See figure 1). Objects can be stored and manipulated directly, there is no need to transform application objects to tables. Data types can be defined by the user, rather than being confined to certain pre-defined types.

b. The database language can be integrated with an object-oriented programming language, so helping the programmer, of say, decision procedures to link them with a single uniform model of the particular objects. This would ensure continuity of information between say basic design and design engineering.

The first factor is instrumental in bringing DBMS capabilities to applications that have complex data (eg CAD, CAM,). Relational databases have not been able to meet the data type scope and performance requirements, for example, representing geometrical entities. The second factor contributes to the improved consistency productivity that may be gained by not having to adapt or re-define information from a variety of sources. This is because the impediments that result when the programming language and database language are different is not an issue with an OODBMS.

The Rapid Acquisition of Manufactured Parts (RAMP) project is a US Navy program employing Computer Integrated Manufacturing (CIM) technologies and Computer Aided Acquisition and Logistics Support (CALS) standards to facilitate parts procurement within the US Navy supply system. Initial development of the system using ORACLE (a relational database) to hold design information has now been superseded with the use of VERSANT, an object oriented database.

Database operations have improved greatly in efficiency. The use of VERSANT has facilitated the incorporation of the STEP geometrical model and allowed information from the CAD environment to be stored in this format. Development time has improved with the more complex information structures naturally represented within the OODBMS.

The move towards developing CAD/CAM and other applications using object oriented design and programming principles linked to a product model definition is fast gathering pace. Recent communications with development staff at Kockums Computer Systems (KCS) has revealed that their shipbuilding and detailing applications will be replaced by a new application called the Ultimate Shipbuilding Systems (USS). This new system is being developed using object oriented methods and the C++ language. The application will use a third party object oriented database to store all data, so showing the way that developments are going in the industry.

The Japanese have over the last two years completed a pilot study and initiated a prototype for Computer Integrated Manufacturing (CIM) for shipbuilding. This system is based around the use of object-oriented languages and databases, but will use a specially developed CAD/CAM environment to drive the applications. Development work is still apace, but is approximately 2-3 years ahead of the European NEUTRABAS Espirit project, in providing usable tools for the user.

6. ELECTRICAL COST ESTIMATING

6.1 Some Computing Considerations

The electrical cost estimating system, which initially focuses on the lighting distribution system for both commercial and naval ship types, is currently under development. This

software system is an advanced prototype technology demonstrator, which is intended to be used alongside traditional estimating methods by electrical cost estimators. The software technology employed uses advanced C++ programming features such as inheritance, encapsulation and polymorphism. An object oriented database VERSANT, is used to store the rich variety of abstract data associated with a complex computer aided design and estimating system. Before examining the electrical cost estimating system a brief explanation by example of some of the C++ language features used, may be of help.

What is an object?
How is it affected by encapsulation?
What is inheritance?
How do we benefit from polymorphism?

- What is an object?

Unfortunately there is no straightforward answer to this question. Is is dependent upon who is answering the question. The important point to note is that objects exist at many levels. At the lowest level, objects are tightly combined at compile time, and have an extremely low overhead for communication with other objects at the same level. However, the tight coupling of objects at this level limits their re-use. At the highest level, objects are very loosely coupled together, communicating via pipes and filters. These objects can be conveniently re-used but there can be a high penalty in execution time overhead during this process. The electrical cost estimating system is built using both of these object types.

- How is an object affected by encapsulation?

Each object encapsulates a private part (its own data) and a part that is shared (a set of methods to access the data) among all objects of the same class.

- What is inheritance?

This is really specialisation. A new class can be defined by taking a more general class and specialising it to meet a particular need. Classes built in this way are organized into what is commonly referred to as an inheritance hierarchy.

- How do we benefit from polymorphism?

Essentially, it allows a method, or operation to take on a form which is specific to an underlying context. For example, a method of time could be defined in three separate ways within a class.

```
time ( );
time (int);
time (int, int, int);
```

The correct method would be invoked dependent upon the number and type of parameters provided.

The electrical cost estimating system is constructed from three types of objects.

- *model* objects are those that represent the underlying application domain.
- *view* objects are those responsible for presenting the information contained in the model to the user.
- *controller* objects are those that manage the interaction between the user and the application.

6.2 Application of the System

The electrical cost estimating system has been designed as an aid for the electrical cost estimator/designer at the concept design stage. This stage of design evaluation is the most fluid in the design process and the electrical cost estimating system is designed to allow rapid re-evaluation of design changes. The primary function of the system is to perform the repetitive quantitation analysis and to check compliance of equipment with required standards. Fig 2. gives a conceptualised view of the system under development. This shows an engineering database, which holds technical information on such items as generators, transformers and electrical cable suppliers. This information is represented within objects, which also combines the design methods necessary to evaluate the data. This facilitates design evaluations to be made. For example, the electrical cable data, will have associated with it, the methods which will allow the correct cable type and size to be selected, dependent upon it's connected function and operational environment.

For each concept design enquiry, a product model is created and this will eventually consist of a diverse range of systems. The current focus of the electrical cost estimating systems is the lighting distribution system, but many of the underlying software principles can be extended into other systems, such as the piping distribution system.

Fig 3. shows a screen shot of the graphical front end, through which the user will communicate with the technical and graphical data of the application.

7. CONCLUDING REMARKS

Clearly it is impossible to cover every aspect of product prototyping during a single lecture. By covering those elements of current research activity dealing with the decision making process, I believe I have been able to highlight some fundamental aspects of prototyping. The application described illustrates the importance of standard, yet flexible data structures. It has been suggested that OODBMS's are an important development and a great deal of current research world-wide is aimed at utilising this new technology in an effective way. The importance of retaining an overall view of the design process cannot be over-emphasised. Individual elements of prototype modelling have to be integrated within practical, working environments. Those features which facilitate connectivity and integration of model elements need to be given a high priority during the earliest stages of product and model development.

Product Constructed By Objects

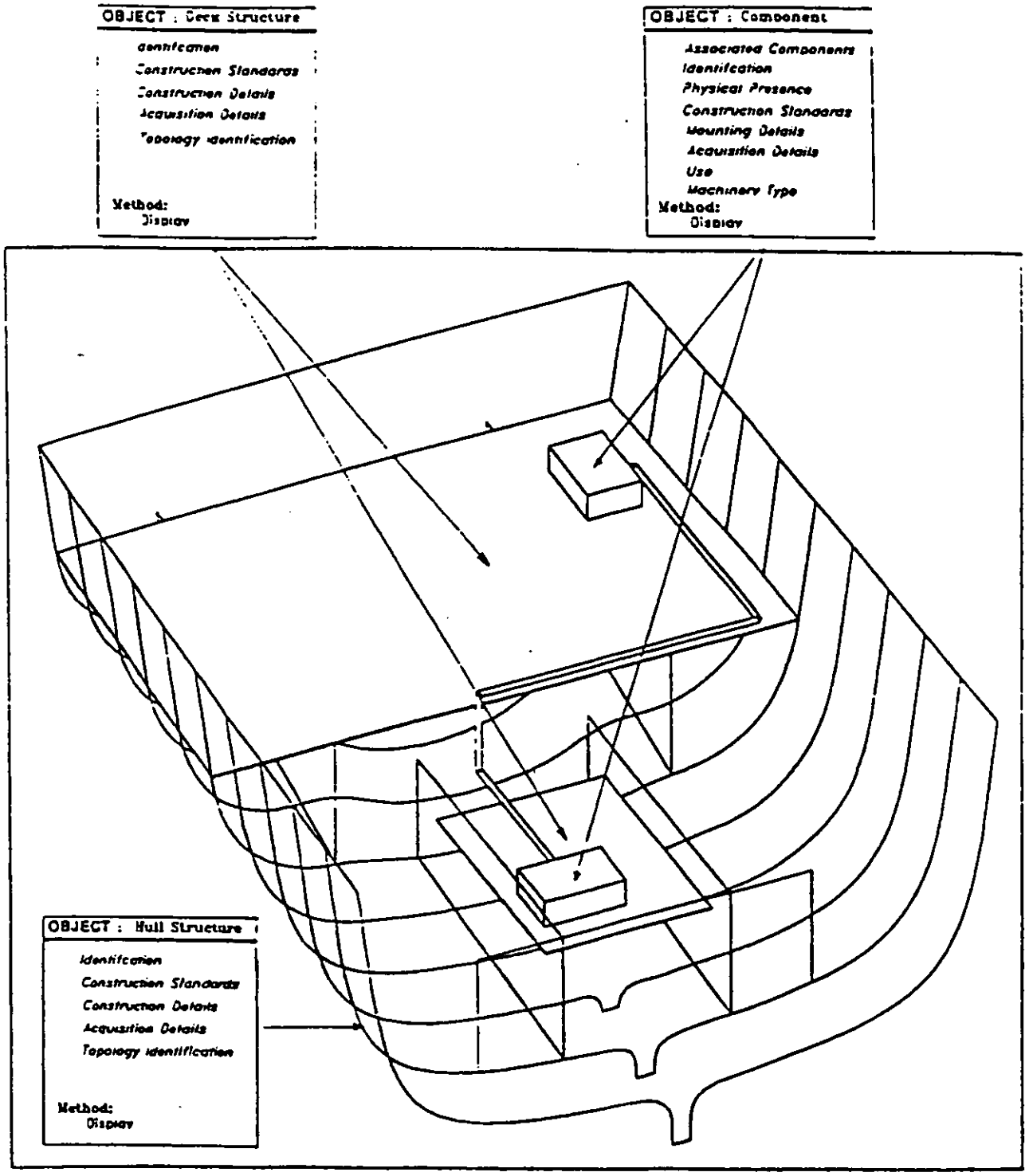

Figure 1

Electrical Cost Estimation Project Database Model

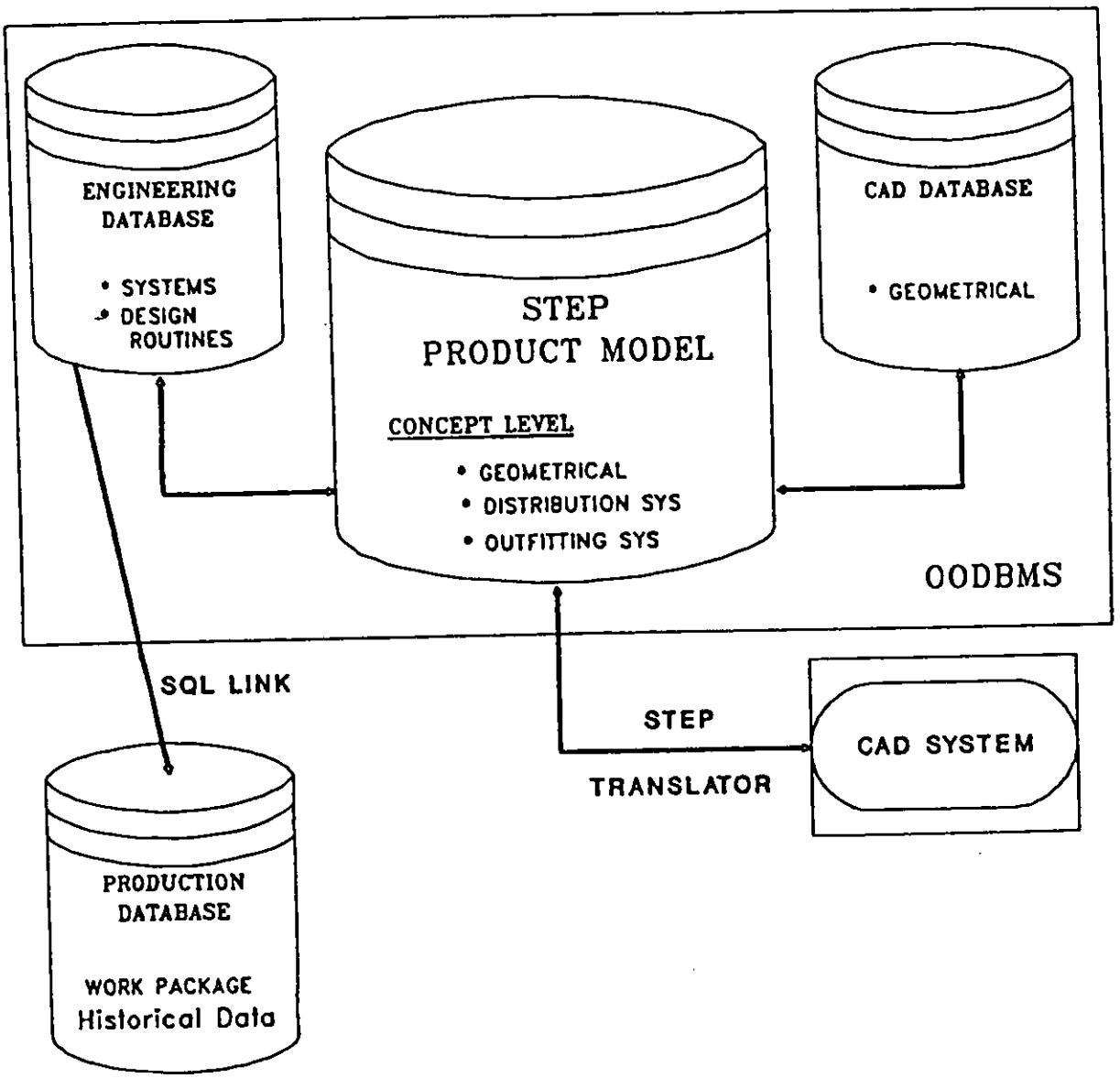

FIG 2

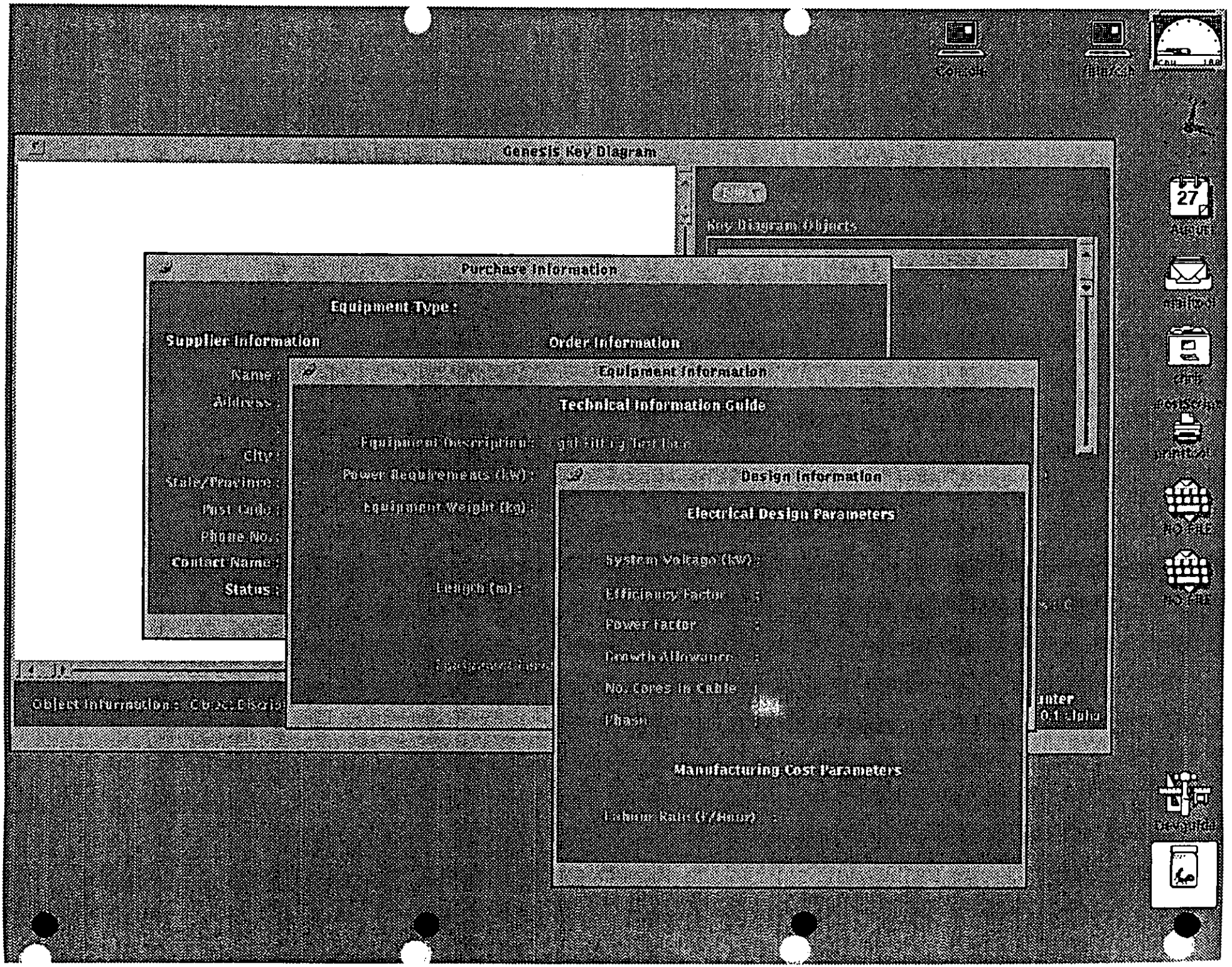
Genesis Key Diagram
Key Diagram Objects
Purchase Information
Equipment Type :
Supplier Information
Order Information
Name :
Address :
City :
State/Province :
Post Code :
Phone No. :
Contact Name :
Status :
Equipment Information
Technical Information Guide
Equipment Description :
Power Requirements (kW) :
Equipment Weight (kg) :
Length (m) :
Design Information
Electrical Design Parameters
System Voltage (kV) :
Efficiency Factor :
Power Factor :
Length Allowance :
No. Cores in Cable :
Phase :
Manufacturing Cost Parameters
Labour Rate ($/Hour) :
Object Information :
Console
Filter/Sch
About
Mail (0)
Drift
Scripts
Printout
No File
No File
Design Aid

FIG. 3

The Use of a Product Modelling Approach to Create a Ship Design and Associated Production Information

1. Introduction

The competitive nature of the shipbuilding industry has for many years and will continue in the future to press shipbuilders to use new methods and techniques to reduce contract elapsed times and manhours.

The paper sets out a method to reduce both of these factors by the adoption of a product modelling approach in design.

2. Shipbuilding Process

The shipbuilding process is very complex with many activities running in parallel. For example the design is still being developed as the production starts. The need for more efficiency means the overlapping of activities must become more and more complex. A new buzz word has been introduced in some industries to describe this situation called "Concurrent Engineering". This is nothing new to the shipbuilding industry as activities have been overlapped for many years. What is interesting is how much activities can be overlapped as this to a large extent controls how efficient any organisation can be.

3. Key Technical Factors for Efficient Shipbuilding

We believe the key technical factors which influence the overlapping of activities and hence the efficiency of ship production are.

Design for production	Try to ensure that the design can be easily produced and so reduce the production manhours for the product
Early unit breakdown	By deciding the units early further design can take this into account to ensure the units can be easily constructed as interim products and the necessary material can be ordered and marshalled to meet the building programme.

Prefabrication	By maximising the level of prefabrication more work can be carried out at an earlier stage in the building process. So for example work can be carried out in workshop conditions as opposed to the building berth and so reduce the cost of the work.
Preoutfitting	By installing outfit items on hull assemblies and sub assemblies before the ship's hull is erected the cost of outfitting can be reduced.
Complete and consistent production information	Production information specifically created for each stage of manufacture can improve the efficiency of the operation as all necessary information is in one document and workers do not have to search for information. Consistent information ensures that when manufactured items are joined at later stages in the building they fit together correctly.
NC, DNC and robotics	The use of NC and robot equipment can reduce the labour costs for items of work. It is important to be able to create the control information for these machines directly from the design and be able to respond quickly to changes in the building programme and design.
Quality Control	The control of quality at each stage of production can reduce the rework at later stages.

4. Systems Philosophies

There are many different solutions using computer aided techniques in the handling of information in the design and building of ships to improve the above key factors. We feel that there are two main approaches. A "General Purpose Computer Aided Design" approach and the "Shipbuilding specific

with Product Model" approach.

The two approaches can look graphically the same when a small part of a project is examined. The general purpose approach concentrates on drawings or files of 2 Dimensional or 3 Dimensional graphical information. These type of systems can also often work in 2D and typically have attributes of some kind attached to the graphical pictures.

Each project will be composed of many drawings or model files. In these systems the graphical drawing or graphical model file is the principle unit of information. All information is grouped by drawing or file and it is difficult to extract the graphical or attribute information without handling it drawing or model file at a time. To reuse information a lot of manual work is necessary to copy between drawings or files. Of course the system can help with this but it is very like the manual process of copying from one drawing or document to another. The main output from these systems is 2D or 3D drawings.

5. Shipbuilding Specific System with Product Model

We believe that the handling of graphics is only part of the job and to make graphical pictures or drawings will not build ships. We think that we are in the business of handling information in the shipbuilding process to achieve reduced manhours and savings in lead time.

Our approach therefore concentrates on the information in the design and stores the information in the form of objects such as pipes, brackets, cables etc. These objects can be sorted in any order and presented on drawings or text reports. The way the objects were created does not effect how the information can be extracted as the objects are in one single database and can be accessed by all in the design process. The objects can be refined as the design continues without rework of data as it is only necessary to add the additional data required. Because the information is stored as objects and not graphics the system knows how each item is to be manufactured so production information can be created automatically. The system ensures that the information necessary to create production information for items is stored in the product model.

To summaries in a general purpose system data is stored as graphics with attributes attached but in the our solutions the information is stored as objects which can be generated easily into graphics pictures or drawings if required. But equally well can be used to create production information.

6. Product Model

Our Product Model is not based on 3 Dimensional graphics but the handling of shipbuilding information that can of course to displayed as graphics but it can also be displayed in lists and reports. We do not store the 3D graphical shapes of all items rather the model database is a description of model objects and graphics are only created to view the model when required. Objects can be displayed as symbolic information, a 2D drawing or as a 3D model depending on the stage of design. By handling the objects as the primary source of information rather than the graphical information the flow of information in the design process is streamlined.

This approach also means that drawings and reports can be easily extracted across a whole project by any selection criterion independent of how the data was created.

The system handles the integration of information and it is not necessary to link your session to new files or drawings or copy files to your session. New model items are instantly available to all users within disciplines and across disciplines (eg Hull and Outfitting) once the items are created.

The building of the product model is a refining process that begins when the first product information is registered in the system. The could simply be an equipment item name and its function. This equipment object is refined during the process as for example its system connections become known this can be added as can the compartment it is location in. Similarly a symbol representation for use on a diagram and the 3D graphical information from a makers drawing can also be added. The principle is that once some information is known it should be registered for use in later stages of design and in should be easy to refine the information. It is quite like the physical process of shaping a piece of wood into a wooden ship model.

Extensive use is made of topology information in the building of the model with the modelling tools. This topology can be used to ensure swift modification of a model item when a topologically referred item used in its construction is modified. The modelling tools which are specifically designed for each type of model item to make modelling as efficient as possible have also been built to make the maximum use of topology when creating and modifying items.

Finally the Product Model because of its nature allows us to produce automatically the many different type of production information needed to build a ship efficiently. Specialised production information creation programs speed up the creation of production information and provide a consistent and efficient type of information.

7. Conventional Organisation

To illustrate why we have chosen a product model approach we need to look at the information flow in a shipyard. In the conventional organisation with a drawing or file based approach the flow of information is very complex. This environment has a lot of documents moving around and the situation is characterised by

- Many organisational units or sections
- Much handling of documents files and drawings
- Considerable double work of copying work from one section before adding data by the next section in the process.
- Easy to make errors and create inconsistent data during copying and handling

A general purpose system can of course help to improve the situation to some extend by reducing the copying work. However it will not significantly effect the manhours required or the leadtime as the same number of steps and operations have to be carried out as in the manual process.

8. Organisation using Product Model approach

With the Product Model approach both manhours and leadtime can be reduced as information is available to all in the design process immediately. This allows many designers to work in parallel so speeding up the process. The situation is characteristed by

- Floating organisation where the designers can work with each stage of design as required as the project progresses. The tools allow the designer to be much wider in the functions he can undertake.
- Much reduced volume of documentation
- Minimal double work. No copying is required as the design is available to all authorised to see it.
- The information is correct first time and consistent across the design.

The net result are considerable savings in design time. In addition the object nature of the data base means that production information can be derived automatically from the model giving further savings in design manhours. The high quality of the production information also means that major benefits can be achieved in production. As the production information is automatically created its generation can be delayed to the last possible moment so that as many changes as possible are incorporated in it. This has the effect of reducing rework in both design and production.

9. Product Model Features

To summarise the Product Model features are

- A shipbuilding object oriented database for all type of object found on a ship. This ensures uniform data across a design created by many designers that can be reused by all.

- Powerful tools to build and change the ship product model using common standards and components. The tools understand the objects and guide the designer in what should be defined each object. The modelling tools also incorporate a range of control and check functions to ensure the product is as easy and therefore as cheap to manufacture as possible. These checks include.
  - modelled items are suitable for manufactured using shipyard facilities (ie can a pipe be bent in an NC pipe bender)
  - collision checks to confirm the layout of modelled items
  - rules for connecting model items (ie ferrous and non ferrous material can not be connected directly)

- Handling of design information at all levels of detail so that information can be registered only once and then refined as the design progresses. This means less duplication of work in the design and a high level of reuse of data. For example equipment item can be registered in the product model directly from the ship specification with no graphical representation. Then later a symbol can be added to the equipment for use on the diagram and later still a 3D graphical image can be added from the makers drawings. All this information goes to up date the object in the database in a refining process.

- Topology information is stored in the product model to speed up changes. Items are placed by references to existing objects so if the first object is changed the second can be updated

- Automatic production information means very little effort is required to produce production information once the design is made. Therefore as this also means production information can be made in a very short time two additional benefits can be had.
  - production information can be made earlier to have an early start of production
  - creating of production information can made just before being required in production so as much design

developments and changes can be incorporated and the information will be as up to date as possible. This means less rework in design and production.

The automatic tools are well tried and tested so the information is very accurate and free of errors which again means less rework in production to make parts fit.

Finally the output information can be easily tailored to the facilities of each shipyard.This ensures that the production information created makes best use of the shipyard facilities such as NC machines etc and hence reduces production costs.

- The model is a true single source of data about all aspects of the design both hull and outfitting which is available to all. In this way design progress and changes can be rapidly passed round the organisation. Also information will be consistent across the design as all are using a common database and so production information will be consistent ensuring that parts and units will fit more accurately to one another.

10. Conclusion

The benefits from our product model approach depend on many factors including how efficient an organisation is to day. However from experience we know the benefits to be

- Reduced elapsed time from contract to delivery
- Reduced manhours in design and production
- Reduced capital employed
- Reduced cost for materials
- More effective utilization of resources

The use of a product model is not just a technique but a complete way of working. Any organisation wishing to use this approach must be prepared to modify its structure to gain the maximum benefits from this way of working.

DESIGN AND THE DICTATES OF PRODUCTION

A Small Shipbuilding Perspective

by

K.G. FULFORD

Ferguson Shipbuilders Limited,
GLASGOW

DESIGN AND THE DICTATES OF PRODUCTION

A small Shipbuilding perspective.

K G Fulford Ferguson Shipbuilders Limited

Topic List

(a) SHIPBUILDING OBJECTIVES

(b) DESIGN OBJECTIVES

(c) THE PRODUCTION PROCESS

- Integrated Systems
- Pre Outfitting
- Pre Fabrication

(d) LEAD TIME

(e) PRELIMINARY DESIGN AND MARGINS

- Weight
- Performance
- Stability

(f) STEELWORK

- Classification
- Rationalisation
- Optimisation

(g) OUTFIT

- Owner Preferences
- Statutory Requirements

(h) MACHINERY

- Owner Preferences
- Statutory Requirements

(i) OPTIMISATION/REGULATION

(j) DELIVERY PROGRAMME

(k) FINAL DESIGN AND MARGINS

(l) DEFENSIVE DESIGN

EQUIPMENT PROCUREMENT SCHEDULE

SYS	PART TYPE	DESCRIPTION	REQUIRED WEEK	LEAD TIME	ORDER BY WEEK
010	PLTA	STEEL PLATES	T.S.P		
010	SECM	STEEL SECTIONS	T.S.P		
030	LADR	LADDERS	F.S.L		
030		STAIRTREADS	20		
040	DRWW	WEATHERTIGHT DOORS	21		
040	MNHS	MANHOLES	F.S.L		
050	PNTA	PAINT	18	10	8
050	CATA	CATHODIC PROTECTION	15	4	11
070	DERM	MASTS	F.S.L		
100	PACI	INSULATION SUPPLY / INSTALL	20	8	12
110	DCKL	TILING & FLOOR COVERING	30	10	20
140	PANA	JOINERS BULKHEADS	21	10	11
140	MANF	ACCOM. OUTFIT INSTALL	21	10	11
140	FRNW	FURNITURE	25	10	15
140	NAMW	NAMEPLATES	25	4	21
140	TIMT	JOINERS TIMBER	T.S.P		
140	IRNH	IRONMONGERY	T.S.P		
150	GARR	GALLEY EQUIPMENT PACKAGE	31	10	21
150		PRESSURE CLEANER	37	10	27
160	WINP	WINDOWS	21	16	5

T.S.P. = TO SUIT PROGRAMME
I.P. = IN PROGRESS

FIG. 5

EQUIPMENT PROCUREMENT SCHEDULE

SYS	PART TYPE	DESCRIPTION	REQUIRED WEEK	LEAD TIME	ORDER BY WEEK
160	WINX	WINDOW BLINDS	25	8	17
170	STOB	OUTFIT TOOLS	37	6	31
200	ANCB	ANCHORS & CABLES	30	16	14
200	WNHW	WINDLASS/CAPSTAN	25	15	10
200	MRGB	BOLLARDS	F.S.L		
200	MRGA	FAIRLEADS	25	5	20
200	RIGT	MOORING ROPES	40	4	36
210	FRDA	FIRE DETECTION	T.S.P	12	
210	FREC	SPRINKLER SYSTEM	T.S.P	12	
210	FRES	CO2 SYSTEM	T.S.P	12	
210	FRFE	FIRE FIGHTING OUTFIT	32	8	24
220	PACV	VENTILATION PACKAGE	T.S.P	12	
220	VENJ	JALOUSIES / LOUVRES	21	12	9
230	DAVR	INFLATABLE BOAT DAVIT	30	10	20
230	LIFD	INFLATABLE BOAT	32	10	22
230	LIFI	LIFERAFTS	32	12	20
230	LIFJ	LSA	32	12	20
410	SPCD	LASHING EYES & SOCKETS	12	8	4
410		HYDRAULIC PIPEWORK INSTALL.	T.S.P		
540	PACA	MACH. AUTOMATION PACKAGE	T.S.P		
540	ALMM	ALARM SYSTEM	25		

T.S.P. = TO SUIT PROGRAMME
I.P. = IN PROGRESS

FIG. 5

SHIP No. 604

EQUIPMENT PROCUREMENT SCHEDULE

SYS	PART TYPE	DESCRIPTION	REQUIRED WEEK	LEAD TIME	ORDER BY WEEK
580	WRKD	WORKSHOP EQUIPMENT	18		
600	PMPU	D.O. TRANSFER PUMP	15	12	3
600	CONV	REMOTE FUEL CONTROL SYSTEM	T.S.P	8	
610	PMPN	L.O. TRANSFER HAND PUMP	15	12	3
660	INSU	EXHAUST INSULATION	T.S.P		
710	PMPO	BALLAST PUMP	23	12	11
710	PMPO	BILGE PUMPS	15	12	3
710	PMPO	OILY BILGE PUMP	15	12	3
710	VLVG	REMOTE BALLAST SYSTEM	T.S.P	12	
720	PACD	DOMESTIC PRESSURE SET	15	10	5
720	HEAW	CALORIFIER	15	10	5
730	PMPS	FIRE PUMPS	15	12	3
740	SANO	SANITARY OUTFIT	25	8	17
810	SUBF	ELECTRICAL INSTALLATION	T.S.P		I.P.
850	PACN	NAVIGATION & COMMUNICATIONS EQUIPTMENT	23	14	9
850	GAUD	DRAUGHT INDICATORS	23		
850	NAIB	COMPASS	37	10	27
860	NASY	WHISTLES	23		
900	MLDS	MODELS	45		

T.S.P. = TO SUIT PROGRAMME
I.P. = IN PROGRESS

FERGUSON SHIPBUILDERS	PLANNING UNITS	SHIP NO.605
	UNIT	1 OF 1

No.	TYPE	DESCRIPTION	FRAMES
001	LM	MAIN DK / SIDE SHELL / BTM UNIT (PORT)	23.5 - 34.5
002	LM	MAIN DK / SIDE SHELL / BTM UNIT (STBD)	23.5 - 34.5
003	GV	FWD SKEG UNIT (PORT)	34 - 46
004	GV	FWD SKEG UNIT (STBD)	34 - 46
005	GV	AFT SKEG UNIT (PORT)	11 - 23
006	GV	AFT SKEG UNIT (STBD)	11 - 23
007	LC	MAIN DK / SIDE SHELL / BTM UNIT (PORT)	34.5 - 43.5
008	LC	MAIN DK / SIDE SHELL / BTM UNIT (STBD)	34.5 - 43.5
009	LC	MAIN DK / SIDE SHELL / BTM UNIT (PORT)	14.5 - 23.5
010	LC	MAIN DK / SIDE SHELL / BTM UNIT (STBD)	14.5 - 23.5
011	LM	MAIN DK / SIDE SHELL / BTM UNIT (PORT)	43.5 - 52.5
012	LM	MAIN DK / SIDE SHELL / BTM UNIT (STBD)	43.5 - 52.5
013	LM	MAIN DK / SIDE SHELL / BTM UNIT (PORT)	5.5 - 14.5
014	LM	MAIN DK / SIDE SHELL / BTM UNIT (STBD)	5.5 - 14.5
015	JA	BRIDGE DK / ACCOMMODATION UNIT (STBD)	29.5 - 39.5
016	JA	BRIDGE DK / ACCOMMODATION UNIT (PORT)	29.5 - 39.5
017	JA	BRIDGE DK / ACCOMMODATION UNIT (STBD)	18.5 - 29.5
018	JA	BRIDGE DK / ACCOMMODATION UNIT (PORT)	18.5 - 29.5
019	HB	BOW UNIT	52.5 - 58
020	HS	STERN UNIT	0 - 5.5
021	LM	WHEELHOUSE	25 - 33
022	WA	PORT BULWARK (CENTRE)	24.5 - 35
023	WA	STBD BULWARK (CENTRE)	21 - 35
024	JA	BRIDGE / GALLERY DK ACCOMMODATION UNIT (S)	39.5 - 50.5
025	JA	GALLERY DK ACCOMMODATION UNIT (P)	39.5 - 50.5
026	JA	BRIDGE / GALLERY DK ACCOMMODATION UNIT (S)	7.5 - 18.5
027	JA	BRIDGE / GALLERY DK ACCOMMODATION UNIT (P)	7.5 - 18.5
028	WB	FWD BULWARK (STBD)	50.5 - 58
029	WB	FWD BULWARK (PORT)	50.5 - 58
030	WS	AFT BULWARK (STBD)	0 - 7.5
031	WS	AFT BULWARK (PORT)	0 - 7.5
032	KM	FUNNEL	22 - 24.5

LEGEND

TYPE

D - CURVED SIDE SHELL
E - FLAT ASSEMBLIES
N - OPEN BTM UNITS
G - CLOSED BTM UNITS
H - BOWS & STERNS
J - DECKHOUSES
K - FUNNELS
C - FLAT SIDE SHELL
L - BLOCK UNITS
W - BULWARKS

AREA

C - CARGO
M - MACHINERY
B - BOW
S - STERN
D - DECK
A - ACCOMMODATION
V - VOID

FIG. 68

FERGUSON SHIPBUILDERS.

SHIP No. 605

FABRICATION PROGRAMME.

DRAFTED BY:- I.HARRIS
CHECKED BY:-
DATE:- 24.02.92

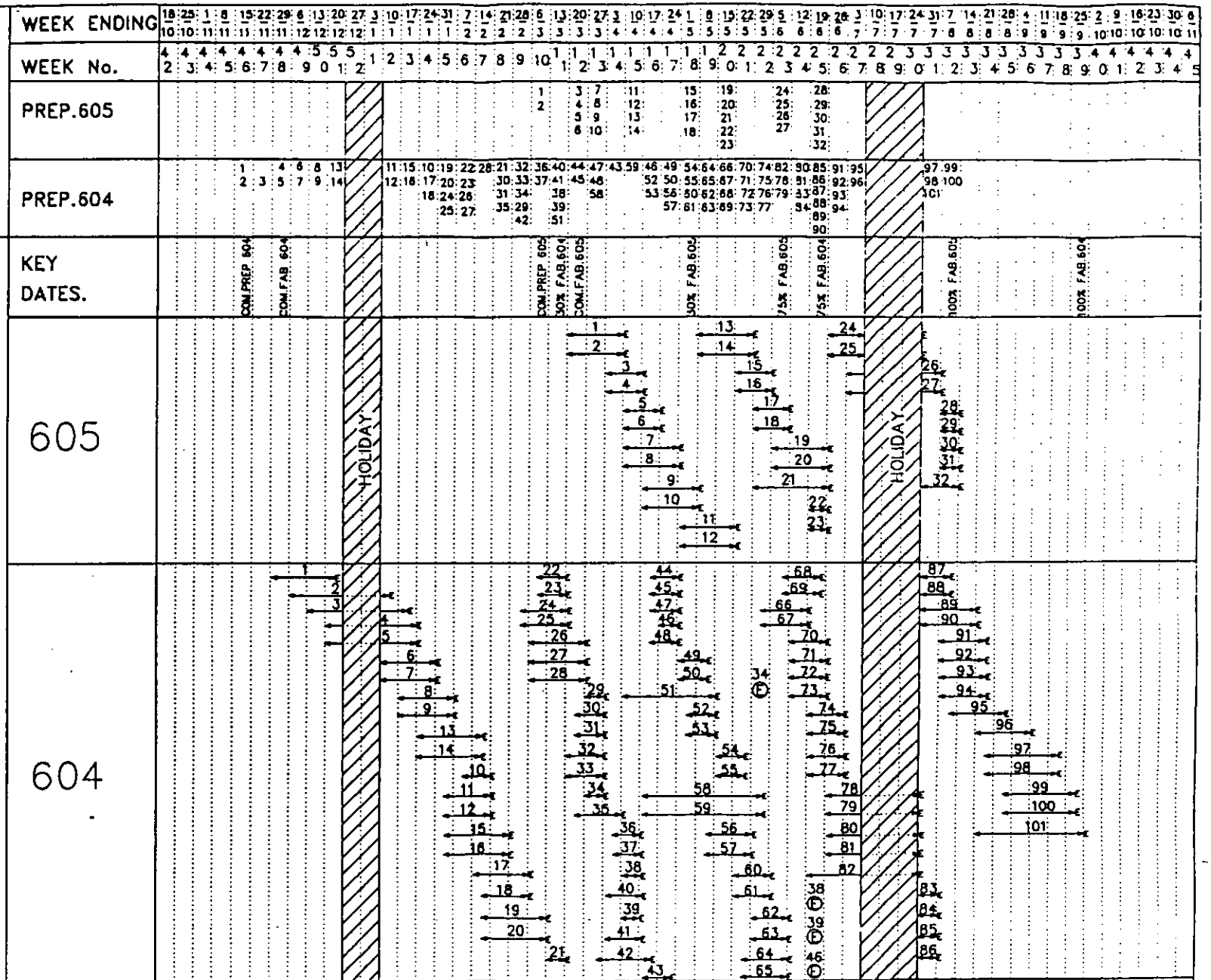

FABRICATION

PROGRAMME SHOWS UNIT BUILD TIME i.e. EXCLUDES MINOR & PANEL ASSEMBLIES

ALLOWANCE FROM WK. 10 TO WK. 27 TAKES INTO ACCOUNT SECOND SHIFT IN OPERATION FOR FABRICATION

ALLOWANCE FROM WK. 5 TAKES INTO ACCOUNT SECOND SHIFT IN OPERATION FOR PREPARATION

Ⓔ – SECOND ERECTION OF PLUGS

ISSUE: 01

FIG.10

SHIP No: 605 SHETLAND ISLES FERRY PRODUCTION CARDINAL DATE PROGRAMME DATE: 31/1/92 ISSUE: 01

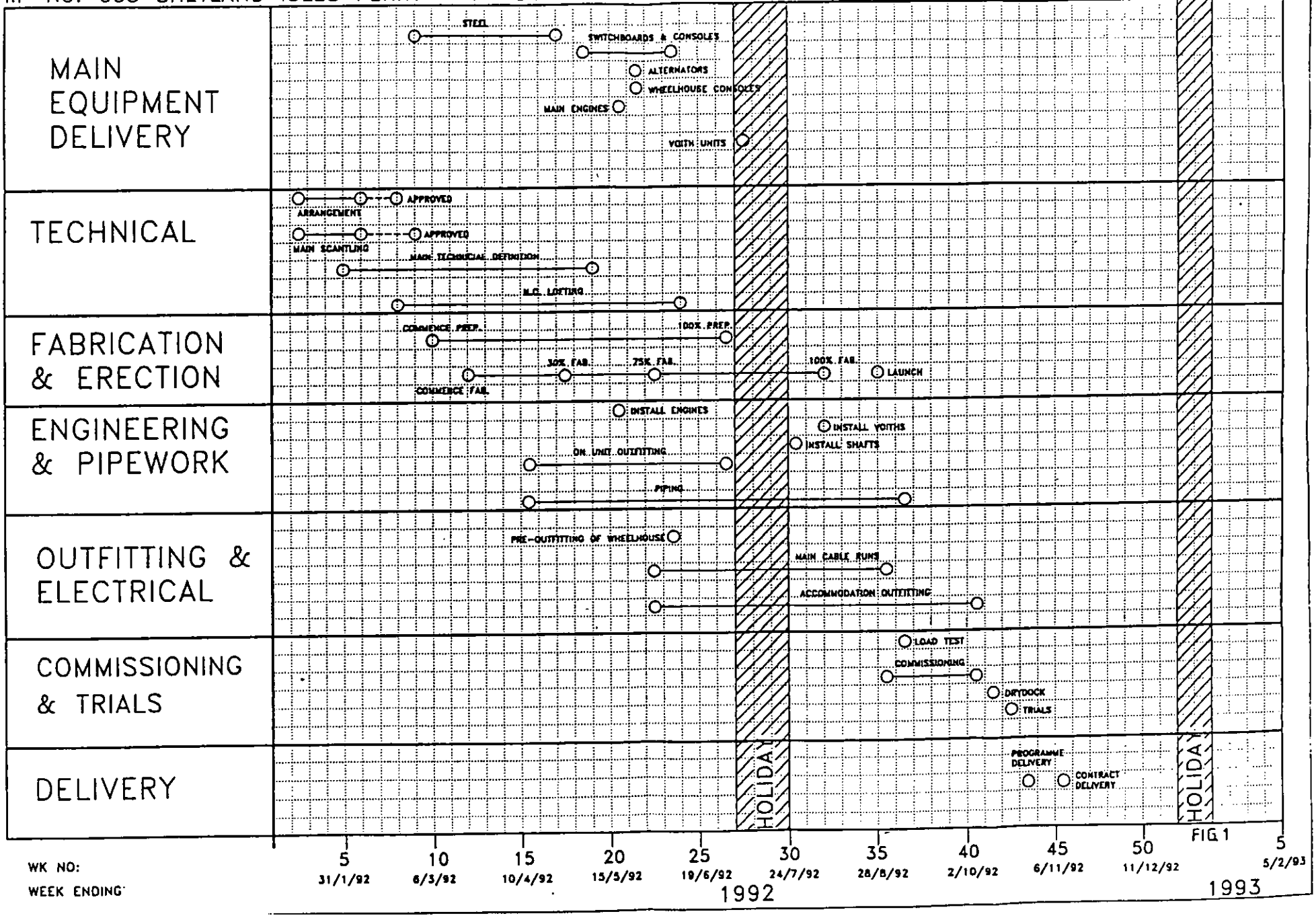

FIG 1

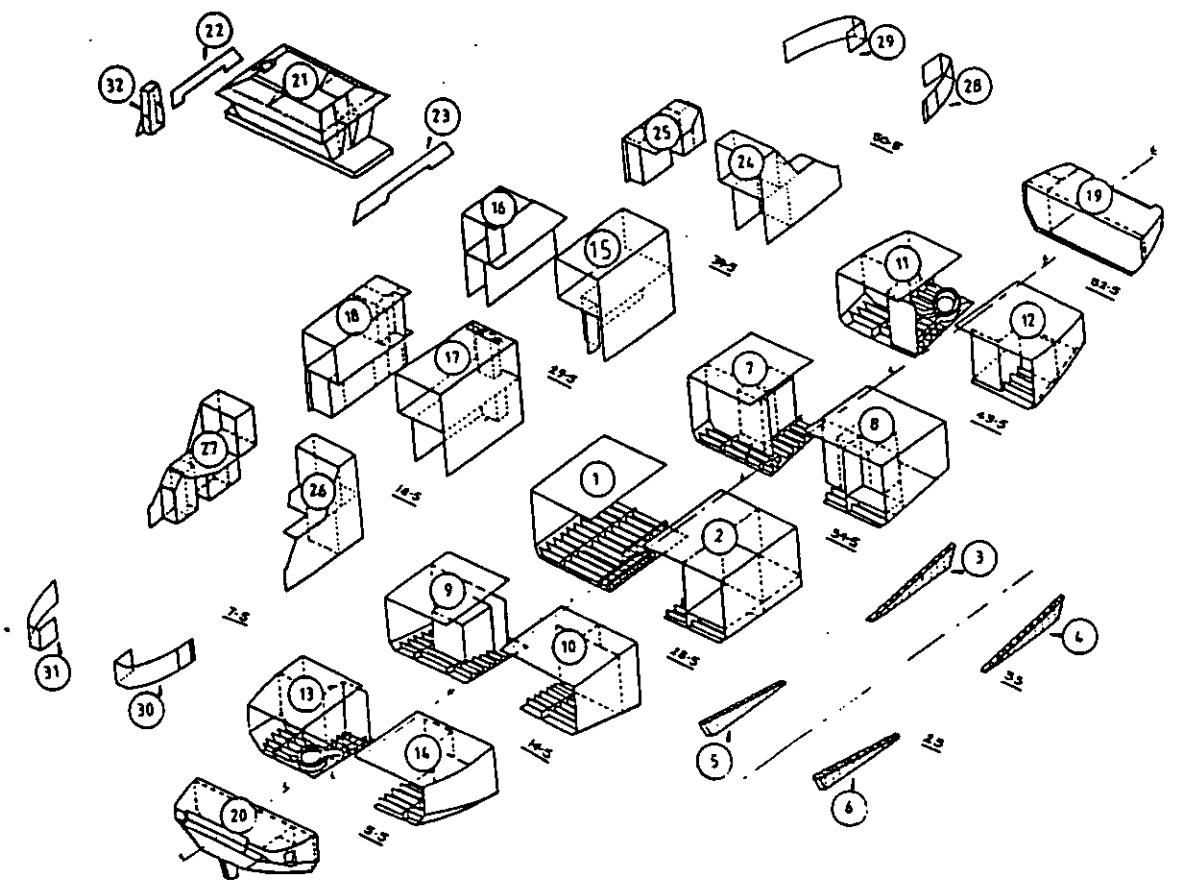

UNIT BUTTS

BELOW MAIN DECK

5.5 , 14.5 , 22.5 , 34.5
43.5 , 52.5

BELOW BRIDGE/GALLERY DECKS

7.5, 18.5 , 29.5 , 39.5 , 50.5

FERGUSON

UNIT BREAKDOWN 505

- 30 -

FIG

DESIGN AND ANALYSIS OF STATION KEEPING SYSTEMS: D.P. SYSTEMS

by

J.A. PINKSTER

DELFT

DESIGN AND ANALYSIS OF STATION KEEPING SYSTEMS: D.P. SYSTEMS

J.A. Pinkster
Delft University of Technology
Ship Hydromechanics Laboratory

Introduction

Since the introduction of Dynamic Positioning systems in the sixties to early seventies, the number of vessels to which it has been applied has steadily increased and now probably numbers about 200. Most of the vessels to which it is applied are relatively small, i.e. Diving Support Vessels, Survey Vessels, Supply Vessels etc. which have displacements of 2-5000 t. Medium size vessels using this positioning system are the monohull drilling vessels which generally are around the 15-2000 t displacement. In recent years, Dynamic Positioning is being applied to large vessels with displacements of up to 125000 t. These are mainly tankers which are being used for offshore loading operations in the North Sea. In Table I a list of the locations in the North Sea at which DP vessels are being used for offloading operations is given. Table II gives a list of tankers equipped with DP systems. The data is taken from a recent paper presented by Omberg [1]. A well known example of a large dynamically positioned vessel is BP's 'Seillean', a purpose-built 70000 tdw, fully dynamically positiotioned oil production and storage vessel which has been in service in the North Sea for over 2 years.See Yuill [2]. See Figure 1. It appears that also for large vessels dynamic positioning is continuing to gain ground as a means of stationkeeping.Omberg [1] surmises that the fleet could grow at the rate of 3 vessels a year for the next 4-5 years. The application at this stage is mainly in the field of offshore loading which requires the vessel to remain on station for periods in the order of up to some days. Seillean can stay on location for several months. As experience is gained, it can be expected that more applications requiring vessels to stay on location for longer times will emerge.

Design of DP-systems.

The purpose of the DP-system is to maintain the position of the vessel in the face of environmental disturbances by means of restoring forces generated by purposely installed thruster units. The forces generated by the thrusters are automatically controlled, mainly on the basis of feed-back of the position error of the vessel. See Figure 2.

In conventional DP-systems, thrusters are positioned at the fore and aft ends of the vessel and are used to generate longitudinal and transverse forces and a yawing moment to maintain the position and heading of the vessel. See Lagers[3]

Pinkster[4] proposed a simplified DP-system which only requires thrusters at one end of the vessel.See Figure 3. This system maintains the horizontal position of a point on the vessel but

allows the environmental forces to dictate the heading of the vessel [weathervaning].
Experiments reported by Hooft [5] confirm-ed the feasibility of the system when applied to a supply vessel.
Further experiments reported by Pinkster and Nienhuis [6] verified the applicability of this weathervaning to a 200 kdwt tanker in a variety of sea conditions.
BP carried out a comprehensive study, including model tests on a DP production vessel based on their 109 kdwt class tankers. See Morris [7]. In this design use was made of the weathervaning concept. The vessel was equiped with three azimuthing thrusters at the bow. Omberg [1] reports the succesful application, in 1988, of the weathervaning system to the 125 kdwt tanker 'Jaguar' which was equiped with one bow-thruster only.

Analysis of DP-systems in the design stage

In Appendix I, a review is given of the elements of a mathematical model used for time domain simulation computations of a dynamically positioned vessel as developed at MARIN, see Nienhuis et al. [8]. Other examples of analysis for DP-systems are given by McClure et al. [9] and Morgan [10].
In this section some general aspects related to the developments of such models is given.

Environmental forces, position error, thruster forces

The environmental forces on the vessel due to waves, wind and current cause the vessel to move away from the required position [set-point]. A major factor governing the design of dynamic positioning systems is the required thrust of the units to be installed.

Initially, the design of DP-systems for smaller vessels was based to a large extent on rather arbitrary estimates of the environmental forces which after applying a factor of safety, became the basis for determining the installed thrust and power.
The environmental forces were assumed to be mainly due to wind and current, wave drift forces were not considered to be of great influence.

Based on improved insight in the nature and magnitude of the environmental forces it is now known that these assumption made for smaller vessels were not unreasonable, however, for the larger vessels, for which wave diffraction effects are stronger, it turns out that in some cases, wave drift forces are the dominant factor in determining the installed power of the DP-system. See Davison et al.[11].

On the basis of such findings it is concluded that in the analysis of DP-systems for large vessels in the design stage, all elements of the environmental forces must be properly accounted for. In the following a brief review will be given with respect to the 'state of the art' in evaluating the environmental forces.

Wind forces.

Mean wind forces on vessels can be determined from wind tunnel testing of the particular vessel or on the basis of available data for similar vessels. In recent years, calculation methods, based on a building-block approach for determining wind forces have been developed. See van Walree and van den Boom[12].
An example of correlation between calculated and measured wind forces is shown in Figure 4.

Unsteady wind forces, especially the low-frequency components also play a roll in the dynamic behaviour of a DP vessel. The effect of wind-gusts is often counteracted by including a wind-feed-forward loop in the DP-control. See Lagers[3]. This is based on real-time wind speed measurement. Little is known of wind dynamics at this stage. Feikema and Wichers [13]
have reviewed the available spectral models of unsteady wind and investigated the effects of unsteady wind forces on a moored tanker by computations and model tests. From the results of model test with and without dynamic wind effects it was concluded that for the tanker considered the representation of wind by means of the 1-minute mean steady wind resulted in larger motions and mooring loads than found for the same sea conditions but using the corresponding dynamic wind based on the wind spectrum. See Figure 5.

Current forces.

As is the case with wind forces, current forces on DP vessels can only be determined based on model tests or on available data for similar vessels. No adequate mathematical model for determining such forces exists as yet.

Mean current forces on tankers have been published by the Oil Companies International Marine Forum [OCIMF].See ref.[14] An example is given in Figure 6. Current force data has also been published by Edwards [15].

Dynamic effects may also be present in current. Shatto and van Calcar [16] reported the necessity to increase the quality of the control of a dynamically positioned drill ship as a result of poor performance under fluctuating current conditions. At present, much less data on the dynamic effects in current is available than for the wind. De Kat and Wichers [17] have investigated the influence of dynamic effects in currents on moored tankers. In Figure 7 an example is given of the effect of current dynamics on vessel motions. On the basis of findings reported in the above mentioned references it may be concluded that dynamic current effects need to be taken into account in the designing DP-systems.

Wave forces.

Much attention has been devoted to the wave action on moored vessels in the past years. The developments in this field will be adressed by other contributions to this course and need not be repeated in detail here. Most of the results of such investigations are directly applicable to DP vessels.

For the design of the control system both wave frequency and low frequency wave forces and the ensuing motion components of the vessel are of importance.
Knowledge of the wave frequency motion components is of importance for the design of the filters used to extract the important low frequency motion components from the total measured motions.

As indicated by Davison et al. [11], the mean and slowly varying wave drift forces on large DP vessels can be a dominant factor in the design of such systems. Theoretical and experimental investigations of the wave drift forces carried out by Pinkster [18] have shown that real-time measurements of the relative wave elevation at a number of locations around the waterline of the vessel can be used to generate a 'wave-feed-forward' control signal which can improve the station keeping performance. See Figure 8. Aalbers and Nienhuis[19] have carried investigations into a simplified form of wave-feed-forward using only three relative wave elevation measurements.

Thrusters.

Thrusters are a very important item in the total DP-system. Two main types are used i.e. tunnel thrusters and azimuthing thrusters. DP-tankers for Offshore loading tend to use main propellers combined with tunnel thrusters. Mork and Lerstad [20] report that Ugland's new generation DP-shuttle tankers will be fitted with one bow-thruster and one azimuth thruster, also at the bow.
The Seillean relies mainly on azimuthing thrusters although tunnel thrusters are also fitted.

The performance of such thrusters with respect to the effective force they can generate needs to be taken into account in the design. Thrust degradation, which ultimately affects the station keeping performance, can take place due to several influences:

- thruster-hull interaction
- thruster-thruster interaction
- thruster-Current interaction
- thruster-wave interaction [ventilation]

English [21] , Chislett and Bjorheden [22], Brix [23] and Nienhuis [24] have carried out investigations on the first three phenomena. An example is given in Figure 9 of thruster-thruster interaction taken from ref.[24].

For thruster-wave interaction information on the relative wave elevation near the thruster location has to be available. On the basis of such information the probability of ventilation can be assessed. Nienhuis et al. [25] have reported results of modeltests on a bow-thruster in waves. It appears that on the occurrence of ventilation the thrust loss is abrupt while the recovery after complete immergence is slow. See Figure 10. It was recommended that systematic model tests be carried out to determine the influence of a number of parameters on the thrust. On the basis of such data approximate models of thruster performance can be based for use in simulation computations.

In table III, taken from ref. [25], an example is given of the effect of bow tunnel thrust degradation on DP accuracy of a supply vessel.
In this table A refers to simulations based on a mean thrust degradation due to wave action while B refers to simulations based on a degradation related to the occurrence of high wave groups. Thrust degradation values of 0%,10% and 23% were used. For the cases investigated the influence of ventilation on the position accuracy was small. The influence was mainly on the heading variations.

Model tests

Model test programs for DP-systems have changed considerably since the first systems were tested in the early 1970's. At first such model tests were limited to tests in still water to determine the current forces for various headings and wind tunnel tests. In some cases thruster-hull interaction tests and thruster-current interaction tests were performed. System performance was then estimated using relatively simple models. Attention was focussed on wind gusts as being a major source of low frequency excitation. See Lagers [3]. If model tests were carried out in waves, the DP-system was simulated by a soft spring mooring system which was given the approximate restoring characteristics of the actual system. To-day, DP model testing can focus on several aspects of the system. In some cases basic testing to determine current loads, wave drift forces and thruster forces are carried out in order to either verify the input to simulation programs. Model testing of the complete system including an active control system and thrusters is within the capability of most major model testing facilities.
In Ref. 6, a description is given of a model test program carried out for the afore-mentioned weathervaning DP-system.

Final remarks

In this contribution a review is given of some of the factors of importance in the design and analysis of DP-systems. Some of the more recent developments regarding additional methods of control and regarding thrusters have been added in order to illustrate that much work still remains to be done in this field.

References

1. Omberg, D;'DP-philosophy in use for different loading operations', Proceedings of 2-day seminar on Offshore Offloading, Stavanger, June 1992

2. Yuill, D.L.;'Operational Aspects of SWOPS over 2-years service', Presented at MARIN Jubilee Meeting, May 1992

3. Lagers, G.;'Development of Dynamic Positioning' OTC Paper No. 1498, Offshore Technology Conference, Houston, 1971

4. Pinkster, J.A.;'Dynamic Positioning of Vessels at Sea', Paper no.105, CISM, Udine, 1971

5. Hooft, J.P.;'Ocean Technology', Presented at the International Jubilee Meeting of NSMB, Wageningen, August, 1972

6. Pinkster, J.A. and Nienhuis, U.;'Dynamic Positioning of Large Vessels at Sea', OTC paper no. 5208,Offshore Technology Conference, Houston, 1986

7. Morris, W.D.M.;'The development of a Bow-DP Production Tanker System', EEC Symposium on New Technologies for the Exploration and Exploitation of Oil and Gas Reserves, Luxembourg, March 1988

8. Nienhuis, U.;'Simulation of Loe Frequency motions of Dynamically Positioned Offshore Structure', RINA, 1986

9. McClure, A.C., McClure, S. and Edwards, R.Y.;'Dynamic Positioning Dynamics', Proceedings of the First Offshore Station Keeping Symposium, Houston, February 1990

10. Morgan, M.J.;'Dynamic Positioning'

11. Davison, N.J. et al.;'A Study on the Hydrodynamic Factors influencing the Workability of the SWOPS vessel', Presented at WEMT Conference on Advances in Offshore Technology, Amsterdam, November, 1986

12. van Walree, F. and van den Boom, H.J.J.;'Wind, wave and current loads on Semi-submersibles', OTC paper no. 6521, Offshore Technology Conference, Houston, 1991

13. Feikema, G.J. and Wichers, J.E.W.;'The Effect of Wind Spectra on the Low-Frequency Motions of a Moored Tanker in Survival Condition', OTC6605, Offshore Technology Conference, Houston, Texas, 1991.

14. Oil Companies International Marine Forum;'Prediction of Wind and Current Loads on VLCC's', Publ.by OCIMF, London, 1977

15. Edwards, R.Y.;'Hydrodynamic Forces on Vessels Stationed in a Current', OTC paper no. 5032, Offshore Technology Conference, Houston, 1985

16. Shatto, H.L. and van Calcar, H.;'Improving Dynamic Positioning Performance in Deep Water, High Current, Rough Water Environment', OTC paper no. 4749, Offshore Technology Conference, Houston, 1984

17. de Kat, J.O. and Wichers, J.E.W.;'Behaviour of a Moored Ship in Unsteady Current, Wind, and Waves', Marine Technology, September 1991.

18. Pinkster, J.A.;'Wave-feed-forward as a means to improve Dynamic Positioning', OTC paper no.3057, Offshore Technology Conference, Houston, 1978

19. Aalbers, A. and Nienhuis, U.;'Recent Developments in Simulation and Real Time Control of Dynamic Positioning and Tracking', Proceedings MARIN Jubilee Meeting, Wageningen, May 1992

20. Mork, K. and Lerstad, A.;'Development of Dynamic Positioning in Relation to Offshore Loading in the Norwegian Sector', Proceedings of MARIN Jubilee Meeting, Wageningen, May 1992

21. English, J.W.;'Propeller Hull Interaction', Report of Propeller Committee, Appendix 2, 14th ITTC, 1975

22. Chislett, M.S. and Bjorheden, O.;'Influence of Ship Speed on Effectiveness of a Lateral Thrust Unit', Hydro- and Aerodynamisk Laboratorium, Report no. HY-8, 1966

23. Brix, J.;'Querstrahl Steuer', Forschungszentrum der Deutscher Schiffbau, Bericht no. 80, 1978

24. Nienhuis, U.;'Analysis of Thruster effectivity for Dynamic Positioning and Low Speed Manoeuvring', Thesis, Technical University Delft, 1992

25. Nienhuis, U., van Walree, F. and Keukens, P.A.A.;'De Effectiviteit van een Boegschroef in Golven', CMO rapport 88 B.2.5.1,1990 [in Dutch]

APPENDIX I

DESCRIPTION OF PROGRAM DPSIM

1. General

For the simulations the three horizontal equations of motion are solved in the time-domain:

$$\sum_{j=1}^{3} (M_{kj} + m_{kj})\, \ddot{x}_j = F_k(\underline{x},\dot{\underline{x}},t) \qquad \ldots\ldots\ldots\ldots (1)$$

where:

x_j = motion in j-direction

$F_k(\underline{x},\dot{\underline{x}},t)$ = arbitrary in time varying forces in the k-mode of motion; F_1 will also be denoted by F_x, similarly F_2 by F_y and F_3 by N

M_{kj} = inertia matrix

m_{kj} = added inertia matrix.

Here m_{kj} are assumed to be frequency independent. Considerations of symmetry lead to: $m_{21} = m_{31} = m_{12} = m_{13} = 0$. Directions 1, 2 and 3 denote respectively surge, sway and yaw. The values of the other added inertia coefficients are dependent on the hull shape and principal particulars. To avoid the necessity of performing model tests regression formulae obtained by Clarke et al. may be used.

The right-hand side of equation (1) consists of environmental forces, hydrodynamic reaction forces other than added mass terms and thruster forces:

$$F(\underline{x},\dot{\underline{x}},t) = F_c(\underline{x},\dot{\underline{x}},t) + F_w(\underline{x},\dot{\underline{x}},t) + F_{wv}(\underline{x},t) +$$

$$+ F_h(\dot{\underline{x}},t) + F_t(\underline{x},\dot{\underline{x}},t) \qquad \ldots\ldots\ldots\ldots (2)$$

Here:

F_c = the current force vector

F_w = the wind force vector

F_{wv} = the wave force vector

F_h = hydrodynamic reaction force vector

F_t = the thruster force vector.

2. Environmental forces

The current forces are derived from:

$$F_{cx} = \tfrac{1}{2}\rho\ v_{cr}^{2}\ B\ \ T\ C_{cx}(\alpha_{cr}) \qquad \ldots\ldots\ldots\ldots (3)$$

$$F_{cy} = \tfrac{1}{2}\rho\ v_{cr}^{2}\ L_{PP}\ T\ C_{cy}(\alpha_{cr}) \qquad \ldots\ldots\ldots\ldots (4)$$

$$N_c = \tfrac{1}{2}\rho\ v_{cr}^{2}\ L_{PP}^{2} T\ C_{cn}(\alpha_{cr}) \qquad \ldots\ldots\ldots\ldots (5)$$

where α_{cr} is the angle between the speed through the water v_{cr} and the ships heading. The resistance coefficients C_{cx}, C_{cy} and C_{cn} are functions of the relative angle α_{cr} and are based on empirical data.

Wind forces are determined by dividing the structure above the waterline into geometric components. For the part of the hull below the upper continuous deck wind resistance coefficients have been derived from existing empirical data. The influence of wind direction is expressed in a Fourier series. The wind forces on the hull result from:

$$F_{wx} = \tfrac{1}{2}\rho_w\ v_{wr}^{2}\ C_{wx}(\alpha_{wr})\ A_T \qquad \ldots\ldots\ldots\ldots (6)$$

$$F_{wy} = \tfrac{1}{2}\rho_w\ v_{wr}^{2}\ C_{wy}(\alpha_{wr})\ A_L \qquad \ldots\ldots\ldots\ldots (7)$$

$$N_w = \tfrac{1}{2}\rho_w\ v_{wr}^{2}\ C_{wn}(\alpha_{wr})\ A_L\ L_{PP} \qquad \ldots\ldots\ldots\ldots (8)$$

where v_{wr} is the instantaneous relative wind velocity including the ship's speed over the ground. Wind forces on the remainder of the superstructure are added to the above forces. These are found by adding the contributions of all superstructure components taking shadowing effects, solidity ratio effects and three-dimensional effects into account. For every component a resistance coefficient is specified (this may be Reynolds number-dependent and direction-dependent) and the local relative velocity is determined using a standard boundary layer profile for the wind velocity:

$$v_{wr}(z) = v_{wr}(z=10)\ (0.1z)^{0.09} \qquad \ldots\ldots\ldots\ldots (9)$$

in which z denotes the vertical position of the component above the waterline.

The variations of wind speed (gusting) have been the subject of research in the past and three different formulations for the wind speed spectrum were suggested. The OCIMF suggested the following spectrum:

$$S_v(\omega) = \frac{4041\ k\ \bar{v}_w}{\left[1 + (202\ \frac{\omega}{\bar{v}_w})^2\right]^{5/6}} \qquad \ldots\ldots\ldots\ldots (10)$$

which differs slightly from the formulation given by Harris:

$$S_v(\omega) = \frac{5268\ k\ \bar{v}_w}{\left[1 + (286\ \frac{\omega}{\bar{v}_w})^2\right]^{5/6}} \qquad \ldots\ldots\ldots\ldots (11)$$

An alternative representation was introduced by Davenport:

$$S_v(\omega) = \frac{916700\ k\ \omega}{\left[1 + (191\ \frac{\omega}{\bar{v}_w})^2\right]^{4/3}} \qquad \ldots\ldots\ldots\ldots (12)$$

In the above formulae k is a turbulence factor and equals 0.005, $\bar{v}_w$ is the average wind speed at a level 10 m above the water surface. To simulate the influence of varying wind forces a wind speed record is generated with a sum of sines approach having random phase.

Wave forces are calculated by scaling drift force transfer functions obtained for other ships. These quadratic transfer functions have been obtained with the help of the 3-D diffraction theory computer program applying the direct integration method. Only the principal diagonals of the in-phase matrices are incorporated in the simulation program. These results are made dimensionless by using:

$$\omega' = \omega\sqrt{\frac{\nabla^{1/3}}{g}} \qquad \ldots\ldots\ldots\ldots (13)$$

and:

$$C_{wvx}(\omega,\alpha_{wv}) = \frac{\overline{F}^{(2)}_{wvx}(\omega,\alpha_{wv})}{\frac{1}{2}\rho g\ \zeta_a^{\ 2}\ \nabla^{1/3}} \qquad \ldots\ldots\ldots\ldots (14)$$

$$C_{wvy}(\omega,\alpha_{wv}) = \frac{\overline{F}^{(2)}_{wvy}(\omega,\alpha_{wv})}{\frac{1}{2}\rho g\ \zeta_a^{\ 2}\ \nabla^{1/3}} \qquad \ldots\ldots\ldots\ldots (15)$$

$$C_{wvn}(\omega,\alpha_{wv}) = \frac{\overline{N}^{(2)}_{wv}(\omega,\alpha_{wv})}{\frac{1}{2}\rho g\ \zeta_a^{\ 2}\ \nabla^{2/3}} \qquad \ldots\ldots\ldots\ldots (16)$$

The average drift forces for the ship under consideration are computed with the help of these coefficients by:

$$\overline{F}^{(2)}_{wv}(\alpha_{wv}) = 2\int_0^\infty S(\omega)\ \left[\frac{\overline{F}^{(2)}_{wv}(\omega,\alpha_{wv})}{\zeta_a^{\ 2}}\right] d\omega \qquad \ldots\ldots\ldots\ldots (17)$$

For the dynamic behaviour the drift force spectral density functions are approximated from the following relationship:

$$S_F^{(2)}(\mu) = 8\int_0^\infty S(\omega)\ S(\omega+\mu)\ \left[\frac{\overline{F}^{(2)}_{wv}(\omega,\omega+\mu)}{\zeta_a^{\ 2}}\right]^2 d\omega \qquad \ldots\ldots (18)$$

in which (similar to the Newman approach):

$$\frac{\overline{F}^{(2)}_{wv}(\omega,\omega+\mu)}{\zeta_a^{\ 2}} = \frac{\overline{F}^{(2)}_{wv}(\omega+\frac{\mu}{2},\omega+\frac{\mu}{2})}{\zeta_a^{\ 2}} \qquad \ldots\ldots\ldots\ldots (19)$$

Here μ is the frequency of a regular wave group originating from a system of regular waves with frequencies ω and $\omega+\mu$. This approximation method assumes relatively large water depths. For limited water depth the off-diagonal elements have to be incorporated in the matrices. In that case the drift force spectrum may be specified in the input to the program.

Using average drift forces and spectral densities a wave drift force record may be generated by a sum of sines approach taking randomly distributed phases.

This leads to a force record having a Gaussian distribution. Experimental and theoretical evidence indicates that an exponential distribution may be more realistic. Therefore a method devised by Pinkster to generate an exponentially distributed force record is also incorporated in the program. This method is based on the fact that:

$$A = \ln\{rnd(x)\} \qquad \ldots\ldots\ldots\ldots (20)$$

has an exponential distribution with average -1 and standard deviation 1. Therefore the following system has the property of having the correct average values and having an exponential distribution.

$$F_{wvx}(\alpha_{wvr}) = - F_{wvxA}(\alpha_{wvr})(A+1) + \overline{F}^{(2)}_{wvx}(\alpha_{wvr}) \qquad \ldots\ldots\ldots (21)$$

$$F_{wvy}(\alpha_{wvr}) = - F_{wvyA}(\alpha_{wvr})(A+1) + \overline{F}^{(2)}_{wvy}(\alpha_{wvr}) \qquad \ldots\ldots\ldots (22)$$

$$N_{wv}(\alpha_{wvr}) = - N_{wvA}(\alpha_{wvr})\ A\ \mathrm{sign}\{rnd(y) - 0.5\} + \overline{N}^{(2)}_{wv}(\alpha_{wvr}) \qquad \ldots\ldots\ldots (23)$$

The inclusion of rnd(y) in (20) assures that $N_{wv}(\alpha_{wvr})$ has a symmetrical exponential distribution, which is coupled to F_{wvx} and F_{wvy} in amplitude but not in phase.

The amplitudes F_{wvxA}, F_{wvyA}, N_{wvA} have to be determined using the derived spectral density $S_F^{(2)}(\mu=0)$. The variance of F_{wvx}, F_{wvy} is given by:

$$\sigma_F^2 = E[F^2] - E^2[F] = F_{wvA}^2 \qquad \ldots\ldots\ldots\ldots (24)$$

Taking a sample frequency of once every Δt, the maximum frequency in the wave drift force record is $\pi/\Delta t$. Assuming that $S_F^{(2)}$ is frequency independent in this case, leads to:

$$\sigma_F^2 = S_F^{(2)}(\mu=0)\,\frac{\pi}{\Delta t} = F_{wvA}^2 \qquad \ldots\ldots\ldots\ldots (25)$$

from which F_{wvA} follows. Similarly it can be derived that:

$$\sigma_N^2 = 2N_{wvA}^2 \qquad \ldots\ldots\ldots\ldots (26)$$

resulting in:

$$N_{wvA} = \sqrt{\frac{\pi\, S_N^{(2)}(\mu=0)}{2\Delta t}} \qquad \ldots\ldots\ldots\ldots (27)$$

An estimate for Δt is derived from:

$$\frac{\pi}{\Delta t}\, S_F^{(2)}(\mu=0) = \sigma_F^2 \approx \{\overline{F}_{wv}^{(2)}\}^2 \qquad \ldots\ldots\ldots\ldots (28)$$

This Δt is different from the simulation time step. By quadratic interpolation a smooth wave drift force record is obtained.

The method described above does not allow for the effects of wave directionality. Therefore it is also possible to use an external drift force record incorporating such effects.

3. Thruster forces

For the actual set points the total force exerted by all propulsors is calculated by taking:

$$F_t(\underline{x},\dot{\underline{x}},t) = F_{az}(\underline{x},\dot{\underline{x}},t) + F_{bt}(\underline{x},\dot{\underline{x}},t) + F_{m,st}(\underline{x},\dot{\underline{x}},t) \quad \ldots\ldots (29)$$

in which F_{az} is the total induced force of all azimuthing thrusters, F_{bt} is the force exerted by all bow thrusters and $F_{m,st}$ is the force of a main propeller/stern thruster arrangement.

All the above forces are split into a thrust and an induced hull force. The thrust is the force transfered by the propeller axis and is always taken to be directed along the axis: propeller side forces caused by oblique flow are not taken into account. The thrust T of each propeller other than the side thrusters is computed from open-water diagrams represented by:

$$K_T = \sum_{i=0}^{6} \sum_{j=0}^{7} C_T(i,j)(P/D)^i J^j \quad \ldots\ldots\ldots\ldots (30)$$

$$K_Q = \sum_{i=0}^{6} \sum_{j=0}^{7} C_Q(i,j)(P/D)^i J^j \quad \ldots\ldots\ldots\ldots (31)$$

in which J denotes the advance ratio based on the axial inflow velocity. For bow thrusters the influence of inflow is not incorporated in the polynomials and K_T refers to the total side force in this case.

The forces exerted by an arbitrary arrangement of azimuthing thrusters are calculated by:

$$F_{az}(\underline{x},\dot{\underline{x}},t) = \sum_{i=1}^{n_{az}} T_{az,i}\, C_{hi}\, l_i \quad \ldots\ldots\ldots\ldots (32)$$

Here l_i depends on the thruster angle and the considered mode (surge, sway, yaw), $T_{az,i}$ is the thrust of azimuthing thruster i including interaction caused by other azimuthing thrusters and C_{hi}

is a correction factor for thruster/hull interactions. C_{hi} is a function of the thrust $T_{az,i}$, the thruster angle and the current speed as well as its direction.

For bollard pull conditions and thruster angles in accordance with normal transit conditions, C_{hi} equals 1-t where t is the thrust deduction factor (t = 0.05 for these conditions). At present empirical data are necessary to determine C_{hi} for other conditions.

Bow thruster performance is significantly influenced by current (or ship's speed). The performance is also dependent on the direction of the current. Therefore detailed model tests were carried out for a number of ships to establish a data base which could be used for prediction purposes. This data base also includes the drift angle as a parameter.

Such tests have been executed for a drill ship, a supply vessel, a container ship and a ferry. For immediate application in the simulation program the results have been made dimensionless by deriving the following coefficients:

$$c_T(v_{cr},\alpha_{cr}) = \frac{T(v_{cr},\alpha_{cr})}{T(o,\alpha_{cr})} \quad \ldots\ldots\ldots\ldots (33)$$

$$c_Q(v_{cr},\alpha_{cr}) = \frac{Q(v_{cr},\alpha_{cr})}{Q(o,\alpha_{cr})} \quad \ldots\ldots\ldots\ldots (34)$$

$$c_{Hy}(m,\alpha_{cr}) = \frac{F_{ty}(v_{cr},\alpha_{cr}) - F_{cy}(v_{cr},\alpha_{cr}) - T(v_{cr},\alpha_{cr})}{F_{ty}(o,\alpha_{cr}) - T(o,\alpha_{cr})} \quad \ldots (35)$$

$$c_{Hx}(m,\alpha_{cr}) = \frac{F_{tx}(v_{cr},\alpha_{cr}) - F_{cx}(v_{cr},\alpha_{cr})}{F_{ty}(v_{cr},\alpha_{cr})} \quad \ldots\ldots\ldots\ldots (36)$$

$$c_{Hn}(m,\alpha_{cr}) = \frac{N_t(v_{cr},\alpha_{cr}) - N_c(v_{cr},\alpha_{cr}) - T(v_{cr},\alpha_{cr})\ x_i}{M_t(o,\alpha_{cr}) - T(o,\alpha_{cr})\ x_i} \quad \ldots (37)$$

where m is the ratio between relative ship speed and jet exit velocity and x_i represents the location of the side thruster relative to the ship's centre of gravity.

Interpolation in the data bases yields the expected induced forces on the hull.

4. Control system

The objective of the control system is to reduce the low frequency horizontal motions by actively employing the thrusters and rudders. The input to the system consists of the motions of the vessel as obtained with the help of the position reference signals, of the actual settings of pitch, numbers of revolutions, rudder angles and thruster angles and of an arbitrary number of other quantities describing the environment in which the vessel operates. Also such quantities as bow hawser tension, mooring buoy position and angle and thrust of fire-fighting equipment may serve as input.

Some of the input signals may be used for feed forward purposes of which wind feed forward is a well-known example. In this case the thruster set points are directly dependent on the input signal (e.g. wind velocity for wind feed forward) instead of being dependent on the resulting ship motion. These feed forward loops neutralize to a great extent the effect which the observed quantity will have on the low frequency motions. Feed forward will also reduce the peak loads of the thrusters increasing safety and reducing wear and tear as well as building and operation costs.

The control mechanism of the present simulation program is a feed back system using position data and includes a wind feed forward system. Based on the position signals the total required thrust vector is determined with a PID controller:

$$F_{treq,x} = -\overline{F}_{ex} + c_{tx}\Delta x + b_{tx}\Delta\dot{x} + i_{tx}\int_{T_{int}} \Delta x \, dt + F_{wffx} \quad . . (38)$$

$$F_{treq,y} = -\overline{F}_{ey} + c_{ty}\Delta y + b_{ty}\Delta\dot{y} + i_{ty}\int_{T_{int}} \Delta y \, dt + F_{wffy} \quad . . (39)$$

$$N_{treq} = -\overline{N}_{e} + c_{tn}\Delta\psi + b_{tn}\Delta\dot{\psi} + i_{tn}\int_{T_{int}} \Delta\psi \, db + N_{wff} \quad . . (40)$$

in which $\overline{F}_e$ is the average environmental force vector, T_{int} is the integration time and Δx, Δy, $\Delta\psi$ are the position deviations, see the figure below. F_{wffx}, F_{wffy} and N_{wff} are the wind feed forward forces.

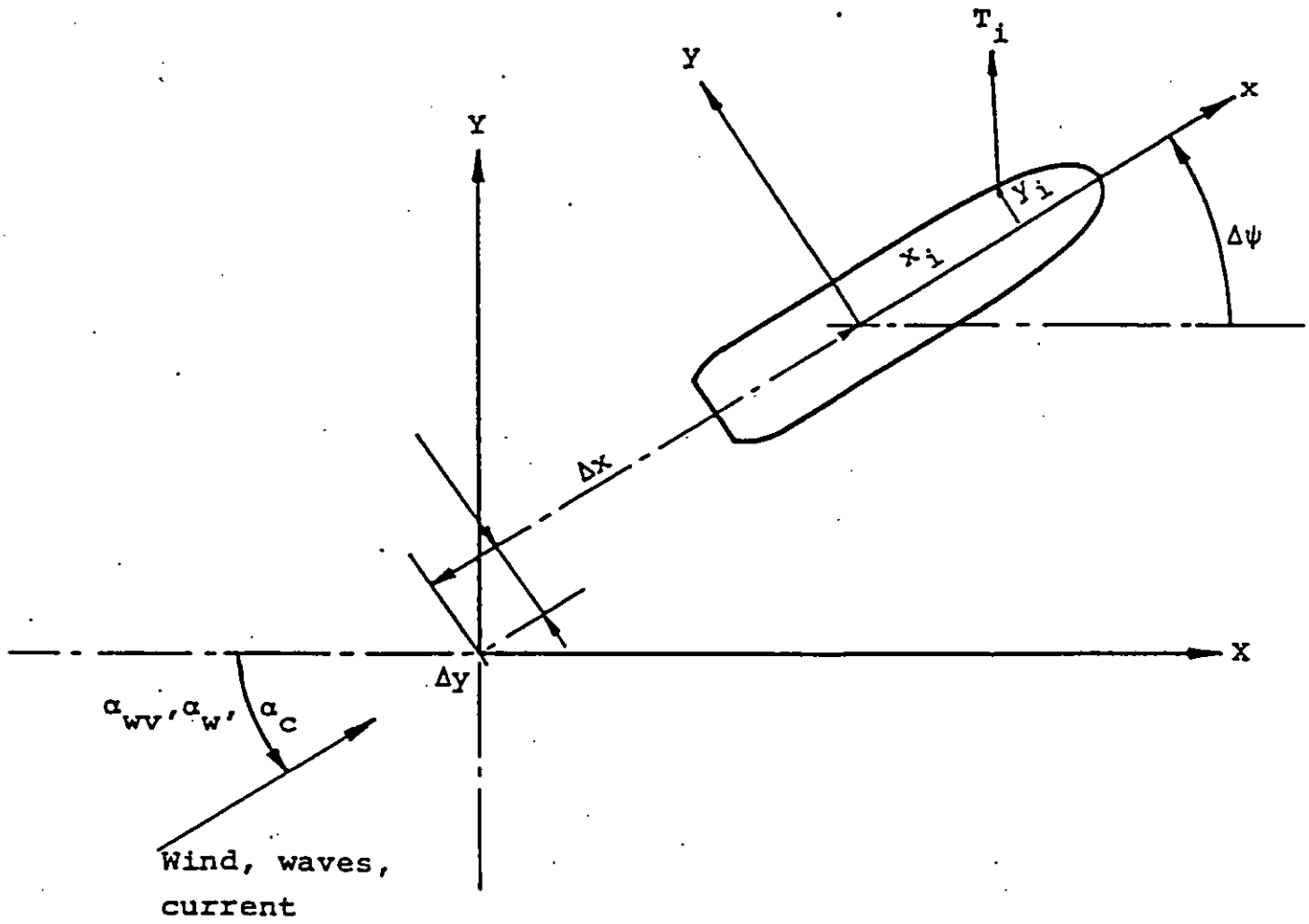

The following formulae were derived for the optimal control coefficients:

$$c_t = \left[\frac{\pi^2 \; S_F^{\;2}}{8\sigma^4 \; (M+m)}\right]^{1/3} \qquad \ldots\ldots\ldots\ldots\ldots (41)$$

$$b_t = \left[\frac{\pi \; S_F \; (M+m)}{\sigma^2}\right]^{1/3} \qquad \ldots\ldots\ldots\ldots\ldots (42)$$

in which (M+m) is the mass plus added mass for the considered mode of motion and σ is the permissible standard deviation of the position of the reference point.

The required forces (eq. (38) to (40)) have to be split into the forces to be delivered by each propulsor. To this end an algorithm has been implemented in the program which minimizes an arbitrary function with an arbitrary number of non-linear constraints.

Three equality constants have to be satisfied, i.e. the total required force has to be met:

$$\sum_{i=1}^{n_p} T_i \cos \alpha_i = F_{treq,x} \qquad \ldots\ldots\ldots\ldots\ldots (43)$$

$$\sum_{i=1}^{n_p} T_i \sin \alpha_i = F_{treq,y} \qquad \ldots\ldots\ldots\ldots\ldots (44)$$

$$\sum_{i=1}^{n_p} \left[x_i \; T_i \cos \alpha_i - y_i \; T_i \sin \alpha_i\right] = N_{treq} \qquad \ldots\ldots (45)$$

where α_i is the thruster angle ($\alpha_i = 0$ for main propellers and $\alpha_i = \pi/2$ for side thrusters), and x_i and y_i are the co-ordinates of the propellers, see Figure I-1. n_p is the total number of propellers.

$2n_p$ inequality constraints are provided by:

$$|T_i| < T_{i,max} \qquad \ldots\ldots\ldots\ldots\ldots (46)$$

where $T_{i,max}$ is determined by the power of each thruster.

The function to be minimized is the power. The power P_i equals approximately $c_i T_i^{3/2}$. To speed up convergence the following function is minimized:

$$f_{obj} = \sum_{i=1}^{n_p} T_i^2 \qquad \ldots\ldots\ldots\ldots (47)$$

Nomenclature

A	: random number with average = -1, standard deviation = 1
A_L	: lateral area of ship between waterline and upper continuous deck
A_T	: transverse area of ship between waterline and upper contiuous deck
B	: breadth
b_{tx}, b_{ty}, b_{tn}	: damping coefficients for thruster control
C_{cx}, C_{cy}, C_{cn}	: resistance coefficients for current
C_{hi}	: correction factor for thruster-hull interaction
C_{Hn}	: dimensionless factor for hull induced turning moment of side thruster
C_{Hx}	: dimensionless factor for hull induced longitudinal force of side thruster
C_{Hy}	: dimensionless factor for hull induced side force of side thruster
c_Q	: dimensionless factor for torque of side thruster
c_{tx}, c_{ty}, c_{tn}	: spring coefficients for thruster control
c_T	: dimensionless factor for thrust of side thruster
C_T, C_Q	: coefficients for thrust and torque polynomials
C_{wx}, C_{wy}, C_{wn}	: resistance coefficients for wind

C_{wvx}, C_{wvy}, C_{wvn}	: dimensionless quadratic transfer functions for drift forces
D	: diameter
F_{az}	: total induced force of azimuthing thrusters
F_{bt}	: total induced force of bow thrusters
F_c	: current force vector
F_{cx}, F_{cy}, N_c	: current forces in surge, sway and yaw direction
$\overline{F}_{ex}$, $\overline{F}_{ey}$, $\overline{N}_e$	: average environmental forces for initial conditions
F_h	: hydrodynamic reaction force vector
F_k	: in time varying force in the k-mode of motion
$F_{m,st}$	: total induced force of a main propeller/stern thruster arrangement
f_{obj}	: object function (power) to be minimized
F_t	: thruster force vector
F_{treqx}, F_{treqy}, N_{treq}	: required total propulsive force
F_w	: wind force vector
F_{wv}	: wave force vector
$\overline{F}^{(2)}_{wvx}$, $\overline{F}^{(2)}_{wvy}$, $\overline{N}^{(2)}_{wv}$	: average second order drift forces
F_{wvxA}, F_{wvyA}, N_{wvA}	: amplitude of exponentially distributed drift force record
F_{wx}, F_{wy}, N_w	: aerodynamic forces in surge, sway and yaw direction
g	: acceleration of gravity, $g = 9.81\ m/s^2$
i_{tx}, i_{ty}, i_{tn}	: integrator coefficients for thruster control
J	: advance coefficient (v/nD)
k	: turbulence factor
K_Q	: torque coefficient, $K_Q = Q/\rho n^2 D^5$
K_T	: thrust coefficient, $K_T = T/\rho n^2 D^4$
l_i	: arm of $T_{az,i}$ for moment calculation
L_{pp}	: length between perpendiculars
m	: ratio of ship speed and jet exit velocity

m_{kj}	: added inertia matrix
M_{kj}	: inertia matrix
n_{az}	: number of azimuthing thrusters
n_p	: number of propellers
P/D	: pitch-diameter ratio
rnd(x), rnd(y)	: random number generator
S	: spectral density
$S_F^{(2)}$, $S_N^{(2)}$	: drift force spectral density function, force (surge and sway) and moment
S_v	: spectral density for wind speed variations
t	: time
t	: thrust deduction factor
Δt	: sample time for generation of exponentially distributed wave force record
T	: draft of ship
T	: thrust of impeller (bow thruster)
$T_{az,i}$	: thrust of azimuthing thruster i
T_i	: thrust of propeller i
$T_{i,max}$	: maximum thrust of propeller i
T_{int}	: integration time for thruster control
v_{cr}	: speed through the water
v_{wr}	: relative wind velocity
$\bar{v}_w$	: average wind speed 10 m above water surface
$\underline{x}$	: position vector = $(x_1, x_2, x_3) = (x, y, \psi)$
Δx, Δy, $\Delta\psi$	: deviations between required and actual ship position
x_i, y_i	: co-odinates of propeller i
x_j	: motion in j-direction (j=1: surge, j=2: sway and j=3: yaw)
z	: vertical co-ordinate above waterline
α_c	: current direction
α_{cr}	: relative current angle
α_i	: direction of the axis of propeller i
α_{wr}	: relative wind angle
α_{wv}	: wave direction

α_{wvr}	: relative wave direction
ζ_a	: wave height
μ	: frequency of slowly varying second order drift force
ρ	: density of water
ρ_w	: density of air
σ	: permissible standard deviation of the position of the ship
σ_F^2, σ_N^2	: variance of drift force
ψ	: heading of ship
∇	: volume displacement
ω	: frequency
ω'	: dimensionless frequency

Table 1 DP used for Offshore Terminal Loading in the North Sea

Field	Offloading Concept
Statfjord A	ALP
Statfjord B	SPM
Statfjord C	SPM
Statfjord A	OLS (Replaced ALP)
Statfjord B	OLS (Replaced SPM)
Gullfaks 1	SPM
Gullfaks 2	SPM
Brent	SPAR
Birch	CALM
Fulmar	Storage tanker
Gullfaks South	Directly from flexible hose

Table 2 Vessels using DP System

Name of Vessel	Vessel Owner	DP System
Esso Fife (Wilnora)	Esso	Single
Bergina	Bergshav A/S	Single
Polyviking	Einar Rasmussen A/S	Single
Polytraveller	Einar Rasmussen A/S	Single
Polytrader	Einar Rasmussen A/S	Single
Norissia (Gerina)	Shell Tankers	Single
Ragnhild Knutsen	Knutsen OAS Shipping	Single
Anna Knutsen	Knutsen OAS Shipping	Single
Sarita	Ugland	Single
Jaguar	Anders Jahre	Single
Juanita (Lisita)	Ugland	Single
Evita	Ugland	Single
Nordic Apollo	NSM	Single
NB-285 (A. Sestao)	Knutsen OAS	Redundant
NB-288 (A. Sestao)	Knutsen OAS	Redundant
NB-289 (A. Sestao)	Knutsen OAS	Redundant
Tove Knutsen	Knutsen OAS	Redundant
NB-1397 Mitsui	Einar Rasmussen A/S	Redundant
NB-1318 (K. Masa)	Neste Oil	Redundant

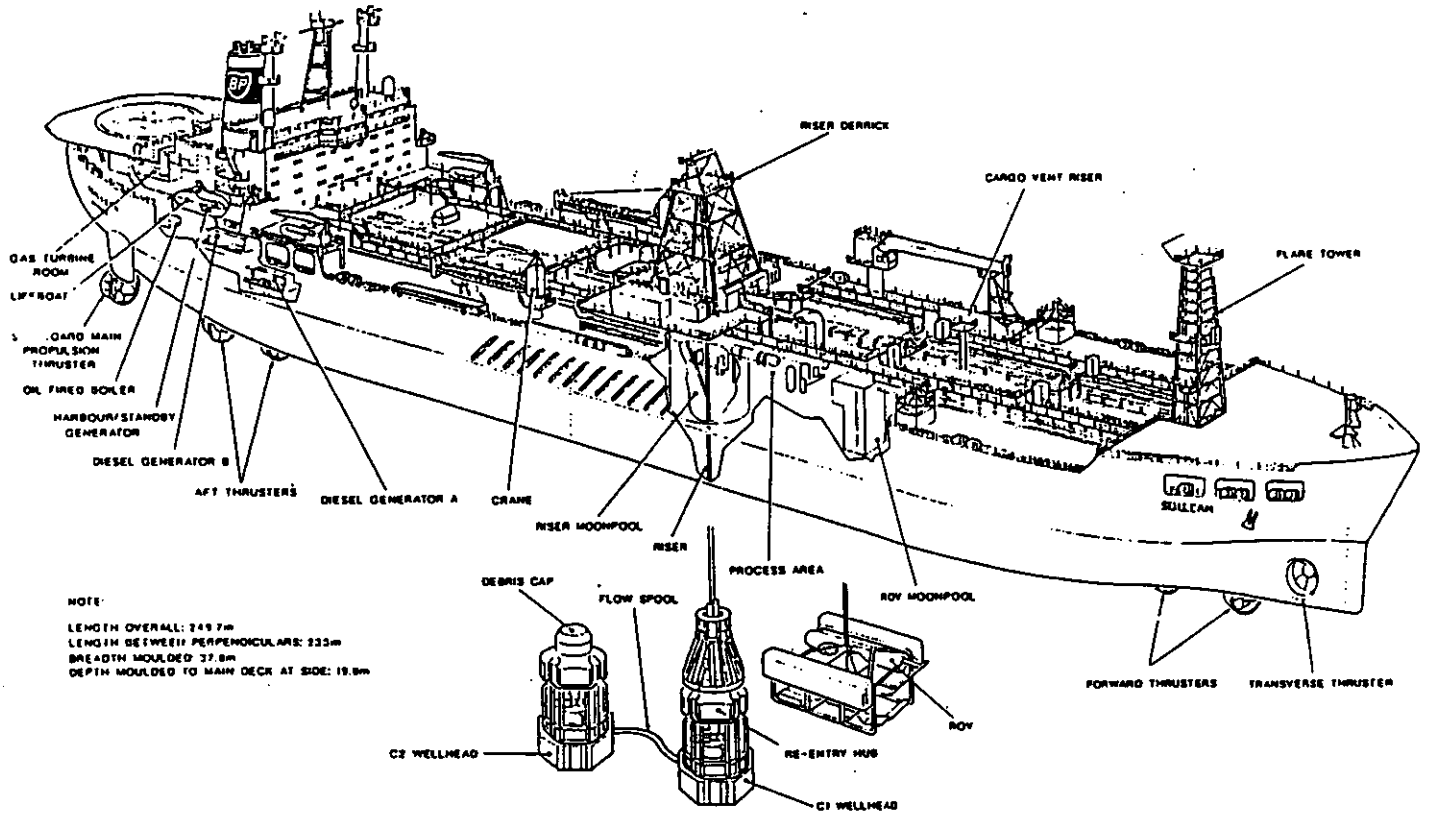

Figure 1: DP vessel SEILLEAN (SWOPS).

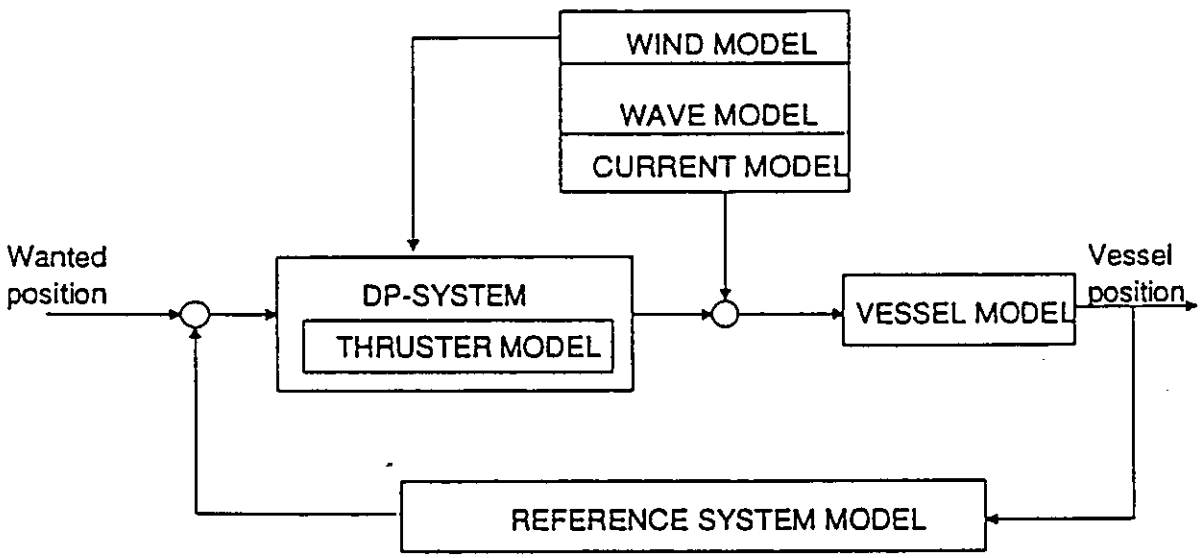

Figure 2: DP-Control

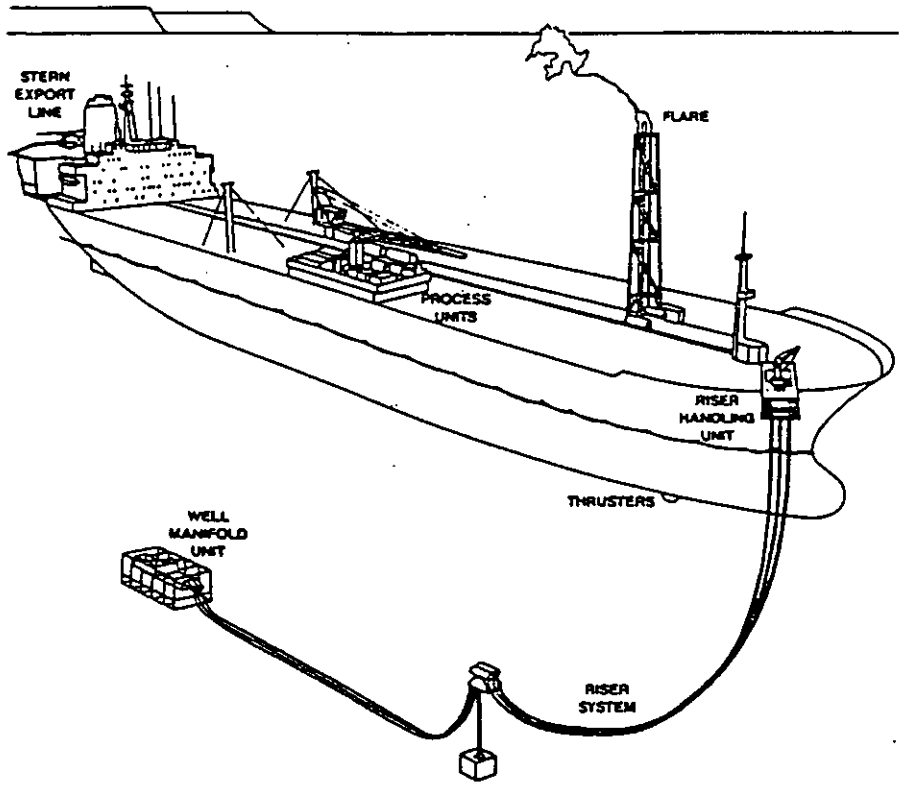

Figure 3: Weathervaning DP-tanker

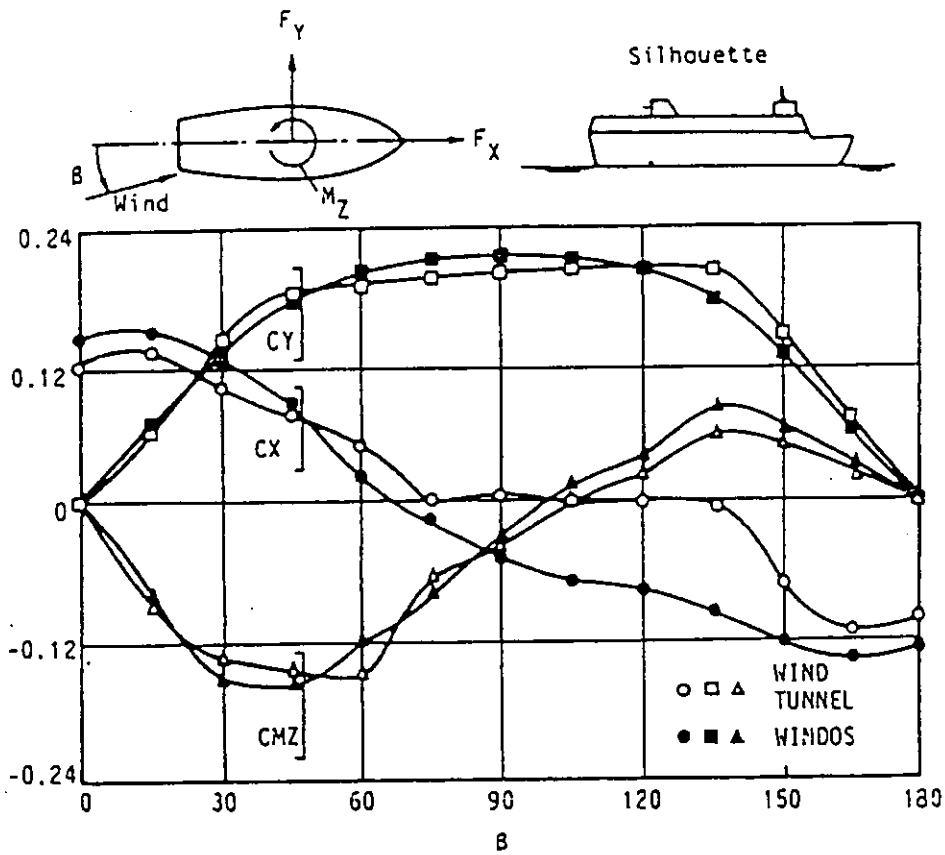

Figure 4: Measured and computed wind forces.

Results of the time-domain computations and model tests

Loaded tanker/"2π-enhanced" Ochi-Shin wind spectrum

Data		Wind spectrum V_w = 30.9 m/s	Wave spectrum	1-minute gust V_w = 39.7 m/s Wave spectrum	Wind spectrum V_w = 30.9 m/s Wave spectrum
TIME DOMAIN (duration 60 hrs)					
$\bar{x}_1$	[m]	-6.9	-8.4	-19.1	-15.3
σ_{x_1}	[m]	9.2	13.4	12.6	13.9
T	[s]	275.0	271.0	271.0	270.0
N (3 hrs)	[-]	39.3	39.9	39.9	40.0
x_{max} (3 hrs)	[m]	-32.9	-48.6	-56.7	-55.4
MODEL TESTS (duration 6 hrs)					
$\bar{x}_1$	[m]	-6.62	-7.8	-18.1	-13.5
σ_{x_1}	[m]	11.95	12.5	12.5	13.9
T	[s]	267.0	254.0	254.0	267.0
N (3 hrs)	[-]	40.4	42.5	42.5	40.5
x_{max} (3 hrs)	[m]	-33.0	-40.0	-52.0	-55.0

Figure 5: Surge motions of a fully loaded 200 Kdwt tanker in head waves and/or wind.

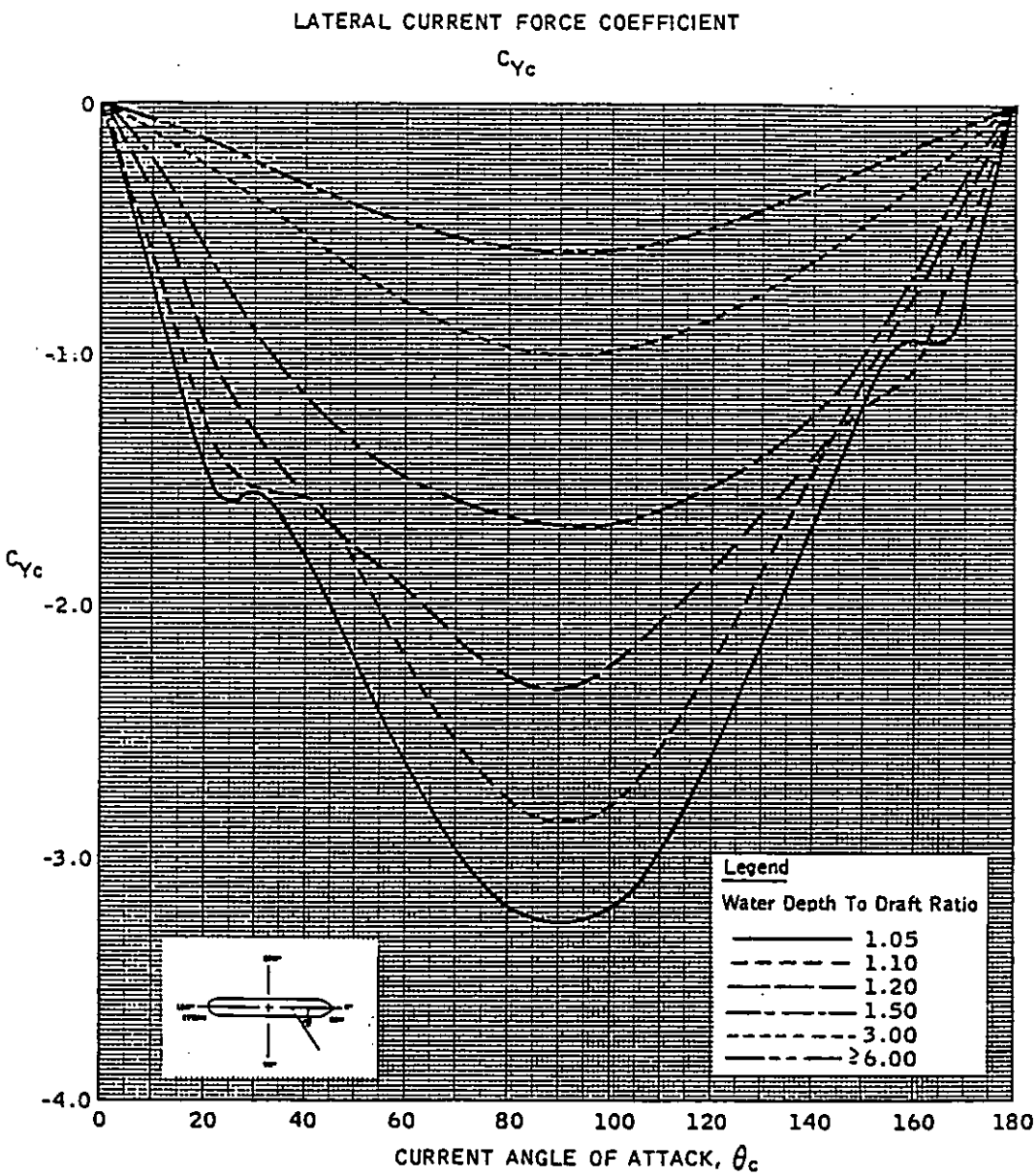

Figure 6: Current forces on a tanker.

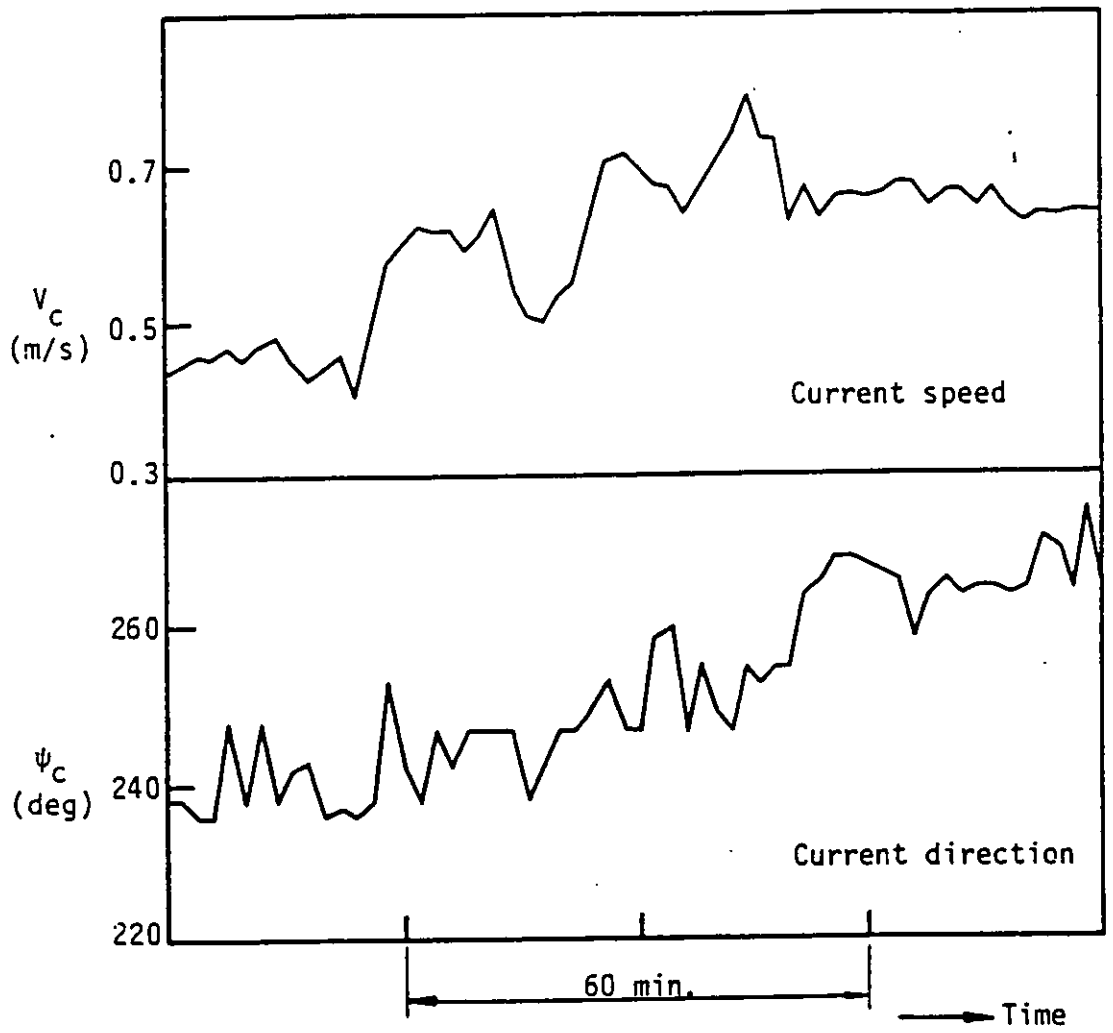

Measurement of current speed and direction in 26.5 m water depth (with courtesy from Tanker Mooring Services Co., Singapore)

Figure 7a: Full scale current speed and direction.

$V_W = 0$

V_C = 1.03 m/s (time-varying direction; 10° block function)

Fully loaded (100%)

Bow hawser length = 75 m

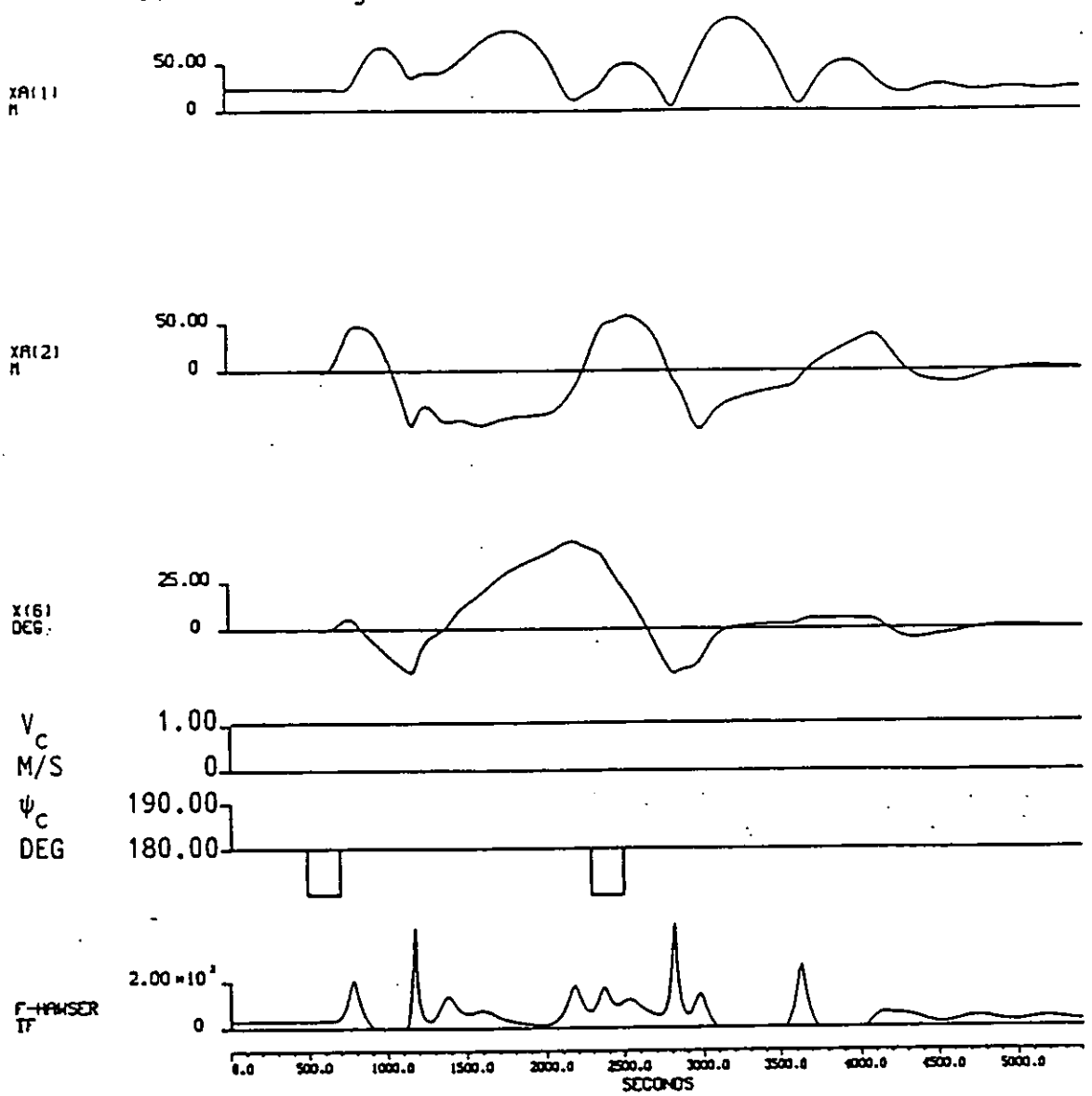

Fully loaded tanker in dynamic environment

Figure 7b: Motion of a tanker moored to a buoy under influence of current direction variations.

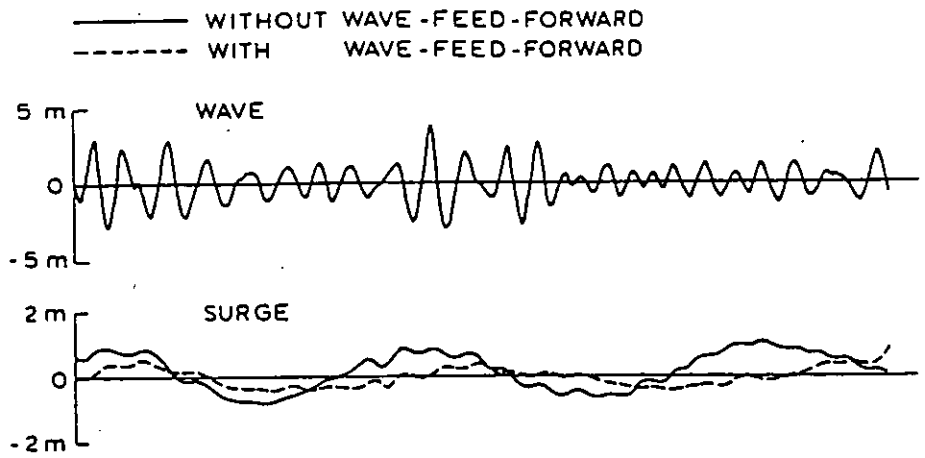

Surge motions in irregular head waves. Significant height 4.9 m.

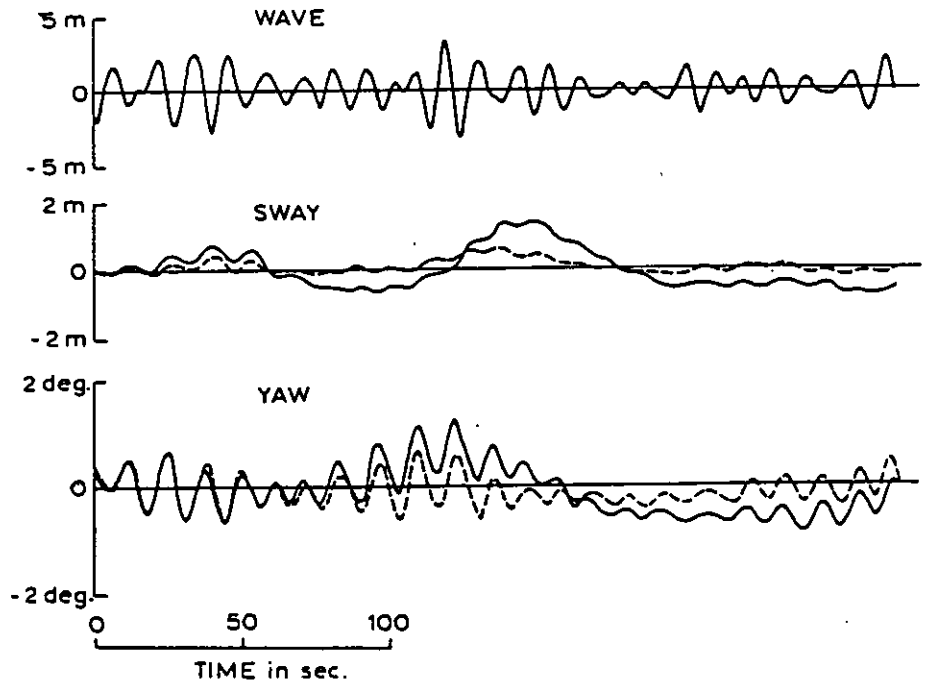

Sway and yaw motions in irregular bow quartering waves. Significant height 4.9 m.

Figure 8: Influence of Wave - Feed - Forward on a horizontal motions of a dynamically positioned tanker.

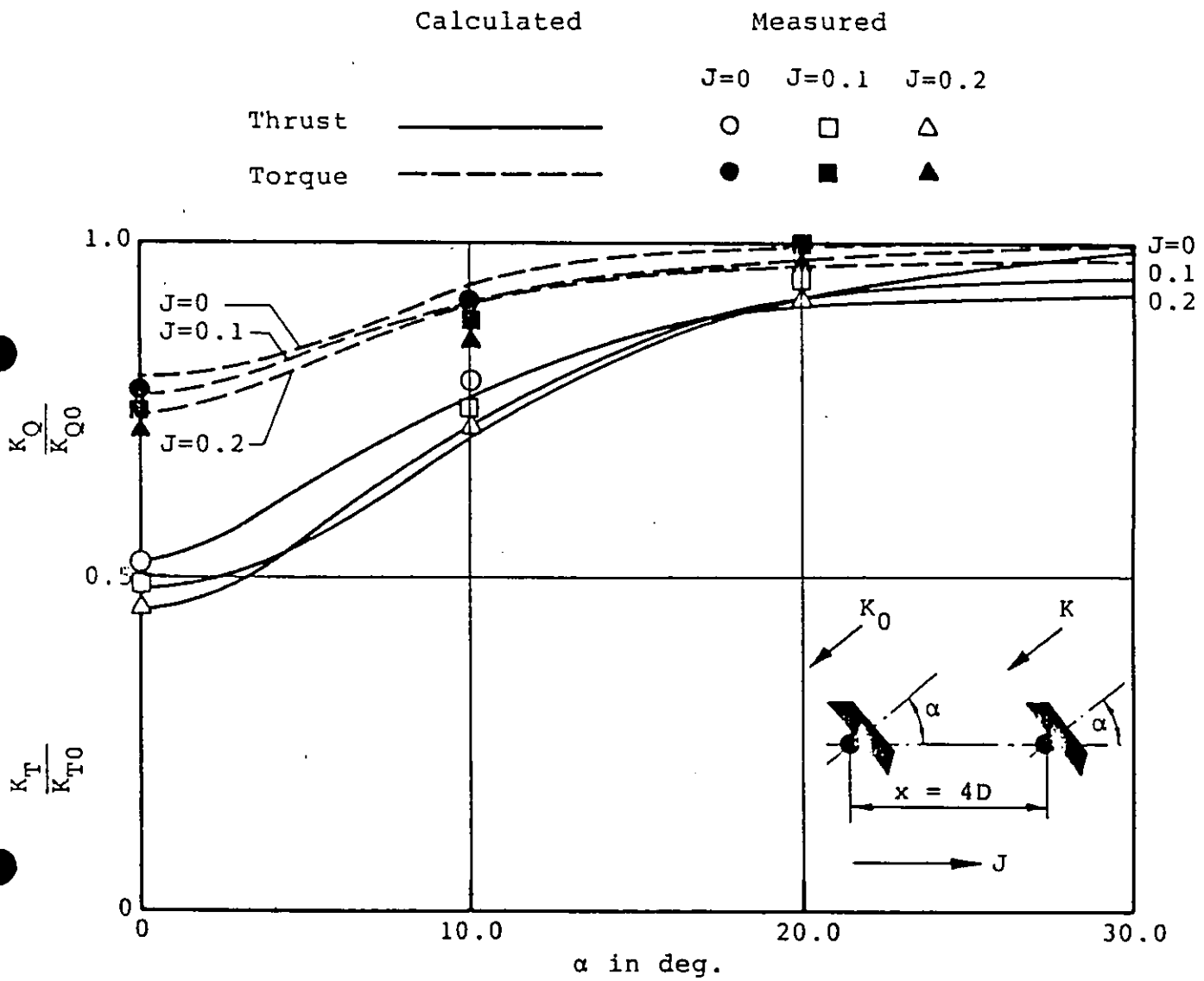

Influence of thruster angle on thruster-thruster interaction

Figure 9: Experimental data on a thruster - thruster interaction.

FULL SCALE TESTING AND MONITORING OF THE BEHAVIOUR OF SHIPS AND FLOATING OFFSHORE STRUCTURES

by

J.A. PINKSTER

DELFT

FULL SCALE MEASUREMENTS

J.A. Pinkster
Delft University of Technology
Ship Hydromechanics Laboratory

Introduction

Full scale measurements of the behaviour of ships and offshore structures are being carried out on an increasing scale. In part this is due to the increasing availability of relatively inexpensive , reasonably manageable equipment for measuring and recording full scale behaviour.Various reasons are put forward for carrying out such measurements. In this contribution the backgrounds to such exercises are discussed and some critical notes are added.

Full scale measurements can be carried out for various reasons. In the following a few of the reasons quoted in literature are given:

- Because there is no other way to obtain such data.
- In order to verify predictions based on model tests and/or computations
- In order to quantify the behaviour as it is influenced by operational decisions.
- In order to verify contractually guaranteed performance
- In order to supply quantitive data on which operational decisions can be based
- In order to quantify the behaviour as it is influenced by unpredictable environmental conditions
- In order to generate a log which is only consulted in the event of the occurrence of misshaps or other sub-standard performance which might lead to litigation
- In order to increase safety margins for operations

As can be inferred from the aforegoing, the actual practice of carrying out full scale measurements of behaviour is greatly influenced by the purpose which they serve. For instance, measurements carried out in order to verify if a ship is achieving the contract speed with the installed power may only require a specialist measurement team with limited portable equipment to be on board for a few hours while measurements carried out in order to obtain long term statistics on ship motions require virtually unattended measuring and data aquisition systems to run uninterrupted for several months at a time. This not only requires high quality measuring equipment in terms of robustness, constant and uninterrupted energy supplies but also places high demands on the data handling. Continuous monitoring of even a few measuring channels may generate enormous amounts of raw data which need to be processed on board in order to remain manageable. It will not come as a surprise to note that extremely large amounts of full scale data measured and recorded in real time have ended up in the garbage can simply because of the lack of facilities to process such large amounts or , for that matter, even to administer the data adequately.

In this contribution attention will be devoted to a number of aspects related to full-scale measurement on ships and offshore structures. A number of cases reported in open literature will be referred to in order to highlight some of the most important , more general, aspects.

Categories of full scale test programs

Full scale measurement programs may be subdivided in categories related to the objectives of the measurements

Long-term monitoring of loads and motions

The objectives in this case are the determination of system behaviour under a wide range of operating conditions encountered over periods of years. The results of measurements, which are carried out on a routine basis by non-dedicated personel, are sometimes incorporated in the day-to-day decision making process on board and, for long-term purposes, the data is analysed to yield statistical information in terms of distribution functions and probabilities of exceedance of extremes. The environmental conditions may, in the case of stationary floating offshore structures, be measured using wave-rider buoys, current meters and anemometers. On board of ships under way visual observations of wave conditions are used. Instrumentation may be quite extensive and large amounts of data collected.

Results of measurements may be used as a log for the system behaviour which can be referred to in case of, for instance, the occurrence of cargo damage. Use has also been made of long-term statistics of measured data in order to verify Classification Societies design criteria.

Finally, long-term data has been used to verify statistically based prediction methods for such quantities as motion acceleration levels etc.

Short-term measurements

As the name implies, short-term measuring programs are carried out to in order to obtain data on the short-term statistics of the behaviour of the structure. Typical of such programs is the desire to carry out measurements under more or less specified environmental conditions. In most cases, this will involve extreme sea-conditions in which it is desired to determine motions and loads in the system. In some cases a calm water condition is required. The objective of such measurements may be to generate motion and load data for verification of design values, to explore the basic nature of the behaviour of the system, or to generate frequency domain data for comparison with theoretical predictions.
For such programs at least part of the instrumentation is installed temporarily for the duration of the program and generally operated by dedicated personel from institutes specialized in this field.

The desire to carry out measurements under specific conditions in which specialist personel is involved requires a very flexible organization of the project.
The specialist may be required to board the vessel at short notice when the conditions appear to be favourable. If it is not possible to carry out measurements when the desired environmental conditions occur, and the program must be scheduled beforehand due to other constraints, the time slot for the program is selected to maximise the probability of meeting the desired conditions. The environmental conditions are generally measured using wave-rider buoys, current meters and anemometers when appropriate.
Measured data is recorded and analysed to yield short-term statistical data and frequency domain data.

Transient measurements

In the first two categories the stationary behaviour of ships and offshore structures in a seaway were the main focus of attention. Measurements of transient behaviour of structures at sea, although requiring many of the measures associated with the previous category, has a number of specific characteristics of its own. The first of these is that the transient event, a launching, a heavy lift, etc. occur within a very short time-frame which, within the constraints of the weather conditions, are governed by the operation. Secondly, the event is sometimes unique and will not be repeated. The success of the measurement depends on all systems being operational at that time. There is ,in such cases, no second chance.
The purpose of carrying out measurements of transient behaviour can be, for instance, to compare the (deterministic) behaviour with time domain computer predictions.

In the following section some examples of measuring programs of all three categories will be given.

Long-term programs

Tension Leg Platform behaviour

Erb et al. [1] describe the data acquisition and Performance monitoring systems in use on the Hutton and Joliet TLP's and the analyses carried out on the measured data. A list of the measurements carried is given in Table I. The disposition of measuring devices on the Joliet TLP is given in Figure 1. Data acquisition takes place in two modes, i.e. the normal mode and the storm mode. In normal mode all signals are sampled at between 1 Hz and 5 Hz for a period of 20 minute. Data is then analysed to yield statistical summaries (mean, max, min, rms values) and written to files. In storm mode additional analyses are also carried out to yield such data as responses and extreme statistics. A routine check is carried out to detect and remove bad data. This may be due to electronic or mechanical interference.
Use is made of commercially available software (Matlab) for carrying out some of the analyses.
According to the authors, the quality and quantity of the data being collected anables two important kinds of analyses and interpretation:

- Long-term assessment of the responses can be treated statisticaly and a good picture of the extreme and cumulative history of the tensiol leg loads determined.
- Input-output relationships can be derived from (short-term) responses and measured wind, wave and current data to compare with and calibrate predictive models(both theoretical and scale model experiments)

From the measured data and the subsequent analyses the following conclusions could be drawn with respect to the TLP behaviour;

- Extreme responsed have been significantly smaller than corresponding design estimates, although the extreme sea states have been up to about 90% of the original design extreme.
- It is apparent that extreme events have not involved simultaneous occurrence of extreme environmental conditions (wind, waves, current, water levels). The need for a rational probabilistic approach to event combination is emphasized.

Dynamically positioned vessel 'Seillean' (SWOPS)

Yuill [2] has given a review of 2 years operation of the BP's SWOPS. See Figure 2. Attention is focussed on the vessel's DP performance in terms of stationkeeping and power consumption.
The performance data is drawn from a DP performance logging system which keeps temporary records which are overwritten after a given time and permanent records. The temporary records perform a so-called Blackbox and Alarm and Event Logger function which are only consulted in emergency situations. The permanent records are retained by the Performance Logger.
Among others, the following data is recorded;

- Pitch
- Roll
- Wave height(infrared)
- Wave rider buoy
- Wind Speed and direction (2 systems)
- Position(Hydro-acoustic, 2 taut-wire systems, 2 gyrocompasses, 2 vertical reference units, Radio position reference)

Other data on power consumption is also measured.Data recording takes place over 20 minute intervals.

According to the author, the comprehensive data logging system incorporated in the DP system has not only provided feedback on faults/incidents but also provided valuable feedback to the designers and has provided a means of comparison between the actual and the predicted performance
From the full scale data some conclusions could be drawn;

- There have been at least two recorded incidents, with the vessel in service, where the vessel has been forced to disconnect due to cross-sea conditions. Model tests had previously highlighted these as an area of concern from the point of view of stationkeeping.

- Power levels have generally been lower than predicted in the design stage. See Figure 3. The main reason for the differences is considered to be due to the differing philosophy between the simulations and the actual operations. The computer simulations assumed wind, waves and current from the same quarter. In practice the DP operator attempts to reduce the transverse forces and turning moment on the vessel by balancing the ship between the wind, waves and current forces.

Dock Express Heavy Lift Ships

Aalbers and Leenaars [3] have give a comprehensive review of the objectives, instrumentation, data recording and data analysis of 2 years measurements carried out on 3 Dock Express vessels, Dock Express 11, 12 and 20. The vessels, with a fully loaded displacement of approximately 18000 t, were instrumented for acceleration measurements in order to investigate the actual level of the safety margins in the design methods proposed by classification societies. Beside using the measured data for the above, the statistical data derived from the measured data were compared with theoretical predictions based on strip theory ship motion computations combined with statistical data derived from Hogben and Lumb [4].
The measurements were carried out mainly with the vessels on the route Japan-Middle East.
The location of the accelerometers is given in Figure 4.
In addition to the measured accelerations, the results of observations of the sea conditions, wind conditions, anemometer readings, ship speed and information about time,date,sea area,route and loading condition were stored on diskette. Data was recorded in 30 minute intervals, analysed and stored.
The quality of the measured data (drop-outs, radio interference) was assessed and in subsequent analyses bad data was discarded.
About 2000 data sets were recorded of which finally 958 were considered suitable for the final analyses.
Two types of analyses were carried out i.e. short-term analyses on board yielding mean, rms, max and min values and long-term analyses which were carried out at MARIN.
An example of results of analyses is given in Figure 5.

One of the main conclusions obtained from the measuring program is that the design level accelerations obtained based on the procedures given by classification societies leads to to predicted transverse accelerations in the loaded condition with a very high confidence level. The magnitude may be a factor 2.5 higher than measured values at the required probability of exceedance. The main reason for the considerable safety margins are the assumptions on wave direction and wave period in the design sea state. Both are required to be the most unfavourable for the mode of acceleration considered.

Prior to installing the measuring equipment and the instrumentation, extensive performance checks were made. Special measures were taken to make it possible to calibrate the instruments on board.
Data acquisition was based on the use of a micro-computer and the data stored on diskettes.

During the two years measuring period no major failures of either the instrumentation or the data acquisition system occurred. The need for extensive and carefull prepara-tions is underlined.

Short-term measurements

Motions of two Frigates in rough weather

The program described by Andrew and Lloyd [5] concerns simultaneous motion and slamming measurements on two Frigates on October 11, 1977 in rough weather off the south-west of Ireland.
The objective of the measurements was to quantify the reported performance differences of the two ships concerned, to provide measured data of behaviour in extreme conditions for correlation with theoretical predictions and to establish a data base of measurements of ship motions at full-scale for different relative wave directions if conditions allowed. The vessels and a summary of the measuring channels is given in Figure 6 and Table II respectively. A number of measuring runs were made at different speeds with the vessels travelling parallel at some distance from each other. The measurements were carried out for 30 minutes in each case and recorded on FM-tape. Results of measurements were analysed to yield, among others, rms values, probablity density functions. Results were compared for both ships with theoretical predictions.
In Figure 7 the wave spectra as obtained from the wave rider buoy are given. In Figure 8 an example is given of the good correlation found between measured and predicted motions.

With respect to the sea conditions it was remarked that the waves were 'strongly unidirectional'. This is a very important observation as in many other full scale measuring programs where considerably worse correlation was found between predicted and observe motion, directional spreading, which is always difficult to quantify, may have been at the root of the differences.

Behaviour of a Tanker-based SPM system

Dogliani et al. [6] have carried out a measuring program on a permanently moored 140 kdwt tanker off Sicily. The objective of the program was to confirm and quantify the existance of low-frequency motion and force components in the mooring system of the tanker. The slow drift behaviour has been verified many times by computations and model tests however this has not been confirmed sufficiently on full scale. This was therefore a rather limited objective and, while it was hoped that measurements would co-incide with rough weather conditions, budgetary reasons prevented an extensive measuring program throughout the winter. The measuring equipment was installed and working for about 15 days. Within this period a important storm developed and the results of the subsequent measurements were presented.
In Figure 9 the configuration of the measuring equipment is shown. The following signals were measured and recorded;

- 4 strain gauges on the lower mooring yoke
- wave elevation using a wave rider buoy
- surge,sway and heave using accelerometers on a stabilized platform

- roll and pitch motions
- wind speed and direction

In view of the fact that low-frequency horizontal motions were the focal point of the program, the measuring interval was set at 8 hours. A sample frequency of 1 Hz was used for wave frequency signals while for low frequency motions were sampled at 1/60 Hz.
In Figure 10 the wave spectrum is given. The time history of the mooring stress, showing large, low frequency components in given in Figure 11.
Cross-bi-spectral analysis of the low-frequency signals was carried out and it was confirmed that the low-frequency motion and stress components were a quadratic function of the wave elevation thus confirming the theoretical predictions.

Behaviour of the semisubmersible Polycastle

Tamaki et al. [7] describe a comprehensive measuring program with the newly-built semisubmersible Polycastle in the North Sea in February 1983.
The objective of the test program was to obtain data to verify the design values of loads and motions. This entails measurement of behaviour in rough weather conditions.
The following signals were measured;

- wave elevation (radar, compensated for local heave motion)
- pitch, roll, yaw using gyroscopes
- surge, sway, heave using accelerometers
- wind using an anemometer
- current using a propeller type current meter
- bracing stresses using strain gauges

The measuring set-up for the strain gauges is shown in Figure 12.
The wave direction was estimated by observations.

Measurements were carried out for 22 days. 88 measurements of 30 minutes duration were made.

From the measurements statistical data and frequency domain data in the form of spectra and motion response functions were obtained. In Figure 13 results are shown of the wave and roll spectra in high seas. The presence of low-frequency components in the roll motions is clear. In Figure 14 the measured heave transfer function is compared with results of computations and model tests. It was concluded that good correlation was obtained for wave frequency components in both motions and stress fluctuations. The presence of low-frequency components in pitch and roll motions which indicates the presence of non-linear excitation components.

Transient measurements

Motion decay of two semi-submersibles.

Morch et al. [8] have carried out motion decay tests on two semi-submersibles the Henrik Ibsen and the Save Concordia. See Figure 15.

The objective of the tests was to obtain full scale motion decay data for comparison with experimental data.
The data was needed in view of more stringent NMD requirements regarding transient motions of a platform after line breakage. In order to obtain the motion decay data, the platforms were given an initial offset by using the mooring winches. A mooring winch is then released rapidly and the vessel carries out a transient horizontal motion to regain its new equilibrium position.
The following data were measured:

- surge and sway by accelerometers and radar or taut-wire system
- yaw by gyrocompas
- line tension by strain gauge equipment

The data sampling rate was 2 Hz.

Each measuring run lasted only a few minutes before the motion died down. The weather conditions were mild with wave heights from 1-1.5 m. The results of the motion measurements were analysed to obtain the damping ratios of the surge, sway and yaw motions.
Examples of results obtained are shown in Figure 16.
The measured results were compared with results of simulations.

Behaviour of two jackets during launching

Aage et al. [9] have reported a novel method for determining the rigid body motions a jacket structure during launching from a transportation barge.
The objective of the measurements was to determine the transient motions of the jacket and to compare these with time-domain computer simulations of the launching operation.
The measurements of the jacket motions were carried out by analysing a sequence of photographs taken using a motor-driven camera and a film made of the launch and from these to obtain 30-40 positions at time intervals of 1-2 s. The positions were obtained by taken film and photographs more or less from the side of the jacket and matching a template of the jacket to each photograph.
Examples of the jacket motions are shown in Figure 17. In Figure 18 examples are shown of comparisons of predicted and recorded motions of both jackets.

This is an example of a full-scale measuring program carried out with creativity and with a very high yield for modest effort and investment costs.

It can be expected that, with the development of video tracking techniques such optical tracking systems will be used more often for this type of full scale measuring programs.

Final remarks

In this contribution, we have looked at a number of examples of the three categories of full scale measuring programs for ships and offshore structures.

Monitoring of system behaviour in a hostile environment and for

longer duration places great demands on equipment and also on the personel using it. In reference [10] which gives a very comprehensive review of aspects of importance related to stress and motion monitoring on ships, reliability of the equipment is named as one of the major causes for concern. It appears that the reliability of the equipment is improving rapidly however, since in the more recent papers little mention is made of equipment failures.
It is now state-of-the-art to use microcomputers for data acquisition and for analysis purposes. Commercially available data acquisition software is becoming well established. Equipment such as the portable GPS systems are available with standardized interfaces to link-up to the micro-computer. GPS cards are also available for directly mounting in the computer.
All these developments will continue to make it easier and less expensive, as far as the equipment is concerned, to carry out trouble-free full scale measurements.
What stil remains however, are the problems associated with the interpretation of full scale data. Undeniably, good full scale data is extremely valuable in establishing real life behaviour. Problems sometimes arise when full scale data is compared with results of theoretical prediction or results of model tests. Although most of the results presented in the aforegoing publications seem to correspond reasonable well with predictions, it is also known that much data is gathered that does not conform well with predictions even though the quality of the measurements are above suspicion. It is these results that must also be brought before the footlight if the discussion is to be carried further.

As far as full scale measurement programs are concerned, what has been learnt is that especially here, thorough preparations must be made before embarking on such programs. The objectives must be clear in order to avoid misunderstanding with respect to the applicability of the data later.
If possible, predictions should be made beforehand for the expected range of conditions in order to be sure the right quantities are being measured.
Equipment should be well-tested and calibrated. Redundancy in both transducers and data acquisition systems is vital. Last but not least, the personel carrying out the program should be knowledgeable not only with respect to the equipment and resourcefull in solving hiccups, but also have insight in the processes which the system is monitoring.

References

1. Erb, P.R., Jefferys, E.R., Mercier, J.A. and Peters, D.J.H.; 'Lessons from TLP Performance Measurements', Proceedings MARIN Jubilee Meeting, Wageningen, May 1992

2. Yuill, D.L.;'Operational Aspects of SWOPS over 2-years Service', Proceedings MARIN Jubilee Meeting, Wageningen, May 1992

3. Aalbers, A. and Leenaars, C.;'Two Years of Acceleration Measurements on Dock Express Heavy Lift Ships compared with Predicted Values from Several Design Methods', RINA, 1987

4. Hogben, N. and Lumb;'Ocean Wave Statistics', NMI publ.67

5. Andrew, R.N. and Lloyd, A.R.J.M.;'Full-scale Comparative Measurements of the Behaviour of Two Frigates in Severe Head Seas', Paper no.7, RINA Spring Meeting, London, 1980

6. Dogliani, M., Monti, S., Sebastiani, L.and Tedeschi, R.;'Full Scale Measurement and Analysis on a SPM System', Proceedings OMAE, Volume I-B, Offshore Technology, 1991

7. Tamaki, I., Sodal, F., Nakayama, K., Inui,T., Kobayashi,M. and Nakamura, K.;'Full-Scale Measurement Tests on the New Semisubmersible Polycastle', OTC paper no.4731, Offshore Technology Conference, Houston, 1984

8. Morch, M., Kaasen, K.E. and Rudi, H.;'Full-Scale Measurements of Free-Oscillation Motions of Two Semisubmersibles', OTC paper no.4532, Offshore Technology Conference, Houston, 1983

9. Aage, C., Christiansen, P.E. and Moller, J.;'A Jacket Launch Computer Program compared with Two Full-Scale Launches', Proceedings Boss'85, 1985

10. Chazal, E.A., Cojeen, H.P., Lindeman, K. and Maclean, W.M.; 'Status Report on the Application of Stress and Motion Monitoring in Merchant Vessels', Paper no.17, SNAME Spring Meeting/STAR Symposium, Coronado, June 1980

11. Spidsoe, H. and Brathaug, H.P.;'Measured Motions of a North Sea Articulated Loading Platform', OTC paper no.4639, Offshore Technology Conference, Houston, 1983

12. Wevers, L.J. and Bos, R.W.;'Measurements of Wave and Drift Induced Line Forces and Motions o/b the Semi-Submersible DB-100', OTC paper no. 4439, Offshore Technology Conference, Houston, 1982

13. Borresen, R.;'Full Scale Experience with Petrojarl I', Proceedings MARIN Jubilee Meeting, Wageningen, May 1992

14. Clarke, J.D.;'Measurement of Hull Stresses in Two Frigates during a Severe Weather Trial', RINA, 1981

15. Bishop, R.E.D., Clarke, J.D. and Price, W.G.;'Comparison of Full Scale and Predicted Responses of Two Frigates in a Severe Weather Trial', RINA, 1983

TABLE 1: VARIABLES, SAMPLING RATES AND STATISTICAL PARAMETERS RECORDED AND ARCHIVED IN HUTTON AND JOLLIET DATA ACQUISITION SYSTEM NORMAL MODE

	Hutton	Jolliet
Wind speed:	mean (1 Hz) mean square	mean (2 Hz) and max gust
Wind Direction:	mean (1 Hz)	mean (2 Hz)
Wave height:	20 min signif value (1 Hz)	20 min signif value (2 Hz) and max indiv wave ht
Wave period:	zero-crossing	zero-crossing, spectral peak and period of max wave
Currents:	not measured	Average speed and direction from ADCP, 10 bins
Water level:	Average draft	Average draft
Tendon tension:	(1 Hz)	(5 Hz)
	For both TLPs, Average and standard deviation of total tension in each tendon and for each column, and maximum and minimum individual tension value.	
Horizontal acceleration:	(1 Hz) Standard deviation x and y components of acceleration and maximum radial acceleration	(2 Hz) Standard deviation of radial acceleration and and maximum radial acceleration and associated direction
Horizontal position:	(0.2 Hz)	(1 Hz)
	For both TLPs, average offset with respect to foundation template.	
Yaw:	(1 Hz)	(2 Hz)
	For both TLPs, average and standard deviation of yaw, and maximum and minimum individual yaw value.	
Riser tilt and stroke:	3 risers (1 Hz)	1 riser (2 Hz)
	For both TLPs, average and standard deviation of stroke and tilt, and maximum and minimum individual values and associated directions.	
Temperature:	not measured	Average air and water temperatures
Air pressure:	not measured	Sea level pressure

Table I: List of measurements on Hutton and Joliet TLPs

TABLE II. List of Measurements

Parameter	Transducer Location	Recording	Authority
Vertical acceleration Lateral acceleration Longitudinal acceleration Roll Pitch Yaw	Amidships (approx)	FM Magnetic tape	AMTE, Haslar
Vertical acceleration	Bridge	FM Magnetic tape	
Relative bow motion	Stem head	FM Magnetic tape	
Rudder angle	Tiller flat	FM Magnetic tape	
Stabiliser angle	Stabiliser compartment	FM Magnetic tape	
Speed	Ships EM Log	UV	
Deck wetness	Bridge (TV camera)	Video tape	
Hull girder strains	Various	FM Magnetic tape	AMTE, Dunfermline
Propeller shaft thrusts*	Engine room	UV	AMTE, Haslar
Propeller shaft torques*		UV	
Propeller shaft rpm*		UV	
Shp*		FM Magnetic tape	
Accelerations of aerials	Foremast	UV	ASWE, Portsdown
Vibration levels	Various in way of equipment	UV	
Green sea loading*	Foredeck	Computer	
Weapon system alignment*	Ring bulkhead	UV	
Green sea loading	Foredeck (one-shot gauges)	Manual	DG Ships
Waves (uni-directional)	Waverider buoy	FM Magnetic tape	AMTE, Haslar
Waves (directional)	IOS buoy	FM Magnetic tape	IOS, Wormley
Motion sickness factors	–	Questionnaire	INM, Alverstoke

*LEANDER only

Table II: List of measurements on two Frigates.

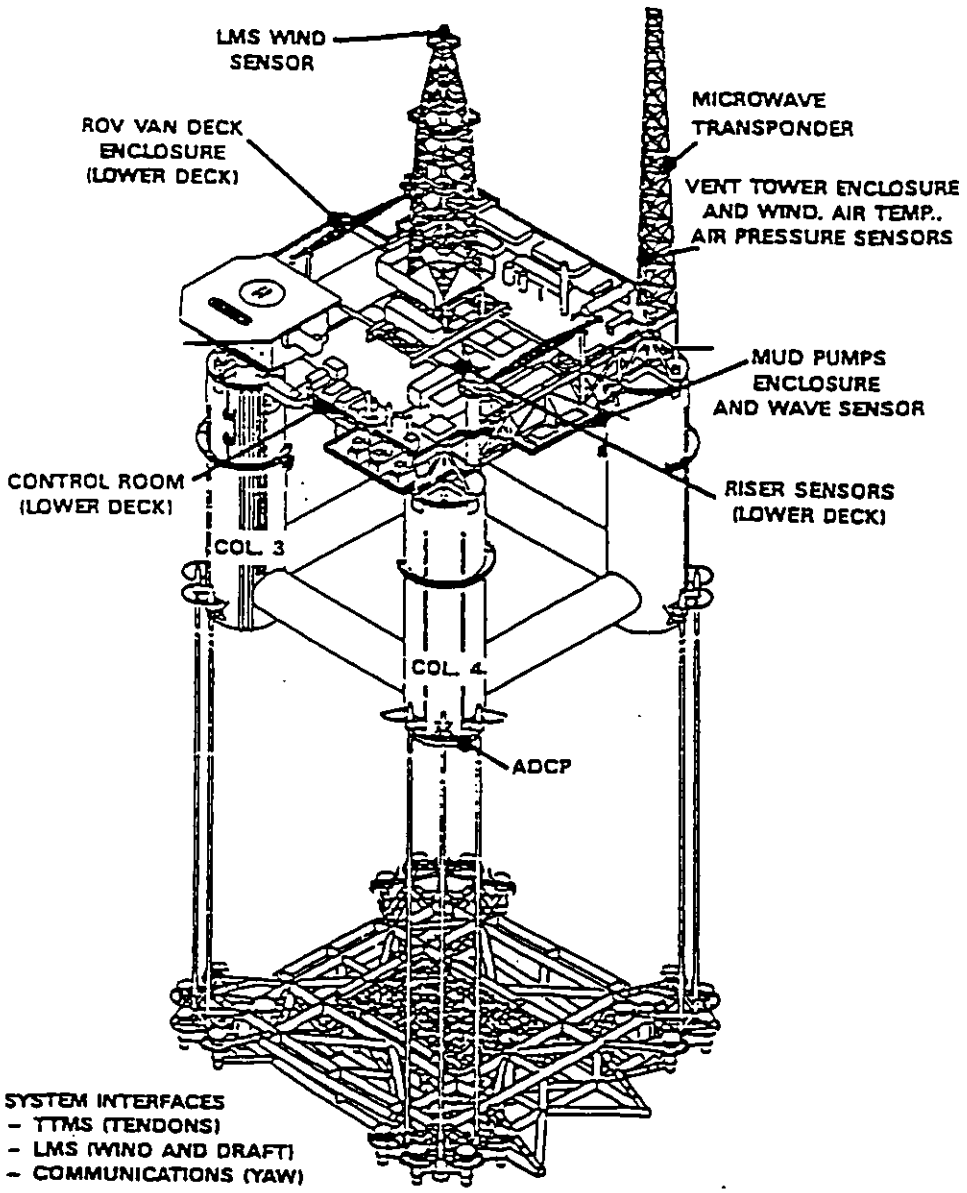

Locations of measurement systems on the Joliet TLWP

Figure 1: Joliet Tension Leg Wellhead Platform

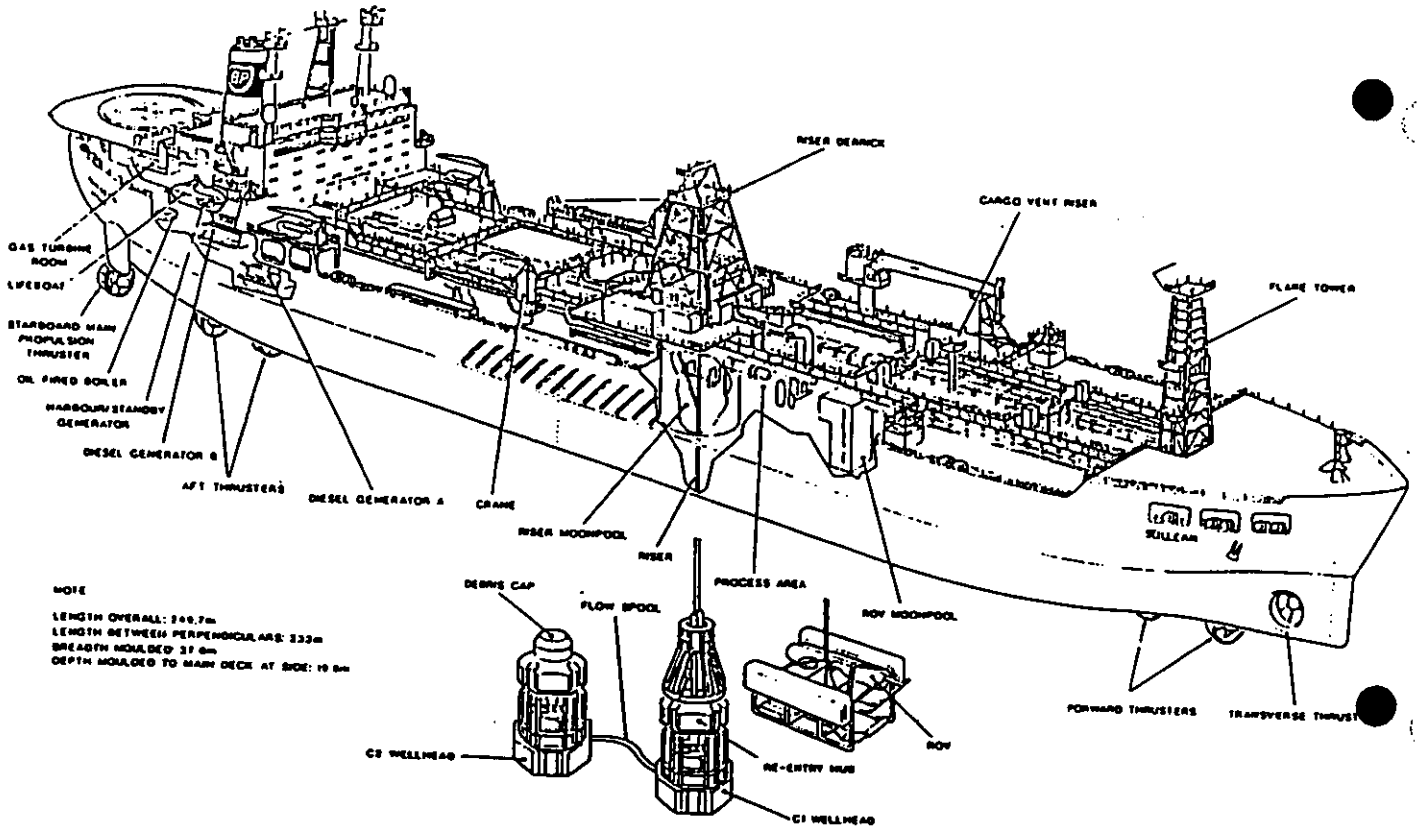

Figure 2: DP-vessel "SEILLEAN" (SWOPS)

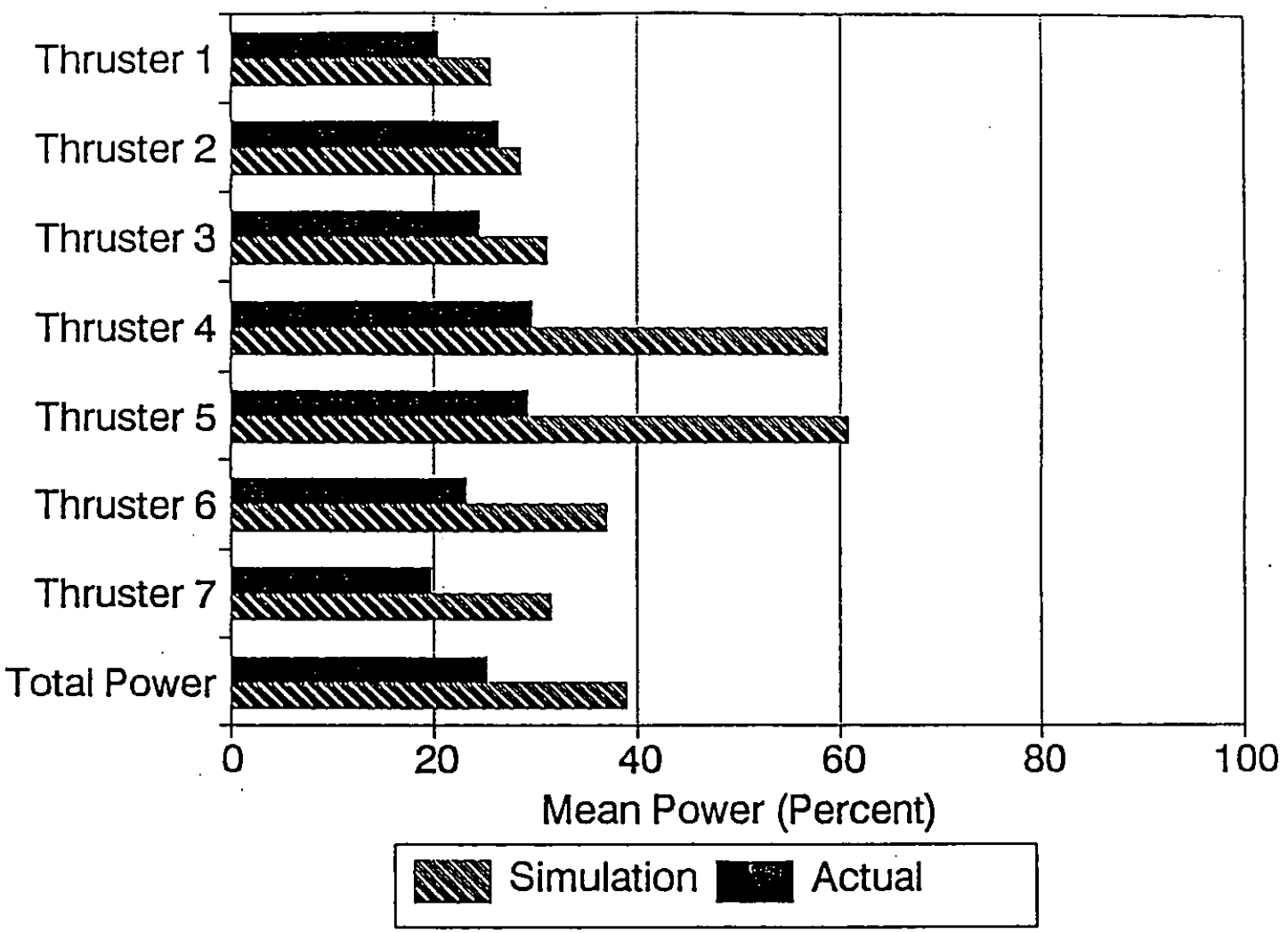

Figure 3: Thruster power SWOPS.

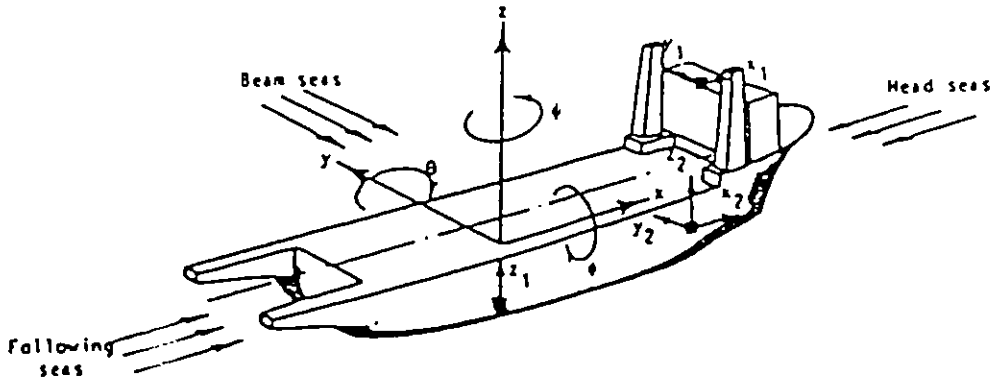

Co-ordinate System and Location of Accelerometers on the Ships

Figure 4: Location measuring devices on Dock Express vessels.

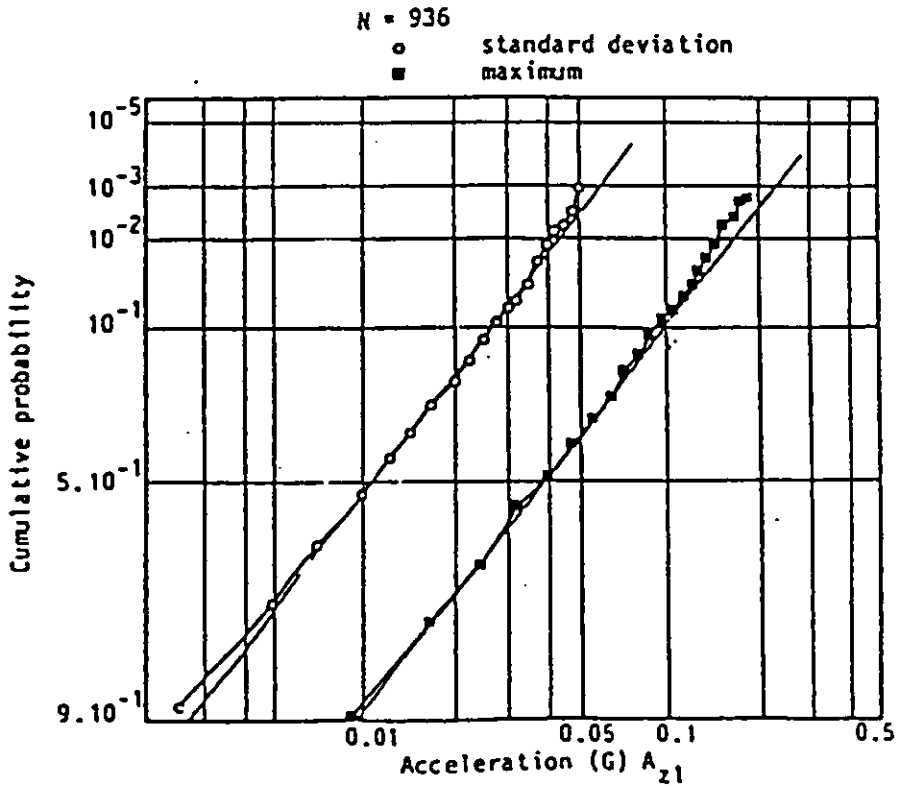

Vertical Acceleration in Engine Room

Figure 5: Probability of exceedance of accelerations on Dock Express.

Outline Ship Particulars

	LEANDER	TRIBAL
Mass (nominal), tonnes	3000	2800
Length, waterline, m	110	107
Beam, m	13	13
Draught, m	5·5	5·3
Longitudinal centre of gravity, percentage LWL aft of amidships	3·60	1·77
Longitudinal radius of gyration, m	25·9	25·4
Trim	TRIBAL has more trim by stern.	
Form	LEANDER waterplane and underwater body finer forward and fuller aft.	
Deadrise	LEANDER has higher deadrise angles forward.	
Freeboard	Similar at FP but raised fo'c'sle of LEANDER provides higher freeboard further aft (Fig. 2).	
Flare	TRIBAL has more flare forward.	
Bridge position, percentage LWL aft of FP	34	21

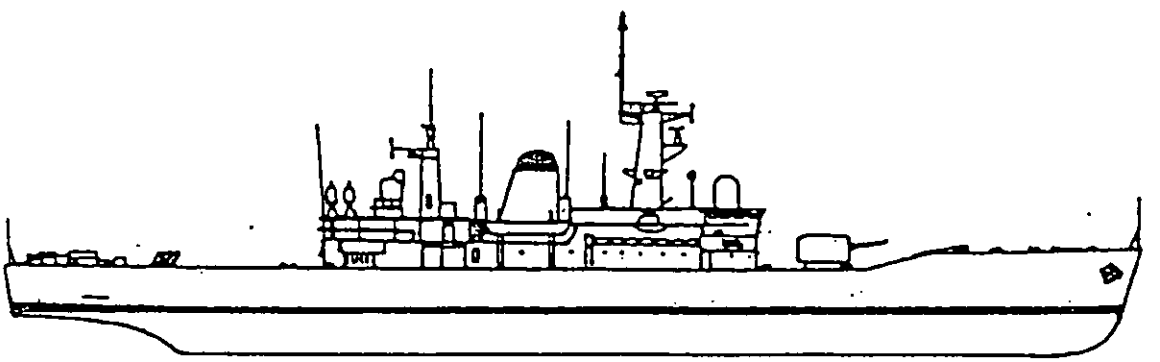

LEANDER

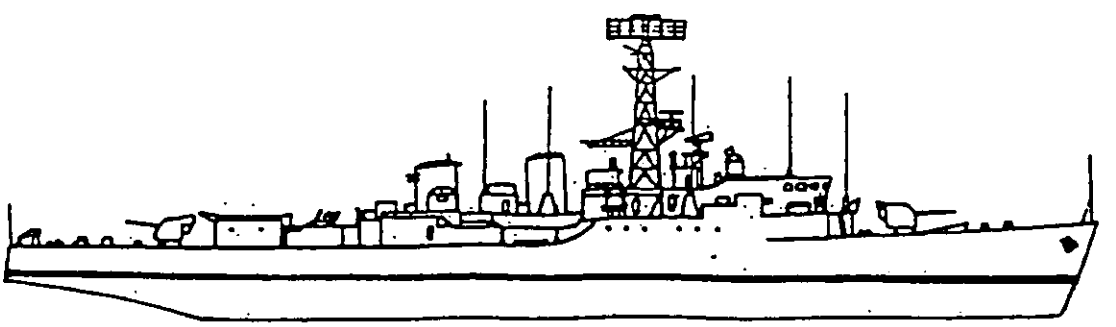

TRIBAL

Figure 6: General arrangement and particulars of two Frigates.

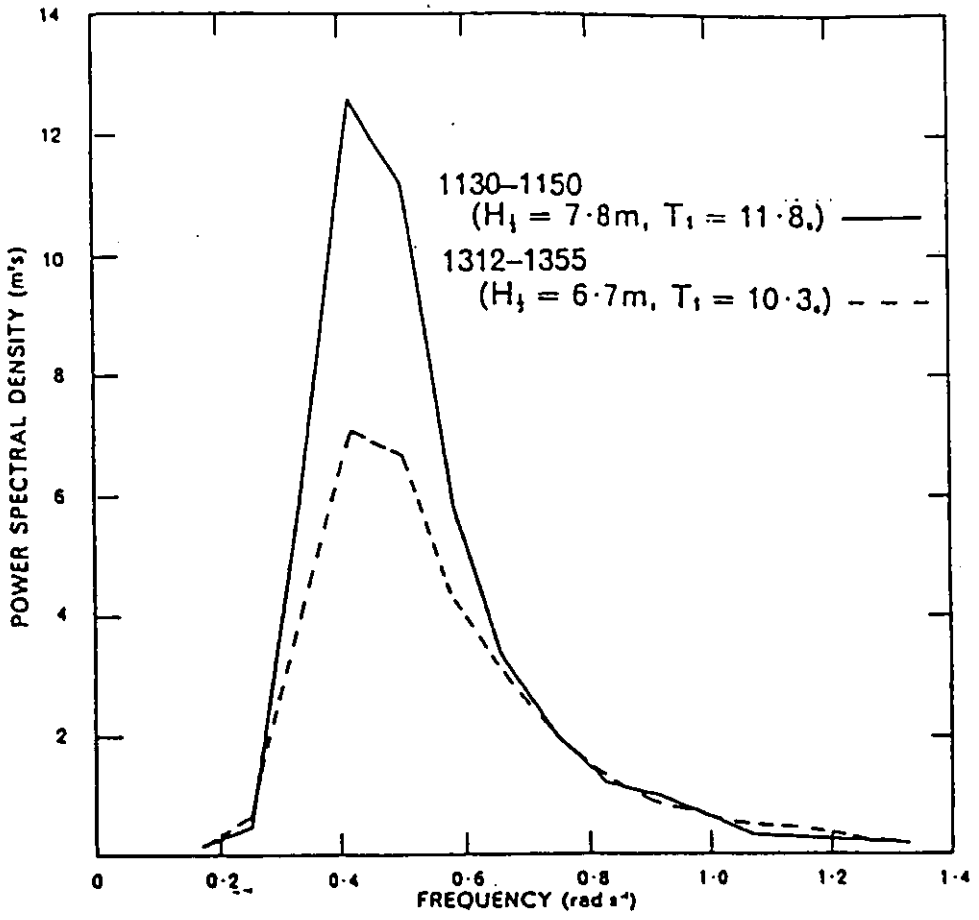

Measured point wave power spectral densities

Figure 7: Wave spectrum from wave rider buoy.

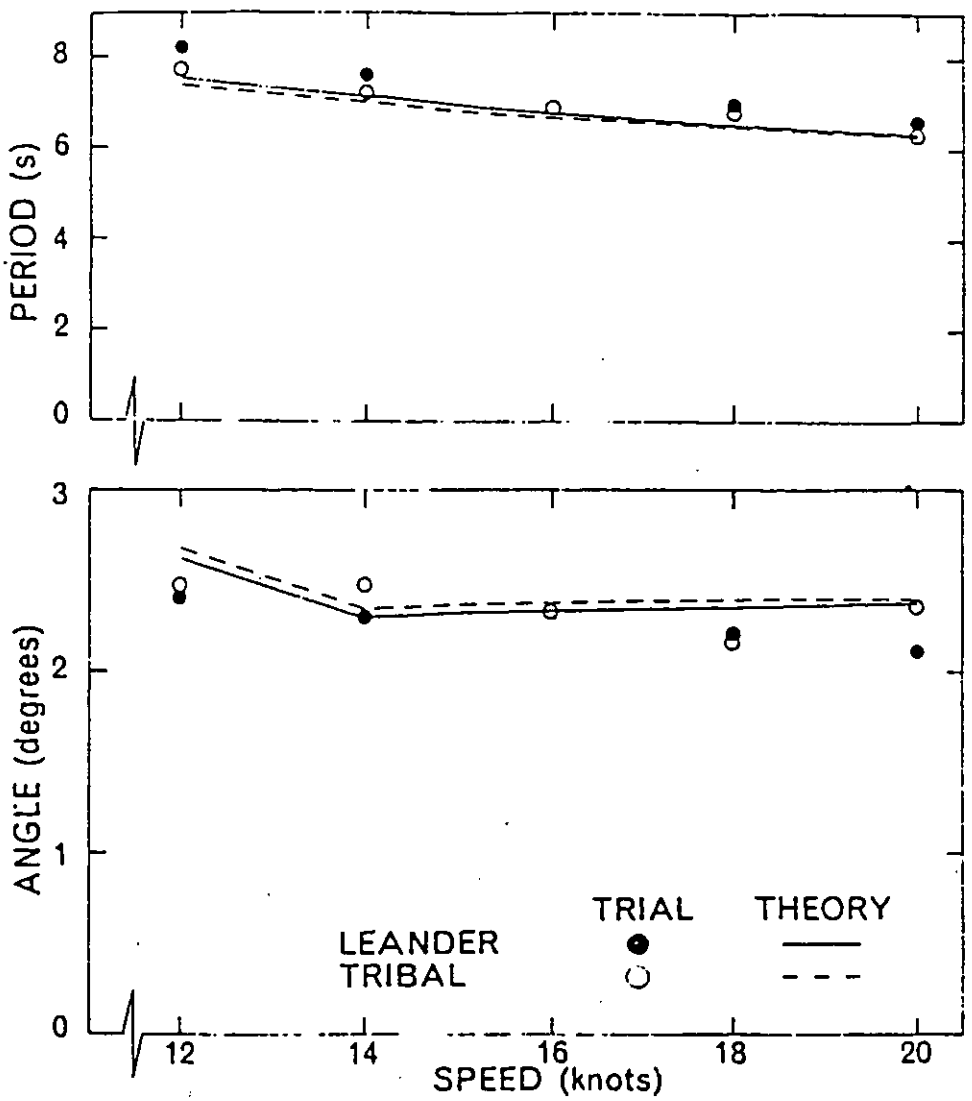

Root mean square pitch angle and mean period
(zero-crossing identity)

Figure 8: Motions of two Frigates.

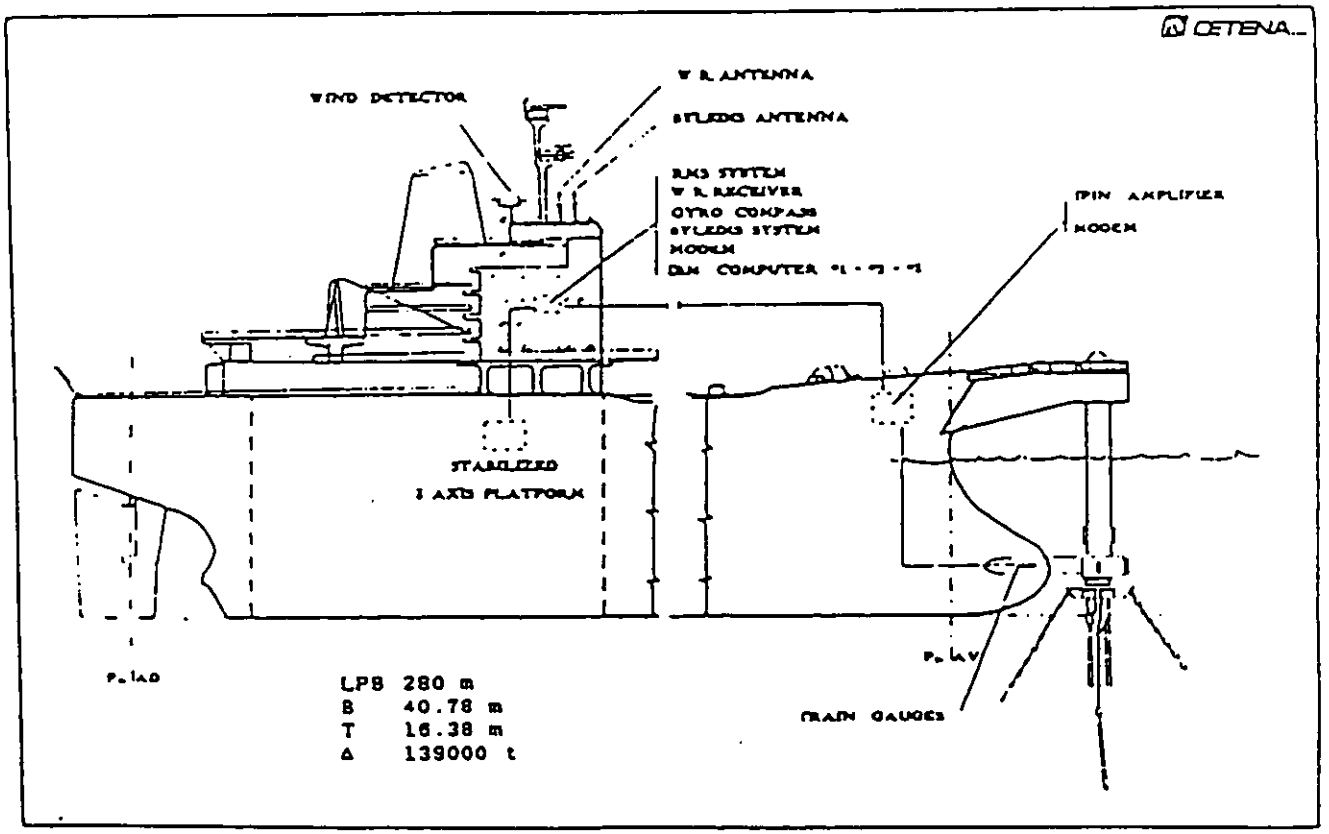

- Configuration of the measurement system

Figure 9: Measuring system on a moored storage and production tanker.

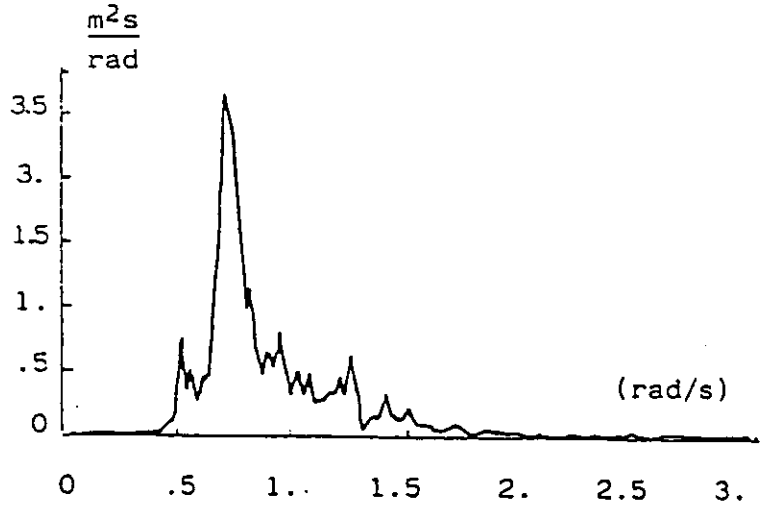

- Power spectrum of wave elevation relevant to Fig. 4.
  Significant wave height: 3.35 m
  Peak frequency: 0.69 rad/s (0.11 Hz)

Figure 10: Wave spectrum from wave rider buoy.

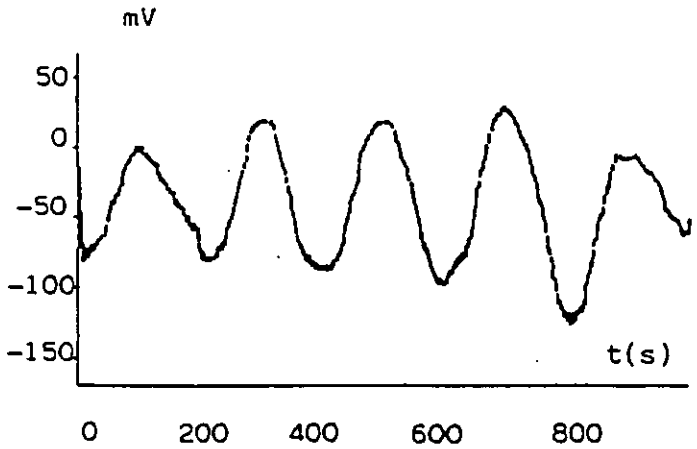

- Time history of a 1024 s record of mooring stresses.
  Zero crossing period: 204.8 s

Figure 11: Stresses in mooring system of storage tanker.

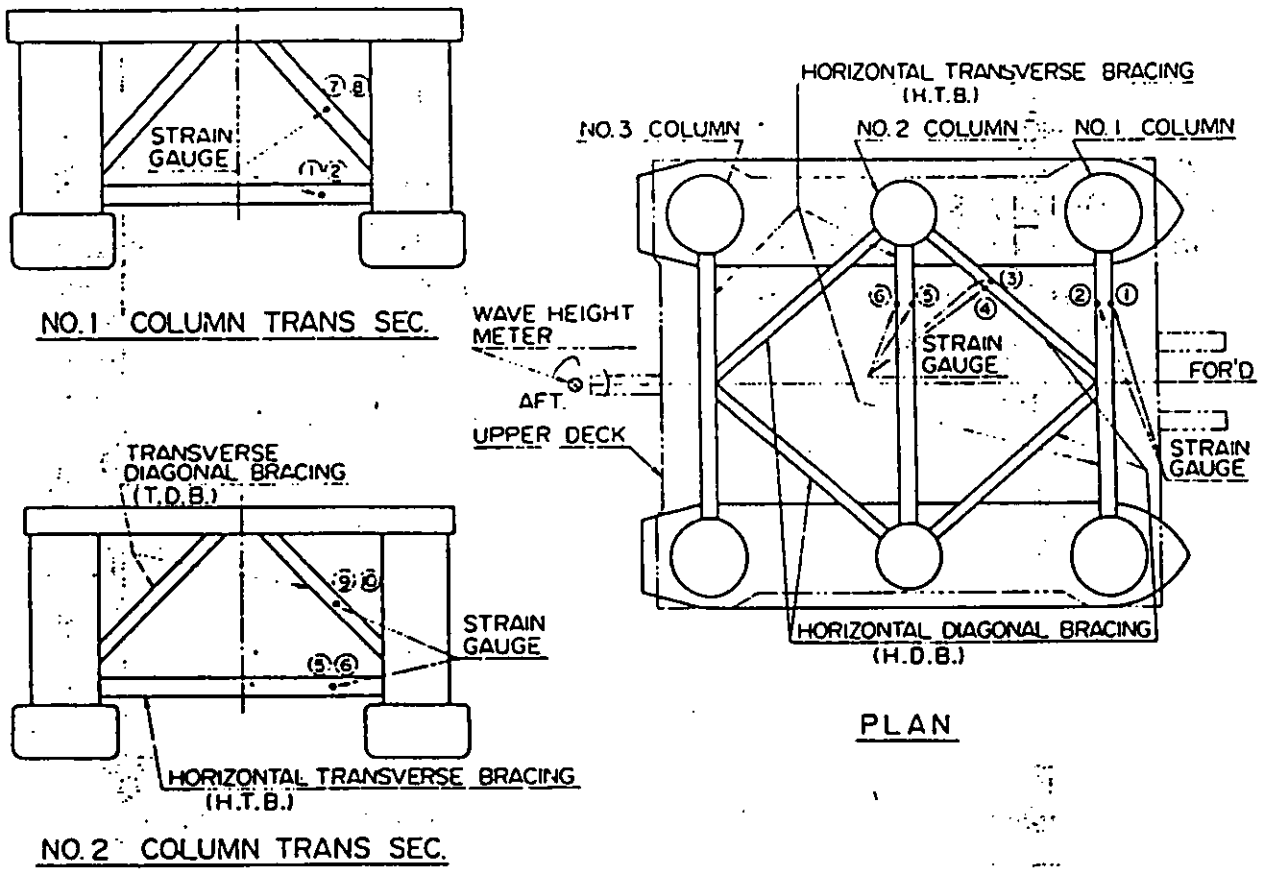

–Location of wave height meter and strain gauges (10 points).

Figure 12: Location measuring devices on semisubmersible Polycastle

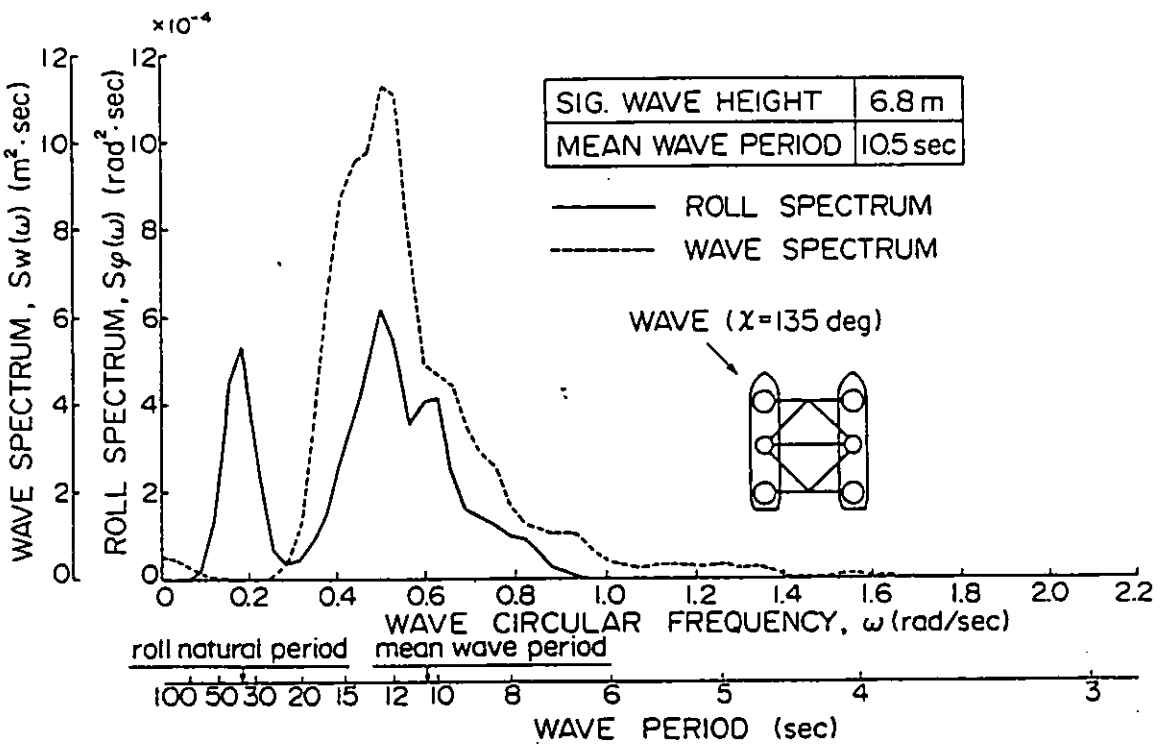

Figure 13: Wave and Roll motion spectra Polycastle

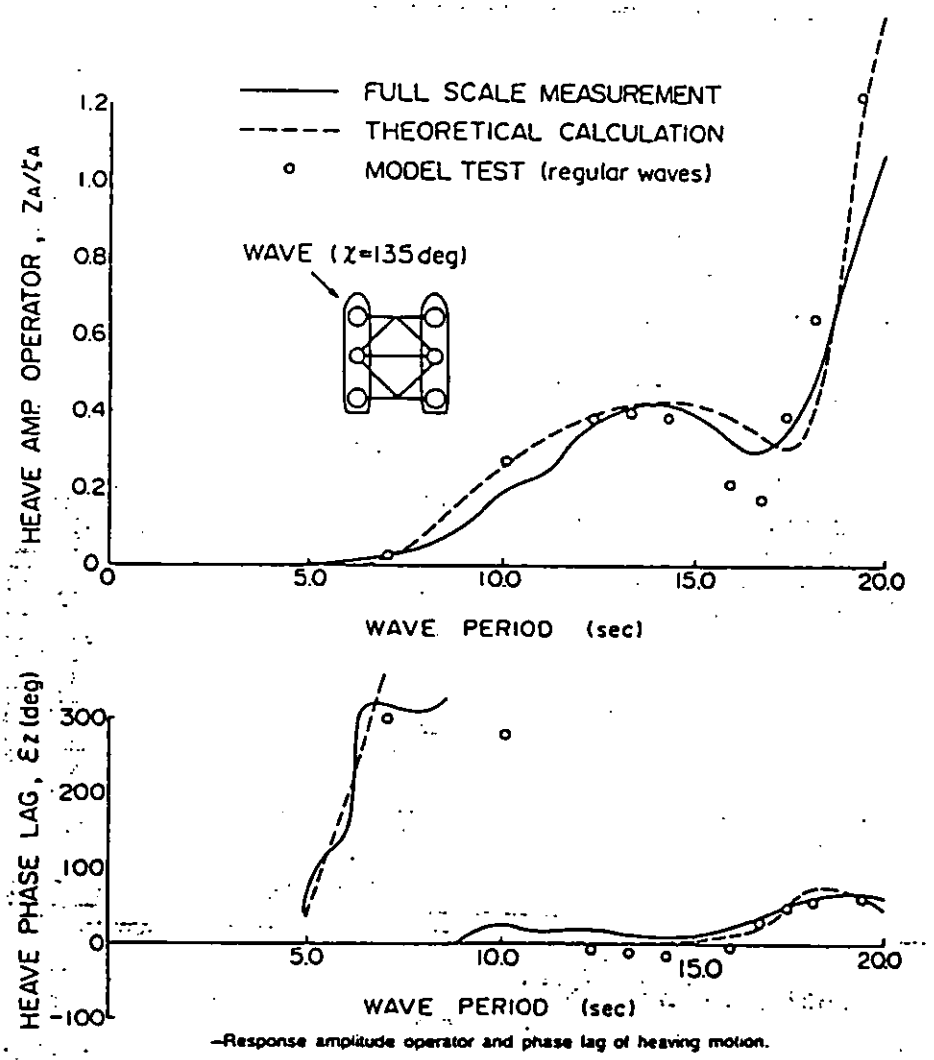

–Response amplitude operator and phase lag of heaving motion.

Figure 14: Measured and predicted heave motions of Polycastle

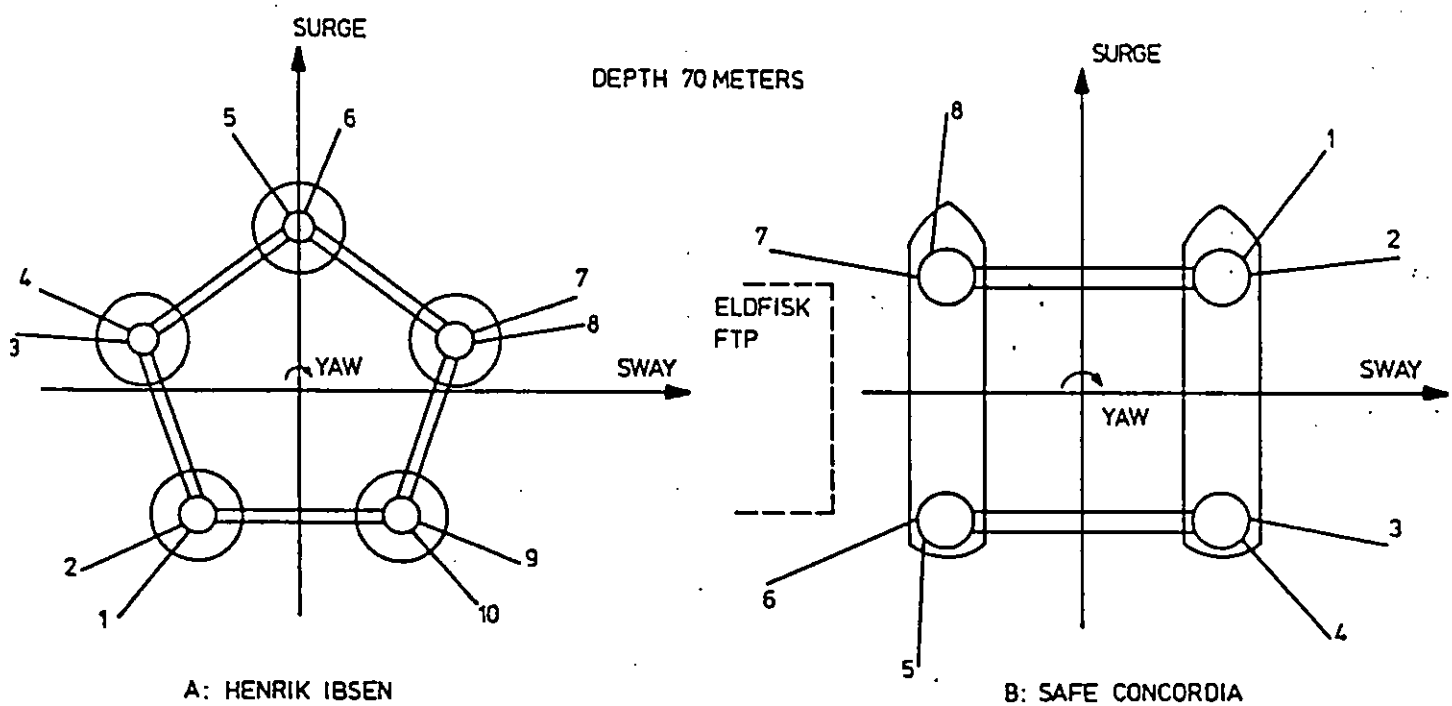

MOORING PATTERNS FOR THE HENRIK IBSEN AND THE SAFE CONCORDIA.

Figure 15: Semisubmersibles Henrik Ibsen and Safe Concordia

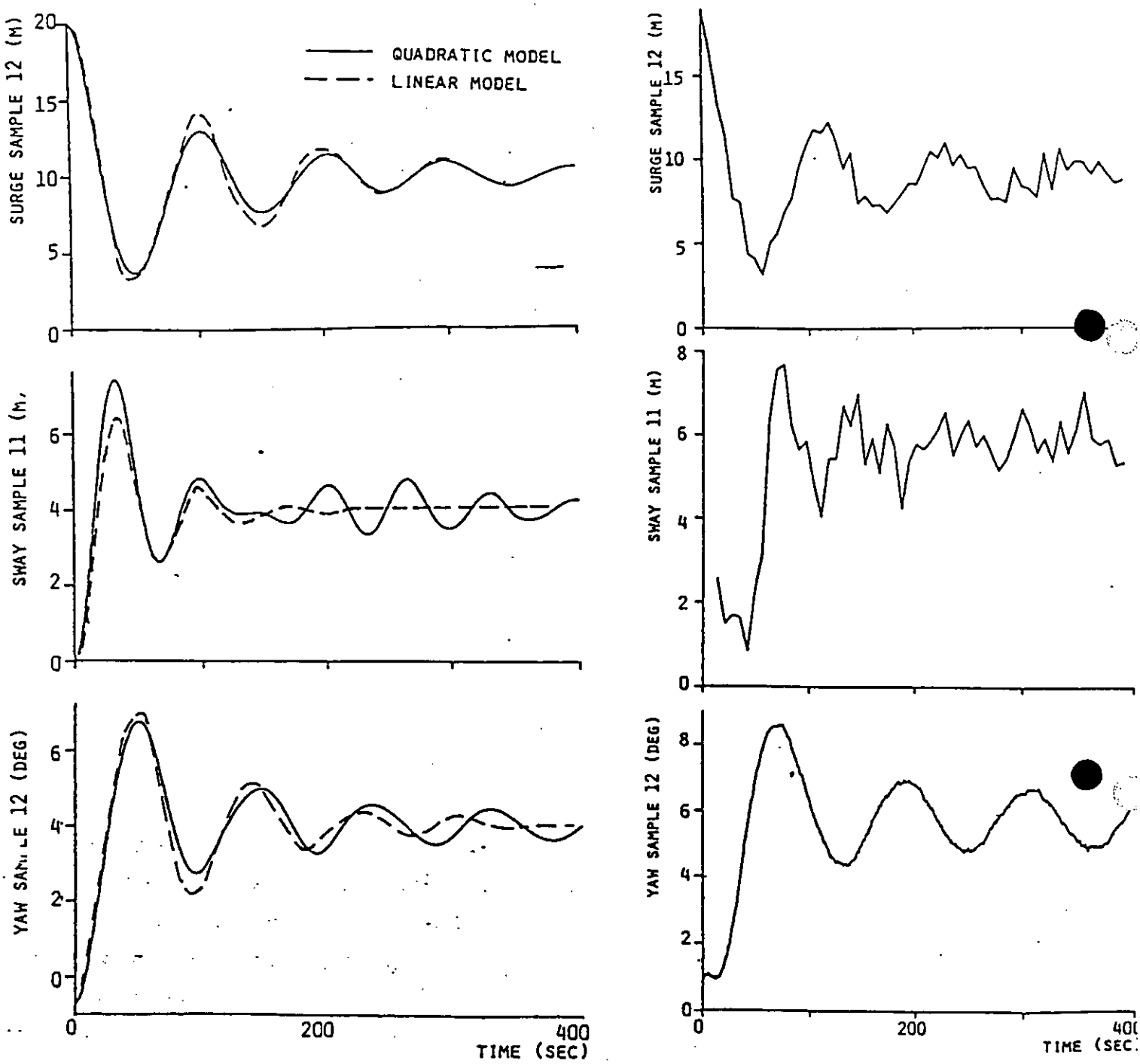

SIMULATED TRANSIENT MOTIONS OF THE HENRIK IBSEN.

MEASURED TRANSIENT MOTIONS OF THE HENRIK IBSEN.

Figure 16: Measured and predicted horizontal motion decay data Henrik Ibsen

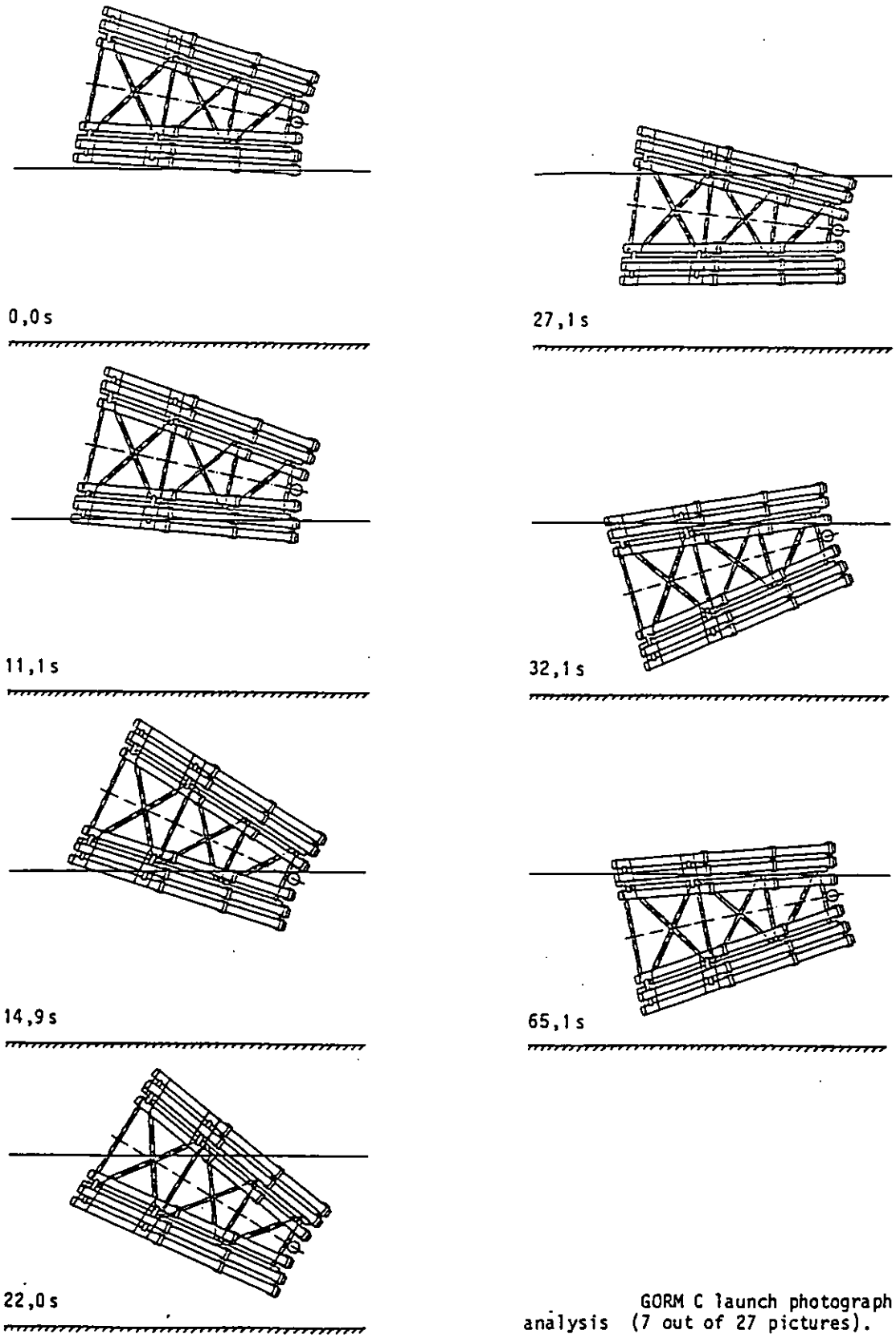

Figure 17: Position of Gorm-C jacket during launching (taken from photographs)

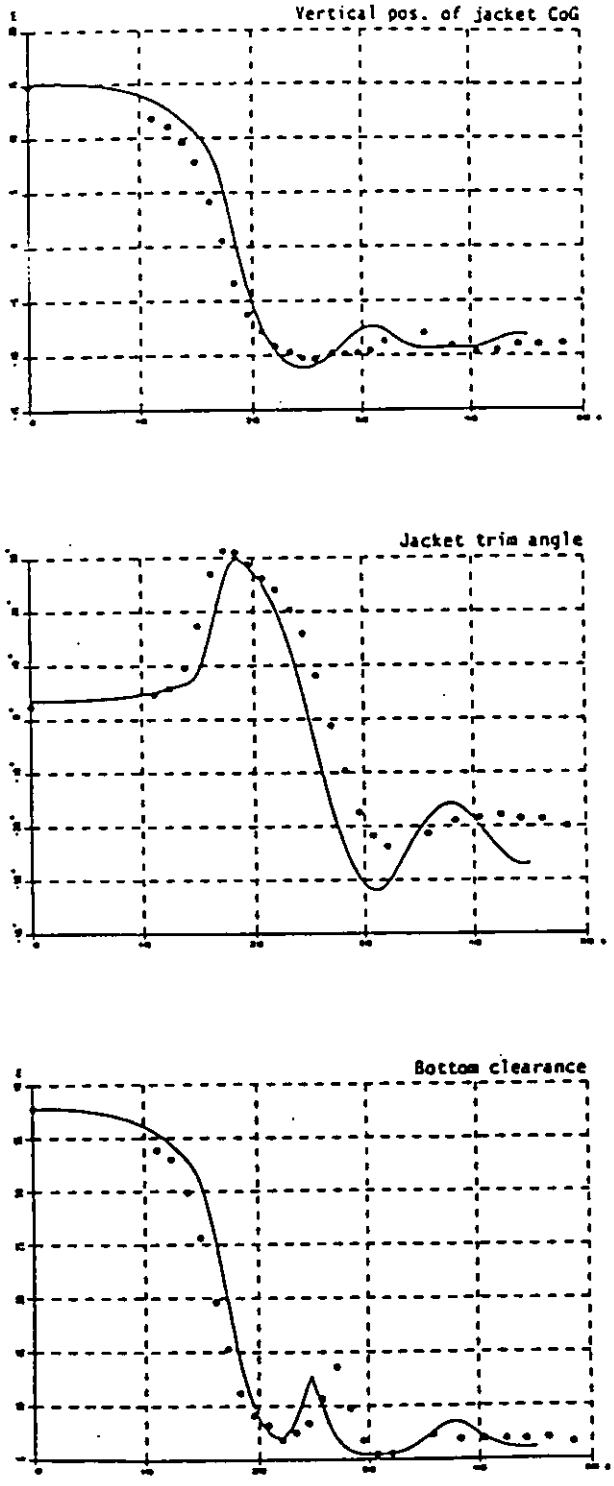

GORM C launch computer
simulation and full-scale measurements.

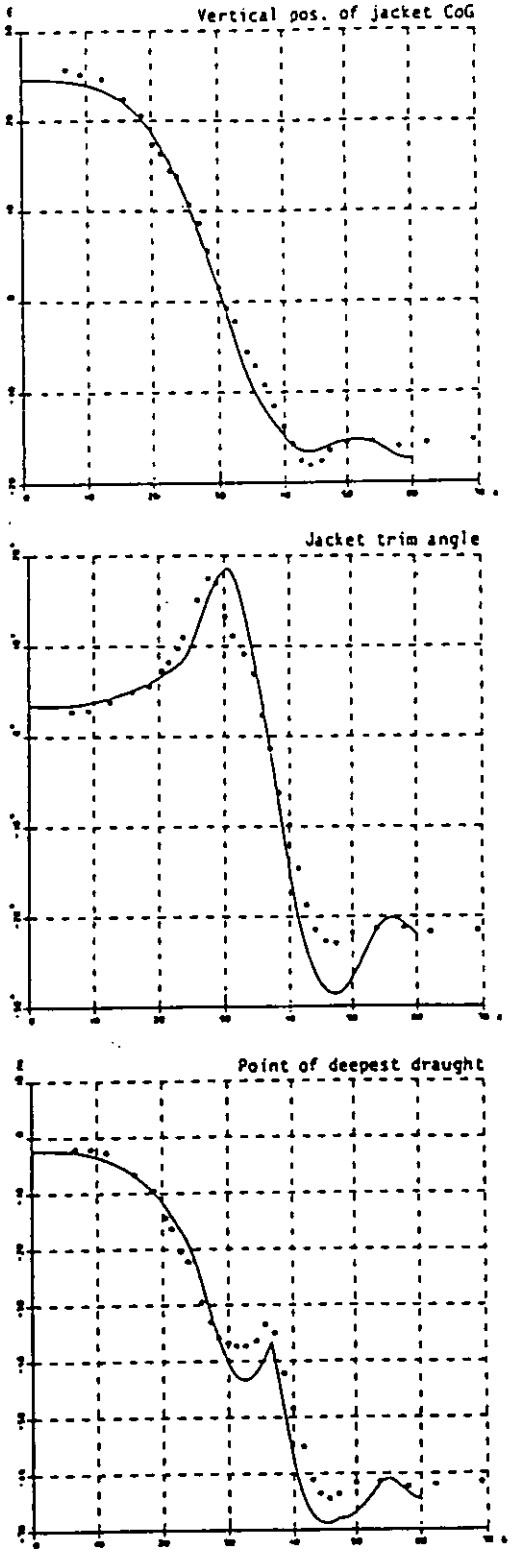

BERYL B launch computer
simulation and full-scale measurements.

Figure 18: Measured and predicted motions of two jackets during launching

MODEL TESTING OF SHIPS AND FLOATING OFFSHORE STRUCTURES

by

J.A. PINKSTER

DELFT

MODEL TESTING OF SHIPS AND OFFSHORE STRUCTURES

J.A. Pinkster
Delft University of technology
Ship Hydromechanics Laboratory

Introduction

Since William Froude introduced the laws by means of which it became possible to translate results of ship model tests into corresponding full scale values, model testing has never lost it's place in the arsenal of means at the disposal of the engineer and naval architect to gain insight into the various hydromechanic aspects of interest.

In recent years with the upsurge of availability of cheap, powerful computers and the corresponding development of software, many of the problems hitherto only to be tackled by means of model tests can now be analysed by means of computations. Since computers are more widely available than model testing facilities , it is natural that much attention is being devoted to developing computational methods and software for the analysis of hydromechanic aspects of ships and offshore structures. Whereas previously model tests were considered to be the only reliable source of quantitative data these are now being preceded and in many cases, replaced, in the design spiral by computations since these are considered to be more flexible in use, cheaper and generally ,in their application, directly under the control of the designer. The quantitative accuracy of results of computations are often considered to be equal to that of model tests.

Model tests however, will continue to occupy a place of great importance in the analysis of hydromechanic aspects. This is due to the fact that the hydrodynamic theory underlying computational methods is in many cases not sufficiently developed to represent the physically important processes sufficiently accurately. For instance, viscous flow about ships and large amplitude motions in waves resulting in green water on deck cannot be assessed sufficiently accurately on the basis of computations alone and often need to be verified by means of model tests. Also the behaviour of more complex systems such as a vessel moored to a spm with a transport tanker moored in tandem in irregular waves, wind and current still defy accurate computer analysis. Nowadays, even when there is sufficient confidence that the computer software has a solid foundation in terms of correct description of the relevant physical phenomenon, model tests may yet be carried out as a totally independent means of generating the same data on the behaviour of a structure and is thus used as a check on computations. This can be the case when the computations themselves are very complex with respect to , for instance, input quantities, and the possibility of human error is very real.

It is very likely therefore that an offshore engineer or naval architect will at some stage be confronted with the need for results of model tests.

It is the intention of this contribution to adress some of the practical aspects related to model tests which he may be confronted with and to discuss some of the common pitfalls.

Classification of model tests

In order to be able to design a meaningfull model test program it is necessary to define the purpose of the tests. To that end it is usefull to classify the some of the major types of model tests and to list some of the main characteristics of these types:

Fundamental tests:

These tests are aimed at giving insight in basic phenomena related to the project at hand for which there may not be a corresponding computational method available. Characteristic of such model tests are:

- Simplified models are used
- Relatively few quantities are measured

Correlation testing:

A computational method is available to determine, for instance, wave loads or wave induced motions. The purpose of the tests is to verify the results of computations.

Feasibility testing:

New concepts of ships or floating structures are being developed and may need verification at an early stage.

Design test:

As the name implies, these tests are aimed at producing data specifically relevant to the design of the vessel or structure.

- Emphasis on extreme survival conditions and limiting operational conditions
- Measurement of quantities relevant for the structural design and motion behaviour in operational and extreme conditions
- Increasing interest in fatigue loads resulting in more testing in low sea conditions
- Interest in statistical behaviour of motions and loads
- Detailed models
- Large number of measuring quantities

Installation tests for offshore structures:

The design of offshore structures is not always fully determined by the in-situ conditions but often considerably influenced by the installation. The installation can involve two or more other vessels such as crane barges and transportation barges.

- Low sea-states
- Multi-bodies
- Launching
- Transient effects

Transportation tests:
- Towing large structures
- Dry tow/Wet tow

Launching tests for ships:
- Transient effects
- Repeated tests

Resistance and Propulsion and flow visualization tests for ships:

Manoeuvring tests:
- Free-running
- Captive

Model testing standards:
At present time there are no mandatory international standards to which model tests have to conform. The International Towing Tank Conference [ITTC], of which many model testing facilities are members, has , from time to time proposed standards for various aspects related to model tests, primarily in the field of ship resistance and propulsion testing. Some guidelines are also given for testing of offshore structures notably in the reports of the Ocean Engineering Committee. Comparative model testing is sometimes carried out by member organisations in order to determine , among others, variability of model test results on the same object [Figuren]. There is a growing tendency for large offshore contractors to demand Quality Control systems to be applied by model testing facilities. Only the larger model testing facilities have the resources to set up the necessary organization and to prepare the required documentation. This entails, among others, that detailed descriptions of model testing preparations, model manufacture, testing procedures , analysis of test results etc be available to the client and that a clear approval procedure with corresponding distribution of responsibility within the facility be established and documented. Regulatory bodies and Classification Societies tend not to specific with regards to model testing other than that , when required, they be carried out by 'recognized institutes'.

Scaling laws

It is well known that ship and offshore model tests are carried out taking into account Froude's Law of Similitude, which is valid when we assume that the governing process is the equilibrium between inertia forces and gravity forces (free-surface effects). We also know that viscous effects can be of great importance with respect to some phenomena such as resistance, drag, lift etc. and that for such effects to be scaled properly, Reynolds Law should be taken into account. In some model test programs, where gravity effects are considered less important, higher Reynolds numbers are aimed for in the model tests than would follow according to Froude scaling. In some instances it was surmised that the best results would be achieved if model tests could be carried out at the full scale Reynolds number.
It can be shown, however, that if the full scale Reynolds number is achieved in the model, then the hydrodynamic forces on the model will equal those on the full scale prototype. This clearly is a totally unrealistic situation!

Preparations for model tests

general

Prior to detailed preparations for model tests, some primary aspects have to be adressed i.e.:

- What is the purpose of the tests
- What data is expected from the tests and in which form
- What is the function of the results of model tests in the whole of the project

Such aspects play an important role in determining the scope of model tests. For instance, instead of carrying out extensive model tests on a new concept, it may be advantageous to carry out limited tests first in order to establish the feasibility of the concept and to get some preliminary data on basis of which the design may be improved. This generally leads to an increased probability of success for the project as a whole and to more optimized test programs.

Particulars of the structure to be tested.

In order to carry out model tests various particulars with respect to the structure need to be established depending on the scope of the tests to be carried out.

First and foremost the lines of the structure need to be known. If the model tests are to be carried out in waves, or instationary behaviour such as occurs during a launching test in still water needs to be determined, particulars of the weight distribution need to be known. This generally entails knowing the position of the Center of Gravity in all three co-ordinates and the roll, pitch and yaw radii of gyration. For ships approximate values of the radii of gyration can be obtained from literature. For more complex structures these data can be determined from the detailed weight distribution of the vessel. If tests to determine internal loads in a structure are considered, the particulars of the weight distributions of the parts into which the structure is to be sub-divided and between which the forces and moments are to be measured must also be known. These data are only available from the detailed weight distribution of the structure in question. Care must be taken to ensure that the required weight distribution of the complete vessel is correct.

In some cases, for instance, upending tests with jacket structures, or ship model tests involving anti-roll tank testing, also the internal dimensions of the structure or part of the structure may need to modelled. This may place stringent demands on the subsequent model construction for instance with respect to wall thicknesses.

It is general practice to include on the underwater part of a model all relevant appendices unless the appendices themselves are part of the investigation. In such cases part of the test program is often carried out without the presence of such elements.

In the case of ship testing the appendices include the rudder, propeller, bilge keels , anti-roll fins, bow-thruster tunnels etc.

Except in the case of resistance and propulsion testing of ships in still water conditions, the models are generally constructed up to the deck-level. In some cases involving tests in wind, or in tests in waves where the shipping of green water is of interest, the main particulars of superstructures need to be determined. Superstructures are often added to models for purely cosmetic purposes.

Construction materials

Models may be constructed of a variety of materials of which a few are mentioned here. The choice of material depends to a large extent on the standard practice developed at the particular facility. This is dictated partly by the availability of the material and also on the particular skills of the craftmen involved.

Generally models should be constructed to be rigid and not deform noticably under the loading to which it may be subjected during the tests. Care should also be taken that, for instance, in the case of slamming pressure measurements, not only the overall rigidity of the model is sufficient, but also the local stiffness of the hull, so that the pressure measurement is influenced as little as possible by elasticity effects. An overall check on the model rigidity is obtained by carrying out impact tests, with the model suspended in air, and also with it lying in still water. A record of, for instance, acceleration components at a number of locations on the model will yield the natural frequencies of the structure. This may be compared with the expected frequency of the excitations during the actual test program. If the frequency ranges are too close, dynamic magnification effects in the measured data may be significant.
Models of ships may be constructed of wood, fibreglass or in some cases, foam. In case wood is used this may be in the form of a sandwich construction of thicker planks which is then given the proper outside dimensions by first milling and then hand-finishing. Alternately, a wooden batten model may be constructed usig plywood frames and bulkheads. The wooden batten models are lighter and it is somewhat more difficult to maintain the required construction tolerances.

Fibreglass models require the construction of a mould from which first a female fibreglass mould is made after which the final model can be made. Fibreglassmodels are often used for smaller models or when model weight becomes a problem. Making fibreglass models places additional requirements on the ventilation of the workshop. In a number of cases, regular manufacture of fibrglass models was stopped due to the possible health hazard to personnel. Models of semi-submersibles and tension leg platforms can be made of sheet metal, PVC, wood, fibreglass or combinations of these materials. When making models with combinations of materials, special attention may be required to ensure watertightness. Models of jacket structures are generally constructed of tubular steel or aluminium. Steel has the advantage of smaller wall thickness thus making it possible to retain the required internal floodable volumes.

Aluminium is sometimes preferred with a view to easier weldability of the pipes due, among others to a greater wall thickness.

Construction tolerances

Models of ships and floating offshore structures are generally constructed to a tolerance of about 0.5 to 1.0 mm for the hull shape. Deck houses and superstructures are often schematized. In the case of jacket structures which are always constructed of commercially available steel or aluminium pipe sections, differences between the required and available diameters may be larger. In such cases an excess of volume in one part of the model is compensated by a reduction in diameter in an adjacent part of the model.

Weight distribution of the models

Depending on the nature of the model tests, one or more properties of the weiht distribution of the structure has to be reproduced in the model.
If resistance and propulsion tests are carried out for a ship model, the static draft, heel and trim have to be reproduced. This is satisfied if the weight and position of the center of gravity in the horizontal plane are correct. The practical way of adjusting these values is to place the model in the water, add ballast weights in the appropriate locations until the model is at the correct drafts, fore, aft and midships. It should be remembered however, that following this procedure, the correct draft etc. are achieved but no direct check is made of the displacement of the model. This may be checked by first weighing the model and then also taking into account the added weights. In this way the total displacement weight at the required draft is checked.
For jacket structures the distribution of the displacement over the vertical is checked by lowering the model, step by step, into the water and measuring the change in total suspended weight of the model.
If tests of a dynamic nature are carried out the center of gravity and radii of gyration of the model have to be adjusted.
For ship models, the radii of gyration for pitch and yaw are assumed to be the same. These are adjusted by placing the model on a horizontal pendulum table which can rotate in pitch direction about the assumed center of gravity of the model. The table has a known statec pitch restoring coefficient [spring coefficient] and the pitch moment of inertia of the tabel about the point of rotation is known [table calibration]. By adding the required pitch moment of inertia of the vessel, the total pitch moment of inertia of table and model is found. Taking into account the known pitch restoring coefficient of the table, the natural pitch period of the table plus ship model is found. The model is ballasted on the tabel to the correct weight appropriate for the particular loading condition and the weights are distributed fore and aft in the model to achieve a horizontally level table. This adjusts the longitudinal position of the center of gravity of the model.
By carrying out a static trim test on the table plus model and adjusting the vertical position of the ballast weights, the vertical center of gravity is adjusted.
Finally, the table is given a static trim angle, released and the natural pitch period of table plus model are measured.

If the value is too low, the ballast weights are moved symmetrically outwards in fore and aft direction thus increasing the moment of inertia. By trial and error process the correct position of the ballast weights are found and noted.

In the case of models or structures which are too large for a pendulum table, or such equipment is not available, the center of gravity is adjusted after weighing the model without ballast added and the center of gravity of the model has been determined by, for instance balancing on a knife-edge. The moments of inertia of the model can be determined by using the bi-filar pendulum principle. The model is suspended by two parellel vertical wires of equal length attached to points placed equal horizontal distance from the center of gravity of the model. Using the known weight of the model, the length of the wires and the location of the attachment points to the model, the moment of inertia of the model about a vertical axis through the center of gravity is found on basis of the measurement of the natural period of angular motion of the suspended model about the vertical axis using the solution of the appropriate second order equation of motion. This can be repeated for the remaining two axes if required. Once the moments of inertia of model are known, the position of the ballast weights may be determined by calculation.
Conversely, the model may be suspended including all ballast weights placed to achieve the correct position of the center of gravity, and which are then shifted to achieve a precalculated natural period of the bi-filar pendulum set-up corresponding to the required moments of inertia.

Up to now the weight distribution has been adjusted with the model in air. In practice, part of the weight distribution may be adjusted with the model in water. This is often the case with ship models when considering the the vertical center of gravity and the roll moment of inertia. Due to the relatively small transverse dimensions of a ship model, using a bi-filar pendulum to measure the roll moment of inertia is impractical. Instead, the model is placed in the water and all ballast weights are added to give the correct draft and trim. The vertical center of gravity is adjusted by carrying out a static heeling test by shifting a known weight in transverse direction and measuring the ensuing heel angle. Ballast weights are shifted vertically until the correct angle of heel for a given heeling moment is achieved. Care has to be taken to ensure that the model is floating freely and that the heel is unrestricted by measuring cables etc. The roll moment of inertia is adjusted indirectly by making use of a roll decay test. Based on existing data or on calculations the natural period of roll of the vessel is assumed to be known. Ballast weights are shifted symmetrically outwards or inwardes in the transverse direction until the roll decay test results of the required period of roll of the model. Care should be taken in this test that the model is sufficiently far away from the basin side so that wall effects are negligible. Due consideration should also be given to the effect of waterdepth in the case of small keel clearance in the model basin. Small keel clearance results in an increase in the natural period of roll for the same roll moment of inertia of the vessel's structure. This is due to the change of added mass moment of inertia of the model.

In the case of wide-beam vessels such as catamaran vessels, roll decay tests may not be quite as suitable for adjusting the roll moment of inertia as for conventional ship shapes. This is related to the fact that in such cases the roll damping may be considerably larger resulting in a very rapid decay of the roll motion and a subsequently less accurate assessment of the natural roll period. In such cases the bi-filar pendulum test may be used.
For the same reason, the pitch moment of inertia is never adjusted for ship or barge shapes with the model in the water. The pitch decay is too rapid to allow a good assessment of the natural period.

For offshore structures such as semi-submersibles the position of the center gravity is generally adjusted with the model in the water. In such cases due care has to be taken that most of the ballast, which is often in the pontoons and therefore relatively in accessible, is placed beforehand and that there is sufficient movable ballast to be able to obtain the correct weiht distribution.

Weight distribution of components of models

As mentioned above, if internal loads in the structure are to be measured during tests in waves, the weight distribution of the components in which the model is subdivided should also be adjusted. Depending on the size of the component parts, the weight of the component, the center of gravity and, for large components, moments of inertia should be adjusted. If, due to practical constraints, the moments of inertia cannot be adjusted, these should be measured. If considered significant, results of internal load measurements may then be corrected during post-processing of the data in order to take into account the correct weight distribution of the components of the structure.

Weight distribution of small models

In practice the adjustment of the weight distribution of small models such as a CALM buoy used in model testing of moored vessels is confined to the adjustment of the weight and center of gravity. In case of elongated spar-type SPM models the center of gravity should be adjusted. The pitch moment of inertia may be adjusted using the bi-filar pendulum system.

Choice and calibration of measuring devices

An extremely important part of the preparations of model tests is the choice of measuring devices and their calibration.

The choice of the measuring devices for any particular quantity is dictated by a number of factors, for instance:

- Size
- Weight
- Stiffness
- Vulnerability

- Temperature sensitivity
- Sensitivity to water
- Expected range of the particular quantity in relation to the maximum capacity of the device
- Linearity of the calibration
- Cross-talk in multi-component force transducers
- Ease of replacement
- Hysteresis effects
- Duration of test program
- Test set-up
- Purpose of the tests
- Availability of devices

A number of the above-mentioned factors are self-evident some, however are not. For instance, a measuring device may be considered to be temperature insensitive for the range of normal temperatures in the test basin. However, when making a film or video of the model tests, powerfull lights are needed to obtain a sufficiently well lit scene. This is especially the case with high-speed filming. In such cases, force transducers which were hitherto considered to be compensated for temparature changes, may display erratic behaviour. This does not necessarily mean that such measuring devices are unsuitable but this may result in the decision not to carry out measurements when making high-speed film or video. When measuring any quantity, be it force, pressure or motion, it is of importance to have an indication of the expected levels of such quantities. If possible, measuring devices should be chosen so that the measured quantities do not result in signals which are in the range of the noise in the measuring system. Ideally, greatest accuracy of the measured signal is achieved when the transducer output is a significant percentage of the maximum range of the output and the signal is properly amplified and digitized taking into account the available digitization range.

This ideal situation is however, strongly modified by practical constraints arising from the requirement that, for instance, a model be transportable through the model facility etc. This may result in loads which are considerably higher than those measured during the actual tests. An example of the way in which a test program may influence the choice of measuring devices is found in the case of the measurements of vessel motions during model tests of moored systems. Measurement of motions of vessels in waves are often based on the use of light lines running from points on the models to pulleys on the shafts of potentiometers. In the past, so-called pantograph systems which consisted of a light tubular parallelogram structure incorporating potentiometers to measure heave, surge and sway of the attachment point to the model were also used.See Pinkster and Remery [1]. Due to the physical connection to the model, such devices exert small forces which may influence significantly the motions of the model in waves. This is not the case with the wave frequency motions of a vessel as the wave frequency forces are an order larger than the forces due to such measuring devices. However, in the case of the low-frequency motions of a moored vessel which are very sensitive to damping effects and for which the exitation forces are small, even small additional forces due to such measuring devices can have a significant influence. As a result, when considering the behaviour of moored objects in waves, measurements of all signals should preferable be based on remote sensing systems.

This type of system has been adopted by most of the major testing facilities for measuring the motions of models. However, at this point in time, the measuring signals of all other quantities measured on the model are still relayed to the data acquisition computer on the edge of the model basin through the use of cables running from the model. In an attempt to minimize the forces due to such cables the last part suspended between the model carriage and the model consists of very light, flexible electric wire.
In future, such physical connections should be eliminated by introducing optical or other suitable data transmission systems.

Calibration of measuring devices can take place either when the measuring devices are located in the model or beforehand. Calibration beforehand has the advantage that the conditions of the calibration are more controlled, i.e. use can be made of a dedicated calibration set-up in a separate laboratory. In such cases the calibration signal of the transducer as measured in the calibration laboratory is recorded and electronically simulated in the rest of the measuring equipment chain in the model test facility in order to yield the calibration of the complete chain.
The more traditional way to calibrate devices is to install these in the model (if appropriate) and construct a temporary calibration set-up in the basin around the model. In this way the complete measuring/recording chain is calibrated at the same time. A disadvantage of this method is the additional basin time needed for the calibration.

Even if the measuring devices are pre-calibrated before installation in the model, some checks should still be carried out when the model is placed on location in the basin. This set-up can, however, be relatively simple.

Choice of the facility

The choice of the facility in which the model tests are to be carried out depends, beside the economical and sometimes the political factor, on a number of technical aspects, for instance:

- System to be tested
- Type of test considered
- Waterdepth
- Environmental conditions
- Measurements envisaged

In some cases, it is not possible to find a facility which is capable of complying with the requirements. For instance if an extremely large waterdepth is required. In such cases compromises have to be made.

Generally, model testing for vessels at non-zero speeds takes place in conventional towing tanks which are often equipped with wave makers so that beside standard resistance and propulsion testing, tests in head and stern waves can be carried out. Roll motion tests can be carried out at zero speed in beam waves. In some cases, special seakeeping basins, which also have the capability to generate bow-quartering and beam waves beside head and stern waves, will be required.

In both types of basin the vessel model is more or less attached to a carriage which follows or tows the model and carries the recording equipment.

When considering testing of moored offshore structures, conventional towing tanks are generally not suitable. This is due to a number of aspects of such systems. i.e.:

- Horizontal dimensions of the mooring system too large for basin width
- Wall effects wave reflections from basin sides and blockage effects when towing large structures. See for instance, Yeung and Sphaier[2]. See also Figure 1.
- No capability to generate non-co-linear environmental conditions (waves perpendicular to current)
- Limited capability to simulate effect of current towing of complete set-up

In some cases however, towing tanks can be used for limited testing of offshore structures when one or more of the above mentioned limitations do not apply. Such may be the case with testing of semi-submersibles or tension leg system. Depending on the actual vessel shape and dimensions and the conditions of the tests, wave reflections may be insignificant.

Selection of sea-conditions

The selection of sea conditions for the model tests requires full scale data. Ewing[2] summarizes existing sources of wind and wave data. Primary sources of data and referral services are National Oceanographic Centers; National Meteorological Services; the World Meteorological Organization; and Unesco. The US National Climatic Data Center and UK Meteorological Office are among the largest collectors of such data. The wave atlas produced by Hogben et al. [3] of British Maritime Technology is also a prime source of data on environmental conditions.

Preparation in the basin: Generation of environmental effects

Prior to placing the models in the basin, calibration of the environmental conditions have to be carried out. For tests for a moored offshore structure this could entail adjustment of waves, wind and current.

With the increasing development of more sophisticated model testing facilities, the increase in the data regarding full scale environmental conditions and the awareness of the environmental factors influencing the behaviour of ships and offshore structures, there is a clear trend discernable towards the generation of more complex environmental conditions in model tanks as well as in computer simulations of offshore structures.
At this point in time state-of-the-art model tests of offshore structures include simultaneous generation of irregular long-crested waves, steady current parallel or perpendicular to waves and steady wind. In some facilities with independently operated wave makers on two sides of a rectangular basin, the test condi-

tions might include simultaneous generation of mutually perpendicular long-crested irregular waves representing wind driven waves and swell waves. In very few instances irregular fully directionally spread seas are generated on a regular basis for industrial test programs.

Regular waves

Regular wave tests are generally used to determine motion transfer functions and mean second order drift force transfer functions.
In deep water the waves are sinusoidal in shape for low to moderate wave heights. As the waterdepth is reduced (or the wavelength increased) higher harmonic components appear in the wave profile. Adjustment of regular waves in terms of the wave frequency is straight forward. If the wave height is incorrect, alinear adjustment of the amplitude of the wave generator generally suffices to obtain the rquired value. An example of regular waves in shallow water showing some of the non-linear, higher order effects are given in Figure 2.

Irregular waves

Irregular waves are usually adjusted to conform with a given wave spectrum. In Figure 3 a number of theoretical spectra are compared. The spectrum of the irregular waves in the basin is obtained on a trial and error basis using a stock spectrum as initial setting. The wave train should be generated and measured for a minimum duration corresponding to about 30 minutes full scale. The measured record is analysed to yield the next iteration. On an average, 2-5 iterations may be required in order to reach the target spectrum. It is necer possible to exactly equal the target spectrum, in practice, depending partly on the type of wave generator, there is a fall-off of energy at the higher frequencies due to mechanical limitations of the wavemakers. The loss in energy is sometimes compensated by increasing the spectral density of the adjusted waves in the remaining part of the spectrum. The rms value of the wave elevations should normally be within about 5% of the nominal value. Spectral density values should, in the more energetic regions of the wave spectrum, generally be within 10%-20% of the nominal value. These values are not to be taken literally, the degree to which the nominal spectrum can be attained also depends on the position of the spectrum in the range of the wavemaker. In Figure 4 examples are given of some adjusted spectra.

Multi-directional sea generation

In the past many papers have been devoted to full scale measurement of directional properties of irregular waves in open sea conditions. In most case attention was devoted to determining the directional spread of waves with a dominant direction. From analyses of measured wave fields models for directional wave spectra have evolved and are ocasionally used in model tests in facilities having the necessary multi-flap wave maker systems.
More recently, attention has been given to crossed sea conditions. tions.

Such sea conditions consist of two or more, more or less unidirectional wave fields propagating into the particular area from discrete, different directions. In a paper given by Grancini et al. [5] evidence is presented of the devastating effect crossed seas may have on the loads on rigid-arm-moored floating storage vessels. As such , the crossed sea condition is considered to be a particularly important particular case of a directionally spread sea condition .

With respect to the generation of directionally spread irregular waves in model tanks it will be clear that such capabilities are becoming more and more desirable as more full scale data on such conditions and their effects on offshore structures become more apparent. Generation of directionally spread seas with one dominant direction are considered to require a rectangular basin with a number of independently controllabel and independently driven wave flaps. See Figure 5. The width of such wave flaps are generally in the range of 0.4 to 0.6 m. Model tests are carried out with the model situated in the middle of the wave generator array situated along one side of the basin. Due to edge effects, the test area in which the directional properties of the waves may be considered to be relatively constant is generally only a fraction of the size of the basin.
Model tests in crossed seas require a rectangular wave basin having independently driven wave generators on two sides of the basin, or a directional wave generator on one long side of the basin which can generate two irregular wave trains with different main directions at the same time. In such cases, each of the crossed sea components is calibrated seperately to conform with the required swell or wind sea spectrum. The combined, crossed sea wave train is realized by generating both trains at the same time. Pinkster [6] has shown results of crossed seas generated in this manner. Results of the superposition of two longcrested irregular waves from mutuallly perpendicular directions are shown which confirm that linear superposition is valid for such cases. See Figure 2.
Takezawa et al. [7] discuss the generation of short crested seas in long towing tanks. Such tanks have hitherto not been considered suitable for the generation of such waves due to the short length of the array of wave flaps which can be installed within the width of such basins. Reflection of the waves on the side walls of the tank , which has always been considered to be a disturbance, is utilized positively to obtain directional irregular waves propagating in the towing tank. Some details are given of the method of generating the wave flap control signal and examples are given of directional spectra of waves generated in the tank. The waves were analysed using a five probe wave measuring system. Measurements confirm that the directional properties of the irregular waves change only slightly over the length of the basin. This is important when testing ship models at service speed. It is concluded that it is feasible to generate symmetrical directional wave spectra in towing tanks.

Regarding the formulations for the directional wave spectra to be used for model tests or for simulations, Niedzwecki and Whatley [8] have carried out a comparative study of some directional sea models.

Wave grouping

Wave grouping effects on ships and offshore structures are of importance from the point of view of several aspects:

- With respect to the behaviour of moored floating systems with low natural frequencies in the horizontal motions, wave group periods invariably have a bandwidth which includes the resonant periods of the moored system. In such instances, a description of the wave group characteristics in a form compatible with the continuous, stationary low-frequency irregular motions of the structure is required.
- With respect to the roll and pitch motions of semi-submersibles which have low natural roll and pitch periods lying outside the range of the frequencies present in the wave spectrum but inside the range of frequencies present in the wave group spectrum.
- With respect to consequences of the occurrence of sequences of discrete waves exceeding a certain wave elevation leading to, for instance, an inadmissible accumulation of water on the deck of a ship or floating production vessel or to fatal events such as the capsizing of a vessel.

For model tests on systems which may be sensitive to wave grouping effects, the wave grouping in the irregular waves generated in the basin can be measured and compared with the recommendations of the ITTC. The report of the Ocean Engineering committee of the 17th ITTC states the following:

- From the point of view of the resonant motions of moored structures with low natural frequencies, a description of wave grouping in terms of the distribution function and the frequency spectrum of the square of the wave envelop contain adequate information on basis of which the waves generated in model tanks can be judged and compared with full scale waves.
- For deep water conditions, the spectrum of the square of the wave envelop [group spectrum] as found on basis of full scale time records of wave elevations conform well with predictions based on random Gaussian theory. By this it is meant that given the ordinary wave spectrum, the wave group spectrum may be directly deduced whereby the only additional assumption to be made is that of the independence of the spectral components of the waves [random phase assumption]. It has been suggested that this conclusion also holds for shallow water waves but there is less evidence to support this assumption.

In Appendix I some relevant data is given on the relationship between the spectrum of the measured wave and the wave grouping. Some examples are also given in Figure 7.

Tikka and Paulling [9] describe a method for predicting the occurrence of conditions which can excite extreme ship motions leading to capsize. Earlier model experiments suggested that large roll motions and capsizing are often associated with the ship encoun-

tering a number of steep and almost regular waves. In this work, the wave conditions encountered by the ship are characterized in terms of wave groups that consist of a high run and an low run of waves. Critical conditions were determined by comparing the period and length of the dominant encountered waves with the characteristics of the ship. The progability of the ship encountering a critical high wave run was then determined for a given speed and seastate.

Wind generation

Steady wind forces are often generated by means of a wind field created by a battery of wind fans situated some distance away from the model. In connection with the possible existence of scale effects the model wind speed is often altered to achieve the correct wind force on the model as predicted from wind tunnel tests with similar vessels. In other cases Froude scaling is applied in order to determine the model wind speed.
Alternate means of generating wind forces have also been used, for instance, by the use of computer controlled fans mounted on the deck of a ship model or by means of weights and pulleys.

Until now , very few attempts have been made to scale dynamic wind fluctuations by means of computer controlled fans. Feikema and Wichers [10] carried out computations and model tests on a moored 200 kdwt tanker in irregular waves and wind. Both steady wind and unsteady wind were generated in order to determine the relative effects on the vessel motions and mooring forces.
For the value of the steady wind speed the 1-minute gust speed was used. Wind was generated using a battery of fans located some distance from the model. The fans produced a relatively homogeneous wind field which was wide enough to cover the test set-up of the tanker and a wind gauge. The wind fans were connected to a computer controlled system which regulated the fan speed. The fan speed was controlled using the wind speed measured next to the tanker model as feed-back signal. This system was able to generate the required wind spectrum. An example is shown in Figure 8. From the results of model test with and without dynamic wind effects it was concluded that for the tanker considered the representation of wind by means of the 1-minute mean steady wind resulted in larger motions and mooring loads than found for the same sea conditions but using the corresponding dynamic wind based on the wind spectrum. It was also concluded that dynamic wind generation using computer controlled wind fans was feasible for model tests of floating offshore structures in irregular waves, wind and current.

Current

In the aforegoing mention was made of the effects of unsteady currents on the behaviour of moored vessels and some data on full scale current speed and simultaneous current direction have been given in reference [11]. In ref.[12] Schaudt,Forristall et al. present data on the occurrence of the Nelson Eddy in the gulf of Mexico. Nelson Eddy was the first major Loop Current Eddy to enter the deep water lease areas offshore Louisiana during active drilling operations.

The paper summarises the history of this eddy, and the hydrographic and curren measurements collected during its intrusion onto the shelf. To date no literature could be found regarding the controlled generation of unsteady current in model tanks. In ref. [12] Pinkster gives and example of current turbulence measured in an offshore model test basin compared with full scale turbulence measurements. The correlation appears satisfactory but is purely co-incidental since no attempt had been made to reproduce the full scale turbulence at the time. See Figure 9.

In model basins current, or the effect of current can be generated in several ways. In normal towing tanks current can be simulated by towing the model at the corresponding speed according to Froude's Law. This requires very good low-speed control of the carriage. The carriage motions should be smooth with no vibrations or variations in the speed since this will result in the setting-up of corresponding low-frequency motion oscillations of the moored structure. Only the effect of current in the wave direction or against the wave direction can be simulated in this way.
Some model basins are equiped with a current pumping system. In these systems the water is withdrawn from the basin, pumped round and re-introduced in the basin on the opposite side. If the pump capacity is sufficiently large, a reasonably homogeneous current field can be generated over a large part of the basin. This type of current generation system is probably the best available but is restricted to use in relatively shallow basins. An example of the current field obtainable in a rectangular shallow water basin is shown in Figure 10. In deep water basins the required pump capacity and current ducting is economically prohibitive.
In deep water basins current is sometimes generated by inducing water circulation within the basin. This is done either by installing pumps in the basin or by driving the water in the basin by means of high speed jets of water issuing from piping at at the side of the basin. By the first method a local current field can be generated in a part of the basin. A disadvantage in this method is that waves generated at the side of the basin propagate over a current field of which the direction and magnitude of the velocity is changing with the location of not in time. This in turn can cause deformation of the wave field.
When using waterjets to drive the current, turbulence is set up within the basin.
If high speeds are employed, the turbulence can extend into the test area and induce additional dynamic effects in the motions of moored structures. This was shown by de Kat and Wichers[11]. See Figure 11.
A simple way of introducing the effect of current is to apply an external force to the model by means of, for instance a wire attached to the model, running over a pulley and attached to a weight corresponding to the estimated current force.
This method has often been applied in cases where other methods are not feasible. Interaction effects of current and waves or the effects of current damping [see ref.[13]]are not modelled by this method.
Current forces have also been simulated by using thrusters attached to the model which produce forces corresponding to the estimated current force. This method is however little used.

Model testing

When the enviromental conditions have been adjusted and the model preparations ready the model is placed in the basin, hooked-up to the restraining system, or mooring system and final preparations are made.

Restraining systems

For model tests with ships, different types of model restraining systems are used. For resistance and propulion tests in still water, the transverse and yaw motions of the vessel are restrained by the use of articulated trim devices. These allow the model to trim freely and exert little longitudinal forces on the model. The resistance is measured by a transducer in the towing wire.
In some cases also for tests in head waves, ship models may be restrained in surge, sway and yaw by a suitable device which allows heave and pitch motions freely.
Ship models which are tested in quartering seas are generally free-running models equipped with their own propulsion and steered by means of an automatic pilot which reacts to the offset of the model from the center line of the basin or, in the case no carriage is present and the basin is of the large rectangular type, may only respond to heading errors.
Except in the case of complete free-running models in basins without carriage, measured signal from the model are transmitted to the data collecting computer by cables. In the former case the signals are transmitted by radio.

For tests with moored offshore structures, the restraining system is part of the model set-up and is modeled to achieve the correct static and if possible, dynamic properties corresponding to full scale. Chains are modeled using chains. The scaling is again according to Froude's Law.

In some cases, for ship model and for offshore structures, the restraining system will consists of a soft-spring system which allows the model to carry out freely wave frequency motions while maintaining a mean position in the basin. This type of set-up is used, among others, for tests to determine mean drift forces and motion response functions. See Figure 12. Care should be taken not to use springs that are too stiff. This may lead to dynamic magnification effects.

Tests aimed at determining mean and low frequency wave drift forces require an active system of restraint in order to restrict as much as possible mean and low frequency motion components while leaving wave frequency motion components unhampered. See Figure 12.

Preliminary tests

Prior to carrying the test program itself, preliminary tests are generally carried out which are either aimed at completing the calibrations/adjustments or aimed at providing basic information which may be an aid in analysing the results of the main test program.

Such tests are:

- Static stability and motion decay tests.
  These tests are part of the adjustments to be carried out with respect to the model.
- Static load testing of mooring systems.
  The static restoring forces of the mooring system of an offshore structure are measured for a number of offsets of the model from the static equilibrium position in still water. This provides a check on the modelling of the mooring system as the results can be checked against static calculations based, for instance, on the catenary equations.
- Motion decay test for moored vessels.
  These test provide the natural frequency of the moored vessel and an indication of the level of still water damping for low frequency motions.

Tests in waves,wind and current

In this section we will briefly run through the procedures followed when carrying out tests and discuss some aspects of the different types of tests.

Prior to starting up the carriage, the wavemaker, wind fans or current pumps etc., the static levels of all measuring signals should be recorded. These are the reference levels for the subsequent test measurements.

For all types of tests excepting those in which the situation of total rest is the initial condition(ship launching tests, there is a transient state between condition whereby the model and the basin are at rest and the conditions during the tests. Generally no measurements are carried out while this transient state exists.

When the model behaviour has become stationary, measurements are carried out. At the end of the measuring interval recording is stopped and preparations carried out for the next test.

This, very briefly summarizes the test procedure. There are, however, a number of parameters which need to be discussed.
For instance, how long does one wait before starting measurements after the wavemakers have been switched on ?, or, what should the duration of a model test be ?.

With respect to the waiting time before measurements start, it can be said that this depends mainly on the time necessary for transient motion response of the model to die out. This takes considerably more time than the time taken by the wave system to become stationary after the first waves have passed the model location. For moored offshore structures the natural periods of the horizontal motions are very low and the motions lightly damped. As a result, considerable time has to be allowed for the transient motion components to become negligible. As a rule of thumb a duration corresponding to 30 minutes full scale is often used.
The test duration itself is dependent on a number of factors:

- Reflections in the basin.
  As time progresses, waves sent into the basin from the wavemaker, impinge upon the model and are partly diffracted in all directions. The primary wave field progresses to the wave absorbing beaches and will lose most of its energy there. Some of the energy (5-10%, depending on wave length, beach, waterdepth etc.) will be reflected back into the basin where a complex combination of primary, diffracted and reflected waves is set up. In some basins a gradual build-up of reflected energy can occur which will distort the primary wave field sufficiently to warrant ending the test after a certain time. In other basins, in our experience, of the rectangular type with beaches on at least two sides, the reflected wave energy does not seem to build up to large proportions so that in such facilities long, uninterrupted test durations can be applied if desired. An example of the time variation of the rms value of the wave elevation in such a basin is shown in Figure 14.
  The fact that reflections can build up in a basin does not however preclude long duration testing. It simply means that statistics of long duration tests have to be obtained from a number of shorter tests in the same wave spectrum.
- Main items of interest in the model system behaviour.
  If wave frequency phenomena are of interest measurements during tests in regular waves need only be carried out for a durations corresponding to 15 - 20 wave oscillations.
  With this amount of data Fourier analyses can be carried out to yield harmonic components of the measuring quantities. Tests in irregular waves in which wave frequency behaviour is the main item of interest, durations corresponding to 30 - 45 minutes full scale seem to be sufficient. For mean wave periods in the region of 10 s this yields an average of about 200 - 250 oscillations at wave frequency. This is considered to be sufficient for achieving reliable results of spectral and statistical analyses of the motion components.

If interest is focussed on low-frequency phenomena in the system behaviour such as those related to the horizontal motions of moored vessels much longer test durations need to be applied in order to obtain statistically reliable results. Just what this constitutes in itself merits a discussion which will not be given here. One way to quantify the statistical variability of the measured data is to determine the variance of the variance of a given signal. In other words to determine the degree to which the rms value changes if the test were repeated under the same wave conditions(same spectrum, not same wave train) for the same duration. Pinkster and Wichers [14] have given an expression on the basis of which an estimate may be made of the test duration required in order to reduce the statistical variability of low-frequency motion of a moored vessel in irregular waves to a given level.

$$\sigma^2_{\sigma^2} = \frac{1}{T\,\omega_e\,\delta}$$

in which T = test duration

ω_e = natural frequency of the motion

δ = system damping

$\sigma^2_{\sigma^2}$ = non-dimensional variance-of-variance of the low frequency motions

The above expression is sometimes interpreted as giving the total number of oscillations of the low frequency motions which would be required for a desired variance-of-variance value.
However, in [15] Pinkster has shown that the correct interpretation of the above equation leads to a required number of oscillations of the envelope of the low-frequency motion components. The number of oscillations of the motion signal itself is of no consequence in this respect.

Data acquisition and analyses

In most modern model testing facilities, data recording takes place using computers which can supply a first analysis of the measured signals directly after the end of a test run. Data is generally sampled at 25 to 50 hz in the case of wave frequency behaviour. Higher sample rates may be needed in the case of impact loads or slamming pressures. The latter may require special measuring equipment with very high data sampling rates.

The first analysis of the data in the basin can be relatively simple and include only maxima, minima, mean and rms values. On the basis of this information, a client can sometimes take the decision to make changes in the model test program.
More comprehensive analyses take place off-line. These can include:

- Harmonic analyses (regular wave testing)
- Spectral analyses (response functions)
- Statistical analyses (distribution functions)
- Filtering (high frequency, low frequency)
- Combination of signals (force components)
- Higher order spectral analyses (bi-spectral analyses)

A more detailed review of model test data analyses is given, among others by Dillingham and Hoste [16].

Scale effects

As stated in the aforegoing, model tests are carried out in accordance with Froude's Law of similitude. As a consequence, scale effects are present in quantities which are influenced by viscous effects.

For resistance and propulsion testing of ships, this is taken into account when scaling-up the measured data to full scale. The principle with respect to, for instance, the resistance, is to deduct the estimated frictional resistance of the model from the total measured resistance using a friction resistance coefficient according to the ITTC recommendations.
The remaining part of the measured resistance called the residual resistance is scaled up by a factor which is the cube of the scale of the model. The frictional resistance of the full scale vessel is calculated again using the ITTC equation for the resistance coefficient given above. This is added to the residual resistance to yield the estimated value for the full scale vessel. This method of predicting the full scale resistance is due to Froude and has, due to the great amount of experience gained by its use during over 100 years, found a solid base in the amount of data available for almost all types of ships.
For offshore vessels, for instance a moored semi-submersible, the flow conditions about the vessel in a wave and current environment are dependent on more parameters than is the case of a ship travelling in still water on which the resistance problem is based. This increased complexity of the flow conditions coupled with the relative lack of full scale and model data and the lack of a rational extrapolation procedure, prevents extrapolation of model test data to full scale whereby such scale effects as are present in model test data are taken into account. Huse[17] has made a first attempt to correct for scale effects in offshore model testing. He carried out some sensitivity analyses for the low-frequency surge motions of a moored tanker in head seas and concluded that the scale effect would influence the motions in the order of a few percent.
In general, model test data for offshore systems are simply extrapolated to full scale based on Froude's law, i.e. the model force values are multiplied by the cube of the scale ratio.
Even though it is not possible to give an extrapolation method which takes into account scale effects in offshore testing, it is stil worthwhile to make estimates of the order of scale effects which may be present in some of the quantities of interest.

Final remarks

In this contribution a broad review is given of a number of aspects related to model testing of ship and offshore structures. It was not intended as a handbook on how to manage model tests but rather as a quick reference guide just to make sure you covered most items.

References

1. Pinkster, J.A. and Remery, G.F.M.;'The role of model tests in the design of single point mooring terminals', Paper No.2212, Offshore Technology Conference, Houston, 1975

2. Yeung, R.W. and Sphaier, S.H.;'Wave-interference effects on a truncated cylinder in a Channel', Journal of Engineering Mathematics 23;95-117, 1989

3. Ewing, J.A.;'Wind, Wave and Current Data for the Design of Ships and Offshore Structures', Marine Structures 3[1990] 421-459

4. Hogben, N., Dacunha, N.M.C. and Oliver, G.F.;'Global Wave Statistics', Unwin Brothers for British Maritime Technology Ltd.,1986

5. Grancini, G., Iovenitti, L.M. and Pastore, P.;'Moored Tanker Behaviour in Crossed Sea. Field Experiences and Model Tests', Symposium on Description and Modelling of Directional Seas, Technical U. of Denmark, Copenhagen, 1984

6. Pinkster, J.A.;'Drift Forces in Directional Seas', Marintec China, Shanghai, 1985.

7. Takezawa, S., Kobayashi, K., Kasahara, A.;'Directional Irregular Waves Generated in a Towing Tank', Japanese Society of Naval Architects, Vol.163, June 1988.

8. Niedzwecki, J.M. and Whatley, C.P.;'A Comparative Study of Some Directional Sea Models', Ocean Engineering, Vol.18, No.1/2, 1991.

9. Tikka, K.K. and Paulling, J.R.;'Prediction of Critical Wave Conditions for Extreme Vessel Response in Random Seas', STAB 90, Stability of Ships & Ocean Vehicles; 4th International Conference, Naples, 1991.

10. Feikema, G.J. and Wichers, J.E.W.;'The Effect of Wind Spectra on the Low-Frequency Motions of a Moored Tanker in Survival Condition', OTC6605, Offshore Technology Conference, Houston, Texas, 1991.

11. de Kat, J.O. and Wichers, J.E.W.;'Behaviour of a Moored Ship in Unsteady Current, Wind, and Waves', Marine Technology, September 1991.

12. Schaudt, K.J., Forristal, G.Z. et.al.;'The Evolution of Nelson Eddy, 1989', OTC 6537, Offshore Technology Conference, Houston, Texas, 1991.

13. Wichers, J.E.W.;'A Simulation Model for a Single Point Moored Tanker', Publication no. 797, MARIN, Wageningen, 1988

14. Pinkster, J.A. and Wichers,J.E.W.;'The Statistical Properties of Low Frequency Motions of Non-linearly Moored Tankers', OTC Paper No.5457, Offshore Technology Conference, Houston, 1987.

15. Pinkster, J.A.;'Statistical Aspects of the Behaviour of Moored Floating Structures', Proceedings MARIN Jubilee Meeting, Wageningen, May 1992

16. Dillingham, J.T. and Hoste, J.H.;'Data Analysis Techniques in Model Testing', Paper presented to 20th American Towing Tank Conference , 1983

17. Huse, E.;'Experimental Prediction of Low Frequency Motions and Mooring Line Tensions of Offshore Structures', Proceedings of the First Offshore Station Keeping Symposium, Houston, February 1990

18. Blok, J.J.;'Motions of Floating Structures', Proceedings Second WEGEMT Graduate School, Aachen, 1979

19. Wichers, J.E.W.;'Some Aspects of Model Tests in Designing Mooring Systems in the Open Sea', Proceedings Second WEGEMT Graduate School, Aachen, 1979

20. de Boom, W.C.;'Model Testing of Large Jacket Platform Installations', RINA, 1984

21. Pinkster, J.A.;'Aspects of Tankers Moored at Sea', International Conference on Floating Production Systems, London, 1989.

SET-DOWN AND GROUPING IN IRREGULAR WAVES

J.A. Pinkster

Maritime Research Institute Netherlands (NSMB)

1.0 INTRODUCTION

The motions and mooring forces of vessels moored in irregular waves can be significantly affected by low frequency second order wave drift forces (Hsu and Blenkarn, 1970).

These forces are small in magnitude and in irregular waves contain frequencies coinciding with the natural frequencies of the horizontal motions of moored vessels. Combined with the fact that the motion damping is generally small this can lead to large amplitude resonant motions. Not only the horizontal motions of moored vessels are affected by such forces. Floating objects with small waterplane area have also displayed such resonant behaviour in the vertical motions. It has also been found that, in shallow water, conventional hull forms such as tankers can display significant low frequency vertical motions at frequencies well below the range of frequencies contained in the spectrum of the irregular wave field.

It can be shown that the characteristic behaviour of the low frequency second order wave drift forces in irregular waves is closely linked with the occurrence of wave groups in the incident irregular wave train (Pinkster and Huijsmans, 1982). When modelling the behaviour of moored vessels by means of either physical or mathematical models, it is therefore of interest to study wave grouping in the incident waves.

In irregular waves the mean surface is depressed under groups of higher waves (set-down) and raised under low waves (set-up). Based on potential theory it can be shown that set-down (and set-up) is at first approximation a second order phenomenon. It has been found that the low frequency waves associated with set-down can, especially in shallow water, contribute significantly to the total low frequency wave drift forces acting on floating vessels. It is therefore also of interest to study the occurrence of set-down in the irregular incident waves.

2.0 WAVE GROUPING

In the aforegoing it was stated that wave drift forces are associated with wave grouping. More specifically it can be shown that these forces are directly related to the low frequency part of the square of the envelope of the incident waves. This quantity also contains information on wave grouping.

Data on wave grouping occurring in reality is scarce. Based on the assumption that the elevation $\zeta(t)$ is a zero mean random Gaussian process, certain properties of the square of the wave envelope can be deduced. For instance, given the spectral density $S_\zeta(\omega)$ of the irregular waves, it can be shown that the expectation of the spectrum of the square of the wave envelope is:

$$S_{A^2}(\mu) = 8 \int_0^\infty S_\zeta(\omega)\, S_\zeta(\omega+\mu)\, d\omega \qquad \ldots\ldots (1)$$

Moreover, it can be shown that the area M_0 under the spectrum $S_{A^2}(\mu)$ is:

$$M_0 = 4m_0^2 \qquad \ldots\ldots\ldots\ldots\ldots\ldots (2)$$

in which:

$$m_0 = \int_0^\infty S_\zeta(\omega)\, d\omega \qquad \ldots\ldots\ldots\ldots (3)$$

This shows that the total energy associated with the wave groups is independent of the form or period of the wave spectrum $S_\zeta(\omega)$.

The distribution function of $A^2(t)$ becomes:

$$p(A^2) = \frac{1}{2m_0} \cdot e^{-\frac{A^2}{2m_0}} \qquad \ldots\ldots\ldots\ldots (4)$$

3.0 WAVE SET-DOWN

In irregular waves, the spectrum of the wave set-down record is found from:

$$S_{\zeta^{(2)}}(\mu) = 8 \int_0^\infty S_\zeta(\omega)\, S_\zeta(\omega+\mu)\, D^2(\omega,\omega+\mu)\, d\omega \qquad \ldots\ldots\ldots\ldots (5)$$

in which $D(\omega,\omega+\mu)$ is the quadratic transfer function of the wave set-down in a regular wave group consisting of two regular waves with frequencies ω and $\omega+\mu$ respectively.

The quadratic transfer function $D(\omega,\omega+\mu)$ can be obtained theoretically based on potential theory or experimentally by means of cross-bi-spectral analysis of time records of measured wave trains. Given the time record of a measured (or synthetic) wave elevation $\zeta(t)$, the corresponding time record of the wave set-down $\zeta^{(2)}(t)$ can be computed from:

$$\zeta^{(2)}(t) = \int_{-\infty}^{\infty}\int_{-\infty}^{\infty} f^{(2)}(t_1,t_2)\, \zeta(t-t_1)\, \zeta(t-t_2)\, dt_1 dt_2 \qquad \ldots\ldots\ldots\ldots (6)$$

in which $f^{(2)}(t_1,t_2)$ is the double Fourier transform of $D(\omega,\omega+\mu)$.

4.0 COMPARISON THEORY AND MEASUREMENTS

Random long-crested irregular waves were generated in shallow and deep water. The time records of the measured waves were analyzed with respect to the wave grouping expressed by the square of the wave envelope and with respect to the wave set-down which was obtained by low-pass filtering of the measured wave records.

The results of analyses of the measured records are compared with prediction based on equations (1) through (6). An example is given in the Figures 1 through 5. The example refers to an irregular wave with a significant height of 6 m and a mean period of 11.5 s. The water depth is 30 m.

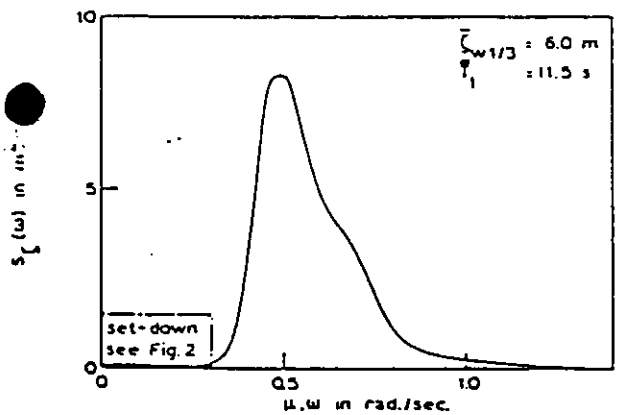

Fig. 1 : Spectrum of measured waves

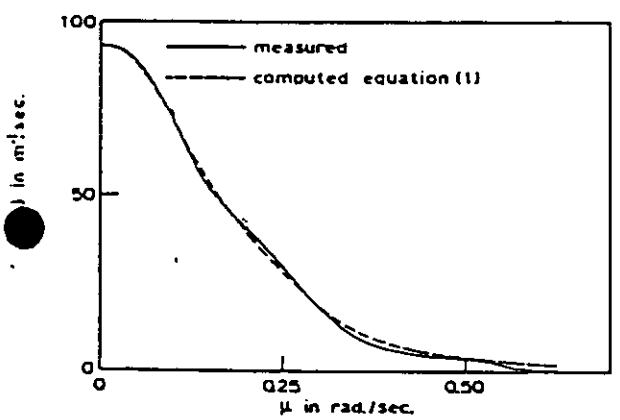

Fig. 3 : Spectra of wave envelope squared

5.0 CONCLUSIONS

The results show that wave set-down can be predicted accurately based on potential theory. Wave grouping in measured random waves also conforms reasonably well with predictions based on random wave theory.

REFERENCES

Hsu, F.H., and K.A. Blenkarn, 1970: Analysis of peak mooring forces caused by slow vessel drift oscillation in random seas. Houston.

Pinkster, J.A., and R.H.M. Huijsmans, 1982: The low frequency motions of a semi-submersible in waves. Proceedings BOSS'82, Boston.

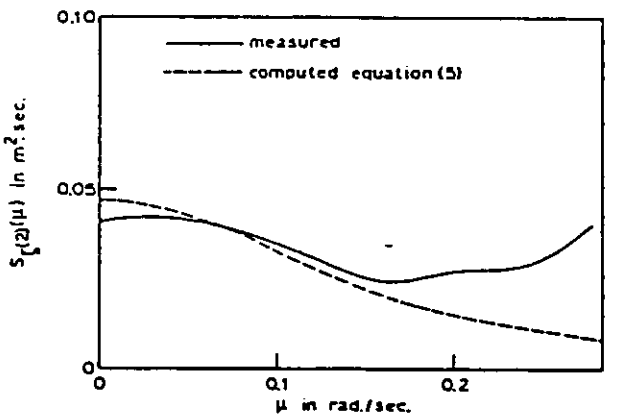

Fig. 2 : Set-down spectra

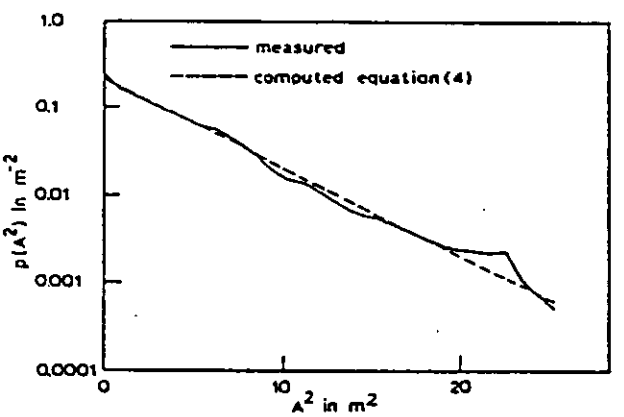

Fig. 4 : Distribution function of wave envelope squared

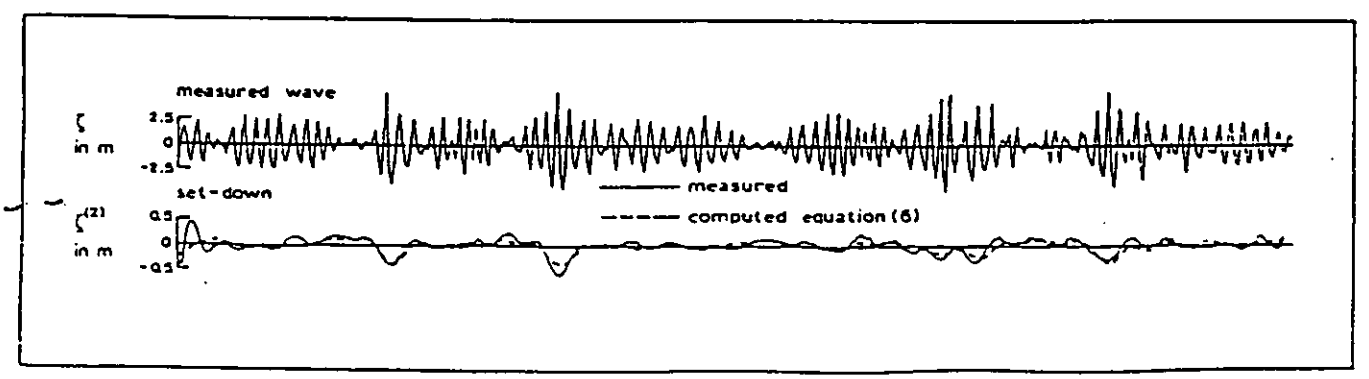

Fig. 5 : Wave and wave set-down records

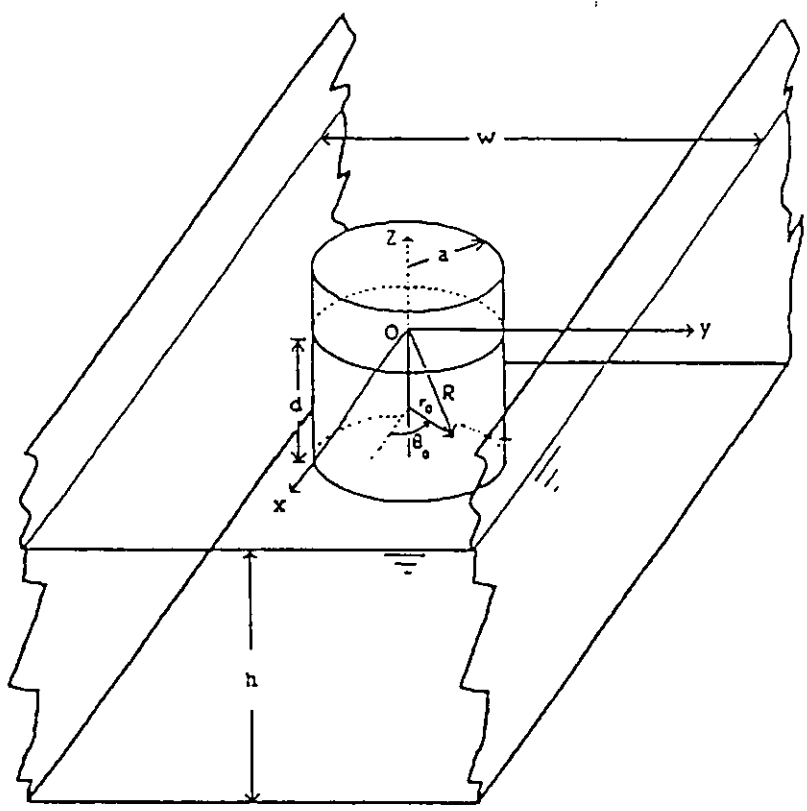

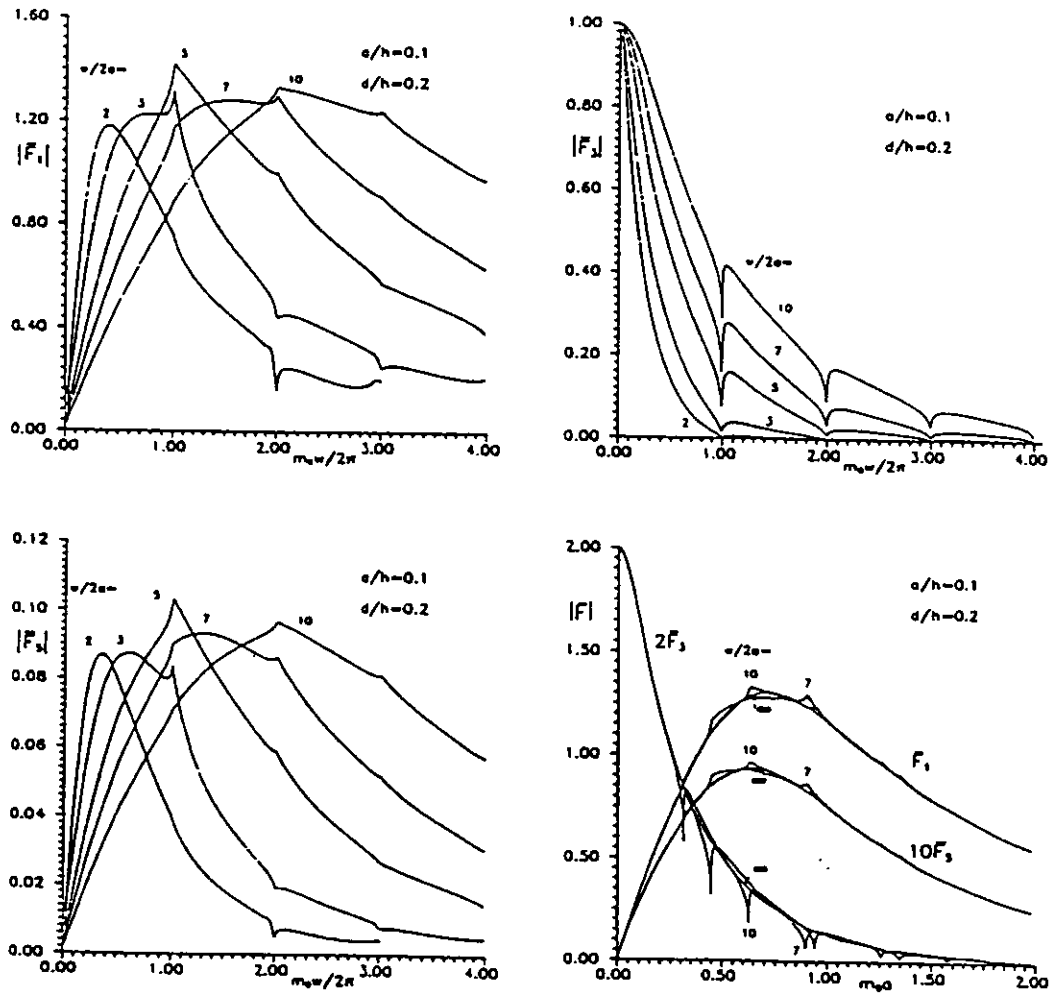

Modulus of nondimensional wave-exciting force/moment: (a) horizontal, (b) vertical, (c) overturning moment, as a function of $m_0w/(2\pi)$, (d) as a function of m_0a; $a/h = 0.1$, $d/h = 0.2$, $w/(2a) = 2, 3, 5, 7$ and 10.

Figure 1: Effects of reflections from basin sides on wave forces on a cylinder

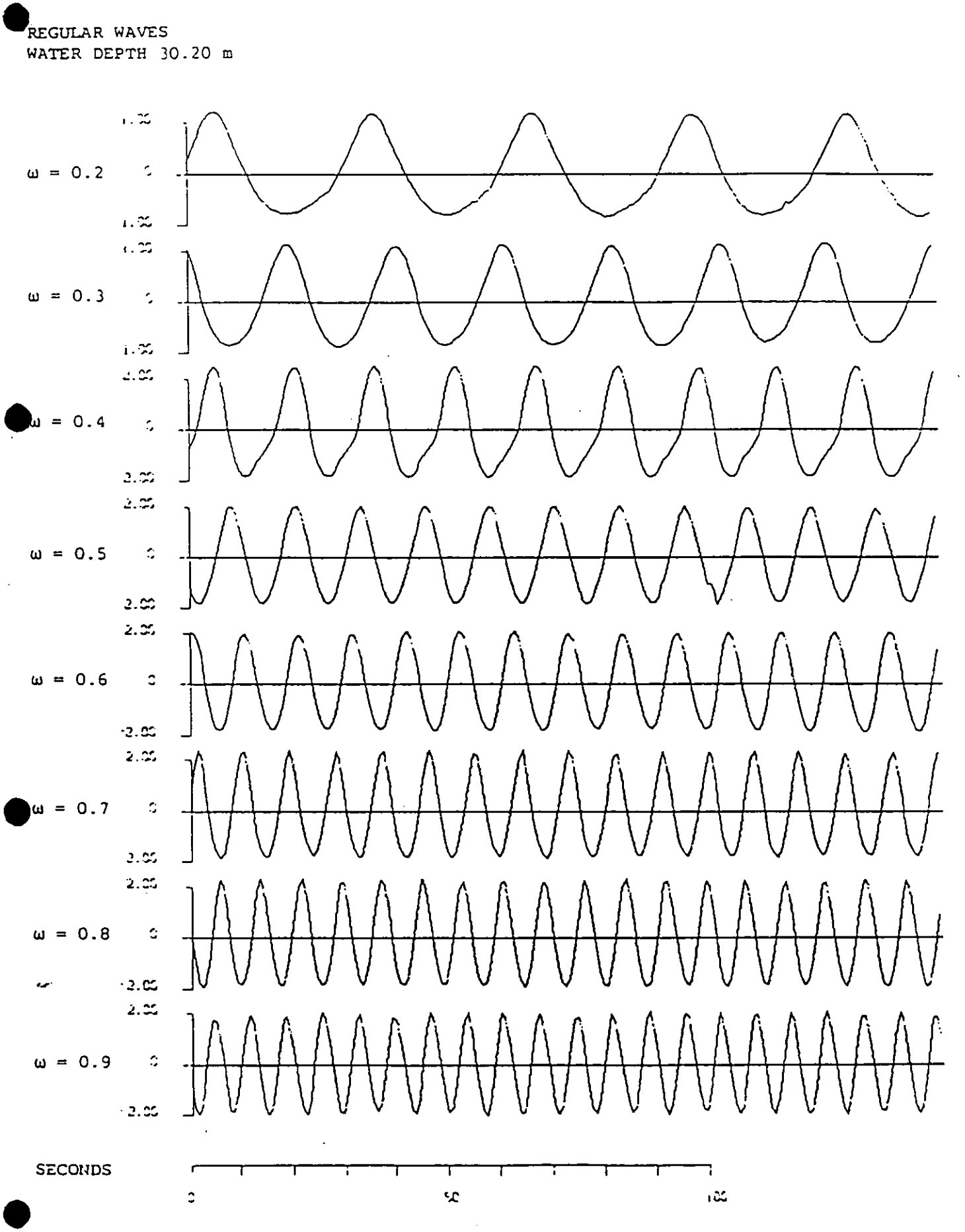

Figure 2: Regular waves in shallow water

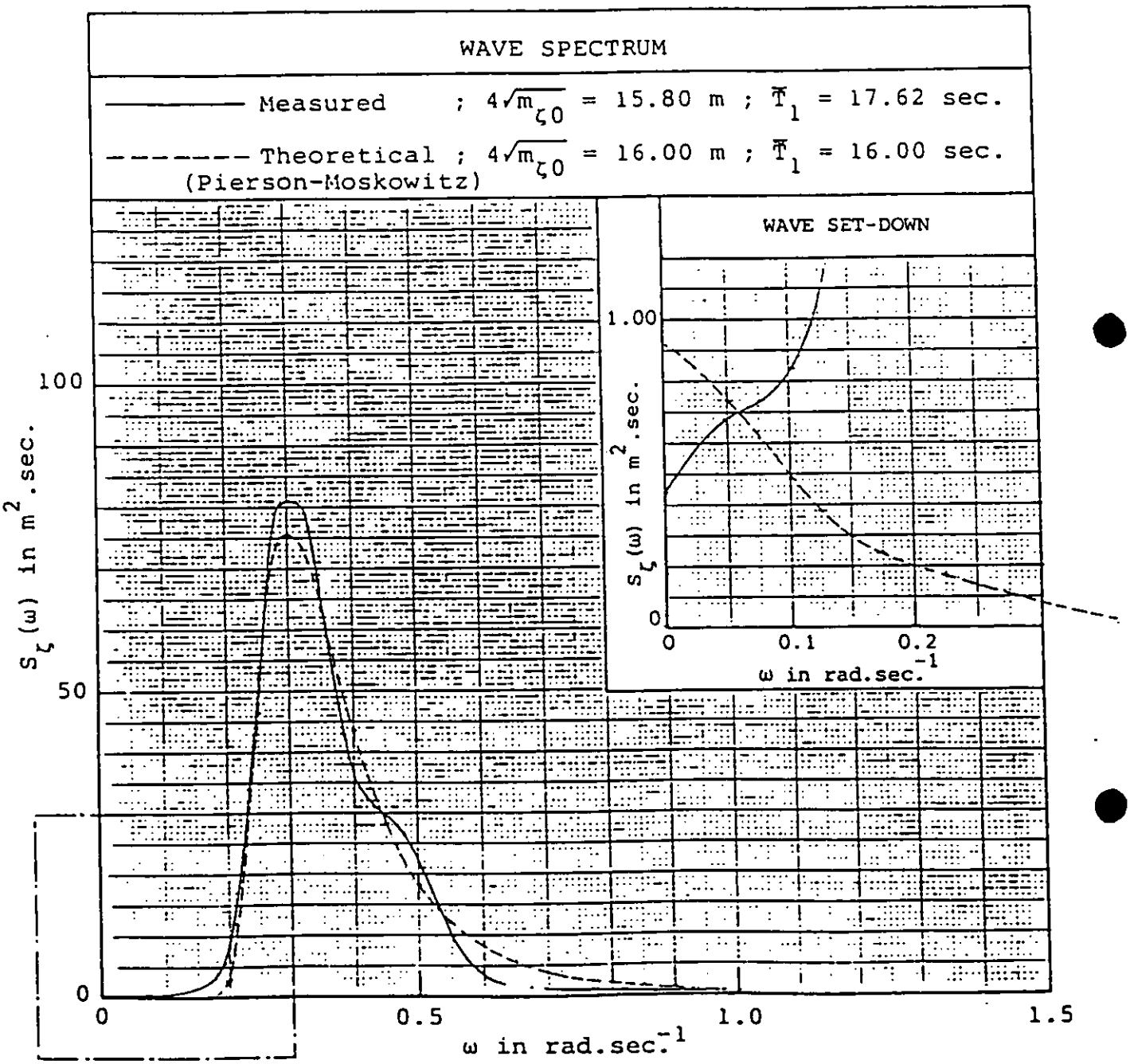

Figure 4: Spectrum of irregular waves

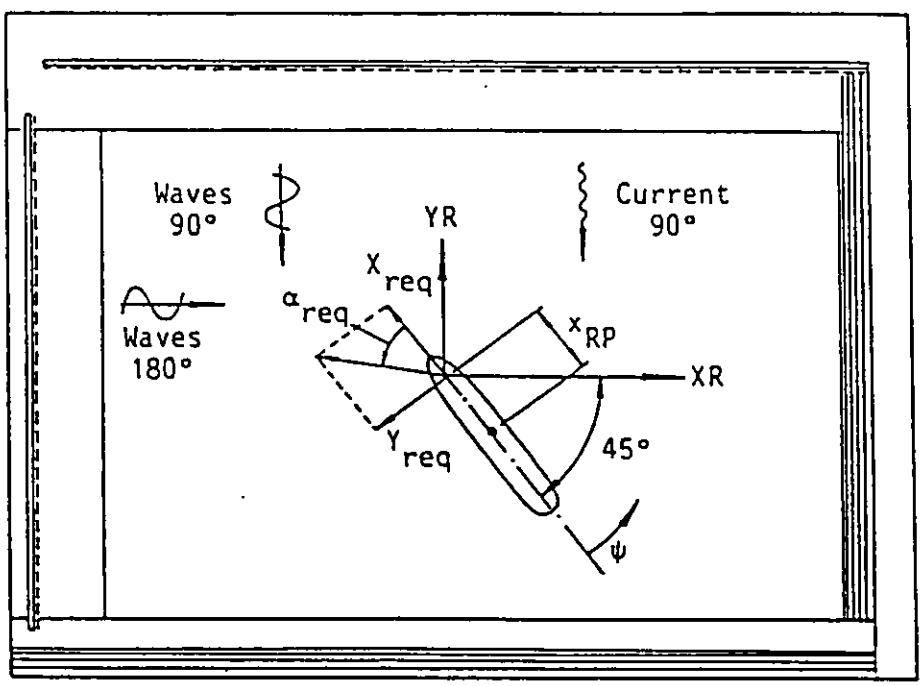

Figure 5: Wave and Current Basin

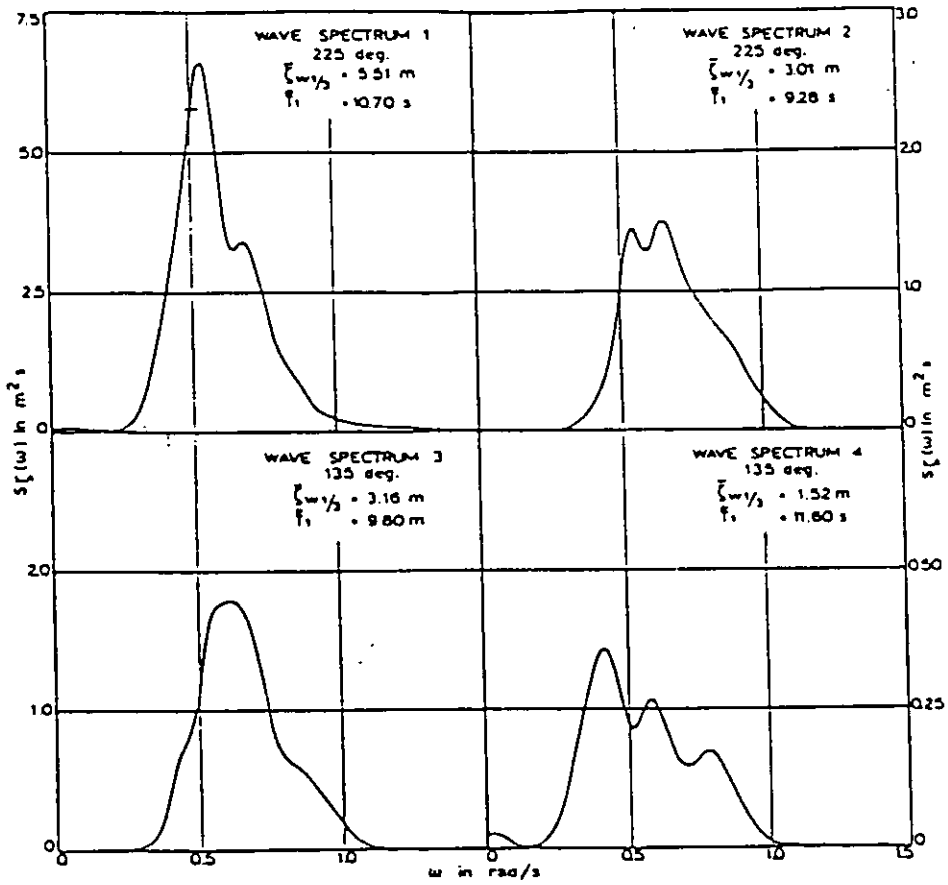

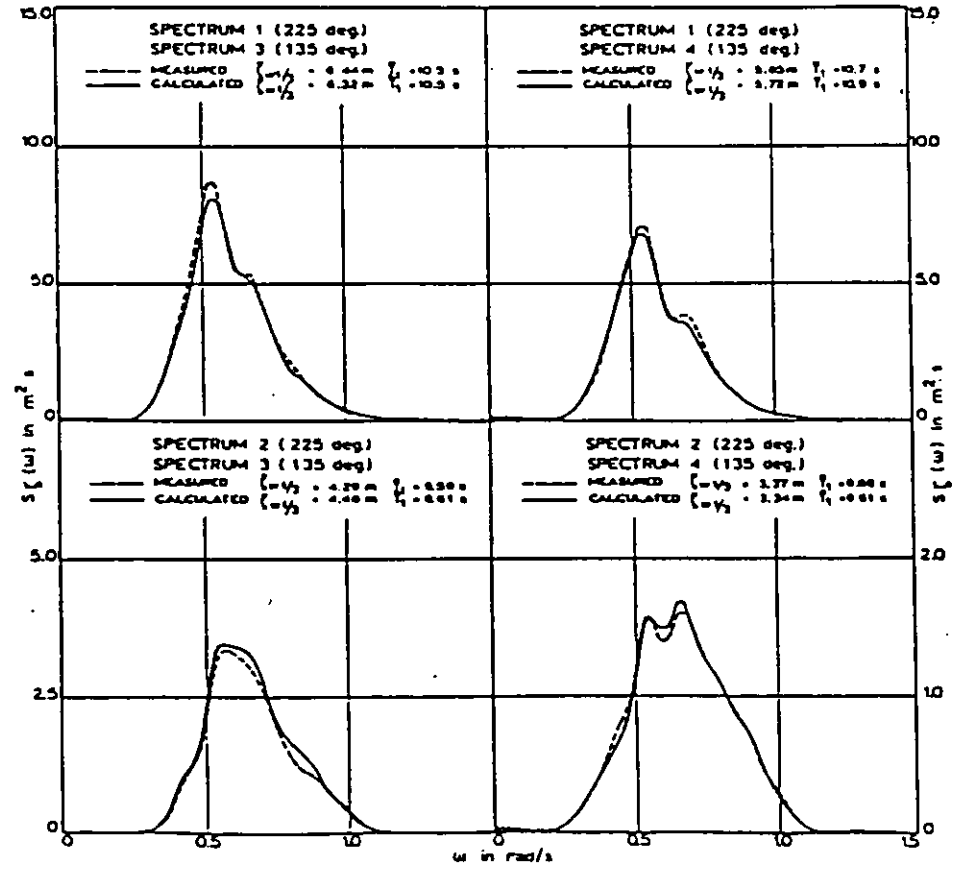

Figure 6: Superposition of irregular wave trains

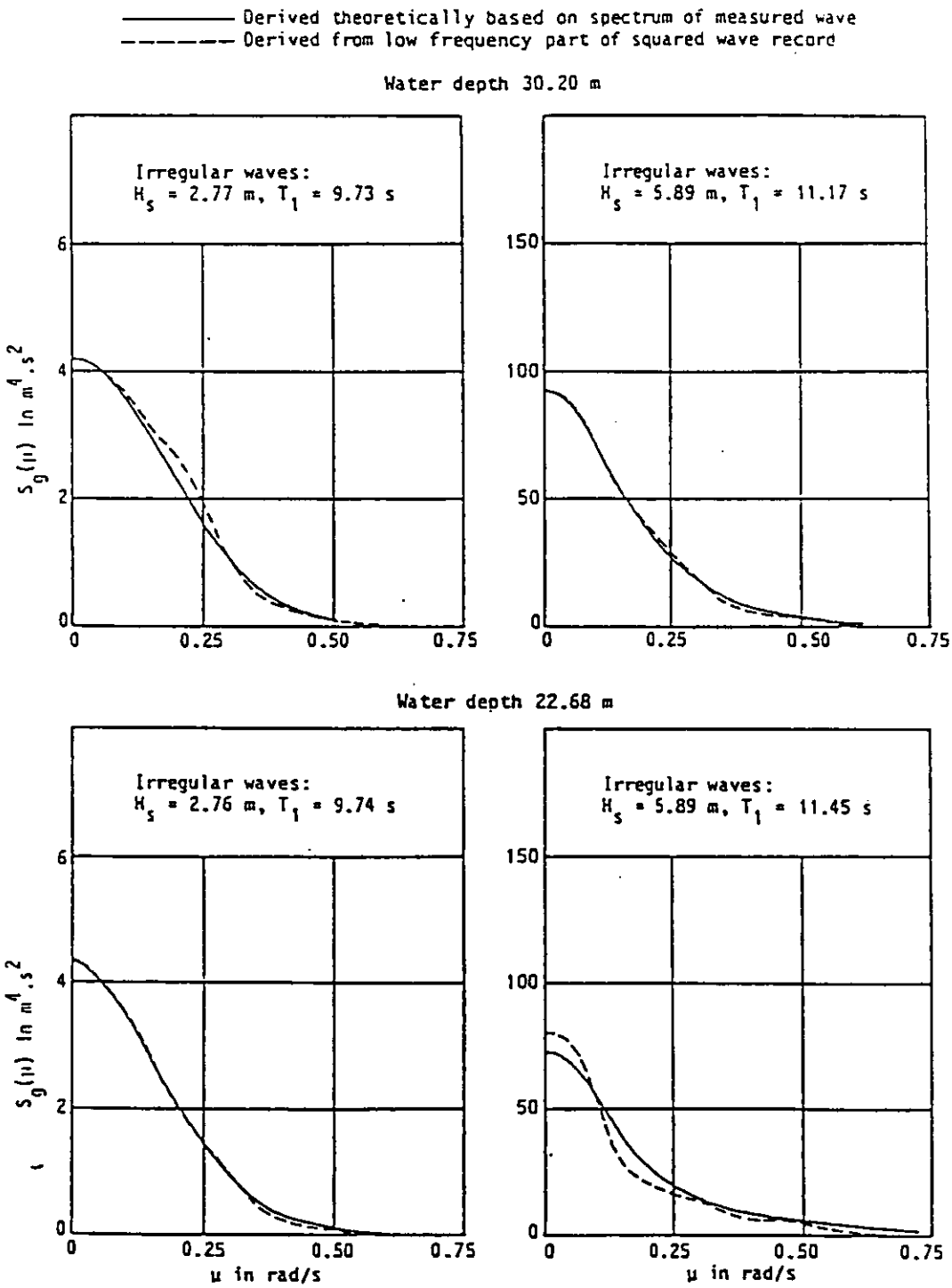

Figure 7: Wave group spectra (envelop squared)

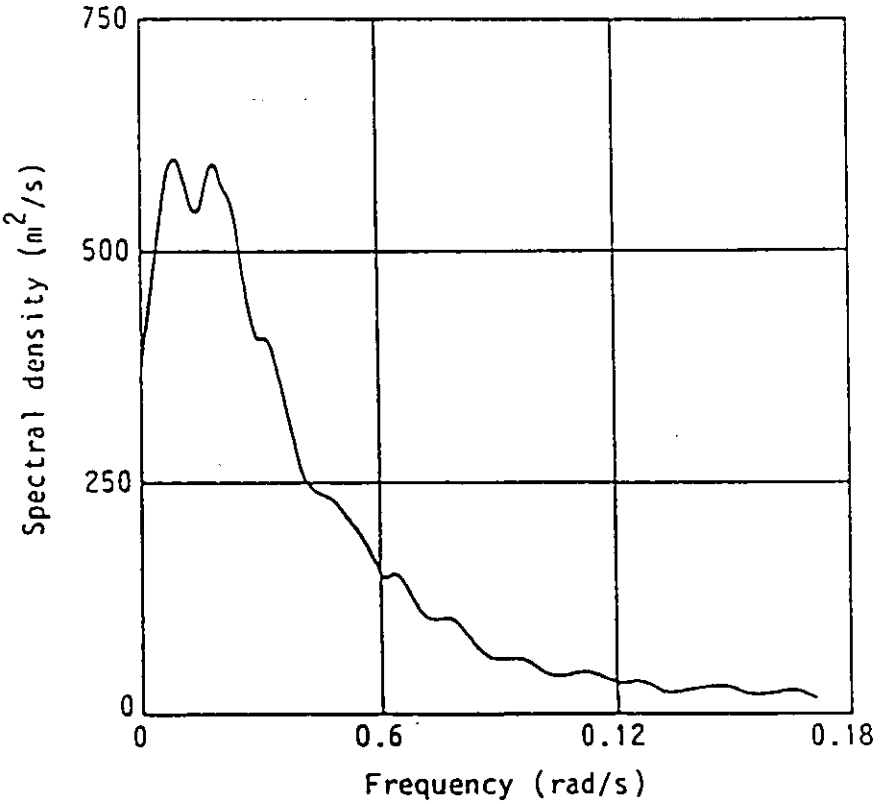

- Generated 2π-enhanced wind spectrum in the basin

Figure 8: Adjusted wind velocity spectrum

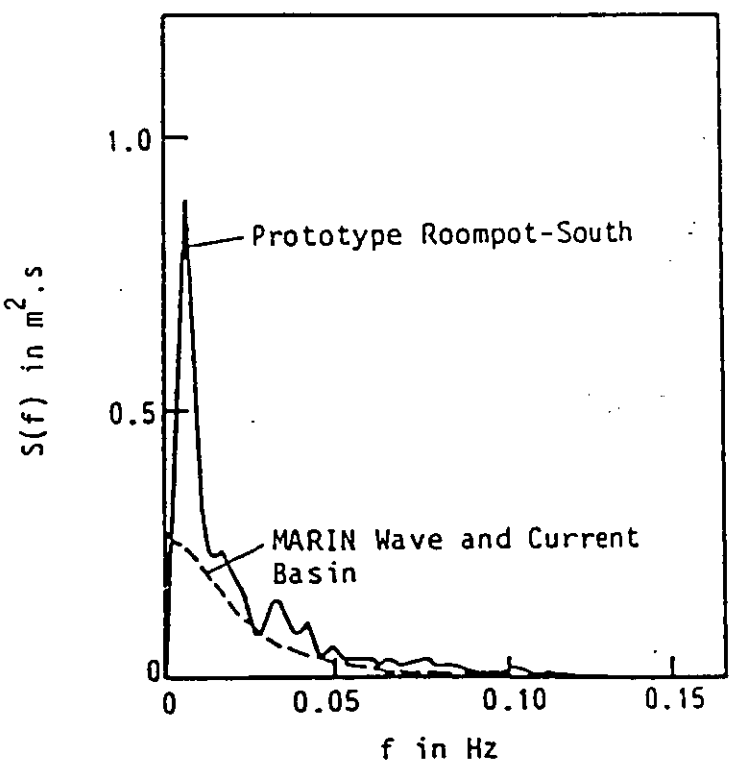

Spectral density of low-frequency current velocity fluctuations

Figure 9: Current velocity spectrum

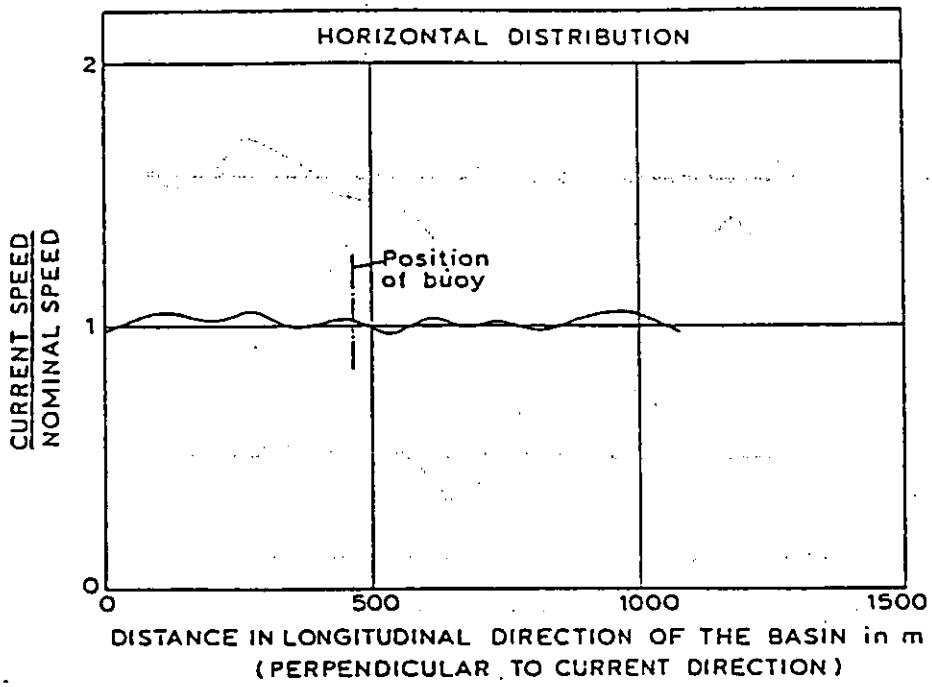

Figure 10: Adjusted current field in basin

$V_W = 0$

V_C = 1.03 m/s (time-varying direction; 10° block function)

Fully loaded (100%)

Bow hawser length = 75 m

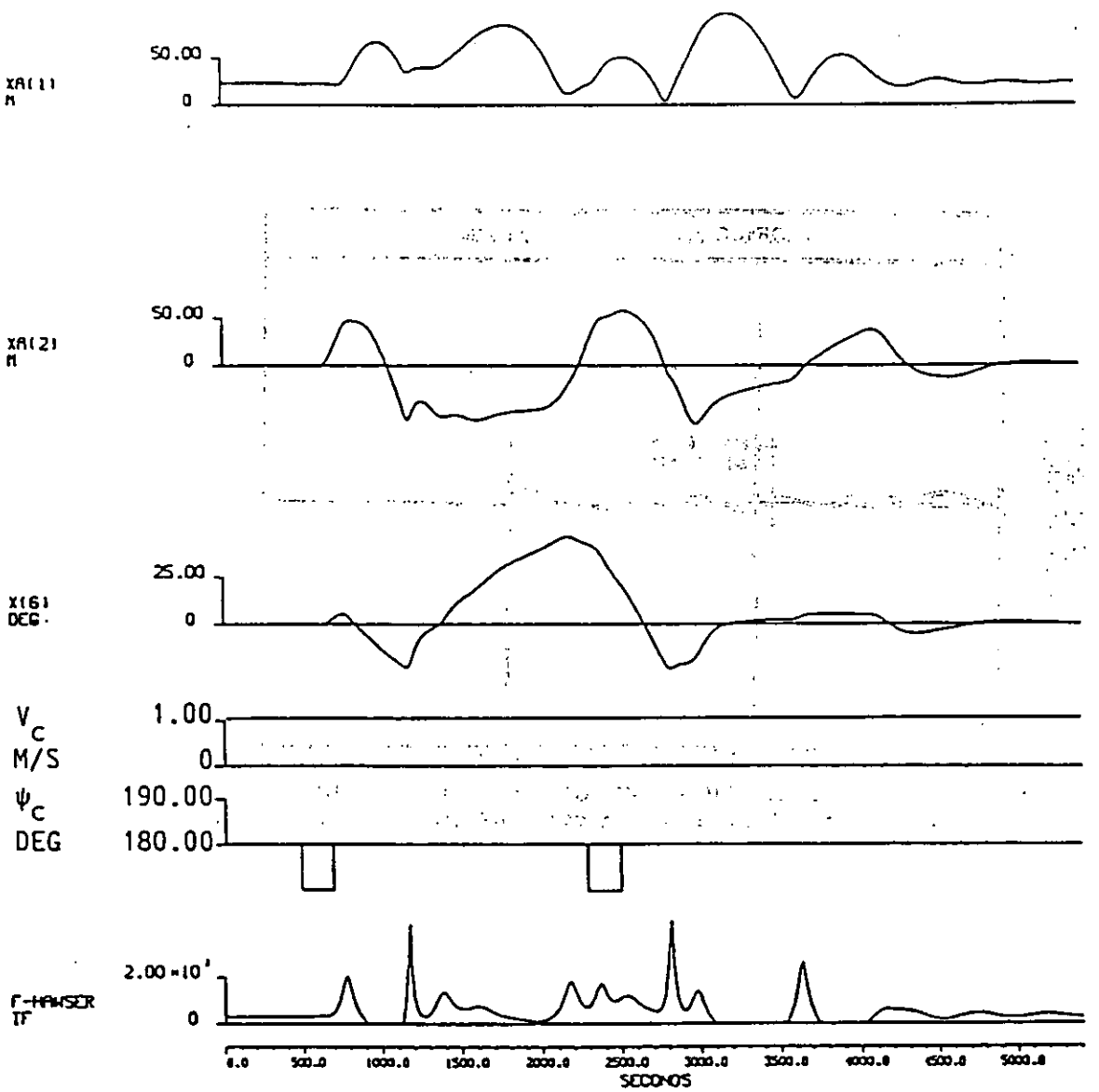

Figure 11: Influence of current dynamics on tanker motions

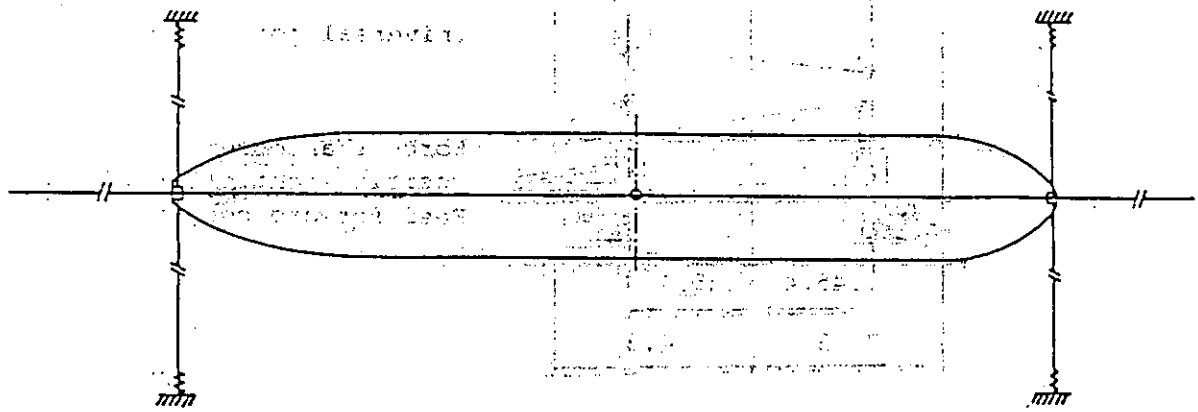

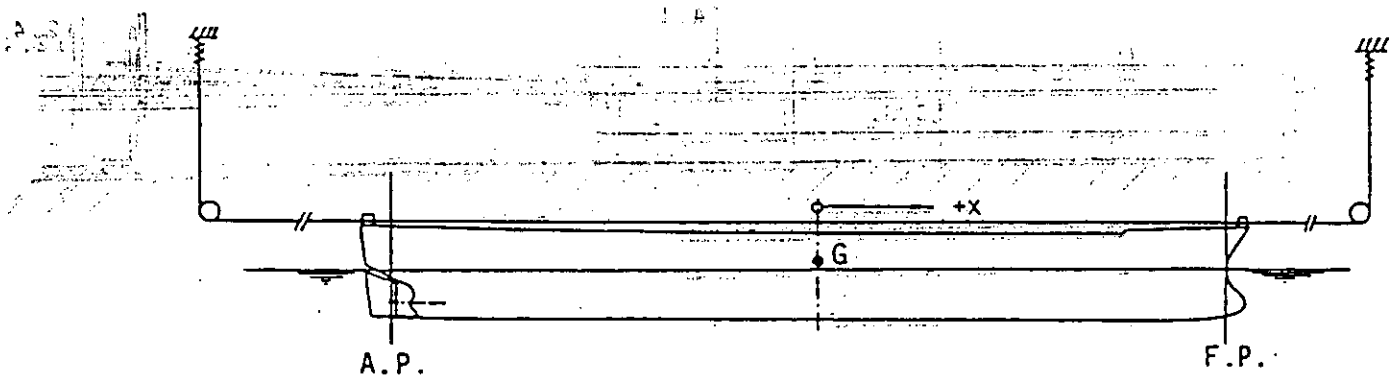

Figure 12: Soft spring mooring system

Dimensions are given in metres (full scale)

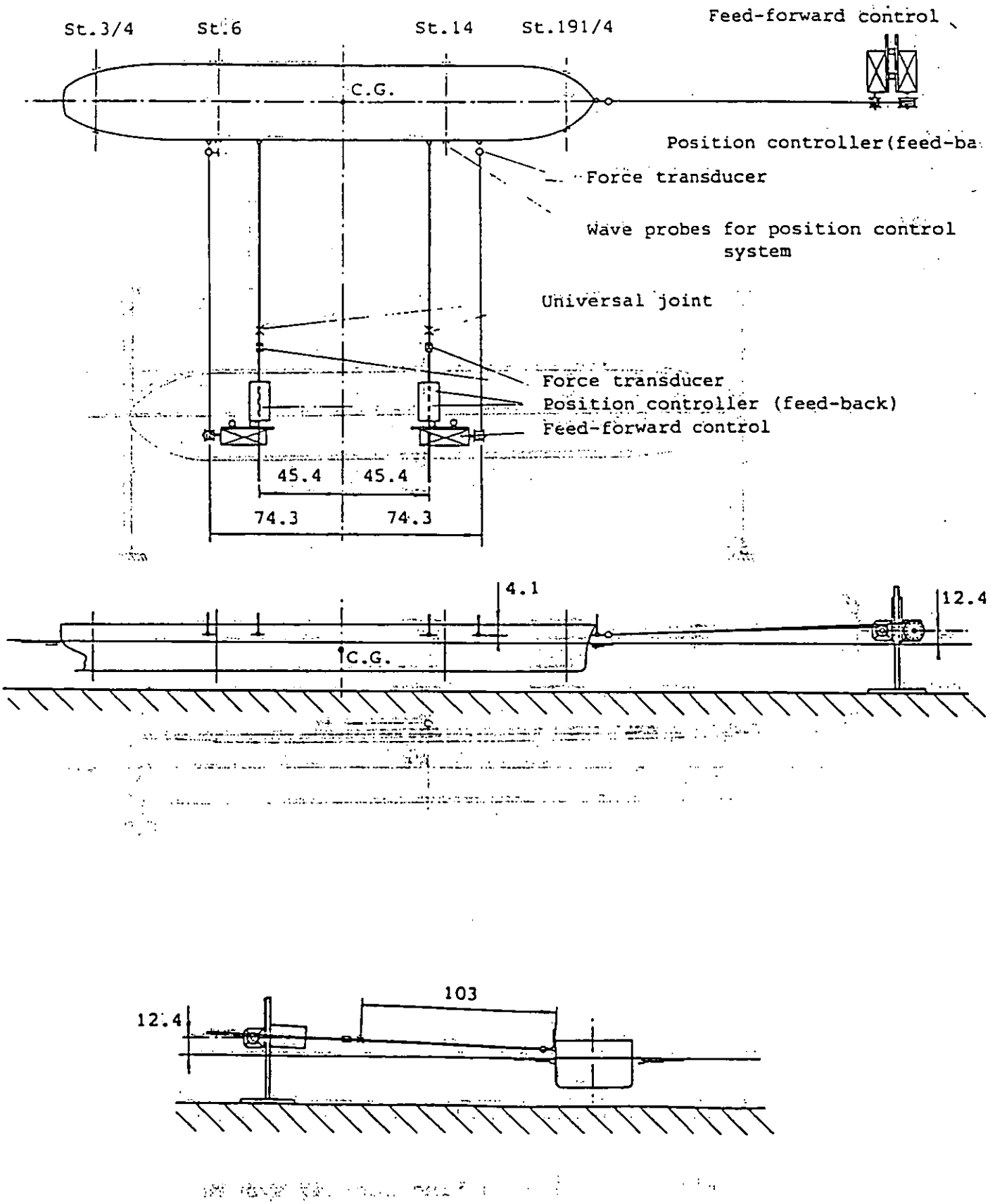

Figure 13: Dynamic system of restraint

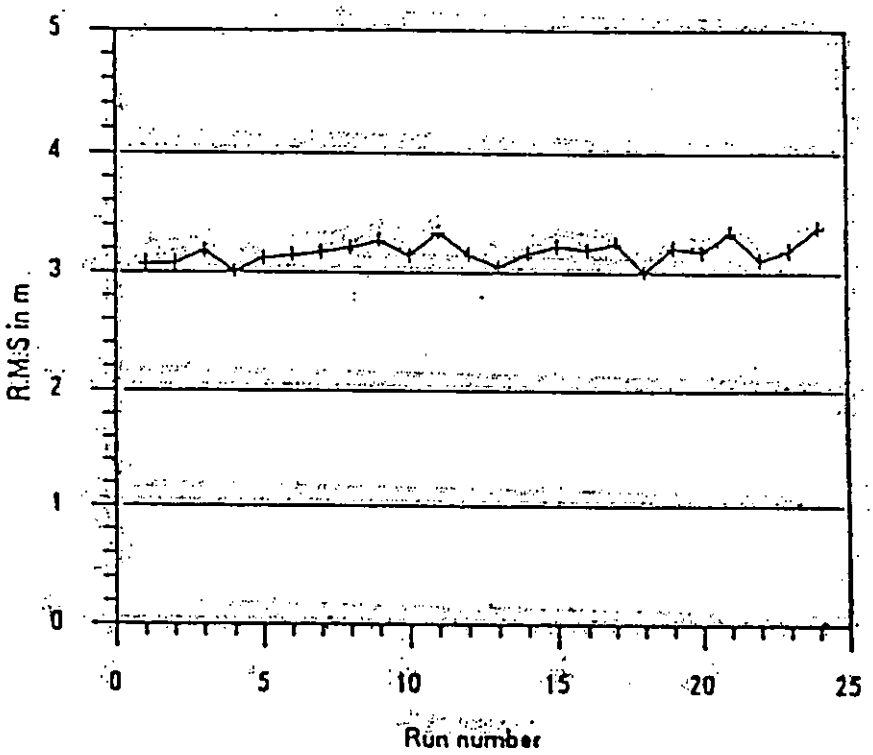

Figure 14: Time dependent wave rms-value during non-stop consecutive 30 minute wave runs